Volume 180 Number 1

THE BIOLOGICAL BULLETIN

FEBRUARY, 1991

Published by the Marine Biological Laboratory

THE BIOLOGICAL BULLETIN

PUBLISHED BY
THE MARINE BIOLOGICAL LABORATORY

FEBRUARY, 1991

Printed and Issued by
LANCASTER PRESS, Inc.
PRINCE & LEMON STS.
LANCASTER, PA

THE BIOLOGICAL BULLETIN

THE BIOLOGICAL BULLETIN is published six times a year by the Marine Biological Laboratory, MBL Street, Woods Hole, Massachusetts 02543.

Subscriptions and similar matter should be addressed to Subscription Manager, THE BIOLOGICAL BULLETIN, Marine Biological Laboratory, Woods Hole, Massachusetts 02543. Single numbers, $25.00. Subscription per volume (three issues), $72.50 ($145.00 per year for six issues).

Communications relative to manuscripts should be sent to Michael J. Greenberg, Editor-in-Chief, or Pamela L. Clapp, Managing Editor, at the Marine Biological Laboratory, Woods Hole, Massachusetts 02543. Telephone: (508) 548-3705, ext. 428. FAX: 508-540-6902.

POSTMASTER: Send address changes to THE BIOLOGICAL BULLETIN, Marine Biological Laboratory, Woods Hole, MA 02543.

Second-class postage paid at Woods Hole, MA, and additional mailing offices.
ISSN 0006-3185

INSTRUCTIONS TO AUTHORS

The Biological Bulletin accepts outstanding original research reports of general interest to biologists throughout the world. Papers are usually of intermediate length (10–40 manuscript pages). A limited number of solicited review papers may be accepted after formal review. A paper will usually appear within four months after its acceptance.

Very short papers (less than 9 manuscript pages including tables, figures, and bibliography) will be published in a separate section entitled "Research Notes." A Research Note in *The Biological Bulletin* follows the format of similar notes in *Nature*. It should open with a summary paragraph of 150 to 200 words comprising the introduction and the conclusions. The rest of the text should continue on without subheadings, and there should be no more than 30 references. References should be referred to in the text by number, and listed in the Literature Cited section in the order that they appear in the text. Unlike references in *Nature*, references in the Research Notes section should conform in punctuation and arrangement to the style of recent issues of *The Biological Bulletin*. Materials and Methods should be incorporated into appropriate figure legends. See the article by Lohmann *et al.* (October 1990, Vol. **179:** 214–218) for sample style. A Research Note will usually appear within two months after its acceptance.

The Editorial Board requests that regular manuscripts conform to the requirements set below; those manuscripts that do not conform will be returned to authors for correction before review.

1. ***Manuscripts.*** Manuscripts, including figures, should be submitted in triplicate. (Xerox copies of photographs are not acceptable for review purposes.) The original manuscript must be typed in no smaller than 12 pitch, using double spacing (*including* figure legends, footnotes, bibliography, etc.) on one side of 16- or 20-lb. bond paper, 8½ by 11 inches. Please, no right justification. Manuscripts should be proofread carefully and errors corrected legibly in black ink. Pages should be numbered consecutively. Margins on all sides should be at least 1 inch (2.5 cm). Manuscripts should conform to the *Council of Biology Editors Style Manual*, 4th Edition (Council of Biology Editors, 1978) and to American spelling. Unusual abbreviations should be kept to a minimum and should be spelled out on first reference as well as defined in a footnote on the title page. Manuscripts should be divided into the following components: Title page, Abstract (of no more than 200 words), Introduction, Materials and Methods, Results, Discussion, Acknowledgments, Literature Cited, Tables, and Figure Legends. In addition, authors should supply a list of words and phrases under which the article should be indexed.

2. ***Title page.*** The title page consists of: a condensed title or running head of no more than 35 letters and spaces, the manuscript title, authors' names and appropriate addresses, and footnotes listing present addresses, acknowledgments or contribution numbers, and explanation of unusual abbreviations.

3. ***Figures.*** The dimensions of the printed page, 7 by 9 inches, should be kept in mind in preparing figures for publication. We recommend that figures be about 1½ times the linear dimensions of the final printing desired, and that the ratio of the largest to the smallest letter or number and of the thickest to the thinnest line not exceed 1:1.5. Explanatory matter generally should be included in legends, although axes should always be identified on the illustration itself. Figures should be prepared for reproduction as either line cuts or halftones. Figures to be reproduced as line cuts should be unmounted glossy photographic reproductions or drawn in black ink on white paper, good-quality tracing cloth or plastic, or blue-lined coordinate paper. Those to be reproduced as halftones should be mounted on board, with both designating numbers or letters and scale bars affixed directly to the figures. All figures should be numbered in consecutive order, with no distinction between text and plate figures. The author's name and an arrow indicating orientation should appear on the reverse side of all figures.

4. ***Tables, footnotes, figure legends, etc.*** Authors should follow the style in a recent issue of *The Biological Bulletin* in preparing table headings, figure legends, and the like. Because of the high cost of setting tabular material in type, authors are asked to limit such material as much as possible. Tables, with their headings and footnotes, should be typed on separate sheets, numbered with consecutive Roman numerals, and placed after

the Literature Cited. Figure legends should contain enough information to make the figure intelligible separate from the text. Legends should be typed double spaced, with consecutive Arabic numbers, on a separate sheet at the end of the paper. Footnotes should be limited to authors' current addresses, acknowledgments or contribution numbers, and explanation of unusual abbreviations. All such footnotes should appear on the title page. Footnotes are not normally permitted in the body of the text.

5. ***Literature cited.*** In the text, literature should be cited by the Harvard system, with papers by more than two authors cited as Jones *et al.*, 1980. Personal communications and material in preparation or in press should be cited in the text only, with author's initials and institutions, unless the material has been formally accepted and a volume number can be supplied. The list of references following the text should be headed Literature Cited, and must be typed double spaced on separate pages, conforming in punctuation and arrangement to the style of recent issues of *The Biological Bulletin*. Citations should include complete titles and inclusive pagination. Journal abbreviations should normally follow those of the U. S. A. Standards Institute (USASI), as adopted by BIOLOGICAL ABSTRACTS and CHEMICAL ABSTRACTS, with the minor differences set out below. The most generally useful list of biological journal titles is that published each year by BIOLOGICAL ABSTRACTS (BIOSIS List of Serials; the most recent issue). Foreign authors, and others who are accustomed to using THE WORLD LIST OF SCIENTIFIC PERIODICALS, may find a booklet published by the Biological Council of the U.K. (obtainable from the Institute of Biology, 41 Queen's Gate, London, S.W.7, England, U.K.) useful, since it sets out the WORLD LIST abbreviations for most biological journals with notes of the USASI abbreviations where these differ. CHEMICAL ABSTRACTS publishes quarterly supplements of additional abbreviations. The following points of reference style for THE BIOLOGICAL BULLETIN differ from USASI (or modified WORLD LIST) usage:

A. Journal abbreviations, and book titles, all underlined (for *italics*)

B. All components of abbreviations with initial capitals (not as European usage in WORLD LIST *e.g. J. Cell. Comp. Physiol.* NOT *J. cell. comp. Physiol.*)

C. *All* abbreviated components must be followed by a period, whole word components *must not* (*i.e. J. Cancer Res.*)

D. Space between all components (*e.g. J. Cell. Comp. Physiol.*, not *J Cell Comp.Physiol.*)

E. Unusual words in journal titles should be spelled out in full, rather than employing new abbreviations invented by the author. For example, use *Rit Vísindafjélags Islendinga* without abbreviation.

F. All single word journal titles in full (*e.g. Veliger, Ecology, Brain*).

G. The order of abbreviated components should be the same as the word order of the complete title (*i.e. Proc* and *Trans.* placed where they appear, not transposed as in some BIOLOGICAL ABSTRACTS listings).

H. A few well-known international journals in their preferred forms rather than WORLD LIST or USASI usage (*e.g. Nature, Science, Evolution* NOT *Nature, Lond., Science, N.Y.; Evolution, Lancaster, Pa.*)

6. ***Reprints, page proofs, and charges.*** Authors receive their first 100 reprints (without covers) free of charge. Additional reprints may be ordered at time of publication and normally will be delivered about two to three months after the issue date. Authors (or delegates for foreign authors) will receive page proofs of articles shortly before publication. They will be charged the current cost of printers' time for corrections to these (other than corrections of printers' or editors' errors). Other than these charges for authors' alterations, *The Biological Bulletin* does not have page charges.

Reference: *Biol. Bull.* **180**: 1–11. (February, 1991)

Chemical Mediation of Larval Release Behaviors in the Crab *Neopanope sayi*

M. C. DE VRIES, D. RITTSCHOF, AND R. B. FORWARD JR.

Duke University Marine Laboratory, Beaufort, North Carolina 28516 and Duke University Zoology Department, Durham, North Carolina 27706

Abstract. Control of egg hatching was investigated in ovigerous females of the crab *Neopanope sayi*. Larval release is a brief event, generally lasting less than 15 min, during which females perform stereotypic behaviors involving vigorous abdomen pumping. Substances released by hatching eggs (pumping factors) of *N. sayi*, *Rhithropanopeus harrisii*, and *Uca pugilator*, but not *Sesarma cinereum*, evoked these stereotypic behaviors (pumping response) in ovigerous *N. sayi*. Spontaneous pumping and responsiveness to pumping factors varied with the age of the embryos. These results indicate that the eggs release pheromones around the time of hatching, which supports the general model for egg-hatching control described for *R. harrisii* (Forward and Lohmann, 1983). The chemistry of *N. sayi* pumping factors was investigated, and the pumping response was used as a bioassay in this study. Pumping factors adsorbed to Amberlite XAD-7 resin and could be eluted from it with methanol. Size fractionation by cascade pressure dialysis showed that the active molecules were <1000 daltons. Acid hydrolysis followed by reverse-phase HPLC amino acid analysis showed that the biologically active fraction contained peptides. Cysteine, glycine, methionine, and isoleucine were the four most common amino acids in these peptides. The responsiveness of *N. sayi* to hatch water from *R. harrisii*, the general similarity of adsorptive characteristics of hatch waters from the two species toward XAD-7 resin, and the amino acid compositional analysis suggest that the pumping factors from both species are similar. This supports the hypothesis that *N. sayi* pumping factors are also small peptides, as was suggested for those of *R. harrisii* (Rittschof *et al.*, 1985, 1989).

Introduction

Rhythms in larval release corresponding to lunar, diel, and tidal cycles have been observed for numerous species of Brachyura (see DeCoursey, 1983; Forward, 1987, for reviews). In species showing rhythms, egg hatching generally occurs during the dark phase of the diel cycle, and often near the high tide of a tidal cycle (Saigusa and Hidaka, 1978; Saigusa, 1981, 1982; Forward *et al.*, 1982; Wolcott and Wolcott, 1982; Christy, 1986; Salmon *et al.*, 1986; De Vries and Forward, 1989). For most warm-water species, such as the xanthid *Neopanope sayi*, larval release is a brief event, usually lasting less than 15 min for an individual (DeCoursey, 1979; Forward *et al.*, 1982; De Vries, 1990). During this time, in general, all of a female's eggs hatch while the female vigorously pumps her abdomen. Occasionally, larvae are released in more than one short burst at the time of consecutive tidal phases or nights (Forward *et al.*, 1982; Christy, 1986; De Vries and Forward, 1989).

The control of egg-hatching time in decapods seems to vary with species. Hatching time has been reported to be controlled by the female (Branford, 1978; DeCoursey, 1979) and alternatively by the developing embryos (Pandian, 1970; Ennis, 1973; Forward and Lohmann, 1983) in crabs and lobsters. The site of egg-hatching control may also be related to adult habitat (De Vries and Forward, 1991a). Control of egg-hatching time has been well studied only in the subtidal xanthid crab *Rhithropanopeus harrisii* (Forward and Lohmann, 1983; Rittschof *et al.*, 1985; Forward *et al.*, 1987; Rittschof *et al.*, 1989). In this species, the developing embryos control the exact timing, while the female controls the synchrony of hatching. Substances associated with hatching eggs are released near the time of hatching and induce the ovigerous female to perform stereotyped larval release behaviors that synchronize hatching. These pheromones are collectively called "pumping factors" and are a heterogeneous group of peptides mostly of <500 daltons.

The present study was performed to investigate the generality of the model for hatching-time control de-

Received 15 December 1989; accepted 28 November 1990.

scribed for *R. harrisii* (Forward and Lohmann, 1983). In particular, we aimed to determine whether active substances from another xanthid, *Neopanope sayi*, are similar to active components from *R. harrisii*. If active molecules from *N. sayi* are similar to those from *R. harrisii*, they should cross react biologically, and produce similar results upon chemical purification and analysis, as done for *R. harrisii* pumping factors (Rittschof *et al.*, 1985).

Neopanope sayi is a subtidal xanthid crab, occurring in coastal and estuarine areas, from the low littoral to the sublittoral zones (Williams, 1984). Experiments were designed to determine whether hatching eggs of *N. sayi* and other crab species produce substances that stimulate ovigerous *N. sayi* to perform larval release behaviors. Pumping factors were indicated, and some of their chemical characteristics were investigated, the crabs' stereotyped larval release behavior serving as an assay for biological activity. Our results suggest that pumping factors from *N. sayi* are similar in composition, but not identical, to those from *R. harrisii*.

Materials and Methods

General collection and maintenance of animals

Ovigerous females of *Neopanope sayi* (Smith) were collected from among the subtidal hard substrate community near the Duke University Marine Laboratory in Beaufort, North Carolina. Crabs were brought into the laboratory and placed into individually numbered culture bowls (diameter, 10.4 cm) containing approximately 160 ml of 5 μm filtered ambient salinity seawater (approximately 32–35‰). Crabs were located in a controlled-environment room (27°C ± 1°C), under a 14 h light:10 h dark cycle, with lights-out at 2000 h. This LD cycle corresponded to the cycle in the field at the time of collection.

The water in each crab's bowl was changed daily between 0900 and 1200 h. At this time, the presence of larvae in the bowls was noted and the date of larval release recorded for each crab. Experiments were performed on ovigerous females and the data were examined in relation to the age of the embryo. Embryonic age at the time of experimentation (expressed as days until hatching) was determined by counting backwards from the subsequent time of hatching. For individuals that released larvae in more than one burst, the release date was considered to be on the day that the first group of eggs hatched. Crabs were not fed while in the laboratory.

Spontaneous levels of pumping

Until they released their larvae, the crabs were placed once each day for 2 min into filtered (0.45 μm) seawater, and the number of spontaneous pumps counted. The spontaneous pumping activities of 62 *N. sayi* carrying embryos of various developmental stages were recorded in this way. These data were collected to determine whether the percentage of crabs that pumped spontaneously, and the absolute frequency of spontaneous pumping varied with embryo age.

Because crabs were brought into the laboratory carrying embryos of all ages, and because their pumping activities were measured repeatedly, the effects on spontaneous pumping activity of length of time in the laboratory and of embryo age might be confounded. To separate the effects of the two variables, plots of frequency of spontaneous abdomen pumping *versus* length of time in the laboratory were made for three groups of crabs (*i.e.*, those carrying embryos that would hatch in 0–1, 2–3, and 4–5 days, respectively). These plots showed no relationship between pumping and time in the laboratory (De Vries, unpub. data). Thus, when embryo age was held constant, the frequency of spontaneous abdomen pumping appeared to be independent of time in the laboratory. Plots were not made for crabs carrying embryos in earlier stages because of the small numbers and extremely low pumping rate of such crabs. *N. sayi* release their larvae within at most 10 days of egg deposition at the laboratory maintenance temperature of 27°C.

Biological assays

An abdomen-pumping bioassay was used to detect chemicals that stimulated larval release behaviors in ovigerous crabs. The assay, a modification of that described in Forward and Lohmann (1983), proceeded as follows. A crab was placed in a bowl (diameter, 7.9 cm) containing 80 ml of filtered, (0.45 μm) ambient salinity seawater, and the frequency of abdomen pumps was counted for 2 min. The crab was then transferred to a second bowl containing 80 ml of test solution, and the count was repeated. If a crab pumped at least five more times in the second bowl than in the first, this was counted as a positive signal or a "response" to that test solution. For any given test solution, 20–60 (but usually 30) animals were assayed. The percentage of crabs tested that responded to each test solution was defined as the % response, and is considered a measure of the biological activity of that solution. Most test solutions were derived from water in which crab larvae were released by females. We used the number of larvae released per ml of water as an indication of the concentration of active substances in that solution. The results of pumping-response assays are shown as dose-response curves (*i.e.*, larvae/ml *vs.* % response), such as that in Figure 2.

The two-bowl protocol, described above, was used to allow for variability in spontaneous pumping activity among individuals, as well as for changes in this parameter within an individual that might occur between 1000 and 1700 h, the interval during which these assays were performed. An assay was also performed in which both bowls

contained filtered seawater—a control of the effects of the experimental procedure upon spontaneous pumping rates. Although pumps were usually vigorous, they were sometimes subtle, and could be unseen if crabs suddenly moved their abdomens out of view. The criterion of a five pump difference to define a positive response was therefore used to preclude potential observational errors that could occur with differences of less than five pumps. A simple proportional increase in pumping between two bowls to define a response was inappropriate, because many crabs pumped 0 times in the first bowl.

Water in the control and test bowls was replaced after every 10 crabs to ensure a minimal change in water composition between crabs (Forward *et al.*, 1987). Individuals were assayed in each concentration of a test solution only once, and were not retested with another concentration within 30 min. Individuals were generally tested 3–5 times/day. Crabs were returned to their home bowls containing filtered seawater between tests. Substances were tested from the lowest to the highest concentrations to reduce adaptation. Significant differences between test and control response levels were established by the use of a Z-statistic for testing differences between two proportions at $\alpha = 0.05$ (Walpole, 1974).

Preparation of hatch water

We collected water into which *N. sayi* had released larvae and determined whether it would stimulate larval release behaviors (*i.e.*, abdominal pumping) in ovigerous crabs. About 1–2 h before the predicted time of larval release (generally evening high tide for *N. sayi;* De Vries and Forward, 1989), ovigerous crabs were placed into individual culture bowls. The bowls were 10.4 or 7.9 cm in diameter (depending upon crab size) and contained 100 or 50 ml (respectively) of 0.45 μm filtered ambient salinity seawater. Just after a female had released her larvae, she was removed from the bowl, and the water was passed through 100 μm plankton netting to remove the larvae. This filtered hatch water was kept on ice only briefly and was then frozen (−20°C) for later use. The titer of pumping factors in a hatch water sample was estimated by counting subsamples of the larvae contributing to it, and is expressed as larvae/ml. Hatch water was collected from three additional crab species, *Sesarma cinereum* (Grapsidae), *Uca pugilator* (Ocypodidae), and *Rhithropanopeus harrisii* (Xanthidae), as described above, except that *R. harrisii* hatch water was collected in 10‰ water, as necessitated by their upper estuarine habitat. For testing in biological assays with *N. sayi,* the hatch water from *R. harrisii* was raised to ambient salinity with Instant Ocean.

The response to hatch water from *N. sayi* was assayed with crabs carrying embryos of different ages to determine whether sensitivity changed with the stage of embryonic development. Crabs with early (>5 days until hatching) embryos and crabs with late-stage (≤3 days until hatching) embryos were tested, and control levels (*i.e.*, percent response) were established for them. For all other assays, however, only crabs with late-stage embryos were used.

Isolation and purification of pumping factors

Adsorption chromatography. The molecular characteristics of *N. sayi* pumping factors were determined by a modification of the adsorption chromatography and size fractionation procedures of Rittschof *et al.* (1985), with the pumping bioassay being used to monitor the process. The pumping factors from hatch water were first concentrated on Amberlite XAD-7 resin. The column of resin (24 cm × 1 cm bed volume) was stored in 100% HPLC-grade methanol (Fisher Chemical Co.), and immediately before being loaded with pumping factors was rinsed with hexane, then back flushed and rinsed with at least 200 ml of deionized water. Loading was done by gravity-feed at approximately 16 ml/min. The passage of hatch water through the column was stopped before the resin was exposed. Methanol was carefully overlaid upon the hatch water. At the first signs of methanol breakthrough in the eluate (decrease in drop size and effervescence), the next 13 ml of solution was collected. The methanol in this sample was then evaporated under a stream of N_2 until approximately 1–2 ml of solution remained. This concentrated pumping factor was stored at −20°C until it was bioassayed or size fractionated.

For bioassays, concentrated pumping factor was diluted with filtered (0.45 μm) seawater to the desired test concentration. The calculation of larval concentrations in the test solutions was based upon that estimated in the original hatch water samples, assuming 100% recovery of pumping factors from the resin.

Cascade pressure dialysis. Hatch water from *N. sayi* that had been concentrated on XAD-7 resin was brought to a volume of about 100 ml with deionized water. This solution was subjected to cascade pressure dialysis (4°C, 40 psi); Amicon YM10 and YM2 Diaflo membranes with nominal cutoffs at 10 and 1 kDa, respectively, were used. The membranes were stored and rinsed according to the manufacturer's instructions. Two additional rinses with 50 ml deionized water were carried out under pressure to insure that all preservatives were washed from the membranes. A sample was first passed through the 10 kDa cutoff membrane. Part of this filtrate was bioassayed, and the remainder was fractionated with the 1 kDa cutoff membrane. When about 10 ml of sample remained above each membrane, three successive 40 ml rinses with distilled water were done. This procedure effectively eliminated small molecules (<10 or <1 kDa) in the original solution that might have been passively retained above the membranes. Rinse water passing through the membranes was discarded. Those solutions that passed through

the membranes, as well as those that were retained, were kept on ice and bioassayed immediately.

For bioassays, size fractionated pumping factor was diluted with filtered (0.45 μm) seawater to the desired test concentration. Larval concentrations in the test solutions were calculated based on those estimated in the original hatch water sample, assuming 100% recovery of pumping factors from size fractionation procedures.

Control solutions

To be certain that substances with biological activity were directly related to the hatching process, two control solutions were subjected to the hatch water purification procedure described above. One solution was 0.45 μm filtered seawater. The other was seawater in which ovigerous crabs had been incubated under conditions similar to those used for crabs releasing larvae (ovigerous crab essence). The filtered seawater was processed to ensure that no stimulatory effects were produced by the adsorption chromatography or cascade pressure dialysis. A volume of seawater equal to the average volume of hatch water processed in each batch was used. The number of larval equivalents in the filtered seawater control was based on the average concentration of all *N. sayi* hatch water processed during the present experiments.

Ovigerous crab essence was included as a control to ensure that substances associated with hatching eggs, and not substances secreted by ovigerous crabs or their embryos at other times, were responsible for the observed pumping activity. Ovigerous crab essence was prepared by placing 20 ovigerous *N. sayi* with embryos of various developmental stages into 2 l of 0.45 μm filtered seawater. After 2 h, the crabs were removed and the water treated as described above for the filtered seawater control. Each crab was assumed to carry 2500 eggs (based on unpublished estimates of egg-mass sizes for *N. sayi*), from which the larval concentrations of this control were calculated. Aliquots of the seawater and ovigerous crab essence controls were diluted such that they contained concentrations equivalent to 20 and 50 larvae/ml and were assayed; these concentrations of crude and size-fractionated hatch water produced strong pumping responses.

To be certain that larger active molecules were not denatured on the column matrix upon elution, hatch water not passed through the column was filtered through a 10 kDa membrane. Dilution series of the <10 kDa and >10 kDa fractions were assayed.

Amino acid analysis

The amino acid composition of *N. sayi* pumping factors was analyzed by Dr. Dano Fiorio at Florida State University. A <1 kDa sample from the release of approximately 19,000 larvae was analyzed. Reverse-phase high-performance liquid chromatography (HPLC) and pre-column derivatization with phenylisothiocyanate were performed using a modification of the method in Henrickson and Meredith (1984). Unhydrolyzed and hydrolyzed (in 6 *N* HCl for 24 h at 110°C) samples were analyzed to determine the initial composition of free amino acids and the composition of the peptides (<1 kDa), respectively. Phenylthiocarbomyl derivatives were separated on an octadecasilyl reverse-phase column and detected spectrophotometrically at 254 nm. Identification and quantification of amino acids was by comparison of derivatized standard amino acids with those in the samples.

Amino acid experiments

Results of the above compositional analysis provided the basis for testing the biological activity of mixtures of pure amino acids (Sigma Chemicals). Pumping assays were performed using a mixture of the four most abundant amino acids in hydrolyzed pumping factor, L-cysteine, glycine, L-isoleucine, and L-methionine. These amino acids were combined in equimolar amounts (as in hydrolyzed factor) and tested at concentrations bracketing those for which hatch water was active. In addition, pumping assays were performed using a combination of glycine and arginine, the most abundant amino acids in *Rhithropanopeus harrisii* pumping factor, in proportions and concentrations bracketing their level in hydrolyzed pumping factor from this species (Rittschof *et al.*, 1985).

Results

Spontaneous pumping rates

Frequency of spontaneous abdomen pumping generally increased with the age of the embryos (Fig. 1A). For crabs with embryos of all ages, at least 25% did not pump at all. However, the percentage of crabs which pumped increased sharply with increasing embryo age (Fig. 1B).

Response to hatch water

The percent pumping response of ovigerous *N. sayi* individuals increased when the animals were exposed to hatch water (Fig. 2A). Responsiveness varied with concentration for crabs with both early- and late-stage embryos. At concentrations lower than 2.5 larvae/ml for crabs with late embryos, and lower than 5.0 larvae/ml for crabs with early embryos, the percentages of crabs responding were not significantly different from controls. At these concentrations and higher, however, the percentages of crabs responding were significantly greater than controls.

For each concentration tested, the percentages of crabs with early embryos that responded were consistently lower than those of crabs with late embryos. This reflects, in part, the greater inclination of crabs with older embryos to spontaneously pump their abdomens (as evidenced by

the increased control levels), but probably also indicates that crabs with older embryos are more sensitive or responsive to pumping factors. The latter is evidenced by the higher concentration of hatch water necessary to elicit a significant percent response for crabs with early embryos compared to those with late embryos. Because crabs with late stage embryos were more responsive to pumping factors, they were used in all subsequent experiments.

N. sayi with late embryos also had significantly higher percent pumping responses upon exposure to hatch water from *Rhithropanopeus harrisii* and *Uca pugilator* at concentrations ≥ 20 larvae/ml (Fig. 3). Exposure of *N. sayi* to hatch water from *Sesarma cinereum* at concentrations from 1 to 60 larvae/ml, however, produced levels of response not significantly different from the control (Fig. 3). These results indicate some, but not complete, cross-reactivity of hatch waters among species, and suggest that active substances from some species are similar in composition.

Adsorption chromatography and cascade pressure dialysis

Hatch water was fractionated into substances with and without affinity for Amberlite XAD-7 resin, and the fractions were bioassayed with crabs bearing late-stage embryos. A concentration of 10 larvae/ml was tested because it produced maximum response (Fig. 2A). When exposed to untreated hatch water, 69% of the crabs responded (Table I), which was significantly greater than the control level (23%; n = 158). After passage of hatch water through the resin however, activity was lost. Only 33% of the crabs responded, which was not significantly different from the control level.

To recover adsorbed activity, the resin was eluted with methanol, which removes lipophilic and proteinaceous substances. Bioassays showed a modest increase in response when tested with the methanol eluate, but at concentrations up to 20 larvae/ml, these responses were not significantly different from those of the control (Fig. 2B, before size fractionation). After passage of the methanol eluate through the 10 kDa and 1 kDa membranes, activity reappeared (Fig. 2B), presumably due to the removal of an inhibitor introduced by, or concentrated by, the resin (see Discussion). In these two fractions, an increase in the percentage of response with concentration was observed, with concentrations ≥ 10 larvae/ml producing levels of response significantly different from control. The fractions from these two filtrations, which were retained above the membranes (the >10 kDa and the <10 kDa but >1 kDa fractions), produced levels of response no different from controls at concentrations up to 20 larvae/ml.

When untreated hatch water was passed through the 10 kDa cutoff membrane, the retained >10 kDa fraction lacked biological activity (Fig. 4). Response levels in the <10 kDa fraction were significantly greater than control levels at ≥10 larvae/ml. The absence of biological activity in the >10 kDa fraction of the untreated hatch water suggests that precipitation of large (>10 kDa), biologically active molecules onto the resin upon methanol elution was unimportant. In summary, pumping factors were adsorbed to XAD-7 resin, eluted with methanol, and were <1 kDa.

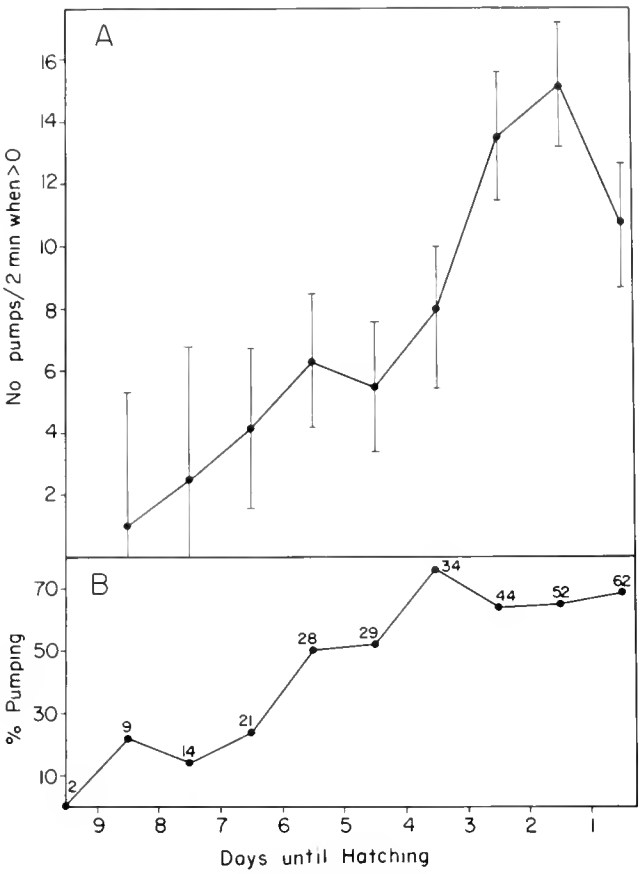

Figure 1. Frequency of spontaneous abdomen pumping (A), and percentage of crabs which pumped (B), as a function of embryo age in ovigerous female *Neopanope sayi*. Means and 95% confidence limits of spontaneous pumping frequency are shown for crabs that pumped at least once. The numbers beside the points are the sample sizes.

Controls demonstrated that biologically active substances originate from hatching eggs. Filtered seawater and ovigerous crab essence were subjected to the adsorption chromatograph and fractionation procedures. At concentrations equivalent to 20 and 50 larvae/ml, neither filtered seawater nor crab essence produced responses significantly greater than the filtered seawater control, either before or after passage of the two solutions through the resin and membranes (Table II). These results show that passage of seawater through the resin and membranes did not add excitatory substances to the water, and that substances associated with ovigerous females, in the absence of egg hatching, did not produce a significant level of pumping response.

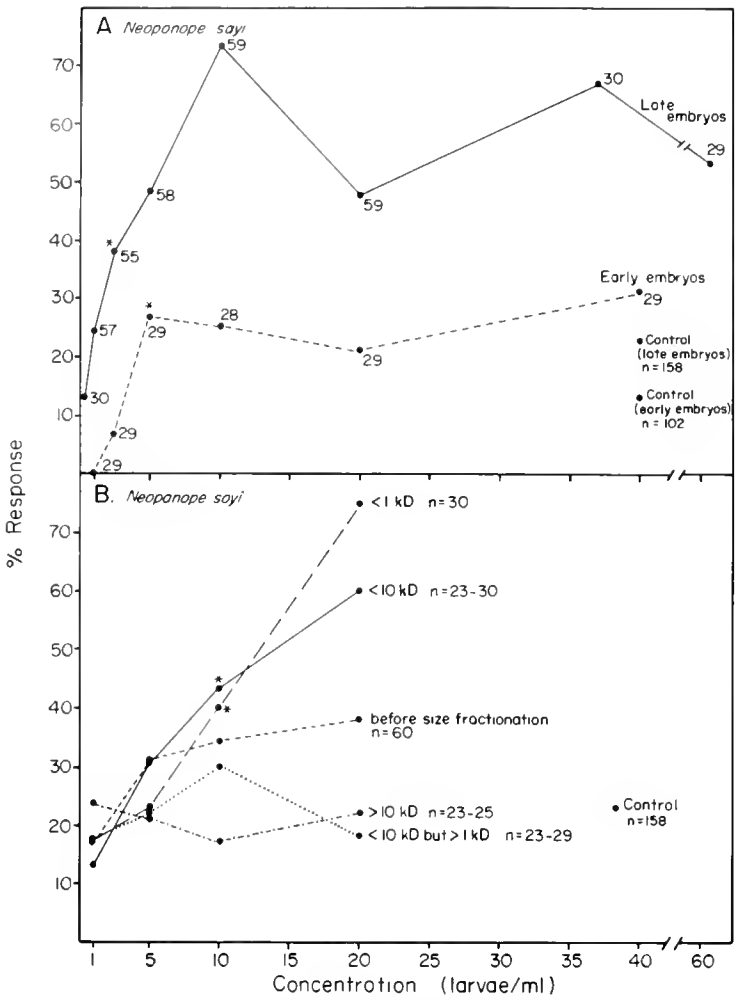

Figure 2. Percentage of ovigerous female *Neopanope sayi* that responded to *N. sayi* hatch water (A) and to various size fractions of a methanol eluate of hatch water after concentration on XAD-7 resin (B). Concentration of active substances (abscissa) was calculated from estimates of larval concentration in the untreated hatch water solutions. Numbers by points are specific sample sizes (A) or a range of sample sizes (B). Asterisks indicate the first concentration at which pumping response was significantly different from controls. Control levels for pumping response were established in filtered seawater. Crabs with late embryos were 0–3 days from larval release, and those with early embryos were >5 days from larval release.

Amino acid analysis

Reverse-phase HPLC analysis of free and hydrolyzable amino acids showed picomolar concentrations of 15 amino acids in the biologically active (<1 kDa) fraction of hatch water concentrated on the resin [calculated to a titer of 160 larvae/ml for comparison with results in Rittschof *et al.* (1985); Table III]. The most abundant amino acids after hydrolysis—cysteine, glycine, isoleucine, and methionine—accounted for 47% of the total free, and 57% of the total hydrolyzable amino acids. These four amino acids were approximately equimolar, at >100 p*M* after acid hydrolysis. Free amino acids before hydrolysis represented 23% of the total amino acids in the sample after hydrolysis. *N. sayi* pumping factors of this titer thus contain picomolar amounts of amino acids, most of which appear to be bound in peptides.

Amino acid experiments

When presented with mixtures of the amino acids most abundant in partially purified hatch water from *N. sayi* and *R. harrisii*, ovigerous *N. sayi* individuals significantly increased their levels of pumping over those of controls, at concentrations > 10^{-4} *M* (Fig. 5). Concentrations at which native pumping factors were effective (10^{-7}–10^{-9} *M*), produced pumping responses no different from controls. These effective concentrations are based on those of the four major amino acids (Table III) in hatch water of titer > 2.5 larvae/ml (*i.e.*, the threshold for crabs carrying late embryos; Fig. 2). In contrast, amino acid mix-

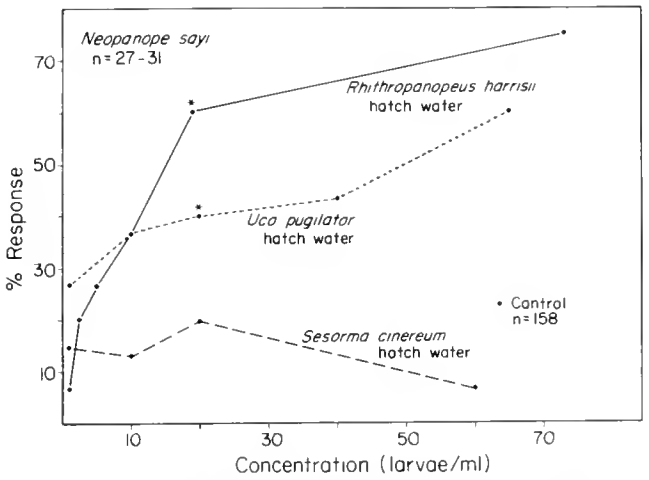

Figure 3. Percentage of ovigerous female *Neopanope sayi* with late embryos that responded to hatch water from three other brachyurans: *Rhithropanopeus harrisii*, *Uca pugilator*, and *Sesarma cinereum*. Asterisks indicate the first concentration at which the pumping response was significantly different from controls. Control levels for pumping response were established in filtered seawater.

tures first produced significant responses at concentrations corresponding to approximately 100,000 larvae/ml (2.5×10^{-4} *M*) for the *N. sayi* mixture, and approximately 7,000 larvae/ml (8.3×10^{-4} *M*) for the *R. harrisii* mixture. These results suggest that simple mixtures of the amino acids most abundant in pumping factors are not the molecules most active in producing abdomen pumping at the time of larval release.

Discussion

Substances associated with hatching eggs evoked stereotyped larval release behaviors in ovigerous females of the crab *Neopanope sayi*. Responsiveness to these pumping factors varied with embryo age, as did the spontaneous pumping activity of ovigerous crabs. The pumping factors adsorbed to Amberlite XAD-7 resin and could be eluted with methanol, but biological activity did not appear in the methanol eluate until after size fractionation. The presence of small peptides was inferred from the size fractionation and amino acid analysis of a partially purified preparation of hatch water.

For *N. sayi*, a clear variation was observed in the frequency of spontaneous abdomen pumping with embryo age. A possible physiological explanation for this phenomenon is that, as nonliving yolk is converted into embryo, metabolic rate increases, causing increased O_2 demand and waste production. Abdomen pumping by crabs is thought to facilitate O_2 transport to, and waste removal from, developing embryos (Templeman, 1937; Ennis, 1973), hence older embryos with higher metabolic rates would require more water pumped around them.

In contrast to those of *N. sayi*, the spontaneous abdomen pumping rates of *R. harrisii* were independent of

Table I

Effect of passing hatch water through Amberlite XAD-7 resin

Fraction	Test concentration larvae/ml	n	Percentage responding
Hatch water before resin	10	59	69
Hatch water after resin	10	30	33
Control	—	158	23

embryo age (Forward and Lohmann, 1983). This species difference may be due in part to the smaller size of *R. harrisii* egg masses (average size, about 1000 eggs; Forward, unpub. data) compared with *N. sayi* (generally 2000–4000 eggs; De Vries unpub. data). Eggs of the two species are of approximately the same diameter [about 400 μm on the day of hatching (De Vries and Forward, 1990b; De Vries, unpub. data)]. Therefore, the egg masses of *N. sayi* are 2–4 times larger in volume than those of *R. harrisii*, and the former would have a greater total metabolic demand and slower diffusion rate of water through the egg mass. These effects may compound one another, leading to a much greater need for water transport around *N. sayi* eggs, and thus a more pronounced increase in pumping rate as the embryos mature. The increase in egg mass size (De Vries and Forward, 1990b) with embryo age may cause the increase in spontaneous pumping rate by stimulating stretch receptors.

The response of *N. sayi* to hatch water of conspecifics is similar to that observed previously for *R. harrisii* (For-

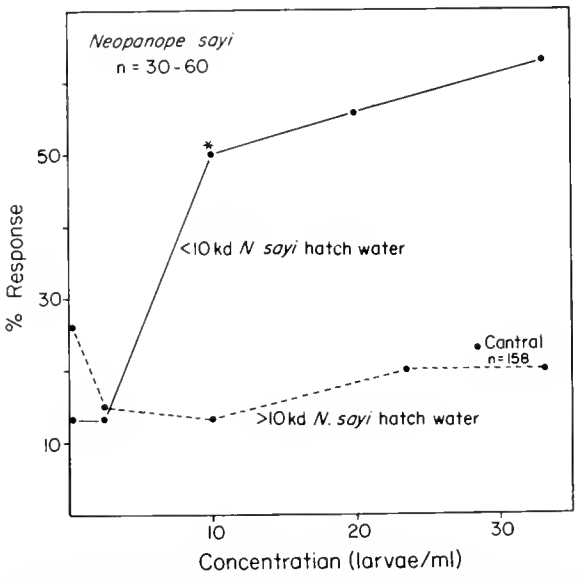

Figure 4. Percentage of ovigerous females of *Neopanope sayi* with late embryos that responded to the retained and non-retained fractions of *N. sayi* hatch water after ultrafiltration with a 10 kDa membrane. The control is for responses in filtered seawater.

Table II

Controls performed for Neopanope sayi *pumping factor experiments*

Solution	Test concentration (larvae/ml)	n	Percentage responding
1. 0.45 μm filtered seawater (FSW) (untreated) (control)	—	158	23
2. 10 kDa fraction MeOH eluate FSW	20	31	23
10 kDa fraction MeOH eluate FSW	50	30	17
3. 1 kDa fraction MeOH eluate FSW	20	30	17
1 kDa fraction MeOH eluate FSW	50	30	17
4. Ovigerous crab essence (OCE) (untreated)	25	25	13
5. 10 kDa fraction MeOH eluate OCE	20	35	26
10 kDa fraction MeOH eluate OCE	50	35	17
6. 1 kDa fraction MeOH eluate OCE	20	35	23
1 kDa fraction MeOH eluate OCE	50	35	6

In all tests, crabs carrying embryos within three days of hatching were used. Test concentrations were calculated as described in the text. Solutions 2–6 produced response rates not significantly greater than control (Solution 1). Ovigerous crab essence was seawater in which ovigerous crabs had been incubated for several hours (details in text).

ward and Lohmann, 1983), which suggests that the model for hatching-time control described for *R. harrisii* also applies for *N. sayi*. In this model, synchronized development of the eggs is believed to result from an unknown interaction between the embryos and the females, but actual hatching time is controlled by the embryos. When the eggs become ready to hatch, several eggs hatch spontaneously, releasing substances into the water that stimulate additional abdomen pumping. This action breaks open the remaining eggs, and the result is the synchronous release of larvae. The release of pheromones by embryos to communicate their readiness to hatch may have adaptive significance. During larval release, female crabs are presumably exposed and therefore at greater risk to predation than at other times (Forward and Lohmann, 1983). In addition, abdominal pumping during larval release is a vigorous, hence an energetically costly activity. Concentration of larval release behaviors to a time when the embryos are ready to hatch may thus decrease the risk of predation and energetic costs to the female.

Substances (pumping factors) that evoke larval release behavior (pumping response) were released at the time of egg hatching and were not released from eggs prior to this time. The effects of different treatments with these pumping factors can be determined by comparing the effective concentrations that evoked a 50% pumping response (EC_{50}; Table IV). When exposed to untreated hatch water, the titer for the EC_{50} was 6 larvae/ml. If this water was passed through a 10 kDa cutoff membrane, the EC_{50} increased to 10 larvae/ml. Because activity could not be detected in the water above the 10 kDa membrane, this decrease in activity did not result from the removal of large active molecules. Two possible explanations are adsorption of active molecules to the membrane during the filtration process, or degradation during the filtration interval by enzymes released by lysed microorganisms during thawing and pressure dialysis of hatch water. Crabs were unresponsive to hatch water that had been passed through the XAD-7 resin, suggesting that active substances

Table III

Amino acid composition of hydrolyzed and unhydrolyzed Neopanope sayi *pumping factor of <1000 daltons*

Amino Acid	Picomolar amount		
	Unhydrolyzed factor	Hydrolyzed factor	Difference
Pro	—	35	35
Cys	53	134	81
Asp	—	13	13
Thr	6	29	23
Ser	15	61	46
Glu	—	47	47
Gly	6	125	119
Ala	6	58	52
Val	28	61	33
Met	3	137	134
Ile	43	123	80
Leu	4	34	30
Tyr	—	—	—
Phe	51	54	3
His	—	—	—
Lys	7	15	8
Arg	—	19	19
Total	222	945	723

Concentrations are calculated for a sample with a titer of 160 larvae/ml.

were removed by the column. The methanol eluate was also inactive. Pressure dialysis of the methanol eluate resulted in a titer of activity comparable to size fractionated (10 kd filtered) hatch water that had not been passed through the resin. This result suggests high recovery of pumping factors from the column, as previously obtained for *R. harrisii* factors (Rittschof *et al.*, 1985).

The apparent absence of activity in the methanol eluate may have resulted because the resin: (1) removed an important component of the pumping factors that was not eluted with methanol; (2) concentrated high molecular weight inhibitory substances in the hatch water; or (3) added inhibitory substances *de novo*. The column did not add inhibitory molecules because XAD-7 resin leaches low molecular weight compounds (Jolley *et al.*, 1981) that would not be removed by size fractionation. Because activity reappeared after passage through the 10 kDa membrane (Fig. 4), the active factors and components were recovered from the resin. Thus, the most likely explanation is that inhibition resulted from concentration of high molecular weight inhibitory substances present in the hatch water.

The EC_{50} for the methanol eluate after passage through the 10 kDa membrane was 13 larvae/ml (Table IV). Because this value is very close to that for untreated hatch water (10 larvae/ml) after passage through the 10 kDa membrane, recovery of active molecules from the XAD-7 column was close to 100%. Rittschof *et al.* (1985) had similar success rates in recovery of active molecules in *R. harrisii* hatch water from an XAD-7 column. The activity of *N. sayi* hatch water remained the same (EC_{50} = 12 larvae/ml) after it had been passed through the 1 kDa membrane, indicating that activity can be attributed solely to molecules that are less than 1 kDa in size.

N. sayi responded to hatch water from *R. harrisii* and *Uca pugilator*, but the EC_{50} values were high at 15 and

Table IV

Effective concentrations for a 50% pumping response (EC_{50}) in crabs carrying late-stage embryos

Hatch water treatment	EC_{50} (larvae/ml)	Data source
Untreated	6	Fig. 2
10 kDa filtered	10	Fig. 4
XAD-7 resin	none	Fig. 2
XAD-7 resin, 10 kDa filtered	13	Fig. 2
XAD-7 resin, 10 kDa, 1 kDa filtered	12	Fig. 2
Rhithropanopeus harrisii hatch water	15	Fig. 3
Uca pugilator hatch water	50	Fig. 3

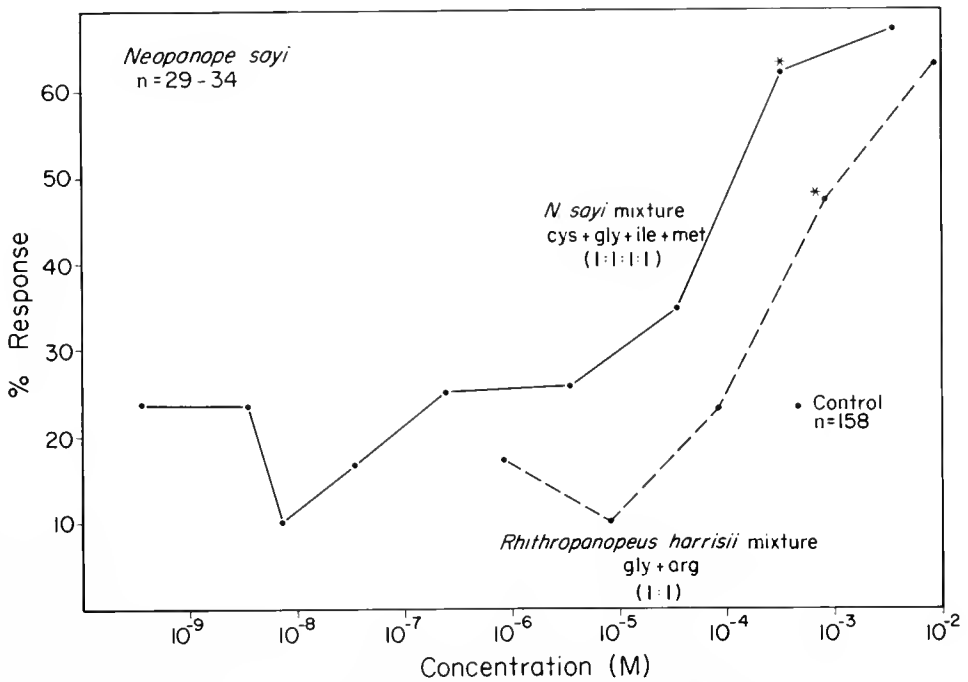

Figure 5. Percentage of ovigerous *Neopanope sayi* with late embryos that responded to different concentrations of mixtures of amino acids. Mixtures represent the main components of hydrolyzed pumping factors of *N. sayi* (equimolar amounts of L-cysteine, glycine, L-isoleucine, and L-methionine) and *Rhithropanopeus harrisii* (equimolar amounts of glycine and L-arginine; Rittschof *et al.*, 1985). Asterisks indicate the first concentration at which the pumping response was significantly different from controls. Control levels for the response were established in filtered seawater.

50 larvae/ml, respectively (Table IV). This result, and the lack of response to *S. cinereum* hatch water, show that cross-reactivity among species occurs, but is incomplete, implying that hatch waters from different species may be similar, but are probably not identical.

Three lines of evidence suggest that the active molecules in hatch water of *R. harrisii* are peptides. First, activity is lost if hatch water is treated with a protease. Second, compositional analysis of partially purified active molecules suggests that they may consist of di- or tripeptides with a neutral amino acid at the amino-terminus and an arginine carboxy-terminus (Rittschof *et al.*, 1985). Third, pure peptides having this structure induce pumping responses (Forward *et al.*, 1987; Rittschof *et al.*, 1989).

Results from the present study support the hypothesis that active substances in hatch water of *N. sayi* are also peptides, though their exact chemical nature is unknown. Evidence for this includes: (1) responsiveness of *N. sayi* to *R. harrisii* hatch water; (2) general similarity in the adsorptive characteristics of *N. sayi* and *R. harrisii* pumping factors toward XAD-7 resin; (3) suggestion of peptides in a partially purified hatch water preparation; and (4) similarity in the response of *N. sayi* and *R. harrisii* to mixtures of amino acids.

The amino acid analysis of *Neopanope sayi* pumping factors indicates that the four main amino acids in the proposed peptides are cysteine, glycine, isoleucine, and methionine. With the exception of glycine, these amino acids have neutral side chains and are hydrophobic. In contrast, the proposed active peptides of *Rhithropanopeus harrisii* contain arginine (present only in low amounts in *N. sayi* factor), which is strongly charged and hydrophilic. Thus the foregoing analysis suggests that the pumping factors of *N. sayi* are more hydrophobic than those of *R. harrisii*.

Bioassays of amino acids suggest that, for both species, simple mixtures of amino acids are not the active components of pumping factors (Rittschof *et al.*, 1985). Mixtures of the amino acids most abundant in the pumping factors produced significant levels of pumping only at concentrations much higher than those present in native hatch waters. The threshold concentrations for responses of *N. sayi* to amino acids were about 10^{-4} *M*, while free amino acid levels based on compositional analysis (Table III) at the threshold concentration of hatch water (2.5 larvae/ml; Fig. 2) were about 3.0×10^{-12} *M* (calculated from Table III). For *N. sayi*, small peptides of undetermined sequence are hypothesized to be the active components of pumping factors as concluded for *R. harrisii* (Rittschof *et al.*, 1985). The source of these peptides is as yet unknown. However we have postulated elsewhere that enzymatic degradation of the egg membranes (De Vries and Forward, 1991b; Rittschof *et al.*, 1990a) produces the pumping factors.

The chemical mediation of a diversity of behaviors has been described in virtually all phyla and may be particularly important in aquatic environments (*e.g.*, Knight-Jones, 1953; Collins, 1975; Trott and Dimock, 1978; Derby and Atema, 1980; Tierney and Dunham, 1982; Rittschof *et al.*, 1983, 1984). In particular, proteins and peptides elicit behaviors in various taxa, including feeding behavior in the snail *Ilyanassa* (=*Nassarius*) *obsoleta* (Carr *et al.*, 1974), creeping in predatory snails (Rittschof *et al.*, 1984), and metamorphosis in the sand dollar *Dendraster excentricus* (Burke, 1984) and the abalone *Haliotis* (Morse, 1988). Among crustaceans, serine protease generated peptides are implicated in hermit crab shell acquisition behavior (Rittschof, 1980; Lepore and Gilchrist, 1988; Rittschof *et al.*, 1990b), barnacle attachment behavior (Rittschof, 1985) and metamorphosis (Tegtmeyer and Rittschof, 1989), and crustacean larval release (Rittschof *et al.*, 1990a). Rittschof and Bonaventura (1986) argue that distinct advantages are inherent in the use of peptides as chemical cues in aquatic systems, including: (1) increased complexity of primary structure (compared to amino acids), allowing opportunity for increased response specificity; (2) background concentrations in marine systems are low (Mopper and Lindroth, 1982), allowing for high signal to noise ratios; and (3) metabolic inexpensiveness, because they need not be synthesized *de novo*, but may be broken down from existing structural and metabolic components.

Acknowledgments

We thank Dr. D. Fiorio for performing the amino acid analysis of *N. sayi* pumping factors. We are grateful to C. Buswell, K. Eisenman, E. Herzog, S. Posey, M. Wachowiak and C. Wellins for technical assistance. This material is based on research supported by the National Science Foundation under Grants No. OCE-8603945 and DCB-8701544.

Literature Cited

Branford, J. R. 1978. The influence of daylength, temperature and season on the hatching rhythm of *Homarus gammarus*. *J. Mar. Biol. Assoc. U.K.* **58:** 639–658.

Burke, R. D. 1984. Pheromonal control of metamorphosis in the Pacific sand dollar, *Dendraster excentricus*. *Science* **225:** 442–443.

Carr, W. E. S., E. R. Hall, and S. Gurin. 1974. Chemoreception and the role of proteins, a comparative study. *Comp. Biochem. Physiol.* **47A:** 559–566.

Christy, J. H. 1986. Timing of larval release by intertidal crabs on an exposed shore. *Bull. Mar. Sci.* **39:** 176–191.

Collins, A. R. S. 1975. Biochemical investigation of two responses involved in the feeding behavior of *Acanthaster planci* (L.) II. Isolation and characterization of chemical stimuli. *J. Exp. Mar. Biol. Ecol.* **17:** 69–86.

DeCoursey, P. J. 1979. Egg hatching rhythms in three species of fiddler crabs. Pp. 399–406 in *Cyclic Phenomena in Marine Plants and Animals*, E. Naylor and R. G. Hartnoll, eds. Pergamon Press, Oxford.

DeCoursey, P. J. 1983. Biological timing. Pp. 107–162 in *The Biology of Crustacea*, Vol. 7, F. J. Vernberg and W. B. Vernberg, eds. Academic Press, New York.

Derby, C. D., and J. Atema. 1980. Induced host odor attraction in the pea crab *Pinnotheres maculatus*. *Biol. Bull.* **158:** 26–33.

De Vries, M. C. 1990. Control of egg hatching in crabs: a comparative study of species from different tidal heights. Ph.D. dissertation, Duke Univ., Durham, NC.

De Vries, M. C., and R. B. Forward Jr. 1989. Rhythms in larval release of the sublittoral crab *Neopanope sayi* and the supralittoral crab *Sesarma cinereum*. *Mar. Biol.* **100:** 241–248.

De Vries, M. C., and R. B. Forward Jr. 1991a. Control of egg-hatching time in crabs from different tidal heights. *J. Crust. Biol.* In press.

De Vries, M. C., and R. B. Forward Jr. 1991b. Mechanisms of crustacean egg hatching: evidence for enzyme release by crab embryos. *Mar. Biol.*

Ennis, G. P. 1973. Endogenous rhythmicity associated with larval hatching in the lobster *Homarus gammarus*. *J. Mar. Biol. Assoc. U.K.* **53:** 531–538.

Forward, R. B., Jr. 1987. Larval release rhythms of decapod crustaceans: an overview. *Bull. Mar. Sci.* **41:** 165–176.

Forward, R. B., Jr., and K. J. Lohmann. 1983. Control of egg hatching in the crab *Rhithropanopeus harrisii*. *Biol. Bull.* **165:** 154–166.

Forward, R. B., Jr., K. J. Lohmann, and T. W. Cronin. 1982. Rhythms in larval release by an estuarine crab (*Rhithropanopeus harrisii*). *Biol. Bull.* **163:** 287–300.

Forward, R. B., Jr., D. Rittschof, and M. C. De Vries. 1987. Peptide pheromones synchronize crustacean egg hatching and larval release. *Chem. Senses* **12:** 491–498.

Henrikson, R. L., and S. C. Meredith. 1984. Amino acid analysis by reverse-phase high-performance liquid chromatography: precolumn derivatization with phenylisothiocyanate. *Anal. Biochem.* **136:** 65–74.

Jolley, R. L. 1981. Concentrating organics in water for biological testing. *Environ. Sci. Technol.* **158:** 874–880.

Lepore, M., and S. Gilchrist. 1988. Hermit crab attraction to gastropod predation sites. *Am. Zool.* **28**(4): 93A.

Knight-Jones, G. W. 1953. Laboratory experiments on gregariousness during setting in *Balanus balanoides* and other barnacles. *J. Exp. Biol.* **30:** 584–598.

Mopper, K., and P. Lindroth. 1982. Diel and depth variations in dissolved free amino acids and ammonium in the Baltic Sea determined by shipboard HPLC analysis. *Limnol. Oceanogr.* **27:** 336–337.

Morse, A. 1988. The role of algal metabolites in the recruitment process. Pp. 463–475 in *Marine Biodeterioration: Advanced Techniques Applicable to the Indian Ocean*, M. Thompson and R. S. Nagabhushanam, eds. Oxford & IBW, Bombay.

Pandian, T. J. 1970. Ecophysiological studies on the developing eggs and embryos of the European lobster *Homarus gammarus*. *Mar. Biol.* **5:** 154–167.

Rittschof, D. 1980. Enzymatic production of small molecules attracting hermit crabs to simulated gastropod predation sites. *J. Chem. Ecol.* **6:** 665–675.

Rittschof, D. 1985. Oyster drills and the frontiers of chemical ecology: unsettling ideas. *Am. Malacolog. Bull.*, Spec. Ed. **1:** 111–116.

Rittschof, D., and J. Bonaventura. 1986. Macromolecular cues in marine systems. *J. Chem. Ecol.* **12:** 1013–1023.

Rittschof, D., L. G. Williams, B. Brown, and M. R. Carriker. 1983. Chemical attraction of newly hatched oyster drills. *Biol. Bull.* **164:** 493–505.

Rittschof, D., D. Keiber, and C. Merrill. 1984. Modification of responses of newly hatched snails by exposure to odors during development. *Chem. Senses* **9:** 181–192.

Rittschof, D., R. B. Forward Jr., and D. D. Mott. 1985. Larval release in the crab *Rhithropanopeus harrisii* (Gould): chemical cues from hatching eggs. *Chem. Senses* **10:** 567–577.

Rittschof, D., R. B. Forward Jr., D. A. Simons, P. Amantha Reddy, and B. W. Erickson. 1989. Peptide analogs of the mud crab pumping pheromone. *Chem. Senses* **14:** 137–148.

Rittschof, D., R. B. Forward Jr., and B. W. Erickson. 1990a. Larval release in brachyuran crustaceans: functional similarity of the peptide receptor and the catalytic site of trypsin. *J. Chem. Ecol.* **16:** 1359–1370.

Rittschof, D., C. M. Kratt, and A. S. Clare. 1990b. Gastropod predation sites: the role of predator and prey in chemical attraction of the hermit crab *Clibanarius vittatus* (Bosc). *JMBA* **70:** 583–596.

Saigusa, M. 1981. Adaptive significance of semilunar rhythm in the terrestrial crab *Sesarma*. *Biol. Bull.* **160:** 311–321.

Saigusa, M. 1982. Larval release rhythm coinciding with solar day and tidal cycles in the terrestrial crab *Sesarma*—harmony with the semilunar timing and its adaptive significance. *Biol. Bull.* **162:** 371–386.

Saigusa, M., and T. Hidaka. 1978. Semilunar rhythms in zoeae-release activity of the land crab *Sesarma*. *Oecologia* **37:** 163–176.

Salmon, M., W. H. Seiple, and S. G. Morgan. 1986. Hatching rhythms of fiddler crabs and associated species at Beaufort, North Carolina. *J. Crust. Biol.* **6:** 24–36.

Tegtmeyer, K., and D. Rittschof. 1989. Synthetic peptide analogs to barnacle settlement pheromone. *Peptides* **9:** 1403–1406.

Templeman, W. 1937. Egg-laying and hatching postures and habits of the American lobster (*Homarus americanus*). *J. Fish. Res. Bd. Canada* **3:** 339–342.

Tierney, A. J., and D. W. Dunham. 1982. Chemical communication in the reproductive isolation of the crayfishes *Orconectes propinquus* and *Orconectes virilis* (Decapoda, Cambaridae). *J. Crust. Biol.* **2:** 544–548.

Trott, T. J., and R. V. Dimock. 1978. Intraspecific trail following by the mud snail *Ilyanassa obsoleta*. *Mar. Behav. Physiol.* **5:** 91–101.

Walpole, R. E. 1974. *Introduction to Statistics*. Macmillan, New York.

Williams, A. B. 1984. *Shrimps, Lobsters, and Crabs of the Atlantic Coast of the Eastern United States, Maine to Florida*. Smithsonian institution Press, Washington DC.

Wolcott, T. W., and D. L. Wolcott. 1982. Larval loss and spawning behavior in the land crab *Gecarcinus lateralis* (Fremenville). *J. Crust. Biol.* **2:** 477–485.

Reference: *Biol. Bull.* **180:** 12–27. (February, 1991)

Particle Captures and the Method of Suspension Feeding by Echinoderm Larvae

MICHAEL W. HART

Department of Zoology, NJ-15, University of Washington, Seattle, Washington, 98195 and Friday Harbor Laboratories, 620 University Road, Friday Harbor, Washington, 98250

Abstract. Motivated by discrepancies between two recent descriptions of the suspension-feeding mechanism employed by echinoderm larvae, I describe particle captures by the larvae of seven species of temperate eastern Pacific echinoderms from four classes. When videotape recordings of free-swimming larvae clearing plastic spheres from suspension were analyzed, two modes of particle capture were observed to operate. The majority of captured spheres were caught at the peripheral ciliated band and then transported to the mouth, often by repeated capture on portions of the band progressively nearer to the mouth. This description is consistent with the ciliary reversal model of suspension feeding described by R. R. Strathmann. A small minority of captured spheres followed broad, curving paths directly into the larval mouth without interception at the ciliated band. These particle paths resemble those described by T. H. J. Gilmour. The videotape recordings also permitted a quantitative comparison of suspension feeding by these larvae. Several aspects of this behavior varied among developmental stages or among types of larvae, including: the distribution of particle captures among different segments of the ciliated band, the number of captures for single particles en route to the mouth, and the frequency of particles lost after initial capture. This variation raises a number of questions regarding the feeding performance of different larval species and the efficacy of these different larvae as elements of a reproductive strategy.

Introduction

The form and function of suspension-feeding aquatic animals is of wide interest, in part because they face a formidable challenge: concentrating materials and energy from a pool of resources that is both patchily distributed and highly dilute. Many different structures for concentrating food from suspension have evolved. These structures range from the relatively simple collar-cell filters of sponges to the morphologically and geometrically complex ciliated gills of bivalves and setose appendages of many crustaceans (Jorgensen, 1966). The method of capturing and concentrating food particles from suspension undoubtedly affects the effectiveness of particle capture and aspects of the growth and metabolism of suspension feeders (Conover, 1968). Inefficient suspension feeding may even limit the range of alternative strategies for growth and reproduction (McEdward and Strathmann, 1987). Thus, even if we were not generally curious about how organic particle filters work, there are particular reasons (the diversity of filters, and the physiological and evolutionary consequences of this diversity) for investigating the nature of different kinds of filters that remove food particles from suspension.

Suspension feeding by the planktonic larvae of echinoderms has been described by a number of authors (Gemmill, 1914, 1916; MacBride, 1914; Runnström, 1918; Meeks, 1927; Tattersall and Sheppard, 1934; Garstang, 1939; Strathmann, 1971, 1975; Strathmann *et al.*, 1972; Gilmour, 1985, 1986, 1988a, b). These larvae develop a band of tightly packed ciliated columnar epithelial cells (the ciliated band) that circumscribes the mouth, dividing the surface of the larva into circumoral and aboral fields (see Strathmann, 1971, 1975). Early workers offered divergent interpretations of the method by which these larvae concentrate suspended particles from seawater. They variously attributed larval feeding abilities to the actions of: (*i*) cilia on the circumoral field, (*ii*) water currents generated by the ciliated band, (*iii*) cilia surrounding

Received 27 November 1989; accepted 30 November 1990.

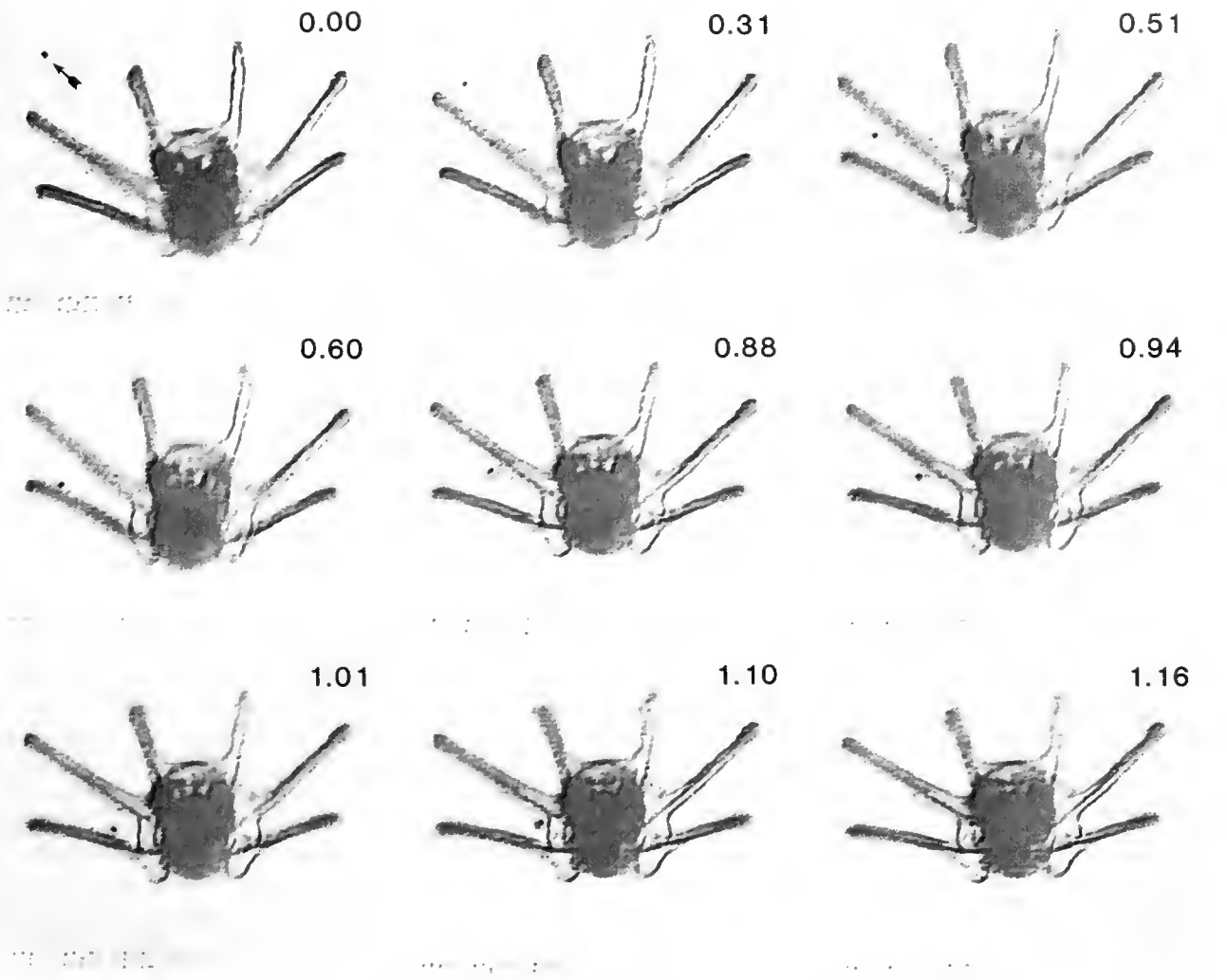

Figure 1. A collage of videotape frames showing the capture of a 20 μm diameter sphere by a six-armed echinopluteus (*Dendraster excentricus*). The number in the upper right of each panel is elapsed time in seconds (starting arbitrarily at 0 s). The arrow in the first panel shows the initial position of the particle. For scale, the arrow is about 135 μm long. The larva is shown in anterior ventral view, moving forward toward the top of each panel. The sphere moved toward the right postoral arm (0.00–0.51 s), was captured on the ciliated band and changed direction toward the base of the same arm (0.60–0.94 s), then was captured a second time near the base of the arm and moved toward the larval midline and mouth (1.01–1.16 s).

the mouth, and (*iv*) mucus secreted between opposed parts of the ciliated band. The more recent studies of Strathmann (1971) and Strathmann *et al.* (1972) resolved many of these conflicting descriptions: these studies suggest that echinoderm larvae remove particles from dilute suspensions by the brief reversal of the direction of the beat of cilia on the ciliated band. Particles are retained on the circumoral field, at the upstream side of the ciliated band, and then are transported toward the larval mouth. However, Gilmour (1985, 1986, 1988a, b) has disputed this interpretation of larval feeding and has suggested two completely different methods of particle capture.

Studies of suspension feeding by marine invertebrates often suffer from the inherent difficulty of relating rates of feeding to mechanisms of particle capture. For example, there is no general agreement on how the naplius larvae of copepods and barnacles capture particles, even though these are among the best-studied suspension feeders (reviewed by R. Strathmann, 1987). The feeding mechanism of nauplii is difficult to study because the movements of the feeding appendages and food particles are swift and complex. Measures of feeding rates of these animals are therefore restricted to indirect observations, such as the depletion of food particles (Paffenhöffer, 1971) or the in-

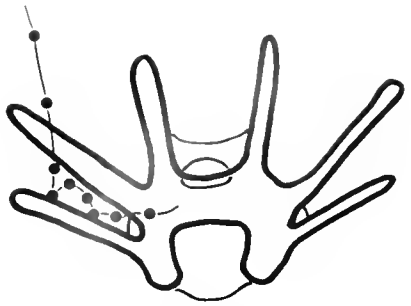

Figure 2. A cartoon of the particle capture sequence shown in Figure 1. The positions of the sphere in each panel of Figure 1 are indicated by the dots, and the particle path between these positions is interpolated by the solid line. The ciliated band of the larva is shown by the heavy lines; the mouth is shown in outline.

corporation of radioactivity from radiolabelled compounds in food particles (Marshall and Orr, 1956). However, without direct observations of feeding, it is difficult to relate variation in feeding rate (*e.g.*, among different naupliar stages) to variation in the morphological features (*e.g.*, the size and number of setae) that determine the feeding mechanism.

Unlike nauplii, the feeding larvae of echinoderms lend themselves to direct observation of particle capture. These larvae are relatively transparent, they swim with slow and continuous movement, and particle captures are sufficiently slow events that they can be counted and described with some precision. Given an accurate description of particle capture by these larvae, one can then interpret quantitative variation in feeding in terms of the particle capture mechanism. Echinoderm larvae are therefore excellent model organisms for comparative studies of form and function in suspension feeding.

In this report, I describe particle captures and suspension feeding by the larvae of seven species from four different echinoderm classes. A qualitative analysis of videotape recording (including still video images of particle captures) of free-swimming larvae clearing a dilute suspension of particles is generally consistent with Strathmann's description of the ciliary reversal suspension feeding mechanism. My observations also refute Gilmour's interpretation of the predominant method of particle capture by echinoderm larvae. However, a quantitative analysis of these recordings (which is difficult without a permanent record of larval behavior) leads to several novel inferences about larval feeding. First, these larvae appear to have two modes of particle capture: most particles are caught by apparent ciliary reversal at the ciliated band, but a small proportion of particles are captured without contacting the peripheral band, and this proportion does not vary among the different larvae examined. Second, changes in the distribution of particle captures on the ciliated bands of larvae do not correspond to changes in the lengths of particular segments of the band as larvae grow; some parts of the band appear to be more effective than others, and this discrepancy changes during larval development. Third, the number of independent ciliary reversals involved in a single particle capture (from the peripheral band to the mouth) varies among segments of the band, among developmental stages, and among species of echinoderms. These analyses also serve as a basis for quantitative comparisons of feeding performance among echinoderm larvae of different size, shape, and developmental stage that will be presented elsewhere.

Materials and Methods

Collection of adults

The sea urchin *Strongylocentrotus purpuratus* (Stimpson, 1857) (O. Echinoida) was collected from tidepools at Botanical Beach, Renfrew County, British Columbia, Canada. All other adults were collected from intertidal or shallow subtidal locations off the San Juan Islands, San Juan County, Washington, USA. *Strongylocentrotus droebachiensis* (O. F. Müller, 1776) and the sea star *Stylasterias forreri* (de Loriol, 1887) (O. Forcipulatida) were collected by dredge from San Juan Channel. The sea star *Dermasterias imbricata* (Grube, 1857) (O. Valvatida) was collected at 10 m depth from a rock wall off Turn Island. The sand dollar *Dendraster excentricus* (Eschscholtz, 1831) (O. Clypeasteroida) was collected from an intertidal bed in East Sound, Orcas Island. The brittle star *Ophiopholis aculeata* (L., 1767) (O. Ophiurida) was collected from a low intertidal cobble beach in Mitchell Bay on San Juan Island. The sea cucumber *Parastichopus californicus* (Stimpson, 1857) (O. Aspidochirotida) was collected at 15 m depth from a silt bottom off Brown Island.

Culture of embryos and larvae

Gametes, embryos, and larvae were treated according to methods described by M. Strathmann (1987). Gametes of echinoids were obtained by intracoelomic injection of 0.5 *M* KCl. Asteroid gonads were obtained by dissection; oocytes were induced to mature by incubation in $10^{-6}M$ 1-methyladenine in seawater. *Parastichopus* gonads were also obtained by dissection: oocytes were matured in a 1 $g \cdot l^{-1}$ solution of lyophilized radial nerve in seawater; and sperm were activated in 10 m*M* NH_4Cl in seawater. The radial nerves were obtained from the asteroid *Pycnopodia helianthoides* (Brandt, 1835). *Ophiopholis* females, in separate glass bowls filled with seawater, were allowed to warm on the benchtop for several hours and were thus induced to spawn; sperm were obtained by dissection.

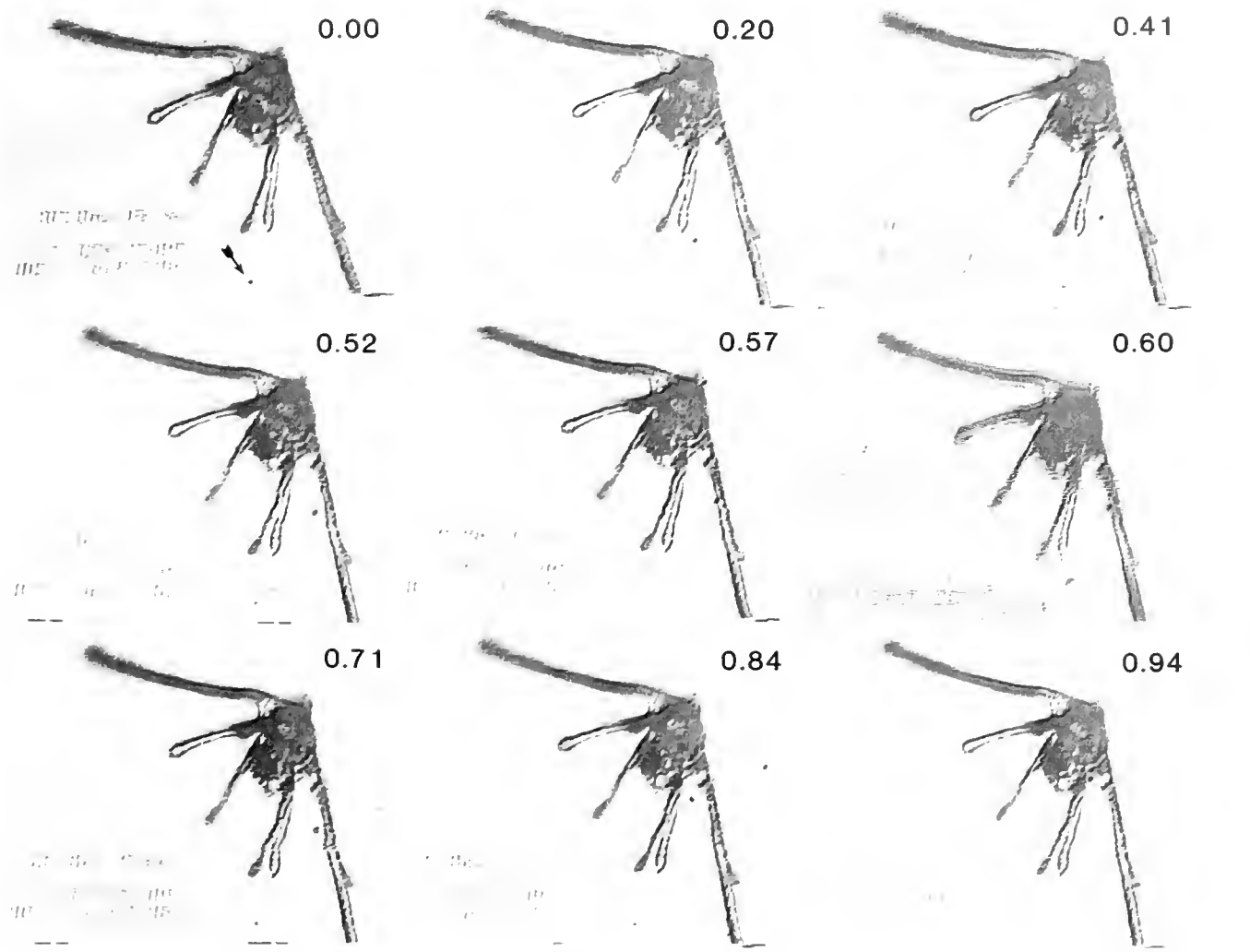

Figure 3. A collage of videotape frames showing the capture of a 20 μm diameter sphere by an eight-armed ophiopluteus (*Ophiopholis aculeata*) (the short postoral arms are not visible in this view). Numbers and arrow as in Figure 1. For scale, the arrow is 87 μm long. The larva is shown in anterior ventral view, moving forward toward the lower left of each panel. The sphere moved past the tips of the right anterolateral and posterodorsal arms (0.00–0.52 s), was captured on the right posterolateral arm (0.57–0.60 s), and changed direction back toward the larval mouth (0.71–0.94 s).

For all species, eggs were washed in 5-μm filtered seawater, fertilized with a few drops of a dilute sperm suspension, then washed again and transferred in groups of a few thousand to 3-l glass jars filled with filtered seawater. The jars were immersed in a flowing seawater bath at temperatures of 9–13°C (near local ambient sea temperature), stirred gently by paddles. Feeding larval stages were fed 2–3 ml per jar from dense cultures of each of three algae (*Dunaliella tertiolecta* Butcher, *Isochrysis galbana* Parke, and *Rhodomonas* sp.) at intervals of five to ten days coincident with water changes. These combinations of algae produced initial algal concentrations of about 10 cells μl^{-1} in the jars. Over five to ten days, groups of several hundred or thousand larvae, clearing 1–2 μl^{-1} min (averaged over time), probably captured most of this food.

Observing larval feeding

Larvae selected at random from the culture jar were placed singly, by pipette, into the bottom of a 63 ml cylindrical glass observation chamber (4.8 cm diameter by 3.5 cm deep) containing a suspension of 20 μm diameter polystyrene divinylbenzene microspheres (Duke Scientific) at a concentration of 2.4 μl^{-1} in filtered seawater. The concentration of spheres was reduced to 1 μl^{-1} for a few very large *Dermasterias* larvae with very high clearance rates. In those cases where the mouths of larvae were

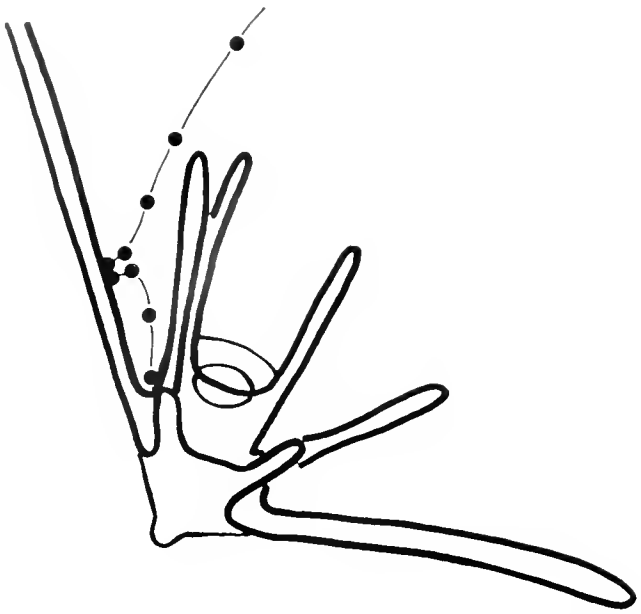

Figure 4. A cartoon of the particle capture sequence shown in Figure 3. The positions of the sphere in each panel of Figure 3 are indicated by the dots, and the particle path between these positions is interpolated by the solid line. The ciliated band of the larva is shown by the heavy lines; the mouth is shown in outline.

too small to ingest 20 μm spheres, or where small larvae were unable to capture these particles, 10 μm diameter spheres were used (these cases include all of the smaller *Ophiopholis* larvae, and several of the smallest *Dendraster*, *Parastichopus*, and *Strongylocentrotus purpuratus* larvae). The larger spheres were used whenever possible, because they were easier to identify and follow on videotape. Larvae of a wide range of sizes and developmental stages were used for all seven species. Temperatures inside the observation chamber could be held within 0.5–1.0°C of ambient seawater temperature because the chamber was equipped with a circulating seawater jacket. The top of the chamber was sealed with a clear plastic lid, eliminating trapped air and preventing image distortion by surface waves. As the larva swam from the bottom to the top of the chamber, several minutes of feeding were observed. For most larvae, several such feeding periods were observed. After each feeding period, the larva was returned to the bottom of the chamber by pipette and observed as it again swam upward.

Some larvae did not swim or capture spheres at high rates. These individuals were not used in subsequent analyses. Slow swimming, frequent stops, infrequent particle captures, or rejection of captured spheres by these larvae were probably the result of disturbance during transfer from the jar to the observation chamber. Under the conditions described, many larvae swam rapidly and had high clearance rates, but readers should not assume that larvae exhibit such behavior continuously, or that all larvae will do so under any conditions of observation.

I tried to get larvae to capture and ingest a number of other kinds of artificial particles, including Sephadex spheres of various sizes, other types of plastic spheres, and ragweed pollen, with variable success. I also used various unicellular algae. Some of these algae [*e.g., Isochrysis galbana, Pavlova lutheri* (Droop)] are small or non-refractile; others (e.g., *Dunaliella tertiolecta*) are larger but tend to clump in suspension. The most promising cultured unicellular organism was the dinoflagellate *Prorocentrum micans* Ehrenb., which is large and highly visible, does not clump, and keeps itself suspended in water by flagellar movements. Unfortunately, many larvae refused to capture or ingest these cells. Strathmann (1971) used the dinoflagellate *Amphidinium carteri* Hulburt, which I did not have in culture. Polystyrene spheres are useful for observations of suspension feeding because they are highly refractile, are available in a range of sizes, do not readily form clumps, settle from suspension slowly, and are readily captured and ingested by echinoderm larvae. An added advantage of indigestible particles is that larvae are unlikely to become quickly satiated as they clear particles from suspension.

Videotape recordings of larvae feeding were made with transmitted light at 30 frames s^{-1} with a videocamera mounted on the trinocular head of a dissecting microscope. I controlled both the focus and field of view manually. Thirteen to forty-four individuals were videotaped for each species, and I made some observations of feeding by larvae that were not taped. For illustrations of particle captures, single video frames were captured from the videotape by a frame grabber. The size and contrast of the sphere were increased in each of these images, and much of the background contrast was removed. These computer-enhanced images were then laser-printed and assembled into collages.

I calculated a clearance rate (volume of water cleared of particles per unit time, in μl min^{-1}) for each larva by counting particle captures and dividing the total number of captures by the length of the observation period, then dividing this capture rate (number min^{-1}) by the concentration of spheres in suspension (number μL^{-1}). Only periods of continuous swimming and feeding were used, therefore the calculated clearance rates represent maximum feeding performance over several minutes. A number of laboratory artifacts, including handling and transfer, high light intensity, and novel food particles, may affect the rate of feeding and the method of particle capture (Strathmann, 1971). Therefore, interpretations of the method of particle capture must be based on observations of larvae clearing particles from suspension at near maximal rates. High clearance rates indicate that the behavior of larvae in the laboratory has not been strongly altered by any of these

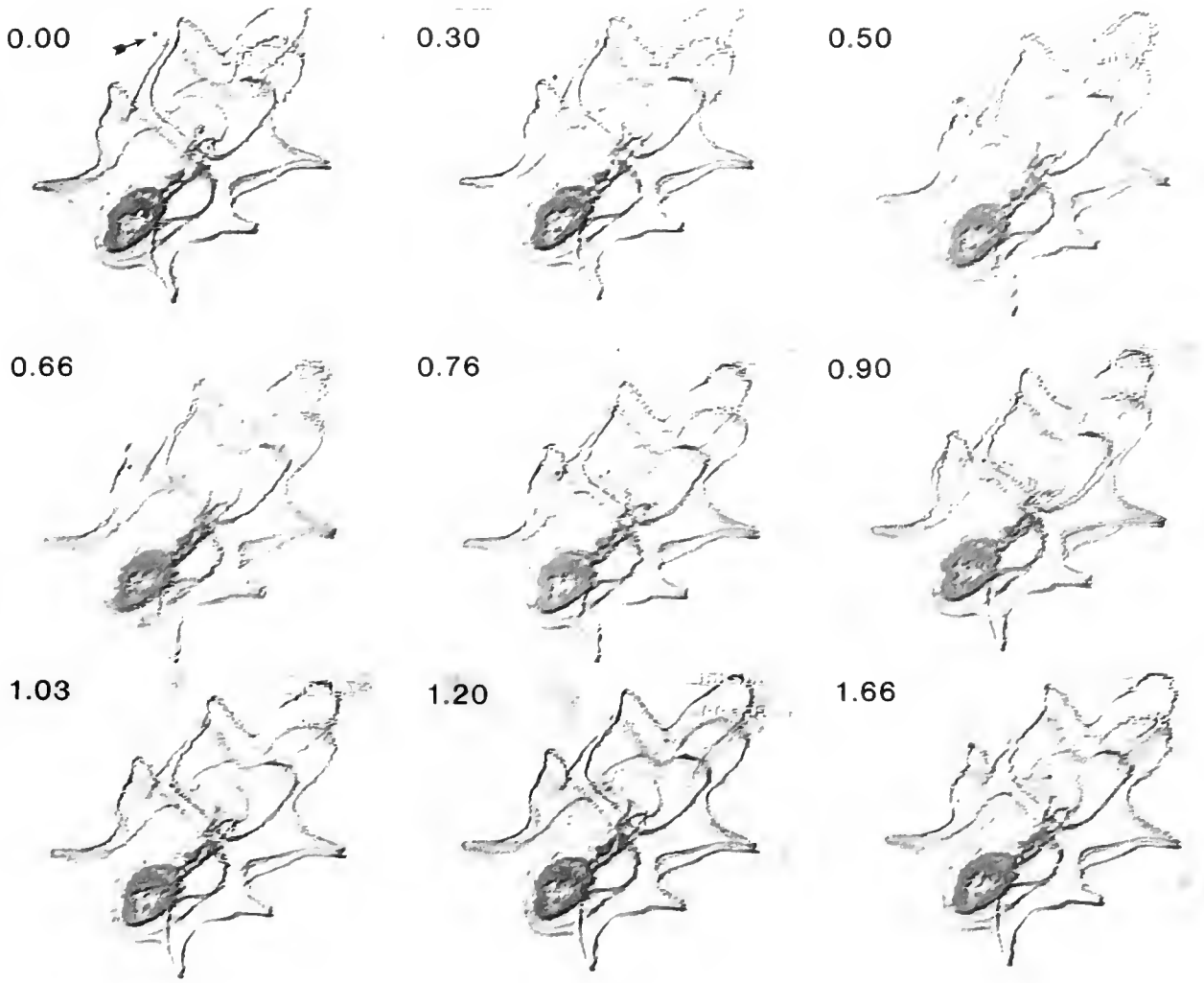

Figure 5. A collage of videotape frames showing the capture of a 20 μm diameter sphere by a bipinnaria (*Dermasterias imbricata*). Numbers (in the upper left) and arrow as in Figure 1. For scale, the arrow is 79 μm long. The larva is shown in ventral view, moving forward toward the upper right of each panel. The sphere approached the ciliated band on the right side lateral to the larval mouth (0.00–0.50 s), was captured there (0.66 s), and changed direction back toward the circumoral field (0.76–0.90 s). The sphere was captured a second time, on the preoral transverse ciliated band (1.03 s) and then swept into the mouth (1.20–1.66 s).

artifacts. Rates of growth and development of larvae in nature are probably often limited by low phytoplankton concentrations (Paulay *et al.*, 1985; but see Olson and Olson, 1989). High clearance rates are probably typical of larvae feeding on these dilute phytoplankton suspensions.

Measuring ciliated band lengths

Larvae were removed from the observation chamber, killed in a dilute solution of formalin in seawater, then mounted in a drop of seawater beneath a raised coverglass. Ciliated band length was estimated by summing the distances between sequential landmark points on the band (such as the tips and bases of the larval arms of plutei). The planar location of each landmark was determined by digitizing a camera lucida tracing of the band for each mounted larva; the location of each landmark in the third dimension, when in focus under the microscope, was determined from the vertical displacement of the microscope stage (McEdward, 1985).

Results

Particle captures

All larvae typically swam with the anterior end uppermost, from the bottom of the observation chamber, up

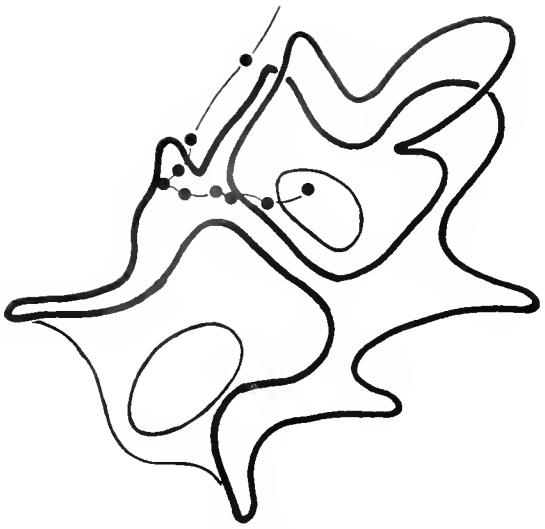

Figure 6. A cartoon of the particle capture sequence shown in Figure 5. The positions of the sphere in each panel of Figure 5 are indicated by the dots, and the particle path between these positions is interpolated by the solid line. The ciliated band of the larva is shown by the heavy lines; the mouth and stomach are shown in outline.

toward the observer and videocamera, capturing spheres as they swam. Runnström (1918) described this and a variety of other swimming postures; I observed some of them (most notably a lateral swimming direction, usually with the ventral side uppermost, as the larva swam slowly along the bottom of the chamber). These alternative swimming patterns were usually associated with low rates of feeding and frequent general ciliary arrests during which the larva came to a halt on the chamber bottom. I am not sure whether these behaviors are likely to be common in the plankton.

The aborally directed beat of cilia on the ciliated band produces water currents with a net posterior component that drives the larva forward while moving water laden with particles toward the ciliated band. Polystyrene spheres entrained in these currents approached the ciliated band on the upstream side of the band (usually on the arms of plutei, or on the loops of band between the bases of the arms, and on the anterior, posterior, and lateral portions of the band on bipinnariae and auriculariae). In cases where the proximity of the particle to the ciliated band could be judged, spheres appeared to approach within about one diameter of the surface of the larva (10–20 μm), less than the length of the cilia on most parts of the ciliated band (20–30 μm; Strathmann, 1971; McEdward, 1984). For larvae that were actively feeding, spheres approached the ciliated band, then abruptly changed direction at the band, and moved back toward the circumoral field rather than passing over the band toward the aboral field. On nearby portions of the band, water continued to pass over the band, while spheres were retained on the circumoral field (thus they were concentrated from suspension). Subsequent to this initial capture, spheres caught near the mouth often were swept immediately into the suboral pocket, probably aided by the beat of cilia on the circumoral field (Runnström, 1918) and by water currents generated by the aboral beat of cilia on the transverse portions of the ciliated band directly anterior and posterior to the mouth (the preoral and postoral transverse bands, respectively; see Strathmann, 1971). Spheres captured at any great distance (more than 50–100 μm) anterior or posterior to the mouth were often captured repeatedly on portions of the ciliated band progressively closer to the mouth; they were then transported to the mouth, probably by the same two mechanisms described above. I observed hundreds of such captures for each species examined; the specific descriptions that follow are for four particular species (one for each larval type), but they apply equivalently to other larvae of the same type.

Figures 1, 3, 5, and 7 show sequences of frames, from videotapes of particle captures like those described above, for an echinopluteus (*Dendraster excentricus*, Fig. 1), an ophiopluteus (*Ophiopholis aculeata*, Fig. 3), a bipinnaria (*Dermasterias imbricata*, Fig. 5), and an auricularia (*Parastichopus californicus*, Fig. 7). The accompanying line drawings (Figs. 2, 4, 6, and 8) depict the paths of spheres shown in the photocollages. These four pictorial accounts of particle captures are representative of almost all of the several thousand captures that I observed. Figures 1 and 2 show the abrupt change in direction of a sphere at the ciliated band of a six-armed echinopluteus, on the right postoral arm (the larva is shown in ventral view). The sphere was captured twice enroute to the mouth, once near the arm tip, and once nearer the base of the arm. A similar pluteus capture, on the right posterolateral arm of an advanced ophiopluteus, is shown in Figures 3 and 4. In this sequence, the sphere was held briefly on the ciliated band on the leading edge of the arm, then moved back toward the circumoral field (between the opposed bands on the arm) and the mouth. Because the oral hood above the mouths of these larvae is opaque, the end of the particle path cannot be followed into the mouth and esophagus. Figures 5 and 6 illustrate the capture of a sphere by a large bipinnaria: the sphere first approached the ciliated band on the right side of the larva, lateral to the suboral pocket and mouth. The sphere crossed the circumoral field, was arrested at the band, and moved back toward the mouth; it was captured again on the anterior transverse ciliated band (near the mouth) and was then swept into the mouth. A similar capture by an auricularia is shown in Figures 7 and 8; the sphere was captured first on the dorsal part of the ciliated band anterior

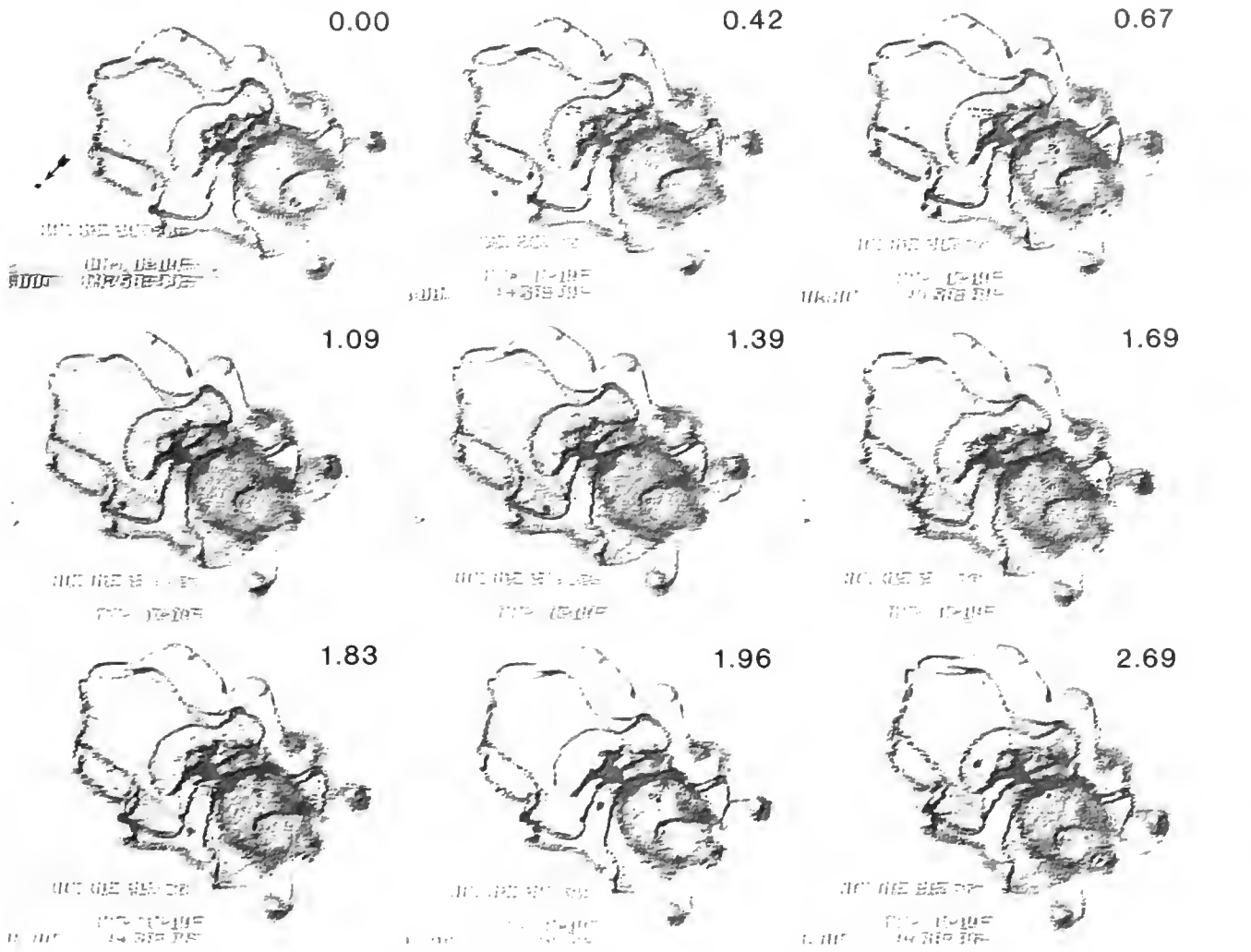

Figure 7. A collage of videotape frames showing the capture of a 20 μm diameter sphere by an auricularia (*Parastichopus californicus*). Numbers and arrow as in Figure 1. For scale, the arrow is 128 μm long. The larva is shown in ventral view, moving forward toward the upper left of each panel. The sphere approached the dorsal ciliated band on the right side anterior to the larval mouth (0.00–0.42 s), was captured there (0.067 s), and changed direction posteriorly along the circumoral field toward the right lateral portion of the band (1.09–1.39 s). The sphere was captured a second time, lateral to the mouth (1.69 s), and then moved toward the larval midline and into the mouth (1.83–2.69 s).

to the mouth, then was recaptured on the lateral ciliated band before entering the suboral pocket and mouth.

Larvae of all species occasionally captured spheres without close approach of the sphere to the ciliated band, and without abrupt change in the direction of movement of the sphere at the band. Such a particle capture (by the same *Dermasterias* larva illustrated in Figs. 5 and 6) is shown in Figures 9 and 10. These few spheres followed broad, curving paths into the suboral pocket of the larva, where they were swept into the larval mouth (probably by the current generated by the circumoral cilia). These particle paths resembled those described by Gilmour (1985, 1986, 1988b). Strathmann (1971) also depicted such particle captures, but did not emphasize their frequency or importance. I observed 44 individuals of *Strongylocentrotus droebachiensis* capture 1594 spheres; of these, only 80 (5.2%) were caught without an approach and a change of direction at the ciliated band. Similar proportions obtained for 13 *Parastichopus* (23 of 438 captures without ciliary reversals, (5.3%) and 17 *Dermasterias* (24 of 504 captures, 4.8%). These proportions do not vary significantly among species (compared by contingency table analysis, $\chi^2 = 0.118$, $P > 0.90$).

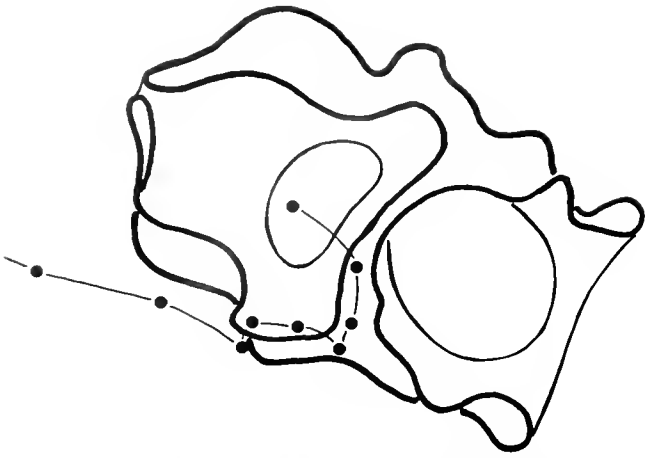

Figure 8. A cartoon of the particle capture sequence shown in Figure 7. The positions of the sphere in each panel of Figure 7 are indicated by the dots, and the particle path between these positions is interpolated by the solid line. The ciliated band of the larva is shown by the heavy lines; the mouth and stomach are shown in outline.

Some readers may be unconvinced that collages of still video frames can accurately represent the dynamic events involved in particle capture by these echinoderm larvae. I encourage such readers to photocopy the collages (enlarging them, if possible), to cut the frames of each collage out of the photocopy, and then to view the frames, as a stack of flip pictures, thus simulating the particle movement that occurs during the capture of spheres. Especially skeptical readers, who will be persuaded by nothing else, can contact me about receiving a copy of a short videotape sequence that demonstrates these particle captures.

The distribution of particle captures on ciliated bands

Spheres were caught on all parts of the ciliated bands of larvae, including the most anterior and posterior portions of the bands of auriculariae and bipinnariae and the tips of the arms of echinoplutei and ophioplutei. For *Parastichopus* larvae, 169 spheres (41.0%) were captured by ciliary reversal on the anterior portions of the ciliated band, 118 (28.5%) on the band lateral to the suboral pocket and mouth, and 127 (30.7%) on the portions of the band posterior to the mouth; for *Dermasterias* larvae, the same distribution was 242 (50.4%) anterior, 122 (25.4%) lateral, and 116 (24.2%) posterior captures (Table I). These distributions vary significantly between species (compared by contingency table analysis, $\chi^2 = 8.471$, $P = 0.015$), perhaps because the lengths of the different segments of the band vary as well. This is a difficult comparison (between the lengths of segments of the band and the proportion of captures by those segments) for bipinnariae and auriculariae, because the same landmarks that can be used to identify the locations of captures on videotape cannot always be precisely identified on the drawings of ciliated bands used to measure band lengths.

A similar comparison is more easily made among different developmental stages of echinoplutei, because such landmarks (the tips and bases of the larval arms) are readily identifiable on these larvae from all aspects. The growth of early pluteus stages involves the addition of ciliated band to only a few portions of the band (especially the postoral and anterolateral arms), whereas larger plutei grow by elongating other arm pairs, as well as that part of the band carried on the body of the larva (see Strathmann, 1971, 1975). All segments of the ciliated band (four arm pairs and the larval body) grew as *Strongylocentrotus droebachiensis* larvae progressed from four- to six- to eight-armed stages (Fig. 11); most of the *post hoc* pairwise contrasts (four- *vs.* six-armed, or six- *vs.* eight-armed) among these mean band lengths were significant (Table II). But in three cases, these size increases led to no measurable increase in the maximum clearance rate of the same segment (determined by counting particle captures on each segment). Eight-armed larvae had longer postoral and anterolateral arms, and longer ciliated bands on the larval body, than did six-armed larvae, but mean clearance rates for these segments of the ciliated band were no greater for the more advanced larval stage (Fig. 11, Table II). In a fourth case, feeding performance for one segment of the band declined: the length of the ciliated band borne on the larval body was similar for four-armed and six-armed stages, but the mean clearance rate for that portion of the band was significantly lower for the later larval stage. The lack of correspondence between size and performance of various parts of the ciliated bands of plutei suggests that some segments of the band are more effective at particle capture than other segments, and that this variation among segments changes as larvae develop.

Repeated capture of particles

One striking aspect of particle capture by echinoderm larvae was the repeated capture of individual spheres on the ciliated band. Figures 1 and 7 show good examples of such events. In many cases, these repeated captures produced a sort of pinball effect as spheres "bounced" from peripheral portions of the band to segments of the band nearer the mouth. I counted as many as 11 distinct capture events for single spheres caught by *Dermasterias* and *Parastichopus* larvae (Table I), though most spheres were captured 1–4 times, and even spheres captured near the most anterior or posterior ends of the band could be transported directly to the mouth after a single capture on the band. The mean number of captures varied among segments of the band (anterior, lateral, and posterior to

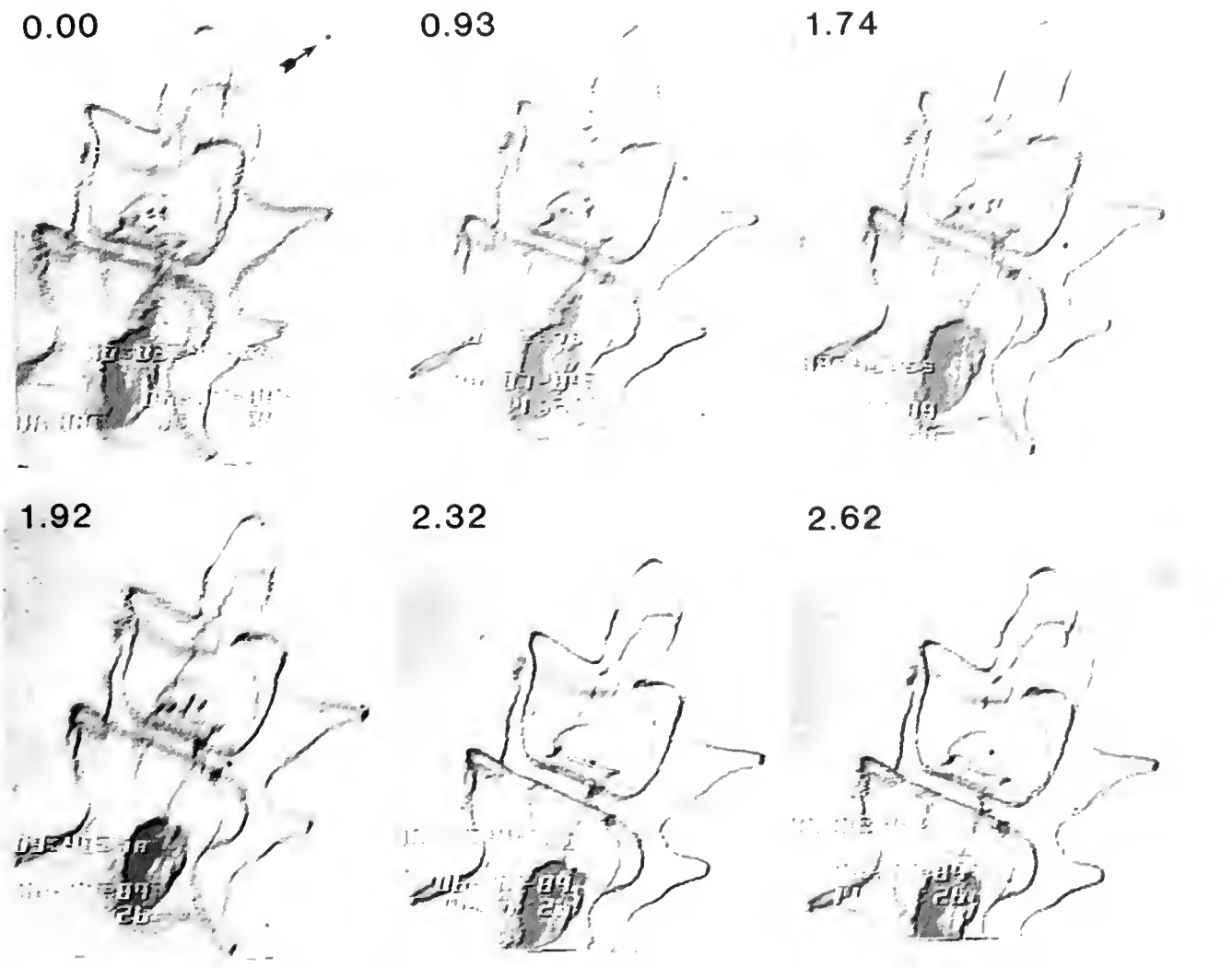

Figure 9. A collage of videotape frames showing the capture of a 20 μm diameter sphere by a bipinnaria (*Dermasterias imbricata*). Numbers and arrow as in Figure 5. For scale, the arrow is 89 μm long. The larva is shown in ventral view, moving forward toward the top of each panel. The sphere approached the left anterior side of the larva (0.00–1.74 s) and was swept directly into the larval mouth (1.92–2.62 s) without close approach to any part of the ciliated band and without changing direction at the band.

the mouth) for both species. Spheres initially caught lateral to the mouth were captured fewer times before ingestion than were spheres caught either anterior, or posterior, to the mouth (comparison of mean capture numbers by analysis of variance and *post hoc* contrasts for *Parastichopus*, $F = 39.60$; for *Dermasterias*, $F = 69.84$; for both comparisons, $P < 0.001$). Spheres caught initially on the anterior part of the ciliated band were also captured more times than those caught initially on the posterior end of the larva (for *Parastichopus*, $F = 16.96$, $P < 0.001$; for *Dermasterias*, $F = 5.60$; $P = 0.018$). The mean (± one standard deviation) number of captures for all spheres was also greater for *Parastichopus* (2.123 ± 1.254) than for *Dermasterias* (1.944 ± 0.890) (compared by *t*-test, $t = 2.488$, $P = 0.013$). These observations support the probable role of cilia on the circumoral field in transporting captured particles to the mouth. Spheres captured several hundred micrometers posterior to the mouth could be moved swiftly to the suboral pocket, in spite of the anterior direction of movement of the whole larva. In similar captures, larvae of *Parastichopus*, which lack circumoral ciliation (Strathmann, 1971), retained captured spheres more often en route to the mouth (see above) than did asteroid larvae, which have abundant circumoral cilia (Gemmill, 1914, 1916; Tattersall and Sheppard, 1934; Strathmann, 1971).

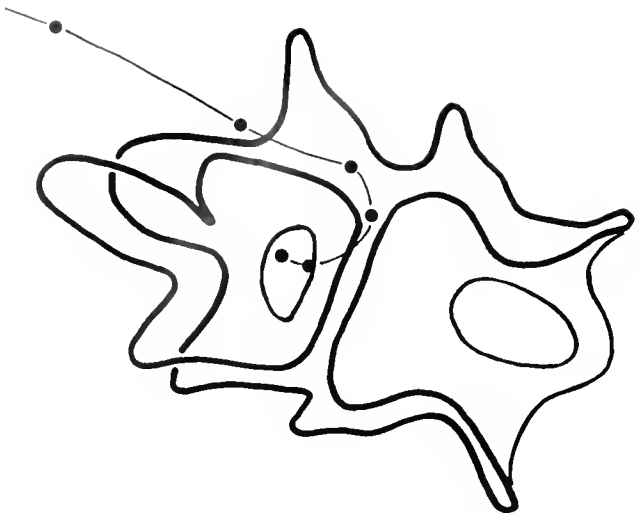

Figure 10. A cartoon of the particle capture sequence shown in Figure 9. The positions of the sphere in each panel of Figure 9 are indicated by the dots, and the particle path between these panels is interpolated by the solid line. The ciliated band of the larva is shown by the heavy lines; the mouth and stomach are shown in outline.

Most spheres caught by echinoplutei were captured just once on the ciliated band, but the incidence of multiple captures of spheres increased for *Strongylocentrotus drobachiensis* as these larvae developed more arms: for four-armed larvae (n = 9), 10.8 ± 2.7% (mean ± S.E.) of spheres captured were retained at more than one location on the ciliated band before entering the mouth; for six-armed larvae (n = 18), 16.1 ± 2.5%; for eight-armed larvae (n = 17), 21.6 ± 2.0%. Analysis of variance of arcsine-transformed proportions suggests that this is a significant increase in the incidence of multiple captures of spheres ($F = 4.11$, $P = 0.023$). Thus the complexity of particle paths to the mouth increases as plutei increase in size and change shape.

Retention of captured particles

Larvae of all species rarely failed to move to the mouth particles that had been removed from suspension at the ciliated band. For example, of 443 spheres captured by *Parastichopus* larvae at the ciliated band (where the site and number of captures for each sphere could be determined), only 29 (6.5%) were lost before reaching the mouth (Table I); *Dermasterias* larvae lost only 11 of 491 such spheres (2.2%). The frequency of loss did not vary significantly among segments of the band (anterior, lateral, and posterior to the mouth) for *Dermasterias* larvae (compared by contingency table analysis, $\chi^2 = 0.71$, $P > 0.25$). The same proportions varied significantly for *Parastichopus* ($\chi^2 = 12.33$, $P < 0.001$), mainly because I observed no spheres lost from the lateral portions of the ciliated bands of these larvae. The certainty of retention and transport from the initial site of capture to the mouth, often a distance of hundreds of micrometers, was remarkable. The exceptions to this generalization include a few small echinoplutei and bipinnariae that were unable to retain the larger spheres at the ciliated band, and some ophiuroid larvae that occasionally captured spheres without ingesting them. In these cases, some spheres approached the ciliated band on the upstream side, changed direction toward the circumoral field, then subsequently passes over the band and were lost. Thus, under some circumstances, some larvae may reject particles before they reach the mouth. Control over particle captures at the ciliated band may allow the collection of food to be inhibited even as the larva continues to swim forward

Table I

Mean number of captures for single spheres caught by larvae of (A) Parastichopus californicus *and (B)* Dermasterias imbricata

A. *Parastichopus californicus*

	Ciliated band segment		
	Anterior	Lateral	Posterior
	(Spheres ingested)		
$\bar{x}$ (range)	2.592 (1–11)	1.517 (1–7)	2.039 (1–5)
SD	1.510	0.855	0.858
n	169	118	127
	(Spheres not ingested)		
$\bar{x}$ (range)	2.643 (1–5)	—	2.733 (1–10)
SD	1.277	—	2.314
n	14	0	15

B. *Dermasterias imbricata*

	Ciliated band segment		
	Anterior	Lateral	Posterior
	(Spheres ingested)		
$\bar{x}$ (range)	2.211 (1–10)	1.369 (1–5)	1.991 (1–4)
SD	0.947	0.619	0.761
n	242	122	116
	(Spheres not ingested)		
$\bar{x}$ (range)	1.200 (1–2)	1.250 (1–2)	1.000 (1)
SD	0.447	0.500	0
n	5	4	2

Observations are tabulated by ciliated band segment (anterior, lateral, or posterior to the mouth of the larva) and by capture success (ingested or not ingested). SD = standard deviation; n = number of spheres.

under conditions where the mouth is jammed with particles, or the particles are not desirable, or the larva is attempting to reject particles from its buccal cavity (Strathmann, 1971).

Clearance rates

Maximum clearance rates ranged from 1–2 μl min^{-1} for early larval stages (four-armed plutei and the simple bipinnaria-shaped larvae of asteroids and holothuroids) with short ciliated bands, to 6–10 μl min^{-1} for late larval stages (the large eight-armed plutei and the bipinnariae and auriculariae with large loops and folds of the ciliated band) with longer bands. Maximum clearance rate increases with the length of the ciliated band in all of these larvae (Strathmann, 1971; M. Hart, unpub. data).

These clearance rates are similar to those of other larvae of comparable size and type, but measured by very different techniques. Strathmann (1971) measured clearance rates for larvae by two methods: counting algal cells entering the mouths of swimming larvae, or counting cells in the guts of larvae left briefly in algal suspensions. Lucas (1982) measured clearance rates for groups of larvae by estimating the depletion of algal cells from suspension in prolonged feeding trials (of about 24 h duration). The similar range of clearance rates estimated for larvae of similar types clearing algal cells or polystyrene spheres from suspension suggests that the use of artificial suspended particles can give accurate estimates of clearance rates. Flavoring particles with some transferable factor from algal cells may enhance the rate of ingestion of polystyrene spheres (Fenaux *et al.*, 1985), but larvae capturing unflavored spheres, in my study, ingested almost all of the spheres captured on the ciliated band (see below). Larvae may respond to particle flavor by altering the rate of forward swimming and water processing.

Although these different measuring techniques produce similar clearance rates, the techniques are not necessarily equivalent. Strathmann (1971) found that maximum clearance rates measured by counting algal cells captured

Table II

F-statistics and probability values for post hoc *paired comparisons of mean lengths and of mean maximum clearance rates among larval stages of* Strongylocentrotus droebachiensis, *for different segments of the ciliated band*

	Larval stage comparison	
Ciliated band segment	Four-armed (9) *vs* six-armed (18)	Six-armed *vs* eight-armed (17)
Postoral arms		
length	F = 34.762***	F = 26.461***
maximum clearance rate	11.826***	3.030^{ns}
Anterolateral arms		
length	50.647***	38.756***
maximum clearance rate	12.149***	0.003^{ns}
Posterodorsal arms		
length	—	48.607***
maximum clearance rate	—	6.384*
Body		
length	0.954^{ns}	12.290***
maximum clearance rate	4.227*	1.617^{ns}

Note that only one set of comparisons for posterodorsal arms is made (four-armed larvae lack these arms). Numbers in parentheses indicate sample sizes for each larval stage. ***, $P \leq 0.001$; *, $P < 0.05$; ns, $P > 0.05$.

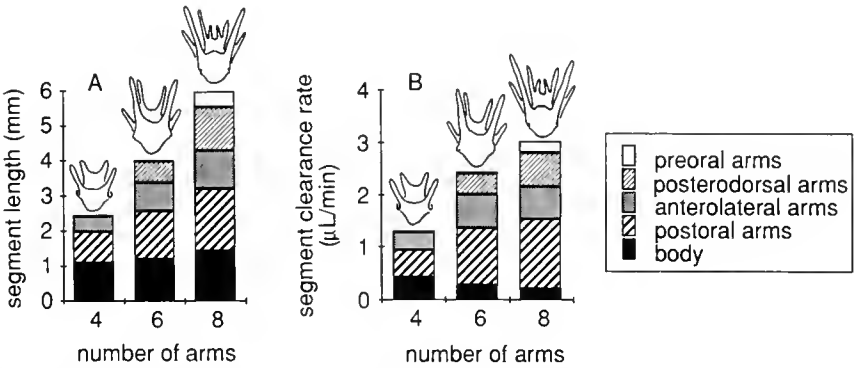

Figure 11. A bar graph showing the (A) length and (B) maximum clearance rate of different segments of the ciliated bands (borne on the larval body and on the postoral, anterolateral, posterodorsal, and preoral arms) for four-, six-, and eight-armed larvae of *Strongylocentrotus droebachiensis*. The total height of each bar indicates the mean ciliated band length or mean maximum clearance rate for whole larvae; for each bar, the height of segments with different shading indicates the same measures for particular segments of the ciliated band. Cartoons of larvae above each bar indicate the approximate changes in size and shape from one stage to the next.

during periods of 1–3 min were generally higher and less variable than those measured by counting algal cells in the guts of larvae left in algal suspensions for 5–13 min, presumably because the latter periods include some intervals when larvae are not feeding rapidly. Lucas' (1982) highest clearance rate for *Acanthaster* larvae (5.8 μl min^{-1} for early brachiolaria larvae) is much lower than the highest maximum rate that I measured for *Dermasterias* larvae of similar stage (10.0 μl min^{-1}). However, because of the large variance in clearance rates measured for different individuals, it is difficult to make precise contrasts among these three studies. Maximum clearance rates measured by watching larvae for a few minutes should usually be greater than rates measured by allowing larvae to feed for many minutes or hours, but other factors may obscure this effect.

One study is not consistent with the above prediction. Rivkin *et al.* (1986) found exceptionally high clearance rates (measured as the incorporation of radiolabel) for echinoderm larvae capturing [^{3}H]thymidine-labelled bacteria. For example, in feeding trials of ~4 h, the mean clearance rate for larvae of *Sterechinus neumayeri* (an echinoid) was 13.8 μl min^{-1}. The largest clearance rates (which were time-integrated *averages*) in their study must have been substantially higher: the mean + 1 SD clearance rate for *Sterechinus* was 18.5 μl min^{-1}. The largest *maximum* clearance rate I measured for an echinopluteus was 5.4 μl min^{-1} for a large *Dendraster excentricus*. This is a substantial difference. The thymidine-incorporation technique appears sound. Unless these Antarctic larvae are exceptionally large, these clearance rates may reflect a dramatic adaptation for the rapid capture of very small (<2 μm) particles. Measures of maximum clearance rates by direct observation of these larvae would be of considerable interest.

Ingestion of particles

Most larvae ingested captured spheres by accumulating a bolus of spheres in the middle and lower esophagus. They then swallowed the bolus into the stomach by a rapid peristaltic contraction accompanied by opening of the cardiac sphincter. Most other workers have observed the same process. Other individuals, at times, did not readily ingest spheres, but instead accumulated them in a whirling mass that rotated within the buccal cavity under the influence of water currents directed into the mouth by the adoral cilia, and out of the suboral pocket by the transverse ciliated bands. If this mass of spheres was not ingested, it was eventually rejected from the buccal cavity, probably by reversal of the direction of beat of the adoral or other cilia of the buccal cavity (MacBride, 1914; Gemmill, 1914, 1916; Runnström, 1918; Strathmann, 1971), and then moved out of the suboral pocket over the postoral transverse band. Rejection of a mass of spheres was not accompanied by a general arrest or reversal of beat of the cilia on the ciliated band (*i.e.*, the larvae did not stop swimming or swim backward), and the rejected mass was not captured again at the postoral transverse band. These events indicate an impressive subtlety of control over ciliary beat that is probably modulated by the larval nervous system (Burke, 1978, 1983).

Discussion

Methods of suspension feeding by echinoderm larvae

My observations of particle capture by echinoderm larvae suggest a resolution of the conflicting accounts of suspension feeding by these larvae. The majority of particle captures (by all of the stages and species of larvae that I examined) were similar to those described by Strathmann (1971). The retention of particles on the upstream side of the ciliated band of larvae, accompanied by a change in the direction of particle movement toward the circumoral field, supports the hypothesis that echinoderm larvae remove particles from suspension mainly by a brief, localized reversal in the direction of beat of cilia on the ciliated band (Strathmann *et al.*, 1972). However, about 5% of all particle captures appeared to occur without the close approach of the particle to the ciliated band and without an abrupt change in the direction of particle movement at the band. This proportion was similar among the three species I examined; larvae of a fourth species (*Stylasterias forreri*) also captured about 5% of the particles that they encountered when prevented from generating ciliary reversals (Hart, 1990). The paths of particles caught by this second method were reminiscent of those described by Gilmour (1985, 1986, 1988b) for echinoplutei and bipinnariae.

The resolution of these conflicting descriptions depends on two factors: the availability of videotape as a permanent record of behavior suitable for quantitative analysis; and high rates of partical clearance, indicating normal larval behavior uncompromised by laboratory artifacts. Lacking any permanent record of larval feeding, Strathmann probably described only the most common mode of particle capture that he observed for free-swimming larvae in relatively large volumes of seawater. For his part, Gilmour has principally described particle captures by larvae attached to suction pipettes or trapped between glass surfaces, and such methods of manipulating and orienting larvae for observation may disrupt normal swimming and feeding behaviors, due to the disturbing effects of strong suction by the pipette, or to the close proximity of surfaces and their large effect on flow patterns at low Reynolds numbers (Vogel, 1981). Larvae may respond to these dis-

turbances with reduced clearance rates. At low clearance rates, a few particles may enter the mouths of echinoderm larvae without apparent change of direction at the ciliated band, but this is not the method of particle capture that is most common when larvae are processing water at high rates (Strathmann, 1971, 1982; Hart, 1990). The particle paths described by Gilmour (1985) also occur in free-swimming larvae, but at a lower frequency than his studies suggest. Because he has not reported clearance rates in any of his studies, it is difficult to interpret Gilmour's observations. Gilmour has probably observed larvae that are not actively feeding. To the extent that larvae exhibit such behavior in nature (perhaps in dense phytoplankton patches, or in response to other disturbances), these observations may indicate the lower limit of the capacity of larvae to reduce clearance rate in situations where feeding is actively suppressed. Gilmour's methods are useful for some kinds of observations, and larvae may feed at high rates under these conditions if care is taken, but the interpretation of observations on methods of suspension feeding made under such conditions also requires careful consideration.

I cannot account for the differences between Gilmour's (1988a) description of particle capture by the auricularia of *Parastichopus californicus* and my own observations of feeding by these larvae. *Parastichopus* larvae in my study removed large numbers of spheres from suspension in a manner identical with that of plutei and bipinnariae. I could not confirm Gilmour's (1988a) observation that an encounter between an auricularia and a particle results in a brief reversal in the direction of rotation of the larva and entry of the particle to the suboral pocket. The rotation of these larvae was not disturbed by particle capture, and they cleared spheres from suspension at rates comparable to those for other larvae of similar size and developmental stage.

The kinds of descriptions I have presented are crucial for the interpretation of quantitative aspects of suspension feeding. For example, the observation that echinoderm larvae retain captured particles at the ciliated band leads to the prediction that the clearance rates of these larvae should increase as their ciliated bands grow longer during development (Strathmann, 1971). Such explicit predictions are more difficult to derive for larvae (or other suspension feeders) where feeding rates cannot be determined by direct observation. For echinoderm larvae, one can now try to interpret ontogenetic and phylogenetic variation in feeding rates as a consequence of the variation in the length and arrangement of the ciliated band (see below).

Larval shapes and the development of ciliated bands

The forms of echinoderm larvae vary among classes, among species within classes, and among developmental stages of single species. Suspension feeding by these larvae covaries in several ways with these form differences. For example, the number of capture events for single particles varied among parts of the ciliated bands of both bipinnariae and auriculariae, and the same measure (averaged over all segments) varied between these two larval forms. The most significant of these differences, I think, are the distribution of particle captures among segments of the ciliated bands of echinoplutei and the change in this distribution during larval development. For *Strongylocentrotus droebachiensis*, the clearance rate of a single segment of the band was not necessarily reflected in the growth of that segment as the larva grows and adds new larval arms. The surprising implication of this result is that some ciliated bands (on a single larva) are more effective suspension-feeding devices than are other bands. LaBarbera (1981) made a similar observation for adult articulate brachiopods. The ciliated lophophore of these animals consists of a pair of lateral arms and a median coil. The area-specific pumping rate (which would be proportional to a clearance rate if LaBarbera had observed particle captures instead of dye stream movement) of the median coil was only about 60% of the rate for the lateral arms. LaBarbera ascribed this difference to the geometrical arrangement of the different parts of the lophophore and the consequences of this geometry for shear stress and viscous energy loss (resulting in lower fluid flow rates) over the median coil.

This inference (of shape effects on feeding performance) could clearly be extended to variations on the pluteus form among echinoid species, or to variation among the basic larval forms of different echinoderm classes. Emlet (1991) has predicted that such effects could arise from ontogenetic changes in larval shape or from phylogenetic variation in ciliated band arrangement. Using scaled models of whole larvae with different shapes, or of isolated ciliated bands with different orientation, Emlet showed that changes in both the gross morphology of larvae and the arrangement of ciliated bands could enhance particle capture rates (by increasing velocity gradients and fluid flow rates over the band). My direct measurements of the feeding performance of different ciliated bands confirm that performance differences among larvae of different development stages do manifest themselves, possibly due to the fluid-mechanical effects described by Emlet. Other observations (M. Hart, unpub. data) suggest that these effects may also extend to comparisons among different types of echinoderm larvae. If the geometrical development of a ciliated band affects the functional performance of that band, then there may be taxonomic biases in performance associated with evolutionarily conserved differences in patterns of larval development.

The evolution of larval form and reproductive strategies

Two general conclusions derive from the previous discussion: all feeding echinoderm larvae employ the same mechanisms to concentrate food particles from suspension; and quantitative aspects of feeding by these larvae change during larval development. These conclusions invite some interesting corollaries. First, the method of particle capture by echinoderm larvae has remained similar among different classes in spite of considerable evolution of larval form. The four types of echinoderm larvae are not necessarily related phylogenetically in a manner obvious from their gross organization. Raff *et al.* (1988), Smiley (1988), Smith (1988), and Strathmann (1988) have all recently proposed phylogenies for the extant echinoderm classes based on different combinations of morphological, embryological, and molecular information. In spite of the apparent similarities in elaboration and organization of the ciliated band between ophiuroid and echinoid larvae, and between holothuroid and asteroid larvae, few of these phylogenies group the pairs of classes together in this way. There are relatively few points of agreement among the different phylogenies or among their authors. One is left to conclude that there may have been both convergent and divergent evolution of larval form in echinoderms. However, the method of suspension feeding by echinoderm larvae has apparently been strongly conserved throughout the evolutionary history of the phylum (though numerous groups have lost the means and requirement to feed during larval development).

Second, quantitative variation in feeding among echinoderm larvae may imply variation in the effectiveness of these different larvae as elements of a reproductive strategy. Echinoderm larvae (and other feeding larval forms) can be thought of as devices for turning small eggs into large juveniles (by concentrating materials and energy from the plankton). The effectiveness of these devices turns on the relative rates of development and mortality during larval life. The availability of food to larvae affects the development of larval and juvenile structures and the duration of the larval period (Fenaux *et al.*, 1985; Paulay *et al.*, 1985; Hart and Scheibling, 1988). Larval duration figures prominently in several theoretical and comparative treatments of life history evolution in marine invertebrates (Vance, 1973; Christiansen and Fenchel, 1979; Strathmann, 1985; Emlet *et al.*, 1987). Although all of the larvae that I have observed use the same methods to remove particles from suspension, they vary considerably in the organization and development of the ciliated band (see Figs. 2, 4, 6, 8). Some quantitative aspects of larval feeding vary as larvae change shape, or vary among larvae of different classes. This variation may be reflected in measures of clearance rates for different larvae. In this case, we could reject the tacit assumption that all larvae are equivalent solutions to the problem of building a large juvenile from a small egg. The functional and life-historical consequences of such a result are the subject of a second paper.

Acknowledgments

The Director and staff of the Friday Harbor Laboratories provided space, facilities, and assistance for which I am grateful. Larry McEdward, Joe Pawlik, Richard Strathmann, Malcolm Telford and the editors of the journal provided encouragement and helpful comments on the manuscript. Larry McEdward generously loaned the equipment and software for measurement of ciliated band lengths. Richard Strathmann provided me with his translation of Runnström (1918). I was supported by NSF grant OCE 8606850 and by an award from the Graduate School Research Fund of the University of Washington, both to Richard Strathmann.

Literature Cited

Burke, R. D. 1978. The structure of the nervous system of the pluteus larva of *Strongylocentrotus purpuratus*. *Cell Tiss. Res.* **191:** 233–247.

Burke, R. D. 1983. The structure of the larval nervous system of *Pisaster ochraceus* (Echinodermata: Asteroidea). *J. Morphol.* **178:** 23–35.

Christiansen, F. B., and T. M. Fenchel. 1979. Evolution of marine invertebrate reproductive patterns. *Theor. Pop. Biol.* **16:** 267–282.

Conover, R. J. 1968. Zooplankton—life in a nutritionally dilute environment. *Am. Zool.* **8:** 107–118.

Emlet, R. B. 1991. Functional constraints on the evolution of larval forms of marine invertebrates: experimental and comparative evidence. *Am. Zool.* in press.

Emlet, R. B., L. R. McEdward, and R. R. Strathmann. 1987. Echinoderm larval ecology viewed from the egg. Pp. 55–136 in *Echinoderm Studies, Vol. 2*, M. Jangoux and J. M. Lawrence, eds. A. A. Balkema, Rotterdam.

Fenaux, L., C. Cellario, and M. Etienne. 1985. Croissance de la larve de l'oursin *Paracentrotus lividus*. *Mar. Biol.* **86:** 151–157.

Garstang, W. 1939. Spolia Bermudiana. I. On a remarkable new type of Auricularia larva (*A. bermudensis*, n. sp.). *Q. J. Microsc. Sci., N. S.* **81:** 321–345.

Gemmill, J. F. 1914. The development and certain points in the adult structure of the starfish *Asterias rubens*, L. *Philos. Trans. R. Soc. Lond. B Biol. Sci.* **205:** 213–294.

Gemmill, J. F. 1916. The larva of the starfish *Porania pulvillus* (O. F. M.). *Q. J. Microsc. Sci., N. S.* **61:** 27–50.

Gilmour, T. H. J. 1985. An analysis of videotape recordings of larval feeding in the sea urchin *Lytechinus pictus* (Verril). *Can. J. Zool.* **63:** 1354–1359.

Gilmour, T. H. J. 1986. Streamlines and particle paths in the feeding mechanisms of larvae of the sea urchin *Lytechinus pictus* Verril. *J. Exp. Mar. Biol. Ecol.* **95:** 27–36.

Gilmour, T. H. J. 1988a. Feeding behaviour of holothurian larvae. *Am. Zool.* **28:** 167A.

Gilmour, T. H. J. 1988b. Particle paths and streamlines in the feeding behaviour of echinoderm larvae. Pp. 253–258 in *Echinoderm Biology*, R. D. Burke, P. V. Mladenov, P. Lambert, and R. L. Parsley, eds. A. A. Balkema, Rotterdam.

Hart, M. W. 1990. Manipulating external Ca^{2+} inhibits particle capture by planktotrophic echinoderm larvae. *Can. J. Zool.*, in press.

Hart, M. W., and R. E. Scheibling. 1988. Heat waves, baby booms, and the destruction of kelp beds by sea urchins. *Mar. Biol.* **99:** 167–176.

Jørgensen, C. B. 1966. *Biology of Suspension Feeding.* Pergamon Press, Oxford.

LaBarbera, M. 1981. Water flow patterns in and around three species of articulate brachiopods. *J. Exp. Mar. Biol. Ecol.* **55:** 185–206.

Lucas, J. S. 1982. Quantitative studies of feeding and nutrition during larval development of the coral reef asteroid *Acanthaster planci* (L.). *J. Exp. Mar. Biol. Ecol.* **65:** 173–193.

MacBride, E. W. 1914. *Text-book of Embryology. Vol. 1. Invertebrata.* Macmillan and Co., London.

Marshall, S. M., and A. P. Orr. 1956. On the biology of *Calanus finmarchicus* IX. Feeding and digestion in the young stages. *J. Mar. Biol. Assoc. U.K.* **35:** 587–603.

McEdward, L. R. 1984. Morphometric and metabolic analyses of the growth and form of an echinopluteus. *J. Exp. Mar. Biol. Ecol.* **82:** 259–287.

McEdward, L. R. 1985. An apparatus for measuring and recording the depth dimension of microscopic organisms. *Trans. Am. Microsc. Soc.* **104:** 194–200.

McEdward, L. R., and R. R. Strathmann. 1987. The body plan of the cyphonautes larva of bryozoans prevents high clearance rates: comparison with the pluteus and a growth model. *Biol. Bull.* **172:** 30–45.

Meeks, A. 1927. *Bipinnaria asterigera* (Echinodermata), from the Northumberland plankton. *Proc. Zool. Soc. Lond., Pt. 1* **1927:** 159–171.

Olson, R. R., and M. H. Olson. 1989. Food limitation of planktotrophic marine invertebrate larvae: does it control recruitment success? *Ann. Rev. Ecol. Syst.* **20:** 225–247.

Paffenhöfer, G. A. 1971. Grazing and ingestion rates of nauplii, copepodids, and adults of the marine planktonic copepod *Calanus helgolandicus*. *Mar. Biol.* **11:** 286–298.

Paulay, G., L. Boring, and R. R. Strathmann. 1985. Food limited growth and development of larvae: experiments with natural sea water. *J. Exp. Mar. Biol. Ecol.* **93:** 1–10.

Raff, R. A., K. G. Field, M. T. Ghiselin, D. J. Lane, G. J. Olsen, N. R. Pace, A. L. Parks, B. A. Parr, and E. C. Raff. 1988. Molecular analysis of distant phylogenetic relationships in echinoderms. Pp. 29–41 in *Echinoderm Phylogeny and Evolutionary Biology*, C. R. C. Paul and A. B. Smith, eds. Clarendon Press, Oxford.

Rivkin, R. B., I. Bosch, J. S. Pearse, and E. J. Lessard. 1986. Bacteriovory: a novel feeding mode for asteroid larvae. *Science* **233:** 1311–1314.

Runnström, J. 1918. Zur Biologie und Physiologie der Seeigellarve. *Bergens Museum Aarbok, Naturvid Raecke, Nr. 1.* 60 pp.

Smiley, S. 1988. The phylogenetic relationships of holothurians: a cladistic analysis of the extant echinoderm classes. Pp. 69–84 in *Echinoderm Phylogeny and Evolutionary Biology*, C. R. C. Paul and A. B. Smith, eds. Clarendon Press, Oxford.

Smith, A. B. 1988. Fossil evidence for the relationships of extant echinoderm classes and their times of divergence. Pp. 85–97 in *Echinoderm Phylogeny and Evolutionary Biology*, C. R. C. Paul and A. B. Smith, eds. Clarendon Press, Oxford.

Strathmann, M. F. 1987. *Reproduction and Development of Marine Invertebrates of the Northern Pacific Coast.* University of Washington Press, Seattle.

Strathmann, R. R. 1971. The feeding behavior of planktotrophic echinoderm larvae: mechanisms, regulation, and rates of suspension feeding. *J. Exp. Mar. Biol. Ecol.* **6:** 109–160.

Strathmann, R. R. 1975. Larval feeding in echinoderms. *Am. Zool.* **15:** 717–730.

Strathmann, R. R. 1982. Comment on Dr. Gilmour's views on feeding by hemichordates and lophophorates. *Can. J. Zool.* **60:** 3466–3468.

Strathmann, R. R. 1985. Feeding and nonfeeding larval development and life-history evolution in marine invertebrates. *Annu. Rev. Ecol. Syst.* **16:** 339–361.

Strathmann, R. R. 1987. Larval feeding. Pp. 465–550 in *Reproduction of Marine Invertebrates, Vol. 9*, A. C. Giese, J. S. Pearse, and V. B. Pearse, eds. Blackwell Scientific Publications and The Boxwood Press, Palo Alto, CA.

Strathmann, R. R. 1988. Larvae, phylogeny, and von Baer's Law. Pp. 53–68 in *Echinoderm Phylogeny and Evolutionary Biology*, C. R. C. Paul and A. B. Smith, eds. Clarendon Press, Oxford.

Strathmann, R. R., T. L. Jahn, and J. R. C. Fonseca. 1972. Suspension feeding by marine invertebrate larvae: clearance of particles by ciliated bands of a rotifer, pluteus, and trochophore. *Biol. Bull.* **142:** 505–519.

Tattersall, W. M., and E. M. Sheppard. 1934. Observations on the bipinnaria of the asteroid genus *Luidia*. Pp. 35–61 in *James Johnstone Memorial Volume*. University of Liverpool Press, Liverpool.

Vance, R. R. 1973. On reproductive strategies in marine benthic invertebrates. *Am. Nat.* **107:** 339–352.

Vogel, S. 1981. *Life in Moving Fluids.* Willard Grant Press, Boston.

Reference: *Biol. Bull* **180**: 28–33. (February, 1991)

Retarded and Mosaic Phenotype in Regenerated Claw Closer Muscles of Juvenile Lobsters

C. K. GOVIND, CHRISTINE GEE, AND JOANNE PEARCE

Life Sciences Division, Scarborough Campus, University of Toronto, 1265 Military Trail, Scarborough, Ontario, Canada M1C 1A4

Abstract. The closer muscle in the paired claws of the lobster *Homarus americanus* become determined into their asymmetric form of a cutter and crusher type claw during the 4th and 5th juvenile stages and differentiate their fiber composition accordingly in subsequent juvenile stages. Our aim was to study the effects of claw loss during this critical juvenile period on muscle regeneration. Hence the fiber composition of the paired closer muscles in newly regenerated claws was examined histochemically following removal of both claws either in the 4th and 5th stages or in the 4th through 7th stages. The newly regenerated muscle was retarded compared to its original counterpart in both cases. In the former case, however, the retardation was temporary as the muscle composition in later stages resembled the original. Recovery in the latter was not apparent in later stages, suggesting that retardation is more permanent. Also in both protocols the newly regenerated closer muscle occasionally displayed a mosaic distribution, with slow fibers interspersed among fast fibers in a central band that is normally homogenously fast. Therefore, loss of the paired claws during a developmentally sensitive period affects the phenotype of the regenerated muscle with the change persisting for shorter or longer periods depending on how often the claws are lost.

Introduction

Crustaceans have an amazing ability of dropping an entrapped or endangered limb by breaking it off at a preformed fracture plane, thus allowing the animal to escape. Because such limb autotomy involves little loss of blood, the animal usually lives to regenerate a new limb. The ability to autotomize a limb varies not only among species, or within a species, but also within an individual, in that the chelipeds autotomize more readily than the walking legs. This is the case in lobsters (*Homarus americanus*) and particularly in their juvenile forms when a gentle pinch to the cheliped will result in autotomy whereas the walking limbs will need greater provocation. Indeed, lobsters with their solitary life-style and aggressive nature often lose claws in the wild and often lose them more than once.

Following the loss of a claw, a new one is regenerated which, in structure and function, resembles its predecessor. Although smaller in size initially, the regenerate limb grows over several molt cycles to assume pristine proportion at which time there is little to distinguish it from the original limb. A similar degree of fidelity applies internally, at least with muscles that regenerate the same fiber types as the original in the claw closer muscles in lobsters (Kent *et al.*, 1989), as well as in snapping shrimps (Govind *et al.*, 1986) and crayfish (Govind and Pearce, 1985).

A variation seen consistently in the newly regenerated closer muscle of the claw in crayfish and occasionally in the major claw of snapping shrimps was the appearance of a central band of fast fibers in a muscle that otherwise comprises 100% slow fibers. Because this regional distribution of fast and slow fibers is reminiscent of an early developmental stage in the closer muscle of crayfish and snapping shrimps, it was assumed that some aspects of ontogeny were recapitulated during regeneration. Such a variation in the phenotype did not persist, and the muscle assumed its pristine character over the next few molt cycles. These regenerative events were recorded in adult crayfish and shrimps where the muscle is fully differentiated. What would be the condition of regenerate muscles that had not yet differentiated their adult phenotype? We studied this question in the lobster *Homarus americanus*

Received 7 August 1990; accepted 6 November 1990.

because we were familiar with the development of its closer muscle (Govind, 1984, 1989).

The paired claws and closer muscles in the lobster, *Homarus americanus*, become determined into a major and minor type early in juvenile development and subsequently differentiate their claw morphology and muscle fiber composition into their final form. While loss of both claws in the critical juvenile stages delays the determination of claw asymmetry to a later stage, more prolonged loss suppresses asymmetry altogether (Govind and Pearce, 1989). With such clear-cut effects of claw loss on the determination of asymmetry, it seemed likely that muscle regeneration might also be affected. The present experiments record the phenotypic variations in the paired claw closer muscles of juvenile lobsters following regeneration.

Materials and Methods

Larval lobsters (*Homarus americanus*) were obtained from the Massachusetts State Lobster Hatchery on Martha's Vineyard and reared communally at the Marine Biological Laboratory, Woods Hole, Massachusetts, by methods described previously (Govind and Kent, 1982). Upon molting to the first post-larval or 4th stage, lobsters were reared individually in plastic trays containing pieces of oyster shells as substrate (Lang, 1975). On a daily basis, the animals were fed frozen brine shrimp and checked for molts to record their juvenile development.

Claws were removed by a gentle pinch, which elicited a reflex autotomy, resulting in the claw breaking off at a preformed fracture plane without much loss of blood. Both claws were so removed within 24 h after the animal had molted.

At the appropriate stages the regenerated paired claws were autotomized and prepared for histochemical examination of their muscles based on the stability of the myofibrillar ATPase enzyme to the pH of the incubating medium (Ogonowski and Lang, 1979). Thus, at pH 8, the enzyme is relatively stable in fast crustacean muscle, and hence these fibers stain more intensely in frozen cross-sections of the claw compared to slow muscle. The histochemically treated cross-sections of the claws were photographed, and the resulting photographs were used to calculate the percentage of fast and slow fibers. These calculations were made from the medial region of the claw, which provides the largest surface area, and hence is most representative of the entire muscle.

Results

Regenerated phenotype is retarded

We have previously shown that juvenile 4th and 5th stage lobsters reared with a substrate of oyster chips develop paired asymmetric (cutter/crusher) claws, while their counterparts reared without a substrate develop paired symmetric (cutter/cutter) claws (Lang *et al.*, 1978). Both rearing conditions were adopted for the present experiments. Thus, in the first experiment with oyster chips as a substrate, the development into asymmetric cutter and crusher type muscles is shown by plotting the percent of fast fibers in the paired original muscles (Fig. 1A). One of the muscles rapidly accumulates fast fibers to make up 90% of its mass and thus becomes a cutter type closer muscle. The slow fibers persist in a small (10%) ventral band (Fig. 2b). The contralateral muscle, which is the putative crusher, shows a more gradual loss of fast fibers, making up 10–20% by the 8th or 9th stage (Fig. 1A) and becoming zero by the 13th to 20th stage. The fast muscle in the putative crusher is restricted to a narrow central region (Figs. 2a).

Following autotomy of the paired claws in the 4th and 5th stages, the regenerated muscles in the 6th stage have a phenotype that is intermediate to the normal asymmetric condition (Fig. 1A). The fast muscle composition of the paired regenerated muscles is 57% and 44%, while that of the paired original muscles is 75% and 28%. The regional distribution of fast and slow fibers, however, is similar between original and regenerated claws in that the fast muscle is restricted to a central band while the slow muscle appears on either side (Fig. 2c, d). The regenerated muscle therefore appears to be retarded in its development. This retardation is temporary because the paired muscles show a normal phenotype by the 8th or 9th stage, despite loss of the paired claws in the 4th and 5th stages. In other words, recovery of the muscle phenotype following claw loss in the 4th and 5th stages occurs within 3 to 4 molts.

Loss of the paired claws for more prolonged periods, such as from the 4th to the 7th stage, successively results in the regenerated muscles in the 8th stage showing a retarded phenotype (Fig. 1A). The percent fast muscle in these regenerated muscles is 52% and 44% compared to the 90% of a normal cutter muscle. In both retarded muscles, the fast fibers are restricted to a central band (Fig. 3c, d) as compared to the normal cutter muscle in which the fast fibers occur over the entire area except for a small ventral band (Fig. 3b). The retardation in this case appears to be more permanent because paired muscles examined in the 10th stage still showed subnormal amounts of fast fibers, between 60–70%. Both muscles remained as putative cutter types as loss of the paired claws successively from the 4th to the 7th stage prevents the determination of bilateral asymmetry (Govind and Pearce, 1989). Recovery to 80–90% fast fiber composition was still not seen by the 13th to 15th juvenile stages, indicating that retardation of the muscle phenotype may be more permanent in these animals.

In the second experiment in which lobsters were reared without a substrate of oyster chips, the development of

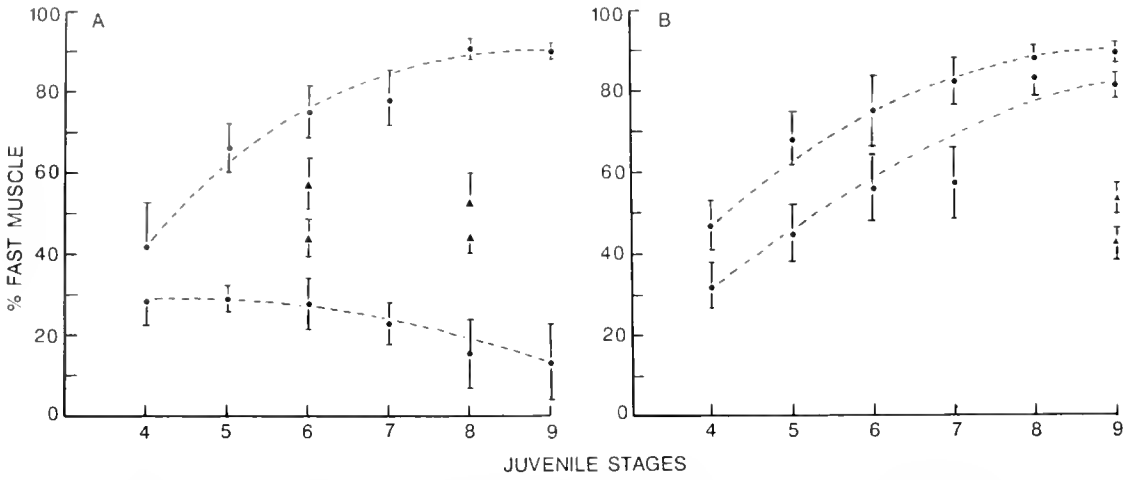

Figure 1. Percent composition of fast fibers in the paired claw closer muscles of original (circles) and regenerated (triangles) claws of juvenile lobsters reared with a substrate of oyster chips (A) and without a graspable substrate (B). For the regenerated condition, the paired claws were removed in all of the previous juvenile stages. Each point represents the mean and standard deviation of five animals. Curves fitting the points for each of the paired claw muscles is drawn by eye. The two curves in (B) were generated by arbitrarily assigning the muscle with the higher percentage of fast fibers to one group (upper curve) while its counterpart was assigned to the second group (lower curve).

the paired closer muscles into symmetric cutter types was followed by plotting the percent fast fibers in the paired original muscles (Fig. 1B). The paired muscles develop in a parallel fashion, accumulating fast fibers until these make up 80–90% of the total mass, and the remainder are slow fibers restricted to a ventral band. In other words, the paired muscles develop as typical cutter type muscles. In comparison, the regenerated phenotype in lobsters that had successively lost their claws from the 4th to the 8th stage, is distinctly retarded (Fig. 1B). The fast fibers in these regenerated muscles is between 40–50% compared to 80–90% in the original muscles. Moreover, as in the first experiment, the retarded condition persists for several subsequent stages at least until the 13th stage, which is as far as we proceeded in this experiment.

Regenerated phenotype shows mosaic pattern

As described above, the distribution of fast fibers in the paired closer muscles is restricted to a distinct central band. In the putative cutter muscle, this fast band during juvenile development rapidly enlarges to occupy almost the entire cross-sectional face, except for a slim ventral band (Figs. 2b, 3b). In the putative crusher, on the other hand, this central fast band gradually diminishes in size until it completely disappears (Figs. 2a, 3a). Throughout these developmental changes, the central band of fast fibers is homogenous and sharply delineated from the adjacent slow fibers.

The homogeneity of the fast band, however, was disrupted to various degrees in some of the regenerated muscles following autotomy of the paired claws. The least disruptive case was where slow fibers were occasionally interspersed among the fast fibers, especially along the lateral edges of the fast band (Fig. 2c, d; 3c, d). This gave the fast band a ragged edge, which was in contrast to its usual sharp edge. Much more disruptive cases involved considerable interspersing of slow fibers in the fast band (Fig. 4a, b), resulting in a distinct mosaic pattern.

Discussion

In a previous study (Kent *et al.*, 1989), we examined the phenotype of the regenerated closer muscle following claw loss in late juveniles and adults, when the claws and closer muscles were well differentiated into cutter and crusher types. In these cases, the regenerated claws and closer muscles resembled their predecessors with considerable fidelity. The present report examines the effect on the regenerate muscle phenotype following the loss of both claws in early juvenile stages when claw type is being determined (Emmel, 1908; Lang *et al.*, 1978) and fiber typing in the closer muscle is being expressed (Govind and Lang, 1978; Ogonowski *et al.*, 1980). Thus removal of paired claws successively either in the 4th and 5th stages or in the 4th through 7th stages resulted in a regenerated phenotype that resembled the undifferentiated condition in the normal 4th stage lobster. In the case where claw loss encompassed only the 4th and 5th stages, the regenerate muscle completes its differentiation into crusher and cutter types in subsequent stages. In the animals subjected to more prolonged claw loss (*i.e.*, from the 4th to the 7th

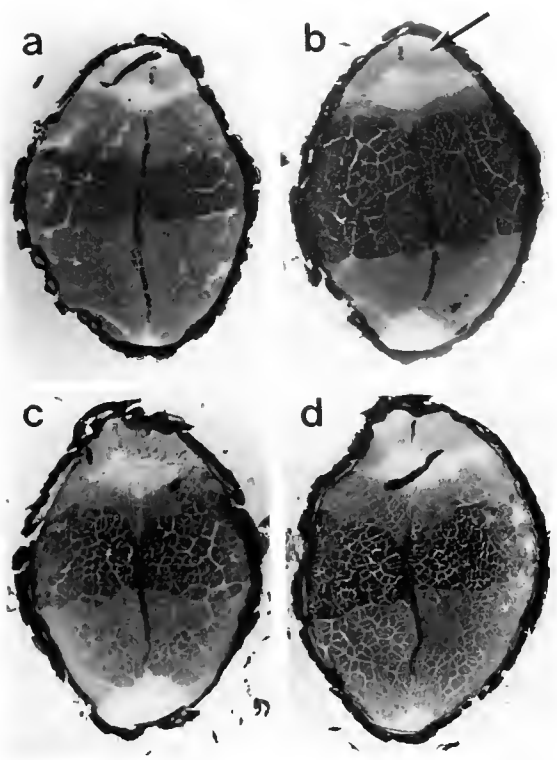

Figure 2. Cross-sections through the paired original (a, b) claws of a juvenile 6th stage lobster and through the paired regenerated (c, d) claws of another 6th stage lobster in which the claws had been removed in the 4th and 5th stages. Histochemical detection of myofibrillar ATPase activity shows fast fibers staining more intensely than slow, and hence the small, dorsally located opener muscle (arrow) is entirely slow while the large closer muscle occupying most of the cross-sectional area has a central band of fast fibers sandwiched dorsally and ventrally by slow fibers. The fast band varies considerably in size between the paired original muscles being narrow in the putative crusher muscle (a) and broad in the putative cutter muscle (b). In the paired regenerate muscles, however, the fast band is similar in size. Magnification 25×.

stage), however, the regenerate muscles have not completely differentiated into cutter types in the subsequent 3–5 stages. Thus the absence of the muscle during the critical juvenile stages results in regenerate phenotype being retarded. How long the muscle is retarded appears to depend on how often the claws are lost; when lost for two successive stages, the retardation is temporary but when lost over several successive stages, the retardation is more permanent.

A few of the regenerate muscles had slow fibers interspersed in the fast muscle band, giving rise to a mosaic distribution of these two types of fibers. This is an unusual distribution of fast and slow fibers in the closer muscle of lobsters as well as other decapod crustaceans. Thus, in the claw closer muscle of lobsters (Ogonowski *et al.*, 1980), crayfish (Govind and Pearce, 1985), snapping shrimps (O'Connor *et al.*, 1984), and hermit crabs (Stephens *et al.*, 1984), fast and slow muscle is regionally distributed; the fast fibers are restricted to a band in the central region. The closer muscle in the more anterior walking limbs in lobsters (Mearow and Govind, 1986) and hermit crabs (Stephens *et al.*, 1984) have a similar pattern. In no instance has a mosaic distribution of fast and slow fibers in the closer muscle been reported in the above mentioned species.

Apart from the closer muscles listed above containing discrete populations of fast and slow fibers, other muscles that have been examined are composed of a single fiber type, *e.g.*, the abdominal extensor and flexor systems that have separate fast and slow muscles in tailed crustaceans (Govind and Atwood, 1982). Consequently, the appearance of a mosaic distribution of fiber types is an uncommon finding among decapod crustaceans. That such a mosaic pattern occurs only in regenerated closer muscles and not in the originals suggests that the instructions for differentiating an entire muscle are not as robust as those

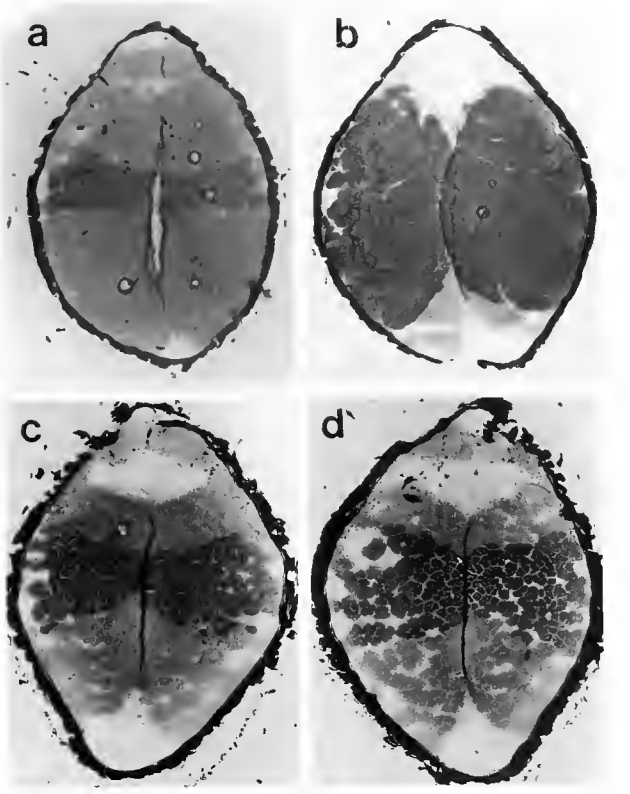

Figure 3. Cross-sections through the paired original (a, b) claws of a juvenile 8th stage lobster and through the paired regenerated (c, d) claws of another 8th stage lobster in which the claws had been removed in the 4th, 5th, 6th, and 7th stages. The proportion of fast fibers is highly asymmetric in the paired original closer muscles being restricted to a narrow central band in the crusher claw (a) but widespread in the cutter claw (b). In the paired regenerate muscles, however, the band of fast fibers is symmetric. Magnification 15×.

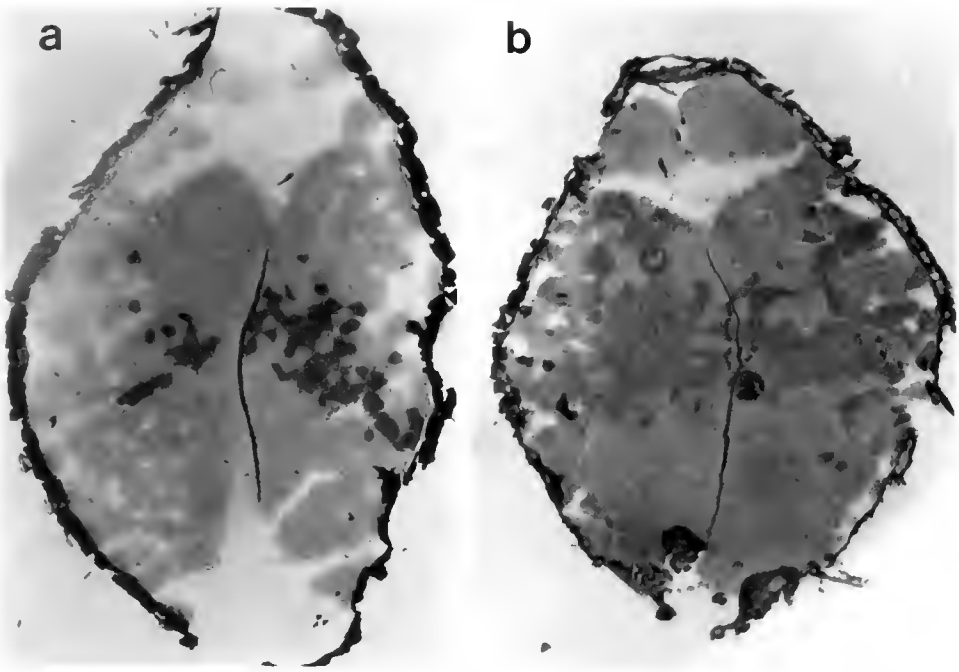

Figure 4. Cross-sections through the claws of two juvenile 8th stage lobsters (a, b) showing different degrees of interspersion of slow fibers (light staining) in the band of fast fibers (dark-staining), resulting in a mosaic appearance in the closer muscle. Magnification 35×.

for differentiating individual fiber types. Perhaps along similar lines is our observation that in the regenerated chelipeds of adult lobsters, the main limb nerve will often travel in a scattered, diffuse fashion rather than in discrete bundles. Although haphazard in appearance, the regenerated nerve contains the requisite motor and sensory neurons.

While a mosaic distribution of fiber types within a muscle occurs rarely in crustaceans, it is commonplace among vertebrates where individual limb muscles are innervated by a large number of motor neurons (Burke, 1981). Despite being randomly distributed within the muscle, fibers comprising a motor unit are of the same type. This has led to the suggestion that the innervating neuron regulates muscle fiber properties. Such neurotrophic regulation in the lobster claw closer muscle is unlikely as there are only two excitor neurons (Wiersma, 1961), both of which distribute to most of the muscle fibers (Govind and Lang, 1974).

Our findings also underscore the very robust nature of the regenerative capacity among juvenile lobsters. Apart from the slowing down in muscle differentiation and the occasional appearance of a mosaic distribution of fiber types, conditions that may be ameliorated, the regenerate muscle otherwise resembles its original counterpart. Thus, the loss of claws seen particularly in the early juvenile stages does not appear, in the long term, to impede the differentiation of a typical phenotype in the closer muscle.

Acknowledgments

We thank Michael Syslow and Kevin Johnson for generous supplies of larval lobsters and the Natural Sciences and Engineering Research Council of Canada for financial support.

Literature Cited

Burke, R. E. 1981. Motor units: anatomy, physiology and functional units. Pp. 345–422 in *Handbook of Physiology: The Nervous System*, Vol. II, J. M. Brookhart and V. B. Mountcastle, eds. Williams and Wilkens, Baltimore.

Emmel, V. E. 1908. The experimental control of asymmetry at different stages in the development of the lobster. *J. Exp. Zool.* **5:** 471–484.

Govind, C. K. 1984. Development of asymmetry in the neuromuscular system of lobster claws. *Biol. Bull.* **167:** 94–119.

Govind, C. K. 1989. Asymmetry in lobster claws. *Am. Sci.* **77:** 468–474.

Govind, C. K., and H. L. Atwood. 1982. Organization of the neuromuscular system. Pp. 63–103 in *The Biology of Crustacea Vol. 3., Neurobiology: Structure and Function*, D. E. Bliss, H. L. Atwood, and D. C. Sandeman, eds. Academic Press, New York.

Govind, C. K., and K. S. Kent. 1982. Transformation of fast fibres to slow prevented by lack of activity in developing lobster muscle. *Nature* **298:** 755–757.

Govind, C. K., and F. Lang. 1974. Neuromuscular analysis of closing in the dimorphic claws of the lobster, *Homarus americanus*. *J. Exp. Zool.* **190:** 281–288.

Govind, C. K., and F. Lang. 1978. Development of the dimorphic claw closer muscles of the lobster *Homarus americanus*. III. Transformation to dimorphic muscles in juveniles. *Biol. Bull.* **154:** 55–67.

Govind, C. K., and J. Pearce. 1985. Enhanced reappearance of fast fibers in regenerating crayfish claw closer muscle. *Dev. Biol* **107:** 206–212.

Govind, C. K., and J. Pearce. 1989. Critical period for determining claw asymmetry in juvenile lobsters. *J. Exp. Zool* **249:** 31–35.

Govind, C. K., K. M. Mearow, and A. Wong. 1986. Regeneration of fiber types in paired asymmetric closer muscle of the snapping shrimp, *Alpheus heterochelis*. *J. Exp. Biol* **123:** 55–71.

Kent, K. S., J. Pearce, C. Gee, and C. K. Govind. 1989. Regenerative fidelity in the paired claw closer muscles of lobsters. *Can. J. Zool* **67:** 1573–1577.

Lang, F. 1975. A simple culture system for juvenile lobsters. *Aquaculture* **6:** 389–393.

Lang, F., C. K. Govind, and W. J. Costello. 1978. Experimental transformation of fiber properties in lobster muscle. *Science* **201:** 1037–1039.

Mearow, K. M., and C. K. Govind. 1986. Neuromuscular properties in the serially homologous lobster limbs. *J. Exp. Zool* **239:** 197–204.

O'Connor, K., P. J. Stephens, and J. M. Leferovich. 1982. Regional distribution of muscle fiber types in the asymmetric claws of California snapping shrimp. *Biol. Bull.* **163:** 329–336.

Ogonowski, M. M., and F. Lang. 1979. Histochemical evidence for enzyme differences in crustacean fast and slow muscle. *J. Exp. Zool* **207:** 143–151.

Ogonowski, M. M., F. Lang, and C. K. Govind. 1980. Histochemistry of lobster claw closer muscles during development. *J. Exp. Zool* **213:** 359–367.

Stephens, P. J., L. M. Lofton, and P. Klainer. 1984. The dimorphic claws of the hermit crab, *Pagurus pollicaris*: properties of the closer muscle. *Biol. Bull* **167:** 713–721.

Wiersma, C. A. G. 1961. The neuromuscular system. Pp. 191–240 in *The Physiology of Crustacea*, Vol. 2, T. H. Waterman, ed. Academic Press, New York.

Reference: *Biol. Bull.* **180:** 34–55. (February, 1991)

Gastropod Egg Capsules and Their Contents From Deep-Sea Hydrothermal Vent Environments

R. G. GUSTAFSON, D. T. J. LITTLEWOOD, AND R. A. LUTZ

Institute of Marine and Coastal Sciences, Rutgers University, New Brunswick, New Jersey 08903

Abstract. Egg capsules from three different prosobranch gastropods were retrieved from the Galapagos Rift and Juan de Fuca Ridge deep-sea hydrothermal vent fields. The morphology of these capsules and their excapsulated embryos and larvae are described and illustrated. Based on their capsule type and the protoconch morphology of their contained larvae, 29 lenticular capsules from the Galapagos Rift could be attributed to a provisionally described neogastropod turrid, *Phymorhynchus* sp. But 3 inflated, triangular capsules from the Galapagos Rift, and 56 different egg capsules from the Juan de Fuca Ridge, each shaped like an inflated pouch, could not be unambiguously assigned to a member of the known vent gastropod fauna. The mode of development and potential for dispersal is inferred from egg capsule type, the number of embryos per capsule, and protoconch characters comparable to those of confamilial shallow-water gastropods for which the type of development is known. These criteria and a comparison to the known juvenile shell morphology of *Phymorhynchus* sp., suggest that, after encapsulation, this species develops planktotrophically and is capable of long-range dispersal. Similar evidence suggests that the larvae contained in the inflated triangular capsules from the Galapagos Rift may also develop planktotrophically after hatching; but the larvae in the pouch-like egg capsules from the Juan de Fuca Ridge probably develop non-planktotrophically without a dispersal stage. These developmental patterns are characteristic of shallow-water members of the systematic groups to which these species belong, indicating, as previous studies have shown, that vent gastropods can persist in these patchy, ephemeral environments in the absence of unique adaptations allowing dispersal between active hydrothermal sites.

Received 14 August 1990; accepted 30 November 1990.

Introduction

Active hydrothermal vent systems accompanied by dense benthic fauna occur at several widely separated sites along active oceanic ridges in the eastern Pacific, from 48°N along the Juan de Fuca Ridge, to 22°S along the East Pacific Rise. Known hydrothermal fields on the Juan de Fuca Ridge are separated by as much as 100 km, whereas separation along transform faults on the East Pacific Rise indicates that vent fields are at least 100 km apart in this region (Crane, 1985; Grassle, 1986). Local vent habitats appear to be transient, with populations being susceptible to intermittent establishment and extinction (Lutz *et al.*, 1985; J. F. Grassle, 1985; Lutz, 1988). Despite their apparent geographic isolation and ephemeral nature, vent areas are characterized by the remarkable similarity of their faunal assemblages (Lutz, 1988). Fundamental biological questions remain regarding both the manner in which these ephemeral habitats are colonized, and the mechanisms of organism dispersal and rates of gene flow between discrete areas of hydrothermal activity associated with contiguous and non-contiguous oceanic ridge systems.

Because laboratory culture of deep-sea organisms is difficult (Turner *et al.*, 1985), many of our perceptions about the development and larval dispersal of vent biota have been, by necessity, inferred from analyses of egg size, fecundity, and morphology of larval structures retained on juvenile and adult specimens. Gastropod mollusks have been widely used for such studies, because a record of the larval developmental pattern can be inferred from the morphology of the initial shell, comprising the Protoconch I in non-planktotrophic species and, also, the Protoconch II shell stages, in planktotrophic species (Powell, 1942; Thorson, 1950; Shuto, 1974; Robertson, 1976; Jablonski and Lutz, 1980).

The mode of larval development in recent (Rodriguez Babio and Thiriot-Quiévreux, 1974; Bandel, 1975a, b, c,

1982; Bouchet, 1976a, b; Scheltema, 1978; Bouchet and Warén, 1979b; Rex and Warén, 1982; Scheltema and Williams, 1983; Lutz *et al.*, 1984, 1986; Turner and Lutz, 1984; Turner *et al.*, 1985; Colman *et al.*, 1986; Lutz, 1988; Lima and Lutz, 1990) and fossil (Jung, 1975; Scheltema, 1978, 1981; Jablonski and Lutz, 1980, 1983; Bouchet, 1981; Hansen, 1982, 1983; Jablonski, 1986) prosobranch gastropods has been classified as either planktotrophic or non-planktotrophic based on criteria of larval shell morphology formulated by Kesteven (1912), Dall (1924), Powell (1942), Thorson (1950), Robertson (1971, 1976), Rodriguez Babio and Thiriot-Quiévreux (1974), Shuto (1974), Sohl (1977), and Jablonski and Lutz (1980, 1983).

Prosobranch species with larval shells having 1.5 to 9 whorls, a distinct fine sculpture, a brown coloration in contrast to a white or gray adult shell, a narrow high spire, a clear difference between the Protoconch I and Protoconch II, and possibly a projection on the outer lip of the larval shell which interdigitates with the velum [("sinusigera" larvae in terminology of Robertson (1976)] are categorized as planktotrophic. Species with larval shells having 0.5 to 1.5 whorls, simple or no ornamentation, the same coloration as the teleoconch, a large bulbous apex, and no evidence of separation between the Protoconch I and Protoconch II are categorized as non-planktotrophic. In the general terminology of Thorson's (1950) "apex theory," shells of the planktotrophic type are termed multispiral or polygyrate and shells of the non-planktotrophic type are termed paucispiral.

Although these criteria allow differentiation between planktotrophic and non-planktotrophic larvae, recent culturing of trochoidean archeogastropods demonstrates that the presence of a paucispiral protoconch is insufficient evidence on which to discriminate between a planktonic and a non-planktonic larval existence (Hadfield and Strathmann, 1990). Of four trochoideans cultured, Hadfield and Strathmann (1990) found two with pelagic development of 7 d or more and two with entirely benthic life histories, although all four produced veliger larvae and had similar inflated paucispiral protoconchs. Although the mode of larval development in shelled opisthobranchs may also be reflected in the larval shell morphology, this relationship has not been demonstrated throughout the group (Rex and Warén, 1982).

Ockelmann (1965) formulated criteria distinguishing between planktotrophic and non-planktotrophic development in a wide range of bivalves based on relatively precise dimensions of the prodissoconch I and II, but the only effort to establish similar criteria for gastropod protoconchs was based on data from comparatively few species (Lima and Lutz, 1990). Nevertheless, Shuto (1974) has shown that, given a complete Protoconch I and II, the ratio of the maximum diameter (D; in mm) of the whole protoconch to the number of whorls or volutions (Vol) provides an index to the developmental type of a marine prosobranch gastropod. A species with more than three whorls and a D/Vol value less than 0.3 suggests planktotrophic development. A D/Vol value between 0.3 and 1.0 with less than three volutions indicates a species with either planktotrophic or non-planktotrophic development, whereas a D/Vol value between 0.3 and 1.0 and less than 2.25 volutions suggests a species with a non-planktotrophic larval type. A D/Vol value higher than 1.0 would suggest a species with direct development (Shuto, 1974). However, Pawlik *et al.* (1988) have shown that the criteria of Shuto (1974) cannot accurately predict the actual mode of development in a majority of cancellariid gastropods.

The type of sculpture or ornamentation on the protoconch has been widely used to infer the mode of development in prosobranch gastropods (Thorson, 1950; Shuto, 1974; Bandel, 1975a, b, c, 1982; Lima and Lutz, 1990). Planktotrophy has been indicated for those larvae with protoconchs possessing a fine reticulate or cancellate pattern, oblique radial ribs or both, whereas a smooth or simply sculptured protoconch suggests that the larvae are non-planktotrophic (Thorson, 1950; Shuto, 1974; Bandel, 1975a, b, c, 1982). A well developed protoconch ornamentation is thought to strengthen the shell, a benefit to planktotrophic larvae spending lengthy periods in the plankton (Bandel, 1975a; Jablonski and Lutz, 1980). Two recent reviews of poecilogony, or intraspecific variation in the mode of larval development, found no evidence for the occurrence of this phenomenon in prosobranch gastropods, indicating that the form of the protoconch is a species-specific character (Hoagland and Robertson, 1988; Bouchet, 1989). Nevertheless, the species variability of protoconch and teleoconch morphologies of cultured meso- and neogastropods led Lima and Lutz (1990) to stress the need for caution when inferring type of development from shell morphology alone.

The most reliable method for determining developmental mode from protoconch morphologies is to compare confamilial or congeneric species with known developmental histories (Scheltema, 1978; Jablonski and Lutz, 1980, 1983). In the case of deep-sea prosobranchs, the comparison must be made with taxonomically related shallow-water species, the assumption being that similar protoconch morphologies result from similar life history patterns in shallow and deep seas (Colman *et al.*, 1986).

Based on the above larval shell criteria, the majority of vent gastropods are believed to have non-planktotrophic development and to have limited larval dispersal capability (Lutz *et al.*, 1984, 1986; Turner *et al.*, 1985), although low temperatures encountered in the deep sea may extend the period available for dispersal of swimming but non-feeding veligers (Turner *et al.*, 1985). This abundance of non-planktotrophy may, in part, be due to the fact that

Table I

DSV "Alvin" dive number, date, location, latitude/longitude, and depth of dives in which gastropod egg capsules were retrieved

Dive #	Date	Location	Latitude; Longitude	Depth (m)
1418	24 July 1984	Juan de Fuca Ridge Endeavour Segment	47°57.0'N; 129°04.0'W	2212
1419	25 July 1984	Juan de Fuca Ridge Endeavour Segment	47°57.0'N; 129°04.0'W	2208
1523	11 March 1985	Galapagos Rift Rose Garden Vent	0°48.3'N; 86°13.5'W	2450
1527	16 March 1985	Galapagos Rift Rose Garden Vent	0°48.3'N; 86°13.5'W	2450
1528	17 March 1985	Galapagos Rift Rose Garden Vent	0°48.3'N; 86°13.5'W	2450
1529	18 March 1985	Galapagos Rift Rose Garden Vent	0°48.3'N; 86°13.5'W	2450
1531	20 March 1985	Galapagos Rift Rose Garden Vent	0°48.3'N; 86°13.5'W	2450
2031	3 May 1988	Galapagos Rift Rose Garden Vent	0°48.3'N; 86°13.5'W	2450

the majority of gastropods found at the vents are limpet-like or coiled archeogastropods. When found in shallow seas, these gastropods appear to be phylogenetically constrained to non-planktotrophy (Anderson, 1960; Heslinga, 1981; Strathmann, 1978a, b; Rex and Warén, 1982; Lutz *et al.*, 1984; Jablonski, 1985; Warén and Bouchet, 1989).

Analysis of developmental stages contained in benthic egg capsules also provides information about the life history of bottom-dwelling gastropods. Although many researchers have described the egg capsules and encapsulated embryos of shallow-water (see reviews in Fretter and Graham, 1962; Robertson, 1976; Webber, 1977; Fretter, 1984; Pechenik, 1986; Soliman, 1987; M. F. Strathmann, 1987) and deep-sea (Thorson, 1940b; Bouchet and Warén, 1979a, 1980, 1985a, 1985b; Colman and Tyler, 1988) marine prosobranch gastropods, only brief mention has been made of the rarely collected egg capsules from hydrothermal vent habitats and their contents (Turner *et al.*, 1985; Berg, 1985). "Lens-shaped" egg capsules measuring 10–12 mm (Turner *et al.*, 1985) or 17.7 ± 3.8 mm (Berg, 1985) in diameter have been reported at the Galapagos Rift, while Berg (1985) has briefly described four small prosobranch egg capsules 4.9 mm in length by 1.7 mm wide and shaped like an "inflated triangle" from Garden of Eden vent on the Galapagos Rift.

When specimens of the previously reported egg capsules from the Galapagos Rift (Turner *et al.*, 1985; Berg, 1985) and numerous egg capsules from the Endeavour Segment of the Juan de Fuca Ridge, came into our possession, it was evident that a more detailed study of these capsules and their contents might yield insights into the life histories and the means of dispersal of these species. This paper is a description of the morphology of three different egg capsules from hydrothermal vents and the embryos and larvae contained in those capsules. Inferences are also made about the dispersal capabilities of the contained larvae, and an attempt is made to predict which of the known hydrothermal vent gastropod species produced each capsule type.

Materials and Methods

Specimens were retrieved with the assistance of DSV "Alvin" during the dives summarized in Table I. Egg capsules were collected: (1) from the surfaces of geological and biological samples brought up in the "Alvin" basket or in insulated retrieval boxes; (2) from sampling gear or markers that had been left at the vents and later retrieved; and (3) from sorted material collected with a "slurp gun" attached to "Alvin."

On board ship, specimens were fixed for 24–48 h in 10% formalin buffered with borax, thoroughly rinsed, transferred to 70% ethanol, and finally to 95% ethanol to prevent corrosion of larval protoconchs. Terminology used in egg capsule descriptions follows that of D'Asaro (1970a). Egg capsule length is the distance between the lateral edges at the widest point parallel to the apical suture; width is the distance between the two sides at the widest point perpendicular to the apical suture; and height is the distance from the apex to the basal membrane through the capsule's central axis.

Photographs, drawings, and measurements were made of pertinent views of the capsules. Capsules containing embryos were then dissected into two equal halves and the embryos were removed. Both capsules and free embryos were critical point dried, placed on stubs, coated with approximately 400 Å of gold-palladium, and examined on an Hitachi S-450 scanning electron microscope (SEM).

Table II

Average dimensions (mean ± standard deviation) of hydrothermal vent gastropod egg capsules collected on specific dives of DSV "Alvin". Number of specimens collected on each dive are in parentheses

Galapagos Rift Lenticular Egg Capsules

"Alvin" Dive #	Length (mm)	Width (mm)	Height (mm)
1528 (2)	14.9 ± 0.8	13.4 ± 0.0	—
1529 (1)	17.4	15.9	—
1531 (4)	16.4 ± 1.3	14.0 ± 0.7	—
2031 (22)	14.4 ± 1.7	13.9 ± 1.8	—

Galapagos Rift Inflated-Triangular Egg Capsules

"Alvin" Dive #	Length (mm)	Width (mm)	Height (mm)
1523 (1)	4.1	1.1	2.4
1527 (1)	3.2	1.1	3.2
1528 (1)	5.0	1.6	3.4

Juan de Fuca Ridge Egg Capsules

"Alvin" Dive #	Length (mm)	Width (mm)	Height (mm)
1418 (8)	3.3 ± 0.6	1.2 ± 0.1	2.7 ± 0.7
1419 (48)	3.7 ± 0.5	1.4 ± 0.3	3.8 ± 0.6

Values for the maximum dimension of the protoconch and the number of volutions of the larval shell were measured directly from scanning electron micrographs by the methods of Shuto (1974). Maximum diameter of the protoconch was defined as the straight-line distance from the protoconch-teleoconch boundary to the opposite side of the protoconch in the region of greatest width. Maximum diameter of the Protoconch I was defined as (1) the greatest straight-line distance from the Protoconch I-Protoconch II boundary in species with planktotrophic development, or (2) from the Protoconch I-teleoconch boundary in non-planktotrophic species lacking a Protoconch II, to the opposite side of the Protoconch I in the region of greatest width [see Lima and Lutz (1990), their figure 1B, for a diagrammatic depiction of these dimensions]. Maximum diameter measurements of the protoconch should not be confused with Robertson's (1971) "first whorl diameter," which is a measurement of the straight-line distance tangent to the straight beginning of the suture and extended in both directions to where it intersects the nearest suture (Lima and Lutz, 1990, their figure 1A). All these values are most accurately determined when the shell is viewed with an apical orientation. Taxonomic terminology and categories are in agreement with those outlined in Vaught (1989).

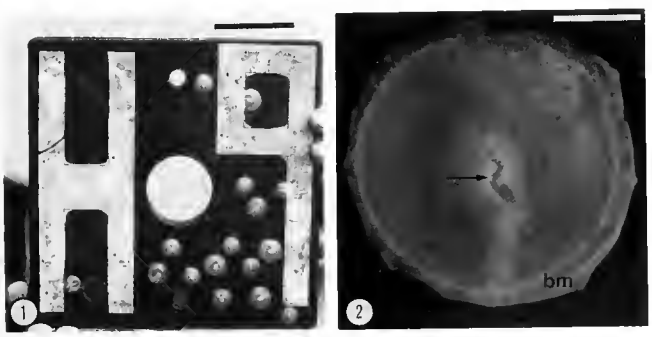

Figures 1–2. Lenticular egg capsules from Rose Garden Vent on the Galapagos Rift. **Figure 1.** Photograph of egg capsules attached to location marker retrieved on "Alvin" Dive 2031. Scale bar = 50 mm. **Figure 2.** Light micrograph of apical view of egg capsule removed from substrate. Arrow marks the escape aperture. Scale bar = 5 mm. bm, basal membrane.

Results

The gastropod egg capsules described in this report consist of three distinct groups: (1) lenticular capsules, with a flattened oval or circular base and a convex upper surface, from the Galapagos Rift; (2) inflated triangular-shaped capsules, from the Galapagos Rift; and (3) inflated oval or pouch-like capsules attached to the substratum by a flattened basal membrane, from the Endeavour Segment of the Juan de Fuca Ridge. Dimensions of each collected capsule are summarized in Table II.

Galapagos Rift lenticular egg capsules

Twenty-nine round to oval, lenticular egg capsules averaging 14.8 ± 1.8 mm in length by 14.0 ± 1.7 mm in width were collected during four separate dives at Rose Garden Vent on the Galapagos Rift (Figs. 1–3; Tables I, II). Height could not be measured due to unequal deformation of the capsules during fixation and dehydration. Twenty-two capsules were found attached to a gray polyethylene marker retrieved on "Alvin" Dive 2031 (Fig. 2), while the remaining specimens were found attached to basaltic rocks by a thin basal membrane that extends beyond the limits of the capsule chamber (Figs. 2, 3).

The outer surface of the whitish to transparent capsules was smooth; there were no apparent ridges (Figs. 2, 3). A transparent elongated escape aperture, centered about the long axis of each capsule, blended into an indistinct apical suture that effectively separated each low capsule into two equal halves (Figs. 2, 3). The capsule wall had three layers consisting of a compact, dense inner layer, a spongy-fibrous middle layer, and a compact, dense outer layer. (Figs. 4–5). The elongated escape aperture was derived from a hollow chamber within the middle spongy-fibrous layer; this chamber caused the capsule wall to bulge outward above the level of the capsule surface (Fig. 5).

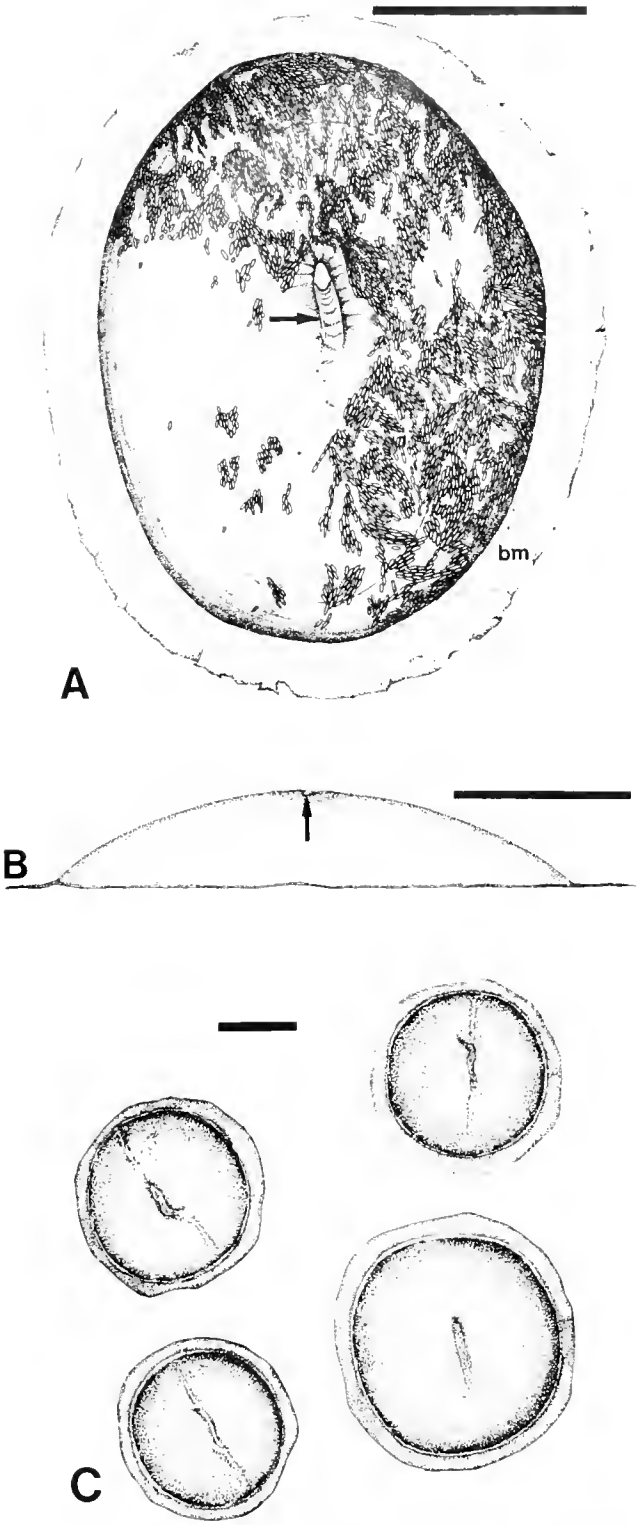

Figure 3. (A) Apical view of lenticular egg capsule from the Galapagos Rift with individual embryos visible through transparent capsule wall. Arrow marks the escape aperture. Scale bar = 5 mm. bm, basal membrane. (B) Lateral view of lenticular egg capsule with peripheral extension of basal membrane. Arrow marks the escape aperture. Scale bar = 5 mm. (C) Group of four lenticular capsules drawn as they appeared attached to location marker in Figure 1, prior to fixation. Scale bar = 5 mm.

Early trochophore and veliger larvae in various stages of development were present in capsules collected during "Alvin" Dives 1528, 1529, and 1531 (Figs. 6–11); one capsule collected during Dive 2031 contained 1052 veliger larvae, all with a fully formed Protoconch I (Figs. 12–14). All other lenticular capsules collected during Dive 2031 were empty. No nurse eggs were observed in lenticular egg capsules.

The following is a chronological reconstruction of developmental stages found in a number of lenticular capsules from the Galapagos Rift. The earliest stage encountered, a late prototroch, was approximately 175 μm in length by 100 μm in width (as measured from electron micrographs), with a prominent apical plate, short pretrochal region, prototroch, long post-trochal region, mouth, and very early larval shell (Figs. 6–10). The apical plate lacked an apical ciliary tuft while the prototrochal cilia appeared to be of the compound type and 15–19 μm in length (Fig. 7). The posterior-dorsal shell field (see Eyster and Morse, 1984, for terminology) had already invaginated in the earliest specimens obtained, and some shell secretion had commenced (Figs. 8–10).

The next observed stage of development was a veliger larva, which had a bi-lobed velum, a mouth leading into the stomadeum, a foot primordium—a protruding knob located immediately posterior to the mouth—an operculum, and a more developed larval shell (Fig. 11). This was a very early veliger because the body was still much too large to be withdrawn into the shell.

One capsule collected during Dive 2031 (Figs. 12–14) contained late Protoconch I larvae that were almost ready to hatch. The embryonic shells of these specimens had a maximum diameter of 234 μm (as measured from electron micrographs). The larval shells of these larvae had a fine reticulate sculpture formed of spiral raised ridges running in the direction of growth, and crossed by regularly spaced perpendicular riblets (Figs. 12–14). An uncalcified operculum was present at this stage (Fig. 13).

Galapagos Rift inflated triangular egg capsules

Three specimens of an egg capsule 4.1 ± 0.9 mm in length by 1.3 ± 0.3 mm in width by 3.0 ± 0.5 mm in height and shaped like an inflated triangle were found attached to basaltic substrates during a series of "Alvin" dives at the Galapagos Rift in 1985 (Figs. 15, 16; Table II). Capsules were attached by a basal membrane that barely extends beyond the limits of the capsule chamber (Fig. 16). A lateral ridge extended up from either end of the long axis of these capsules to meet at the capsule's slightly off-center apex (Figs. 15, 16). Except for the prominent lateral ridge, the surfaces of these capsules were smooth. Capsules fixed in 10% buffered formalin and subsequently stored in ethanol, ranged in color from white

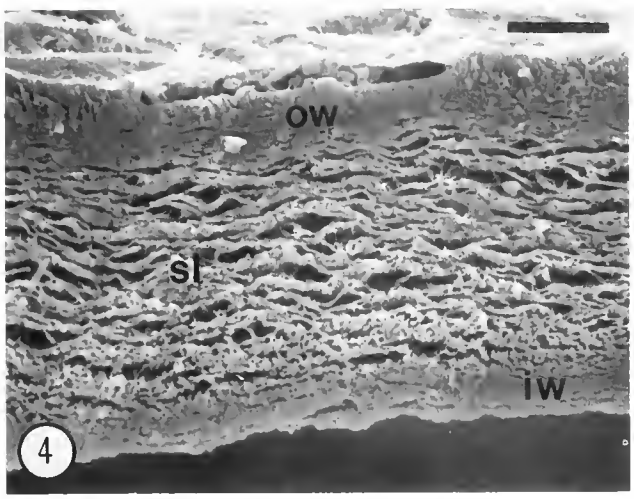

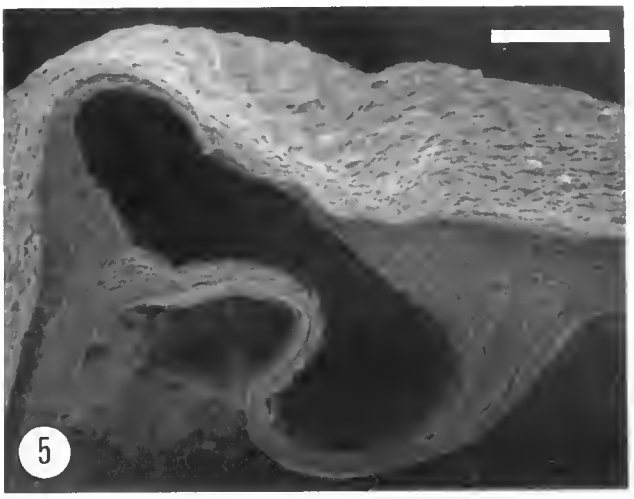

Figures 4–5. Scanning electron micrographs of lenticular egg capsule wall from Galapagos Rift. **Figure 4.** Cross-section of capsule wall. Scale bar = 10 μm. ow, outer capsule wall; iw, inner capsule wall; sl, spongy layer. **Figure 5.** Cross-section through the escape aperture chamber. The outer surface of the capsule is towards the top. Scale bar = 100 μm.

to yellowish-white to almost orange. The capsule wall was composed of what appeared to be one spongy-fibrous layer (Fig. 17).

Each capsule contained several hundred early veliger larvae approximately 165 μm in length by 98 μm in width, as measured from electron micrographs. Larvae in all three capsules were at the same relative stage of development and were characterized by a bi-lobed velum, an apical sensory region with cephalic cilia, a mouth, a foot primordium with attached operculum, and an early Protoconch I (Figs. 18, 19). Velar compound cilia were approximately 30 μm long. The early protoconch was overlaid by a membrane that obscured a sculpture of radially arranged rows of short tubercules intersected by weak concentric raised ridges or lines (Figs. 19–21). Distal to this membrane, the sculpture consisted of parallel raised ridges running in the direction of growth, crossed by radial riblets, and forming a cancellate or net-like pattern (Fig. 19). Nurse eggs were not present in the three inflated triangular egg capsules.

Juan de Fuca Ridge egg capsules

Fifty-six orange egg capsules, each shaped like an inflated oval or pouch and measuring 3.6 ± 0.5 mm in length, 1.3 ± 0.3 mm in width, and 3.6 ± 0.7 mm in height were collected during "Alvin" Dives 1418 and 1419 on the Endeavour Segment of the Juan de Fuca Ridge in 1984 (Tables I, II). Each capsule was attached to the substrate by a flattened basal membrane (Figs. 22, 23). A lateral ridge rose abruptly from the thin basal membrane at either end of the capsule. About 2 mm above the substratum, the ridges at either end of the capsule split into two wing-like extensions forming a saddle-shaped structure around the central oval escape aperture (Fig. 23B). In most cases an amorphous, poorly fixed, orange embryonic mass, containing an indeterminate number of embryos, occupied the capsule chamber (Figs. 22, 23C). In other cases, from one to six, but most often five, larvae were observed through the capsule walls. The Juan de Fuca Ridge egg capsule wall consisted of two compact dense layers: an outer and an inner layer separated by a sharp boundary (Fig. 24).

Examination of the amorphous yolk mass present in most capsules revealed that some larval shell had been secreted, but structural details were indeterminable. Nurse eggs may have been present, but fixation was too poor for this to be determined. However, more advanced larvae were present in a few capsules, which revealed a paucispiral protoconch that was large and bulbous and lacked ornamentation other than that due to weak growth lines (Figs. 25, 26).

Discussion

Although some archeogastropods embed their eggs in a benthic gelatinous mass or ribbon, the majority of shallow-water archeogastropods do not produce benthic egg capsules (Fretter and Graham, 1962; Hyman, 1967; Robertson, 1976; Webber, 1977; Bandel, 1982; Fretter, 1984; Soliman, 1987; M. F. Strathmann, 1987). Therefore, egg capsules described in this paper from hydrothermal vents are most likely the spawn of prosobranchs of the higher orders Mesogastropoda or Neogastropoda. Various authors (Anderson, 1960; Amio, 1963; Bandel, 1976a, b; Soliman, 1987) have stressed that the general form of the

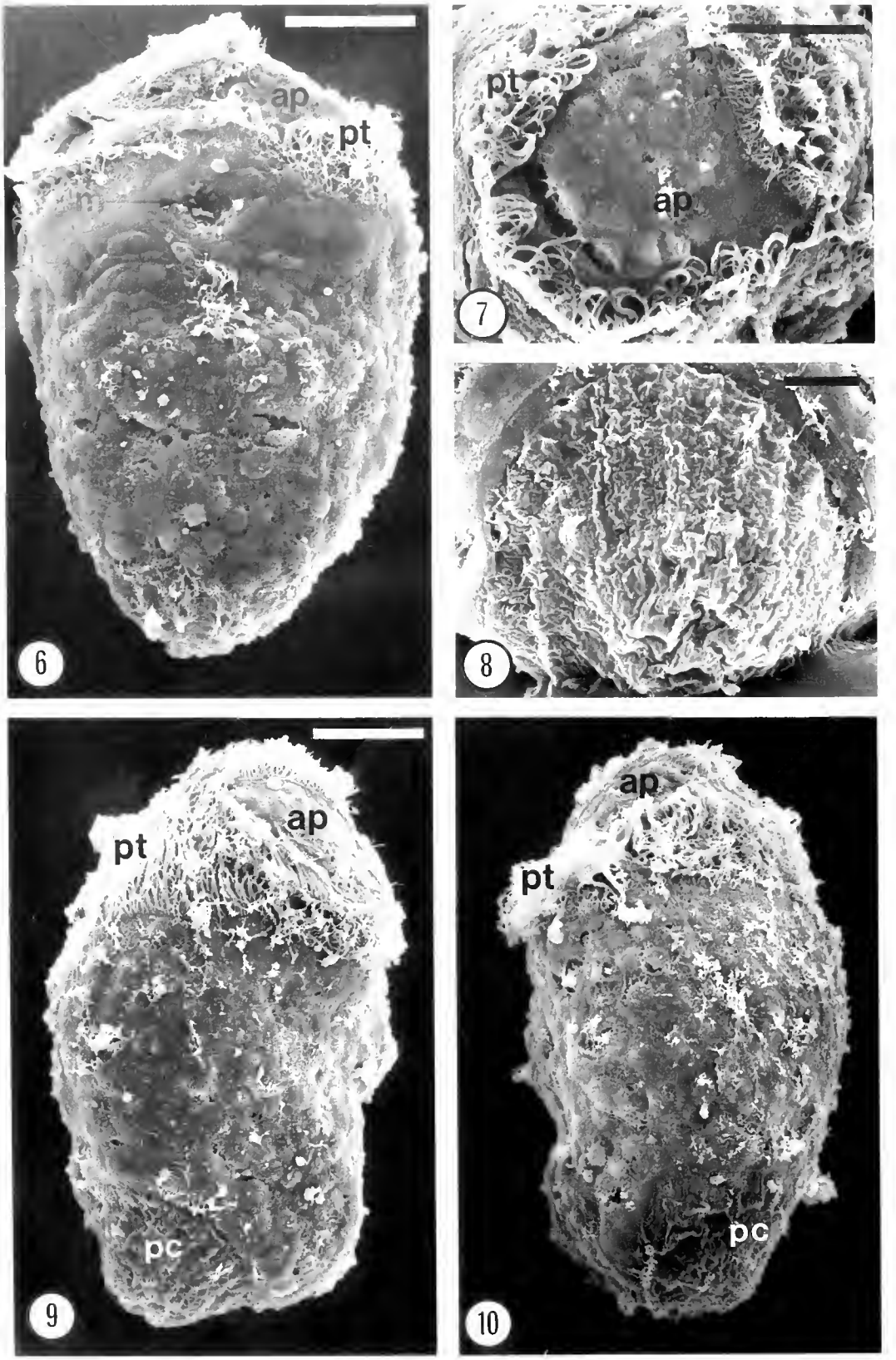

Figures 6–10. Scanning electron micrographs of early trochophore larvae removed from Galapagos Rift lenticular egg capsules. **Figure 6.** Ventral view showing apical plate (ap), prototroch (pt), and mouth (m). Scale bar = 25 μm. **Figure 7.** Apical view showing apical plate (ap) and prototroch (pt). Scale bar = 20 μm. **Figure 8.** Early protoconch at extreme posterior end. Scale bar = 10 μm. **Figure 9.** Right lateral aspect showing apical plate (ap), prototroch (pt), and protoconch (pc). Scale bar = 25 μm. **Figure 10.** Left lateral aspect of different specimen to that shown in Figure 9. Scale as in Figure 9. ap, apical plate; pt, prototroch; pc, protoconch.

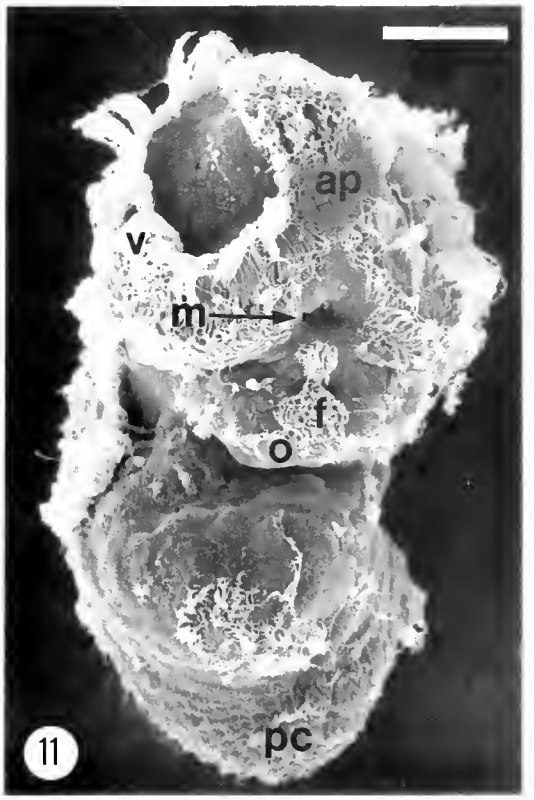

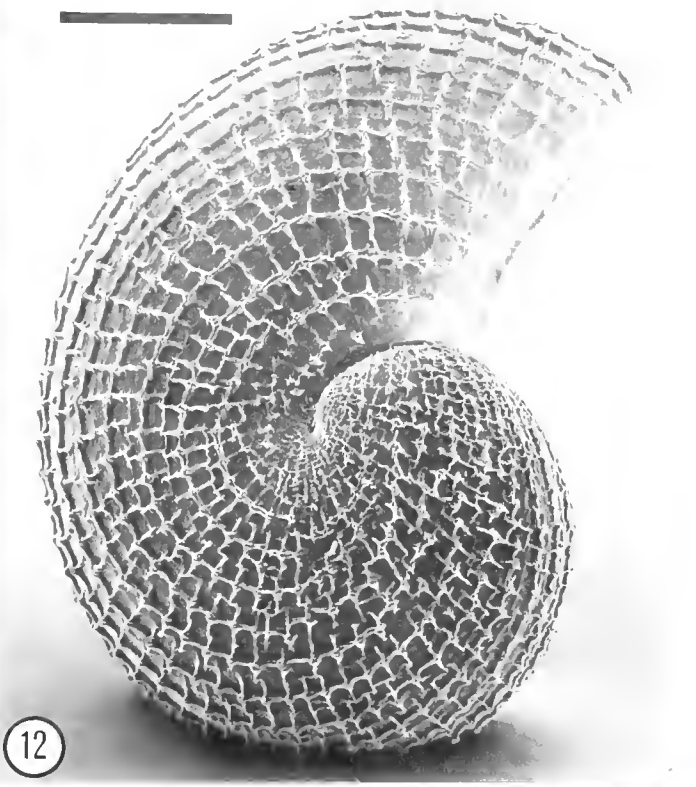

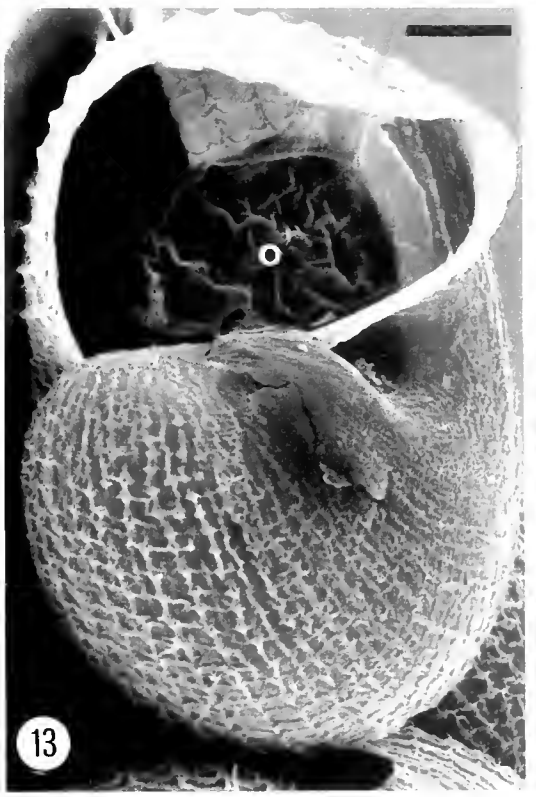

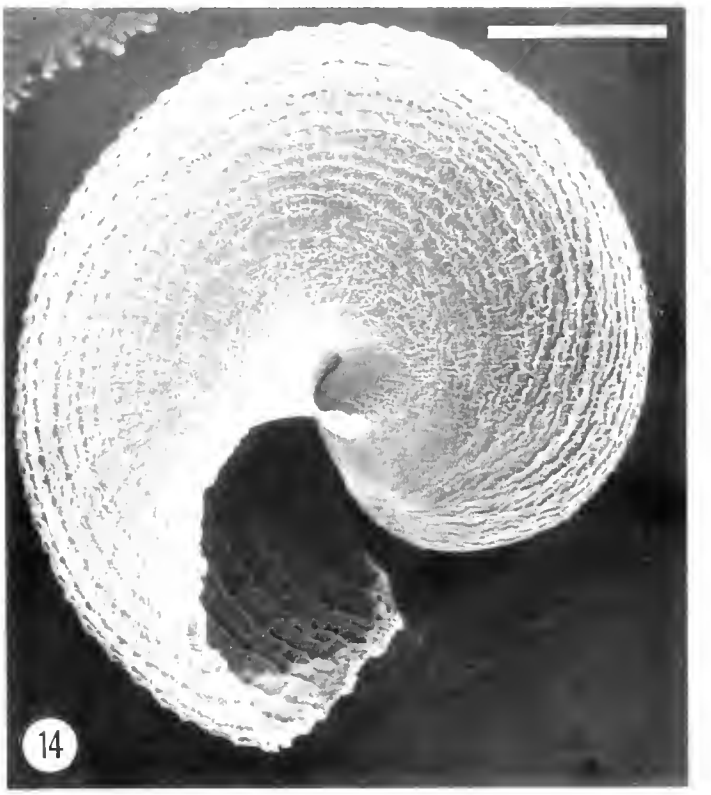

Figures 11–14. Scanning electron micrographs of early and late veliger larvae extracted from lenticular egg capsules from the Galapagos Rift. **Figure 11.** Early veliger larva showing apical plate (ap), velum (v), mouth (m), foot primordium (f), operculum (o), and protoconch (pc). Scale bar = 25 μm. **Figure 12.** Apical view of Protoconch I in larva near hatching. Scale bar = 50 μm. **Figure 13.** Apertural view of Protoconch I in larva near hatching. Scale bar = 25 μm. o, operculum. **Figure 14.** Ventral view of Protoconch I in larva near hatching. Scale bar = 50 μm.

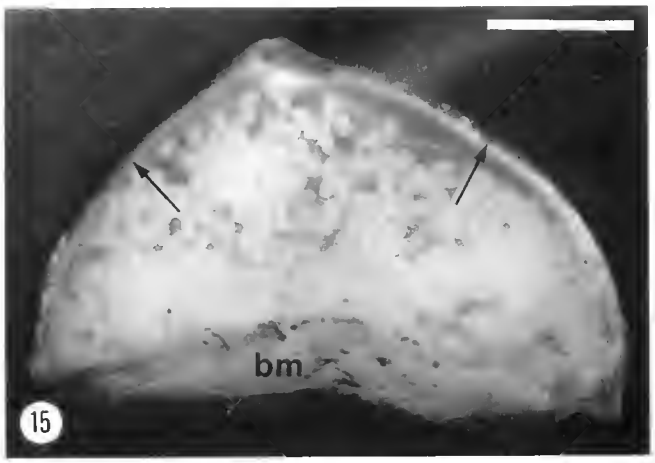

Figure 15. Light micrograph of convex side of Galapagos Rift inflated triangular egg capsule with embryos visible through the transparent capsule wall. Arrows mark the lateral ridges. Scale bar = 1 mm. bm, basal membrane.

oothecae in different gastropod taxa is characteristic of the species, and in some cases, of higher orders of classification, and may be valuable in taxonomy. It should be noted, however, that similar capsules may be produced by taxonomically diverse species, while in other cases interspecific variation in capsule morphology is insufficient to differentiate closely related species (Kohn, 1961).

Galapagos Rift lenticular egg capsules

Flattened lenticular egg capsules with a centrally located escape aperture are known from the neogastropod families Muricidae, Fasciolariidae, and Turridae. Dimensions and other statistics pertaining to selected lenticular egg capsules from these families are presented in Table III. The only member of these families known to occur at the Galapagos Rift hydrothermal vents is a large turrid, provisionally described as *Phymorhynchus* sp. (Warén and Bouchet, 1989). A similar species occurs at 13°N and 21°N on the East Pacific Rise (Turner *et al.*, 1985; Warén and Bouchet, 1989). Both the six egg capsules described by Turner *et al.* (1985) and the five "lens-shaped" egg cases described by Berg (1985) as characteristic of turrids, as well as, the lenticular egg capsules described in this paper, may all belong to *Phymorhynchus* sp. from the Galapagos Rift. Differences in reported average size between these three groups of capsules is not unexpected, because capsule size in neogastropods is proportional to adult size. Capsule size is also correlated with female foot width; the capsule is formed and manipulated by the foot during deposition (Robertson, 1976; Shimek, 1986).

Berg (1985) estimated that "lens-shaped" oothecae from the Garden of Eden and Mussel Bed hydrothermal vent sites along the Galapagos Rift contained from 500–1000

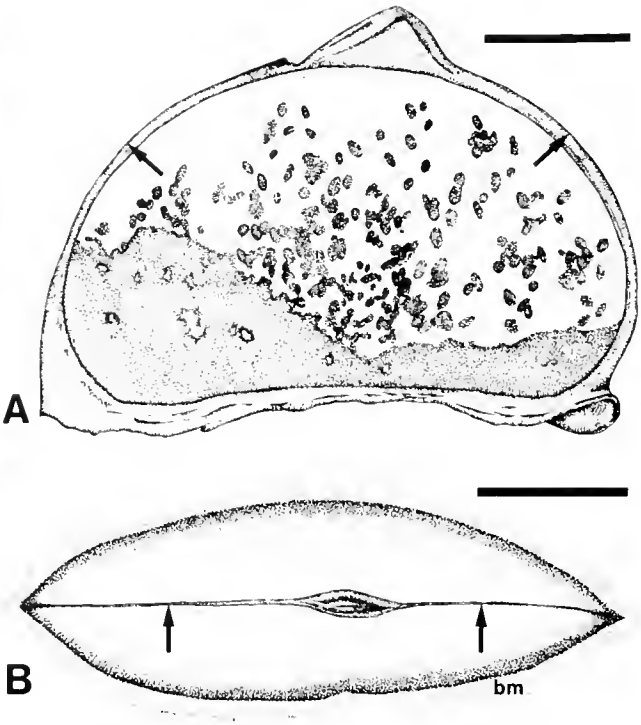

Figure 16. (A) View of the convex side of Galapagos Rift inflated triangular egg capsule with individual embryos visible through transparent membrane. Arrows mark the lateral ridges. Scale bar = 1 mm. (B) Apical view of Galapagos Rift inflated triangular egg capsule. Arrows mark the lateral ridges. Scale bar = 1 mm. bm, basal membrane.

eggs with a mean size of 192.1 ± 13.5 μm by 136.2 ± 10.1 μm. This agrees well with our count of 1052 larvae in one capsule from Dive 2031 and with the size of larvae both from this capsule (234 μm maximum diameter) and from

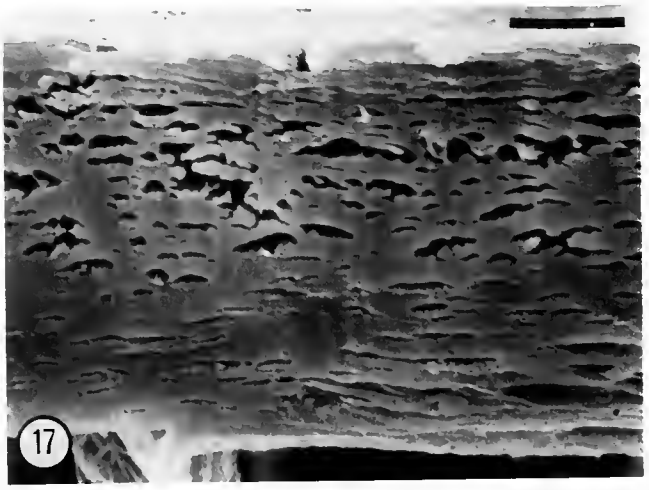

Figure 17. Scanning electron micrograph of cross-section of single-layered spongy capsule wall of inflated triangular egg capsule from Galapagos Rift. The outer surface is towards the top. Scale bar = 5 μm.

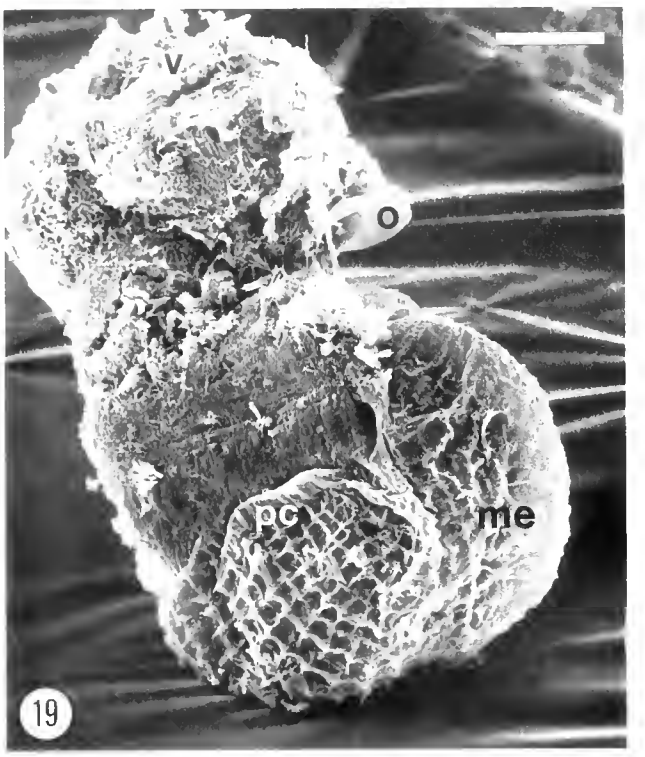

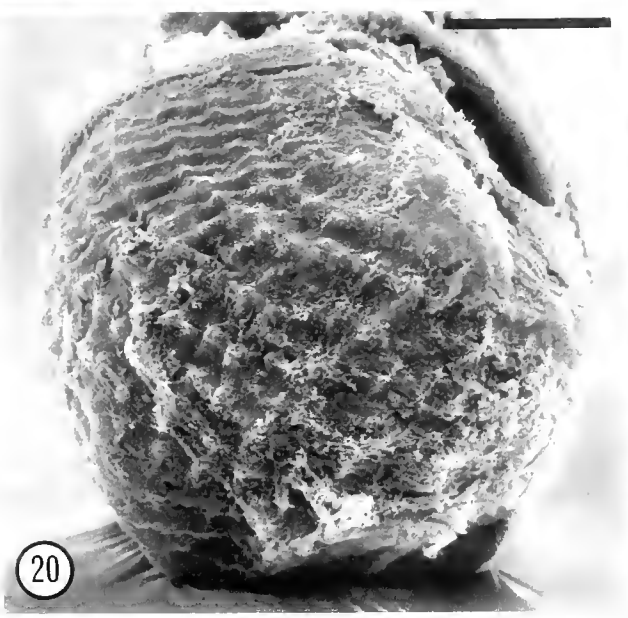

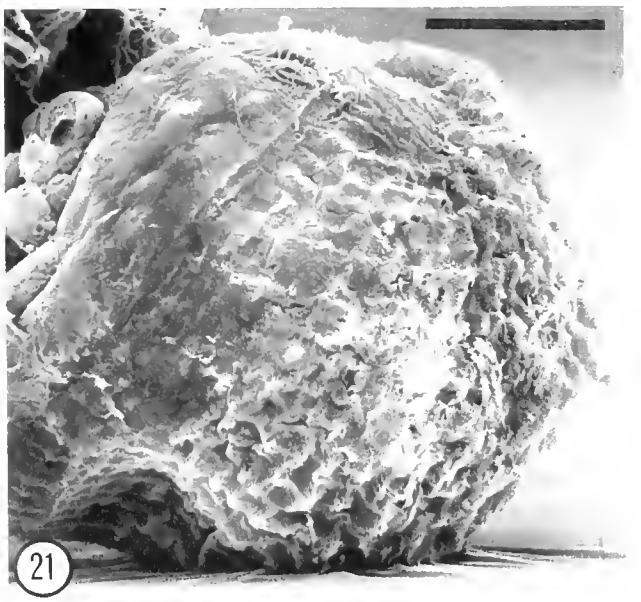

Figures 18–21. Scanning electron micrographs of veliger larvae extracted from inflated triangular egg capsules from Galapagos Rift. **Figure 18.** Lateral ventral view showing velum (v), apical plate (ap), mouth (m), foot primordium (f), and early protoconch (pc). Scale bar = 25 μm. **Figure 19.** Lateral view showing cancellate or net-like early protoconch (pc) sculpture and obscuring membrane (me). Scale bar = 25 μm. o, operculum; v, velum. **Figure 20.** Apical view of early protoconch. Scale bar = 20 μm. **Figure 21.** Dorsal view of early protoconch. Scale bar = 20 μm.

capsules with larvae in earlier stages of development (175 μm in length by 100 μm in width). The absence of nurse eggs further suggests these capsules were laid by a turrid, because nurse eggs are unknown in the Turridae (Table III).

Although the basal diameter of lenticular egg capsules described herein (14.8 × 14 mm) is larger than the 2–6 mm of normal turrid egg capsules, it is not unprecedented. Egg capsules of the turrid *Mangelia plicosa* are 30–33

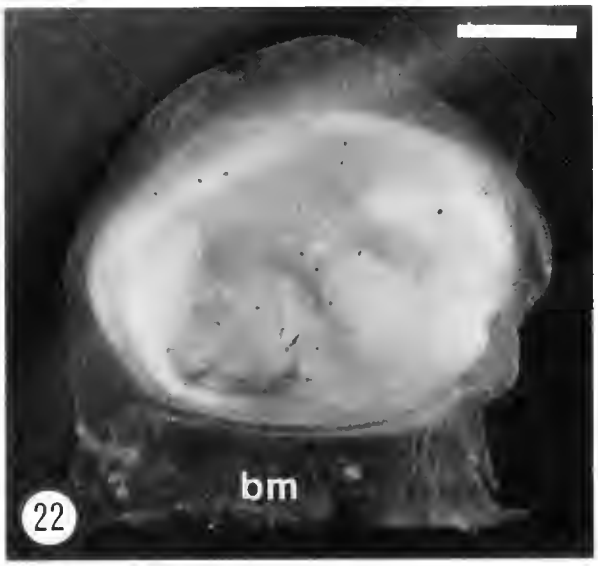

Figure 22. View of the convex side of Juan de Fuca Ridge pouch-like egg capsule containing amorphous embryonic mass. Scale bar = 1 mm. bm, basal membrane.

mm in diameter, while those of *Polystira barretti* measure up to 10.7 mm in basal diameter (Table III). Furthermore, the large size of the Galapagos Rift turrid (up to 74 mm in height, pers. obs., RGG) is consistent with the large size of the egg capsules. Although turrid egg capsule wall structure has not been previously studied, the three-layered capsule wall (Fig. 4) is similar to that described for the closely related Conidae (D'Asaro, 1988). This is consistent with the designation of these capsules as belonging to a turrid, because lenticular capsules of the Muricoidea have four layers (D'Asaro, 1988). Some degree of reproductive synchrony may occur in the population of the Galapagos Rift turrid provisionally described as *Phymorhynchus* sp., because eggs, embryos, and larvae contained in different lenticular capsules collected during March 1985 and May 1988 in the present study (Tables I, II), and by Berg (1985), were at the same relative stage of development on each collection date but were at different stages of development between collection dates.

Galapagos Rift inflated triangular capsules

Berg's (1985) account of four egg capsules, each "shaped like a small inflated triangle," retrieved from a larval trap in 1979 at the Garden of Eden vent on the Galapagos Rift, agrees in every respect with the description found here of the inflated triangular capsules from Rose Garden vent. Although Berg (1985) does not give a measure of the egg capsule's height, the average length of 4.9 mm and width of 1.7 mm of his capsules is similar to the average length of 4.1 mm and width of 1.3 mm for the three inflated triangular capsules described in this report.

Inflated triangular capsules from the Galapagos Rift vent fields are similar in morphology, but not in size, to those from 5480 m in the Kermadec Trench illustrated by Bouchet and Warén (1985a) and attributed to the buccinid *Calliloconcha knudseni* Bouchet and Warén. These 15 mm long by 12 mm high *C. knudseni* capsules were empty and had been drilled by a predator. Certain small capsules similar to the inflated triangular capsules found at the Galapagos Rift, but without a prominent lateral and apical ridge, are produced by members of the neogastropod family Columbellidae (Petit and Risbec, 1929; Thorson, 1940a; Bacci, 1947; Amio, 1955; Bandel, 1974a). Capsules of this group contain no more than 60 eggs, which are usually reduced in number through oophagy (Bandel, 1974a). Small capsules attributed to the buccinid *Tacita danielsseni* (Friele) and to the turrid *Oenopota ovalis* (Friele) from abyssal parts of the Norwegian Sea resemble the inflated triangular capsules in size but appear to lack the lateral ridge and strong off-center apex (Bouchet and Warén, 1979a). The egg capsule attributed to *O. ovalis* in Bouchet and Warén (1979a, Fig. 15) is unlike any known for the genus *Oenopota* (Thorson, 1935; Shimek, 1983b, 1986) or for any other turrid. Capsules belonging to *T. danielsseni* contained thousands of small eggs, although only one large embryo (4 mm in maximum dimension) developed in each capsule. A large protoconch (840–880 μm) is also present in *O. ovalis*, which is indicative of direct development (Bouchet and Warén, 1979a; Rex and Warén, 1982). By comparison to the above species, several hundred veligers were present in each of the triangular capsules from the Galapagos Rift examined in this study. Neither a buccinid nor a columbellid has as yet been reported from the Galapagos Rift hydrothermal vents.

Gastropods that are large enough to have laid these capsules at the Galapagos Rift vent sites include *Phymorhynchus* sp., *Provanna ios* Warén and Bouchet and *P. muricata* Warén and Bouchet (Warén and Bouchet, 1986, 1989). The turrid *Phymorhynchus* is an unlikely candidate because the capsule type for this species has been provisionally assigned in the present study. Although the inflated triangular capsules from the Galapagos Rift are unlike the typical lenticular capsules of turrids, a similar capsule from the deep-sea has been attributed to the turrid *Oenopota ovalis* (Bouchet and Warén, 1979a; see discussion above). Either species of *Provanna* is also an unlikely choice, because the recent placement of *Provanna* within the Littorinoidea (Warén and Bouchet, 1989) suggests that the production of such an elaborate egg capsule is unlikely, because all known littorinoids spawn either a benthic, amorphous gelatinous mass, a single pelagic capsule containing a single egg, or release veligers or fully formed juveniles from an internal brood pouch (Thorson, 1946; Anderson, 1960, 1962; Amio, 1963; Pilkington,

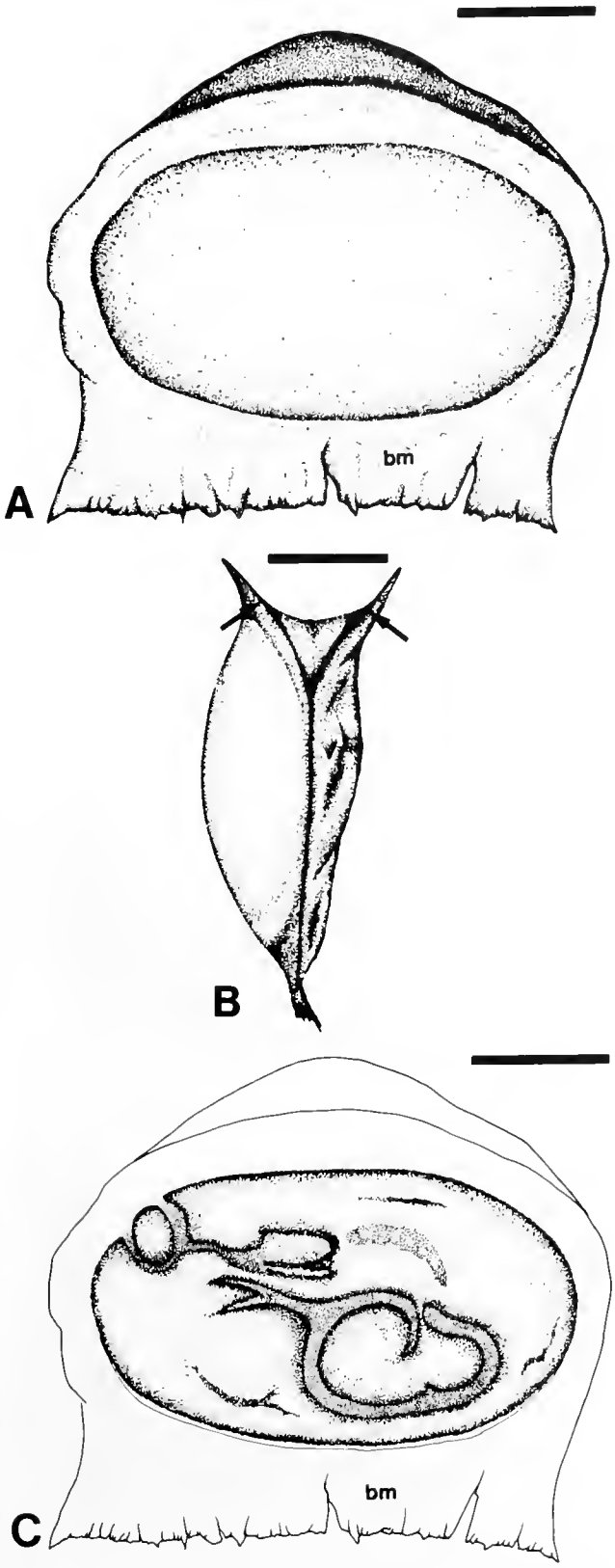

Figure 23. (A) View of the convex side of Juan de Fuca Ridge egg capsule. Scale bar = 1 mm. bm, basal membrane. (B) Lateral view of Juan de Fuca capsule showing lateral ridge running into two apical wing-like extensions (arrows) forming a saddle-like structure. Scale bar = 1 mm. (C) View of the convex side of Juan de Fuca egg capsule with amorphous embryonic mass visible through transparent capsule wall. Scale bar = 1 mm. bm, basal membrane.

1974; Robertson, 1976; Bandel, 1974b, 1975b, 1982; Soliman, 1987; M. F. Strathmann, 1987). Based on egg capsule morphology, we cannot assign the inflated triangular egg capsules from the Galapagos Rift to a particular species. A more definitive statement on the taxonomic affiliation of the inflated triangular capsule must await additional collections of organisms from the Galapagos Rift vent fields and further taxonomic examination of existing material.

The wall structure of the inflated triangular egg capsules from the Galapagos Rift is similar to that seen in several species within the Muricoidea (Roller and Stickle, 1988; D'Asaro, 1988), although too little is known of egg capsule wall structures at this time to make a definitive statement as to this capsule's affinity. Because all three inflated triangular capsules collected from Galapagos Rift on three separate dives in 1985 contained early veligers at the same stage of development, it is possible that some degree of reproductive synchrony occurs in this population.

Juan de Fuca Ridge egg capsules

Egg capsules strikingly similar in size and shape to the Juan de Fuca Ridge capsules described in the present study are produced by the cancellariid neogastropod, *Admete viridula* (Fabricius) [Thorson, 1935: fig. 71 (mistakenly attributed to *Velutina undata* Brown, see Thorson, 1944: 108); Bouchet and Warén, 1985b: fig. 687]. The capsules described herein and those of *A. viridula* both possess parallel wing-like extensions, a flattened base, and an apical escape aperture. Species of *Admete* have been described from 6700 m deep in the Kermadec Trench, whereas *A. viridula*, which is circumpolar, has a depth range of 4–2,295 m, according to Clarke (1962). The small number (1–6) of large larvae present in Juan de Fuca capsules is consistent with the 6–7 larvae per capsule found in *Admete viridula* by Thorson (1935) and the 6 larvae per capsule found in *Admete* sp. by MacGinitie (1955). However, a species of *Admete* has not been collected from the Juan de Fuca Ridge.

Other pouch-like egg capsules, with or without a flattened base, but without wing-like extensions, are found in the neogastropod families Muricidae and Buccinidae (Thorson, 1935, 1940b; Anderson, 1960; Golikov, 1961; Cowan, 1964; Radwin and Chamberlin, 1973; MacIntosh, 1979, 1986; D'Asaro, 1986). However, buccinids typically form their capsules into clusters (Thorson, 1935; Cowan, 1964), in contrast to the pouch-like capsules from Juan

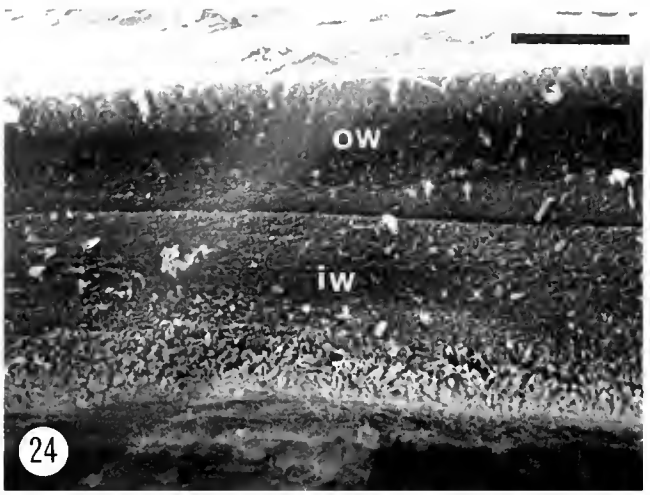

Figure 24. Scanning electron micrograph of cross-section of double-layered capsule wall of Juan de Fuca Ridge egg capsule. Scale bar = 5 μm. ow, outer wall; iw, inner wall.

de Fuca, which are individually attached to the substrate. Capsules secreted by members of the neogastropod family Columbellidae frequently possess apical collars that surround a central escape aperture somewhat similar to the wing-like extensions seen in capsules from the Juan de Fuca Ridge described in the present study (Thorson, 1940a; Perry and Schwengel, 1955; Amio, 1955, 1963; Marcus and Marcus, 1962; Scheltema, 1969; D'Asaro, 1970b; Bandel, 1974a).

Only two gastropods, *Buccinum viridum* Dall and *Provanna variabilis* Warén and Bouchet, which are large enough to have secreted these capsules, have been recorded from the Juan de Fuca Ridge system (Warén and Bouchet, 1986; Tunnicliffe *et al.*, 1985; Tunnicliffe and Fontaine, 1987; Tunnicliffe, 1988). Dall (1890) described *B. viridum* as having a maximum shell height of 46 mm, while *P. variabilis* reaches a maximum height of 8.7 mm (Warén and Bouchet, 1986). Warén and Bouchet (1989) have recently placed *P. variabilis* within the Superfamily Littorinoidea. No members of the Littorinoidea have as yet been shown to produce complex egg capsules (see discussion above of inflated triangular capsules), which suggests that *P. variabilis* is not the source of the egg capsule from the Juan de Fuca Ridge. The Buccinidae produce egg capsules either singly or in clusters, each containing many nurse eggs; only a few of these survive (Thorson, 1935, 1946; Lebour, 1937; Anderson, 1960). Encapsulated

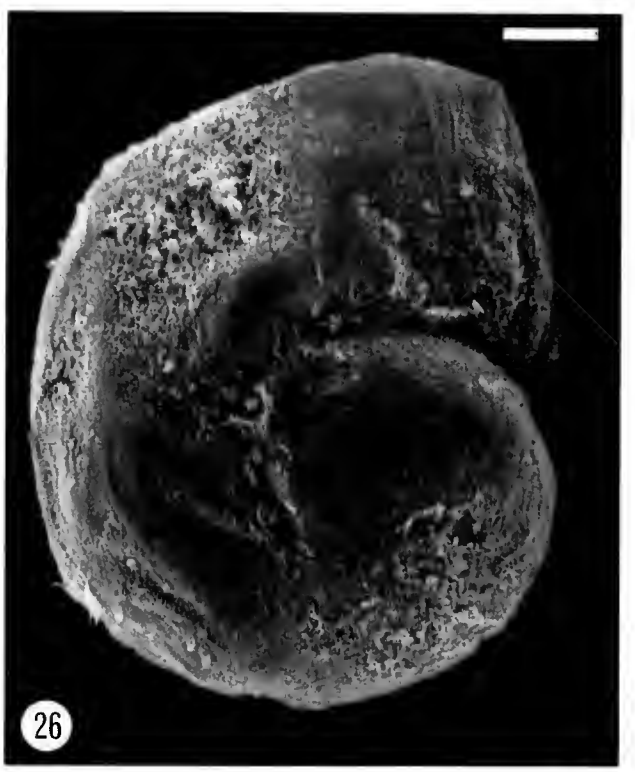

Figures 25–26. Scanning electron micrographs of larvae extracted from Juan de Fuca Ridge egg capsules. **Figure 25.** Lateral view of protoconch showing height of the first whorl and weak concentric growth lines. Scale bar = 200 μm. **Figure 26.** Apical view showing unsculptured appearance of protoconch. Scale bar = 200 μm.

Table III

Taxonomic affiliation, dimensions, number of eggs, egg size, and number of veligers present at hatching for lenticular egg cases as reported in selected references

Species	Size (mm)		Number of eggs	Egg size (μm)	Number of veligers at hatching	Post-hatching development type	Reference
	Basal diameter	Height					
Order Neogastropoda							
Muricoidea							
Family Muricidae							
Bedeva hanleyi (Angas)	3.0	—	50–70	250	15	N	Anderson, 1965
Bedevina (Lataxiena) birileffi (Lischke)	3.0	0.85	60–90	190	—	P	Amio, 1963
Ergalatax constractus (Reeve)	2.5–3.0	—	130	—	—	?	Habe, 1960
Ergalatax calcareus (Dunker)	3.5–4.5	—	130	—	—	?	Habe, 1960
Trophon clathratus (L.)	6–7	—	—	—	9–18	N	Thorson, 1940b
Trophon muricatus (Montagu)	2.5	—	—	—	2–9	N	Lebour, 1936
Trophon truncatus (Strom.)	1.8–3.1	—	—	—	6–11	N	Thorson, 1946
Zeatrophon (Xymene) ambiguus (Philippi)	6–10	1.0–1.5	—	—	600	N-P	Pilkington, 1974
Family Fasciolariidae							
Glaphyrina vulpicolor (Sowerby)	12	—	—	—	10	N	Pilkington, 1974
Conoidea							
Family Turridae							
Clavus japonicus (Lischke)	2.5	1.8	2–4	650	2–4	N	Amio, 1963
Crassispira sp.	1.5	—	2–5	—	2–5	N	Bandel, 1976b
Drillia crenularis (Lamarck)	6–7	—	150–170	230–300	150–170	P	Thorson, 1940a
Drillia solida (C. B. Adams)	4	1	2–7	—	2–7	?	Bandel, 1976b
Kurtziella plumbea (Hinds)	2.3 ± 0.3	—	180 ± 43	137 ± 8	180 ± 43	?	Shimek, 1983c
Mangelia nebula (Montagu)	1.6	—	—	—	60	P	Lebour, 1934, 1936, 1937
Mangelia plicosa (C. B. Adams)	30.1–33.0	0.32	60	160	—	?	Perry and Schwengel, 1955
Oenopota simplex (Midd.)	2–3	—	—	—	5–6	N	Thorson, 1935
Oenopota exarata (Moller)	3.0–4.5	—	—	—	5–21	N	Thorson, 1935
Oenopota bicarinata (Couth.)	2.25–3.25	—	—	—	3–11	N	Thorson, 1935
Oenopota pyramidialis (Strom.)	3.5–6	—	—	—	4–20	N	Thorson, 1935
Oenopota nobilis (Moller)	4.5–4.75	—	—	—	3–7	N	Thorson, 1935
Oenopota trevelyana (Turton)	3.1–3.3	—	—	—	25–31	N-P	Thorson, 1946
Oenopota turricola (Montagu)	2.5	—	100–150	—	100–150	?	Vestergaard, 1935
Oenopota elegans (Moller)	3.02	—	250	150	250	P	Shimek, 1983b
Oenopota excurvata (Carpenter)	2.08	1.08	30	212	—	?	Shimek, 1983b
Oenopota fidicula (Gould)	2.24	0.98	20	371	—	?	Shimek, 1983b
Oenopota levidensis (Carpenter)	5.30	1.38	175 ± 85	286	175 ± 85	P	Shimek, 1983b
Ophiodermella inermis (Hinds)	4.68 ± 0.99	1.44 ± 0.29	208 ± 61	222 ± 15	208 ± 61	P	Shimek, 1983a
Philbertia gracilis (Montagu)	3.4	—	—	—	40–80	P	Lebour, 1934, 1936, 1937
Philbertia linearis (Montagu)	1.5–2.0	—	60–80	140–150	—	P	Lebour, 1934, 1936, 1937
	—	—	51–114	150	—	P	Thorson, 1946
Philbertia purpurea (Montagu)	5.3	0.6	350–400	100	—	P	Franc, 1950
Polystira barretti (Guppy)	5.0–10.7	—	32–126	438	32–126	N	Penchaszadeh, 1982
Raphitoma (Teretia) amoena (Sars)	1.25–1.5	—	—	—	2	N	Thorson, 1935
Unknown turrid	2–3.5	—	—	—	—	?	Arnaud and Zibrowius, 1973
Unknown turrid	2.6	—	—	—	—	?	Bouchet and Warén, 1980
Unknown turrid	4.0–4.2	—	—	—	—	?	Bouchet and Warén, 1980

direct development is universal within this group (Lebour, 1937; Robertson, 1976; Colman *et al.*, 1986; Warén and Bouchet, 1989), although planktotrophic buccinids are known from the Early Tertiary (Hansen, 1982). Capsule wall morphology of the Juan de Fuca egg capsule described in the present study is similar to that seen in certain Buccinidae and Muricidae (D'Asaro, 1988), although a definitive statement is not possible until the micromorphology

of a wider taxonomic grouping of capsules is known. On the basis of egg capsule morphology we are unable to assign the pouch-like egg capsules from the Juan de Fuca Ridge to any species that has as yet been collected from this site. However, the similarity of the Juan de Fuca Ridge capsules to those produced by species of *Admete* (Thorson, 1935; Bouchet and Warén, 1985b) is so striking that it leads us to predict that a member of this genus may soon be found associated with this hydrothermal vent.

Egg size, fecundity, and protoconch morphology

The size of the ovum in those prosobranch gastropods that do not provide nurse eggs or albumen in the egg capsule regulates the amount of nutrition supplied to the larva and has a close relationship with the type of larval development [Thorson 1946, 1950; Shuto, 1974; Bandel, 1975a; Lima and Lutz, 1990; but see discussion on this topic in Vance (1973, 1974), Underwood (1974), Steele (1977), Strathmann (1977), Perron (1981), Todd and Doyle (1981), and Hines, (1986)]. Planktotrophic prosobranch gastropod larvae typically have a small pointed apex, often with delicate sculpture, reflecting an originally small ovum. However, non-planktotrophic larvae typically have a large rounded apex reflecting a large ovum with plenty of yolk available for the larva to grow to a large size (Ockelmann, 1965; Shuto, 1974). This relationship may become obscured in those non-planktotrophs that feed on nurse eggs or other forms of extraembryonic nutrition and emerge as large juveniles, because they often have egg diameters no larger than those of free-swimming, non-planktotrophs (Bandel, 1975a, c; Jablonski, 1986). Similarly, Hadfield and Strathmann (1990) have shown that egg size is not a reliable indicator for differentiating between a pelagic and a benthic mode of development in non-planktotrophic trochoidean archeogastropods. In addition, although archeogastropods are purported to be exclusively non-planktotrophic (Anderson, 1960; Heslinga, 1981; Strathmann, 1978a, b; Rex and Warén, 1982; Lutz *et al.*, 1984; Jablonski, 1985; Warén and Bouchet, 1989), many species develop from relatively small eggs between 110 and 230 μm in diameter (Amio, 1963), and as small as 80 μm in some cases (Bandel, 1982). Unfortunately, egg size criteria could not be applied in the present study, because ova were not encountered.

In the absence of nurse eggs, the number of eggs produced by a gastropod species is also indicative of its mode of larval development (Thorson, 1950; Crisp, 1978; Shuto, 1974; Bandel, 1975a). A large number of eggs suggests planktotrophic development, because many free-swimming embryos and larvae are assumed to be lost to predation, whereas few eggs suggest non-planktotrophic development (Thorson, 1950; Jablonski and Lutz, 1983). Estimates of fecundity in the present study are complicated by the fact that we have no way of knowing how many capsules were produced by each laying female. However, the over 1000 larvae contained in the lenticular capsules from the Galapagos Rift, when compared to information on the number of eggs per capsule, total fecundity, and development type in other species with lenticular egg capsules (Table III), suggests that this species develops planktotrophically following hatching. The apparent absence of nurse eggs and the presence of several hundred embryos in the inflated triangular capsules from the Galapagos Rift also suggests the potential for planktotrophic development after hatching; while the small number of embryos (1–6) in pouch-like capsules from the Juan de Fuca Ridge is strongly indicative of non-planktotrophic development.

Non-planktotrophic development is the most common strategy among prosobranchs in the deep-sea, soft-sediment environment of the western North Atlantic (Rex and Warén, 1982). However, an examination of bathyal and abyssal prosobranch larval shells reveals that roughly 30% may develop planktotrophically below 1000 m in the north-eastern Atlantic (Bouchet, 1976a, b; Bouchet and Warén, 1979b) and that the incidence of planktotrophic development in this group increases with depth below the continental shelf (Rex and Warén, 1982). About 50% of mesogastropod and neogastropod prosobranch species on the abyssal plain may have planktotrophic development based on their protoconch morphologies (Rex and Warén, 1982). Bouchet (1976a, b) and Bouchet and Warén (1979b) have proposed that deep-sea prosobranch larvae with protoconchs, indicative of planktotrophy, migrate to feed and undergo development in surface waters. In addition, ^{18}O and ^{13}C isotope analyses of larval shells from deep-sea gastropods have suggested that at least some larvae of abyssal species may migrate upwards into warmer waters during development (Bouchet and Fontes, 1981; Killingley and Rex, 1985).

Protoconch 1 sculpture of the type seen in larvae from lenticular egg capsules at the Galapagos Rift (Figs. 12–14) is characteristic of many turrid species with putative planktotrophic development in both shallow waters [*Philbertia linearis* (Montagu) (Rodriguez Babio and Thiriot-Quiévreux, 1974), *Raphitoma* spp. (Richter and Thorson, 1975)] and in the deep sea [*Pleurotomella* spp., *Teretia* spp., *Xanthodaphne* spp., *Phymorhynchus* spp., *Gymnobela* spp., *Theta* spp. (Bouchet and Warén, 1980), *Gymnobela subaraneosa* (Dautzenberg and Fischer) (Colman *et al.*, 1986)]. The Turridae includes species with larval shell morphologies that are indicative of both planktotrophic and non-planktotrophic development (Rex and Warén, 1982; Shimek, 1983a, b, c, 1986). The maximum diameter of the Protoconch 1 in certain planktotrophic-type turrid species can be roughly estimated from published micrographs, including the species *Phil-*

bertia linearis (260 μm) (Rodriguez Babio and Thiriot-Quiévreux, 1974), *Raphitoma reticulata* (Renier) (220 μm), *R.* (*Philbertia*) *purpurea* (Montagu) (245 μm), *R.* (*Cirilla*) *linearis* (Montagu) (245 μm), *R.* (*Leufroyi*) *leufroyi* (Michaud) (225 μm) (Richter and Thorson, 1975), *Pleurotomella coeloraphe* (Dautzenberg and Fischer) (265 μm), *Pleurotomella demosia* (Dautzenberg and Fischer) (355 μm), *Pleurotomella megalembryon* (Dautzenberg and Fischer) (280 μm), *Pleurotomella bureaui* (Dautzenberg and Fischer) (220 μm), *Pleurotomella sandersoni* Verrill (195 μm), *Teretia teres* (Forbes) (260 μm), *Xanthodaphne dahnasi* (Dautzenberg and Fischer) (215 μm), *Theta chariessa* (Watson) (240 μm) (Bouchet and Warén, 1980), and *Gymnobela subaraneosa* (Dautzenberg and Fischer) (180 μm) (Colman *et al.*, 1986).

Assuming that the larvae in lenticular egg capsules from the Galapagos Rift retrieved on "Alvin" Dive 2031 were near hatching and represent the complete Protoconch I stage, then measurements made from electron micrographs reveal that this species has a Protoconch I maximum diameter of approximately 235 μm (Figs. 12–14). This compares favorably with the Protoconch I maximum diameters above, estimated for various turrid species (195–280 μm), with the exception of the large Protoconch I in *Pleurotomella demosia* (355 μm) and the small Protoconch I in *Gymnobela subaraneosa* (180 μm). The maximum diameter of the Protoconch I in larvae from the lenticular capsules also agrees well with the size of the Protoconch I (as estimated from published micrographs) in both the unnamed, newly settled turrid from the Galapagos Rift (205–225 μm) and the unnamed newly settled turrid from 21°N on the East Pacific Rise (260 μm) (Turner *et al.*, 1985; their figs. 27a–e and 26a–e, respectively). Unfortunately, pre-juvenile development is incomplete for larvae in lenticular capsules in the present study, and the final Protoconch II maximum diameter and number of whorls cannot be determined, which precludes the estimation of D/Vol values for these samples. However, as estimated from Fig. 27a in Turner *et al.* (1985), the unnamed newly settled turrid from the Galapagos Rift has a Protoconch II with approximately 4 whorls and a maximum diameter of 950 μm (giving a D/Vol value of 0.19). Similarly, the unnamed newly settled turrid from 21°N (Turner *et al.*, 1985) has a Protoconch II maximum diameter of approximately 775 μm with about 4 whorls (giving a D/Vol value of 0.19), as estimated from Fig. 26d in Turner *et al.* (1985). The number of volutions, D/Vol values, clear demarcation between Protoconch I and II, and the protoconch ornamentation of spiral threads crossed by axial riblets of both unnamed newly settled turrids from the Galapagos Rift and 21°N, depicted in Turner *et al.* (1985), are all indicative of planktotrophic development.

Although the Protoconch I sculpture of the unnamed newly settled turrid from the Galapagos Rift, depicted in Turner *et al.* (1985, their figs. 27a–e), and Protoconch I larvae from lenticular egg capsules in the present study, also from the Galapagos Rift (Figs. 12–14), cannot be directly compared due to corrosion of the former, the similarly sized Protoconchs I (205–225 μm and 235 μm, respectively) suggest that these specimens are taxonomically related. Because the only turrid to be collected at the Galapagos Rift is the provisionally classified *Phymorhynchus* sp. (Warén and Bouchet, 1989), it is likely that both the turrid juvenile from the Galapagos Rift described by Turner *et al.* (1985), and the lenticular egg capsules and larvae within, belong to this species. However, adult or juvenile *Phymorhynchus* sp. with intact, non-corroded protoconchs, characteristics that would verify this identification, have not been collected at the Galapagos Rift.

Although it is not possible to determine the maximum diameter of the Protoconch I stage or the D/Vol value for larvae from the inflated triangular egg capsules from the Galapagos Rift due to the incomplete development of the larval shell, the initial reticulate sculpture (Figs. 19–21) is indicative of planktotrophic development, following the encapsulated phase. This type of sculpture is similar to that seen on the Protoconch I of some members of the mesogastropod families Rissoidae (Lebour, 1936, 1937; Amio, 1963) and Cypraeidae (Richter and Thorson, 1975), as well as the neogastropod families Columbellidae (Colman *et al.*, 1986) and Turridae (Lebour, 1934; Amio, 1963; Rodriguez Babio and Thiriot-Quiévreux, 1974; Richter and Thorson, 1975; Bouchet, 1976a; Bouchet and Warén, 1980). Members of the Cypraeidae have not been collected in the deep-sea (Clarke, 1962), and no member of this family or of the Rissoidae has been collected at the Galapagos Rift. The columbellid *Anachis haliaeeti* (Jeffreys) from the Rockall Trough has an ornately sculptured Protoconch I and has been designated a planktotrophic developer (Colman *et al.*, 1986). Shallow-water species of this genus produce small egg capsules similar to the inflated triangular type from the Galapagos Rift but with a circular collar around the capsule's apex and containing only 10–30 embryos (Scheltema, 1969) in contrast to the several hundred larvae seen in capsules from the Galapagos Rift. Likewise, the morphology of the inflated triangular egg capsule is unlike that seen in most Turridae. However, the egg capsule attributed to the turrid *Oenopota ovalis* (Bouchet and Warén, 1979a) resembles the inflated triangular capsules, but contains only one embryo with an unsculptured protoconch, in contrast to the several hundred highly ornamented larvae encountered in the inflated triangular capsules from the Galapagos Rift. Given the incomplete formation of the larval shell and unique structure of the egg capsule, it has proved impos-

sible to assign the inflated triangular capsules from the Galapagos Rift to any known gastropod species from this site.

Larvae from the Juan de Fuca Ridge egg capsules have a large, paucispiral protoconch devoid of sculpture (Figs. 25, 26), which suggests that this species develops non-planktotrophically. Assuming that these larvae have a nearly fully developed protoconch, with a maximum diameter of approximately 1.3 mm and 1.5 whorls (as estimate from Fig. 26), their calculated D/Vol value of 0.87 in concert with the small number of whorls is also indicative of non-planktotrophic development. This type of protoconch, lacking ornamentation, is similar to that produced by members of the neogastropod superfamilies Muricoidea and Cancellaroidea (Thorson, 1935; Radwin and Chamberlin, 1973; Bandel, 1975a, b, c; Bouchet and Warén, 1985a; Colman *et al.*, 1986; Colman and Tyler, 1988), however taxonomic placement of these larvae is uncertain using protoconch morphology alone. The protoconch of the cancellaroid *Admete viridula* (Thorson, 1935: fig. 72), the species with the most similar egg capsule morphology to the specimens described in this study from the Juan de Fuca Ridge, has a maximum diameter of about 0.88 mm [as estimated from Thorson (1935: fig. 72)] and 1.25 whorls, for a D/Vol value of 0.77, which also compares favorably with that calculated for encapsulated larvae from the Juan de Fuca Ridge (0.87). Bouchet and Warén (1985a) give the protoconch maximum diameters and number of whorls for the deep-sea buccinids *Eosipho thorybopus* Bouchet and Warén (0.7 mm, 1 whorl, D/Vol = 0.7), *Manaria lirata* Kuroda and Habe (0.8 mm, 1+ whorl, D/Vol = 0.8), and *M. clandestina* Bouchet and Warén (0.7 mm, 1+ whorl, D/Vol = 0.7). Colman *et al.* (1986) also provide protoconch maximum diameters, whorl number, and D/Vol values for the deep-sea buccinids *Tacita abyssorum* (Locard) (0.75 mm, 1.2 whorls, D/Vol = 0.63), *Colus jeffreysianus* (Fischer) (2.5 mm, 1.25 whorls, D/Vol = 2), and the muricid *Trophon* sp. (1.1 mm, 1.5 whorls, D/Vol = 0.73). All of these species lack protoconch ornamentation. Ornamentation is also lacking on some members of the mesogastropod families Rissoidae (Richter and Thorson, 1975) and Cerithiidae (Rodriguez Babio and Thiriot-Quiévreux, 1974), as well as the neogastropod families Nassariidae (Richter and Thorson, 1975) and Turridae (Bouchet and Warén, 1980; Colman *et al.*, 1986).

Protoconchs retained on adult specimens of the two known gastropod species from the Juan de Fuca Ridge, large enough to have laid the capsules from this site [*Buccinum viridum* (pers. obs.) and *Provanna variabilis* (Warén and Bouchet, 1986)], were badly corroded, precluding comparison with larvae extracted from the Juan de Fuca Ridge egg capsules. The potential for either of these two species to be the source of the pouch-like capsules from the Juan de Fuca Ridge is discussed above.

Molluscan larval dispersal at hydrothermal vents

Despite the ephemeral nature and patchy distribution of hydrothermal vent environments, an analysis of the developmental mode of 30 species of mollusks (gastropods and bivalves) present at three deep-sea hydrothermal vents (13°N, 21°N and Galapagos Rift; Lutz *et al.*, 1980, 1984, 1986; Turner and Lutz, 1984; Turner *et al.*, 1985; Lutz, 1988) suggested that only three species (two turrids and a mytilid) have larvae capable of long-range dispersal. The other 27 species have larval shell morphologies indicative of non-planktotrophic, low-dispersal modes of development. These developmental patterns are all typical of the shallow-water members of the systematic group to which these vent species belong. Although some unusual adaptations may be present among larvae of vent organisms, such as prolonged delay of metamorphosis in response to low deep-sea temperatures (Lutz *et al.*, 1980, 1984, 1986; Turner and Lutz, 1984; Turner *et al.*, 1985; Lutz, 1988), inferences made from egg size, fecundity, and larval morphology suggest that unique adaptations to ensure successful larval dispersal between vent habitats have not evolved in hydrothermal vent mollusks (Turner *et al.*, 1985; Warén and Bouchet, 1989). However, many of the molluscan morpho-species described from vents in the eastern Pacific are present at more than one vent field (9 are shared by Galapagos Rift and 13°N; 10 are shared by Galapagos Rift and 21°N; 18 are shared by 13°N and 21°N; 2 are shared by Juan de Fuca and Explorer Ridges; and 7 are shared by Galapagos Rift, 13°N and 21°N) (Boss and Turner, 1980; Kenk and Wilson, 1985; Schein-Fatton, 1985; McLean and Haszprunar, 1987; McLean, 1988, 1989a, b; Warén and Bouchet, 1986, 1989). This paradox may be partially explained by recent findings of vent fauna on or near whale carcasses (Smith *et al.*, 1989; but see Tunnicliffe and Juniper, 1990) and at cold methane and sulfide seeps (Paull *et al.*, 1984; Kennicutt *et al.*, 1985, 1989; Juniper and Sibuet, 1987; Mayer *et al.*, 1988), which may serve as stepping-stone habitats for dispersal between vents. In addition, Johannesson (1988), and to a lesser degree others (Palmer and Strathmann, 1981; Burton, 1983; Highsmith, 1985; Hedgecock, 1986; Jackson, 1986; R. R. Strathmann, 1987; Safriel and Hadfield, 1988; O'Foighil, 1989), question the effective dispersal benefits of the planktotrophic *versus* the non-planktotrophic mode of development, over long distances. It is suggested that a small founder group of direct developers or hermaphroditic individuals, passively transported to a new site as adults or in a drifted egg mass, would have an advantage over planktonic developers in establishing a new colony, because their offspring would remain in the

immediate vicinity of the founder group where the encounter rate with mates would be high. On the other hand, the offspring of planktonic developers are free-swimming for weeks and may settle far from the founder group, and from each other, where the encounter rate with mates is low (Johannesson, 1988).

Similar, if not identical, species of *Phymorhynchus* occur at the Galapagos Rift and at 13°N and 21°N on the East Pacific Rise (Warén and Bouchet, 1989). The planktotrophic-type larvae found in turrid egg capsules from the Galapagos Rift, putatively identified as the spawn of *Phymorhynchus* sp., suggests that this species has a great potential for disperal and may explain its apparent wide distribution (but see discussion above). Shimek (1983a, b, 1986) has cultured three shallow-water turrids, *Ophiodermella inermis* (Hinds), *Oenopota levidensis* (Carpenter), and *Oenopota elegans* (Möller), with encapsulated periods of 50 days, 50 days, and 42–49 days, respectively, and free-swimming periods of 35 days, 7–10 days, and 42–49 days, respectively. In addition, *Oenopota levidensis* assumes a benthic existence and develops for a further 25 days prior to metamorphosis as a "demersal-planktotrophic larva," using the terminology of Shimek (1986). If parallel conditions obtain in deep-sea turrids the potential for dispersal of larvae during a 1–7 week planktonic phase, given known bottom currents on the East Pacific Rise (Lonsdale, 1977), would be on the order of hundreds of kilometers (Lutz *et al.*, 1980). A maximum current speed of 18 cm s^{-1} was recorded at a site 50 m above the crest of the East Pacific Rise within 350 m of a suspected hydrothermal plume (Lonsdale, 1977). In addition, a decrease in developmental rate in response to cold ambient bottom waters away from the vents may increase the length of larval life and further enhance disperal (Lutz *et al.*, 1980, 1984, 1986; Turner and Lutz, 1984; Turner *et al.*, 1985; Lutz, 1988). Based on comparison of the stable isotope compositions (^{18}O:^{16}O ratios) of adult and larval shells, Killingley and Rex (1985) reported that three deep-sea turrids with similar protoconch sculpture to that seen in *Phymorhynchus* (*Theta lyronuclea, T. chariessa* and *Pleurotomella sandersoni*), migrate vertically, as larvae, to develop in warm surface waters. At present, it is indeterminable whether *Phymorhynchus* larvae complete their development as demersal feeders, ascend to feed on plankton in surface waters, or undergo some combination of these developmental modes. The fact that *Phymorhynchus* is either a predator or scavenger at the vents (Warén and Bouchet, 1989) indicates that it may not be restricted to vent habitats, although it is able to tolerate the extreme vent environment and exploit the abundant food energy available at these sites. Adult *Phymorhynchus* are mobile and the extent to which movements of adults aid in dispersal is unknown.

Although it has not been possible to unambiguously identify the species to which the inflated triangular egg capsules from the Galapagos Rift or the pouch-like egg capsules from the Juan de Fuca Ridge belong, we can infer something about the mode of development of these two organisms. The presence of several hundred veliger larvae in inflated triangular capsules from the Galapagos Rift and the intricate sculpture on the early protoconch both suggest that this species may develop planktotrophically. On the other hand, the small number of larvae (1–6) in capsules from the Juan de Fuca Ridge and the protoconch's large size, inferred value of D/Vol, and unsculptured appearance all suggest that this species has a non-planktotrophic mode of development.

How relatively sedentary organisms at deep-sea hydrothermal vents locate and colonize these geographically isolated environments remains an open question. With the exception of a few preliminary population genetic studies (J. P. Grassle, 1985; Bucklin, 1988), our knowledge of colonization, gene flow and dispersal of organisms between hydrothermal vents has been obtained from inferences drawn from egg capsule type, egg size, fecundity, and larval morphologies retained on adults (Lutz, 1988). Further zoogeographic data and systematic descriptions are needed before we can provide more rigorous answers to questions involving the mechanisms of dispersal and rates of gene flow between isolated areas of deep-sea hydrothermal vent activity. Laboratory culture of these unusual deep-sea molluscan taxa is also necessary to confirm the link between larval shell characteristics and the mode of development. If we assume that the majority of the vent fauna is endemic to the hydrothermal vent habitat [(but see contrasting opinion of Clarke (1986)], and that larval dispersal in non-planktotrophic species is a stepwise process, then each ridge axis should be a discrete dispersal corridor. Given these assumptions, genetic relatedness of the most widely separated non-planktotrophic species' populations along a single ridge axis should be more homogeneous than among populations that are equally separated but belong to two different ridge axes. On the other hand, genetic relatedness of species with planktotrophic development should be more homogenous in the prevailing direction of bottom currents and less reliant on the configuration of ridge systems. The studies of J. P. Grassle (1985) and Bucklin (1988) provide highly paradoxical results. In *Bathymodiolus thermophilus*, a species reported to have a lengthy dispersal stage (Lutz *et al.*, 1980), populations from the Galapagos Rift and 13°N (separated by 2200 km) are genetically distinct. Yet in *Riftia pachyptila*, a non-molluscan species that is believed to have lecithotrophic, demersal larvae with limited dispersal abilities, more widely separated populations from the Galapagos Rift and 21°N along the East Pacific Rise (separated by 3300 km) are genetically similar (Bucklin,

1988). Clearly, an expanded research effort using electrophoretic and molecular techniques to ascertain population structure within species and genetic relatedness among species, coupled with analyses of molluscan larval shell morphology, will be needed to answer questions concerning the rates of gene flow between discrete areas of hydrothermal activity associated with contiguous and noncontiguous oceanic ridge systems, as well as the validity of using larval shell morphology to ascertain dispersal capability in the deep sea.

Acknowledgments

We thank the pilots and crew of "Atlantis II"/"Alvin" for invaluable technical assistance with the retrieval of specimens; Robert Hessler of Scripps Institution of Oceanography for his extraordinary powers of observation which led to retrieval of marker H9 and its attached egg capsules from the Galapagos Rift; John Grazul of the Electron Microscopy Facility, Nelson Biological Laboratories, Rutgers University, for assistance with SEM; Meridith L. Jones of the Smithsonian Institution, for samples from Juan de Fuca Ridge; and Lowell Fritz for critical comments throughout this study and for critically reading early versions of the manuscript. This is Contribution #90-30 of the Institute of Marine and Coastal Sciences, Rutgers University and New Jersey Agricultural Experiment Station Publication No. D-32402-1-90, supported by State funds and by NSF Grants OCE-87-16591 and OCE-89-17311.

Literature Cited

Amio, M. 1955. On the eggs and early life histories of Pyrenidae (Columbellidae) in marine gastropods. *J. Shimonoseki Coll. Fish.* **4:** 231–238.

Amio, M. 1963. A comparative embryology of marine gastropods, with ecological considerations. *J. Shimonoseki Coll. Fish.* **12:** 229–358.

Anderson, D. T. 1960. The life histories of marine prosobranch gastropods. *J. Malacol. Soc. Aust.* **4:** 16–29.

Anderson, D. T. 1962. The reproduction and early life histories of the gastropods *Bembicium auratum* (Quoy and Gaimard) (Fam. Littorinidae), *Cellana tramoserica* (Sower.) (Fam. Patellidae) and *Melanerita melanotragus* (Smith) (Fam. Neritidae). *Proc. Linn. Soc. N. S. W.* **87:** 62–68.

Anderson, D. T. 1965. Further observations on the life histories of littoral gastropods in New South Wales. *Proc. Linn. Soc. N. S. W.* **90:** 242–251.

Arnaud, P. M., and H. Zibrowius. 1973. Capsules ovigères de gastéropodes Turridae et corrosion du squelette des scléractinaires bathyaux des Açores. *Rev. Fac. Ciênc. Univ. Lisb. Sér. C Ciênc. Nat.* **17:** 581–597.

Bacci, G. 1947. Le capsule ovigere di *Columbella rustica* (L.) e di *Fasciolaria lignaria* (L.) (Prosobranchia, Stenoglossa). *Boll. Zool.* **14:** 75–81.

Bandel, K. 1974a. Spawning and development of some Columbellidae from the Caribbean Sea of Colombia (South America). *Veliger* **16:** 271–282.

Bandel, K. 1974b. Studies on Littorinidae from the Atlantic. *Veliger* **17:** 92–114.

Bandel, K. 1975a. Embryonalgehäuse karibischer Meso- und Neogastropoden (Mollusca). *Abhandlungen der Mathematisch-Naturwissenschaftlichen Klasse, Akademie der Wissenshaften und der Literatur, Mainz, Jahrgang 1975, Nr. 1*, 133 pp.

Bandel, K. 1975b. Embryonale und larvale Schale einiger Prosobranchier (Gastropoda, Mollusca) der Oosterschelde (Nordsee). *Hydrobiol. Bull.* **9:** 3–22.

Bandel, K. 1975c. Das Embryonalgehäuse mariner Prosobranchier der Region von Banyuls-sur-Mer. *Vie Milieu Sér. A Biol. Mar.* **25:** 83–118.

Bandel, K. 1976a. Observations on spawn, embryonic development and ecology of some Caribbean lower Mesogastropoda. *Veliger* **18:** 249–270.

Bandel, K. 1976b. Spawning, development and ecology of some higher Neogastropoda from the Caribbean Sea of Colombia (South America). *Veliger* **19:** 176–193.

Bandel, K. 1982. Morphologie und Bildung der frühontogenetischen Gehäuse bei conchiferan Mollusken. *Facies* **7:** 1–198.

Berg, C. J., Jr. 1985. Reproductive strategies of mollusks from abyssal hydrothermal vent communities. In *The Hydrothermal Vents of the Eastern Pacific: An Overview*, M. L. Jones, ed. *Biol. Soc. Wash. Bull.* **6:** 185–197.

Boss, K. J., and R. D. Turner. 1980. The giant white clam from the Galapagos Rift, *Calyptogena magnifica*, species novum. *Malacologia* **20:** 161–194.

Bouchet, P. 1976a. Mise en évidence de stades larvaires planctoniques chez des Gastéropodes Prosobranches des étages bathyal et abyssal. *Bull. Mus. Natl. Hist. Nat. Zool.* **277:** 947–971.

Bouchet, P. 1976b. Mise en évidence d'une migration de larves véligères entre l'étage abyssal et la surface. *C. R. Hebd. Seances Acad. Sci. Sér. D Sci. Nat.* **283:** 821–824.

Bouchet, P. 1981. Evolution of larval development in Eastern Atlantic Terebridae (Gastropoda), Neogene to Recent. *Malacologia* **21:** 363–369.

Bouchet, P. 1989. A review of poecilogony in gastropods. *J. Moll. Stud.* **55:** 67–78.

Bouchet, P., and J-C. Fontes. 1981. Migrations verticales des larves de Gastéropodes abyssaux: arguments nouveaux dûs à l'analyse isotopique de la coquille larvaire et postlarvaire. *C. R. Hebd. Seances Acad. Sci. Sér. III* **292:** 1005–1008.

Bouchet, P., and A. Warén. 1979a. The abysal molluscan fauna of the Norwegian Sea and its relation to other faunas. *Sarsia* **64:** 211–243.

Bouchet, P., and A. Warén. 1979b. Planktotrophic larval development in deep-water gastropods. *Sarsia* **64:** 37–40.

Bouchet, P., and A. Warén. 1980. Revision of the north-east Atlantic bathyal and abyssal Turridae (Mollusca, Gastropoda). *J. Moll. Stud. Suppl.* **8:** 1–119.

Bouchet, P., and A. Warén. 1985a. Mollusca Gastropoda: Taxonomical notes on tropical deep water Buccinidae with descriptions of new taxa. *Mem. Mus. Natl. Hist. Nat. Sér. A Zool.* **133:** 457–499.

Bouchet, P., and A. Warén. 1985b. Revision of the north-east Atlantic bathyal and abyssal Neogastropoda, excluding Turridae. *Boll. Malacol. Suppl.* **1:** 121–296.

Bucklin, A. 1988. Allozymic variability of *Riftia pachyptila* populations from the Galapagos Rift and 21°N hydrothermal vents. *Deep-Sea Res.* **35:** 1759–1768.

Burton, R. S. 1983. Protein polymorphisms and genetic differentiation of marine invertebrate populations. *Mar. Biol. Lett.* **4:** 193–206.

Clarke, A. H. 1962. Annotated list and bibliography of the abyssal marine molluscs of the world. *Bull. Natl. Mus. Canada* **181:** 1–114.

Clarke, A. H. 1986. Some alternative views about deep-sea mollusks from the Arctic and from hydrothermal vents. *Malacology Data Net* **1:** 49–57.

Colman, J. G., and P. A. Tyler. 1988. The egg capsules of *Colus jeffreysianus* (Fischer, 1868) (Prosobranchia: Neogastropoda) from the Rockall Trough, North East Atlantic. *Sarsia* **73:** 139–145.

Colman, J. G., P. A. Tyler, and J. D. Gage. 1986. Larval development of deep-sea gastropods (Prosobranchia: Neogastropoda) from the Rockall Trough. *J. Mar. Biol. Assoc. U.K.* **66:** 951–965.

Cowan, I. M. 1964. The egg capsule and young of *Beringius eyerdami* Smith. *Veliger* **7:** 43–44.

Crane, K. 1985. The distribution of geothermal fields along the mid-ocean ridge: an overview. In *The Hydrothermal Vents of the Eastern Pacific: An Overview*, M. L. Jones, ed. *Biol. Soc. Wash. Bull.* **6:** 3–18.

Crisp, D. J. 1978. Genetic consequences of different reproductive strategies in marine invertebrates. Pp. 257–273 in *Marine Organisms: Genetics, Ecology, and Evolution*, B. Battaglia and J. A. Beardmore, eds. Plenum Press, New York.

Dall, W. H. 1890. Scientific results of explorations by the U.S. Fish Commission steamer "Albatross." VII. Preliminary report on the collection of Mollusca and Brachiopoda. *Proc. U.S. Natl. Mus.* **12:** 219–362.

Dall, W. H. 1924. On the value of nuclear characters in the classification of marine gastropods. *J. Wash. Acad. Sci.* **14:** 177–180.

D'Asaro, C. N. 1970a. Egg capsules of prosobranch mollusks from South Florida and the Bahamas and notes on spawning in the laboratory. *Bull. Mar. Sci.* **20:** 414–440.

D'Asaro, C. N. 1970b. Egg capsules of some prosobranchs from the Pacific coast of Panama. *Veliger* **13:** 37–43.

D'Asaro, C. N. 1986. Egg capsules of eleven marine prosobranchs from northwest Florida. *Bull. Mar. Sci.* **39:** 76–91.

D'Asaro, C. N. 1988. Micromorphology of neogastropod egg capsules. *Nautilus* **102:** 134–148.

Eyster, L. S., and M. P. Morse. 1984. Early shell formation during mollusean embryogenesis, with new studies on the surf clam, *Spisula solidissima*. *Am. Zool.* **24:** 871–882.

Franc, A. 1950. Ponte et larves planctoniques de *Philbertia purpurea* (Montagu). *Bull. Lab. Marit. Dinard* **33:** 23–25.

Fretter, V. 1984. Prosobranchs. Pp. 1–45 in *The Mollusca, Vol. 7, Reproduction*, A. S. Tompa, N. H. Verdonk and J. A. M. van den Biggelaar, eds. Academic Press, New York.

Fretter, V., and A. Graham. 1962. *British Prosobranch Molluscs: Their Functional Anatomy and Ecology*. Bartholomew Press, London. 755 pp.

Golikov, A. N. 1961. Ecology of reproduction and the nature of egg capsules in some gastropod molluscs of the genus *Neptunea* (Bolten). *Zool. Zh.* **40:** 997–1008.

Grassle, J. F. 1985. Hydrothermal vent animals: distribution and biology. *Science* **229:** 713–725.

Grassle, J. F. 1986. The ecology of deep-sea hydrothermal vent communities. *Adv. Mar. Biol.* **23:** 301–362.

Grassle, J. P. 1985. Genetic differentiation in populations of hydrothermal vent mussels (*Bathymodiolus thermophilus*) from the Galapagos Rift and 13°N on the East Pacific Rise. In *The Hydrothermal Vents of the Eastern Pacific: An Overview*, M. L. Jones, ed. *Biol. Soc. Wash. Bull.* **6:** 429–442.

Habe, T. 1960. Egg masses and egg capsules of some Japanese marine prosobranchiate gastropod. *Bull. Mar. Biol. Station Asamushi* **10:** 121–126.

Hadfield, M. G., and M. F. Strathmann. 1990. Heterostrophic shells and pelagic development in trochoideans: implications for classification, phylogeny and palaeoecology. *J. Moll. Stud.* **56:** 239–256.

Hansen, T. A. 1982. Modes of larval development in Early Tertiary neogastropods. *Paleobiology* **8:** 367–377.

Hansen, T. A. 1983. Modes of larval development and rates of speciation in Early Tertiary neogastropods. *Science* **220:** 501–502.

Hedgecock, D. 1986. Is gene flow from pelagic larval dispersal important in the adaptation and evolution of marine invertebrates? *Bull. Mar. Sci.* **39:** 550–564.

Heslinga, G. A. 1981. Larval development, settlement and metamorphosis of the tropical gastropod *Trochus niloticus*. *Malacologia* **20:** 349–357.

Highsmith, R. C. 1985. Floating and algal rafting as potential dispersal mechanisms in brooding invertebrates. *Mar. Ecol. Prog. Ser.* **25:** 169–179.

Hines, A. H. 1986. Larval problems and perspectives in life histories of marine invertebrates. *Bull. Mar. Sci.* **39:** 506–525.

Hoagland, K. E., and R. Robertson. 1988. An assessment of poecilogony in marine invertebrates: phenomenon or fantasy? *Biol. Bull.* **174:** 109–125.

Hyman, L. H. 1967. *The Invertebrates, Vol. VI, Mollusca I*. McGraw-Hill, New York. 790 pp.

Jablonski, D. 1985. Molluscan development. Pp. 33–49 in *Mollusks, Notes For a Short Course*, T. W. Broadhead, ed. University of Tennessee Studies in Geology 13, University of Tennessee Press, Knoxville.

Jablonski, D. 1986. Larval ecology and macroevolution in marine invertebrates. *Bull. Mar. Sci.* **39:** 565–587.

Jablonski, D., and R. A. Lutz. 1980. Molluscan larval shell morphology: ecological and paleontological applications. Pp. 323–377 in *Skeletal Growth of Aquatic Organisms*, D. C. Rhoads and R. A. Lutz, eds. Plenum Press, New York.

Jablonski, D., and R. A. Lutz. 1983. Larval ecology of marine benthic invertebrates: paleobiological implications. *Biol. Rev.* **58:** 21–89.

Jackson, J. B. C. 1986. Modes of dispersal of clonal benthic invertebrates: consequences for species' distributions and genetic structure of local populations. *Bull. Mar. Sci.* **39:** 588–606.

Johannesson, K. 1988. The paradox of Rockall: why is a brooding gastropod (*Littorina saxatilis*) more widespread than one having a planktonic dispersal stage (*L. littorea*)? *Mar. Biol.* **99:** 507–513.

Jung, P. 1975. Quaternary larval gastropods from leg 15, site 147, deep sea drilling project. Preliminary report. *Veliger* **18:** 109–126.

Juniper, S. K., and M. Sibuet. 1987. Cold seep benthic communities in Japan subduction zones: spatial organization, trophic strategies and evidence for temporal evolution. *Mar. Ecol. Prog. Ser.* **40:** 115–126.

Kenk, V. C., and B. R. Wilson. 1985. A new mussel (Bivalvia, Mytilidae) from hydrothermal vents in the Galapagos Rift zone. *Malacologia* **26:** 253–271.

Kennicutt, M. C., II, J. M. Brooks, R. R. Bidigare, T. L. Wade, and R. R. Faye. 1985. Vent type taxa in a hydrocarbon seep region on the Louisiana slope. *Nature* **317:** 351–353.

Kennicutt, M. C., II, J. M. Brooks, R. R. Bidigare, S. J. McDonald, and D. L. Adkison. 1989. An upper slope "cold" seep community: northern California. *Limnol. Oceanogr.* **34:** 635–640.

Kesteven, H. L. 1912. The constitution of the gastropod protoconch: its value as a taxonomic feature and the significance of some of its forms. *Proc. Linn. Soc. New South Wales* **37:** 49–82.

Killingley, J. S., and M. A. Rex. 1985. Mode of larval development in some deep-sea gastropods indicated by oxygen-18 values of their carbonate shells. *Deep-Sea Res.* **32:** 809–818.

Kohn, A. J. 1961. Studies on spawning behavior, egg masses, and larval development in the gastropod genus *Conus*. II. Observations in the Indian Ocean during the Yale Seychelles Expedition. *Bull. Bingham Oceanogr. Collect. Yale Univ.* **17:** 3–51.

Lebour, M. V. 1934. The eggs and larvae of some British Turridae. *J. Mar. Biol. Assoc. U.K.* **19:** 541–554.

Lebour, M. V. 1936. Notes on the eggs and larvae of some Plymouth prosobranchs. *J. Mar. Biol. Assoc. U.K.* **20:** 547–564.

Lebour, M. V. 1937. The eggs and larvae of the British prosobranchs with special reference to those living in the plankton. *J. Mar. Biol. Assoc. U.K.* **22:** 105–166.

Lima, G. M., and R. A. Lutz. 1990. The relationship of larval shell morphology to mode of development in marine prosobranch gastropods. *J. Mar. Biol. Assoc. U.K.* **70:** 611–637.

Lonsdale, P. 1977. Clustering of suspension-feeding macrobenthos near abyssal hydrothermal vents at oceanic spreading centers. *Deep-Sea Res.* **24:** 857–863.

Lutz, R. A. 1988. Dispersal of organisms at deep-sea hydrothermal vents. Pp. 23–29 in *Proceedings of the Hydrothermalism, Biology and Ecology Symposium,* Paris, 4–7 November 1985. *Oceanol. Acta* Special Vol. No. 8.

Lutz, R. A., P. Bouchet, D. Jablonski, R. D. Turner, and A. Warén. 1986. Larval ecology of mollusks at deep-sea hydrothermal vents. *Am. Malacol. Bull.* **4:** 49–54.

Lutz, R. A., L. W. Fritz, and D. C. Rhoads. 1985. Molluscan growth at deep-sea hydrothermal vents. In *The Hydrothermal Vents of the Eastern Pacific: An Overview,* M. L. Jones, ed. *Biol. Soc. Wash. Bull.* **6:** 199–210.

Lutz, R. A., D. Jablonski, D. C. Rhoads, and R. D. Turner. 1980. Larval dispersal of a deep-sea hydrothermal vent bivalve from the Galapagos Rift. *Mar. Biol.* **57:** 127–133.

Lutz, R. A., D. Jablonski, and R. D. Turner. 1984. Larval development and dispersal at deep-sea hydrothermal vents. *Science* **226:** 1451–1454.

MacGinitie, G. E. 1955. Distribution and ecology of the marine invertebrates of Point Barrow, Alaska. *Smithson. Misc. Collect.* **128**(9): 1–201.

MacIntosh, R. A. 1979. Egg capsule and young of the gastropod *Beringius beringii* (Middendorff) (Neptuneidae). *Veliger* **21:** 439–441.

MacIntosh, R. A. 1986. Egg capsule and young of the gastropod *Beringius* (*Neoberingius*) *frielei* (Dall) (Neptuneidae). *Veliger* **28:** 426–428.

Marcus, E. B.-R., and E. Marcus. 1962. Studies on Columbellidae. *Bol. Fac. Filos. Cienc. Let. Univ. Sao Paulo Ser. Zool* **24:** 335–402.

Mayer, L. A., A. N. Shor, J. Hughes Clarke, and D. J. W. Piper. 1988. Dense biological communities at 3850 m on the Laurentian Fan and their relationship to the deposits of the 1929 Grand Banks earthquake. *Deep-Sea Res.* **35:** 1235–1246.

McLean, J. H. 1988. New archaeogastropod limpets from hydrothermal vents. Superfamily Lepetodrilacea. Part 1: Systematic descriptions. *Philos. Trans. R. Soc. Lond. B Biol. Sci.* **319:** 1–32.

McLean, J. H. 1989a. New archaeogastropod limpets from hydrothermal vents: New family Peltospiridae, new superfamily Peltospiracea. *Zool. Scr.* **18:** 49–66.

McLean, J. H. 1989b. New slit limpets (Scissurellacea and Fissurellacea) from hydrothermal vents. Part 1. Systematic descriptions and comparisons based on shell and radular characters. *Contrib. Sci. (Los Angel.)* **407:** 1–29.

McLean, J. H., and G. Haszprunar. 1987. Pyropeltidae, a new family of cocculiniform limpets from hydrothermal vents. *Veliger* **30:** 196–205.

Ockelmann, K. W. 1965. Developmental types in marine bivalves and their distribution along the Atlantic coast of Europe. Pp. 25–35 in *Proceedings of the First European Malacological Congress, London, 1962,* L. R. Cox and J. F. Peake, eds. Conchological Society of Great Britain and Ireland and the Malacological Society of London, London.

O'Foighil, D. 1989. Planktotrophic larval development is associated with a restricted geographic range in *Lasaea,* a genus of brooding, hermaphroditic bivalves. *Mar. Biol.* **103:** 349–358.

Palmer, A. R., and R. R. Strathmann. 1981. Scale of dispersal in varying environments and its implications for life histories of marine invertebrates. *Oecologia* **48:** 308–318.

Paull, C. K., B. Hecker, R. Commeau, R. P. Freeman-Lynde, C. Neumann, W. P. Corso, S. Golubic, J. E. Hook, E. Sikes, and J. Curray. 1984. Biological communities at the Florida Escarpment resemble hydrothermal vent taxa. *Science* **226:** 965–967.

Pawlik, J. R., J. B. O'Sullivan, and M. G. Harasewych. 1988. The egg capsules, embryos, and larvae of *Cancellaria cooperi* (Gastropoda: Cancellariidae). *Nautilus* **102:** 47–53.

Pechenik, J. A. 1986. The encapsulation of eggs and embryos by molluscs: an overview. *Am. Malacol. Bull.* **4:** 165–172.

Penchaszadeh, P. E. 1982. Reproductive aspects of *Polystira barretti* (Guppy, 1866) (Gastropoda, Turridae) from Golfo Triste, Venezuela. *Veliger* **25:** 160–162.

Perron, F. E. 1981. Larval biology of six species of the genus *Conus* (Gastropoda: Toxoglossa) in Hawaii, USA. *Mar. Biol.* **61:** 215–220.

Perry, L. M., and J. S. Schwengel. 1955. Marine shells of the western coast of Florida. *Bull. Am. Paleontol.* **26:** 1–318.

Petit, G., and J. Risbec. 1929. Sur la ponte de quelques Gastéropodes Prosobranches. *Bull. Soc. Zool. Fr.* **54:** 564–570.

Pilkington, M. C. 1974. The eggs and hatching stages of some New Zealand prosobranch molluscs. *J. R. Soc. N.Z.* **4:** 411–431.

Powell, A. W. B. 1942. The New Zealand recent and fossil Mollusca of the family Turridae. *Bull. Auckl. Inst. Mus.* **No. 2:** 1–188.

Radwin, G. E., and J. L. Chamberlin. 1973. Patterns of larval development in stenoglossan gastropods. *Trans. San Diego Soc. Nat. Hist.* **17:** 107–118.

Rex, M. A., and A. Warén. 1982. Planktotrophic development in deep-sea prosobranch snails from the western North Atlantic. *Deep-Sea Res.* **29:** 171–184.

Richter, G., and G. Thorson. 1975. Pelagische prosobranchier-larven des Golfes von Neapel. *Ophelia* **13:** 109–185.

Robertson, R. 1971. Scanning electron microscopy of planktonic larval marine gastropod shells. *Veliger* **14:** 1–12.

Robertson, R. 1976. Marine prosobranch gastropods: larval studies and systematics. *Thalass. Jugoslav.* **10:** 213–238.

Rodriguez Babio, C., and C. Thiriot-Quiévreux. 1974. Gastéropodes de la Région de Roscoff. Étude particulière de la protoconque. *Cah. Biol. Mar.* **15:** 531–549.

Roller, R. A., and W. B. Stickle. 1988. Intracapsular development of *Thais haemastoma canaliculata* (Gray) (Prosobranchia; Muricidae) under laboratory conditions. *Am. Malacol. Bull.* **6:** 189–197.

Safriel, U. N., and M. G. Hadfield. 1988. Sibling speciation by life-history divergence in *Dendropoma* (Gastropoda; Vermetidae). *Biol. J. Linn. Soc.* **35:** 1–13.

Schein-Fatton, E. 1985. Découverte sur la ride du Pacifique oriental à 13°N d'un Pectinidae (Bivalvia, Pteromorpha) d'affinités paléozoiques. *C. R. Hebd. Seances Acad. Sci. Sér. III* **301:** 491–496.

Scheltema, A. H. 1969. Pelagic larvae of New England gastropods. IV. *Anachis translirata* and *Anachis avara* (Columbellidae, Prosobranchia). *Vie Milieu Sér. A Biol. Mar.* **20:** 94–104.

Scheltema, R. S. 1978. On the relationship between dispersal of pelagic veliger larvae and the evolution of marine prosobranch gastropods. Pp. 303–322 in *Marine Organisms,* B. Battaglia and J. A. Beardmore, eds. Plenum, New York.

Scheltema, R. S. 1981. The significance of larval dispersal to the evolution of benthic marine species. Pp. 130–145 in *Genetics and Reproduction of Marine Organisms,* V. L. Kasyanov and A. I. Poduvkin, eds. Proc. XIV Pacific Sci. Congr. Khabarovsk, Aug. 1979, Section Marine Biology, Issue 2, Acad. Sci. USSR.

Scheltema, R. S., and I. P. Williams. 1983. Long-distance dispersal of planktonic larvae and the biogeography and evolution of some Polynesian and western Pacific mollusks. *Bull. Mar. Sci.* **33:** 545–565.

Shimek, R. L. 1983a. Biology of the Northeastern Pacific Turridae. I. *Ophiodermella. Malacologia* **23:** 281–312.

Shimek, R. L. 1983b. Biology of the Northeastern Pacific Turridae. II. *Oenopota J. Moll. Stud.* **49:** 146–163.

Shimek, R. L. 1983c. Biology of the Northeastern Pacific Turridae. III. The habit and diet of *Kurtziella plumbea* (Hinds, 1843). *Veliger* **26:** 10–17.

Shimek, R. L. 1986. Biology of the Northeastern Pacific Turridae. IV. Demersal development, synchronous settlement and other aspects of the larval biology of *Oenopota levidensis*. *Int. J. Invert. Reprod.* **10:** 313–333.

Shuto, T. 1974. Larval ecology of prosobranch gastropods and its bearing on biogeography and paleontology. *Lethaia* **7:** 239–256.

Smith, C. R., H. Kukert, R. A. Wheatcroft, P. A. Jumars, and J. W. Deming. 1989. Vent fauna on whale remains. *Nature* **341:** 27–28.

Sohl, N. F. 1977. Utility of gastropods in biostratigraphy. Pp. 519–539 in *Concepts and Methods in Biostratigraphy*, E. G. Kauffman and J. E. Hazel, eds. Dowden, Hutchinson & Ross, Stroudsburg, Pennsylvania.

Soliman, G. N. 1987. A scheme for classifying gastropod egg masses with special reference to those from the northwestern Red Sea. *J. Moll. Stud.* **53:** 1–12.

Steele, D. H. 1977. Correlation between egg size and developmental period. *Am. Nat.* **111:** 371–372.

Strathmann, M. F. 1987. Phylum Mollusca, Class Gastropoda, Subclass Prosobranchia. Pp. 220–267 in *Reproduction and Development of Marine Invertebrates of the Northern Pacific Coast*. Univ. of Washington Press, Seattle and London.

Strathmann, R. R. 1977. Egg size, larval development, and juvenile size in benthic marine invertebrates. *Am. Nat.* **111:** 373–376.

Strathmann, R. R. 1978a. The evolution and loss of feeding larval stages of marine invertebrates. *Evolution* **32:** 894–906.

Strathmann, R. R. 1978b. Progressive vacating of adaptive types during the Phanerozoic. *Evolution* **32:** 907–914.

Strathmann, R. R. 1987. Larval feeding. Pp. 465–550 in *Reproduction of Marine Invertebrates, Vol. IX, General Aspects: Seeking Unity in Diversity*. Blackwell, Palo Alto, California and Boxwood Press, Pacific Grove, California.

Thorson, G. 1935. Studies on the egg-capsules and development of arctic marine prosobranchs. *Medd. Grønl.* **100:** 1–71.

Thorson, G. 1940a. Studies on the egg masses and larval development of Gastropoda from the Iranian Gulf. *Dan. Invest. Iran* **2:** 159–238.

Thorson, G. 1940b. Notes on the egg capsules of some North-Atlantic Prosobranchs of the genus *Troschelia, Chrysodomus, Volutopsis, Sipho* and *Trophon*. *Vidensk. Medd. Dan. Naturhist. Foren.* **104:** 251–266.

Thorson, G. 1944. The zoology of east Greenland: Marine Gastropoda Prosobranchiata. *Medd. Grønl.* **121:** 1–181.

Thorson, G. 1946. Reproduction and larval development of Danish marine bottom invertebrates, with special reference to the planktonic larvae in the Sound (Oresund). *Medd. Dan. Fisk. Havunders. Serie Plankton* **4:** 1–523.

Thorson, G. 1950. Reproduction and larval ecology of marine bottom invertebrates. *Biol. Rev.* **25:** 1–45.

Todd, C. D., and R. W. Doyle. 1981. Reproductive strategies of marine benthic invertebrates: a settling-timing hypothesis. *Mar. Ecol. Prog. Ser.* **4:** 75–83.

Tunnicliffe, V. 1988. Biogeography and evolution of hydrothermal-vent fauna in the eastern Pacific Ocean. *Proc. R. Soc. Lond. B* **233:** 347–366.

Tunnicliffe, V., and S. K. Juniper. 1990. Cosmopolitan underwater fauna. *Nature* **344:** 300.

Tunnicliffe, V., and A. R. Fontaine. 1987. Faunal composition and organic surface encrustations at hydrothermal vents on the southern Juan de Fuca Ridge. *J. Geophys. Res.* **92**(B11): 11,303–11,314.

Tunnicliffe, V., S. K. Juniper, and M. E. de Burgh. 1985. The hydrothermal vent community on Axial Seamount, Juan de Fuca Ridge. In *The Hydrothermal Vents of the Eastern Pacific: An Overview*, M. L. Jones, ed. *Biol. Soc. Wash. Bull.* **6:** 199–210.

Turner, R. D., and R. A. Lutz. 1984. Growth and distribution of molusks at deep-sea vents and seeps. *Oceanus* **27:** 55–62.

Turner, R. D., R. A. Lutz, and D. Jablonski. 1985. Modes of molluscan larval development at deep-sea hydrothermal vents. In *The Hydrothermal Vents of the Eastern Pacific: An Overview*, M. L. Jones, ed. *Biol. Soc. Wash. Bull.* **6:** 167–184.

Underwood, A. J. 1974. On models for reproductive strategy in marine benthic invertebrates. *Am. Nat.* **108:** 874–878.

Vance, R. R. 1973. On reproductive strategies in marine benthic invertebrates. *Am. Nat.* **107:** 339–352.

Vance, R. R. 1974. Reply to Underwood. *Am. Nat.* **108:** 879–880.

Vaught, K. C. 1989. *A Classification of the Living Mollusca*. Melbourne, Florida, American Malacologists. 189 pp.

Vestergaard, K. 1935. Über den Laich und die Larven von *Scalaria communis* (Lam.), *Nassarius pygmaeus* (Lam.) und *Bela turricola* (Mont.). *Zool. Anz.* **109:** 217–222.

Warén, A., and P. Bouchet. 1986. Four new species of *Provanna* Dall (Prosobranchia, Cerithiacea?) from East Pacific hydrothermal sites. *Zool. Scr.* **15:** 157–164.

Warén, A., and P. Bouchet. 1989. New gastropods from East Pacific hydrothermal vents. *Zool. Scr.* **18:** 67–102.

Webber, H. H. 1977. Gastropoda: Prosobranchia. Pp. 1–97 in *Reproduction of Marine Invertebrates, Vol. 4, Molluscs: Gastropods and Cephalopods*, A. C. Giese and J. S. Pearse, eds. Academic Press, New York.

Reference: *Biol Bull* **180**: 56–64. (February, 1991)

Expansion of the Sperm Nucleus and Association of the Maternal and Paternal Genomes in Fertilized *Mulinia lateralis* Eggs

FRANK J. LONGO[1] AND JOHN SCARPA[2]

[1]*Department of Anatomy, The University of Iowa, Iowa City, Iowa 52242 and* [2]*Rutgers Shellfish Research Laboratory, Port Norris, New Jersey 08349*

Abstract. Sperm nuclear expansion, meiotic maturation of the maternal chromatin, and events involving the association of the male and female pronuclei leading to the two-cell stage were observed in *Mulinia* zygotes using the fluorochromes DAPI and Hoechst. The effects of ultraviolet irradiation on the fertilizing sperm were also examined. Incorporated sperm nuclei underwent changes in diameter that were temporally correlated with meiotic processes of the maternal chromatin. Following its entry, the sperm nucleus underwent a rapid, initial enlargement, which was correlated with germinal vesicle breakdown. Sperm nuclear expansion ceased during the period in which the egg was engaged in polar body formation and was re-initiated with formation and enlargement of the female pronucleus. The rates of enlargement of the male and female pronuclei were 0.59 and 0.65 μm/min, respectively. Following their migration into apposition with one another, the male and female pronuclei synchronously underwent events characteristic of prophase as separate structures; *i.e.*, chromosome condensation, and nuclear envelope breakdown. The two groups of chromosomes that formed became organized on the metaphase plate in preparation of the first cleavage division; hence, there was no fusion of pronuclei. Ultraviolet irradiation of fertilizing sperm had no apparent affect on sperm nuclear transformations leading to the development of a male pronucleus or on female pronuclear development. However, events subsequent to the apposition of the pronuclei were affected and included asynchrony of prophase and the nondisjunction of chromosomes at anaphase. These observations are discussed in relationship to events regulating transformations of the sperm nucleus and experiments to generate gynogenetic bivalve embryos.

Received 17 September 1990; accepted 29 November 1990.

Introduction

For the eggs of most animals insemination occurs at an arrested stage of meiosis; *i.e.*, meiotic prophase (the germinal vesicle stage), metaphase I, or metaphase II (Longo, 1987a). Representatives of these three stages include the eggs of annelids, mollusks, and chordates, respectively. In comparison, the eggs of relatively few organisms are fertilized following the completion of meiotic maturation (the pronuclear stage). The most notable example of the latter group are eggs of echinoids. Although processes of fertilization are fundamentally the same in eggs inseminated at different stages of meiotic maturation, there are prominent differences, particularly during the transformation of the sperm nucleus into a male pronucleus and pronuclear association (Wilson, 1925; Longo, 1985).

In eggs inseminated at the completion of meiotic maturation, the female pronucleus is already present and "waiting" for the entry and transformation of the sperm nucleus into a pronucleus. In contrast, in eggs inseminated at an arrested stage of meiotic maturation, the sperm nucleus, following its entry into the egg cytoplasm, must "wait" for the maternal chromatin to complete its meiotic maturation. Observations carried out with the gametes of a variety of organisms (sea urchin, surf clam, mussel, hamster, rabbit, and mouse) have shown that both the kinetics of sperm nuclear enlargement into a male pronucleus and events attending pronuclear association are correlated with the stage of meiosis at which the egg is inseminated and the length of time the sperm nucleus spends in the egg cytoplasm before pronuclear association

(Wilson, 1925; Longo, 1985). For example, in eggs inseminated at the pronuclear stage, the rate of sperm nuclear expansion is uniform, whereas in eggs inseminated at an arrested stage of meiosis, the rate of expansion is much more complex and shows different phases that are correlated with stages of meiotic maturation of the maternal chromatin (Luttmer and Longo, 1987, 1988; Wright and Longo, 1988; Longo, 1989).

In eggs inseminated at an arrested stage of meiosis, pronuclear fusion does not occur as in eggs fertilized at the pronuclear stage. The paternally and maternally derived chromatin do not become associated with one another until prophase of the first cleavage division when chromosomes derived from the male and female pronuclei intermix and become aligned on the metaphase plate of the mitotic spindle (Longo, 1985). Evidence suggests that differences in the kinetics of sperm nuclear expansion and pronuclear association are related to cell cycle events associated with meiotic maturation and mitosis of the first mitotic division (Luttmer and Longo, 1988; Wright and Longo, 1988; Longo, 1989).

Because analyses of sperm nuclear expansion and its relationship to meiotic events of the maternal chromatin have been carried out in relatively few organisms (see Longo, 1989), and to further explore possible relationships between these processes of fertilization and cell cycle phenomena, we have initiated studies with a variety of organisms, the eggs of which are inseminated at an arrested stage of meiosis. Here we describe the course of meiotic maturation of the maternal chromatin, corresponding events of sperm nuclear enlargement, and association of the male and female pronuclei in *Mulinia lateralis* (dwarf surf clam or coot clam) eggs, which are inseminated at meiotic prophase. The effects of ultraviolet irradiation on sperm nuclear transformations and events involving and subsequent to male and female pronuclear association are also presented.

Material and Methods

Sexually mature individuals of *Mulinia lateralis*, collected from Massey's Landing, Delaware, were kept at 15°C in a recirculating seawater system. Spawning was induced by placing individual animals into 100 ml beakers containing seawater at 30°C. Eggs from 1 to 3 spawned females were pooled, washed in fresh seawater, inseminated and permitted to develop at 20°C. Unfertilized eggs and samples of fertilized ova, taken at 5 min intervals up to 1 to 1.5 h after the addition of sperm, were fixed in 1% formalin in seawater. In some experiments, eggs and sperm were incubated with 10 μM Hoechst 33342 (Hoechst) in seawater, washed in fresh seawater, and used for insemination (Luttmer and Longo, 1986).

To examine the effects of ultraviolet irradiation on sperm nuclear transformations leading to pronuclear development, sperm were irradiated with ultraviolet light as previously described (Nace *et al.*, 1970; Chourrout and Quillet, 1982; Scarpa and Bolton, 1988). Sperm suspended in a plastic Petri dish were exposed for 20 min, at a distance of 20 cm, to a 15-watt tube generating ultraviolet light ranging from 200 nm to 295 nm, with 60% of the ultraviolet light concentrated at 254 nm. Irradiated sperm were mixed with a suspension of eggs; samples were taken and fixed as described above for non-irradiated specimens.

Fixed specimens were washed in seawater and stained with one of the following DNA intercalating fluorochromes: 1 μg/mL 4′,6-diamidino-2-phenylindole (DAPI) in seawater, or 10 μM Hoechst in seawater. Stained specimens were washed once in seawater, placed into a droplet of glycerol on a glass slide, and covered with a glass coverslip. To improve microscopic observation, some specimens were compressed. Specimens were observed with a Nikon Diaphot microscope equipped with epifluorescence. Photographs were taken of specimens using 40× or 100× objectives and Kodak T-Max film.

Because *Mulinia* sperm nuclei are spheroid, and their transformations leading to male pronuclei produced a symmetrical distribution of chromatin (*i.e.*, spheroid), changes in the size of incorporated sperm nuclei were measured throughout the period of fertilization. To measure incorporated sperm nuclei at different periods after insemination, as well as the developing spheroid female pronucleus, stained specimens were placed into droplets of glycerol as described above. A coverslip, bearing a thin layer of Vaseline along its edges, was lowered over the droplets such that the eggs or zygotes were suspended between the slide and coverslip. Images of the cross-sectional diameters of transforming sperm nuclei and male and female pronuclei were projected onto the screen of a video monitor, checked for linearity, and traced onto plastic sheets with a felt tip pen. The traced images were analyzed with a Micro-plan II Image Analysis System (Laboratory Computer Systems, Cambridge, Massachusetts). Diameters and maximum cross-sectional areas of transforming sperm nuclei and male and female pronuclei were measured (mean ± standard deviation) at 5-min intervals following insemination and temporally correlated with the progression of meiotic maturation, female pronuclear development, and first mitosis. Twenty to forty specimens were measured at each time point.

Results

Structure of the unfertilized egg and spermatozoon

Unfertilized *Mulinia* eggs measured 46.4 ± 0.4 μm in diameter. When viewed with phase or Nomarski optics they were seen to possess a large, meiotic prophase nucleus (29.7 ± 1.4 μm in diameter), the germinal vesicle, which usually contained a single, spheroid nucleolus (10.4 ± 0.8

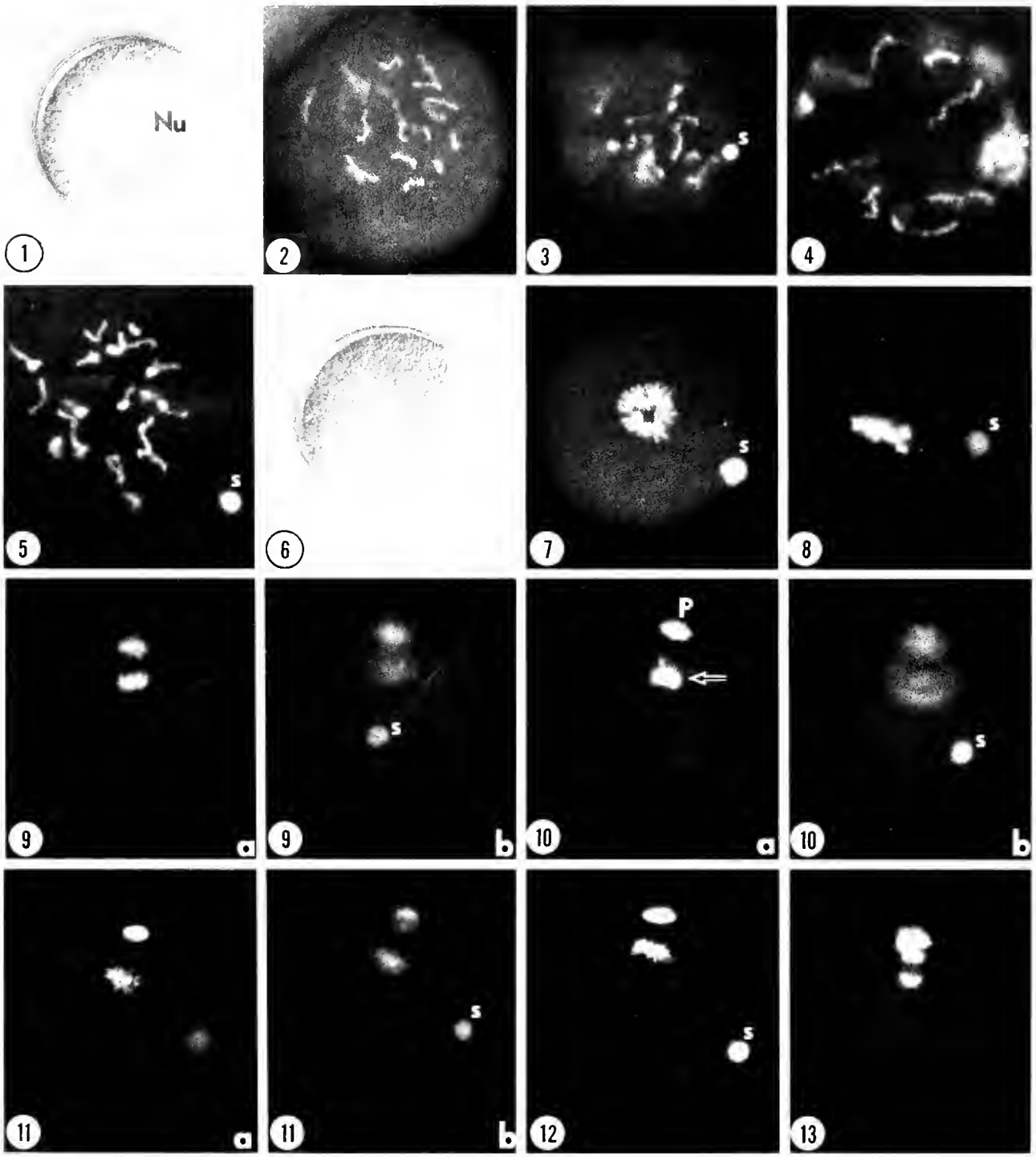

Figures 1 and 2. Nomarski (Fig. 1) and fluorescent (Fig. 2) preparations of unfertilized *Mulinia* eggs showing germinal vesicles, nucleoli (Nu) and meiotic chromosomes. Figure 1, · 760; Figure 2, · 960.

Figures 3 and 4. Fertilized *Mulinia* eggs depicting incorporated sperm nuclei (S) and meiotic chromosomes which are distributed throughout the germinal vesicle (5 min pf). Figure 3, · 960; Figure 4, · 1500.

Figure 5. Zygote (10 min pf) in which the meiotic chromosomes are condensing and the sperm nucleus (S) is dispersing. · 1800.

Figures 6–8. Zygotes (15 min pf) in which the meiotic chromosomes have become condensed and organized on the same optical plane (Fig. 7). The chromosomes move as a group to the cortex in preparation for polar body formation (Fig. 8). Figure 6 is a Nomarski preparation in which the meiotic chromosomes and incorporated sperm nucleus are difficult to discern; these structures are intensely stained in Hoechst- or DAPI-prepared specimens. Figure 6, · 760; Figures 7 and 8, · 960.

μm in diameter) suspended in a nucleoplasm (Fig. 1). Occasionally, specimens containing two large nucleoli were observed. Unfertilized eggs prepared with DAPI (fixed eggs) or Hoechst (fixed or unfixed eggs) observed with epi-fluorescence were essentially identical. Two features were apparent with both methods: (1) a low background staining of the cytoplasm, and (2) a relatively intense staining of the maternal tetrad chromosomes. Tetrads were distributed throughout the interior of the germinal vesicle such that chromosome number and individual chromosomal features (*e.g.*, chiasma) could be ascertained (Fig. 2). Examination of whole mounts and compressed specimens revealed that the number of meiotic chromosomes in *Mulinia* eggs; *i.e.*, the haploid number, was 19 (see also Menzel, 1968; Scarpa and Bolton, 1988; Wada *et al.*, 1990).

The structure of *Mulinia* sperm as examined by light microscopy was similar to that of other pelecypods (Franzen, 1955). The sperm nucleus was spheroidal, 1.7 ± 0.15 μm in diameter, and contained a uniform distribution of DNA as determined in fluorochrome stained preparations.

As was found for the surf clam, *Spisula* (Luttmer and Longo, 1986), living *Mulinia* sperm or eggs treated with Hoechst 33342 could inseminate and develop with no apparent ill-effects. In living *Mulinia* zygotes in which only one of the gametes was treated with Hoechst dye prior to insemination, staining of both the maternal and paternal genomes was found consistently after fertilization, indicating that the dye was not remaining confined to the nucleus of one gamete. Unlike the situation in *Spisula* (Luttmer and Longo, 1986), we were unable to achieve exclusive staining of only one genome in *Mulinia* zygotes. The following account is based on experiments employing fixed and unfixed, stained specimens.

Meiotic maturation of the maternal chromatin leading to development of the female pronucleus

The interaction of the sperm with the egg initiated the resumption of meiotic maturation and development of the female pronucleus in *Mulinia*. Resumption of meiotic maturation was heralded by the breakdown of the nuclear envelope of the germinal vesicle and the disappearance of the nucleolus (Figs. 3–6). These characteristic features of germinal vesicle breakdown were readily apparent with Nomarski and phase contrast optics (Fig. 6), but changes in the structure and location of the tetrads were much more difficult to ascertain. Meiotic events of the maternal chromosomes and transformations of the sperm nucleus were readily apparent with fluorochrome stained *Mulinia* preparations and epi-fluorescence microscopy (Figs. 3, 4, 5, 7). Concomitant with germinal vesicle breakdown was the condensation of the tetrads (Figs. 5, 7). The tetrads formed a cluster within the center of the egg; eventually they were organized on the metaphase plate of the first meiotic spindle (Figs. 7, 8). The spindle and tetrads then moved to one pole of the egg where completion of meiosis and polar body formation occurred (Fig. 9). In almost all cases examined, more than 90% of the specimens were in synchrony and had developed to metaphase I by 15 min postinsemination (pi).

Anaphase I followed localization of the meiotic spindle to the egg cortex and was seen as the separation of two fluorescent masses of chromosomes (Figs. 9, 10). With the completion of anaphase I, the chromosomes emitted within the first polar body formed a compact mass; those within the egg became reorganized on a metaphase plate in preparation for second polar body formation (Figs. 11, 12).

Anaphase II quickly followed formation of the first polar body (Fig. 13) and appeared as the separation of two fluorescent masses that were of less intensity than the chromosomal masses that formed at anaphase I, reflecting the decrease in DNA. After anaphase II, chromosomes within the second polar body formed a densely stained cluster (Fig. 14). The first and the second polar bodies became positioned side by side and remained at the pole of the egg where the meiotic divisions took place.

By 35 min pi, more than 95% of the specimens examined had completed polar body formation and were engaged in the formation of a female pronucleus (Figs. 14–16). The maternal chromosomes remaining in the egg dispersed, forming an irregularly shaped nucleus that eventually expanded to become a spheroidal female pronucleus. Measurements of the female pronucleus at different times following its formation (35 to 45 min pi) indicated that its rate of expansion was 0.65 μm/min (Fig. 23). Its average maximal size, measured at 45 min pi,

Figures 9a, b. Zygote (25 min pi) at two optical planes depicting anaphase I (Fig. 9a) and the incorporated sperm chromatin (S). Note that the latter has ceased dispersion and is smaller than the sperm nucleus depicted in Figure 7. ×960.

Figures 10a,b and 11a, b. Zygotes (30 min pi) at two optical planes in which the first polar body (P) has formed and the chromosomes remaining in the zygote are preparing for the second meiotic division (Figs. 10a, 11a). Figures 10b and 11b are at the level of the incorporated sperm nucleus which has ceased its enlargement. ×960.

Figures 12 and 13. Zygotes (35 min pi) at metaphase II (Fig. 12) and anaphase II (Fig. 13). S, sperm nucleus. ×820.

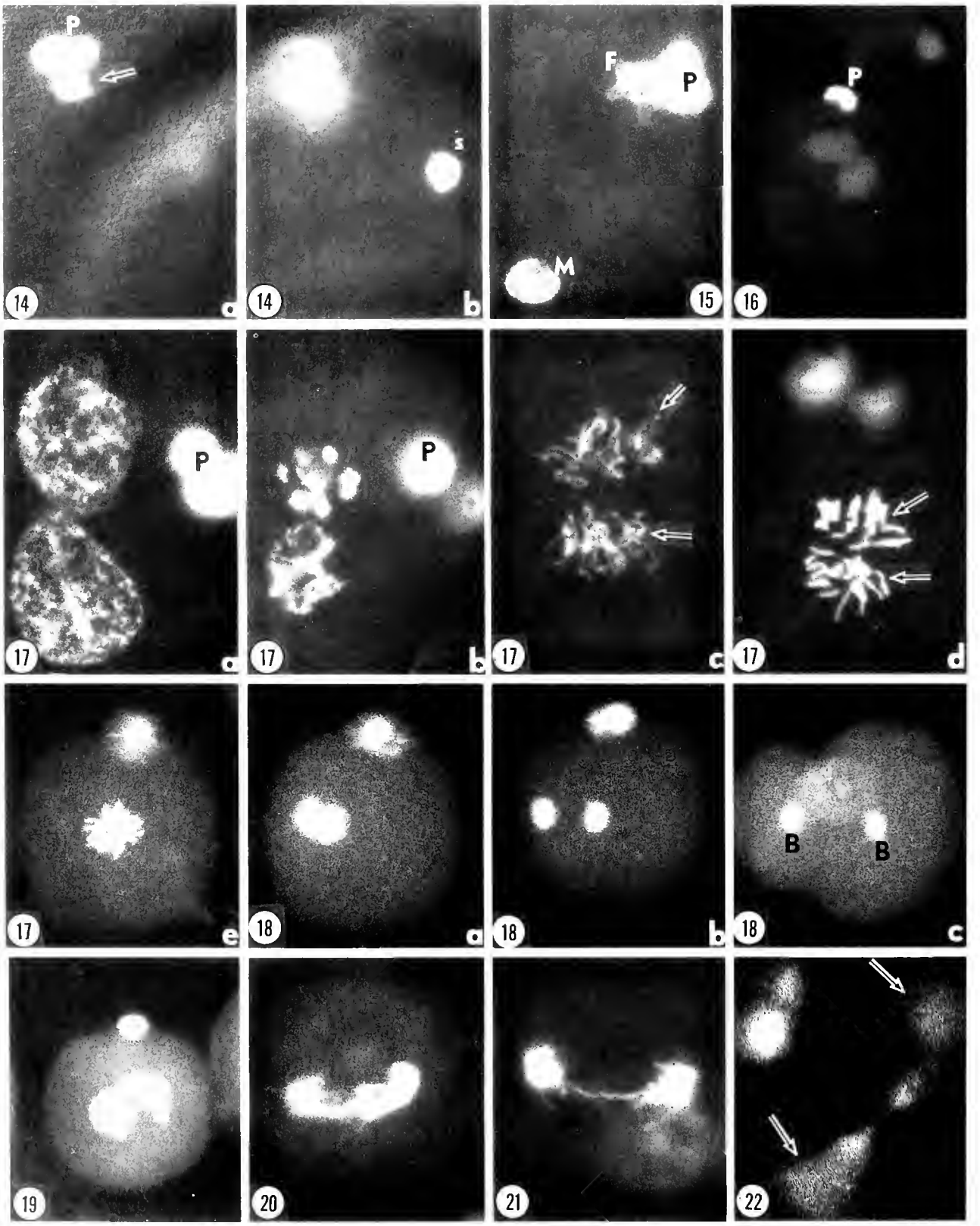

Figures 14a, b. Zygote (35 min pi) at two optical planes depicting the maternal chromosomes (arrow) that have just completed their second meiotic division and are dispersing to form the female pronucleus (Fig. 14a). Figure 14b shows the sperm nucleus (S), which is enlarging. P, first and second polar bodies. ×1500

Figure 15. Zygote (40 min pi) at a slightly later stage of pronuclear development than the egg depicted in Figure 14 in which the male (M) and female (F) pronuclei are expanding. P, first and second polar bodies. ×1900

was 9.8 ± 1.4 μm. By 50 min pi the female pronucleus had decreased in diameter (9.4 ± 1.1 μm) and was engaged in prophase of the first mitotic (cleavage) division (Figs. 17, 23).

Transformations of incorporated sperm nuclei leading to the development of male pronuclei

Upon its incorporation into the egg cytoplasm, the sperm nucleus underwent an expansion from 1.7 ± 0.15 to 3.7 ± 0.28 μm in diameter (Figs. 3–5, 7, 23). This initial expansion occurred symmetrically while the maternal tetrads were condensing and becoming aligned on the metaphase plate of the first meiotic spindle (Figs. 5, 7). From 20 to 35 min pi, coincident with the period in which the maternal chromosomes were engaged in polar body formation, the incorporated sperm nucleus did not expand and, in fact, decreased slightly in size to 3.5 ± 0.28 μm in diameter (Figs. 9–12, 23). With the completion of meiosis and the development of the female pronucleus there was a dramatic enlargement in the sperm nucleus (rate = 0.59 μm/min; Figs. 14–16, 23). At the completion of its expansion (45 min pi), the male pronucleus measured 9.7 ± 1.4 μm in diameter. Subsequent changes in the male pronucleus included its reduction in size (9.6 ± 0.8 μm) as a part of prophase of the first cleavage division.

Morphogenesis of the male and female pronuclei leading to the first cleavage division

By 45 min pi, both the male and female pronuclei had reached their maximal sizes (Fig. 23) and individually and synchronously undergone prophase events leading to the first cleavage division (Fig. 17). By 50 min pi condensing chromosomes appeared in the two pronuclei. As the chromosomes condensed, the nuclear envelopes broke down, forming two distinct groups of chromosomes in the midregion of the zygote, one derived from the female pronucleus and the other from the male (Fig. 17). The two groups of chromosomes moved together, intermixed, and became positioned on the metaphase plate of the first mitotic spindle (Fig. 17). Subsequent morphogenesis of the maternally and paternally derived chromosomes involved their participation in the first cleavage division, which was asymmetric with respect to cytokinesis (Fig. 18). That is, the metaphase plate was displaced from the center of the zygote and, as a consequence, two unequally sized blastomeres formed upon cleavage.

Effects of ultraviolet irradiation on male pronuclear development and morphogenesis

Effects of ultraviolet irradiation were not apparent during transformation of the sperm nucleus into a male pronucleus, nor was there any apparent effect on meiotic maturation and development of the female pronucleus. Irradiated sperm nuclei expanded into pronuclei of a size comparable to those of control preparations. Effects of ultraviolet irradiation on sperm nuclei were not observed until the male pronucleus was engaged in prophase events of the first cleavage division. In eggs inseminated with ultraviolet irradiated sperm, mitotic prophase events in the two pronuclei were asynchronous (Fig. 19). The maternally and paternally derived chromosomes eventually became aligned on a metaphase plate, but anaphase of mitosis was abnormal as evidenced by chromosomal nondisjunction (Figs. 20, 21). The number of chromosomes that failed to move to the spindle poles was not constant. Consequently, material of varying fluorescent intensity was seen between the spindle poles at telophase, and between interconnecting blastomere nuclei at subsequent stages of development (Fig. 22).

Discussion

The results presented here demonstrate nuclear changes that occur in fertilized *Mulinia* eggs and lead to the two-

Figure 16. Expanded male and female pronuclei that have become associated with one another in the center of a zygote (45 min pi). P, polar bodies. ×820.

Figures 17a–e. Morphogensis of the male and female pronuclei following their apposition. Initiation of prophase in each pronucleus is evident by chromosome condensation (Fig. 17a, b). Two groups of chromosomes are produced (arrows, Fig. 17c, d) which become closely associated and positioned on the metaphase plate of the first mitotic spindle (Fig. 17e). P, polar bodies. Figure 17a, c, and d, ×2000; Figure 17b, ×1830; Figure 17e, ×870.

Figures 18a–c. First cleavage division of *Mulinia* leading to unequal size blastomers (Fig. 18c). Figures 18a and b depict early and late anaphase. P, polar bodies; B, developing blastomere nuclei. ×870.

Figure 19. Asynchronous pronuclear morphogenesis in an egg fertilized with an ultraviolet irradiated sperm. ×750.

Figure 20. Nondisjunction of mitotic chromosomes in an egg inseminated with an ultraviolet irradiated sperm. ×1400.

Figure 21. Cleaving egg which was inseminated with an ultraviolet irradiated sperm. Chromatin is spread between the two developing blastomere nuclei. ×1400.

Figure 22. Cleaved zygote that was fertilized by an ultraviolet irradiated sperm. DAPI staining material (*i.e.*, DNA) connects the two blastomere nuclei (arrows). ×1700.

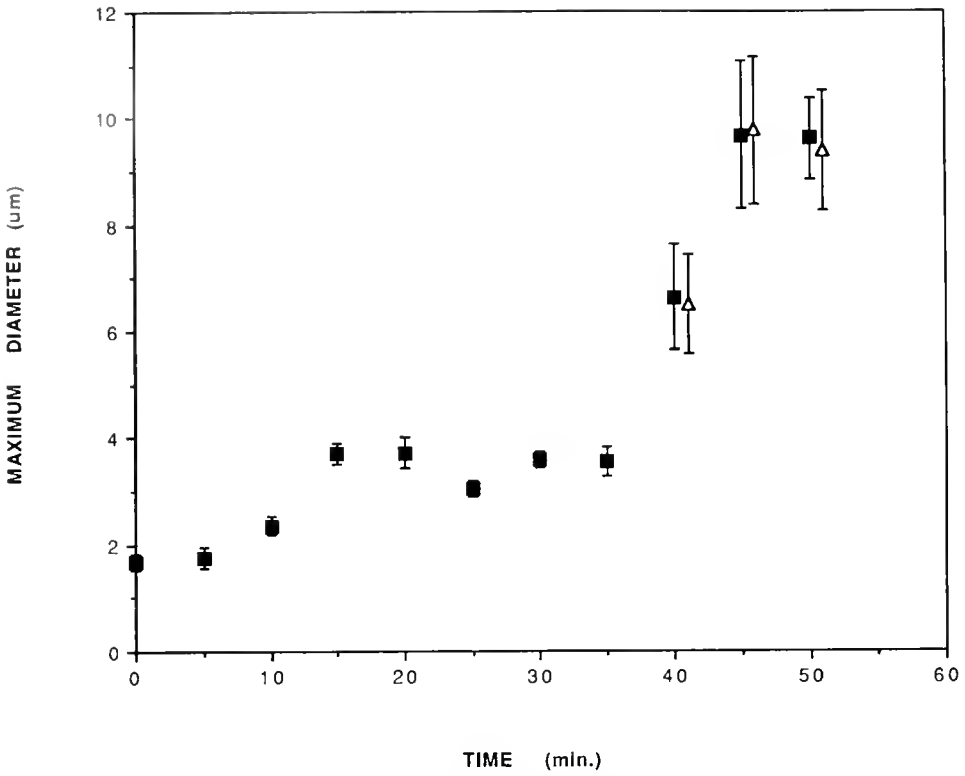

Figure 23. Expansion (mean ± S.D.) of incorporated sperm nuclei (■) and female pronuclei (△) of *Mulinia* zygotes. The sperm nucleus shows three periods of transformation: 0 to 15, 15 to 35, and 35 to 45 min pi corresponding to periods encompassing germinal vesicle breakdown, polar body formation, and female pronuclear development, respectively. The decrease in size of the male and female pronuclei from 45 to 50 min pi is correlated with the onset of mitotic prophase in both pronuclei.

cell stage. Meiosis of the maternal chromatin, transformations of the sperm nucleus, and pronuclear development and association are readily amenable to analysis in specimens prepared with the DNA intercalating dyes DAPI and Hoechst. This suitability is due to a combination of factors, such as low background of the egg cytoplasm, and chromosome size, number and structure (Wada *et al.*, 1990).

Meiotic maturation of the maternal chromatin of *Mulinia* eggs is similar to that previously described for other mollusks (Longo, 1983; Luttmer and Longo, 1988). Interaction of the sperm with the egg induces germinal vesicle breakdown. The chromosomes become organized on the metaphase plate of the first meiotic spindle apparatus which then moves to, and becomes positioned within, the egg's cortex. The mechanism by which this movement takes place has not been established, although investigations demonstrating that cytochalasin B inhibits the cortical localization of the meiotic spindle suggests that it may be an actin-mediated process (Longo, 1987b).

Anaphase I and II, as well as the formation of the first and second polar bodies, followed in quick succession, as occurs in the surf clam *Spisula* (see Longo, 1983). Formation of the female pronucleus was evident subsequent to the formation of the second polar body by the formation of an expanding mass of material staining with either DAPI or Hoechst. The rate of expansion of the forming female pronucleus was comparable to that of the male pronucleus, suggesting that the two chromatin masses may be regulated by similar mechanisms. A corresponding relationship has also been demonstrated in polygynic and polyspermic *Spisula* zygotes (Luttmer and Longo, 1988).

The kinetics of sperm nuclear expansion in fertilized *Mulinia* eggs is in agreement with previous studies demonstrating that sperm nuclear transformations share a temporal relationship with changes of the maternal chromatin (Das and Barker, 1976; Da-Yuan and Longo, 1983; Yamashita, 1985; Luttmer and Longo, 1987, 1988; Wright and Longo, 1988; Longo, 1989). Measurements of sperm nuclear expansion in *Mulinia* zygotes indicates that this process takes place in three distinct phases temporally correlated with meiotic maturation of the maternal chromatin. In previous studies, as well as in the one reported here, the incorporated sperm nucleus undergoes a period of rapid expansion followed by one of no enlargement or condensation. This is succeeded by a

dramatic expansion of the sperm nucleus leading to a male pronucleus similar in size to that of the female. The three phases of sperm nuclear enlargement in *Mulinia* correlate with germinal vesicle breakdown, polar body formation, and female pronuclear development, respectively. The kinetics of sperm nuclear expansion is similar to that described in the surf clam, *Spisula solidisima*, where four phases were observed based on closer sampling times than those taken during the course of the present study (Luttmer and Longo, 1988). In *Spisula*, the sperm nucleus, upon incorporation, underwent little change in size until germinal vesicle breakdown. Additionally, during the period of polar body formation, the expanded sperm nucleus of *Spisula* underwent a significant reduction in size; *i.e.*, it condensed. A reduction (one time point) in size of the expanded sperm nucleus of *Mulinia* zygotes was observed during polar body formation. We suspect that with closer sampling times, this reduction, as well as the status of the incorporated sperm nucleus prior to germinal vesicle breakdown, would become apparent in *Mulinia* zygotes.

Expansion of the sperm nucleus following germinal vesicle breakdown is consistent with other studies demonstrating that mixing of germinal vesicle substances with the cytoplasm precedes sperm nuclear changes (Masui and Clarke, 1979; Longo, 1981; Schuetz and Longo, 1981; Hirai *et al.*, 1981; Yamada and Hirai, 1984). This change in the sperm nucleus may be a manifestation of sperm basic protein replacement by histones present in the oocyte cytoplasm. Histone changes that occur with the early onset of sperm chromatin dispersion have been demonstrated (Poccia *et al.*, 1978, 1981; see Poccia, 1986). Because agents affecting meiotic maturation of the maternal chromatin also affect the kinetics of sperm nuclear expansion (Luttmer and Longo, 1988; Wright and Longo, 1988), factors regulating the status of the maternal chromatin during polar body formation probably act on the transformed sperm nucleus such that it ceases expansion and in some instances condenses; *e.g.*, surf clam, hamster, and starfish (Luttmer and Longo, 1988; Wright and Longo, 1988; Longo, 1989).

The second expansion of the sperm nucleus, which is correlated with enlargement of the maternal chromatin and female pronuclear formation (Zirkin *et al.*, 1989), is set into motion as a result of cell cycle changes within the fertilized egg that affect both the maternally and paternally derived chromation (Longo, 1989). In the case of *Mulinia*, as well as other species that have been studied to date, both chromatin masses undergo dramatic rates of expansion to form enlarged pronuclei (Luttmer and Longo, 1988; Wright and Longo, 1988). Unlike the situation seen in mammalian zygotes (Wright and Longo, 1988), expansion of the maternally and paternally derived chromatin resulted in pronuclei of nearly equal size (see also Luttmer and Longo, 1989).

Results presented here demonstrate that pronuclear fusion in *Mulinia* does not occur as in sea urchins (fertilized at the completion of meiotic maturation) or as in other cellular systems (Longo and Anderson, 1968). Rather, both the male and female pronuclei, as separate bodies, synchronously undergo prophase events in preparation for first mitosis. The chromosomes from each pronucleus, which replicated during the period following polar body formation, become aligned on the metaphase plate of the mitotic spindle and separate at anaphase into two masses consisting of both maternally and paternally derived chromosomes. Hence, maternal and paternally derived chromosomes do not become enclosed within the same nucleus until formation of the two-cell stage.

The effects of ultraviolet irradiation on sperm transformations that lead to the development of male pronuclei in *Mulinia* are consistent with what has been shown in other systems (Onozato and Yamaha, 1983; Arai *et al.*, 1984). Ultraviolet irradiation disrupts the DNA helix and thus interferes with the proper duplication of chromosomes prior to first cleavage (Strickberger, 1976). We anticipated that the effects of ultraviolet irradiation might be manifested at two periods during fertilization: (1) during transformation of the sperm nucleus into a male pronucleus, indicative of gross DNA disruption; and (2) subsequent to DNA replication, during the period in which the paternally derived chromosomes were engaged in mitosis. Alterations were not apparent during any of the stages leading to a male pronucleus, possibly due to an insensitivity of the method of analysis, or more likely to an inability to achieve concomitant high levels of irradiation and fertilization. (Higher doses of ultraviolet irradiation were tested but resulted in an inhibition of fertilization.) Radiation effects were seen only after pronuclear association—*i.e.*, during prophase and anaphase of the first cleavage division—and involved variable numbers of chromosomes. The manner in which the male and female pronuclei become associated in *Mulinia* and other molluscan eggs (see Longo, 1983), as well as parameters affecting both the quantity and quality of ultraviolet irradiation, call into question the effectiveness of using ultraviolet irradiation to form gynogenetic molluscan embryos. Induction of gynogenesis with variable results has been achieved by a variety of techniques, including irradiation of sperm with ultraviolet light (Chourrout, 1980; Streisinger *et al.*, 1981; Onozato and Yamaha, 1983; Lou and Purdom, 1984; Onozato, 1984; Suzuki *et al.*, 1985). Variability in cases employing ultraviolet irradiation (Chourrout, 1980; Onozato and Yamaha, 1983; Arai *et al.*, 1984) appeared to be due to difficulties in controlling parameters associated with the exposure of sperm to ultraviolet rays

and an inability to uniformly and effectively destroy all of the paternally derived DNA.

Acknowledgments

The assistance of Tena Perry and Lori Mathews is greatfully appreciated. Portions of the study presented here were supported by funds from the NIH. Support for John Scarpa was provided by the New Jersey Agricultural Experiment Station grant to Standish K. Allen, Jr.

Literature Cited

Arai, K., F. Naito, H. Sasaki, and K. Fujino. 1984. Gynogenesis with ultraviolet ray irradiated sperm in the Pacific abalone. *Bull. Jpn Soc. Sci. Fish.* **50:** 2019–2023.

Das, N. K., and C. Barker. 1976. Mitotic chromosome condensation in the sperm nucleus during postfertilization maturation division in *Urechis* eggs. *J. Cell Biol.* **68:** 155–159.

Da-Yuan, C., and F. J. Longo. 1983. Sperm nuclear dispersion coordinate with meiotic maturation in fertilized *Spisula solidissima* eggs. *Dev. Biol.* **99:** 217–244.

Chourrout, D. 1980. Thermal induction of diploid gynogenesis and triploidy in the eggs of the rainbow trout (*Salmo gairdneri*). *Reprod. Nutr. Dev.* **20:** 727–733.

Chourrout, D., and E. Quillet. 1982. Induced gynogenesis in the rainbow trout: sex and survival of progenies production of all-triploid populations. *Theor. Appl. Genet.* **63:** 201–205.

Franzen, A. 1955. Comparative morphological investigations into the spermiogenesis among Mollusca. *Zool. Bidrag.* **30:** 399–456.

Hirai, S., Y. Nagahama, and H. Kanatani. 1981. Cytoplasmic maturity revealed by the structural changes in incorporated spermatozoan during the course of starfish oocyte maturation. *Dev. Growth Differ.* **23:** 465–478.

Longo, F. J. 1981. Regulation of pronuclear development. Pp. 529–557 in *Bioregulators of Reproduction*, G. Jagiello and C. Vogel, eds. Academic Press, New York.

Longo, F. J. 1983. Meiotic maturation and fertilization. Pp. 49–89 in *The Mollusca*, Vol. 3, N. H. Verdonk and J. A. M. van den Biggelaar, eds. Academic Press, New York.

Longo, F. J. 1985. Pronuclear events. Pp. 251–298 in *Biology of Fertilization*, Vol. 3, C. B. Metz and A. Monroy, eds. Academic Press, NY.

Longo, F. J. 1987a. *Fertilization.* Chapman and Hall, New York.

Longo, F. J. 1987b. Egg cortical architecture. Pp. 108–138 in *The Cell Biology of Fertilization*, G. Schatten and H. Schatten, eds. Academic Press, Inc.

Longo, F. J. 1989. Dynamics of sperm nuclear transformations at fertilization. Pp. 297–307 in *Fertilization in Mammals*, B. D. Bavister, J. Cummins and E. R. S. Roldan, eds. Serono Symposia, Norwell, MA.

Longo, F. J., and E. Anderson. 1968. The fine structure of pronuclear development and fusion in the sea urchin *Arbacia punctulata*. *J. Cell Biol.* **39:** 335–368.

Lou, Y. D., and C. E. Purdom. 1984. Diploid gynogenesis induced by hydrostatic pressure in the rainbow trout, *Salmo gairdneri*. *J. Fish Biol.* **24:** 665–670.

Luttmer, S. J. and F. J. Longo. 1986. Examination of living and fixed gametes and early embryos stained with supervital fluorochromes (Hoechst 33342 and 3,3′-dihexyloxacarboxyanine iodide). *Gamete Res.* **15:** 267–283.

Luttmer, S. J., and F. J. Longo. 1987. Rates of male pronuclear enlargement in sea urchin zygotes. *J. Exp. Zool.* **243:** 289–298.

Luttmer, S. J., and F. J. Longo. 1988. Sperm nuclear transformations consist of enlargement and condensation coordinate with stages of meiotic maturation in fertilized *Spisula solidissima* oocytes. *Dev. Biol.* **128:** 86–96.

Masui, Y., and H. Clarke. 1979. Oocyte maturation. *Int. Rev. Cytol.* **57:** 185–282.

Menzel, R. W. 1968. Chromosome number in nine families of marine pelecypod mollusks. Nautilus **82:** 45–58.

Nace, G. W., C. M. Richards, and J. H. Asher Jr. 1970. Parthenogenesis and genetic variability. I. Linkage and inbreeding estimations in the frog, *Rana pipiens*. *Genetics* **66:** 349–368.

Onozato, H. 1984. Diploidization of gynogenetically activated salmonid eggs using hydrostatic pressure. *Aquaculture* **43:** 91–97.

Onozato, H., and E. Yamaha. 1983. Induction of gynogenesis with ultraviolet rays in four species of salmoniformes. *Bull. Jpn. Soc. Sci. Fish.* **49:** 693–699.

Poccia, D. 1986. Remodeling of nucleoproteins during gametogenesis, fertilization and early development. *Int. Rev. Cytol.* **105:** 1–65.

Poccia, D., G. Krystal, D. Nishioka, and J. Salik. 1978. Controls of sperm chromatin structure by egg cytoplasm in the sea urchin. *ICN-UCLA Symp. Mol. Cell. Biol.* **12:** 197–206.

Poccia, D., J. Salik, and G. Krystal. 1981. Transitions in histone variants of the male pronucleus following fertilization and evidence for a maternal stage of cleavage-stage histones in sea urchin eggs. Dev. Biol. **82:** 287–296.

Scarpa, J., and E. T. Bolton. 1988. Experimental production of gynogenetic and parthenogenetic *Mulinia lateralis* (Say). *J. Shellfish Res.* **7:** 132.

Schuetz, A., and F. J. Longo. 1981. Hormone-cytoplasmic interaction controlling sperm nuclear decondensation and male pronuclear development in starfish oocytes. *J. Exp. Zool.* **215:** 107–111.

Streisinger, G., C. Walker, N. Dower, C. Dnauber, and F. Singer. 1981. Production of clones of homozygous diploid zebra fish *Brachydanio rerio*. *Nature* **291:** 293–296.

Strickberger, M. W. 1976. *Genetics.* Macmillan Pub. Co., New York.

Suzuki, R., T. Oshiro, and T. Nakanishi. 1985. Survival, growth and fertility of gynogenetic diploids induced in the cyprinid loach, *Misgurnus anguillicaudatus*. *Aquaculture* **48:** 45–55.

Wada, K. T., J. Scarpa, and S. K. Allen Jr. 1990. Karyotype of the dwarf surf clam *Mulinia lateralis* (Mactridne, Bivalvia). *J. Shellfish Res.* **9:** in press.

Wilson, E. B. 1925. *The Cell in Development and Heredity.* McMillian, New York.

Wright, S. J., and F. J. Longo. 1988. Sperm nuclear enlargement in fertilized hamster eggs is related to meiotic maturation of the maternal chromatin. *J. Exp. Zool.* **247:** 155–165.

Yamada, H., and S. Hirai. 1984. Role of contents of the germinal vesicle in male pronuclear development and cleavage of starfish oocytes. *Dev. Growth Differ.* **26:** 479–487.

Yamashita, M. 1985. Electron microscopic analysis of the sperm nuclear changes in meiosis inhibited eggs of the brittle star, *Amphipholis kochii*. *J. Exp. Zool.* **235:** 105–117.

Zirkin, B., S. D. Perrault, and S. J. Naish. 1989. Formation and function of the male pronucleus during mammalian fertilization. Pp. 91–114 in *The Molecular Biology of Fertilization*, H. Schatten and G. Schatten, eds. Academic Press, New York.

Reference: *Biol Bull* **180**: 65–71. (February, 1991)

Putative Molt-Inhibiting Hormone in Larvae of the Shore Crab *Carcinus maenas* L.: An Immunocytochemical Approach

S. G. WEBSTER[1] AND H. DIRCKSEN*

*School of Biological Sciences, University College of North Wales, Bangor, Gwynedd LL57 2UW, UK, and *Institut für Zoophysiologie, Universität Bonn, Endenicher Allee 11-13, D-5300 Bonn 1, Germany.*

Abstract. Immunocytochemical investigations of the eyestalk of *Carcinus maenas* zoeal larval stages, using an antiserum directed against putative *Carcinus* molt-inhibiting hormone (MIH), revealed immunopositive neuronal structures. These structures included perikarya associated with the medulla terminalis X-organ, parts of the sinus gland tract, and the neurohemal organ—the sinus gland. Apart from an increase in volume of the sinus gland between zoeal stage I and II, no striking changes in the topography or morphology of the MIH neurosecretory system were observed. Immunopositive structures were found in similar locations to those seen in adult crabs. Our results suggest that the control of molting by MIH in crustacean larvae may be similar to the currently accepted model of molt control in adult decapod crustaceans.

Introduction

A current model of molt control in decapod crustaceans involves regulation of ecdysteroid synthesis by a molt-inhibiting hormone (MIH), released by neurosecretory neurons in the eyestalk. Much evidence has now accumulated suggesting that increased synthesis and titers of circulating ecdysteroids necessary for induction of premolt are directly repressed by this neuropeptide, thus inhibiting proecdysis and molting. Nevertheless, alternative hypotheses have implicated processes such as metabolism and excretion of ecdysteroids in molt regulation (see Skinner, 1985; Webster and Keller, 1988; Watson *et al.*, 1989 for recent reviews). Despite recent advances in our knowledge concerning mechanisms of molt control in adult decapod crustaceans, little is known about the regulation of molting in larval crustaceans. This deficiency has been reiterated in a recent review by Christiansen (1988).

Evidence for molt regulation by MIH in crustacean larvae has, until recently, been obtained by eyestalk ablation experiments (for references see Charmantier *et al.*, 1988; Christiansen 1988), which have given equivocal results, suggesting that in some instances, the larval molt is not regulated by MIH until shortly before metamorphosis. However, with regard to morphological correlates of neurosecretory structures in larval eyestalks, several reports (Orlamünder, 1942; Pyle, 1943; Hubschman, 1953; Dahl, 1957; Matsumoto, 1958; Little, 1969; Zielhorst and Van Herp, 1976; Bellon-Humbert *et al.*, 1978; Gorgels-Kallen and Meij, 1985) detail the ontogeny of larval neurosecretory systems in a wide variety of crustaceans. With the exception of studies by Gorgels-Kallen and Meij (1985), Beltz and Kravitz (1987), and Beltz *et al.*, (1990), there are no other studies in which neurosecretory systems containing immunocytochemically defined neuropeptides have been described in crustacean larvae.

Recently, we have characterized a neuropeptide from the sinus gland of *Carcinus maenas*, which, by virtue of its ability to repress ecdysteroidogenesis by Y-organs cultured *in vitro*, could be described as a *putative* MIH (Webster, 1986; Webster and Keller, 1986). It should be stressed that the precise significance and function of this neuropeptide as a molt-inhibitor *in vivo* has not yet been elucidated, and until suitable *in vivo* bioassays are developed, the status of MIH must remain "putative." Re-

Received 23 May 1990; accepted 6 November 1990.

[1] To whom correspondence should be sent.

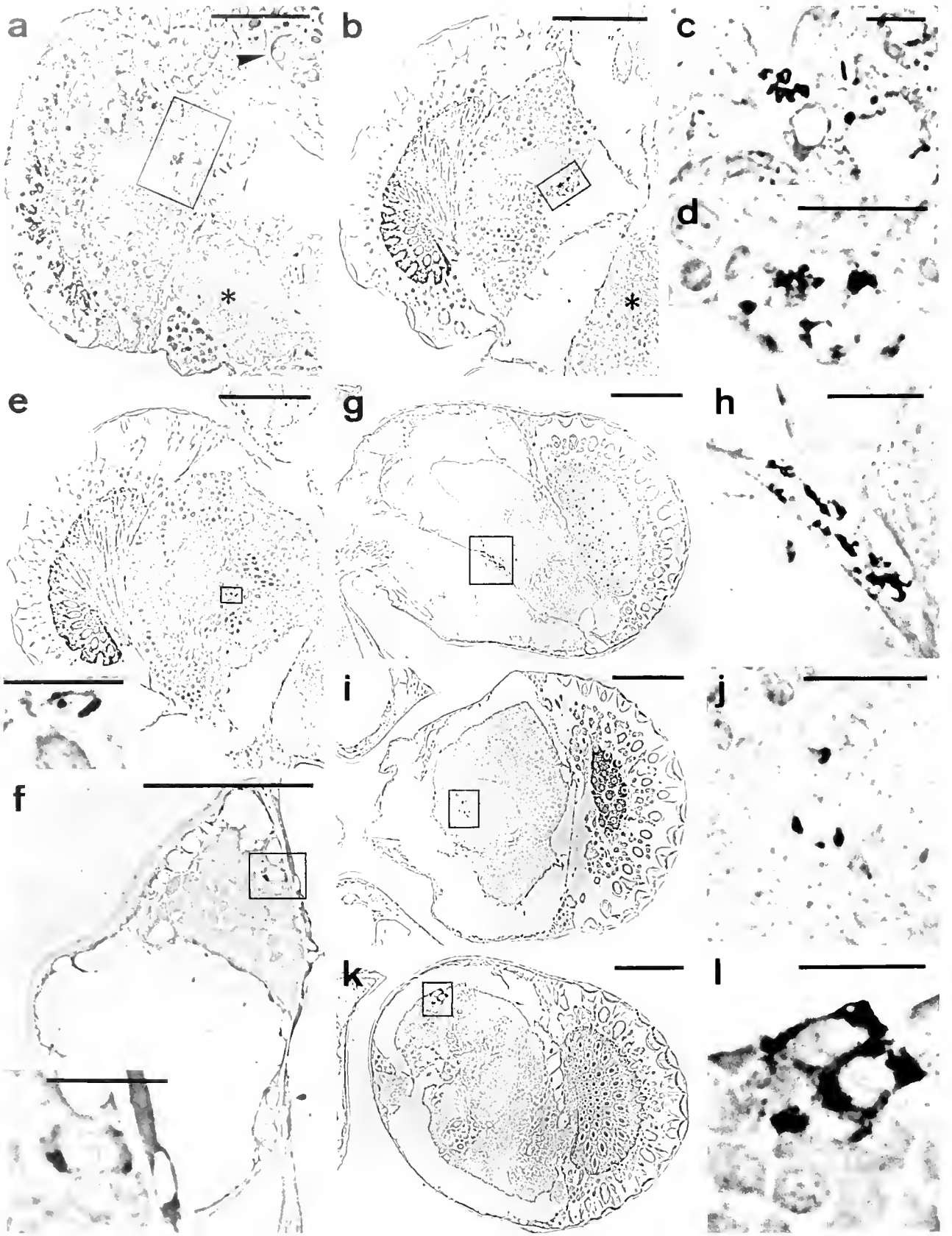

Figure 1. Characteristic structures of MIH-immunoreactive (IR) neurons in prezoeal (a, c), stage I zoea (b, d–f, left eye), and stage II zoea (g–l) eyes of *Carcinus maenas* larvae. Phase contrast micrographs of immunostained semithin (1 μm) transverse sections. (Orientation of dorsal parts of larvae to the tops of micrographs.)

cently, we demonstrated that the neurosecretory system produced putative MIH in the eyestalk ganglia of several adult brachyuran crustaceans (Dircksen *et al.*, 1988). Because these studies provide compelling evidence to suggest that MIH is a secretable neuropeptide, and in view of our earlier observations on the nature and mode of action of this neuropeptide on ecdysteroid synthesis in *Carcinus* (Webster and Keller, 1986; Lachaise *et al.*, 1989), it seemed opportune to examine the larval eyestalk neurosecretory system immunocytochemically, using antibodies raised against *Carcinus* MIH. Evidence presented here suggests that a functional MIH-like neurosecretory system exists in all larval stages of *Carcinus*.

Materials and Methods

Laboratory rearing of larvae

Ovigerous *Carcinus maenas* L. females were collected from the Menai Strait, North Wales, between May and July, and maintained in the laboratory until larvae were released. Only positively phototropic, rapidly swimming larvae were collected. Rearing techniques were initially based upon those of Rice and Ingle (1975), but were found to be inadequate. Successful rearing to first crab with a high survival was achieved using a mixed diet of (A) phytoplankton (*Tetraselmis chuii*), (B) rotifers (*Brachionus plicatilis*), (C) barnacle nauplii (*Elminius modestus*), and (D) brine shrimp nauplii (*Artemia salina*). During each larval stage, prey ratios were supplied as follows: Zoea I (A):1, (B):1, (C):1. Zoea II (A):1, (B):1, (C):1, (D):1. Zoea III (C):1, (D):1. Zoea IV, Megalopa and First crab (D):1. With the exception of phytoplankton (culture density *ca.* 10^6 cells ml^{-1}: 1 part = 15 ml), the total prey concentration was around 25–50 items per ml. Larvae were reared in 50-ml plastic containers in constantly aerated, filtered seawater (33‰) under ambient temperature (15–18°C) and photoperiod (L 15–18 h: D 9–6 h). Maximum density of larvae was 1 per 5 ml. Water and food were changed every two days, at which time instars were staged according to Rice and Ingle (1975). Under these maintenance conditions, survival was good (80%), and instar durations were approximately: Z I: 7, Z II: 5, Z III: 6, Z IV: 7, M: 8, days. Samples of larvae were taken at the middle of each instar, which was considered to be during intermoult.

Tissue processing and immunocytochemistry

Fixations were carried out in a mixture of 2% paraformaldehyde, 2% glutaraldehyde, and 0.1% saturated picric acid in 0.1 *M* sodium cacodylate buffer, pH 7.4, supplemented with 0.5 *M* sucrose and 5 m*M* $CaCl_2$ for 2–4 h at 4°C according to Dircksen *et al.* (1987). Tissues were washed extensively in the same buffer, dehydrated, and embedded in low viscosity resin (Spurr, 1969). Semithin frontal cross-sections (1 μm) through the whole animal were cut on a LKB Ultrotome III or a Reichert Ultracut E, and processed for immunocytochemistry using a rabbit antiserum (code R1TB) directed against HPLC-purified MIH of *Carcinus* (Dircksen *et al.*, 1988), diluted 1:4000 in 0.01 *M* phosphate buffered saline (PBS) and PAP staining techniques (Dircksen *et al.*, 1987). Micrographs were taken with a Zeiss Axioskop using phase contrast optics and documented on Agfapan 25 film.

Results

Despite several attempts to improve the penetration of fixative into the eyestalks (for example, by piercing the exoskeleton behind the eyestalks, using other fixatives or fixation times), adequate fixation of megalopae and first crab stages was impossible. Thus, by necessity, this study is restricted to the zoeal stages of *Carcinus*, and in later zoeal stages problems with fixation and tissue shrinkage were encountered. A sometimes confusing feature of the zoeal eyestalk was the presence of a pigmented perineural sheath (Fig. 2c, 2f), which could have been identified as an immunopositive structure. This problem was resolved by using normal bright field optics, under which immunopositive material appears brownish, or by higher mag-

(a) MIH-IR axon profiles within the sinus gland (center of *rectangle*) of a prezoea. Note ommatidial primordia, brain (*) and yolk droplets (*arrowhead*). (b) MIH-IR axon profiles within the sinus gland (*rectangle*) of a stage I zoea. Note dense pigmentation at the base of the ommatidia, and well-developed neuropiles of the lamina ganglionaris (LG), medulla externa (ME), and the brain (*). (c, d) Higher magnifications of sinus glands corresponding to *rectangles* in a, b. (e) Cross-sectioned MIH-IR axons (inset enlarged from the *rectangle*). (f) Two MIH-IR perikarya in an anterior dorsal cell group of the left eyestalk ganglia (inset enlarged from the *rectangle*). (g) MIH-IR axon profiles in the sinus gland (*rectangle*) of a stage II zoea adjacent to the ME and large hemolymph spaces. Note stalk formation of the eye at this stage. (i) Cross-sectioned MIH-IR axons in the medulla terminalis. (k) Three clustered MIH-IR perikarya in an anterior dorsal position of the presumptive X-organ cell group. Note well-developed ganglia and neuropiles in the eye. (h, j, l) Higher magnifications of *rectangles* outlined in g, i, k. Note axon profiles and putative terminals abutting on the surface of the sinus gland (h) and dark PAP reaction products restricted to the cytoplasm of the perikarya (l) of MIH-IR neurons.

Scale bars: 50 μm in a, b, e, f, g, i, k. 10 μm in c, d, h, j, l, and insets in e, f.

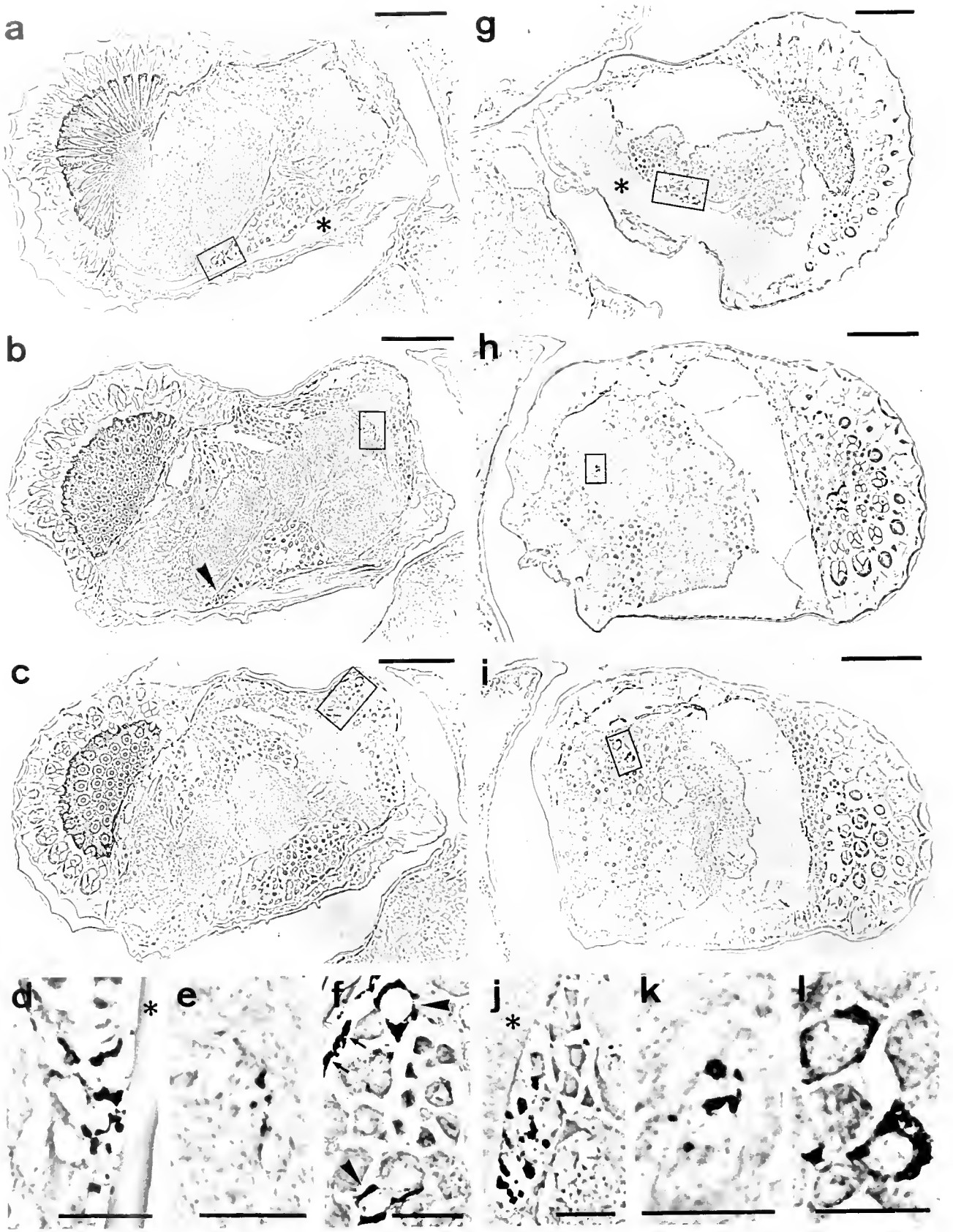

Figure 2. Characteristic structures of MIH-immunoreactive (IR) neurons in stage III zoea (a–f, left eye) and stage IV zoea (g–l, right eye) eyes of *Carcinus maenas* larvae. Phase contrast micrographs of immunostained semithin (1 μm) transverse sections. (Orientation of dorsal parts of the larvae to the tops of the micrographs.)

nification (Fig. 2f) when the black pigment granules could be clearly resolved by phase contrast optics.

MIH immunoreactivity was found in all zoeal stages examined, including the so-called prezoeal stage, which, in view of its brevity (*ca.* 30 min), and association with hatching, could well be described as an embryonic molt. (Fig. 1a, c). In general, MIH immunoreactivity was found in structures similar to those found in the adult, including perikarya in a position similar to the X-organ in adults, an X-organ sinus gland tract, and a sinus gland (Figs. 1, 2). In several preparations the sinus gland appeared to be in close proximity to a large hemolymph vessel (Figs. 1h, 2a, d). By serially sectioning through the entire eyestalk, a maximum of four immunopositive perikarya of about 8–10 μm in diameter were observed in all zoeal stages localized in a cluster of neuroblasts in an anterior dorsal position of the eyestalk, with large nuclei and scarce cytoplasm (Figs. 1f, k, l. 2c, f, i). Axonal projections were found in the medulla terminalis of the well-developed eyestalk ganglia in a typical circular arrangement of four cross-sectioned axons (Figs. 1j, 2e, k), reminiscent of the axonal arrangement in the adult crab. This pattern was found in all zoeal stages. Despite exhaustive investigation, the only discernable change in the morphology of the neurosecretory structures was the size of the sinus gland, which appeared to increase in volume between zoea I and II, when the eye became stalked and mobile. Indeed, it was frequently difficult to observe the sinus gland in zoea I due to its small size, but in zoea II, the sinus gland was often the most striking immunopositive structure (Fig. 1b, d, g, h). In control incubations, preabsorbtion of the antiserum with 2 nmoles of MIH per μl of crude antiserum completely abolished immunostaining, thus proving the specificity of the immunocytochemical detection (results not shown).

Discussion

In the present study, the location of perikarya, axons, and sinus gland terminals immunopositive for MIH have been demonstrated in all zoeal instars of *Carcinus* larvae. Surprisingly, larval immunopositive structures were topographically and morphologically similar to those found in the adult crab. However, very few (maximum 4) MIH-immunoreactive perikarya were observed in any larval stage, compared to the adult crab where there are 32–36 MIH-immunoreactive perikarya (Dircksen *et al.*, 1988). It is likely that the increase in number of immunopositive cells during larval to juvenile/adult development is due to increased MIH gene expression rather than by cell division because neuroblasts are generally considered to be too highly differentiated to undergo further division. A striking similarity of the larval MIH immunopositive structures to those of the adult concerns the morphology of the X-organ sinus gland tract. In the adult, MIH immunoreactive axons form a peripheral tract around the central axon bundle containing crustacean hyperglycemic hormone (CHH) immunopositive axons (Dircksen *et al.*, 1988). Although we did not determine CHH in the present study, the similarity in the arrangement of the four MIH-immunoreactive axons around a central tract was clearly suggestive of the adult morphology.

Several studies have reported the general development of neural systems in the crustacean eyestalk. Cells corresponding to the X-organ have been found in the first larval stages of all species examined (*Birgus*, Orlamünder, 1942; *Homarus, Pinnotheres*, Pyle, 1943; *Crangon*, Dahl, 1957; *Potamon*, Matsumoto, 1958; *Palaemonetes*, Hubschman, 1963; *Palaemon*, Little, 1969, Bellon-Humbert *et al.*, 1978; *Astacus*, Zielhorst and Van Herp, 1976, Gorgels-Kallen and Meij, 1985). With regard to the development of the sinus gland, for freshwater crustaceans, which hatch at an advanced developmental stage, the sinus gland is present in the first larval stage (Matsumoto, 1958; Gorgels-Kallen and Meij, 1985). In marine crustaceans, which hatch at a relatively early stage of development, and which often undergo a lengthy planktonic existence prior to a dramatic metamorphosis, all studies suggest that the sinus gland develops (or can first be observed) late in larval life, at about the time

(a) MIH-IR axon profiles in the sinus gland (*rectangle*) adjacent to the large hemolymph vessel (*) of the eyestalk. (b) Section slightly anterior to (a) showing the sinus gland (*arrowhead*) and cross-sectioned MIH-IR axons (*rectangle*) in the medulla terminalis. (c) Four MIH-IR perikarya (*rectangle*) are found in an anterior dorsal position of the presumptive X-organ cell group. (d, e, f) Higher magnifications of *rectangles* outlined in a, b, c. MIH-IR putative axon terminals adjacent to the hemolymph vessel (*) are found in the sinus gland (d). Note also cross-sectioned MIH-IR axons (e) in the medulla terminalis and strong immunoreactivity of three perikarya (f, *arrowheads*). *Arrows* in (f) point to dark pigments usually found in perineural sheaths of eyestalk ganglia. (g) MIH-IR axon profiles in the sinus gland (*rectangle*) adjacent to the large hemolymph vessel (*) of the eyestalk. (h) Cross-sectioned axons of the presumptive X-organ sinus gland (XO-SG) tract in the medulla terminalis. (i) Two MIH-IR perikarya in the presumptive X-organ cell group in a dorsal anterior position of the proximal eyestalk ganglia. (j, k, l) Higher magnification of *rectangles* outlined in g, h, i. MIH-IR axon profiles and putative axon terminals abutting on the surface of the sinus gland, (*) indicates hemolymph vessel. (j), MIH-IR axons in the XO-SG tract (k) and two strongly immunopositive XO perikarya (l). Note unstained axons in the center of the XO-SG tract (k).

Scale bars: 50 μm in a–c, g–i. 10 μm in d–f, j–l.

of metamorphosis (stage V *Palaemonetes,* Hubschman, 1963, *Palaemon,* Bellon-Humbert *et al.,* 1978; stage III *Homarus,* Pyle 1943). Apart from a report by Jaques (1975) demonstrating the presence of a sinus gland in stage I *Squilla mantis* larvae, this paper reports the first demonstration of a sinus gland in first stage larvae of a marine decapod crustacean, and is undoubtedly due to the great resolving power of immunocytochemical techniques compared to conventional histochemical staining methods. To our knowledge, the only other reports using immunocytochemical techniques to identify larval neurosecretory structures are those by Gorgels-Kallen and Meij (1985), demonstrating the neurosecretory structures containing CHH immunoreactivity in *Astacus leptodactylus* larvae, and Beltz and Kravitz (1987) and Beltz *et al.* (1990), demonstrating proctolin-like immunoreactivity in the CNS of larval *Homarus americanus.*

While immunocytochemical evidence indicates that *Carcinus* zoeae possess a MIH neurosecretory system, which may participate in the control of larval molting, experiments involving eyestalk ablation in several species of crustacean larvae (see specific examples in Charmantier *et al.,* 1988; Christiansen, 1988) have demonstrated that, in general, eyestalk ablation is only effective in accelerating proecdysis and molting when performed during the last instar before metamorphosis. Although the deficiencies of these experiments have been commented upon by Freeman and Costlow (1980), particularly with regard to difficulties in determining the precise duration of instars and the time of initiation of proecdysis in rapidly moulting larvae, it has been suggested (Freeman *et al.,* 1983) that the larval molt cycle is not regulated by MIH until metamorphosis. However, studies demonstrating that larval ecdysteroid titers cycle in a molt-stage-dependent manner in much the same way as adults (Chang and Bruce, 1981; Spindler and Anger, 1986), and a report by Snyder and Chang (1986), demonstrating that increases in proecdysial ecdysteroid titer induced by eyestalk removal of Stage II *Homarus* zoeae can be repressed by the injection of adult sinus gland extracts, strongly support the hypothesis that larval molting (or at least, initiation of proecdysis) is regulated by MIH, and the results presented here would also support this hypothesis. However, it should be stressed that no firm inferences as to the function of the immunoreactive MIH can yet be made; it is not known whether larval MIH-immunoreactive material is identical to that in adults, although the antiserum used displays a very high specificity in immunodot assays (Dircksen *et al.,* 1988), RIA, and ELISA (Webster, unpub.), or whether it is released during the zoeal stages. Although *in vivo* experiments involving injection of MIH or sinus gland extracts into zoeal larvae and subsequent monitoring of proecdysis or instar length would undoubtedly strengthen hypotheses concerning larval molt control, the small size of most crab zoeae argues against the success of such experiments in crab larvae. A further problem, which remains unresolved, concerns the increase in number of immunoreactive perikarya between the last zoeal stage and the adult. It is possible that this transition occurs during metamorphosis (a phenomenon we could not elucidate due to difficulties in achieving adequate fixation of megalopae and first crab stages). If the MIH secretory system became synthetically active at this time, and stored MIH was released, then previous observations regarding the failure to accelerate molting in zoeal larvae, and the appearance of the sinus gland as a structure stainable by conventional histochemical methods prior to metamorphosis, could be reconciled with the model of molt control suggested by Freeman *et al.* (1983).

Acknowledgments

We are grateful to Mr. M. Budd, School of Ocean Sciences, Menai Bridge, UK, for culturing the phytoplankton and rotifers used in this study, and for much useful advice concerning larval rearing techniques. This work was supported by a Royal Society University Research Fellowship (S.G.W.). Financial support from the British Council for travel to Bangor (H.D.) is gratefully acknowledged.

Literature Cited

Bellon-Humbert, C., M. J. P. Thijssen, and F. Van Herp. 1978. Development, location and relocation of sensory and neurosecretory sites in the eyestalks during the larval and postlarval life of *Palaemon serratus* (Pennant). *J. Mar. Biol. Assoc. U.K.* **58:** 851–868.

Beltz, B. S., and E. A. Kravitz. 1987. Physiological identification, morphological analysis and development of identified serotonin-proctolin containing neurons in the lobster ventral nerve cord. *J. Neurosci.* **7:** 533–546.

Beltz, B. S., M. Pontes, S. M. Helluy, and E. A. Kravitz. 1990. Patterns of appearance of serotonin and proctolin immunoreactivities in the developing nervous system of the American lobster. *J. Neurobiol.* **21:** 521–542.

Chang, E. S., and M. J. Bruce. 1981. Ecdysteroid titers of larval lobsters. *Comp. Biochem. Physiol.* **70A:** 239–241.

Charmantier, G., M. Charmantier-Daures, and D. E. Aiken. 1988. Larval development and metamorphosis of the American lobster *Homarus americanus* (Crustacea, Decapoda): effect of eyestalk ablation and juvenile hormone injection. *Gen. Comp. Endocrinol.* **70:** 319–333.

Christiansen, M. E. 1988. Hormonal processes in decapod crustacean larvae. *Symp. Zool. Soc. Lond.* **59:** 46–68.

Dahl, E. 1957. Embryology of X-organs in *Crangon allmanni. Nature* **179:** 482.

Dircksen, H., C. A. Zahnow, G. Gaus, R. Keller, K. R. Rao, and J. P. Riehm. 1987. The ultrastructure of nerve endings containing pigment dispersing hormone (PDH) in crustacean sinus glands: identification by an antiserum against synthetic PDH. *Cell Tiss. Res.* **250:** 377–387.

Dircksen, H., S. G. Webster, and R. Keller. 1988. Immunocytochemical demonstration of the neurosecretory systems containing putative

molt-inhibiting hormone and hyperglycemic hormone in the eyestalk of brachyuran crustaceans. *Cell Tiss. Res.* **251:** 3–12.

Freeman, J. A., and J. D. Costlow. 1980. The molt cycle and its hormonal control in *Rhithropanopeus harrisi* larvae. *Dev. Biol.* **74:** 479–485.

Freeman, J. A., T. L. West, and J. D. Costlow. 1983. Postlarval growth in juvenile *Rhithropanopeus harrisii*. *Biol. Bull.* **165:** 409–415.

Gorgels-Kallen, J. L., and J. T. A. Meij. 1985. Immunocytochemical study of the hyperglycemic hormone (CHH)-producing system in the eyestalk of the crayfish *Astacus leptodactylus* during larval and postlarval development. *J. Morphol.* **185:** 155–163.

Hubschman, J. H. 1963. Development and function of neurosecretory sites in the eyestalks of larval *Palaemonetes* (Decapoda, Natantia). *Biol. Bull.* **125:** 96–113.

Jaques, F. 1975. Découverte de la glande du sinus chez la larve de *Squilla mantis* (stade I) (Crustacé, Stomatopodes). Ultrastructure. *C. R. Acad. Sci. (D) (Paris)* **280:** 1575–1577.

Lachaise, F., M. Hubert, S. G. Webster, and R. Lafont. 1988. Effect of molt-inhibiting hormone on ketodiol conversion by crab Y-organs. *J. Insect Physiol.* **34:** 557–562.

Little, G. 1969. The larval development of the shrimp, *Palaemon macrodactylus* Rathbun, reared in the laboratory, and the effect of eyestalk extirpation on development. *Crustaceana* **17:** 69–87.

Matsumoto, K. 1958. Morphological studies on the neurosecretion in crabs. *Biol. J. Okayama Univ. (Japan)* **4:** 103–176.

Orlamünder, J. 1942. Zur Entwicklung und Formbildung des *Birgus latro* L. mit besonderer Berücksichtigung des X-Organs. *Z. Wiss. Zool.* **155:** 280–316.

Pyle, R. W. 1943. The histogenesis and cyclic phenomena of the sinus gland and X-organ in Crustacea. *Biol. Bull.* **85:** 87–102.

Rice, A. L., and R. W. Ingle. 1975. The larval development of *Carcinus maenas* (L.) and *C. mediterraneus* Czerniavsky (Crustacea, Brachyura, Portunidae) reared in the laboratory. *Bull. Brit. Mus. (Nat. Hist.)* **28:** 103–119.

Skinner, D. M. 1985. Interacting factors in the control of the crustacean molt cycle. *Am. Zool.* **25:** 275–284.

Snyder, M. J., and E. S. Chang. 1986. Effects of sinus gland extracts on larval molting and ecdysteroid titers of the American lobster, *Homarus americanus*. *Biol. Bull.* **170:** 244–254.

Spindler, K. D., and K. Anger. 1986. Ecdysteroid levels during the larval development of the spider crab *Hyas araneus*. *Gen. Comp. Endocrinol.* **64:** 122–128.

Spurr, A. R. 1969. A low-viscosity epoxy resin embedding medium for electron microscopy. *J. Ultrastruc. Res.* **26:** 31–43.

Watson, R. D., E. Spaziani, and W. E. Bollenbacher. 1989. Regulation of ecdysone synthesis in insects and crustaceans: a comparison. Pp. 188–203 in *Ecdysone: From Chemistry to Mode of Action*, J. Koolman, ed. Georg Thieme Verlag, Stuttgart.

Webster, S. G. 1986. Neurohormonal control of ecdysteroid biosynthesis by *Carcinus maenas* Y-organs *in vitro* and preliminary characterization of the putative moult-inhibiting hormone (MIH). *Gen. Comp. Endocrinol.* **61:** 237–247.

Webster, S. G., and R. Keller. 1986. Purification, characterization and amino acid composition of the putative moult-inhibiting hormone (MIH) of *Carcinus maenas* (Crustacea, Decapoda). *J. Comp. Physiol. B* **156:** 617–624.

Webster, S. G., and R. Keller. 1988. Physiology and biochemistry of crustacean neurohormonal peptides. Pp. 173–196 in *Neurohormones in Invertebrates*, M. C. Thorndyke and G. J. Goldsworthy, eds. Cambridge University Press.

Zielhorst, A. J. A. G., and F. Van Herp. 1976. Développement du système neurosécréteur du pedoncle oculaire des larves d' *Astacus leptodactylus salinus* Nordmann (Crustacea, Decapoda, Reptantia): Microscopie photonique. *C. R. Acad. Sci. (D) (Paris)* **283:** 1755–1758.

(J)
Reference: *Biol. Bull.* **180:** 72–80. (February, 1991)

The First Historical Extinction of a Marine Invertebrate in an Ocean Basin: The Demise of the Eelgrass Limpet *Lottia alveus*

JAMES T. CARLTON[1], GEERAT J. VERMEIJ[2], DAVID R. LINDBERG[3], DEBBY A. CARLTON[1], AND ELIZABETH C. DUDLEY[4]

[1]*Maritime Studies Program, Williams College—Mystic Seaport, Mystic, Connecticut 06355;* [2]*Department of Geology, University of California, Davis, California 95616;* [3]*Museum of Paleontology, University of California, Berkeley, California 94720; and* [4]*Department of Zoology, University of Maryland, College Park, Maryland 20742*

Abstract. *Lottia alveus*, a gastropod limpet once found only on the blades of the eelgrass *Zostera marina* from Labrador to New York in the western Atlantic Ocean, is the first marine invertebrate known to have become extinct in an ocean basin in historical time. The last known specimens were collected in 1929, immediately prior to the catastrophic decline of *Zostera* in the early 1930s in the North Atlantic Ocean. The brackish water refugium of *Zostera* throughout the decline was apparently outside of this gastropod's physiological range, and the limpet became extinct. Few marine invertebrates have habits as specialized and ranges and tolerances as narrow as did *L. alveus*. The fact that most marine invertebrates have large effective population sizes may account for their relative invulnerability to extinction.

Introduction

There are no reports of the post-Pleistocene extinction of any marine invertebrate, in spite of the fact that hundreds of terrestrial and freshwater species of animals and plants have become extinct as human activity has increased around the world (Martin and Klein, 1984; Vermeij, 1986; McNeely *et al.*, 1990). This is perhaps even more remarkable given the widespread perception that many marine invertebrate species have suffered extensive decimation and that a number of them are on endangered species lists (for example, Gee and Wilson, 1981; Franz, 1982; Wells *et al.*, 1983; Wicksten, 1984).

Received 18 July 1990; accepted 24 November 1990.

We report here the first historical extinction of a marine invertebrate from an ocean basin. The limpet *Lottia alveus* (Fig. 1), a once abundant stenotopic species that ranged from southern Labrador to Long Island Sound and lived only on the blades of the eelgrass *Zostera marina* (Conrad, 1831; Couthouy, 1839; Gould and Binney, 1870), is now extinct in the Atlantic Ocean. Here we consider the evidence for this conclusion and suggest why this extinction occurred.

Materials and Methods

Field studies

Eelgrass populations were searched specifically for limpets in the following locations: Cape Cod, Massachusetts, between 1979 and 1982; along the eastern Connecticut shore (Fishers Island and Long Island Sounds) between 1982–1987 and 1989–1990, and at Vinalhaven (25 km east of Rockland), central Maine in 1984 (J.T.C. and D.A.C.); at Boothbay Harbor (45 km southwest of Rockland), central Maine in 1971, and in Newfoundland (Come by Chance, in Placentia Bay, and at Norris Point, Bonne Bay, in the Gulf of St. Lawrence) in 1990 (G.J.V.). We contacted biologists who are familiar with the common Atlantic limpet *Tectura testudinalis* (= *Acmaea testudinalis*) and who have sampled *Zostera* epiphytes in Quebec (Rimouski), Nova Scotia (Halifax), Maine, Massachusetts, Rhode Island, and Connecticut. Since 1965, *L. alveus* has been searched for without success in south-central Nova Scotia, and in Labrador and Newfoundland (D. Davis and R. Noseworthy, pers. comm., respectively). We examined

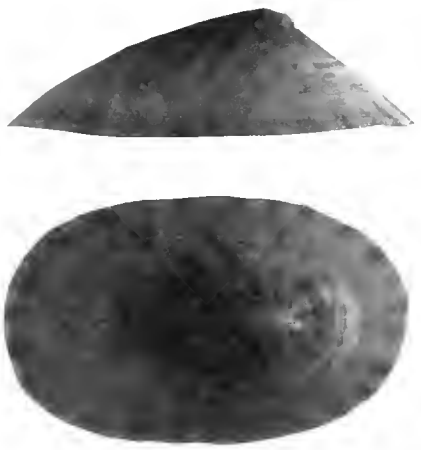

Figure 1. Dorsal and lateral views of the extinct Atlantic limpet *Lottia alveus* (a pre-1900 specimen from Massachusetts, ANSP 39044, 1.6×). The laterally compressed shell of this limpet precisely fitted the narrow blade of the eelgrass *Zostera marina*.

all published records (from 1831 to 1989) of shallow-water marine mollusks and eelgrass biota from the Arctic Ocean to the central Atlantic coast of the United States.

Museum studies

We examined 14 museum malacological collections in search of specimens of *L. alveus*. For systematic purposes and for trophic analyses, we studied radulae of alcohol preserved and rehydrated specimens of *L. alveus*, as well as radulae of *L. alveus parallela* and illustrations of the radula of *L. alveus angusta*.

These collections are located in the following museums (abbreviations are given for museums cited later in the text): Academy of Natural Sciences, Philadelphia (ANSP); American Museum of Natural History, New York; British Columbia Provincial Museum, Victoria (BCPM); California Academy of Sciences, San Francisco; Los Angeles County Museum of Natural History; Museum of Comparative Zoology, Harvard University (MCZ); Museum of Paleontology, University of California, Berkeley; National Museums of Canada, Ottawa; New York State Museum, Albany (NYSM); Natural History Museum, London [formerly British Museum (Natural History)]; Nova Scotia Museum, Halifax; Santa Barbara Museum of Natural History, Santa Barbara, California; United States Museum of Natural History, Smithsonian Institution, Washington, DC (USNM); University of Alaska Museum, Fairbanks (UAM).

In addition, a number of major United States herbarium collections of the eelgrass *Zostera marina* from North America were examined in an independent study on eelgrass wasting diseases by F. Short, who has provided us with his records of dried limpets found on herbarium sheets.

Results

Systematics and biogeography

The limpet *Lottia alveus* (Conrad) was described in 1831 from Massachusetts. It is more commonly known as *Acmaea alveus* or *Collisella alveus*. We follow the nomenclatural revision of Lindberg (1986) in referring this species to *Lottia*. Two situations led to the previously overlooked history of this limpet in the North Atlantic Ocean. First, there was a persistent belief that *L. alveus* was an ecotype of the rocky intertidal limpet *Tectura testudinalis* (Müller, 1776) (Dall, 1871; Johnson, 1928; Abbott, 1974), and that it was thus not a separate species. Second, there are continued reports of its presumed presence on the Atlantic coast in molluscan checklists and books (for example, Abbott, 1954, 1974; Emerson and Jacobson, 1976).

However, as Jackson (1907) and Morse (1910, 1921) clearly demonstrated, *L. alveus* is distinct from *T. testudinalis* in anatomy, behavior, shell shape, sculpture, and color. Morse (1910) noted that shells of the two species could be distinguished at "a millimeter or more" in length, by sculpture, apex shape, and color. McLean (1966) further noted that *L. alveus* was not a form of *T. testudinalis* that had settled on eelgrass blades, as both *T. testudinalis* and the eelgrass *Zostera marina* are common in European waters, where *L. alveus* does not occur. William Healey Dall, whose opinion was widely regarded by contemporary malacologists, also concluded, in a reversal of his earlier belief (Dall, 1871), that *L. alveus* was "a good species" (Sumner *et al.*, 1913). He was apparently influenced by the findings of Jackson (and perhaps Morse), but his opinion apparently did not reach the general malacological community.

McLean (1966) and Lindberg (1986) have shown that *L. alveus* and *T. testudinalis* are properly placed in different genera. The genus *Lottia* possesses a single pair of reduced marginal teeth (uncini) that are present at the posterior end of the ribbon segment. The genus *Tectura* lacks these marginal teeth on the radula. Lindberg (1981, 1986, 1988) discusses the phylogenetic importance of these radular characters in diagnosing limpet genera. Jackson (1907) detailed other differences between the radulae of the two species, although he failed to illustrate the uncini.

Lottia alveus originated in the North Pacific Ocean from an ancestral lineage represented in the Mio-Pliocene of Japan by *Lottia angustitesta* (Yokoyama, 1926) (Yokoyama, 1926; Kotaka and Ogasawara, 1974; D.R.L., in prep.). The Western North Pacific Ocean is also considered the center of origin in the Tertiary of *Zostera* (McRoy, 1968; den Hartog, 1970). Both *L. alveus* and *Zostera* invaded the North Atlantic Ocean through the Bering Strait and the Arctic Ocean in the late Tertiary,

as did numerous other marine organisms (Durham and MacNeil, 1967; G.J.V., in prep.).

Pleistocene glaciation subsequently created three allopatric subspecies: *Lottia alveus parallela* (Dall, 1914) in the Northeast Pacific, *Lottia alveus angusta* (Moskalev, 1967) in the Northwest Pacific, and *Lottia alveus alveus* (hereafter, *L. alveus*) in the Northwest Atlantic. The three subspecies are distinguished on the basis of external morphology and radulae (D.R.L., in prep.). In addition, the Atlantic subspecies had markedly less variation in color and shell pattern than Pacific populations, and also possessed a widespread radular abnormality (an extra first lateral tooth on the left side of the radula) absent in Pacific individuals. These characteristics in the Atlantic subspecies suggest a founder effect. Mitochondrial DNA analysis (of the extant North Pacific populations and of preserved material of the North Atlantic populations) may aid in resolving whether these three taxa should be treated as full species.

Lottia alveus parallela occurs only on *Zostera* between Kazuna Bay, Cook Inlet (60° North Latitude) in southern Alaska (UAM, N. Foster collections, 1975) and Smith's Inlet in Queen Charlotte Sound, British Columbia (51° North Latitude) (BCPM, late nineteenth century specimens). Dall (1921) cites a southern Pacific coast limit of *L. a. parallela* as Victoria, British Columbia (48° North Latitude), but the specimen lot in BCPM upon which this record is apparently based indicates that the material may also have been collected at Skidegate Inlet, on the east coast of Queen Charlotte Island. Burch (1946) cites what appears to be an independent Victoria record, but without data, and we have been unable to locate supporting material. We know of no formal searches in Alaska or British Columbia that have attempted to establish the exact distribution of *L. a. parallela*. *Lottia a. angusta* has been recorded only from Sakhalin Island, Sea of Japan (46° North Latitude), on *Zostera* (Moskalev, 1967).

Lottia alveus was known as far west (south) on the Atlantic coast as Long Island Sound, where it was recorded from New York by De Kay (1843) and Letson (1905) (see also Table I, herein) and from Stratford, Connecticut by Linsley (1845). It occurred as far east (north) as Egg Harbor, Labrador (USNM, O. Bryant collections, 1908) (Fig. 2).

The last known populations

No eelgrass limpets have been collected in the Atlantic Ocean since 1929 (Table I). The previous known range of this limpet (Labrador to New York) has been searched thoroughly by us and others. Given the planktotrophic larva that lottiid limpets possess (Lindberg, 1981), and the now widespread occurrence and availability of *Zostera* as a habitat, we do not believe that there are refugial, isolated "pockets" of this limpet in remote coves, offshore islands, or similar sites.

Two live collected USNM specimens (13.0 and 9.3 mm in length) of *L. alveus* bear a label indicating the place of collection as Cape Ann, Massachusetts (50 km northeast of Boston) and a date of 14 July 1953. We have excluded this record from Table I for the following reasons. In contrast to the records listed in Table I, we have been unable to verify that this is the date of collection (for example, by other species collected at the same time and place by the same collector, by knowledge of the collector's specific activities at the time and place of collection, and so forth). The collector (J. A. Weber) specialized (as a hobby) in collecting gastropod radulae, and obtained material from many sources. Thus he may, for example, have obtained preserved or dried material of this limpet from another shell collector (Weber made a long trip up the coast in 1953, visiting shell collectors and collecting specimens). The specimens were received at the Smithsonian Institution in 1966; while the Latin name and location are part of the original writing, the date has been added in black ink at a later time. Dexter (1968) systematically sampled the mollusks at five widely separated stations at Cape Ann from 1933 to 1937 and from 1956 to 1961, and in many intervening years through 1967. While finding many uncommon and rare species, he never found *L. alveus* (R. Dexter, pers. comm., 1990). Dexter specifically examined the mollusks on eelgrass blades at Cape Ann in 1949 (Dexter, 1950), again without finding *L. alveus*. Dexter was also at Cape Ann in July 1953, where he did not find *L. alveus* in informal surveys of the eelgrass, nor did he meet Weber there (R. Dexter, pers. comm., 1990).

We do not discount this record because it occurs after 1929, nor because it does not fit our view of the timing of the extinction of this mollusk. The possible persistence of *L. alveus* until the early 1950s does not alter our conclusion that this limpet is extinct. Many extinctions are characterized by a lengthy and slow decline of a species, rather than by the precipitous disappearance documented here. Thus, one scenario for the demise of *L. alveus* would have been a catastrophic bottleneck followed by the eventual disappearance of the last remnant populations over subsequent decades. Rather, we reject this record because decades of sampling and collecting mollusks specifically at Cape Ann, and in the Boston area in general, before and after 1953 have failed to discover this limpet. It is not infrequent to find on museum labels transmittal dates, exchange dates, and cataloging dates, and we thus suggest, pending other confirmation, that "1953" is one of these dates-of-record.

The last verifiable report of living eelgrass limpets in the Atlantic Ocean is that of Proctor (1933). Collecting in 1929 (*fide* Johnson, 1929) at Bar Harbor on Mt. Desert

Figure 2. Former populations (dots) of the limpet *Lottia alveus* in the Northwest Atlantic Ocean. Triangles represent other localities mentioned in text.

Island on the northeastern Maine coast, Proctor reported that "One may go to the Narrows [near Bar Harbor] at low tide today and find . . . thousands of individuals readily accessible . . ." Proctor believed (evidently on the basis of shell color and shape) that *L. alveus* and *T. testudinalis* were identical species. Their abundance may have been a source of his confusion. It is possible that he found dislodged *L. alveus* individuals upon rocks and errant *T. testudinalis* individuals on eelgrass blades. There are reports of *L. alveus* from rocks (Stimpson, 1851; Jackson, 1907; Morse, 1910) that Morse (1910) believed to be the result of specimens detached by waves and storms. *Lottia alveus* was on occasion also found on other substrates. There is, for example, a specimen (MCZ) collected in 1897 at Isle au Haut, Maine, attached to the periwinkle *Littorina littorea* (Linnaeus, 1758), bearing the label, "living thus on this specimen of *L. littorea* which was on (a) float . . . in bed of eelgrass." The typically rock-dwelling limpet *Lottia pelta* (Rathke, 1833) can be found occasionally in California on the blades of the surfgrass *Phyllospadix* when dense stands of the latter overlap intertidal rocks (J.T.C., pers. observ.)

Reconstruction of the biology of Lottia alveus

The morphology, anatomy, habitat, and collection records of *Lottia alveus* permit a partial reconstruction of the biology and natural history of this extinct Atlantic species. There are no studies of the extant subspecies in the North Pacific Ocean.

Abundance

As with many now uncommon animals and plants reported as "common" or "abundant" in the nineteenth

century, there are no quantitative analyses of the population size or structure of *Lottia alveus*. However, a sense of the abundance of this eelgrass limpet can be gleaned from the literature (Table II). It is clear that this limpet was sufficiently common throughout much of northern New England that it could be collected "on demand" between the 1860s and the late 1920s. While workers continued to refer to *L. alveus* in later years [for example, Miner's (1950) statement, "found abundantly on eelgrass"], it is clear that these are references to older literature and collections.

Trophic ecology

The radula of *L. alveus* was illustrated by Jackson (1907). We find it to be an accurate figure, with the exception of the missing uncini. Analysis of the radular morphology of *L. alveus* indicates that it was a trophic specialist, feeding upon the epithelial cells of the eelgrass, rather than upon epiphytic diatoms and algae. The radula of all *alveus* subspecies has broad, straight cutting edges on its first and second lateral teeth. It is analogous to the radula of the Northeast Pacific Ocean stenotopic surfgrass (*Phyllospadix*) limpet *Tectura paleacea* (Gould, 1853), which eats only the epithelial cells of that grass (Fishlyn and Phillips, 1980). With the exceptions of specimens that presumably wandered off or were dislodged from eelgrass, all reliable literature reports and museum material indicate that *Lottia alveus* was restricted to, and by our analysis ate only, the eelgrass *Zostera marina*. We predict that the extant subspecies in the North Pacific feed upon the epithelial cells of *Zostera*.

Distributional ecology

We have studied all reported localities (including consideration of their probable nineteenth century shoreline configurations) for *Lottia alveus* from Long Island Sound to Labrador to reconstruct aspects of the distributional ecology of this limpet.

Although no authors reported the salinity of the water in which they collected, it appears that all localities in which *L. alveus* was collected were and are characteristic of fully marine (32–33‰ or greater), rather than estuarine, habitats. Of course it is difficult to establish the salinity of a locality without actual records, but no collections indicate that populations of *L. alveus* were maintained on eelgrass in low salinity (brackish water) sites. Further evidence may be sought in the associated biota: the mollusks reported to have been collected with or in the immediate vicinity of *L. alveus* (for example, Rathbun, 1881; Jackson, 1908; Winkley, 1909; Thompson, 1921; Lermond, 1922) include strictly marine species, as well as euryhaline species, but never was the co-occurring molluscan fauna (nor authors' site descriptions) characteristic of strictly brackish water.

We conclude that *L. alveus* was probably a stenohaline species of open coastal waters. We predict that extant sub-

Table I

Final records of the limpet Lottia alveus *in the Atlantic Ocean*

Locality	Last known collection	Reference
New York: Long Island: Noyack Bay	1926	(1)
Massachusetts: Boston region	1921	(2)
Maine: Rockland	1922	(3)
Maine: Mt. Desert Island	1929	(4)
New Brunswick: Bay of Fundy: Grand Manan	1920	(5)
Quebec: Saguenay County: Sept-Iles	1925	(6)

References: (1) NYSM, R. C. Latham, collector; (2) Thompson, 1921; (3) Lermond, 1922; (4) Johnson, 1929; (5) ANSP, H. S. Colton, collector; (6) ANSP, on *Zostera* herbarium sheet.

Table II

Records of the abundance of the limpet Lottia alveus *on the Atlantic coast of North America*

Locality and date	Remarks	Reference
"New England", 1860s	"Found abundantly on the eel-grass"	Gould and Binney, 1870
Grand Manan Island, Bay of Fundy, 1890	"very abundant on eel-grass at low water"	Ganong, 1890
Isle au Haut, Maine, 1893–1897	[>1000 specimens in many lots]	MCZ
North Haven, Maine [25 km east of Rockland], 1908	"very common on *Zostera marina*"	Jackson, 1908
"Maine", 1909	"very common all along the coast, on eel grass and occasionally on rocks"	Lermond, 1909
Boston region, 1910	"in certain places hundreds may be collected in a short time"	Morse, 1910
Rockland, Maine, 1922	75 specimens taken on eel grass in one afternoon, incidental to other collections	Lermond, 1922
Mt. Desert Island, Maine, 1929	"thousands of individuals readily accessible" at low tide	Proctor, 1933

species of *L. alveus* in the North Pacific will be found to be stenohaline.

Discussion

An extinction scenario

What factors led to the extinction of this limpet? We suggest a scenario that focuses upon a combination of the stenotopic habitat of this species and its apparently narrow physiological range.

Between 1930 and 1933, *Zostera* precipitously disappeared from both the eastern and western North Atlantic Ocean on a scale and in geographic breadth far exceeding any previous historical declines (Rasmussen, 1973, 1977). The dramatic decline of this eelgrass led to extensive disruptions in neritic ecosystems, including large reductions in migratory waterfowl populations, loss of commercial scallop fisheries, and alterations for decades of nearshore soft sediment habitats (Rasmussen, 1977; Short *et al.*, 1987). Until now, however, no extinctions have been attributed to this decline. The primary cause of this decline was probably a "wasting disease" caused by the slime mold *Labyrinthula* (Muehlstein *et al.*, 1988; Short *et al.*, 1986, 1987, 1988). More than 90% of the standing stock of *Zostera* was eliminated with concomitant and often striking changes in associated biota (Stauffer, 1937; Dreyer and Castle, 1941).

Populations of *Zostera marina* survived, however, in low-salinity refugia (Short *et al.*, 1986). As argued above, we suggest that *Lottia alveus* was probably a stenohaline species; collection records indicate that it did not, unlike *Zostera*, extend into brackish waters. We speculate that the presumably narrow salinity range of this limpet may have prevented it from surviving on refugial eelgrass populations in lower salinity waters.

In contrast, the sacoglossan opisthobranch *Elysia catulus* Gould, 1870, similarly restricted to and feeding solely upon eelgrass (Clark, 1975), did not become extinct. This small sea slug ranges from Boston, Massachusetts (Johnson, 1915) to Virginia (Clark, 1975), and probably south to the southern limit of *Zostera* in the Carolinas (Jensen and Clark, 1983). Eelgrass populations were similarly eliminated throughout *Elysia*'s range, except, as noted, in brackish water. We suggest that *Elysia* did not become extinct because it lives in salinities at least as low as 17‰ (Marcus, 1972), and thus survived the eelgrass blight in the estuarine eelgrass refugia.

It remains possible, of course, that factors other than the putative osmoregulatory abilities (which cannot now be experimentally determined for Atlantic populations) prevented *L. alveus* from extending into brackish waters. These factors could include respiratory intolerance of the clay-silt loads typical of estuarine environments, or the build-up of sediments or epiphytes in brackish water on eelgrass blades that may have inhibited the limpet's feeding. For whatever reasons, the evidence suggests that *L. alveus* did not occur in the upper bay environments in which *Zostera* survived.

Further evidence for this scenario is gained by the observation that other eelgrass-associated gastropods also found refugia in other habitats or on *Zostera* in lower salinity waters. Snails typically found on eelgrass in New England and the middle Atlantic coast include the prosobranchs *Lacuna vincta* (Montagu, 1803), *Bittium alternatum* (Say, 1822), *Bittium varium* (Pfeiffer, 1840), *Crepidula convexa* Say, 1822, and *Mitrella lunata* (Say, 1826) (Nagle, 1968; Marsh, 1973). None of these is restricted to *Zostera*, and none became extinct, although there are reports of changes in microhabitat and abundance following the eelgrass decline (Dexter, 1962; O'Connor, 1972). Russell-Hunter and Tashiro (1985) have similarly noted the decline of the *Zostera*-associated infaunal bivalve *Cumingia tellinoides* following the disappearance of eelgrass beds.

The survival of *Lottia alveus parallela* and *Lottia alveus angusta* may result from the fact that no extensive areas of eelgrass were eliminated in the North Pacific Ocean (den Hartog, 1987).

Other reported marine mollusk extinctions

Other marine mollusks have been reported as possibly extinct. We have found no records of any other documented historical marine invertebrate extinctions.

A single living specimen of the limpet "*Collisella*" *edmitchelli* was collected in the early 1860s in southern California (Lindberg, 1984). Nothing is known further of the Holocene history or habitat of this otherwise Pleistocene species. The Caribbean bivalve *Pholadomya candida* was believed extinct (Runnegar, 1979), but it is extant in waters off Venezuela (Gibson-Smith and Gibson-Smith, 1981). The nudibranch sea slug *Doridella batava*, once believed to be endemic to the Netherlands, is reported as possibly extinct (Wells *et al.*, 1983), but has been found living in France (Platts, 1985). Moreover, *D. batava* may represent an introduction of a previously described species from elsewhere in the world (Wells *et al.*, 1983; T. Gosliner, pers. comm., 1990).

Six to eight species of brackish water hydrobiid snails were reported as possibly extinct on the United States Atlantic coast by Morrison (1970). The distinction of these undescribed species from still living and closely related taxa has not been demonstrated (F. Thompson, pers. comm., 1986), nor is it clear that searches were made for still extant populations.

The most intriguing record that we have found is that of the Californian potamidid estuarine snail *Cerithidea fuscata*, which Taylor (1981) reported as "possibly ex-

tinct." This high intertidal, mudflat-dwelling horn snail is known only from San Diego Bay in southern California; it was last collected in 1935. Taylor (1981) suggested that threats to its existence were "pollution, dredging, and land fill." Taylor (1981) treated *C. fuscata* Gould, 1857, as a distinct species, with *Cerithidea sacrata hyporhyssa* Berry, 1906, in synonymy. Grant and Gale (1931) and Bequaert (1942) considered the latter a synonym of *Cerithidea californica* (Haldeman, 1840). The status of *C. fuscata* as a species distinct from *Cerithidea californica*, rather than either an ecophenotype or subspecies, has not been clarified (J. McLean, pers. comm., 1986). *Cerithidea fuscata* differs from other populations of *Cerithidea* by virtue of its smooth, tapered shell with flat whorls (Berry, 1906). While *C. californica* is common and widespread both to the north and south, the smooth-shell population has long been considered to occur only in San Diego Bay (Burch, 1945). There are no details of population declines or disappearances of *C. fuscata* as yet documented, nor is there published evidence that searches have been made for extant populations. Nevertheless, that populations of *Cerithidea*, whose life history is characterized by non-planktonic larvae (Race, 1981), are susceptible to bay-wide extinctions has been documented elsewhere (Carlton, 1976).

It is clear from these and other reports that there are historical records of marine and estuarine mollusks with small and geographically limited populations, and that some of these populations are believed to have disappeared. There are also many species of crustaceans, annelids, flatworms, hydroids, and other invertebrates that have never been reported since the nineteenth century. Some of these are from coastal localities that have been obliterated during the course of human population expansion and concomitant littoral urbanization. Finally, at both local (state) and international levels, various marine invertebrates have been reported as "endangered." Listings for marine mollusks have been achieved in part due to the collecting activities of shell collectors. We distinguish all of these records from demonstrably extinct taxa.

Conclusions

With its specialized feeding habits and narrow habitat range, *Lottia alveus* conforms well to the profile of species that are believed to be highly susceptible to extinction (Martin and Klein, 1984; Vermeij, 1986). The limited geographic range (a consequence of Pleistocene glaciations), the limited trophic range (an adaptation dating from the Mio-Pliocene), and the presumably limited physiological range (a phylogenetic constraint shared by almost all lottiid limpets and perhaps dating from the Paleozoic origin of the group) were interwoven and cascading attributes that set the stage to make this species vulnerable to extinction. We suggest that the refugia of *Lottia*'s sole food source during a period of catastrophic decline were outside of this limpet's habitat range, and the limpet became extinct.

Most marine invertebrates whose biology and distribution are well-known do not have habits as specialized and ranges as narrow as did *Lottia alveus*. (There are, of course, a great many species described from only one locality, but whose actual ranges are not known). Most of those taxa that are known from one or a few host species have much wider geographical ranges than did this limpet. The fact that most marine invertebrates have large effective population sizes, often over broad ranges, may account further for their relative invulnerability to extinction in historical time. In contrast, small and geographically restricted populations of species (short-range endemics, for example) may be particularly vulnerable to extinction. Those species whose life history combines non-planktonic larvae with juvenile or adult stages not likely to be associated with drifting algae or wood may be specifically susceptible to extinction.

While our records to date indicate that marine invertebrates in general have escaped historical extinctions by the end of the twentieth century, human activities have been and are clearly capable of severely reducing and completely eliminating populations of marine invertebrates from extensive parts of their ranges. These actions have and will continue to fundamentally alter the structure of natural communities.

Acknowledgments

We thank numerous museum curators and correspondents for aid in establishing the status of this small snail. Frederick Short (University of New Hampshire) provided the herbarium-based record from Quebec. Ralph Dexter (Kent State University) provided valuable information and references on his mollusk collections at Cape Ann, Massachusetts. Terrence Gosliner (California Academy of Sciences), James McLean (Los Angeles County Museum of Natural History), and Fred Thompson (Florida State Museum, Gainesville) provided valuable comments on the taxonomic status of certain mollusks. Peter Frank (University of Oregon), Peter Petraitis (University of Pennsylvania), and Janie Wulff (Williams College) commented upon various versions of the manuscript.

Literature Cited

Abbott, R. T. 1954. *American Seashells.* D. Van Nostrand Company, Inc., Princeton, NJ.

Abbott, R. T. 1974. *American Seashells,* 2nd ed. Van Nostrand Reinhold Company, New York City, NY.

Bequaert, J. 1942. Random notes on American Potamididae. *Nautilus* **56:** 20–30.

Berry, S. S. 1906. Note on a new variety of *Cerithidea sacrata* Gld., from San Diego, Cal. *Nautilus* **19:** 133.

Burch, J. Q. 1945. *Cerithidea californica hyporhyssa. Min. Conchological Club So. Calif.* **54:** 34–35.

Burch, J. Q. 1946. Family Acmaeidae. *Min. Conchological Club So. Calif.* **57:** 5–16.

Carlton, J. T. 1976. Extinct and endangered populations of the endemic mudsnail *Cerithidea californica* in northern California. *Bull. Am Malacol. Union* **1975:** 65.

Clark, K. B. 1975. Nudibranch life cycles in the Northwest Atlantic and their relationship to the ecology of fouling communities. *Helgol. Wiss Meeresunters.* **27:** 28–69.

Conrad, T. 1831. Descriptions of fifteen new species of Recent, three of fossil shells, chiefly from the coast of the United States. *J Acad Nat. Sci. Philadelphia* **6:** 256–268.

Couthouy, J. P. 1839. Monograph on the family Osteodesmacea of Deshayes, with remarks on two species of Patelloidea, and descriptions of new species of marine shells, a species of *Anculotus*, and one of *Eolis. Boston J Nat. Hist.* **2:** 129–189.

Dall, W. H. 1871. On the limpets; with special reference to the species of the west coast of America, and to a more natural classification of the group. *Am J Conch* **6:** 228–282.

Dall, W. H. 1914. Notes on some northwest coast acmaeas. *Nautilus* **28:** 13–15.

Dall, W. H. 1921. Summary of the marine shell-bearing mollusks of the northwest coast of Alaska. *Bull. U. S Natl Mus.* **112:** 1–217.

De Kay, J. E. 1843. *Zoology of New York. Part V Mollusca.* Carroll and Cook, Albany.

den Hartog, C. 1970. *The Sea Grasses of the World* North-Holland Publishing Company, Amsterdam.

den Hartog, C. 1987. "Wasting disease" and other dynamic phenomena in eelgrass beds. *Aquat. Bot.* **27:** 3–14.

Dexter, R. W. 1950. Restoration of the *Zostera* faciation at Cape Ann, Massachusetts. *Ecology* **31:** 286–288.

Dexter, R. W. 1962. Further studies on the marine mollusks of Cape Ann, Massachusetts. *Nautilus* **76:** 63–70.

Dexter, R. W. 1968. Distribution of the marine molluscs at Cape Ann, Massachusetts. *Proc. Symp. Mollusca* (Mar. Biol. Assoc. India, Cochin, Symp. Ser. 3) **I:** 214–222.

Dreyer, W. A., and W. A. Castle. 1941. Occurrence of the bay scallop, *Pecten irradians. Ecology* **22:** 425–427.

Durham, J. W., and F. S. MacNeil. 1967. Cenozoic migrations of marine invertebrates through the Bering Strait region. Pp. 326–349 in *The Bering Land Bridge,* D. M. Hopkins, ed. Stanford University Press, Stanford, CA.

Emerson, W. K., and M. K. Jacobson. 1976. *The American Museum of Natural History Guide to Shells.* Alfred A. Knopf, New York.

Fishlyn, D. A., and D. W. Phillips. 1980. Chemical camouflaging and behavioral defenses against a predatory seastar by three species of gastropods from the surfgrass *Phyllospadix* community. *Biol. Bull.* **158:** 34–48.

Franz, D. R. 1982. An historical perspective on molluscs in lower New York harbor, with emphasis on oysters. Pp. 181–197 in *Ecological Stress and the New York Bight: Science and Management,* G. F. Mayer, ed. Estuarine Research Federation, Columbia, SC.

Ganong, W. F. 1890. Article III. Zoological notes. Report of the Committee on Marine Invertebrate Zoology. I. Mollusca. *Bull. Nat. Hist. Soc. New Brunswick* **9:** 1–14.

Gee, J. H. R., and K. Wilson. 1981. The littoral Mollusca of Greenisland, Co Antrim: 40 years of change in Belfast Lough. *Ir. Nat. J* **20:** 343–345.

Gibson-Smith, J., and W. Gibson-Smith. 1981. The status of *Pholadomya candida* G. B. Sowerby, I, 1823. *Veliger* **23:** 355–356.

Gould, A. A., and W. G. Binney. 1870. *Report on the Invertebrata of Massachusetts.* Wright and Potter, Boston, MA.

Grant, U. S., and H. R. Gale. 1931. Catalogue of the marine Pliocene and Pleistocene Mollusca of California and adjacent regions. *Mem. San Diego Soc. Nat Hist.* **1:** 1–1036.

Jackson, H. 1907. The differences between the two New England species of *Acmaea. Nautilus* **21:** 1–5, 24.

Jackson, H. 1908. The Mollusca of North Haven, Maine. *Nautilus* **21:** 142–144.

Jensen, K., and K. B. Clark. 1983. Annotated checklist of Florida ascoglossan Opisthobranchia. *Nautilus* **97:** 1–13.

Johnson, C. W. 1915. Fauna of New England. List of Mollusca. *Occ. Pap. Boston Soc. Nat Hist.* **13:** 1–231.

Johnson, C. W. 1928. A review of the New England limpets. *Nautilus* **41:** 109–117.

Johnson, C. W. 1929. *Acmaea testudinalis* (Mull.). *Nautilus* **42:** 103.

Kotaka, T., and K. Ogasawara. 1974. A new abalone from the Miocene of Aomori Prefecture, northeast Honshu, Japan. *Venus* **33:** 117–128.

Lermond, N. W. 1909. Shells of Maine. A catalogue of the land, freshwater and marine Mollusca of Maine. *Fourth Ann. Rept State Entomologist,* Augusta, ME, Pp. 217–262.

Lermond, N. W. 1922. One haul of the dredge. *The Maine Naturalist, Journal of the Knox Academy of Arts and Sciences* **2:** 138–140.

Letson, E. 1905. Check list of the Mollusca of New York. *Bull. New York State Museum* **88,** Zoology 11, Pp. 1–112.

Lindberg, D. R. 1981. *Acmaeidae Gastropoda Mollusca* Invertebrates of the San Francisco Bay Estuary System. The Boxwood Press, Pacific Grove, CA.

Lindberg, D. R. 1984. A recent specimen of *Collisella edmitchelli* from San Pedro, California (Mollusca: Acmaeidae). *Bull. So. Calif. Acad Sci.* **83:** 148–151.

Lindberg, D. R. 1986. Name changes in the "Acmaeidae." *Veliger* **29:** 142–148.

Lindberg, D. R. 1988. The Patellogastropoda. *Malacol. Rev.,* Suppl. **4:** 35–63.

Linsley, J. H. 1845. Catalogue of the shells of Connecticut. *Am. J Sci* **48:** 271–286.

Marcus, E. d. B.-R. 1972. Notes on some opisthobranch gastropods from the Chesapeake Bay. *Ches. Sci.* **13:** 300–317.

Marsh, G. A. 1973. The *Zostera* epifaunal community in the York River, Virginia. *Ches. Sci* **14:** 87–97.

Martin, P. S., and R. G. Klein, eds. 1984. *Quarternary Extinctions: A Prehistoric Revolution.* University of Arizona Press, Tucson, AZ.

McLean, J. H. 1966. West American prosobranch Gastropoda: superfamilies Patellacea, Pleurotomariacea, and Fissurellacea. Ph.D. dissertation, Stanford University, Stanford, CA.

McNeely, J. A., K. R. Miller, W. V. Reid, R. A. Mittermeier, and T. B. Werner. 1990. *Conserving the World's Biological Diversity.* International Union for Conservation of Nature and Natural Resources, Gland, Switzerland, and Washington, D. C.

McRoy, C. P. 1968. The distribution and biogeography of *Zostera marina* (eelgrass) in Alaska. *Pac. Sci.* **22:** 507–513.

Miner, R. W. 1950. *Field Book of Seashore Life.* G. P. Putnam's Sons, New York City, NY.

Morrison, J. P. E. 1970. Brackish water mollusks. *Malacologia* **10:** 55–56.

Morse, E. S. 1910. An early stage of *Acmaea. Proc. Bos. Soc. Natl. Hist.* **34:** 313–323.

Morse, E. S. 1921. *Observations on the Living Gasteropods of New England.* Peabody Museum, Salem, Massachusetts.

Moskalev, L. I. 1967. *Collisella angusta,* n. sp. Pp. 18–19 in A. N. Golikov and O. A. Scarlato. Molluscs of the Possiet Bay (the Sea of Japan) and their ecology. *Trudy Zool. Inst. Leningrad* **42:** 5–154 (in Russian).

Muehlstein, L. K., D. Porter, and F. T. Short. 1988. *Labyrinthula* sp., a marine slime mold producing the symptoms of wasting disease in eelgrass, *Zostera marina*. *Mar. Biol.* **99:** 465–472.

Nagle, J. S. 1968. Distribution of the epibiota of macroepibenthic plants. *Contrib. Mar. Sci.* **13:** 105–144.

O'Connor, J. S. 1972. The benthic macrofauna of Moriches Bay, New York. *Biol. Bull.* **142:** 84–102.

Platts, E. 1985. An annotated list of the North Atlantic Opisthobranchia, excluding Thecosomata and Gymnosomata. *Ophelia* Supplement **2:** 150–170.

Proctor, W. 1933. Biological survey of the Mount Desert region. Part V. Wistar Institute of Anatomy and Biology. Philadelphia, PA.

Race, M. S. 1981. Field ecology and natural history of *Cerithidea californica* (Gastropoda: Prosobranchia) in San Francisco Bay. *Veliger* **24:** 18–27.

Rasmussen, E. 1973. Systematics and ecology of the Isefjord marine fauna (Denmark). (With a survey of the eelgrass (*Zostera*) vegetation and its communities). *Ophelia* **11:** 1–495

Rasmussen, E. 1977. The wasting disease of eelgrass (*Zostera marina*) and its effects on environmental factors and fauna. Pp. 1–52 in *Seagrass Ecosystems. A Scientific Perspectives*. C. P. McRoy and C. Helfferich, eds. Marcel Dekker, New York.

Rathbun, R. 1881. The littoral marine fauna of Provincetown, Cape Cod, Massachusetts. *Proc. U. S. Natl. Mus.* **3:** 116–133.

Runnegar, B. 1979. *Pholadomya candida* Sowerby: the last cadaver unearthed. *Veliger* **22:** 171–172.

Russell-Hunter, W. D., and J. S. Tashiro. 1985. Life-habits and infaunal posture of *Cumingia tellinoides* (Tellinacea, Semelidae): an example of evolutionary parallelism. *Veliger* **27:** 253–260.

Short, F. T., A. C. Mathieson, and J. I. Nelson. 1986. Recurrence of the eelgrass wasting disease at the border of New Hampshire and Maine, USA. *Mar. Ecol. Prog. Ser.* **29:** 89–92.

Short, F. T., L. K. Muehlstein, and D. Porter. 1987. Eelgrass wasting disease: cause and recurrence of a marine epidemic. *Biol. Bull.* **173:** 557–562.

Short, F. T., B. W. Ibelings, and C. den Hartog. 1988. Comparison of a current eelgrass disease to the wasting disease of the 1930s. *Aquat. Bot.* **30:** 295–304.

Stauffer, R. C. 1937. Changes in the invertebrate community of a lagoon after disappearance of the eelgrass. *Ecology* **18:** 427–431.

Stimpson, W. 1851. *Shells of New England. A Revision of the Synonymy of the Testaceous Mollusks of New England*. Phillips, Sampson, and Co., Boston.

Sumner, F. B., R. C. Osburn, and L. J. Cole. 1913. A biological survey of the waters of Woods Hole and vicinity. Section III. A catalogue of the marine fauna. *Bull. Bur. Fisheries* **31:** 545–794.

Taylor, D. W. 1981. Freshwater mollusks of California: a distributional checklist. *Calif. Fish Game* **67:** 140–163.

Thompson, L. D. 1921. Collecting at Nahant Beach, Mass. *Nautilus* **34:** 100–101.

Vermeij, G. J. 1986. The biology of human-caused extinction. Pp. 28–49 in *The Preservation of Species*, B. G. Norton, ed. Princeton University Press, Princeton, NJ.

Wells, S., R. Pyle, and N. Collins. 1983. *The IUCN Invertebrate Red Data Book*. International Union for Conservation of Nature, Switzerland.

Wicksten, M. K. 1984. Early twentieth century records of marine decapod crustaceans from Los Angeles and Orange counties, California. *Bull. So. Calif. Acad. Sci.* **83:** 12–42.

Winkley, H. W. 1909. Essex County notes. *Nautilus* **23:** 86–87.

Yokoyama, M. 1926. Fossil shells from Sado. *J. Fac. Sci. Imp. Univ. Tokyo*, Sec. 2, **1:** 249–312.

Reference: *Biol. Bull.* **180**: 81–92. (February, 1991)

Passive Suspension Feeding by an Octocoral in Plankton Patches: Empirical Test of a Mathematical Model

MARK R. PATTERSON

Division of Environmental Studies, University of California, Davis, California 95616

Abstract. Feeding rate in the octocoral, *Alcyonium siderium*, was investigated as a function of colony size, flow speed, and prey concentration. The feeding rate decreases with time in high prey concentrations. A model of passive suspension feeding is formulated that successfully predicts feeding behavior. At low prey concentrations, the model predicts a linear feeding response as particle flux or colony size increases. The dominant constraint on feeding is the "handling time" required to transfer prey from tentacle to pharynx and to re-extend the tentacle. The time constant of prey capture shows no relation to particle flux, in agreement with the model. Another constraint, the "filtration time," is inversely related to colony size and flow speed. Filtration time becomes important only during feeding in sparse prey concentrations, when feeding rate is proportional to flow speed, colony size, and prey concentration. In the field, *Alcyonium* colonies reduce filtration time by orienting at right angles to the dominant flow direction. Feeding efficiency on prey patches is low and inversely related to flow speed, colony size, and prey concentration. Feeding in patches is not a simple process for this octocoral, because colonies will "saturate" with prey before all polyps have successfully captured a single prey item.

Introduction

Suspension feeding occurs in nearly all animal groups (Jørgensen, 1966), and virtually every body of water possesses a guild of organisms making a living by filtering the soup in which they live. Groups that have received the greatest amount of attention in the literature are active suspension feeders, *i.e.*, those organisms that generate their own feeding currents. Organisms that rely exclusively on environmentally produced currents to bring them food are termed passive suspension feeders.

Experimental studies on active suspension feeders led to the formulation of the first mathematical models of suspension feeding. Decreases in the concentration of particles in closed systems containing these animals could be easily monitored; use of a decreasing exponential model of filtration allowed calculation of pumping rate (Jørgensen, 1943). Coughlan (1969) reviews the use of the exponential model in calculating pumping rates (sometimes erroneously called filtration rates) for active suspension feeders. Filtration efficiency was assumed to be 100% in his treatment. Williams (1982) showed that if this assumption is seriously violated, the decline in cell concentration will be a double exponential, and measured declines cannot be easily converted into a filtration or pumping rate. His formulation of suspension feeding also predicts that the apparent filtration rate will be a function of time as physical limitations of the system with respect to filtration efficiency become important. Thus, apparent variations in filtration rate may be nothing more than manifestations of how sieving and other means of particle capture (Rubenstein and Koehl, 1977) interact with the population of cells of different sizes available for capture. Behavioral modifications of pumping rate need not be invoked to explain variation in pumping rate. Williams (1982) provides a prescription for measuring pumping rate accurately and testing for any behavioral modifications; this involves finding a particle that is filtered with 100% efficiency by the organism under investigation. Most active suspension feeders such as bivalves (Jørgensen, 1975; Mohlenberg and Riisgard, 1978; Palmer and Williams, 1980) and ascidians (Fiala-Medioni, 1973, 1978a, b, c, d) attain remarkable capture efficiencies for the small

Received 15 September 1989; accepted 6 November 1990.

particles on which they feed (bacterio- and phytoplankton). Efficiencies can often reach 100% for particles on the order of 10 μm in diameter, and thus pumping rates can be easily measured following the recommendations of Williams (1982).

Predictions of mathematical models

Mathematical models have also been used to clarify the control of suspension feeding. Two complementary and not entirely separable approaches have been: (1) to predict how an organism's feeding rate should relate to the density or quality of the food it encounters (Holling, 1965; Emlen, 1973; Doyle, 1979; Seale, 1982) and, (2) to see whether suspension feeding organisms maximize the rate of energy gain (Lehman, 1976; Lam and Frost, 1976).

Both Holling (1965; functional response type I) and Lehman (1976) predict that ingestion or filtering rate should show a linear dependence on prey availability or density up to some saturation value in organisms such as cnidarians, where encounter rate with the prey is determined by organism size and environment (in this case, flow speed). The saturation level is presumably set by the digestive physiology of the organism, *e.g.*, the "packed gut" assumption of Townsend and Hughes (1981). An implicit assumption is that all prey encountered, or at least some constant fraction of them, are retained by the organism (constant efficiency); symbolically, $\frac{dN}{dt} = K$, where N = number of prey caught, and K is a constant. K can be further decomposed: $K = U \times V \times SA$, where U = flow speed, V = prey concentration, and SA is the surface area of the organism available for prey capture. I term this hypothesis the "linear" model of passive suspension feeding, which is typically used in analyzing passive suspension feeding.

The "linear" model predicts that for a given prey density below the saturation level, feeding rate should be constant. Figure 1A gives the solution to the linear model and shows how doubling the prey concentration, flow speed, or projected surface area (size) of the organism should affect the feeding "response." Note that this "filling" curve gives the cumulative number of prey caught as a function of time; it assumes that prey density is not changing as the organisms feeds. The "filling" curve is mathematically isomorphic with the functional response type I of Holling (1965) at a given prey concentration. The curve is also conceptually equivalent to viewing filtration as a Poisson process, *i.e.*, the probability (P) of capture during a small increment of time (Δt) is constant, and the magnitude of P is the product of U, V, and SA (Fig. 1B). Furthermore, the interval between capture events is large at low prey concentrations, for reasons to be discussed below, and hence capture events are rare.

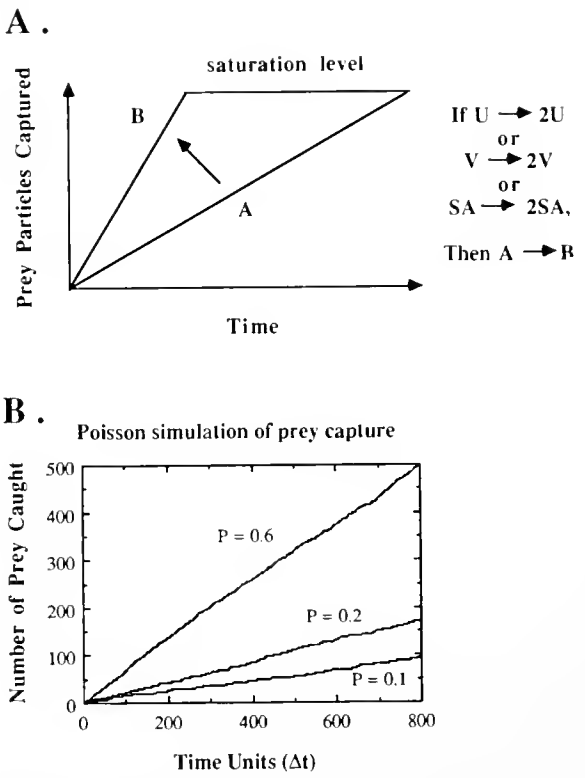

Figure 1. The classical view of passive suspension feeding. (A) The "linear" deterministic model of passive suspension feeding, which assumes prey encounter rate is proportional to the projected surface area normal to the flow (SA), the flow speed (U), and concentration of prey present (V_i). The feeding rate is constant until some saturating level of prey inside the organism is attained. This curve is implicit in Holling's (1965) type I functional response curve for predator-prey systems similar to passive suspension feeding. (B) The previous model is functionally equivalent to a process governed by the Poisson interval distribution, *i.e.*, a process where the probability of capture (P) during a small interval of time (Δt) is constant. The filling curves were generated by computer simulation for three levels of P, corresponding to increasing levels of flow, colony size, or particle concentration. Note the linear dependence between the number of particles captured and the time the suspension feeder has been exposed to a current carrying prey items.

Energy maximization arguments (*cf.* Townsend and Hughes, 1981) argue that filter feeders should feed preferentially on particles with the higher nutritional value, unless the cost of sorting and rejection are too high. The few tests in the literature (Doyle, 1979, amphipod; Seale, 1982, anuran tadpole larvae) indicate that these suspension feeders do behave in a manner consistent with energy maximization. Some work has addressed whether models formulated for other organisms make predictions compatible with observations of feeding rate as a function of prey density for passive suspension feeding in cnidarians (Clayton and Lasker, 1982). Sebens (1979, 1984) formulated a cost/benefit model for cnidarians using energy maximization as a means of predicting optimum organism size in a given habitat. The model has had good success

in predicting maximum organism sizes observed in the field. However, little attention has been paid to modeling the response of passive suspension feeders to dense prey concentrations, which may change suddenly in time, *i.e.*, what happens when a plankton patch sweeps by a cnidarian colony?

A dynamic mathematical model of passive suspension feeding

The limitations of the "linear" model are those imposed by its assumptions. Feeding rates may not be constant over time, especially if the handling of individual particles, or digestive or neurally mediated behavior becomes important. A more robust model of suspension feeding for cnidarian colonies was formulated and tested against real feeding in "patch" concentrations in the laboratory. The model takes a systems analysis view of passive suspension feeding; the input to the system (colony) is prey in the water column, the output is prey inside the organism. The model allows sudden changes in prey concentration and predicts the time course of feeding using two parameters. Congruence between the observed and predicted parameters of the model implies the assumptions used in the formulation are not too far from reality, *i.e.*, identification has been made of the salient features of the filtration system that determine feeding performance.

There are three model assumptions. (1) The colony "fills" up with prey at a rate proportional to the difference between the ambient plankton concentration (V_i) and the amount of prey already in the colony (V_o); symbolically, $(V_i - V_o)$. (2) The colony fills at a rate inversely proportional to the time necessary to handle the particles caught during filtering (R_1) and the time needed to filter the water containing the particles (R_2); symbolically, $\frac{1}{(R_1 + R_2)}$. Operationally, R_1 is the time taken to transfer, from tentacle to polyp mouth, the particle caught from a unit volume of water and to re-extend the tentacle; R_2 is the inverse of the filtration rate, which depends on the projected area of the organism perpendicular to the flow, and the flow speed. (3) A sudden jump in the plankton concentration results in a jump in the number of particles caught. The size of the jump is directly proportional to the jump in the particle concentration, $\frac{dV_i}{dt}$, the colony volume (C), and the proportion of time spent filtering particles during feeding, $\frac{R_2}{(R_1 + R_2)}$; symbolically, $C \frac{dV_i}{dt} \frac{R_2}{(R_1 + R_2)}$.

The first and second assumptions address the steady-state behavior of the passive suspension feeder, while the third deals with the dynamic aspect of prey capture. Expressed as a differential equation, passive suspension feeding may obey:

$$C \frac{dV_o}{dt} = \frac{(V_i - V_o)}{(R_1 + R_2)} + C \frac{R_2}{(R_1 + R_2)} \frac{dV_i}{dt}, \qquad \text{(Eq. 1)}$$

where $C \frac{dV_o}{dt}$ is the time change in the total number of particles caught by the organism.

Dividing by the size of the colony yields:

$$\frac{dV_o}{dt} = \frac{(V_i - V_o)}{(R_1 + R_2) C} + \frac{R_2}{(R_1 + R_2)} \frac{dV_i}{dt}. \qquad \text{(Eq. 2)}$$

Eq. (2) can be rearranged algebraically to:

$$\tau \frac{dV_o}{dt} + V_o = \alpha\tau \frac{dV_i}{dt} + V_i, \qquad \text{(Eq. 3)}$$

where $\tau = (R_1 + R_2) C$, and $\alpha = \frac{R_2}{(R_1 + R_2)}$. τ is the time constant of colony "filling," while α is the measure of how many prey are caught as the edge of the patch sweeps by the colony.

The solution to Eq. (3) depends on the nature of the change in the plankton concentration in the water column or laboratory flume. An electrical circuit that mimics exactly the behavior of this mathematical feeding model is called a lag-lead network (Milsum, 1966) and is shown in Figure 2. Formulation of the resistive-capacitive analog is motivated by the observation that prey filtration and prey handling are discrete processes. They are modeled as "resistances" through which the "current" of prey must pass to fill the organism's "capacity" (the etymological root of capacitance). This circuit can be easily wired up with variable resistors, $R_{1,2}$ and variable capacitor, C, allowing exploration of the model's qualitative behavior. A change in plankton concentration would be simulated by

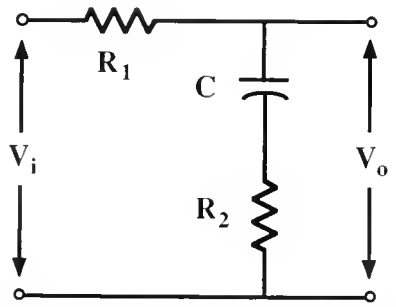

Figure 2. Electrical analog to the differential equations used to model the process of passive suspension feeding. The behavior of this circuit exactly mimics the model. R_1 is the handling time "resistance" and R_2 is the filtration time "resistance." The concentration of particles in the water column is a "voltage" (V_i) that may cause a "current" of particles to enter and reside inside the organism (V_o); this is controlled by the resistances, $R_{1,2}$ and the volume "capacitance" (C) of the animal.

a change in the input voltage (V_i); simulation of colony feeding response predicted by the model can be seen by watching the behavior of V_o as a function of time on an oscilloscope.

Applying Kirchoff's law to this circuit, I obtain:

$$iR_1 + \frac{1}{C}\int idt + iR_2 = V_i(t) \qquad \text{(Eq. 4)}$$

and

$$\frac{1}{C}\int idt + iR_2 = V_o(t), \qquad \text{(Eq. 5)}$$

where i is the "current" of particles.

Taking the Laplace transform of Eqs. (4) and (5) yields:

$$\left(R_1 + R_2 + \frac{1}{Cs}\right)i(s) = V_i(s) \qquad \text{(Eq. 6)}$$

and

$$\left(R_2 + \frac{1}{Cs}\right)i(s) = V_o(s), \qquad \text{(Eq. 7)}$$

where s is the frequency-domain variable. Some algebra then results in:

$$\frac{V_o(s)}{V_i(s)} = \frac{R_2 + \frac{1}{Cs}}{R_1 + R_2 + \frac{1}{Cs}} = \frac{a(s+b)}{b(s+a)} \qquad \text{(Eq. 8)}$$

where $a = \frac{1}{(R_1 + R_2)C}$, and $b = \frac{1}{R_2C}$.

Eq. (8) is the Laplace transform of Eq. (3). It can be rearranged to:

$$V_o(s) = s\frac{R_2C}{(\tau s + 1)}V_i(s) + \frac{V_i(s)}{(s+1)} \qquad \text{(Eq. 9)}$$

To solve Eq. (9), the nature of the input change in plankton concentration must by specified. For a *step* increase in the plankton availability to level V_i, caused by a patch of plankton flowing past the colony, $V_i(s) = \frac{V_i}{s}$. Substituting, I obtain:

$$V_o(s) = s\frac{R_2C\frac{Vi}{s}}{(\tau s + 1)} + \frac{V_i(s)}{(\tau s + 1)}, \qquad \text{(Eq. 10)}$$

which can be rearranged to:

$$V_o(s) = s\frac{R_2CV_i}{(\tau s + 1)} + \frac{V_i}{s(\tau s + 1)}. \qquad \text{(Eq. 11)}$$

Taking the inverse Laplace transform, I obtain:

$$V_o(t) = V_i\{1 - (1 - \alpha)e^{(-1/\tau)}\}, \qquad \text{(Eq. 12)}$$

the solution in the time domain.

Since α and τ can be computed from known quantities, it is possible to compare predicted with observed values of these two model parameters. In particular, τ will be an important descriptor of how quickly a colony can use a change in plankton concentration. Figure 3A shows the "filling" curve for colonies of different size (C), while Figure 3B shows identically sized colonies as the ratio between "handling" time (R_1) and "filtration" time (R_2) changes. The implications of the behavior of this model, its decomposition into the "linear" model (Type 1 functional response) under certain conditions, and the extent of its congruence with reality will be more fully developed in the Discussion section.

I experimentally tested this model by measuring feeding rates for a colonial cnidarian in the laboratory. *Alcyonium siderium*, an octocoral, is a dominant zooplanktivore on subtidal hard rock substrates in New England (Sebens and Koehl, 1984; Sebens, 1986). Colonies assume a variety of shapes varying from fingers to globose forms to compressed ellipsoids (Patterson, 1980). In plankton-rich

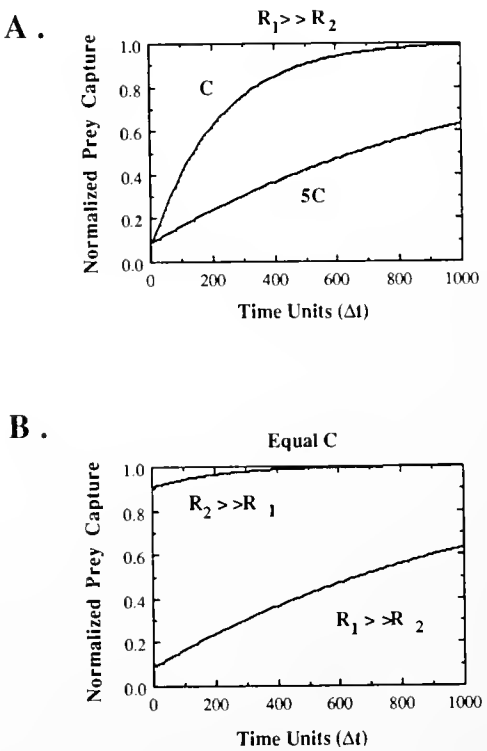

Figure 3. The time course of organism feeding as predicted by the model. (A) Colonies differing in size by a factor of five (C, 5C) and with handling time (R_1) much greater than filtration time (R_2), as occurs during feeding in plankton patches. (B) Colonies of identical size where the handling time (R_1) is much greater than filtration time (R_2) and *vice versa*. The ordinates for both graphs are normalized for the effects of colony size. Note that if R_2 becomes much larger than R_1, *i.e.*, the particle flux drops, then the filling curve tends toward a step function. Since particle flux is low, each passing particle is caught, and the model decomposes to the "linear" model of Figure 1.

habitats, fully expanded globose colonies can reach 10 cm in diameter. Previous work with *Alcyonium* colonies feeding in a closed system has shown that they readily accept prey particles (Patterson, 1984). This octocoral might be expected to follow the "linear" filling curve if prey concentration is held constant, and obey the changes predicted in Figure 1 as size and flow speed are varied. The aim of this laboratory feeding study was to test the "linear" model and the proposed alternative model for feeding in plankton patches. An intensive study of the diet of this species over a diel cycle (Sebens and Koehl, 1984) provides information useful in analyzing the results of this study.

Materials and Methods

Colony collection, maintenance, and flow generation and measurement

Feeding rate experiments were conducted at the Marine Science Center (MSC), Northeastern University, Nahant, Massachusetts, and in the biomechanics laboratory at the University of California, Davis. Colonies of *Alcyonium siderium* were collected by SCUBA diving and maintained in flowing seawater tables or recirculating chilled aquaria. Feeding observations were made in a recirculating flume described in Patterson (1984). All experiments were performed with the flow straighteners installed, which removed turbulence of length scales greater than 1 cm. Flow speeds and turbulence intensities were measured with a two channel thermistor flowmeter circuit modified from LaBarbera and Vogel (1976). The voltage output of the flowmeter was either connected to an eight-bit successive approximation A/D convertor (Mountain Computer) connected to an Apple IIe, or to a MacADIOS A/D convertor (GW Instruments) connected to an Apple Macintosh Plus. The sampling rate was 10 Hz.

Octocoral colonies attached to horse mussels (*Modiolus modiolus*) were collected subtidally from 15–23 m depth. Mussel shell fragments bearing *Alcyonium* colonies were mounted in the flow tank working section. The prey offered to the colonies were cysts of the brine shrimp, *Artemia salina*. Characteristics of the cysts are described in Patterson (1984). Capture of the cysts on individual tentacles of this species is readily observed. At the end of each feeding bout, three 60-ml samples were withdrawn isokinetically using a Cole-Parmer peristaltic pump (model no. 7568) smoothed with hydraulic capacitors. Samples were filtered onto gridded Millipore filters, the number of cysts was counted, and a mean concentration of particles present in the flow was calculated. The concentration of cysts offered (0.056–0.40 part./ml) was of the order of plankton concentrations seen in the field (Sebens and Koehl, 1984). However, even greater concentrations may be typical of dense patches of plankton that are seasonally and spatially abundant (Fasham, 1978; Grosberg, 1982).

Documenting the time course of prey capture

Alcyonium colonies were introduced individually into the working section of the flume and allowed to acclimate to the flow. Prey were not introduced until the polyps were fully expanded. A standard volume concentration (0.45 g dry cysts/l) of *Artemia* cysts was added all at once to the flume. Observations of capture events were made at a magnification of 35X through a dissecting microscope suspended over the flume. A watch glass floating on the water and anchored over the colony prevented blurring of the image from capillary waves at the air/water interface. An interval timer program (0.05 s resolution) running on an Apple IIe microcomputer measured the time between capture events. The time required for a tentacle to transfer a captured particle to the pharynx ($\{R_1\}$ in the above model) was timed with a stop watch during separate experiments.

Filtration time for an individual particle was calculated using the projected surface area of the organism, and the flow speed measured 4 cm upstream of the top of the colony. Specimen volume was measured by volumetric displacement of water in a graduated cylinder. The number of prey caught as a function of time was plotted for each specimen; the observed values for the model parameters τ and α were obtained using a least squares algorithm, and then compared with the values predicted by the model calculations through linear regression.

Feeding efficiency

Efficiency of prey capture at the colony level was computed as follows: the number of particles caught by a colony during a standard feeding bout of 10 min was divided by the number of particles that would pass through the cross-sectional area occupied by the colony if the colony were not there. This is the standard engineering definition of efficiency of particle capture (Dorman, 1966). Because feeding rate at dense concentrations of prey is non-linear (Fig. 4), efficiency will be a function of time. Hence, for purposes of comparison, efficiency is computed over the time necessary to reach "saturation." Saturation is defined as the point at which capture events drop to less than one prey item caught per 5 min period *per colony*.

Field measurements of flow and orientation to flow

Field observations of orientation to flow in *Alcyonium* colonies and flow regime were made at the following sites (depths) in the subtidal of Massachusetts Bay: (1) Dive Beach site (8 m), located near Nahant, Massachusetts (42°25′N: 70°54′W), (2) Shag Rocks inner wall (7 m)

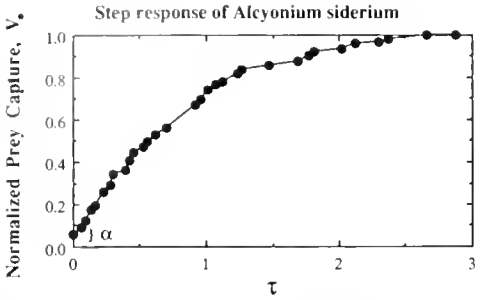

Figure 4. Typical feeding response of an *Alcyonium* colony to a step increase in the plankton concentration (*Artemia* cysts). The time axis (abscissa) is expressed in units of τ, a model parameter defined as the time necessary for the cumulative prey capture to reach $(1 - e^{-1}) = 63\%$ of the saturating value. The ordinate, V_*, is the cumulative number of prey captured normalized to the saturation level. Note that the response is curvilinear and can be characterized by two parameters, the time constant, τ, and α, the initial jump in plankton caught as the concentration changes.

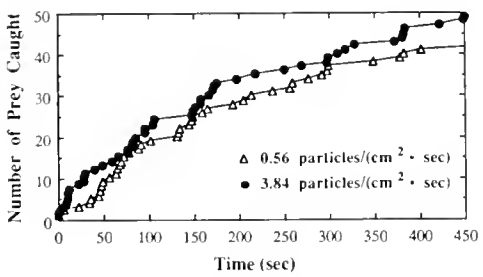

Figure 5. Feeding response of the same colony of *Alcyonium* to *Artemia* cysts offered at very different flux rates (flow speed {U} X particle concentration {V_1}). This effect is not predicted by the linear model (Fig. 1).

located near Dive Beach, (3) Shag Rocks outer wall (9 m), and (4) Halfway Rock (14 m) (42°30′N: 70°46′W). Orientation to the direction of current flow by colonies on subtidal rock walls was measured with a protractor and plumb line. The direction of current flow was determined with a filament of dye, and was parallel to the bottom and the wall. Flow measurements were made *in situ* at 1.0 cm and 10.0 cm height over *Alcyonium* colonies using a submersible thermistor flowmeter recording a digital signal on magnetic tape. Flow measurements were made over a three year period in all kinds of weather throughout the year. The sampling rate was 3 Hz.

Results

Feeding response to plankton patch concentrations

When *Alcyonium* colonies were subjected to sharp (step) increases in the plankton concentration, the "filling" curve was markedly curvilinear and showed an asymptote (see Fig. 4 for a typical example). Similar results were obtained with the sea anemone *Metridium senile* (unpub. data). At these high prey concentrations, doubling the flow speed and hence the particle flux typically had little effect on the feeding curve for a given colony (Fig. 5), providing evidence that the linear model of passive suspension feeding doesn't apply very well in patch concentrations.

Figure 4 gives the graphical interpretation of τ and α. Figure 6 shows how closely the model formulated in the Introduction predicts τ, the time constant, [time needed to reach $(1\text{-}e^{-1})$ of saturation], and α, the proportion of prey caught as the edge of the patch sweeps past the colony at the start of feeding bout. Model I linear regression was used to test the ability of the predicted (calculated) model parameters to forecast the observed values. This type of regression analysis is appropriate since the x values (the computed model parameters) were known precisely and fixed by the choice of colony (Sokal and Rohlf, 1981). Alpha values were log transformed before calculations of the regression to eliminate problems with non-normality. The aim of the model was to predict feeding behavior in dense suspensions to within a factor of two. The model achieves this goal in predicting τ and α. Linear regressions are $\tau_{obs} = 6.9 + 1.04 \ln (\tau_{pred})$ and $\ln \alpha_{obs} = -1.93 + 0.28 \ln (\alpha_{pred})$. R^2 values for these regressions for α and τ are 0.33 ($P = 0.05$) and 0.70 ($P = 0.0006$), respectively.

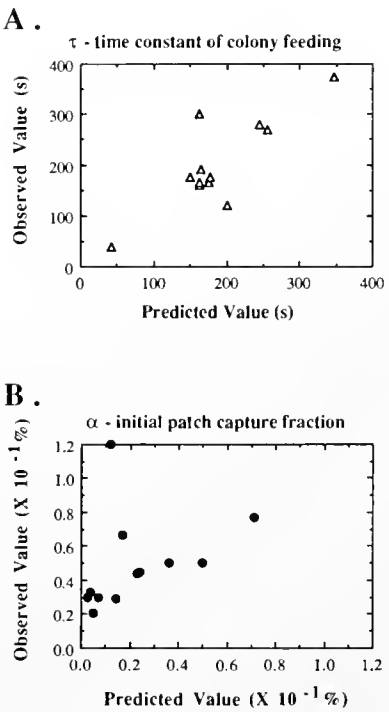

Figure 6. Predicted and observed values of (A) the time constant, τ, and (B) the patch edge capture fraction, α, for particle filtration by colonies of *Alcyonium siderium*. Predicted values of the model parameters were computed from the handling time (R_1), filtration time (R_2), and the colony volume (C).

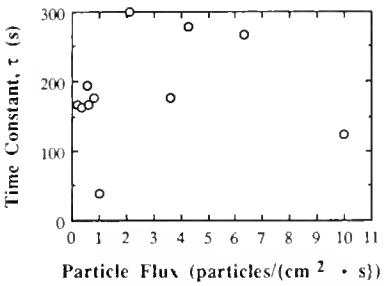

Figure 7. Plot of the time constant of colony filling, τ, as a function of the particle flux (flow speed $\{U\}$ X particle concentration $\{V_1\}$). The data do not have a slope significantly different from zero ($P < 0.001$) showing the lack of dependence of τ on particle flux at high flux rates.

Because $R_1 \gg R_2$ at the prey concentrations used, and $\tau = (R_1 + R_2)\,C$, R_2 will have little effect on τ. Thus a corollary to the model is that particle flux past the colony for high prey densities will have no correlation with the time constant (τ) or organism filling. This indeed was the case (Fig. 7). The model has slightly lower success in predicting the magnitude of α, which measures the degree to which a colony can "grab" the edge of a plankton patch as it sweeps by. Alpha is consistently overestimated; it is probably sensitive to colony shape and the precise patterns of flow obtained for a particular shape, and these aspects of passive suspension feeding were not part of the model formulation.

Colony size and feeding efficiency

Figure 9 demonstrates an inverse relationship between efficiency of capture (as defined in the Materials and Methods) and colony size. Smaller colonies are more efficient filters, although all sizes have very low efficiencies when feeding in dense concentrations. Figure 10 shows that there is also an inverse relationship between efficiency and flow speed, and hence particle flux, for a given particle concentration, for feeding by colonies.

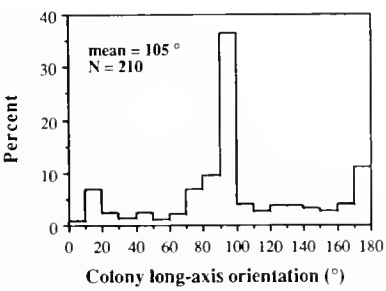

Figure 8. Orientation of the longest dimension of *Alcyonium* colonies to the local direction of current flow at four subtidal sites in Massachusetts Bay. Angles were measured with protractor and plumb line; current direction was determined with a filament of sodium fluorescein dye.

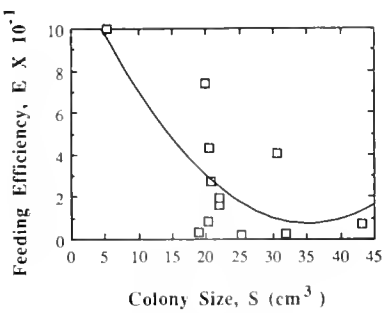

Figure 9. Efficiency of particle capture *per* colony (E) in *Alcyonium* as a function of colony size (S). Efficiency is defined as the number of particles caught by the colony in the time interval to saturation of the colony divided by the number of particles that would have passed through the space occupied by the colony. The regression is given by the equation: $E = 12.8 - 0.68S + (9.62 \times 10^{-3})S^2$ ($P < 0.05$; $R^2 = 0.55$; df = 11).

Discussion

The dynamics of cnidarian passive suspension feeding

Most cnidarians use passive suspension feeding, even though many forms such as scleractinian corals also possess symbiotic dinoflagellates that supply them with some large fraction of their nutrition (Muscatine and Porter, 1977). While the independence of zooplankton capture from autotrophy has been questioned (Clayton and Lasker, 1982), there is no doubt that for most boreal cnidarians lacking zooxanthellae, capture of particulate prey from the water column is of prime importance in their biology. Hence, modeling of the passive suspension feeding process is worthwhile because (1) it is ubiquitous in marine systems, (2) the particles filtered from the water column are patchy (Wiebe, 1970, 1971; Ortner *et al.*, 1984), *i.e.*, discontinuously distributed in space and time,

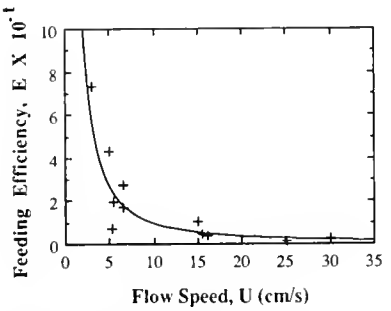

Figure 10. Efficiency (E) of particle capture *per* colony in *Alcyonium* as a function of flow speed (U). Efficiency is defined as the number of particles caught by the colony in the time interval to saturation of the colony divided by the number of particles that would have passed through the space occupied by the colony. The regression is given by the equation: $E = 32.30U^{-1.62}$ ($P < 0.05$; $R^2 = 0.81$; df = 11). These flow speeds correspond to a Reynolds number (Re) range of 800–12,000 calculated using the greatest dimension of each colony.

Table I

Field measurements of flow speed 1.0 cm and 10.0 cm above colonies of Alcyonium *at four subtidal sites in Massachusetts Bay (December 1981–September 1984)*

		1.0 cm			10.0 cm		
Site	Depth (m)	Dives	Flow speed (cm/s)	Re × 10^2	Dives	Flow speed (cm/s)	Re × 10^2
Halfway Rock	14	10	18.8 (9.8)	90.8 (47.3)	11	18.4 (10.6)	88.9 (51.2)
Shag Rocks Inner	7	18	8.7 (7.2)	42.0 (34.8)	18	10.2 (9.7)	49.3 (46.9)
Shag Rocks Outer	9	20	10.5 (8.5)	50.7 (41.1)	21	11.3 (8.2)	54.6 (39.6)
Dive Beach	8	23	9.3 (7.1)	44.9 (34.3)	24	9.3 (7.6)	44.9 (36.7)

Flow was sampled at 3 Hz for 6 minutes per date.
Reynolds number (Re) was calculated for a colony 5 cm in greatest dimension.
Values are mean (standard deviation).

and the feeding response of these organisms to patches may have important effects on growth and metabolism (Szmant-Froelich and Pilson, 1984), or competition for food and space (Okamura, 1984), and (3) any predictive model must make assumptions that will offer insight into which features of the system are the most important.

Patchiness of particles is a common phenomenon in aquatic systems; the causes can be both biological (nutrient tracking, mass spawning) and abiotic (eddy entrainment) in origin (reviewed in Okubo, 1980). Passive suspension feeders respond to patchiness in interesting ways. Leversee (1976) found that an octocoral could alter its feeding rate in response to jumps in prey concentration. Crowell (1957) observed that a hydroid grew better on a single large daily ration of food than more frequent feedings, implicating more efficient digestion in a packed gut (coelenteron). Lasker *et al.* (1982) discovered that *Hydra* interrupts its feeding to digest its prey; therefore a single large feeding (dense prey) is just as good as a continuous supply. The response of *Alcyonium* to patch concentrations is interesting, especially when contrasted with the capture of prey in the field under more dilute conditions (Sebens and Koehl, 1984).

Lasker *et al.* (1982) used prey concentrations more than an order of magnitude greater than those used in this study. Plankton densities over coral reefs (Alldredge and King, 1977) and near boreal subtidal rock walls (K. Sebens, Northeastern University, pers. comm.) can often be greater than those in the water column nearby. Densities of plankton in freshwater aquatic systems are typically on the order of tens of plankters *per* liter (Wetzel, 1975); comparable densities are found in New England inshore waters (Sebens, 1984). The concentrations used in this study were on the order of 100/l. By comparison, oligotrophic oceanic waters usually have less than one zooplankter *per* liter (Ortner, *et al.*, 1981). Feeding on high densities of prey resulted in a curvilinear feeding response for the octocoral species investigated in this study. *Alcyonium* did not feed markedly faster at enhanced levels of prey density, in contrast to previous work with scleractinians (Lasker, 1976; Clayton and Lasker, 1982).

Handling time, filtration time, and flow in the field

Part of the error in the predictions of the parameter values of the model (Fig. 6) can be attributed to the variation in handling time (R_1). The mean handling time for a particle was 8.0 s (SD = 3.0; n = 20 colonies). It was not possible to measure handling time and capture events simultaneously, so the mean handling time was used to calculate the model parameters. The filtration resistance (R_2), is not subject to as wide a variation within a colony unless the organism changes its size by pumping water into its gastrovascular spaces. Size change is usually a response to severe hydromechanical stress (*cf.* Patterson, 1980); these organisms do not appear to regulate feeding rate through size changes except to turn feeding on and off. Robbins and Shick (1980) found similar behavior in the sea anemone *Metridium senile*. Colonies did not change size during the course of these feeding experiments. During ontogeny, the potential exists for *Alcyonium* colonies to reduce the value of the filtration time, R_2, by growing in an oriented fashion to the predominant direction of flow. This indeed seems the case (Fig. 8).

The flow regime experienced by these colonies over a three year period at the four sites demonstrates a wide range of flow speeds (Table I), with mean flows on the order of 10–20 cm/s. This corresponds to a whole colony Reynolds number of *ca.* 5,000 to 10,000. The flow at these depths is tidally driven and is often dominated by wave-induced oscillations (Patterson and Sebens, 1989). Colonies generally do not feed as velocities approach 50 cm/s (unpubl. obs.) and instead begin contraction.

The time constant of organism "filling" (τ) depends on colony size, handling time, and filtration time. Handling time was so much larger than filtration time for the particle

fluxes tested, that it dominated the time constant. For example, at the lowest particle flux tested {0.25 part./($cm^2 \cdot s$)}, the handling time was three orders of magnitude greater than the filtration time for a typical colony with a projected surface area of 10 cm^2. At what particle flux would the handling time and the filtration time become comparable in magnitude, *i.e.*, at what particle concentration and flow speed would passive suspension feeding be expected to be *responsive* to the *changes* in particle flux? For the same size colony considered above, the handling time will equal the filtration time at a particle flux of 0.01 part./($cm^2 \cdot s$). What are particle fluxes like in the field?

Comparison with field data: do colonies become more efficient at lower particle fluxes?

Using the data of Sebens (1984) and Sebens and Koehl (1984), it is possible to calculate how many particles are caught by *Alcyonium* in the field, and make some order of magnitude calculations of the particle flux they are experiencing. Knowing the prey caught and the particle flux, we can calculate efficiency of capture. Particle flux is the product of prey concentration and flow speed. Flow speeds have been measured (Sebens, 1984; Table I) and Sebens (1984) reports plankton concentrations averaging about 3500 zooplankters/m^3, or 3.5 particles/l, in the warmer months of the year at the Nahant, Massachusetts, sites. Flow speeds are on the order of about 10–20 cm/s measured 1.0 cm above the tops of *Alcyonium* colonies. The integrated flow over the colony will show a lower mean value, since the flow speed is reduced as one approaches the substrate through the logarithmic boundary layer (Denny, 1988).

Calculations show that a mean particle flux of 0.04 particles/($cm^2 \cdot s$) occurs around these colonies in the field, not far from the value necessary for equality of the handling time and filtration time for *Alcyonium* [0.01 particles/($cm^2 \cdot s$)]. If the mean flow speed is *ca.* 1 cm/s, the particle flux will be reduced another order of magnitude. Now the filtration time will be much greater than the handling time. Under such conditions, increases in the flow speed or prey concentration will cause an increase in the feeding rate, and a quasi-linear response will be found, similar to that predicted by the linear model! The model described in the Introduction decomposes to the "linear" model of passive suspension feeding described above when the particle flux past the organism is low. When R_2 (filtration time) is large compared to R_1 (handling time), α becomes almost one. The second term of Eq. (12) goes to zero; hence prey in the water becomes prey in the organism. In essence, as the particle flux becomes lower (through slower flow or lower prey concentrations), the model predicts instantaneous step responses (capture) of single plankters or 100% efficiency. Are field data on feeding consistent with this prediction of high feeding efficiency?

Sebens and Koehl (1984) sampled gut contents of the sea anemone, *Metridium* and *Alcyonium* over a diel cycle. Using Sebens (1984), the plankton concentration for the site averages about 4 plankters/l during the warmer months. Assume the prey inside the organisms were caught during the previous two hours as *per* Sebens and Koehl (1984). Their data give a mean number of prey per colony of *Alcyonium* (n = 90). Assume each *Alcyonium* colony had a projected surface area normal to the flow capable of capturing prey of 10 cm^2. Given the above plankton density, and an efficiency of 100%, a current of 2.1 cm/s would be needed to account for the gut contents. This flow speed is within the typical range of speeds seen above these organisms (Table I). Of course, these calculations are crude estimates because (1) different sizes and types of plankton are lumped in particle counts, and (2) both species prefer certain types of plankton over others. But high efficiencies for prey capture in *Alcyonium* seem reasonable for field values of flow and prey concentration (non-patch conditions).

Efficiencies measured under very high particle concentrations in the flume were an order of magnitude lower than these field estimates. *This dichotomy is predicted by the model;* at very high plankton concentrations, feeding becomes uncoupled from particle flux; under field conditions, efficiencies skyrocket, presumably due to the lower particle flux and hence favorable (R_2/R_1) ratio. Why couldn't these feeding experiments be repeated in the laboratory using particle fluxes representative of non-patch concentrations? In the flume, feeding was studied at high concentrations over short period of time for two reasons: (1) concentration and hence particle flux remained constant in the flume only over a period of 30 min; after that time, gravitational settlement significantly affects concentration, and (2) at realistic concentrations, capture events are on the order of minutes to large fractions of an hour apart, and would be tedious to document, even if concentration could be kept constant. Using SCUBA, I did spend several hours observing colonies of *Alcyonium* feeding *in situ* at the four sites sampled for flow speed. Because the particles on which they feed are only a few hundred micra in length, this requires approaching within 30 cm of the colony to observe capture events; this necessarily alters the flow around the colony. Only rarely in the field did I see "rapid" capture of prey at a rate comparable to that seen in the flume (seconds between captures); during these rare events there was an easily discerned "cloud" of copepods near the colonies. However, most of the time, the interval between prey capture events (visible particle adhesion followed by movement of the tentacle towards the pharynx) was several minutes in

length, with occasional mind (and body) numbing pauses of up to 10 min between capture events.

An examination of the data of Sebens and Koehl (1984) shows that even under the best conditions, the interval between capture events must be over a minute for *Alcyonium* and 2 min for *Metridium*. Barange and Gili (1988) sampled the coelenteron contents of a benthic hydroid over a diel cycle. From their data [mean prey items captured *per* (polyp · day), number of polyps *per* colony], I calculated the average interval between capture events to be about 1.3 min. Thus, passive suspension feeding for these organisms is a *slow* process for non-patch concentrations of prey. Cnidarian colonies snag particles slowly from the water when a patch isn't around, unlike some vertebrate suspension feeders that capture enormous quantities of particles in the same period of time (Sanderson and Wassersug, 1990).

Saturation of colonies remains a puzzling phenomenon

The utility of this model is that it points out some new directions for work with passive suspension feeding cnidarians. An unanswered question is why are these filters not adapted for high efficiency filtration under high particle fluxes? Is there a biological constraint on the system that limits feeding? Constraints found in other suspension feeding systems include saturation of the filter (Parker, 1975; Real, 1977) or gut-filling (Doyle, 1979). Neither of these constraints appears likely for this species. *Alcyonium* colonies began slowing their feeding rate long before most polyps had successfully fed once. They are also capable of packing many prey items into a single polyp (Patterson, 1984). Lasker *et al.* (1982) showed that in single-polyped *Hydra*, the ingestion of prey was controlled by previous feeding events, *i.e.*, prey captured later in a feeding bout were less likely to be ingested than prey caught near the beginning. Burnett *et al.* (1960) and Hand (1961) showed that nematocyst discharge in *Hydra* is inhibited by food in the gastrovascular cavity, and Lasker *et al.* (1982) speculate that this may be important in limiting ingestion rate. But Ruch and Cook (1984) have demonstrated inactivation of nematocyst discharge even in the absence of food in the gut. This startling observation was explored further by Clark and Cook (1986) using a colonial hydroid. They provide evidence from lab feeding experiments that the accumulation of discharge products from the stenotele nematocysts used by this hydroid in prey capture is sufficient to inhibit further feeding, and that it is not necessary to invoke waste product accumulation from digestion, or depletion of nematocysts, to explain the phenomenon. For those cnidarians exhibiting this interesting feedback, the second assumption of the model (see Introduction) could easily be reformulated to incorporate a term specifying the diffusion time of the nematocyst discharge products. It is unknown whether nematocyst discharge products affect *Alcyonium* in a similar fashion.

The nerve net is also probably involved in the process of modulating prey capture in cnidarians (McFarlane, 1978). Deformation of the tentacle by repeated particle impactions may be important in producing inhibition of nematocyst discharge during feeding in plankton patches. On a larger scale, flow induced deformation of the entire colony may be important in regulating the rate process of prey capture. Best (1988) found that feeding rate in a sea pen, *Ptilosarcus*, increased then decreased with flow speed and attributed this behavior to changes in volume flow rate that occurred as the filtering surfaces changed their orientation. A similar phenomenon was noted in a crinoid (Leonard *et al.*, 1988).

Some experiments that would help solve the mystery of why colonies saturate long before all filtering units (polyps) have fed would include (1) stealing particles from the tentacles after capture but before transfer to the mouth, while monitoring frequency of capture and attempted ingestion events, (2) eliciting repeated nematocyst discharge by micromolar diffusion clouds of amino acids from a micropipette near tentacle tips or mechanical stimulation of tentacles while the cnidarian colony is simultaneously feeding, (3) separating a cnidarian colony into two halves except for a strip of tissue and examining feeding rates in the two halves before and after the connection is severed [Clark and Cook (1986) found no effect for a hydroid], and (4) offering digestible and non-digestible prey to a species that will ingest both types of particles (*cf.* Lasker *et al.*, 1983) and measuring feeding rates on both types of particles separately and together while nematocyst discharge products are monitored.

It is very intriguing that this colonial octocoral saturates after a few minutes of feeding in high prey densities at about the same number of prey that would be caught over a 2–4 h period in the field (Sebens and Koehl, 1984). Digestion of prey items renders them unidentifiable after 4–6 h (Sebens and Koehl, 1984). Have these colonial suspension feeders evolved to "charge their capacitance" on a time scale of approximately two hours because they are limited by the activity of their digestive enzymes? For boreal cnidarians in the Atlantic, the strongest tidal flows will be obtained for a 2–4 h period between slack tides. Because plankton patches are the exception rather than the rule, the feeding response may have evolved to cope with sparse prey moving past the colony over a 2–4 h period. During periods of flow dominated by wave-driven oscillations, *e.g.*, slack tides, colonies will re-filter water already low in prey. Feeding in a bi-directional flow can actually increase feeding success in a hydroid exposed to high (patch) concentration of prey (Hunter, 1989). At present, it is unknown for this species whether feeding

effectiveness is higher in bi-directional flow at *low* prey concentrations.

Application of this model to other passive suspension feeders will test its generality and provide evidence for whether the dichotomy in feeding behavior characteristic of this species when feeding in low and high prey concentrations is a widespread phenomenon. Future developments in the measurement and description of plankton patchiness on a small scale in nearshore waters (Pieper and Holliday, 1985) and description of the benthic boundary layer in which these organisms live (Jumars and Nowell, 1984) will improve our ability to model and understand this fascinating process.

Acknowledgments

Discussions with P. Basser, B. Best, R. Etter, T. Givnish, R. Grosberg, S. Kleinhaus, W. McFarland, T. McMahon, R. Olson, S. L. Sanderson, K. Sebens, R. Turner, the HUMP seminar group, and the Aquatic Sciences group at M. I. T., have improved the paper greatly. P. Rudy, Acting Director, Marine Science Center, Northeastern University, Nahant, Massachusetts, kindly provided laboratory space. C. Alexander and B. Otteson provided technical assistance. Financial support for this project was provided by the Richmond Fund of Harvard University, the Lerner-Gray Fund for Marine Research of the American Museum of Natural History, NSF OCE-8308958 to K. Sebens of Harvard University, a Faculty Research Award from UC Davis, and NSF OCE-8716427 to the author.

Literature Cited

Alldredge, A. A., and J. M. King. 1977. Distribution, abundance, and substrate preferences of demersal reef zooplankton at Lizard Is., Great Barrier Reef. *Mar. Biol.* **41:** 317–334.

Barange, M., and J. M. Gili, 1988. Feeding cycles and prey capture in *Eudendrium racemosum* (Cavolini, 1785). *J. Exp. Mar. Biol. Ecol.* **115:** 281–293.

Best, B. A. 1988. Passive suspension feeding in a sea pen: effects of ambient flow on volume flow rate and filtering efficiency. *Biol. Bull.* **175:** 332–342.

Burnett, A. L., T. Lentz, and M. Warren. 1960. The question of control of the nematocyst discharge reaction by fully fed hydra. *Ann. Soc., Roy. Zool. Blg.* **90:** 247–268.

Clark, S. D., and C. B. Cook. 1986. Inhibition of nematocyst discharge during feeding in the colonial hydroid *Halocordyle disticha* (=*Pennaria tiarella*): the role of previous prey killing. *Biol. Bull.* **171:** 405–416.

Clayton, W. S., Jr., and H. R. Lasker, 1982. Effects of light and dark treatments on feeding by the reef coral *Pocillopora damicornis* (Linnaeus). *J. Exp. Mar. Biol. Ecol* **63:** 269–279.

Coughlan, J. 1969. The estimation of filtering rate from the clearance of suspensions. *Mar. Biol.* **2:** 356–358.

Crowell, S. 1957. Differential responses of growth zones to nutritive level, age and temperature in the colonial hydroid, *Campanularia. J. Exp. Zool.* **134:** 63–90.

Denny, M. 1988. *Biology and the Mechanics of the Wave-Swept Environment.* Princeton University Press, Princeton.

Dorman, R. G. 1966. Filtration. Pp. 195–222 in *Aerosol Science,* C. N. Davies, ed. Academic Press, New York.

Doyle, R. W. 1979. Ingestion rate of a selective deposit feeder in a complex mixture of particles: testing the energy-optimization hypothesis. *Limnol. Oceanogr.* **24:** 867–874.

Emlen, J. M. 1973. *Ecology: An Evolutionary Approach.* Addison-Wesley, Reading, Massachusetts.

Fasham, M. J. R. 1978. The statistical and mathematical analysis of plankton patchiness. *Oceanogr. Mar. Biol. Ann. Rev.* **16:** 43–79.

Fiala-Medioni, A. 1973. Éthologie alimentaire d'invertébrés benthiques filtreurs (ascidies). I. Dispotif experimental. Taux de filtration et de digestion chez *Phallusia mammillata. Mar. Biol.* **23:** 137–145.

Fiala-Medioni, A. 1978a. Filter feeding ethology of benthic invertebrates (ascidians). III. Recording of water current *in situ*–rate and rhythm of pumping. *Mar. Biol.* **45:** 185–190.

Fiala-Medioni, A. 1978b. Filter feeding ethology of benthic invertebrates (ascidians). IV. Pumping rate, filtration rate, filtration efficiency. *Mar. Biol.* **48:** 243–249.

Fiala-Medioni, A. 1978c. Filter feeding ethology of benthic invertebrates (ascidians). V. Influence of temperature on pumping, filtration and digestion rates and rhythms in *Phallusia mammillata. Mar. Biol.* **48:** 251–259.

Fiala-Medioni, A. 1978d. A scanning electron microscope study of the branchial sac of benthic filter-feeding invertebrates (ascidians). *Acta Zool. (Stockholm)* **59:** 1–10.

Grosberg, R. K. 1982. Intertidal zonation of barnacles: the influence of planktonic zonation of larvae on vertical distribution of adults. *Ecology* **63**(4): 894–899.

Hand, C. 1961. Present state of nematocyst research types, structure, and function. Pp. 187–202 in *The Biology of Hydra,* H. M. Lenhoff and W. F. Loomis, eds. Univ. of Miami Press, Miami.

Holling, C. S. 1965. The functional response of predators to prey density and its role in mimicry and population regulation. *Mem. Entomol. Soc. Canada* **No. 45,** 60 pp.

Hunter, T. 1989. Suspension feeding in oscillating flow: the effect of colony morphology and flow regime on plankton capture by the hydroid *Obelia longissima. Biol. Bull.* **176:** 41–49.

Jorgensen, C. B. 1943. On the water transport through the gills of bivalves. *Acta Physiol. Scand.* **5:** 277–304.

Jorgensen, C. B. 1966. *Biology of Suspension Feeding.* Pergamon Press, Oxford.

Jorgensen, C. B. 1975. On gill function in the mussel *Mytilus edulis* L. *Ophelia* **13:** 187–232.

Jumars, P. A., and A. R. M. Nowell. 1984. Fluid and sediment dynamic effects on marine benthic community structure. *Am. Zool.* **24:** 45–55.

LaBarbera, M., and S. Vogel. 1976. An inexpensive thermistor flowmeter for aquatic biology. *Limnol. Oceanogr.* **21:** 750–756.

Lam, R. K., and B. W. Frost. 1976. Model of copepod filtering response to changes in size and concentration of food. *Limnol. Oceanogr.* **21:** 490–500.

Lasker, H. R. 1976. Intraspecific variability of zooplankton feeding in the hermatypic coral *Montastrea cavernosa.* Pp. 101–109 in *Coelenterate Ecology and Behavior,* G. O. Mackie, ed. Plenum, New York.

Lasker, H. R., J. A. Syron, and W. S. Clayton, Jr. 1982. The feeding response of *Hydra viridis:* effects of prey density on capture rates. *Biol. Bull.* **162:** 290–298.

Lasker, H. R., M. D. Gottfried, and M. A. Coffroth. 1983. Effects of depth on the feeding capabilities of two octocorals. *Mar. Biol.* **73:** 73–78.

Lehman, J. T. 1976. The filter-feeder as an optimal forager, and the predicted shapes of feeding curves. *Limnol. Oceanogr.* **21:** 501–516.

Leonard, A. B., J. R. Strickler, and N. D. Holland. 1988. Effects of current speed on filtration during suspension feeding in *Oligometra serripinna* (Echinodermata: Crinoidea). *Mar. Biol.* **97:** 111–122.

Leversee, G. J. 1976. Flow and feeding in fan-shaped colonies of a gorgonian coral, *Leptogorgia*. *Biol. Bull.* **151:** 344–356.

McFarlane, I. D. 1978. Multiple conducting systems and the control of behaviour in the brain coral *Meandrina meandrites* (L.). *Proc. Roy. Soc. Lond. B* **200:** 193–216.

Milsum, J. H. 1966. *Biological Control Systems Analysis.* McGraw-Hill, New York.

Mohlenberg, F., and H. U. Riisgard. 1978. Efficiency of particle retention in 13 species of suspension feeding bivalves. *Ophelia* **17:** 239–246.

Muscatine, L., and J. W. Porter. 1977. Reef corals: mutualistic symbioses adapted to nutrient-poor environments. *BioScience* **27**(7): 454–460.

Okamura, B. 1984. The effects of ambient flow velocity, colony size, and upstream colonies on the feeding sucess of Bryozoa., I. *Bugula stolonifera* Ryland, an arborescent species. *J. Exp. Mar. Biol. Ecol.* **83:** 179–193.

Okubo, A. 1980. *Diffusion and Ecological Problems: Mathematical Models.* (Biomathematics, Vol. 10). Springer Verlag, New York.

Ortner, P. B., L. C. Hill, and H. E. Edgerton. 1981. *In-situ* silhouette photography of Gulf Stream zooplankton. *Deep-Sea Res.* **28A**(12): 1569–1576.

Ortner, P. B., R. L. Ferguson, S. R. Piotrowicz, L. Chesal, G. Berberian, and A. V. Palumbo. 1984. Biological consequences of hydrographic and atmospheric advection within the Gulf Loop Intrusion. *Deep-Sea Res.* **31**(9): 1101–1120.

Palmer, R., and L. Williams. 1980. Effect of particle concentration on filtration efficiency of the Bay Scallop *Argopecten irradians* and the oyster *Crassostrea virginica*. *Ophelia* **19:** 163–174.

Parker, M. 1975. Similarities between the uptake of nutrients and the ingestion of prey. *Verh. Internat. Verein. Limnol.* **19:** 56–59.

Patterson, M. R. 1980. Hydromechanical adaptations in *Alcyonium siderium* (Octocorallia). Pp. 183–201 in *Biofluid Mechanics 2*, D. J. Schneck, ed. Plenum, New York.

Patterson, M. R. 1984. Patterns of whole colony prey capture in the octocoral, *Alcyonium siderium*. *Biol. Bull.* **167:** 613–629.

Patterson, M. R., and K. P. Sebens. 1989. Forced convection modulates gas exchange in cnidarians. *Proc. Nat. Acad. Sci. (USA)* **86:** 8833–8836.

Pieper, R. E., and D. V. Holliday. 1985. Acoustic measurements of zooplankton distributions in the sea. *J. Cons. Cons. Int. Explor. Mer* **41**(3): 226–238.

Real, L. A. 1977. The kinetics of functional response. *Am. Natur.* **111:** 289–300.

Robbins, R. E., and J. M. Shick. 1980. Expansion-contraction behavior in the sea anemone *Metridium senile*: environmental cues and energetic consequences. Pp. 101–116 in *Nutrition in the Lower Metazoa*, D. C. Smith and Y. Tiffon, eds. Pergamon, New York.

Rubenstein, D. J., and M. A. R. Koehl. 1977. The mechanism of filter feeding: some theoretical considerations. *Am. Natur.* **111:** 981–994.

Ruch, R. J., and C. B. Cook. 1984. Nematocyst inactivation during feeding in *Hydra littoralis*. *J. Exp. Biol.* **111:** 31–42.

Sanderson, S. L., and R. Wassersug. 1990. Suspension-feeding vertebrates. *Sci. Am.* **262:** 96–101.

Seale, D. B. 1982. Obligate and facultative suspension feeding in anuran larvae: feeding regulation in *Xenopus* and *Rana*. *Biol. Bull.* **162:** 214–231.

Sebens, K. P. 1979. The energetics of asexual reproduction and colony formation in benthic marine invertebrates. *Am. Zool.* **19:** 683–697.

Sebens, K. P. 1984. Water flow and coral colony size: interhabitat comparisons of the octocoral *Alcyonium siderium*. *Proc. Natl. Acad. Sci. (USA)* **81:** 5473–5477.

Sebens, K. P., and M. A. R. Koehl. 1984. Predation on zooplankton by the benthic anthozoans, *Alcyonium siderium* (Alcyonacea) and *Metridium senile* (Actiniaria) in the New England subtidal. *Mar. Biol.* **81:** 255–271.

Sebens, K. P. 1986. Spatial relationships among encrusting marine organisms in the New England subtidal zone. *Ecol. Monogr.* **56:** 73–96.

Sokal, R. R., and F. J. Rohlf. 1981. *Biometry.* W. H. Freeman, San Francisco.

Szmant-Froelich, A., and M. E. Q. Pilson. 1984. Effects of feeding frequency and symbiosis with zooxanthellae on nitrogen metabolism and respiration of the coral *Astrangia danae*. *Mar. Biol.* **81:** 153–162.

Townsend, C. R., and R. N. Hughes. 1981. Maximizing net energy returns from foraging. Pp. 86–108 in *Physiological Ecology: An Evolutionary Approach*, C. R. Townsend and P. Calow, eds. Sinauer Associates, Sunderland, Massachusetts.

Wetzel, R. G. 1975. *Limnology.* W. B. Saunders, Philadelphia.

Wiebe, P. H. 1970. Small-scale spatial distribution in oceanic zooplankton. *Limnol. Oceanogr.* **15:** 205–217.

Wiebe, P. H. 1971. A computer model study of zooplankton patchiness and its effects on sampling error. *Limnol. Oceanogr.* **16:** 29–38.

Williams, L. G. 1982. Mathematical analysis of the effects of particle retention efficiency on determination of filtration rate. *Mar. Biol.* **66:** 171–177.

Reference: *Biol. Bull.* **180**: 93–102. (February, 1991)

The Effects of Flow on Polyp-Level Prey Capture in an Octocoral, *Alcyonium siderium*

MARK R. PATTERSON

Division of Environmental Studies, University of California, Davis, California 95616

Abstract. Particle capture by individual polyps and tentacles of the octocoral, *Alcyonium siderium*, was investigated in flows of different speed and turbulence intensity. In low flow (U_{mean} = 2.7 cm/s; u′ = 1.2 cm/s, where u′ is the root mean square of the fluctuations from U_{mean}), tentacles on the upstream side of a polyp capture the most prey. In intermediate flow (U_{mean} = 12.2 cm/s; u′ = 6.0 cm/s), downstream tentacles within a polyp catch the most prey. In high flow (U_{mean} = 19.8 cm/s; u′ = 4.0 cm/s), polyps are bent downstream, eddies form over the tentacular surfaces, and the capture distribution over tentacles becomes radially symmetric. At all flow speeds tested, particles are caught with increasing frequency nearer the tip of the tentacle relative to locations near the pharynx. At the highest flow speed tested, no particles are caught on the segment of each tentacle closest to the pharynx. The per polyp capture efficiency is low and drops markedly with increasing Reynolds number. The capture mechanism for this species appears to be direct interception; inertial impaction is shown to be unimportant. Flow modulation of particle capture by polyps is probably a general phenomenon among octocorals.

Introduction

The application of modern engineering theory to the analysis of particle capture by suspension feeding organisms began with a review of the engineering and fluid mechanics literature by Rubenstein and Koehl (1977). The medical community has long been interested in the related problem of how particles are deposited in the tracheobronchial tree of mammalian lungs (Findeisen, 1935; Landahl, 1950, 1963). The theory invoked was the same (McMahon *et al.*, 1977), and importance of flow pattern in affecting the location of particle capture inside lungs was recognized (Bell, 1974). Particle capture mechanisms used by biological filters include direct interception (the particle comes within one particle radius of a filtering surface), inertial impaction (the particle contacts the filter because particle inertia causes it to deviate from a fluid streamline around the filter), diffusive deposition (both Brownian and eddy-enhanced—the motion of the particle across streamlines leads to contact with the filter), sieving (the particle is too large to pass through gaps in the filter geometry), electrostatic attraction (requires net surface charges of opposite sign on filter and particle), and gravitational deposition (a particle denser than the fluid sinks and contacts the filter). Aerosol filtration theory allows estimation of the relative importance of these mechanisms by calculating the ratios of relevant forces acting on particles of different charge, size, and density, in flows of different velocity and viscosity (LaBarbera, 1984).

Recent work in organisms as diverse as conifers (Niklas, 1982a,b), dipteran larvae (Ross and Craig, 1980), polychaetes (Taghon *et al.*, 1980; Merz, 1984), veliger larvae of mollusks (Strathmann and Liese, 1979), ophiuroids (LaBarbera, 1978), bryozoans (Okamura, 1984, 1987), hydroids (Harvell and LaBarbera, 1985; Hunter, 1989), and crinoids (Holland *et al.*, 1987) has extended our knowledge of how biological filters work and how flow speed can affect the geometric pattern of particle capture at the level of the colony or individual. An important generalization from these works is that the coupling between an organism's filter morphology and the resulting flow field, whether generated actively or passively, is extremely important in the particle capture process.

Few studies have examined the mechanics of zooplankton capture by passive suspension feeding cnidarians at the level of the filtering elements themselves, the polyps composed of tentacles. Lewis and Price (1976) investigated mucus feeding in corals. Hunter (1989) demonstrated that feeding effectiveness of hydroid polyps was greater in os-

Received 30 August 1989; accepted 6 November 1990.

cillatory flow compared to steady, unidirectional flow. Harvell and LaBarbera (1985) examined how flexibility affects local flow speeds over polyps in hydroid colonies. Best (1988) has investigated prey capture in the sea pen, *Ptilosarcus gurneyi*, a species that has the polyps arranged at the ends of cantilevered support tissue through which flowing seawater passes. She found that the deformability of the organism strongly affected filtration efficiency and volume of water filtered; in effect the organism could tune its feeding performance by maintaining a variable porosity filter.

While some workers have investigated the location of prey capture on the surface of cnidarian colonies (Leversee, 1976; Lasker, 1981; Patterson, 1984), no studies have addressed the location of prey capture within individual polyps or tentacles. *Alcyonium siderium* Verrill is a planktivorous colonial octocoral common on hard rock substrate in the New England subtidal (Sebens, 1986). Its diet consists largely of small zooplankton; invertebrate eggs, foraminiferans, ascidian larvae, nematodes, harpacticoid and calanoid copepods, barnacle nauplii and cyprids, ostracods, and crustacean fragments were common, although algal material is often present (Sebens and Koehl, 1984). It readily captures and eats live zooplankton and *Artemia* cysts in a laboratory flume (Patterson, 1984). Prey capture events by individual tentacles are easily observed by the naked eye. The subtidal habitats it occupies can differ greatly in water motion (Sebens, 1984; Patterson, 1985), and there is a change in colony morphology of local populations that is correlated with flow regime, with finger-like colonies found in slower flow areas, and lobate ellipsoids and roughly spherical forms found in higher flows (Patterson, 1980). The present study tested whether the location of prey capture within individual polyps and tentacles of the boreal octocoral, *Alcyonium siderium*, is affected by flow patterns over the colony.

Materials and Methods

Colony collection, maintenance, and flow generation and measurement

Polyp feeding experiments were conducted at the Marine Science Center (MSC), Northeastern University, Nahant, Massachusetts, and at the University of California, Davis. Colonies of *A. siderium* were collected and maintained in flowing seawater tables or recirculating chilled aquaria. A recirculating Plexiglas flume (98 liters; 15 cm × 15 cm working section; 1.9 m long) patterned after a design published by Vogel and LaBarbera (1978) and equipped with a chiller (Aquanetics) enabled colonies to feed in flows of various speeds and turbulence intensities at 15°C. Patterson (1984) gives a quantitative description of flow in this particular flume. All experiments were performed with the flow straighteners removed, resulting in higher turbulence in the flow tank and a closer approximation to the flow seen over the colonies in the field (Patterson and Sebens, 1989). Seawater for the flume was obtained from the MSC seawater system and was filtered twice (sand, cotton mesh) to remove particles greater than 20 μm diameter or was made fresh using InstantOcean, and adjusted to a salinity of 34‰.

Flow speeds and turbulence intensities were measured with a two channel thermistor flowmeter circuit modified from LaBarbera and Vogel (1976). The frequency response of the probe plus circuit is 5 Hz at −6 dB down from maximum response. The turbulence intensities may underestimate the true turbulence in the flume, if there is significant energy at frequencies above 5 Hz; this aspect of flume flow regime was not evaluated. The velocity signal was converted into an FM signal for transmission over a distance of several meters to a frequency-to-voltage (f/v) convertor. The output of the f/v convertor was sent to a signal conditioner (custom-made) and eight bit successive approximation A/D convertor (Mountain Computer) connected to an Apple IIe microcomputer. The sampling rate was 10 Hz.

Octocoral colonies attached to mussels (*Modiolus modiolus*) were collected subtidally. Mussel shell fragments bearing *Alcyonium* were mounted securely in the flow tank working section. The prey offered to the colonies were cysts of the brine shrimp, *Artemia*. Characteristics of the cysts are described in Patterson (1984). The cysts are about the same size as the mean prey size taken by *Alcyonium* in the field (Sebens and Koehl, 1984).

Location of prey capture

The spatial location of prey capture on individual polyps of *Alcyonium* was studied in flows of high turbulence levels and differing mean flow speeds. Colonies used ranged from 2 to 8 cm in greatest dimension when expanded. Colonies were all roughly spherical. Prior to an observation period, a single colony was introduced to the flow tank and allowed to acclimate to the flow regime and expand its polyps. A standard volume of seawater (1l) and weight of hydrated cysts (0.45 g) were added to the flow tank at the beginning of the observation period. The flow 1 cm above the observed polyp was adjusted to have a mean value of 2.7, 12.2, or 19.8 cm/s (4 s average achieved through an electronic integrator) by adjusting the speed control on the flume motor. Five minutes into the experiment, three 60-ml samples were withdrawn isokinetically (Brodkey and Hershey, 1988) using a Cole-Parmer peristaltic pump (model no. 7568) smoothed with hydraulic capacitors. Each sample was filtered onto gridded Millipore filters, the cysts counted, and the mean concentration of particles calculated. The range of particle concentrations encountered by the colony among experiments ranged from 0.13 to 0.53 cysts/ml.

Figure 1A shows a typical top view of a polyp after a feeding bout and the coordinate system used to assess location of capture around the polyp's circumference. Note that the coordinate system for the top projections paired tentacles from the bilaterally symmetric halves of the polyp (Fig. 1A). The coordinate variable (x) used for describing capture along individual tentacles is shown in Figure 1B; note that the distance along the tentacle (x) is normalized to the tentacle length (L). Capture events on individual polyps were observed at a magnification of 35× through a dissecting microscope suspended over the flume. A watch glass floating on the water and anchored over the colony prevented blurring of the image from capillary waves at the air/water interface. As a feeding bout progressed, composite maps of capture sites of cysts from individual polyps were made (Fig. 1A). All polyps censused were located near the top of the colony; polyps chosen for observation had their tentacles oriented to the flow (Fig. 1A).

An ocular micrometer permitted measurement of relative position of capture along the length of a tentacle. Only particles caught on the oral side of the tentacles were noted; particles were very rarely captured on the aboral side of the tentacles. The tentacle capture maps were divided into five non-dimensional length sectors. Particle counts in the tentacle length sectors were normalized within a tentacle to the projected area available for particle capture. Surface areas of polyps were computed using a camera lucida and an interactive digitizing tablet (Apple Graphics Tablet). The area of the pinnules was not measured in calculating areas available for capture. Projected surface area of the entire colony was measured similarly.

Feeding efficiency

A dimensionless measure of feeding effectiveness, the efficiency of prey capture at the polyp level was computed as follows: the number of particles caught per polyp during a standard feeding bout was divided by the number of particles passing through the cross-sectional area occupied by the colony (divided by the number of polyps), if the colony were not there. This result is the standard definition of filtration efficiency from engineering theory (Dorman, 1966). The number passing through the cross-sectional area was calculated by integrating the flow over the height and width of the colony and multiplying by the sampled particle concentration. Feeding rate in the dense concentrations of prey used in the flume is not constant, but decreases with time (Patterson, 1991). These concentrations were similar to zooplankton patch concentrations in the field. Hence, efficiency is a function of time. For purposes of comparison, efficiency was computed over the time necessary to reach saturation. Saturation is defined as the point at which capture events drop to less than one prey item caught per 5-min period *per colony*.

Results

Prey capture around the periphery of a polyp

Figure 1C shows the distribution of particle capture around the polyps on the different tentacles as one moves in the downstream direction; the histograms have been adjusted for the amount of surface area available for prey capture. At low flow speeds (U_{mean} = 2.7 cm/s), prey capture is remarkably asymmetric, with upstream tentacles capturing the most prey [Kolmogorov-Smirnov (K-S) test; $P < 0.001$; df = 207]. At intermediate flow speeds (U_{mean} = 12.2 cm/s), the distribution is again asymmetric, but in the opposite direction, with downstream tentacles favored in particle capture (K-S test; $P < 0.001$; df = 205). At the highest flow speed tested (U_{mean} = 19.8 cm/s), the distribution is indistinguishable from an even distribution of prey capture around the tentacles (K-S test; $P > 0.5$; df = 70). The distribution of capture events is thus markedly affected by flow speed. Only at the highest speeds can capture be modeled by a Poisson process.

Prey capture by tentacles

When prey capture events are examined over the length of individual tentacles, an additional pattern emerges (Fig. 2). At low speeds (U_{mean} = 2.7 cm/s), the distribution is significantly asymmetric, with the outer segments of the tentacles capturing the most prey (K-S test; $P < 0.001$; df = 207). The same pattern is found at intermediate flow speeds (U_{mean} = 12.2 cm/s), with the asymmetry shifted even further in the direction away from the pharynx (K-S test; $P < 0.001$; df = 205). Finally, at the highest speed used in the flume (U_{mean} = 19.8 cm/s), the distribution is still asymmetric with a bias toward the tentacle tips (K-S test; $P < 0.001$; df = 70), but with some differences. Capture in the innermost 20% of the tentacle's length has disappeared, and the outermost 20% experiences much more variable prey capture success.

Feeding efficiency

When the efficiency of filtration for individual polyps is examined with respect to Reynolds number (Re) computed for flow around a polyp, a significant inverse relationship is found ($P < 0.05$; df = 11), and the efficiency is remarkably low at all speeds tested for feeding in dense concentrations of prey (Fig. 3). $Re = U_{mean}d/\nu$, where d = polyp oral disk diameter, and ν = kinematic viscosity of seawater. Because polyp size is relatively constant, Re can be viewed as a dimensionless flow speed.

Discussion

Mechanisms of particle impaction

Rubenstein and Koehl (1977) presented dimensionless indices for various mechanisms of particle capture by sus-

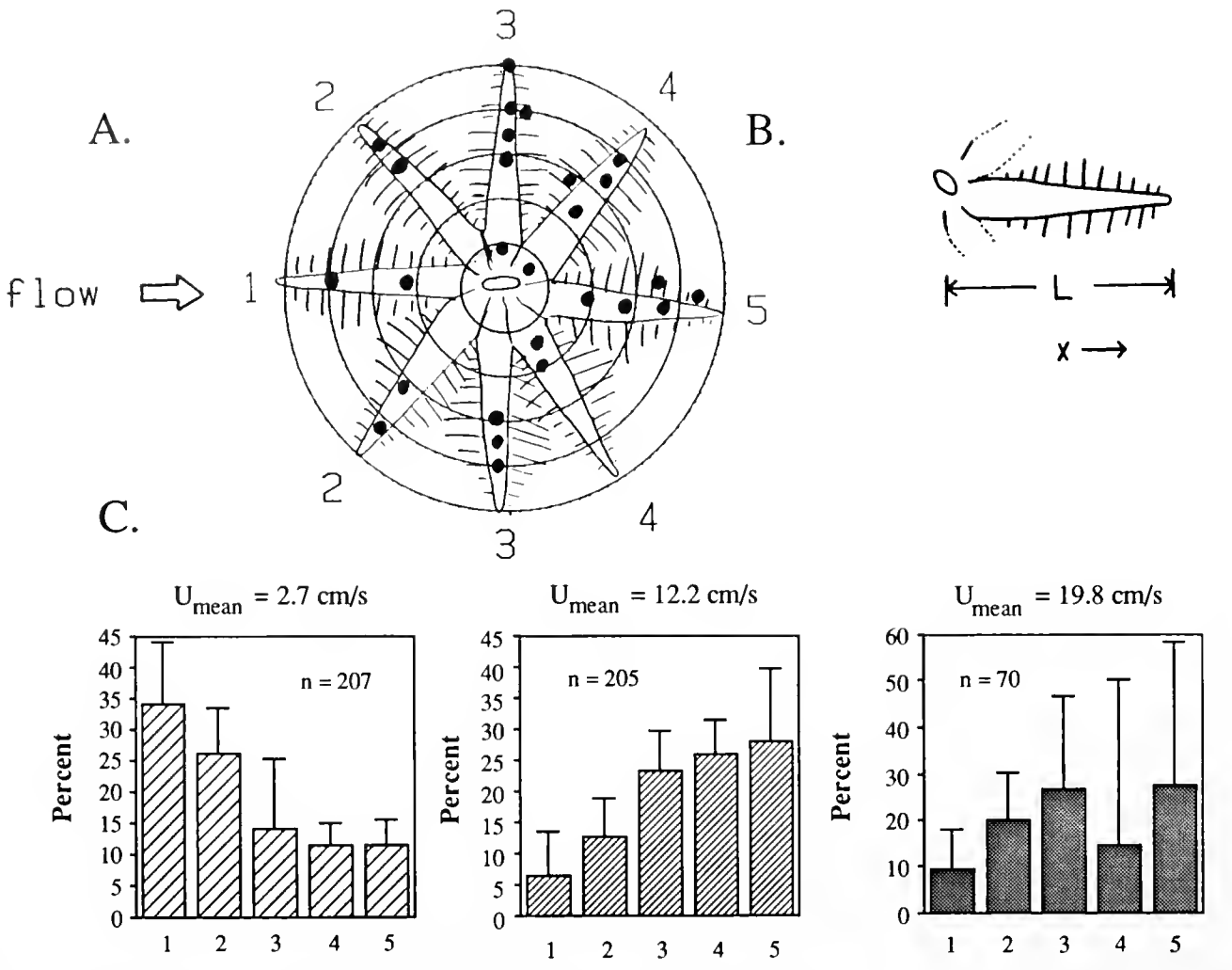

Figure 1. Coordinate system used to quantify prey capture in individual polyps in colonies of *Alcyonium*. (A) Quantification in the circumferential direction around the polyp. Note the pairing of tentacles from the bilaterally symmetric halves of the polyp, *i.e.*, prey caught on tentacles with the same identification number were paired. The five concentric rings delineate the dimensionless length coordinate used for assessing capture by individual tentacles. (B) The distance from the pharynx toward the tentacle tip (X) is divided by the overall length of the tentacle (L) to generate the dimensionless distance (X/L) used as the independent variable (abscissa) in Figure 2. (C) Circumferential position of prey capture events in individual polyps of *Alcyonium* at three different flow speeds. Data from the bilateral halves of the colony are pooled; see Figure 1A for interpretation of abscissa. Capture frequencies are normalized relative to the amount of tentacle area assigned to the numbers one through five. Data were arc-sine transformed and then back-transformed for graphical portrayal. Vertical bars are 95% confidence intervals. For flow speeds of 2.7, 12.2, and 19.8 cm/s, the total numbers of cysts caught were 207, 205, and 70, respectively.

pension feeding organisms. Table I gives these values for polyps of *Alcyonium* feeding on *Artemia* cysts. Note that direct interception or "geometric" interception (Chang, 1973) has the highest value and is thus most likely to be the dominant mechanism of particle capture. For a *rigid* filter, the efficiency of capture by direct interception should be independent of flow speed (Fuchs, 1964); this is contrary to the pattern observed. A formulation of the model more appropriate to aqueous suspensions invokes the importance of short-range (London-van der Waals) forces and does not ignore the hydrodynamic resistance that occurs as the particle squeezes fluid from the space between itself and the filter element (Chang, 1973; La-Barbera, 1984). This more refined theory predicts an in-

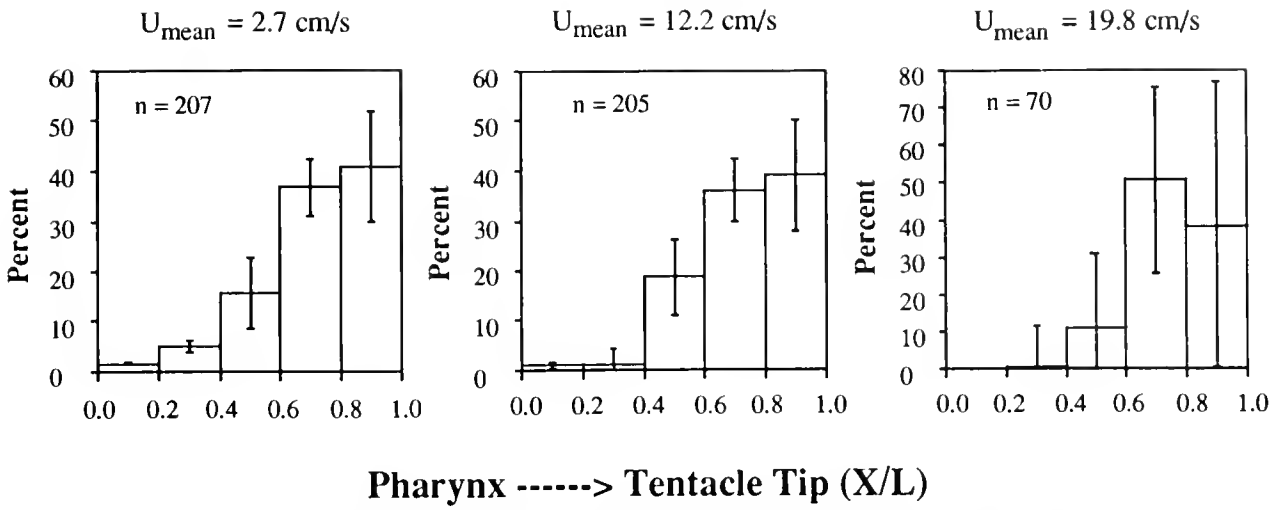

Figure 2. Location of prey capture events along the length of tentacles of polyps in the octocoral *Alcyonium* at three different flow speeds. See Figure 1A for interpretation of abscissa. Capture frequencies are normalized relative to the amount of tentacle area available for prey capture. Data were arc-sine transformed and then back-transformed for graphical portrayal. Vertical bars are 95% confidence intervals. For flow speeds of 2.7, 12.2, and 19.8 cm/s, the total numbers of cysts caught were 207, 205, and 70, respectively.

verse relationship between flow speed at the surface of the filter and efficiency of particle capture and is here observed in *Alcyonium* (Fig. 3). Rubenstein and Koehl (1977) originally predicted that direct interception would be the dominant mode of feeding in aquatic suspension feeders and subsequent work with a diversity of organisms seems to be bearing out their hypothesis (LaBarbera, 1984).

Alcyonium could sieve particles larger than the spacing between pinnules on the tentacles (200–280 μm) as suggested by Sebens and Koehl (1984). However, *Artemia* cysts sieved on the aboral side of a tentacle were almost always dislodged subsequently by the flow and lost to the polyp (pers. obs.). *Artemia* cysts were occasionally sieved by tentacles on the downstream side of the polyp. For larger prey items, sieving may be an important capture mechanism, but probably only for tentacles on the downstream side of a polyp.

The parameter for diffusive deposition assumes the particle has a diffusion coefficient (D) predicted by Brownian motion for a particle of a certain size in a given liquid of a certain temperature and viscosity. If eddy-enhanced diffusion is allowed, the value for D is no longer a constant, but will be a property of the flow speed and eddy size (Richardson, 1926; Okubo, 1971); it can be as much as 10^4 larger than the diffusion coefficient for laminar or "Fickian" diffusion (Okubo, 1980). Turbulent diffusive deposition would increase by a similar factor and would be comparatively more important as the size of the particle of interest decreased, perhaps becoming very important as a mechanism for suspension feeders eating phyto- and bacterioplankton. Schrijver *et al.* (1981) studied particle collection efficiencies by small glass fibers of about the same diameter as the tentacles in *Alcyonium*. For small particles (*ca.* 5 μm), diffusive deposition was a very significant mechanism. More work is needed in this area, which is technically difficult, because eddy diffusivities near surfaces must be measured (Denny, 1988), and

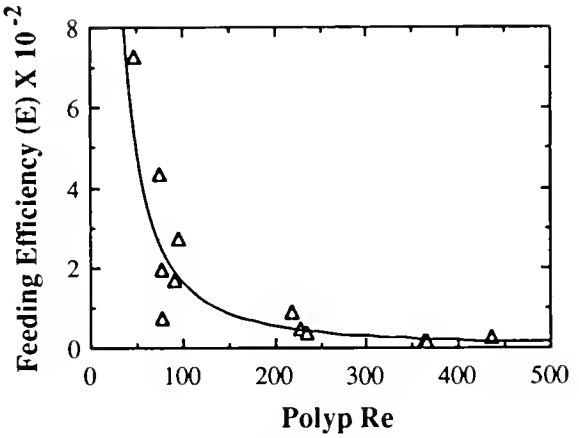

Figure 3. Efficiency (E) of particle capture per polyp in colonies of *Alcyonium* as a function of polyp Reynolds number (Re). Efficiency is defined as the number of particles caught by the polyp in the time interval to saturation of the colony, divided by the number of particles that would have passed through the space occupied by the polyp. Reynolds number was calculated using the oral disk diameter of the polyp and flow speed measured 1.0 cm above the oral disk. Whole colony Re for the specimens used was 10–40 × greater than polyp Re. The regression is given by the equation: $E = 2066\ Re^{-1.55}$; $P < 0.05$; $r = 0.92$; $df = 11$.

the convection of unfiltered water to the vicinity of the filter should be considered. Methods of carefully releasing dye and studying its motion near filter feeders using image processing techniques are being developed to allow better investigation of microscale turbulent diffusive deposition (unpub. obs.).

Rates of particle encounter and possible capture by gravitational deposition are independent of flow speed but directly proportional to settling velocity. The settling velocity for *Artemia* cysts is absolutely low, so the total flux of particles to the polyps via this mechanism is much lower than the contribution provided by direct interception. It is unlikely that natural food particles have settling velocities appreciably greater than *Artemia* cysts. The contribution of inertial impaction to the capture of particles at higher Reynolds number could be a potentially important mechanism if particle inertia is appreciable. The upstream side of an individual tentacle will have a stagnation point and the flow will split at this point (Fig. 4) and flow around the tentacle at low flow speeds or up and over the tentacular crown at higher Re (Patterson, 1984). A calculation in the Appendix demonstrates that this mechanism is highly unlikely to be an important mode of particle capture by polyps in this octocoral.

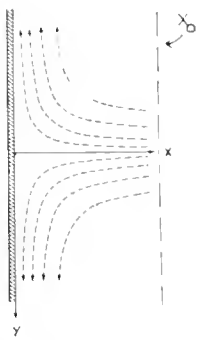

Figure 4. Streamlines of fluid flow near the upstream stagnation point of a filter (Bird *et al.*, 1960), where inertial impaction is most likely to occur. X and Y are directional coordinates. The upstream plane (indicated by X_0) marks where particles carried by the flow have not yet deviated from the streamlines due to their inertia. See the Appendix for a derivation showing how inertial impaction is not likely to be an important capture mechanism for cnidarians that use passive suspension feeding.

Feeding efficiency of cnidarian filters

The filtration efficiency as calculated *per* Dorman (1966) is very low for individual polyps (Fig. 3); a possible explanation involves partitioning capture efficiency into collection efficiency and adhesion efficiency (Weber *et al.*, 1983). Many particles that appear to strike the surface of *Alcyonium* tentacles are not trapped; relatively few are lost if they initially adhere, although J. Miles (Northeastern Univ. pers. comm.) found that adhesion and loss was significantly affected by flow speed in the sea anemone, *Metridium senile*, and Leonard *et al.* (1988) found that flow speed affected capture probabilities in a crinoid. My study of capture at the level of the polyp addresses successful prey capture events only.

Future work on the mechanisms of particle capture by cnidarians should investigate the role of unsuccessful adhesions. In particular, the importance of London-van der Waals forces *versus* nematocyst firing should be ex-

Table I

Values of dimensionless parameters for four potential modes of particle capture (cf. Rubenstein and Koehl, 1977) in the octocoral Alcyonium siderium *feeding on* Artemia *cysts at two different flow speeds commonly encountered in nature*

	Gravitational deposition $N_{gd} = \frac{U_g}{U_0}$	Direct interception $N_{di} = \frac{d_p}{d_f}$	Inertial impaction $N_{ii} = \frac{(\rho_p - \rho_m)\, d_p^2}{18\, \mu d_f}$	Diffusive deposition $N_{dd} = \frac{D}{d_f U_0}$
U_0 = 3.0 cm/s	0.027	0.67	4.0×10^{-6}	8.2×10^{-11}
U_0 = 30.0 cm/s	0.003	0.67	4.0×10^{-5}	8.2×10^{-12}

d_p = particle diameter = 0.02 cm (Patterson, 1984).
d_f = filter element diameter = 0.03 cm (Sebens and Koehl, 1984).
U_g = Stokes' settling velocity = 0.08 cm/s (Gibbs, 1985).
ρ_p = density of particle = 1.05 g/ml (Gibbs, 1985).
ρ_m = density of seawater = 1.02 g/ml at 10°C (Zerbe and Taylor, 1953).
μ = dynamic viscosity of seawater = 1.4×10^{-2} g/(cm·s) at 10°C (Sverdrup *et al.*, 1942).
U_0 = flow near the tentacle (two values used in table above; *cf.* Patterson, 1984; Patterson and Sebens, 1989).
D = diffusion coefficient of an *Artemia* cyst = $\frac{KT}{6\pi\mu d_p} = 7.4 \times 10^{-12}$ cm²/s.
KT = energy of thermal fluctuation = 3.9×10^{-14} (g·cm²)/s².

plored, as current data are insufficient to address this issue. The subject bears further attention because Best (1988) also found that feeding efficiency was an inverse function of flow speed (read Reynolds number) in the sea pen, *Ptilosarcus gurneyi*. She attributed this decline to the predicted behavior of particles that are caught by direct interception (Spielman, 1977), perhaps aided by a deformation of the filter elements as the hydrodynamic drag increased. *Alcyonium* polyps on the upstream side of colonies deform in strong flows while polyps in the wake undergo little deformation (Patterson, 1984). The octocorals she studied are more efficient than *Alcyonium* by a factor of five at a similar flow speed. This study used only polyps located near the top of the colony. Increasing mechanical deformation of this subpopulation of polyps occurred at higher flows, resulting in less surface area available for prey capture, but the reduction was detected in the measurements of projected colony surface area. The reasons for this interspecific difference in feeding effectiveness are presently unknown.

Particle capture locations

The patterns of prey capture seen (Figs. 1C, 2) are in agreement with a direct interception model of prey capture. Polyps resemble inverted umbrellas (see photograph in Sebens and Koehl, 1984); they do not hold their tentacles in a flat canopy as the top view in Figure 1A might imply. At low speeds, the first tentacles to encounter particles are the upstream ones, and here capture is more likely. As the flow speed increases, the polyps are bent by the flow (*cf.* Patterson, 1984), and the aboral side of the upstream polyps is presented to the flow. For prey particles the size of *Artemia* cysts (*ca.* 200 μm; close in value to the mean size of natural zooplankton prey, Sebens and Koehl, 1984), few particles are caught on these upstream tentacles because particles do not adhere to the aboral side. The downstream tentacles then begin feeding. In strong flows, the polyp is severely bent downstream, and a small eddy forms over the tentacular disk (pers. obs.); the distribution becomes roughly symmetric again. The relative roles that attached eddy formulation and turbulent diffusion play in this smoothing out of the particle capture distribution are unknown.

These experiments were conducted under turbulent but steady flow conditions. *Alcyonium* occurs over a range of depths and habitats in the shallow subtidal; it is exposed to both oscillatory flow from wind-driven waves and to steady tidal flows (Patterson, 1984, 1985). The particle capture behavior of individual polyps and tentacles might be quite different in an oscillating flow. Hunter (1989) found that the feeding effectiveness of the hydroid *Obelia longissima* was much greater in an oscillating flow relative to a steady current. *Alcyonium* colonies are inherently more rigid than those of *Obelia*, and hence it is not clear without further experimentation whether oscillatory flow would result in enhanced feeding in *Alcyonium*. Thus these results should be applied only to feeding in the field under steady flow conditions when wind-driven oscillations have a small contribution to the flow field.

The distribution of particle capture over the length of an individual tentacle is also in agreement with a geometric (direct) interception model. Parts of the tentacle furthest out of the boundary layer of the polyp intercept the most prey. Patterns of prey capture discerned through flume experiments using non-motile particles such as *Artemia* cysts may be different from those measured using live prey, but only if the loss rate of captured particles differs between the two types of food or the motility of live prey causes the diffusive deposition mechanism to increase capture preferentially at a location different from direct interception. Loss of captured particles is most likely caused by hydrodynamic drag forces exceeding the breaking strength of the attachment between particle and tentacle. Live zooplankton prey and *Artemia* cysts will experience very similar amounts of drag because size and shape are similar. The motility of live zooplankton should result in an increase in the diffusive particle flux relative to *Artemia* cysts, but it should not affect the geometric location of capture on tentacles if movement is random in all directions.

This study has shown how flow regime can dramatically affect patterns of particle capture at the level of the filtering elements in an octocoral. Variation in feeding ability at the level of the polyp caused by hydrodynamics may help explain the variation Lasker (1981) observed in prey capture between polyps and branches in colonies of tropical gorgonians. Capture events in the three species Lasker studied did not fit a Poisson distribution, and he invoked differential feeding ability of the polyps as the cause of the variation. He offered no explanation for the differential feeding ability other than to note that other authors had also seen asymmetric patterns in prey capture by cnidarians (*e.g.*, Leversee, 1976). I have demonstrated that momentum transport (fluid flow) directly affects mass transport (particle capture) at the level of the individual feeding elements, polyps. Upon closer inspection, other passive suspension feeding cnidarians may exhibit similar patterns.

Acknowledgments

This paper has benefited from discussions with P. Basser, T. Givnish, M. Koehl, M. LaBarbera, T. McMahon, R. Olson, S. L. Sanderson, K. Sebens, and R. Turner. T. McMahon provided inspiration and insight into the mechanics of particle deposition through his graduate course on fluid flow in the human body. P. Rudy, Acting Di-

rector, Marine Science Center, Northeastern University, Nahant, Massachusetts, kindly provided laboratory space. C. Alexander provided technical assistance. Financial support for this project was provided by the Richmond Fund of Harvard University, the Lerner-Gray Fund for Marine Research of the American Museum of Natural History, a Faculty Research Award from UC Davis, and NSF OCE87-16427.

Literature Cited

Bell, K. 1974. Aerosol deposition in models of a human lung bifurcation. Ph.D. Dissertation, California Institute of Technology, Pasadena.

Berg, H. C. 1983. *Random Walks in Biology.* Princeton University Press, Princeton.

Best, B. A. 1988. Passive suspension feeding in a sea pen: effects of ambient flow on volume flow rate and filtering efficiency. *Biol. Bull.* **175:** 332–342.

Bird, R. B., W. E. Stewart, and E. N. Lightfoot. 1960. *Transport Phenomena.* John Wiley, New York.

Brodkey, R. S., and H. C. Hershey. 1988. *Transport Phenomena: A Unified Approach.* McGraw-Hill, New York.

Chang, D. P. Y. 1973. Particle collection from aqueous suspensions by solid and hollow single fibers. Ph.D. Dissertation, California Institute of Technology, Pasadena.

Denny, M. 1988. *Biology and the Mechanics of the Wave-Swept Environment.* Princeton University Press, Princeton.

Dorman, R. G. 1966. Filtration. Pp. 195–222 in *Aerosol Science,* C. N. Davies, ed. Academic Press, New York.

Findeisen, W. 1935. Uber das Abstetzen kleiner, in der Luft suspendierter Teilchen in der menschlichen Lunge bei der Atmung. *Pfluger Arch. Ges. Physiol.* **236:** 367–379.

Fuchs, N. A. 1964. *The Mechanics of Aerosols.* Pergamon Press, New York.

Gibbs, R. J. 1985. Estuarine flocs: their size, settling velocity, and density. *J. Geophys. Res.* **90(C2):** 3249–3251.

Glauert, M. 1940. A method of constructing the paths of raindrops of different diameters moving in the neighbourhood of (1) a circular cylinder, (2) an aerofoil, placed in a uniform stream of air; and a determination of the rate of deposit of the drops on the surface and the percentage of drops caught. *Aeronaut. Res. Council, Reports and Memoranda No. 2025,* London.

Harvell, D., and M. LaBarbera. 1985. Flexibility: a mechanism for control of local velocity in hydroid colonies. *Biol. Bull.* **168:** 312–320.

Holland, N. D., A. B. Leonard, and J. R. Strickler. 1987. Upstream and downstream capture during suspension feeding by *Oligometra serripinna* (Echinodermata: Crinoidea) under surge conditions. *Biol. Bull.* **173:** 552–556.

Hunter, T. 1989. Suspension feeding in oscillating flow: the effect of colony morphology and flow regime on plankton capture by the hydroid *Obelia longissima. Biol. Bull.* **176:** 41–49.

Koehl, M. A. R., and J. R. Strickler. 1981. Copepod feeding currents: food capture at low Reynolds number. *Limnol. Oceanogr.* **26:** 1062–1093.

LaBarbera, M. 1978. Particle capture by a Pacific brittle star: experimental test of the aerosol suspension feeding model. *Science* **201:** 1147–1149.

LaBarbera, M. 1984. Feeding currents and particle capture mechanisms in suspension feeding animals. *Am. Zool.* **24:** 71–84.

LaBarbera, M., and S. Vogel. 1976. An inexpensive thermistor flowmeter for aquatic biology. *Limnol. Oceanogr.* **21:** 750–756.

Landahl, H. D. 1950. On the removal of air-borne droplets by the human respiratory tract: I. The lung. *Bull. Math. Biophys.* **12:** 43–56.

Landahl, H. D. 1963. Particle removal by the respiratory system: note on the removal of airborne particulates by the human respiratory tract with particular reference to the role of diffusion. *A. M. A. Arch. Ind. Hyg. Occup. Med.* **25:** 29–39.

Lasker, H. R. 1981. A comparison of the particulate feeding abilities of three species of gorgonian soft coral. *Mar. Ecol. Prog. Ser.* **5:** 61–67.

Leversee, G. J. 1976. Flow and feeding in fan-shaped colonies of a gorgonian coral, *Leptogorgia. Biol. Bull.* **151:** 344–356.

Leonard, A. B., J. R. Strickler, and N. D. Holland. 1988. Effects of current speed on filtration during suspension feeding in *Oligometra serripinna* (Echinodermata: Crinoidea). *Mar. Biol.* **97:** 111–122.

Lewis, J. B., and W. S. Price. 1976. Patterns of ciliary currents in Atlantic reef corals and their functional significance. *J. Zool.* **178:** 77–89.

McMahon, T. A., J. D. Brain, and S. Lemott. 1977. Species differences in aerosol deposition. Pp. 23–33 in *Inhaled Particles IV,* W. H. Walton, ed. Pergamon Press, Oxford.

Merz, R. 1984. Self-generated versus environmentally produced feeding currents: a comparison for the Sabellid polychaete *Eudistylia vancouveri. Biol. Bull.* **167:** 200–209.

Niklas, K. J. 1982a. Pollination and airflow patterns around conifer ovulate cones. *Science* **217:** 442–444.

Niklas, K. J. 1982b. Simulated and empiric wind pollination patterns of conifer ovulate cones. *Proc. Nat. Acad. Sci. USA* **79:** 510–514.

Okamura, B. 1984. The effects of ambient flow velocity, colony size, and upstream colonies on the feeding success of Bryozoa., I. *Bugula stolonifera* Ryland, an arborescent species. *J. Exp. Mar. Biol. Ecol.* **83:** 179–193.

Okamura, B. 1987. Particle size and flow velocity induce an inferred switch in bryozoan suspension-feeding behavior. *Biol. Bull.* **173:** 222–229.

Okubo, A. 1971. Oceanic diffusion diagrams. *Deep-Sea Res.* **18:** 789–802.

Okubo, A. 1980. *Diffusion and Ecological Problems: Mathematical Models.* (Biomathematics, Vol. 10). Springer Verlag, New York.

Patterson, M. R. 1980. Hydromechanical adaptations in *Alcyonium siderium* (Octocorallia). Pp. 183–201 in *Biofluid Mechanics 2,* D. J. Schneck, ed. Plenum, New York.

Patterson, M. R. 1984. Patterns of whole colony prey capture in the octocoral, Alcyonium siderium. *Biol. Bull.* **167:** 613–629.

Patterson, M. R. 1985. The effects of flow on the biology of passive suspension feeders: prey capture, feeding rate, and gas exchange in selected cnidarians. Ph.D. dissertation, Harvard University, Cambridge. Massachusetts.

Patterson, M. R., and K. P. Sebens. 1989. Forced convection modulates gas exchange in cnidarians. *Proc. Nat. Acad. Sci. USA* **86:** 8833–8836.

Patterson, M. R. 1991. Passive suspension feeding by an octocoral in plankton patches: empirical test of a mathematical model. *Biol. Bull.* **180:** 81–92.

Richardson, L. F. 1926. Atmospheric diffusion shown on a distance-neighbor graph. *Proc. Roy. Soc. London A* **110:** 709–727.

Ross, D. H., and D. A. Craig. 1980. Mechanisms of fine particle capture by larval black flies (Diptera: Simuliidae). *Can. J. Zool.* **58:** 1186–1192.

Rubenstein, D. J., and M. A. R. Koehl. 1977. The mechanism of filter feeding: some theoretical considerations. *Am. Nat.* **111:** 981–994.

Schrijver, J. H. M., C. Vreeker, and J. A. Wesselingh. 1981. Deposition of particles on a cylindrical collector. *J. Coll. Interf. Sci.* **81:** 249–256.

Sebens, K. P. 1984. Water flow and coral colony size: interhabitat comparisons of the octocoral *Alcyonium siderium*. *Proc. Nat. Acad. Sci. (USA)* **81:** 5473–5477.

Sebens, K. P. 1986. Spatial relationships among encrusting marine organisms in the New England subtidal zone. *Ecol. Monogr.* **56:** 73–96.

Sebens, K. P., and M. A. R. Koehl. 1984. Predation on zooplankton by the benthic anthozoans, *Alcyonium siderium* (Alcyonacea) and *Metridium senile* (Actiniaria) in the New England subtidal. *Mar. Biol.* **81:** 255–271.

Spielman, L. A. 1977. Particle capture from low-speed laminar flows. *Annu. Rev. Fluid Mech.* **9:** 297–319.

Strathmann, R. R., and E. Liese. 1979. On feeding mechanisms and clearance rates of molluscan veligers. *Biol. Bull.* **157:** 524–535.

Sverdrup, H. U., M. W. Johnson, and R. H. Fleming. 1942. *The Oceans: Their Physics, Chemistry, and Biology.* Prentice-Hall, New York.

Taghon, G. L., A. R. M. Nowell, and P. A. Jumars. 1980. Induction of suspension feeding in spionid polychaetes by high particle fluxes. *Science* **210:** 562–564.

Taylor, G. I. 1940. Notes on possible equipment and technique for experiments on icing on aircraft. *Aeronaut. Res. Council, Reports and Memoranda No. 2024,* London.

Vogel, S., and M. LaBarbera. 1978. Simple flow tanks for research and teaching. *BioScience* **10:** 638–643.

Weber, M. E., D. C. Blanchard, and L. D. Syzdek. 1983. The mechanism of scavenging of waterborne bacteria by a rising bubble. *Limnol. Oceanogr.* **28(1):** 101–105.

Zerbe, W. B., and C. B. Taylor. 1953. Sea water density reduction tables. Pp. 18–19 *in Coast and Geodetic Survey, Special Publ. no. 298.* U. S. Dept. of Commerce, Washington, DC.

Appendix

The following derivation, developed from the work of Glauert (1940) on raindrop capture by airfoils and from Taylor (1940) on aircraft icing, shows how unlikely it is that inertial impaction will be an important mechanism for passive suspension feeding cnidarians for the range of velocities normally encountered in the field.

Consider the motion of a solid particle (*e.g.*, a plankter), moving with a velocity relative to the seawater, as it approaches the upstream end of a filtering organism (Fig. 4). In other words, the particle does not follow the streamlines perfectly. If the Reynolds number (Re) of the particle is on the order of one or less, as it would be for plankton-size particles (Koehl and Strickler, 1981), the forces acting on the particle are due solely to the Stokes' drag (Berg, 1983). The equation governing the motion of the particle in the x-direction is:

$$\frac{4}{3}\pi r^3 \rho_s \frac{dU_p}{dt} = 6\pi r\mu(U - U_p) \qquad \text{(Eq. 1)}$$

where r = particle radius, ρ_s = particle density, μ = dynamic viscosity, U_p = velocity component of the particle in the x-direction, and U = velocity component of the seawater in the x-direction.

The velocity components in the y- and z-directions are V and W, respectively, and the equations of motion are similar. If I define:

$$k_0 = \frac{2\rho_s r^3}{9\mu} \qquad \text{(Eq. 2)}$$

then (Eq. 1) becomes:

$$k_0 \frac{dU_p}{dt} = U - U_p \qquad \text{(Eq. 3)}$$

and other directions can be transformed similarly.

The equations of motion must be solved subject to the initial conditions. Let me introduce a scaled time variable,

$$T = \frac{t}{k_0} \qquad \text{(Eq. 4)}$$

and the differential operator,

$$\frac{d}{dT} = k_0 \frac{d}{dt} \qquad \text{(Eq. 5)}$$

Now (Eq. 3) becomes

$$\frac{dU_p}{dT} = U - U_p \qquad \text{(Eq. 6)}$$

and similarly for the other directions.

Flow near the upstream stagnation point of the filter will look like Figure 4 (Bird *et al.*, 1960). The velocity field near the stagnation point is given by:

$$U = -cx \qquad \text{(Eq. 7)}$$

and

$$V = cy \qquad \text{(Eq. 8)}$$

Substituting into (Eq. 6), I obtain:

$$\frac{d^2x}{dT^2} + \frac{dx}{dT} + ck_0x = 0 \qquad \text{(Eq. 9)}$$

It is reasonable to assume that upstream of the tentacle a certain distance, X_0, the flow field is not distorted by the presence of the tentacle and the particle is following the streamlines of the moving seawater (see Fig. 4). If the time at which the particle starts to deviate from the streamlines of flow is called T = 0, I obtain:

$$x(0) = -X_0 \qquad \text{(Eq. 10)}$$

$$\frac{dx}{dt} = ck_0X_0 \qquad \text{(Eq. 11)}$$

A reasonable guess to the solution of (Eq. 11) is one of the form $x(t) = Ae^{pt}$, where A = constant. The characteristic equation is thus,

$$p^2 + p + ck_0 = 0 \qquad \text{(Eq. 12)}$$

The roots of the equation are:

$$p_{1,2} = \frac{-1 \pm \sqrt{1 - 4ck_0}}{2} \qquad \text{(Eq. 13)}$$

When one of the roots is imaginary, the solution to the equation of motion of the passing particle will be oscillatory, *i.e.*, the particle position and the filter position will eventually coincide ($x = 0$). This condition will occur when:

$$4ck_0 > 1 \qquad \text{(Eq. 14)}$$

Glauert (1940) showed for a cylindrical geometry that a negligible number of particles will impact if $k_0c \leq 0.125$, where $c = 2$ and the definition of k_0 is as follows:

$$k_0 = \frac{2\rho_s r^2 RU}{9\rho R^2 \nu} \qquad \text{(Eq. 15)}$$

where R = radius of the filter, and $\nu = \mu/\rho$, the kinematic viscosity of the seawater.

Using reasonable values for flow around an *Alcyonium* colony, I obtain $k_0c = 0.003$, for $\rho = 1.024$ g/cm^3, (Zerbe and Taylor, 1953), $\rho_s = 1.049$ g/cm^3, (Gibbs, 1985), $r = 100 \times 10^{-4}$ cm, R = 5 cm, U = 5 cm/s, $\nu = 1.36 \times 10^{-2}$ cm^2/s for seawater at 10°C (calculated from Sverdrup *et al.*, 1942). If the flow speed increases by an order of magnitude to U = 50 cm/s, then $k_0c = 0.034$. Appreciable impaction will not occur until U = 185 cm/s, far above the range of speeds normally encountered near this species (Patterson and Sebens, 1989). Such a flow would only be found under stormy conditions in the subtidal or in tidal currents in fjords. *Alcyonium* contracts its prey-capturing surfaces long before this flow speed is obtained (Patterson, 1980).

Reference: *Biol. Bull.* **180**: 103–111. (February, 1991)

Differential Ingestion and Digestion of Bivalve Larvae by the Scyphozoan *Chrysaora quinquecirrha* and the Ctenophore *Mnemiopsis leidyi*

JENNIFER E. PURCELL[1], FRANCES P. CRESSWELL[1], DAVID G. CARGO[2], AND VICTOR S. KENNEDY[1]

The University of Maryland

Abstract. We investigated predation on bivalve veligers by the scyphozoan *Chrysaora quinquecirrha* and the ctenophore *Mnemiopsis leidyi*. We found that the medusa stage of *C. quinquecirrha* captures, but does not digest, veliger larvae: 99% of oyster veligers (*Crassostrea virginica*) caught by medusae were egested alive within 7 h of capture, and 98% survived for 24 h after egestion; 98% of oyster, mussel (*Mytilus edulis*), and clam (*Mulinia lateralis*) veligers placed on the oral arms of medusae were rejected; all bivalve veligers in field-collected medusae were closed and full of tissue. Our laboratory evidence suggests that the shell of larval bivalves probably offers protection from medusae: 23% of dead, open veligers were ingested by medusae compared with 0.7% of live, closed veligers; open veligers were retained longer than closed veligers; and tissue excised from recently settled oyster larvae was ingested and digested. Freeswimming *C. quinquecirrha* ephyrae ingested but did not digest veligers. By contrast, the benthic scyphistoma stage ingested 69% of veligers that contacted their tentacles and digested 48% of those ingested. Each scyphistoma consumed an average of 1 veliger/day at densities of 0.3 veligers ml^{-1}. However, larval settlement was not reduced on oyster shells bearing scyphistomae. By contrast to the results on *C. quinquecirrha*, ctenophores egested only 4% of veligers alive, and 25% of the veligers in their gut contents were digested. Predation on veligers by ctenophores was estimated to be 0.2 to 1.7%/day in Chesapeake Bay. We conclude that *C. quinquecirrha* medusae are not important predators of bivalve veligers, but rather may reduce their mortality by consuming ctenophores, which do eat veligers.

Received 14 August 1990; accepted 6 November 1990.

[1] Horn Point Environmental Laboratories, P. O. Box 775, Cambridge, Maryland 21613.

[2] Chesapeake Biological Laboratory, Box 38, Solomons, Maryland 20688-0038.

Introduction

Predation on planktonic larvae is one of the least understood factors affecting abundance of adult benthic invertebrates (Young and Chia, 1987). Early studies reported that the scyphomedusan *Chrysaora quinquecirrha* (DeSor) and the ctenophore *Mnemiopsis leidyi* A. Agassiz may prey heavily upon the larvae of the eastern oyster *Crassostrea virginica* (Gmelin) (Truitt and Mook, 1925; and Nelson, 1925, 1953, respectively). Both species are seasonally abundant in Atlantic coast estuaries, and co-occur with oyster larvae. Their effects on survival of oyster larvae have not been documented.

In several Atlantic coast estuaries, *M. leidyi* has been shown to be an important predator of crustacean zooplankton (*e.g.*, Cronin *et al.*, 1962; Cargo and Schultz, 1967; Bishop, 1967; Burrell, 1968; Herman *et al.*, 1968; Kremer, 1979; Deason and Smayda, 1982; Feigenbaum and Kelly, 1984; Olson, 1987) and bivalve veliger larvae (Nelson, 1925; Truitt and Mook, 1925; Burrell and Van Engel, 1976). Bivalve veligers were 75% of the prey of *M. leidyi* in New Jersey waters, and high larval settlement of three bivalve species, including oysters, occurred in years when ctenophore densities were low (Nelson, 1925). In the York River, Virginia, bivalve larvae were inversely related to the biomass of ctenophores (Burrell and Van Engel, 1976).

Studies on the feeding of scyphomedusae have shown them to eat a variety of zooplankton (reviewed in Larson, 1978; Clifford and Cargo, 1978; Feigenbaum and Kelly, 1984; Larson, 1987; Fancett, 1988; Brewer, 1989). Al-

though *C. quinquecirrha* medusae were reported to feed on oyster larvae (Truitt and Mook, 1925; Loosanoff, 1974), high numbers of oyster larvae and medusae often co-occurred (Truitt and Mook, 1925). This apparent paradox may be due to the fact that *C. quinquecirrha* medusae prey heavily upon ctenophores (Cargo and Schultz, 1967; Burrell, 1968; Miller, 1974; Feigenbaum and Kelly, 1984; Larson, 1986), thus decreasing ctenophore predation on oyster larvae.

Nothing is known of the trophic ecology of the inconspicuous benthic scyphistoma or early free-swimming ephyra stages of scyphozoans. Large numbers of *C. quinquecirrha* scyphistomae are found on oyster shell (Cargo and Schultz, 1966, 1967), which is a preferred settling substrate for oyster larvae (Kennedy and Breisch, 1981). Therefore, these scyphistomae may be predators of oyster pediveliger larvae that are preparing to settle upon oyster shells.

To test the potential importance of *C. quinquecirrha* and *M. leidyi* as predators of bivalve larvae, we compare (1) medusa and ctenophore digestion of oyster veligers, (2) rejection or ingestion of oyster, blue mussel (*Mytilus edulis* L.), and coot clam [*Mulinia lateralis* (Say)] veligers by medusae, and (3) rejection, or ingestion and digestion of oyster trochophores and veligers by the ephyra and scyphistoma stages of *C. quinquecirrha*. We also present data on bivalve veligers in gut contents of medusae and ctenophores, and *in situ* densities of those predators and veligers, to estimate the importance of predation by gelatinous zooplankton on bivalve larvae in the mesohaline region of Chesapeake Bay.

Materials and Methods

During June through August, 1987, 1988, and 1989, *C. quinquecirrha* medusae and *M. leidyi* were collected in jars from the boat basin of the Horn Point Environmental Laboratories (HPEL) on the Choptank River. In the laboratory, we used 30 μm filtered Choptank River water at ambient salinity (11–12‰) and temperature (20–27°C). After collection, medusae and ctenophores were held in 20-l plastic containers of water, and fed on *Artemia salina* nauplii for at least 12 h to clear their guts of natural zooplankton. Oyster larvae from trochophore (60 μm long) to pediveliger (270 μm) stages, and clam veligers (100–260 μm) were obtained from the HPEL hatchery. For the following experiments, veligers were separated into size fractions on screens of different mesh sizes. Mussel veligers (180 μm) were supplied by the University of Delaware, College of Marine Studies in Lewes, DE.

Digestion and survival of oyster veligers after capture by medusae and ctenophores

Individual medusae and ctenophores were exposed for 10 min either to high densities of oyster veligers alone (2–9 ml^{-1}), or to oyster veligers (0.1 ml^{-1}) with copepods (*Acartia tonsa*) as alternative prey in 4-l containers. The predators then were gently transferred twice with sieves (1 mm mesh) at 5-min intervals to 4-l containers with filtered water to remove prey adhering to their external surfaces and to dilute swimming zooplankton possibly transferred with the predators. Each predator was subsequently transferred at hourly intervals to new containers of filtered water. After the predator was removed from each container, the water was poured through a 60-μm screen, and live oyster veligers, larval shells, live copepods, and copepod exoskeletons were counted with a dissecting microscope, thus recording all prey egested each hour. Egestion times were calculated from the midpoint of each interval, so the accuracy is ±0.5 h. Living veligers that were retrieved after egestion by the medusae were put in beakers of water with food (phytoplankton *Isochrysis galbana*) to determine their survival after 24 h.

Rejection and ingestion of bivalve veligers by medusae

To examine the feeding reactions of *C. quinquecirrha* medusae to bivalve veligers and copepods, we placed medusae (15–90 mm in bell diameter) exumbrellar surface down in fingerbowls with less than 100 ml water. In this position, medusae continued to take food, and were easily examined with a dissecting microscope. Individual prey were placed by pipette on the oral arms, where prey are captured and transferred to the gastric pouches (Larson, 1986). The length of time it took prey to reach a gastric pouch (ingestion) or to be rejected from the oral arm was measured during continuous observation.

Prey in this experiment included live (closed) and freshly killed (gaping) oyster veligers, live clam and mussel veligers, live and heat-killed copepods (*Acartia tonsa*), and tissue removed from 2- to 3-day-old oyster spat (recently settled larvae). Gaping veligers were used to determine whether the larval shell caused the rejection of veligers by medusae. To obtain gaping veligers, we anaesthetized them by gradually adding seltzer water (CO_2) until the shells opened, and then rapidly heating the water to kill them. To ensure that the medusae were feeding well, live copepods, which were readily accepted, were alternated with other prey.

C. quinquecirrha ephyrae 2 to 3 mm in diameter, budded from scyphistomae in the laboratory, were placed singly in a depression slide with 0.5 ml of water and a few live oyster trochophores or live oyster or clam veligers; the process of rejection or ingestion was timed after contact occurred. Scyphistomae attached to plastic slides in the laboratory were offered live oyster trochophores or veligers in 25-ml dishes, and rejection or ingestion was timed after contact.

Effect of scyphistomae on veliger settlement

To determine if *C. quinquecirrha* scyphistomae reduced oyster settlement, field-collected oyster shells containing

scyphistomae were cut into 5 to 8 cm^2 pieces and cleaned of other epifauna. Seven pieces of shell with scyphistomae (9.3 ± 3.7 individuals per shell for all experiments) and seven without were placed in 3 l of 11‰ water at 24° to 27°C in dishes of 143 cm^2 bottom area. Shell pieces were oriented so that scyphistomae were on the underside, which is their preferred location in nature (Cargo and Schultz, 1966, 1967). About 500 oyster pediveligers (179–250 μm long) were added to the dishes, plus algae (*Isochrysis galbana*) as food for the larvae and *Artemia salina* nauplii as alternate prey for the scyphistomae. The dishes were gently aerated and were covered with black plastic, because oyster veligers prefer low light levels for settlement (Ritchie and Menzel, 1969). The shell pieces were checked at 24 and 48 h for newly settled larvae. Six trials, each with two replicates, were run with different pieces of shell. There were 4 controls, each with 14 shell pieces without scyphistomae.

Scyphistoma predation and digestion rates on veligers

Predation by scyphistomae on oyster veligers was determined at the end of each trial (24 or 48 h) by counting the empty larval shells retrieved from the experimental containers. In additional predation experiments at the Chesapeake Biological Laboratory (CBL), containers were filled with 150 ml of estuary (Patuxent River) water. Each container had one plastic slide that was raised off the bottom by fishing weights so that the 3 to 20 attached scyphistomae were on the lower surface. Fifty oyster veligers (179 to 250 μm long) and algal food were added to each container. After 24 and 48 h, larvae inside scyphistomae and clear shells were counted. There were 159 trials, and 26 controls without scyphistomae to check for veliger death due to experimental manipulations. In combination with the preceding experiment, 171 predation measurements were taken.

The length of time required by scyphistomae for digestion of both closed (live) and gaping (anaesthetized and killed) oyster larvae was determined by pipetting the larvae into the tentacles and mouth region of the scyphistomae. The times of ingestion were recorded, then containers were checked at intervals for empty larval shells.

Field studies on medusae and ctenophores

In 1987, we sampled medusae, ctenophores, and bivalve veligers weekly from May to September in two tributaries of Chesapeake Bay [Broad Creek (38° 40′, 76°15′W) and Tred Avon River (38°40′N, 76°05′W)], and on three dates in both May and August, and on one day in both June and July at five stations across the Bay at the same latitude. At each station, we collected individual medusae and ctenophores by dip net and immediately preserved them in 5% formalin for dietary analysis with a dissecting microscope. All bivalve veligers in these samples were counted. Empty and open larval shells were counted separately from closed shells that contained tissue.

Densities of *C. quinquecirrha* and *M. leidyi* were measured with a 1 m diameter, 1.6-mm mesh net with flowmeter towed at 1 m depth in the tributaries (bottom depth < 4 m), and above the pycnocline in the Bay (<11 m). Medusae and ctenophores were counted from samples preserved in 5% formalin (Purcell, 1988). Densities of bivalve larvae were determined from plankton samples taken at the same times as the net tows at 1 m depth in the tributaries with a portable bilge pump, and at 1-m intervals above 11 m depth in the Bay with a submersible pump. Pump samples were filtered through a 64 μm plankton net in the field, then preserved in 5% formalin, and veligers were counted in the laboratory from whole samples or subsamples taken with a Hensen Stempel pipette.

Rates of ctenophores feeding on bivalve veligers *in situ* were estimated from individual clearance rates (Kremer, 1979) times the numbers of ctenophores per cubic meter.

Statistics

Our results are presented as the mean ± one standard deviation. Comparisons on the numbers of prey rejected or ingested were by contingency tables and Chi-square tests, and comparisons of the retention times of different prey species were by one-way analysis of variance. In results reported here as significantly different, the statistical probability is less than 0.001, unless stated otherwise.

Results

Digestion and survival of oyster veligers after capture by medusae and ctenophores

Chrysaora quinquecirrha medusae captured copepods and oyster veligers (80–270 μm long). Ninety-three percent of the copepods were digested, compared with only 1% of the veligers (Table I). Medusae egested copepod remains in less than 5 h, and the few undigested copepods were

Table I

Numbers of copepods and oyster veligers digested after capture by Chrysaora quinquecirrha *medusae and* Mnemiopsis leidyi

Species	Captured	Digested	Predators tested
C. quinquecirrha			
copepods	12,143	11,276 (93%)	110
oyster veligers	4,800	48 (1%)	100
M. leidyi			
oyster veligers	333	316 (96%)	28

Table II

Percentages of oyster veligers of different sizes surviving for 24 h after egestion by Chrysaora quinquecirrha *medusae. Numbers of egested veligers are in parentheses*

	Time inside medusa (h)					
Veliger size	<1	1–2	2–3	3–4	4–5	5–6
<100 μm	96.3	88.9	75.0	72.7	—	100
	(164)	(18)	(12)	(11)	(0)	(2)
100–200 μm	99.6	95.2	97.1	94.1	71.4	91.7
	(1559)	(272)	(102)	(51)	(14)	(12)
>200 μm	99.4	100	93.9	81.8	100	66.7
	(335)	(65)	(33)	(11)	(6)	(3)

dead. Undigested veligers were egested in less than 7 h, with over 90% egested in less than 2 h. Medusae egested shells of the 48 veligers that were digested in 3.4 ± 1.8 h at 22 to 27°C. Digested veligers included 31 small (<100 μm) and 17 medium (100–200 μm), but no large (>200 μm) veligers. These numbers represent 0.03%, 0.006%, and 0% of the numbers of veligers ingested in each size class. Medusae digested veligers less than 100 μm long significantly more frequently than those in both larger size classes. More medium sized veligers were digested than large ones ($P < 0.05$). Ctenophores digested significantly more oyster veligers (96%) than did medusae (1%) (Table I), and egested 333 empty larval shells in 2.0 ± 1.0 h at 19.5 to 20.5°C.

Many veligers egested by medusae were alive. Overall, 98.4% of 2670 veligers that we retrieved after egestion by medusae survived for 24 h afterward. Veligers smaller than 100 μm long showed significantly lower survival than larger veligers (Table II). Veligers retained for more than 2 h showed significantly lower survival than those retained for less than 2 h (Table II). Differences between the <1 h and the 1–2 h groups, and among the groups >2 h were not significant ($P > 0.2$ for all comparisons).

Rejection and ingestion of bivalve veligers by medusae

Prey placed on an oral arm of *C. quinquecirrha* medusae were immediately rejected, or they were taken briefly inside the oral arm by the medusae before rejection, or they were transported inside the oral arm and then to a gastric pouch (ingestion). Medusae rejected significantly more live oyster veligers (99.3%) from the oral arms than live copepods (1.5%) (Table III). The numbers of live oyster, mussel, and clam veligers rejected were not significantly different ($P = 0.2$ to 0.8).

The closed shell protected veligers from ingestion and digestion by medusae. Open oyster veligers were rejected significantly less than closed, live ones, but the difference between closed and open mussel larvae was not significant

Table III

Numbers of oyster, mussel, and clam veligers, copepods, and oyster spat tissue rejected, ingested, and digested by Chrysaora quinquecirrha *medusae, ephyrae, and scyphistomae*

Prey	Rejected	Ingested	Digested	Specimens tested
Medusae				
Veligers				
Oyster—live	134	1	1	22
Oyster—dead	41	12	—	12
Oyster—shells	22	0	0	2
Mussel—live	91	4	—	8
Mussel—dead	16	0	0	1
Clam—live	74	1	0	14
Oyster spat tissue	6	27	≥10	9
Copepods—live	7	451	451	57
—dead	20	137	—	8
Ephyrae				
Veligers				
Oyster—live	18	26	0	28
Clam—live	77	7	5	14
Trochophores	3	117	≥105	26
Scyphistomae				
Veligers				
Oyster—live	9	32	12	19
Clam—live	9	8	7	12

— = Not quantified because we were unable to track the prey.

(Table III). Open oyster veligers also were retained significantly longer in the oral arms than were closed veligers (Table IV). Empty larval shells were never ingested (Table III). Oyster spat tissue was ingested significantly more frequently than either open or closed oyster veligers (Table III). Dead copepods were rejected significantly more often

Table IV

Percentages of bivalve veligers that were retained for five time intervals in the oral arms of Chrysaora quinquecirrha *medusae. The numbers of veligers tested are in the "Rejected" column in Table III*

	Time inside oral arm (min)					
Prey	<1	1–2	2–4	4–10	>10	Maximum time (min)
Oysters						
live	16	31	19	19	16	45
dead	12	24	20	5	39	156
Mussels						
live	9	31	12	24	24	70
Clams						
live	2	10	8	15	65	91

than live ones (Table III), but most dead ones were still accepted as food.

Although nearly all veligers were eventually rejected from the oral arms of *C. quinquecirrha* medusae, differences in retention time existed among the three bivalve species tested (Table IV). Most live veligers were rejected in less than 10 min. Live mussel veligers were retained somewhat longer than live oysters, but the difference was not significant ($P = 0.2$). Clams were retained significantly longer before rejection than were oysters and mussels.

Comparisons among life history stages of *C. quinquecirrha* showed that ephyrae and scyphistomae ingested proportionately more oyster and clam veligers than did the medusae (Table III). Ingestion of oyster veligers differed significantly between medusae and ephyrae, and between medusae and scyphistomae; however, differences between ephyrae and scyphistomae were not significant ($P = 0.1$). Ingestion of clam veligers differed significantly between scyphistomae and medusae, and between scyphistomae and ephyrae; however the difference between medusae and ephyrae was not significant ($P = 0.1$).

Of the ingested veligers, scyphistomae digested significantly more oysters than did ephyrae (Table III), but not clams ($P = 0.9$). Thus, ephyrae behaved more like medusae than scyphistomae in that they digested few oyster veligers. Ephyrae digested five clam veligers in 1.8 to 20.6 h (mean 10.6 ± 8.3 h).

Comparisons between types of veligers showed that ephyrae ingested significantly more oyster than clam veligers (Table III), but digested significantly more clams than oysters. In contrast, scyphistomae ingested significantly more clam than oyster veligers ($P < 0.05$), and digested significantly more clams than oysters ($P < 0.05$). These results suggest that clam and oyster veligers are captured with different success by ephyrae and scyphistomae, and that oyster veligers show greater resistance to digestion than do clam veligers once captured.

Because individual oyster trochophore larvae were difficult to observe due to their small size (<60 μm), we were successful at offering them only to ephyrae, which ingested and digested significantly more trochophores than veligers (Table III).

Effect of scyphistomae on veliger settlement

No settlement of oyster veligers occurred in three of six experiments. Veligers in three experiments and one control settled preferentially on the lower surfaces of the shell pieces, even those with *C. quinquecirrha* scyphistomae. Numbers of spat on the upper/lower shell surfaces were: shells with scyphistomae 19/69; without scyphistomae 22/49; control 22/77. No significant differences in spat settlement were seen among shell pieces with or without scyphistomae, which were on the lower surfaces ($P > 0.2$ for all comparisons). Total settlement was greater in the control container (average of seven veligers settled per shell), where there were no scyphistomae, as compared with the experimental containers (average settlement of two per shell), probably because predation by scyphistomae reduced the numbers of veligers.

Scyphistoma predation and digestion rates on veligers

A total of 4409 oyster veligers were consumed by *Chrysaora quinquecirrha* scyphistomae in 171 predation experiments, as evidenced by the presence of empty shells. In contrast, only 9 empty shells were retrieved from 27 controls without scyphistomae. No significant differences existed between the ingestion rates measured at 24 and 48 h, therefore the results were pooled. The initial densities of larvae in the experimental and control containers averaged 0.31 ± 0.06 veligers ml^{-1}. Over the range of prey density (0.1–0.7 veligers ml^{-1}), the number of larvae consumed per scyphistoma per day (range 0–13) was positively correlated with larval density ($r = 0.26$, $P < 0.01$). On average, each scyphistoma consumed 0.9 ± 0.6 veligers/day. As many as 15 larvae were observed within a single scyphistoma. These results indicate that scyphistomae are more effective predators on oyster veligers than are medusae. However, we observed that after a few hours, scyphistomae sometimes expelled ingested larvae, which began swimming again. These larvae then were available for recapture.

Closed bivalve veligers were very resistant to digestion by scyphistomae. Closed D-stage clam veligers were digested in 37.5 to 41 h (mean 39.2 ± 1.2 h, n = 34), and clam pediveligers were digested in 4 to 47 h (mean 30.6 ± 15.6 h, n = 6). Scyphistomae that had ingested one or two closed oyster pediveligers egested empty shells in 24 to 67 h (mean 34.6 ± 12.9 h, n = 13). Three pediveligers removed from scyphistomae after 18.5 h appeared to be healthy. In contrast, open oyster pediveligers were digested in only 1.3 to 5.1 h (mean 3.7 ± 0.8 h, n = 32).

Field studies on medusae and ctenophores

Field-collected *M. leidyi* and *C. quinquecirrha* medusae both contained bivalve veligers. In 67 medusae, the shells of all 77 veligers were closed and full of tissue, indicating that they had not been digested. By contrast, 19 of 76 (25%) of the shells in 9 ctenophores were open and empty, indicating complete digestion. The proportions of open and closed shells in medusae and ctenophores were significantly different. Ctenophores contained more veligers (an average of six each) than did medusae (about one each). This may be because the ctenophores were collected in Chesapeake Bay, where veliger densities were much greater than in the tributaries, which was where the medusae were collected for diet studies (Table V).

Table V

Densities (numbers m^{-3}) of Chrysaora quinquecirrha *medusae,* Mnemiopsis leidyi, *and bivalve veligers in Chesapeake Bay and the Broad Creek and Tred Avon River tributaries from May to August, 1987, and the percentages of veligers consumed per day by* Mnemiopsis

	Chesapeake Bay				Tributaries			
Month	Medusae	Ctenophores	Veligers	Veligers* consumed per day (%)	Medusae	Ctenophores	Veligers	Veligers* consumed per day (%)
May	0	0.3 ± 0.5	13,826 ± 11,491	0.2 ± 0.2	0–0.3	0.2–33.1	—	—
June	0	2.7 ± 1.6	14,210 ± 8,145	1.0 ± 0.6	5.4 ± 5.8	0	1786 ± 1550	0
July	0.1 ± 0.1	0.1 ± 0.1	60,032 ± 97,380	0.2 ± 0.2	9.6 ± 4.2	0	419 ± 279	0
August	0.6 ± 0.7	0.7 ± 0.8	12,284 ± 15,234	1.7 ± 1.9	7.2 ± 3.7	0	1421 ± 1060	0

* Percentage daily consumption estimated from ctenophore filtering rates (Kremer, 1979).
— = No data.

To estimate the importance of predation on veligers by medusae and ctenophores in nature, we measured *in situ* densities of *M. leidyi, C. quinquecirrha,* and bivalve veligers in May through August, 1987 (Table V). Ctenophores occurred in the Bay throughout this period, but they were excluded from the tributaries by high densities of medusae that fed on them from June through August. Medusae were much less abundant in the Bay than in the tributaries. Sampled densities of bivalve veligers were much greater in the Bay than in the tributaries, possibly due to different efficiencies of the pumps used to collect them. If we assume that only ctenophores ate the bivalve veligers, then 0.2 to 1.7% of the veligers were consumed daily in the main Bay, and none were eaten in the tributaries during that period (Table V).

Discussion

A surprising result of this study is that *Chrysaora quinquecirrha* medusae do not ingest or digest bivalve veliger larvae. Three lines of evidence lead to this conclusion. (1) Medusae that caught swimming veligers egested them alive. (2) Veligers placed on oral arms were subsequently rejected. (3) Veligers in the gut contents of field-collected medusae were closed and full of tissue. The ephyra stage ingested oyster veligers but did not digest them. By contrast, scyphistomae egested some living veligers, but many were retained and eventually digested.

The larval shell may protect bivalve veligers from ingestion by *C. quinquecirrha* medusae. The rapid rejection of veligers from the oral arms suggests that medusae either do not recognize veligers as food items because of the shell, or that veligers provide a "distasteful" stimulus. Larvae of an echinoderm (*Acanthaster planci*) and an ascidian (*Ecteinascidia turbinata*) contain chemicals that make them unpalatable to planktivorous fishes (Lucas *et al.*, 1979; Young and Bingham, 1987).

The sensing and recognition of food must take place in the oral arms of the medusae, as indicated by the differences in ingestion of copepods and veliger larvae. This recognition may involve a mechanical stimulus from active prey, as suggested by the facts that more living, active copepods were ingested than dead ones, and that immobile veligers nearly always were rejected. Recognition also may be due to chemical stimuli, because more open oyster veligers, which presumably leaked body fluids, were ingested than closed ones. The various bivalve species also may present different stimuli, as suggested by the different retention times of oyster, mussel, and clam veligers in the medusae.

The larval shell probably protects veligers from digestion as long as they remain closed within the predators. Veligers were retained for up to 7 h in medusae, and then egested alive. Veligers were removed alive from scyphistomae after 18 h, but closed oyster pediveligers eventually were digested in over 24 h. By contrast, newly killed veligers with open shells were digested by scyphistomae in 3 to 5 h. Therefore, open veligers apparently are more susceptible to digestion than closed ones. Digestion of some veligers may be due to their injury by the scyphistomae's nematocysts at capture, causing the shells to open. Presumably, this also could explain why a few veligers were digested by the medusae.

Suspension-feeding benthic invertebrates can be important predators of pelagic larvae (Thorson, 1946). Bivalve larvae have been found in the stomach contents of their own and other bivalve species (summarized in Mileikovsky, 1974; Young and Chia, 1987). However, oyster larvae taken into the mantle cavities of six mollusk species were rejected in the pseudofeces, from which they may be able to escape (MacKenzie, 1981). A few veligers were ingested and eliminated in the feces of these mollusks, from which they could not escape (MacKenzie, 1981).

Oyster veligers also were rejected unharmed by a barnacle (*Balanus eburneus*) and a polychaete (*Polydora ligni*) (in MacKenzie, 1981), but the common barnacle (*Balanus improvisus*) ate oyster veligers in Chesapeake Bay (Steinberg and Kennedy, 1979).

From earlier studies, Mileikovsky (1974) concluded that bivalve veligers often could pass alive through the guts of primarily herbivorous feeders. However, no larvae were known to pass alive through primarily carnivorous feeders, although protectively coated gametes of a polychaete (*Melinna palmata*) passed through fish (*Acipenser stellatus*) feeding on the adult worms (in Mileikovsky, 1974). Numerous examples exist of benthic cnidarians feeding on bivalve veligers (Young and Chia, 1987). Also, oyster veligers were eaten by the common sea anemone *Diadumene leucolena* in Chesapeake Bay (Steinberg and Kennedy, 1979). To our knowledge, our study presents the first evidence of bivalve veligers passing alive through a carnivorous predator, the medusa stage of *Chrysaora quinquecirrha*.

The diets of several species of pelagic cnidarians are reported to include bivalve veligers, but the numbers of veligers in siphonophores (Purcell, 1981) and hydromedusae (reviewed in Purcell and Mills, 1988) usually were less than 1% of the prey items. Similarly, the scyphomedusae *Aurelia aurita* and *Stomolophus meleagris* in the Gulf of Mexico, and *Mastigias* sp. in Jellyfish Lake, Palau, contained small numbers of bivalve veligers (Purcell, unpub. data). However, bivalve veligers were 25 to 67% of the prey in the hydromedusan *Proboscidactyla flavicirrata* (Purcell and Mills, 1988), and 40 to 80% of the prey in the scyphomedusan *Cyanea* sp. (Brewer, 1989). None of the above studies distinguished between digested or undigested veligers.

The importance of predation on oyster larvae by scyphistomae in nature is difficult to predict because there are few density estimates for scyphistomae or for oyster veligers near the estuary bottom. Only 2.8 ± 3.1% of oyster shells had scyphistomae in the York River, Virginia (Cones and Haven, 1969). One third of those shells had an average of more than 10 scyphistomae per shell (maximum 21), and densities were <1 to 53 scyphistomae m^{-2} of bottom. However, 53.4 ± 25.3% of oyster shells contained scyphistomae in eleven tributaries of the Chesapeake Bay in Maryland, and 70% of those shells had more than 10 individuals (maximum 200; Cargo, unpub. data). Predation by scyphistomae on oyster veligers in those tributaries probably would be higher than in the York River.

The predation rate of one oyster veliger scyphistoma^{-1} day^{-1} from our laboratory experiments should be applied to field conditions with caution, because the experimental larval densities (100–700 l^{-1}, mean 300 l^{-1}) were generally high in comparison with densities of pediveligers in bottom waters. Oyster veliger densities were generally less than 14 l^{-1} near the bottom in Broad Creek and the Tred Avon River, but one sample had 134 l^{-1} (Seliger *et al.*, 1982). Densities of oyster veligers > 200 μm long were 23 to 215 l^{-1} near the bottom in the James River, Virginia (Andrews, 1983). Mortality in our laboratory experiments could be higher than in the field because veligers that were expelled undigested by scyphistomae in our experiments could have been repeatedly ingested, eventually resulting in death, while veligers in nature might have escaped.

Molluscan trochophore larvae lack a shell, and are probably vulnerable to predation by all life history stages of *C. quinquecirrha*. We could only follow the fate of trochophores offered to ephyrae, which did ingest and digest them. In nature, trochophores may be distributed throughout the water column, and may seldom encounter benthic scyphistomae. Although medusae do consume some copepod nauplii and rotifers of the same size as trochophores (about 60 μm), such small animals were only a few percent of the prey items (Purcell, unpub. data). Therefore, medusae probably do not capture many trochophores in nature. Depending on temperature, the trochophore stage lasts only 24 to 30 h, so this period of vulnerability to predators is short, compared with the 6 to 18 day veliger stage of various bivalve species (Loosanoff and Davis, 1963). Ctenophores readily ingested and digested veligers, and they probably also eat trochophores, because they consume many copepod nauplii (Purcell, unpub. data) and ciliates (Stoecker *et al.*, 1987) of the same size.

Quaglietta (1987) studied potential predation by *Mnemiopsis leidyi* on larvae of the hard clam *Mercenaria mercenaria* in Great South Bay, New York. Clam veligers and ctenophores co-occurred in July through December, and were most abundant in August through September. Ctenophore feeding reached a maximum in September, with an average of 11 and 36% of the water cleared of prey per day in 1985 and 1986, respectively. Both the biomass of ctenophores and their estimated predation on veligers were greater during Quaglietta's (1987) study in Great South Bay than during our study in Chesapeake Bay.

Predation on bivalve veligers by *M. leidyi* during our study was apparently limited to Chesapeake Bay, because the ctenophores were not found in Broad Creek and Tred Avon River after the appearance of *C. quinquecirrha* medusae in June. Predation by medusae on *M. leidyi* also may have reduced ctenophore densities in the main Bay. We conclude that not only do *C. quinquecirrha* medusae not consume bivalve veligers, but the medusae may reduce other predation on them by feeding on ctenophores.

In the mesohaline region of Chesapeake Bay, *C. quinquecirrha* medusae are present during June through September or October (Cargo and Schultz, 1966). Therefore,

medusae could reduce ctenophore predation on veligers of *Crassostrea virginica*, as well as other bivalves such as *Ischadium recurvum* Rafinesque, *Macoma mitchelli* Dall, *Mulinia lateralis*, *Mytilopsis congeria* (Conrad), and *Tagelus plebeius* (Lightfoot) which spawn throughout the summer (Shaw, 1965; Kennedy, pers. obs.). However, bivalve species that spawn only in the spring and autumn in Chesapeake Bay, *e.g.*, *Macoma balthica* (L.) and *Mya arenaria* (L.) (Shaw, 1965), would be most vulnerable to predation by *M. leidyi*.

Acknowledgments

We thank T. Dean, C. Densmore, C. Kalafus, L. Hill, and V. Steele-Perkins for their excellent assistance in the laboratory, and C. A. Miller and J. R. White for their comments on the manuscript. We are also grateful to Drs. R. I. E. Newell, G. S. Alspach, and T. C. Malone for allowing us to sample during their cruises, to Dr. J. H. Waite of the College of Marine Studies of the University of Delaware for providing mussel veligers, and to Dr. M. R. Roman and J. R. White, who provided data on bivalve veliger densities from Chesapeake Bay. This research was partially funded by the Maryland Department of Natural Resources, and the NSF Research Experiences for Undergraduates Grant OCE-8900707 to the University of Maryland Sea Grant College. UMCEES Contribution No. 2175.

Literature Cited

Andrews, J. D. 1983. Transport of bivalve larvae in James River, Virginia. *J. Shellfish Res.* **3:** 29–40.

Bishop, J. W. 1967. Feeding rates of the ctenophore, *Mnemiopsis leidyi*. *Chesapeake Sci.* **8:** 259–261.

Brewer, R. H. 1989. The annual pattern of feeding, growth, and sexual reproduction in *Cyanea* (Cnidaria:Scyphozoa) in the Niantic River Estuary, Connecticut. *Biol. Bull.* **176:** 272–281.

Burrell, V. G., Jr. 1968. The ecological significance of the ctenophore (*Mnemiopsis leidyi* A. Agassiz) in a fish nursery grounds. M. S. Thesis, College of William and Mary, Williamsburg, VA. 61 pp.

Burrell, V. B., Jr., and W. A. Van Engel. 1976. Predation by and distribution of a ctenophore, *Mnemiopsis leidyi* A. Agassiz, in the York Estuary. *Estuarine Coastal Mar. Sci.* **4:** 235–242.

Cargo, D. G., and L. P. Schultz. 1966. Notes on the biology of the sea nettle, *Chrysaora quinquecirrha*, in Chesapeake Bay. *Chesapeake Sci.* **7:** 95–100.

Cargo, D. G., and L. P. Schultz. 1967. Further observations on the biology of the sea nettle and jellyfishes in Chesapeake Bay. *Chesapeake Sci.* **8:** 209–220.

Clifford, H. C., and D. G. Cargo. 1978. Feeding rates of the sea nettle *Chrysaora quinquecirrha*, under laboratory conditions. *Estuaries* **1:** 58–61.

Cones, H. N., Jr., and D. S. Haven. 1969. Distribution of *Chrysaora quinquecirrha* in the York River. *Chesapeake Sci.* **10:** 75–84.

Cronin, L. E., J. C. Daiber, and E. M. Hulbert. 1962. Quantitative seasonal aspects of zooplankton in the Delaware River estuary. *Chesapeake Sci.* **3:** 63–93.

Deason, E. E., and T. J. Smayda. 1982. Ctenophore-zooplankton-phytoplankton interactions in Narragansett Bay, Rhode Island, USA, during 1972–1977. *Plankton Res.* **2:** 203–218.

Fancett, M. S. 1988. Diet and prey selectivity of scyphomedusae from Port Phillip Bay, Australia. *Mar. Biol.* **98:** 503–509.

Feigenbaum, D., and M. Kelly. 1984. Changes in the lower Chesapeake Bay food chain in presence of the sea nettle, *Chrysaora quinquecirrha* (Scyphomedusa). *Mar. Ecol. Prog. Ser.* **19:** 39–47.

Herman, S. S., J. A. Mihursky, and A. M. McErlean. 1968. Zooplankton and environmental characteristics of the Patuxent River estuary 1963–1965. *Chesapeake Sci.* **9:** 67–82.

Kremer, P. 1979. Predation by the ctenophore *Mnemiopsis leidyi* in Narragansett Bay, R. I. *Estuaries* **2:** 97–105.

Kennedy, V. S., and L. L. Breisch. 1981. *Maryland's Oysters. Research and Management.* Univ. of MD Sea Grant Program, College Park, MD Publ. No. UM-SG-TS-81-04.

Larson, R. J. 1978. Aspects of feeding and functional morphology of scyphomedusae. M. S. Thesis, University of Puerto Rico. 132 pp.

Larson, R. J. 1986. The feeding and growth of the sea nettle, *Chrysaora quinquecirrha* (Desor), in the laboratory. *Estuaries* **9:** 376–379.

Larson, R. J. 1987. A note on the feeding, growth, and reproduction of the epipelagic scyphomedusa *Pelagia noctiluca* (Foskal). *Biol. Oceanogr.* **4:** 447–454.

Loosanoff, V. L. 1974. Factors responsible for the mass mortalities of molluscan larvae in nature: a review. *Proc. Ann. Mtg. World Mariculture Soc.* **5:** 297–309.

Loosanoff, V. L., and H. C. Davis. 1963. Rearing of bivalve mollusks. *Adv. Mar. Biol.* **1:** 1–135.

Lucas, J. S., R. J. Hart, M. E. Howden, and R. Salathe. 1979. Saponins in eggs and larvae of *Acanthaster planci* (Asteroidea) as chemical defenses against planktivorous fish. *J. Exp. Mar. Biol. Ecol.* **40:** 155–165.

MacKenzie, C. L., Jr. 1981. Biotic potential and environmental resistance in the American oyster (*Crassostrea virginica*) in Long Island Sound. *Aquaculture* **22:** 229–268.

Mileikovsky, S. A. 1974. On predation of pelagic larvae and early juveniles of marine bottom invertebrates by adult benthic invertebrates and their passing alive through their predators. *Mar. Biol.* **26:** 303–311.

Miller, R. J. 1974. Distribution and biomass of an estuarine ctenophore population, *Mnemiopsis leidyi* (A. Agassiz). *Chesapeake Sci.* **15:** 1–8.

Nelson, T. C. 1925. On the occurrence and food habits of ctenophores in New Jersey inland coastal waters. *Biol. Bull.* **48:** 92–111.

Nelson, T. C. 1953. Some observations on the migrations and setting of oyster larvae. *Proc. Natl. Shellfish. Assoc.* **(1952):** 99–104.

Olson, M. M. 1987. Zooplankton. Pp. 38–81 in *Ecological Studies in the Middle Reach of Chesapeake Bay*, K. L. Heck, Jr., ed. Springer Verlag, Berlin.

Purcell, J. E. 1981. Dietary composition and diel feeding patterns of epipelagic siphonophores. *Mar. Biol.* **65:** 83–90.

Purcell, J. E. 1988. Quantification of *Mnemiopsis leidyi* (Ctenophora, Lobata) from formalin preserved plankton samples. *Mar. Ecol. Prog. Ser.* **45:** 197–200.

Purcell, J. E., and C. E. Mills. 1988. The correlation between nematocyst types and diets in pelagic Hydrozoa. Pp. 463–485 in *The Biology of Nematocysts*, D. A. Hessinger and H. M. Lenhoff, eds. Academic Press, Inc., San Diego.

Quaglietta, C. E. 1987. Predation by *Mnemiopsis leidyi* on hard clam larvae and other natural zooplankton in Great South Bay, N.Y. M. S. Thesis, State University of New York, Stony Brook. 66 pp.

Ritchie, T. P., and R. W. Menzel. 1969. Influence of light on larval settlement of American oyster. *Proc. Natl. Shellfish. Assoc.* **59:** 116–120.

Seliger, H. H., J. A. Boggs, R. B. Rivkin, W. H. Biggley, and K. R. H. Aspden. 1982. The transport of oyster larvae in an estuary. *Mar Biol* **71:** 57–72.

Shaw, W. N. 1965. Seasonal setting patterns of five species of bivalves in the Tred Avon River, Maryland. *Chesapeake Sci* **6:** 33–37.

Steinberg, P. D., and V. S. Kennedy. 1979. Predation upon *Crassostrea virginica* (Gmelin) larvae by two invertebrate species common to Chesapeake Bay oyster bars. *Veliger* **22:** 78–84.

Stoecker, D. K., P. G. Verity, A. E. Michaels, and L. H. Davis. 1987. Feeding by larval and post-larval ctenophores on microzooplankton. *J Plankton Res* **9:** 667–683.

Thorson, G. 1946. Reproduction and larval development of Danish marine bottom invertebrates with special reference to planktonic larvae in the Sound (Oresund). *Meddr Danm Fisk -og Havunders (Ser Plankton)* **4:** 1–523.

Truitt, R. V., and P. V. Mook. 1925. Oyster problem inquiry of Chesapeake Bay. *Third Ann Rep Conserv Dept. of MD* Pp. 25–55.

Young, C. M., and B. L. Bingham. 1987. Chemical defense and aposematic coloration in larvae of the ascidian *Ecteinascidia turbinata Mar Biol* **96:** 539–544.

Young, C. M., and F.-S. Chia. 1987. Abundance and distribution of pelagic larvae as influenced by predation, behavior, and hydrographic factors. Pp. 385–463 in *Reproduction of Marine Invertebrates. Vol. IX. General aspects seeking unity in diversity*, A. C. Giese, J. S. Pearse, and V. B. Pearse, eds. Boxwood Press, Pacific Grove, CA.

Reference: *Biol. Bull.* **180**: 112–118. (February, 1991)

Settlement, Refuges, and Adult Body Form in Colonial Marine Invertebrates: A Field Experiment

LINDA J. WALTERS[1] AND DAVID S. WETHEY[1,2]

[1]*Department of Biological Sciences and* [2]*Marine Science Program, University of South Carolina, Columbia, South Carolina 29208*

Abstract. We examine the relationship between adult body form (sheet *vs.* arborescent) and larval settlement in colonial animals. Because thin sheet forms are more susceptible to overgrowth than arborescent forms, we predict that larvae of sheet forms should preferentially settle in refuges from competitors. On both natural and artificial substrata, the larvae of the sheet form (*Membranipora membranacea*) settled more often on high spots, which could serve as refuges from competition. The arborescent forms (*Bugula neritina* and *Distaplia occidentalis*) settled around the bases of bumps more frequently than would be expected by chance. For many arborescent forms, their most vulnerable periods are the days immediately following settlement, when individuals can be consumed easily by predators or dislodged by physical disturbances. Settlement in a crevice (base of a bump) would provide protection from the bulky mouthparts of predators. Moreover, dislodgment would be less likely than if settlement had occurred on flat locations, such as the tops of bumps or the areas between bumps.

Introduction

Striking patterns of spatial distribution are characteristic of many marine invertebrates sessile on algae, rocks, and other hard surfaces. Individuals are often found in aggregations relative to each other (*e.g.*, Knight-Jones, 1951; Crisp, 1961; Wethey, 1984), relative to topographic features of the substrata (*e.g.*, Crisp and Barnes, 1954; Ryland, 1959; Crisp, 1961; Wisely, 1960; Hayward and Harvey, 1974; Keough and Downes, 1982; Wethey, 1986; LeTourneux and Bourget, 1988), or relative to microflora (*e.g.*, Crisp and Ryland, 1960; Brancato and Woollacott, 1982; Strathmann *et al.*, 1981). These patterns may arise at the time of larval settlement or develop later as a result of differential mortality. The distribution of individuals at the time of larval settlement has a strong influence on their future success. Individuals that settle near dominant competitors are more likely to die quickly, as are those that settle within the range of predators or where disturbance events frequently occur.

There are a number of potential escapes from sources of biotic mortality, including simple avoidance of settlement near enemies (*e.g.*, Grosberg, 1981; Young and Chia, 1981) and recruitment to spatial refuges (*e.g.*, Connell, 1961; Dayton, 1971; Paine, 1974; Wethey, 1983; Walters and Wethey, 1986). Organisms located in spatial refuges increase their chances of survival against competitors, predators, and disturbance events. Size can also be protective to colonies once they have grown to certain dimensions unaffected by competitors; this is the size refuge. Potential morphological escapes may also exist. Among colonial organisms attached to hard substrata, one can distinguish a number of morphological types, including sheet and tree forms (Jackson, 1979). The outcomes of competitive interactions can be strongly influenced by the morphologies of the competitors. Tree forms are relatively isolated from the substratum-associated competitors (Jackson, 1979; Grosberg, 1981), whereas sheet forms encrust the substratum and may suffer competitive interactions along their edges. Thin sheets tend to lose to thicker forms (Buss, 1980; Seed and O'Connor, 1981; Russ, 1982; Sebens, 1985, 1986; Walters and Wethey, 1986) unless they have a height advantage in the zone of contact (Walters and Wethey, 1986). Therefore, one would predict that animals with thin, sheet-like growth forms should preferentially settle on or near locations where they have a height advantage (Walters and Wethey, 1986).

Although tree forms are less likely to be overgrown by competitors, they can be more visible to predators and

Received 27 July 1990; accepted 29 November 1990.

are more susceptible to total colony mortality than sheet forms. On irregular substrata, a potential settlement refuge location would be found around the bases of bumps. Here, certain predators may not be able to reach newly settled individuals. Here they are also protected from more disturbance events than they would be if they were located on a flat surface or on the top of a bump.

We examined the patterns of larval settlement in three species of encrusting colonial animals with different growth forms. We asked whether the settlement patterns were consistent with our prediction that species with thin sheet morphologies should choose spatial refuges from competitors, whereas species with tree morphologies should choose refuge locations that would reduce the risk of predation and disturbance. The encrusting cheilostome bryozoan *Membranipora membranacea* was our example of a thin sheet morphology, and the arborescent bryozoan *Bugula neritina* and the pedunculate ascidian *Distaplia occidentalis* were our examples of tree morphologies. We examined two kinds of substrata. The kelp *Laminaria saccharina* is a substratum commonly colonized by all three species. Settlement plates cast from bumps on Lego toy building blocks and pits created from bubble plastic served as model topographies of the same spatial scale as those found on *Laminaria*. Our analysis was carried out in two phases: (1) we examined the extent to which settlement on our model substrata mimicked that on natural surfaces; and (2) we examined in detail the spatial pattern of settlement on the model substrata.

Materials and Methods

Study organisms

The bryozoans *Membranipora membranacea* and *Bugula neritina* have small, ciliated larvae (*Membranipora:* 750 μm; *Bugula:* 200 μm, from Reed, 1987) that have limited swimming abilities in the ocean (Chia *et al.*, 1984). However, these larvae can choose their settlement locations. When competent, they move closely over the substrata and test it (Woollacott and Zimmer, 1978, for *Bugula;* Atkins, 1955, for *Membranipora*). During this phase, *Bugula* larvae form temporary attachments using adhesives that are sufficiently strong to prevent the individual from being mechanically dislodged (Loeb and Walker, 1977). *Bugula* can quickly dissolve the adhesive or change its viscosity to detach from, or reject the surface (Reed and Woollacott, 1982).

In the plankton, *Distaplia occidentalis* larvae are much larger than those of the other two species, measuring up to 3.2 mm in length (Cloney and Torrence, 1984). Most encounter a number of surface locations before metamorphosing on one of them (R. A. Cloney, pers. comm.). Torrence and Cloney (1988) suggest that sensory neurons in the adhesive papillae may be common in ascidians. In the laboratory, adhesion in *Distaplia* occurs within 30 s at 15°C (Cloney, 1978). Tail resorption reduces the size of the newly settled individual to approximately 650 μm within 7 min (Cloney, 1978).

For the purposes of this study, it was important to distinguish between newly settled and metamorphosed individuals. Newly metamorphosed *Membranipora* colonies have only the twin ancestrula skeleton fully formed, and *Bugula* has only the first zooid skeleton completed. *Distaplia* colonies were considered new individuals if they occupied less than 1 mm^2.

Experimental procedure

To study larval settlement on natural substrata, we examined the alga *Laminaria saccharina*. Plants were collected on the floating docks at the Friday Harbor Laboratories, San Juan Island, Washington state (48° 32′ 42″ N; 123° 0′ 39″ W) and on the floating public docks at Fisherman's Bay on Lopez Island, Washington state (48° 30′ 30″ N; 122° 54′ 51″ W). Entire blades were either placed in running seawater tables and a census taken within 48 h, or frozen immediately for a later census. Random pieces of the alga (20 × 20 cm) were cut from the central portion of large (1.0–2.0 m in length) *Laminaria* fronds. All new settlers were recorded on each algal square. As the topographies of the blades are quite variable, we could not distinguish a pit from a bump. Instead, each topographical feature on the blade was defined as a continuous slope extending from a lowest to a highest point (Fig. 1). The lowest point on one side of an algal blade is the highest point on the reverse side. The diameter (base) and the height of each topographic feature were recorded with vernier calipers. The slopes ranged in length from 1 to 20 mm. The location of each animal was determined by cre-

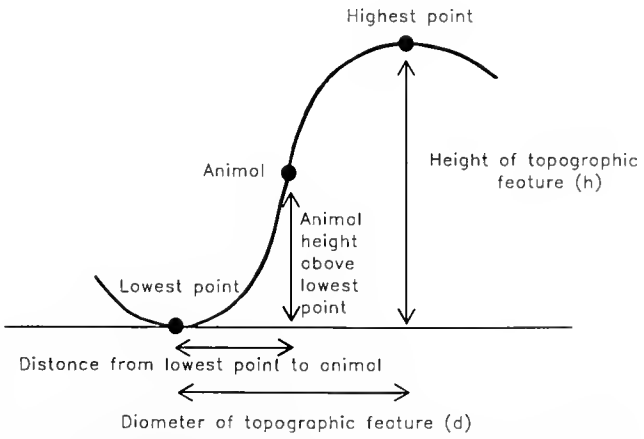

Figure 1. Each colony was mapped in relation to the nearest topographic high and low point. The dimensions of the topographic feature were measured.

ating a right triangle with the animal location and the lowest point as two of the points (Fig. 1). The distance from the lowest point to the animal and the animal height above the lowest point were measured (Fig. 1).

Using the diameter (d) and height (h) of each topographic feature, we calculated:
(1) the radius of curvature (rc) of the topographic feature:

$$rc = \frac{h^2 + (d/2)}{2*(1 + d)*(d/(2*h))}$$

(2) the vertical position (vp) of the animal, which we use to determine the location (top, side or base) of the organism on the topographic feature:

$$vp = (\text{animal height}/h).$$

Wilcoxon rank sum tests were used to determine if there were differences in locations occupied by larvae of the three common species. We examined the effects of size and shape of topographic features (height, diameter, and radius of curvature) as well as larval position (animal height and vertical position). When differences were found, pairwise Wilcoxon rank sum tests were run to determine which species were significantly different. Data from the Friday Harbor Laboratories and Lopez Island were pooled after Wilcoxon rank sum tests showed that there were no differences between the two sites.

To model the kinds and size scales of topographic features found on natural substrata, such as the alga *Laminaria saccharina,* we constructed three types of plastic plates 8.9 cm in diameter: (1) small Lego (Lego Systems Inc.) building block bumps (cylindrical, 2 mm high, 5 mm diameter) simulated small algal bumps; (2) large Lego building block bumps (cylindrical, 5 mm high, 9 mm diameter) simulated large algal bumps; and (3) bubble plastic pits (hemispherical, 2 mm deep, 5 mm diameter) simulated small algal pits. These materials were used because their topographic features were of the appropriate spatial scale and were uniformly spaced. We produced settlement plates by pouring polyester resin into silicone rubber molds (Sylgard 184 Silicone Elastomer, Dow Corning Corp.). Black resin pigment (Titan Corp.) was added to the uncatalyzed resin to make newly settled larvae more visible on the plates.

The settlement plates were attached to wooden boards with stainless steel screws. These were hung beneath the floating docks with polypropylene rope. The plates were oriented face down to prevent algal colonization. Six replicates of each surface were submerged in each trial. Plates were arranged in a Latin square design, with one replicate of each type of plate on each board. Six trials were run during the summers of 1987 and 1989.

Photographs were taken every two days at the Friday Harbor Laboratories and once or twice a week at Lopez Island during 1987. Additional data were collected by direct observation at Lopez Island in 1989. Flash-lit photographs were taken underwater using Kodak Technical Pan 2415 film and a Nikonos 5 camera equipped with a 5:1 extension tube and focal framer. Negatives were observed under a dissecting microscope equipped with an ocular micrometer to determine the specific locations of newly settled individuals. We distinguished among four kinds of locations on the plates with bumps: (1) top of bump; (2) side of bump; (3) touching the base of the bump; and (4) on the flat surface not touching the base of the bump. On the pitted surface, we distinguished among three kinds of locations: (1) in the pit; (2) touching the edge of the pit, and (3) on the flat surface not touching the pit. Individual larvae were scored as touching a topographic feature if they were within 250 μm of the feature. This distance represents approximately one body length of the settled larvae (200 to 750 μm in length).

To determine whether larvae settled preferentially in relation to topographic features, we compared our observations to a random distribution. For example, if larvae settled randomly, then the proportion of larvae settling in pits should be equal to the proportion of space accounted for by pits. In this way we calculated the number of larvae expected to settle in each of our classes of locations (on or in pits or bumps, touching pits or bumps, away from pits or bumps). Paired simultaneous *t*-tests were used to compare the observed *versus* expected number of individuals in each location on a settlement plate. The simultaneous *t*-tests were weighted because the estimates of proportions of larvae were all based on samples of different sizes. The estimate p of a proportion has a gaussian distribution with a variance $p(1 - p)/N$, where N is the sample size (Snedecor and Cochran, 1967: p. 208). We weighted our estimates by the reciprocal of this variance because we have higher confidence in estimates with the lowest variance. Plates with less than two individuals were not included. We used the Bonferroni inequality to make the tests simultaneous (Miller, 1966). For example, when we compared three settlement locations, to maintain an overall error rate of 0.05, we used an error rate of $0.05/3 = 0.016$ in each individual comparison.

To determine whether settlement preference changed as space became occupied, we examined the relationship between the proportion of larvae settling in the feature and the proportion of unoccupied space accounted for by that feature. On all dates we calculated the space available for settlement by subtracting from the total the area occupied by settled individuals. We assumed that all newly metamorphosed larvae occupied 1 mm^2. We compared settlement in samples with more than the average amount of free space, to settlement in samples with less than the average amount of free space.

Stoloniferous hydrozoan (primarily *Obelia dichotoma* and *Obelia geniculata*) and entoproct (*Barentsia benedeni*) colonies were present on all of the plates within 10 days, and at least a few stolons rapidly covered the entire surface of most plates. To determine whether the stolons affected settlement of *Bugula*, *Distaplia*, and *Membranipora*, the tops of the Lego bumps were divided into ten pie-shaped wedges. Similarly, the bases of the Lego bumps were divided into ten equal sections. If settlement was random with respect to stolons, then the ratio of wedges where stolons and larvae co-occur, to wedges with larvae, should equal the ratio of wedges with stolons to total wedges. Paired simultaneous *t*-tests were used to determine whether the observed and expected ratios were equal.

Very few individuals of other species settled on our experimental plates. Approximately 75% of the plates of each type had no other species settling on them. The remaining 25% had an average of two individuals of other species on them. These other species included: the bryozoans *Tegella armifera* and *Schizoporella unicornis*, the ascidian *Diplosoma macdonaldi*, the barnacle *Balanus crenatus*, the serpulid polychaete worm *Pseudochitonopoma occidentalis*, and spirorbid polychaetes.

Results

Natural alga substrata

Bugula neritina, *Distaplia occidentalis*, and *Membranipora membranacea* settled in locations with similar diameters and radii of curvature (Table I). *Bugula* and *Distaplia* settled in significantly lower elevations relative to topographic features than did *Membranipora* (Table I: Vertical Position). *Bugula* settled on topographic features that were significantly taller than those on which the other two species settled (Table I).

Settlement plate experiments

On the Lego settlement plates, settlement was non-random for all species (Table II). *Distaplia* and *Bugula* were found most often around the bases of bumps (Table II). These locations covered less than 5% of the total surface area of the settlement plates, yet more than 50% of the larvae of *Distaplia* and *Bugula* settled there.

Both arborescent forms, *Distaplia* and *Bugula*, were found significantly less often than expected on flat surfaces of the large and small Legos and the flat surfaces of plates with small pits (Table II). *Distaplia* settled more than expected by chance in the pits. In contrast, *Bugula* significantly avoided pits (Table II). The sheet form, *Membranipora*, was found more than expected on the tops of bumps and on the flat surfaces away from the topographic features in the large Lego treatment, but less than expected around the bases of bumps (Table II). On the pitted surfaces, *Membranipora* settled significantly less than expected in the pits and more than expected around the edges of the pits. *Bugula* and *Distaplia* settled preferentially around the bases of bumps, while *Membranipora* appeared to avoid this location. To estimate whether there was preemption of space by *Bugula* and *Distaplia*, we compared *Membranipora* settlement in samples with more than the average percent free space to settlement in samples with less than the average. Free space around the bumps decreased during the settlement season from 2.0% to 1.5% on the small Legos and from 4.3% to 3.6% on large Legos. *Membranipora* settlement was independent of availability of free space on both large Lego plates ($F = 0.24$; d.f. = 1, 23; $P = 0.63$), and small Lego plates ($F = 0.16$; d.f. = 1, 19; $P = 0.69$).

The settling larvae were not affected by the presence of hydrozoan or entoproct stolons (Table III). The larvae neither preferentially settled in locations where stolons were present nor did they significantly avoid these locations.

Table I

Settlement locations of Membranipora membranacea, Bugula neritina *and* Distaplia occidentalis *on the alga* Laminaria saccharina

Species	N	Mean	Group
	Height of Topographic Feature		
Bugula	64	9.22	A
Distaplia	95	7.81	B
Membranipora	147	7.80	B
	Diameter of Topographic Feature		
Bugula	64	26.30	A
Distaplia	95	28.13	A
Membranipora	147	27.12	A
	Radius of Curvature of the Topographic Feature		
Bugula	64	213.62	A
Distaplia	95	446.45	A
Membranipora	147	453.29	A
	Animal Height Above Lowest Point		
Bugula	64	1.80	A
Distaplia	95	1.44	A
Membranipora	147	5.32	B
	Vertical Position of the Animal		
Bugula	64	0.23	A
Distaplia	95	0.18	A
Membranipora	147	0.71	B

N = the number of individuals. Mean = the mean in millimeters, and Group = the results of Wilcoxon rank sum tests. Different letters refer to significant differences ($P < 0.05$). For explanation of the measured values, see Figure 1 and the text.

Table II

Test of randomness of settlement locations, the results of simultaneous paired t-tests comparing the expected versus the observed number of settlers

Species	Location	N	Difference	S.E.	Sign.
		Large Lego			
Bugula	Top	16	−2.14	0.33	Less
	Base	16	5.28	0.64	More
	Flat	16	−2.60	0.96	Less
Distaplia	Top	25	−2.60	0.36	Less
	Base	25	11.05	1.33	More
	Flat	25	−1.18	0.46	Less
Membranipora	Top	16	5.47	1.16	More
	Base	16	−0.65	0.13	Less
	Flat	16	3.92	0.57	More
		Small Lego			
Bugula	Top	16	−2.75	0.43	Less
	Base	16	7.01	1.30	More
	Flat	16	−2.57	0.77	Less
Distaplia	Top	25	−4.05	0.49	Less
	Base	25	15.78	1.99	More
	Flat	25	−5.67	0.90	Less
Membranipora	Top	15	1.21	0.88	n.s.
	Base	15	−0.20	0.08	n.s.
	Flat	15	1.26	0.84	n.s.
		Small Pits			
Bugula	Pit	11	−1.86	0.60	Less
	Edge	11	3.22	0.96	More
	Flat	11	−1.51	0.43	Less
Distaplia	Pit	19	3.99	0.82	More
	Edge	19	1.38	0.29	More
	Flat	19	−4.57	0.85	Less
Membranipora	Pit	9	−3.23	0.78	Less
	Edge	9	1.64	0.52	More
	Flat	9	2.15	0.95	n.s.

N = the number of plates on which at least two larvae settled; Difference = the mean for N plates of the observed − expected values; S.E. = the standard error of the Difference; and Sign. = the direction of the significance value with n.s. = not significant ($P > 0.05$). A Bonferonni comparisonwise error rate of 0.016 was used to keep the experimentwise error rate = 0.05.

Discussion

In this study we examined the relationship between larval settlement pattern and adult growth form in colonial epifauna on hard substrata. We asked whether larvae of species with thin sheet morphologies chose different settlement locations from those of larvae of species with arborescent morphologies. We argued that species with thin sheet growth forms should be more susceptible to overgrowth by competitors than species with tree morphologies. Because topographic high spots may serve as spatial refuges from competitors (Walters and Wethey 1986), we expected species with thin sheet morphologies to settle preferentially on topographic high spots.

In the present study, the thin sheet species, *Membranipora membranacea*, preferentially settled on the highest available locations on topographically complex surfaces (tops of bumps and flat areas between pits: Table II). This is consistent with our predictions, because the tops of bumps and the flat areas on a pitted surface are both locations where a colony has a height advantage over competitors, and thus has a potential refuge from competition. This result indicates that physical cues may allow larvae to escape from competitors, much as biogenic cues (*e.g.*, Grosberg, 1981; Young and Chia, 1981) allow larvae to avoid recruitment near enemies.

We argued that species with arborescent growth forms should be relatively immune to competitors, but that they might suffer damage from mobile predators like fish. In North Carolina, for example, filefish feed voraciously on newly settled colonies of *Bugula stolonifera* growing on flat surfaces (L.J.W., pers. obs.). Thus, tree forms might be expected to settle in cracks and crevices. In the present study, the arborescent forms, *Distaplia occidentalis* and *Bugula neritina*, settled preferentially around the bases of topographic irregularities (Table II). This result is consistent with our predictions, because the bases of bumps on our experimental plates are the locations most like crevices.

Similar spatial partitioning occurred on the alga *Laminaria saccharina* (Table I). Arborescent *Distaplia* and *Bugula* were found low on the slopes of the alga, while the thin sheet *Membranipora* was found significantly higher (Table I: Animal Height). The algal low spots,

Table III

Test of response of larvae to hydroid and entoproct stolons

Species	Location	N	Diff.	S.E.	p Value	Sign.
Bugula	Top	1	0.00	N.A.	N.A.	N.A.
Bugula	Base	22	−0.53	0.50	0.3293	n.s.
Distaplia	Top	4	2.50	2.50	0.3910	n.s.
Distaplia	Base	43	−1.10	3.11	0.7243	n.s.
Membranipora	Top	50	3.25	2.82	0.2553	n.s.
Membranipora	Base	10	−2.14	8.86	0.8144	n.s.

If settlement is random with respect to stolons, then the ratio of wedges with stolons and larvae, to wedges with larvae, should be equal to the ratio of wedges with stolons to total wedges. N = the number of individuals; Diff. = the mean of the difference: [(wedges with stolons)/(total wedges)] − [(wedges with larvae + stolons)/(wedges with larvae)]; S.E. = the standard error of the Difference; and Sign. = the sign of the significance value if $\alpha < 0.05$. A negative difference denotes bumps that had more larvae settling than it had stolons, and N.A. = not applicable.

where *Bugula* and *Distaplia* settled, are functionally equivalent to the bases of Lego bumps and the pits in the artificial settlement surfaces (Table II). Similarly, the high positions on algal slopes where *Membranipora* settled are functionally equivalent to the elevated locations where they settled on the settlement plates (Table II). However, topography does not fully control settlement pattern, because neither previously settled individuals, nor the stolon mats of hydrozoans and entoprocts, affected settlement by the larvae (Table III), even though the presence of any organisms on the substratum alters the local microtopography.

An alternative mechanism that could account for the settlement patterns is passive transport of larvae by hydrodynamic forces. Because of their limited swimming abilities (Chia *et al.*, 1981), larvae are often passively transported in boundary layer flows (*e.g.*, Butman, 1987). One can model passive larval transport as analogous to sediment transport (*e.g.*, Middleton and Southward, 1984). The patterns of transport are influenced by the turbulent motion of the water and by the topography of the substratum. When the surface topography protrudes beyond the 'viscous sublayer' into the turbulent overlying water, turbulent eddies can cause erosion. The roughness Reynolds number, Re*, is a measure of the degree to which roughness elements protrude above the viscous sublayer:

$$\mathrm{Re}^* = u^* L \rho / \mu$$

where u* is the shear velocity of the fluid flow regime, L is the height of the roughness element, ρ is the density of seawater, and μ is the dynamic viscosity of seawater.

In a wave-influenced environment, u* is approximately 10% of the maximum water velocity (Denny, 1988; Denny and Shibata, 1989; Svenden, 1987). We estimate u* to be in the range of 1.6 to 2.4 cm/s, yielding Re* values of 30–50 for the small Legos and 75–120 for the large Legos. If the roughness Reynolds number is less than 5, the bumps lie within the viscous sublayer. Thus, in all cases, the bumps on our settlement plates are in a potentially erosional regime. Larvae differ from sediment particles in their ability to adhere to surfaces. In flume experiments with our settlement plates, sediment never accumulated on the tops of the Lego bumps, presumably because the erosional forces are very high in these locations. Therefore, if the pattern were passive, larvae would not have accumulated on the tops of bumps. However, the tops of the bumps are the locations where *Membranipora* larvae did accumulate. Thus, we believe that the passive model cannot explain our patterns.

Competitive interactions were infrequent on these settlement plates, because recruitment rates were low and space did not become limiting during our experiments. The only common encounters were between the entoproct and hydrozoan stolons and the three species, with the later arrival always growing over the previously established colony. Neither colony appeared to be affected by these interactions. Although space was not filled on our settlement plates during the time course of this study, little bare space existed on the docks from which the plates were suspended. Because so little free space existed on the persistent hard substrata, we believe that competition could act as a selective agent on larval behavior.

The results of these studies are consistent with our prediction that adult body form should be correlated with larval settlement pattern. The arborescent forms (*Bugula* and *Distaplia*) settled preferentially in the small amount of space touching the bases of the bumps, potentially hidden from predators and disturbance events. The thin sheet form (*Membranipora*) settled most frequently on the highest available locations on topographically complex surfaces. Thus *Membranipora*, the adult growth form of which is most susceptible to overgrowth, had larvae that settled in potential refuges from competitors. Adult competitive ability and susceptibility to predation and disturbance may be an important influence on selection for larval settlement behavior.

Acknowledgments

This study was supported by the University of South Carolina, grants from the Office of Naval Research (Contract N00014-82-K-0645) and the National Science Foundation (Grant OCE86-00531) to D. Wethey and grants from the Lerner-Gray Fund for Marine Research, Sigma Xi, and the International Women's Fishing Association to L. Walters. We are grateful to all at the Friday Harbor Laboratories for providing us with space and facilities. D. Padilla, D. Pencheff, L. Muehlstein, A. Kettle, S. Cohen, A. Sewell, and countless others assisted with the field work. J. Sutherland and A. Underwood assisted with the statistical analyses. S. Woodin, J. Sutherland, R. Showman, and two anonymous reviewers made helpful comments on the manuscript.

Literature Cited

Atkins, 1955. The cyphonautes larvae of the Plymouth Area and the metamorphosis of *Membranipora membranacea*. *J. Mar. Biol. Assoc. U.K.* **34:** 441–449.

Brancato, M. S., and R. S. Woollacott. 1982. Effect of microbial films on settlement of bryozoan larvae (*Bugula simplex*, *B. stolonifera* and *B. turrita*). *Mar. Biol.* **71:** 51–56.

Buss, L. W. 1980. Bryozoan overgrowth interactions—the interdependence of competition for space and food. *Nature* **281:** 475–477.

Butman, C. A. 1987. Larval settlement of soft-sediment invertebrates: the spatial scales of pattern explained by active habitat selection and the emerging role of hydrodynamic processes. *Oceanogr. Mar. Biol. Ann. Rev.* **25:** 113–165.

Chia, F-S., J. Buckland-Nicks, and C. M. Young. 1984. Locomotion of marine invertebrate larvae: a review. *Can. J. Zool.* **62:** 1205–1222.

Cloney, R. A. 1978. Ascidian metamorphosis: review and analysis. Pp. 255–282 in *Settlement and Metamorphosis of Marine Invertebrate Larvae*, F-S. Chia and M. E. Rice, eds. Elsevier, New York.

Cloney, R. A., and S. A. Torrence. 1984. Ascidian larvae: structure and settlement. Pp. 103–126 in *Marine Biodeterioration*, J. D. Costlow and R. C. Tipper, eds. Naval Institute Press, Annapolis.

Connell, J. H. 1961. The effects of competition, predation by *Thais lapillus*, and other factors on natural populations of the barnacle, *Balanus balanoides*. *Ecol. Monogr.* **31:** 61–104.

Crisp, D. J. 1961. Territorial behavior in barnacle settlement. *J. Exp. Biol.* **38:** 569–590.

Crisp, D. J., and H. Barnes. 1954. The orientation and distribution of barnacles at settlement with particular reference to surface contour. *J. Anim. Ecol.* **23:** 142–162.

Crisp, D. J., and J. S. Ryland. 1960. Influence of filming and of surface texture on the settlement of marine organisms. *Nature* **185:** 119.

Dayton, P. 1971. Competition, disturbance, and community organization: the provision and subsequent utilization of space in the rocky intertidal community. *Ecol. Monogr.* **41:** 351–389.

Denny, M. W. 1988. *Biology and Mechanics of the Wave-Swept Environment.* Princeton University Press, Princeton, NJ.

Denny, M. W., and M. F. Shibata. 1989. Consequences of surf-zone turbulence for settlement and external fertilization. *Am. Nat.* **134:** 859–889.

Grosberg, R. K. 1981. Competitive ability influences habitat choice in marine environments. *Nature* **290:** 700–702.

Hayward, P. J., and P. H. Harvey. 1974. The distribution of settled larvae of the bryozoans *Alcyndium hirsutum* (Fleming) and *Alcyndium polyoum* (Hassall). *J. Mar. Biol. Assoc. U. K.* **54:** 665–676.

Jackson, J. B. C. 1979. Morphological strategies of sessile animals. Pp. 499–555 in *Biology and Systematics of Colonial Organisms*, G. Larwood and B. R. Rosen, eds. Academic Press, New York.

Keough, M. J., and B. J. Downes. 1982. Recruitment of marine invertebrates: the role of active larval choices and early mortality. *Oecologia* **54:** 348–352.

Knight-Jones, E. W. 1951. Gregariousness and some other aspects of the settling behavior of *Spirorbis*. *J. Mar. Biol. Assoc. U. K.* **30:** 201–222.

LeTourneux, F., and E. Bourget. 1988. Importance of physical and biological settlement cues used at different spatial scales by the larvae of *Semibalanus balanoides*. *Mar. Biol.* **97:** 57–66.

Loeb, M. J., and G. Walker. 1977. Origin, composition and function of secretions from pyriform organs and internal sacs of four settling cheilo-ctenostome bryozoan larvae. *Mar. Biol.* **42:** 37–46.

Middleton, G. V., and J. B. Southward. 1984. *Mechanics of Sediment Movement.* 2d ed. Society of Economic Paleontologists and Mineralogists, Tulsa, Okla.

Miller, R. G. 1966. *Simultaneous Statistical Inference.* McGraw-Hill, Inc., New York.

Paine, R. T. 1974. Intertidal community structure: experimental studies on the relationship between a dominant competitor and its principal predator. *Oecologia* **15:** 93–120.

Reed, C. G. 1987. Phylum Bryozoa. Pp. 494–510 in *Reproduction and Development of Marine Invertebrates of the Northern Pacific Coast*, M. F. Strathmann, ed. University of Washington Press, Seattle.

Reed, C. G., and R. M. Woollacott. 1982. Mechanisms of rapid morphogenetic movements in the metamorphosis of the bryozoan *Bugula neritina*. *J. Morphol.* **172:** 335–348.

Ryland, J. S. 1959. Experiments on the selection of algal substrates by polyzoan larvae. *J. Exp. Biol.* **36:** 613–631.

Russ, G. R. 1982. Overgrowth in a marine epifaunal community: competitive hierarchies and competitive networks. *Oecologia* **53:** 12–19.

Sebens, K. P. 1985. Community ecology of vertical rock walls in the Gulf of Maine, U.S.A.: small scale processes and alternative stable states. Pp. 346–371 in *The Ecology of Rocky Coasts*, P. G. Moore and R. Seed, eds. Hodder and Stroughton, London.

Sebens, K. P. 1986. Spatial relationships among encrusting marine organisms in the New England subtidal zone. *Ecol. Monogr.* **56:** 73–96.

Seed, R., and R. J. O'Connor. 1981. Community organization in marine algal epifaunas. *Ann. Rev. Ecol. Syst.* **12:** 49–74.

Snedecor, G. W., and W. G. Cochran. 1967. *Statistical Methods.* Iowa State University Press, Ames, Iowa.

Strathmann, R. R., E. S. Branscomb, and K. Vedder. 1981. Fatal errors in set as a cost of dispersal and the influence of intertidal flora on set of barnacles. *Oecologia* **48:** 13–18.

Svenden, I. A. 1987. Analysis of surf zone turbulence. *J. Geophys. Res.* **92:** 5115–5124.

Torrence, S. A., and R. A. Cloney. 1988. Larval sensory organs of ascidians. Pp. 151–163 in *Marine Biodeterioration, Advanced Techniques Applicable to the Indian Ocean*, M-F. Thompson, R. Sarogini, and R. Nagabhushanam, eds. Oxford and IBH Publishing Company Pvt. Ltd., New Dehli.

Walters, L. J., and D. S. Wethey. 1986. Surface topography influences competitive hierarchies on marine hard substrata: a field experiment. *Biol. Bull.* **170:** 441–449.

Wethey, D. S. 1983. Geographic limits and local zonation: the barnacles Semibalanus (Balanus) and Chthamalus in New England. *Biol. Bull.* **165:** 330–341.

Wethey, D. S. 1984. Spatial pattern in barnacle settlement: day to day changes during the settlement season. *J. Mar. Biol. Assoc. U. K.* **64:** 687–698.

Wethey, D. S. 1986. Ranking of settlement cues by barnacle larvae: influence of surface contour. *Bull. Mar. Sci.* **39:** 393–400.

Wisely, B. 1960. Observations on the settling behavior of larvae of the tubeworm *Spirorbis borealis* Daudlin (Polychaete). *Aust. J. Mar. Freshwat. Res.* **11:** 55.

Woollacott, R. M., and R. L. Zimmer. 1978. Metamorphosis of cellularioid bryozoans. Pp. 49–64 in *Settlement and Metamorphosis of Marine Invertebrate Larvae*, F-S. Chia and M. E. Rice, eds. Elsevier, New York.

Young, C. M., and F. S. Chia. 1981. Laboratory evidence for delay of larval settlement in response to a dominant competitor. *Int. J. Invert. Reprod.* **3:** 221–226.

Reference: *Biol Bull* **180**: 119–124. (February, 1991)

GABA-Like Immunoreactivity in the Nervous System of *Oikopleura dioica* (Appendicularia)

TOMAS BOLLNER[1,*], JON STORM-MATHISEN[2], AND OLE PETTER OTTERSEN[2]

[1]*Department of Zoology, Stockholm University, S-106 91, Sweden, and* [2]*Anatomical Institute, University of Oslo, Karl Johans gt. 47, N-0162 Oslo 1, Norway*

Abstract. The cellular localization of γ-aminobutyric acid (GABA) has been visualized immunocytochemically in the nervous system of *Oikopleura dioica* by using an antiserum to glutaraldehyde fixation complexes of GABA. The results show GABA-like immunoreactivity in neurons of the brain, in cells of the sensory vesicle, in the caudal ganglion, and in the nerve cord. Positive reactions were also found at the neuromuscular terminals in the tail.

Introduction

Amino acids are considered to be important neurotransmitters in the vertebrate central nervous system (review: Ottersen and Storm-Mathisen, 1984a). Among these, γ-aminobutyric acid (GABA) is a dominant inhibitory neurotransmitter in the brain and spinal cord, and even occurs in the peripheral nervous system (Jessen *et al.*, 1986). GABA has also been reported to be a major inhibitory neurotransmitter in a wide variety of the invertebrate phyla (Gerschenfeld, 1973; Meyer *et al.*, 1986; Vitellaro-Zuccarello and De Biasi, 1988). But no information is available concerning this amino acid in the Urochordata, a group that is often considered to be a phylogenetic link between invertebrates and vertebrates.

The organization of the nervous system of *Oikopleura dioica* has been investigated by several authors (Galt and Mackie, 1971; Holmberg, 1984; Bollner *et al.*, 1986), and the presence of acetylecholinesterase in this species has been reported (Durante, 1959; Flood, 1973). The aim of this investigation was to establish whether *Oikopleura dioica* exhibits GABA immunoreactivity in its central or peripheral neurons.

Received 22 January 1990; accepted 6 November 1990.

* Present address: Department of Biology, University of London, Royal Holloway and Bedford New College, Egham Hill, Egham, Surrey TW20 OEX, UK.

Materials and Methods

Specimens of *O. dioica* Fol, 1872, were collected at the Kristineberg Marine Biological Station and at the Tjärnö Marine Biological Laboratory, both on the west coast of Sweden. For immunocytochemistry the following fixatives were used: (1) 5% glutaraldehyde, (2) 3% glutaraldehyde and 1% paraformaldehyde, or (3) 1% glutaraldehyde and 1% paraformaldehyde, all in 0.1 *M* sodium-phosphate buffer at pH 7.4. After 1 h fixation at room temperature, animals were kept and transported in cold sodium-phosphate buffer with 0.5% glutaraldehyde added. Free floating whole tissues were processed for immunocytochemistry as described by Storm-Mathisen *et al.* (1983) and Dale *et al.*, (1986); the primary anti-serum was diluted 1:300 before processing according to the peroxidase-anti peroxidase technique (Sternberger, 1979).

After fixation in 3% glutaraldehyde and 1% paraformaldehyde or 1% glutaraldehyde alone, both in 0.1 *M* sodium-phosphate buffer at pH 7.4, animals were embedded in Epon resin and cut with a glass knife. One-μm sections were processed on glass slides previously coated with either chrome alum gelatin or poly-L-lysine, and processed by the immunogold-silver (IGS) method, as follows.

The sections were etched for 45 min in sodium-ethanolate, washed 3 × 5 min in absolute alcohol, followed by 2 × 5 min in distilled water, and rinsed briefly in 20 m*M* Tris buffer at pH 7.4 containing 155 m*M* NaCl, 0.1% BSA, and 20 m*M* NaN_3. The same medium was also used for subsequent rinses and for diluting sera. The sections were then incubated with a droplet of 5% normal goat serum in a moist chamber for 20 min. Thereafter they were incubated overnight in 50 μl primary anti-serum diluted 1:100. After a rinse in buffer, followed by washes 3 × 10 min in buffer at pH 8.2, the sections were incubated for 60 min with GAR G5 (goat anti-rabbit immunoglob-

ulin adsorbed to 5 nm colloidal gold, Janssen, Belgium) diluted 1:80 in the same buffer. Finally the sections were washed with the same medium as after primary serum, rinsed in distilled water several times (5 min each at least), developed in 100 μl silver enhancer kit (Janssen), washed in water, and coverslipped.

Indirect immunofluorescense as well as the peroxidase-antiperoxidase (PAP) method of Sternberger (1979) were also tried; the same primary antibodies were visualized by either a second layer of FITC-conjugated sheep anti-rabbit serum (SIGMA), or by unlabeled sheep anti-rabbit serum (Statens Bakteriologiska Laboratorium, Stockholm) followed by PAP complex (Dakopatts).

The antiserum against glutaraldehyde-conjugated γ-aminobutyric acid (GABA antiserum 26) was raised, purified, and characterized as described previously (Ottersen and Storm-Mathisen, 1984b; Ottersen *et al.*, 1986). For all methods used, the controls included absorption of GABA antiserum with GABA-glutaraldehyde complexes (GABA-G) and glutamate complexes (Glu-G) at final concentrations of 300 μ*M*, or replacement of the primary antiserum with normal rabbit serum. Furthermore, the immunoreactivity of the antiserum used was tested according to the filter disc method described by Ottersen and Storm-Mathisen (1984b). The fixation conjugates spotted on the discs were made from macromolecules extracted from rat brain homogenate and from homogenate of the neural complex from the ascidian *Ciona intestinalis*.

Results

The central nervous system of *Oikopleura dioica* consists of an anterior ganglion (brain) and tail ganglia. The anterior part of the brain is extended into paired bulbs, and in the mid-region it has a sensory vesicle. The brain is connected to several ganglia in the tail by a solid nerve cord. The largest of these tail ganglia is referred to as the caudal ganglion (Figs. 1, 2).

Although the brain is hard to see in whole mounts due to the thick oikoplast epithelium, GABA-like immunoreaction was observed in the paired anterior bulbs described by Bollner *et al.*, (1986). In semithin sections, a positive reaction is easily seen in some of the neurons in the bulbs (Fig. 3). In the rest of the brain, staining with the GABA anti-serum were found: in one cell located ventrally in the mid region, in one of the most caudal cells (Figs. 2, 4), and in a dorsal cell close to the sensory vesicle (Fig. 5). Furthermore, immunopositive staining was seen in the epithelial cells referred to as the "brain vesicle cells" by Holmberg (1984) (Fig. 6).

Two immunostained cell bodies situated in the caudal part of the caudal ganglion were observed in semithin sections (Fig. 7) and in the whole mount preparations (Fig. 8). Immunoreactive fibers were seen in both semithin

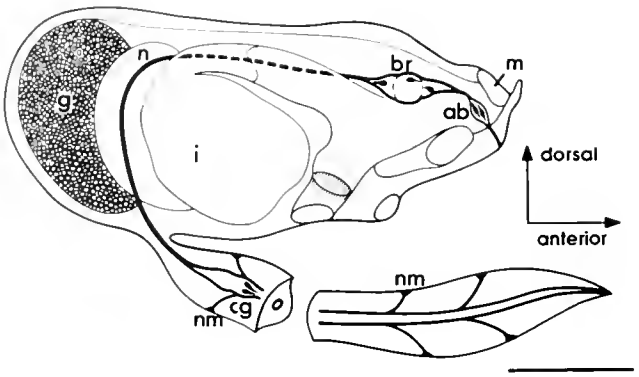

Figure 1. Schematic drawing of *Oikopleura dioica* showing the position of the nervous system with the immuno-positive neurons indicated, the position of the sensory vesicle is indicated by the dotted circle. ab, anterior bulb; br, brain; cg, caudal ganglion; g, gonads; i, intestine; m, mouth; n, nerve cord; nm, neuromuscular junction. Bar = 200 μm.

sections (Fig. 7) and in whole mounts. Transverse semithin sections through the tail showed GABA-like immunoreactivity in the large nerve terminals (Fig. 9) innervating the muscles (*cf.* Flood, 1973, 1975) and in fibers of the dorsal nerve cord. Furthermore, positive staining was often seen in the epithelial cells of the notochord. Because the tail of the animal is twisted 90° counter-clockwise, the dorsal nerve cord is seen to the right of the notochord in a frontal view of a transverse section of tail.

The semithin sections from animals fixed with 1% glutaraldehyde processed using the immunogold technique gave a stronger reaction than any other method. The PAP-method showed weak staining in the anterior bulbs and in the caudal ganglion, whereas the FITC-incubated sections showed clear label in the same regions as did the immunogold method. However, all methods showed similar patterns of immunoreactivity.

The anti GABA serum, either absorbed with glutamate-glutaraldehyde complex (Glu-G) or not, produced selective staining of the GABA conjugates on the filter discs, but no significant staining could be seen after pretreatment of the GABA antiserum with GABA-glutaraldehyde complex (GABA-G) (Fig. 8). Similar results were obtained with spots of amino acids conjugated to macromolecules from rat and *Ciona*, suggesting that the previously demonstrated specificity is valid also for urochordates. In whole mounts as well as in semithin sections, the reaction was virtually abolished when antisera treated with GABA-G or normal rabbit serum were used instead of GABA antiserum. Treatment of the anti serum with Glu-G did not have this effect.

Discussion

Many investigations have established the presence of either GABA or glutamic acid decarboxylase (GAD),

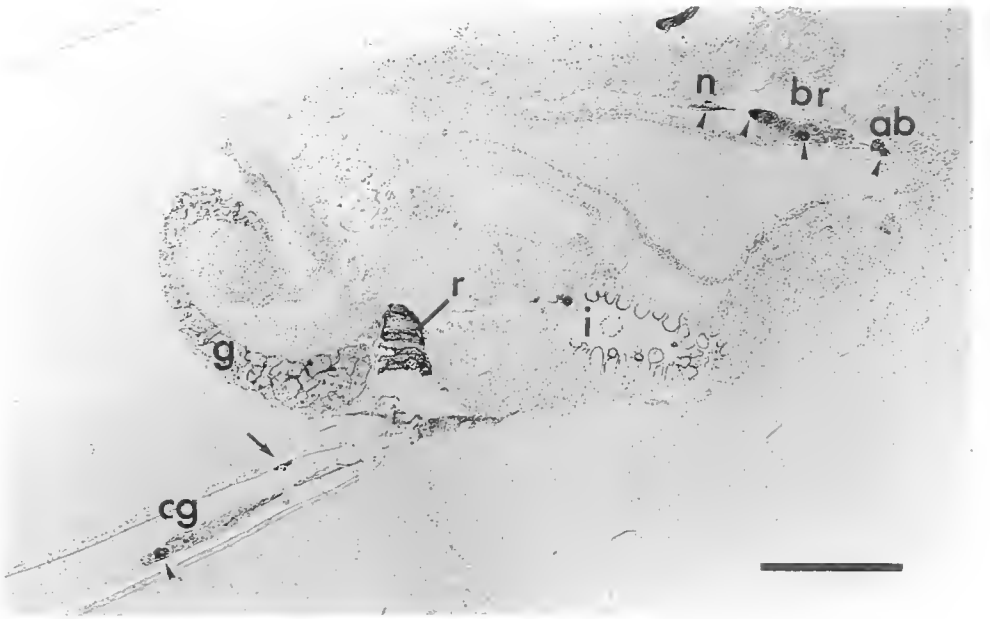

Figure 2. Sagittal section through the whole animal showing the localization and GABA-like immunoreactivity (arrowheads) of the brain (br), one of the anterior bulbs (ab), the nerve cord (n), the caudal ganglion (cg) and in a neuromuscular junction of the tail (arrow). Staining can also be seen in the gonads (g), at the apical surface of some of the intestinal cells (i), and in the rectum (r). No staining could be seen in an adjacent section treated with anti-GABA/GABA-G. IGS method. Differential interference contrast. Bar = 100 μm.

which catalyzes the synthesis of GABA from glutamate, in lower chordates and in invertebrates (Osborne, 1972; Osborne *et al.*, 1979; De Biasi, 1986). More recently, the use of specific antibodies (Storm-Mathisen *et al.*, 1983) has led to a more precise knowledge about the cellular localization of GABA in both vertebrates (Ottersen and Storm-Mathisen 1984, a, b; Roberts *et al.*, 1987) and invertebrates (Bicker *et al.*, 1985; Meyer *et al.*, 1986; Homberg *et al.*, 1987). This is, to our knowledge, the first immunocytochemical study on the occurrence of amino acids in the nervous system of a protochordate. Using biochemical analyses, Osborne *et al.* (1979) found GABA and several other putative amino acid neurotransmitters in homogenates of the cerebral ganglion of another protochordate, the tunicate *Ciona intestinalis*.

The present investigation shows the cellular localization of a GABA-like substance in the nervous tissue of *O. dioica*. The GABA-positive cells in the anterior bulbs and in the rest of the brain are thought to be neurons judging from their location and their ultrastructural appearance previously described by Bollner *et al.*, (1986, unpubl.). Also, most of the cells in the caudal ganglion are considered to be neurons. However, one of its anterior cells, a large ependymal cell, produces the Reissner's fiber (Holmberg and Olsson, 1984). The significance of GABA-like immunoreactivity in the neurons of the central nervous system is difficult to evaluate. Although they may be neurons with inhibitory functions, it should be remembered that GABA may also have depolarizing effects (Alger and Nicoll, 1982). In addition to the neural localization, GABA was clearly present in epithelial cells. This agrees with the situation in vertebrates, where GABA has been demonstrated in non-neural epithelial cells (Orensanz *et al.*, 1986; Davanger *et al.*, 1989). Amino acids in general are also known to modulate osmoregulation (see Gilles, 1979, for review). Synthesis of GABA has been reported to occur in fish erythrocytes where it may participate in the maintenance of a constant cell volume (Fugelli *et al.*, 1970). *O. dioica* is an isosmotic animal, and the vesicle and the chorda are the only internal structures not totally surrounded by hemolymph, and therefore might use GABA for regulating the intracellular osmolarity.

The muscles in the tail are innervated both by fibers branching directly from the nerve cord and from perikarya along the cord (Flood, 1973). These nerves have elaborate end-arborizations on the surface of the muscle cells and are thought to be cholinergic (Flood, 1975; Bone and Mackie, 1982). Cholinergic neuromuscular transmission is widely distributed throughout the animal kingdom, but GABA-ergic inhibition of muscles is only known in invertebrate phyla (Gerschenfeld, 1973). GABA-like immunoreactivity has been demonstrated in inhibitory nerves in insect muscle (Bicker *et al.*, 1988; Robertson

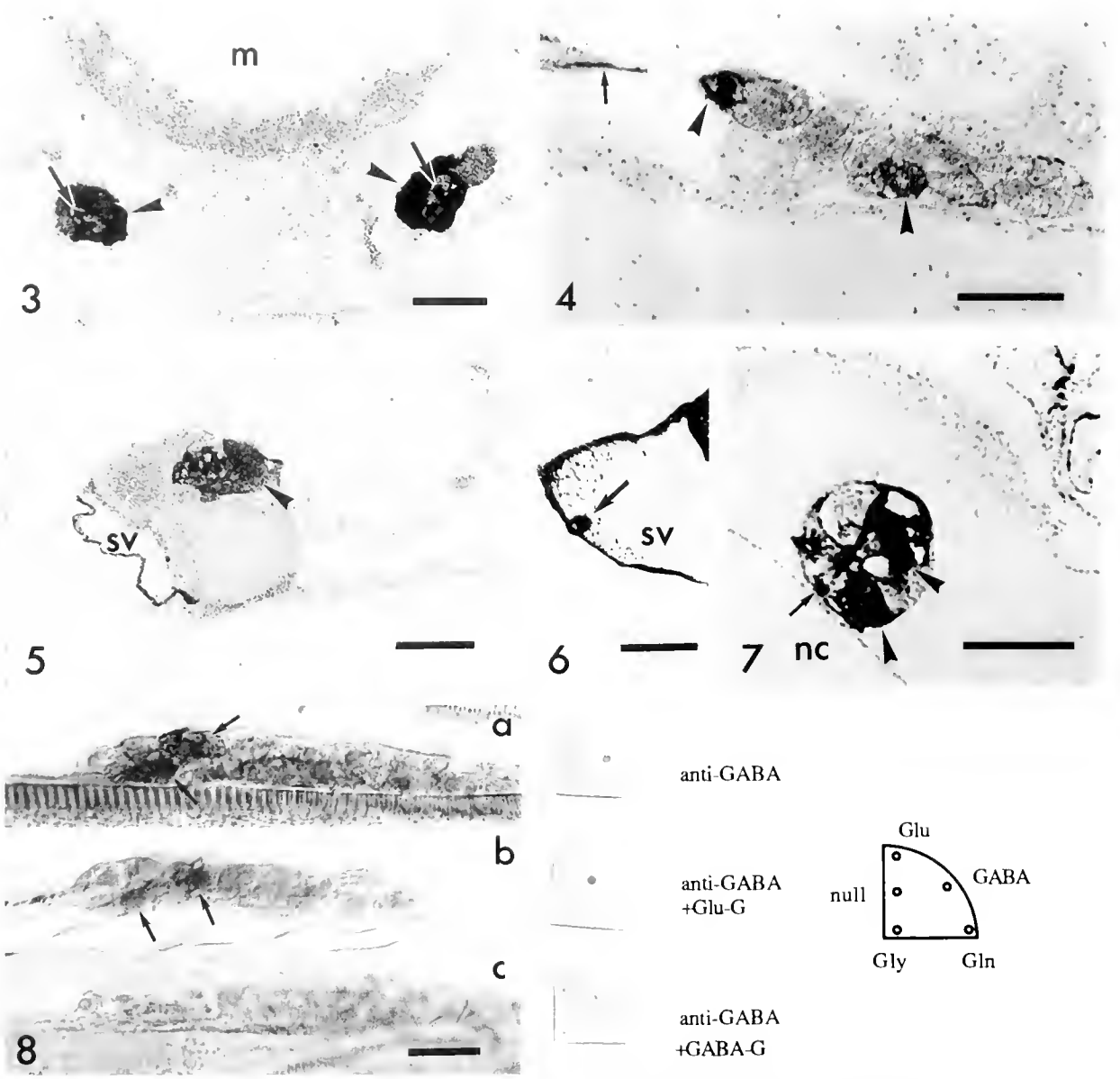

Figure 3. Transverse section through the anterior bulbs with staining in neurons (arrowheads) and in some of the fibers of the neuropile (arrows). m, mouth. IGS method. Differential interference contrast. Bar = 15 μm.

Figure 4. Sagittal section showing positive staining in one cell in the mid part and in one cell in the rear part of the brain (arrowheads) and also in a fiber of the nerve cord (arrow). IGS method. Differential interference contrast. Bar = 15 μm.

Figure 5. Transverse section through the brain in the region of the sensory vesicle (sv), with staining in one cell body (arrowhead). IGS method. Differential interference contrast. Bar = 15 μm.

Figure 6. Section through the sensory vesicle (sv) showing positive staining in one of the brain vesicle cells (arrowhead) and in the epithelial cells forming the vesicle wall. IGS method. Differential interference contrast. Bar = 15 μm.

Figure 7. Transverse section through the caudal ganglion showing positive staining in cell somata (arrowheads) and in neuropile fibers (arrow); nc, notochord. IGS method. Differential interference contrast. Bar = 10 μm.

Figure 8. Whole-mount preparations of the caudal ganglion showing positive reaction in neurons (*arrows*) after treatment with anti-GABA (a) and anti-GABA/Glu-G (b) and no reaction after treatment with anti-GABA/GABA-G (c), corresponding control filter discs with amino acids conjugated to macromolecules from *Ciona* neural tissue by glutaraldehyde are shown at the right. Gln, glutamine; Gly, glycine; null, glutaraldehyde-treated protein with no amino acid added. PAP method. Bar = 15 μm.

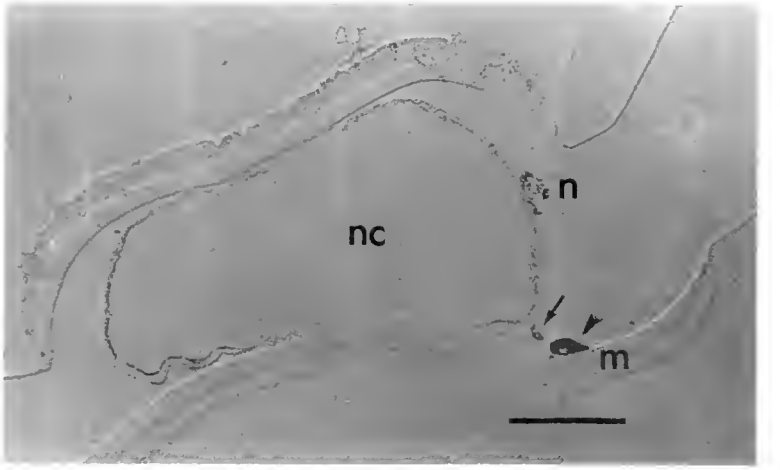

Figure 9. Transverse section through the tail near the trunk, frontal view. GABA-like immunoreaction can be seen in a neuromuscular terminal (arrowhead) and in the nerve cord (n). This section also shows staining in a part of the fiber between the nerve cord and the neuromuscular terminal (arrow). m, muscle; nc, notochord. IGS method. Differential interference contrast. Bar = 20 μm.

and Wisniowski, 1988). Our finding that neuromuscular synapses of *O. dioica* show GABA-like immunoreactivity is the first indication that GABA may also act as neuromuscular inhibitory substance in some chordates.

More work is needed to establish whether GABA is a neurotransmitter in *O. dioica*. Its possible role in osmoregulation in the vesicle should also be subject to further investigation.

Acknowledgments

We are grateful to A. T. Bore and Y. Lilliemark for technical assistance. This investigation was supported by the Hierta-Retzius and Lars Hiertas Minne foundations.

Literature Cited

Alger, B. E., and R. A. Nicoll. 1982. Pharmacological evidence for two kinds of GABA receptor on rat hippocampal pyramidal cells studied *in vitro*. *J. Physiol.* **328:** 125–141.

Bicker, G., S. Schäfer, and T. G. Kingan. 1985. Mushroom body feedback inter neurons in the honeybee show GABA-like immunoreactivity. *Brain Res.* **360:** 394–397.

Bicker, G., S. Schäfer, O. P. Ottersen, and J. Storm-Mathisen. 1988. Glutamate-like immunoreactivity in identified neuronal populations of insect nervous systems. *J. Neurosci.* **8:** 2108–2122.

Bollner, T., K. Holmberg, and R. Olsson. 1986. A rostral sensory mechanism in *Oikopleura dioica* (Appendicularia). *Acta Zool.* **67:** 235–241.

Bone, Q., and G. O. Mackie, 1982. Urochordata. Pp. 473–535 in *Electrical Conduction and Behavior in "Simple" Invertebrates*, G. A. B. Shelton, ed. Oxford University Press, Oxford.

Dale, N., O. P. Ottersen, A. Roberts, and J. Storm-Mathisen. 1986. Inhibitory neurons of a motor pattern generator in *Xenopus* revealed by antibodies to glycine. *Nature* **324:** 255–257.

Davanger, S., O. P. Ottersen, and J. Storm-Mathisen. 1989. GABA immunoreactive cells in the rat gastrointestinal epithelium. *Anat. Embryol.* **179:** 221–226.

De Biasi, S., C. Frassoni, and L. Vitellaro Zuccarello. 1986. Glutamic acid decarboxylase (GAD)-like immunoreactivity in the pedal ganglion of *Mytilus galloprovincialis*. *Cell Tissue Res.* **244:** 591–593.

Durante, M. 1959. Sulla localizzazione istochimica della acetilcolinesterasi lungo lo sviluppo di alcune ascidie e in appendicularie. *Acta Embryol. Morphol. Exp.* **2:** 234–243.

Flood, P. R. 1973. Ultrastructural and cytochemical studies on the muscle innervation in Appendicularia, Tunicata. *J. Microsc.* **18:** 317–326.

Flood, P. R. 1975. Scanning electron microscope observations on the muscle innervation of *Oikopleura dioica* Fol (Appendicularia, Tunicata) with notes on the arrangement of connective tissue fibers. *Cell Tissue Res.* **164:** 357–369.

Fol, H. 1872. Etudes sur les appendiculaires du détroit de Messine. *Mém. Soc. Phys. Hist. Nat. Geneve* **21:** 445–449.

Fugelli, K., J. Storm-Mathisen, and F. Fonnum. 1970. Synthesis of γ-aminobutyric acid in fish erythrocytes. *Nature* **228:** 1001.

Galt, C. P., and G. O. Mackie. 1971. Electrical correlates of ciliary reversal in *Oikopleura*. *J. Exp. Biol.* **55:** 205–212.

Gerschenfeld, H. M. 1973. Chemical transmission in invertebrate central nervous system and neuromuscular junctions. *Physiol. Rev.* **53:** 1–119.

Gilles, R. 1979. Intracellular organic osmotic effectors. Pp. 11–154 in *Mechanisms of Osmoregulation in Animals*, R. Gilles, ed. Wiley Chichester, New York.

Holmberg, K. 1984. A transmission electron microscopic investigation of the sensory vesicle in the brain of *Oikopleura dioica* (Appendicularia). *Zoomorphology* **104:** 298–303.

Holmberg, K., and R. Olsson. 1984. The origin of Reissner's fibre in the appendicularian, *Oikopleura dioica*. *Viddensk. Medd. Dan. Naturhist. Foren.* **145:** 43–52.

Homberg, U., T. G. Kingan, and J. G. Hildebrand. 1987. Immunocytochemistry of GABA in the brain and suboesophageal ganglion of *Manduca sexta*. *Cell Tissue Res.* **248:** 1–24.

Jessen, K. R., J. M. Hills, and J. Saffrey. 1986. Immunohistochemical demonstration of GABA ergeic neurons in the enteric nervous system. *J. Neurosci.* **6:** 1628–1634.

Meyer, E. P., C. Matute, P. Streit, and D. R. Nässel. 1986. Insect optic lobe neurons identifiable with monoclonal antibodies to GABA. *Histochemistry* **84:** 207–216.

Orensanz, L. M., I. Fernández, R. Martín del Río, and J. Storm-Mathisen. 1986. Gamma-aminobutyric acid in the rat oviduct. *Adv. Biochem. Psychopharmacol.* **42:** 265–274.

Osborne, N. N. 1972. Occurrence of glycine and glutamic acid in the nervous system of two fish species and some invertebrates. *Comp. Biochem. Physiol.* **43B:** 579–585.

Osborne, N. N., V. Neuhoff, E. Ewers, and H. A. Robertson. 1979. Putative neurotransmitters in the cerebral ganglia of the tunicate *Ciona intestinalis*. *Comp. Biochem. Physiol.* **63C:** 209–213.

Ottersen, O. P., and J. Storm-Mathisen. 1984a. Neurons containing or accumulating transmitter amino acids. Pp. 141–146 in *Classical Transmitters and Transmitter Receptors in the CNS Part II*, A. Bjorklund, T. Hökfelt, and M. J. Kuhar, eds. Handbook of Chemical Neuroanatomy, Vol. 3 Elsevier, Amsterdam.

Ottersen, O. P., and J. Storm-Mathisen. 1984b. Glutamate- and GABA-containing neurons in the mouse and rat brain, as demonstrated with a new immunocytochemical technique. *J. Comp. Neurol.* **229:** 374–392.

Ottersen, O. P., J. Storm-Mathisen, S. Madsen, S. Skumlien, and J. Strømhaug. 1986. Evaluation of the immunocytochemical method for amino acids. *Med. Biol.* **64:** 147–158.

Roberts, A., N. Dale, O. P. Ottersen, and J. Storm-Mathisen. 1987. The early development of neurons with GABA immunoreactivity in CNS of *Xenopus laevis* embryos. *J. Comp. Neurol.* **261:** 435–449.

Robertson, R. M., and L. Wisniowski. 1988. GABA-like immunoreactivity of identified inter neurons in the flight system of the locust, *Locusta migratoria*. *Cell Tissue Res.* **254:** 331–340.

Sternberger, L. A. 1979. *Immunocytochemistry*, Second Edition. John Wiley and Sons, New York, Chichester.

Storm-Mathisen, J., A. K. Leknes, A. T. Bore, J. L. Vaaland, P. Edminson, F-M. S. Haug, and O. P. Ottersen. 1983. First visualization of glutamate and GABA in neurons by immunocytochemistry. *Nature* **301:** 517–520.

Vitellaro Zuccarello, L., and S. De Biasi. 1988. GABA-like immunoreactivity in the pedal ganglia of *Mytilus galloprovincialis*: light and electron microscopic study. *J. Comp. Neurol.* **267:** 516–524.

Reference: *Biol. Bull.* **180:** 125–134. (February, 1991)

Ontogeny of Osmoregulation and Salinity Tolerance in *Cancer irroratus;* Elements of Comparison with *C. borealis* (Crustacea, Decapoda)

G. CHARMANTIER AND M. CHARMANTIER-DAURES

Laboratoire d'Ecophysiologie des Invertébrés, Université des Sciences, Montpellier 2, Place E. Bataillon, 34095 Montpellier cedex 05, France

Abstract. Osmoregulation and salinity tolerance were studied in zoeae, megalopae, first crab stage (osmoregulation only), and adults of *Cancer irroratus*, and in zoeae and adults of *C. borealis*.

In *C. irroratus*, salinity tolerance was moderate in zoeae, decreased in late zoeae 5, was at a minimum in megalopae, and increased in adults. The lower and upper lethal salinities for 50% of the animals (48 h LS 50) at 15°C were about 13–17‰/42–50‰ in zoeae, 24‰/37‰ in megalopae, and 8.5‰/65‰ in adults.

In *C. borealis*, the corresponding values of LS 50s were 16–20‰/46–50‰ in zoeae and 12‰/65‰ in adults.

In both species, zoeae were hyper-osmoconformers; adults were isosmotic in high salinities and slightly hyper-regulators in low salinities. In *C. irroratus*, the change from larval to adult type of regulation occurred from megalopa (hyper-osmoconformer) to first crab stage (hyper-regulator in dilute media), *i.e.*, after the completion of metamorphosis.

Osmoregulation and salinity tolerance appear correlated and are modified at metamorphosis. These results are discussed with an emphasis on the effects of metamorphosis on osmoregulation of developing decapods.

Introduction

While osmoregulation has been extensively studied in adult crustaceans (review in Mantel and Farmer, 1983), relatively few data are available on larval or post-larval osmoregulation, in the following species: *Rhithropanopeus harrisii* (Kalber and Costlow, 1966), *Cardisoma guanhumi* (Kalber and Costlow, 1968), *Callinectes sapidus*, *Hepatus epheliticus*, *Libinia emarginata* (Kalber, 1970), *Sesarma reticulatum* (Foskett, 1977), *Clibanarius vittatus* (Young, 1979), *Callianassa jamaica* (Felder *et al.*, 1986), *Macrobrachium petersi* (Read, 1984), *Uca subcylindrica* (Rabalais and Cameron, 1985), *Homarus americanus*, and *Penaeus japonicus* (Charmantier, 1986; Charmantier *et al.*, 1984a, 1988).

For different reasons, including culture difficulties in late larval stages, osmoregulation was frequently studied in larval stages only, particularly in brachyuran crabs. However, in the four latter species, osmoregulation was studied throughout the post-embryonic development including post-metamorphic stages, thus osmoregulation in larvae, postlarvae, and adults could be compared. The ability to osmoregulate did not change along the development in some species. In other species, metamorphosis marked the appearance of the adult type of regulation; among brachyurans, this case has been so far documented in only one species, *U. subcylindrica*, the adults of which are strong hyper-hypo-regulators (Rabalais and Cameron, 1985).

Consequently, one of the objectives of this study was to determine whether comparable changes in osmoregulation at metamorphosis exist in brachyurans with lower abilities to osmoregulate, particularly in species of the genus *Cancer*, which slightly hyper-regulate in low salinities. Experiments designed to study the ontogeny of osmoregulation were performed on the most abundant *Cancer* species of the Canadian East coast, the rock crab *Cancer irroratus* Say 1817. Comparative data were also obtained from some developmental stages of a sympatric species, the Jonah crab *Cancer borealis* Stimpson, 1859.

Numerous studies have dealt with the tolerance to salinity of crustacean larvae and postlarvae, but the corre-

Received 11 June 1990; accepted 27 November 1990.

lation between the salinity tolerance of different developmental stages and their corresponding osmoregulatory capabilities has only been experimentally investigated in a few species, *U. subcylindrica* (Rabalais and Cameron, 1985), *H. americanus* and *P. japonicus* (Charmantier *et al.*, 1988).

Thus, the second objective of this study was to determine the salinity tolerance of larval, postlarval, and adult stages of *C. irroratus* (and, for the purpose of comparison, of *C. borealis*), and to attempt to correlate their osmoregulatory abilities and their salinity tolerance. This is of particular interest in *Cancer* species, the larvae of which are submitted to different patterns of salinity changes: in *C. irroratus*, zoeae hatch offshore and, as development proceeds, late larvae and postlarvae are found nearer to shore (Sandifer, 1973).

In both species, the early post-embryonic development comprises one prezoea, five zoeal stages, one megalopal stage, and several early crab stages (Sastry, 1977a, b). Following a wide acceptance, zoeae are larval stages, and the following stages, beginning with the megalopa, are considered postlarvae (Felder *et al.*, 1985).

In *C. irroratus*, osmoregulation has been studied in adults and large juveniles (Thurberg *et al.*, 1973; Cantelmo *et al.*, 1975; Neufeld and Pritchard, 1979), and preliminary data on osmoregulation are also available in the early post-embryonic stages (Charmantier *et al.*, 1989).

Materials and Methods

Animals

Adult *C. irroratus* and *C. borealis* were caught by SCUBA diving in summer and autumn in Passamaquoddy Bay and transferred to the culture facility at the Biological Station, St Andrews, New Brunswick, Canada. They were kept in tanks supplied with running seawater ($S \cong 29$–$32‰$; $T \cong 12°C$) under natural photoperiod, and were fed cod, squid, and shrimp (*Pandalus borealis*). In September, two weeks before the experiments, four groups of crabs were selected: large and small *C. irroratus* [cephalothoracic width (CTW): 91 to 115 mm and 45 to 70 mm, respectively], and large and small *C. borealis* (CTW: 80–110 mm and 57–71 mm). Males and females were equally represented in each group. They were transferred to 250-l tanks with charcoal-filtrated recirculated seawater kept at 15°C. Only animals in molt stages C or Do (according to the nomenclature of Drach, 1939) were retained for survival and osmoregulatory experiments.

Larvae of both species were obtained in spring and summer from some of the aforementioned crabs. After hatching, larvae were transferred to 40-l planktonkreisels (Hughes *et al.*, 1974) supplied with flow-through seawater at a salinity of 29–32‰ under natural photoperiod. The planktonkreisels, normally used for culturing lobster larvae, were modified for the culture of crab larvae. Seawater was filtered to 50 μm during the zoea development then suppressed; flow-rate was set at 2.5–3 l min^{-1} from zoeae 1 to early megalops, then at 1.–1.5 l min^{-1}; a 280 μm mesh screen was used around the overflow system. Water temperature was set at 15°C during the zoeal development, then at 19°C. Cephalothoracic length was about 0.56 mm in zoeae 1, 1.5 mm in zoeae 5, 2.2 mm in megalopae, and CTW was 2.3 mm in first crab stage (Charmantier-Daures and Charmantier, 1991). Crab larvae were fed three times a day with live *Artemia* nauplii. Larvae of *C. irroratus* were cultured to the second crab stage, and those of *C. borealis* to the third zoea. As each larval stage lasts several days, molting stages were obtained according to the time elapsed from the preceeding molt, and three groups of animals, postmolt stage A, stage C, and premolt stage D, were selected.

Preparation of media

Experimental media were prepared in compartmented 250-l tanks for adults and 0.5-l plastic containers for larvae and young crabs. Dilute media were prepared by adding tap water to seawater, and high salinity media were prepared by adding "Instant Ocean Synthetic Sea Salts" (Aquarium Systems, Inc.) to seawater. All experiments were conducted at 15°C. Salinities were expressed according to the osmotic pressure in mosm · kg^{-1}, and to the salt content in the medium in ‰. A value of 3.4‰ is equivalent to 100 mosm · kg^{-1}. Osmotic pressure was measured with an Advanced Instruments 31 LA or Wescor 5000 osmometer, and salinity on a YSI 33 salinometer.

Survival bioassays

Due to the small number of available animals, salinity tolerance in adults was evaluated only from the number of surviving and dead animals in media of different salinities. Adult crabs were progressively adapted from seawater to diluted or concentrated media by adding freshwater or Instant Ocean salts to the original medium; each change of 100 mosm · kg^{-1} in the salinity required about 24 h. Between two changes of salinity, they were kept for two days at constant salinity in each test medium, which differed from one another by increments of 100 mosm · kg^{-1} ($\cong 3.4‰$).

Acute static 48–96 h bioassays were conducted with zoeae and megalopae held in test media ranging from 100 mosm · kg^{-1} to seawater ($\cong$900–1000 mosm · kg^{-1}) and to 1600 mosm · kg^{-1}, and differing by increments of 100 mosm · kg^{-1}. Each bioassay was run on a group of 10 individuals and replicated. Animals were counted and dead animals removed at 0.5, 1, 3, 6, 12, 24, 36, 48, 72, 96 h according to the prescriptions of Sprague (1969) in toxicity studies. The criteria for death were total lack of

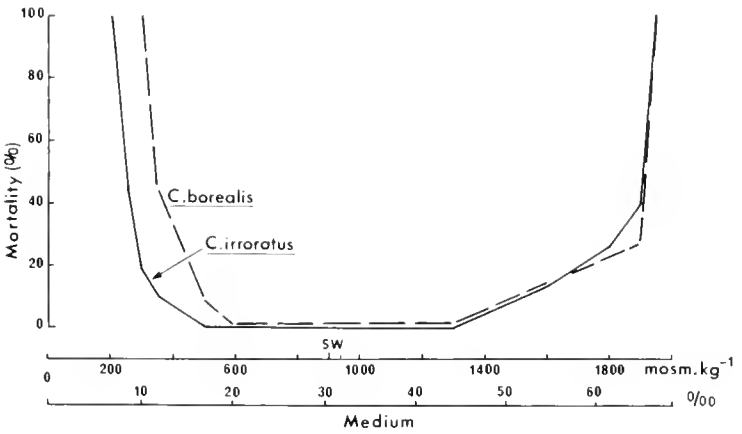

Figure 1. Salinity tolerance in adult *Cancer irroratus* and *C. borealis* at 15°C. Percent mortality of animals according to the salinity of the medium. Number of animals at the start of the experiments in seawater (SW): *C. irroratus:* 16 (to low salinity media) and 8 (to high salinity media); *C. borealis.* 19 and 7.

movement, immobility of appendages and heart, and lack of response after repeated touches with a probe. Median lethal salinities (LS 50) and 95% confidence intervals were calculated by techniques of probit analysis (Lichtfield and Wilcoxon, 1949; Finney, 1962) computerized on the Letcur program (Zitko, 1982; Lieberman, 1983). LS 50s were calculated at 24, 48, and 96 h. Survival bioassays were not run in first and second crab stages due to the small number of available animals.

Osmoregulation

The hemolymph was collected from adult crabs via a hypodermic needle inserted through the articulation membrane at the basis of the fourth or fifth pereiopods. At least seven days elapsed between hemolymph samples were taken from the same animal.

Zoeae, megalopae, and young crabs were quickly dried on filter paper and immersed in mineral oil to avoid evaporation and desiccation. The hemolymph was then sampled with a glass micropipette inserted in the heart.

Osmotic pressure of hemolymph was measured on an Advanced Instruments 31 LA or Wescor 5000 osmometer (adults) or on a Kalber-Clifton micro-osmometer, with reference to the osmotic pressure of the medium (young stages). Student *t* tests were used for statistical comparisons.

Results

Salinity tolerance

The ability of *C. irroratus* and *C. borealis* to tolerate low and high salinities varied with post-embryonic development.

Adults of *C. irroratus* survived without mortality in media ranging from 500 mosm · kg^{-1} to 1300 mosm · kg^{-1} (≅17‰ to 44‰). The LS 50 s were about 250 and 1900 mosm · kg^{-1} (≅8.5 and 65‰). In adult *C. borealis,* no mortality was observed between 600 and 1300 mosm · kg^{-1} (≅20.4 and 44‰), and LS 50s were about 350 and 1900 mosm · kg^{-1} (12 and 65‰) (Fig. 1). No difference in salinity tolerance was detected between large and small crabs of either species.

In larvae and postlarvae of *C. irroratus* the 48 h LS 50 in low salinity media varied around 450 ± 60 mosm · kg^{-1} (≅15 ± 2‰) in zoeal stages 1 to 4 and early 5, then increased from the end of stage zoea 5 through early megalopae (≅600 mosm · kg^{-1}, 20‰) to a highly significant maximum value (corresponding to a minimum tolerance) of 700 mosm · kg^{-1} (≅24‰) in intermolt megalopae. The 24 h and 96 h LS 50s were, respectively, generally lower and higher than the 48 h value but followed the same pattern of variation. Maximum LS 50s at 24, 48, and 96 h occurred in megalopae with respective values of 520, 700, and 820 mosm · kg^{-1} (18, 24, and 28‰), differing significantly from one another.

In high salinity media, the 48 h LS 50 of *C. irroratus* young stages varied around 1350 ± 120 mosm · kg^{-1} (≅46 ± 4‰) in zoeal stages 1 to 5, then decreased in early megalopae (≅1240 mosm · kg^{-1}, ≅42‰) to a highly significant minimum value of 1100 mosm · kg^{-1} (≅37‰) in intermolt megalopae. The 24 h and 96 h LS 50s were respectively higher and lower than the 48 h value; they followed the same pattern of variation, decreasing to minima of 1150 mosm · kg^{-1} (24 h: 39‰) and 1000 mosm · kg^{-1} (96 h: 34‰) in megalopae (Fig. 2).

In zoeae of *C. borealis,* the 48 h LS 50 varied around 530 ± 60 mosm · kg^{-1} (≅18 ± 2‰) in low salinities. The 24 h and 96 h LS 50s were markedly lower and higher than the 48 h LS 50. The differences between 96 h and 24 h LS 50s were more important than in *C. irroratus:* in

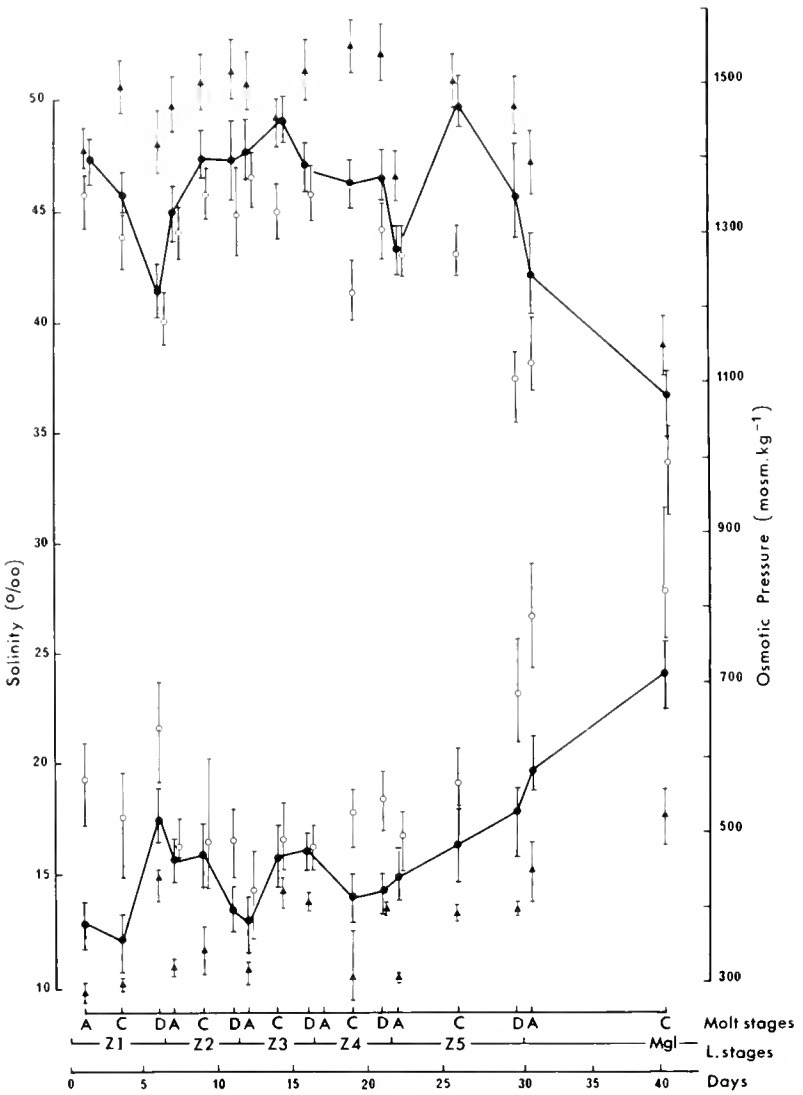

Figure 2. Salinity tolerance in zoeae 1–5 and megalopae of *Cancer irroratus* at 15°C. Variations in LS 50 in ‰ and mosm · kg^{-1} according to larval and molt stages and to days of development, in high and low salinities (upper and lower traces). Each point represents the mean value of at least two determinations from 10 animals, with 95% confidence interval. Closed triangles: 24 h LS 50. Closed circles: 48 h LS 50; open circles: 96 h LS 50.

some instances (early zoea 1 and zoea 2), the 24 LS 50 was about 300 mosm · kg^{-1} (10‰), the 96 h LS 50 reaching about 740 mosm · kg^{-1} (25‰). In high salinities, the 48 h LS 50 varied around 1420 ± 60 mosm · kg^{-1} (≅48 ± 2‰); 24 h and 96 h LS 50s were respectively higher and lower (Fig. 3).

Osmoregulation

Adaptation time. The time of adaptation after a change in the environmental salinity was evaluated in stage C zoeae 1 and 5 and in adults of *C. irroratus*. After a rapid transfer from seawater at 920 mosm · kg^{-1} (31‰) to a dilute medium of 500 mosm · kg^{-1} (17‰), the hemolymph osmotic pressure stabilized within 1 to 2 h in zoeae 1 and 5. In adults transferred from seawater to a dilute medium of 677 mosm · kg^{-1} (23‰), the corresponding time was 24 h (Fig. 4). The time of osmotic adaptation to concentrated media was not tested; in other species, it was shorter than the time of adaptation to dilute media (Charmantier *et al.*, 1988). In all subsequent experiments and in both species, we kept the young stages 6–24 h and the adults 3–4 days in each medium before sampling.

Osmoregulation. Adults of *C. irroratus* and *C. borealis* were almost osmoconformers in high salinities and

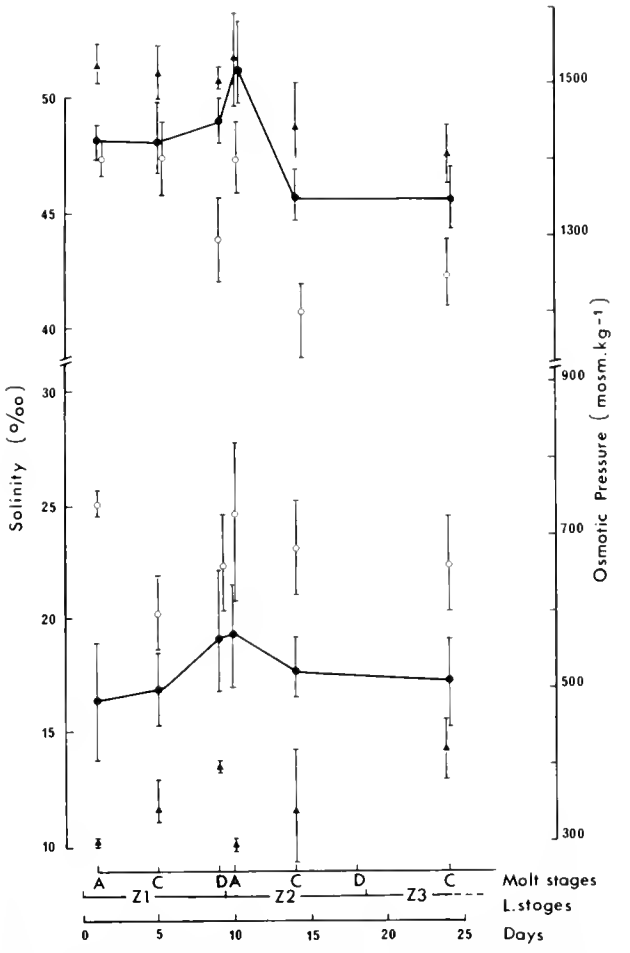

Figure 3. Salinity tolerance in zoeae 1–3 of *Cancer borealis* at 15°C. Variations in LS 50 in ‰ and mosm · kg^{-1} according to larval and molt stages and to days of development, in high and low salinities (upper and lower traces). Each point represents the mean value of two determinations from 10 animals, with 95% confidence interval. Closed triangles: 24 h LS 50; closed circles: 48 h LS 50; open circles: 96 h LS 50.

seawater, and their regulation was slightly hyper-osmotic in dilute media (Fig. 5). No difference of hyper-regulation was detected between large and small adults in *C. borealis*. In *C. irroratus* large crabs were significantly stronger regulators than small crabs (hemolymph-medium differences of 71 ± 7 and 55 ± 13 mosm · kg^{-1} respectively, $P < 0.005$, in a 500 mosm · kg^{-1}; 17‰, medium). The ability to hyper-regulate in dilute media was significantly higher in *C. irroratus* than in *C. borealis* (in large crabs, hemolymph-medium differences of 71 ± 7 and 37 ± 5 mosm · kg^{-1}, $P < 0.001$, in a 500 mosm · kg^{-1}, 17‰, medium).

Zoeae 1 to 5 of *C. irroratus* in molting stage C hyper-osmoconformed at almost all tested salinities, *i.e.*, their hemolymph osmotic pressure varied as a function of external osmotic pressure but remained above external by about 15–50 mosm · kg^{-1}; at the lowest tested salinity (300 mosm · kg^{-1}), zoeae were isosmotic. In some zoeal stages, regulation in dilute media was slightly more hyper-osmotic in premolt (zoeae 1,4 at 500 mosm · kg^{-1}: $P < 0.05$) and less hyper-osmotic in post-molt (zoeae 2, 3, 4 at 500 and 900 mosm · kg^{-1}: $P < 0.01$). Megalopae were also hyper-osmoconformers. The pattern of osmoregulation seemed to change after the completion of metamorphosis. First crab stages were almost osmoconformers in seawater and their regulation was slightly hyper-osmotic in a dilute medium of 500 mosm · kg^{-1}, 17‰ (hemolymph-medium difference of 55 ± 16 mosm · kg^{-1}) (Fig. 6).

Zoeae 1 to 3 of *C. borealis* had the same pattern of hyperosmoconforming regulation as zoeae of *C. irroratus* (Fig. 7).

Discussion

Salinity tolerance

In *Cancer irroratus*, the interval of tolerable salinities tends to decrease at the end of the larval development and is minimum in megalopae. At this stage, the 96 h LS 50s are about 28‰ and 34‰, which means that megalopae are almost restricted to seawater. In adults, approximate 48 h LS 50s are 8.5‰ and 65‰. The wide euryhalinity demonstrated by adults could be partly related to the relatively short time of exposure to the different media and to the progressive adaptation to changing salinities. Long-term exposure to extreme salinities could yield more restrictive results.

These results are in agreement with previous data. Sastry (1970) found that at 15°C, only 5.5% of megalopae of *C. irroratus* molted to the first crab stage in a medium of 15‰, while this molt was successful in a higher percentage of megalopae in media ranging from 20 to 35‰, with a maximum rate of 76% in a medium of 30‰. Complete development from zoea 1 to first crab stage was found possible at 15°C between 20 and 35‰ (Sastry and McCarthy, 1973) or 25 and 35‰, but survival exceeded 50% only in 30–35‰. (Johns, 1981). In adults, McCluskey (1975, cited in Bigford, 1979) found survival was possible for three days at 5–8°C in salinities ranging from 10 to 20‰ (the upper limit was not tested).

Compared to the larvae of *C. irroratus*, zoeae of *C. borealis* were less tolerant to prolonged exposure to low salinities. In *C. borealis*, Sastry and McCarthy (1973) found that complete larval development was only possible in a medium of 30‰ at 20°C. These and our results demonstrate that *C. borealis* is more stenohaline than *C. irroratus*, and, in particular, less tolerant to low salinities during the larval development and in adults.

Adaptation time

In *C. irroratus*, the time of osmotic equilibration in a dilute medium is about 1 to 2 h in larvae and 24 h in

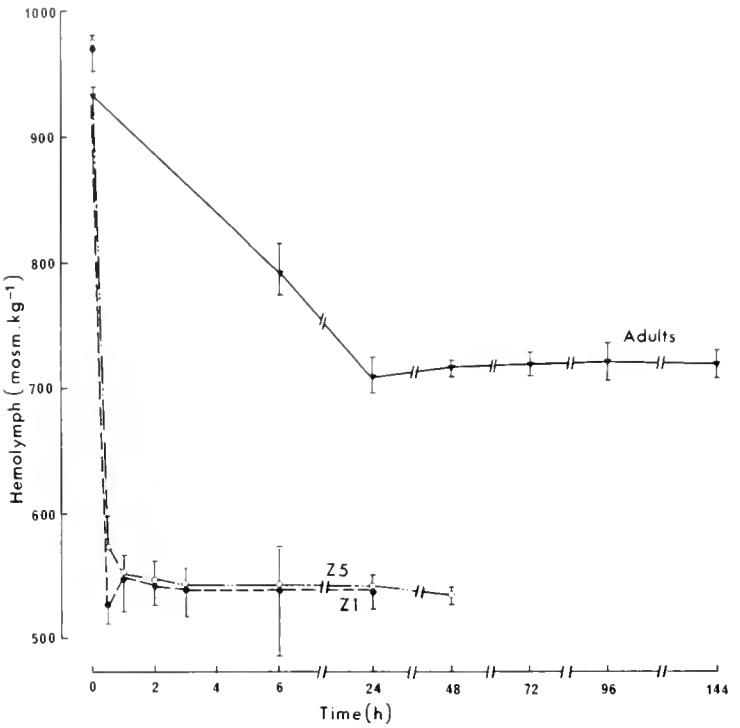

Figure 4. Change in hemolymph osmotic pressure in stages zoeae 1 and 5 of *Cancer irroratus* after rapid transfer from seawater (920 mosm · kg^{-1}, 31‰) to a dilute medium (500 mosm · kg^{-1}, 17‰), and in adults of *C. irroratus* after rapid transfer from seawater to 677 mosm · kg^{-1}, 23‰, at 15°C. Each point represents the mean value of determinations from 3 to 5 zoeae or 5 adults, with 95% confidence interval.

adults. Adaptation time is thus size-dependent, which could be related to differences in the volumes of water and ion exchanges and to differences in tegument permeability between development stages. These times of adaptation are similar to those of the corresponding stages of other species (see Charmantier *et al.*, 1988).

Osmoregulation

In *C. irroratus* and *C. borealis*, adults osmoconform in high salinities and seawater and slightly hyper-regulate in dilute media. The ability to hyper-regulate is higher in *C. irroratus*.

A similar pattern of osmoregulation has been described in *C. irroratus* and other species of *Cancer*, but the ability to hyper-regulate varies with the species, although other factors such as size and temperature can affect this parameter. In media of approximately 500 mosm · kg^{-1}, 17‰, at temperatures of ≅15–20°C, the difference between the osmotic pressures of hemolymph and medium expressed in mosm · kg^{-1} is about 15 in *C. antennarius* (Jones, 1941), 30–40 in *C. borealis* (this study), 50 in *C. pagurus* (Wanson *et al.*, 1983), 50–120 in *C. irroratus* (Thurberg *et al.*, 1973; Cantelmo *et al.*, 1975; Neufeld and Pritchard, 1979; this study), 150–250 in *C. magister* (Jones, 1941; Engelhardt and Dehnel, 1973; Hunter and Rudy, 1975).

Zoeae of *C. irroratus* hyper-osmoconform in all tested salinities. Most decapod larvae that have been studied

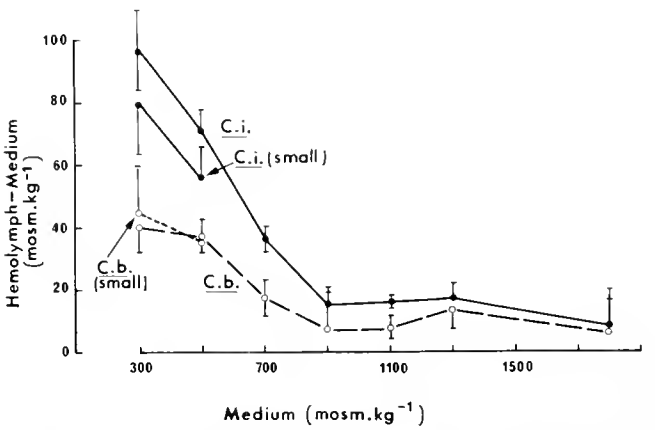

Figure 5. Variations in the difference between the osmotic pressures of hemolymph and medium according to the osmotic pressure of the medium in large and small adults of *Cancer irroratus* and *C. borealis* at 15°C. Each point represents the mean value of determinations from 7 to 10 animals (exception in lowest salinity: 4–6 animals) with 95% confidence interval.

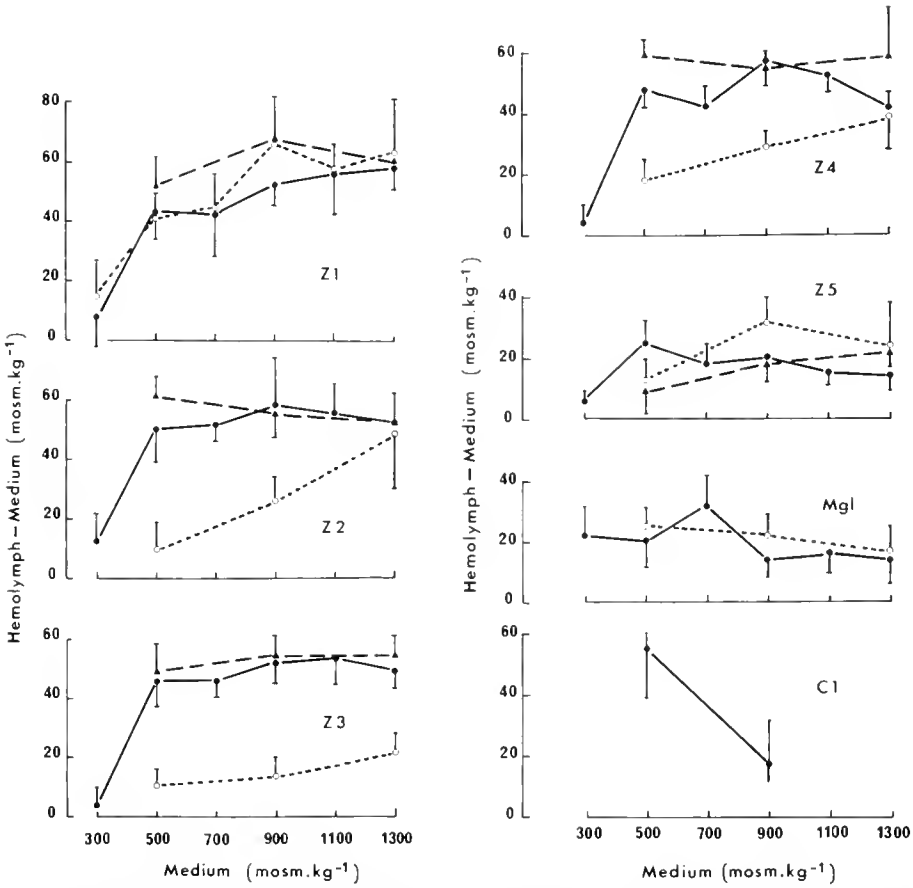

Figure 6. Variations in the difference between the osmotic pressures of hemolymph and medium according to the osmotic pressure of the medium in zoeae 1–5, megalopae, and first crab stage of *Cancer irroratus* at 15°C. Each point represents the mean value of determinations from 9–15 animals (5–10 animals in extreme salinities) with 95% confidence interval. O-----O: post-molt; ● —— ●: stage C; ▲ – – ▲: premolt.

hyper-osmoconform in salinities that they normally encounter in their environment (Charmantier *et al.*, 1988). This could be considered an adaptation of small organisms to planktonic or pelagic life. The slight positive difference in osmotic pressure between hemolymph and medium maintains an osmotic influx of water, which in turn favors the turgescence of the body and particularly of the extended appendages and exopodites involved in the buoyancy of the larvae. In a few zoeal stages of *C. irroratus*, the osmotic pressure of hemolymph is affected by the molting stage, increasing in premolt and decreasing in postmolt but much less regularly than in other species like *Rhithropanopeus harrisii* (Kalber and Costlow, 1966), *Cardisoma guanhumi* (Kalber and Costlow, 1968), *Homarus americanus* and *Penaeus japonicus* (Charmantier *et al.*, 1988). Like zoeae, megalopae of *C. irroratus* hyper-osmoconform in all media. First crab stages osmoconform in seawater, but they hyper-regulate in a dilute medium. Thus, the adult type of osmoregulation seems to be acquired at the first crab stage. However, the ability to hyper-regulate, evaluated by the difference between the osmotic pressures of hemolymph and medium in a dilute medium, increases with size in adults: in a medium of 500 mosm · kg^{-1}, 17‰, this difference was 55 ± 16 mosm · kg^{-1} in first crab stage, 55 ± 13 mosm · kg^{-1} in small adults, and 71 ± 7 mosm · kg^{-1} in large adults. As in *C. irroratus*, zoeae of *C. borealis* hyper-osmoconform, while adults have a slight hyper-isoregulation. In a preliminary study, Brown and Terwilliger (1989) found that megalopae and first crabs of *C. magister* were weaker osmoregulators than adults, after 8 h exposure to dilute media. A comparison with our results is difficult due to the lack of numerical data. Additionally, it is possible that the short time of exposure did not allow for complete osmotic equilibration in adults.

In a recent study, we reviewed the evolution of osmoregulatory abilities that have been described for the post-embryonic development of decapod crustaceans (Charmantier *et al.*, 1988). Most decapod larvae that have been studied, including zoeae of *C. irroratus* and *C. bo-*

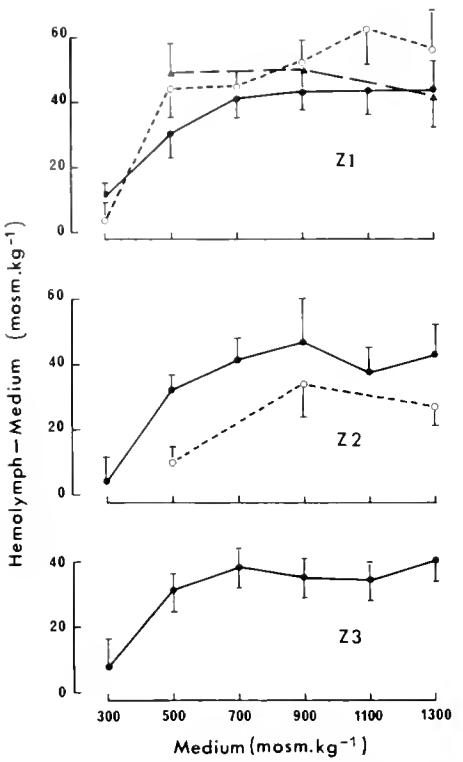

Figure 7. Variations in the difference between the osmotic pressures of hemolymph and medium according to the osmotic pressure of the medium in zoeae 1–3 of *Cancer borealis* at 15°C. Each point represents the mean value of determinations from 10 animals with 95% confidence interval. ○-----○: post-molt; ● —— ●: stage C; ▲ – – ▲: premolt.

realis, are hyper-osmoconformers or weak regulators, an exception being the larvae of *Macrobrachium petersi* (Read, 1984), which are confronted with very low salinities in their natural environment and which can efficiently regulate the osmotic concentration of their hemolymph. During or after the larval phase, different patterns of ontogeny of osmoregulation have been described, which we proposed to separate into three groups (Charmantier *et al.*, 1988). In one group of species, osmoregulation varies little with developmental stage; the adults of these species are often weak regulators or osmoconformers, like *Hepatus epheliticus* and *Libinia emarginata* (Kalber, 1970). In *M. petersi* (Read, 1984), which lives in variable salinities due to its migration, the adult type of regulation is established as early as the first larval stage. In a third group of species, which includes *Uca subcylindrica* (Rabalais and Cameron, 1985), *Homarus americanus, Penaeus japonicus* (Charmantier *et al.*, 1988), and *Cancer irroratus* (this study), metamorphosis marks the appearance of the adult type of regulation. In other species that do not still fit in those three categories, in which "no clear trend toward development of adult osmoregulatory patterns toward the end of larval life" was found (Foskett, 1977), this could be due to the lack of information about the osmoregulatory capacity of early post-metamorphic stages. For example, in *Sesarma reticulatum* studied by Foskett, 1977, zoeae and megalopae were hyper-osmoconformers and adults were hyper-hyporegulators, but early crab stages were not studied. Foskett stated: ". . . even by late megalops the adult osmoregulatory response is still not attained. Examination of osmoregulation in early juvenile crab stages may reveal osmoregulatory responses that are transitional between the larval and adult forms."

The few studies that were conducted in decapods throughout the post-embryonic development, including post-metamorphic stages, confirm this statement. The transition from larval to adult type of osmoregulation may occur rapidly when metamorphosis itself is sudden, as in *H. americanus*, or may be progressive when metamorphosis is spread over several post-larval stages as in *P. japonicus* (Charmantier *et al.*, 1988). There is a lack of agreement on the exact timing of metamorphosis in brachyurans: it has been located either at the molt from megalopa to first crab stage (Costlow, 1968), or at the molt from last zoea to megalopa (Felder *et al.*, 1985). Actually, most morphological changes result from the molt separating the last zoea and the megalopa and, in *U. subcylindrica*, the type of osmoregulation also changes at this molt (Rabalais and Cameron, 1985). However, this physiological modification occurs only after the molt separating the megalopa and the first crab stage in *C. irroratus* (this study), and possibly in *S. reticulatum* (Foskett, 1977). Additionally, as stated by Felder *et al.*, (1985), "in almost all the Decapoda, some ontogenic changes in locomotion, feeding, and habitat coincide with early postlarval growth." Thus, in our opinion, metamorphosis in brachyurans requires two molts to be completed and the megalopa, while clearly postlarval, is a transitional stage between the larvae and the postmetamorphic stages starting with the first crab stage.

In summary, studies conducted on the species of the third group of decapods cited above demonstrate that the completion of metamorphosis yields a change to the adult type of osmoregulation. We propose the hypothesis that, in most species in which larvae are hyper-osmoconformers or weak regulators and adults are efficient osmoregulators, the transition from the larval type to the adult type of osmoregulation occurs at metamorphosis. More generally, metamorphosis can be considered a combination of morphological, ecological, behavioral, and physiological changes (Costlow, 1968; Charmantier *et al.*, 1984b).

Relation between osmoregulation and salinity tolerance

In *C. irroratus* and *C. borealis*, zoeae are weak regulators and their salinity tolerance is comparatively moderate or low. In megalopae of *C. irroratus*, salinity tolerance is minimum just before the pattern of osmoregula-

tion changes. Under natural conditions, developing brachyurans are known to settle on the bottom during the megalopal stage, usually near the shores (Sandifer, 1973), *i.e.*, in an environment subjected to possible variations of salinity. The limited salinity tolerance of megalopae could cause high rates of mortality, which have been noted in different species of *Cancer*, at least under culture conditions (Charmantier-Daures and Charmantier, 1991). Unsufficient number of available animals prevented us from determining the salinity tolerance of early crab stages, in which the pattern of osmoregulation has changed. We may suppose that their salinity tolerance has correlatively increased. In adults of both species, the ability to osmoregulate is higher and so are their salinity tolerances. Compared to *C. borealis*, adult *C. irroratus* are stronger hyper-regulators in dilute media and are more tolerant to low salinity. Thus, as previously noted in *Macrobrachium petersi* (Read, 1984), *Uca subcylindrica* (Rabalais and Cameron, 1985), *Homarus americanus* and *Penaeus japonicus* (Charmantier *et al.*, 1988), there is a strong correlation between increased ability to osmoregulate and improved salinity tolerance.

Acknowledgments

Part of this study was supported by a grant from NATO. We thank Dr. D. E. Aiken for providing lab space and facilities, and Ross Chandler, Jay Parsons, David Robichaud, and Wilfred Young-Lai for their help in capturing and rearing crabs.

Literature Cited

Bigford, T. E. 1979. Synopsis of biological data on the Rock Crab, *Cancer irroratus* Say. *NOAA Techn. Rep.* NMFS 426, FAO Synopsis n° 123, 26 pp.

Brown, A. C., and N. B. Terwilliger. 1989. Developmental changes in osmotic and ionic regulation in the Dungeness crab, *Cancer magister*. *Am. Zool.* **29:** 156A.

Cantelmo, A. C., F. R. Cantelmo, and D. M. Langsam. 1975. Osmoregulatory ability of the rock crab, *Cancer irroratus*, under osmotic stress. *Comp. Biochem. Physiol.* **51A:** 537–542.

Charmantier, G. 1986. Variation des capacités osmorégulatrices au cours du developpement post-embryonnaire de *Penaeus japonicus* Bate, 1888 (Crustacea Decapoda). *C. R. Acad. Sci. Paris* **303:** 217–222.

Charmantier, G., M. Charmantier-Daures, and D. E. Aiken. 1984a. Variation des capacités osmorégulatrices des larves et postlarves de *Homarus americanus* H. Milne-Edwards, 1837 (Crustacea, Decapoda). *C. R. Acad. Sci. Paris* **299:** 863–866.

Charmantier, G., M. Charmantier-Daures, and D. E. Aiken. 1984b. Neuroendocrine control of hydromineral regulation in the American lobster *Homarus americanus* H. Milne-Edwards, 1837 (Crustacea, Decapoda). 2. Larval and post-larval stages. *Gen. Comp. Endocrinol.* **54:** 20–34.

Charmantier, G., M. Charmantier-Daures, N. Bonaricha, P. Thuet, D. E. Aiken, and J.-P. Trilles. 1988. Ontogeny of osmoregulation and salinity tolerance in two decapod crustaceans: *Homarus americanus* and *Penaeus japonicus*. *Biol. Bull.* **175:** 102–110.

Charmantier, G., M. Charmantier-Daures, N. Bonaricha, P. Thuet, J.-P. Trilles, and D. E. Aiken. 1989. Ontogeny of osmoregulation and salinity tolerance in *Homarus americanus*, *Penaeus japonicus* and *Cancer irroratus*. *Am. Zool.* **29:** 155A.

Charmantier-Daures, M., and G. Charmantier. 1991. Mass-culture of *Cancer irroratus* larvae (Crustacea, Decapoda): adaptation of a flow-through sea water system. *Aquaculture*.

Costlow, J. D., Jr. 1968. Metamorphosis in crustaceans. Pp. 3–41 in *Metamorphosis*, W. Etkin and L. I. Gilbert, eds. Appleton-Century-Crofts, New York.

Drach, P. 1939. Mue et cycle d'intermue chez les Crustacés Décapodes. *Ann. Inst. Océanogr., Monaco* **19:** 103–391.

Engelhardt, F. R., and P. A. Dehnel. 1973. Ionic regulation in the Pacific edible crab, *Cancer magister* (Dana). *Can. J. Zool.* **51:** 735–743.

Felder, J. M., D. L. Felder, and S. C. Hand. 1986. Ontogeny of osmoregulation in the estuarine ghost shrimp *Callianassa jamaicense* var. *louisianensis* Schmitt (Decapoda, Thalassinidea). *J. Exp. Mar. Biol. Ecol.* **99:** 91–105.

Felder, D. L., J. W. Martin, and J. W. Goy. 1985. Patterns in early postlarval development of decapods. Pp. 163–225 in *Larval Growth*, A. M. Wenner, ed. A. A. Balkema, Rotterdam, Boston.

Finney, D. J. 1962. *Probit Analysis: A Statistical Treatment of the Sigmoid Response Curve*. Second Edition, Cambridge Univ. Press, London.

Foskett, J. K. 1977. Osmoregulation in the larvae and adults of the grapsid crab *Sesarma reticulatum* Say. *Biol. Bull.* **153:** 505–526.

Hughes, J. T., R. A. Shleser, and G. Tchobanoglous. 1974. A rearing tank for lobster larvae and other aquatic species. *Progr. Fish. Cult.* **36:** 129–132.

Hunter, K. C., and P. P. Rudy Jr. 1975. Osmotic and ionic regulation in the Dungeness crab, *Cancer magister* Dana. *Comp. Biochem. Physiol.* **51A:** 439–447.

Johns, D. M. 1981. Physiological studies on *Cancer irroratus* larvae. I. Effects of temperature and salinity on survival, development rate and size. *Mar. Ecol. Progr. Ser.* **5:** 75–83.

Jones, L. L. 1941. Osmotic regulation in several crabs of the Pacific coast of North America. *J. Cell. Comp. Physiol.* **18:** 79–92.

Kalber, F. A. 1970. Osmoregulation in decapod larvae as a consideration in culture techniques. *Helgol. Wiss. Meeresunters.* **20:** 697–706.

Kalber, F. A., and J. D. Costlow. 1966. The ontogeny of osmoregulation and its neurosecretory control in the decapod crustacean, *Rhithropanopeus harrisii*. *Am. Zool.* **6:** 221–229.

Kalber, F. A., and J. D. Costlow. 1968. Osmoregulation in larvae of the land crab, *Cardisoma guanhumi* Latreille. *Am. Zool.* **8:** 411–416.

Lichtfield, J. T., and F. Wilcoxon. 1949. The reliability of graphic estimates of relative potency from dose-percent effect curves. *J. Pharmacol. Exp. Theor.* **108:** 18–25.

Lieberman, H. R. 1983. Estimating LD 50 using the probit technique: a basic computer program. *Drug Chem. Toxicol.* **6:** 111–116.

Mantel, L. H., and L. L. Farmer. 1983. Osmotic and ionic regulation. Pp 53–161 in *The Biology of Crustacea, Vol. 5*. Internal Anatomy and Physiological Regulation, L. H. Mantel, ed. Academic Press, New York.

McCluskey, W. J. 1975. The effects of hyposaline shocks on two species of *Cancer*. Unpubl. manuscr., 15 p. Narragansett Marine Laboratory, University of Rhode Island, Narragansett, RI 02882.

Neufeld, G. J., and J. B. Pritchard. 1979. Osmoregulation and gill Na^+, $K^\pm$ ATPase in the rock crab, *Cancer irroratus*: response to DDT. *Comp. Biochem. Physiol.* **62C:** 165–172.

Rabalais, N. N., and J. N. Cameron. 1985. The effects of factors important in semi-arid environments on the early development of *Uca subcylindrica*. *Biol. Bull.* **168:** 147–160.

Read, G. H. L. 1984. Intraspecific variation in the osmoregulatory capacity of larval, post-larval, juvenile and adult *Macrobrachium petersi* (Hilgendorf). **Comp. Biochem. Physiol. 78A:** 501–506.

Sandifer, P. A. 1973. Distribution and abundance of decapod crustacean larvae in the York River estuary and adjacent Chesapeake Bay, Virginia, 1968–1969. *Chesapeake Sci.* **14:** 235–257.

Sastry, A. N. 1970. Culture of brachyuran crab larvae using a re-circulating sea water system in the laboratory. *Helgol. Wiss. Meeresunters.* **20:** 406–416.

Sastry, A. N. 1977a. The larval development of the rock crab, *Cancer irroratus* Say, 1817, under laboratory conditions (Decapoda Brachyura). *Crustaceana* **32:** 155–168.

Sastry, A. N. 1977b. The larval development of the Jonah crab, *Cancer borealis* Stimpson, 1859, under laboratory conditions (Decapoda Brachyura). *Crustaceana* **32:** 290–303.

Sastry, A. N., and J. F. McCarthy. 1973. Diversity in metabolic adaptation of pelagic larval stages of two sympatric species of brachyuran crabs. *Netherl. J. Sea Res.* **7:** 434–446.

Sprague, J. B. 1969. Measurement of pollutant toxicity to fish. I. Bioassay methods for acute toxicity. *Water Res.* **3:** 793–821.

Thurberg, F. P., M. A. Dawson, and R. S. Collier. 1973. Effects of copper and cadmium on osmoregulation and oxygen consumption in two species of estuarine crabs. *Mar. Biol.* **23:** 171–175.

Wanson, S., A. Pequeux, and R. Gilles. 1983. Osmoregulation in the stone crab *Cancer pagurus*. *Mar. Biol. Lett.* **4:** 321–330.

Young, A. M. 1979. Osmoregulation in larvae of the striped hermit crab *Clibanarius vittatus* (Bosc) (Decapoda: Anomoura, Diogenidae). *Est. Coast. Mar. Sci.* **9:** 595–601.

Zitko, V. 1982. Letcur, the lethality curve program. *Can. Tech. Rep. Fish. Aquat. Sci.* **1134:** 10 pp.

Reference: *Biol. Bull.* **180:** 135–153. (February, 1991)

Sulfide-Driven Autotrophic Balance in the Bacterial Symbiont-Containing Hydrothermal Vent Tubeworm, *Riftia pachyptila* Jones

J. J. CHILDRESS[1], C. R. FISHER[2], J. A. FAVUZZI[1], R. E. KOCHEVAR[1], N. K. SANDERS[3], AND A. M. ALAYSE[4]

[1]*Department of Biological Sciences and Marine Science Institute, University of California, Santa Barbara, California 93106,* [2]*Department of Biological Sciences, Pennsylvania State University, University Park, Pennsylvania 16802,* [3]*Bamfield Marine Station, Bamfield, British Columbia, Canada V0R 1B0, and* [4]*Department Environment Profond, IFREMER, Centre de Brest, B. P. 70-29263 Plouzane, France*

Abstract. Hydrothermal vent tubeworms, *Riftia pachyptila* Jones, were maintained alive and studied on board ship using flow-through pressure aquaria. Simultaneous measurements of O_2, ΣCO_2, ΣH_2S fluxes showed that the intact symbioses reach maximum rates of uptake of ΣCO_2 (>2 μmole g^{-1} h^{-1}) at about 90 μM ΣH_2S. Measurements were made of hemolymph and coelomic fluid ΣCO_2, ΣH_2S, thiosulfate, pH, and hemoglobin concentrations in worms kept under various conditions of O_2 and ΣH_2S. Normal hemolymph pH appears to be about 7.5 and is not affected by ΣH_2S and ΣCO_2 concentrations within the ranges observed. We conclude that *Riftia* is specialized to provide sulfide to its symbionts with minimal interaction of sulfide with the animal metabolism. The uptake of sulfide is apparently by diffusion into the hemolymph, facilitated by the sulfide-binding properties of the hemoglobins. Both ΣCO_2 and P_{CO_2} are elevated in the hemolymph above their levels in the medium, although they are reduced under autotrophic conditions. Thus inorganic carbon is apparently concentrated from the medium into the hemolymph by an unknown mechanism.

Introduction

The giant hydrothermal vent tubeworm, *Riftia pachyptila* Jones, is perhaps the most distinctive of the animals living around the deep-sea hydrothermal vents. Like all vestimentiferan tubeworms, adults of this species lack a mouth and a gut (Jones, 1981, 1988; Jones and Gardiner, 1988; Southward, 1988). The adult worms appear to derive their nutritional needs from the large population of sulfur-oxidizing chemolithoautotrophic bacterial symbionts that live in cells within a specialized organ—the trophosome—in their trunk (Cavanaugh *et al.*, 1981; Felbeck, 1981). The trophosome is a highly vascularized organ lying between two coelomic cavities that contain a hemoglobin-rich fluid (Jones, 1988). This anatomy requires that the animal supply the needs of the symbionts through its circulatory system (Arp *et al.*, 1985; Felbeck and Childress, 1988). Because these symbionts are sulfide-oxidizing autotrophs (Felbeck, 1981; Belkin *et al.*, 1986; Fisher *et al.*, 1989), the worm must take up sulfide, oxygen, and carbon dioxide from the medium and transport them to the symbionts. These substances can be taken up from the water by the large obturacular plume, a highly vascularized organ that has a large surface area and brings the hemolymph very close to the surrounding water (Arp *et al.*, 1985; Jones, 1988). The hemolymph and the coelomic fluid both have abundant extracellular hemoglobins which are believed to play a key role in the transport of all three of these metabolites (Childress *et al.*, 1984; Arp *et al.*, 1985).

Two hemoglobins are found in the extracellular fluids of these worms. One has a molecular weight of about 1.7×10^6 M_r and is found primarily in the hemolymph, while the second is smaller (0.4×10^6 M_r) and is found in both the coelomic and vascular compartments (Terwilliger *et*

Received 10 September 1990; accepted 24 November 1990.

al., 1980; Arp and Childress, 1981; Terwilliger and Terwilliger, 1985; Arp *et al.*, 1987). Both hemoglobins bind oxygen and sulfide reversibly with a high affinity (Arp and Childress, 1981, 1983; Childress *et al.*, 1984; Arp *et al.*, 1987; Fisher *et al.*, 1988a). The sulfide binding does not affect the simultaneous binding of oxygen, and appears to occur at a site removed from the heme (Childress *et al.*, 1984; Arp *et al.*, 1987). When sulfide and oxygen are below saturation in the hemolymph, their normally rapid, spontaneous reaction is suppressed (Fisher and Childress, 1984). Further, the hemoglobin can protect the animal tissues from sulfide toxicity by binding the sulfide with a higher affinity than does the site of toxic effects, cytochrome-c-oxidase (Powell and Somero, 1983, 1986). The hemoglobin does, however, release sulfide to the symbionts while simultaneously protecting them from sulfide toxicity by holding free sulfide concentrations down (Fisher and Childress, 1984; Fisher *et al.*, 1988a, 1989). The hemoglobins also buffer the hemolymph for carbon dioxide transport (Childress *et al.*, 1984). Thus, the hemolymph apparently has the properties required to take oxygen, carbon dioxide, and sulfide from the medium and to transport them to the endosymbionts.

Most of the experiments described in this paper were performed to test the role of the hemolymph in gas uptake and transport in intact, living *Riftia pachyptila* individuals. In particular, we were concerned with demonstrating the continuous uptake and oxidation of sulfide by the intact organisms, evaluating the role of the hemoglobins in concentrating sulfide from the medium, looking for the possible roles of other forms of sulfur in the symbiosis, examining the impact of sulfide and symbiont autotrophy on internal CO_2 pools and pH, and observing the pattern of exchange of gases between the coelomic fluid and the hemolymph.

A consistent chemical terminology will be used throughout this paper. Sulfide and inorganic carbon refer to these substances without specifying the chemical species involved. ΣH_2S and ΣCO_2 refer to the amounts of these gases analyzed from acidified samples using the analytical methods described below. They are measures of the sum of the various chemical forms in which these substances are found. H_2S, HS^-, S^{2-}, S^0, CO_2, HCO_3^- and any other chemical formulae refer only to the chemical species symbolized. "Free" refers to that fraction of a substance in the body fluids that is not bound to the hemoglobins.

Materials and Methods

The tubeworms used in these studies were collected from depths of about 2600 m at sites on the Galapagos Rift (00°48.247′N, 86°13.478′W) and the East Pacific Rise (12°48′N, 108°57′W) by deep submersibles (*Alvin* at the Galapagos Rift site and *Nautile* at the East Pacific Rise site). Both submersibles pulled the worms off the rocks using their manipulators, placed them in thermally insulated containers, and brought them to the surface about 2 to 8 h after capture. Once at the surface the worms were quickly transferred to cold seawater (7°C) where undamaged worms were set apart for the whole animal experiments described here. The worms chosen were then carefully removed from their natural tubes and placed in straight plastic tubes of appropriate size so they could be fitted into the pressure vessels necessary for their maintenance. They were then quickly placed in pressure aquaria.

The worms were routinely maintained in flowing-water pressure aquaria (Quetin and Childress, 1980) at 200 atm pressure, 8°C, and more than 100 μM O_2. Water was pumped through these stainless steel pressure vessels at about 12 l/h. Previous studies (Childress *et al.*, 1984) and preliminary observations during this study indicate that although the worms live at a hydrostatic pressure of about 260 atm at these sites, they are able to survive and display apparently "normal" behavior at pressures as low as about 100 atm. The symbionts themselves do not show significant effects of pressure on carbon fixation rates within the pressure range used here (Fisher *et al.*, 1989). In the present study pressures as low as 120 atm were used in some experiments, but the experience cited above suggests that these lower pressures should have little effect on the results.

Studies involving the maintenance of the worms at known sulfide concentrations were carried out in flowing-water aquaria (120 atm, about 4 l/h) using transparent acrylic pressure vessels (Quetin and Childress, 1980), allowing the activity of the worms to be observed during the experiments. Anaerobic sulfide stock solution (5 or 10 mM sodium sulfide in seawater at ph 7.0 or 7.5) was added continuously at the intakes of the pressure pumps with low pressure metering pumps to achieve stable sulfide concentrations in the pressure vessels. The effluent water from the vessels was periodically sampled with a 0.5 ml glass syringe, and the gases were analyzed by gas chromatography (Childress *et al.*, 1984). The pH of the effluent water was measured with a double junction electrode and was between 7. and 8.1, depending on the experiment.

Metabolism measurements

Measurements of whole animal metabolism were made in a flowing water system similar to that used by Anderson *et al.*, (1987), but adapted for use at the high pressures required for the survival of the worms. The system pumped seawater through the respirometer chambers using HPLC pressure pumps with small acrylic pressure vessels as respirometer chambers. The water in this system was first passed through a series of filters (5.0 and 0.2 μm) and a UV sterilizer. It was then continuously mixed by

means of metering pumps with an antibiotic solution to achieve a final concentration of 150 mg penicillin-G per liter and with a sulfide solution (pH 7.5 in seawater) to achieve the desired sulfide concentration. It then went to a vertically oriented column measuring 1 × 0.1 m, with the seawater entering at the top and exiting near the bottom. The pH of the water in the column was maintained at 7.5 by a pH controller that pumped 1 *M* acid (HCL) or base (NaOH) into the column. Oxygen and N_2 bubbled via the bottom of the column mixed the water in the column while maintaining the desired O_2 concentration. The water was then pumped through the respirometer chambers to a gas chromatograph for analysis. Two respirometer streams were continuously used in these measurements, one with animals in the respirometer chamber and the other an identical system without animals, which served as a control for spontaneous oxidation of sulfide. Fluxes of the measured gases due to the animals were calculated from the differences in gas concentrations in the water exiting the experimental and control chambers. These experiments were carried out at 130 atm hydrostatic pressure.

Ammonium flux was measured for several worms while they were in the respirometer system described above. The ammonium concentrations in the effluents from the two chambers were measured by flow injection analysis (Willason and Johnson, 1986).

Dissection procedure

Worms were dissected so that samples of hemolymph, coelomic fluid, and trophosome could be obtained for further analysis. Worms to be sacrificed were quickly removed from the pressure aquaria and the plastic tubes and then stretched out in a dissecting tray. The body wall below the vestimentum was carefully slit for a few centimeters parallel to the main axis of the worm on the ventral side. A sample of coelomic fluid (1–5 ml) was quickly drawn, with a blunt needle, from the pool of this fluid in the coelomic space and placed on ice. Subsamples for the various analyses were quickly taken. The remaining coelomic fluid was then drained from the worm, and a 1-ml syringe with a 30-ga needle was used to remove hemolymph from the major dorsal vessel leading from the trophosome to the plume of the worm. Aliquots of this post-trophosome (pre-branchial) hemolymph sample were quickly taken for the various analyses. Samples of trophosome tissue were also frozen for later analysis of elemental sulfur. If the trophosome appeared "unhealthy" [the pinkish appearance correlated with lack of CO_2 fixation in trophosome preparations (Fisher *et al.*, 1989), occurred in 7 of the 50 animals used] for an individual worm, the data from that worm were excluded from further consideration. These unhealthy worms were always characterized by low (<7.0) hemolymph pH values.

Analytical methods

Gas chromatographic methods similar to those described by Childress *et al.* (1984) were used to analyze gases in body fluids and seawater. Briefly, water samples were acidified with phosphoric acid, and gases were stripped from them using a glass and teflon extractor, inline with a thermal conductivity gas chromatograph. This system allowed the analysis of the O_2, CO_2, H_2S, N_2, CH_4, and CO concentrations in fluid samples of 0.2 to 1.0 ml. The limit of sensitivity for these gases was between 1 and 20 μM, depending on the gas and the sample size. Throughout this paper, the terms ΣH_2S and ΣCO_2 refer to the amounts measured using this analytical method without regard for the chemical species present at the very different pH values and conditions in the worms.

To measure pH, a sample of hemolymph or coelomic fluid was drawn from an animal with a syringe. The dead space of the syringe was filled with blood by drawing a small amount of sample into the syringe and then expelling the air and excess blood before drawing the sample for analysis. Without air exposure, the sample was immediately injected into a Radiometer glass capillary electrode (Radiometer America G298A) used in conjunction with a reference electrode (Radiometer K171) in a water jacketed chamber. Precision buffers (Radiometer S1500 & S1510) were used to calibrate the electrode.

The abundances of the two hemoglobins in the hemolymph were quantified by separating them by HPLC gel filtration and measuring the absorbance as they eluted from the column (Arp *et al.*, 1987). A TSK-50 column, 7.5 mm in diameter and 300 mm long, was used with a TSK guard column (7.5 mm by 75 mm). The eluent was a citric acid/phosphate buffer (1.63 g citric acid and 26.17 g KH_2PO_4/l) at pH 7.5, pumped at 0.3 ml/min at 5°C. The run time was about 40 min, and an undiluted 1-μl sample was used. The absorbance was measured at 415 nm as the eluent left the column.

Determinations of thiosulfate and other unbound thiols in the body fluids were made by HPLC analysis of samples derivatized by monobromobimane using the methods of Newton *et al.* (1981) and Fahey *et al.* (1983) as modified by Vetter *et al.* (1989). Derivatives were separated on a 15 cm C-18 reversed phase column and detected using a 235 nm filter for excitation and a 442 nm filter for detection of fluorescence. The eluent flow rate was 1.5 ml per min, using an increasing hydrophobic gradient of HPLC grade methanol and 2% acetic acid, starting at 10% methanol and increasing to 100% during the run.

Elemental sulfur in the extracts was quantified by gas chromatography according to the method of Richard *et al.* (1977) as modified by Fisher *et al.* (1988b). Pieces of tissue (0.5–2.0 g wet weight) were dried for 18 h in a 100°C drying oven, and then extracted for 24 h with cyclohexane

in a micro-Soxhlet apparatus. The extracts were "cleaned up" by passing them through a fluorosil column to remove lipids, and concentrated by evaporation. The injector temperature was 240°C, and the initial column temperature was 150°C, programmed to 220°C during the separation. A six foot (1.8 m) glass column with a 2 mm bore, packed with 5% SP2401 on 100/120 mesh Supelcoport, was used to separate sulfur. The sulfur was detected and quantified using a thermal conductivity detector. The detection limit for elemental sulfur was *ca.* 0.001% of the dry weight of the sample (depending somewhat on sample size). The identity of the separated sulfur was confirmed by the distinctive smell of sulfur vapor coming out of the gas chromatograph detector at the time of the putative sulfur peak.

Estimation of free ΣH_2S and H_2S

Because ΣH_2S, pH, and hemoglobin contents were measured, it was possible, using previously published data, to estimate the concentration of free (unbound) ΣH_2S as well as the various species of sulfide. Free ΣH_2S was estimated by using the Hill equation describing the relationship between fractional saturation and free sulfide measured at 6°C, pH 7.5 in a mixture of coelomic fluid and hemolymph (Fisher *et al.*, 1988a): ln [% saturation/(100 − % saturation)] = 0.737(ln free ΣH_2S μM) − 1.778.

To use this equation, the capacity of each fluid sample to bind sulfide was estimated by multiplying the small hemoglobin aggregate concentration by one sulfide/heme and the large aggregate concentration by three sulfides/heme. These estimates were derived from a multiple regression of the sulfide concentrations in nine coelomic fluid samples dialyzed at saturating sulfide concentrations against the concentrations of the two aggregates in those samples (data from Arp, 1987). This regression had an r^2 of 0.97 and gave coefficients of 0.90 ± 0.27 (95% C. I.) and 2.97 ± 0.86, respectively, for the two hemoglobins. From the estimated capacity for binding sulfide and the measured ΣH_2S in the fluid, the percent saturation was approximated, and the above equation was solved for free sulfide. This approximation of free sulfide was then used with the estimated sulfide binding capacity [% saturation = 100 (bound sulfide/binding capacity)] in the Hill equation to estimate the sulfide bound to the hemoglobin. This procedure was then carried through several iterations until the estimates converged on a single value for free sulfide. This value was then used to calculate the percentage saturation of the fluid.

The free H_2S in each sample was calculated from the free ΣH_2S using a pK_1 value (8°C, 35‰ and 120 atm) of 6.784 (Millero, 1986; Millero *et al.*, 1988) and the pH measured in that particular sample.

Estimation of P_{CO_2}

Because ΣCO_2, pH, and hemoglobin contents were measured, it was possible, using previously published data, to estimate the P_{CO_2} in the fluids. The data relating pH, ΣCO_2, and P_{CO_2} in *Riftia* coelomic fluid at 10°C (Childress *et al.*, 1984) were used as the basis of a family of curves that predict P_{CO_2} from pH and ΣCO_2. However, although the coelomic fluid and hemolymph are quite similar in ionic composition, the hemolymph often has much higher hemoglobin content. Because hemoglobin is the only protein in any concentration in the hemolymph (Arp *et al.*, 1987), we used the concentration of heme as an indicator of protein content in these fluids. An approximate correction factor for hemoglobin concentration was developed by equilibrating subsamples, brought to different concentrations in *Riftia* saline, of the same hemolymph sample with gases of known P_{CO_2} and then measuring the ΣCO_2 in these subsamples using the gas chromatographic method. These subsamples (0.909 and 3.554 mM heme) were equilibrated with 2.09 torr P_{CO_2} and a final pH of 7.70 (Arp *et al.*, 1987). These measurements indicated that the effect of heme concentration on ΣCO_2 in this range was 0.50 mmole ΣCO_2/mmole heme. This was added to the final equation used to calculate P_{CO_2} as a factor that changed the slope of the relationship between P_{CO_2} and ΣCO_2 at different pH values. The equation was: P_{CO_2} = (4.199 − 0.537 pH) + ΣCO_2[(e^(−1.845 pH + 13.396)] + 0.0667(heme − 0.79). P_{CO_2} in the medium was estimated from the medium pH and ΣCO_2 with the pK_{app} estimated from the equation given by Heisler (1984), and αCO_2 (0.06345) at 8°C (Skirrow, 1975).

Statistical methods

Statistical analyses were carried out using Statview SE+ and SuperANOVA (Abacus Concepts) and Fastat (Systat Inc.). The Kendall rank correlation was used to test for a relationship between two parameters without any assumptions about the form or linearity of the relationship. Testing for differences in the medians in paired data sets employed the Wilcoxon signed rank test. The Mann-Whitney U test was used to test for differences in medians between unpaired datasets. Simple and multiple linear regressions of raw and in transformed data were used to describe the relationships between parameters.

Results

Whole animal metabolism

Due to a variety of equipment problems, only one such experiment was successfully conducted. In this experi-

ment, two worms (8.7 and 5.0 g) were run in their natural tubes in one chamber for 68 h. This experiment was started at 13.5°C without sulfide. After 6 h, sulfide was added continuously and 14 h later the animals showed net ΣCO_2 uptake (autotrophy). For the next 20 h the effects of different sulfide concentrations on the fluxes of O_2, ΣH_2S and ΣCO_2 were measured while maintaining O_2 between 105 and 209 μM (Fig. 1B). After that time the temperature of the system was lowered to 8.4°C over 2 h, and a similar set of measurements repeated at O_2 concentrations between 72 and 211 μM during the next 24 h (Fig. 1A). The set of observations at 8.4°C started at 92 μM ΣH_2S, decreased in steps to 0.0 μM ΣH_2S, and then was then raised to 41–49 μM ΣH_2S for 6 h. As can be seen in Figure 1A, the lower ΣH_2S concentrations resulted in less uptake of ΣCO_2, and without added sulfide the ΣCO_2 balance was fully heterotrophic (+3.05 μmoles ΣCO_2 $g^{-1}h^{-1}$). For the first three hours after the reintroduction of sulfide, this balance remained heterotrophic (+1.93 μmoles ΣCO_2 $g^{-1}h^{-1}$, high point at 43 μM ΣH_2S in Fig. 1A), but autotrophy was reached in the next 3 h (−0.64 μmoles ΣCO_2 g^{-1} h^{-1}, at 49 μM ΣH_2S in Fig. 1A). The worms were then removed and their tubes replaced in the vessels. The tubes alone did not show significant ΣCO_2 flux (<0.1 μmole ΣCO_2 g^{-1} worm h^{-1}) in the presence of 130 μM ΣH_2S. When the worms were dissected after the experiment, S° was visible in their trophosomes.

These data demonstrate that these worms were dependent on ΣH_2S levels greater than about 50 μM to break even on carbon flux and more than 90 μM was required for maximum uptake of ΣCO_2. They also show that the lag-time for changes in ΣCO_2 flux when ΣH_2S was removed was short, suggesting that use of stored S° was not quantitatively very important. In contrast, when sulfide was introduced after an absence, the lag time was relatively long (3–14 h).

Both O_2 and ΣCO_2 flux were significantly dependent on the ΣH_2S flux (Fig. 1C). The slope of the line relating ΣCO_2 flux to ΣH_2S flux was 0.92 ± 0.18 (95% C. I.) indicating that 0.92 mole CO_2 was fixed for each mole H_2S consumed. The slope of the line relating O_2 flux to ΣH_2S flux (Fig. 1C) was 1.14 ± 0.17 (95% C. I.), indicating that 1.14 mole O_2 was consumed for each mole ΣH_2S consumed. The lines relating ΣCO_2 and O_2 fluxes to ΣH_2S flux both intercept the y-axis at virtually the fluxes found for the worms in the absence of sulfide. This indicates that sulfide does not interact with the metabolism of carbon or O_2 by the animal tissues. The R. Q. in the absence of sulfide is 0.83 suggesting a metabolism based on a mixture of the major substrates.

The autotrophic *Riftia* experiment described above failed to show net uptake of N_2, supporting other negative data that this species' symbionts do not fix N_2. A preliminary study has also been carried out on ammonia flux

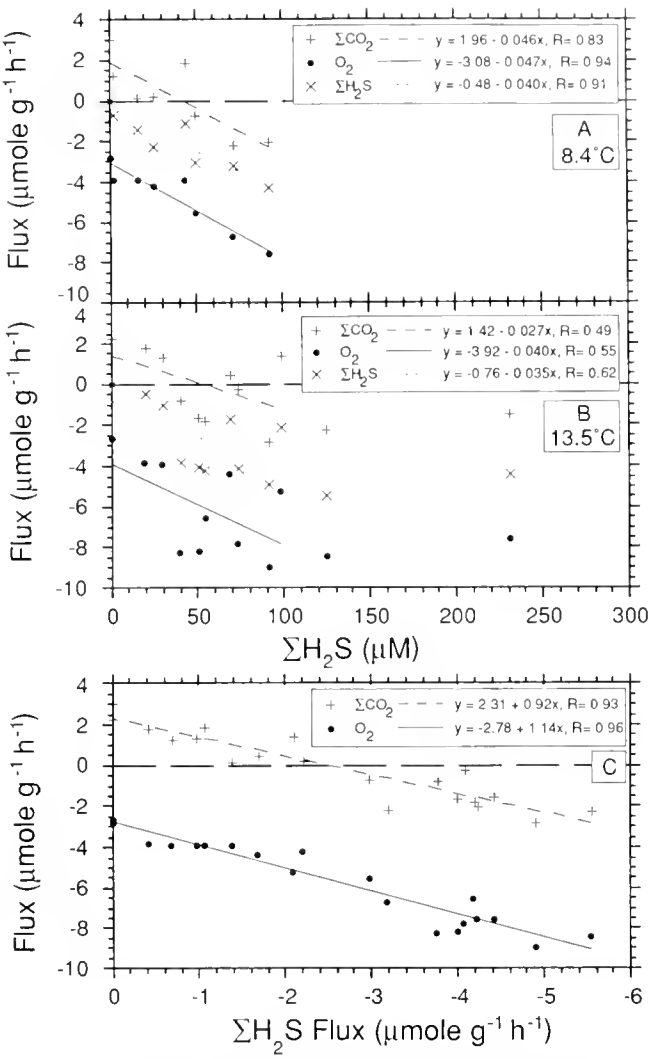

Figure 1. *Riftia pachyptila* metabolic fluxes in a flowing water, pressure respirometer system. Closed circles are oxygen fluxes, x symbols are sulfide fluxes, and crosses are CO_2 fluxes. (A) Fluxes presented as functions of the ambient sulfide concentrations measured at 8.4°C. (B) Fluxes presented as functions of the ambient sulfide concentrations measured at 13.5°C. (C) Fluxes at both temperatures combined, presented as functions of sulfide consumption rate as manipulated by controlling the sulfide concentration around the worms.

in *Riftia*. Three different animals (3.3, 6.1, and 17.2 g wet weight) in flowing water pressure respirometers in heterotrophic carbon balance showed appreciable rates of ammonia excretion (0.07, 0.19, and 0.27 μmol g^{-1} h^{-1}, respectively).

Hemolymph parameters after capture and maintenance without sulfide

In these experiments, several properties related to autotrophic metabolism in *Riftia pachyptila* were followed over time, after capture and recovery of the tubeworms.

Five worms were sacrificed immediately after capture, and their hemolymph and coelomic fluid pH, ΣCO_2, ΣH_2S, and $S_2O_3^{2-}$ as well as trophosome S° concentrations were measured. Nine other *R. pachyptila* were placed in high-pressure, flowing-water aquaria immediately after recovery and maintained, under pressure (120 atm), in seawater without added sulfide for varying periods of time before sacrifice and analysis. The initial values found (Table I) were comparable to those found previously for this species (Childress *et al.*, 1984) with ΣCO_2 being quite elevated and pH values being quite low. This indicated that the worms were probably withdrawn into their tubes and anaerobic while they were being brought to the surface. Data following recovery in the aquarium system supports the same conclusion. Hemolymph and coelomic pH rose and ΣCO_2 concentration declined (from very high levels found immediately after capture) after the animals were maintained for one or more days under pressure (Table I). Hemolymph ΣH_2S concentrations in the freshly collected animals were substantial, ranging up to 1.75 m*M* (mean of 0.71 m*M* Table I), decreased rapidly in animals maintained under pressure in the absence of added sulfide, and was undetectable after three and five days (Table I). Trophosome S° declined significantly with time as well, approaching zero after 3 to 5 days (Table I). Thiosulfate concentrations in the hemolymph of *R. pachyptila* were always very low (less than 36 μM, average = 24 μM) and did not decline during the five days in captivity (Table I).

To examine the hypothesis that the pattern of high ΣCO_2 and low pH found in the hemolymph of freshly recovered worms resulted from oxygen deprivation, we maintained two individuals for 24 h in the flowing water aquarium system at 14 μM O_2 and 15 μM ΣH_2S. Prior to this experiment these worms had been kept in the aquarium system for 2 days with no sulfide and more than 100 μM O_2. The hemolymph pH was depressed (6.48 and 6.82), supporting the suggestion that depressed pH values after recovery are the result of anaerobic metabolism (Childress *et al.*, 1984). The ΣCO_2 values were low (3.357 and 3.280 *mM*), but at the low pH values these represent high P_{CO_2} values (13.9 and 8.0 torr). The failure of these worms to accumulate the higher ΣCO_2 concentrations found in freshly recovered worms (Table I) probably resulted from their plumes remaining extended and thus continuing to exchange CO_2 with the medium during the experiment. In contrast, during recovery from the bottom, worms were constrained in a box and could not extend their plumes to exchange gases. This is consistent with observations that *Riftia pachyptila* individuals release substantial amounts of ΣCO_2 to the medium under hypoxic conditions (Childress *et al.*, 1984). The hemolymph ΣH_2S contents were substantial (5.497 and 5.013 m*M*)

Table I

Riftia pachyptila *hemolymph, coelomic fluid, and trophosome parameters immediately after capture and after maintenance in the absence of sulfide in flowing water, pressure (120 atm) aquaria*

Days after capture	n	Tissue	pH	ΣCO_2 (mmoles/l)	ΣH_2S (mmoles/l)	$S_2O_3^{2-}$ (mmoles/l)	S° (%wet wt.)
0	5	Hemolymph	7.07 ± 0.07	10.37 ± 1.05	0.714 ± 0.332	0.024 ± 0.004	
	5	Coelomic	7.14 ± 0.78	11.56 ± 2.81	0.089 ± 0.087	0.013 ± 0.017	
	5	Trophosome					2.76 ± 1.38
1	1	Hemolymph	7.39	7.78	0.066	0.000	
	1	Coelomic	7.48	8.67	0.000	0.000	
	1	Trophosome					1.94
3	2	Hemolymph	7.38, 7.47	5.48, 9.45	0.000, 0.000	0.000, 0.013	
	2	Coelomic	7.42, 7.39	6.39, 9.17	0.000, 0.000	0.000, 0.000	
	2	Trophosome					1.75, 0.03
5	5	Hemolymph	7.49 ± 0.40	5.91 ± 0.25	0.000 ± 0.000	0.014 ± 0.013	
	5	Coelomic	7.59 ± 0.12	5.91 ± 0.56	0.000 ± 0.000	0.003 ± 0.006	
	5	Trophosome					0.092 ± 0.21
Test of change over time in captivity (Kendall rank correlation *tau*, P =)							
		Hemolymph	0.67, 0.0014	−0.77, 0.0005	−0.70, 0.0009	−0.29, 0.19	
		Coelomic	0.71, 0.0007	−0.77, 0.0005	−0.55, 0.0085	−0.20, 0.35	
		Trophosome					−0.54, 0.0097

"n" indicates the number of worms and samples at each time period and the parameter values are shown as mean ± standard error of the mean. ΣCO_2 and ΣH_2S indicate the total concentration of all forms of these substances, released by acidification of the samples in the process of analysis. The Kendall rank correlation tests the significance of changes over time in captivity (underlined *tau* values indicate $P < 0.05$) and are listed beneath each parameter tested.

Table II

Coelomic fluid hemoglobin concentrations as functions of hemolymph hemoglobin concentrations in Riftia pachyptila *after maintenance (24 h) in high-pressure (120 atm), flowing-water aquaria at various fixed ΣH_2S concentrations ≥0.0 and ≤800 μM. Data on freshly collected worms from Arp* et al. *(1987)*

Parameter	n	[coelomic] = a + b[hemolymph]				Wilcoxon signed-rank	
		b ± 95% CI	a	r^2	*P*	Coel:Hemo +, =, −	*P*
All Worms							
Heme (m*M*)	34	0.304 ± 0.204	0.873	0.47	0.005	1, 0, 33	<0.0001
Hemoglobin FI (m*M*)	34			0.04	0.145	0, 0, 34	<0.0001
Hemoglobin FII (m*M*)	34			0.02	0.187	18, 0, 16	0.228
Data from Arp *et al.* (1987)							
Hemoglobin FI (m*M*)	18			0.05	0.70	0, 0, 18	0.0002
Hemoglobin FII (m*M*)	18	0.413 ± 0.276	0.633	0.39	0.0059	11, 0, 7	0.013

"n" indicates the number of worms and samples and the regression coefficients are shown ±95% confidence intervals (CI). FI is the large hemoglobin aggregate (1,700,000 M_r) and FII is the smaller aggregate (400,000 M_r) described by Terwilliger *et al.* (1980) and Arp *et al.* (1987). Underlined regression coefficients and Wilcoxon distributions are significant at the level of at least $P < 0.05$. Not all analyses were completed on all specimens. Regressions are given only when they are significant at the level of at least $P < 0.05$.

and apparently in equilibrium (0.52 and 0.57 fractional sulfide saturation) with the external ΣH_2S (Fig. 5A, B). This is consistent with uptake being due solely to the binding of sulfide by the hemoglobins.

Functioning of tubeworms exposed to various concentrations of oxygen and sulfide

To test the existing hypotheses concerning carbon dioxide and sulfide transport in the hemolymph (Rau and Hedges, 1979; Arp and Childress, 1983; Childress *et al.*, 1984; Arp *et al.*, 1985; Felbeck, 1985; Fisher *et al.*, 1989; Fisher *et al.*, 1990) and to examine responses of this species to different external sulfide concentrations, a series of experiments were conducted in which individual tubeworms were maintained under different conditions before dissection and analysis. In these experiments, *R. pachyptila* individuals were maintained in the high-pressure flowing-seawater aquaria in the absence of sulfide for two days after capture. This allowed the worms to recover from capture and to metabolize most of their internal stores of inorganic sulfur compounds. These worms were then exposed continuously to constant concentrations of sulfide (0–805 μ*M* ΣH_2S) for 24 to 36 h while in the high-pressure (120 atm) flowing-seawater aquaria at 8°C. Oxygen concentrations in the seawater during these experiments were between 0 and 276 μ*M*. After the sulfide exposure, the worms were dissected and samples taken. The hemolymph and coelomic fluid samples were analyzed for pH, ΣCO_2, ΣH_2S, $S_2O_3^{2-}$, and the two hemoglobin fractions. Trophosome samples were analyzed for S°. Upon dissection, seven of the worms were found to have substantial amounts of trophosome that appeared to be in poor condition (see Materials and Methods), and these were dropped from further consideration, leaving 43 worms in the study. Extensive exploration of the data with scatterplots suggested that the data could best be presented in two groups; one of these consisted of 28 animals kept at O_2 concentrations greater than 42 μ*M* and whose hemolymph pH was greater than 7.2. These worms showed evidence of autotrophy and blood circulation (to be discussed below). The other group of 15 worms consisted of individuals kept at O_2 concentrations of 42 μ*M* or less (8 worms) and individuals whose hemolymph pH was less than or equal to 7.2 (11 worms). The low O_2 apparently limited sulfide oxidation while the low pH values apparently indicated anaerobic metabolism in the worms due to behavioral (remaining contracted in the tubes) or undetected physiological constraints. In the figures and tables to be presented, the numbers for each analysis are often less than the total number of individuals, because not all analyses were successfully executed on all specimens.

The heme contents of the hemolymph and coelomic fluid samples of the worms were significantly correlated, but the hemolymph samples had much higher heme concentrations than did the coelomic fluid ones (Table II). There was no significant correlation between the concentrations of the large hemoglobin (FI) in the two compartments, but the concentration in the hemolymph was always much higher (Table II, Fig. 2). In contrast, there was no significant difference in the concentrations of the small hemoglobin (F II) between the two compartments (Table II). However, because there was no significant correlation between the concentrations in the two compartments, it is apparent that they are not confluent. Arp *et al.* (1987) suggested that these two compartments may be

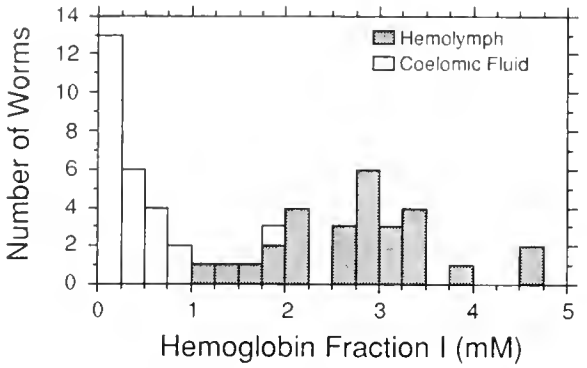

Figure 2. Frequency distributions of the concentrations of the large hemoglobin [FI, 1.7×10^6 M_r, (Terwilliger *et al.*, 1980; Arp *et al.*, 1987)] in coelomic fluid and hemolymph of *Riftia pachyptila* kept for 24 h at different external sulfide and O_2 concentrations.

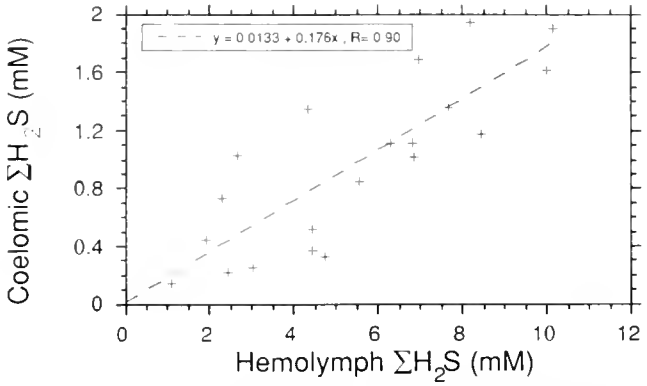

Figure 3. Coelomic fluid ΣH_2S as a function of hemolymph ΣH_2S in *Riftia pachyptila* kept for 24 h at different external sulfide concentrations and >42 μM O_2.

confluent at the size of the smaller hemoglobin, because the concentrations in the two compartments were significantly correlated. However, re-analysis showed that while the concentrations were significantly correlated in their data, the coelomic fluid had higher concentrations precluding confluence for this size molecule (Table II).

Although the two compartments do not exchange hemoglobin molecules, it is apparent that small dissolved molecules are readily exchanged, because the higher O_2, higher pH group had highly significant correlations between the values of all of the measured parameters between the two compartments (Table III). In addition, there were significant differences in the values of all of these parameters, except thiosulfate, between the compartments, apparently resulting from their interactions with the hemoglobins. ΣH_2S was in much higher concentrations in the hemolymph (Fig. 3) than in the coelomic fluid because of the much higher concentrations of hemoglobin FI, which binds 3 moles of sulfide per mole of heme, although this binding is not to the heme group itself (Arp *et al.*, 1987), *versus* 1 mole of sulfide per mole of heme for F II (Fig. 2). These correlations and distributions indicate that these worms were circulating their blood effectively. In contrast, the low O_2, low pH group had no significant correlations between the two compartments for these parameters, and the values were sig-

Table III

Riftia pachyptila *coelomic fluid parameters as a function of the same parameters in hemolymph after maintenance (24 h) of the worms in flowing water, pressure (120 atm) aquaria at various fixed* ΣH_2S *concentrations between 0.0 and 600* μM *with external* O_2 *concentrations > 42* μM *and hemolymph pH > 7.2*

		[coelomic] = a + b[hemolymph]				Wilcoxon signed-rank	
Parameter	n	b ± 95% CI	a	r^2	*P*	Coel:Hemo +, =, −	*P*
pH	26	0.841 ± 0.394	1.223	0.45	0.0002	16, 2, 8	0.042
ΣCO_2 (m*M*)	27	0.990 ± 0.105	0.520	0.94	<0.0001	25, 0, 2	<0.0001
P_{CO_2} (torr)	20	0.744 ± 0.171	0.638	0.82	<0.0001	6, 0, 14	0.04
ΣH_2S (m*M*)	27	0.176 ± 0.034	0.013	0.81	<0.0001	0, 7, 20	<0.0001
% Hb sulfide saturation	20	0.759 ± 0.123	−0.019	0.90	<0.0001	0, 7, 13	0.0015
Free ΣH_2S (m*M*)	19	0.140 ± 0.031	0.002	0.84	<0.0001	0, 6, 13	0.0015
Free H_2S (m*M*)	19	0.133 ± 0.024	0.0003	0.89	<0.0001	1, 6, 12	0.0024
$S_2O_3^{2-}$ (m*M*)	22	1.54 ± 0.25	−0.021	0.89	<0.0001	7, 3, 12	0.41

"n" indicates the number of worms and samples and the regression coefficients are shown ±95% confidence intervals (CI). ΣCO_2 and ΣH_2S indicate the total concentration of all forms of these substances, bound and free, released by acidification of the samples in the process of the analyses. Free ΣH_2S is an estimate of the free sulfide of all molecular species. Free H_2S is an estimate of the free (*i.e.*, unbound) concentration of this molecular species. Underlined Wilcoxon distributions are significant at the level of at least $P < 0.05$. These data include observations for all parameters for seven animals that were not exposed to sulfide during the experiment and had internal sulfide concentrations of zero. Not all analyses were completed on all individuals studied.

nificantly different for only three of the parameters (Table IV). Such lack of equilibration indicates a lack of opportunity for exchange between the two fluids, suggesting that circulation was impaired in this group of worms.

Because the hemolymph and coelomic fluid parameters were always parallel and closely correlated, and because the low O_2, low pH worms do not, for the most part, show signs of autotrophy and effective circulation, the hemolymph parameters from the higher O_2, higher pH worms will be emphasized in considering the responses of the internal parameters to external sulfide (Table V). The low O_2, low pH group (Table VI) will be considered primarily in contrast to the other group.

In the higher O_2 group, hemolymph and coelomic ΣH_2S were correlated with external ΣH_2S. They were at least one order of magnitude higher than the external concentration in all cases (Table V, VII, Fig. 4A), clearly demonstrating the ability of this worm to concentrate sulfide from its environment. However, their hemoglobin was maintained well below sulfide saturation at all external sulfide concentrations tested (Fig. 5A) showing 50% saturation at an external ΣH_2S of 122 μM as compared to an *in vitro* affinity of 50% saturation at 11.2 μM ΣH_2S (Fisher *et al.*, 1988a). The hemolymph free ΣH_2S and free H_2S also increased with external ΣH_2S, but remained about an order of magnitude lower than the external concentrations (Table V, Fig. 5B, C). Thus, although the ΣH_2S concentration in the hemolymph was much higher than outside the worm, there was a significant gradient from the outside to the inside for the free chemical species. The latter gradient could only be maintained by the consumption of sulfide within the worm, presumably by the symbionts.

In contrast, the low O_2, low pH group shows only three barely significant correlations between external ΣH_2S and any of the hemolymph sulfide parameters (Table VI). Further, the hemolymph sulfide saturation is close to that expected *in vitro*, and 50% saturation is close to the *in vitro* value (3.3 and 11.2 μM ΣH_2S, respectively, Fig. 5A). Thus, the ability of these worms to concentrate ΣH_2S in their hemolymph appears to be explained entirely by the binding of sulfide by the hemoglobins. In addition, the hemolymph free ΣH_2S and free H_2S were essentially in equilibrium distributions with the corresponding external parameters (Fig. 5B, C) indicating that no gradient for passive uptake exists in these worms. Symbiont sulfide oxidation had apparently essentially ceased under these conditions so the hemoglobins could no longer function to depress free sulfide concentrations.

It is also apparent from the data that sulfide is the only sulfur compound of importance in the hemolymph. Although thiosulfate was found in both groups, and increases significantly in the presence of external sulfide (Table V), it is typically less than hemolymph ΣH_2S by more than one order of magnitude (Fig. 4).

The hemolymph ΣCO_2 and P_{CO_2} values are both reduced at higher external ΣH_2S concentrations in the higher O_2 group (Table V, VII, Fig. 6A, B), suggesting the removal of inorganic carbon by the autotrophic symbionts. There were no significant relations between these parameters for the low O_2, low pH group (Table V, Fig. 6A, B). In addition, the internal P_{CO_2} was higher than the external under virtually all conditions (Fig. 6B, Table V, VI) precluding uptake by passive diffusion into the hemolymph.

Table IV

Coelomic fluid parameters as a function of the same parameters in hemolymph of Riftia pachyptila *after maintenance (24 h) in high-pressure (120 atm), flowing-water aquaria at various fixed sulfide concentrations between 0.13 and 800* μM *with* O_2 *concentrations* $\leq$ *42* μM *or hemolymph pH* $\leq$ *7.2*

		[coelomic] = a + b[hemolymph]				Wilcoxon signed-rank	
Parameter	n	b ± 95% CI	a	r^2	*P*	Coel:Vasc +, =, −	*P*
pH	15			0.19	0.105	11, 0, 4	0.125
ΣCO_2 (mM)	14			0.45	0.054	10, 0, 3	0.022
P_{CO_2} (torr)	13			0.05	0.47	0, 0, 13	0.0015
ΣH_2S (mM)	14			0.00	0.96	2, 0, 12	0.0019
% Hb sulfide saturation	13			0.03	0.56	5, 0, 8	0.34
Free ΣH_2S (mM)	13			0.04	0.49	5, 0, 8	0.60
Free [H_2S] (mM)	13			0.03	0.55	4, 0, 9	0.34
$S_2O_3^{2-}$ (mM)	7			0.04	0.691	5, 0, 2	0.13

"n" indicates the number of worms and samples and the regression coefficients are shown ±95% confidence intervals (CI). ΣCO_2 and ΣH_2S indicate the total concentration of all forms of these substances, released by acidification of the samples in the process of the analyses. Free ΣH_2S is an estimate of the unbound sulfide of all molecular species. Free [H_2S] is an estimate of the concentration of this molecular species. Underlined Wilcoxon distributions are significant at the $P < 0.05$ level. No regressions were significant at the $P < 0.05$ level and therefore none are listed.

Table V

Riftia pachyptila hemolymph parameters and S° in trophosome as functions of external conditions after maintenance (24 h) in high-pressure (120 atm), flowing-water aquaria at various fixed ΣH_2S concentrations greater than 0.0 and less than 600 μM (external O_2 concentrations > 42 μM and hemolymph pH > 7.2). Kendall correlations, but not the regressions or Wilcoxon tests, include seven individuals at 0.0 ΣH_2S

X Variable	Kendall correlation			[hemolymph parameter] = aX^b					Wilcoxon signed-rank	
Hemolymph Parameter	n	*tau*	*P* =	n	b ± 95% CI	a	r^2	*P*	External:Hemo +, =, −	*P*
X = External ΣH_2S										
pH	26	−0.165	0.24	19			0.05	0.38		
ΣCO_2 (m*M*)	27	−0.629	<0.0001	20	−0.224 ± 0.124	1.565	0.44	0.0014		
P_{CO_2} (torr)	26	−0.529	<0.0001	19	−0.170 ± 0.150	1.525	0.25	0.031		
ΣH_2S (m*M*)	27	0.826	<0.0001	20	0.448 ± 0.121	12.53	0.76	<0.0001	0, 0, 20	<0.0001
Sulfide saturation	19	0.772	<0.0001	18	0.417 ± 0.138	1.057	0.72	<0.0001		
Free ΣH_2S (m*M*)	25	0.861	<0.0001	18	1.05 ± 0.41	0.105	0.65	<0.0001	17, 0, 1	0.0002
Free H_2S	25	0.832	<0.0001	18	1.086 ± 0.438	0.0219	0.63	<0.0001		
$S_2O_3^{2-}$ (m*M*)	22	0.487	0.0015	15			0.11	0.13		
S° (% wet wt.)	24	0.504	0.0006	14			0.017	0.66		
X = External H_2S										
Free H_2S	25	0.694	<0.0001	18	1.053 ± 0.593	0.179	0.47	0.016	17, 0, 1	0.0004
X = External P_{CO_2}										
P_{CO_2} (m*M*)	25	−0.361	0.011	18			0.007	0.74	1, 0, 17	0.0002
X = External pH										
pH	26	0.123	0.38	19			0.018	0.68	14, 0, 5	0.0079

"n" indicates the number of worms and samples and the regression coefficients are shown ±95% confidence intervals (CI). ΣCO_2 and ΣH_2S indicate the total concentration of all forms of these substances, released by acidification of the samples in the process of the analyses. H_2S indicates only this chemical species itself. "Free" indicates an estimate of quantity present in a fluid but not bound to the hemoglobin. Only regressions that were significant at the $P < 0.05$ level are shown.

Hemolymph pH appeared to be unaffected by external or internal sulfide or external pH (Table V, VI, VII, Fig. 6C), although it is somewhat variable. This lack of interaction suggests that pH is not apt to be a significant factor in the uptake and distribution of sulfide or inorganic carbon from the environment into the hemolymph. The strong effect of low O_2 on hemolymph pH is probably due to the accumulation of acidic endproducts of anaerobic metabolism.

These various parameters followed the same trends in the coelomic fluid. However, the multiple regression analyses consistently showed that the strongest predictor of a chemical parameter in the coelomic fluid is not an external parameter but the corresponding parameter in the hemolymph. This indicates that the route of transport to the coelomic fluid is via the hemolymph and not the body wall.

Discussion

Autotrophy

Riftia pachyptila, like all vestimentiferan tubeworms, lacks a mouth and a gut as an adult, and as a result, its nutrition has been a matter of considerable investigation and speculation. While net ΣCO_2 uptake (autotrophy) by the intact symbioses between sulfur-oxidizing, autotrophic bacteria and marine invertebrates living around deep-sea hydrothermal vents has been widely assumed (Cavanaugh *et al.*, 1981; Felbeck, 1981, 1985; Felbeck *et al.*, 1981; Cavanaugh, 1985; Southward, 1987), the data presented here are the first actually to demonstrate this in a vestimentiferan tubeworm or any hydrothermal vent animal. Actual autotrophic balance for the tubeworm symbiosis of course depends on the reasonable assumptions that much of the fixed carbon is available to the animal tissues, and the production of mucus and loss of small organic molecules are not large compared to the rate of carbon fixation.

The only previous demonstration of autotrophic balance in an animal/bacterial symbiosis was for the shallow-living, gutless protobranch bivalve, *Solemya reidi* (Anderson *et al.*, 1987). In that case, the clams showed a maximum net ΣCO_2 uptake of 0.89 μmole g^{-1} h^{-1} which equals about 0.24% of the clam's total organic carbon per day. In contrast, *Riftia pachyptila* apparently has a considerably higher maximum rate of net ΣCO_2 uptake (2.74 μmole g^{-1} h^{-1} maximum in this study). This high rate, combined with the relatively low carbon content of 5.5%

Table VI

Hemolymph parameters and S° in trophosome as functions of external sulfide in Riftia pachyptila *after maintenance (24 h) in high-pressure (120 atm), flowing-water aquaria at various fixed ΣH_2S concentrations between 0.013 and 800 μM (external O_2 concentrations ≤ 42 μM or hemolymph pH ≤ 7.2)*

X Variable	Kendall correlation			[hemolymph parameter] = aX^b					Wilcoxon signed-rank	
Hemolymph Parameter	n	tau	P =	n	b ± 95% CI	a	r^2	P	External:Hemo +, =, −	P
X = External ΣH_2S										
pH	15	−0.154	0.42	15			0.00	0.97		
ΣCO_2 (m*M*)	15	−0.174	0.37	15			0.10	0.26		
P_{CO_2} (torr)	14	−0.223	0.91	14			0.02	0.61		
ΣH_2S (m*M*)	15	0.385	0.045	15			0.08	0.30	0, 0, 15	0.0007
Sulfide saturation	14	0.425	0.034	14	0.098 ± 0.088	0.885	0.33	0.033		
Free ΣH_2S (m*M*)	14	0.438	0.029	14	0.646 ± 0.523	0.270	0.38	0.020	8, 0, 6	0.55
Free H_2S	14	0.402	0.040	14	0.669 ± 0.562	0.100	0.36	0.023		
$S_2O_3^{2-}$ (m*M*)	7	−0.410	0.20	7			0.56	0.053		
S° (% wet wt.)	11	−0.185	0.94	11			0.028	0.62		
X = External H_2S										
Free H_2S	14	0.291	0.148	14			0.20	0.106	4, 0, 10	0.177
X = External P_{CO_2}										
P_{CO_2} (m*M*)	14	−0.205	0.31	14			0.005	0.82	0, 0, 14	0.001
X = External pH										
pH	15	−0.216	0.26	15			0.021	0.87	13, 0, 2	0.002

"n" indicates the number of worms and samples and the regression coefficients are shown ±95% confidence intervals (CI). ΣCO_2 and ΣH_2S indicate the total concentration of all forms of these substances, released by acidification of the samples in the process of the analyses. H_2S indicates only this chemical species itself. "Free" indicates an estimate of quantity present in a fluid but not bound to the hemoglobin.

of wet weight of this species (Fisher *et al.*, 1988b), results in a much higher estimate of 1.4% of the tubeworm's total organic carbon per day. This suggests a high potential growth rate in this species, which is supported by some evidence of growth in length *in situ* (Roux *et al.*, 1989). Very rapid growth has been hypothesized to be important in this species' apparent domination of young vent sites (Childress, 1988; Fustec *et al.*, 1988; Hessler *et al.*, 1988).

The maximum rate of carbon fixation (2.74 μmole ΣCO_2 g $worm^{-1}h^{-1}$) for the intact symbiosis corresponds to a rate of 17.9 μmole ΣCO_2 g $trophosome^{-1}h^{-1}$, assuming that trophosome accounts for 15.3% of the wet weight of the intact symbiosis (Childress *et al.*, 1984). This rate is in good agreement with the maximum rates of fixation of $H^{14}CO_3^-$ (13 to 28 μmol ΣCO_2 g $trophosome^{-1}h^{-1}$) observed in preparations of trophosome tissue from *Riftia pachyptila* containing viable endosymbiotic bacteria using sulfide as a substrate (Fisher *et al.*, 1989).

Substrates used by the symbiosis

Studies of the isolated symbionts of *Riftia pachyptila* have indicated that these symbionts use only sulfide and not thiosulfate as a source of externally derived reducing power (Belkin *et al.*, 1986; Fisher *et al.*, 1989; Wilmot and Vetter, 1990). The data presented in this paper support the view that vestimentiferan tubeworms are specialized to supply only sulfide to their symbionts (Childress *et al.*, 1984), because sulfide is concentrated from the medium and is quickly used by the symbionts (Fig. 4, 5, Table I). In contrast, thiosulfate, an endproduct of animal sulfide oxidation (Vetter *et al.*, 1987; O'Brien and Vetter, 1990), is always at a very low concentration in the hemolymph (Fig. 4) and is not quickly used by the symbiosis (Table I). The lack of interaction (either inhibition or utilization as substrate) of sulfide with the animal metabolism is also shown by the fact that the regressions of O_2 and ΣCO_2 fluxes *versus* ΣH_2S flux pass essentially through the values of O_2 and CO_2 flux measured in the absence of ΣH_2S (Fig. 1C). The low levels of sulfide oxidase activity reported from the body wall of *R. pachyptila* (Powell and Somero, 1986) are apparently of little significance in the overall metabolism of this species because so little thiosulfate is found in the body fluids. Thus, the animal metabolism has little interaction with sulfide, delivering it intact to the symbionts.

This arrangement is quite different from that of symbiont-containing bivalves, which appear to oxidize sulfide to thiosulfate and to supply this to the symbionts. *Solemya reidi* mitochondria can produce ATP from the oxidation of sulfide to thiosulfate (Powell and Somero, 1985; O'Brien and Vetter, 1990), which can then be supplied

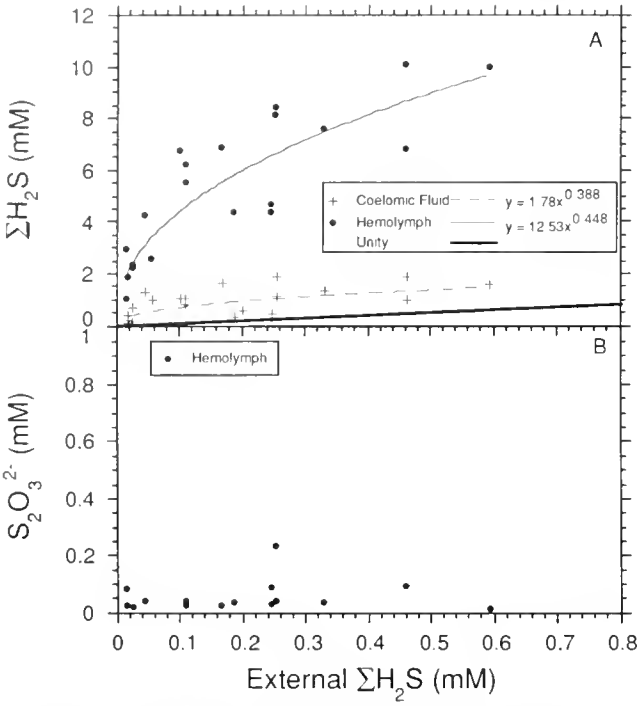

Figure 4. ΣH_2S and thiosulfate concentrations in hemolymph and coelomic fluid in *Riftia pachyptila* kept for 24 h at different external sulfide concentrations and >42 μM O_2. (A) The broad solid line represents equal concentrations of ΣH_2S outside the worm and in its fluids. The narrow solid line and the closed circles apply to the hemolymph while the dashed line and crosses apply to the coelomic fluid. (B) The closed circles represent the concentrations of thiosulfate in the hemolymph in these same worms.

to the symbionts to support their metabolism (Anderson *et al.*, 1987; Vetter *et al.*, 1989). In this species, the oxidation of sulfide apparently has substantial effects on the animal metabolism, reducing the animal carbon oxidation, which indicates that the sulfide oxidation is of metabolic significance to the animal tissues (Anderson *et al.*, 1987). Similarly, the symbionts of *Bathymodiolus thermophilus*, the vent mussel, and *Calyptogena magnifica*, the vent clam, both appear to be able to use thiosulfate to drive carbon-fixation (Belkin *et al.*, 1986; Childress *et al.*, 1991), and the animals involved accumulate substantial thiosulfate in their body fluids (Fisher *et al.*, 1988c; Childress *et al.*, 1991). Whether these other animals can obtain energy from the oxidation of sulfide remains to be tested.

Riftia pachyptila symbionts are dependent on the immediate availability of sulfide to drive significant rates of autotrophy. While the symbionts do store S° at concentrations up to 3200 μg atoms/g fresh weight (Fisher *et al.*, 1988b) and can oxidize the stored S° in the absence of external ΣH_2S (Table 1), the metabolism experiment reported here demonstrated that both O_2 and autotrophic ΣCO_2 fluxes were dependent upon an external supply of ΣH_2S. The stored S° did not support a detectable rate of ΣCO_2 uptake for even a few hours. This is the same situation found in the bivalve *Solemya reidi* (Anderson *et al.*, 1987). Thus, it appears that while the substantial S° stores often found associated with sulfur-oxidizing symbionts (Vetter, 1985; Somero *et al.*, 1989) can be used by the symbionts, these rates are only a small fraction of the rates of oxidation of sulfide or thiosulfate. This may well be the case for free-living sulfur-oxidizing bacteria as well (Nelson *et al.*, 1986). S° sulfur stores may be of significance for the survival of the symbionts during times of sulfide deprivation, but apparently do not represent a significant store to support the symbiosis.

Respiratory fluxes in response to sulfide

Oxygen and ΣCO_2 fluxes in *Riftia pachyptila* are dependent upon the sulfide flux. Net ΣCO_2 uptake requires the presence of both O_2 and sulfide. About 90 μM ΣH_2S was necessary to reach the maximum ΣCO_2 uptake rate (Fig. 1), and external O_2 concentrations greater than 42 μM appeared to be necessary for the use of sulfide by the symbionts (Fig. 5). These concentrations are similar to those that stimulate maximal autotrophy in *S. reidi* (Anderson *et al.*, 1987). However, autotrophic ΣCO_2 uptake by the *R. pachyptila* symbionts in the intact symbiosis did not appear to be inhibited by external sulfide concentrations up to 600 μM (Fig. 5B), unlike that of the symbionts of *S. reidi*, which are inhibited in the intact symbiosis at external ΣH_2S concentrations of about 250 μM (Anderson *et al.*, 1987).

These environmental requirements of *R. pachyptila* appear to match closely the environmental conditions where the species is found. Where *Riftia* is in abundance, the flow of vent water is high, ΣH_2S can approach 350 μM in the vent water and O_2 in the ambient water is around 110 μM (Fisher *et al.*, 1988b; Johnson *et al.*, 1988b). *In situ* measurements of sulfide and O_2 distributions around the tubeworms have suggested that they take up sulfide from concentrations above about 60 μM and O_2 from concentrations above 70 μM, with maximal uptake rates from concentrations around 100 μM in both cases (Johnson *et al.*, 1988b). The worms gain access to both substrates at high concentrations because the water around them is not well mixed, and they are therefore exposed to conditions that fluctuate between vent water (15°C, 350 μM ΣH_2S, 0 μM O_2) and ambient water (2°C, 0 μM ΣH_2S, 110 μM O_2) on time scales of fractions of a second and longer (Johnson *et al.*, 1988a). This species then appears to be specialized for high rates of autotrophic function, and, as a result, it requires the high concentration and supply of sulfide associated with rapid venting. These stringent habitat requirements make *Riftia pachyptila* vulnerable to either natural reduction in vent flow over time or diversion of vent flow by mussels. *R. pachyptila*

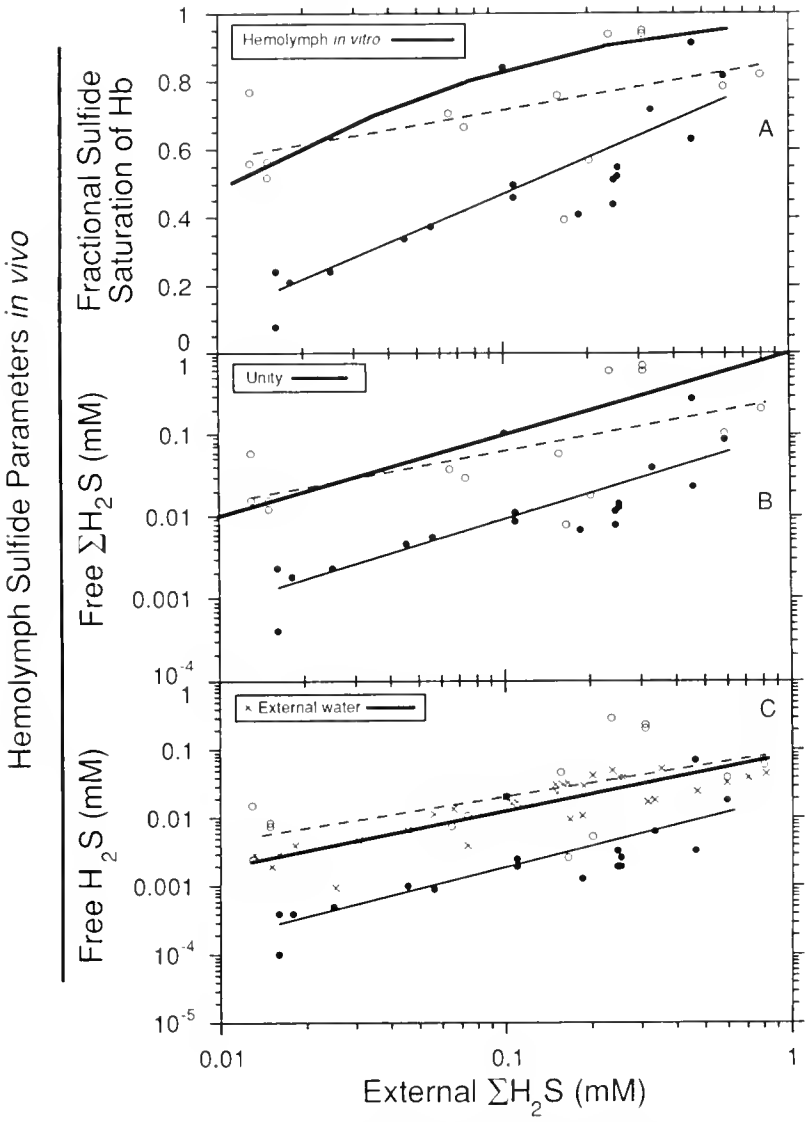

Figure 5. *Riftia pachyptila* hemolymph sulfide parameters as a function of external ΣH_2S concentrations in worms kept for 24 h at fixed ΣH_2S concentrations. Closed circles and narrow solid lines represent values from worms that were kept at >42 μM O_2 and had hemolymph pH values > 7.2. Open circles and dashed lines represent values from worms that were kept at ≤42 μM O_2 or had hemolymph pH values ≤7.2. Regression equations for the plotted lines may be found in Tables V and VI. (A) The fractional saturation of the hemoglobins *in vivo* with sulfide as estimated from the hemoglobin concentrations, hemolymph ΣH_2S and *in vitro* sulfide binding properties. The broad solid line is the saturation *versus* ΣH_2S relationship determined *in vitro* (Fisher *et al.*, 1988a). (B) The relationship between free (unbound) ΣH_2S and external ΣH_2S in hemolymph. The broad solid line represents equal concentrations in the hemolymph and outside. (C) The relationship between free (unbound) H_2S and external ΣH_2S. The x symbols and broad solid line represent the external H_2S concentrations in these same experiments.

numbers might therefore decline at a vent site long before venting ceased, as has been observed at the Galapagos Rift Rose Garden site (Hessler *et al.*, 1988).

Molar ΣCO_2:O_2:ΣH_2S ratios

The maximal measured uptake rates of O_2, ΣH_2S, and ΣCO_2 by *Riftia pachyptila* are high (Fig. 1); they are about twice those of *S. reidi* for O_2 and ΣH_2S and three times that of *S. reidi* for ΣCO_2 (Anderson *et al.*, 1987). The relationships between the O_2 and ΣCO_2 fluxes and the ΣH_2S flux provide quantitative estimates of the dependences of the former fluxes upon the latter (Fig. 1C). As noted earlier, these relationships suggest that there is little direct interaction of the animal metabolism and the ΣH_2S flux, and thus they apparently reflect the symbiont me-

Table VII

Comparisons of hemolymph and coelomic fluid parameters in Riftia pachyptila *after maintenance (24 h) in high pressure (120 atm), flowing-water aquaria either in the absence or presence (0.016 to 0.593 mM, mean = 0.19 mM ΣH_2S) of sulfide*

	Hemolymph		Coelomic fluid		Wilcoxon Coel:Hemo +, =, −	
Parameter	0 sulfide	sulfide	0 sulfide	sulfide	0 sulfide	sulfide
pH	7.47 (±0.32,7)	7.40 (±0.26, 19)	7.54 (0.05, 7)	7.44 (0.03, 20)	5, 0, 2	14, 0, 5
ΣCO_2 (m*M*)	5.76 (±0.66, 7)	2.78 (±0.25, 20)	6.44 (±0.049, 7)	2.78 (0.26, 21)	6, 0, 1	19, 0, 1
P_{CO_2} (torr)	5.81 (±0.78, 7)	3.16 (±0.28, 18)	4.95 (±0.00, 7)	2.92 (±0.00, 19)	1, 0, 6	1, 0, 17
ΣH_2S (m*M*)	0.0 (7)	5.38 (±0.61, 20)	0.0 (7)	0.95 (±0.12, 21)	0, 7, 0	0, 0, 20
$S_2O_3^{2-}$ (m*M*)	0.01 (±0.01, 7)	0.06 (±0.01, 15)	0.00 (±0.00, 7)	0.06 (±0.02, 17)	0, 3, 4	7, 0, 8

Parameter values are shown as means with the standard errors of the means and the number of observations in parentheses. For the hemolymph and coelomic fluid comparisons with and without external sulfide, the data sets were compared using the Mann-Whitney U test. Single underlined pairs of means are from groups that have null hypothesis P values < 0.05. Double underlining indicates P values < 0.005. The relative concentrations of each substance were compared between the coelomic and vascular compartments using the Wilcoxon signed-rank test. Single and double underlining have the same meanings for this test as for the Mann-Whitney.

tabolism. The regression analyses of the metabolism experiment (Fig. 1C) indicate that these symbionts fix 0.92 mole ΣCO_2 using 1.14 mole O_2 and 1 mole ΣH_2S. Using the calculation methods of Kelly (1982), the thermodynamic efficiencies implicit in these ratios can be determined. Given a requirement of 496 kJ to reduce CO_2 to hexose, and a $\Delta G = -716$ kJ for the oxidation of sulfide to sulfate, the resulting efficiency is 63%. The molar ratio observed for *S. reidi*, 0.38 ΣCO_2:0.92 O_2:1 ΣH_2S, gives an efficiency of 40% if one assumes that the bacteria are using thiosulfate ($\Delta G = -936$ kJ for two S atoms) (Anderson *et al.*, 1987). In contrast, studies of the thermodynamic efficiencies of free-living bacteria have been done using very different methods, and they have shown lower efficiencies. The studies of free-living bacteria have used the y_{max} or "true growth yields" to estimate fixation independent of maintenance metabolism (Kelly, 1982). *Thermothrix thiopara* has the highest ratios yet determined for aerobic sulfur-oxidizers (0.58 ΣCO_2:1 thiosulfate at 72°C), corresponding to a thermodynamic efficiency of 29% (Mason *et al.*, 1987). While the ratios and efficiencies for the *S. reidi* and *R. pachyptila* symbionts seem unusually high, this may be a result of the symbiotic lifestyle.

Measurements of the y_{max} in free-living bacteria are generally made in a chemostat that maintains constant, optimal conditions for the growth of the bacteria. The production of bacterial biomass is then measured. This situation is very different from that in a symbiosis in that microbial growth involves the synthesis of a variety of complex compounds, not primarily the production of small organic molecules as is typical of animal/algal symbioses and is probably typical of most animal/bacterial symbioses as well. In *S. reidi*, the symbionts "leak" newly fixed carbon within seconds and are apparently held at a very low rate of growth (Fisher and Childress, 1986). While much less is known about this aspect of the *R. pachyptila* symbiosis, it too is believed to operate primarily by the "leakage" of small organic compounds from the bacteria to the animal with the bacteria being held in a state of slowed reproduction (Felbeck, 1985). Under the conditions present in these symbioses (low microbial growth rates, synthesis of small organic compounds, and maintenance in an environment controlled by the host) it may be possible for bacteria to achieve unusually high efficiencies for CO_2 fixation.

The internal consistency of the molar ratios for *Riftia pachyptila* can also be evaluated from the O_2:ΣH_2S ratios. The ratio of 1.14:1 falls well short of the expected 2:1 if all of the sulfide is oxidized to sulfate in the absence of other reductive processes. However, because carbon fixation is a reductive process, the reducing equivalents used in carbon fixation must also be taken into account. Following the reasoning of Kelly (1982), each CO_2 fixed to the level of CH_2O *via* the Calvin-Benson cycle requires $4e^-$ and $4H^+$. For our ratio of 0.92 ΣCO_2:1 ΣH_2S, CO_2 fixation requires $0.92 \times 4(H) = 3.68$ of the 8(H) available from complete oxidation of sulfide. Thus, $8 - 3.68 = 4.32(H)$ remain for the reduction of O_2, and the predicted O_2 uptake would be $4.32/8 \times 2 = 1.08$ O_2, compared with our value of 1.14. This agreement supports the validity of the observed ratios.

In contrast, the ratios determined for *S. reidi* showed a considerable discrepancy (0.92 O_2:1ΣH_2S observed *versus* 1.62:1 calculated as above) with insufficient O_2 consumption seemingly to account for the observed fixation

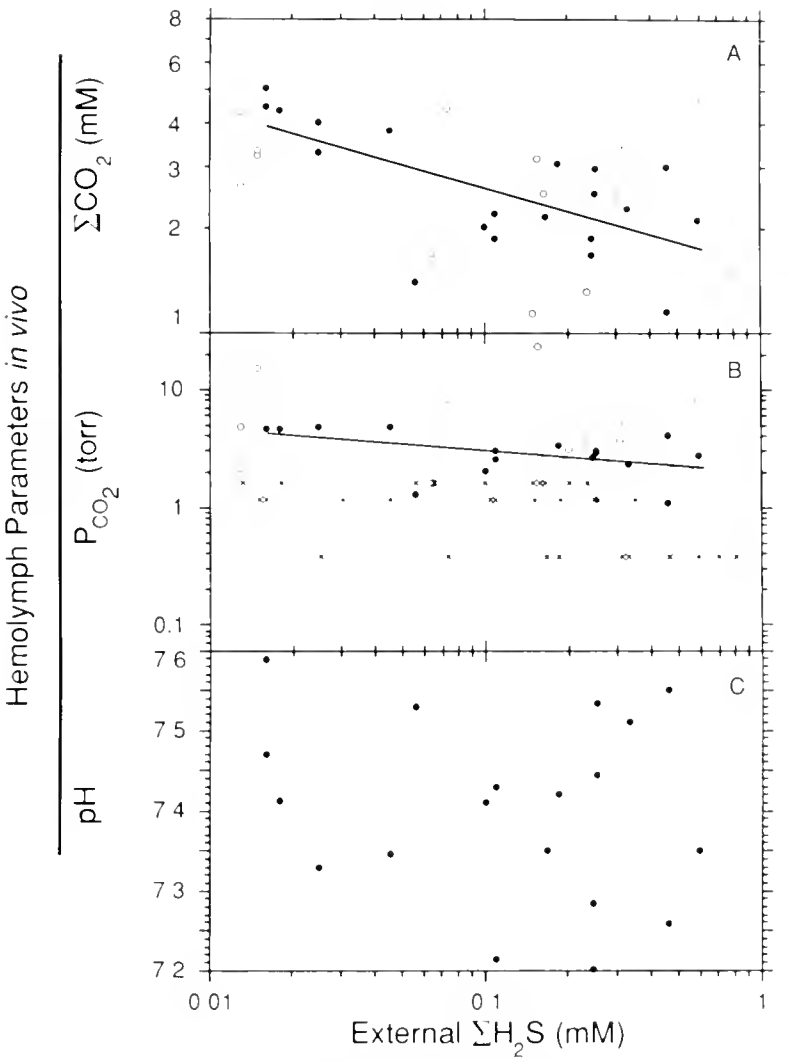

Figure 6. *Riftia pachyptila* hemolymph parameters as a function of external ΣH_2S in worms kept for 24 h at a given ΣH_2S. Closed circles and solid lines represent values from worms which were kept at >42 μM O_2 and had hemolymph pH values >7.2. Open circles represent values from worms which were kept at ≤42 μM O_2 or had hemolymph pH values ≤7.2. Regression equations for the plotted lines may be found in Table V. Where no line is plotted, the relationship was not significant (Tables V and VI). (A) Hemolymph ΣCO_2 as a function of external ΣH_2S. (B) P_{CO_2} as a function of external ΣH_2S in hemolymph and in the external water (x symbols). (C) Hemolymph pH as a function of external ΣH_2S.

of carbon and oxidation of sulfide (Anderson *et al.*, 1987). This discrepancy was attributed to the interactions between the animal sulfide and carbon metabolism. Therefore, the agreement observed for *R. pachyptila* may be yet another indicator of the degree to which the animal metabolism is isolated from the sulfur metabolism of the symbiosis.

Uptake and transport processes

The data presented here provide much new information on the processes for the uptake and transport of sulfide and carbon dioxide that are operative in these worms. The central role of the sulfide-binding hemoglobins in sulfide uptake, transport, and toxicity control (Arp and Childress, 1983; Powell and Somero, 1983; Childress *et al.*, 1984; Powell and Somero, 1986; Fisher *et al.*, 1988a, 1989) is fully supported by these data. In particular, the worms can bind sulfide reversibly *in vivo* (Table I); they can concentrate ΣH_2S from the medium by a factor of 1 to 2 orders of magnitude (Fig. 4A); and when the worms are not in autotrophic balance (low O_2, low pH group), the hemolymph hemoglobins approach equilibrium sulfide binding (half saturation near 11 μM ΣH_2S) at all sulfide concentrations tested (Fig. 5A). In addition, free ΣH_2S and free H_2S in the hemolymph of these worms is in equi-

librium with the same parameters in the external medium (Fig. 5B, C). Because the endpoint, in the absence of autotrophy, appears to be sulfide equilibrium between the hemolymph and the medium, no mechanism other than diffusion appears to be functioning to bring sulfide into the hemolymph.

When the worms are in autotrophic balance, the symbionts remove sulfide from the hemolymph at a sufficient rate to keep the hemoglobins below equilibrium binding of sulfide, resulting in an apparent *in vivo* affinity of 122 μM ΣH_2S for half saturation of the hemoglobins (Fig. 5A). This uptake by the symbionts is sufficient to maintain the hemolymph free ΣH_2S and free H_2S about an order of magnitude below the values of those parameters in the external medium (Fig. 5B, C). This provides a gradient to drive the diffusion of sulfide into the hemolymph. The available evidence indicates that this gradient is sufficient for the uptake of sulfide by the worms. Once the sulfide is transported to the trophosome, it presumably diffuses from the hemolymph into the bacteriocytes and subsequently to the bacteria. A sulfide binding factor found in the trophosome may also be important in this process (Childress *et al.*, 1984).

The cooperative role of the hemoglobin sulfide-binding and the symbiont sulfide consumption in controlling hemolymph free ΣH_2S concentrations to prevent sulfide toxicity to either the host tissues or the symbionts can be appreciated from Figure 4 and Figure 5. For example, at an external ΣH_2S of 100 μM, the internal ΣH_2S is 4.5 mM, however, the hemoglobins are only 47% saturated, and, as a result, the free ΣH_2S is only 9.3 μM and the free H_2S is 1.8 μM. Above 300 μM external ΣH_2S, the internal free sulfide rises rapidly due to the increasing saturation of the hemoglobins. Because 50% inhibition of *R. pachyptila* cytochrome c oxidase activity occurs at about 25 μM ΣH_2S *in vitro* at pH 7.0 (Powell and Somero, 1986), the observed hemolymph free ΣH_2S concentrations indicate a significant degree of protection for this critical enzyme at the usual external ΣH_2S concentrations found in this species' environment, with 50% inhibition being reached at about 250 μM external ΣH_2S concentration (Fig. 5B). While the sensitivity of the *R. pachyptila* symbionts to sulfide *in vitro* has not been precisely defined, the onset of inhibition of carbon fixation at pH 7.5 appears to occur at about 300 μM free ΣH_2S (Fisher *et al.*, 1989). In autotrophic worms, such concentrations would not be reached until the hemoglobin was more than 90% saturated, which would not be expected until external ΣH_2S concentrations reached more than 900 μM ΣH_2S (Fig. 5). Thus, the proposed protective role of the hemoglobin sulfide binding activity, both for the tubeworm tissues and the symbionts, is supported by these observations of *in vivo* sulfide concentrations.

The uptake and transport of inorganic carbon appear to be very different from those for sulfide. The environmental pH around the worms ranges from 7.0 in vent water to 7.9 in ambient water, and the ΣCO_2 is about the same in both (K. Johnson, pers. comm.). While O_2 must be taken up primarily from ambient water and ΣH_2S from vent water, inorganic carbon could be taken up from either or both, although the P_{CO_2} values would be higher in the vent water. The hemolymph pH of the worms appears to be somewhat variable, with typical values being between 7.4 and 7.55. The hemolymph pH does not appear to be affected even by the large ΣH_2S concentrations that it carries at high external sulfide concentrations. This is very different from the situation described for nonsymbiotic organisms where H_2S diffuses into the organism and then dissociates causing a drop in pH (Jaques, 1936; Groenendaal, 1981). It suggests that either the uptake mechanism is different in *Riftia* or the binding mechanism does not result in the release of H^+ from H_2S. Hemolymph pH is apparently also not affected by the ΣCO_2 concentration variations or the H^+ produced by sulfide oxidation. Hemolymph ΣCO_2 and P_{CO_2} values in *R. pachyptila* were unusually high for a worm under oxic conditions (pH = 7.47, ΣCO_2 = 5.76 mM, P_{CO_2} = 5.81 torr at 8°C in the absence of sulfide and 7.4, 2.78, and 3.16, respectively, in the presence of sulfide, Table VII). For comparison, *Arenicola marina* has a hemolymph pH of about 7.53, a ΣCO_2 of about 2.5 mM, and a P_{CO_2} of about 1.1 torr at 7.5°C (Toulmond, 1977). Thus, it appears that, in spite of its apparently large respiratory surface and effective circulation (Arp *et al.*, 1985; Jones, 1981), *R. pachyptila* has unusually high internal ΣCO_2 and P_{CO_2} levels. When the worms were in apparent autotrophic balance, the hemolymph ΣCO_2 and P_{CO_2} were decreased significantly as a function of external ΣH_2S, with minimal values approaching 1 mM and 1 torr, respectively, but were still above the environmental values (Table VII, Fig. 6A, B). While we believe that the observed distributions represent conditions in the worms under net autotrophy, it is possible that the observed distribution could result from the experimental worms not being in net autotrophic balance. The decrease in ΣCO_2 under autotrophic conditions is most likely due to the demand of the symbionts, because they have been shown to readily fix inorganic carbon (Belkin *et al.*, 1986; Fisher *et al.*, 1989). The implication of the observed distributions is that these tubeworms concentrate ΣCO_2 to relatively high P_{CO_2} values in the hemolymph and then depend on diffusion through the bacteriocytes to supply the symbionts.

This hypothesis is supported by the unusual $\delta^{13}C$ values of *Riftia pachyptila* of between −9 and −15.6‰ (Rau, 1981; Fisher *et al.*, 1988b, 1990). These workers have suggested that these low values of isotope discrimination result from carbon fixation in this species operating under

conditions approaching carbon limitation, as can happen in marine plankton (Degens *et al.*, 1968). Because the K_m for the carbon fixation by the *Riftia* symbionts is between 400 and 700 μM ΣCO_2 at pH 7.5 (Fisher *et al.*, 1988d), the hemolymph carbon dioxide values (as low as 1100 μM ΣCO_2 in the presence of sulfide) might well be low enough to limit carbon isotope discrimination under conditions of active autotrophy.

Relationship between coelomic fluid and hemolymph

The data presented here support the view that there is free exchange of small molecules between the coelomic fluid and hemolymph (Childress *et al.*, 1984), although this exchange does not extend to molecules as large as the hemoglobins. The much higher hemoglobin concentration in the hemolymph is clearly responsible for the much higher ΣH_2S in that fluid, and may well be responsible for differences in pH, ΣCO_2, and P_{CO_2} as well. However, the cause of the consistently lower percent sulfide saturation, free ΣH_2S, and free H_2S in the coelomic fluid is not apparent at this time. The new data reported here support the concept that the coelomic fluid is a reservoir of O_2, ΣCO_2, and ΣH_2S which the worms can use to buffer the effects of brief fluctuations in vent flow (Arp and Childress, 1981; Childress *et al.*, 1984).

Model of the functioning of the intact symbiosis

Riftia pachyptila appears to have the greatest autotrophic potential and as a result the fastest growth rate of any of the sulfur-oxidizing symbioses investigated to date. It, and probably all vestimentiferans, appears to be unique among the studied species in that the animal is specialized to minimize the interaction of the animal metabolism with sulfide and to provide only sulfide to symbionts that are only capable of using sulfide. Central to the ability of the vestimentiferan symbioses to use sulfide are the hemoglobins, which reversibly bind both sulfide and oxygen to different sites simultaneously. These hemoglobins enable the worms to concentrate sulfide from the medium and by almost two orders of magnitude. Yet, because of the high affinity of the hemoglobins for sulfide as well as the consumption of sulfide by the symbionts, which holds the hemoglobins well below sulfide saturation, the worms can maintain their hemolymph free ΣH_2S concentrations an order of magnitude lower than external ΣH_2S concentrations. The high capacitance of the hemolymph for sulfide is essential for the transport of sufficient quantities of sulfide to the symbionts *via* the circulatory system. The low free sulfide concentrations are essential for preventing the inhibition of animal metabolism or symbiont carbon fixation by sulfide. Diffusion of sulfide across the plume into the hemolymph appears sufficient to explain the movement of sulfide into the worms. Because the symbionts can take sulfide from the hemoglobins, diffusion from the hemolymph into the bacteriocytes in the highly vascularized trophosome may well be sufficient to supply the needs of the symbionts.

The uptake and supply of O_2 to both the symbionts and the worm tissues is apparently accounted for by the high affinity of the hemoglobins for oxygen and the ability of the symbionts and the tissues to use O_2 at low P_{O_2} values. The combination of the high O_2 affinity and the high sulfide affinity is responsible for the ability of these hemoglobins to suppress the spontaneous oxidation of sulfide by O_2 (Fisher and Childress, 1984).

About half the inorganic carbon fixed by the symbionts is potentially derived from the heterotrophic metabolism of the symbiosis, while the remaining half requires the uptake of inorganic carbon from the medium. The hemolymph ΣCO_2 and P_{CO_2} are apparently elevated above the medium by some mechanism, other than a pH-based one, which concentrates carbon dioxide in the hemolymph. This elevated hemolymph inorganic carbon can then diffuse into the bacteriocytes and to the bacteria, although the available evidence indicates that, at maximal rates of autotrophy, this supply may approach values limiting the rate of carbon fixation. The supply of fixed carbon from the symbionts to the host is presumably predominantly *via* small organic molecules transported in the hemolymph.

Using the available data, one can evaluate this model by creating a hypothetical 100-g worm that has 5 ml of hemolymph and 15 g of trophosome (Childress *et al.*, 1984). At 200 μM external ΣH_2S, one would expect 5.9 mM ΣH_2S, 5 mM O_2, and 2 mM ΣCO_2 in the hemolymph. At an uptake rate of 5 μmole ΣH_2S $g^{-1}h^{-1}$, the O_2 uptake rate would be 8 μmole $g^{-1}h^{-1}$ and the net ΣCO_2 uptake would be 2 μmole g^{-1} h^{-1}. If one assumes that the hemolymph makes one circuit per minute, one can calculate that 27% of the ΣH_2S, 53% of the O_2, and 33% of the ΣCO_2 must be exchanged on each circuit. These numbers are not unreasonable, while at the same time the similarity of the percentages provides some confidence that the values used for the hemolymph concentrations are approximately correct.

Acknowledgments

This work was supported by NSF grants OCE-8609202 and OCE-9012076 to J.J.C. and OCE-8610514 to J.J.C. and C.R.F. and funding from IFREMER to A.-M. Alayse. Some travel support was provided by NATO grant D.880423 to H. Felbeck. We would like to thank R. Van Buskirk, V. Vanderveer, and D. Gage for technical assistance during the cruises. Thanks are also due to the captains and crews of the *RV Melville, RV Thomas Thompson,* and *N/O Nadir,* as well as the sub crews and pilots

of the submersibles *Alvin* and *Nautile*, without whom this work would not have been possible. This manuscript has benefited from discussions with and comments by A. Anderson, H. Felbeck, R. Trench, and J. Feigenbaum.

Literature Cited

Anderson, A. E., J. J. Childress, and J. Favuzzi. 1987. Net uptake of CO_2 driven by sulfide and thiosulfate oxidation in the bacterial symbiont-containing clam *Solemya reidi*. *J. Exp. Biol* **133:** 1–31.

Arp, A. J., and J. J. Childress. 1981. Blood function in the hydrothermal vent vestimentiferan tube worm. *Science* **213:** 342–344.

Arp, A. J., and J. J. Childress. 1983. Sulfide binding by the blood of the hydrothermal vent tube worm *Riftia pachyptila*. *Science* **219:** 295–297.

Arp, A. J., J. J. Childress, and C. R. Fisher Jr. 1985. Blood gas transport in *Riftia pachyptila*. *Bull. Biol. Soc. Wash* **6:** 289–300.

Arp, A. J., J. J. Childress, and R. D. Vetter. 1987. The sulfide binding protein in the blood of *Riftia pachyptila* is the extracellular hemoglobin. *J. Exp. Biol.* **128:** 139–158.

Belkin, S., D. C. Nelson, and H. W. Jannasch. 1986. Symbiotic assimilation of CO_2 in two hydrothermal vent animals, the mussel *Bathymodiolus thermophilus* and the tube worm *Riftia pachyptila*. *Biol. Bull.* **170:** 110–121.

Cavanaugh, C. M. 1985. Symbiosis of chemoautotrophic bacteria and marine invertebrates from hydrothermal vents and reducing sediments. *Bull. Biol. Soc. Wash.* **6:** 373–388.

Cavanaugh, C. M., S. L. Gardiner, M. L. Jones, H. W. Jannasch, and J. B. Waterbury. 1981. Prokaryotic cells in the hydrothermal vent tube worm *Riftia pachyptila*: possible chemoautotrophic symbionts. *Science* **213:** 340–342.

Childress, J. J. 1988. Biology and chemistry of a deep-sea hydrothermal vent on the Galapagos Rift; the Rose Garden in 1985, an introduction. *Deep-Sea Res.* **35:** 1677–1680.

Childress, J. J., A. J. Arp, and C. R. Fisher Jr. 1984. Metabolic and blood characteristics of the hydrothermal vent tube worm *Riftia pachyptila*. *Mar. Biol.* **83:** 109–124.

Childress, J. J., C. R. Fisher, J. A. Favuzzi, and N. K. Sanders. 1991. Factors affecting the uptake of sulfide and carbon dioxide by the hydrothermal vent clam, *Calyptogena magnifica*. *Physiol. Zool.* In press.

Degens, E. T., R. R. L. Guillard, W. M. Sackett, and A. Hellebust. 1968. Metabolic fractionation of carbon isotopes in marine plankton—1. Temperature and respiration experiments. *Deep-Sea Res.* **15:** 1–9.

Fahey, R. C., R. D. Dorian, G. L. Newton, and J. Utley. 1983. Determination of intracellular thiol levels using monobromobimane fluorescent labeling: applications involving radioprotective drugs. Pp. 103–120 in *Radioprotectors and Carcinogens*, O. F. Nygaard, and M. G. Simic, ed. Academic Press, New York.

Felbeck, H. 1981. Chemoautotrophic potential of the hydrothermal vent tube worm, *Riftia pachyptila* Jones (Vestimentifera). *Science* **213:** 336–338.

Felbeck, H. 1985. CO_2 fixation in the hydrothermal vent tube worm *Riftia pachyptila* (Jones). *Physiol. Zool.* **53:** 272–281.

Felbeck, H., and J. J. Childress. 1988. *Riftia pachyptila*: a highly integrated symbiosis. *Oceanol. Acta Special Vol.* **8:** 131–138.

Felbeck, H., G. N. Somero, and J. J. Childress. 1981. Calvin-Benson cycle sulphide oxidation enzymes in animals from sulphide rich habitats. *Nature* **293:** 291–293.

Fisher, C. R., Jr., and J. J. Childress. 1984. Substrate oxidation by trophosome tissue from *Riftia pachyptila* Jones (Phylum Pogonophora). *Mar. Biol. Lett.* **5:** 171–184.

Fisher, C. R., and J. J. Childress. 1986. Translocation of fixed carbon from symbiotic bacteria to host tissues in the gutless bivalve, *Solemya reidi*. *Mar. Biol.* **93:** 59–68.

Fisher, C. R., J. J. Childress, and N. K. Sanders. 1988a. The role of vestimentiferan hemoglobin in providing an environment suitable for chemoautotrophic sulfide-oxidizing endosymbionts. *Symbiosis* **5:** 229–246.

Fisher, C. R., J. J. Childress, A. J. Arp, J. M. Brooks, D. Distel, J. A. Favuzzi, S. A. Macko, A. Newton, M. A. Powell, G. N. Somero, and T. Soto. 1988b. Physiology, morphology, and composition of *Riftia pachyptila* at Rose Garden in 1985. *Deep-Sea Res.* **35:** 1745–1758.

Fisher, C. R., J. J. Childress, A. J. Arp, J. M. Brooks, D. Distel, J. A. Favuzzi, H. Felbeck, R. Hessler, K. S. Johnson, M. C. Kennicutt II, S. A. Macko, A. Newton, M. A. Powell, G. N. Somero, and T. Soto. 1988c. Microhabitat variation in the hydrothermal vent mussel *Bathymodiolus thermophilus*, at Rose Garden vent on the Galapagos rift. *Deep-Sea Res.* **35:** 1769–1792.

Fisher, C. R., J. J. Childress, and J. M. Brooks. 1988d. Are hydrothermal-vent vestimentifera carbon-limited? *Am. Zool.* **28:** 128A.

Fisher, C. R., J. J. Childress, and E. Minnich. 1989. Autotrophic carbon fixation by the chemoautotrophic symbionts of *Riftia pachyptila*. *Biol. Bull.* **177:** 372–385.

Fisher, C. R., M. C. Kennicutt II, and J. M. Brooks. 1990. Stable carbon isotopic evidence for carbon limitation in hydrothermal vent vestimentiferans. *Science* **247:** 1094–1096.

Fustec, A., D. Desbruyéres, and L. Laubier. 1988. Biomass estimation of animal communities associated with deep-sea hydrothermal vents near 13°N/EPR. *Oceanol. Acta Spec. Vol.* **8:** 15–22.

Groenendaal, M. 1981. The adaptation of *Arenicola marina* to sulphide solutions. *Neth. J. Sea Res.* **15:** 65–77.

Heisler, N. 1984. Acid-base regulation in fishes. Pp. 315–392 in *Fish Physiology*, W. S. Hoar, and D. J. Randall, ed. Academic Press, Orlando.

Hessler, R. R., W. M. Smithey, M. A. Boudrias, C. H. Keller, R. A. Lutz, and J. J. Childress. 1988. Temporal change in megafauna at the Rose Garden hydrothermal vent. *Deep-Sea Res.* **35:** 1681–1710.

Jaques, A. G. 1936. The kinetics of penetration: XII. Hydrogen sulfide. *J. Gen. Physiol* **19:** 397–418.

Johnson, K. S., J. J. Childress, and C. L. Beehler. 1988a. Short term temperature variability in the Rose Garden hydrothermal vent field. *Deep-Sea Res.* **35:** 1711–1722.

Johnson, K. S., C. M. Sakamoto-Arnold, J. J. Childress, and C. L. Beehler. 1988b. The biogeochemistry of hydrothermal vent communities in the Galapagos Rift. *Eos* **69:** 1271.

Jones, M. L. 1981. *Riftia pachyptila*, new genus, new species, the vestimentiferan tubeworm from the Galapagos Rift geothermal vents. *Proc. Biol. Soc. Wash.* **93:** 1295–1313.

Jones, M. L. 1988. The Vestimentifera, their biology, systematic and evolutionary patterns. *Oceanol. Acta Spec. Vol.* **8:** 69–82.

Jones, M. L., and S. L. Gardiner. 1988. Evidence for a transient digestive tract in Vestimentifera. *Proc. Biol. Soc. Wash.* **101:** 423–433.

Kelly, D. P. 1982. Biochemistry of the chemolithotrophic oxidation of inorganic sulphur. *Phil. Trans. Roy. Soc. Lond. Ser. B* **298:** 499–528.

Mason, J., D. P. Kelly, and A. P. Wood. 1987. Chemolithotrophic and autotrophic growth of *Thermothrix thiopara* and some thiobacilli on thiosulphate and polythionates, and a reassessment of the growth yields of *T. thiopara* in chemostat culture. *J. Gen. Microbiol.* **133:** 1249–1256.

Millero, F. J. 1986. The thermodynamics and kinetics of the hydrogen sulfide system in natural waters. *Mar. Chem.* **18:** 121–147.

Millero, F. J., T. Plese, and M. Fernandez. 1988. The dissociation of hydrogen sulfide in seawater. *Limnol. Oceanogr.* **33:** 269–274.

Nelson, D. C., B. B. Jorgensen, and N. P. Revsbach. 1986. Growth pattern and yield of a chemoautotrophic *Beggiatoa* sp. in oxygen-sulfide microgradients. *Appl. Environ. Microbiol.* **52:** 225–233.

Newton, G. L., R. Dorian, and R. C. Fahey. 1981. Analysis of biological thiols by derivatization with monobromobimane and separation by reverse-phase high performance liquid chromatography. *Anal. Biochem.* **114:** 383–387.

O'Brien, J., and R. D. Vetter. 1990. Production of thiosulfate during sulphide oxidation by mitochondria of the symbiont-containing bivalve *Solemya reidi*. *J. Exp. Biol.* **149:** 133–148.

Powell, M. A., and G. N. Somero. 1983. Blood components prevent sulfide poisoning of respiration of the hydrothermal vent tubeworm *Riftia pachyptila*. *Science* **219:** 297–299.

Powell, M. A., and G. N. Somero. 1985. Sulfide oxidation occurs in the animal tissue of the gutless clam, *Solemya reidi*. *Biol. Bull.* **169:** 164–181.

Powell, M. A., and G. N. Somero. 1986. Adaptations to sulfide by hydrothermal vent animals: sites and mechanisms of detoxification and metabolism. *Biol. Bull.* **171:** 274–290.

Quetin, L. B., and J. J. Childress. 1980. Observations on the swimming activity of two bathypelagic mysid species maintained at high hydrostatic pressures. *Deep-Sea Res.* **27A:** 383–391.

Rau, G. H. 1981. Hydrothermal vent clam and tubeworm $^{13}C/^{12}C$: Further evidence of nonphotosynthetic food sources. *Science* **213:** 338–340.

Rau, G. H., and J. I. Hedges. 1979. Carbon-13 depletion in a hydrothermal vent mussel: suggestion of a chemosynthetic food source. *Science* **203:** 648–649.

Richard, J. J., R. D. Vick, and G. A. Junk. 1977. Determination of elemental sulfur by gas chromatography. *Env. Sci. and Technol.* **11:** 1084–1086.

Roux, M., M. Rio, E. Schein, R. Lutz, L. Fritz, and L. Ragone. 1989. Mesures *in situ* de la croissance des bivalves et des vestimentiferes et de la corrosion des coquilles au site hydrothermal de 13°N (dorsale du Pacifique oriental). *C. R. Acad. Sci. Paris Sér. III* **308:** 121–127.

Skirrow, G. 1975. The dissolved gases—carbon dioxide. P. 1 in *Chemical Oceanography*, J. P. Riley, and G. Skirrow, ed. Academic Press, New York.

Somero, G. N., J. J. Childress, and A. E. Anderson. 1989. Transport, metabolism and detoxification of hydrogen sulfide in animals from sulfide rich marine environments. *Crit. Rev. Aquat. Sci.* **1:** 591–614.

Southward, E. C. 1987. Contribution of symbiotic chemoautotrophs to the nutrition of benthic invertebrates. Pp. 83–118 in *Microbes in the Sea*, M. A. Sleigh, ed. Horwood Ltd., Chichester.

Southward, E. C. 1988. Development of the gut and segmentation of newly settled stages of *Ridgeia* (Vestimentifera): implications for relationship between Vestimentifera and Pogonophora. *J. Mar. Biol. Assoc. U. K.* **68:** 465–487.

Terwilliger, R. C., and N. B. Terwilliger. 1985. Respiratory proteins of hydrothermal vent animals. *Bull. Biol. Soc. Wash.* **6:** 273–288.

Terwilliger, R. C., N. B. Terwilliger, and E. Schabtach. 1980. The structure of hemoglobin from an unusual deep-sea worm (Vestimentifera). *Comp. Biochem. Physiol.* **65B:** 531–535.

Toulmond, A. 1977. Temperature-induced variations of blood acid-base status in the lugworm, *Arenicola marina* (L.): I. *In vitro* study. *Respir. Physiol.* **31:** 139–149.

Vetter, R. D. 1985. Elemental sulfur in the gills of three species of clams containing chemoautrophic symbiotic bacteria: a possible inorganic energy storage compound. *Mar. Biol.* **88:** 33–42.

Vetter, R. D., P. A. Matrai, B. Javor, and J. O'Brien. 1989. Reduced sulfur compounds in the marine environment: analysis by HPLC. Pp. 244–261 in *Biogenic Sulfur in the Environment*, E. S. Saltzman, and W. J. Cooper, ed. American Chemical Society, Washington.

Vetter, R. D., M. E. Wells, A. L. Kurtsman, and G. N. Somero. 1987. Sulfide detoxification by the hydrothermal vent crab *Bythograea thermydron* and other decapod crustaceans. *Physiol. Zool.* **60:** 121–137.

Willason, S. W., and K. S. Johnson. 1986. A rapid, highly sensitive technique for the determination of ammonia in seawater. *Mar. Biol.* **91:** 285–290.

Wilmot, D. B. J., and R. D. Vetter. 1990. The bacterial symbiont from the hydrothermal vent tubeworm *Riftia pachyptila* is a sulfide specialist. *Mar. Biol.* **106:** 273–283.

Reference: *Biol. Bull.* **180:** 154–166. (February, 1991)

Distribution and Characterization of Ion Transporting and Respiratory Filaments in the Gills of *Procambarus clarkii*

JOHN S. DICKSON, RICHARD M. DILLAMAN, ROBERT D. ROER, AND DAVID B. ROYE

Center for Marine Science Research, University of North Carolina at Wilmington, 7205 Wrightsville Ave., Wilmington, North Carolina 28403

Abstract. Individual gill filaments of the freshwater crayfish *Procambarus clarkii* were determined to be either predominantly respiratory or transporting. Silver staining revealed that the filaments within the central bed of the gills formed silver deposits whereas filaments at the margins and the entire sixth pleurobranch formed no deposits. Designation of the silver staining gills as predominantly transporting and unstained filaments as predominantly respiratory was substantiated by ultrastructural analyses and measurements of ATPase and transepithelial potentials. Presumptive transporting filaments had an epithelium subjacent to the cuticle that was relatively thick and dominated by abundant mitochondria. Lacunae were delineated by pillar structures and served as collateral pathways for the movement of blood from the afferent to efferent blood channels, which were separated by a thin septum. Presumptive respiratory filaments had an extremely thin epithelium with few organelles, but a relatively thick septum. Present in both types of filaments were nerves and podocytes. The values for Na, K-ATPase were significantly higher in the transporting filaments than in those designated as respiratory. The measurement of transepithelial potentials showed both filaments to be cation selective with the respiratory filaments slightly more positive and the transporting filaments slightly more negative than the diffusion potential for Na.

Introduction

Gills are a site for exchange between the blood of the organism and the external medium and, as such, are involved in the separate but interrelated functions of gas exchange, acid/base balance, and ion regulation. Those substances exchanged may include oxygen, electrolytes, carbon dioxide, and ammonia. To produce a large surface area for such exchange, gills are often branched along one or more axes. In the crabs (Crustacea, Decapoda) lamellar gills are present (Copeland, 1963, 1968; Copeland and Fitzjarrell, 1968; Taylor and Greenaway, 1979; Finol and Croghan, 1983) and consist of a parallel afferent and efferent blood vessel between which are broad flattened sheets. In branchipod crustaceans, such *Artemia salina* and *Daphnia magna* (Copeland, 1967 and Kikuchi, 1983), amphipods and isopods (Milne and Ellis, 1973; Bubel and Jones, 1974) gills are flat, oval, sac-like extensions of thoracic appendages or modified pleopods. In crayfish and shrimp the gills are filamentous (Morse *et al.*, 1970; Bielawski, 1971; Fisher, 1972; Burggren *et al.*, 1974; Foster and Howse, 1978). In crayfish the gills are trichobranchiate and have a central stalk from which hundreds of tiny finger-like filaments arise. The podobranchia (outermost gills) are attached to the coxae of the appendages. A membranous lamina, devoid of filaments, extends from the inner side of the podobranch and lies against the thoracic body wall; its distal tip is flattened into a plate bearing a few filaments. The arthrobranchia, which are attached to the articular membrane between the body wall and the appendages, and the pleurobranchia, which are attached to the pleural wall of each somite, lie beneath the podobranchia and have no distal plate structure (Huxley, 1986; Burggren *et al.*, 1974).

Despite variations in gill anatomy, the ultrastructure of the gill epithelium in those species that are capable of osmoregulation is similar, and can be placed into one of

Received 28 June 1990; accepted 9 November 1990.

two categories. Both categories consist of a single layered epithelium that separates blood spaces from the uncalcified cuticle. One type of epithelium is relatively thick and has the characteristics of an ion transporting epithelium (see Cioffi, 1984, for a review of arthropod ion transporting epithelia). Briefly, it consists of cells with highly folded apical and basal processes, a prominent basal lamina and cytoplasm containing abundant mitochondria as well as golgi apparati, smooth and rough endoplasmic reticulum and glycogen. The second type of epithelium consists of very thin squamous cells subjacent to the cuticle. The cells are only one tenth the thickness of the previously described type, and the cytoplasm contains very few organelles (Copeland and Fitzjarrell, 1968). This ultrastructure would appear to favor diffusion of gases between the external and internal media and consequently this epithelium has been categorized as being respiratory in function.

Studies on a variety of species of decapod crustaceans have demonstrated the existence of a partitioning of ion regulatory and respiratory functions among different gills or within different regions of gills. Both morphological and biochemical (Na, K-ATPase distribution) studies have provided evidence that the anterior gills are dedicated to gas exchange while the posterior gills are involved in ion regulation in the euryhaline brachyurans *Eriocheir sinensis* (Péqueux and Gilles, 1978, 1981), *Uca pugnax* (Holliday, 1985), *Uca minax* (Wanson *et al.*, 1984), *Callinectes sapidus* (Copeland and Fitzjarrell, 1968; Neufeld *et al.*, 1980; Towle, 1984), and *Carcinus maenas* (Mantel and Landesman, 1977). Although we and other investigators realize that gill tissues possessing transport epithelia are also engaged in gas exchange, and that ions move across respiratory surfaces, we still use, for simplicity, the predominant function to designate that of the entire filament. Henceforth, we will refer to those gill filaments that possess a typical transporting epithelium as "transport" types and those gill filaments with a squamous epithelium as "respiratory" types.

Crayfish, like the euryhaline brachyurans in dilute media, exist in a hypoosmotic medium, and must maintain their ion balance by actively transporting electrolytes across the gills (Maluf, 1940; Bryan, 1959; Shaw, 1960a, b; Ehrenfeld, 1974). Unlike the euryhaline brachyurans studied, however, most crayfish are stenohaline freshwater crustaceans and possess filamentous, rather than lamellate, gills. The partitioning of respiratory and ion transporting function in the gills of crayfish is still in question. While Wheatly and Henry (1987) have used biochemical analyses of pooled gill sets to show that the distribution of Na, K-ATPase was similar among gills of *Pacifastacus leniusculus*, Morse *et al.* (1970) used silver staining and reported a partitioning of respiratory and transport functions among the gill filaments of the same species. Dunel-Erb *et al.* (1982), on the other hand, observed only respiratory epithelial tissues in the filaments and ion transporting epithelial tissues in the podobranch lamina of *Astacus pallipes* and therefore assigned the appropriate function to the two structures. The only ultrastructural observations of filaments have been of transporting epithelia (Morse *et al.*, 1970; Burggren *et al.*, 1974; Bielawski, 1971; Fisher, 1972).

This investigation was therefore directed at determining—within a single filament, within a single gill, and among gills—the distribution and frequency of the two types of epithelia of the freshwater crayfish *Procambarus clarkii*. The methods employed in this study were silver staining (Maluf, 1940), an indicator of ion transporting tissue; transmission electron microscopy (TEM), which reveals the striking difference between the morphology of the two types of epithelia; analysis for Na, K-ATPase, an effector of ion movement; and measurement of transepithelial potentials in individual filaments, which reflects possible differences in transport or permeability of the combined epithelial and cuticular layers.

Materials and Methods

The crayfish (*Procambarus clarkii*), obtained from Carolina Biological Supply, were kept in aquaria of artificial pond water (Roer and Shelton, 1982), maintained between 20°C and 25°C, and fed 2–3 times a week. Only active crayfish in the intermolt stage, as determined by the criteria of Drach and Tchernigovtzeff (1967) and Stevenson (1972), were used in this study.

Silver staining

Crayfish subjected to silver staining were first rinsed in deionized water and placed in a 0.05% $AgNO_3$ solution at 25°C for 30 min. The volume of the solution was sufficient to completely submerge the crayfish. Crayfish were then rinsed with deionized water. The branchiostegites were removed to expose the gills, and the crayfish were placed in Kodak Microdol-X developer (diluted 3:1 to lower the osmolarity to 630 mOsm) for one hour with frequent agitation. After the gills were thoroughly washed and placed in distilled water, one or two drops of NH_4S were added to intensify the stain.

Preparation of gill filament tissues for electron microscopy

Silver treated filaments were fixed in 3% glutaraldehyde in 0.1 *M* cacodylate buffer (pH 7.2) containing 5% sucrose (osmolarity = 640 mOsm) at 25°C for at least 1 h. To facilitate penetration of the various solutions, the tips were cut off the filaments and the tissue was gently agitated at each step of the preparation. The filaments were then

rinsed in buffer and postfixed with 2% osmium tetroxide in 0.1 *M* cacodylate buffer (pH 7.2) plus 5% sucrose at 25°C for 2 h. After another rinse with buffer, tissues were dehydrated with a graded series of ethanol and propylene oxide, and embedded in Spurr low viscosity embedding medium (Spurr, 1969).

Filaments not silver-treated were fixed in 2% glutaraldehyde in 0.15 *M* cacodylate buffer, pH 7.4, with 5 m*M* $CaCl_2$ for 1 h, rinsed in buffer, and post-fixed in fresh 0.5% OsO_4 with 0.8% $K_4Fe(CN)_6$ in 0.1 *M* cacodylate buffer, pH 7.4, with 5 m*M* $CaCl_2$ at 25°C for 1 h. After rinsing again in cacodylate buffer, the tissues were placed in 0.15% tannic acid in 0.15 *M* cacodylate buffer, pH 7.4, with 5 m*M* $CaCl_2$ for 5 min. Following a short rinse in buffer and distilled water, the tissues were stained *en bloc* with 2% aqueous uranyl acetate for 2 h. After a distilled water rinse, tissues were dehydrated through a graded series of acetone and embedded in Spurr.

Cross-sections were cut in the basal, medial, and distal regions of the filaments. Sections were post-stained with 4% uranyl acetate in 50% ethanol and Reynolds lead citrate (Reynolds, 1963), and were viewed with a Zeiss EM 9S transmission electron microscope operated at 60 kV.

Na, K-ATPase assay of filaments

Na, K-ATPase assays were done according to the method of Horiuchi (1977). After washing excised gills in 0.25 *M* sucrose buffered to pH 7.5 with 100 m*M* Tris-HCl, predicted transporting or respiratory filaments were removed from the gills, pooled by type, and homogenized at 4°C in 2 volumes of the buffered sucrose solution during 35 passes in a glass tissue homogenizer. The homogenate was centrifuged at 3000 × *g* for 15 min and the supernatant was assayed for activity.

The reaction mixture consisted of 60 m*M* NaCl, 20 m*M* KCl, 2 m*M* $MgCl_2$ and 30 m*M* Tris-HCl, pH 7.5, in 0.8 ml. This reaction mixture was preincubated at 32°C before 0.1 ml of the enzyme solution and 0.1 ml of the 3.0 m*M* Tris-ATP were added. The enzymatic reaction was allowed to proceed for 45 min, being terminated by the addition of cold 3% trichloroacetic acid. The amount of inorganic phosphate, hydrolyzed from ATP, present in the supernatant was measured according to Wheeler (1975). Mg-ATPase activity was determined as above with the substitution of 10 m*M* ouabain for KCl in the reaction mixture to inhibit Na, K-ATPase. Na, K-ATPase activity was calculated as the difference between the total ATPase and Mg-ATPase values. The amount of protein was determined according to Peterson's (1977) modified Lowry protein assay using a Bausch and Lomb Spectronic 710 spectrophotometer and bovine serum albumin as a standard. The specific activities were recorded as micromoles of inorganic phosphate per milligram of protein per hour.

Transepithelial potential measurements

Crayfish were submerged in ¼ strength Van Harreveld's Ringer solution (final concentrations: NaCl = 51.3 m*M*; KCl = 1.3 m*M*; $CaCl_2$ = 3.4 m*M*; $MgCl_2$ = 0.3 m*M*) in a finger bowl, and restrained by rubber bands attached to a notched plexiglass plate. Diluted Ringer's solution was used to provide sufficient electrolytes for electrode conduction. Potentials measured with pond water as the external medium were unreliable. The branchial region of the carapace was cut away from one side of the animal to expose the gills. In this position, individual gill filaments could easily be impaled by glass microelectrodes using a micromanipulator.

Microelectrodes were drawn from glass capillary tubing and filled with 3 *M* KCl. A Ag-AgCl reference electrode was immersed in the bathing medium. Both electrodes were connected by shielded cables to a WPI model 701 microprobe system and a Tectronix 5111 storage oscilloscope.

Only filaments of the podobranchs were impaled and the assignment of putative transport and respiratory filaments was based upon the results of the silver staining experiments. Transepithelial potentials (TEP's) and the position of the electrode tip within the filament were recorded each time a gill was impaled. Sodium concentrations of the medium and crayfish hemolymph were measured by flame photometry (Turner model 510).

Results

Silver staining

In six crayfish subjected to silver staining all showed some staining in all gills except pleurobranch 6. Staining occurred only in the filaments. That is, no staining was observed in the central gill stalk, in the lamina, in the distal plate of the podobranchia, nor at the base of the gills. Figure 1 is representative of the filament staining patterns. The podobranchs had the largest proportion of stained filaments, whereas the pleurobranchs had the least for each set of gills. All gills showed the same basic pattern, a population of stained filaments in the central area of the filament bed surrounded by lateral rows of unstained filaments, with the exception of the pleurobranch of the sixth gill set, which showed no silver staining. Silver stained filaments had precipitate distributed evenly over the length of the filament.

Transmission electron microscopy of silver stained filaments showed that most of the precipitate was within the gill cuticle, although lesser amounts were observed outside or beneath the cuticle (Fig. 2). Precipitate within the cuticle was localized almost exclusively in a layer corresponding to the exocuticle, rarely being found in the epicuticle or endocuticle. While the treatment employed

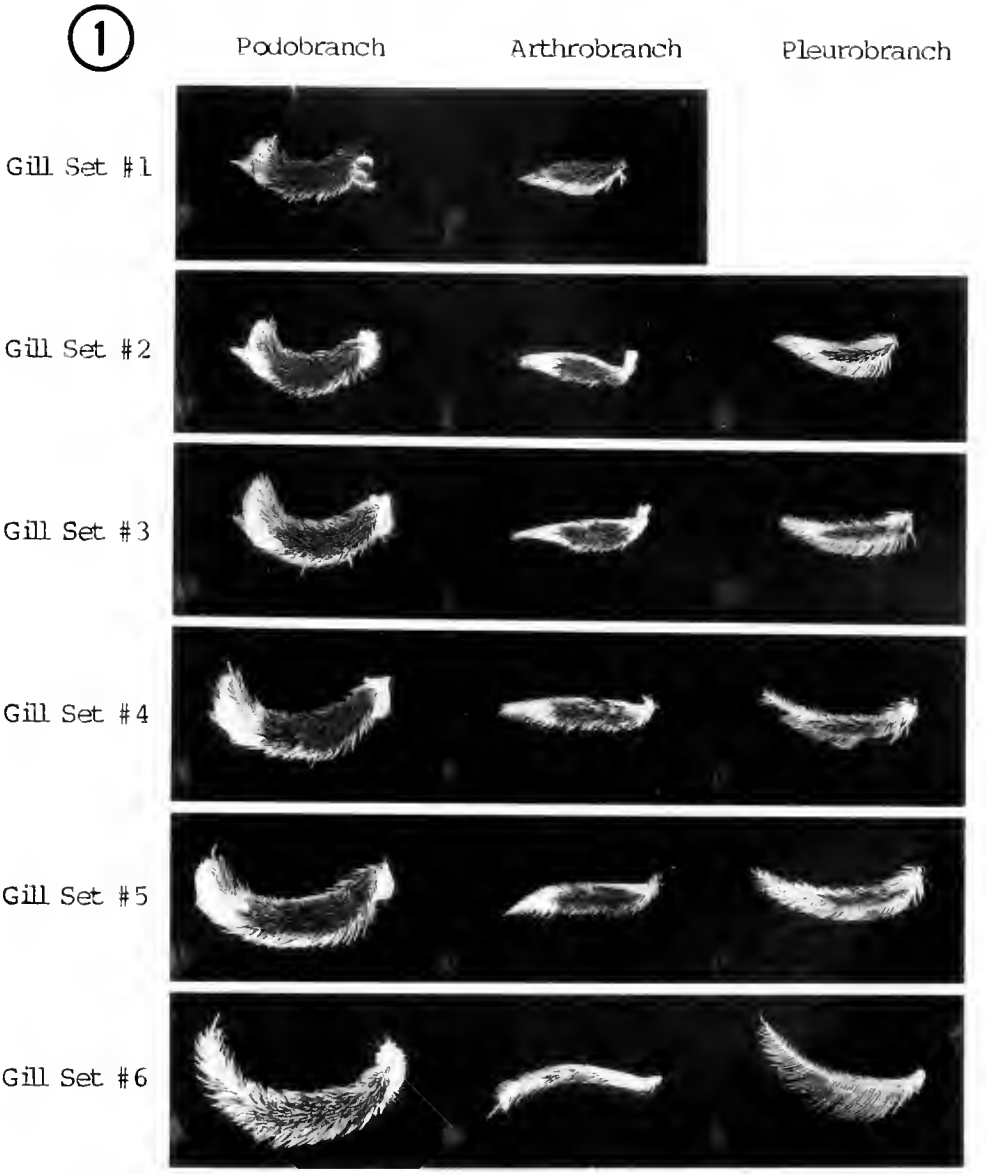

Figure 1. Light micrographs of six sets of gills from the right side of a crayfish after silver staining. Each gill is oriented with the base to the right. Dark staining indicates silver deposition.

in the silver staining disrupted the soft tissues, it was possible to note that the epithelium underlying the cuticle was relatively thick and had numerous basal and apical infoldings. Filaments containing no precipitate after silver treatment (Fig. 3) had an epithelium subjacent to the cuticle that was markedly thinner than that of the silver stained filaments and had few, if any, basal and apical infoldings.

Ultrastructure of the gill filaments

Choice of filaments for ultrastructural analysis of presumptive ion-transporting and respiratory tissue was based upon the distribution of the two types as indicated by silver staining (Fig. 1) and proved to be accurate in all 20 of the filaments examined. No differences were observed among sections from proximal, medial, or distal regions of a filament. Diagrammatic representations of cross sections through the two types of filaments are seen in Figures 4 and 5. The transporting filaments, regardless of the gill set, had a diameter of 0.1 mm to 0.2 mm, while the respiratory filaments were 0.2 mm to 0.3 mm in diameter. Both types of filaments contained an afferent and an efferent blood channel and lateral lacunae. The afferent channel was on the side of the filament that faced toward the gill stalk, and the efferent channel on the side that

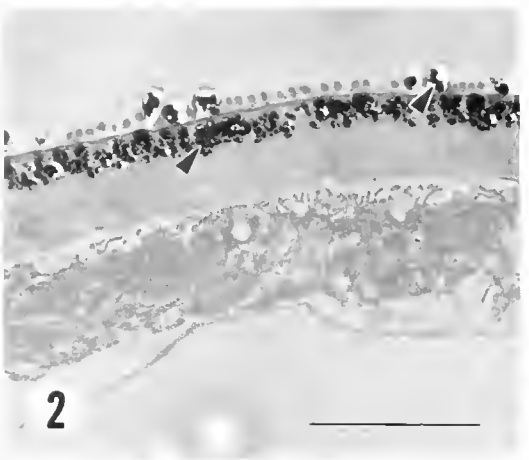

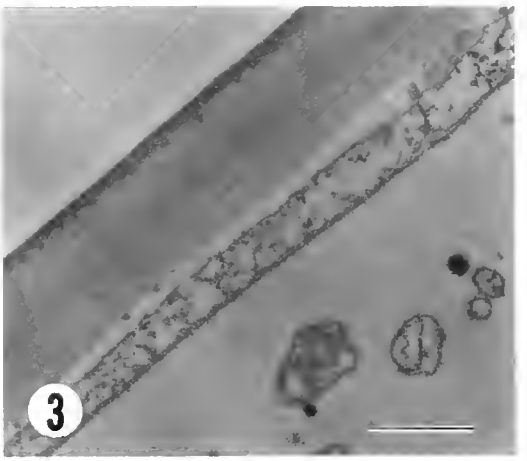

Figure 2. TEM of transporting gill filament after silver staining. Note crystals within and on the cuticle (arrows). Bar = 5 μm.

Figure 3. TEM of respiratory gill filament after silver staining. Bar = 1.0 μm.

faced away from the stalk. A septum and the surrounding connective tissue separated the two major blood spaces. An epithelium, 80–90% of which occurred in the lacunar blood space, lined the noncalcified cuticle of the filaments. Epithelial cells extended across the lacunae forming pillar structures with their basal portion embedded in loose connective tissue. Also depicted is the marked difference in epithelial thickness within and between the filament types.

In the transporting filaments, the cuticle epithelium bordering the afferent channel was the thickest (approximately 6 μm) (Fig. 4). Numerous mitochondria, generally oriented perpendicular to the cuticle, were observed and were most abundant in the apical portion of the cells (Figs. 6, 7, 8). Apical microvillar processes were approximately 80 nm wide and varied in length from 0.4 μm to 1.2 μm (Fig. 8). Electron-dense material was observed between the tips of the microvilli and the overlying cuticle (Fig. 9). Numerous infoldings and interdigitations occurred in the basal region of the epithelium (Figs. 6, 7). The microtubules observed within the cytoplasm were oriented nearly perpendicular to the cuticle and were often closely apposed to mitochondria (Fig. 8). Occasional golgi apparati were observed in the epithelium lining the outer margin of the afferent canal (Fig. 6), as well as a thin basal lamina (Figs. 6, 9). Adhering junctions occurred apically on lateral cell membranes, below which were septate junctions. Gap junctions were observed below the septate junctions (Fig. 6).

The portion of the epithelium lateral to the septum and on the efferent side of the filament was thinner (approximately 1.5 μm) than that portion bordering the afferent canal, but also contained numerous mitochondria and microvillar processes (Fig. 9).

The epithelial cells forming the pillar structures had a highly convoluted basal nucleus (Fig. 7) and were usually rich in mitochondria, rough endoplasmic reticulum, and golgi apparati (Fig. 8).

The cuticle of the transporting gill filaments was of uniform thickness (approximately 1.8 μm) around their entire circumference. An outer thin epicuticle, the thin lamellae of the exocuticle, and the thicker lamellae of the endocuticle were easily differentiated in most sections (Figs. 6, 9). The approximate thicknesses of the exocuticle and the endocuticle were 0.8 μm and 0.6 μm, respectively.

The septum traversed the central blood space, joining the loose connective tissue on either side of the filament, thereby forming a partition between the afferent and efferent blood channels (Figs. 4, 5, 10, 16). Along the efferent channel the septum was relatively smooth, whereas the side facing the afferent channel possessed processes that extended into the channel (Figs. 10, 16). In the transporting filaments the septum was relatively thin (approximately 1.1 μm) (Fig. 10) and became shorter as the filament tapered in its distal portions. Numerous membranes were observed along the length of the septum, some of which constituted the cell membranes of loose connective tissue cells on either side of the filament. A thin basal lamina was observed on the efferent side of the septum, and a thicker fibrous basement membrane covered the afferent septal process (Figs. 10, 16).

The epithelium of the respiratory filament varied in thickness, ranging from 0.7 μm opposite the septum to 3.0 μm in regions adjacent to pillar structures (Figs. 5, 11). A few scattered round or oval mitochondria were observed in the granular cytoplasm whereas thicker regions of the epithelium adjacent to the pillar cells also had some glycogen granules (Figs. 12, 13). The regions of

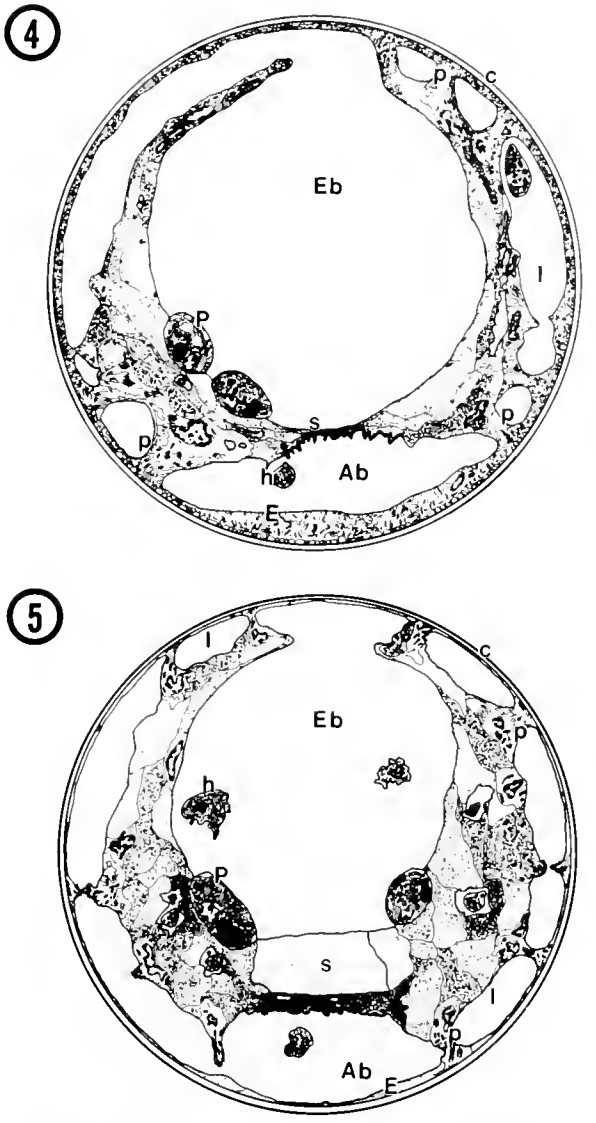

Figures 4 and 5. Diagrammatic representations of cross sections through a transporting (Fig. 4) and respiratory (Fig. 5) gill filament. Note the afferent blood channel (Ab), efferent blood channel (Eb), epithelium (E), cuticle (c), septum (s), podocyte (P), hemocyte (h), pillar structure (p), and lacuna (l).

the epithelium lateral to the septum and on the efferent side of the filament were much thinner, having a width as small as 0.08 μm (Figs. 11, 14). The epithelium was lined by a thin basal lamina and had a sparse cytoplasm containing microtubules. Fibrous material was also seen between the basal lamina and the epithelium. No apical microvillar processes or basal infoldings were observed in the respiratory filament epithelia.

The most prominent feature of the cells in the pillar regions was the bundles of microtubules observed in their cytoplasm (Figs. 12, 13). These bundles were generally oriented perpendicular to the cuticle, apparently attached to extensions of the cuticle that penetrated into the epithelial cells (Fig. 13). The pillar cytoplasm contained some mitochondria, rough endoplasmic reticulum, and golgi, but noticeably fewer than in the transporting filament tissues (Fig. 12).

The cuticle of the respiratory filaments was thickest on the side of the afferent channel (approximately 2.0 μm) (Fig. 14) and thinnest on the efferent side of the filament (approximately 0.5 μm) (Fig. 15). The attenuation of the cuticle from the afferent to the efferent side was observed lateral to the septum of the filament. It appeared as if no endocuticle had been deposited on the afferent side of the filament, the side facing the carapace.

The septum of the respiratory filament was thicker than the transporting filament septum, possessing afferent septal projections, a thick afferent basement membrane, and a thin efferent basal lamina. The septum had a width of about 5 μm, with an abundance of cell membrane interdigitations (Figs. 5, 16). A thick layer of fibrous material frequently lined the inside of the cell membrane on the afferent side of the septum (Fig. 16). Thicker septa observed in these filaments usually had loose connective tissue extending across the septum on the afferent side (Fig. 5).

Neural tissue was often observed in both filament types (Fig. 17). The small nerves were located within one of the small blood spaces of the connective tissue lateral to the septum. Usually there was one nerve per filament, though a few filaments were observed that contained two or three nerves, each in a separate blood space. The nerve was continuous throughout the length of a filament. Nerves ranged from 1.0 μm to 2.7 μm in diameter and contained two to six neurons. The neurons, which ranged from 0.16 μm to 1.5 μm in diameter, contained numerous, evenly spaced neurotubules. No cell bodies, neurosecretory granules, or synapses were observed in any section.

Also occurring in both types of filaments were cells resembling "podocytes" (Morse *et al.*, 1970). They were observed near the septum, attached to the loose connective tissue bordering the afferent channel (Figs. 4, 5, 18) and were surrounded by a basal lamina. These cells possessed an interdigitating cell membrane, or pedicels, which formed extracellular spaces between the pedicels and the cell body. Much of the cytoplasm contained an abundance of smooth endoplasmic reticulum. Coated pits and vesicles were often observed along or near the cell membrane and numerous dense granules, varying in size and number, occurred within the cytoplasm along with golgi apparati consisting of thin, curved cisternae (Fig. 19).

ATPase determinations

As shown in Figure 20, the mean for total ATPase activity was higher in the transporting than in the respiratory

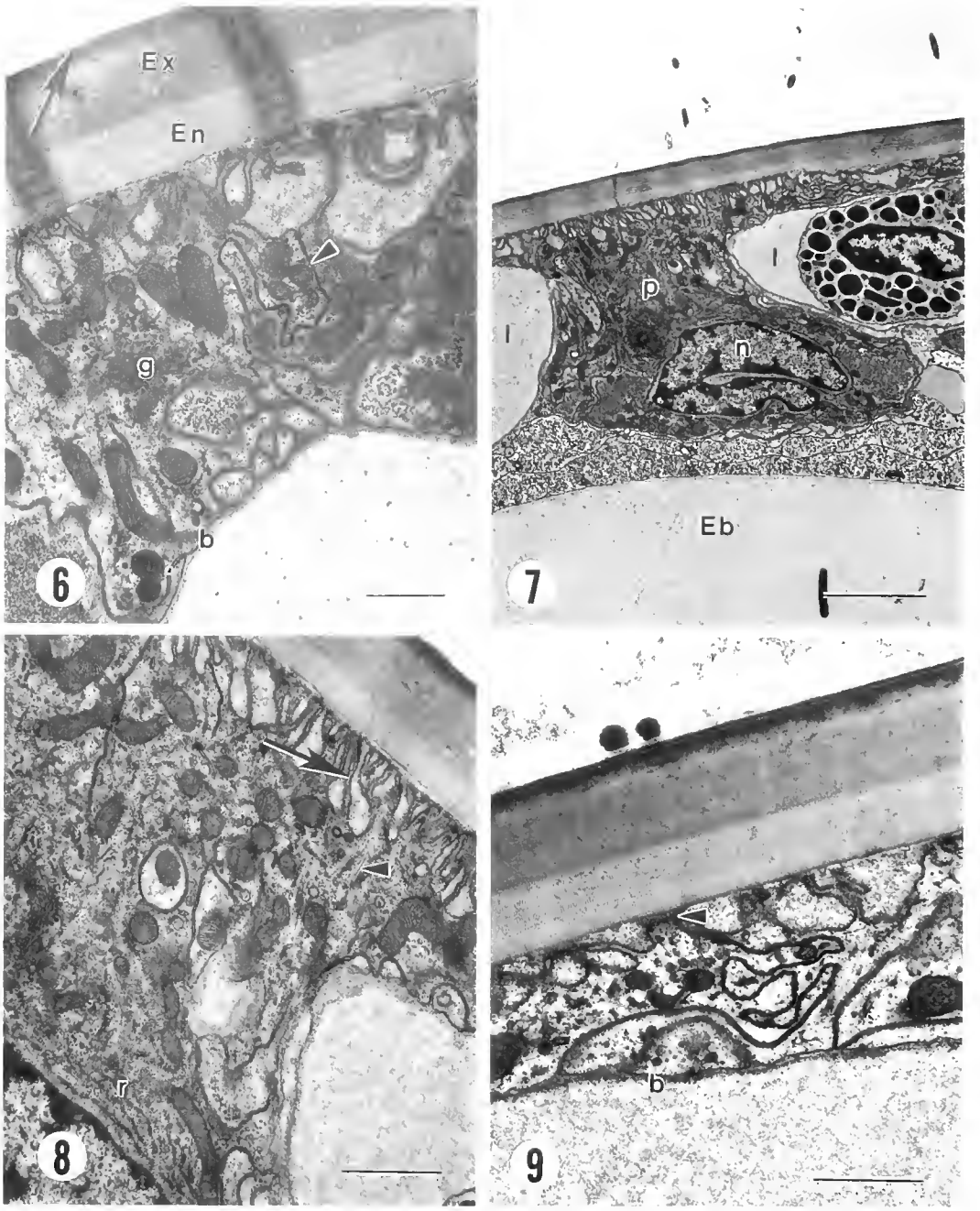

Figures 6–9. TEM of transporting filaments. **Figure 6.** Section showing the cuticle with its three layers, the epicuticle (arrow), the exocuticle (Ex) and the endocuticle (En). Also note a Golgi apparatus (g), the basal lamina (b), and a junctional complex (arrowhead). Bar = 1.0 μm. **Figure 7.** Section showing a pillar structure (p) separating two lacunar spaces (l) from an efferent blood channel (Eb). Note heterochromatic nucleus (n). Bar = 5.0 μm. **Figure 8.** Section of epithelium under cuticle showing microtubules (arrowheads) and rough endoplasmic reticulum (r) in the cytoplasm. Also note the apical microvillar structures (arrow) immediately below the cuticle. Bar = 1.0 μm. **Figure 9.** Section of epithelium between cuticle and lacuna showing the electron dense material at the tip of the microvillar processes (arrowhead) and the thin basal lamina (b). Bar = 1.0 μm.

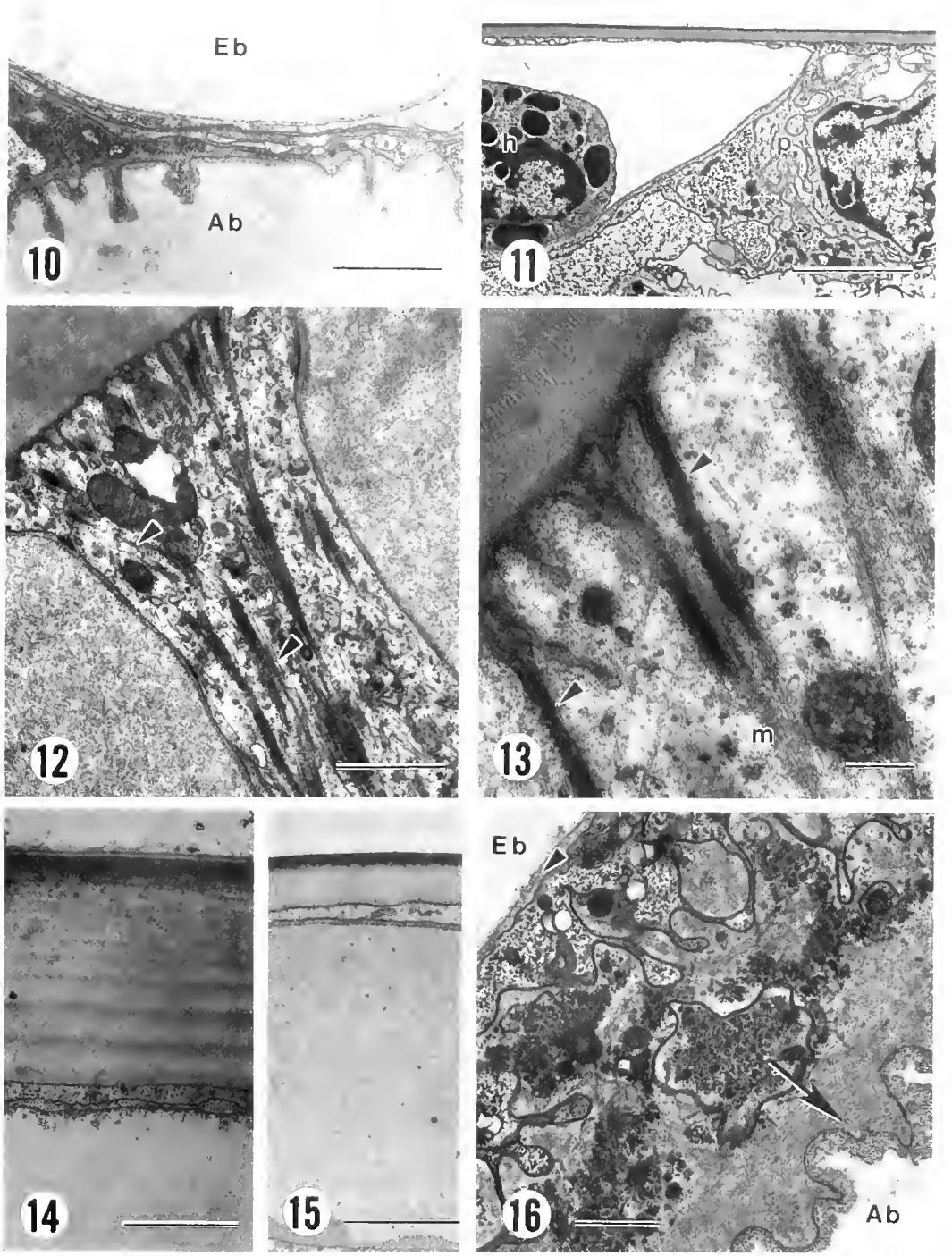

Figures 10–16. TEM of transporting (10) and respiratory (11–16) filaments. **Figure 10.** Section of a septum in a transporting filament that separates the afferent (Ab) from the efferent (Eb) blood channel. Bar = 2.0 μm. **Figure 11.** Section of a respiratory filament showing the thin epithelium underlying the cuticle. Also note the pillar structure (p) and a hemocyte (h). Bar = 5.0 μm. **Figure 12.** Pillar structure of a respiratory filament showing the bundles of microtubules running perpendicular to the cuticle (arrowheads). Bar = 1.0 μm. **Figure 13.** Section showing relationship of microtubules (m) to extensions of the cuticle (arrowheads). Bar = 0.2 μm. **Figure 14.** Cuticle on side of afferent channel. Bar = 1.0 μm. **Figure 15.** Cuticle on side of efferent channel. Bar = 1.0 μm. **Figure 16.** Septum from respiratory filament separating the afferent blood channel (Ab) from the efferent blood channel (Eb). Note the thin basal lamina on the efferent side (arrowhead) as compared with the thick layer on the afferent side (arrow). Bar = 1.0 μm.

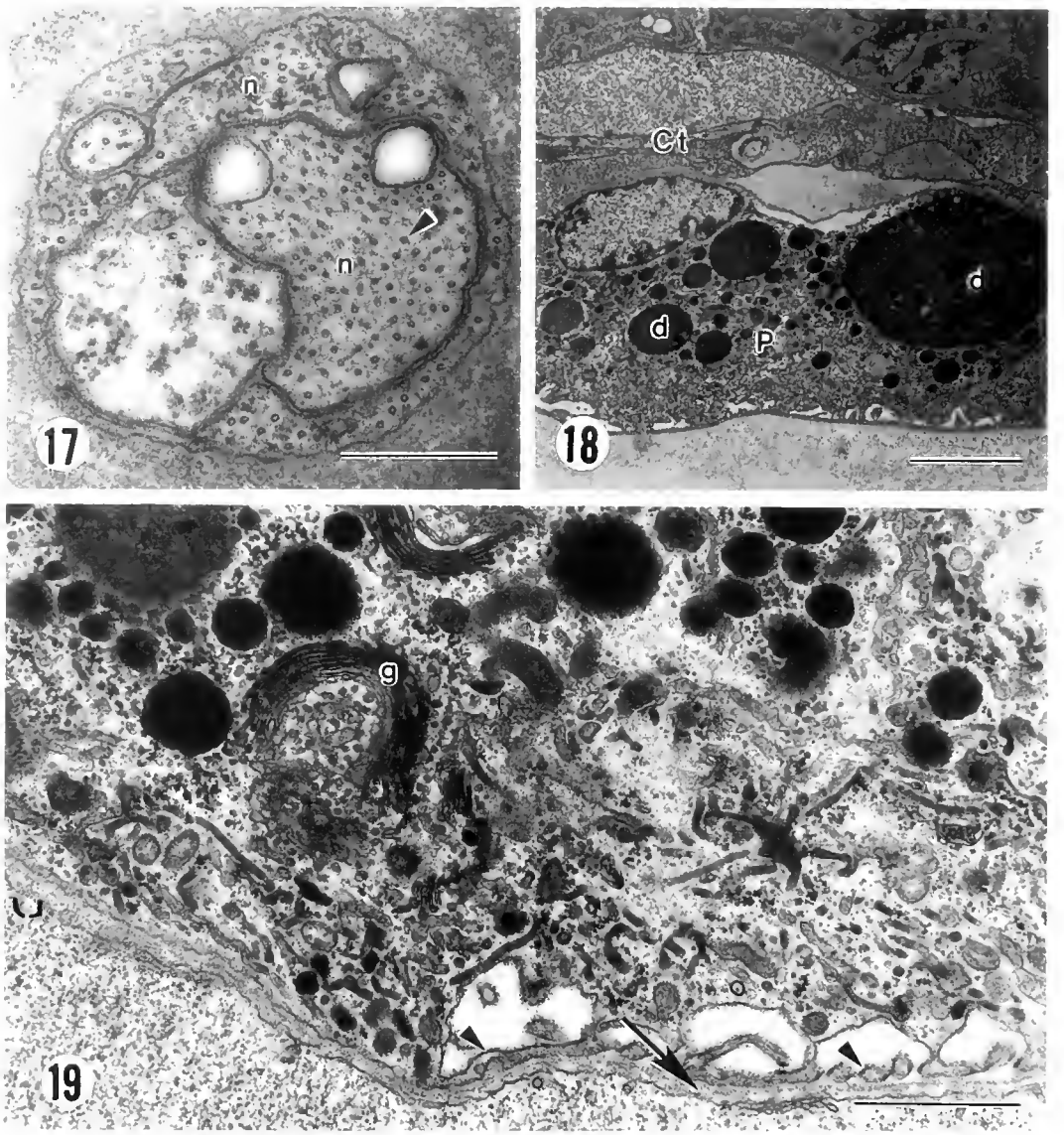

Figures 17–19. TEM of filaments. **Figure 17.** Cross section of nerve showing individual neurons (n) having evenly spaced neurotubules (arrowheads). Bar = 0.5 μm. **Figure 18.** Podocyte (P) in loose connective tissue (Ct). Note electron-dense inclusions (d). Bar = 5.0 μm. **Figure 19.** Podocyte cytoplasm showing pedicels (arrowheads) golgi (g) and basal lamina (arrow). Bar = 1.0 μm.

filaments; however, the difference between the means was not significant. Mean values for Mg-ATPase were very similar between respiratory and transporting filaments and were likewise not significantly different. The means for Na, K-ATPase, in contrast, were significantly different ($P < 0.001$, Mann-Whitney U test), with the transporting filaments having more than five times as much mean activity as the respiratory filaments.

Transepithelial potentials

The values of the TEP's in the filaments were independent of the region (proximal, medial, or distal) of the filament impaled and of the podobranch upon which the filament was located. The TEP's of filaments that were presumed to be respiratory (based upon the silver staining results) ranged from −6 to −18 mV (−11.9 ± 3.2 mV, mean ± S.D., n = 19). The TEP's measured in presumptive transport filaments ranged from −21 to −36 mV (−28.1 ± 4.7 mV, mean ± S.D.; n = 21). There was no overlap in the frequency distributions of the ranges of TEP's (Fig. 21) and the difference between the means was highly significant ($P < 0.001$, two-tailed t test). The sodium concentration of the medium was 51 m*M* and that of the hemolymph was 107.5 ± 15.0 m*M* (mean ± S.D., n = 11).

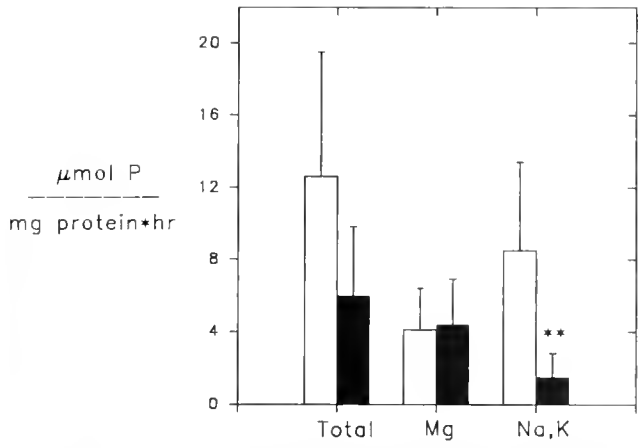

Figure 20. Mean (± standard deviation) ATPase activity comparing pooled transporting (open bars) and respiratory (solid bars) filaments. ** = $P < 0.001$

Discussion

The results of silver staining, ultrastructural analyses, ATPase measurements, and measurements of TEP all indicate that the gills of *P. clarkii* are not homogeneous in structure, but contain filaments dedicated to ion transport and filaments dedicated to respiration. No filaments had both characteristics; rather individual filaments were uniquely respiratory or transporting. Respiratory filaments occurred on the lateral rows of most gills, whereas the transporting filaments predominated in the central bed of the gills. This distribution of the two filament types in discrete regions of the gill placed the respiratory filaments in the path of the most rapid water flow (Burggren *et al.*, 1974).

The respiratory filaments had a very thin, squamous epithelium, whereas the ion transporting filaments possessed a markedly thicker epithelium. The ultrastructure of the ion transporting epithelia observed in *P. clarkii* gill filaments was similar to ion transporting epithelia described in other crayfish (Morse *et al.*, 1970; Bielawski, 1971; Fisher, 1972), in isopods (Bubel and Jones, 1974), in crabs (Copeland and Fitzjarrell, 1968; Taylor and Greenaway, 1979; Finol and Croghan, 1983), in shrimp (Foster and Howse, 1978), and in *Daphnia* (Kikuchi, 1983). Apical microvillar processes were present to increase the surface area over which ions could be transported as well as numerous basal infoldings with associated mitochondria. Such basal infoldings are reported to be the major site of Na, K-ATPase (Diamond and Bossert, 1968; Ernst, 1972; Ernst *et al.*, 1981; Towle, 1985; Towle and Kays, 1986). This would be consistent with the higher Na, K-ATPase activity measured in transporting filaments, because few basal infoldings or mitochondria were observed in the epithelia of the respiratory filaments.

The structure of the thin squamous epithelia in *P. clarkii* respiratory filaments was similar to the respiratory epithelia described in other crayfish (Dunel-Erb *et al.*, 1982) in crabs (Copeland and Fitzjarrell, 1968; Taylor and Greenaway, 1979), and in shrimp (Foster and Howse, 1978). The paucity of organelles observed in the epithelium and pillar structures indicates that little cellular activity occurs in these cells other than maintenance of cell components. The thin epithelial layer may serve as a permeability barrier to the diffusive loss of ions and blood proteins, while the thin cytoplasm would allow efficient gas exchange to occur.

Large bundles of microtubules were observed in the pillar structures of the respiratory filaments, whereas single microtubules were the rule in the transporting epithelia of this crayfish and in most gill epithelia of other crustaceans (Copeland and Fitzjarrell, 1968; Bielawski, 1971; Foster and Howse, 1978; Taylor and Greenaway, 1979; Finol and Croghan, 1983; Compère *et al.*, 1989). These microtubules appear to anchor the epithelium to the cuticle. Finol and Croghan (1983) have proposed that the microtubules function to stabilize the gill epithelium against the hydrostatic pressure of the blood. Because the respiratory epithelium contains very little cytoplasm, additional microtubules, in the form of bundles near the periphery of the pillar structures, may give the additional support needed to withstand the shear forces of the blood flow in these filaments.

The loose connective tissue in the gills of *P. clarkii* is similar to that observed in *Callinectes sapidus* (Johnson, 1980). The cells within the loose connective tissue, with their abundant glycogen rosettes and granules, may regulate the blood glucose levels as suggested by Finol and Croghan (1983) for *Uca morda*.

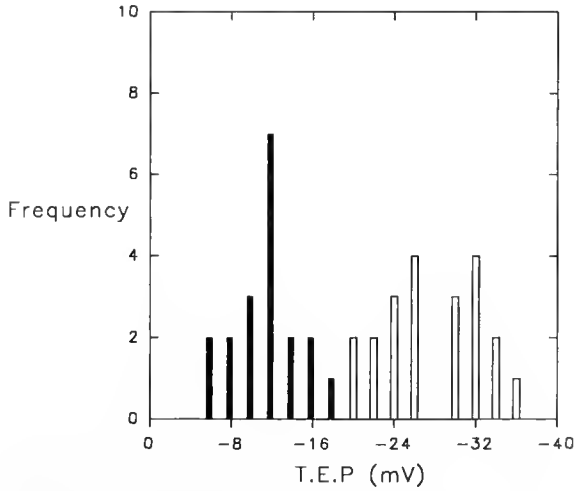

Figure 21. Transepithelial potentials (TEP) for respiratory (solid bars, n = 19) and transporting (open bars, n = 21) filaments.

The observed difference in the size and structure of the septum in the two types of filaments suggests its function may likewise differ. The thicker septum in the respiratory filaments may make the vascular canals more rigid, or it may also be a more substantial barrier to diffusion between the two compartments.

The neurons observed in the filaments of *P. clarkii* were similar to those constituting the branchial nerve observed in *A. pallipes* and *A. leptodactylus* (Dunel-Erb *et al.*, 1982). While those authors have described the nerve cell bodies and described structures resembling neurosecretory granules, the role of the nerve is uncertain. Massabuau *et al.* (1980) and Ishii *et al.* (1989) have suggested that the nerve may serve peripheral sensory elements involved in oxygen sensing. While the presence of the nerve in both the respiratory and transporting filaments would seem to question this function, the absence of any description of a transducing element leaves this question unresolved.

The "podocytes" observed in the filament tissues possessed the same ultrastructure as "podocytes" observed in other crustacean gills (Wright, 1964; Strangeways-Dixon and Smith, 1970; Doughtie and Rao, 1981). The presence of coated vesicles and large storage vacuoles gives support to the hypothesis that these cells take up toxic substances and blood components from the hemolymph for degradation or storage (Strangeways-Dixon and Smith, 1970; Doughtie and Rao, 1981).

ATPase measurements supported the silver staining and morphological observations in that values were highest in the transporting filaments. These data represent an apparent contradiction to the conclusion of Wheatly and Henry (1987) who reported that enzyme activity was homogeneously distributed throughout the branchial tissue. However, Wheatly and Henry (1987) pooled tissue from entire gill sets, and, therefore, could not have detected differences at the level of individual filaments. In fact, their data would represent a mean of respiratory and transporting filaments, assuming that *Pacifastacus* has a distribution of filament types similar to *Procambarus*. Our values for Na, K-ATPase activity in respiratory filaments are comparable to theirs, but the values we obtained for transport filaments are fivefold higher, reflecting the enrichment of transport tissue resulting from analyses of selected filaments.

While the *in situ* measurements of TEP's in the gill filaments were not intended to supply extensive data on the mechanisms of transport, a few interesting conclusions may be made. The data clearly suggest two functionally different populations of filaments. These data are qualitatively similar to those of Péqueux and Gilles (1988) who found positive TEP's in isolated, anterior, respiratory gills of *Eriocheir*, but negative potentials in the posterior, transporting gills.

The fact that the TEP's were negative with respect to the dilute medium, suggests that under the experimental circumstances the integumental barrier is preferentially cation conductive. The TEP's of the respiratory filaments were slightly more positive and those of the transport filaments slightly more negative than the diffusion potential for Na (−19 mV) calculated from the measured concentration difference. Cation selectivity is consistent with the data from other gill potential studies (*Austropotamobius* = *Astacus pallipes*, Croghan *et al.*, 1965; *Callinectes*, Mantel, 1967) and a study on the isolated gill cuticle of *Carcinus* (Lignon, 1987). Only a study by Avenet and Lignon (1985) presented data showing anion selectivity in the isolated cuticle from the gill lamina (plate) of *Astacus leptodactylus*. Whether the TEP's arise from diffusion potentials or from electrogenic transport is unknown, however, the contribution of transport-generated potentials is generally small in gills in the presence (Siebers *et al.*, 1985) or in the absence of concentration gradients (Siebers *et al.*, 1985; Drews and Graszynski, 1987). Avenet and Lignon (1985) and Lignon (1987) suggested that the ion selectivity of the integumental barrier resided in the epicuticle. Such cation selectivity of the epicuticle of the gill of *Procambarus* would be consistent with the location of the silver precipitate within the exocuticle. Presumably, the divalent silver cations could easily cross the outer cuticular barrier to precipitate with higher internal concentrations of chloride or, more likely, bicarbonate. If the observed TEP's are the result of diffusion potentials, the differences in TEP's between the respiratory and transport filaments would suggest either different ion permeabilities or different local ion concentrations within the two types of filaments.

The circulation of hemolymph within the gill filament has been described by Bock (1925), Fisher (1972), and Burggren *et al.* (1974). They describe hemolymph as flowing toward the tip of the filament in the afferent channel and down the filament toward the gill stalk in the efferent channel. Hemolymph may also be shunted from the afferent to the efferent channels via the lateral lacunae. The thick septum of connective tissue in respiratory filaments may act as a permeability barrier to counter-current gas exchange between the deoxygenated afferent hemolymph and the oxygenated efferent hemolymph, because this type of exchange would result in deoxygenated blood being returned to the body. The thin septum of the transporting filaments, on the other hand, may promote counter-current diffusion of ions from the afferent to the efferent channel, preventing further diffusive ion loss from the lacunae.

The observations in the present study indicate that there is a precise partitioning of structural and functional epithelium types within the gills of *Procambarus clarkii*, a thin squamous epithelium functioning in respiration and

a thick, mitochondria-rich epithelium functioning in ion transport. It is important to remember, however, that the integument consists not only of the underlying epithelium, but also of the overlying cuticle. Because this cuticle must periodically be shed to permit growth, the question arises as to whether the specialized functions of the filaments are disrupted during the period surrounding ecdysis. During premolt the hypodermis is normally engaged in cuticular synthesis, and prior to ecdysis the preexuvial cuticle exists as an additional barrier to the movement of substances. A more complete understanding of gill function must await examination of gills not only during intermolt, but also during the molt.

Literature Cited

Avenet, P., and J. M. Lignon. 1985. Ionic permeabilities of the gill lamina of the crayfish, *Astacus leptodactylus* (E). *J. Physiol.* **363:** 377–401.

Bielawski, J. 1971. Ultrastructure and ion transport in gill epithelium of the crayfish, *Astacus leptodactylus* Esch. *Protoplasma* **73:** 177–190.

Bock, F. 1925. Die Respirationsorgane von *Potamobius astacus* Leach. (*Astacus fluviatilis* Fabr.) Ein Beitrag zur Morphologie der Decapoden. *Z. Wiss. Zool.* **124:** 51–117.

Bryan, G. W. 1959. Sodium regulation in the crayfish *Astacus fluviatilis*. I. The normal animal. *J. Exp. Biol.* **37:** 83–99.

Bubel, A., and M. B. Jones. 1974. Fine structure of the gills of *Jaera nordmanni* (Rathke) [Crustacea, Isopoda]. *J. Mar. Biol. Assoc. U.K.* **54:** 737–743.

Burggren, W. W., B. R. McMahon, and J. W. Costerton. 1974. Branchial water- and blood-flow patterns and the structure of the gill of the crayfish *Procambarus clarkii*. *Can. J. Zool.* **52:** 1511–1518.

Cioffi, M. 1984. Comparative ultrastructure of arthropod transporting epithelia. *Am. Zool.* **24:** 139–156.

Compère, P., S. Wanson, A. Péqueux, R. Gilles, and G. Goffinet. 1989. Ultrastructural changes in the gill epithelium of the green crab *Carcinus maenas* in relation to the external salinity. *Tissue Cell* **21:** 299–318.

Copeland, D. E. 1963. Possible osmoregulatory cells in crab gills. *J. Cell Biol.* **19:** 16A.

Copeland, D. E. 1967. A study of salt secreting cells in the brine shrimp (*Artemia salina*). *Protoplasma* **63:** 363–384.

Copeland, D. E. 1968. Fine structure of salt and water uptake in the land-crab, *Gecarcinus lateralis*. *Am. Zool.* **8:** 417–432.

Copeland, D. E., and A. T. Fitzjarrell. 1968. The salt absorbing cells in the gills of the blue crab (*Callinectes sapidus* Rathbun) with notes on modified mitochondria. *Z. Zellforsch.* **92:** 1–22.

Croghan, P. C., R. A. Curra, and A. P. M. Lockwood. 1965. The electrical potential difference across the isolated gills of the crayfish *Austropotamobius pallipes* (Lereboullet). *J. Exp. Biol.* **42:** 463–474.

Diamond, J. M., and W. H. Bossert. 1968. Functional consequences of ultrastructural geometry in "backwards" fluid-transporting epithelia. *J. Cell Biol.* **37:** 694–702.

Doughtie, D. G. and K. R. Rao. 1981. The syncytial nature and phagocytic activity of the branchial podocytes in the grass shrimp, *Palaemonetes pugio*. *Tissue Cell* **13:** 93–104.

Drach, P., and C. Tchernigovtzeff. 1967. Sur la méthode de détermination des stades d'intermue et son application générale aux crustacés. *Vie Milieu* **18:** 595–610.

Drews, G., and K. Graszynski. 1987. The transepithelial potential difference in the gills of the fiddler crab, *Uca tangeri*: influence of some inhibitors. *J. Comp. Physiol.* **157B:** 345–353.

Dunel-Erb, S., J.-C. Massabuau, and P. C. Laurent. 1982. Organisation fonctionelle de la branchie d'ecrevisse. *C. R. Seances Soc. Biol.* **176:** 248–258.

Ehrenfeld, J. 1974. Aspects of ionic transport mechanisms in crayfish *Astacus leptodactylus*. *J. Exp. Biol.* **61:** 57–70.

Ernst, S. A. 1972. Transport adenosine triphosphatase cytochemistry. II. Cytochemical localization of ouabain-sensitive, potassium-dependent phosphatase activity in the secretory epithelium of the avian salt gland. *J. Histochem. Cytochem.* **20:** 23–28.

Ernst, S. A., C. V. Riddle, and K. J. Karnaky, Jr. 1981. Relationship between localization of Na^+-K^+-ATPase, cellular fine structure, and reabsorptive and secretory electrolyte transport. Pp. 355–385 in *Current Topics in Membranes and Transport*, V. 30, F. Bronner and A. Kleinzeller, eds. Academic Press, New York.

Finol, H. J., and P. C. Croghan. 1983. Ultrastructure of the branchial epithelium of an amphibious brackish-water crab. *Tissue Cell* **15:** 63–75.

Fisher, J. M. 1972. Fine-structural observations on the gill filaments of the freshwater crayfish, *Astacus pallipes* Lereboullet. *Tissue Cell* **4:** 287–299.

Foster, C. A., and H. D. Howse. 1978. A morphological study on gills of the brown shrimp, *Penaeus aztecus*. *Tissue Cell* **10:** 77–92.

Holliday, C. W. 1985. Salinity-induced changes in gill Na, K-ATPase activity in the mud fiddler crab, *Uca pugnax*. *J. Exp. Zool.* **233:** 199–208.

Horiuchi, S. 1977. Characterization of gill Na, K-ATPase in the freshwater crayfish, *Procambarus clarkii* (Girard). *Comp. Biochem. Physiol.* **56B:** 135–138.

Huxley, T. H. 1896. *The Crayfish—An Introduction to the Study of Zoology*. The Internat. Scientific Series. Paul, Trench and Trubner. London.

Johnson, P. T. 1980. *The Histology of the Blue Crab, Callinectes sapidus. A Model for the Decapoda*. Praeger. New York. Pp. 34–40.

Ishii, K., K. Ishii, J.-C. Massabuau, and P. Dejours. 1989. Oxygen-sensitive chemoreceptors in the branchio-cardiac veins of the crayfish, *Astacus leptodactylus*. *Resp. Physiol.* **78:** 73–81.

Kikuchi, S. 1983. The fine structure of the gill epithelium of a freshwater flea, *Daphnia magna* (Crustacea: Phyllopoda) and changes associated with acclimation to various salinities. I. Normal fine structure. *Cell Tissue Res.* **229:** 253–268.

Lignon, J. M. 1987. Ionic permeabilities of the isolated gill cuticle of the shore crab *Carcinus maenas*. *J. Exp. Biol.* **131:** 159–174.

Maluf, N. S. R. 1940. The uptake of inorganic electrolytes by the crayfish. *J. Gen. Physiol.* **24:** 151–167.

Mantel, L. H. 1967. Asymmetry potentials, metabolism and sodium fluxes in gills of the blue crab, *Callinectes sapidus*. *Comp. Biochem. Physiol.* **20:** 743–753.

Mantel, L. H., and J. Landesman. 1977. Osmotic regulation and Na-K-activated ATPase in the green crab, *Carcinus maenas* and the spider crab *Libinia emarginata*. *Biol. Bull.* **153:** 437–438.

Massabuau, J.-C., B. Elancher, and P. Dejours. 1980. Ventilatory reflex response to hypoxia in the crayfish, *Astacus pallipes*. *J. Comp. Physiol.* **140:** 193–198.

Milne, D. J., and R. A. Ellis. 1973. The effect of salinity acclimation on the ultrastructure of the gills of *Gammarus oceanicus* (Segerstrale, 1947) (Crustacea: Amphipoda). *Z. Zellforsch.* **139:** 311–318.

Morse, H. C., P. J. Harris, and E. J. Dornfield. 1970. *Pacifastacus leniusculus*: fine structure of the arthrobranch with reference to active ion uptake. *Trans. Am. Micr. Soc.* **89:** 12–27.

Neufeld, G. J., C. W. Holliday, and J. B. Pritchard. 1980. Salinity adaptation of gill Na, K-ATPase in the blue crab, *Callinectes sapidus*. *J. Exp. Zool.* **211:** 215–224.

Péqueux, A., and R. Gilles. 1978. Osmoregulation of the euryhaline Chinese crab *Eriocheir sinensis* Ionic transports across isolated perfused gills as related to the salinity of the environment. Pp. 105–111 in *Proc. 12th EMBS, Stirling, Scotland* Pergamon Press, Oxford.

Péqueux, A., and R. Gilles. 1981. Na^+ fluxes across isolated perfused gills of the Chinese crab *Eriocheir sinensis*. *J. Exp. Biol.* **92:** 173–186.

Péqueux, A., and R. Gilles. 1988. The transepithelial potential difference of isolated perfused gills of the Chinese crab *Eriocheir sinensis* acclimated to fresh water. *Comp. Biochem. Physiol.* **89A:** 163–172.

Peterson, G. L. 1977. A simplification of the protein assay method of Lowry *et al.* which is more generally applicable. *Anal. Biochem.* **83:** 346–356.

Reynolds, E. S. 1963. The use of lead citrate at high pH as an electron opaque stain in electron microscopy. *J. Cell Biol.* **17:** 208–212.

Roer, R. D., and M. G. Shelton. 1982. The effects of hydrostatic pressure on sodium transport in the crayfish, *Procambarus clarkii*. *Comp. Biochem. Physiol.* **71A:** 271–276.

Shaw, J. 1960a. The absorption of sodium ions by the crayfish, *Astacus pallipes* Lereboullet. II. The effect of the external anion. *J. Exp. Biol.* **37:** 534–547.

Shaw, J. 1960b. The absorption of sodium ions by the crayfish *Astacus pallipes* Lereboullet. III. The effect of other cations in the external solution. *J. Exp. Biol.* **37:** 548–556.

Siebers, D., A. Winkler, C. Lucu, G. Thedens and D. Weichart. 1985. Na-K-ATPase generates an active transport potential in the gills of the hyperregulating shore crab *Carcinus maenas*. *Mar. Biol.* **87:** 185–192.

Spurr, A. R. 1969. A low-viscosity epoxy resin embedding medium for electron microscopy. *J. Ultrastruct. Res.* **26:** 31–43.

Stevenson, J. R. 1972. Changing activities of the crustacean epidermis during the molt cycle. *Am. Zool.* **12:** 373–380.

Strangeways-Dixon, J., and D. S. Smith. 1970. The fine structure of the gill "podocytes" in *Panulirus argus* (Crustacea). *Tissue Cell* **2:** 611–624.

Taylor, H. H., and P. Greenaway. 1979. The structure of the gills and lungs of the arid-zone crab, *Holthuisana* (*Austrothelphusa*) *transversa* (Brachyura: Sundathelphusidae) including observation on arterial vessels within the gills. *J. Zool.* **189:** 359–384.

Towle, D. W. 1984. Membrane-bound ATPases in arthropod ion-transporting tissues. *Am. Zool.* **24:** 177–185.

Towle, D. W. 1985. Localization of $Na^+ + K^+$-ATPase in basolateral membranes of crab (*Carcinus maenas*) gill epithelium. *Bull. MDIBL* **25:** 80–83.

Towle, D. W., and W. T. Kays. 1986. Basolateral localization of $Na^+ + K^+$-ATPase in gill epithelium of two osmoregulating crabs, *Callinectes sapidus* and *Carcinus maenas*. *J. Exp. Zool.* **239:** 311–318.

Wanson, S. A., A. J. R. Péqueux, and R. D. Roer. 1984. Na^+ regulation and the $(Na^+ + K^+)$ATPase activity in the euryhaline fiddler crab *Uca minax* (Le Conte). *Comp. Biochem. Physiol.* **79A:** 673–678.

Wheatly, M. G., and R. P. Henry. 1987. Branchial and antennal gland Na^+/K^+-dependent ATPase and carbonic anhydrase activity during salinity acclimation of the euryhaline crayfish *Pacifastacus leniusculus*. *J. Exp. Biol.* **133:** 73–86.

Wheeler, A. P. 1975. Oyster mantle carbonic anhydrase: evidence for plasma membrane bound activity and for a role in bicarbonate transport. Ph.D. Dissertation, Duke University. Durham, North Carolina.

Wright, K. A. 1964. The fine structure of the nephrocyte of the gills of two marine decapods. *J. Ultrastructure Res.* **10:** 1–13.

Reference: *Biol. Bull.* **180**: 167–184. (February, 1991)

Nutrient Translocation during Early Disc Regeneration in the Brittlestar *Microphiopholis gracillima* (Stimpson) (Echinodermata: Ophiuroidea)

WILLIAM E. DOBSON[1,*], STEPHEN E. STANCYK, LEE ANN CLEMENTS[2], AND RICHARD M. SHOWMAN

Department of Biology, University of South Carolina, Columbia, South Carolina, 29208; [1]Department of Biology, Claflin College, Orangeburg, South Carolina 29115; and [2]Division of Science and Mathematics, Jacksonville University, Jacksonville, Florida 32211

Abstract. *Microphiopholis gracillima* can autotomize and then regenerate the autotomized central disc, including integument, gut, and gonads. Experiments were carried out to determine the relative importance of internal nutrient reserve translocation and exogenous nutrient uptake during the regeneration process. Approximately 60% of the dry body weight of *M. gracillima* is organic material. Intact animals held for three weeks in natural seawater did not change significantly in weight, caloric content, or relative concentration of protein, carbohydrates, or lipids. Intact animals held for three weeks in artificial seawater devoid of nutrients lost weight and caloric content. The rate of loss was rapid initially, but slowed after about eight days. Animals regenerated in natural seawater lost weight initially, then regained the lost weight. Animals regenerated in artificial seawater lost weight constantly and at a higher rate than either the artificial seawater control or natural seawater regenerated animals. All weight losses were attributable to significant changes in the protein and carbohydrate fractions of the organic body component. The lipid fraction and ash components did not change significantly in any treatment. *M. gracillima* appears to be adapted to regenerate the lost disk rapidly, even under conditions of food deprivation.

Introduction

Autotomy (self-mutilation by casting off body parts), followed by regeneration of the lost parts, is widespread among the echinoderms, and these animals are known to have superb wound-healing and regenerative capacities (see review by Emson and Wilkie, 1980; Brown, 1982). The few published studies of echinoderm regeneration have dealt almost exclusively with the capacity of an individual species to regenerate, descriptions of the appearance of new structures, or measurements of regeneration rates (Gibson and Burke, 1983). Although two recent studies have estimated the environmental energy production represented by regenerating brittlestar arms (Duineveld and Van Noort, 1986; O'Conner *et al.*, 1986), the energetic costs to the regenerating animal of autotomy, and the sources of nutrition for regeneration in echinoderms, have not been evaluated.

Members of at least five families of ophiuroid echinoderms (brittlestars) autotomize arms or the aboral disc (including digestive tract, gonads, and disc epithelium) when disturbed. They can regenerate these tissues within a few weeks in the laboratory (Emson and Wilkie, 1980; pers. obs.). The rate of tissue replacement must be related to the amount of stored nutrients available and the rate at which the animal can accumulate and allocate additional nutrients for tissue regeneration. The ophiuroid disc begins to regenerate before the gut has been replaced, but the sources of the nutrients that support that process are uncertain. To date, no specific nutrient storage organ other than the disc has been found, although the interstices of the arm ossicles may be repositories for nutrients (Turner and Murdoch, 1976). The ability of many echinoderms to translocate nutrients during gametogenesis (Lawrence, 1987) suggests that the same mechanism could be used during regeneration. Echinoderms may also take up dis-

Received 26 February 1990; accepted 26 November 1990.

Contribution #830 from the Belle W. Baruch Institute for Marine Biology and Coastal Research.

* To whom all correspondence and reprint requests should be sent.

solved organic matter (DOM) from the surrounding seawater, or process exogenous particulate nutrients by external digestion (Lawrence, 1987; Clements, 1988).

Theoretically, use of either DOM alone or external digestion alone would result in a net gain of organic matter by regenerating animals with no concomitant tissue loss from non-regenerating portions of the body. In contrast, internal nutrient translocation would result in the decrease of tissue in non-regenerating portions of the animal, with no net gain of organic matter during regeneration. There should even be a net loss of tissue due to catabolism of tissue constituents for respiration during regeneration. But translocation of stored nutrients, external digestion, and DOM uptake are not mutually exclusive and may operate sequentially or simultaneously. Other echinoderms lacking special storage organs resorb body parts under starvation conditions (Ebert, 1967; Feral, 1985; Lawrence, 1987). We hypothesize that early disc regeneration (prior to reformation of the functional gut) relies heavily on translocation of internal nutrient stores that are mobilized from the non-regenerating somatic tissues. The purpose of this paper is to estimate the relative contribution of internal nutrient translocation to disc regeneration.

Material and Methods

Individuals of *Microphiopholis gracillima* were collected from intertidal mud flats in the North Inlet Estuary just north of Georgetown, South Carolina (37°20′N, 79°10′W). After collection, animals were taken to the laboratory and sorted to eliminate all but individuals with complete (or almost completely regenerated) discs. Animals were then placed in autoclaved all-glass aquaria in an environmental chamber held at 25°C with a 12:12 light:dark cycle. The aquaria contained Millipore-filtered (0.45 μm) natural seawater (30‰). All aquaria were constantly aerated. The seawater was changed daily to control bacterial contamination (Clements *et al.*, 1988). Field-collected animals may have large differences in their nutritional states; therefore all animals were allowed to acclimate to the above conditions for seven days before the start of the experiments to help equalize nutritional differences. Animals were then randomly assigned to experimental groups.

The amount of nutrients translocated during regeneration was estimated in the following treatments. Intact and autotomized individuals were held in autoclaved all-glass aquaria containing either Millipore-filtered (0.45 μm) natural seawater without sediment; artificial seawater alone (Cavanaugh, 1956; trace minerals formula 5); or artificial seawater with approximately 125 μmol/l glucose, 125 μmol/l palmitic acid, and 12.5 μmol/l of each of 21 amino acids (alanine, arginine, asparagine, aspartic acid, cysteine, cystine, glutamic acid, glutamine, glycine, histidine, isoleucine, leucine, lysine, methionine, phenylalanine, proline, serine, threonine, tryptophan, tyrosine, and valine) added, for a total DOM concentration of approximately 513 μmol/l. This represents about a five-fold increase over natural DOM levels. (Clements, 1988; Williams, 1975). All aquaria were constantly aerated and kept in an environmental chamber at 25°C with a 12:12 light: dark lighting regimen. All media were changed daily. At 4-day intervals, 10 animals were removed from each treatment and dissected into the following body fractions: proximal, medial, and distal thirds of the arms, the oral frame, and the regenerated (or intact) discs. All of these fractions were dried to constant weight *in vacuo* over anhydrous calcium carbonate. About half of each fraction was ashed at 400°C for 6 h and its ash-free dry weight determined. The remaining three parts were subjected to biochemical analyses for protein, carbohydrate, and lipid, respectively. Before biochemical analysis, each part was split into three replicates, weighed, and ground to a dry powder in a hand-held all-glass homogenizer. In this way, replicated estimates of protein, carbohydrate, and lipid were obtained for each body fraction, as well as estimates of ash-free dry weight and caloric content. Because the tissue samples were small, colorimetric techniques were used in the biochemical analyses.

Total carbohydrate levels (as reducing sugars) were estimated by the phenol-sulfuric acid method of Dubois *et al.* (1956), with a 1:1 glucose:maltose solution as the standard. Total proteins were quantified by the Bio-Rad (Richmond, CA) modification of the Bradford (1976) method, with a 1:1 mixture of bovine serum albumin and purified mollusk protein (Sigma) as the standard. Lipids were extracted from the fraction homogenate with a 2:1 (v:v) chloroform:methanol solution. The extract was processed according to the sulphophosphovanillin method of Barnes and Blackstock (1973), with purified *Microphiopholis gracillima* lipid as the standard. The purified standard was prepared according to the procedures outlined in Barnes and Blackstock (1973). To compensate for the possibility of significant variation in total weights of the specimens used in this study, and to control for the inevitable loss of tissue during the fractioning of the samples for the different biochemical assays, all biochemical measures are reported as units per gram dry weight of specimen rather than as absolute quantities per body part.

To determine the relative translocation rate of proteins, carbohydrates, and lipids during regeneration, 300 animals were incubated in artificial seawater with either ^{14}C-leucine (specific activity 348.0 mCi/mmol), ^{14}C-glucose (3.5 mCi/mmol), or ^{14}C-palmitic acid (850.0 mCi/mmol) added at concentrations of 0.03 μCi/ml, 0.04 μCi/ml, and 0.04 μCi/ml, respectively. After 48 h, the animals were removed from the medium and rinsed in several changes of artificial seawater. One half of the animals in each nu-

trient treatment were induced to autotomize following the procedure of Dobson (1984, 1985). Five animals from each of the six treatments were immediately processed (see below). The remaining specimens were held in autoclaved all-glass aquaria containing constantly aerated artificial seawater in an environmental chamber at 25°C with a 12:12 light:dark cycle. The seawater was changed daily. At 4-day intervals, for 20 days, 8 animals were removed from each treatment and dissected to separate the distal half of the arms, the proximal half of the arms (including the oral frame), and the regenerated (or intact) disc tissue. Each fraction of five individuals was dried to constant weight at 80°C and placed in a separate glass scintillation vial containing 1 ml of 1:1 ProtoSol (New England Nuclear) tissue solublizer:ethanol. Five ml of AquaSol liquid scintillation cocktail (New England Nuclear) was added to each solublized specimen vial, and the samples were counted with a Beckman liquid scintillation counter with internal quench correction. The other three individuals were dried to constant weight at 80°C, ashed at 400°C for 6 h, and weighed again. We normalized all counts by computing the counts per minute (CPM) per gram dry weight and per gram ash-free dry weight of the tissue.

All data were analyzed by one-way or two-way ANOVA, Tukey's multiple comparison procedure (Ostle and Mensing, 1975; Sokal and Rohlf, 1981), or least-squares linear regression using the General Linear Models Procedure of the Statistical Analysis System (Carey, North Carolina). The probability of making any type I error at all in the entire series of tests was held at a = 0.05 or less [= Experimentwise error rate (Sokal and Rohlf, 1981, pg. 241)].

Results

Biochemical composition of the intact brittlestar

Normal values for organic and inorganic constituents of whole and individual regions of *Microphiopholis gracillima* were obtained by pooling all of the initial (time = 0) biochemical measurements from each experiment. The results are summarized in Table I. About 60% of the total dry body weight is organic tissue (as ash-free dry weight), and most of it is located in the arms. The central disc has the highest organic content (74%) relative to inorganic material, but this represents only 7% of the total dry body weight and 10% of the total organic tissue weight. The proximal, medial, and distal arm parts and the oral frame region contain 50 to 60% organic material, which accounts for 90% of the total organic material. The arms have a higher percentage of organic material at their bases than at their tips.

The central disc and oral frame have higher concentrations (per gram dry weight) of all organic components than do any of the arm regions. The disc has the highest concentration (per gram dry weight) of protein and lipid, whereas the oral frame has the highest concentration of carbohydrates. All arm fractions are similar in their protein, carbohydrate, and lipid concentrations. Interestingly, the assayed total protein, carbohydrate, and lipid content of the body accounts for only 30% of the total ash-free dry weight (= organic content) of the brittlestar. The relative underrepresentation of organic material is constant between body fractions with the exception of the oral frame, which has a relatively lower underrepresentation. Most of the total missing organic material is located in the arm parts. Although colorimetric assays commonly underestimate the actual amount of material present (Dubois *et al.*, 1956; Barnes and Blackstock, 1973; Davis, 1988), the magnitude of the underrepresentation in this case is unusual. We assume that, as has been reported for other echinoderms (Geise, 1966; Feral, 1985), the majority of the missing material represents insoluble organic material (such as connective tissue), organics tied up in the stromal spaces of the ossicles, complexed biochemicals (*e.g.*, glycoproteins and lipoproteins) that were not detected by the assays, and nucleic acids.

Change in biochemical composition of tissues during regeneration

Body weight changes. The changes in total dry weight (DW), total organic weight (= ash-free dry weight, AFDW) and total inorganic material weight (=ASH) fractions with time in individuals in the natural seawater control (NC), artificial seawater control (AC), natural seawater regenerated (NR), and artificial seawater regenerated (AR) treatments are shown in Figure 1. Animals in artificial seawater with added organics did not survive the experiment and thus were not analyzed. Animals in the NC group did not exhibit any significant change in total DW ($P = 0.3919$), ASH weight ($P = 0.9406$), or AFDW ($P = 0.4805$) during the course of the experiment (Fig. 1A). AC animals showed a rapid initial drop in both total DW ($P = 0.0466$) and AFDW ($P = 0.0002$) until day eight, after which both weight measures remained relatively constant. Total ASH weight did not change significantly at any time in the AC group ($P = 0.0828$) (Fig. 1B). NR animals did not lose significant amounts of total DW ($P = 0.0546$) or ASH weight ($P = 0.4458$) with time, but gradually lost AFDW ($P = 0.0022$) until about day 12, after which AFDW gradually increased through day 20 (Fig. 1C). The NR and AC groups lost as much as 40% of their initial AFDW values at some point during the 20-day experiment. AR animals displayed a rapid initial drop in total DW ($P < 0.0001$) and AFDW ($P < 0.0001$) from day 0 to day 4, followed by a slower constant decrease in these values. The maximum loss of DW during the ex-

Table I

Normal biochemical composition of Microphiopholis gracillima

Constituent	Whole	Disc	Body Part: Proximal arms	Medial arms	Distal arms	Oral frame
DRY WEIGHT	91.32 ± 10.87	8.85 ± 1.44	29.27 ± 3.57	27.50 ± 4.76	22.32 ± 4.71	2.26 ± 0.26
(% total body part DW)	100	100	100	100	100	100
(% whole DW)	100	9.7	32	30.0	24.5	2.4
ASH-FREE DRY WEIGHT	52.47 ± 7.78	6.52 ± 1.05	15.96 ± 2.64	16.32 ± 2.87	12.35 ± 2.58	1.35 ± 0.22
(% total body part DW)	100	74	54.5	59.3	55.3	59.7
(% whole DW)	58	7.1	17.5	17.8	13.5	1.47
(% whole AFDW)	100	12	30.4	31.1	23.5	2.5
ASH WEIGHT	37.70 ± 4.81	2.33 ± 0.42	13.31 ± 1.30	11.19 ± 3.72	9.97 ± 2.14	0.91 ± 0.14
(% total body part DW)	100	26	45.5	40.6	44.6	40.3
(% whole DW)	42	2.6	14.6	12.3	10.9	0.9
(% whole Ash weight)	100	6.2	35.4	29.7	26.4	2.4
PROTEIN	6.53 ± 0.35	1.59 ± 0.18	2.04 ± 0.05	1.44 ± 0.03	1.17 ± 0.09	0.21 ± 0.01
(% total body part DW)	7.15	18.02	7.00	5.27	5.27	9.60
(% whole DW)	7.15	1.74	2.23	1.57	1.28	0.23
(% total protein)	100	24.35	31.24	22.05	17.91	3.21
CARBOHYDRATES	2.88 ± 0.26	0.74 ± 0.07	0.91 ± 0.13	0.65 ± 0.14	0.33 ± 0.04	0.11 ± 0.01
(% total body part DW)	3.15	8.42	3.08	2.37	1.48	8.80
(% whole DW)	3.15	0.81	0.99	0.71	0.36	0.12
(% total carbohydrates)	100	25.69	31.59	22.56	11.45	3.81
LIPIDS	3.46 ± 0.33	0.74 ± 0.05	1.05 ± 0.24	0.94 ± 0.08	0.60 ± 0.17	0.10 ± 0.01
(% total body part DW)	3.79	8.36	3.58	3.41	2.68	4.50
(% whole DW)	3.79	0.81	1.14	1.02	0.65	0.11
(% total lipids)	100	21.40	30.60	27.10	17.60	2.89
UNACCOUNTED ORGANICS	39.60 ± 3.89	3.45 ± 0.09	11.96 ± 0.96	13.29 ± 1.13	10.25 ± 0.76	0.42 ± 0.02
(% total body part DW)	43.36	38.90	40.86	48.30	45.93	18.58
(% whole DW)	43.36	3.77	13.09	14.50	11.22	0.46
(% whole AFDW)	65.47	6.57	22.79	25.32	19.53	0.80
(% total UO)	100	8.71	30.20	33.56	25.88	1.06
CALORIC CONTENT (calc.) (kCal/g dry weight)	0.93 ± 0.04	2.40 ± 0.06	0.83 ± 0.08	0.70 ± 0.03	0.58 ± 0.08	1.08 ± 0.07

All values are averages ± one standard deviation. All units are milligrams unless otherwise noted.
DW = Dry Weight, AFDW = Ash-Free Dry Weight, UO = Unaccounted Organics.

periment occurred in this group, which lost as much as 40% of the initial DW and 50% of the initial AFDW. Ash weight did not change significantly in the AR group ($P = 0.4893$) (Fig. 1D).

When the total DW measurements were broken down by body part, the following trends were observed. In the NC group, no significant DW change occurred in any body part with time ($P > 0.05$ in all fractions) (Fig. 2A). In the AC group, the DW of the medial ($P = 0.4247$) and proximal ($P = 0.4928$) regions of the arms remained relatively constant, but the disc, distal arm regions, and oral frame lost DW until about day eight, after which their dry weights remained constant ($P = 0.0003$, $P = 0.0029$, $P = 0.0025$, respectively) (Fig. 2B). Animals in the NR group exhibited no overall change in DW in any body part ($P > 0.05$) after first appearance of the disc tissue, although the weight of the oral frame on day 16 was significantly different from all other days. Animals in the AR group lost DW throughout the experiment in all non-regenerating body parts ($P < 0.05$). This loss was rapid until approximately day eight, after which the decline proceeded at a slower rate.

Ash-free dry weight and ASH weight measurements by body part with time indicate that the loss in DW is due to loss exclusively from the organic fraction (Fig. 3). There were no significant changes in the ASH weights of any body parts in any experimental treatment over the 20-day period with the exception of first appearance of the discs (between days zero and four) in the regenerating groups (Fig. 4). There was no significant change in AFDW in anybody part with time ($P > 0.05$) in the NC group (Fig. 3A). In the AC group, all body parts with the exception of the proximal arm fractions lost AFDW until approximately day eight, after which AFDW remained relatively

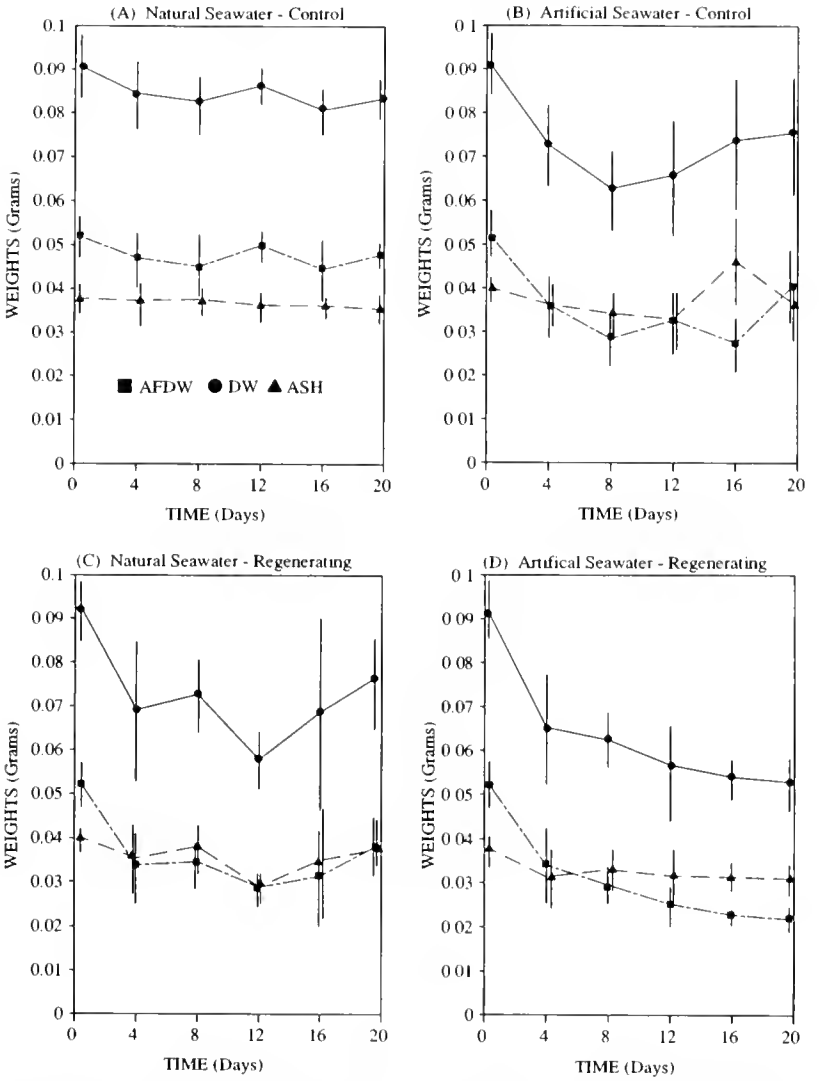

Figure 1. Total body weight changes during early disc regeneration. (A) Natural seawater control group. (B) Artificial seawater control group. (C) Natural seawater regenerating group. (D) Artificial seawater regenerating group. Error bars represent 95% confidence intervals. Error bars and points offset slightly for graphical clarity.

constant in all body fractions (Fig. 3B). The most rapid drop in AFDW occurred between day zero and day four. Although the proximal arm fractions did lose AFDW over the course of the experiment, the loss was not significant at any time ($P = 0.1443$). Animals in the NR group lost AFDW from all non-regenerating body fractions until approximately day 12, after which AFDW increased (Fig. 3C). Because of the high variability in the data, the changes in AFDW of the proximal and medial arm fractions were not statistically significant from day zero at any other time ($P = 0.0566$ and $P = 0.0853$, respectively). The AFDW of all non-regenerating body part fractions in the AR group declined continuously until day 16 of the experiment ($P < 0.05$) (Fig. 3D). The most rapid decrease occurred between day zero and day four, except in the proximal arm regions, where tissue was lost at a constant rate. The disc tissue in both the NR and AR groups did not increase in AFDW content significantly after first appearing.

Protein content changes. The changes in total body protein concentration over time are shown in Figure 5A. The natural seawater control group did not change in total protein concentration over the course of the experiment ($P = 0.4717$). The artificial seawater control group exhibited a slight decline in protein concentration with time ($P = 0.0121$), but the only day that was significantly different from the others in this group was day eight. The groups regenerating in natural seawater and in artificial seawater both changed slightly in total protein concen-

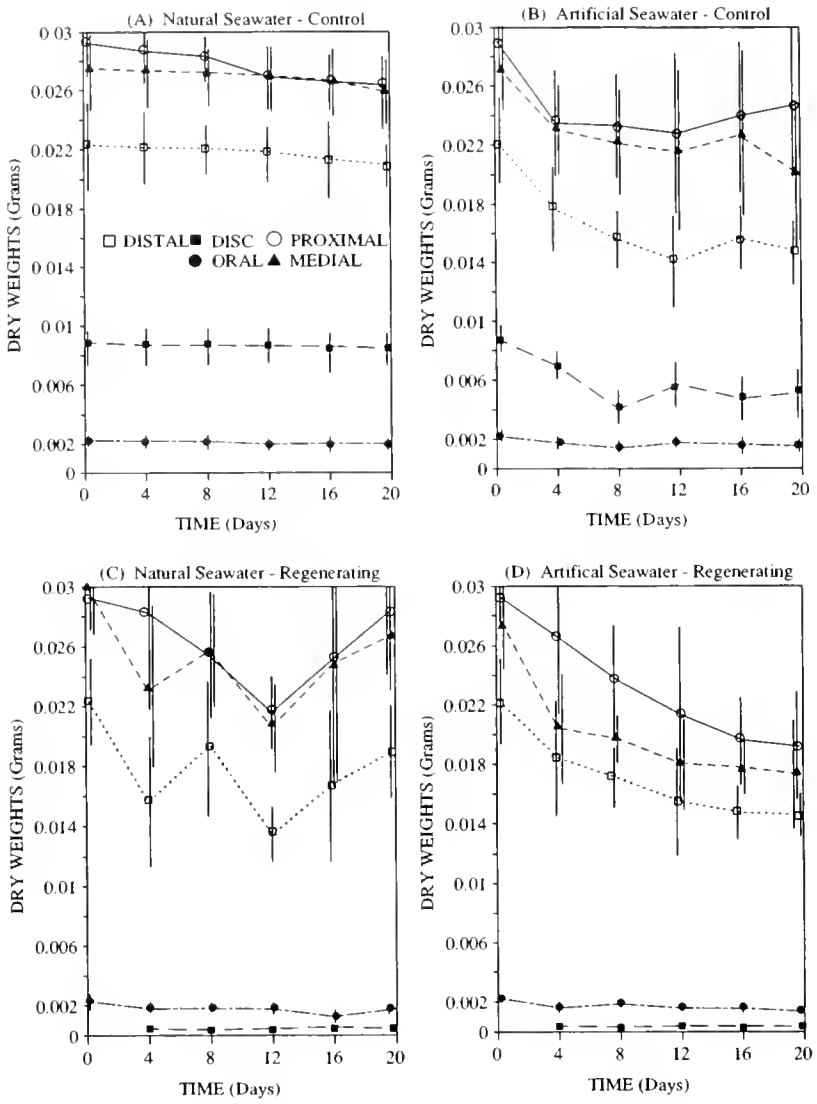

Figure 2. Changes in dry weights by body parts during early disc regeneration. (A) Natural seawater control group. (B) Artificial seawater control group. (C) Natural seawater regenerating group. (D) Artificial seawater regenerating group. Error bars represent 95% confidence intervals. Error bars and points offset slightly for graphical clarity.

tration over the course of the experiment ($P < 0.001$ in both). The protein concentration increased at the same rate in both the NR and AR groups until day eight, after which the NR group continued to gradually increase while the AR group began to decline. By the end of 20 days, the protein concentration in the AR group was the same as its initial (day zero) protein concentration.

The change in protein concentration over time by treatment group and body part is shown in Figure 6. There was no change in protein concentration in any body part in the NC group over the course of the experiment ($P > 0.05$) (Fig. 6A). The AC group lost protein in significant amounts from the disc ($P = 0.0012$), distal arm fractions ($P < 0.0001$), and oral frame ($P < 0.0001$). The protein concentration of the medial and proximal arm fractions did not change ($P = 0.0675$, $P = 0.7822$, respectively) (Fig. 6B). There was no change in the protein concentration of any arm fractions in the NR group ($P > 0.05$), but the oral frame lost significant amounts of protein relative to its dry weight ($P = 0.0003$), while the disc rapidly increased in protein concentration ($P < 0.0001$) (Fig. 6C). The AR treatment group lost protein from all non-regenerating body parts ($P < 0.05$) (Fig. 6D). The protein concentration of the disc in the AR group increased rapidly until day 12 ($P < 0.0001$), then fell off rapidly through day 20 ($P < 0.0001$). The rate of increase to day 12 was the same as in the NR treatment ($P > 0.05$). The rate of protein loss from the oral frame was slower in the AR

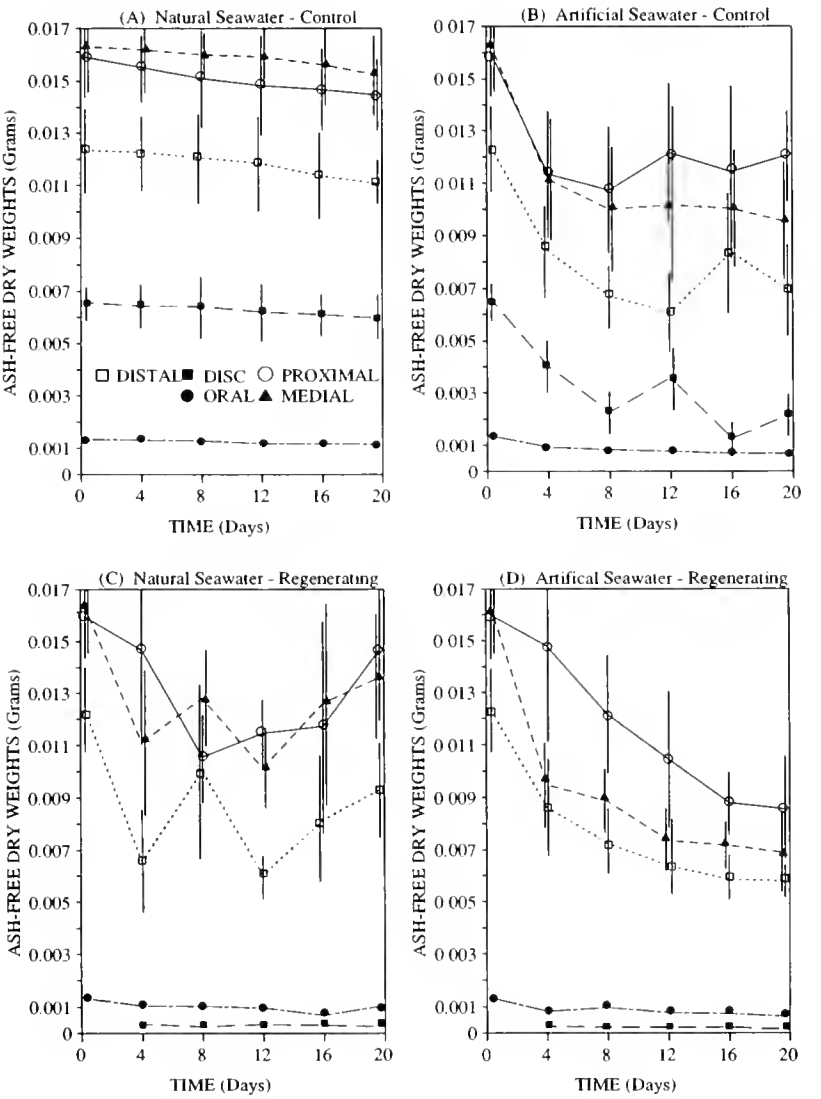

Figure 3. Changes in ash-free dry weights by body parts during early disc regeneration. (A) Natural seawater control group. (B) Artificial seawater control group. (C) Natural seawater regenerating group. (D) Artificial seawater regenerating group. Error bars represent 95% confidence intervals. Error bars and points offset slightly for graphical clarity.

and NR groups than in the AC group ($P < 0.0001$), but loss occurred throughout the experiment, whereas the AC group stopped losing protein from the oral frame at about day 8. The AR and NR treatment groups lost protein from the oral frame at the same rate throughout the experiment ($P = 0.0931$). The AR treatment lost protein from the distal arms at a higher rate than did the AC treatment group ($P < 0.0001$).

Carbohydrate content changes. The results of the total body carbohydrate assays are graphed by day in Figure 5B. The NC and NR groups did not exhibit any significant change in total carbohydrate concentration with time ($P = 0.0877$, $P = 0.4784$). The AC and AR groups did exhibit changes in total carbohydrate concentration ($P = 0.0063$, $P < 0.0001$) over the course of the experiment. There was no difference in the rate of loss between the AC and AR groups ($P = 0.5675$).

The changes in carbohydrate concentration of the various body parts with time in the different treatments is graphed in Figure 7. The NC, AC, and NR groups lost significant amounts of carbohydrates only from the oral frame ($P = 0.0173$, $P = 0.0002$, $P = 0.0075$, respectively). Although there were fluctuations in the carbohydrate concentration of the other non-regenerating body parts in each of these groups, they did not represent significant changes in concentration with time (Fig. 7A, B, C). The AR group lost significant amounts of carbohydrates from the distal and medial arm parts and the oral frame (P

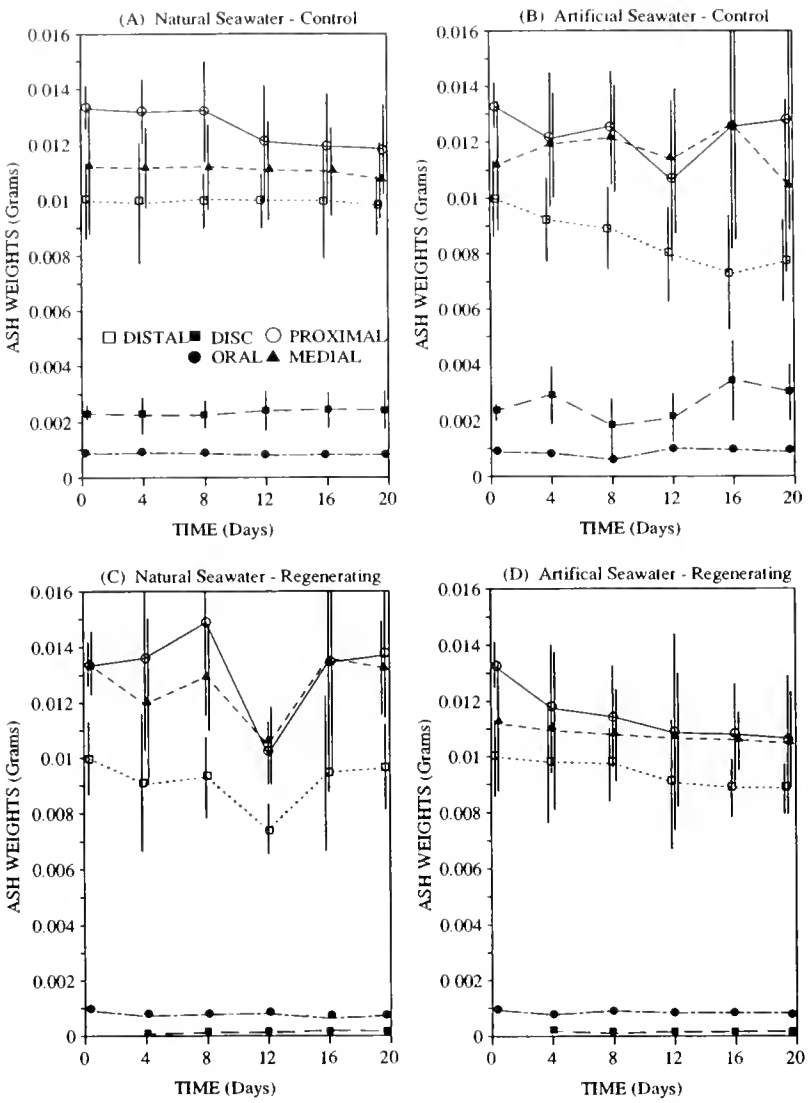

Figure 4. Changes in ash weights by body parts during early disc regeneration. (A) Natural seawater control group. (B) Artificial seawater control group. (C) Natural seawater regenerating group. (D) Artificial seawater regenerating group. Error bars represent 95% confidence intervals. Error bars and points offset slightly for graphical clarity.

< 0.05). The proximal arm parts did not exhibit a significant change, although there appeared to be a gradual decline in carbohydrate concentration ($P = 0.0623$, Fig. 7D). Both the NR and AR groups exhibited a rapid increase in the carbohydrate content of the regenerating disc, with rate of increase being the same in both groups through day 12. After day 12, the disc continued to increase in carbohydrate concentration in the NR group, while the carbohydrate concentration in the disc tissue of the AR group began to decline. The rate of decline in oral frame carbohydrate concentration was identical across all treatments ($P > 0.05$) until day 20, when the NC treatment was different from the AC, NR, and AR treatments, which were still the same ($P < 0.05$).

Lipid content changes. The changes in total body lipid concentration over time are shown in Figure 5C. There were no significant changes in the total lipid concentration within any of the treatments with time ($P > 0.05$). Between treatments, the NC and AC treatments were identical on all days. In addition, the NR and AR treatments were identical through day 12. The NR treatment was different from the AR treatment and the same as the NC and AC treatments at day 16. All treatments had the same lipid concentrations by day 20.

The changes in lipid concentration by day and body part are illustrated in Figure 8. There was no significant change in lipid concentration in any non-regenerating body part in the NC, AC, and NR groups ($P > 0.05$) (Fig.

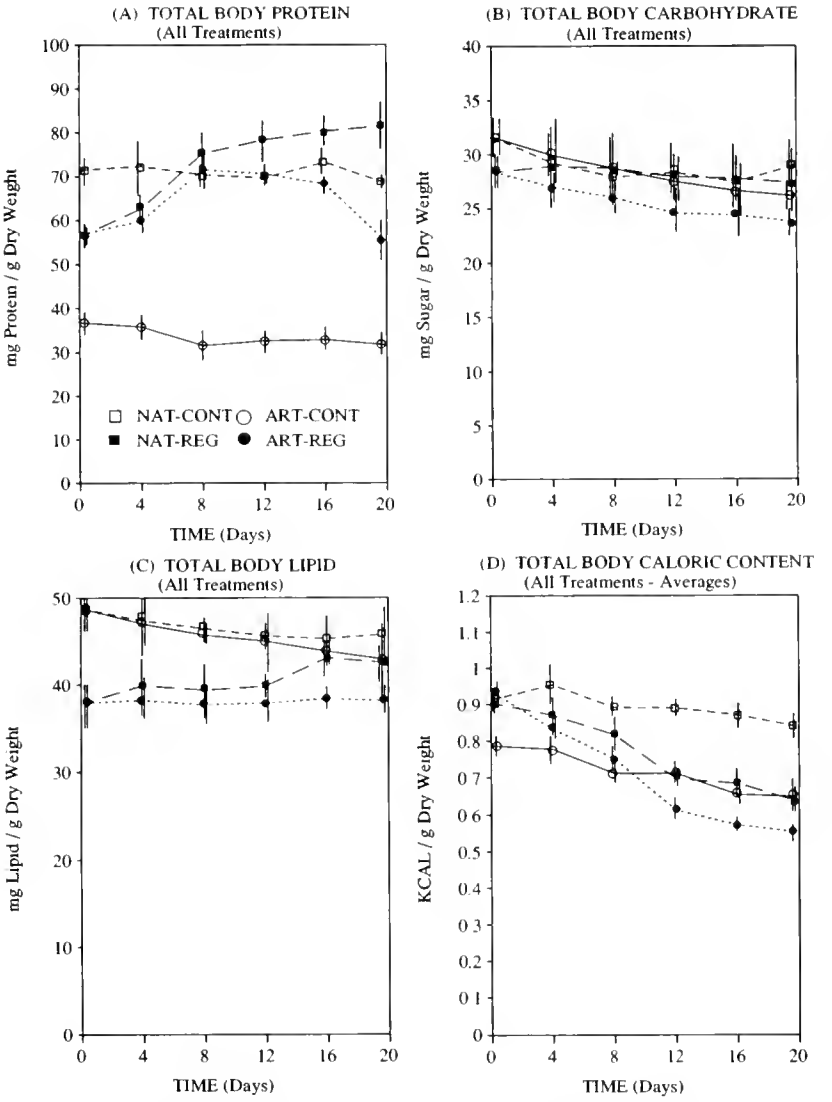

Figure 5. Total body biochemical concentration changes during early disc regeneration. (A) Total body protein by treatment group. (B) Total body carbohydrate by treatment group. (C) Total body lipid by treatment group. (D) Total body caloric content (calculated) by treatment group. Error bars represent 95% confidence intervals. Error bars and points offset slightly for graphical clarity.

8A, B, C). Although the AC and NR groups showed a constant decline in lipid concentration in all body parts except the regenerating disc of the NR treatment, the overall changes were not statistically significant. The AR group showed a significant decrease in lipid concentration in the medial arm fraction ($P = 0.0235$) as well as the same non-significant concentration decline in all other non-regenerating body parts shown by the AC and NR groups. The NR and AR groups exhibited rapid increases in lipid concentration in the disc tissue fragment, which were the same through day 16 ($P > 0.05$). The NR group had a higher lipid concentration in the disc fraction by day 20 ($P = 0.2430$).

Caloric content changes. Caloric values presented here were calculated from the biochemical data using caloric-conversion values (protein, 5.65 kcal/g; carbohydrate, 4.10 kcal/g; lipid, 9.45 kcal/g;) (Brody, 1964; Ekert and Randall, 1978). Although the current trend in physiological research is to use the SI unit of energy (joules), we determined energy content as calories and present the data here in calories for ease of comparison with previous literature. However, one calorie equals 4.184 joules (Crisp, 1984), so direct conversion between units is relatively simple. Although there is potential for error in using calculated values instead of real values for caloric content (Giese, 1966; Cummins and Wuy-

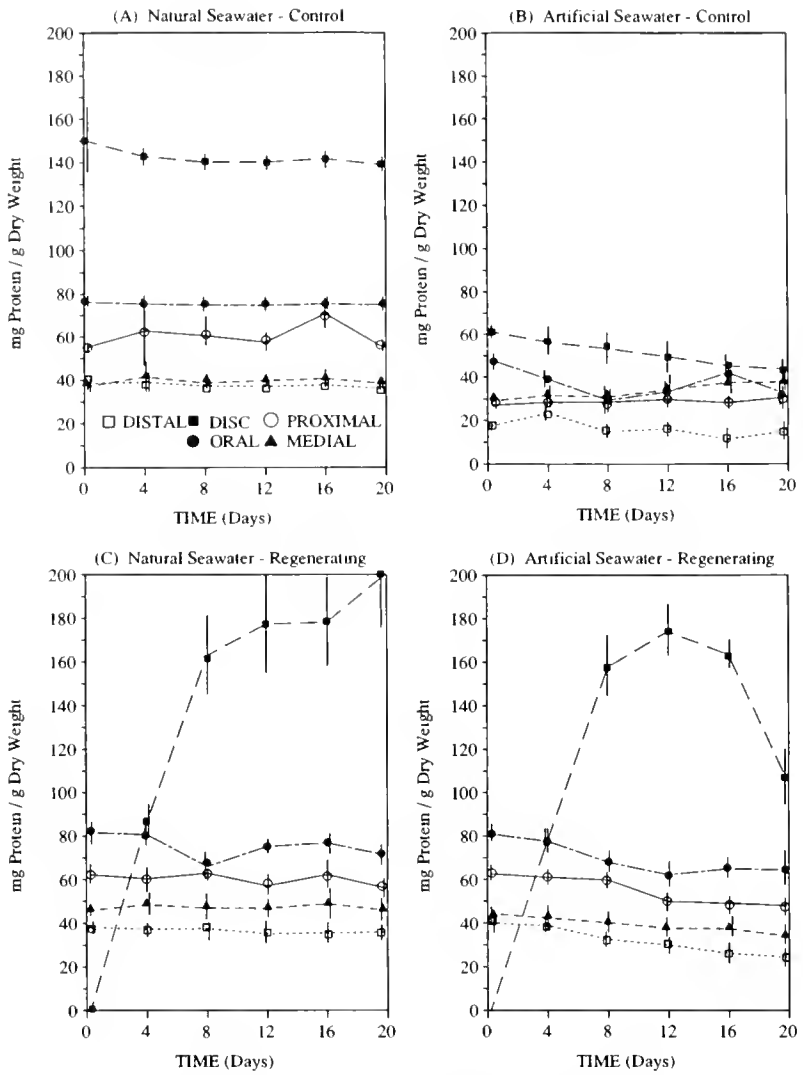

Figure 6. Protein content changes by body part during early disc regeneration. (A) Natural seawater control group. (B) Artificial seawater control group. (C) Natural seawater regenerating group. (D) Artificial seawater regenerating group. Error bars represent 95% confidence intervals. Error bars and points offset slightly for graphical clarity.

check, 1971; Feral, 1985), the calculated caloric values are probably closer to the "true" values than the actual calorimetry data due to procedural errors in obtaining the micro-bomb calorimetry data and the resulting wide variations in the actual caloric values. The total calculated caloric content of the body in the different treatments is illustrated in Figure 5D. With the exception of day four in the AC group (which was only different from day 20), there were no statistically significant differences in caloric content with time in either of the NC and AC groups ($P > 0.05$). The caloric content of the NR and AR groups declined constantly ($P < 0.0001$), with the AR group losing caloric content faster than the NR group ($P < 0.0001$).

The caloric content changes with time by body part are diagrammed in Figure 9. The natural seawater control group lost calories only in the disc fraction ($P = 0.0310$) (Fig. 9A). All other body parts maintained their caloric levels ($P > 0.05$). The artificial seawater control group lost calories only from the disc and oral frame ($P = 0.0045$, $P = 0.0050$), not the arm fractions ($P > 0.05$) (Fig. 9B). The NR treatment group lost calories from the oral frame and distal arm fractions ($P = 0.0017$, $P = 0.0064$) but not the medial and proximal arm fractions ($P > 0.05$) (Fig. 9C). The AR group lost calories from every non-regenerating body part ($P < 0.0001$) (Fig. 9D). The NR and AR groups both increased the caloric content of their disc tissue until day 16. By day 20, the AR group had begun

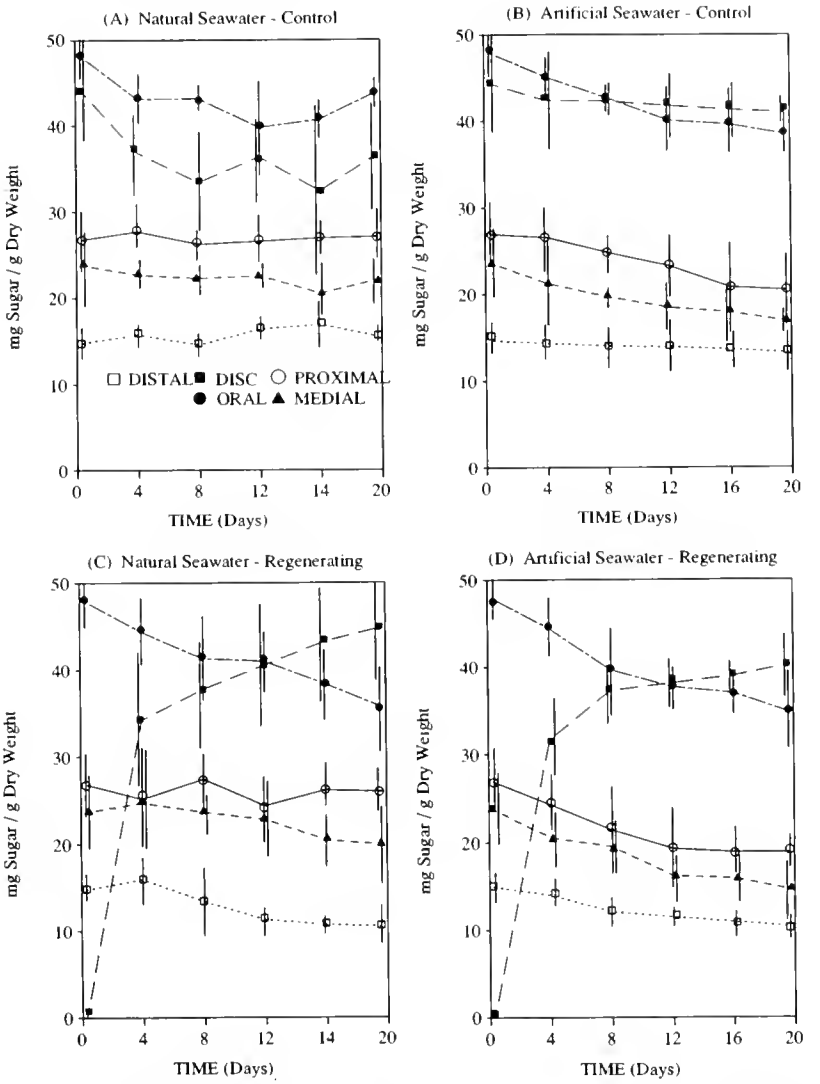

Figure 7. Carbohydrate content changes by body part during early disc regeneration. (A) Natural seawater control group. (B) Artificial seawater control group. (C) Natural seawater regenerating group. (D) Artificial seawater regenerating group. Error bars represent 95% confidence intervals. Error bars and points offset slightly for graphical clarity.

to lose calories from the disc tissue, whereas the NR group continued to add calories to the disc tissue. The rate of increase in caloric content was the same in the NR and AR groups through day 12.

Rate of nutrient translocation

All brittlestars took up statistically significant amounts of ^{14}C-leucine and ^{14}C-glucose during the pulse portion of the experiment (Fig. 10, 11). Counts of the individual body parts indicated that all body parts absorbed label in approximately the same quantities per gram of dry body weight ($P = 0.5740$). However, the animals only accumulated significant amounts of ^{14}C-palmitic acid in the disc region of the body. This result was somewhat unexpected, because other echinoderms are known to take up lipids, especially exogenous palmitic acid, from their environment across their dermal surfaces (Beijnink and Voogt, 1984).

During the post-absorption portion of the experiment, ^{14}C-leucine and ^{14}C-glucose label counts decreased rapidly and in approximately linear fashion in all the experimental treatments (Fig. 10, 11). ^{14}C-palmitic acid concentration changes were not followed because the animals failed to take up the material in non-regenerating body parts. Counts of the individual body parts indicated that ^{14}C-leucine and ^{14}C-glucose labels were lost in approximately the same proportions from all non-regenerating fractions

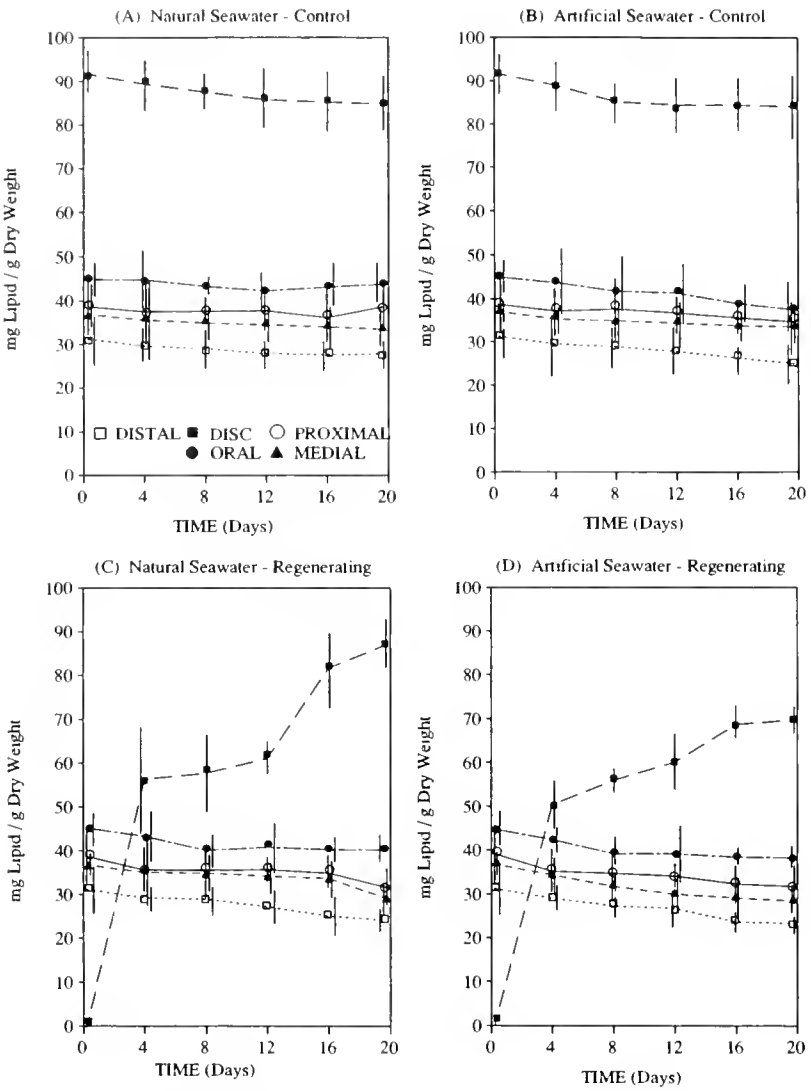

Figure 8. Lipid content changes by body part during early disc regeneration. (A) Natural seawater control group. (B) Artificial seawater control group. (C) Natural seawater regenerating group. (D) Artificial seawater regenerating group. Error bars represent 95% confidence intervals. Error bars and points offset slightly for graphical clarity.

of the body, including the disc of intact specimens. However, little of the label lost from the non-regenerating tissues of regenerating animals was incorporated into the regenerating disc tissue. Although counts of the regenerating disc tissue showed that some radiolabel was incorporated into the disc tissue, the levels were not significantly different from background counts throughout the course of the experiment ($P > 0.05$).

Discussion

The experimental treatments used to study the amount of nutrients translocated during disc regeneration can be described in terms of nutrient availability. The NC group represented control animals that were given access to dissolved organic material (DOM), but not particulate food, to determine the effect of maintenance metabolism on the body's biochemical composition when both stored nutrient catabolism and DOM uptake were available as energy sources. The AC group represented control animals that had to rely on stored nutrients alone to supply energy for maintenance. The NR group were animals that had to supply energy for both maintenance metabolism and regeneration, as well as building materials for regeneration. These animals had access to both stored nutrients and DOM uptake sources of nutrients. The AR group represented animals that had to both maintain metabolism and regenerate

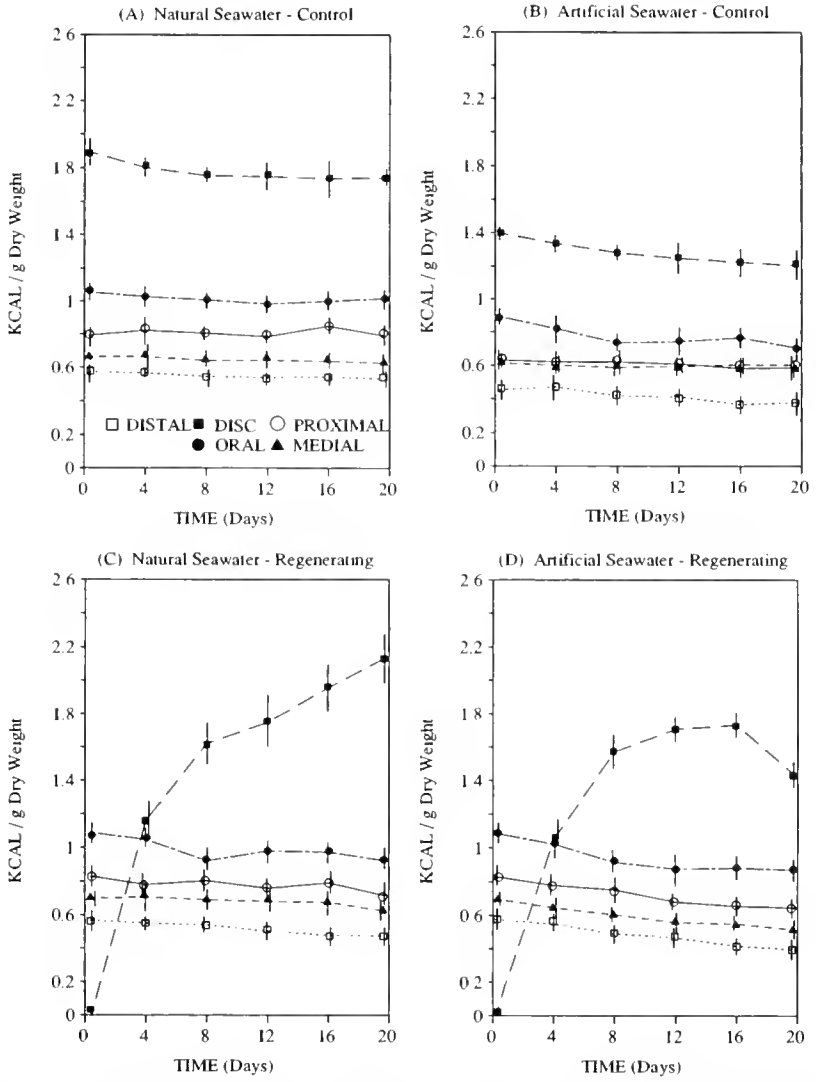

Figure 9. Tissue caloric content changes by body part during early disc regeneration. (A) Natural seawater control group. (B) Artificial seawater control group. (C) Natural seawater regenerating group. (D) Artificial seawater regenerating group. Error bars represent 95% confidence intervals. Error bars and points offset slightly for graphical clarity.

in the absence of any external nutrient source (*i.e.*, only stored nutrients were available).

Under natural seawater control conditions, animals survived for at least four weeks (one week of acclimation plus three weeks of experimentation) with no significant change in the overall biochemical composition of the body. The only localized changes in body constituents occurred in the oral frame region, which lost small amounts of carbohydrates during the experiment. Although the animals probably lost stored nutrients from all body parts under these conditions, the losses were below the limits of detection. The total energy content of the animal did not change. The only localized caloric content change occurred in the disc region and could not be attributed to changes in any measured biochemical component. This indicates that, although animals deprived of particulate food may be stressed, they probably are not starving (*i.e.*, they are obtaining nutrients by direct uptake from the environment). This result is consistent with previous studies showing that echinoderms, including brittlestars, can obtain up to 58% of their energetic requirements from DOM (Ferguson, 1982a, b; Feral, 1985; Lawrence, 1987; Clements, 1988).

When deprived of all exogenous food (artificial seawater treatments), control animals initially lost stored material at a rapid rate. The material was lost from the disc, oral frame, and distal arm regions of the body, and was attributable to losses of protein and carbohydrates, but not

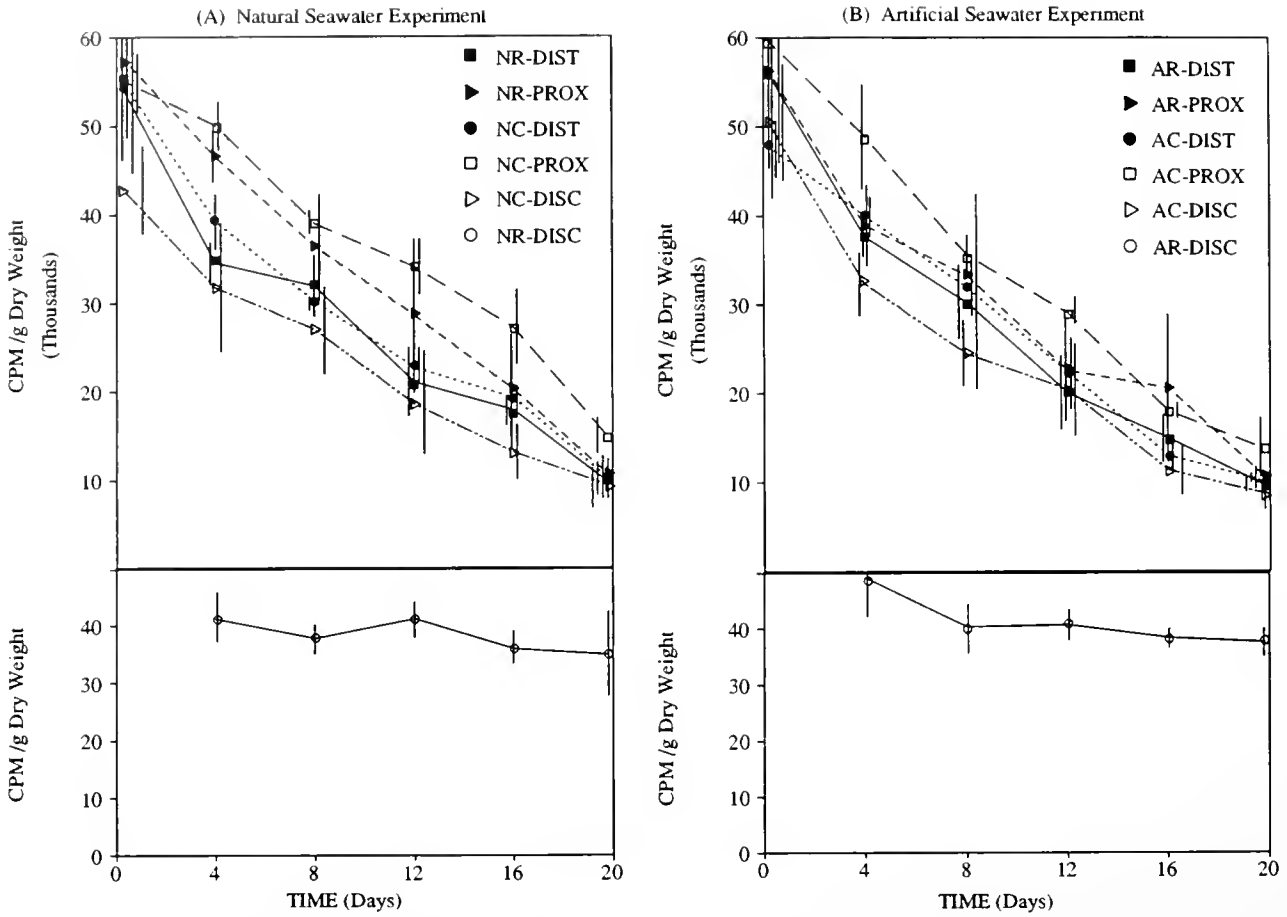

Figure 10. ^{14}C-Leucine tracer content of tissues during early disc regeneration. (A) Natural seawater experiment. (B) Artificial seawater experiment. AC = Artificial seawater control, AR = Artificial seawater regenerating, NC = Natural seawater control, NR = Natural seawater regenerating, DIST = Distal arm, PROX = proximal arm and oral frame. Error bars represent 95% confidence intervals. Error bars and points offset slightly for graphical clarity.

lipids. The loss of total caloric content in the various body parts followed the same pattern, with no significant loss in any other body parts. After four days, these animals appeared to acclimate to the lack of food such that the rate of overall materials loss was reduced; (*i.e.*, they apparently adjusted to food deprivation by reducing their consumption of stored material). The temporal pattern of material loss may also represent a rapid initial use of stored resources followed by a breakdown of essential body tissues to maintain metabolism. As tissue mass decreased, the metabolic load due to those tissues decreased, and the rate of tissue loss declined. Because mass-specific metabolic rates were not obtained during this experiment, these observations could not be empirically verified.

There are two possible explanations for the spatial pattern of material loss in the artificial seawater control group. The first is that the disc, oral frame, and arm tips are preferentially resorbed when the animal is forced to catabolize tissue for maintenance. Turner and Murdoch (1976) described such a pattern of arm tissue loss during regeneration of the disc in *Ophiophragmus filograneus*. This mechanism would leave the majority of the arm tissue undisturbed so that normal feeding activity would not be impaired when feeding conditions improved. The second possibility is that the absolute rate of loss is the same from all body parts, but there is less material in the disc, oral frame, and arm tips to begin with, so the material available within them is exhausted sooner than that in other body parts. The latter possibility is the more likely, because the medial and proximal arms have the highest total amounts of all biochemical constituents (Table I).

Animals regenerating in natural seawater showed an initial decrease in organic mass followed by a gradual increase. This indicates that the use of material during early regeneration exceeded the rate at which DOM uptake from the medium could compensate for it, and thus must have been at least partially independent of external nutrient availability. Loss of organic material occurred in

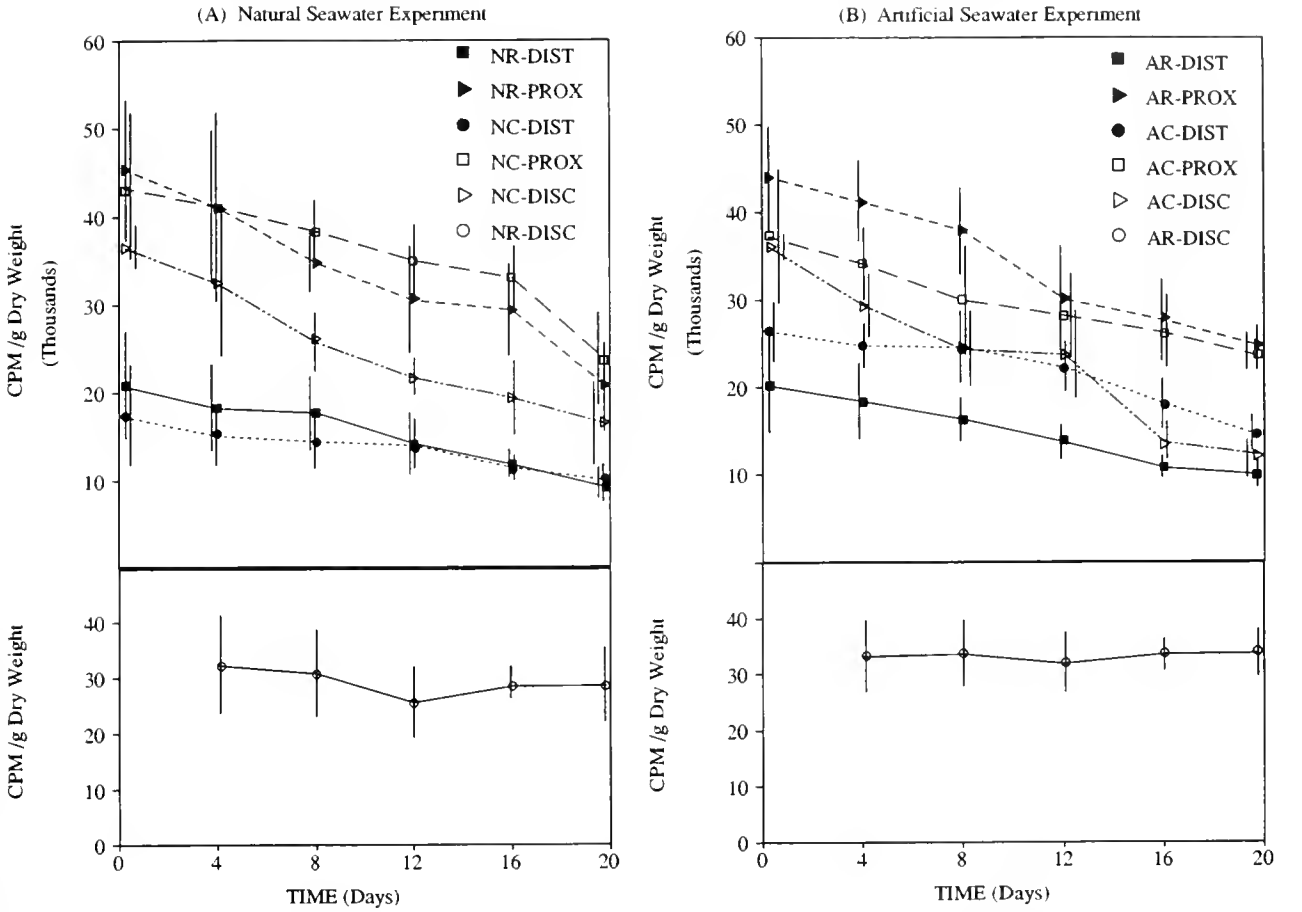

Figure 11. ^{14}C-Glucose tracer content of tissues during early disc regeneration. (A) Natural seawater experiment. (B) Artificial seawater experiment. AC = Artificial seawater control, AR = Artificial seawater regenerating, NC = Natural seawater control, NR = Natural seawater regenerating, DIST = Distal arm, PROX = proximal arm and oral frame. Error bars represent 95% confidence intervals. Error bars and points offset slightly for graphical clarity.

all non-regenerating body parts, but the overall trend was similar to that exhibited by the artificial seawater control group in that most of the loss was from the oral frame and arm tips. The subsequent increase in organic material appeared to be localized in the arms. The relative protein content of the body increased constantly during regeneration, indicating either a net gain of protein during regeneration, or a loss of minerals as tissue breakdown occurred. This gain could be due to a net uptake of proteins (or amino acids) from the medium, or a combination of uptake and overall loss of other body biochemical constituents during regeneration. Although the carbohydrate and lipid content of the body did not change significantly over the same period, the latter explanation is more likely, because the animals lost total caloric content constantly during regeneration. The increase in organic material in the non-regenerating portions of the body after day 12 is problematical, because no corresponding increase in biochemical constituents in those parts could be demonstrated. This increase might be explained as the summation of non-significant increases in each biochemical constituent to make a significant increase in total organics.

Animals regenerating in the absence of exogenous nutrients constantly lost organic material from non-regenerating body parts. The rate of loss was relatively rapid through day 8, and slower from day 12 through day 20. This change was related to the constant decrease in protein, carbohydrate, and lipid content of the non-regenerating tissues. Although lipid content loss was statistically significant only in the medical portions of the arms, all non-regenerating body parts showed a trend toward lipid loss. The regenerating disc tissue increased in protein, carbohydrate, and lipid content through day 12, after which protein and carbohydrate content dropped dramatically, while lipid content remained the same or slightly increased (the continued proportional lipid increase was probably due to the loss of protein and carbohydrates). The caloric content of these animals dropped

constantly, and consistently faster than that in the experimental group regenerating in natural seawater. All non-regenerating parts of the body lost calories throughout the experiment. The caloric content of the disc increased through day 16, then dropped dramatically.

The data on the consumption of biochemicals and disc tissue production in the regeneration experimental groups, especially the artificial seawater regeneration group, seems to indicate that the process of regeneration runs at a set rate, and may be independent of the nutritional state of the animal (at least for the first two weeks of disc regeneration). A similar phenomenon has recently been reported in crinoids under field conditions (Meyer, 1988). These observations imply that early replacement of initial disc tissues and structures has priority over the maintenance of body mass. Since these observations coincide temporally with appearance of the functional gut (Dobson and Stancyk, in prep), one can conclude that the animal tries to replace the gut so it can feed again regardless of its initial nutritional state. Only when resources drop below some critical level (*i.e.*, the actual onset of starvation) do they stop regenerating the disc. This experiment should be repeated with animals that have been held without food sources for varying lengths of time to determine whether regeneration is even initiated after the critical point in the food withdrawal period has passed.

Regeneration appears to require a set amount of nutrients, which are transported from the deep tissues of all the non-regenerating body parts. If food is present (as DOM in this case) the loss of material due to translocation may be offset by uptake. Further, after the gut lining is reformed and becomes functional, ingestion of particulates, including small bacteria, may ameliorate the loss of stored nutrients.

A previous attempt to verify and quantify nutrient translocation into the disc from somatic body parts during disc regeneration in *M. gracillima* was unsuccessful (Clements, 1988). That study relied on the assumption that loss of organic material from the arms would result in a decrease in total arm size. This assumption was based on the results of Turner and Murdoch (1976) and the observation that echinoid test diameter decreases during starvation (Ebert, 1967). However, a loss of arm tissue without a reduction in overall arm size has been demonstrated in starving asteroids (Lawrence *et al.*, 1986). Thus, the internal soft tissues of asteroid arms are scavenged while leaving the calcified structures in place. Indeed, the arms of asteroids have been implicated as general nutrient storage organs (Beijnink and Voogt, 1984; Lawrence, 1987). If the non-regenerating body parts of *M. gracillima* are fulfilling a similar role, then translocation of organic material from the non-regenerating body parts should occur without an overall decrease in body part size or inorganic (=ASH) weight. The calcification of tissues in marine invertebrates is also a relatively expensive process compared to the production of soft tissues, due to the energetics of mineralization and the cost of producing the skeletal matrix (Simkiss, 1976; Palmer, 1983; Lawrence, 1987). Consequently, we would expect the calcified structures of *M. gracillima* to be conserved even as its soft tissues are degraded to supply catabolic and regenerative nutrients. Because the entire external surface of *M. gracillima* is covered with plate ossicles and spines, the shape and size of body parts would not change much as the soft tissues are degraded inside the structures. The absence of change in the ash weight of all the body parts of all animals in the current study supports this hypothesis.

Abnormal regeneration and death of specimens in the nutrient-enriched experimental groups is perplexing, but has been verified by repeated experimentation (Clements, 1988; K. Fielman, pers. comm.). Because preliminary experiments indicated that these conditions promoted bacterial growth (Clements, 1988), we took care to inhibit such growth by completely changing the medium each day. Several researchers have proposed that echinoderm regeneration requires the presence of functional nerve fibers that produce recognition and regulatory molecules (Bisgrove *et al.*, 1988; P. Mladenov, pers. comm.). Abnormally high ambient concentrations of nutrients (especially amino acids, which can act as neurotransmitters) may have directly affected the regeneration process by interfering with the actions of these recognition molecules.

Uptake of ^{14}C-leucine and ^{14}C-glucose indicated that dissolved organic material is taken up in statistically significant amounts in all treatments. The results agree closely with those of Clements (1988) for net uptake of the amino acids leucine and glycine by *M. gracillima.* However, her study showed significant retention of the labeled compound over time. The current results indicate that the initially retained labeled molecules are rapidly turned over or leaked back into the medium, with little permanent incorporation of the labeled molecules into the tissues and no translocation of the labeled material to the active regeneration site. The labeled compounds may have been transported in quantities below the detected threshold of the assay method. We do not know whether the loss of label from non-regenerating tissues is due to leakage or respiration, because the experiment was not designed to test for respired $^{14}CO_2$ or for an increase in the label content of the medium with time. We would understand this process better if the ^{14}C-leucine, ^{14}C-glucose, and $^{14}CO_2$ evolved in the medium during the post-absorption portion of the experiment had been assayed to determine what fraction of the material taken up by the animals was catabolized or leaked out.

The absence of detectable translocation of radiolabeled material into regenerating tissue indicates that, if the labeled material is not simply leaking out of the body [which

is not expected to be the case based on the results obtained by Clements (1988)], then the material may have been absorbed only into the surface tissue layers of the body, and not subsequently transported into the deeper tissues. Several investigators have proposed such DOM absorption as a mechanism by which echinoderms, which have poor circulatory systems, maintain their external tissues (Ferguson, 1982b; Bamford, 1982). In these models, DOM feeds the external tissues, but is not transported into the deep tissues, whereas material ingested and digested is not transported to the surface layers but supplies nutrients only to the internal tissues. Because the current results, and the results of previous work on regeneration (Dobson and Stancyk, in prep), indicate that nutrients are translocated from the deep tissues of the non-regenerating body parts—probably by coelomocytes of the water-vascular system—the lack of label in the regenerating disc may be ascribed to its inability to migrate into the deep tissues and thus to be available for regeneration.

Disc autotomy is probably a predator avoidance mechanism (Turner *et al.*, 1981). Because the disc (or at least the gut) is needed for feeding, some mechanism should be available to replace it after escape-response disc autotomy, irrespective of the nutritional state of the animal. Such an effect has been demonstrated in this and a previous set of experiments (Dobson, Stancyk, and Clements, in prep). In addition, because *M. gracillima* is a seasonal spawner (pers. obs.), selection for rapid replacement of the disc structures to facilitate replacement of gonads and gametes would be expected. Because these animals lose up to one-fourth of their available body organic mass during early regeneration, a massive amount of body reserves must enter the process. However, a significant amount of the reserves must be used for maintenance metabolism. This study shows that, although these animals do have some energy storage resources (because the starving and regenerating animals still produce disc tissue), there is still no specific nutrient storage organ or tissue. Without additional exogenous nutrient input, these stores are depleted within about two weeks, a sufficient time for replacement of the gut and initiation of feeding, even when particulate and dissolved exogenous organic material is absent.

Acknowledgments

This work would not have been possible without the facilities of the Biology Department of U.S.C. and the Belle W. Baruch Institute. This work was supported in part by a Grant from the Slocum-Lunz Foundation of South Carolina to W. E. Dobson, and in part from a National Institute of Health Biomedical Research Support Grant (grant #BSR-8514326) to S. E. Stancyk, W. E. Dobson, R. M. Showman, and L. A. Clements. Field assistance was provided by K. Zimmerman and K. Fielman. Special thanks to L. F. Dobson for gestalt support.

Literature Cited

Bamford, D. 1982. Epithelial absorption. Pp. 317–330 in *Echinoderm Nutrition*, M. Jangoux and J. M. Lawrence, eds. A. A. Balkema, Rotterdam.

Barnes, H., and J. Blackstock. 1973. Estimation of lipids in marine animals and tissues: detailed investigation of the sulphophosphovanillin method for "total" lipids. *J. Exp. Mar. Biol. Ecol.* **12:** 103–118.

Beijnink, F. B., and P. A. Voogt. 1984. Nutrient translocation in the sea star: whole-body and microautoradiography after ingestion of radiolabeled leucine and palmitic acid. *Biol. Bull.* **167:** 669–682.

Bisgrove, B. W., P. V. Mladenov, S. K. Asotra, and R. D. Burke. 1988. Wound healing and regeneration following arm-tip amputation in the sea star *Leptasterias hexactis*. P. 788 in *Echinoderm Biology: Proceedings of the Sixth International Echinoderm Conference*, R. D. Burke, P. V. Mladenov, P. Lambert, and R. L. Parsley, eds. Victoria, 23–28 August.

Bradford, M. M. 1976. A rapid and sensitive method for the quantification of protein utilizing the principle of protein dye-binding. *Anal. Biochem.* **72:** 248–254.

Brody, S. 1964. *Bioenergetics and Growth.* Hafner, New York. 1023 pp.

Brown, B. K. 1982. Gut replacement during disc regeneration of the autotomized disc of *Ophiophragmus filograneus* (Echinodermata: Ophiuroidea). Unpublished master's thesis, Florida Institute of Technology, Melbourne, 90 pp.

Cavanaugh, G. M. 1965. *Formulae and Methods V. of the Marine Biological Laboratory Chemical Room.* Mar. Biol. Lab., Woods Hole, Mass. 87 pp.

Clements, L. A. J. 1988. Uptake and utilization of dissolved free amino acids by the brittlestar *Microphiopholis gracillima* (Say, 1852) (Echinodermata: Ophiuroidea). Unpublished Ph.D. dissertation, University of South Carolina. 116 pp.

Clements, L. A. J., Fielman, K. T., and S. E. Stancyk. 1988. Regeneration by an amphiurid brittlestar exposed to different concentrations of dissolved organic material. *J. Exp. Mar. Biol. Ecol.* **122:** 47–61.

Crisp, D. J. 1984. Energy flow measurements. Pp. 284–372 in *Methods for the Study of Marine Benthos*, N. A. Holme and A. D. McIntyre, eds. Blackwell Scientific Publications, Oxford.

Cummins, K. W., and Wuycheck, J. C. 1971. Caloric equivalents for investigations in ecological energetics. *Int. Ass. Theor. App. Limnol.* Vol 18. 162 pp.

Davis, E. M. 1988. Protein assays: a review of common techniques. *Am. Biotech. Lab.* **5:** 28–37.

Dobson, W. E. 1984. Nervous mediation of disc autotomy in *Ophiophragmus filograneus* (Echinodermata: Ophiuroidea). M.S. Thesis, Florida Institute of Technology, Melbourne. 68 pp.

Dobson, W. E. 1985. A pharmacological study of neural mediation of disc autotomy in *Ophiophragmus filograneus* (Lyman) (Echinodermata: Ophiuroidea). *J. Exp. Mar. Biol. Ecol.* **94:** 223–232.

Dubois, M., K. A. Gilles, J. K. Hamilton, P. A. Rebers, and F. Smith. 1956. Colorimetric method for determination of sugars and related substances. *Anal. Chem.* **28:** 350–356.

Duineveld, G. C. A., and G. J. Van Noort. 1986. Observations on the population dynamics of *Amphiura filiformis* (Ophiuroidea: Echinodermata) in the southern North Sea and its exploitation by the Dab, *Limanda limanda*. *Neth. J. Sea Res.* **20:** 85–94.

Ebert, T. A. 1967. Negative growth and longevity in the purple sea urchin *Strongylocentrotus purpuratus* (Stimpson). *Science* **157:** 557–558.

Ekert, R., and D. Randall. 1978. *Animal Physiology.* Freeman, San Francisco. 558 pp.

Emson, R. H., and I. C. Wilkie. 1980. Fission and autotomy in echinoderms. *Oceanogr. Mar. Biol. Ann. Review* **18:** 155–250.

Feral, J.-P. 1985. Effect of short-term starvation on the biochemical composition of the apodous holothurian *Leptosynapta galliennei* (Echinodermata): possible role of dissolved organic material as an energy source. *Mar. Biol.* **86:** 297–306.

Ferguson, J. C. 1982a. A comparative study of the net metabolic benefits derived from the uptake and release of free amino acids by marine invertebrates. *Biol. Bull.* **162:** 1–17.

Ferguson, J. C. 1982b. Support of metabolism of superficial structures through direct uptake of dissolved primary amines in echinoderms. Pp. 345–351 in *Echinoderm Biology: Proceedings of the International Echinoderm Conference,* J. M. Lawrence, ed. Tampa Bay, 14–17 September.

Gibson, A. W., and R. D. Burke. 1983. Gut regeneration by morphallaxis in the sea cucumber *Leptosynapta clarki* (Heding, 1928). *Can. J. Zool.* **61:** 2720–2732.

Giese, A. C. 1966. On the biochemical constitution of some echinoderms. Pp. 757–796 in *Physiology of Echinodermata,* R. A. Boolootian, ed. John Wiley, New York.

Lawrence, J. 1987. *A Functional Biology of Echinoderms.* Johns Hopkins University Press, Baltimore. 340 pp.

Lawrence, J., T. S. Klinger, J. B. McClintock, S. A. Watts, C. P. Chen, A. March, and L. Smith. 1986. Allocation of nutrient resources to body components by regenerating *Luidia clathrata* (Say) (Echinodermata: Asteroidea). *J. Exp. Mar. Biol. Ecol.* **102:** 47–53.

Myer, D. L. 1988. Crinoids as renewable resources: rapid regeneration of the visceral mass in a tropical reef-dwelling crinoid from Australia. Pp. 519–522 in *Echinoderm Biology: Proceedings of the Sixth International Echinoderm Conference,* R. D. Burke, P. V. Mladenov, P. Lambert, and R. L. Parsley, eds. Victoria, 23–28 August. 818 pp.

O'Conner, B., T. Bowmer, D. McGrath, and R. Raine. 1986. Energy flow through an *Amphiura filiformis* (Ophiuroidea: Echinodermata) population in Galway Bay, west coast of Ireland: a preliminary investigation. *Ophelia* **26:** 351–357.

Ostle, B. and R. W. Mensing. 1975. *Statistics in Research,* 3rd ed. Iowa State University Press. 596 pp.

Palmer, A. R. 1983. Relative cost of producing skeletal organic matrix versus calcification: evidence from marine gastropods. *Mar. Biol.* **75:** 287–292.

Simkiss, K. 1976. Cellular aspects of calcification. Pp 1–32 in *The Mechanisms of Mineralization in the Invertebrates and Plants,* N. Watabe and K. M. Wilbur, eds. Univ. of South Carolina Press.

Sokal, R. R., and F. J. Rohlf. 1981. *Biometry.* Freeman, New York, 859 pp.

Turner, R. L., and J. D. Murdoch. 1976. Potential of arms as a nutrient source for disc regeneration in brittlestars. *Am. Zool.* **16:** 288 (Abstract).

Turner, R. L., D. W. Heatwole, and S. E. Stancyk. 1981. Ophiuroid discs in stingray stomachs: evasive autotomy or partial consumption of prey? Pp. 331–335 in *Echinoderm Biology: Proceedings of the International Echinoderm Conference,* J. M. Lawrence, ed. Tampa Bay, 14–17 September.

Williams, P. J. LeB. 1975. Biological and chemical aspects of dissolved organic material in seawater. Pp. 301–363 in *Chemical Oceanography,* Vol. 2, Riley, J. P. and G. Skirrow, eds. Academic Press, London.

Reference: *Biol. Bull* **180**: 185–195. (February, 1991)

Calcium-Proton Exchange During Algal Calcification

TED A. McCONNAUGHEY[1]* AND RICHARD H. FALK[2]

[1]*Marine Biological Laboratory, Woods Hole, Massachusetts 02543, and* [2]*Botany Department, University of California, Davis, California 95616*

Abstract. Extracellular calcification by the giant celled alga *Chara corallina* may involve active Ca^{2+} extrusion from the cell in exchange for protons. The following evidence is presented: $CaCO_3$ incrustations accrete largely along the inside, facing the cell, as revealed by X-ray microanalysis using Sr^{2+} and Mn^{2+} as tracers for new mineralization. Inward proton currents are inhibited by the Ca^{2+} transport antagonists Gd^{3+} and La^{3+}. Low Ca^{2+} concentrations inhibit pH banding and photosynthesis, and solutions of low Ca^{2+} activity support more photosynthesis in the presence of additional buffered calcium. The ratio of calcification to photosynthesis in moderately alkaline solutions containing sufficient calcium remains stable at about 1.0 independent of solution Ca^{2+} concentration. Ion specific microelectrodes placed close to the calcified surface sometimes detect increases in Ca^{2+} activity coincident with decreases in proton activity. As the pCa of solution increases, the maximum pH observed at the alkaline surface increases, as does the maximum solution pH which supports electrochemical currents by the cell. Combinations of extracellular pH and pCa approach the calculated thermodynamic limits for ATP driven $2H^+/Ca^{2+}$ exchange against the cytosol.

Introduction

Ca^{2+} ATPase appears to be associated with calcification in various animals and plants (*e.g.*, Klaveness, 1976; Okazaki, 1977; Okazaki *et al.*, 1984; Kingsley and Watabe, 1985). This report explores the possibility that extracellular calcification in characean algae involves active calcium-proton exchange.

Characeans calcify as a by-product of bicarbonate assimilation from alkaline waters (Spear *et al.*, 1969; Raven *et al.*, 1986; Okazaki and Tokita, 1988). The plants extract proton equivalents from the medium along parts of their giant cells, forming alkaline patches or bands that may become heavily calcified. The proton equivalents are extruded elsewhere, forming acidic patches or bands. There, HCO_3^- is apparently protonated to form CO_2, which the plant absorbs (Walker *et al.*, 1980; Smith and Walker, 1980; Price and Badger, 1985). Pericellular carbonic anhydrase and complicated invaginations of the plasma membrane within the acid zones may facilitate CO_2 generation and absorbtion (Price *et al.*, 1985).

Characeans can be more than half $CaCO_3$ by dry weight, and as will be shown here, calcification is often stoichiometric to photosynthesis. Nevertheless, calcification physiology has been largely neglected, and calcification is generally assumed to be independent of active Ca^{2+} transport (*e.g.*, Raven *et al.*, 1986). Various evidence nevertheless suggests that active Ca^{2+} transport might be involved. First, Ca^{2+} ATPases apparently catalyze Ca^{2+} extrusion from cells in exchange for protons (Niggli *et al.*, 1982; Villalobo and Roufogalis, 1986; Rasi-Caldogno *et al.*, 1987; Dixon and Haynes, 1989). Ca^{2+} ATPase could therefore catalyze proton uptake at the site of calcification in *Chara*. Second, characeans are functionally analogous to coccolithophorid algae, which also calcify in an approximate ratio of 1:1 to photosynthesis, but do so intracellularly (*e.g.*, Sikes *et al.*, 1980). Ca^{2+} and carbon presumably traverse the cytoplasm to reach the vesicular site of calcification, and Ca^{2+} ATPase seems to be involved (Klaveness, 1976; Okazaki *et al.*, 1984). Third, molecular CO_2 apparently provides most of the precipitating carbon during calcification by various plants and animals (McConnaughey, 1989a, b, c), including *Chara* (Mc-

Received 3 April 1990; accepted 6 November 1990.

*Address communications to: Dr. Ted McConnaughey, U.S. Geological Survey, Box 25046 MS 413, Lakewood, CO 80225.

Abbreviations: CAPS = 3-(cyclohexylamino)propanesulfonate; CHES = 2-(N-cyclohexylamino)ethanesulfonate; MOPS = 2-(N-morpholino)propanesulfonate; PIPES = 1,4-piperazinediethane-sulfonate; TAPS = tris(hydroxymethyl)methylaminopropane sulfonate; TRIS = tris(hydroxymethyl)aminomethane.

Connaughey, in prep). Since HCO_3^- is more abundant in alkaline solutions, its unimportance in calcification suggests that the calcifying region can be fairly isolated from solution. The calcifying cell must therefore supply calcium, and remove the protons generated by the reaction $Ca^{2+} + CO_2 + H_2O = CaCO_3 + 2H^+$. And finally, Ca^{2+} is well known to affect characean photosynthesis and membrane properties associated with pH banding (*e.g.*, Lucas, 1976; Wiesenseel and Ruppert, 1977; Luhring and Tazawa, 1985; Bisson, 1984; Tazawa *et al.*, 1987).

A Ca^{2+} ATPase model and a more conventional proton channel model for characean calcification are illustrated in Figure 1. Both models are elaborated to fit the available data. Ca^{2+} influx into the cell, in the Ca^{2+} ATPase model, occurs within the alkaline band (Fig. 1b) to produce the observed electrogenic character of pH banding (Walker and Smith, 1977). Figure 1c, e shows the use of molecular CO_2 from the plant as the major carbon source for calcification (McConnaughey, in prep.) and the accretion of extracellular calcium deposits from the inside (demonstrated here). Figures 1d and 1f depict non-calcifying conditions, such as when Ca^{2+} or carbon levels are too low to sustain much $CaCO_3$ precipitation. The non-calcifying condition can be experimentally useful, because the H^+ fluxes measured extracellularly then reflect cellular H^+ transport most closely.

The energy (E) required for proton uptake under both models is given by:

$$E = FV(aZ_{Ca} - bZ_H) + RT \ln (Ca_i/Ca_0)^a/(H_i/H_0)^b \quad (1)$$

The terms on the right represent work done against the membrane electrical potential V, and against the membrane chemical gradients. F is the Faraday constant, "a" and "b" are the numbers of Ca^{2+} and H^+ ions transported per cycle, Z is ionic charge, R is the gas constant, and T is Kelvin temperature. Cytoplasmic and external Ca^{2+} and H^+ activities are subscripted "i" and "o," respectively.

For the proton channel model, protons are drawn into the cell by the membrane electrical potential. The thermodynamic limit for passive (E = 0) proton uptake occurs when the membrane electrical and chemical gradient energies balance, yielding a proton Nernst equation:

$$0 = FV + 2.3\ RT(pH_0 - pH_i) \quad (2)$$

For an illuminated cell in alkaline solution, the membrane potential might be around −200 mV and cytoplasmic pH_i might be about 7.5–8.0 (Smith and Raven, 1979; Spanswick and Miller, 1977; Mimura and Kirino, 1984;

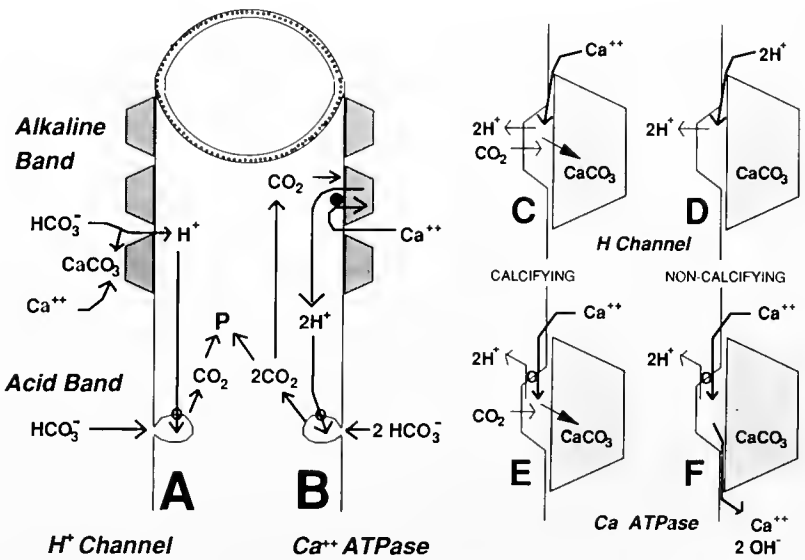

Figure 1. Models of extracellular calcification and its coupling to bicarbonate utilization in *Chara*. Left: schematic of a cell, showing alkaline band at top (with trapezoidal $CaCO_3$ incrustations), and acid band below (with plasmalemmasomes, participating in bicarbonate use). "P" represents photosynthesis. (a) Proton channel model. HCO_3^- diffuses to the alkaline surface and donates a proton, becoming converted to $CO_3^=$, which precipitates with Ca^{2+}. (b) Ca^{2+} ATPase model. ATP driven $2H^+/Ca^{2+}$ exchange alkalinizes the external medium and locally increases its Ca^{2+} concentration. CO_2 diffuses from the cell and reacts with water to yield the protons needed for exchange with Ca^{2+}, and the $CO_3^=$ which precipitates as $CaCO_3$. A 1:1 ration of calcification to photosynthesis is shown for both models. Right: elaborations on the H^+ channel and Ca^{2+} ATPase models for the alkaline band, incorporating inward accretion of $CaCO_3$ incrustations, using CO_2 as the carbon source. Proton channel (c, d) and Ca^{2+} ATPase models (e, f) showing the alkaline band under calcifying (c, e) and non-calcifying conditions (d, f). The ion fluxes detectable externally are highlighted.

Smith, 1984a, b). The maximum pH in the alkaline band would then be about 10.9–11.4, independent of solution Ca^{2+} activity.

For ATP-driven $2H^+/Ca^{2+}$ exchange, the energy of ATP hydrolysis (E) is about −50 to −55 KJ/mol (*e.g.*, Kishimoto *et al.*, 1984). The electrical term in eq. (1) drops out, leaving

$$E/2.3RT = (pCa_0 - pCa_i) - 2(pH_0 - pH_i) \quad (3)$$

Cytoplasmic $pCa_i = -\log\{Ca^{2+}_i\}$ is about 6.9 (Miller and Sanders, 1987). Equation 3 describes a line in (pH_0, pCa_0) space having a slope of 1/2, and displaced from the composition of the cytosol, (pH_i, pCa_i), by 4.4 to 4.8 pH units.

The present experiments look for evidence that $CaCO_3$ incrustations accrete from the inside, as would be expected if the plant supplies the precipitating calcium and carbon. Proton and calcium specific microelectrodes search for regions of elevated Ca^{2+} and depressed H^+ activities along the calcifying surface. The combinations of calcium and proton activities are compared with the thermodynamic constraints of ATP driven $2H^+/Ca^{2+}$ exchange against the cytosol. Calcium transport antagonists are used to inhibit proton uptake. And the stoichiometry of calcification to photosynthesis is examined to see if calcium merely diffuses to the calcification site. In the end, the Ca^{2+} ATPase model offers some advantages, but presents some interesting difficulties. The discussion touches on how the plant uses calcification as a photosynthetic adaptation.

Materials and Methods

The present experiments used male plants of *Chara corallina* from South Australia, provided by Bill Lucas. Plants were maintained in the laboratory, in aquaria initially containing "CPW/B" solution (in m*M*, $CaCl_2$ 0.2, $NaHCO_3$ 1, NaCl 1, KCl 0.2) overlying 5–20 cm mud. Nutrients and additional calcium and carbon were sometimes added to stimulate growth and calcification. Cool white fluorescent lights provided illumination.

Regions of new mineralization were identified by X-ray microanalysis. Plants first accumulated $CaCO_3$ in a medium containing (in m*M*) $CaCl_2$ 2, $NaHCO_3$ 2, $CaSO_4$ 0.2, KCl 0.2, and NaCl 1, and were then transferred to media containing additional $SrCl_2$ 1, and $MnSO_4$ 0.1, to label regions of new mineralization. Cells showing heavy calcification and good cytoplasmic streaming were rapidly frozen in liquid nitrogen slush, fractured, and given a thin coating of aluminum by vacuum evaporation (Emscope SP2000) at −196°C, to increase surface conductivity. Frozen hydrated specimens were transferred under vacuum to the cryostage of a scanning electron microscope (Hitachi S800) equipped with a solid state X-ray spectrometer (Kevex 8000 series). Secondary electron mode images provided details of surface morphology. X-ray maps, line scans, and area scans made with an accelerating voltage of 15 KeV revealed distributions of Ca, Sr, and Mn.

Rates of calcification and photosynthesis were estimated from changes in the alkalinity and total dissolved inorganic carbon content of solution. Alkalinity was measured by acidometric titration using the Gran method (Stumm and Morgan, 1970). Heavily calcified plants were incubated in stoppered flasks at 25°C under a mixture of fluorescent and incandescent lights for 6–8 h. Solutions initially contained (in m*M*/l) $NaHCO_3$ 1, NaCl 1, KCl .2, and 0–50 m*M* $CaCl_2$, pH 8 to 8.2, adjusted with NaOH. Calcification was calculated as half the change in alkalinity, and photosynthesis was calculated as the change in total carbon minus calcification.

In experiments designed to see whether buffered Ca^{2+} stimulated photosynthesis in solutions of low Ca^{2+} activity, photosynthesis was monitored using an oxygen electrode (Orion 97–08). Wide mouth jars (500 ml) containing about 5 g of algae were filled with solutions prepared from partially degassed, deionized water, and capped underwater to exclude air bubbles. Control solutions contained (in m*M*) $CaCl_2$ 0.05, KCl 0.1, NaCl 1, $NaHCO_3$ 1.8, and Na_2CO_3 0.2. Test solutions contained an additional 0.8 m*M* $CaCl_2$ and sodium citrate (1.5 m*M*). These solutions exhibited the same Ca^{2+} activity, using a Ca^{2+} specific microelectrode. A relatively high pH (9.1) ensured that the plants obtained most of their carbon through the physiology associated with pH banding. Half of the plants had been mostly decalcified before the experiment by soaking them for 2 days in a solution containing 10 m*M* MES buffer, initial pH 5.2. Cool white fluorescent lights provided illumination during 2–3 h incubations at about 25°C.

The effect of calcium transport antagonists on inward proton currents were investigated by exposing an illuminated cell to $LaCl_3$ or $GdCl_3$, while measuring proton uptake with an extracellular vibrating H^+ specific microelectrode (Kühtrieber and Jaffe, 1990). The cell was mounted in an open Petri dish (solution volume about 3 ml) and perfused at a rate of 0.08 ml/s with a solution containing, in m*M*: $CaCl_2$ 0.2, KCl 0.2, NaCl 1.0, TRIS 5, pH adjusted to 8.3 with NaOH. Fiberoptic lights provided illumination. The proton electrode vibrated perpendicularly to the cell over an excursion of 10 μ, at a frequency of 0.5 Hz, at a distance of about 10 μm from the cell. 4 μMoles of the lanthanide was added to the input stream without changing flow rate. The signal here is the voltage difference registered by the electrode as it moves back and forth near the cell. A proton gradient of one pH unit within the sampled region ideally yields a signal of about 58 mV, although in practice the signal is smaller. Fluxes of proton equivalents carried by H^+, OH^-, and protonated TRIS buffer were calculated from Fick's

first law, using diffusion coefficients 93, 53, and 7×10^{-6} cm^2/s, respectively, and concentrations calculated from the measured pH. In the case illustrated, the pH at the electrode was about 9 before adding the lanthanides. The voltage field arising from net charge uptake by the alkaline band introduces only a small bias to the pH signal; relative to background solution, the alkaline band might show a voltage differential of about −4 mV, while the pH gradient of around 2 units produces a voltage signal of about −120 mV.

Ca^{2+} and H^+ activities at the alkaline surface of the cell were measured using stationary ion specific microelectrodes, constructed as described by Borelli *et al.* (1985). Electrodes were connected to a high impedance amplifier (World Precision Instruments FD223), with output to a chart recorder. Additional potential sensing electrodes were sometimes used as well. The pericellular electrical field (about −4 mV relative to background) biased pH and pCa measurements by about +.07 and 0.14 pCa unit, respectively. The cells were exposed to buffered solutions of various calcium concentrations, usually lacking dissolved inorganic carbon to discourage calcification. Fiber optic lights provided illumination.

In experiments comparing pericellular pH against a thermodynamic model for $2H^+/Ca^{2+}$ exchange, the pH data represent the highest values observed during electrode scans of the cell surface, and during observations of several minutes duration at particularly alkaline locations. Solution pCa was calculated from solution Ca^{2+} concentrations and ionic strength, using Davies' individual ion activity coefficient (see Stumm and Morgan, 1970), or measured using an Orion 93–20 electrode for solutions containing citrate. In experiments comparing simultaneous variations in pericellular pH and pCa, H^+ and Ca^{2+} electrodes were placed close together near the alkaline surface of the cell, and the intensity of pH banding either fluctuated spontaneously or was modulated by turning the light off and on. In the examples shown, the medium contained MOPS (5 m*M*) and citrate (2 m*M*), plus NaOH and $CaCl_2$ to produce pH 7.98, pCa 3.89.

Extracellular electrical currents were measured using a vibrating probe electrometer (Jaffe and Nuccitelli, 1974). The probe vibrated perpendicular to the cell surface, approximately 30–50 μm from the cell while the cell moved by on a motorized stage. Fiberoptic lights provided illumination. Most experiments used nominally carbon-free solutions containing (in m*M*) KCl 0.2, NaCl 1, and a zwitterionic buffer (MOPS, PIPES, EPPS, CHES, or CAPS, 5 m*M*), pH adjusted to the desired value using NaOH. At the chosen concentration of $CaCl_2$ (0.1–50 m*M*), the cell was repeatedly scanned along its length for electrical activity while solutions of progressively higher pH or Ca^{2+} concentration were added. The cell was allowed to adjust in each solution for at least 30 min. Electrical currents were calculated from the electrical conductivity of solution, using Ohm's law. The example shown used a divided chamber, so that opposite halves of the cell were exposed to different solutions. Cytoplasmic streaming between the two halves was uninterrupted. The "control" half was bathed in CPW/B, while the "test" half went from CPW/B to carbon-free solutions containing zwitterionic buffers and 20 m*M* $CaCl_2$ at progressively higher pH.

Results

Mineralization patterns

Calcified cells exposed to solutions enriched in Sr and Mn accumulate significant Sr and Mn mainly along the inward surface of $CaCO_3$ incrustations (Figs. 2, 3, 4). This distribution suggests metal transport from the cell to the extracellular site of deposition, although diffusion along the cell wall is also possible. Mn/Sr ratios are spatially variable, suggesting some elemental segregation during transport or precipitation. This is indicated by variations in the relative intensities of their X-ray peaks observed in area scans. Some of this variability is visible in the X-ray maps presented in Figure 3.

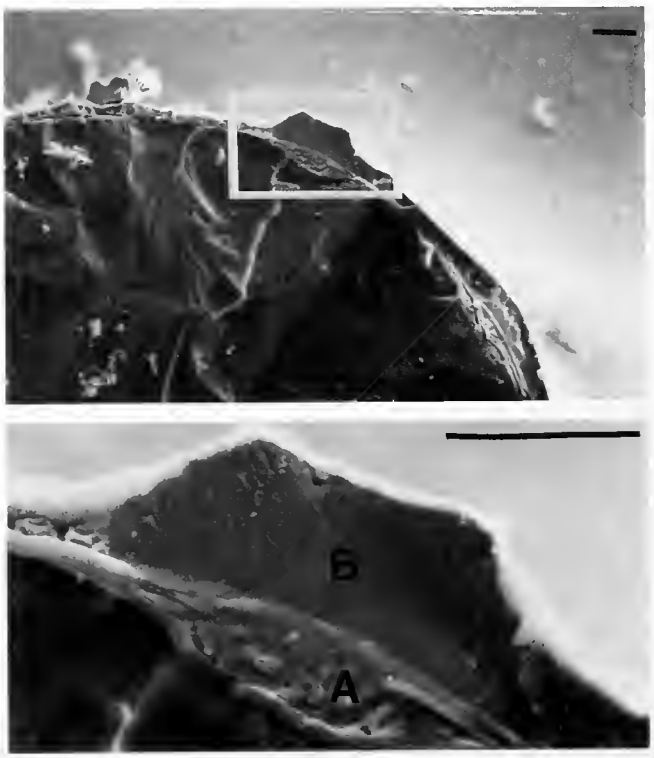

Figure 2. Scanning electron micrograph of frozen, hydrated cell labeled with Sr^{2+} and Mn^{2+}, showing extracellular $CaCO_3$ incrustations, with inward dimpling of the cell and apparent duplication of the cell wall. Magnification: top 162×, bottom 830×. Scale bar = 30 μ.

Figure 3. Distributions of Ca (yellow), Sr (blue), and Mn (red) in an extracellular $CaCO_3$ deposit, visualized by X-ray mapping of a frozen, hydrated cell exposed to Sr^{2+} and Mn^{2+} after first accumulating significant $CaCO_3$.

Sr and Mn accumulations presumably consist of divalent metal carbonates and MnO_2, the latter inferred from its dark color. Manganese oxidation, $Mn^{2+} + H_2O + \frac{1}{2}O_2 = MnO_2 + 2H^+$, is favored in the alkaline, oxygen-rich environment of the plant surface. More or less pure Mn accumulations, based on relative X-ray counts for

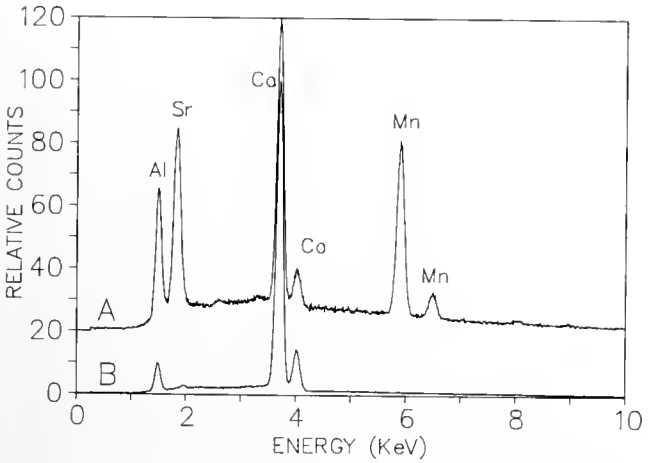

Figure 4. X-ray spectra taken at points "A" and "B" of cell shown in Figure 2. Spectra correspond to materials deposited after (A) and before (B) addition of Sr^{2+} and Mn^{2+} to the medium. X-ray counts are scaled relative to the Ca peak (100%); spectrum A has been shifted upwards by 20% for clarity.

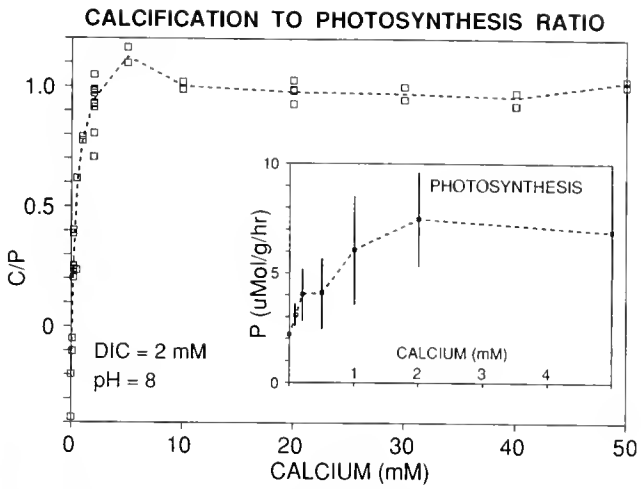

Figure 5. Ratio of calcification to photosynthesis near pH 8 as a function of Ca^{2+} concentration. Inset: inhibition of photosynthesis by low Ca^{2+} concentrations. Error bars: 1 S.D.

Mn, Sr, and Ca, sometimes occur beneath $CaCO_3$ incrustations, even when the incubating medium contains considerably more Ca^{2+} and Sr^{2+}. Mn enrichment may reflect kinetics of transport or precipitation, and was probably assisted by oxidation of Mn^{2+} to Mn^{4+}, thus producing a less soluble, non-transportable cation.

Indentations of the cell and apparent duplications of the cell wall sometimes occur underneath $CaCO_3$ incrustations (Fig. 2). Non-calcified regions of the cell lack such features. Calcification within the cell wall may force the plasma membrane inward, followed by the secretion of a new wall. This scenario again suggests $CaCO_3$ accretion to the inward side of $CaCO_3$ incrustations, and $CaCO_3$ adhesion to the cell wall.

Physiological stoichiometry

The molar ratio of calcification to photosynthesis (C/P), determined using the pH-alkalinity method, is relatively constant at about 1.0 for Ca^{2+} concentrations between 2 and 50 m*M* (pH 8, 1 m*M* $NaHCO_3$) (Fig. 5). Controls (dark, no algae, or boiled algae) show little calcification, even at 50 m*M* $CaCl_2$.

The Ca^{2+} ATPase model (Fig. 1) correctly predicts the 1:1 C/P ratio, provided the calcifying region is fairly isolated from bulk solution. Each CO_2 precipitated at the alkaline band yields $2H^+$, which the plant uses to generate $2CO_2$ at the acid band. Calcification uses one CO_2, leaving one for photosynthesis, yielding a 1:1 C/P ratio. The proton channel model would predict lower C/P ratios, increasing with Ca^{2+} concentration, because a diffusion pathway must exist to the calcifying region. OH^- and $CO_3^=$ can therefore diffuse away. These results consequently favor the Ca^{2+} ATPase model.

Proton cycling involves calcium

Low Ca^{2+} concentrations inhibit photosynthesis (Fig. 5, inset). This inhibition appears to involve Ca^{2+} fluxes, because plants incubated at the same low Ca^{2+} activity show more photosynthesis if additional buffered Ca^{2+} is added to solution (Table I). The rate of photosynthesis and the stimulation by buffered Ca^{2+} are greater with calcified than with decalcified plants (two way ANOVA, both factors and interactions significant at $P < 0.05$).

Proton uptake at the alkaline band, measured using a vibrating H^+ specific electrode, is inhibited by the Ca^{2+} transport antagonists Gd^{3+} and La^{3+} (Fig. 6). In this example, the electrode was positioned over a point showing particularly strong alkalinization. Gd^{3+} reduced the signal registered by the vibrating electrode by about half, but the cell soon recovered about 80–90% of its former signal. Subsequent treatment with La^{3+} reduced the signal more strongly, and H^+ uptake did not recover for over an hour. Before adding the lanthanides, the voltage difference signal registered by the vibrating electrode (about 7 mV at pH 9) corresponds ideally to a flux of proton equivalents around 2 nMoles cm^{-2}/s, carried mostly by OH^- and TRIS buffer (calculation, Fig. 6 inset).

The alkaline bands of *Chara* can turn on and off independently, sometimes without obvious provocation, so reductions in the pH gradient are not necessarily proportional to pathology. The pH gradient is also affected by $CaCO_3$ dissolution at the plant surface, and by ion pairing and precipitation of the introduced lanthanides. The effects here appear to be mostly physiological, however. Perfusion of the chamber should have brought solution pH back to normal within a few minutes (theoretical dilution time about 38 s).

An approximately 2–3 min oscillation in apparent H^+ influx is observed in this experiment (Fig. 6). Such oscillations are detected using various techniques (Fisahn *et al.*, 1989), and can sometimes be induced by adding Ca^{2+} to the medium.

Electrochemical detection of calcium efflux

Both the Ca^{2+} ATPase and proton channel models predict Ca^{2+} diffusion toward the alkaline surface under calcifying conditions. The Ca^{2+} ATPase model also predicts localized Ca^{2+} efflux, which, in principle, should be detectable with Ca^{2+} specific microelectrodes. This efflux might be difficult to detect, however. It may occur underneath $CaCO_3$ crystals or within an endomembrane system, and calcification may consume it before it is detected externally. More importantly, Ca^{2+} influx and efflux must both occur within the alkaline band to produce its electrogenic character (Fig. 1b), regionally cancelling the Ca^{2+} efflux signal. Therefore, detection requires a local asymmetry between Ca^{2+} influx and efflux under non-calcifying conditions (Fig. 1f).

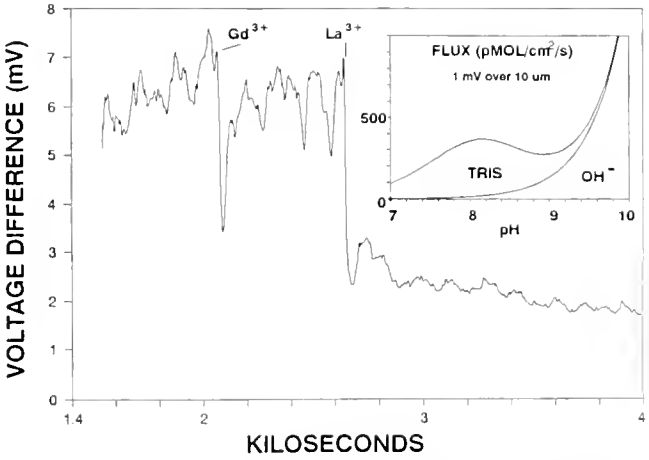

Figure 6. Inhibition of proton influx by La^{3+} and Gd^{3+}, measured with a vibrating proton specific electrode. Ordinate: voltage difference registered by the electrode between the extremes of its 10 micron excursion perpendicular to the cell. Inset: apparent proton influx calculated from a diffusion model, as a function of pH at the probe, for a signal of 1 mV over an excursion of 10 microns. Fluxes scale almost linearly with excursion and voltage.

Such conditions encourage $CaCO_3$ dissolution and Ca^{2+} leaching from the cell wall. The resulting increase in pericellular Ca^{2+} concentration may be confused with the effects of $2H^+/Ca^{2+}$ exchange. The former effect will be most pronounced at low pH, while the latter will be associated with high pH. Simultaneous pH observations are therefore needed to distinguish these two cases.

Increases in Ca^{2+} activity (pCa decreases) are often observed coincident with pH decreases (Fig. 7a), suggesting Ca^{2+} leaching or $CaCO_3$ dissolution. Small drops in pCa are also observed coincident with pH increases (Fig. 7b), suggesting $2H^+/Ca^{2+}$ exchange. At one point in the case illustrated, the apparent pericellular Ca^{2+} activity increases about 30% as the pH rises from 8.2 to 9.8. The actual Ca^{2+} activity presumably increased even more, because the alkaline band develops a pericellular electrical field of around −4 mV when it turns on. This biases the Ca^{2+} electrode toward higher apparent pCa by about $-4/-28 = 0.14$ pCa unit. The increase in pericellular Ca^{2+} due to

Table I

Stimulation of photosynthesis by buffered calcium, at low solution calcium activity. Photosynthesis estimated by oxygen evolution, in micromoles O_2 per gram wet weight per hour, with standard deviation (n = 10)

	Solution		
	Unbuffered	Buffered	Change
Calcified	6.43 ± 0.67	8.11 ± 0.68	+26%
Decalcified	4.48 ± 0.10	5.29 ± 0.41	+18%

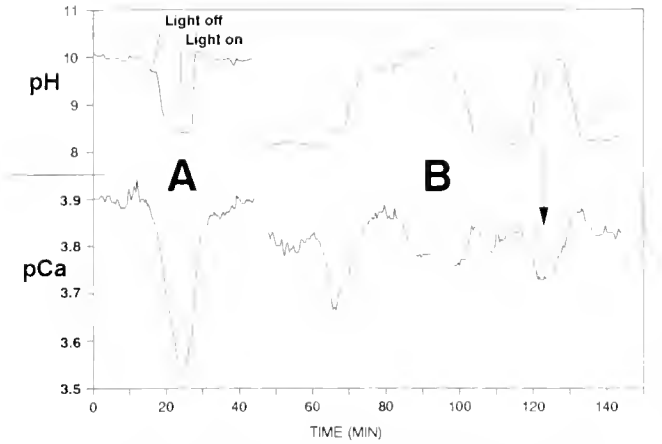

Figure 7. Extracellular pH and pCa measured with stationary ion specific electrodes placed close to the calcified surface of a cell under non-calcifying conditions. (A) Positive correlation between pH and pCa, probably caused by increased $CaCO_3$ dissolution or leaching at low pH. (B) Anticorrelation between pH and pCa, suggesting calcium-proton exchange.

$2H^+/Ca^{2+}$ exchange must also be sufficient to overcome the decrease in pericellular Ca^{2+} at high pH, caused by reductions in $CaCO_3$ dissolution and Ca^{2+} leaching from the cell wall.

Thermodynamics

The maximum pH observed at the alkaline surface using microelectrodes approaches the thermodynamic limit for ATP driven $2H^+/Ca^{2+}$ exchange, calculated using eq. 3 (Fig. 8). The approach is closest at high solution Ca^{2+} activities (low pCa). As pCa^{2+} increases, the maximum pH also increases, although not as much as allowed by thermodynamics. At pCa >4, higher pH readings are obtained in the presence of the weak Ca^{2+} buffer citrate, suggesting that the rate of Ca^{2+} supply to the cell may limit proton uptake. All pericellular pH, pCa observations fall within the thermodynamic constraints for ATP driven $2H^+/Ca^{2+}$ exchange, and the Ca^{2+} dependence for pericellular pH provides some support for the Ca^{2+} ATPase model.

The pH and pCa in large culture vessels containing *Chara* also approach the calculated thermodynamic limits for $2H^+/Ca^{2+}$ exchange (Fig. 8). The most extreme conditions observed (pH 10.78, pCa 4.30) are close to the most extreme conditions observed at the cell surface with microelectrodes. Rather high pericellular pH (about 10.7) is observed transiently in Ca^{2+} free solutions, but pH banding eventually collapses, consistent with a Ca^{2+} requirement for banding. Internal Ca^{2+} stores, perhaps supplemented by $CaCO_3$ dissolution and Ca^{2+} leaching from the cell wall, may support banding for awhile.

Extracellular electrical currents

The ion fluxes associated with pH banding create extracellular current loops which can be measured with a vibrating probe electrometer. These currents persist until solution pH is raised above a critical value, at which point the currents cease or may reverse with much diminished amplitude. The solution pH at which current cessation occurs varies with solution Ca^{2+} activity in more or less the same way as the extracellular pH data in Figure 8. The Ca^{2+} dependence suggests that proton uptake is coupled to Ca^{2+} expulsion.

Presumably, as $2H^+/Ca^{2+}$ exchange becomes impossible, cytosolic Ca^{2+} rises and inhibits Ca^{2+} influx (see Eckert and Chad, 1984). The proton ATPase of the acid band shuts down as the cytoplasm becomes alkalinized (due to cessation of proton uptake) and the membrane potential increases (due to cessation of Ca^{2+} uptake). Consequently, even though $2H^+/Ca^{2+}$ exchange is electrically silent, preventing this exchange can stop extracellular electrical activity.

Figure 9 illustrates an experiment in which a cell is placed in a divided chamber, and increasingly alkaline solutions containing 20 m*M* $CaCl_2$ (pCa = 2.1) are applied to the right (test) side. The left (control) side remains at pH 8.2, pCa = 3.8. Cytoplasmic streaming between the two sides is uninterrupted. As the test side approaches the calculated thermodynamic limits for ATP driven $2H^+/Ca^{2+}$ exchange, its currents diminish, but currents on the control side are unaffected. In the last test solution (pH 10.0, pCa 2.1), banding is strongly suppressed and an ap-

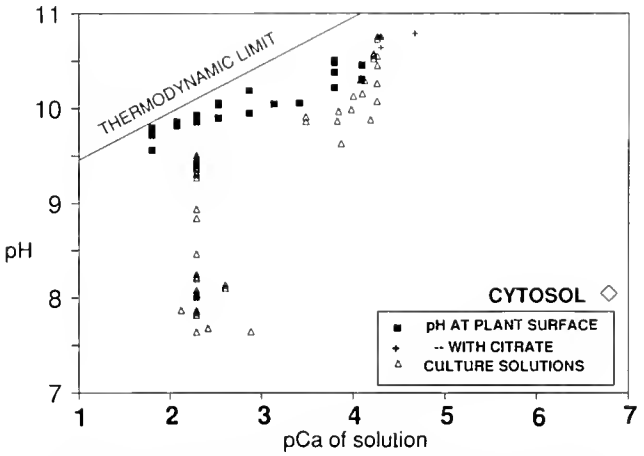

Figure 8. pH observations at the alkaline surface as a function of solution Ca^{2+} activity. Diagonal line: calculated thermodynamic limits for ATP driven $2H^+/Ca^{2+}$ exchange between the cytosol and external solution, assuming E(ATP) = 50 KJ/mol. Symbols: (Diamond) assumed cytosolic composition, pH = 8, pCa = 6.9. (Squares) maximum pH observed at alkaline surface under experimental conditions, without citrate. (+) Same, with citrate. (△) Combinations of solution pH and pCa observed in large vat cultures.

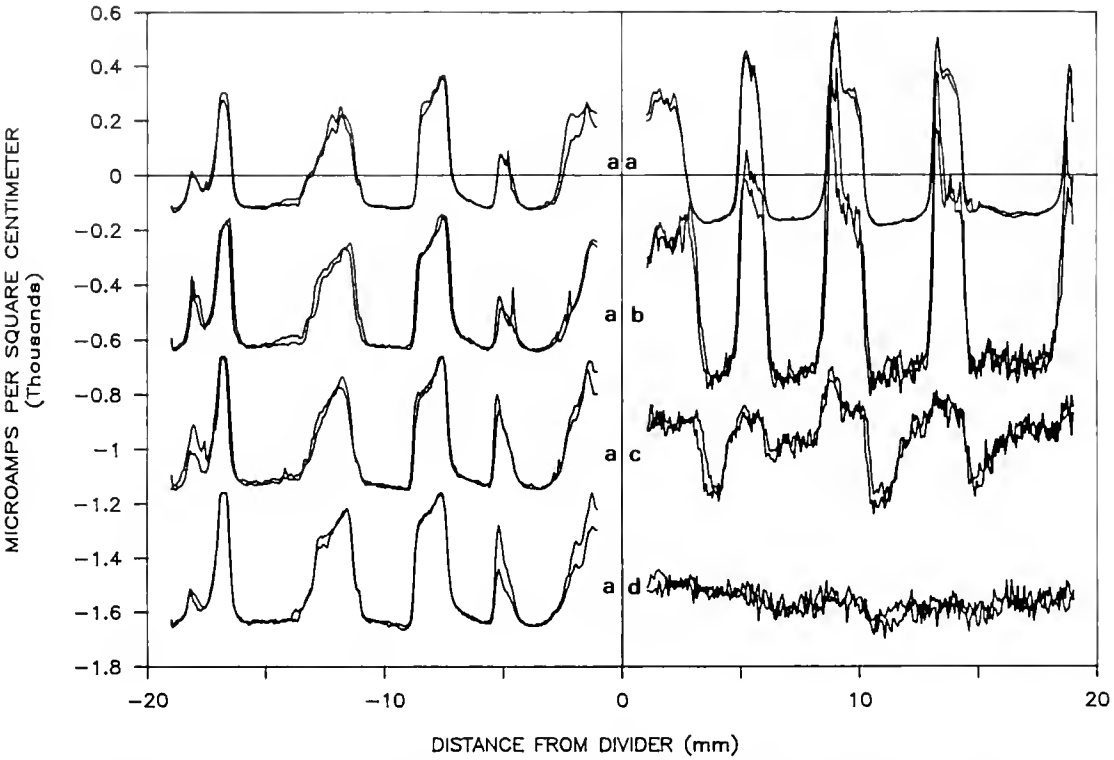

Figure 9. Extracellular currents measured using a vibrating voltage probe. Cell was placed in a divided chamber, and solution on the right side was replaced with solutions having higher Ca^{2+} activity and progressively higher pH. Duplicate scans are shown in each medium, and cell responses to different media are offset by $-500\ \mu A/cm^2$. Positive currents denote regions of positive current influx to cell (alkaline bands). Solutions contained (in m*M*) NaCl 1, KCl 0.2, plus the following additions: (a) $CaSO_4$ 0.2, $NaHCO_3$ 1, pH 8.2, (b) $CaCl_2$ 20, CHES 5, pH 9.0, (c) $CaCl_2$ 20, CAPS 5, pH 9.8, (d) $CaCl_2$ 20, CAPS 5, pH 10.0).

parent efflux of positive charge prevails over the test side of the cell. The control side does not appear to compensate, so if real, this current efflux should hyperpolarize the cell.

Discussion

Antecedents to the Ca^{2+} ATPase model for *Chara* extend back at least to 1829, when Bishoff (cited in Pringsheim, 1888) suggested that characean lime deposits grow from the inside. Classical works on bicarbonate use also favored calcium and carbon movement through the polarized leaves of calcareous aquatic angiosperms and characeans to reach the site of mineralization (Arens, 1933, 1938, 1939). Kishimoto *et al.* (1984) suggested that proton uptake in *Chara* might occur through an electroneutral proton cotransport or countertransport system. Many aspects of the Ca^{2+} ATPase model have therefore been discussed.

The Ca^{2+} ATPase model correctly predicts the data presented here. Sr^{2+} and Mn^{2+} accumulate largely along the inner surface of $CaCO_3$ incrustations, facing the cell. Increasing the Ca^{2+} concentration in solution (from 2 to 50 m*M*) has a minimal effect on the ratio of calcification to photosynthesis, suggesting that diffusion to the calcification site can be minimal. Ca^{2+} transport antagonists interfere with H^+ uptake. In solutions of low Ca^{2+} activity, additional "buffered" Ca^{2+} enhances photosynthesis and proton uptake. Pericellular Ca^{2+} activities sometimes increase simultaneously with stronger alkalization. Combinations of extracellular Ca^{2+} and H^+ activities are thermodynamically compatible with ATP driven $2H^+/Ca^{2+}$ exchange, and the maximum pH at the alkaline band increases with pCa, as would be expected if Ca^{2+} extrusion accompanies proton uptake.

Most of the precipitating carbon also appears to be supplied by the cell as CO_2 (McConnaughey, in prep.). This further implies that the calcifying region can become isolated from bulk solution. Consequently, the cell must supply Ca^{2+}, and remove protons in 1:2 stoichiometry, as indicated by the reaction $Ca^{2+} + CO_2 + H_2O = CaCO_3 + 2H^+$.

The data are less supportive of the proton channel model, which offers no explanation for the Ca^{2+} dependence of photosynthesis, or the elevations of pericellular Ca^{2+} coincident with H^+ depletion. The diffusion pathway

to the site of calcification creates additional conceptual problems. Why won't it accept OH^- and $CO_3^=$, which should diffuse away from the cell, reducing the ratio of calcification to photosynthesis to values below 1.0, and making it dependent on the Ca^{2+} concentration, or phosphate, which fails to precipitate where Sr and Mn do (McConnaughey, in prep.)?

Most of the published data appears compatible with the Ca^{2+} ATPase model. Both models attribute the extracellular current influx in the alkaline band largely to Ca^{2+} under calcifying conditions, and to H^+ equivalents under non-calcifying conditions (Fig. 1). Membrane hyperpolarizations are caused by electrogenic H^+ extrusion in the acid band under either model. Increased membrane conductivity at high pH (Bisson and Walker, 1980, 1982) might result from more favorable thermodynamics for the proton ATPase of the acid band, reversibility of $2H^+/Ca^{2+}$ exchange, and perhaps opening of additional ion channels (*e.g.*, Kikuyama *et al.*, 1984).

Calcium transport

Certain caveats apply to the thermodynamic analysis of Ca^{2+} transport attempted here. Pericellular pCa varies locally, and depressions relative to solution values are likely at high pCa (Fig. 7). Cytoplasmic pH and pCa may also vary. Extracellular and intracellular activity scales may be offset with respect to each other. The slope of the extracellular pH data is closer to 1/3 than 1/2, but pH is too high for ATP driven $3H^+/Ca^{2+}$ exchange. $4H^+/2Ca^{2+}$ exchange is likewise excluded. Several factors may contribute to the fall-off from the limits calculated for $2H^+/Ca^{2+}$ exchange at high pCa. As noted above, Ca^{2+} extrusion may locally depress pCa below ambient values. Ca^{2+} diffusion toward the cell may limit the rate of Ca^{2+} and H^+ cycling, as suggested by the higher pH values and photosynthetic rates obtained with buffered Ca^{2+}. Finally, the diffusion of alkalinity from the plant surface increases enormously as pericellular pH increases (see Fig. 6 inset), so if the proton flux remains constant, diffusion should reduce pericellular pH most strongly at high pCa. In summary, there are many reasons why the data might fall short of the thermodynamic limit, even if the plant operates close to the limit. The more interesting feature is that the plant apparently approaches the thermodynamic limit.

Why are extracellular H^+ fluxes so much easier to detect than Ca^{2+} fluxes? The difference, presumably, is that Ca^{2+} influx and efflux occur close together, while proton fluxes must be separated to create the acid bands needed for bicarbonate assimilation. Proton electrodes are also twice as sensitive as Ca^{2+} electrodes, and proton fluxes should be twice as large.

The Ca^{2+} ATPase model postulates high rates of Ca^{2+} cycling through the cell, around 100 pMol cm^{-2} s^{-1} within the alkaline band of *Chara*. $^{45}Ca^{2+}$ exchange rates are generally less than 3 pMol cm^{-2} s^{-1}, measured over the whole cell (Spanswick and Williams, 1965, Hayama *et al.*, 1979; MacRobbie and Banfield, 1988). Some experiments employed conditions unfavorable to pH banding, but the disparity between inferred and published steady state $^{45}Ca^{2+}$ fluxes nevertheless requires further study. Low Ca^{2+} exchange rates may be caused by containment of fluxes to the cortical cytoplasm of the alkaline band, with little exchange into major cellular Ca^{2+} reservoirs such as the vacuole, chloroplasts, or mitochondria. The available evidence supports this possibility. Extracellular electrical currents presumably reflect Ca^{2+} uptake mainly within the alkaline bands. When cells are placed in a divided chamber with Mn^{2+} on one side, Mn precipitation is visible only on that side, suggesting minimal transport along the cell. $^{45}Ca^{2+}$ fluxes measured during repeated electrical stimulation yield values around 60 pMol cm^{-2} s^{-1}, measured over the whole cell, at 1 m*M* external Ca^{2+} (Hayama *et al.*, 1979). The metabolic machinery needed for large fluxes therefore appears to be present.

An analogy to coccolithophorid algae is instructive. Calcification in these algae occurs within intracellular vesicles, so both calcium and carbon presumably traverse the cytoplasm to reach the calcification site. Ca^{2+} ATPase apparently participates in calcification (Klaveness, 1976; Okazaki *et al.*, 1984). Sufficient data are sometimes available to estimate Ca^{2+} fluxes. For example, *Emiliania huxleyi* calcifies at a rate of around $5–7 \times 10^{-18}$ moles/s, and the surface area of the finished coccolith is around $1–1.5 \times 10^{-7}$ cm^2 (Paasche, 1964; Klaveness, 1976; Sikes *et al.*, 1980). Therefore, the trans-membrane Ca^{2+} flux may be 30–50 pMol cm^{-2} s^{-1}. This is of the same magnitude as estimated for *Chara*.

Because cytosolic "free" Ca^{2+} concentrations are uniformly rather low, large trans-cellular Ca^{2+} fluxes presumably involve Ca^{2+} rich vesicles, vacuoles, reticula, etc. Total Ca^{2+} concentrations in characean cytoplasm and vacuoles is in the millimolar range (Okihara and Kiyosawa, 1988). To the extent that cytosolic free ion concentrations pose a transport problem, the issue may be more acute with protons. The proton fluxes are presumably twice as large and involve longer distances.

Applicability to other organisms

If Ca^{2+} ATPase underlies extracellular calcification in *Chara* and intracellular calcification in coccolithophorids, it might contribute similarly elsewhere. For example, large Ca^{2+} dependent proton influxes, sensitive to lanthanides, also occur at the calcified rhizoid of the siphonaceous marine alga *Acetabularia* (McConnaughey, in prep.).

Coupling calcification to photosynthesis

Although a photosynthetic organism may loose CO_2 to calcification, it gains two protons for each carbon lost. In

mildly alkaline waters, these $2H^+$ potentially enable it to convert $2HCO_3^-$ to $2CO_2$, yielding a net gain of one CO_2 for photosynthesis. An approximately 1:1 ratio of calcification to photosynthesis is observed not only in *Chara*, but sometimes also in coccolithophorid algae (Paasche, 1964; Sikes *et al.*, 1980), calcareous seaweeds (Pentecost, 1978), and invertebrate-algae symbioses (Goreau, 1963; Barnes and Taylor, 1973; Duguay and Taylor, 1978; Kuile *et al.*, 1989). In the symbioses, the animal calcifies while the algae use the CO_2. Rapid and massive calcification may exceed structural or defensive uses for $CaCO_3$, and coccolithophorids, for example, discard excess scales to remain suspended in the water. Corals build up huge skeletal mounds but occupy only the top few millimeters. No structural or defensive use of $CaCO_3$ is obvious in *Chara*.

Proton cycling theoretically allows organisms to generate pericellular CO_2 concentrations well above ambient (Walker *et al.*, 1980). Photosynthesis generally saturates at CO_2 concentrations higher than the atmospheric equilibrium value (*e.g.*, Smith and Walker, 1980), and far higher than present in many natural waters subjected to strong photosynthesis. Elevating CO_2 concentrations (by protonating HCO_3^-) therefore increases carboxylation rate. Many aquatic plants and invertebrate-algae apparently promote photosynthesis through proton cycling. In this context, protons, rather than $CaCO_3$, may be the principle product of calcification.

From a geochemical perspective, biologically precipitated carbonates comprise one of the more abundant crustal materials, and represent the principle biogeochemical reservoir for carbon (Garrels *et al.*, 1976). Because organisms often calcify much faster than the ambient media in which they live, biological calcification may provide an important brake on the photosynthetic alkalinization of natural waters, and thereby affect such processes as the partitioning of CO_2 between the oceans and the atmosphere.

Aeknowledgments

Primary funding was provided through NSF fellowship DCB-8807613 to Ted McConnaughey. W. J. Lucas and L. F. Jaffe contributed laboratory facilities. The authors are grateful to J. Fisahn, W. Kühtreiber, A. Miller, and A. Shipley, for their assistance, and to D. McCorkle, A. Kuzerian, C. Barr, and others for their enthusiasm and helpful comments.

Literature Cited

Arens, K. 1933. Physiologisch polarisierter Massenaustausch und Photosynthese bei submersen Wasserpflanzen. I. *Planta* **20:** 621–658.

Arens, K. 1938. Manganablagerungen bei Wasserpflanzen als Folge des Physiologisch polarisierten Massenaustausches. *Protoplasma* **30:** 104–129.

Arens, K. 1939. Physiologische Multipolaritat der zelle von *Nitella* wahrend der Photosynthese. *Protoplasma* **33:** 295–300.

Barnes, D. J., and D. L. Taylor. 1973. *In situ* studies of calcification and photosynthetic carbon fixation in the coral *Montastrea annularis*. *Helgol Wiss Meeresunters* **24:** 284–291.

Bisson, M. A. 1984. Calcium effects on electrogenic pump and passive permeability of the plasma membrane of Chara corallina. *J. Membrane Biol.* **81:** 59–67.

Bisson, M. A., and N. A. Walker. 1980. The *Chara* plasmalemma at high pH. Electrical measurements show rapid specific passive uniport of H^+ or OH^-. *J. Membrane Biol.* **56:** 1–7.

Bisson, M. A., and N. A. Walker. 1982. Control of passive permeability in the *Chara* plasmalemma. *J. Exp. Bot.* **33:** 520–532.

Borelli, M. M., W. G. Carlini, W. C. Dewey, and R. R. Ransom. 1985. A simple method for making ion-selective microelectrodes suitable for intracellular recording in vertebrate cells. *J. Neurosci. Methods* **15:** 141–154.

Dixon, D. A., and D. H. Haynes. 1989. Ca^{2+} pumping ATPase of cardiac sarcolemma is insensitive to membrane potential produced by K^+ and Cl^- gradients but requires a source of counter-transportable H^+. *J. Membr. Biol.* **112:** 169–183.

Duguay, L. E., and D. L. Taylor. 1978. Primary production and calcification by the soritid foraminiferan *Archais angulatus* (Fichtel & Moll). *J. Protozool.* **25:** 356–361.

Eckert, R., and J. E. Chad. 1984. Inactivation of Ca channels. *Prog. Biophys. Molec. Biol.* **44:** 215–267.

Fisahn, J., T. McConnaughey, and W. J. Lucas. 1989. Oscillations in extracellular current, external pH, and membrane potential and conductance in the alkaline bands of *Nitella* and *Chara*. *J. Exp. Bot.* **40:** 1185–1193.

Garrels, R. M., A. Lerman, and F. T. Mackenzie. 1976. Controls of atmospheric CO_2 and O_2: past, present, and future. *Am. Sci.* **64:** 306–315.

Goreau, T. F. 1963. Calcium carbonate deposition by coralline algae and corals in relation to their roles as reef-builders. *Ann. N. Y. Acad. Sci.* **107:** 127–167.

Hayama, T., T. Shimmen, and M. Tazawa. 1979. Participation of Ca^{2+} in cessation of cytoplasmic streaming induced by membrane excitation in *Characeae* internodal cells. *Protoplasma* **99:** 305–321.

Jaffe, L. F., and R. Nuccitelli. 1974. An ultrasensitive vibrating probe for measuring extracellular currents. *J. Cell. Biol.* **63:** 614–628.

Kingsley, R. J., and N. Watabe. 1985. Ca-ATPase localization and inhibition in the gorgonian *Leptogorgia virgulata* (Lamarck) (Coelenterata; Gorgonacea). *J. Exp. Mar. Biol. Ecol.* **93:** 157–167.

Kishimoto, U., N. Kami-iki, Y. Takeuchi, and T. Ohdawa. 1984. A kinetic analysis of the electrogenic pump of *Chara corallina*: I. Inhibition of the pump by DCCD. *J. Membrane Biol.* **80:** 175–183.

Klaveness, D. 1976. *Emiliania huxleyi* (Lohman) Hay and Mohler. 3. Mineral deposition and the origin of the matrix during coccolith formation. *Protistologica* **12:** 217–224.

Kühtreiber, W. M., and L. F. Jaffe. 1990. Detection of extracellular calcium gradients with a calcium specific vibrating electrode. *J. Cell Biol.* **110:** 1565–1573.

Kuile, B. ter, J. Erez, and E. Padan. 1989. Mechanisms for the uptake of inorganic carbon by two species of symbiont-bearing foraminifera. *Mar. Biol.* **103:** 241–251.

Lucas, W. J. 1976. The influence of Ca^{2+} and K^+ on $H^{14}CO_3^-$ influx in internodal cells of *Chara corallina*. *J. Exp. Bot.* **27:** 32–42.

Lühring, H. and M. Tazawa. 1985. Effect of cytoplasmic Ca^{2+} on the membrane potential and membrane resistance of Chara plasmalemma. *Plant Cell Physiol.* **26:** 635–646.

MacRobbie, E. A. C., and J. Banfield. 1988. Calcium influx at the plasmalemma of *Chara corallina*. *Planta* **176:** 98–108.

McConnaughey, T. A. 1989a. Biomineralization mechanisms. Pp. 57–73 in *The Origin, Evolution, and Modern Aspects of Biomineralization in Animals and Plants*, R. E. Crick, ed. Plenum Press, New York.

McConnaughey, T. A. 1989b. ^{13}C and ^{18}O isotopic disequilibrium in biological carbonates. I. Patterns. *Geochim. Cosmochim. Acta* **53:** 151–162.

McConnaughey, T. A. 1989c. ^{13}C and ^{18}O isotopic disequilibrium in biological carbonates. II. *In vitro* simulation of kinetic isotope effects. *Geochim. Cosmochim. Acta* **53:** 163–171.

Miller, A. J., and D. Sanders. 1987. Depletion of cytosolic free calcium induced by photosynthesis. *Nature* **326:** 397–400.

Mimura, T., and Y. Kirino. 1984. Changes in cytoplasmic pH measured by ^{31}P-NMR in cells of *Nitellopsis obtusa*. *Plant Cell Physiol.* **25:** 813–820.

Niggli, V., E. Sigel, and E. Carafoli. 1982. The purified Ca^{2+} pump of human erythrocyte membranes catalyzes an electroneutral Ca^{2+}-H^+ exchange in reconstituted liposomal systems. *J. Biol. Chem.* **257:** 2350–2356.

Okazaki, M. 1977. Some enzymatic properties of Ca^{2+}-dependent adenosine triphosphatase from a calcareous marine alga, *Serraticardia maxima* and its distribution in marine algae. *Bot. Mar.* **20:** 347–354.

Okazaki, M., M. Fujii, Y. Usuda, and K. Furuya. 1984. Soluble Ca^{2+} activated ATPase and its possible role in calcification in the coccolithophorid *Cricosphaera roscoffensis var. Haptonemofera* (Haptophyta). *Bot. Mar.* **27:** 363–369.

Okazaki, M., and M. Tokita. 1988. Calcification of *Chara braunii* (Charophyta) caused by alkaline band formation coupled with photosynthesis. *Jpn. J. Phycol.* **36:** 193–201.

Okihara, K., and K. Kiyosawa. 1988. Ion composition of the *Chara* internode. *Plant Cell Physiol.* **29:** 21–25.

Paasche, E. 1964. A tracer study of the inorganic carbon uptake during coccolith formation and photosynthesis in the coccolithophorid *Coccolithus huxleyi*. *Physiol. Plant. Supp.* **III:** 5–82.

Pentecost, A. 1978. Calcification and photosynthesis in *corallina officinalis* L. using the $^{14}CO_2$ method. *Br. Phycol. J.* **13:** 383–390.

Price, G. D., and M. R. Badger. 1985. Inhibition by proton buffers of photosynthetic utilization of bicarbonate in *Chara corallina*. *Aust. J. Plant Physiol.* **12:** 257–267.

Price, G. D., M. R. Badger, M. E. Bassett, and M. I. Whitecross. 1985. Involvement of plasmalemmasomes and carbonic anhydrase in photosynthetic utilization of bicarbonate in *Chara corallina*. *Aust. J. Plant Physiol.* **12:** 241–256.

Pringsheim, N. 1888. Uber die Entstehung der Kalkencrustationen an Susswasserpflanzen. *Jahrb. Wissensch. Bot.* **19:** 138–154.

Rasi-Caldogno, F., M. C. Pugliarello, and M. I. De Michelis. 1987. The Ca^{2+}-transport ATPase of plant plasma membrane catalyzes a nH^+/Ca^{2+} exchange. *Plant Physiol.* **83:** 994–1000.

Raven, J. A., F. A. Smith, and N. A. Walker. 1986. Biomineralization in the Charophyceae *sensu lato*. Pp. 125–139 in *Biomineralization in Lower Plants and Animals*, B. S. C. Leadbeater and R. Riding, eds. Clarendon Press, Oxford.

Sikes, C. S., R. D. Roer, and K. M. Wilbur. 1980. Photosynthesis and coccolith formation: inorganic carbon sources and net inorganic reaction of deposition. *Limnol. Oceanogr.* **25:** 248–261.

Smith, F. A. 1984a. Regulation of the cytoplasmic pH of *Chara corallina*: response to changes in external pH. *J. Exp. Bot.* **35:** 43–50.

Smith, F. A. 1984b. Regulation of the cytoplasmic pH of *Chara corallina* in the absence of external Ca^{2+}: its significance in relation to activity and control of the H^+ pump. *J. Exp. Bot.* **35:** 1525–1536.

Smith, F. A., and J. A. Raven. 1979. Intracellular pH and its regulation. *Ann. Rev. Plant Physiol.* **30:** 289–311.

Smith, F. A., and N. A. Walker. 1980. Photosynthesis by aquatic plants: effects of unstirred layers in relation to assimilation of CO_2 and HCO_3^- and to carbon isotope discrimination. *New Phytol.* **86:** 245–259.

Spanswick, R. M., and A. G. Miller. 1977. Measurement of the cytoplasmic pH in *Nitella translucens*. *Plant Physiol.* **59:** 664–666.

Spanswick, R. M., and E. J. Williams. 1965. Ca fluxes and membrane potentials in *Nitella translucens*. *J. Exp. Bot.* **16:** 463–473.

Spear, D. G., J. K. Barr, and C. E. Barr. 1969. Localization of hydrogen ion and chloride ion fluxes in *Nitella*. *J. Gen. Physiol.* **54:** 397–414.

Stumm, W., and J. J. Morgan. 1970. *Aquatic Chemistry*. Wiley-Interscience, New York. 583 pp.

Tazawa, M., T. Shimmen, and T. Mimura. 1987. Membrane control in the characeae. *Ann. Rev. Plant Physiol.* **38:** 95–117.

Villalobo, A., and B. D. Roufogalis. 1986. Proton countertransport by the reconstituted erythrocyte Ca^{2+}-translocating ATPase: evidence using ionophoretic compounds. *J. Membr. Biol.* **93:** 249–258.

Walker, N. A., and F. A. Smith. 1977. Circulating electrical currents between acid and alkaline zones associated with HCO_3^- assimilation in *Chara*. *J. Exp. Bot.* **28:** 1190–1206.

Walker, N. A., F. A. Smith, and I. R. Cathers. 1980. Bicarbonate assimilation by fresh-water charophytes and higher plants: I. Membrane transport of bicarbonate ions is not proven. *J. Membr. Biol.* **57:** 51–58.

Wiesenseel, M. H., and H. K. Ruppert. 1977. Phytochrome and calcium ions are involved in light-induced membrane depolarization in *Nitella*. *Planta* **137:** 225–229.

CONTENTS

Volume 180 Number 2

THE BIOLOGICAL BULLETIN

APRIL, 1991

Published by the Marine Biological Laboratory

THE
BIOLOGICAL BULLETIN

PUBLISHED BY
THE MARINE BIOLOGICAL LABORATORY

APRIL, 1991

Printed and Issued by
LANCASTER PRESS, Inc.
PRINCE & LEMON STS.
LANCASTER, PA

Erratum

The Biological Bulletin, Volume **179**, Number 3, pages 358 and 363

The following corrections should be made in the article by William J. Kuhns *et al.* titled, "Biochemical and functional effects of sulfate restriction in the marine sponge, *Microciona prolifera*" (*Biol. Bull.* **179:** 358–365). Due to a printing error, the last two lines of the abstract on page 358 were transposed from the first column (abstract) to the second column (introduction). We apologize for the error.

On page 363, the sentence beginning on line 7 of Figure 5 should now read "The *upper two lines* depict uptake of $^{35}SO_4$ by cells pretreated in MBL-SO_4." The words "upper two lines" replace the words "solid lines."

Reference: *Biol. Bull.* **180:** 197–199. (April, 1991)

Integrative Neurobiology and Behavior of Mollusks Symposium: Introduction, Perspectives, and Round-Table Discussion

ROGER T. HANLON

The Marine Biomedical Institute, University of Texas Medical Branch, Galveston, Texas 77550

The objective of this symposium was to bring together molluscan researchers from a wide variety of disciplines to consider the behavior of mollusks, particularly in relation to their evolutionary history and to their neural structure and function. For that reason, the symposium was convened during the 56th Annual Meeting of the American Malacological Union (AMU), attended by 280 persons and held at the Marine Biological Laboratory (MBL) in Woods Hole from 3–7 June 1990. The AMU membership includes many researchers interested primarily in systematics, phylogeny, and evolution; the MBL enjoys a long and distinguished history as a global center for molluscan neurobiological research. Thirty-two papers and seven posters were presented at this symposium, which was held concurrently with The Behavior of Mollusks symposium in which 26 papers and 12 posters were presented; selected papers from the latter symposium will be published in the *American Malacological Bulletin* during 1991. Support for the symposia was provided by the National Science Foundation (BNS 9007661) and the AMU Symposium Endowment Fund. The organizers and participants greatly appreciate this funding as well as the assistance of *The Biological Bulletin* and the hospitality of the MBL.

Perspectives

The Phylum Mollusca is large (about 100,000 living species), diverse, well represented in the fossil record (approx. 35,000 species dating to the Cambrian), and richly studied (*cf.,* Tasch, 1973; Wilbur, 1983–1988; Barnes, 1987). It is also important to man; its uses range from food to models in biomedicine. In the latter instance it has been mainly species with unusually large or easily identified neurons that have been studied so intensively. These species were well represented in the symposium; *e.g., Aplysia, Hermissenda, Navanax, Pleurobranchaea, Tritonia, Lymnaea,* and *Loligo* among several others.

Molluscan diversity offers fertile grounds for thought among evolutionary biologists, ethologists, and neurobiologists. In what other phylum can you find organisms as different as chitons, with their simple nervous system and behavior, and cephalopods, with their immensely complex nervous system and correspondingly complex and varied behavior that rival vertebrates? In the middle of this continuum, consider the marine opisthobranchiate gastropod *Aplysia* and some of its cousins, whose relatively simple behaviors are being studied even at molecular levels by thousands of researchers worldwide. The challenge, of course, is to make some sense of this dazzling diversity.

The scope and goals of the relatively new field of Neuroethology have been well reviewed by Hoyle (1984) and Bullock (1990). As Bullock (1990) explains eloquently, although neurobiologists mainly study proximate mechanisms of neural function, the implications of their findings are basic to the philosophy of science and to evolutionary biology because it is likely that the nervous system and behavior represent the system most responsible for large evolutionary leaps in the grade of complexity among higher taxa. Notwithstanding this provocative assertion, most neurobiologists do not spend much time mingling with evolutionary biologists, especially those who study the same phylum, because their professional organizations and journals are usually quite distinct. Conversely, evolutionary biologists do not often consider

proximate mechanisms of neural control of behavior or its implications in evolution. This meeting and its round-table discussion were organized to help bridge this gap among molluscan researchers.

Round-Table Discussion

Are round-table discussions worthwhile? While controversial, they are worthwhile in forcing the consideration of differing views and alternative hypotheses in a less binding way than a paper or poster presentation. I include here the briefest synopsis of our recorded 3-h session.

Can the comparative method bridge studies involving neurobiology, behavior, and evolution?

There was some consensus that proper use of homologies could provide common ground to test hypotheses across these disciplines. However, gaps in our knowledge in each broad discipline are considerable, and future progress was anticipated to be slow unless workers were willing to take evidence from many disciplines (including molecular and neural biology, behavior and ecology) and integrate it into analyses of convergence and parallelism in the Mollusca. This was one of the few points of general consensus!

Are there any uniquely molluscan behaviors?

As a matter of perspective, only a dozen or so species are being studied in detail, so generalizations about molluscan behavior seem inappropriate; no unique behaviors were mentioned. It was noted that some groups of mollusks have similar nervous system organization but apparently very different behaviors.

What is the role of behavior in evolution?

Some researchers consider behavior to be the phenotype upon which selection occurs, and the corollary is that the neural, endocrine, and related systems exist to produce behavior. Perhaps, then, homologies at different levels of organization can be used to study the role of behavior in evolution. However, several concerns were voiced about the seemingly endless variability of molluscan behavior that would make it difficult to discern homologs in any concrete fashion. How, for example, do we account for phenotypic plasticity, and what is the role of ecological constraint? One related subject of interest to many in attendance was the future need for analyses of the evolution of behavior in mollusks, taking advantage of what has been learned from paleobiology and taphonomy (Tasch, 1973) as well as recent behavioral and ecological studies of extant molluscs.

How did the nervous system evolve?

The action potential is a common feature throughout the animal phyla, from the simplest organisms to the most complex. However, pharmacological sensitivities and other properties are different in various groups and it was suggested that molecular analysis of specific differences in the relevant ion channels may eventually lead to meaningful phylogenetic relationships among different phyla. The role of peptides and other neurotransmitters in producing behavior (*e.g.*, egg laying in many mollusks) may lead to complementary findings (see recent papers in *Biological Bulletin* Vol. **177**, 1989).

Why do we find large neurons in some mollusks, and what is their functional and evolutionary significance?

One obvious function for large cells is the rapid transmission of a signal; additionally, cells must be large if they have to spread over large distances to communicate with many places. If both needs must be satisfied, giant cells like the squid axon can obviously evolve. Perhaps many of these cells are associated with relatively "simple" behaviors. There does seem to be an emerging trend that small neuron size is a requirement for complex information processing. For example, consider the cephalopod CNS and its complex integrative abilities in comparison with the vertebrate, and especially the mammalian, CNS. It is apparent that existing and future neurobiological techniques will dictate to some extent what can be studied and learned from small *versus* large neurons. There will probably continue to be philosophical disagreement about the reductionist *versus* the integrative approach to understanding how behavior is produced by the nervous system.

A thread throughout the discussion was the amazing diversity of mollusks and the difficulty in agreeing on many generalizations about neural organization and how it relates to behavior. It was suggested several times that we should appreciate this diversity and not rush to apply our findings to evolutionary principles. As Bullock (1990) has pointed out "Must we assume everything is adaptive?" Various participants echoed a recent thought that evolution does not necessarily work with the logic of engineering, but perhaps more like a tinkerer. The papers in this volume include many examples of neurobiologists evaluating evolutionary considerations of the systems that they study. Perhaps the discussions facilitated this in some small way.

Dedication

We were honored to have Professor J. Z. Young, F.R.S., of Oxford University, enrich our meeting. In the 1930s,

Figure 1. Professor J. Z. Young presenting his review of the cellular basis of learning in cephalopods.

Professor Young rediscovered the squid giant axon and performed the critical experiments demonstrating that these neurons transmitted an electrical signal; this pioneering work (performed partly at the MBL) led to the Nobel Prize by Hodgkin and Huxley in 1962 and made the squid *Loligo* a preferred research organism for thousands of neuroscientists, a trend that continues apace today. In addition to recounting this story at the banquet, Professor Young gave a rousing lecture on learning in cephalopods (Fig. 1). Delivered with panache and his usual scientific fervor, he earned a standing ovation by a packed audience in Whitman Auditorium. For his innumerable contributions to molluscan biology, Professor Young was awarded Honorary Life Membership in the AMU, a distinction bestowed upon only five members in the 56-year history of the organization. We hereby dedicate this volume to him and thank him for inspiring so many students and researchers throughout his brilliant career.

Literature Cited

Barnes, Robert D. 1987. *Invertebrate Zoology.* Fifth Edition. CBS College Publishing/Holt, Rinehart and Winston, Philadelphia, PA.

Bullock, Theodore Holmes. 1990. Goals of neuroethology. *Bioscience* **40**(4): 244–248.

Hoyle, Graham. 1984. The scope of neuroethology. *Behav. Brain Sci.* **7**: 367–412.

Tasch, Paul. 1973. *Paleobiology of the Invertebrates: Data Retrieval from the Fossil Record.* Wiley and Sons, New York.

Wilbur, Karl M. 1983–1988. *The Mollusca.* Volumes 1–12. Academic Press, New York.

Reference: *Biol. Bull.* 180: 200–208. (April, 1991)

Computation in the Learning System of Cephalopods

J. Z. YOUNG

Department of Experimental Psychology, University of Oxford, South Parks Road, Oxford OX1 3UD, United Kingdom

Abstract. The memory mechanisms of cephalopods consist of a series of matrices of intersecting axes, which find associations between the signals of input events and their consequences. The tactile memory is distributed among eight such matrices, and there is also some suboesophageal learning capacity. The visual memory lies in the optic lobe and four matrices, with some re-exciting pathways. In both systems, damage to any part reduces proportionally the effectiveness of the whole memory. These matrices are somewhat like those in mammals, for instance those in the hippocampus.

The first matrix in both visual and tactile systems receives signals of vision and taste, and its output serves to increase the tendency to attack or to take with the arms. The second matrix provides for the correlation of groups of signals on its neurons, which pass signals to the third matrix. Here large cells find clusters in the sets of signals. Their output re-excites those of the first lobe, *unless* pain occurs. In that case, this set of cells provides a record that ensures retreat.

There is experimental evidence that these distributed memory systems allow for the identification of categories of visual and tactile inputs, for generalization, and for decision on appropriate behavior in the light of experience.

The evidence suggests that learning in cephalopods is not localized to certain layers or "grandmother cells" but is distributed with high redundance in serial networks, with recurrent circuits.

Introduction

Responding appropriately in a complex environment depends upon the categorization of events and a decision of what to do. Animals with good brains have the ability to learn the useful responses to particular events that they encounter. They may not be born with receptors tuned to identify objects or situations, say a rock or a tree or a fish, but learn the classification of particular sets of stimuli by virtue of the large number of their neurons. It has been claimed that this involves simply "the spontaneous emergence of new computational capabilities from the collective behaviour of large numbers of simple processing elements" (Hopfield, 1982). Biologists will probably suspect that a genetic component is involved in the organization.

Cephalopods have such nervous systems with numerous neurons, and there is sufficient information about their arrangement to suggest how they function. Formerly, I have emphasized that the circuits in their brains must allow for the outputs from feature detectors to produce alternative effects after learning (Fig. 1). I proposed that the feature detectors must become restricted during learning to establish units of memory or mnemons. This view is correct in that it emphasizes the possibility of alternative outputs from feature detectors, but it is much too restrictive. Emphasis on units obscures the essential fact that these are systems with numerous parallel, interacting channels. It is now evident that the various lobes of the brain provide sequences of matrices of intersecting axes, with feedback. They enable the identification of categories of input and storage of records of the probable value of each, in the form of bias to particular directions of action to each set of input signals.

The principle of the matrices is to provide for selection of paths that are used and inhibition of those that are not used. This is accomplished by various means that allow interaction between pathways. One of the best analyzed systems is in the mammalian hippocampus (Fig. 2) (Rolls, 1990). In a competitive learning matrix such as the dentate gyrus, "different input patterns on the horizontal axons will tend to activate different output neurons. The tendency for each pattern to select different neurons can be enhanced by providing inhibition between the output neurons. . . . Synaptic modification then occurs . . . and

Received 7 August 1990; accepted 18 January 1991.

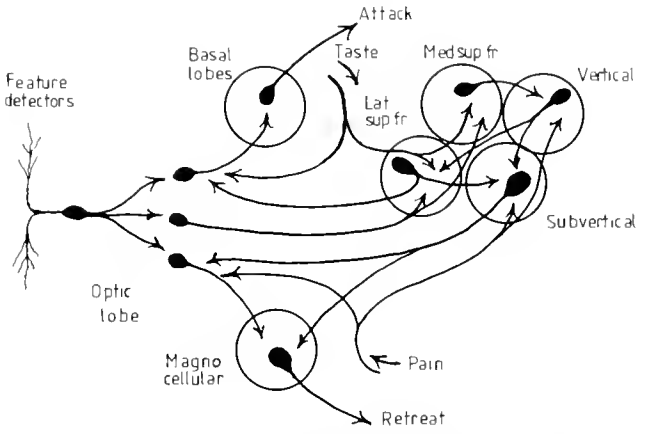

Figure 1. Scheme to show alternative pathways from the visual feature detectors of an octopus. There are output pathways for attack or retreat. A third pathway leads to the four matrices of the vertical lobe system. Here particular patterns of visual signals are combined with those of taste to increase the future tendency to attack, or with signals of pain to reduce it.

the response of the system as a categorizer climbs over repeated iterations" (Rolls, 1990).

In autocorrelation networks, such as the CA_3 cells (Fig. 2), the preferred pathways are reinforced by mutually strengthening each other. In this case, the cells of the matrix have collaterals that feed back to their own inputs. These recurrent synapses follow the Hebb rule so that "any strongly activated cell or set of cells becomes linked by strengthened synapses with any other conjunctively activated cell or set of cells" (Rolls, 1990). As a result, during recall "presentation of even part of the original pattern . . . comes to elicit the firing of the whole set of cells that were originally conjunctively activated."

In the hippocampus, this result is achieved by the collaterals of the CA_3 cells, which reactivate the dendrites of their own and a large number of other CA_3 cells. It may be that in cephalopods a similar effect is achieved by passing the signals through a series of lobes, each serving as a matrix whose output may be returned to a previous member of the series (Fig. 3). The functioning of any such matrix system depends on the particular anatomical arrangements and details of synaptic functioning and its alteration with use. We do not know enough about such factors in cephalopods to be able to specify precisely how they operate. However, the system is simple enough to allow us to follow the whole sequence through these lobes, from sense organs to motor output, and at least to speculate about its functioning.

Matrix systems of this sort have the properties that we associate with complex animal behavior. They ensure that there is *generalization:* presentation of even a part of the original figure, or one like it, activates the firing of the whole set of cells that were conjunctively activated ("*completion*"). Moreover, the system continues to operate even if some of the cells fail to operate or are removed ("*fault tolerance*"). We can show that these essential

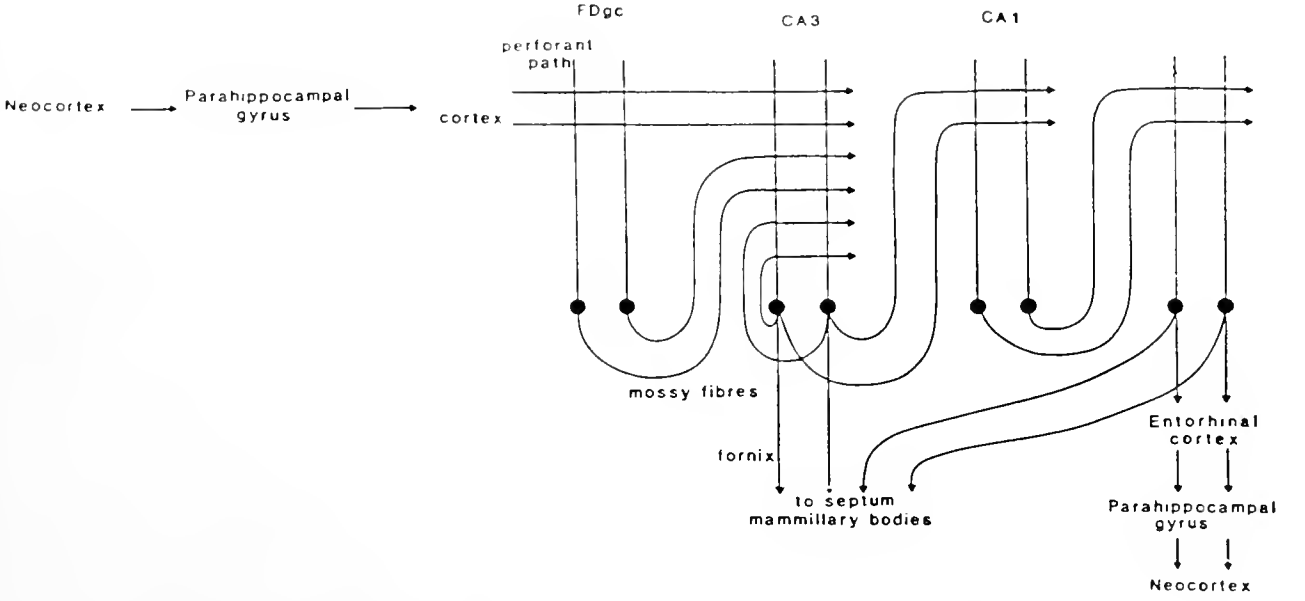

Figure 2. Schematic representation of the scheme of matrices and connections within the primate hippocampus and with the neocortex. The competitive matrix in the dentate gyrus leads to an auto association matrix formed by the CA_3 cells, which in turn lead to a competitive matrix on the CA_1 cells (From Rolls, 1990, with permission).

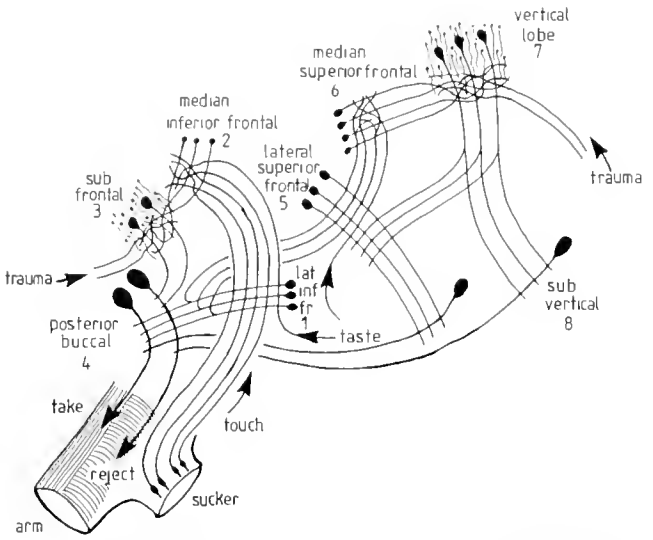

Figure 3. Diagram of the connections of the tactile memory system of *Octopus*. The successive matrices are labelled 1 to 8. In addition, there is some learning capacity in the suboesophageal centers.

properties of memory systems are present in the nervous system of octopuses.

The nervous system of an octopus provides for categorization and setting up of memories both for vision and touch. There are two distinct systems, each made up of four lobes, with elements whose arrangement can now be seen to constitute sequences of matrices (Fig. 3, 4). It was thought at one time that these were independent visual and tactile systems, but it is now clear that in tactile learning all eight lobes are involved (Young, 1983). This, therefore, constitutes a remarkable example of a distributed memory system using a series of networks. This model is rather similar to that suggested by Wells (1978). It does not depend on detailed preformed connections and so avoids problems of complex morphogenesis.

The Chemo-Tactile Memory System

Octopuses readily recognize differences in the chemical nature and texture of objects by touch, although they cannot discriminate between shapes (Wells, 1978). The receptors for touch are in the rims of the suckers (see Graziadei in Young, 1971). Their axons proceed through synapses in the arm, but no details are known of the coding signals that are sent to the brain.

In our experiments, Wells and I train octopuses to distinguish between plastic balls, either smooth or with up to thirteen incised rings (Wells, 1978; Young, 1983). We train an animal by giving it food when it takes one ball (say a smooth one) and by giving it no reward or a small electric shock for taking the other (rough) (Fig. 5). In critical experiments, the optic nerves are cut to avoid possible visual discrimination. Many of the experiments are done after the whole supraoesophageal lobe has been bisected. The arms of the two sides then learn independently and can even be trained in opposite directions.

Afferent fibers from the arms and also taste fibers from the lips cross the dendrite systems of the first tactile lobe, the lateral inferior frontal (Fig. 6, 7). The axons of the cells of this first lobe pass partly to the fourth lobe, the posterior buccal, and partly to the lateral *superior* frontal and so to the vertical lobe system (below). The fibers from the arms and lips then pass on to the second matrix, in the median inferior frontal, where they interweave and cross the trunks of a large sample of the 10^6 cells, this allows maximum opportunity for any cell of the lobe to receive signals from a variety of input fibers (Fig. 7). These median inferior frontal cells then send their axons to the third matrix, the subfrontal lobe, which contains relatively few large cells with twisted trunks and many bushy dendrites and, in addition, a great number (5×10^6) of very small amacrine cells. The subfrontal also receives numerous fibers from below, presumed to signal trauma. The large subfrontal cells send their axons to the fourth lobe, the posterior buccal, from which, in turn, large axons pass directly to the arms and cause them either to draw in or reject the object touched (Budelmann and Young, 1985). These cells must be of two sets, some causing the object touched to be drawn in, the others to reject it.

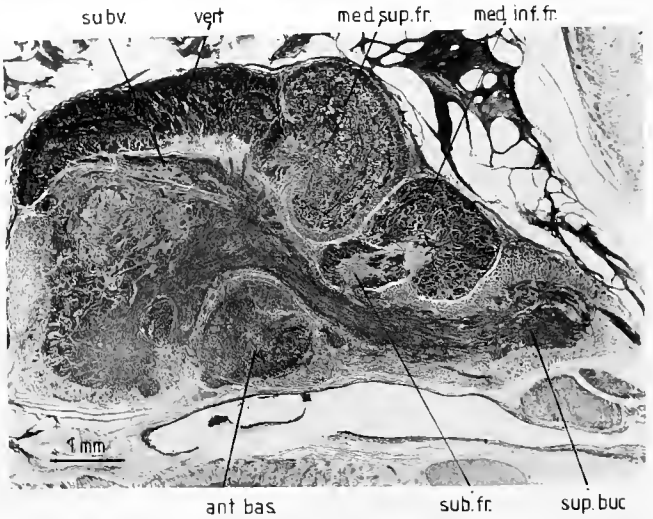

Figure 4. Sagittal section of the supraoesophageal lobe of *Octopus vulgaris* stained with Cajal's silver method. Abbreviations for all figures: ant. bas., anterior basal; b. med., median basal; buc. p., posterior buccal; cer. br. con., cerebrobrachial connective; cer. tr., cerebral tract; lat. inf. fr., lateral inferior frontal; lat. sup. fr., lateral superior frontal; mag., magnocellular; med. inf. fr., median inferior frontal; med. sup. fr., median superior frontal; op., optic; ped., peduncle; post. buc., posterior buccal; plex., plexiform layer; prec., precommissural; pv., palliovisceral; ret., retina; subfr., subfrontal; sup. buc., superior buccal; subv., subvertical; vert., vertical.

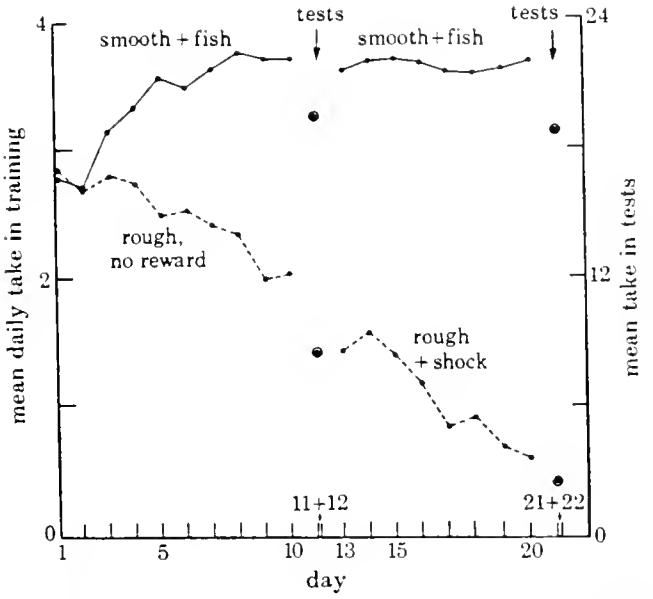

Figure 5. Sequence of learning by 129 control half brains to take a smooth ball and reject a rough. Four trials daily. On days 11 and 12, and 21 and 22, the figure shows mean takes out of 24 unrewarded tests with each ball (Young, 1983).

The basic action of the system is that an arm cautiously and slowly draws in an unfamiliar object that it touches. If this proves to provide food, the taste signals from the lips activate cells of the lateral inferior frontal, which increase the tendency to take and perhaps operate as a competitive learning matrix (like the dentate gyrus). The pattern of input and taste signals is then passed on to the median inferior frontal where that proportion of cells that receive this pattern of signals of touch and taste is activated. This can be considered a re-coding of the input pattern on to a more sparse set of cells.

The axons of these cells then proceed through the interweaving bundles to the subfrontal, where they make connection with a still smaller set of large cells with complex dendritic fields, having also an input of fibers indicating pain. If trauma occurs and these pain fibers are also activated, then the large cells of the subfrontal operate the rejection neurons of the posterior buccal lobe. The synapses activated by this particular pattern of input become consolidated, presumably by the action of the large number of amacrine cells whose short axons end among the dendrites of the larger cells of the subfrontal lobe (Fig. 6).

The basic operation of the system is thus to take objects touched *unless* signals of pain arrive. Signals of taste set up a greater tendency to take by competitive learning in the lateral inferior frontal lobe. Signals of pain set up a tendency to reject that pattern of touch by modification of synapses in the subfrontal lobe. As good evidence of this it was found that, after lesions destroyed all the small amacrine cells, an octopus failed to learn not to take objects from which shocks were received (see this paper and Wells, 1978).

The Vertical Lobe System and Touch Learning

The inferior frontal system contains the major tactile memory, but the vertical lobe also contributes. Experiments show that removal of the vertical lobe impairs the tactile memory, but removal of the median inferior frontal has no effect on visual learning.

The tactile signals enter the vertical lobe circuit through fibers from the lateral inferior frontal that enter the outer plexus of the lateral *superior* frontal lobe (Fig. 3). The vertical lobe system contains four lobes precisely similar to those we have described in the inferior frontal. The lateral superior frontal sends fibers to the subvertical lobe and from there fibers pass down the cerebral tract to the posterior buccal lobe (Fig. 6). This circuit through the lateral superior frontal is thus in a position to increase still further the tendency to take objects that have been associated with taste reward.

The signals for touch are then passed on from the lateral to the median superior frontal. Here the bundles are again interwoven, exactly as in the median *inferior* frontal. The 1.8×10^6 cells thus receive varied combinations of signals of touch and taste, and these are passed on again through

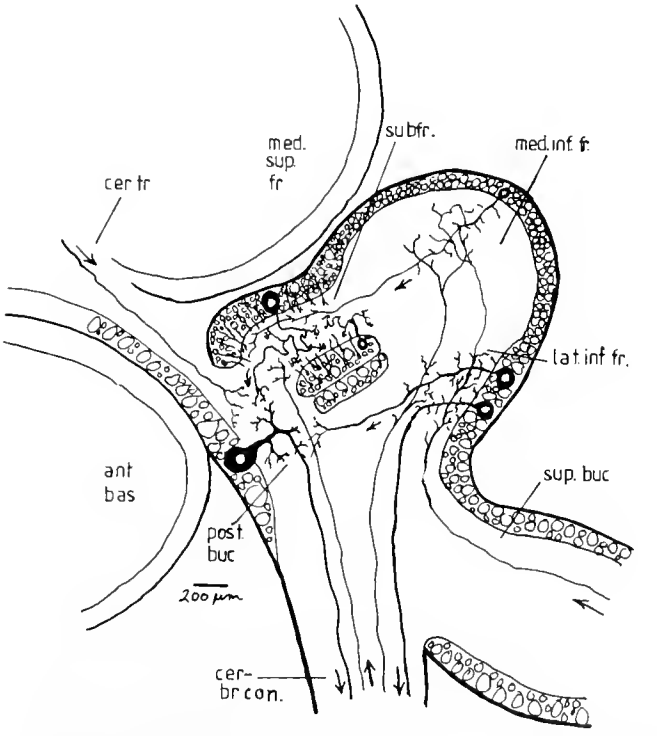

Figure 6. Diagram of connections in the inferior frontal system of an octopus (Young, 1971).

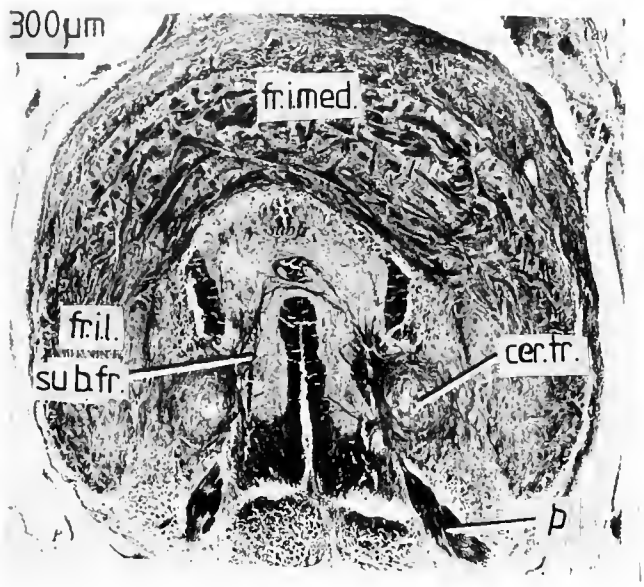

Figure 7. Transverse section of the inferior frontal system of *Octopus vulgaris* stained with Cajal's silver method. Abbreviations as Figure 4. cr. tr., cerebral tract (from subvertical lobe); p. tract of probably pain fibers from hind end of body.

a complex plexus to the vertical lobe. Here there are relatively few large cells (65,000), with complex dendrites, exactly like those of the subfrontal, and no less than 25 million amacrine cells.

The large cells send their axons down to the subvertical lobe and so to the posterior buccal, but also back to the lateral superior frontal (Fig. 3). This circuit evidently plays some part in re-enforcing the conjunctions, possibly by maintaining particular patterns by re-excitation.

The Distributed Tactile Learning System

The system for touch learning thus includes no less than eight distinct lobes with matrix structure (Fig. 3). The relative parts played by the various lobes was studied over a number of years in a large number of animals with divided brains. Lesions were made on one side, and the other was left as a control. In many of the experiments, discrimination was between completely smooth balls (0 rings) and those with 13 incisions. The sequence of training for 129 normal sides is shown in Figure 5.

A useful measure of the extent and reliability of discrimination is to give a series of 24 extinction tests with balls of differing roughness, shown at short intervals (1–3 min) without any reward. Such tests are arduous to give, but they show that habituation proceeds more slowly in proportion to similarity of each ball to the one for which reward was previously given (Fig. 8). The capacity for discrimination was also tested by using more nearly similar balls, with 4 and 7 rings. With long training, octopuses could probably make some discrimination even between a difference of one ring.

By such tests we can compare the discrimination by animals after various lesions. Without the median inferior frontal there is still discrimination, but it is much less accurate than in control animals (Fig. 9). Removal of the vertical lobe also reduces accuracy, although to a lesser extent. Clearly each of the lobes through which the information passes adds something to the effectiveness of the representations that are formed, as would be expected from a system of matrices.

Animals without vertical lobes show errors largely when they take the negative ball, showing again that this lobe serves to increase the effectiveness of shocks. In normal octopuses, learning is possible even if rewards are delayed for up to 30 s after the ball has been removed. In animals without vertical lobes, such delay is no longer possible (Wells and Young, 1968). The re-excitation within the vertical lobe system serves to maintain the necessary excitability for a Hebb type of learning.

We have used this technique to make a large number of experiments, leaving one side as a control. With this technique it is possible to remove the subfrontal lobe, which cannot be approached laterally. The effect is to produce a complete inability to learn on that side: there is a strong and irreversible preference for the rougher balls (Young, 1983). The lobe evidently has some specific effect on the coding and discrimination process.

After cutting the cerebro-brachial tract (Fig. 6), the whole influence of the inferior frontal and vertical systems is removed. Nevertheless, there is still a slight capacity for learned discrimination (Fig. 10), which must lie in the suboesophageal ganglia, or in the arms themselves. This residual learning is difficult to study. Animals with these

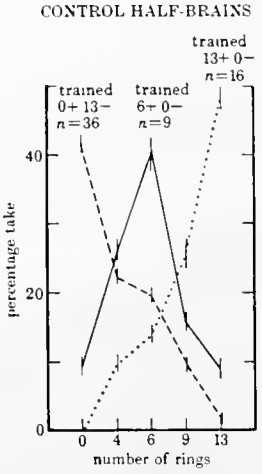

Figure 8. Tests after training in three different directions. Means and standard errors of ratios of takes of each ball to total takes, with 24 trials with each ball. The bars show standard errors.

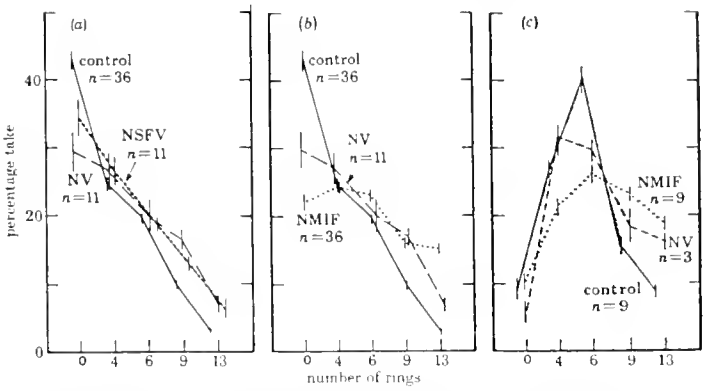

Figure 9. Tests after training. Comparison of results (a): 11 animals after cutting the tract between superior frontal and vertical lobes on one side (NSFV) and removing the vertical lobe (NV) on the other side; 36 controls for comparison (b): 36 animals after removing the median inferior frontal (NMIF); controls and NV added for comparison. In a & b, all training was with smooth balls positive and 13 rings negative. In (c) balls with six rings were positive and smooth balls negative. The figure shows the results for nine animals with the median inferior frontal removed on one side three animals with no vertical lobe on one side added for comparison. Note that here (and Fig. 8) the balls with 9 and 13 rings were seldom taken, although they had not been associated with shock.

large operations do not feed well and tend to hold pieces of food and other objects close to the mouth. Nevertheless, the differences in numbers of takes of the balls during tests are significant and show that some learning has occurred.

Some measure of the accuracy of the memory after the various lesions is given by the difference between the takes of the rough and smooth balls in the tests (Table I). Using the difference in controls as a standard (100%), we can judge that animals without vertical lobes are rather less than half as efficient, without the median inferior frontal are one third as efficient, and that the suboesophageal contribution is about one sixth. Damage to the subfrontal produces a perverse effect.

The Visual Memory System

The vertical lobe system, which plays a part in tactile learning, forms, with the optic lobes, the main and only component of the visual learning system. The existence of this double capacity is a striking demonstration of the power of such a distributed matrix system to store a variety of inputs. It will be very interesting to investigate whether individual cells of the vertical lobe system play a part in both systems. In a study of combined visual and tactile training, no mutual interactions between the two modalities was seen (Allen *et al.*, 1986).

The study of visual memory is made difficult by the complexity of the connections in the optic lobes, which are not fully understood. Cells with large tangential dendrites in the plexiform layer probably act as feature detectors (Fig. 11). Their axons form columns proceeding to the center of the lobe, where they interact in an interweaving matrix of cells and fibers. Second or third order visual neurons then send axons to the central nervous

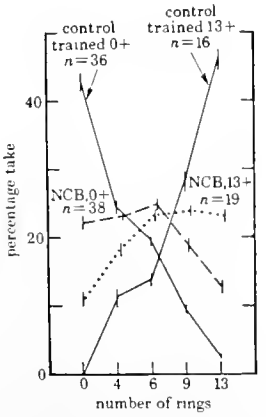

Figure 10. Tests after training. Comparison of control sides with those with the cerebrobrachial tracts cut (NCB).

Table I

Mean takes in final tests after various lesions

Lobe removed	Smooth ball (positive)	Rough ball (negative)	Difference	Percent accuracy remaining
None (controls)	20.22	2.44	17.78	100
Vertical	17.68	10.55	7.13	40
Median inferior frontal	16.32	10.69	5.63	32
Cerebro-brachial tract	13.78	10.94	2.84	16
Subfrontal	7.89	8.42	−0.53	—

The last column indicates the capacity for learned discrimination that remains after the lesions, estimated as a percentage of the differences in the controls.

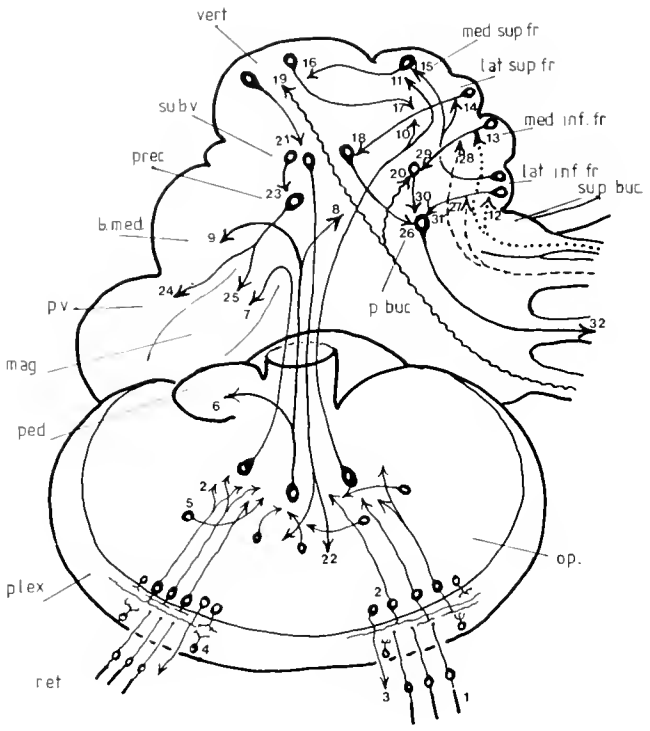

Figure 11. Diagram of the connections of the visual and tactile learning system of an octopus. 1, retina; 2, second order visual cells (feature detectors); 3, centrifugal cells; 4, amacrine cells; 5, tangential cells; 6, optic-peduncle; 7, optic-magnocellular; 8, optic-anterior basal; 9, optic-median basal; 10, optic-lateral superior frontal; 11, optic-median superior frontal; 12, taste fibers-lateral inferior frontal; 13, taste fibers median inferior frontal; 14, lateral inferior frontal-lateral superior frontal; 15, lateral inferior frontal-median superior frontal; 16, median superior frontal-vertical; 17, vertical-lateral superior frontal; 18, lateral superior frontal-subvertical; 19, pain fibers-vertical; 20, pain fibers-subfrontal; 21, vertical-subvertical; 22, subvertical-optic; 23, subvertical-precommissural; 24, precommissural-palliovisceral; 25, precommissural-magnocellular; 26, subvertical-posterior buccal; 27, chemo-tactile fibers-lateral inferior frontal; 28, chemo-tactile fibers-median inferior frontal; 29, median inferior frontal-subfrontal; 30, subfrontal-posterior buccal; 31, lateral inferior frontal-posterior buccal; 32, motor fibers from posterior buccal to arms.

system (Fig. 11). Some pass to the magnocellular lobe, and this is probably a pathway for rapid escape reactions. Other fibers pass to the peduncle and basal lobes, which together regulate movement, including attack. A third pathway leads to the superior frontal, and so to the vertical lobe, and is responsible for learned behavior.

The system is organized exactly as we have seen for tactile learning. In the lateral superior frontal, the visual fibers interact with those of taste, and this is a pathway that promotes attack. After removing this lobe from one side, an octopus will no longer attack when that eye has been used to see a crab, for instance, at a distance (Boycott and Young, 1955). The median superior frontal and vertical lobes provide a system that prevents visual attack when trauma occurs. After removal of these lobes or an interruption of the circuit, an octopus will continue to make attacks, even at crabs, in spite of receiving shocks, *unless these shocks are given at intervals of five minutes or less.* "The setting-up of a memory representing association of a given situation with a shock is therefore a property of the optic and basal lobes but persistence of the representation depends upon the presence of the vertical lobe" (Boycott and Young, 1955).

Many other experiments have confirmed that learning of visual discrimination is impaired by lesions of the vertical lobe system (Young, 1961, 1965). If part of the vertical lobe is removed, the accuracy of the memory is proportionately reduced. This "graceful degradation" is a property to be expected in such a distributed system. Incidentally, Boycott and I were able to show that the same is true of the optic lobes. Memories are retained after removal of at least 50% of the lobe or after making lesions in several places with a cataract knife.

Discussion

The two memory systems of an octopus thus work on precisely similar principles. The input signals are passed through a series of matrices of intersecting axes allowing for particular groupings of signals to interact and to be directed to the pathways for attack or retreat. The systems are tuned to produce exploratory investigation of novel situations. If the results are favorable, the particular set of connections in the lateral frontal lobes are re-enforced by signals of taste, and this set later produces more rapid attacks or takes by the arms. The inputs are given further opportunity for interaction in the matrices of the median frontal lobes. In the vertical and subfrontal lobes, particular sets are then concentrated into rather few large cells. The recurrent output from these to the lateral superior frontal lobe presumably re-enforces the tendency to positive action, unless pain occurs. In that case, the other outputs from these large cells of the vertical or subfrontal prevent further investigation of that configuration of inputs. The numerous amacrine cells in these lobes are evidently concerned with establishing the conjunction between particular sets of input signals and the pathways of retreat.

The organization of these lobes, and the effects of removing them, suggests that learning in these animals is not localized to one or two "hidden layers" or to a few essential "grandmother cells," but is distributed with high redundancy in a series of matrices networks, with recurrent circuitry, up to a late stage where funneling to a few cells occurs.

We can gain some insight into how this process has evolved by considering the differences between octopods and decapods. Cuttlefishes and squids have a system of matrices for visual learning similar to that of octopods

Figure 12. Sagittal section of the brain of *Sepia*. Note that there is no median inferior frontal or subfrontal. The superior frontal has a matrix structure like that of *Octopus*. The vertical lobe has a rather different structure. Cajal silver stain. b.a., anterior basal; b. med., median basal; fr. i., inferior frontal; fr. s., superior frontal; prec., precommissural; subv., subvertical; v., vertical.

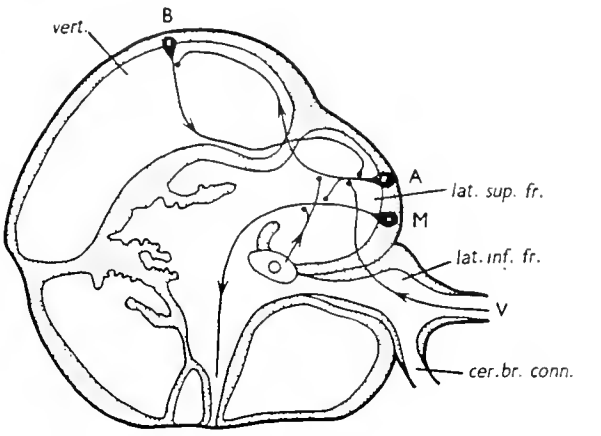

Figure 13. An early suggestion of re-excitation as the basis of memory. Diagram of *Sepia* to show how circulation between the lateral superior frontal (lat. sup. fr.) and vertical (vert.) might facilitate the firing of a motorneuron (M) by conjunctive excitation from the optic lobe (O) and taste fibers (V) (Young, 1938).

(Fig. 12). In an early experiment it was shown that interruption of the vertical lobe circuit damages the visual memory system of *Sepia* (Young, 1938; Sanders and Young, 1940). This was the first suggestion that the circulation of impulses around a circuit provides a basis for memory (Fig. 13). There has been little further progress because the experiments are more difficult than in octopods. In decapods, the inferior frontal system is much simpler than in octopods: there is no median inferior frontal or subfrontal lobe. These animals detect the prey visually and often seize by ejection of the tentacles. It seems likely that they have, at best, only a small capacity for learned tactile discrimination; the operations of manipulating and eating the prey are complex, but are probably largely reflex. Nevertheless, there must be a mechanism for release of any object that gives pain when it is held. Probably all reflex systems have some method of inhibition, especially if they involve muscles acting reciprocally, such as flexors and extensors in mammals, where the inhibition is produced by Golgi type II cells in the spinal cord. In cephalopods, reciprocal inhibition is probably produced by the smaller amacrine neurons that are common among the larger motorneurons of the superior buccal and suboesophageal centers (Fig. 14). These microneurons have processes restricted to a limited field, where they may serve to repress activity in the larger cells. In this context, it is especially interesting that we found some simple capacity for tactile memory in the suboesophageal lobes.

It is suggested that the amacrine cells of the subfrontal and vertical lobes of octopods have evolved from inhibitors of the reciprocal feeding reflexes. The inferior frontal and vertical lobe systems are backward extensions of the superior buccal lobes (see Fig. 4). The matrices that are responsible for learning have evolved by the modification of these simpler reflex centers. The incoming afferent fibers have become marshalled into rows crossing the axons of cells of the lobe, allowing the formation of conjunctive response to the incoming patterns of stimuli. The amacrine cells became collected together in distinct lobes, serving to prolong the effects, perhaps especially of inhib-

Figure 14. Drawing of a single large cell from the pedal lobe of *Loligo*, accompanied by very small cells with branches in the neighborhood.

itory inputs. The details are far from clear, but this provides a possible scenario for the evolution of memory mechanisms, at least among cephalopods.

Acknowledgments

The work reported here has been helped by many colleagues. I am especially grateful to Brian Boycott, Martin Wells, Marion Nixon, and Pamela Stephens. The Stazione Zoologica at Naples provided excellent conditions for experiment over many years. Recently, work has been helped by grants from The Wellcome Trust and University College, London. I am grateful to Professor L. Weiskrantz, F.R.S., for accommodation in the Psychology Department at Oxford and to my wife Raye for her secretarial help and typing. Dr. M. J. Wells kindly commented on an early draft of the paper.

Literature Cited

Allen, A., J. Michels, and J. Z. Young. 1986. Possible interactions between visual and tactile memories in octopus. *Mar. Behav. Physiol.* **12:** 81–97.

Boycott, B. B., and J. Z. Young. 1955. A memory system in *Octopus vulgaris* Lamark. *Proc. R. Soc. B* **143:** 449–480.

Budelmann, B.-U., and J. Z. Young. 1985. Central nervous pathways for the arms and mantle of *Octopus*. *Phil. Trans. R. Soc. B* **310:** 109–122.

Hopfield, J. J. 1982. Neural networks and physical systems with emergent collective computational abilities. *Proc. Natl. Acad. Sci. USA* **79:** 2554–2558.

Rolls, E. T. 1990. The representation and storage of information in neural networks in the primate cerebral cortex and hippocampus. In *The Computing Neuron*, R. Durbin, C. Miall, and G. Mitchison, eds. Addison-Wesley, Wokingham.

Sanders, F. K., and J. Z. Young. 1940. Learning and other functions of the higher nervous centres of *Sepia*. *J. Neurophysiol.* **3:** 501–526.

Wells, M. J. 1978. Octopus. In *Physiology and Behaviour of an Advanced Invertebrate*. Chapman and Hall, London.

Wells, M. J., and J. Z. Young. 1968. Learning with delayed rewards in *Octopus*. *Z. Vergl. Physiol.* **61:** 103–128.

Young, J. Z. 1938. The evolution of the nervous system and of the relationship of organism and environment. Pp. 179–204 in *Evolution*, essays presented to E. S. Goodrich, G. R. de Beer, ed. Clarendon Press, Oxford.

Young, J. Z. 1961. Learning and discrimination in the octopus. *Biol. Rev.* **36:** 32–96.

Young, J. Z. 1965. The organization of a memory system. The Croonian Lecture. *Proc. R. Soc. B* **163:** 285–320.

Young, J. Z. 1971. *The Anatomy of the Nervous System of* Octopus vulgaris. Clarendon Press, Oxford.

Young, J. Z. 1983. The distributed tactile memory system of *Octopus*. *Proc. R. Soc. B* **218:** 135–176.

Reference: *Biol. Bull* **180**: 209–220. (April, 1991)

Development of Giant Motor Axons and Neural Control of Escape Responses in Squid Embryos and Hatchlings

W. F. GILLY, BRUCE HOPKINS, AND G. O. MACKIE*

Hopkins Marine Station, Department of Biological Sciences, Stanford University, Pacific Grove, California 93950

Abstract. Anatomical development of the third-order giant axons was studied in conjunction with ontogeny of the escape response and the underlying neural control. Stimulated escape jetting appears at stage 26 (Segawa *et al.*, 1988); such responses are driven solely by a small axon motor system. Giant axons become morphologically identifiable in the more posterior stellar nerves that effect jetting by stage 28, and electrical activity in the stellate ganglia associated with the giant axons is first recordable at this time. Maturation of the giant axons is accompanied by a marked improvement in temporal aspects of escape behavior up to the time of hatching. In embryonic and hatchling *Loligo*, all escape responses, regardless of the mode of stimulation, are fast-start responses with latencies less than the minimum value displayed by adults (50 ms). Giant axon activity recorded in the stellate ganglion always precedes small axon motor activity; this is not true for adults which display two distinct modes of giant axon use. Both giant and non-giant motor systems are thus functional in embryonic and hatchling squid, and both contribute to escape jetting. However, these animals do not yet display the concerted interplay of the two motor systems characteristic of adults.

Introduction

Lolliginid squid possess giant neurons with very large axons that are important components of the motor pathways mediating jet-propelled escape responses (Young, 1938). Anatomical details of the giant fiber pathway were beautifully described at the light microscope level over 50 years ago by Young (1939). In brief, two bilaterally symmetrical first order interneurons lie in the magnocellular lobe of the brain and receive massive sensory inputs from many sources, including the statocysts, optic lobes, and mechanoreceptors in the tentacles. These cells are unusual in that their short axons are fused via a cytoplasmic bridge. Each first-order giant axon contacts seven second-order giant cells in the palliovisceral lobe. The largest of these cells are interneurons, and each projects a giant axon via the pallial nerve to the ipsilateral stellate ganglion where it contacts the third-order giant motor axons of the stellar nerves. The six other second-order giant cells are motoneurons that innervate the musculature associated with head retraction, siphon aiming, and ink ejection.

This basic plan is straightforward, but oversimplified. Each of the above giant cells receives numerous other synaptic inputs, about which little is known (Boyle, 1986). The first-order giants also receive major inputs from higher-order centers such as the cerebral ganglia. Integrated outputs from these regions must influence activity of the first-order giants, which are likely to be an important decision-making element, given the commanding anatomical position they hold. Complexity in the giant fiber pathway and the biological necessity to strictly control giant fiber excitation was clearly recognized by Young (1939), who pointed out that lack of such control ". . . would lead to behavior by the squid even more 'nervous' than that for which the animals have a reputation."

Despite the wealth of anatomical data, physiological studies of squid escape behavior have lagged far behind work on many other preparations (Eaton, 1984; Mackie, 1990). The pioneering work of Young [1938; Prosser and Young (1937)], in which reflex activation of escape jetting was inferred from studies of nerve-mantle preparations, was followed up only much later by Wilson (1960), who studied control of mantle contractions by a small axon

Received 15 August 1990; accepted 6 November 1990.

* Permanent Address: Department of Biology, University of Victoria, Victoria, B.C., Canada.

system as well as by the giant axons. Since that time it has become widely accepted that (1) high-pressure escape jetting is mediated solely by the giant axon pathway essentially as a reflex and that (2) low-pressure respiratory 'jetting' is the primary, if not only, function of the small axon (non-giant) motor system.

Reinvestigation of these ideas has revealed a more complex picture (Otis and Gilly, 1990). Recordings of stellar nerve activity during escape responses *in vivo* show that strong escape jets can be driven by the small axon system acting independently or in concert with the giant axons. Moreover, the giant axon pathway can be used in two distinct modes. One produces a short latency startle response, whereas the second leads to a complex delayed escape response. In the latter case, critically timed excitation of the giants provides a potent, but secondary boost to the jet.

The present study investigates the neural control of escape jetting in embryonic and hatchling squid. All three neural elements of the giant fiber pathway are highly developed at the time of hatching (Young, 1939), and escape jetting capabilities are respectable (Packard, 1969). Embryonic development of the first-order giant neurons has been studied in detail (Martin, 1965, 1969, 1977), but much less is known about the second- and third-order giants (Marthy, 1987). Behavioral and neurophysiological studies concerning development of the giant fiber pathway are completely lacking.

This paper describes the ontogeny of the escape response in relation to development of the giant fiber system, with emphasis on the role of the third-order motor axons. Several questions are addressed, answers to which provide the framework for future studies. When do the giant motor axons develop morphologically, and when do they begin to mediate escape responses? What functional consequences are manifested in parallel with growth of the giant axons? How does the pattern of giant axons use compare to that in the adult animal? Finally, when does controlled interplay between the giant and non-giant motor systems develop?

Materials and Methods

Animals

Loligo opalescens was collected from Monterey Bay and maintained in holding tanks plumbed with flow-through seawater (~13°C). Spawning occurred in these tanks, and clusters of fertilized eggs were maintained in small mesh enclosures in gently flowing seawater until natural hatching occurred (~30 days). Staging of animals was carried out following criteria of Segawa *et al.* (1988) with only minor modifications (see Results and Table I).

Sepioteuthis lessoniana was supplied by the Marine Biomedical Institute, University of Texas Medical Branch, Galveston, where the animals had been reared. Animals ranging from 5 to 21 days post-hatching were shipped overnight and studied the following day.

Behavioral experiments

Loligo from stage 24 through post-hatching was used for studying development of escape-jetting behavior. To obtain animals for each experiment, a "finger" of eggs was disrupted, the eggs were dispersed in seawater, and the chorionic membranes were ruptured to release the embryos. Individual embryos were chosen from this pool and staged under a stereomicroscope.

After staging, an animal was placed in a 35 mm culture dish lined with Sylgard (Dow-Corning, Midland, Michigan) and filled with seawater at room temperature (16–20°C). The animal was lightly restrained (ventral surface up) with a wire yoke, which was formed to fit over the base of the arms and inserted into the Sylgard. Electrical stimuli (20–60 V, 6 ms duration) were delivered via a seawater-filled micropipette positioned near the ventral midline in the area of the brachial ganglion (see Fig. 2A).

Behavioral responses were recorded on conventional videotape. The stimulating pulse also triggered a small light source beneath the experimental chamber, which served as a timing marker. Although the exact frame when the stimulus occurred is identifiable with this method, stimuli were not synchronized with the video framing and uncertainty therefore exists about precisely when in the frame the pulse occurred (each video frame spans 33 ms). Data were later sampled in blocks of 16 real-time frames with an image-analysis system (Megavision 1024 XM, Santa Barbara, California) and analyzed on a frame-by-frame basis to determine the time course of the change in mantle diameter following stimulation (see Fig. 2B).

Electrophysiological experiments: adult squid

Adult specimens of *Loligo* were lightly anesthetized in 0.4% urethane in aerated seawater at 15°C. The mantle was slit ventrally along the midline, exposing the gills, and the squid was pinned ventral side up through the outspread mantle flaps to the bottom of a Sylgard-filled glass dish. A pin through the region of the mouth prevented head retraction. The left pallial nerve was cut proximal to the stellate ganglion, thereby immobilizing the mantle musculature on that side. On the right side, the stellate ganglion was exposed by removing the thin layer of skin that covers it. The larger, more posterior stellar nerves were severed close to their emergence from the ganglion, but the pallial nerve was left intact. This paralyzed the right side of the animal but retained synaptic transmission at the giant synapses and motor outputs in the stellar nerve stumps. Throughout these operations, chilled seawater was kept flowing over the gills. Upon completion of surgery, the urethane-seawater was ex-

changed for O_2-saturated seawater (12–15°C) which was thereafter perfused continuously over the gills.

Conventional extracellular recording techniques were used. One polyethylene suction electrode was attached to the pallial nerve for *en passant* recording. A second electrode was used to record from a stellar nerve by sucking the proximal stump into the lumen of the electrode. Voltage was measured differentially between Ag:AgCl wires, one in the electrode's lumen and the other wrapped around the tip. Polarity of the recordings was arranged so that the initial phase of activity in the third-order giant axon was positive-going. AC-coupled amplifiers served to amplify and low-pass filter (3–10 KHz) the signals, which were displayed on a digital oscilloscope or recorded onto videotape via a digital audio processor (sampling at 44 KHz; Unitrade, Philadelphia, Pennsylvania) for subsequent analysis using a laboratory computer.

Electrophysiological experiments: embryonic and hatchling squid

Recording techniques were adapted from those used with the adult animals. Hatchlings and embryos (removed from their chorions and staged as in the behavioral experiments) were pinned out with fine cactus spines, ventral side up, after slitting the ventral mantle wall to allow access to the stellate ganglia. No nerves were cut, and recordings from the stellate ganglion were made with a suction electrode applied directly over the ganglion through the overlying tissue. Recordings from the magnocellular lobe (site of the first-order giant neurons) required removal of the skin and cartilaginous material just anterior to the statocysts, and the recording electrode was applied directly to the nervous tissue thereby exposed. It was also necessary to remove some of the mass of small cells, presumably undifferentiated neuroblasts (Martin, 1965), which overlie the first-order giant cells by sucking or blowing water jets through the electrode tip before attaching it.

For all neurophysiological recordings, electrical stimuli were delivered through a fine coaxial metal electrode, and a triggered strobe light was used for delivering photic stimuli. Shocks of 1–3 ms, 20–80 V were most effective in stimulating adults and 0.1–0.4 ms, 10–50 V in hatchlings and embryos. All experiments were carried out at 12–15°C in the case of *Loligo* and 21°C with *Sepioteuthis*.

Electron microscopy

Staged embryos were fixed in a 0.965 osmolar solution of 1% glutaraldehyde, 0.1% tannic acid, 0.2 *M* sodium cacodylate and sucrose (pH 7.4) and post-fixed in 2% osmium tetroxide, 0.8% potassium ferrocyanide, and 0.2 *M* sodium cacodylate (pH 6.8). Fixed material was dehydrated in graded hexalene glycol and embedded in Spurr's resin. Animals were sectioned both perpendicular and oblique to the long body axis to obtain transverse sections of the posterior stellar nerves. *En bloc* staining was carried out in saturated uranyl acetate at 60°C for 3 h. Thin sections were examined in a Philips 301 transmission electron microscope operating at 60 kV.

Results

Developmental timetable of giant motor axons and jetting behavior

Loligo opalescens develops embryologically in close correspondence to *L. forbesi*, and staging criteria for the latter species (Segawa *et al.*, 1988) can be directly applied. Stages 24 through hatching (30), representing approximately half of the total developmental period, are relevant to the present study, and selected characteristics applicable to our staging of *L. opalescens* are summarized in Table I. Based on our work with hundreds of embryos in this study, ontogeny of jetting behavior can be related to these anatomical stages with a high degree of confidence, and this information is included in Table I and covered in detail below.

Electron microscopic examination of conventionally fixed and embedded material reveals that axons in stellar nerves which can be labeled 'giant' (*i.e.*, distinctly larger than any other processes) first occur at stage 26, but only in the more anterior nerves emanating from the stellate ganglion (Fig. 1A). The more posterior stellar nerves do

Table I

Staging characteristics employed and development of escape behavior in embryonic Loligo opalescens. *Developmental staging follows the criteria described by Segawa* et al. *(1988) for* Loligo forbesi, *except in our work we lumped stages 27 and 27+ (into 27) and 28 and 28+ (into 28)*

Stage 25:	1. Spontaneous, symmetrical mantle contractions begin.
Stage 26:	1. Eyes are brilliant red. 2. Ink sac is visible. 3. Chromatophores are on dorsal side of head. 4. Electrical and mechanical stimulation of escape response is possible.
Stage 27:	1. Ink is barely visible in ink sac. 2. Eyes are dark, but not black. 3. Edge of primary lid covers half of optic vesicle.
Stage 28:	1. Eye is completely covered by primary lid. 2. Mid-gut gland is visible. 3. Yellow chromatophores are on arms. 4. Head retraction occurs during escape responses.
Stage 29:	1. Olfactory organ is visible as thickened disk. 2. Light flashes stimulate escape responses.
Stage 29+:	1. External yolk sac is equal to arm length.
Stage 29++:	1. Spontaneous vigorous jetting occurs.
Stage 30:	1. Natural hatching occurs; no external yolk sac.

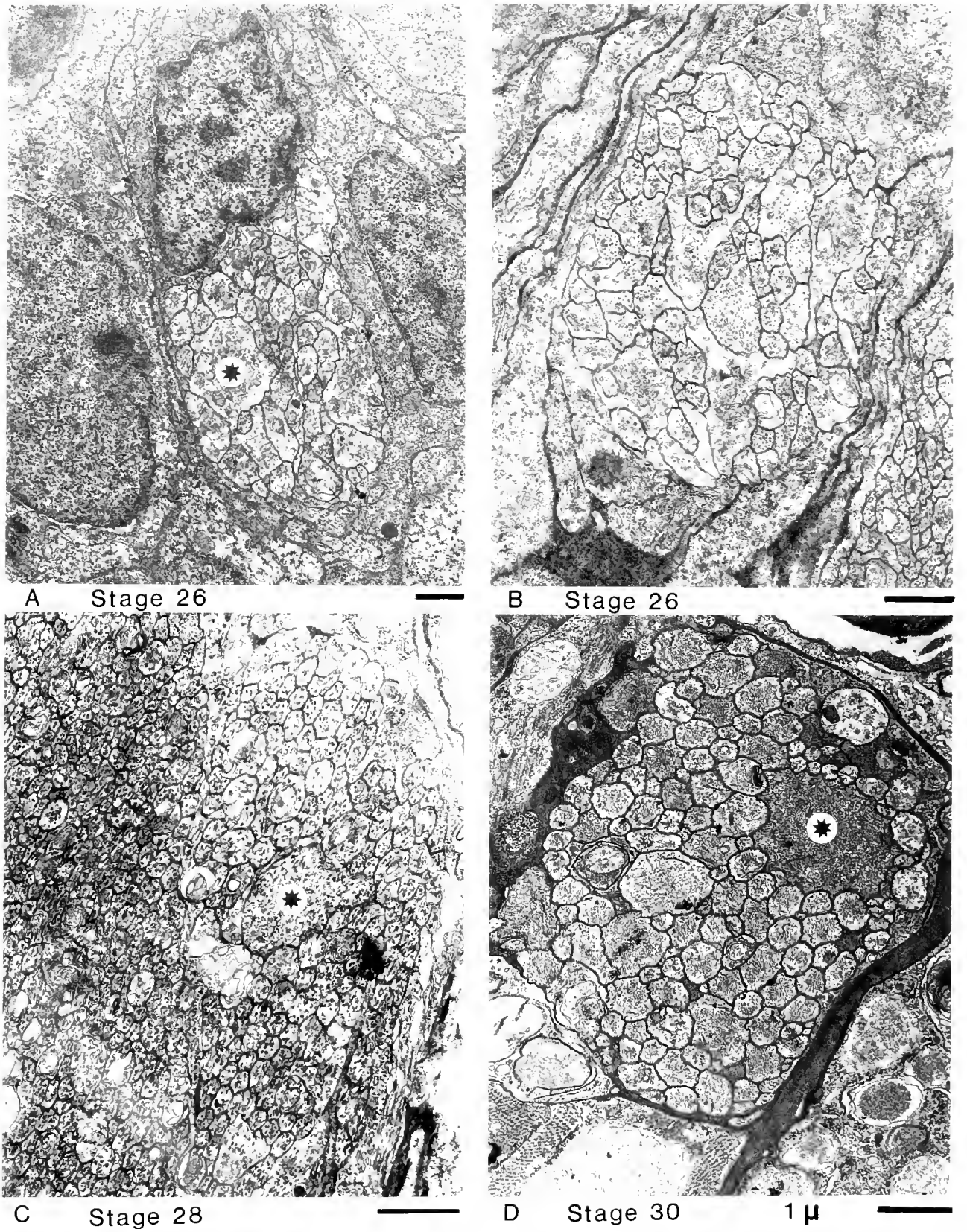

Figure 1. Anatomical development of the giant axons in stellar nerves of embryonic *Loligo opalescens*. Each panel shows a cross-section of a stellar nerve at the indicated developmental stage. (A) A single large axonal process is first identifiable in an anterior stellar nerve at stage 26 (*), although other processes are

not display a singularly large axon leading to the mantle muscle at this time (Fig. 1B), but clearly do so by stage 28 (Fig. 1C). As discussed below, stage 28 is the first time at which giant axon activity could be recorded from the stellate ganglion. Well-developed giant axons exist in all stellar nerves at the time of hatching, and an example of a hind-most nerve is shown in Figure 1D.

We have not characterized the apparent anterior to posterior wave of giant axon maturation in detail, nor do we at this time have a complete picture of where, when, and how the axons of giant fiber lobe motoneurons actually fuse to form the giant axons prior to stage 28. Giant processes can be identified in all stellar nerves at stage 27, but (in every case examined) only proximal to the first branch point of a stellar nerve shortly after it enters the mantle tissue.

Development of escape response: behavioral studies

Escape responses in embryonic and hatchling squid were stimulated with electrical shocks, strobe light flashes, or mechanical stimuli and videotaped for analysis. An example of such data from a stage 29 embryo is shown in Figure 2A. Sequential video frames, photographed from the display monitor of the image analysis system, are numbered −3 through 4. A brief electrical stimulus was applied during frame 0, and the timing is identifiable by a light flash marker (*). Mantle diameter is indicated by arrowheads in each panel, and Figure 2B illustrates the time course of mantle contraction (1 frame equals 33 ms). After a delay of one frame, mantle diameter decreases to 40% of its original (time 0) value over the subsequent four frames.

Peak response, delay, and time to peak (as indicated in Fig. 2B) were measured for electrically stimulated jets in 3–4 animals of every developmental stage from 25 through several days post-hatching. Mean data are summarized in Figures 3A–B, along with values obtained in similar experiments on adult animals in a previous study (Otis and Gilly, 1990).

Escape jetting increases in strength (Fig. 3A) smoothly up to hatching and then begins to slowly decline. Electrical stimuli (●) can elicit relatively strong responses at stages 26–27, a time when there is no anatomical sign of giant axons in the more posterior stellar nerves that innervate the mantle area in which diameter was monitored. Presumably these responses are mediated by the small motor axon system, which also can drive strong escape jets in adults. There is no dramatic sign of increased strength in the response accompanying the appearance of functional posterior giant axons by stage 28. Mechanical stimulation (▲; taps with a fine probe) also leads to strong escape jets, and light flashes (○) become effective at stage 29.

A functional correlate of the development of the giant axons in the posterior stellar nerves is suggested in Figure 3B. Both time-to-peak response (●) and delay (■) decrease dramatically between stage 29 and hatching. As described below, giant axon activity can be first recorded in the stellate ganglion at stage 28, and the developmental decrease in behavioral delay (Fig. 3B) is also evident in the electrical recordings (Fig. 10A).

Development of giant axons thus improves temporal aspects of jetting performance. Acceleration of a squid through water is a function of both intra-mantle pressure and the rate of change in pressure (O'Dor, 1988). Rate of change in mantle diameter is thus an important determinant of escape performance. Figure 3C plots the maximum change in mantle diameter (data in Fig. 3A) divided by the frames to peak change (data in Fig. 3B) for each developmental stage. A sharp rise in the rate of mantle contraction occurs just before hatching, and performance then declines towards the adult level.

Recordings of motor activity in adult Loligo

In a previous study examining the functional role of the giant motor axons (third-order) in escape jetting (Otis and Gilly, 1990), adult squid were attached to a plastic support platform by their dorsal mantle surface but were otherwise free to make unrestrained respiratory and swimming movements. Under these relatively natural conditions, it was demonstrated that squid show apparently normal behavioral responses in regard to escape-jetting when compared with free-swimming animals in large tanks. The present study goes a step further and shows that similar neural responses can be obtained with dissected, pinned, and inverted animals.

Electrical stimulation directly over the magnocellular lobe in an adult squid leads to a large, short latency action potential in the pallial nerve (2) followed by a spike in an ipsilateral stellar nerve (3) as illustrated in Figure 4A. These 'directly' evoked events are assumed to result from direct activation of the first-order giant cells and represent the sequential firing of the second- and third-order giant axons, respectively, as described by Bryant (1959).

The electrode on the stellar nerve also picks up a small potential just before the third-order spike, and this pre-

almost as large. (B) No singularly large axon exists in the hind-most stellar nerve at stage 26. (C) By stage 28, a distinctly large 'giant' axon is present in the hind-most stellar nerve (*). The fin nerve lies to the left of the stellar nerve and is composed entirely of small axons. (D) The hind-most stellar nerve at the time of hatching shows a well-developed giant axon (*).

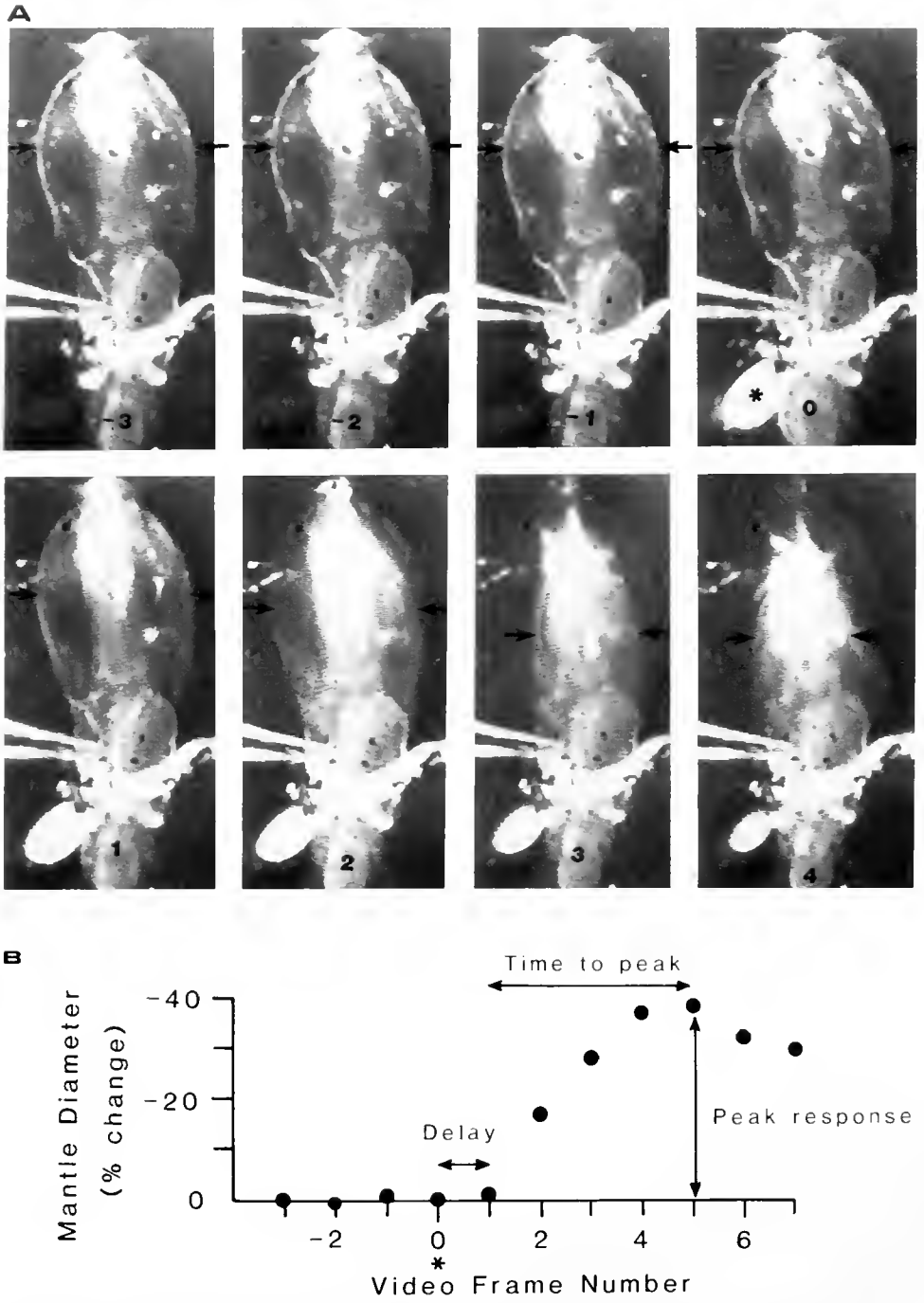

Figure 2. Escape behavior of a stage 29 *Loligo* embryo in response to an electric shock. (A) Sequential video frames are illustrated; the stimulus was applied via the pipette during frame 0 (*). Arrows indicate mantle diameter (measured at the widest point). See text for additional details. (B) Data from the experiment in Figure 2A is plotted in graphical form, and the parameters measured are indicated.

sumably represents the arrival of the second-order wave in the stellate ganglion. The delay between its peak and the start of the third-order event is approximately 1 ms and represents synaptic delay at the giant synapse. This characteristic short-latency pattern of activity in the stellate ganglion was consistently observed in adults (Fig. 4A), hatchlings (Fig. 4B), and embryos (Fig. 6A) only when stimuli were applied directly over the magnocellular lobe. When the squid is stimulated by a light flash (Fig. 5A, B) or by electrical shocks in regions other than the immediate vicinity of the first-order giant cells, *e.g.*, the tentacles (Fig. 5C, D), 'indirect' responses are obtained. These occur after

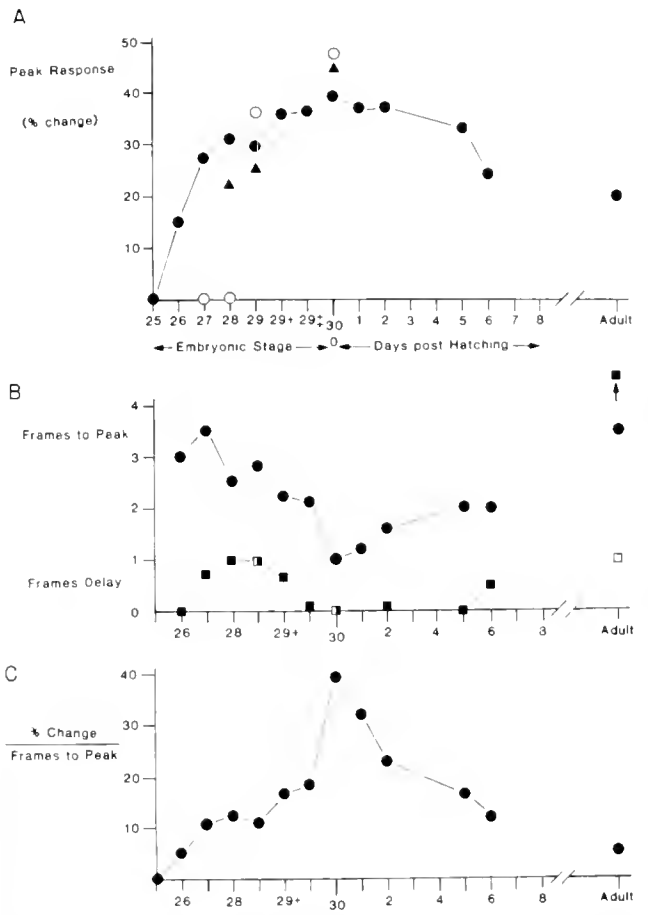

Figure 3. Ontogeny of escape jetting in *Loligo*. Three or four animals at each developmental stage were studied as described in conjunction with Figure 2, and mean values are plotted. Adult values are from data obtained in a previous study (Otis and Gilly, 1990). Electrical (●, ■), tactile (▲), and photic (○, □) stimuli are individually plotted. (A) Peak mantle contraction rises smoothly from stage 25 until hatching. Each of the stimulus modes yields strong escape jets. (B) Temporal aspects of escape performance [frames to peak (●) and delay (■, □)] improve markedly between stages 28 and 30. The adult value for delay with an electrical stimulus (■ over arrow) has a minimum value of 7–8 frames (Otis and Gilly, 1990). (C) Rate of mantle contraction, approximated as maximum diameter change divided by frames to peak, shows a sharp increase before hatching (stage 30) and a post-hatching decline towards the adult level.

sizable delays and represent activation through more physiological pathways.

General features of indirectly stimulated motor activity due to giant and non-giant (small) axon pathways observed in the present study closely resemble those previously reported for tethered, intact squid. In escape responses evoked by light flashes, the giant axons fire either after a 50 ms delay at the start of a burst of small axon activity (Figs. 5A, B) or not at all. In an indirect response stimulated by an electric shock, the giant axons fire only after a much longer delay (several hundred ms) and always during a burst of small-axon activity (Figs. 5C, D). Giant axons do not fire in every jet cycle, and the small-axon

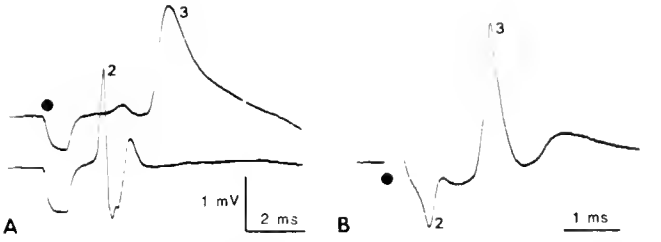

Figure 4. 'Direct' responses to electrical stimulation (●) applied over the magnocellular lobe in an adult *Loligo* (A) and a 7-day post-hatching *Sepioteuthis* (B). (A) The electrode on the pallial nerve (lower trace) records the second-order giant axon spike (2) *en passant*, while a second electrode on a posterior stellar nerve stump (upper trace) records the third-order spike (3) of the giant motor axon. (B) A single electrode placed over the stellate ganglion records both second- and third-order events. See text for additional details.

system acting alone can generate intense episodes of motor activity (second cycle in Fig. 5C). In all these respects our findings agree with Otis and Gilly (1990).

Recordings of motor outputs in hatchling and embryonic Loligo

Recordings from the stellate ganglion of late-stage embryos and hatchlings after electrical stimulation of the head show activity associated with both giant and non-

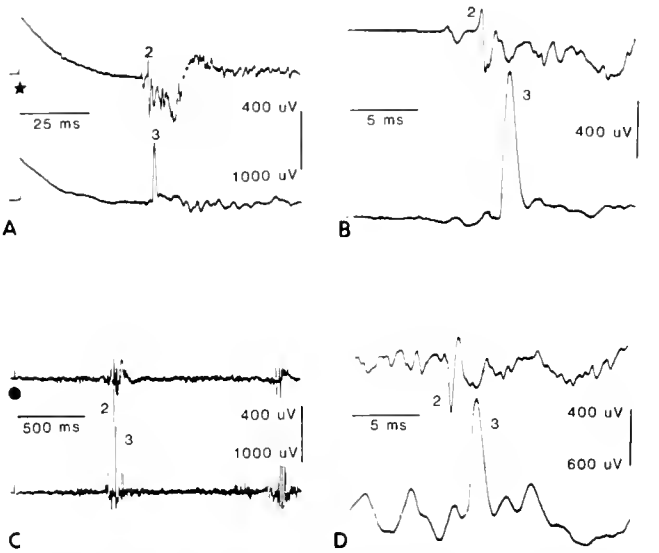

Figure 5. Bursts of motor activity associated with escape jetting in adult *Loligo*. In each panel (A–D) the upper trace is from the pallial nerve, and the lower trace is from a stellar nerve. (A) A light flash stimulus (*) results in firing of the giant axons (2 and 3) after a delay of ~50 ms and before the onset of the non-giant motor burst. (B) Portions of the records in (A) are displayed on an expanded time scale to illustrate the time course of the giant axon spikes. (C) An electrical stimulus (●) leads to giant axon activation after a long delay (>500 ms). In this case, the burst of small axon motor activity commences before the giant spike. A second escape cycle at the end of the record is driven by non-giant axons acting alone and shows no giant spike. (D) The first cycle in (C) is displayed at an expanded time base.

giant motor systems. Figure 6A illustrates such recordings from a stage 29+ embryo. Giant fiber excitation is indicated by an initial small, negative-going spike (2) followed by a larger positive event (3). As discussed above, the first component (2) represents arrival of the impulse in the second-order giant fiber entering the stellate ganglion via the pallial nerve, whereas the second component (3) reflects the summed action potentials from proximal parts of the third-order giants lying within the ganglion. Thus, moving the recording electrode anteriorly along the pallial nerve amplifies the second-order event and eliminates the third (Fig. 6B), whereas moving the electrode posteriorly along the larger stellar nerves isolates activity in the third-order giant fiber (Fig. 6C). Moving the electrode peripherally along one of the smaller (anterior) stellar nerves out into the muscle field shows the third-order spike followed by a large muscle potential (m, Fig. 6D).

Following stimulation over the brachial ganglion, activity can be recorded at all three stages in the giant fiber pathway by placing one recording electrode over the magnocellular lobe and a second on the stellate ganglion. The first electrode records the first-order giant spike (1) while the other records the second- and third-order events in sequence (Figs. 7A, B).

Firing of the first-order cell is invariably followed by activation of the other two elements, and the delay from the peak of the first-order spike to the start of the third-order event is only 2.0–2.5 ms. The delay that precedes firing of the first-order spike during an indirect response is much longer (*e.g.*, 26 ms in Fig. 7A or 13 ms in Fig.

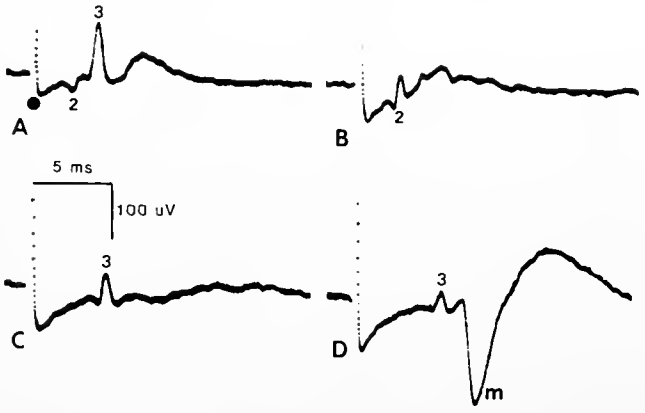

Figure 6. Electrical activity in the second- and third-order giant axons in a stage 29+ *Loligo* embryo. Direct responses of the giant fiber pathway were generated by stimulation over the magnocellular lobe. (A) The recording electrode was placed directly over the stellate ganglion, and the incoming second-order spike (2) and the out-going third-order wave (3) are recorded. (B) The electrode was positioned on the pallial nerve just proximal to the stellate ganglion, and the second-order spike is thereby isolated. (C) The electrode was placed on the emergence of the posterior stellar nerves from the ganglion; this isolates activity in the third-order giant axons. (D) The electrode was placed over an anterior stellar nerve in the muscle field of the mantle. This reveals the third-order giant axon spike and a large muscle potential (m).

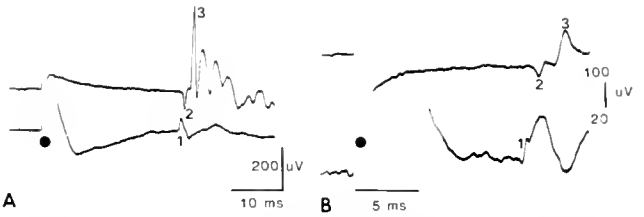

Figure 7. Timing of electrical activity from all three stages of the giant fiber pathway following indirect electrical stimulation over the brachial ganglion in a stage 29++ (A) or 30 (B) *Loligo*. In each panel the lower trace is recorded with an electrode on the magnocellular lobe, and a composite event including the first-order giant spike is obtained (1). Upper traces are recorded from the stellate ganglion, where second- (2) and third-order (3) events are detected.

7B) and presumably reflects 'processing' time in the central nervous system. Small potentials precede the initiation of the first-order spike in Figure 7B and must represent summed activity in pathways leading into the magnocellular lobe. There is also generally an outburst of small-unit activity coincident with and following the first-order giant spike, which itself appears difficult to resolve except for the rising phase (1 in Fig. 7B).

Indirectly stimulated escape responses in hatchlings produce the pattern of second- and third-order giant spikes discussed above (Figs. 8A, B), and the subsequent activity in the small motor axons takes the form of flurries of irregular, compound action potentials (Fig. 8A). Unit activity is generally difficult to resolve, and these potentials probably represent the firing of dozens of axons in rough synchrony. Although these compound events may approach third-order giant spikes in amplitude, they are readily distinguished from the latter by their irregular and variable waveforms and slower rise times. Bursts of small unit activity can be elicited by weak stimulation without excitation of the giant fiber system (upper trace in Fig. 8A) and would be associated in nature with non-giant escape jetting, as occurs in adults.

Two consistent and striking features characterize neural recordings of indirectly stimulated escape responses in late-stage embryos and hatchlings and clearly differentiate them from analogous records obtained in adults. First, the minimum latency for excitation of the third-order giant axons in hatchlings by photic stimulation is considerably shorter than that in adults (~15 ms in Figs. 8B, 9F *vs.* 50 ms for adults in Fig. 5A), and the latency following electrical stimulation in hatchlings can be nearly as brief (Fig. 8A). In adult animals, this latency is at least several hundred ms (Fig. 5C; *c.f.* Otis and Gilly, 1990).

A second and more pronounced difference is that when the third-order giants fire in hatchlings, their impulses arise in the stellate ganglion several ms before those of the small motor axons. This is true regardless of whether stimulation is via electric shocks (Fig. 8A) or light flash (Fig. 8B). This pattern of giant *versus* non-giant activity

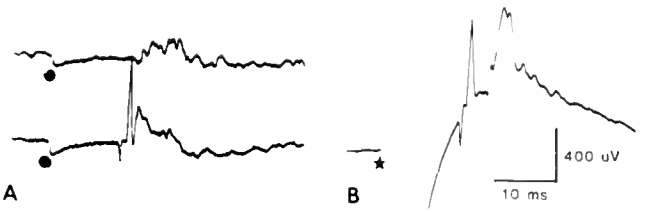

Figure 8. Comparison of motor outputs from a stage 30 *Loligo* in response to an electrical shock at the base of the tentacles (●, A) and to a light flash (*, B). (A) Upper trace shows activity of small axon system acting alone; stimulus was sub-threshold for giant fiber activation. Lower trace was recorded with a slightly stronger shock, which led to indirect excitation of the giant fiber pathway. The giant axon spike arrives in the stellate ganglion before the small axon activity. (B) A light flash produces a similar pattern of motor activity in which the small axon wave follows the giant fiber response.

for electrically stimulated responses is thus temporally inverted in comparison to the picture in adults, where giant axon spikes always fire 50–75 ms after the onset of the burst of non-giant activity (Fig. 5C, D; Otis and Gilly, 1990).

Development of motor patterns prior to hatching

Small axon control of jetting behavior is demonstrable at stage 26 (the earliest examined). Intermittent bouts of spontaneous rhythmic activity occur and represent normal respiratory cycles. Electrical stimulation evokes bursts of small unit activity resembling these respiratory bursts, but stimulated activity is generally more intense and long-lasting (Fig. 9A). Latency for small axon excitation appears to be brief at this stage, but this may reflect direct stimulation of these pathways in the small embryos at this early stage. Small axon responses continue with little change in the above pattern throughout subsequent developmental stages, except for an apparent increase in latency to 30–50 ms by stages 27–28 (Fig. 9C).

Light flashes are ineffective at triggering escape jets or neural activity in the stellar nerves at stages 26 (Fig. 9B) or 27 (not illustrated). Photic stimulation does produce bursts of small axon activity in the stellate ganglion by stage 28 (Fig. 9D), coincident with anatomical maturation of the eye (Segawa *et al.*, 1988).

Giant axon responses can first be evoked by electrical stimuli at stage 28 in embryonic squid (Fig. 9E) and by light flashes around the time of hatching (Fig. 9F). Generally, the picture of functional development of the giant fiber system from stage 28 through hatching is one of progressive maturation, in terms of speeding of the action potential waveform, reduced response latencies, and decreased synaptic delay. The immaturity of the giant fiber pathway at stages 28–29 is suggested by: (i) the small amplitudes and long durations of both second- and third-order giant spikes; (ii) the relatively long response latency—the second-order spike takes more than 20 ms to arrive in the stellate ganglion compared with a delay of ~12 ms at stages 29++ or 30 (Fig. 10A), and (iii) the progressive decrease for second- to third-order synaptic transmission during development (Fig. 10B). These changes parallel the improvement in behavioral performance as indicated by the square symbols and dashed curve in Figure 10A, which are behavioral data replotted from Figure 3B.

Post-hatching development of giant and non-giant motor patterns

Although the embryonic pattern of giant axon use is evident at the time of hatching, several distinctive features of the adult motor patterns (Otis and Gilly, 1990) may emerge shortly thereafter. Figure 11A shows stellar nerve discharge of a 2-week-old *Sepioteuthis* in response to an electric shock applied to the tentacles. A burst of small unit activity follows the stimulus at short latency; this is a pattern typical of embryonic and hatchling *Loligo*. The lower trace is plotted at an expanded time base. A stronger shock produced the response pictured in Figure 11B. A short latency, non-giant burst again occurs, but in this case it is followed by a giant axon spike after 80 ms. Timing of giant axon activation in relation to that of the small axons is adult-like (Fig. 5D), although the overall latency

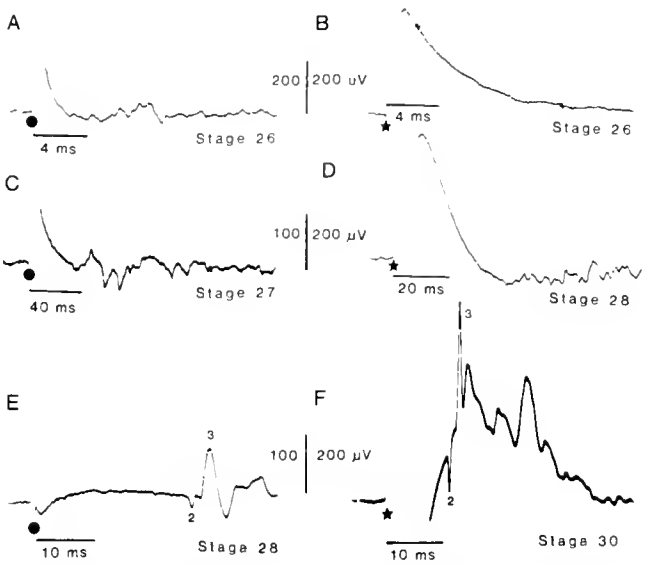

Figure 9. Functional maturation of the giant fiber pathway in embryonic *Loligo*. Indirect electrical (●) or light flash (*) stimuli were used to elicit escape responses at various stages of development; all recordings illustrated were obtained from the stellate ganglion. (A) At stage 26, electrical stimulation elicits only small axon activity. (B) A light flash is ineffective at stimulating escape responses or producing any detectable motor outputs at stage 26. (C) Giant axon activity is still not produced by electrical stimuli at stage 27. (D) Photic stimulation produces small axon activity but no giant spikes at stage 28. (E) Giant axon responses are first detectable at stage 28 with electrical stimuli. (F) A light flash stimulus at stage 30 produces a giant axon response. See text for additional details.

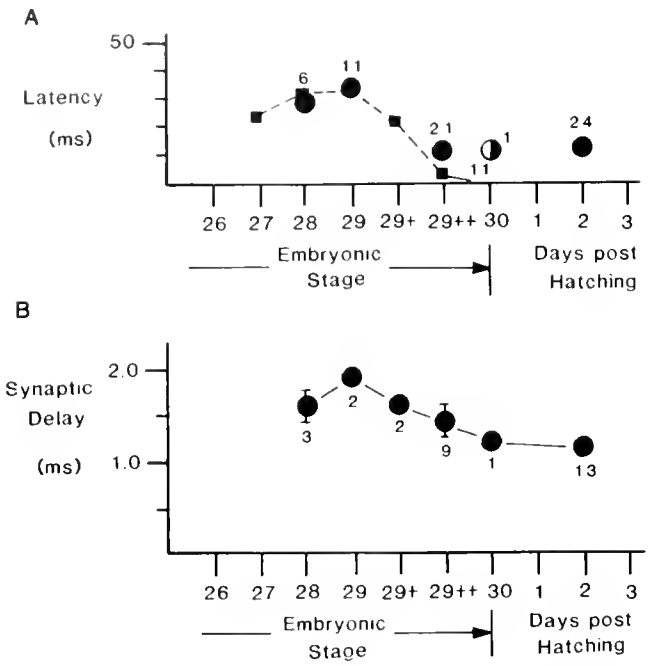

Figure 10. Improvement in performance of the giant fiber pathway during late embryogenesis in *Loligo*. (A) Response latency (time to second-order giant spike) decreases between stage 28 (time of first detectable giant axon activity) and 30 (hatching). Filled circles were obtained with indirect electrical stimuli; open symbol was obtained with light flashes. Mean values and the number of experiments are given; standard error of the mean is smaller than the symbols. Squares and dashed curve are behavioral data which has been replotted from Figure 3B. (B) Synaptic delay between the second- and third-order giants (across the giant synapse in the stellate ganglion) also decreases between stages 28 and 30. Means, number of experiments, and standard error are indicated.

is much less than that in adults (Fig. 5C). The motor pattern underlying the escape response in Figure 11B thus shows both embryonic and adult qualities.

More complex escape responses with the long delays characteristic of the adult can also be generated shortly after hatching in some animals. Results from another *Sepioteuthis* (~5 days post-hatching) are shown in Figure 12. Delayed escape jets driven by only the small axon system (Fig. 12A) and by both small and giant axons acting in concert (Fig. 12B) are well developed. Adult-like multiple cycle responses showing both of the above types of motor patterns are also evident (Fig. 12C). When the giant axons are used during such delayed escape responses, their firing is timed to occur after the non-giant system initiates the jet cycle. In every respect, the motor patterns in Figure 12 are adult-like. We do not yet know precisely when the adult-like motor patterns appear in *Sepioteuthis* after hatching, but stage 29–29++ embryos display only the fast-start embryonic pattern seen in *Loligo* (data not illustrated).

In addition to the delayed bouts of motor activity in Figure 12, an initial brief burst of activity occurs with a delay of ~20 ms in every case illustrated. The origin of this activity is presently unknown, and recordings in adult squid also reveal similar short-latency activity in stellar nerves following an electrical stimulus (*cf.* Fig. 3 in Otis and Gilly, 1990). In the latter case, there is no detectable short-latency mantle contraction. Comparable behavioral experiments have not been carried out with juvenile *Sepioteuthis*.

Discussion

Motor control of escape behavior in late-stage embryos and hatchlings shows important similarities to the corresponding situation in adult squid. In both cases, escape jetting is under the influence of two parallel motor pathways: the giant fiber system and a small axon (non-giant) system. Strong escape jets can be driven by the small-axon system acting alone, with no giant fiber involvement whatsoever (Figs. 9C, 8A). The small axon pathway is the first to develop anatomically and become functional during embryonic development, and vigorous escape jets are possible before the giant axons appear.

Giant axon excitation provides a potent boost to the small axon system, however, and this greatly improves escape jetting performance. This was directly demonstrated in adult animals (Otis and Gilly, 1990). It is also evident in embryonic development (stages 28–30) as a marked decrease in response latency [seen behaviorally

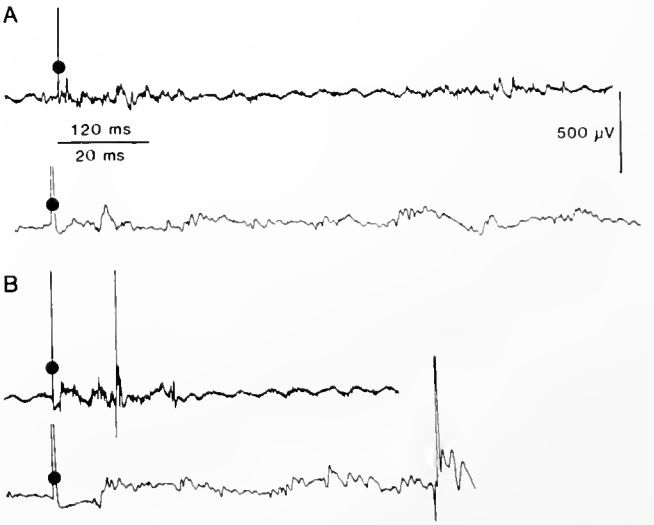

Figure 11. Partial development of adult-like use of the giant fiber pathway in a 14-day post-hatching *Sepioteuthis*. (A) Upper trace was recorded from the stellate ganglion following an electrical stimulus delivered to the base of the tentacles (●). Small unit activity only is generated, and the latency is brief. Lower trace shows the initial portion of the response following the shock displayed at an expanded time scale. (B) A stronger shock to the same site as in (A) produces a stronger burst of small axon activity at a short latency and a single giant axon spike in the middle of this burst. Lower trace shows the expanded version to identify the giant fiber spike. The occurrence of the giant spike well after the onset of the small unit burst is thus adult-like, but the brief latency (<20 ms) for the non-giant burst is characteristic of embryos.

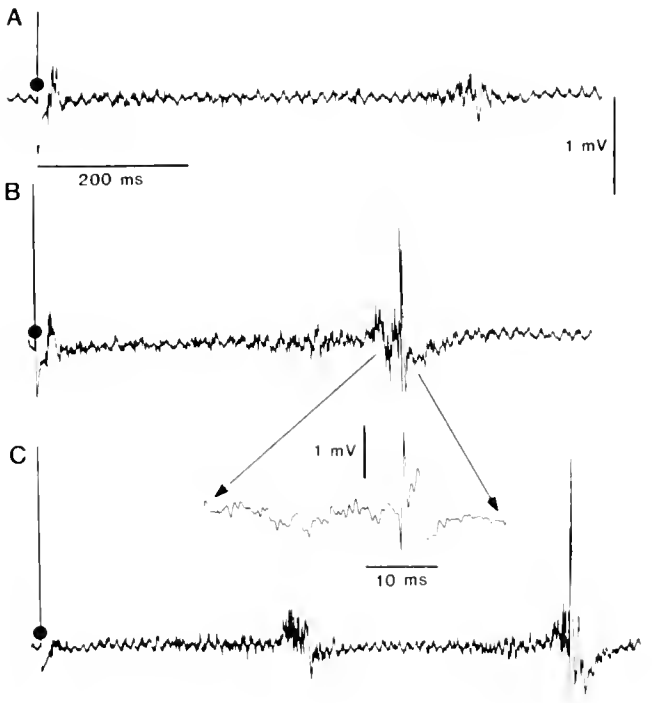

Figure 12. Fully developed adult-like interplay of giant and non-giant motor systems in escape responses of a 5-day post-hatching *Sepioteuthis*. (A) An electrical stimulus (●) to the side of the head produces an escape jet at a latency of ~500 ms that is driven only by small motor axons. (B) A stronger stimulus to the same site produces a delayed escape jet driven by both small axons and giant axons acting in concert. Non-giant activity precedes giant axon activation. Lower trace shows an expansion of the record around the giant fiber spike. (C) Stimulation on the ventral surface of the head just anterior to the eye produces a multiple cycle escape response at a long latency. The first cycle is driven by the small axon motor system acting alone, whereas the second also involves the giant axon pathway.

(Fig. 3B) or neurophysiologically (Fig. 10A)], time to peak mantle contraction (Fig. 3B), and rate of contraction (Fig. 3C). The time course of this improvement, beginning at stage 28–29, coincides closely with the anatomical appearance and maturation of the third-order giant motor axons in the more posterior stellar nerves that control jetting. Performance peaks at hatching. Presumably this is a valuable capability, because the embryonic squid must jet vigorously to escape from the confines of the egg mass in order to hatch.

At present it is not known how the neural portions of these giant and non-giant motor systems are associated with the two types of circular muscle fibers in adult squid mantle (Bone *et al.*, 1981; Mommsen *et al.*, 1981). Developing embryos and hatchlings would provide a valuable system in which to pursue this question, because the two motor systems do not develop in perfect synchrony. We have not carried out an anatomical analysis of the muscle fiber types in these young animals.

Although the overall picture of dual motor control of escape jetting is similar in embryos, hatchlings, and adults, details of how the two motor systems are employed when they act together are strikingly different. In embryos and hatchlings, activity in the third-order giant axons always precedes the burst of small unit motor activity by several ms. This is true regardless of whether stimulation is by electric shock or light flash. Latency to firing for the giant axon varies from ~40 to 10 ms, depending on the exact stage of development (Fig. 10A). This delay basically represents the time required to excite the first-order giant cell (Fig. 7). Once this cell fires, the second- and third-order giants follow within 2–3 ms. In embryos and hatchlings, all escape responses are thus of the fast-start variety, although the latency is never so brief as with artificial direct stimulation of the first-order giant (Fig. 4).

In our experiments on adult squid, only sudden visual stimuli (*e.g.* light flash) have been effective in producing a fast-start pattern of giant axon excitation (Fig. 5A) like that seen in embryos or hatchlings, where giant axon firing precedes the burst of non-giant activity. Latency for giant axon activation, even in this fastest case, is much longer than that in hatchlings (50 ms *versus* 10 ms) and presumably again represents the time before the first-order giant fires.

Electrical stimuli in adults produce a second pattern of giant axon use that is not seen in the embryo. This delayed-escape mode shows a minimum latency of several hundred ms and, more significantly, a burst of non-giant motor output that commences 50–100 ms before the giant axons fire (Fig. 5C). The small-axon system thus appears to be the primary effecter of this type of escape jet, and the giant axons are booster elements that are optionally recruited during any given cycle of a delayed-type response.

Otis and Gilly (1990) have argued that a great deal of complex processing in the central nervous system underlies effective use of the giant fiber pathway in this delayed-escape mode. This idea is in consonance with results on embryonic and hatchling *Loligo* presented in this paper. Much of the brain at these stages is not yet differentiated (Young, 1939; Martin, 1965), and these animals do not yet have the capability of orchestrating complex escape behavior, despite the functional presence of all the necessary peripheral motor components. Presumably, development of higher order neural centers is necessary to coordinate the interplay of giant and non-giant motor systems.

When and how does the strictly fast-start embryonic pattern in escape jetting evolve into the complex capabilities of the adult? This is not yet clear in *Loligo*. We have seen no indication of delayed escape responses in either behavioral or neurophysiological experiments for up to 6 days post-hatching. Preliminary work on post-hatching *Sepioteuthis* is also described in this paper. In this case, perfectly normal, adult-like firing patterns of the giant and non-giant motor systems were observed in an-

imals only 5 days old (Fig. 12), and other animals showed a curious mixture of embryonic and adult-like characteristics (Fig. 11).

The specimens of *Sepioteuthis* that we studied differed from our *Loligo* subjects in two important respects. First, *Sepioteuthis* is a much larger and possibly more developed (*i.e.*, neurologically) animal at birth. Second, the *Sepioteuthis* had been actively feeding and growing for the entire time after hatching (5–21 days), whereas *Loligo* was provided with no (for the neurophysiological work) or minimal food (for the behavioral work) and was maintained for no more than 6 days. Either or both of these factors could be relevant to the early attainment of coordinated delayed-escape jetting in young *Sepioteuthis*. In the first case, *Sepioteuthis* may simply develop the adult-like motor patterns more quickly after birth than does *Loligo*. The second possibility is more intriguing, however.

Hatchling squid have limited energy reserves sufficient only for several days (O'Dor *et al.*, 1986) during which time the animals must learn to capture prey or face starvation (Hurley, 1976; Yang *et al.*, 1983, 1986). Because prey items consist largely of fast-moving copepods, and high speed pursuit is involved in prey-capture, it would seem advantageous to employ the giant fiber pathway in this activity. To do this effectively, however, strict control over excitation of the first order giants must be necessary to provide the giant axon-mediated boost precisely at the correct moment. This capability—critically timed excitation of the giant fiber pathway—is the basic feature of the adult delayed-escape response that differentiates it from the fast-start response. The possibility that such a profound change-over in the pattern of giant axon use in hatchling squid might be associated with the perfection of feeding behavior is a prospect that we are currently pursuing.

Acknowledgments

We thank Natasha Fraley and Patricia Gosling for performing the behavioral experiments, and Dr. Roger Hanlon's group at U.T.M.B., Galveston, Texas, for providing living *Sepioteuthis*. This work was supported by grants from the Whitehall Foundation (J86-110) the Office of Naval Research (N00014-89-J-1744) and the N.I.H. (NS-17510).

Literature Cited

Bone, Q., A. Pulsford, and A. D. Chubb. 1981. Squid mantle muscle. *J. Mar. Biol. Assoc. U.K.* **61:** 327–342.

Boyle, P. R. 1986. Neural control of cephalopod behavior. Pp. 1–97 in *The Mollusca*, vol. 9, part 2, A. O. D. Willows, ed. Academic Press, New York.

Bryant, S. H. 1959. The function of the proximal synapses of the squid stellate ganglion. *J. Gen. Physiol.* **42:** 609–616.

Eaton, R. C. 1984, ed. *Neural Mechanisms of Startle Behavior.* Plenum, New York.

Hurley, A. C. 1976. Feeding behavior, food consumption, growth, and respiration of the squid *Loligo opalescens* raised in the laboratory. *Fish. Bull.* **74:** 176–182.

Mackie, G. O. 1990. Giant axons and control of jetting in the squid *Loligo* and the jellyfish *Aglantha*. *Can. J. Zool.* **68:** 1421–1431.

Marthy, H.-J. 1987. Ontogenesis of the nervous system in cephalopods. Pp. 443–459 in *Nervous Systems in Invertebrates*, M. A. Ali, ed. Plenum, New York.

Martin, R. 1965. On the structure and embryonic development of the giant fibre system of the squid *Loligo vulgaris*. *Z. Zellforsch.* **67:** 77–85.

Martin, R. 1969. The structural organization of the intracerebral giant fiber system of cephalopods. *Z. Zellforsch.* **97:** 50–68.

Martin, R. K. 1977. The giant nerve fibre system of cephalopds. Recent structural findings. *Symp. Zool. Soc. Lond.* **38:** 261–275,443.

Messenger, J. B. 1983. Multimodal convergence and the regulation of motor programs in cephalopods. *Fortschr. Zool.* **28:** 77–97.

Mommesen, T. P., J. Ballantyne, D. MacDonald, J. Gosline, and P. W. Hochachka. 1981. Analogues of red and white muscle in squid mantle. *Proc. Natl. Acad. Sci. USA* **78:** 3274–3278.

O'Dor, R. K. 1988. The forces acting on swimming squid. *J. Exp. Biol.* **137:** 421–442.

O'Dor, R. K., E. A. Foy, P. A. Helm, and N. Balch. 1986. The locomotion and energetics of hatchling squid, *Ilex illecebrosus*. *Am. Malacol. Bull.* **4:** 55–60.

Otis, T. S., and W. F. Gilly. 1990. Jet-propelled escape in the squid *Loligo opalescens:* concerted control by giant and non-giant motor axon pathways. *Proc. Natl. Acad. Sci. USA* **87:** 2911–2915.

Packard, A. 1969. Jet propulsion and the giant fibre response of *Loligo*. *Nature* **221:** 875–877.

Prosser, C. L., and J. Z. Young. 1937. Responses of muscles of the squid to repetitive stimulation. *Biol. Bull.* **73:** 237–241.

Segawa, S., W. T. Yang, H.-J. Marthy, and R. T. Hanlon. 1988. Illustrated embryonic stages of the eastern Atlantic squid *Loligo forbesi*. *Veliger* **30:** 230–243.

Wilson, D. 1960. Nervous control of movement in cephalopods. *J. Exp. Biol.* **37:** 57–72.

Yang, W. T., R. F. Hixon, P. E. Turk, M. E. Krejci, W. H. Hulet, and R. T. Hanlon. 1986. Growth, behavior, and sexual maturation of the market squid, *Loligo opalescens*, cultured through the life cycle. *Fish. Bull.* **84:** 771–798.

Yang, W. T., R. T. Hanlon, M. E. Krejci, R. F. Hixon, and W. H. Hulet. 1983. Laboratory rearing of *Loligo opalescens*, the market squid of California. *Aquaculture* **31:** 77–88.

Young, J. Z. 1939. Fused neurons and synaptic contacts in the giant nerve fibres of cephalopods. *Philos. Trans. R. Soc. Lond. Ser. B.* **229:** 465–503.

Young, J. Z. 1938. The functioning of the giant nerve fibres of the squid. *J. Exp. Biol.* **15:** 170–185.

Reference: *Biol. Bull.* **180:** 221–227. (April, 1991)

Factors Affecting the Sensory Response Characteristics of the Cephalopod Statocyst and their Relevance in Predicting Swimming Performance

RODDY WILLIAMSON

The Marine Biological Association, Citadel Hill, Plymouth PL1 2PB, England

Abstract. The statocyst in cephalopods is the main organ of balance and operates in a manner similar to the vestibular system of vertebrates. This paper reviews the principal factors affecting the sensitivity and frequency response of the statocyst. These include morphological features, such as the size and shape of the statocyst, its canal structure, and the size of the cupulae and maculae, as well as physiological features, such as the electrotonic coupling of sensory cells, the impact of the efferents, and the motility of some cells. The use of statocyst characteristics in predicting the locomotory performance of different cephalopod species is discussed.

Introduction

For spatial control of locomotion, an animal needs information about its orientation with respect to gravity and its motion relative to its surroundings. This information could be derived from a variety of sensory systems, ranging from vision to electroreception, but most animals have developed specific sense organs responding to linear and angular accelerations; *e.g.*, the vestibular system in vertebrates and the statocysts of cephalopods. It has been proposed that the sensory response characteristics of these receptor systems are matched to their likely inputs; *i.e.*, that the frequency response range and sensitivity of the system reflect the accelerations imposed by an animal's own movements (Jones and Spells, 1963; Jones, 1984). Thus the vestibular system of a small agile animal (*e.g.*, a bird) is more sensitive to higher frequencies of movement than that of a slower moving animal living in a denser medium (*e.g.*, a fish) (Correia *et al.*, 1981). This idea can also be applied to cephalopods where, by looking at the statocysts, we can try to predict what kind of locomotion is used by the animal (Maddock and Young, 1984; Morris, 1988; Young, 1989). This is a particularly valuable approach to animals with unstudied lifestyles. This paper reviews some of the evidence for this proposition and identifies some of the features that are likely to influence the sensitivity and response characteristics of cephalopod statocysts.

The parameters affecting statocyst sensitivity can be divided into two main areas, morphological features and physiological features. For convenience these are considered separately, but of course, they act in concert within the living animal.

Received 22 August 1990; accepted 27 November 1990.

Morphological Features

The general morphology of each of the paired right and left statocysts is a fluid-filled cavity within the cranial cartilage (Fig. 1). The statocyst itself varies considerably in shape in different cephalopods; in *Octopus* (Fig. 1A) it is almost spherical, whereas in *Vampyroteuthis* it is short, wide, and shallow (Young, 1960, 1989). Many statocysts have sac-like protrusions into the surrounding cartilage (Stephens and Young, 1982), or cartilaginous pegs or hooks (the anticristae and hamuli) that project into the statocyst interior (Fig. 1B); these projections presumably constrict or direct the flow of the endolymph. Again, this can vary from the single anticrista in *Octopus*, to the 38 anticristae and 5 hamuli in *Egea* (Young, 1984).

Each statocyst has two main areas of receptor epithelium (Fig. 1). The first is a macula or plate of sensory hair cells with an overlying statolith. All coleoids have a macula carrying a single compact statolith, but decapods have two additional maculae carrying numerous small statoconia. Where three maculae are present, they are set in different planes, thus being able to resolve linear accelerations in any direction.

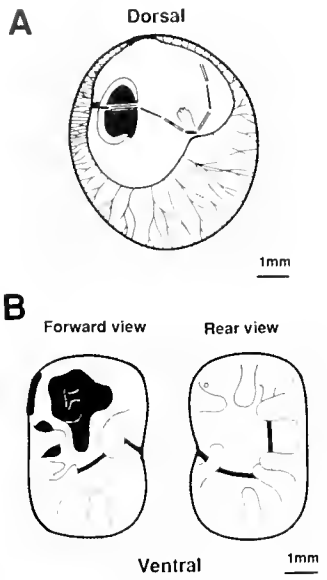

Figure 1. (A) Diagram of the statocyst of *Octopus* viewed from the side. The statocyst sac is suspended within the statocyst cavity by fibrous strands. There are two areas of receptor epithelium: a single, oval shaped macula with an attached statolith, and a crista strip that passes around the inside of the sac, such that it covers all three planes. The crista strip is divided into 9 segments, each segment carries a cupula (not shown). After Budelmann, 1980. (B) A forward and rear view of the cut open statocyst of *Sepia officinalis* There are 3 maculae, arranged in 3 different planes, and the crista strip is divided into 4 segments. Anticristae and hamuli project into the cavity of the statocyst. After Budelmann, 1980.

The second area of receptor epithelium consists of a narrow strip of sensory hair cells that runs around the inside of the statocyst such that it covers all three planes (Fig. 1). This strip is usually divided into segments: the crista segments, each carrying a cupula attached along the length of the crista segment. Octopods (excluding cirroctopods) have nine crista segments, whereas decapods have four, each with its own cupula. Rotational movements of the animal cause a flow of endolymph relative to the statocyst wall; this flow in turn deflects the cupula and stimulates the underlying hair cells. A transverse section through a crista segment (Fig. 2) reveals three main types of cells in the sensory epithelium: primary sensory hair cells, secondary sensory hair cells, and afferent neurons. This combination of primary sensory hair cells and secondary sensory hair cells in a single epithelium is unique to cephalopods (Budelmann *et al.*, 1987). Although the crista/cupula system responds principally to angular accelerations, it may also respond to linear accelerations (Budelmann and Wolff, 1973; Williamson and Budelmann, 1985a). Because the crista/cupula system is crucial for signalling most of the animal's movements, and because this system is dependent upon the physical parameters of the statocyst, we will concentrate on the responses of the crista.

Statocyst size and shape

The idea that the size and shape of the statocyst are correlated with its likely response characteristics, and hence with the animal's locomotory performance, arises from the physical models of the operation of the vertebrate semicircular canal system (Steinhausen, 1933; Wilson and Jones, 1979) and from comparisons of canal dimensions in different animals (Jones and Spells, 1963; Jones, 1984; Gauldie and Radtke, 1990) and in animals of different sizes (Curthoys, 1983). The Steinhausen torsion pendulum model (Steinhausen, 1933; Oman *et al.*, 1987) identifies the radius of curvature of the canal, the bore radius of the canal duct, the viscosity and density of the endolymph, and the stiffness of the cupula as being important factors determining the vestibular response characteristics. Although, in vertebrates, there is a good correlation between the frequency sensitivity predicted from measurements of the radius of curvature of the canal and the bore radius of canal duct, and the actual response characteristics (Correia *et al.*, 1981), the statocyst position is much less clear.

The use of such a model in cephalopods is supported by the relatively large size of the statocysts in newly hatched coleoids. Those statocysts are more than a quarter of the mantle length, but grow at a much lower rate than the animal; *i.e.*, they increase in size by about 29 times while the mantle length is increasing by 390 times (Maddock and Young, 1984). This relative conservation of statocyst size fits well with the idea that statocyst size is constrained by the physical principles under which the organ operates, and that the dimensions of the system are adjusted to the speed at which the animal turns. In addition, Maddock and Young (Maddock and Young, 1984; Young, 1984, 1989) have described a number of correlations between statocyst morphology and probable swimming performance, including data showing that the faster moving squids tend to have a narrower canal, thus

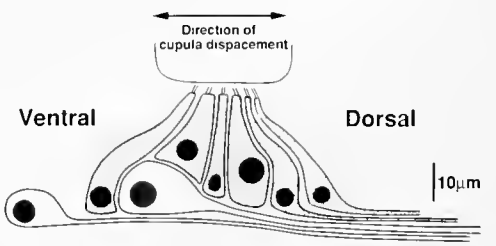

Figure 2. Diagram of a cross-section through the crista strip of the squid, *Alloteuthis subulata*. Three main cell types are present: the primary sensory hair cells (lightly stippled), the secondary sensory hair cells (darkly stippled), and the afferent neurons (unstippled). After Williamson, 1989a.

presumably improving the high frequency response, whereas slow moving cephalopods tend to have relatively large statocysts, thus increasing their low frequency sensitivity.

As pointed out by Young (1984), the main difficulties in applying this idea to cephalopod statocysts is that the radius of curvature can only be approximated as the cross-sectional diameter of the statocyst, and there is only rarely a canal-like structure in the statocyst formed by the anticrista and hamuli. In addition, although there are recognizable patterns of anticristae and hamuli in different groups of cephalopods, it is unclear how these projections affect the flow of endolymph. Clearly, we need a more realistic model of how the endolymph flows within the statocyst, and how this is influenced by the various morphological features of the statocyst.

Cupula parameters

Other morphological features likely to effect the frequency response and sensitivity of the statocyst angular acceleration receptor system are the size, shape, and attachment of the cupulae. The cupulae are gelatinous, flap-like structures, projecting towards the middle of the statocyst, and attached to the crista ridge along the whole length of a segment. The cupulae however, appear to be irregular in shape, often being much taller in the center of the crista segment than at the edges; this is particularly prominent in the squid, *Alloteuthis* (Fig. 3a). The center of the cupula will therefore present a much greater area of resistance to endolymph flow than the edges and hence, unless the cupula is very rigid, will more easily stimulate the underlying hair cells. This likely differential sensitivity in different parts of a single crista segment may be a method of fractionating the sensitivity range of the system. In *Octopus* this is even more pronounced (Fig. 3b,c). Here, the nine crista segments have alternating large and small cupulae, with the tall cupulae having narrower bases than the small ones (Budelmann *et al.*, 1987). This, again, is likely to fractionate the range over which the system operates and, indeed, recordings from the afferent neurons in representatives of these two different segments indicate that the segment with the large cupula is up to 10 times more sensitive than that with the small cupula (Williamson and Budelmann, 1985a,b). The increase in sensitivity means, however, that the afferents from the large segment can be driven into response saturation at a much lower stimulus intensity than those from the small cupula segment. This arrangement could be correlated with *Octopus'* two forms of locomotion, the high sensitivity, large cupulae being needed during slow crawling movements, and the low sensitivity, small cupulae during jet propelled movements.

Like the statoliths, anticristae, and hamuli, the cupulae are also likely to have an effect on the pattern of endolymph flow within the statocyst. Although Young (Maddock and Young, 1984; Young, 1989) has used a vertebrate semicircular canal model to predict endolymph flow, and hence sensory response characteristics, this is unlikely to be adequate. Recent vertebrate models have shown that even a good canal structure, with the three canals orthogonally arranged, is likely to have a complicated pattern of endolymph flow with crosstalk between the canals (Oman *et al.*, 1987; Muller and Verhagen, 1988). In cephalopods, which rarely have a single canal structure, endolymph flow patterns are extraordinarily difficult to predict (Govardovskii, 1971; Muller, pers. comm.). Even the manner of movement of the cupula is unknown; *i.e.*, whether it pivots like a lever, or slides like a piston, or flexes like a diaphram, although recent modelling work has suggested that the cupula does not operate as a simple pivot (Morris, 1988).

Another unknown with respect to cupula movement is the strength of its attachment to the crista and the restoring force it develops when displaced. This will have a

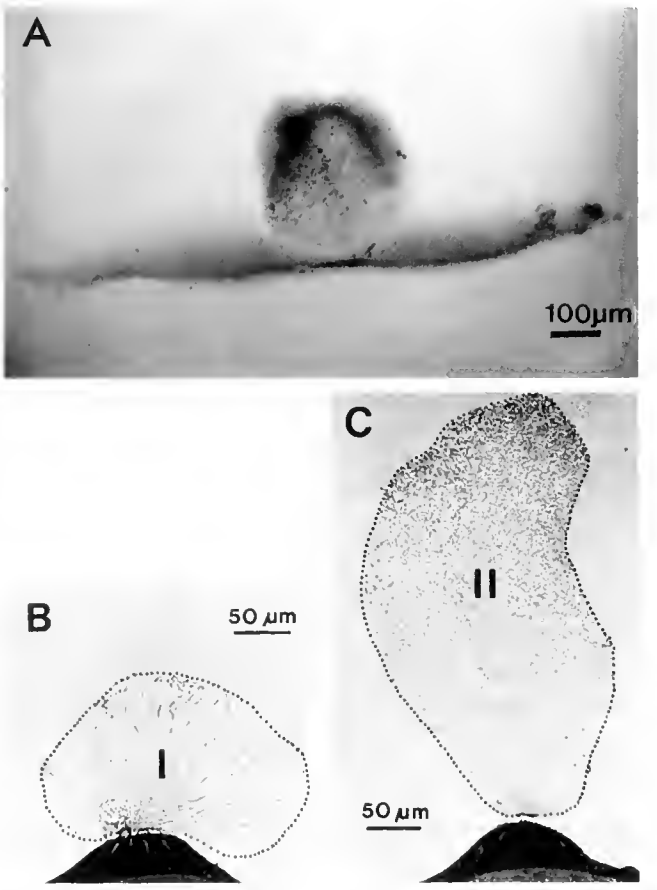

Figure 3. (A) Crista cupula from the squid, *Alloteuthis subulata*. The cupula has been fixed in osmium and then detached from the crista segment. Note that it has a large central mass and is much shorter at the edges. From Williamson 1990a. (B and C) Transverse sections through two different crista segments in the statocyst of *Octopus* showing a small, wide-based cupula type and a large, narrow-based cupula type. From Williamson and Budelmann, 1985b.

major impact on the frequency response characteristics of the crista/cupula system, and any variation between crista segments, or between different animals, would have to be taken into account in a model describing statocyst response characteristics.

The presence or absence of a perilymphatic space may also affect the sensitivity of the statocyst. The octopods, cirroctopods, and *Vampyroteuthis* all have a lymph-filled space between the cartilaginous wall of the statocyst cavity and the statocyst sac containing the sensory epithelia. Anliker and van Buskirk (1971), dealing with the vertebrate semicircular canal system, have argued that the movement of perilymph may have a major effect on the dynamic response characteristics of the system. Although any perilymph flow in the statocyst would be restricted by the fibers supporting the statocyst sac, there may well be an effect in cephalopods from this source.

Physiological Features

Extracellular recordings from statocyst afferents have shown that the crista/cupula system in *Octopus* acts as a velocity transducer over a middle range of frequencies and has response characteristics similar to those of the vertebrate semicircular canal system (Williamson and Budelmann, 1985a). There is as yet no data on afferent response characteristics from decapod statocysts. Recent intracellular recordings from hair cells in the statocyst of the squid, *Alloteuthis subulata*, have provided the first measurements of the sensitivities of cephalopod hair cells (Williamson, 1991a). This work (Fig. 4) has shown that the secondary sensory hair cells in the crista have sensitivities of at least 0.5 mV per degree of cilia deflection. This compares with sensitivities of about 3 mV per degree for frog saccular hair cells (Hudspeth and Corey, 1977), 10 mV per degree for turtle basilar papillar hair cells (Crawford and Fettiplace, 1985), and 30 mV per degree for mouse cochlear hair cells (Russell *et al.*, 1986). This work has also confirmed morphological studies (Budelmann *et al.*, 1987) showing that at least some of the secondary hair cells are physiologically polarized in the opposite direction to the primary hair cells (Fig. 4). This bipolar sensitivity does not occur in vertebrate vestibular cristae and, although it may be more energy efficient (Williamson, 1991a), it is not clear if it will have any effect on the sensitivity or frequency bandwidth of the system.

Differences in hair cell sensitivity

There may well be differences in the intrinsic sensitivities of the individual crista hair cells. In *Octopus*, there are at least three different morphological types of crista hair cells: the primary sensory hair cells, the small secondary sensory hair cells, and the large secondary sensory hair cells. In addition, there are different types of afferent

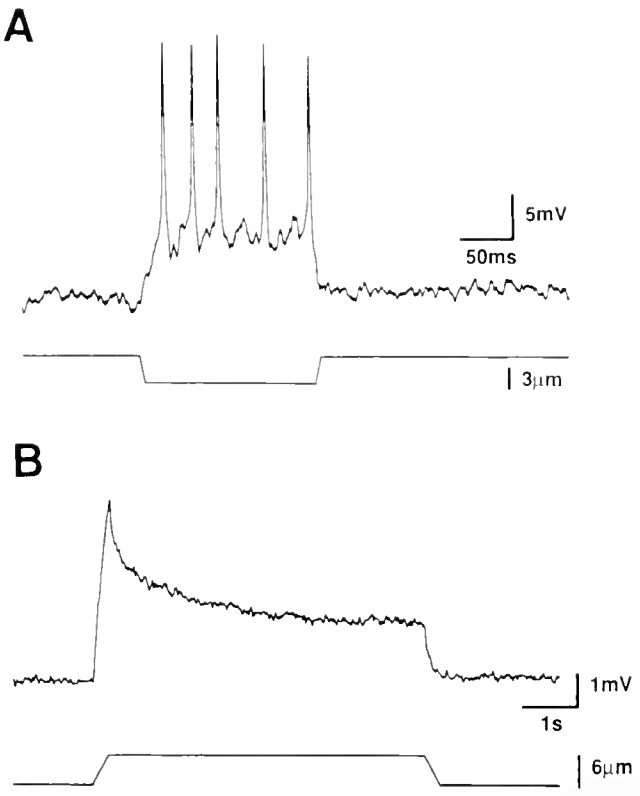

Figure 4. Intracellular recordings from a primary sensory hair cell (A) and a secondary sensory hair cell (B) in the crista of the squid statocyst, showing their responses to small mechanical displacements of the overlying cupula (displacements shown in lower traces). Note that the primary and secondary hair cell depolarizations are caused by cupula displacements of opposite directions, indicating that the cells are polarized in opposing directions, and that only the primary hair cell carries action potentials. From Williamson, 1991a.

neurons, and there may also be subdivisions of the hair cells types (Budelmann *et al.*, 1987). These morphological differences are likely to be reflected in physiological cell parameters, such as input impedance and cell conductance, and therefore result in differences in the sensitivities of the various cell types (Williamson and Budelmann, 1985a).

Electrical coupling

At least some of the secondary sensory hair cells in the squid statocyst cristae are known to be electrically coupled along the length of the crista segment (Fig. 5) (Williamson, 1989a). It has been argued that this coupling will lead to an improvement in the signal to noise ratio of the system and hence enhance its overall sensitivity. However, such coupling is also likely to lower the high frequency response of the system. Clearly, if the coupling could be varied under direct nervous control, this would be a powerful mechanism for changing the sensitivity and frequency response of the system. A comparable sensory system with

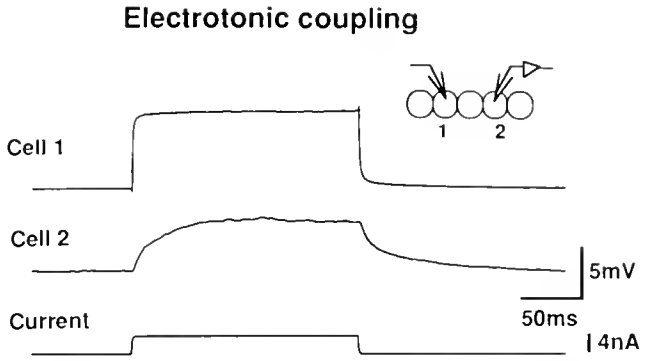

Figure 5. Intracellular recordings from two nearby secondary sensory hair cells in the statocyst crista of the cuttlefish, *Sepia officinalis*, showing their electrotonic coupling. A small current (bottom trace) is injected into Cell 1 (top trace), producing a depolarization, and this causes a simultaneous, but smaller, depolarization in the neighboring cells (Cell 2, middle trace). This provides evidence that the secondary sensory hair cells in a crista segment are electrotonically coupled along the segment. From Williamson, 1991b.

neurally controlled electrical coupling is in the vertebrate retina, where the neurotransmitter dopamine alters the coupling ratio between retinal horizontal cells (Knapp and Dowling, 1987). Dopamine has been located in the retinal efferents in *Octopus* (Suzuki and Tasaki, 1983) and has also been tentatively identified in the statocyst efferents (Budelmann and Bonn, 1982; Williamson, 1989b). It would be an astonishing example of parallel evolution if these two disparate sense organs, the eye and the statocyst, used dopaminergic control of electrical coupling to regulate their sensory input.

Efferent system

The statocysts have an exceptionally large efferent innervation; of the axons in the *Octopus* statocyst crista nerves, 75% are efferent fibers travelling from the brain to the statocyst (Budelmann *et al.*, 1987). In contrast, about 8% of axons in a vertebrate vestibular nerve are efferents (Goldberg and Fernandez, 1980). This efferent innervation forms a plexus running beneath the crista epithelium and makes synaptic contact with primary and secondary sensory hair cells, as well as with the afferent and other efferent neurons (Budelmann *et al.*, 1987). The efferent fibers are active during movements of the animal's head (Williamson, 1986) and can depress or enhance (Fig. 6) the afferent output from the statocyst (Williamson, 1985). These effects are due to direct synaptic hyperpolarization, or to depolarization, of the secondary sensory hair cells, their first-order afferent neurons, and possibly, the primary sensory hair cells (Williamson, 1989c). The inhibitory response is probably due to cholinergic synapses (Auerbach and Budelmann, 1986; Williamson, 1989b), and the excitatory response to catecholaminergic synapses (Budelmann and Bonn, 1982; Williamson, 1989b).

Such a widespread and complex efferent innervation provides the animal with direct and independent control of both the hair cell receptor potential and the level of activity of the afferent neurons. Thus, not only can the gain of the overall system be increased or decreased, but the responses of individual elements can also be varied. This permits an extension of the dynamic range of the system by allowing adjustments to the membrane potentials of the hair cells and afferent neurons, so that the cells' responses are maintained within their operating ranges and at their maximum sensitivities.

Motile cilia and cells

Another feature that may have an impact on the sensitivity of the statocyst hair cells is the presence of motile cilia. Ciliated cells are distributed all over the inner surface of the statocyst, as well as in Kölliker's canal (Young, 1960); these cells have beating cilia that set up minute endolymph currents within the statocyst (Budelmann, 1990). The biological significance of these cells is not clear, but the fluid flow that they produce may be sufficient to increase the background noise within the system and thus reduce the overall sensitivity of the receptor system.

In addition to these ciliated cells, which are motile, some of the sensory hair cells within the crista or macula epithelia may also have a motor capability. Sensory cells with motile beating cilia are present in the statocysts of other mollusks (Stommel *et al.*, 1980), and some circum-

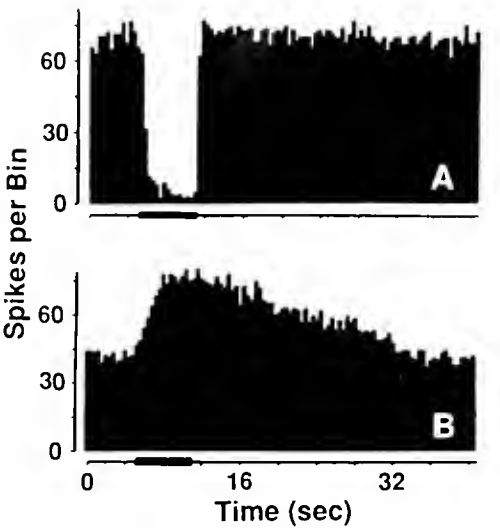

Figure 6. Peristimulus time histograms showing the effect of efferent activity on the statocyst afferent activity. Extracellular recordings were obtained from afferent neurons from the *Octopus* crista and then efferents to this segment activated by electrical stimulation (duration and time indicated by heavy bar on time axes). This caused an inhibition of the activity of unit A, but an increase in the activity of unit B. This provides evidence that there are both inhibitory and excitatory efferents innervating the statocyst crista. Bin width, 400 ms; stimulus, 50 Hz pulses for 6 s. From Williamson, 1985.

stantial evidence suggests that part of the membrane potential noise in recordings from some secondary sensory hair cells in squid crista may be due to ciliary movement (Williamson, 1991a). If some of the hair cells in the crista or macula do have a motor capability, this could have a large impact on the responses of the system. Recent work on vertebrate hair cells has shown that motility in the outer hair cells of the cochlea can change the response characteristics of the sensory system by altering the micromechanics of the basilar membrane responses (Hudspeth, 1989). This is thought to be due to changes in the length of the cells rather than an active beating of their cilia. Such a system, operating under efferent control, could also be present in the cephalopod statocyst.

Central processing

A final feature that can influence the characteristics of the statocyst input is the central processing of the statocyst information. This has two major functions: first, the central control of the statocyst efferents, and second, the analytical processing of the statocyst afferent information.

As has already been discussed, the efferents can have a major impact on the response characteristics of the statocyst. This can operate through a variety of mechanisms. In a feed-forward system, for example, where the animal makes a voluntary movement such as a jet propelled escape, the efferents can be used to suppress, peripherally, the massive input from the statocysts that may saturate the afferent system. This could also be achieved centrally by an efference copy mechanism, as has been proposed for fish electroreception (Bell, 1981). Additionally, the system may operate in a feedback mode, whereby the afferent input feeds back through the efferents to dynamically adjust the sensitivity of the system (Williamson, 1986). This may be important in sustained swimming or in movements imposed by external water currents. Where the efferents are acting at the periphery, the frequency response of the system may well be limited by the conduction velocities of the efferents. The efferent axons are small, unmyelinated fibers (Budelmann *et al.*, 1987) and are likely to have much slower conduction velocities than the larger afferent fibers.

The statocyst afferents project to the ipsi- and contralateral lateral pedal, pedal, and ventral magnocellular lobes within the suboesophageal mass of the octopus brain (Budelmann and Young, 1984; Plän, 1987). Probably, the sensitivity of the sensory system can be improved centrally by summing multiple afferent inputs. For example, where ipsi- and contralateral statocyst inputs are from receptors responding to the same direction of movement, then these multiple channel inputs could be combined to improve the sensitivity of the system or to reduce the noise in the system (Aidley, 1971). This could also occur at the periphery, where some afferent neurons, in both crista and macula, receive multiple inputs from a number of nearby hair cells (Colmers, 1981; Budelmann *et al.*, 1987).

Future research

The idea of being able to predict the locomotory performance of a cephalopod solely from the morphology of its statocysts is very attractive, especially because all but a few species are unavailable for free swimming studies or for physiological testing. However, although such prediction based on a study of the vestibular system is now feasible for vertebrates, only generalized statements can be made about cephalopods.

There are two main reasons for this. First, there is no hydrodynamic model of endolymph flow within the statocyst that takes into account the special features of the statocysts. Although vertebrate semicircular canal models are a good starting point, we can have only limited confidence in the accuracy of predictions transported directly into the cephalopod domain. Second, there is no base of physiological work on cephalopods to provide the constants needed for a mathematical description of statocyst performance, or to test and refine any model predictions. For example, even the best model based on morphological studies, could not predict the effects of electrical coupling or motile cilia on the afferent response characteristics.

Future work, therefore, should be concentrated on developing an adequate model of statocyst endolymph flow, including a description of cupula movement. This should be complemented by an investigation of the afferent response characteristics of representatives of the different cephalopod groups. These data, together with a description of the swimming styles and the likely accelerations produced in a few species of cephalopods, should give us sufficient information to predict with some confidence the probable locomotory performance of an animal, based only on the morphology of its statocyst.

Acknowledgments

I would like to thank Prof. J. Z. Young for his unending stimulation, enthusiasm, and encouragement. Much of this work was supported by the Alexander von Humboldt Stiftung and the Wellcome Trust.

Literature Cited

Aidley, D. J. 1971. *The Physiology of Excitable Cells.* Cambridge University Press, London. Pp. 306–333.

Anliker, M., and W. van Buskirk. 1971. The role of perilymph in the responses of the semicircular canals to angular accelerations. *Acta Otolaryngol.* **72:** 93–100.

Auerbach, B., and B. U. Budelmann. 1986. Evidence for acetylcholine as a neurotransmitter in the statocyst of *Octopus vulgaris*. *Cell Tissue Res.* **243:** 429–436.

Bell, C. C. 1981. An efference copy which is modified by reafference input. *Science* **214:** 450–453.

Budelmann, B. U. 1980. Equilibrium and orientation in cephalopods. *Oceanus* **23:** 34–43.

Budelmann, B. U. 1990. The statocysts of squid. In *Squid as Experimental Animals,* D. L. Gilbert, W. J. Adelman and J. M. Arnold, eds. Plenum Press, New York.

Budelmann, B. U., and U. Bonn. 1982. Histochemical evidence for catecholamines as neurotransmitters in the statocyst of *Octopus vulgaris. Cell Tissue Res.* **227:** 475–483.

Budelmann, B. U., M. Sachse, and M. Staudigl. 1987. The angular acceleration receptor system of the statocyst of *Octopus vulgaris.* morphometry, ultrastructure, and neuronal and synaptic organization. *Phil. Trans. R. Soc. Lond. B* **315:** 305–343.

Budelmann, B. U., and H. G. Wolff. 1973. Gravity response from angular acceleration receptors in *Octopus vulgaris. J. Comp. Physiol.* **85:** 283–290.

Budelmann, B. U., and J. Z. Young. 1984. The statocyst-oculomotor system of *Octopus vulgaris:* extraocular eye muscles, eye muscle nerves, statocyst nerves and the oculomotor centre in the central nervous system. *Phil. Trans. R. Soc. Lond. B.* **306:** 159–189.

Colmers, W. F. 1981. Afferent synaptic connections between hair cells and the somata of intramacular neurons in the gravity receptor system of the statocyst of *Octopus vulgaris. J. Comp. Neurol.* **197:** 385–394.

Correia, M. J., J. P. Landolt, M.-D. Ni, A. R. Eden, and J. L. Rae. 1981. A species comparison of linear and nonlinear transfer characteristics of primary afferents innervating the semicircular canal. In *The Vestibular System: Function and Morphology,* T. Gualtierotti, ed. Springer Verlag, New York.

Crawford, A. C., and R. Fettiplace. 1985. The mechanical properties of ciliary bundles of turtle cochlear hair cells. *J. Physiol.* **364:** 359–380.

Curthoys, I. S. 1983. The development of function of primary vestibular neurons. Pp. 425–461 In *Development of Auditory and Vestibular Systems,* E. Romand, ed. Academic Press, New York.

Gauldie, R. W., and R. L. Radtke. 1990. Using the physical dimensions of the semicircular canal as a probe to evaluate inner ear function in fishes. *Comp. Biochem. Physiol.* **96A:** 199–203.

Goldberg, J. M., and C. Fernandez. 1980. Efferent vestibular system in the squirrel monkey: anatomical location and influence on afferent activity. *J. Neurophysiol.* **43:** 986–1025.

Govardovskii, V. I. 1971. Some characteristics and dynamics of the endolymph in cephalopod statocysts. *J. Evol. Biochem. Physiol.* **7:** 347–351.

Hudspeth, A. J. 1989. How the ear's ear works. *Science* **341:** 397–404.

Hudspeth, A. J., and D. P. Corey. 1977. Sensitivity, polarity and conductance change in the response of vertebrate hair cells to controlled mechanical stimuli. *Proc. Natl. Acad. Sci. USA.* **74:** 2407–2411.

Jones, G. M. 1984. The functional significance of semicircular canal size. In *Handbook of Sensory Physiology,* Vol. 6 (part 1), H. H. Kornhuber, ed. Springer-Verlag, New York.

Jones, G. M., and K. E. Spells. 1963. A theoretical and comparative study of the functional dependence of the semicircular canal upon its physical dimensions. *Proc. R. Soc. Lond. B.* **157:** 403–419.

Knapp, A. G., and J. E. Dowling. 1987. Dopamine enhances excitatory amino acid-gated conductances in cultured retinal horizontal cells. *Nature* **325:** 437–439.

Maddock, L., and J. Z. Young. 1984. Some dimensions of the angular acceleration receptor systems of cephalopods. *J. Mar. Biol. Assoc. U.K.* **64:** 55–79.

Morris, C. C. 1988. Statolith growth lines and statocyst function in the cephalopoda. Ph.D. thesis, University of Cambridge, U.K.

Muller, M., and J. H. G. Verhagen. 1988. A new quantitative model of total endolymph flow in the system of semicircular ducts. *J. Theor. Biol.* **134:** 473–501.

Oman, C. M., E. N. Marcus, and I. S. Curthoys. 1987. The influence of semicircular canal morphology on endolymph flow dynamics. *Acta Otolaryngol. (Stockh.)* **103:** 1–13.

Plän, T. 1987. Functional neuroanatomy of the sensory-motor lobes of the brain of *Octopus vulgaris* Ph.D. thesis, University of Regensburg, West Germany.

Russell, I. J., A. R. Cody, and G. P. Richardson. 1986. The responses of inner and outer hair cells in the basal turn of the guinea-pig cochlea and in the mouse cochlea grown in vitro. *Hearing Res.* **22:** 199–216.

Steinhausen, W. 1933. Über die Beobachtung der Cupula in den Bogengangsampullen des Labyrinths des lebenden Hechts. *Pflügers Arch. Ges. Physiol.* **232:** 500–512.

Stephens, P. R., and J. Z. Young. 1982. The statocysts of the squid *Loligo. J. Zool. Lond.* **197:** 241–266.

Stommel, E. W., R. E. Stephens, and D. L. Alkon. 1980. Motile statocyst cilia transmit rather than directly transduce mechanical stimuli. *J. Cell Biol.* **87:** 652–662.

Suzuki, H., and K. Tasaki. 1983. Inhibitory retinal efferents from dopaminergic cells in the optic lobe of the *Octopus. Vision Res.* **23:** 451–457.

Williamson, R. 1985. Efferent influences on the afferent activity from the octopus angular acceleration receptor system. *J. Exp. Biol.* **119:** 251–254.

Williamson, R. 1986. Efferent activity in the *Octopus* statocyst nerves. *J. Comp. Physiol. A* **158:** 125–132.

Williamson, R. 1989a. Electrical coupling between secondary hair cells in the statocyst of the squid, *Alloteuthis subulata. Brain Res.* **486:** 67–72.

Williamson, R. 1989b. Electrophysiological evidence for cholinergic and catecholaminergic efferent transmitters in the statocyst of *Octopus. Comp. Biochem. Physiol.* **93C:** 23–27.

Williamson, R. 1989c. Secondary hair cells and afferent neurones of the squid statocyst receive both inhibitory and excitatory efferent inputs. *J. Comp. Physiol. A.* **165:** 847–860.

Williamson, R. 1991a. The responses of primary and secondary sensory hair cells in the squid statocyst to mechanical stimulation. *J. Comp. Physiol. A* **167:** 655–664.

Williamson, R. 1991b. The responses of the sensory hair cells in the statocyst of *Sepia.* In *The Cuttlefish,* E. Boucaud-Camou, ed. University de Caen Press, Caen, France.

Williamson, R., and B. U. Budelmann. 1985a. The responses of the *Octopus* angular acceleration receptor system to sinusoidal stimulation. *J. Comp. Physiol. A* **156:** 403–412.

Williamson, R., and B. U. Budelmann. 1985b. An angular acceleration receptor system of dual sensitivity in the statocyst of *Octopus vulgaris. Experientia* **41:** 1321–1323.

Wilson, V. J., and G. M. Jones. 1979. *Mammalian Vestibular Physiology,* Plenum Press, New York.

Young, J. Z. 1960. The statocyst of *Octopus vulgaris. Proc. R. Soc. Lond. B.* **152:** 3–29.

Young, J. Z. 1984. The statocysts of cranchiid squids (Cephalopoda). *J. Zool. Lond.* **203:** 1–21.

Young, J. Z. 1989. The angular acceleration receptor system of diverse cephalopods. *Phil. Trans. R. Soc. Lond.* **325:** 189–238.

Reference: *Biol. Bull* **180**: 228–233. (April, 1991)

Neural Control of Speed Changes in an Opisthobranch Locomotory System

RICHARD A. SATTERLIE

Department of Zoology, Arizona State University, Tempe, Arizona 85287-1501 and Friday Harbor Laboratories, Friday Harbor, Washington 98250

Abstract. Three forms of forward locomotion have been described in the pteropod mollusk *Clione limacina*, including slow, fast, and escape swimming. The neuromuscular organization of the swimming system suggests that a two-geared system operates for slow and fast swimming, while the escape response is superimposed on fast swimming. In addition to escape, changes in locomotory speed can occur through a dramatic "change-of-gears," or through a more subtle change of speed within gears. The former involves reconfiguration of the central pattern generator and recruitment of previously inactive motor units. The latter can be due to: changes in tonic inputs to the central neurons, central modulation that is not sufficient to "change gears," endogenous properties of muscle cells, and peripheral modulation of muscle contractility. The initial ballistic phase of escape swimming is believed to be triggered by activity in a newly identified pair of swim motor neurons that neither receive information from, nor provide input to, the central pattern generator. These neurons appear to produce a startle response. Evidence presented suggests that most, if not all, of these variables help produce locomotory plasticity in *Clione*.

Introduction

Locomotory speed is a function of several factors, most notably the frequency of movements of locomotory appendages and the force of appendage movements. A change in either of these factors can directly trigger a change in locomotory speed. The former is the provence of the central pattern generator circuitry, whereas the latter can be linked to modifications of the neuromuscular system, and can conceivably include purely peripheral plasticity. Furthermore, activity of central and peripheral modulators can serve to increase the richness of locomotory variability.

Few preparations are conducive to simultaneous electrophysiological monitoring of both central and peripheral activity during both dramatic and subtle changes in propulsive activity. One preparation that combines similar behavioral variability with the typical advantages of the molluscan nervous system—relatively simple neural organization coupled with large cell size—is the locomotory system of the pteropod mollusk *Clione limacina*. Thus far, the majority of work on *Clione* has centered on the central generation of rhythmic locomotory activity (Arshavsky *et al.*, 1985a, b, c, d, 1986, 1989; Satterlie, 1985, 1989; Satterlie and Spencer, 1985; Satterlie *et al.*, 1985), although recent work has focussed on peripheral neuromuscular physiology (Satterlie, 1987, 1988; Satterlie *et al.*, 1990). The purpose of this review is to summarize current work and present new data that relate to the neurobiological basis of locomotory plasticity in the *Clione* swimming system.

Results and Discussion

Locomotory movements of *Clione* include relatively simple two-phase flapping movements of wing-like parapodia (wings). Three forms of locomotion have been described including slow, fast, and escape swimming (Arshavsky *et al.*, 1985a; Satterlie *et al.*, 1985, 1990; Satterlie, 1989). The predominant form is slow swimming, which allows the animal to maintain position in the water column or to move forward (upward) slowly. Wing beat frequencies observed during slow swimming ranged from 1 to 4 Hz. Changes in the rate of forward movement within the slow speed occur both with and without a change in the frequency of wing movements. The latter cases presumably involve changes in wing contractility, as sug-

Received 17 August 1990; accepted 23 January 1991.

gested by behavioral observations in which noticeable changes in the vigor of wing movements have been observed in the absence of a change in wing beat frequency. The change to fast swimming is a triggered, typically dramatic change in the frequency (range: 3–8 Hz) and force of wing movements. In addition to these two basic forms of swimming, a ballistic escape response can be triggered following vigorous stimulation of the tail (Satterlie *et al.*, 1990). The initial phase of escape swimming involves one or two wing cycles characterized by massive contractions of the swim musculature. This "startle" phase is followed by a variable period of enhanced fast swimming. While fast swimming can be triggered without an escape response being activated, escape is always followed by fast swimming.

Despite the three-phase swimming behavior, both the central and peripheral organization of the swimming system appears to be based on two speeds. Evidence presented later suggests that escape swimming is merely superimposed on the fast swimming system. Centrally, the change from slow to fast swimming involves a "change-of-gears," defined here as a change in pattern generator output that results in recruitment (or dropping out) of motor units that have significantly different biochemical and contractile properties than those that were previously (or continuously) active. Peripherally, *Clione* has two types of striated swim muscle fibers: slow-twitch fatigue-resistant and fast-twitch fatigable fibers (Satterlie, 1987; Satterlie *et al.*, 1990). To complement the peripheral organization, two types of swim motor neurons have been described: one associated with slow-twitch muscle activity (and slow swimming), and the other associated with both types of muscle fibers. The latter motor units, which include two large swim motor neurons in each pedal ganglion, are recruited into activity during fast swimming (Satterlie, 1987, 1988, 1989).

With the two-geared arrangement of the *Clione* swimming system before us, three categories of locomotory speed changes will be described, with evidence presented to suggest neurobiological mechanisms for each. Categories of speed change mechanisms include: (1) change-of-gears, (2) change of speed within gears, and (3) escape swimming.

Speed changes due to a "change-of-gears"

Centrally, the change-of-gears from slow to fast swimming involves reconfiguration of the central pattern generator (Arshavsky *et al.*, 1985d, 1989), as previously inactive pedal interneurons become active elements of the swim pattern generator. During slow swimming, a two-phase motor drive is produced by activity in two antagonistic groups of pedal interneurons that interact through reciprocal inhibitory connections (Arshavsky *et al.*, 1985b, c; Satterlie, 1985, 1989). One group of interneurons (V-phase interneurons) produces a single action potential during ventral bending of the wings, whereas the other group (D-phase interneurons) spikes during dorsal bending of the wings. Alternating activity of these two groups of interneurons continues during fast swimming, but two additional interneuron types become active (Arshavsky *et al.*, 1985d, 1989). Delayed V-phase interneurons, which receive only inhibitory input from D-phase interneurons during slow swimming, produce slightly delayed (with respect to normal V-phase interneurons) V-phase spikes during fast swimming. Spikes in the delayed V-phase interneurons trigger activity in the second type of interneuron, called interneurons 12 (Arshavsky *et al.*, 1985d, 1989). Each interneuron 12 produces a plateau potential that is turned on by excitatory input from delayed V-phase interneurons, and is turned off by inhibitory input from D-phase interneurons. Plateau potentials of interneurons 12 inhibit V-phase interneurons and excite D-phase interneurons. Addition of the delayed V-phase and type 12 interneurons to the swim pattern generator thus produces an early termination of V-phase activity coupled with onset of the next D-phase. This change increases the cycle frequency of pattern generator output (Arshavsky *et al.*, 1985a) and is associated with a recruitment of previously inactive large motor neurons (Fig. 1). As mentioned previously, recruitment of these motor neurons is associated with the activation of the fast-twitch musculature of the wings. The change-of-gears is also associated with a 5–15 mV tonic depolarization in "normal" D- and V-phase interneurons of the swim pattern generator (Fig. 1). The combination of increased cycle frequency and increased force of wing contractions through recruitment of "fast-twitch" motor units produces a dramatic increase in forward propulsion speed.

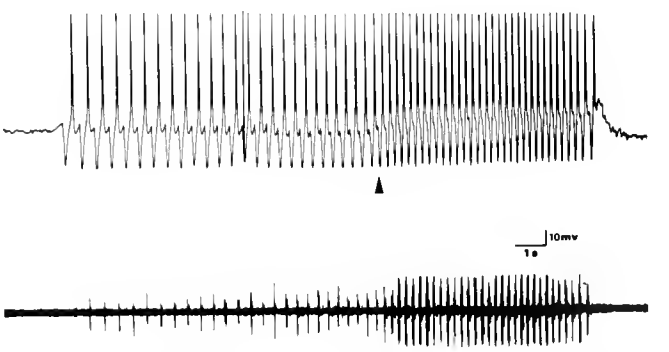

Figure 1. Intracellular recording from a pattern generator interneuron of *Clione* (top trace) with a simultaneous extracellular recording from the wing nerve (bottom trace). The record shows a change-of-gears (arrow) involving an increase in cycle frequency and a tonic depolarization in the interneuron. The change recruits large spikes in the wing nerve recording. These large spikes have been shown to reflect activity in large swim motor neurons. Recording by A. N. Spencer, University of Alberta.

Rewiring of a central pattern generator is certainly not a new concept. The pyloric central pattern generator of the lobster stomatogastric system can exhibit at least four distinct functional circuits and thus four distinct motor activities (Flamm and Harris-Warrick, 1986a, b; Harris-Warrick *et al.*, 1989). In addition to the unmodulated circuit, the amine modulators dopamine, octopamine, and serotonin can each produce a dramatically distinct functional circuit (see Harris-Warrick *et al.*, 1989, for a review). In the opisthobranch mollusk *Tritonia*, variable output in the body wall motor systems can be produced by varying the types and intensities of triggering sensory inputs. According to the polymorphic network concept (Getting and Dekin, 1985), different inputs can activate different configurations of motor control systems to produce unique motor outputs as distinctive as body wall withdrawal and swimming movements. These two examples demonstrate that a motor control system, or part of it, can be used for more than one behavior. In comparison, reconfiguration of the *Clione* swim pattern generator appears to involve exclusively frequency modulation rather than changes in the phase relationships or functional wiring of the pattern generator.

The change from slow to fast swimming in *Clione* is induced in both intact and reduced preparations when the preparations are bathed in 10^{-5} to 10^{-6} *M* serotonin (Arshavsky *et al.*, 1985a, d; Satterlie 1989). Under these conditions, fast swimming continues as long as serotonin remains in the bath. At the level of individual pattern generator interneurons, serotonin produces a 5–10 mV tonic depolarization similar to that seen during spontaneous fast swimming. The source of these tonic depolarizations is not known. Serotonin has also been implicated in the initiation of swimming activity in the leech (Kristan and Weeks, 1983; Nusbaum and Kristan 1986; Nusbaum, 1986) and of *Aplysia brasiliana* (Parsons and Pinsker, 1989), as well as pedal locomotion in non-swimming *Aplysia* (Mackey and Carew, 1983). Serotonin also modulates ongoing rhythmic activity in a number of preparations, including lamprey swimming (Harris-Warrick and Cohen, 1985), feeding in *Aplysia* (Kupfermann and Weiss, 1982), insect flight (Claassen and Kammer, 1986), and the pyloric rhythm of the lobster (Flamm and Harris-Warrick, 1986a, b). Serotonin can also have system-wide behavioral effects, as in the regulation of posture in lobsters (Kravitz *et al.*, 1985).

Changes of swimming speed within gears

Although the possibilities for changes of speed within gears are numerous, four possibilities will be considered here: (1) changes in tonic input to swim interneurons and motor neurons, (2) central modulation of the pattern generator (*e.g.*, with serotonergic inputs) at a level not sufficient to change gears, (3) the role of endogenous properties of muscle cells, and (4) peripheral modulation of muscle contractility. The first two involve central modifications while the last two modify peripheral activity.

Changes in tonic input to swim neurons

Despite the description of pedal neurons that show variable tonic activity associated with changes in pattern generator activity in *Clione* (Arshavsky *et al.*, 1984), little is known about the variety and sources of tonic influences over pattern generator activity. Inasmuch as tonic depolarization of isolated pattern generator interneurons is related to spontaneous firing frequency (Arshavsky *et al.*, 1986), then tonic inputs can presumably modify the frequency of pattern generator output. Provided that the inputs do not cause pattern generator reconfiguration, the change in cycle frequency will be translated into a change of locomotory speed within the appropriate "gear." Tonic input could exert this influence in either slow or fast swimming gears.

Central modulation not sufficient to change gears

The source of central serotonergic inputs to the pattern generator that are responsible for reconfiguration and gear change have not yet been identified. But circumstantial evidence now in hand has led us to investigate descending serotonergic inputs from the cerebral ganglia. Serotonin-immunoreactive neurons have been found in the medial posterior and medial anterior regions of the cerebral ganglia. Axons from some of these cells run from the cerebral ganglia to the pedal ganglia via the cerebro-pedal connectives. Focal extracellular stimulation of the medial posterior region of a pedal ganglion results in acceleration of pattern generator activity, or with strong stimuli, changes in pattern generator activity identical to changes associated with activation of fast swimming activity. Transection of the cerebro-pedal connective greatly reduces these responses. Assuming that the central modulation does not operate in an all-or-none manner, subthreshold levels of modulation (subthreshold for change of gears) might trigger a change of swimming speed within the slow gear, and different levels of supra-threshold modulation might produce variable pattern generator activity in the fast gear. Such changes of swimming speed should be expressed as a change in cycle frequency, unless swim motor neurons are also affected by the central modulatory subsystem. In the latter case, changes in both cycle frequency and force of wing movements will be seen. A further, purely speculative possibility allows for separate modulation of pattern generator interneurons and swim motor neurons, a condition that would add greatly to the complexity of the behavioral output. Potential central

modulators other than serotonin are not being considered here, but should not be discounted.

Intrinsic properties of muscle cells

Intrinsic properties of muscle cells, particularly related to repetitive firing activity, can influence the force of swim muscle contractions. Such intrinsic properties could be synaptic or non-synaptic, the latter including changes in passive or active membrane properties, or in excitation-contraction coupling. Both slow-twitch and fast-twitch fibers of the *Clione* swimming system exhibited non-synaptic facilitation of the amplitude of spike-like responses with repetitive, direct depolarization of individual muscle cells (Satterlie, 1988). The facilitation was strongly frequency-dependent, so that both overall amplitude of spike-like responses and initial rate of change of spike-like response amplitude showed a positive correlation with frequency of induced activity over the range of frequencies normally encountered during slow and fast swimming (in prep.). Provided that the contractile force of whole muscles is related to changes in spike-like response amplitude recorded from individual cells, overall muscle force should change in parallel with changes in pattern generator frequency.

Peripheral modulation of contractile force

A cluster of 7–10 serotonin-immunoreactive neurons have been found in the medial margin of each pedal ganglion of *Clione* (Fig. 2). At least two neurons from this cluster send axons to the ipsilateral wing via the wing nerve. Induced activity in these two neurons produced no direct motor response; but when activity was triggered during ongoing swimming activity, muscle contractions

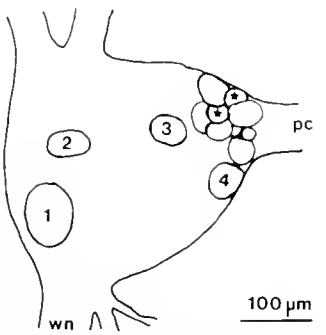

Figure 2. Schematic diagram of the dorsal surface of the left pedal ganglion of *Clione*. The two large motor neurons (major landmarks of the ganglion) are indicated by cells 1 and 2. Cells 3 and 4 represent motor neurons that initiate escape swimming. The remaining cells represent serotonin-immunoreactive cells. The two cells marked with an asterisk have been electrophysiologically identified; they send axons into the ipsilateral wing via the wing nerve (wn). These cells enhance muscle contractility as shown in Figure 3. pc–pedal-pedal commissure.

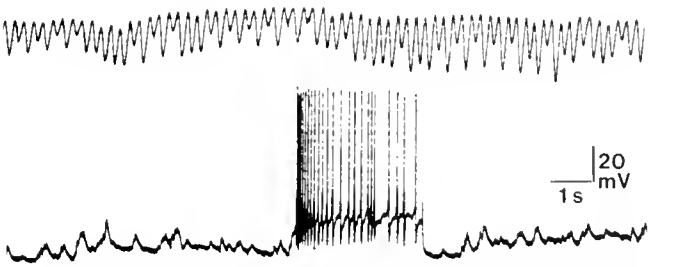

Figure 3. Dual recording from a serotonin-immunoreactive neuron (bottom trace) and a wing force transducer (top trace—not calibrated). Following a burst of action potentials in the neuron, muscle contractions are enhanced. The latency of the response is approximately one second, and the duration is 5 s. The neuron was hyperpolarized by a −1 nA current during the recording to prevent spiking. The burst was triggered by switching to a +1 nA current.

were enhanced (Fig. 3). The response latency was approximately one second from the initiation of the induced burst, and the effect lasted from 3–10 s. Preliminary evidence suggests that this enhancement was due to an increased amplitude of the spike-like response in some, but not all, of the muscle cells.

Peripheral modulation, including both pre- and post-synaptic effects, have been noted in numerous preparations (*e.g.*, Kravitz *et al.*, 1985; Kobayashi and Hasimoto, 1982; Maranto and Calabrese, 1984; Weiss *et al.*, 1978). Induced bursts in the pedal serotonin-immunoreactive neurons of *Clione* produced no apparent synaptic activity in either pattern generator or motor neurons, and produced no changes in frequency or intensity of spike activity in either neuron type. This suggests an interesting dichotomy in serotonin modulation of swimming in *Clione*: *i.e.*, pedal serotonin-immunoreactive neurons modulate muscle activity, whereas proposed cerebral serotonergic neurons modulate pattern generator activity. A similar separation of central and peripheral modulation is seen in the leech heartbeat system (Calabrese and Arbas,

Table I

Summary of four possible modulatory states in the swimming system of Clione limacina *based on separate central and peripheral modulatory subsystems*

Modulatory state	Swimming activity
No modulation	Slow swimming, normal muscle contractility
Peripheral modulation only	Slow swimming, enhanced muscle contractility
Central modulation only	Fast swimming, normal muscle contractility
Central and peripheral modulation	Fast swimming, enhanced muscle contractility

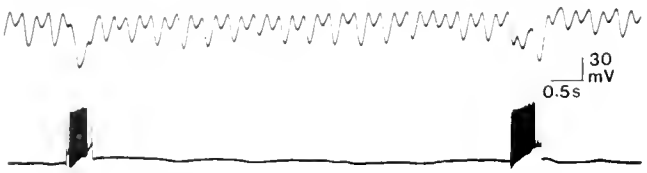

Figure 4. Dual recording from a "startle" motor neuron (bottom trace) and an uncalibrated wing force transducer (top trace). Note the absence of pattern generator input to the neuron despite the ongoing swimming activity. Bursts of action potentials were triggered in the neuron with +12 nA injected currents (through the recording electrode). The resultant bursts of activity induced strong contractions of the wing.

1985). Assuming the simplest case of supra-threshold modulation in both central and peripheral subsystems of *Clione*, the separation of pattern generator and muscle modulatory subsystems allows four possible states with respect to serotonin modulation of swimming activity (Table 1). As mentioned previously, central modulation will primarily affect cycle frequency, whereas peripheral modulation will affect contractile force.

This discussion takes into account only one peripheral modulatory system. The possibility of other modulatory inputs, as well as the release of multiple transmitters or modulators from the serotonin-immunoreactive neurons, could add further complexity to the swimming system.

Escape swimming

An interesting pair of motor neurons have recently been identified from each pedal ganglion of *Clione* (Fig. 4). These motor neurons activate both slow-twitch and fast-twitch fibers of the swim musculature, but do not receive input from the swim pattern generator. The neurons were originally overlooked, because they are electrically silent during normal swimming activity and have extremely high firing thresholds. In some preparations, it is very difficult to stimulate electrical activity from these cells with intracellular current injection. Induced bursts of spikes in the motor neurons produce massive contractions of the ipsilateral wing. Despite this strong peripheral input, the cells have no inputs to, or influence over, the activity of interneurons of the pattern generator or swim motor neurons. Their powerful effect on swim musculature, their total independence from the swim pattern generator, and their high firing threshold suggest that these motor neurons may participate in the primary phase of escape swimming by triggering the initial ballistic movement; indeed, the ballistic movement may function as a startle response. The maintenance of escape swimming, involving the variable period of enhanced fast swimming, could represent activation of both central and peripheral serotonergic modulatory subsystems (see Table 1). Multiple recordings from "startle" neurons and serotonin-immunoreactive neurons following tail stimulation in intact preparations have not yet been completed due to technical difficulties, but should help clarify this relationship.

The foregoing discussion introduces several levels at which changes of locomotory speed can occur in the swimming system of *Clione*. Some of the results are preliminary, while a few are purely speculative. It is clear, however, that both central and peripheral modulatory influences are operating, and that significant changes in both frequency and strength of wing movements can contribute to locomotory speed changes. With this information, we are beginning to gain an appreciation for the neurobiological complexity involved in locomotory plasticity in this relatively "simple" swimming system. Our comprehension of the neuronal bases of speed changes involves changes of gears, changes of speed within gears, and superimposed inputs, such as escape. This understanding is providing a good starting point for further investigation of other forms of input and modulation, as well as detailed descriptions of the intrinsic properties of all cells involved in swimming behavior.

Acknowledgments

I thank Lou and Alison Satterlie for help collecting experimental animals, Dr. A. O. D. Willows for providing space and facilities at Friday Harbor Laboratories, and Dr. A. N. Spencer for the use of Figure 1. Research covered in this paper was supported by a National Science Foundation grant (BNS85-11692) and a research grant from the Whitehall Foundation.

Literature Cited

Arshavsky, Yu.I., I. N. Beloozerova, G. N. Orlovsky, G. A. Pavlova, and Yu.V. Panchin. 1984. Neurons of pedal ganglia of pteropodial mollusc controlling activity of the locomotor generator. *Nejrofiziologia* **16:** 543–546.

Arshavsky, Yu.I., I. N. Beloozerova, G. N. Orlovsky, Yu.V. Panchin, and G. A. Pavlova. 1985a. Control of locomotion in marine mollusc *Clione limacina*. I. Efferent activity during actual and fictitious swimming. *Exp. Brain Res* **58:** 255–262.

Arshavsky, Yu.I., I. N. Beloozerova, G. N. Orlovsky, Yu.V. Panchin, and G. A. Pavlova. 1985b. Control of locomotion in marine mollusc *Clione limacina*. II. Rhythmic neurons of pedal ganglia. *Exp. Brain Res.* **58:** 263–272.

Arshavsky, Yu.I., I. N. Beloozerova, G. N. Orlovsky, Yu.V. Panchin, and G. A. Pavlova. 1985c. Control of locomotion in marine mollusc *Clione limacina*. III. On the origin of locomotory rhythm. *Exp. Brain Res.* **58:** 273–284.

Arshavsky, Yu.I., I. N. Beloozerova, G. N. Orlovsky, Yu.V. Panchin, and G. A. Pavlova. 1985d. Control of locomotion in marine mollusc *Clione limacina*. IV. Role of type 12 interneurons. *Exp. Brain Res.* **58:** 285–293.

Arshavsky, Yu.I., T. G. Beliagina, G. N. Orlovsky, Yu.V. Panchin, G. A. Pavlova, and L. B. Popova. 1986. Control of locomotion in marine mollusc *Clione limacina*. VI. Activity of isolated neurons of pedal ganglia. *Exp. Brain Res.* **63:** 106–112.

Arshavsky, Yu.I., G. N. Orlovsky, Yu.V. Panchin, and G. A. Pavlova. 1989. Control of locomotion in marine mollusc *Clione limacina* VII. Reexamination of type 12 interneurons. *Exp Brain Res* **78:** 398–406.

Calabrese, R. L., and E. A. Arbas. 1985. Modulation of central and peripheral rhythmicity in the heartbeat system of the leech. Pp. 69–85 in *Model Neural Networks and Behavior*, A. I. Selverston, ed. Plenum, New York.

Claassen, D. E., and A. E. Kammer. 1986. Effects of octopamine, dopamine and serotonin on production of flight motor output by thoracic ganglia of *Manduca sexta*. *J Neurobiol* **17:** 1–14.

Flamm, R. E., and R. M. Harris-Warrick. 1986a. Aminergic modulation in the lobster stomatogastric ganglion. I. Effects on the motor pattern and individual neurons within the pyloric circuit. *J Neurophysiol.* **55:** 847–865.

Flamm, R. E., and R. M. Harris-Warrick. 1986b. Aminergic modulation in the lobster stomatogastric ganglion. II. Target neurons of dopamine, octopamine and serotonin within the pyloric circuit. *J. Neurophysiol.* **55:** 866–881.

Getting, P. A., and M. S. Dekin. 1985. *Tritonia* swimming. A model system for integration within rhythmic motor systems. Pp. 3–20 in *Model Neural Networks and Behavior*, A. I. Selverston, ed. Plenum, New York.

Harris-Warrick, R. M., and A. H. Cohen. 1985. Serotonin modulates the central pattern generator for locomotion in the isolated lamprey spinal cord. *J Exp. Biol.* **116:** 27–46.

Harris-Warrick, R. M., R. E. Flamm, B. R. Johnson, and P. S. Katz. 1989. Modulation of neural circuits in crustacea. *Am Zool* **29:** 1305–1320.

Kobayashi, M., and T. Hasimoto. 1982. Antagonistic responses of the radular protractor and retractor to the same putative neurotransmitters. *Comp. Biochem Physiol.* **72C:** 343–348.

Kravitz, E. A., B. Beltz, S. Glusman, M. Goy, R. Harris-Warrick, M. Johnston, M. Livingstone, T. Schwarz, and K. K. Siwicki. 1985. The well-modulated lobster. The roles of serotonin, octopamine and proctolin in the lobster nervous systems. Pp. 339–360 in *Model Neural Networks and Behavior*, A. I. Selverston, ed. Plenum, New York.

Kristan, W. B., Jr., and J. C. Weeks. 1983. Neurons controlling the initiation, generation, and modulation of leech swimming. Pp. 243–260 in *Neural Origin of Rhythmic Movements*, A. Roberts and B. L. Roberts, eds. Cambridge University Press, Cambridge.

Kupfermann, I., and K. R. Weiss. 1982. Activity of an identified serotonergic neuron in free moving *Aplysia* correlates with behavioral arousal. *Brain Res* **241:** 334–337.

Mackey, S., and T. J. Carew. 1983. Locomotion in *Aplysia*: triggering by serotonin and modulation by bag cell extract. *J Neurosci* **3:** 1469–1477.

Maranto, A. R., and R. L. Calabrese. 1984. Neural control of the hearts in the leech, *Hirudo medicinalis* II. Myogenic activity and its control by heart motor neurons. *J. Comp Physiol.* **154:** 381–391.

Nusbaum, M. P. 1986. Synaptic basis of swim initiation in the leech. III. Synaptic effects of serotonin-containing interneurones (cells 21 and 61) on swim CPG neurones (cells 18 and 208). *J Exp. Biol.* **122:** 303–321.

Nusbaum, M. P., and W. B. Kristan. 1986. Swim initiation in the leech by serotonin-containing interneurones, cells 21 and 61. *J Exp. Biol.* **122:** 277–302.

Parsons, D. W., and H. M. Pinsker. 1989. Swimming in *Aplysia brasiliana*: behavioral and cellular effects of serotonin. *J. Neurophysiol.* **62:** 1163–1176.

Satterlie, R. A. 1985. Reciprocal inhibition and postinhibitory rebound produce reverberation in a locomotor pattern generator. *Science* **229:** 402–404.

Satterlie, R. A. 1987. Neuromuscular organization for two-speed swimming in a pteropod mollusc. *Soc. Neurosci. Abstr* **13:** 1061.

Satterlie, R. A. 1988. Peripheral organization of the swimming system in a pteropod mollusc. *Soc. Neurosci. Abstr* **14:** 1001.

Satterlie, R. A. 1989. Reciprocal inhibition and rhythmicity: swimming in a pteropod mollusc. Pp. 151–171 in *Neuronal and Cellular Oscillators*, J. W. Jacklet, ed. Dekker, New York.

Satterlie, R. A., and A. N. Spencer. 1985. Swimming in the pteropod mollusc, *Clione limacina* II. Physiology. *J Exp Biol.* **116:** 205–222.

Satterlie, R. A., M. LaBarbera, and A. N. Spencer. 1985. Swimming in the pteropod mollusc *Clione limacina*. I. Behaviour and morphology. *J Exp. Biol* **116:** 189–204.

Satterlie, R. A., G. E. Gaslow Jr., and A. Reyes. 1990. Two types of striated muscle suggest two-geared swimming in the pteropod mollusc *Clione limacina*. *J Exp. Zool* **255:** 131–140.

Weiss, K. R., J. L. Cohen, and I. Kupfermann. 1978. Modulatory control of buccal musculature by a serotonergic neuron (metacerebral cell) in *Aplysia*. *J Neurophysiol.* **41:** 181–203.

Reference: *Biol. Bull.* 180: 234–240. (April, 1991)

On the Significance of Neuronal Giantism in Gastropods

RHANOR GILLETTE

Department of Physiology & Biophysics and The Neuroscience Program, 524 Burrill Hall, 407 S. Goodwin Ave., University of Illinois, Urbana, Illinois 61801

Abstract. Neurons of the central ganglia of opisthobranch and pulmonate gastropods increase in size as the animals grow, some becoming veritable giants. The origins and functions of neuronal giantism are considered here from a comparative viewpoint. A review of the properties of identified neurons in a variety of opisthobranch and pulmonate species indicates that neuronal size is directly related to the extent of postsynaptic innervation. DNA endoreplication, resulting in partial or complete polyploidy, supports giantism in molluscan neurons as it does in eukaryotic cells elsewhere. Apparently, the functional significance of giantism is enhanced synthesis and transport of materials to serve an expanded presynaptic function.

Giant neurons are found in larger snails where they innervate large areas of the periphery; interneurons and sensory neurons are enlarged to a lesser degree, probably to that which enables load-matching to the peripheral effectors. Neuronal giantism may be an adaptation for the innervation of the periphery in large animals with simple behaviors and uncomplex sensoria, this adaptation enabling growth of body and CNS without a proportionate increase in neuronal number. A more complete understanding of the evolutionary and adaptive significance of neuronal giantism should be sought in comparative studies of the cellular properties of simple and complex molluscan brains.

Introduction

The condition of neuronal giantism in the pulmonate and opisthobranch gastropods has been a point of marvel at least since Buchholz' observations in 1863 (reviewed by Bullock, 1965). The conveniences offered by giant nerve cells to experimenters have also invited numerous biophysical and neuroethological studies; these have contributed greatly to our knowledge of nerve cell function and behavioral mechanisms. Even so, the significance of neuronal giants to the animals in which they are found has not been satisfactorily understood.

The question of neuronal giantism is particularly open to the methods of comparative analysis. The physiology, anatomy, and behavioral roles of giant neurons have been analyzed from a wide variety of species, and homologous neurons have been identified across species. The following paragraphs marshal evidence that supports several hypotheses for the origin and functional significance of neuronal giantism.

Received 7 August 1990; accepted 25 January 1991.

The Molluscan Neuron

The typical molluscan neuron is a monopolar or bipolar cell with its soma lying in the ganglion periphery (Fig. 1). An axon enters the neuropil in the core of the ganglion where it branches off neurites that both receive and make synaptic contacts. Neurites generally sprout close to the cell body and even originate from it in opisthobranch and pulmonate neurons. Action potentials are initiated in the axon and regulated by synaptic inputs to the neurites; the region of spike initiation and synaptic activity is referred to here as the *integrating region.*

Neuronal Giantism: The Condition

The condition of "giantism" is one of degree. The central ganglia of opisthobranch and pulmonate snails commonly possess 10–20 distinct and identifiable nerve cells with cell bodies so large that they stand out from their neighbors as relative giants. Aside from the obvious giant neurons, the entire central nervous system of such animals contains only several tens of thousands of neurons, several

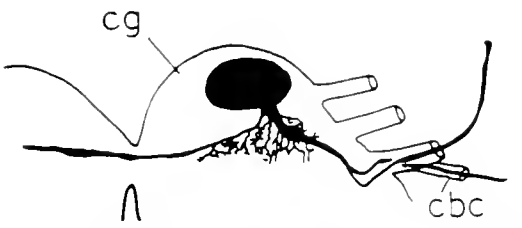

Figure 1. Typical morphology of giant neurons of pulmonates and opisthobranchs, as exemplified by this drawing of the serotonergic giant of the cerebral ganglion of *Tritonia hombergi* (from Dorsett, 1986). The large excitable soma is close to the integrating region of axon and fine neurites, where synaptic potentials occur and spikes are initiated. The large axons, with high specific membrane resistances, favor current spread from integrating region to soma.

hundred of which may be identified on the basis of position, color, synaptic and axonal connections (*cf.* Bullock, 1965; Coggeshall, 1967; Frazier *et al.*, 1967). In the larger pulmonates, the biggest neurons have somata approaching 100 μm in diameter, whereas in the larger sea slugs, certain neuronal somata reach over 700–800 μm. Moreover, as the animals increase in size, all of their identifiable neurons also grow in diameter.

Neuronal Size is Related to Postsynaptic Innervation

In approaching the nature of neuronal giantism, the first relevant observation is that neuron giants must innervate larger postsynaptic target areas than non-giants. The evidence that neuronal size is directly related to the extent of postsynaptic innervation comes from the literature characterizing a variety of identified neurons in opisthobranch and pulmonate snails. The largest neurons of the central ganglia act as effectors that innervate large areas of the periphery.

Prominent examples are a bilateral pair of giant serotonergic neurons identified in many opisthobranch and pulmonate snail species. These neurons are commonly the largest neuronal somata of the cerebral ganglion (Senseman and Gelperin, 1973; Berry and Pentreath, 1976; Weiss and Kupfermann, 1976; Gillette and Davis, 1977; Granzow and Kater, 1977). Approaching 400–500 μm in size in the larger opisthobranchs, these giant effectors send large axons down the cerebrobuccal connectives; the axons ramify within the buccal ganglion so that an axonal branch is sent out in each nerve. These axons innervate large areas of the muscular buccal mass and the esophagus; the neurons also send branches out the lip or mouth nerves of the cerebral ganglion to innervate the oral region (Fig. 2). In addition, the giant serotonergic neurons have some synaptic output in the buccal ganglia (*ibid.*).

Other well-studied giants are two of the largest neurons known, the neurons R2 and LPl1 of the anaspid opisthobranch *Aplysia californica*. R2 and LPl1 are bilaterally homologous and cholinergic, attaining soma diameters nearly 1000 μm in large animals. Due to assymetrical ganglionic fusion in the embryo, R2 is found in the abdominal ganglion, and LPl1 in the left parietal ganglion. The cell bodies give off giant axons that send branches to most ganglia and out many nerves thence innervating extensive areas of the skin (Hughes and Tauc, 1963; Cobbs and Pinsker, 1979). Their electrical activity stimulates mucus secretion (Rayport *et al.*, 1983).

Among the motorneurons innervating the gills of nudibranchs and notaspids are some of the largest neurons of the pedal, pleural, and cerebral ganglia (Blackshaw and Dorsett, 1976; Dickinson, 1979, 1980).

The well-studied buccal ganglia provide more examples of giantism. The largest neurons of opisthobranch buccal

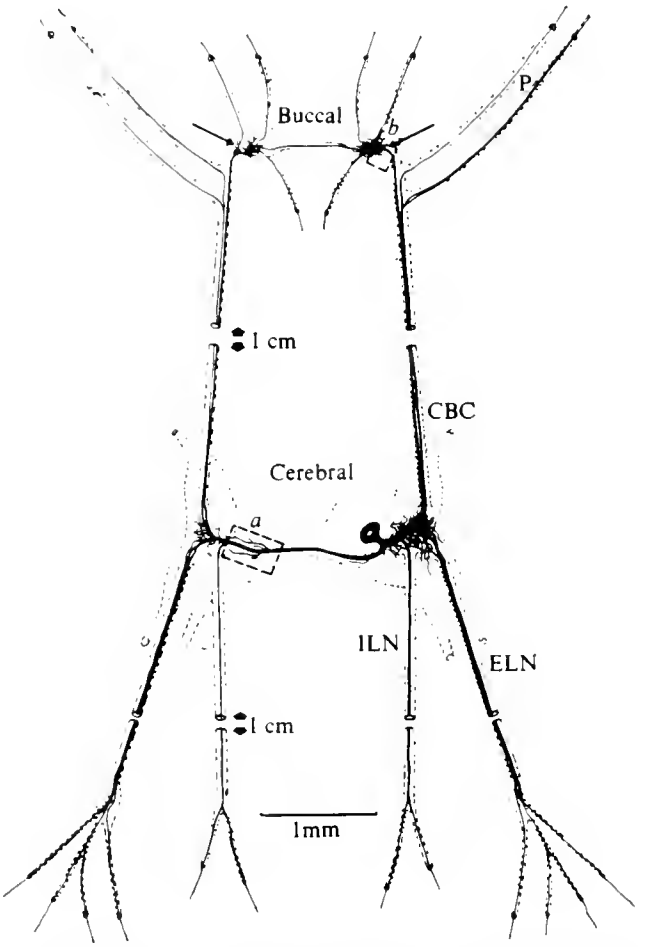

Figure 2. Extensive innervation of the periphery by the serotonergic cerebral giant neurons of *Helix pomatia* (from Berry and Pentreath, 1974). Aside from some interneuronal function in the CNS, these giants send many branches to the buccal ganglion and out the nerves to innervate the musculature of the buccal mass and esophagus. Other branches leave anterior nerves to innervate the feeding musculature of the oral region. This general plan is found in the homologous giant cells of many pulmonate and opisthobranch species.

ganglia are typically motorneurons; sensory neurons are, on the average, much smaller (Byrne *et al.*, 1974; Siegler, 1977; Spray *et al.*, 1980; Dorsett and Sigger, 1981). The largest known buccal cells may be those of the buccal ganglion of the cephalaspid *Navanax*. These neurons innervate the musculature of the large pharynx, driving its expansion during prey-capture (Spira and Bennett, 1972). In aeolid and doridacean buccal ganglia, the largest neurons are often a bilateral pair called the Dorsal White Cells (Bulloch and Dorsett, 1979). The Dorsal White Cells are peptidergic neurons that send axons out the gastroesophageal nerve to ramify over, and innervate, the large esophagus (Masinovsky and Lloyd, 1985).

Interneurons with only central synaptic outputs tend to be smaller than interneurons of dual function, *i.e.*, with both CNS output and peripheral axons innervating muscle. For instance, both the identified VWC and B31 neurons of *Pleurobranchaea* can drive intense cyclic motor output in the buccal oscillator network; but the VWC also innervates the muscular esophagus, and the diameter of its soma is nearly three times that of the B31 soma (Gillette *et al.*, 1980). Identified neurons with purely central outputs also may differ in size according to the extent of their postsynaptic output. The paired SO interneurons of the buccal ganglion of the pulmonate *Lymnaea* have a large dendritic field, and their somata are three times the size of the interneurons of the N1, N2, and N3 populations, which have collectively rather similar functions as oscillator elements, but smaller dendritic fields in the ganglion and weaker effects, individually, on the network (Elliot and Benjamin, 1985a, b).

Sensory neurons can innervate large peripheral areas, but their presynaptic function is largely confined to central ganglia, and they tend to be small. Sensory neurons of the buccal ganglia of *Pleurobranchaea* tend to have smaller somata than motorneurons innervating the same muscles of the buccal mass (Siegler, 1977). Similarly, the buccal ganglia of *Navanax* contain mechanosensory neurons that serve the pharynx and are much smaller than their postsynaptic giant motorneurons that drive the pharyngeal musculature (Spray *et al.*, 1980a, b). Sensory neurons carrying mechanosensory information from the skin of *Tritonia* are quite smaller than the interneurons and motorneurons they drive (Getting, 1977). The abdominal ganglion of *Aplysia* contains sensory neurons that innervate the gill and siphon and that are much smaller than the gill and siphon motorneurons they drive (Byrne *et al.*, 1974). In each case, the sensory neurons have smaller dendritic fields, and thus may make fewer synaptic contacts, than the larger motorneurons and interneurons.

A direct relationship between the field of postsynaptic innervation of a neuron and its soma size has been previously recognized by some workers in arthropod neurobiology. Mittenthal and Wine (1978) showed that the soma diameter of serially homologous motorneurons in the segmental nervous system of crayfish is roughly proportional to the area of the serially homologous muscle they innervate. Mellon *et al.* (1981) showed that amputation of the specialized snapping claw of the snapping shrimp *Alpheus* causes the contralateral claw and its musculature to enlarge into a larger snapping claw at subsequent molts; the soma of the claw opener motorneuron enlarges with the size of its target organ.

Finally, the peripheral effector neurons of the opisthobranch central nervous system increase in size with the growth of their target organs. The size of identified neurons, in soma diameter, axon diameter, and dendritic field, increases with the size of the animal during growth (Coggeshall, 1967; Frazier *et al.*, 1967). Accordingly, sensory interneurons monitoring the peripheral effectors and the smaller interneurons also increase in size; this is a form of load matching. All of these observations argue for a trophic relationship between the area of the innervated structure and the size of the presynaptic neuron. It is assumed here, notwithstanding the lack of direct evidence, that increases in innervated area and extent of presynaptic branching are accompanied by increases in synaptic contact area, number of synaptic sites, or both. Therefore, the beginning of the answer to the question: "Why do some neurons become giants?" is probably that their size is related to the actual total area of synaptic contact.

The Mechanism of Giantism: DNA Endoreplication

For certain cell types in many animals, an increase in cell size is generally accompanied by an increase in the actual mass of the genomic DNA and of RNA (Mirsky and Osawa, 1961; *cf.* Cavalier-Smith, 1978); this is effected either through polyploidy or polyteny. An increase in polyploidy with neuronal size has been demonstrated in molluscan neurons. The nuclei of the largest neurons of mature *Aplysia* (*e.g.*, R2) contain >0.2 μg of DNA—more than 200,000 times the haploid amount (Lasek and Dower, 1971). Neurons of the terrestrial pulmonate *Achatina*, with soma diameters of >9 μm (nuclear diameter > 7 μm), were found to be polyploid (Chase and Tolloczko, 1987). The frequency distribution of the DNA content in *Achatina* (Chase and Tollockzo, 1987) and *Planorbis* (Lombardo *et al.*, 1980) neurons indicates that endoreplication during growth probably represents selective gene amplification, rather than simple sequential doubling. However, sequential doubling may occur during growth in *Aplysia* (Coggeshall *et al.*, 1970; Lasek and Dower, 1971). Giantism in molluscan neurons is thus like giantism in other metazoan cells, and is simply based on increased amounts of nucleic acids and proteins.

Polyploid neurons of varying sizes may be common to the nervous systems of molluscs in general; *i.e.*, increasing

neuron size and ploidy may be a usual feature of growth within all of the molluscan classes; one that is, perhaps, carried to the extreme in the pulmonates and opisthobranchs.

The Functions of Giantism: Synthesis and Transport

Neuronal giants apparently innervate larger postsynaptic target areas than non-giants. Neuronal giantism, therefore, may allow an increase in animal size without a proportional increase in the number of central neurons. Giant cells in most tissues are more metabolically active than smaller cells and are frequently associated with transport and secretory processes. Familiar examples are the giant polytene cells of dipteran salivary glands, malpighian tubules, and gut, all of which are notably active in ion and peptide transport and exocytotic secretion. Thus, elaboration of DNA, RNA, and protein in many giant cells is indicative of enhanced synthetic capacity, presumably to serve the needs of increased cell activity. In giant neurons, these needs are likely to be connected with increased axon transport and secretion processes at their extensively distributed synaptic terminals.

Thus, the picture of the giant neuron becomes one where the size, synthetic capacity, and axonal transport traffic is adapted to the extent of postsynaptic innervation. The giant cells do the work of many smaller cells in other nervous systems.

The Evolutionary Origin and Integrative Significance of Neuronal Giantism in Gastropods

The occurrence of giant neurons in snails is explained in one sense by the observation that the giant neurons must innervate large postsynaptic areas. The imposing question that looms is: why do the pulmonates and opisthobranchs display such pronounced neuron giantism whereas other gastropod taxa do not? The best answer will probably rest on future comparative observations on species chosen for particular nervous system characters, but the context for such comparative observations can be set here. The approach is to enumerate the specific set of behavioral and neurophysiological characteristics that may place the opisthobranch/pulmonate line apart from other gastropods; in the process, perhaps, a few useful speculations may be generated.

Those gastropods that are distinguished by possession of a score or more of large neurons are also distinguished by the combination of the following characteristics:

1. relatively large body size;
2. motile, foraging lifestyles sustained by relatively simple behavior;
3. simple nervous systems lacking, for the most part, complex sensoria;
4. a fairly high degree of centralization within the CNS; and
5. excitable neuron cell bodies.

Although one or more of these characteristics may appear in various gastropod taxa, the appearance of all five may be relatively specific to the opisthobranch/pulmonate line.

The gastropods crept into the fossil record around 580 million years ago as minute animals 1–2 mm in shell diameter, and today most are still smaller than 5 mm. The larger modern gastropods are thus truly somatomorphic giants; their greater body size demands enhanced innervation of the periphery. In most large species, this need is met largely by an increase in brain size and neuron number; even in the opisthobranch/pulmonate line, the number of neurons (and the number of peripheral axons) increases with body size, in parallel with the striking increase in size of identified neurons (Coggeshall, 1967). But if, as has been argued, giant neurons are an adaptation for increased area of innervation, then during evolution these snails have made a trade of neuron size for neuron number in the innervation of an enlarging periphery. This trade has apparently not been made by the other larger gastropods belonging to the prosobranchs.

Large body size in gastropods is associated with a motile, foraging lifestyle, as opposed to the sedentary life of a parasite or filter feeder. Motile foragers are generally expected to exhibit a certain complexity in their behavior, complexity that would emerge from corresponding complexity in the nervous system. However, I suggest that the behavior of the opisthobranchs and pulmonates, relative to that of the larger advanced prosobranchs, is both simpler and underlain by a simpler nervous system.

CNS development is directly associated with sensory and behavioral ability. The behavior of opisthobranchs and pulmonates, like their nervous systems, probably lacks the complexity shown by the larger prosobranch snails; the number of behavioral sub-routines they use in daily living is obviously smaller than those of animals living in more complex ecological niches. Larger, more complex brains, with large numbers of small neurons, are associated with the development of sense organs for high-resolution analysis of the environment and greater complexity of behavior. In the predatory prosobranch whelks, the many tiny neurons, relatively large ganglia, and eyes are likely to mediate similarly complex behaviors. The whelk *Fusitriton oregonensis* devotes considerable behavioral strategy to reproduction. Mating pairs form seasonally and persist for as long as 4 months. Subsequently, a parent attaches its clutch of eggs to a rock surface and patrols them against predators (Eaton, 1972). Potential predators may be sensed in part by the whelk's well-developed eyes; the whelk, with twisting movements of its shell, attempts to attack and dislodge the preditor; failing that, the whelk

may directionally squirt an aversive acid secretion. The opisthobranchs and pulmonates, with their rudimentary-at-best vision and small numbers of CNS neurons, come nowhere near such complexity of behavior. Indeed, the behavior of the opisthobranchs and pulmonates really seems simple.

The relative lack of complex sensoria and their attendant complex central processing may allow the opisthobranch/pulmonate lines to live successfully with a highly reduced CNS. Their eyes are very small and quite limited in both the number and resolution of photoreceptors; in many opisthobranch species, the eyes are even internalized. Their function may be largely limited to setting the circadian rhythms of animal activity (Jacklet, 1969). High resolution eyes in the cephalopods are associated with comparably high resolution, visually directed motor behavior (*cf.*, Wells, 1978). High resolution in sensory-motor systems requires larger numbers of neurons, as are found in the cephalopod optic lobes. The opisthobranchs get along mostly with the environmental information provided by chemosensory and tactile abilities. The opisthobranchs and pulmonates do have specialized chemosensory sites for detecting food: the rhinophores, and the tentacles and other regions about the oral area. These sites appear to be served by peripheral ganglia that may take the burden of a great deal of sensory-motor processing (*cf.*, Mpitsos and Lukowiak, 1986), leaving the central nervous system to process simple tactile information and to integrate motivational and learning processes with the expression of behavior.

Contrasting examples support this interpretation. Some pulmonates and prosobranchs have developed accessory CNS ganglionic lobes; these structures are associated with chemosensation and are composed of many smaller neurons (*cf.*, Bullock, 1965; Chase and Tolloczko, 1989). In the terrestrial slug *Limax*, the structure is the procerebral lobe, and it shows oscillating electrical field potentials characteristic of rather complex sensory feature extraction systems in vertebrates (Gelperin and Tank, 1990). Outside of the gastropods, the obvious example is the complexity of sensoria and sensory processing in the complex brains of cephalopods. In the opisthobranchs and pulmonates, the lack of complexity in sensoria and underlying neural processing underscores their simplicity of brain and lifestyle.

Finally, the opisthobranch and pulmonate nervous systems show a relatively high degree of centralization into a few discrete ganglia. Although centralization and cephalization have not proceeded as far as in the cephalopods, these characteristics still distinguish them from the mostly sessile bivalves and the parasitic or filter-feeding gastropods that rely heavily on peripheral control of reflexes and show generally less centralization. It also distinguishes them from large, motile mollusks like the giant chitons, from which giant neurons are not reported. The chitons attain large size in some cases, and are slowly motile, but their nervous system is only poorly centralized relative to that of the opisthobranchs and pulmonates. Amphineuran ganglia are simply formed nodes lying on a major nerve ring, and many neuronal somata are simply dispersed along the nerves and connectives in a primitive medullary condition (*cf.*, Bullock, 1965).

Thus, snails with giant neurons constitute a group that has grown large in body size, but has retained an uncomplicated behavioral repertory and sensory-motor capacities. To serve the innervation needs of the enlarged body, the nervous system has favored an increase in neuron size relative to neuron number.

The above characters provide the context within which I think we must seek the evolutionary reasons that some snails chose the architecture of neuronal giantism in their nervous systems. Why didn't they choose instead to innervate their enlarged periphery with many smaller central neurons, like their large prosobranch cousins? The developmental simplicity of innervating a large area with one neuron rather than many may be a useful consideration. Another is that neuronal giantism allows increased animal size without a proportional increase in central neuron number.

A potential answer lies in the electrophysiological properties of neurons of simple and complex gastropod brains. In molluscan ganglia, the neurons lie peripherally and send axons into a central neuropil to make synaptic connections. For the opisthobranch and pulmonate snails the neuronal somata are excitable and are placed spatially and electrically quite close to the integrating region (Gorman and Mirolli, 1972; Graubard, 1975); they are thus able to follow almost synchronously the spike activity of the integrating region (*cf.*, Fig. 1). In larger ganglia, the distances from the synaptic integrating region in the neuropil, where spikes are initiated, to soma also become longer. Thus, for a neuron that grows in pace with the whole ganglion, the larger axon diameter would enhance the synchrony of soma and integrating region. In this manner, the continuing enlargement of neuronal somata with the growth of the organism may not only adapt the cells to the innervation of an enlarged periphery, but also to an increased separation of the soma from the integrating region.

Some data suggest that the very small neuronal somata of advanced cephalopod ganglia are inexcitable (Gilly and Brismar, 1989; Williamson and Budelmann, 1991; Robertson *et al.*, 1990), like those of arthropods. Many of these somata lie rather distant from the neuropil integrating regions, because they are packed on top of many intervening cells in the cell body layer (*cf.*, Young, 1971). For a small neuron, this longer distance could cause a disadvantageous desynchronization of the action potential

currents between the soma and integrating region, with the result that the late somatic currents would interfere with ongoing integration (in the worst case, by reflecting spikes). Thus, for the nervous systems having a high proportion of such small neurons, it might be functionally advantageous if the cellular mechanisms of somatic excitability were turned off. We would then wonder, in general, whether large brains with many small neurons have inexcitable somata. Do gastropods, such as the larger whelks with large central ganglia and many small neuron somata distant from the integrating neuropil, have spiking or non-spiking somata? Few intracellular recordings have been made in the complex nervous systems of the advanced giant prosobranchs, but if their small neuron somata were also inexcitable, a strong case could be made that the simplicity and small neuronal numbers of the opisthobranch/pulmonate central nervous system permits the retention, in evolution, of excitable somata with an increase in the size of ganglia.

Conclusion

The opisthobranch and pulmonate gastropods constitute large and successful taxa. In the picture drawn here, selection during evolution has tightly interwoven neuronal giantism in the CNS with the physiology and behavior of the animal. A number of testable hypotheses have been proposed, and each can be verified or falsified by more detailed, quantitative observations. The hoped-for result, a more complete resolution of the adaptive significance of neuronal giantism, may one day make a useful contribution to our understanding of how the nervous system has evolved in tandem with behavior.

Acknowledgment

The observations leading to this paper were made while the author was supported by NSF grant BNS 86-03816.

Literature Cited

Berry, M. S., and V. W. Pentreath. 1976. Properties of a symmetric pair of serotonin-containing neurones in the cerebral ganglia of *Planorbis*. *J. Exp. Biol.* **80:** 119–135.

Blackshaw, S. E., and D. A. Dorsett. 1976. Behavioural correlates of activity in the giant cerebral neurons of *Archidoris*. *Proc. R. Soc. Lond. (Biol.)* **192:** 393–419.

Buchholz, R. 1863. Bemerkungen über den histologischen Bau des Zentralnervensystems der Susswassermollusken. *Arch. Anat. Physiol. LPZ* **1863:** 234–264.

Bulloch, A. G. M., and D. A. Dorsett. 1979. The integration of the patterned output of buccal motorneurones during feeding in *Tritonia hombergi*. *J. Exp. Biol.* **79:** 491–508.

Bullock, T. H. 1965. The Mollusca. Pp. 1273–1515 in *Structure and Function in the Nervous Systems of Invertebrates*, v. 2., T. H. Bullock and G. A. Horridge, eds. Freeman Press, San Francisco.

Byrne, J. H., V. Castellucci, and E. R. Kandel. 1974. Receptive fields and response properties of mechanoreceptor neurons innervating siphon skin and mantle shelf in *Aplysia*. *J. Neurophysiol.* **37:** 1041–1064.

Cavalier-Smith, T. 1978. Nuclear volume control by nucleoskeletal DNA, selection for cell volume and cell growth rate, and the solution of the DNA C-value paradox. *J. Cell Sci.* **34:** 247–279.

Chase, R., and B. Tolloczko. 1987. Evidence for differential DNA endoreplication during the development of a molluscan brain. *J. Neurobiol.* **18:** 395–406.

Chase, R., and B. Tolloczko. 1989. Interganglionic dendrites constitute an output pathway from the procerebrum of the snail *Achatina fulica*. *J. Comp. Neurol.* **283:** 143–152.

Cobbs, J. S., and H. M. Pinsker. 1979. *In vivo* responses of paired giant mechanoreceptor neurons in *Aplysia* abdominal ganglion. *J. Neurobiol.* **9:** 121–141.

Coggeshall, R. E. 1967. A light and electron microscope study of the abdominal ganglion of *Aplysia californica*. *J. Neurophysiol.* **30:** 1263–1287.

Coggeshall, R. E., B. A. Yaksta, and F. J. Swartz. 1970. A cytophotometric analysis of the DNA in the nucleus of the giant cell, R-2, in *Aplysia*. *Chromosoma* **32:** 205–212.

Dickinson, P. S. 1979. Homologous neurons control movements of diverse gill types in nudibranch molluscs. *J. Comp. Physiol.* **131:** 277–283.

Dickinson, P. S. 1980. Gill control in the notaspidean *Pleurobranchaea* and possible homologies with nudibranchs. *J. Comp. Physiol.* **139:** 11–16.

Dorsett, D. A. 1986. Brains to cells: the neuroanatomy of selected gastropod species. Pp. 101–187 in *The Mollusca*, K. M. Wilbur, ed., v. 9, *Neurobiology and Behavior, part 2*, A. O. D. Willows, ed., Academic Press, New York.

Dorsett, D. A., and J. N. Sigger. 1981. Sensory fields and properties of the oesophageal proprioceptors in the mollusc, *Philine*. *J. Exp. Biol.* **94:** 77–93.

Eaton, C. M. 1972. The reproductive and feeding biology of the prosobranch gastropod *Fusitriton oregonensis* (Redfield) (Fam. Cymatiidae). University of Washington M.S. thesis. 40 pp.

Elliot, C. J. H., and P. R. Benjamin. 1985a. Interactions of pattern-generating interneurons controlling feeding in *Lymnaea stagnalis*. *J. Neurophysiol.* **54:** 1396–1411.

Elliot, C. J. H., and P. R. Benjamin. 1985b. Interactions of the slow oscillator interneuron with feeding pattern-generating interneurons in *Lymnaea stagnalis*. *J. Neurophysiol.* **54:** 1412–1421.

Frazier, W. T., E. R. Kandel, I. Kupfermann, R. Waziri, and R. E. Coggeshall. 1967. Morphological and functional properties of identified neurons in the abdominal ganglion of *Aplysia californica*. *J. Neurophysiol.* **30:** 1288–1351.

Gelperin, A., and D. W. Tank. 1990. Odour-modulated collective network oscillations of olfactory interneurons in a terrestrial mollusc. *Nature* **345:** 437–440.

Getting, P. A. 1977. Afferent neurons mediating escape swimming of the marine mollusc *Tritonia*. *J. Comp. Physiol.* **110:** 271–286.

Gillette, R., and W. J. Davis. 1977. The role of the metacerebral giant neurone in the feeding behaviour of *Pleurobranchaea*. *J. Comp. Physiol.* **116:** 129–159.

Gillette, R., M. U. Gillette, and W. J. Davis. 1980. Action potential broadening and endogenously sustained bursting are substrates of command ability in a feeding neuron of *Pleurobranchaea*. *J. Neurophysiol.* **43:** 669–685.

Gilly, W. F., and T. Brismar. 1989. Properties of appropriately and inappropriately expressed sodium channels in squid giant axon and its somata. *J. Neurosci.* **9:** 1362–1374.

Gorman, A. L. F., and M. Mirolli. 1972. The passive electrical properties of the membrane of a molluscan neurone. *J. Physiol. (Lond.)* **227:** 35–49.

Granzow, B., and S. B. Kater. 1977. Identified higher-order neurones controlling the feeding motor program of *Helisoma*. *Neuroscience* **2:** 1049–1063.

Graubard, K. 1975. Voltage attenuation within *Aplysia* neurons: the effect of branching pattern. *Brain Res.* **88:** 325–332.

Hughes, G. M., and L. Tauc. 1963. An electrophysiological study of the anatomical relations of two giant nerve cells in *Aplysia depilans*. *J. Exp. Biol.* **40:** 469–486.

Jacklet, J. W. 1969. Circadian rhythm of optic nerve impulses recorded in darkness from isolated eye of *Aplysia*. *Science* **164:** 562–563.

Lasek, R. J., and W. J. Dower. 1971. *Aplysia californica*: analysis of nuclear DNA in individual nuclei of giant neurons. *Science* **172:** 278–280.

Lombardo, F., O. Sonetti, and E. Baraldi. 1980. Differential staining and fluorescence of chromatin in populations of neuronal nuclei from *Planorbis*. *Nucleus* **23:** 30–36.

Masinovsky, B., and P. E. Lloyd. 1985. Morphology of two pairs of identified peptidergic neurons in the buccal ganglia of the mollusc *Tritonia diomedea*. *J. Neurobiol.* **16:** 27–39.

Mellon, DeF., Jr., J. A. Wilson, and C. E. Phillips. 1981. Modification of motor neuron size and position in the central nervous system of adult snapping shrimps. *Brain Res.* **223:** 134–140.

Mittenthal, J. E., and J. J. Wine. 1978. Segmental homology and variation in flexor motoneurons of the crayfish abdomen. *J. Comp. Neurol.* **177:** 311–334.

Mirsky, A. E., and S. Osawa. 1961. The interphase nucleus. Pp. 677–770 in *The Cell*, J. Brachet and A. E. Mirsky, eds. Academic Press, New York.

Mpitsos, G. J., and K. Lukowiak. 1986. Learning in gastropod molluscs. Pp. 95–267 in *The Mollusca*, K. M. Wilbur, ed., v. 8, *Neurobiology and Behavior, part 1*, A. O. D. Willows, ed., Academic Press, New York.

Rayport, S. G., R. T. Ambron, and J. Babiarz. 1983. Identified cholinergic neurons R2 and LPl_1 control mucus release in *Aplysia*. *J. Neurophysiol.* **49:** 864–876.

Robertson, J. D., R. Gillette, P. Lee, S. Meadows, and J. Zitz. 1990. CNS neuronal somata of octopus are inexcitable and label retrogradely with carbocyanine dyes. *Soc. Neurosci. Abs.* **16:** 249.7.

Senseman, D., and A. Gelperin. 1973. Comparative aspects of the morphology and physiology of a single identifiable neurone in *Helix aspersa*, *Limax maximus*, and *Ariolimax californica*. *Malacol. Rev.* **7:** 51–52.

Siegler, M. V. S. 1977. Motor neurone coordination and sensory modulation in the feeding system of the mollusc *Pleurobranchaea californica*. *J. Exp. Biol.* **71:** 27–48.

Spray, D. C., M. E. Spira, and M. V. L. Bennett. 1980a. Peripheral fields and branching patterns of buccal mechanosensory neurons n the opisthobranch mollusc *Navanax inermis*. *Brain Res.* **182:** 253–270.

Spray, D. C., M. E. Spira, and M. V. L. Bennett. 1980b. Synaptic connections of buccal mechanosensory neurons in the opisthobranch mollusc *Navanax inermis*. *Brain Res.* **182:** 271–286.

Spira, M. E., and M. V. L. Bennett. 1972. Synaptic control of electrotonic coupling between neurons. *Brain Res.* **37:** 294–300.

Weiss, K. R., and I. Kupfermann. 1976. Homology of the giant serotonergic neurones (metacerebral cells) in *Aplysia* and pulmonate molluscs. *Brain Res.* **117:** 33–49.

Wells, M. J. 1978. *Octopus: Physiology and Behaviour of an Advanced Invertebrate*. Chapman and Hall, London.

Williamson, R., and B. U. Budelmann. 1991. Convergent inputs to octopus oculomotor neurones demonstrated in a brain slice preparation. *Neurosci. Lett.* **121:** 215–218.

Young, J. Z. 1971. *The Anatomy of the Nervous System of* Octopus vulgaris. Oxford University Press, London.

Reference: *Biol. Bull.* **180**: 241–251. (April, 1991)

A Functional, Cellular, and Evolutionary Model of Nociceptive Plasticity in *Aplysia*

EDGAR T. WALTERS

Department of Physiology and Cell Biology, University of Texas Medical School at Houston, Houston, Texas 77225

Abstract. Nociceptive plasticity is defined as behavioral and cellular modification produced by activation of nociceptors. A brief survey of nociceptive plasticity in *Aplysia* reveals a puzzling mixture of behavioral modifications of opposite sign and widely varying durations. These include general sensitization, site-specific sensitization, response-specific facilitation, and inhibition of defensive responses. This behavioral complexity is more than matched by the complexity of cellular correlates reported for the behavioral modifications. A functional model is proposed linking complex patterns of behavioral and neural plasticity in *Aplysia* to potentially general principles of nociceptive function. This model is centered around three overlapping but functionally distinct phases: injury detection, escape, and recuperation. A hypothesis about the early origin of nociceptive plasticity in primitive mechanosensory neurons is then developed, based on similarities in the organization and modifiability of nociceptive systems in evolutionarily divergent groups (primarily mollusks and mammals) and on inferences about the early adaptiveness of postinjury behavioral plasticity. Preliminary evidence suggests that aspects of nociceptive plasticity, and perhaps other forms of memory, may have been derived from cellular repair and signal compensation mechanisms.

Introduction

Neuronal mechanisms controlling withdrawal responses in the opisthobranch mollusc, *Aplysia californica*, have been studied extensively by neurobiologists for over two decades. Investigators have been attracted to the gill, siphon, and tail withdrawal responses of *Aplysia*, in part because the CNS can be readily analyzed in this animal, but largely because these responses and their underlying neurophysiology display a remarkable degree of modifiability. The rare opportunity, provided by *Aplysia* and several other gastropod mollusks, to link behavioral and cellular alterations has been used to advantage by several laboratories and has led to the discovery of various mechanisms contributing to learning and memory in this species.

Although we presume that some mechanisms from gastropod "model systems" are general, the possibility that a given mechanism will be common to groups as evolutionarily divergent as are the mollusks and mammals requires serious scrutiny. As a first step in examining the potential generality of mechanisms contributing to learning and memory in *Aplysia*, I will discuss some nociceptive functions of these mechanisms, propose a three-phase model of nociceptive plasticity, and consider the possibility that mechanisms of nociceptive plasticity evolved in primitive mechanosensory neurons and have been conserved in diverse phyla. Central to this discussion is that most cellular mechanisms of behavioral modification revealed to date in *Aplysia* have been produced either by noxious stimulation, or by manipulations that mimic effects of noxious stimulation. The behavioral and cellular modifications are thus examples of *nociceptive plasticity*, which I define as modifications induced by the activation of nociceptors. Nociceptors are defined as sensory neurons that are activated maximally by stimuli that, if sufficiently prolonged, cause tissue damage (Sherrington, 1906).

Forms of Nociceptive Plasticity

Noxious stimuli, such as strong pinch or shock, were at first assumed to have only two major effects on *Aplysia*:

Received 14 August 1990; accepted 22 January 1991.

Abbreviations: Activity-dependent extrinsic modulation, ADEM; central nervous system, CNS; Excitatory postsynaptic potential, EPSP; Phe-Met-Arg-Phe-NH_2, FMRFamide; serotonin, 5-HT.

to trigger vigorous defensive responses, and to cause general sensitization of the animal for several minutes. The term "sensitization" has been used independently by psychologists and physiologists to describe an increase in sensitivity or magnitude of, respectively, a behavioral or physiological response. I define nociceptive sensitization as sensitization produced by noxious stimulation, where sensitization is defined physiologically as an increase in sensitivity or responsiveness of the organism to a constant test stimulus. Such hypersensitivity after noxious stimulation need not be expressed as overt behavior, but is often expressed as a decrease in threshold and an increase in the magnitude of defensive responses evoked by a test stimulus. By this definition, sensitization may also be expressed as inhibition of ongoing behavior (usually nondefensive) by the test stimulus. Nociceptive sensitization can be general (expressed by changes in response to a broad range of test stimuli and stimulation sites) or, as discussed below, specific to a warning signal or to a restricted site on the body. The apparent function of general nociceptive sensitization is to prime the animal for continued defense, so that it responds rapidly and energetically to a wide range of stimuli that might presage an attack.

The first clue that nociceptive plasticity involves more than a brief, general sensitization came from the observation that repeated application of noxious stimuli over hours or days causes general sensitization of siphon withdrawal that can last for weeks (Pinsker *et al.*, 1973; Frost *et al.*, 1985). It was then discovered that sensitization can be conditioned to a warning signal; a variety of defensive responses are selectively facilitated by a chemosensory cue (*e.g.*, shrimp extract) if it is repeatedly paired with noxious shock (Walters *et al.*, 1981; Colwill *et al.*, 1988). Further links between sensitization and associative processes were indicated by behavioral data (Carew *et al.*, 1981, 1983; Hawkins *et al.*, 1983) and neuronal data (see next section), suggesting considerable overlap of sensitization and putative classical conditioning mechanisms within individual sensory neurons.

The next discovery, site-specific sensitization, is crucial to the functional and evolutionary arguments of this paper. Noxious stimulation enhances siphon and tail withdrawal test responses; but responses evoked by test stimuli applied near the site of noxious stimulation are more dramatic than those evoked by test stimuli applied at other sites on the body (Walters, 1987a). The site-specific behavioral plasticity is particularly potent; a single 45 s noxious stimulation sequence that is insufficient to cause long-term general sensitization produces site-specific sensitization lasting a week or more (Fig. 1).

The complexity of nociceptive plasticity was underscored recently when several groups found that noxious stimulation can inhibit, as well as enhance, defensive responses (Krontiris-Litowitz *et al.*, 1987; Mackey *et al.*, 1987; Marcus *et al.*, 1988). The most complete behavioral study of nociceptive inhibition was reported by Marcus *et al.* (1988), who showed that inhibition of siphon withdrawal occurs following noxious but not innocuous stimuli, and that net inhibition has a brief duration.

These various forms of nociceptive plasticity differ in the sign, duration, and stimulus specificity of behavioral modulation. Yet another dimension of plasticity was revealed by the discovery that particular siphon responses are modulated selectively by noxious stimulation of dif-

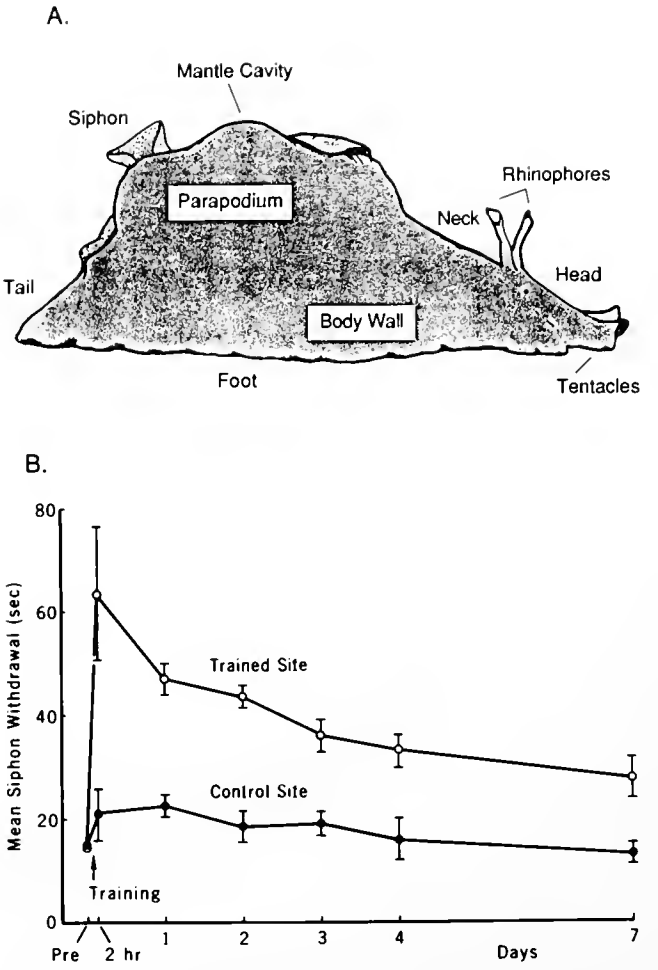

Figure 1. Site-specific sensitization following noxious tail stimulation in freely moving *Aplysia*. (A) Diagram of unrestrained animal used for testing and training. Before and after site-specific sensitization training, weak test stimuli were applied with a hand-held electrode to a site on each side of the tail that had been marked with a suture (not shown). Training consisted of a 45 s sequence of strong shocks to one of the test sites. During each test, the duration of siphon withdrawal was timed, and the magnitude of tail withdrawal was estimated. (B) Site-specific sensitization of siphon withdrawal. Siphon withdrawal was significantly greater when tested at the trained site than the contralateral control site. Similar differences were seen in tail withdrawal (not shown) and when other parts of the body were trained and tested (Walters, 1987a).

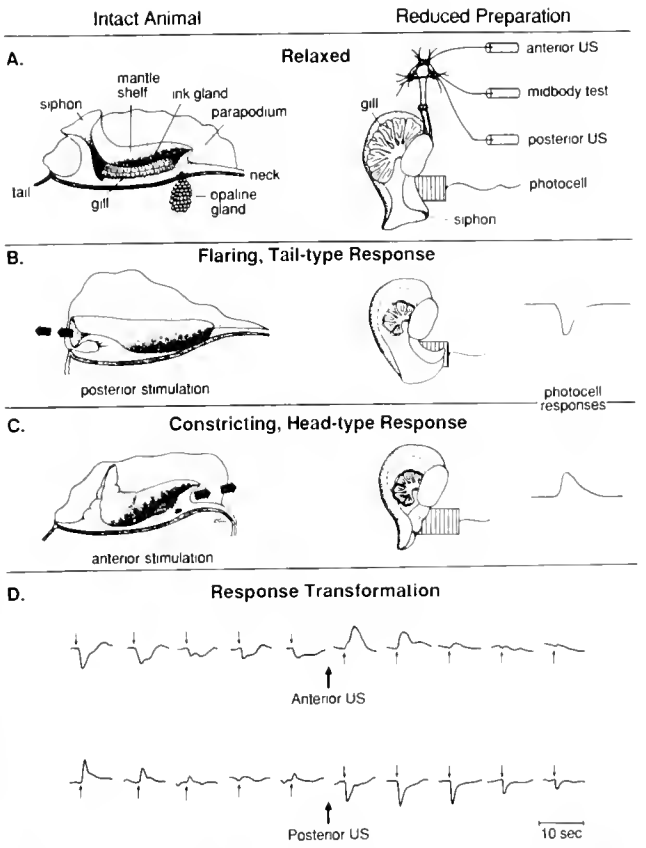

Figure 2. Transformation of siphon responses following noxious stimulation. The left column shows a cutaway view of the siphon and mantle organs in the intact animal (compare Fig. 1A). The right column shows the mantle organs and CNS in a reduced preparation. The photocell monitors the breadth but not the length of the siphon. (A) Relaxed siphon. Weak test stimuli were applied to a midbody nerve at 1 min intervals. A noxious unconditioned stimulus (US), a 15 s sequence of strong shock, was delivered to either a tentacle nerve or a tail nerve. (B) Flaring response, typical of posterior stimulation. The photocell shows a negative deflection. (C) Constricting response typical of anterior stimulation. The photocell shows a positive deflection. (D) Examples of transformed responses. Top—flaring responses are converted to constricting responses after noxious anterior stimulation. Bottom—constricting responses are converted to flaring responses after noxious posterior stimulation (Erickson and Walters, 1988).

ferent regions of the body. This response-specific nociceptive plasticity is expressed most clearly when noxious stimulation causes the animal to respond to a test stimulus with a qualitatively different response than it did before noxious stimulation (Erickson and Walters, 1988). Figure 2 shows examples of siphon responses being transformed into opposite responses following intense stimulation of nerves from the head or tail. Like sensitization, response transformation can be enhanced by associative training. The incidence and degree of transformation of motor responses to particular test stimuli are preferentially increased if the test stimulus is repeatedly paired with a noxious stimulus (Walters, 1989; Hawkins *et al.*, 1989).

Mechanisms of Nociceptive Plasticity

Mechanisms of general sensitization in *Aplysia* have received detailed analysis. Here I briefly describe selected aspects of cellular mechanisms, focusing on those that have been closely linked to changes in defensive behavior. For reviews of subcellular mechanisms of sensitization, see Kandel and Schwartz (1982) and Byrne (1987).

In principle, sensitization might involve alterations in any of various classes of neurons known to contribute to defensive behavior in *Aplysia* (Fig. 3). Although some interneurons and motor neurons show alterations during general sensitization (*e.g.*, Frost *et al.*, 1988), analysis has centered on mechanosensory neurons: the LE cluster, which innervates the siphon (Byrne *et al.*, 1974); and the VC clusters, which innervate most of the rest of the body (Walters *et al.*, 1983a). No major differences between these sensory clusters have been described in their response properties or plasticity. Cells in both clusters show a wide dynamic range, responding weakly to stimuli of moderate intensity and more strongly as stimulus intensity is in-

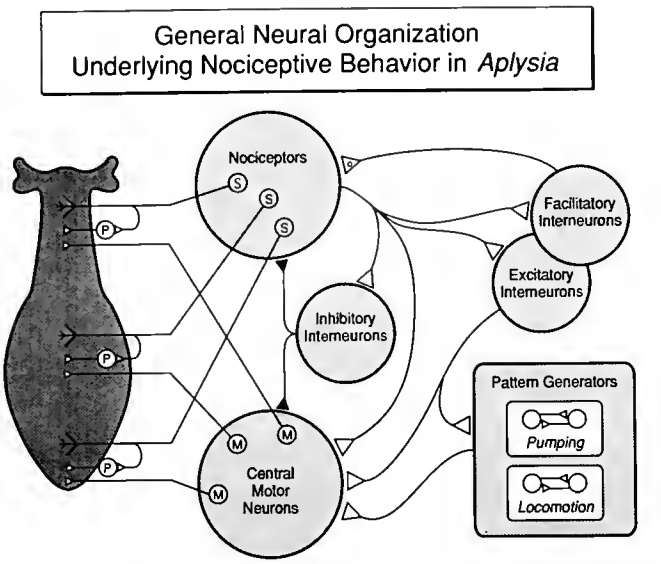

Figure 3. General pattern of neural organization controlling nociceptive behavior in *Aplysia*. Each indicated population of cells may include hundreds of neurons distributed throughout the nervous system. Wide-dynamic range nociceptive sensory neurons (S) innervate the entire body surface. Each cell connects to peripheral motor neurons (P), to central motor neurons (M) innervating the same region, and to inhibitory, excitatory, and facilitatory interneurons. Sensory neurons also make connections (largely polysynaptic) to complex pattern generating networks responsible for rhythmic defensive behaviors such as mantle pumping (used to eject ink and to increase respiration and blood circulation) and escape locomotion. Relatively little is known about interconnections among the various types of interneurons. A further complication is that some interneurons are multifunctional (*e.g.*, having both excitatory and facilitatory effects on the same follower neuron). Based on data from Bailey *et al.* (1979), Byrne (1980, 1983), Hawkins *et al.* (1981), Frost *et al.* (1988), and Hickie and Walters (unpub. obs.).

creased (Byrne *et al.*, 1978; Walters *et al.*, 1983a). Both clusters have nociceptive functions, because they respond maximally to noxious pinching stimuli (Walters *et al.*, 1983a; Walters and Clatworthy, unpub. obs.), and they are therefore indicated, in Figure 3, within the circle labeled "nociceptors".

Sensory neurons in the LE cluster (Bailey *et al.*, 1979), and probably in other central nociceptive clusters (*e.g.*, Walters, 1987b), make some synaptic connections to peripheral motor neurons (Fig. 3). But with few exceptions (see Clark and Kandel, 1984), analysis of synaptic plasticity in these sensory populations has focused on their strong monosynaptic connections to identified motor neurons within the CNS. Because of these connections and others to excitatory, facilitatory, and inhibitory interneurons involved in defensive responses (Fig. 3), changes in the signalling properties of LE and VC sensory neurons should have potent effects on behavioral responses elicited by moderate to strong cutaneous stimuli. Short-term behavioral sensitization is correlated with general facilitation of synapses from sensory neurons to motor and interneurons (Kandel and Schwartz, 1982; Walters *et al.*, 1983b) and with increased excitability of peripheral branches of the sensory neuron (Clatworthy and Walters, 1990). The presynaptic facilitation is mediated, at least in part, by 5-HT (Glanzman *et al.*, 1989), which can also enhance excitability of the central and peripheral parts of the sensory neuron (Walters *et al.*, 1983b; Klein *et al.*, 1986; Billy and Walters, 1989b). Many of the effects of 5-HT are mediated by cyclic AMP-dependent protein kinase (Kandel and Schwartz, 1982), and some are mediated by protein kinase C (Braha *et al.*, 1990). The most notable effects involve the depression of K^+ conductances (Klein *et al.*, 1982; Baxter and Byrne, 1989; Walsh and Byrne, 1989), which increase transmitter release and excitability by broadening spikes and decreasing spike accomodation (Kandel and Schwartz, 1982; Walters *et al.*, 1983b; Klein *et al.*, 1986). Noxious stimulation also appears to enhance a Ca^{2+} conductance (Edmonds *et al.*, 1990).

The expression of long-term sensitization in sensory neurons involves some of the same mechanisms as short-term sensitization: depressed K^+ conductances, increased transmitter release, and increased excitability (Frost *et al.*, 1985; Scholz and Byrne, 1987; Walters, 1987b). Specific morphological changes also occur in the sensory neuron, including the growth of new synaptic varicosities and active zones within the CNS (Bailey and Chen, 1983, 1988; Nazif *et al.*, 1989), and possibly the growth of peripheral processes that expand the size of the receptive field (Billy and Walters, 1989a). Considerable effort is being made to identify molecular mechanisms involved in inducing and maintaining long-term changes in these sensory neurons (*e.g.*, Barzilai *et al.*, 1989; Eskin *et al.*, 1989).

Associative enhancement of withdrawal responses to mechanosensory cues and site-specific sensitization appears to involve the same basic mechanism: activity-dependent enhancement of the mechanisms of general sensitization, as described above (Walters and Byrne, 1983a; Hawkins *et al.*, 1983; Walters, 1987b). Figure 4 illustrates two of the sensory neuron alterations contributing to long-term site-specific sensitization: synaptic facilitation and increased soma excitability; the latter is expressed dramatically as a prolonged afterdischarge to brief depolarization. During the induction of site-specific sensitization, the sensory neuron is activated by the noxious stimulus. In associative conditioning, the sensory neuron is activated by a cue presented immediately before the noxious stimulus. In both cases, the activity enhances the effects of extrinsic chemical modulators (*e.g.*, 5-HT) on the sensory neuron, and thus this general class of plasticity is termed activity-dependent extrinsic modulation (ADEM). Activation of sensory neurons opens Ca^{2+} channels (Walters and Byrne, 1983b; Edmonds *et al.*, 1990). The resulting Ca^+ influx enhances adenylate cyclase activity, increasing the rate of cyclic AMP synthesis, and thus amplifying the degree and duration of plasticity induced by neuromodulators released during noxious stimulation (Abrams and Kandel, 1988). Ca^{2+} might also enhance plasticity in other ways; for example, Ca^{2+}-dependent kinases may directly phosphorylate transcription factors (*cf.* Dash *et al.*, 1990).

The cellular mechanisms of nociceptive inhibition have also been studied. Mackey *et al.* (1987) reported that tail shock causes presynaptic inhibition and spike narrowing in siphon sensory neurons, and that these effects are partly mediated by an identified interneuron containing the neuropeptide FMRFamide. Application of FMRFamide to the sensory cell soma and synaptic region in the CNS causes hyperpolarization, spike narrowing, and presyn-

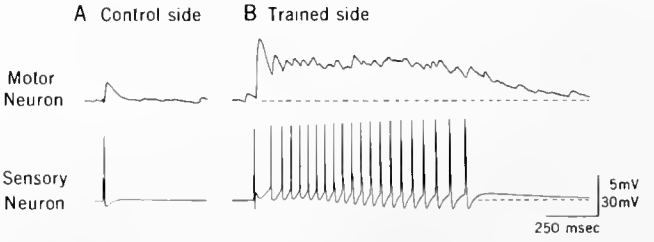

Figure 4. Example of synaptic facilitation and afterdischarge in a sensory neuron after site-specific sensitization. The intact animal was trained with strong noxious shock delivered to one side of the body. One day later, the CNS was removed and sensory and motor neurons innervating the trained side and corresponding regions on the contralateral side were examined. (A) Typical connection between a tail sensory neuron and tail motor neuron innervating the untrained side of the tail. The connection was tested by activating the sensory neuron with a 10 ms depolarizing pulse injected into the soma. (B) The same test procedure on the trained side elicits a larger synaptic potential and an afterdischarge of 20 spikes (Walters, 1987b).

Table I

Three-phase model of the functions and general mechanisms of nociceptive plasticity in Aplysia

	Phase 1. Injury detection	Phase 2. Escape	Phase 3. Recuperation
Period:	0.1 s–10 min	1 s–30 min	10 min–1 month
Functions:	• Severity appraisal • Localization • Compensation for destruction of nociceptive channels • Defensive response triggering • Anticipation	• Flight • Inhibition of competing responses	• General inactivity (healing) • Defensive readiness (sensitization) a. General b. Wound specific c. Cue specific
Mechanisms:	• Nociceptor activation a. Frequency code b. Wide dynamic range • Activation of defensive circuits (Somatotopic organization) • Nociceptor facilitation a. Afterdischarge b. PTP c. HSF d. Hyperexcitability e. ADEM • Motor facilitation	• Activity in circuits generating escape behavior • Nociceptor inhibition a. Presynaptic inhibition (neuromodulation) b. Activity-dependent reduction in excitability • Inhibition of motor and interneurons controlling other behaviors	• Inhibition of circuits controlling feeding, reproduction, etc. • Nociceptor facilitation a. ADEM b. Axon injury signals c. Lower threshold d. Less accomodation e. Afterdischarge f. Synaptic facilitation g. Sprouting • Motor facilitation

The times for each phase indicate the approximate beginning and end of the phase relative to the beginning of the noxious stimulus. ADEM—activity-dependent extrinsic modulation; HSF—heterosynaptic facilitation; PTP—posttetanic potentiation.

aptic inhibition in sensory neurons (Belardetti *et al.*, 1987), whereas peripheral application increases mechanosensory threshold (Billy and Walters, 1989b). Extrapolation from studies in other mollusks suggests that other neuromodulators may also contribute to nociceptive inhibition of defensive responses in *Aplysia*. For example, pharmacological evidence suggests that inhibition of a defensive response in another gastropod, the snail *Cepaea*, may involve opiate-like modulators (Kavaliers, 1987). In *Aplysia*, noxious stimulation also produces activity-dependent reduction in the excitability of sensory neuron axons and receptive fields (Clatworthy and Walters, 1990), and can sometimes block afferent spikes (Clatworthy and Walters, 1989). The presynaptic inhibition produced by FMRFamide is also activity-dependent (Small *et al.*, 1989). Recently, Wright *et al.* (1989) suggested that interneurons may be more important loci than sensory neurons for inhibition in the siphon withdrawal system. They found that tail shock suppressed polysynaptic (interneuronal) components of a complex test EPSP in siphon motor neurons under conditions in which no inhibition of the monosynaptic EPSP from the sensory neurons was detected.

Mechanisms of response-specific nociceptive plasticity are not yet known. However, tests of several potential mechanisms have recently begun in identified neurons within siphon control circuits (Erickson and Walters, 1988; Frost *et al.*, 1988; Hickie and Walters, 1990; Fang and Clark, 1990).

A Functional Model of Nociceptive Plasticity

These findings show that noxious stimulation causes highly complex behavioral and neuronal alterations in *Aplysia*. Two issues have not been clear: the functional significance of this complexity, and the integration of apparently opposing forms of plasticity to produce adaptive behavior. General similarities between the patterns of nociceptive behavior observed in *Aplysia* and in other species (primarily rats and humans) suggest that forms of nociceptive plasticity in *Aplysia* might represent common behavioral adaptations to ubiquitous selection pressures; namely, escape from a source of bodily injury, and optimization of recuperation. This possibility encouraged the formulation of a model linking potentially general principles of nociceptive function to patterns of behavioral and neural plasticity that have been described in *Aplysia*. In a functional model of pain and fear in mammals, Bolles and Fanselow (1980) divided nociceptive responses into perceptual, defensive, and recuperative phases. Somewhat similar phases can be used in a functional model to explain much of the complexity of behavioral and neuronal plasticity observed in *Aplysia* following noxious stimulation (Table I). These overlapping phases of injury detection,

escape, and recuperation correspond to periods of immediate facilitation, short-term inhibition, and long-term facilitation of defensive responses.

Phase 1—injury detection

How does an animal know it is injured, or about to be injured? False negative answers mean an animal will fail to initiate escape and recuperative behavior, jeopardizing its life. False positive answers also reduce biological fitness by committing the animal unnecessarily to energy-consuming escape behavior, and possibly to a long period of recuperative behavior during which important activities such as reproduction and feeding are inhibited. One way for a CNS to decide whether an injury has occurred is to interpret any activity on nociceptive labeled lines from the body as proof of injury. However, because an animal needs to match its responses to the severity and location of its injuries, nociceptive signals should also carry intensity and spatial information. In addition, if the severity of an injury is represented by the number of active nociceptive fibers and by their degree of activity, there should be some way of compensating for the loss of signal strength during and after injury severe enough to destroy or damage nociceptive fibers from the injured region. Finally, a nociceptive system would be highly adaptive if it could recognize noxious stimuli prior to actual injury.

These general functional considerations are reflected in the organization of the nociceptive system of *Aplysia* and in the alterations of this system that immediately follow moderate intensity or noxious cutaneous stimulation (Table I). LE and VC sensory neurons trigger defensive withdrawal responses, and the magnitude of the responses thus evoked depends upon the number of LE or VC neurons activated, upon the number and frequency of spikes generated, and upon the amount of transmitter released per spike (Byrne *et al.*, 1978; Walters *et al.*, 1983a; Walters, unpub. obs.). Therefore, the likelihood and severity of body wall injury in *Aplysia* appear to be coded, at least in part, by the total level of activity in these nociceptive channels and by the strength of nociceptive connections to interneurons and motor neurons. As in mammals, the relatively small size of nociceptive receptive fields and the somatotopic organization of sensory and motor pathways in *Aplysia* (Walters *et al.*, 1983a) contribute to the localization of noxious stimuli.

How does this system compensate for the destruction of nociceptive axons during severe injury? The VC and LE sensory neurons provide labeled lines to the CNS from the periphery, but their wide dynamic range and response properties also make possible a frequency code for the severity of injury. A brief, punctate, moderately intense stimulus to the tail, which does not cause injury unless greatly prolonged, typically evokes one to five spikes in each of three to five VC neurons, the receptive fields of which are estimated to overlap any given point on the tail (Walters *et al.*, 1983a; Billy and Walters, 1989a). The total activity in these sensory neurons (10–20 spikes over about 0.5 s) leads to a relatively brief withdrawal of the tail and siphon, and perhaps to escape locomotion. A strong, punctate, pinching stimulus of the same duration, which may cause some cutaneous damage but does not destroy major axons of VC sensory neurons, causes high frequency activation of each sensory neuron, but the activation rarely outlasts a moderately noxious stimulus. Thus, a 0.5 s stimulus might lead to a 0.5 s barrage of perhaps 75 spikes across the same 5 VC neurons, leading to strong, long-lasting withdrawal of the tail and siphon, as well as to inking and vigorous escape locomotion. Finally, a severe, crushing stimulus of the same duration will probably destroy some of the sensory axons innervating the region. Assuming, for illustrative purposes, that axons from three of the five sensory neurons are destroyed, how is the CNS informed of the severity of the injury? First, the remaining fibers will fire at maximal frequency (about 50 Hz) during the stimulus. Second, the crushed axons will produce an injury discharge of high frequency spikes. Third, very strong stimuli produce an afterdischarge in VC sensory neurons (see Fig. 4) that can last 0.1 to 3 s (Clatworthy and Walters, 1988, and unpub. obs.). The afterdischarge is generated, at least in part, within the CNS (Clatworthy and Walters, 1988), raising the possibility that both the intact VC neurons, and the VC neurons with injury-destroyed axons, fire at high frequency during the noxious stimulus and for 1 to 2 s afterwards. Thus, even with a majority of the sensory fibers from the injured region disconnected from the CNS by the injury, a barrage of 100–200 high frequency sensory spikes may reach central synaptic terminals onto defensive motor and interneurons. The mechanism of afterdischarge is not yet known, but it appears to depend upon both the initial spike activity and the extracellular release of chemical modulators, *i.e.*, ADEM (Clatworthy and Walters, unpub. obs.). Finally, under natural conditions, more severe stimuli usually affect larger areas of body wall and thus activate more nociceptors.

How does the system anticipate injury during moderate intensity cutaneous stimulation that threatens but does not immediately produce tissue damage? Stimuli sufficiently intense to activate LE and VC neurons, but not severe enough to cause immediate body wall injury, have transient facilitatory effects upon defensive responses. This facilitation involves brief (seconds to minutes) heterosynaptic facilitation (Carew *et al.*, 1971; Walters *et al.*, 1983b), post-tetanic potentiation (Walters and Byrne, 1984; Clark and Kandel, 1984), and enhanced peripheral excitability (Clatworthy and Walters, 1990) in the sensory neurons. The facilitation of peripheral excitability, as well

as facilitation of synaptic transmission (Hawkins *et al.*, 1983; Walters and Byrne, 1983a), is greatest in sensory neurons activated by the noxious stimulus. As a consequence, continued or repeated application of a moderately noxious stimulus to the same region should cause increasing activation of the nociceptors, increasing synaptic facilitation (Walters *et al.*, 1983b), and increasingly effective sensory input to the CNS. Temporal summation of excitatory and facilitatory inputs to defensive interneurons and motor neurons occurs (Carew and Kandel, 1977; Walters, unpub. obs.), facilitating motor responsiveness. These effects also increase the spontaneous firing rates of some motor neurons, which can lead to neuromuscular facilitation (*e.g.*, Frost *et al.*, 1988). All of these sensory and motor facilitation mechanisms produce "windup" of neural responses to repeated or prolonged stimulation that is intense enough to be threatening. Windup has two consequences: withdrawal and escape responses are triggered before a prolonged, moderately noxious stimulus injures the animal; and the animal is prepared to respond maximally if more severe stimulation follows. Windup of responses to noxious stimuli in mammals appears to involve some of the same mechanisms (Woolf and Walters, 1991). Brief habituating and inhibitory effects, reported for relatively weak cutaneous stimuli in *Aplysia* (*e.g.*, Kupfermann *et al.*, 1970; Mackey *et al.*, 1987), should oppose and delay these facilitatory effects, reducing the chances of overreaction to innocuous stimuli.

Phase 2—escape

When the CNS interprets a stimulus as injurious or potentially injurious, escape behavior is initiated, and the second phase of nociceptive plasticity begins. It has long been observed that animals in the act of fleeing or fighting ignore their injuries. Nociceptive responses are inhibited, and this inhibition prevents less urgent behavior patterns from interfering with emergency responses critical for escaping from, or repelling, mortal threats (Wall, 1979; Bolles and Fanselow, 1980). In *Aplysia*, strong shock or pinching stimuli inhibit withdrawal reflexes and associated neural activity in an intensity-dependent manner, and the inhibitory effects generally last for 1 to 15 min (Marcus *et al.*, 1988; Walters, Erickson, and Clatworthy, unpub. obs.). This time course and intensity dependence roughly parallel those of escape locomotion (Walters and Erickson, 1986). Because massive withdrawal of any region of the body interferes with escape locomotion, a major function of nociceptive inhibition in this animal is probably to prevent the disruption of escape behavior that would occur if strong withdrawal responses were triggered during flight. As described above, inhibition of defensive responses appears to involve neuromodulation of sensory neurons, interneurons, and perhaps motor neurons, with some of the inhibition being activity-dependent (Table I).

Phase 3—recuperation

After several minutes of escape locomotion, *Aplysia* stop (in a crevice if available), contract into a tight spherical shape, and remain motionless. If the injury is severe, an animal may show little sign of activity for up to several days. If the animal is touched during this time, it will show exaggerated withdrawal responses and a low threshold for escape locomotion, especially if contact is made near the wound (Walters, 1987a, and unpub. obs.). Inactivity during wound healing presumably involves inhibition of circuits controlling active behaviors, such as feeding and mating, which are not immediately essential and which would subject the wound to further stress. Inhibitory signals may include neuroendocrine substances and factors released into the blood from ruptured cells at the site of trauma (Krontiris-Litowitz *et al.*, 1989).

While little is known about mechanisms underlying inhibition of nonessential behaviors during the recuperative phase, a great deal has been learned about the enhancement of defensive responses during this phase. The various mechanisms of sensitization reviewed earlier in this article serve to increase the animal's readiness for defensive action while the wound heals (Table I). This sensitization is functionally equivalent to long-term hyperalgesia in mammals. Hypersensitivity is especially important around the region of injury because a wound may leak substances that can invite further attack from predators or parasites, and because a wounded region is likely to be weakened and vulnerable to further disturbance. Persistent general sensitization in *Aplysia* is mediated, at least in part, by long-term heterosynaptic facilitation of wide-dynamic range nociceptors (Frost *et al.*, 1985; Walters, 1987b). Wound-specific sensitization involves at least three basic mechanisms. First, long-term site-specific sensitization is produced by ADEM of nociceptors activated during wounding. This selectively decreases peripheral mechanosensory threshold (Billy and Walters, 1989a), enhances nociceptor afterdischarge, and produces synaptic facilitation in sensory neurons innervating the wounded region (Walters, 1987b). Second, signals generated at a site of axonal injury may be carried by retrograde axonal transport to the soma and synapses, where they induce the same set of hyperexcitability and facilitatory effects as are triggered by ADEM (Walters, Alizadeh, and Castro, unpub. obs.). The generation of signals at sites of axonal injury may involve interactions with extracellular factors associated with immunocytes aggregating at damaged tissue (Alizadeh *et al.*, 1990). In each case, persistent sensitization may involve growth of new synapses and sprouting of new branches from central and peripheral sensory arbors (Bailey and Chen, 1988; Billy and Walters, 1989a). A third basic mechanism of long-term wound-specific sensitization has been implicated by behavioral

experiments (Fig. 2), but has not yet been demonstrated within the nervous system—selective enhancement of the responsiveness of elements within motor control circuits controlling specific defensive responses appropriate for the wounded region (motor facilitation; Erickson and Walters, 1988).

An interesting feature of nociceptive systems in *Aplysia* and in mammals is the prominence of wide-dynamic range neurons. Results from *Aplysia* suggest that this feature may be important for the induction of nociceptive behavior by innocuous stimuli during nociceptive sensitization (an effect functionally equivalent to allodynia in humans—pain evoked by innocuous stimuli). In *Aplysia* the severity of an injury is partially encoded by the total output of nociceptors representing the injured region (*i.e.*, the number of cells activated × firing rate per cell × transmitter release per spike). Thus, a moderately intense stimulus that would normally be innocuous will be interpreted by the CNS as noxious if transmitter release or spike frequency are enhanced in wide-dynamic range nociceptors after an injury. Presumably, innocuous tactile stimulation near a serious wound is often sufficiently threatening to evoke nociceptive behavior during recuperation in both *Aplysia* and mammals.

The ADEM mechanism in LE and VC sensory neurons may contribute, not only to site-specific sensitization around a wound, but also to classical conditioning of a cutaneous warning cue distant from a wound, provided that the warning cue is at least moderately intense and is delivered shortly before wounding (Walters and Byrne, 1983; Hawkins *et al.*, 1983). However, this cue-specific sensitization mechanism would only be useful if the cue were subsequently to contact the same receptive field. Given the small size of these cells' receptive fields (decreasing the chances of repeated contact), conditioned enhancement of their signals would seem to provide an undependable warning cue (see Walters, 1987b). Cue-specific sensitization mechanisms should be more effective in sensory neurons that have global receptive fields and that can detect a threat at a distance (before contact), allowing more time for avoidance of a threatening situation. Chemosensory neurons have these properties, and chemical stimuli may thus be more effective cues for aversive conditioning than tactile cues. Aversive conditioning with chemosensory cues occurs readily in *Aplysia* (Walters *et al.*, 1981; Colwill *et al.*, 1988), but whether such conditioning is more rapid or potent than conditioning with tactile cues is not yet known (*e.g.*, Carew *et al.*, 1981).

A Hypothesis About the Evolution of Nociceptive Plasticity

Although nociceptive neurons and nociceptive responses have been examined in a variety of species (*e.g.*, Nicholls and Baylor, 1968; Kavaliers, 1988), investigations of behavioral and neuronal *plasticity* following noxious stimulation have largely been restricted to mammalian and molluscan preparations. Nociceptive plasticity in these two groups shows a number of interesting similarities (reviewed by Walters, 1987a,b; Kavaliers, 1988; Woolf and Walters, 1991). In both groups, facilitatory and inhibitory alterations occur in the first stages of nociceptive processing—within wide dynamic range nociceptors in *Aplysia*, and in primary nociceptors and secondary wide-dynamic range spinal interneurons in mammals. Similarities include: intensity-dependent enhancement and inhibition of central excitability, enhanced peripheral sensitivity, enlargement of nociceptive receptive fields, and activity-dependent plasticity. Furthermore, preliminary evidence suggests that aspects of the underlying subcellular mechanisms (*e.g.*, depressed K^+ conductances, mediation by common protein kinases, and activation of "immediate-early" genes) might also be shared (see Woolf and Walters, 1991). In principle, the similarity of any given feature may be due to either convergent evolution of independent mechanisms in response to common environmental pressures (analogy), or to conservation of primitive mechanisms that had evolved in ancestors common to both mollusks and mammals (homology). The ancestors of mollusks and mammals diverged very early in the history of the animal kingdom, before the protostome and deuterostome lineages split during the Precambrian era. Thus, homologous features in mollusks and mammals must be very primitive, having descended from small, soft-bodied animals that lived more than 600 million years ago, before the hard shells or skeletons that would leave a fossil record had evolved (Avers, 1989).

To what extent are mechanisms of nociceptive plasticity homologous in mollusks and mammals? Undoubtedly many similarities are due to analogous adaptations developed independently by these groups in response to a ubiquitous pressure—the dangers that follow sublethal injury in a hostile environment. On the other hand, two arguments suggest that this same pressure existed during the evolution of primitive common ancestors of mollusks and mammals, and could have supported the early evolution of adaptations to optimize defensive behavior following noxious stimulation. First, the presence of predators during early periods of animal evolution is suggested by the occurrence of withdrawal and escape responses in virtually all existing animal groups, including protozoans (Kavaliers, 1988). Unfortunately, almost nothing is known about predators in the Precambrian world except that they, like their prey, would have been small and soft-bodied, and probably lacked specialized feeding appendages (Vermeij, 1987). Nevertheless, Precambrian predators probably existed (Hickman *et al.*, 1984) and would not have needed specialized appendages. For example, prey

may have been captured with nets of mucus, and eaten with simple grasping and extracellular digestion methods, similar to those used by some flatworms today. Second, injury could have also been produced by random assaults from the environment, such as wave action. An injured animal would have been more vulnerable to further physical disturbance, and to detection and attack by predators.

If early mechanisms of nociceptive plasticity did, in fact, originate in primitive animals having very simple nervous systems, an attractive possibility is that some of these mechanisms first appeared in primary mechanosensory neurons. These cells were among the earliest neurons (*e.g.*, Bullock and Horridge, 1965). Because they are directly exposed to surface trauma, they provide a single locus for both recognizing noxious stimulation and altering the responses of an animal to subsequent mechanical stimulation. Exposure of the peripheral branches of mechanosensory neurons to surface trauma suggests a specific cellular hypothesis for the origin of some mechanisms of nociceptive plasticity. Trauma to the body surface (or even wear on soft body parts in a turbulent environment) can damage peripheral sensory branches. The ubiquity of cellular repair processes in modern cells suggests that such processes appeared very early in the evolution of life and were available to repair damaged sensory branches in primitive animals. For an organism to take mechanisms that had evolved to regenerate and maintain excitability in damaged neuronal branches, and use these mechanisms in undamaged neurons where they could amplify the neurons' normal signalling effectiveness, seems a small step. For example, mechanisms of cellular repair, growth, and signal compensation triggered by intracellular signals of cellular injury might become inducible by extracellular neuromodulators released during noxious stimulation, or by interactions of such neuromodulators with spike activity in the neuron (*i.e.*, ADEM).

Recently we tested whether a close relationship exists between mechanisms of general and site-specific sensitization on the one hand (*i.e.*, involving neuromodulation and ADEM), and responses to axonal injury on the other (Walters, Alizadeh, and Castro, unpub. obs.). We studied the effects of axonal injury by crushing nerves containing sensory neuron axons under conditions in which synaptic release of neuromodulators (such as 5-HT) and ADEM were blocked. Tests of the sensory neurons after nerve crush revealed profound hyperexcitability and synaptic facilitation, lasting weeks, that were specific to cells with axons in the crushed nerves. The long latency of the effects (1–2 days) suggested that signals from axonal damage were conveyed back to the soma and synapses by axonal transport. Of particular interest was the qualitative identity of the set of changes produced by axon crush with the alterations produced by neuromodulation and ADEM. One interpretation of these results is that a common set of mechanisms underlying long-term hyperexcitability and synaptic facilitation can be triggered by two signalling pathways from the periphery to the soma. The more primitive pathway would be provided by intracellular signals conveyed slowly by axonal transport from damaged axons. ADEM (conjoint electrical activation and extrinsic neuromodulation) of the soma during injury would provide a much more rapid signal of peripheral injury in nociceptors activated by injurious stimuli (see Billy and Walters, 1989a). ADEM may have evolved later, when the increased size of animals and resulting distances between nociceptor somata and their receptive processes selected for faster signals, so that regulation of protein synthesis necessary for injury-induced plasticity would not be delayed.

Although highly speculative, this hypothesis and our preliminary indications of links between cellular injury responses and long-term sensitization in *Aplysia* raise the possibility that some of the earliest forms of memory may have evolved from cellular repair and signal compensation mechanisms in primitive mechanosensory neurons. If, as brains became increasingly complex, these cells served as evolutionary precursors of other neuronal types, then primitive mechanisms of nociceptive plasticity might have been important for the evolution of other forms of memory as well. Indeed, both axon damage (*e.g.*, Janig, 1988; Kelly *et al.*, 1988) and learning (*e.g.*, Disterhoft *et al.*, 1986) have been associated with long-term hyperexcitability in mammalian neurons.

Evolutionary arguments have obvious weaknesses, especially when they deal with eras that left almost no fossil record. Nevertheless, such arguments can lead to fresh perspectives and novel physiological and molecular predictions. The present hypothesis makes three testable predictions: (1) that common cellular mechanisms (involving homologous molecules) contribute to nociceptive sensitization in a broad range of species; (2) that critical molecular steps are shared with mechanisms involved in cellular repair and signal compensation following axonal damage; and (3) that some of these molecular steps are shared with mechanisms involved in traditional forms of learning and memory. Systematic comparison of learning-related mechanisms and injury-related mechanisms in diverse animals will put these predictions to the test, and may provide insight into the evolution of some forms of memory.

Acknowledgments

I am grateful to Dr. Andrea Clatworthy and Mr. Chris Hickie for their comments and for allowing me to discuss some of their unpublished data. I also thank Dr. Bill Frost for his comments and Mr. Jim Pastore and Ms. Linda Eshelman for preparing the illustrations. Supported by

National Institute of Mental Health grant MH38726 and National Science Foundation grant BNS9011907.

Literature Cited

Abrams, T. W., and E. R. Kandel. 1988. Is contiguity detection in classical conditioning a system or a cellular property? Learning in *Aplysia* suggests a possible molecular site. *Trends Neurosci.* **11:** 128–135.

Alizadeh, H., Clatworthy, A. L., Castro, G. A., and E. T. Walters. 1990. Induction of an immune reaction in *Aplysia* is accompanied by long-term enhancement of sensory neuron excitability. *Soc. Neurosci. Abstr.* **15:** 597.

Avers, C. J., 1989. *Process and Pattern in Evolution.* Oxford University Press, New York. 590 pp.

Bailey, C. H., V. F. Castellucci, J. Koester, and E. R. Kandel. 1979. Cellular studies of peripheral neurons in siphon skin of *Aplysia californica*. *J. Neurophysiol.* **42:** 530–557.

Bailey, C. H., and M. Chen. 1983. Morphological basis of long-term habituation and sensitization in *Aplysia*. *Science* **220:** 91–93.

Bailey, C. H., and M. Chen. 1988. Long-term memory in *Aplysia* modulates the total number of varicosities of single identified sensory neurons. *Proc. Nat. Acad. Sci. USA* **85:** 2373–2377.

Barzilai, A., T. E. Kennedy, J. D. Sweatt, and E. R. Kandel. 1989. 5-HT modulates protein synthesis and the expression of specific proteins during long-term facilitation in *Aplysia* sensory neurons. *Neuron* **2:** 1577–1586.

Baxter, D. A., and J. H. Byrne. 1989. Serotonergic modulation of two potassium currents in the pleural sensory neurons of *Aplysia*. *J. Neurophysiol.* **62:** 665–679.

Belardetti, F., E. R. Kandel, and S. A. Siegelbaum. 1987. Neuronal inhibition by the peptide FMRFamide involves opening of S K^+ channels. *Nature* **325:** 153–156.

Billy, A. J., and E. T. Walters. 1989a. Long-term expansion and sensitization of mechanosensory receptive fields in *Aplysia* support an activity-dependent model of whole-cell sensory plasticity. *J. Neurosci.* **9:** 1254–1262.

Billy, A. J., and E. T. Walters. 1989b. Modulation of mechanosensory threshold in *Aplysia* by 5-HT, small cardioactive peptideB (SCPB), FMRFamide, acetylcholine, and dopamine. *Neurosci. Lett.* **105:** 200–204.

Bolles, R. C., and M. S. Fanselow. 1980. A perceptual-defensive-recuperative model of fear and pain. *Behav. Brain Sci.* **3:** 291–323.

Braha, O., N. Dale, B. Hochner, M. Klein, T. W. Abrams, and E. R. Kandel. 1990. Second messengers involved in the two processes of presynaptic facilitation that contribute to sensitization and dishabituation in *Aplysia* sensory neurons. *Proc. Nat. Acad. Sci. USA* **87:** 2040–2044.

Bullock, T. H., and G. A. Horridge. 1965. *Structure and Function in the Nervous Systems of Invertebrates,* Vol. 1. W. H. Freeman and Co., San Francisco. 798 pp.

Byrne, J. H., 1980. Identification of neurons contributing to presynaptic inhibition in *Aplysia californica*. *Brain Res.* **199:** 235–239.

Byrne, J. H., 1983. Identification and initial characterization of a cluster of command and pattern-generating neurons underlying respiratory pumping in *Aplysia californica*. *J. Neurophysiol.* **49:** 491–508.

Byrne, J. H., 1987. Cellular analysis of associative learning. *Physiol. Rev.* **67:** 329–439.

Byrne, J. H., V. Castellucci, and E. R. Kandel. 1974. Receptive fields and response properties of mechanoreceptor neurons innervating siphon skin and mantle shelf in *Aplysia*. *J. Neurophysiol.* **37:** 1041–1064.

Byrne, J. H., V. F. Castellucci, T. J. Carew, and E. R. Kandel. 1978. Stimulus-response relations and stability of mechanoreceptor and motor neurons mediating defensive gill-withdrawal reflex in *Aplysia*. *J. Neurophysiol.* **41:** 402–417.

Carew, T. J., V. F. Castellucci, and E. R. Kandel. 1971. An analysis of dishabituation and sensitization of the gill-withdrawal reflex in *Aplysia*. *Intern. J. Neurosci.* **2:** 79–98.

Carew, T. J., R. D. Hawkins, and E. R. Kandel. 1983. Differential classical conditioning of a defensive withdrawal reflex in *Aplysia californica*. *Science* **219:** 397–400.

Carew, T. J., and E. R. Kandel. 1977. Inking in *Aplysia californica*. III. Two different synaptic conductance mechanisms for triggering central program for inking. *J. Neurophysiol.* **40:** 721–734.

Carew, T. J., E. T. Walters, and E. R. Kandel. 1981. Classical conditioning in a simple withdrawal reflex in *Aplysia californica*. *J. Neurosci.* **1:** 1426–1437.

Clark, G. A., and E. R. Kandel. 1984. Branch-specific heterosynaptic facilitation in *Aplysia* siphon sensory cells. *Proc. Nat. Acad. Sci. USA* **81:** 2577–2581.

Clatworthy, A. L., and E. T. Walters. 1988. Sensitization and sensory signals in *Aplysia* II. Modulation of central bursting and spike conduction. *Soc. Neurosci. Abstr.* **14:** 609.

Clatworthy, A. L., and E. T. Walters. 1989. Activity-dependent block of central sensory conduction during inhibition of tail withdrawal reflex in *Aplysia*. *Soc. Neurosci. Abstr.* **15:** 1263.

Clatworthy, A. L., and E. T. Walters. 1990. Modulation of the excitability of peripheral receptive fields and axons in sensory neurons of *Aplysia*. *Soc. Neurosci. Abstr.* **16:** 20.

Colwill, R. M., R. A. Absher, and M. L. Roberts. 1988. Context-US learning in *Aplysia californica*. *J. Neurosci.* **8:** 4434–4439.

Dash, P. K., B. Hochner, and E. R. Kandel. 1990. Injection of the cAMP-responsive element into the nucleus of *Aplysia* sensory neurons blocks long-term facilitation. *Nature* **345:** 718–721.

Disterhoft, J. F., D. A. Coulter, and D. L. Alkon. 1986. Conditioning-specific membrane change of hippocampal neurons *in vitro*. *Proc. Nat. Acad. Sci. USA* **83:** 2733–2737.

Edmonds, B., M. Klein, N. Dale, and E. R. Kandel. 1990. Contributions of two types of calcium channels to synaptic transmission and plasticity. *Science* **250:** 1142–1147.

Erickson, M. T., and E. T. Walters. 1988. Differential expression of pseudoconditioning and sensitization by siphon responses in *Aplysia*: novel response selection after training. *J. Neurosci.* **8:** 3000–3010.

Eskin, A., K. S. Garcia, and J. H. Byrne. 1989. Information storage in the nervous system of *Aplysia*: specific proteins affected by 5-HT and cAMP. *Proc. Nat. Acad. Sci. USA* **86:** 2458–2462.

Fang, X., and G. A. Clark. 1990. Neural mechanisms of response specificity. I. Tail and mantle nerve shock produce differential effects on the siphon-withdrawal neuronal circuit in *Aplysia*. *Soc. Neurosci. Abstr.* **16:** 596.

Frost, W. N., V. F. Castellucci, R. D. Hawkins, and E. R. Kandel. 1985. Monosynaptic connections made by the sensory neurons of the gill- and siphon-withdrawal reflex in *Aplysia* participate in the storage of long-term memory for sensitization. *Proc. Nat. Acad. Sci. USA* **82:** 8266–8269.

Frost, W. N., G. A. Clark, and E. R. Kandel. 1988. Parallel processing of short-term memory for sensitization in *Aplysia*. *J. Neurobiol.* **19:** 297–334.

Glanzman, D. L., S. L. Mackey, R. D. Hawkins, A. M. Dyke, P. E. Lloyd, and E. R. Kandel. 1989. Depletion of 5-HT in the nervous system of *Aplysia* reduces the behavioral enhancement of gill withdrawal as well as the heterosynaptic facilitation produced by tail shock. *J. Neurosci.* **9:** 4200–4213.

Hawkins, R. D., T. W. Abrams, T. J. Carew, and E. R. Kandel. 1983. A cellular mechanism of classical conditioning in *Aplysia*: activity-dependent amplification of presynaptic facilitation. *Science* **219:** 400–404.

Hawkins, R. D., V. F. Castellucci, and E. R. Kandel. 1981. Interneurons involved in mediation and modulation of gill- withdrawal reflex in *Aplysia* I. Identification and characterization. *J. Neurophysiol.* **45:** 304–314.

Hawkins, R. D., N. Lalevic, G. A. Clark, and E. R. Kandel. 1989. Classical conditioning of the *Aplysia* siphon-withdrawal reflex exhibits response specificity. *Proc. Nat. Acad. Sci. USA* **86:** 7620–7624.

Hickie, C., and E. T. Walters. 1990. Identified central motor neurons are necessary for directional siphon responses in *Aplysia*. *Soc. Neurosci. Abstr* **16:** 19.

Hickman, C. P., L. S. Roberts, and F. M. Hickman. 1984. *Integrated Principles of Zoology* Mosby, St. Louis, Missouri. 1065 pp.

Janig, W. 1988. Pathophysiology of nerve following mechanical injury. Pp. 89–108 in *Proceedings of the Vth World Congress on Pain* R. Dubner, G. F. Gebhart, and M. R. Bond, eds. Elsevier, Amsterdam.

Kandel, E. R., and J. H. Schwartz. 1982. Molecular biology of learning: modulation of transmitter release. *Science* **218:** 433–444.

Kavaliers, M. 1987. Evidence for opioid and non-opioid forms of stress-induced analgesia in the snail, *Cepaea nemoralis*. *Brain Res* **410:** 111–115.

Kavaliers, M. 1988. Evolutionary and comparative aspects of nociception. *Brain Res. Bull.* **21:** 923–931.

Kelly, M. E., M. A. Bisby, and K. Lukowiak. 1988. Regeneration restores some of the altered electrical properties of axotomized bullfrog B-cells. *J. Neurobiol.* **19:** 357–372.

Klein, M., J. Camardo, and E. R. Kandel. 1982. Serotonin modulates a specific potassium current in the sensory neurons that show presynaptic facilitation in *Aplysia*. *Proc. Nat. Acad. Sci. USA* **79:** 5713–5717.

Klein, M., B. Hochner, and E. R. Kandel. 1986. Facilitatory transmitters and cAMP can modulate accomodation as well as transmitter release in *Aplysia* sensory neurons: evidence for parallel processing in a single cell. *Proc. Nat. Acad. Sci. USA* **83:** 7994–7998.

Krontiris-Litowitz, J. K., B. F. Cooper, and E. T. Walters. 1989. Humoral factors released during trauma of *Aplysia*. I. Body wall contraction, cardiac modulation, and central reflex suppression. *J. Comp. Physiol. B* **159:** 211–223.

Krontiris-Litowitz, J. K., M. T. Erickson, and E. T. Walters. 1987. Central suppression of defensive reflexes in *Aplysia* by noxious stimulation and by factors released from body wall. *Soc. Neurosci. Abstr.* **13:** 815.

Kupfermann, I., V. Castellucci, H. Pinsker, and E. R. Kandel. 1970. Neuronal correlates of habituation and dishabituation of the gill-withdrawal reflex in *Aplysia*. *Science* **167:** 1743–1745.

Mackey, S. L., D. L. Glanzman, S. A. Small, A. M. Dyke, E. R. Kandel, and R. D. Hawkins. 1987. Tail shock produces inhibition as well as sensitization of the siphon-withdrawal reflex of *Aplysia*: possible behavioral role for presynaptic inhibition mediated by the peptide Phe-Met-Arg-Phe-NH_2. *Proc. Nat. Acad. Sci. USA* **84:** 8730–8734.

Marcus, E. A., T. G. Nolen, C. H. Rankin, and T. J. Carew. 1988. Behavioral dissociation of dishabituation, sensitization, and inhibition in *Aplysia*. *Science* **241:** 210–212.

Nazif, F., J. H. Byrne, and L. J. Cleary. 1989. Intracellular injection of cAMP produces a long-term (24 hr) increase in the number of varicosities in pleural sensory neurons of *Aplysia*. *Soc. Neurosci. Abstr* **15:** 1283.

Nicholls, J. G., and D. A. Baylor. 1968. Specific modalities and receptive fields of sensory neurons in the CNS of the leech. *J. Neurophysiol* **31:** 740–756.

Pinsker, H. M., W. A. Hening, T. J. Carew, and E. R. Kandel. 1973. Long-term sensitization of a defensive withdrawal reflex in *Aplysia*. *Science* **182:** 1039–1042.

Scholz, K. P., and J. H. Byrne. 1987. Long-term sensitization in *Aplysia*: biophysical correlates in tail sensory neurons. *Science* **235:** 685–687.

Sherrington, S. C. 1906. *The Integrative Action of the Nervous System* 2nd Ed. 1947, University Press, Cambridge, U. K. 433 pp.

Small, S. A., E. R. Kandel, and R. D. Hawkins. 1989. Activity-dependent enhancement of presynaptic inhibition in *Aplysia* sensory neurons. *Science* **243:** 1603–1606.

Vermeij, G. J. 1987. *Evolution and Escalation: An Ecological History of Life*. Princeton University Press, New Jersey.

Wall, P. D., 1979. On the relation of injury to pain. *Pain* **6:** 253–264.

Walsh, J. P., and J. H. Byrne. 1989. Modulation of a steady-state Ca^{2+}-activated, K^+ current in tail sensory neurons of *Aplysia*: role of 5-HT and cAMP. *J. Neurophysiol.* **61:** 32–44.

Walters, E. T. 1987a. Site-specific sensitization of defensive reflexes in *Aplysia*: a simple model of long-term hyperalgesia. *J. Neurosci.* **7:** 400–407.

Walters, E. T. 1987b. Multiple sensory neuronal correlates of site-specific sensitization in *Aplysia*. *J. Neurosci* **7:** 408–417.

Walters, E. T. 1989. Transformation of siphon responses during conditioning of *Aplysia* suggests a model of primitive stimulus-response association. *Proc. Nat. Acad. Sci. USA* **86:** 7616–7619.

Walters, E. T., and J. H. Byrne. 1983a. Associative conditioning of single sensory neurons suggests a cellular mechanism for learning. *Science* **219:** 405–408.

Walters, E. T., and J. H. Byrne. 1983b. Slow depolarization produced by associative conditioning of *Aplysia* sensory neurons may enhance Ca^{2+} entry. *Brain Res.* **280:** 165–168.

Walters, E. T., and J. H. Byrne. 1984. Post-tetanic potentiation in *Aplysia* sensory neurons. *Brain Res* **293:** 377–380.

Walters, E. T., J. H. Byrne, T. J. Carew, and E. R. Kandel. 1983a. Mechanoafferent neurons innervating tail of *Aplysia*. I. Response properties and synaptic connections. *J. Neurophysiol* **50:** 1522–1542.

Walters, E. T., J. H. Byrne, T. J. Carew, and E. R. Kandel. 1983b. Mechanoafferent neurons innervating tail of *Aplysia*. II. Modulation by sensitizing stimulation. *J. Neurophysiol.* **50:** 1543–1559.

Walters, E. T., T. J. Carew, and E. R. Kandel. 1981. Associative learning in *Aplysia*: evidence for conditioned fear in an invertebrate. *Science* **211:** 504–506.

Walters, E. T., and M. T. Erickson. 1986. Directional control and the functional organization of defensive responses in *Aplysia*. *J. Comp. Physiol. A* **159:** 339–351.

Woolf, C. J., and E. T. Walters. 1991. Common patterns of plasticity contributing to nociceptive sensitization in mammals and *Aplysia*. *Trends In Neurosci.* **14:** 74–78.

Wright, W. G., E. A. Marcus, and T. J. Carew. 1989. Dissociation of monosynaptic and polysynaptic contributions to dishabituation, sensitization and inhibition in *Aplysia*. *Soc. Neurosci. Abstr.* **15:** 1265.

Reference: *Biol Bull* **180**: 252–261. (April, 1991)

Neural Mechanisms Underlying Sensitization of a Defensive Reflex in *Aplysia*

L. J. CLEARY, D. A. BAXTER, F. NAZIF, AND J. H. BYRNE

Department of Neurobiology and Anatomy, University of Texas Medical School, P. O. Box 20708, Houston, Texas 77225

Introduction

One of the last frontiers in modern biology is understanding the neural basis of behavior and its modification by processes such as learning. While the ultimate goal for many is to understand human behavior, other model systems are more commonly used in the laboratory with the expectation that general principles of neuronal function will be conserved across phyla. Mollusks in particular have proven to be valuable model systems because of their relatively simple and accessible nervous systems. *Aplysia californica* is a gastropod mollusk with a simple behavioral repertoire and a relatively simple nervous system (see Kandel, 1979). Nevertheless, a detailed understanding of more complex phenomena, such as the modification of behaviors by learning (Kandel and Schwartz, 1982) and arousal (Weiss *et al.*, 1982) has also emerged from study of this animal. One class of behaviors that has been studied extensively in *Aplysia* is that of defensive withdrawal reflexes. We have focused on the tail-siphon withdrawal reflex, which is elicited by mechanical stimulation of the tail. The features of this reflex are similar to those of the siphon-gill withdrawal reflex, which is elicited by stimulation of the siphon. Moreover, both of these reflexes, or their *in vitro* analogues, can be modulated in several ways, including habituation, sensitization, and classical conditioning (Pinsker *et al.*, 1970; Carew *et al.*, 1983; Walters and Byrne, 1983; Walters *et al.*, 1983b). In this paper, the focus will be on sensitization of the tail-siphon withdrawal reflex.

Tail-Siphon Withdrawal Reflex

Weak mechanical stimulation of the tail elicits a coordinated contraction of the tail, siphon, and also the gill (Fig. 1; Walters *et al.*, 1983a; Walters and Erickson, 1986). A more intense stimulus may also elicit the release of ink from glands in the mantle cavity. Weak electrical stimulation through implanted electrodes elicits contraction of the tail and siphon (Fig. 2). The strength of the reflex response is estimated by measuring the duration of siphon withdrawal. When weak test stimuli are delivered at 5 min intervals, the strength of the response is fairly constant at approximately 7 s. After delivery of a strong stimulus through a hand-held electrode over the tail and lateral body wall, the strength of the response to subsequent weak stimuli is enhanced significantly. This enhancement is called sensitization. In general, the time course of sensitization depends on the training protocol and can last for a relatively short time, such as 15 minutes to an hour (Pinsker *et al.*, 1970), or for a relatively long time, greater than 24 hours (Pinsker *et al.*, 1973; Frost *et al.*, 1985; Scholz and Byrne, 1987).

Neural Circuit for Tail-Siphon Withdrawal

To approach this phenomenon at the cellular level, the neurons that mediate the behavior must be identified (Fig. 3). Sensory neurons innervating the tail (TSN) are located in the pleural ganglion. The main axon from these neurons projects to the pedal ganglion, but there are numerous fine branches within the pleural ganglion as well. The tail component of the withdrawal response is mediated by a monosynaptic circuit. Tail motor neurons (TMN) are located in the pedal ganglion (Walters *et al.*, 1983a). The monosynaptic circuit is sufficiently strong to elicit tail withdrawal (Walters *et al.*, 1983a), but other neurons also contribute. For example, interneurons (IN) in the pleural ganglion receive excitatory input from sensory neurons and, in turn, project to the pedal ganglion where they

Received 18 October 1990; accepted 24 January 1991.

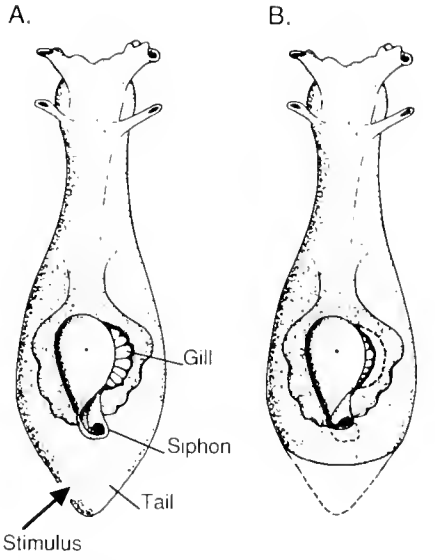

Figure 1. Dorsal view of *Aplysia* illustrating the tail-siphon withdrawal reflex. (A) Relaxed. (B) Stimulation of the tail elicits a coordinated set of defensive responses including reflex withdrawal of the tail, siphon, and gill.

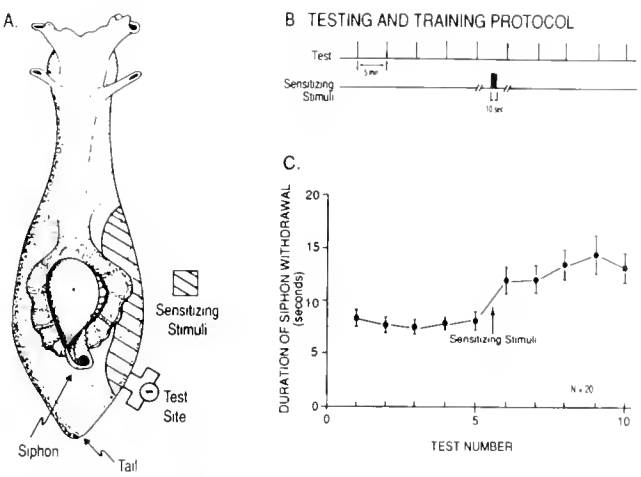

Figure 2. Sensitization of the tail-siphon withdrawal reflex. (A) Sites for delivering test and sensitizing stimuli. (B) Testing and training protocol. (C) Behavioral results. A single brief train (10 s) of sensitizing stimuli leads to an enhancement of siphon withdrawal elicited by stimuli to the tail. (From McClendon, Goldsmith and Byrne, in prep.)

excite motor neurons, forming a second, parallel pathway for tail withdrawal (Cleary and Byrne, 1985). The siphon withdrawal component of the reflex is mediated by a polysynaptic pathway. The population of interneurons in the pleural ganglion that receives input from tail sensory neurons also projects to the abdominal and cerebral ganglia. The siphon component of the response is mediated by motor neurons (SMN) in the abdominal ganglion (Perlman, 1979; Frost *et al.*, 1988). Motor neurons for other mantle organs such as the gill and the ink gland are located in this ganglion as well (Kupfermann *et al.*, 1974; Carew and Kandel, 1977). When stimulated, the pleural interneurons excite siphon (LSF), gill (LD_{G2}), and ink (L14) motor neurons. In addition, they may also trigger a burst in the L25 neurons. L25 is a group of pattern-generating neurons that appears to control respiratory pumping, a behavior that also involves contraction of the gill and siphon (Byrne, 1983; Koester, 1989). L25 neurons have extensive connections throughout the abdominal ganglion. Therefore, interneurons in the pleural ganglion appear to integrate sensory input from tail stimulation and coordinate the total behavioral response.

One characteristic of the connection between pleural interneurons and tail motor neurons is a biphasic excitation of the tail motor neurons. While a single spike frequently produces a fast excitatory postsynaptic potential (EPSP), a short burst in the interneuron produces a long-lasting excitation that appears to have two components (Fig. 4). The first component is the fast EPSP and lasts for the duration of the interneuron burst, whereas the second component is a slow EPSP that can last over one minute. This slow EPSP is sufficient in some preparations to prolong the burst elicited by the first component. In addition, the slow EPSP increases the effectiveness of synaptic input produced by subsequent stimulation of peripheral nerves. Thus, this population of pleural interneurons plays a modulatory role by using a conventional postsynaptic mechanism, temporal summation of excitatory synaptic inputs.

Delivery of a sensitizing stimulus activates conventional interneurons, but, in addition, a separate modulatory circuit must be recruited. This circuit has not been identified

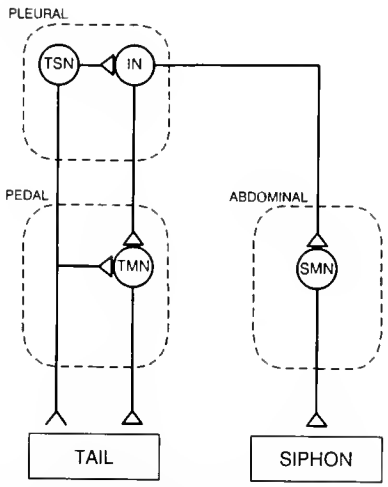

Figure 3. Simplified schematic diagram of the neural circuit controlling the tail-siphon withdrawal reflex.

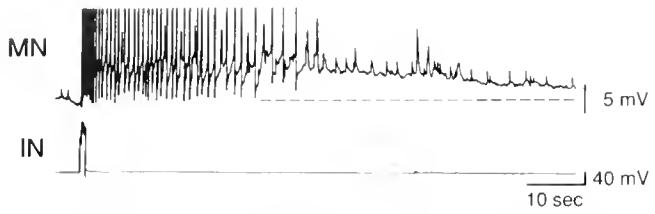

Figure 4. Simultaneous intracellular recordings from isolated pleural-pedal ganglia. A brief (1 s) depolarization of a pleural interneuron (IN) elicits a long-lasting depolarization in a tail motor neuron (MN) in the pedal ganglion. The slow EPSP was of sufficient amplitude to prolong the high-frequency burst of action potentials produced directly by the interneuron. (From Cleary and Byrne, in prep.)

for the tail-siphon withdrawal reflex. The pleural interneurons, however, provide a link to interneurons in the abdominal ganglion that modulate the neural circuit mediating the gill-siphon withdrawal reflex. The strength of the synapse between siphon sensory and motor neurons is enhanced by the activation of at least three cells in the abdominal ganglion: L22, L28, and L29 (Hawkins *et al.*, 1981). One of these, L29, is excited by pleural interneurons (Cleary and Byrne, 1986). Moreover, the pleural interneuron to L29 connections are reciprocal. Thus, a positive feedback loop exists that could prolong and enhance the effects of a sensitizing tail stimulus.

Serotonin as a Facilitatory Transmitter

Modification of the tail-siphon withdrawal reflex by sensitization is due to changes in the properties of neurons that mediate the reflex. The tail sensory neurons in particular have been characterized as a site of plasticity (Walters *et al.*, 1983b; Scholz and Byrne, 1987). Sensitizing stimuli increase synaptic efficacy and alter membrane properties of the sensory neurons, such as resting membrane potential, excitability, and action potential kinetics (Walters *et al.*, 1983b). These changes are similar to those occurring in siphon sensory neurons as a result of sensitization (Castellucci and Kandel, 1976; Kandel and Schwartz, 1982).

Interneurons whose activity modifies the properties of the tail-siphon withdrawal circuit have not been identified. Several lines of evidence indicate that serotonin is one of the modulatory transmitters released by sensitizing stimuli. Serotonin mimics many of the short- and long-term effects of sensitization. Serotonin is necessary for sensitization to occur. In addition, serotonergic circuitry is available in the nervous system to mediate sensitization.

Serotonin mimics several of the biochemical and electrophysiological correlates of sensitization. In a semi-intact preparation, the selective application of serotonin to the pleural-pedal ganglia increases the intensity of the tail withdrawal reflex, just as the application of a sensitizing stimulus to the tail does (Walters *et al.*, 1983b). At the cellular level, serotonin enhances the size of the monosynaptic EPSP elicited in a follower motor neuron by the sensory neuron. A slow depolarization is produced in the sensory neuron, and this depolarization is associated with an increase in membrane input resistance (Ocorr and Byrne, 1985). Membrane excitability is increased as well (Baxter and Byrne, 1990). Finally, serotonin increases the amplitude and duration of the sensory neuron action potential (Baxter and Byrne, 1990).

The mechanism by which serotonin exerts these physiological effects appears to be due to its ability to mimic at least one of the biochemical correlates of sensitization. Using a symmetrical experimental design, the level of cAMP is higher in the cell bodies of tail sensory neurons that innervate the body wall exposed to sensitizing stimuli than in cell bodies of sensory neurons innervating the contralateral unstimulated side (Ocorr *et al.*, 1986). Similarly, application of serotonin to isolated clusters of sensory neurons increases the cAMP content compared to contralateral controls (Ocorr and Byrne, 1985; Pollock *et al.*, 1985; Sweatt *et al.*, 1989). The dose-response relationship indicates that the half-maximal concentration of serotonin is about 15 μM.

To test the hypothesis that serotonin acts by activating adenylyl cyclase, the effects of serotonin on two membrane properties, excitability and action potential duration, were examined and compared with the effects of an analogue of cAMP (Baxter and Byrne, 1990). Neuronal excitability was measured as the number of action potentials elicited by injecting constant depolarizing current pulses of 1 s duration and of increasing magnitude. For example, in artificial seawater, a test pulse of 2 nA elicited an average of three action potentials. Application of serotonin increased the average number of spikes during the depolarizing pulse by a factor of 1.8. Application of a membrane-permeable, phosphodiesterase-resistant analogue of cAMP (8-4-parachlorophenylthio-cAMP, 8-pcpt-cAMP) increased the excitability of the sensory neuron and doubled the number of action potentials elicited by an identical current pulse (Fig. 5A). Addition of serotonin to the bath, which still contained the cAMP analogue, failed to produce a further increase in excitability. Thus, cAMP has potent effects on excitability, and these cAMP-mediated effects are sufficient to fully account for the effects of serotonin on neuronal excitability.

The effects of 8-pcpt-cAMP on action potential duration did not parallel the effects of serotonin, however. Action potential duration was measured as the time between the peak of the action potential and its repolarization to the resting membrane potential. Application of the analogue of cAMP increased the duration of the action

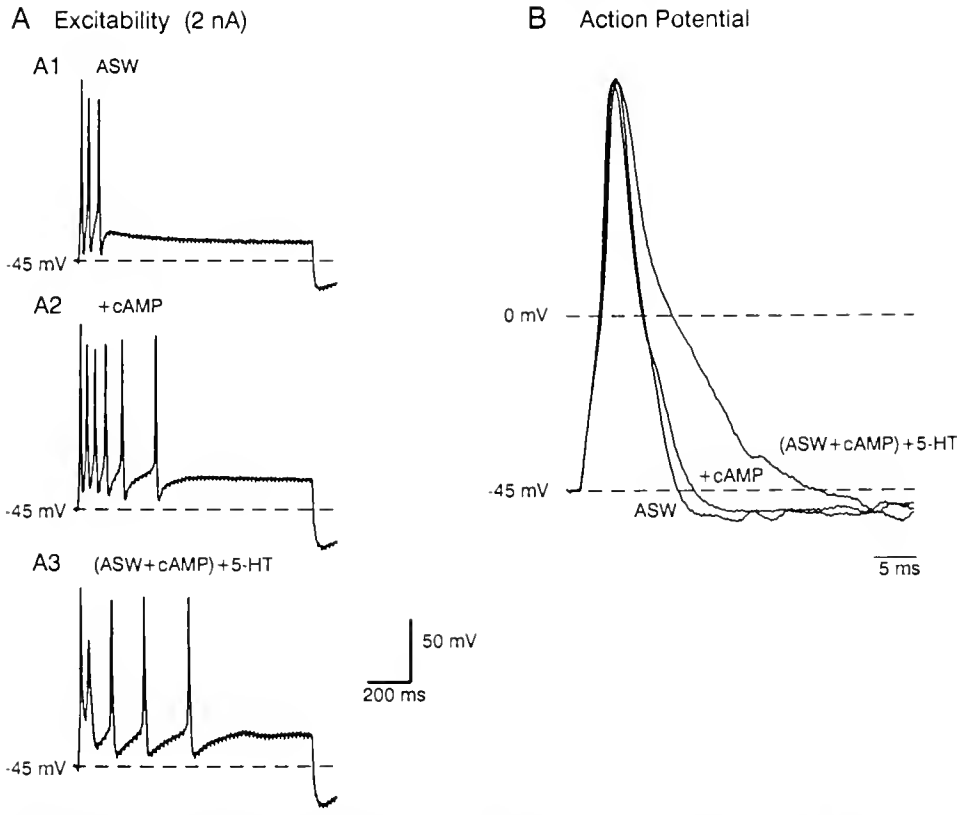

Figure 5. Differential effects of an analogue of cAMP and 5-HT on the duration of the action potential and excitability in tail sensory neurons. Recordings were made from somata that had been isolated surgically from the pleural ganglion. (A) A 1 s, 2 nA depolarizing current pulse elicited three action potentials in artifical seawater (A1). An identical current pulse elicited twice as many action potentials after bath application of 8-pcpt-cAMP (A2). The subsequent addition of serotonin to the bath, which still contained 8-pcpt-cAMP, did not increase further the number of spikes during the pulse (A3). (B) In the same sensory neuron, bath application of 8-pcpt-cAMP (50 μM) increased the duration of the somatic action potential by a modest amount. The subsequent addition of serotonin (50 μM) to the bath, which still contained 8-pcpt-cAMP, dramatically increased the duration of the action potential. (From Baxter and Byrne, 1990).

potential by an average of 17% (Fig. 5B). The subsequent addition of serotonin to the bath, which still contained the cAMP analogue, further increased the duration of the action potential by an additional 230%, on average. Thus, cAMP has modest effects on spike broadening that are not sufficient to occlude the effects of serotonin.

The differential effects of serotonin and cAMP can be accounted for by the actions of these compounds on specific membrane currents. Use of voltage-clamp and computer-subtraction techniques has shown that cAMP reduces a potassium current, the S-current, that is activated at relatively negative membrane potentials, does not inactivate and is relatively insensitive to block by TEA (Klein *et al.*, 1982; Pollock *et al.*, 1985; Shuster and Siegelbaum, 1987; Baxter and Byrne, 1989; Walsh and Byrne, 1989). cAMP activates a protein kinase that phosphorylates the S-channel or a protein associated with it (Siegelbaum *et al.*, 1982; Shuster *et al.*, 1985). This phosphorylation results in an all-or-nothing closure of the S-channel and thus a suppression of the macroscopic S-current. The kinetics of the outward currents reduced by cAMP are qualitatively similar at all levels of depolarization. At low levels of depolarization (*i.e.*, −20 mV or below), the subsequent addition of serotonin to the bath, which still contained the cAMP analogue, did not produce any further reduction in membrane current (Fig. 6A). Thus these results and others indicate that the suppression of the S-current by 5-HT is mediated by cAMP.

In addition, serotonin appears to modulate a second current in tail sensory neurons that is not affected by cAMP and is activated only at depolarized levels (Baxter and Byrne, 1989, 1990). The addition of cAMP changes the currents produced by voltage-clamp steps to +20 mV by decreasing the outward current at the end of the pulse (Fig. 6B). Subsequent addition of serotonin to the bath results in a reduction in outward current at the beginning of the pulse and

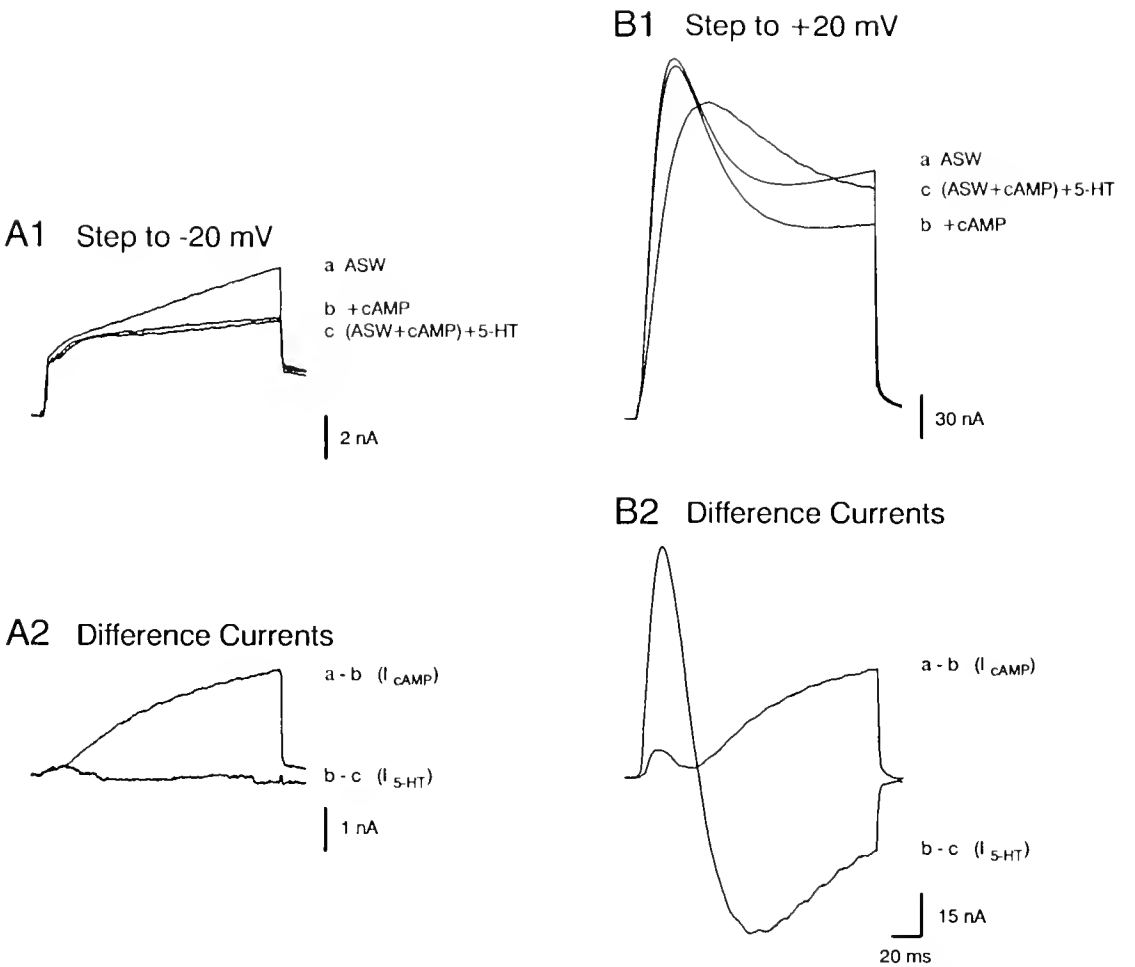

Figure 6. Differential effects of an analogue of cAMP and serotonin on membrane current in tail sensory neurons. In all panels, the label for an individual trace is aligned with the current level at the end of the voltage-clamp pulse. (A1) Current responses were elicited by voltage-clamp pulses from −70 to −20 mV in artificial seawater (*trace a*), after application of 8-pcpt-cAMP (50 μM) (*trace b*), and after addition of serotonin (50 μM) to the bath, which still contained the analogue (*trace c*). Note that the membrane currents do not return to the preclamp level because the cell was clamped from a holding potential of −70 to −20 mV and then back to −50 mV. (A2) The cAMP difference current (I_{cAMP}) was isolated by subtracting *trace b* from *trace a*. The cAMP-independent component of the serotonin difference current ($I_{5\text{-}HT}$) was isolated by subtracting *trace c* from *trace b*. (B1) Current responses from the same cell were elicited by voltage-clamp pulses from −70 to +20 mV in artificial seawater (*trace a*), after bath application of 8-pcpt-cAMP (*trace b*) and after adding serotonin to the bath, which still contained the analogue (*trace c*). (B2) The cAMP difference current (I_{cAMP}) was isolated by subtracting *trace b* from *trace a*. The cAMP-independent component of the serotonin difference current ($I_{5\text{-}HT}$) was isolated by subtracting *trace c* from *trace b*. The qualitative features of the cAMP difference currents (I_{cAMP}) that were isolated from voltage-clamp pulses to −20 mV (A2) and +20 mv (B2) were similar (note the change in scale). In contrast, the qualitative features of the cAMP-independent component of the serotonin difference current ($I_{5\text{-}HT}$) were very different at the two potentials. At −20 mV, the presence of 8-pcpt-cAMP completely occluded further modulation of membrane current by serotonin (A2). At +20 mV, however, serotonin modulated an additional component of membrane current (B2). This additional component probably represents modulation of the kinetics of the delayed potassium current. (From Baxter and Byrne, 1990).

an increase in outward current at the end of the pulse. The voltage-dependence and sensitivity to potassium channel blockers of the cAMP-independent effects of serotonin suggest that the current affected by serotonin under these conditions is the delayed potassium current. The effects of serotonin appear to be produced by a mechanism in which the kinetics of activation and inactivation are slowed, rather than one in which the conductance of channels is blocked.

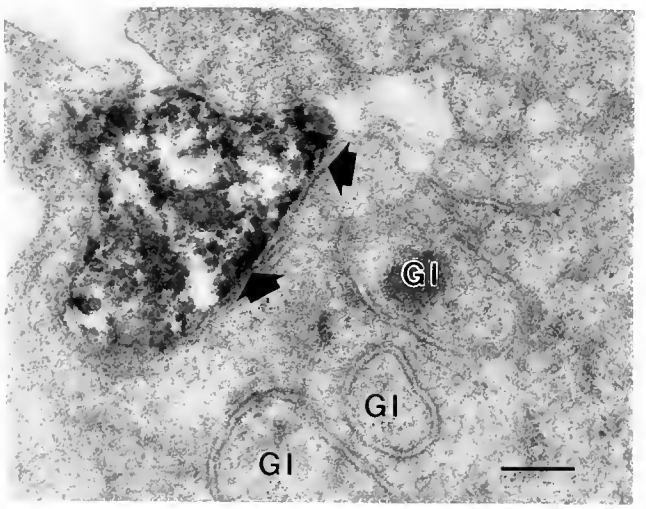

Figure 7. Electron micrograph through the cell body of a pleural sensory neuron illustrating a direct contact between a serotonergic process and the plasma membrane of the sensory neuron. The straight pre- and postsynaptic membrane (arrowheads) and the widened synaptic cleft suggest that this section is through an active zone, a possible site of transmitter release. Numerous glial processes (GI) invaginate the sensory neuron membrane. Pleural ganglia were fixed and incubated in primary antisera to serotonin (Incstar, Inc.) for 1 week. Distribution of the antibody was revealed by an avidin-peroxidase technique (Vectastain ABC, Vector, Inc.). The tissue was then osmicated, embedded in plastic, and cut into thin (100 nm) sections. The scale bar represents 250 nm. (From Zhang, Cleary, Marshak and Byrne, in prep.)

Thus, the differential effects of serotonin and cAMP suggest that the cAMP-mediated modulation of the membrane current is primarily responsible for the effects of serotonin on neuronal excitability. cAMP-independent modulation of the delayed potassium current appears to be primarily responsible for the effects of serotonin on action potential duration. The mechanism underlying this component of the serotonin response is not yet known. Other second messenger pathways may be involved, however. For example, protein kinase C appears to contribute to presynaptic facilitation of the siphon sensory-motor synapse after it has been depressed (Hochner *et al.*, 1986; Braha *et al.*, 1990; Sacktor and Schwartz, 1990).

For sensitization to occur, intact serotonergic neurons must be present in the nervous system. When serotonin is selectively depleted from the nervous system by injection of 5,7-dihydroxytryptamine (5,7-DHT), the effects of subsequent sensitizing stimuli on the siphon-gill withdrawal reflex are blocked (Glanzman *et al.*, 1989). While the average amplitude of the EPSP evoked in a follower neuron by the sensory neuron is not affected by 5,7-DHT treatment, facilitation of PSPs by sensitizing stimuli is drastically reduced. These experiments do not reveal, however, whether the endogenous serotonin acts directly or indirectly on the sensory neurons.

Evidence supporting a direct action of serotonin in the tail-siphon withdrawal reflex comes from the observation that serotonergic fibers are in close proximity to pleural sensory neurons (Lo *et al.*, 1987; Zhang *et al.*, 1988). Although there are no serotonergic neurons in the pleural ganglion itself (Tritt *et al.*, 1983; Ono and McCaman, 1984; Longley and Longley, 1986), there are many serotonin-containing axons within the neuropil that originate from neurons in other ganglia. Some of these serotonergic axons send fine processes up to surround the cell bodies of the pleural sensory neurons. Subsequent examination using electron microscopic immunocytochemistry has shown that these serotonergic axons contain varicosities that are in direct contact with the plasma membrane of sensory neurons (Fig. 7). Moreover, serotonergic contacts may occur on either the cell body or the axon hillock. We have not yet performed double-labeling experiments to examine the distribution of serotonergic contacts along the axons and processes of sensory neurons in the neuropil of the pleural and pedal ganglia.

Although neurons that give rise to serotonergic processes in the pleural ganglion have not been identified, there are several candidates. Most promising among these are the serotonergic cells in the cerebral B cluster (Mackey *et al.*, 1989; Cleary and Byrne, unpub.). These cells appear to send axons that project through the cerebral-pleural connective into the pleural ganglion and continue to the abdominal ganglion through the pleural-abdominal connective. Stimulation of the serotonergic B cell produces both spike broadening in siphon sensory cells in the abdominal ganglion and facilitation of the PSP between siphon sensory and follower motor neurons.

We have focused on the role of serotonin, but other modulatory transmitters may also be involved. For example, the peptide SCP_b mimics many of the effects of serotonin, although it binds to a different receptor (Abrams *et al.*, 1984; Ocorr *et al.*, 1986). Moreover, some identified neurons that produce facilitation of the synapse between siphon sensory and motor neurons do not contain serotonin (Kistler *et al.*, 1985; Hawkins and Schacher, 1989). Future research will be necessary to elaborate the roles of other transmitters in sensitization.

Role of the Cell Body in Modulation

Activation of interneurons that provide serotonergic input to the cell bodies of tail sensory neurons may have multiple modulatory effects. For example, changes in somatic membrane potential would propagate passively to proximal axon branches within the pleural ganglion. In addition, elevation of cAMP levels in cell bodies may be sufficient to elevate cAMP in proximal axonal branches, producing local changes in membrane properties that

could contribute to enhanced release of transmitter as observed in siphon sensory neurons (Brunelli *et al.*, 1976; Castellucci *et al.*, 1982). Because of the limits imposed by diffusion, however, somatic alterations may not be sufficient to account for the effects of sensitizing stimuli at distal sites of transmitter release. Enhancement by serotonin of synaptic transmission at the sensory to tail motor neuron synapse in the pedal ganglion does not require an intact connection between the axon of the sensory neuron in the pedal ganglion and the cell body in the pleural ganglion (Hammer *et al.*, 1989). Similarly, application of serotonin to a peripheral synapse in the siphon selectively enhances transmission from that synapse (Clark and Kandel, 1984). Therefore, facilitation at sites distant from the cell body is probably due to the local action of the modulatory transmitter.

That the cell body is functionally independent from some regions of the neuron suggests that serotonergic input to the cell body is specialized to activate mechanisms that are localized there. Mechanisms that might be regulated by somatic serotonin receptors include mRNA synthesis, which is restricted to the nucleus, and protein synthesis, which is restricted to the somatic cytoplasm. These mechanisms are of particular interest because of their role in long-term forms of facilitation and sensitization (Montarolo *et al.*, 1986; Castellucci *et al.*, 1989).

Some features of long-term sensitization are similar to those of short-term; the major difference is in the duration of the behavioral change. To alter the time course from 1 to 24 h or more, however, a longer training period is required (Pinsker *et al.*, 1973; Frost *et al.*, 1985; Scholz and Byrne, 1987). Nevertheless, the cellular correlates of long-term sensitization are nearly identical to those of short-term. The amplitude of EPSPs at synapses between siphon sensory and motor neurons is enhanced (Frost *et al.*, 1985), and membrane properties of tail sensory neurons are altered (Scholz and Byrne, 1987). The similarities between short- and long-term modifications of sensory neurons suggest that correlates of long-term sensitization are due to the action of a common mediator. Several lines of evidence suggest that cAMP can by itself produce long-term changes in the properties of sensory neurons. Transient elevation of the intracellular level of cAMP leads to altered membrane currents (Scholz and Byrne, 1988) and enhanced synaptic transmission (Schacher *et al.*, 1988) that each persist for at least 24 h.

An additional cellular correlate of long-term sensitization in siphon sensory neurons is a change in the morphology of sensory neuron axons and synapses (Bailey and Chen, 1983; Bailey and Chen, 1988). To examine its role in producing these changes, cAMP was injected iontophoretically, over a period of 15 min, into the cell bodies of tail sensory neurons. These neurons were subsequently

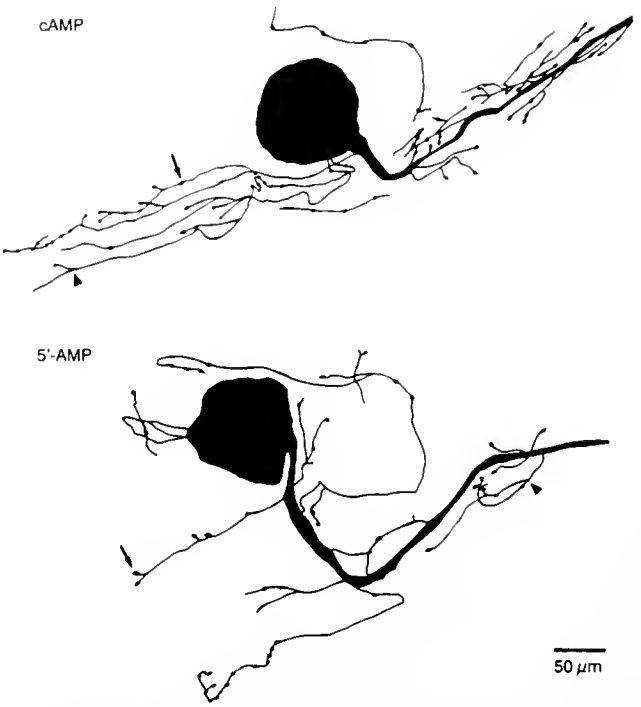

Figure 8. *Camera lucida* drawings of two HRP-filled sensory neurons from the same animal. The cell in the top panel was injected with cAMP approximately 24 h before fixation; the cell in the lower panel was injected with 5′-AMP. In each cell, a single large axon extends from the cell body to the pleural-pedal connective. Because we analyzed only their number, varicosities (arrows) were drawn slightly larger than scale to enhance visibility. Varicosities counted in the cAMP-filled cell were 78 and in the 5′-AMP-filled cell 46. Branch points (arrowheads) counted in the cAMP-filled cell were 32 and in the 5′-AMP-filled cell 24. Not all the branch crossings in these drawings are branch points since these are three-dimensional objects drawn in two dimensions. Some branches appear disconnected as a consequence of the tissue processing procedure. (From Nazif *et al.*, 1991.)

labeled with HRP and fixed 24 h after cAMP injection (Fig. 8). Close analysis of the structure of these neurons revealed that both the number of varicosities was doubled and the number of branch points was increased by 50% compared to neurons that had been injected with 5′-AMP, the inactive metabolite of cAMP. The significance of these morphological changes lies in the hypothesis that sensory neurons make more synapses with follower neurons in the pleural ganglion as a result of sensitization. This implies that connections between sensory neurons and their followers are strengthened. Additional followers might also be recruited by the formation of new connections. Changes in both of these morphological features could contribute to the enhanced strength of the reflex. In future experiments, it will be interesting to test the role of cAMP in producing other morphological changes such as increases in the number, size, and vesicle complement of synaptic active zones (Bailey and Chen, 1983).

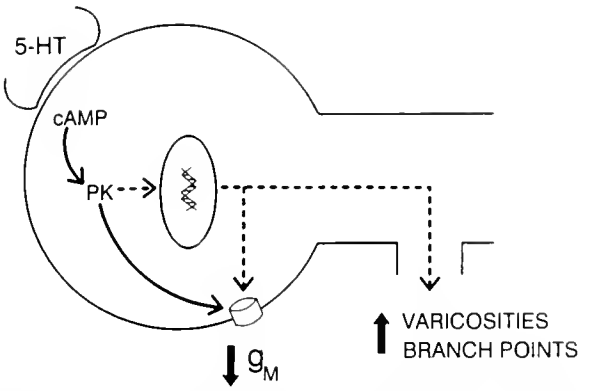

Figure 9. Simplified diagram illustrating the activation of parallel cAMP-dependent pathways by neurites that release serotonin (5-HT) onto the cell bodies of sensory neurons. Transient elevation of cAMP in the soma produces rapid but short-lasting effects on membrane conductance (*solid lines*) via activation of protein kinase (PK). In addition, it produces persistent effects on membrane conductance and neuronal structure (*dashed lines*). The mechanism underlying these long-term effects is not known, but regulation of gene expression and protein synthesis appears to be involved.

Because cAMP in sensory neurons is broken down rapidly (Bernier *et al.*, 1982; Schwartz *et al.*, 1983), long-term changes must depend on a more persistent cellular process. A likely model, then, is one in which the transient cAMP signal activates at least two pathways (Fig. 9). cAMP produces a rapid but short-lasting modulation of membrane currents, decreasing membrane conductance. In addition, a slower but more enduring mechanism is also activated, producing long-term changes in membrane conductance and cell structure. The mechanisms underlying these long-term alterations are not known, but regulatory pathways that alter protein synthesis or gene expression are presumably involved. Indeed, long-term enhancement of synaptic transmission and membrane excitability are affected by inhibitors of protein and RNA synthesis (Montarolo *et al.*, 1986; Dale *et al.*, 1987; Schacher *et al.*, 1988). In addition, serotonin appears to activate regulatory proteins that bind to DNA (Dash *et al.*, 1990). As a consequence, messenger RNA is synthesized (Zwartjes *et al.*, 1990), and the incorporation of amino acids into proteins of sensory neurons is altered (Barzilai *et al.*, 1989; Eskin *et al.*, 1989). Other mechanisms, such as post-translational modification of proteins (Greenberg *et al.*, 1987), may be used as a result of sensitization, providing an intermediate time course.

Acknowledgments

Supported by Texas Higher Education Co-ordination Board Grant 1945 (L.J.C.), National Research Service Award F31 MH09956 (F.A.N.), NIMH Award KO2 MH00649 (J.H.B.), and NIH Grant RO1 NS19895 (J.H.B.).

Literature Cited

Abrams, T. W., V. F. Castellucci, J. S. Camardo, E. R. Kandel, and P. E. Lloyd. 1984. Two endogenous neuropeptides modulate the gill and siphon withdrawal reflex in *Aplysia* by presynaptic facilitation involving cAMP-dependent closure of a serotonin-sensitive potassium channel. *Proc. Natl. Acad. Sci. USA* **81:** 7956–7960.

Bailey, C. H., and M. Chen. 1983. Morphological basis of long-term habituation and sensitization in *Aplysia*. *Science* **220:** 91–93.

Bailey, C. H., and M. Chen. 1988. Long-term memory in *Aplysia* modulates the total number of varicosities of single identified sensory neurons. *Proc. Natl. Acad. Sci. USA* **85:** 2373–2377.

Barzilai, A., T. E. Kennedy, J. D. Sweatt, and E. R. Kandel. 1989. 5-HT modulates protein synthesis and the expression of specific proteins during long-term facilitation in *Aplysia* sensory neurons. *Neuron* **2:** 1577–1586.

Baxter, D. A., and J. H. Byrne. 1989. Serotonergic modulation of two potassium currents in the pleural sensory neurons of *Aplysia*. *J. Neurophysiol.* **62:** 665–679.

Baxter, D. A., and J. H. Byrne. 1990. Differential effects of cAMP and serotonin on membrane current, action potential duration, and excitability in somata of pleural sensory neurons of *Aplysia*. *J. Neurophysiol.* **64:** 978–990.

Bernier, L., V. F. Castellucci, E. R. Kandel, and J. H. Schwartz. 1982. Facilitatory transmitter causes a selective and prolonged increase in adenosine 3′:5′-monophosphate in sensory neurons mediating the gill and siphon withdrawal reflex in *Aplysia*. *J. Neurosci.* **2:** 1682–1691.

Braha, O., N. Dale, B. Hochner, M. Klein, T. W. Abrams, and E. R. Kandel. 1990. Second messengers involved in two processes of presynaptic facilitation that contribute to sensitization and dishabituation in *Aplysia* sensory neurons. *Proc. Nat. Acad. Sci. USA* **87:** 2040–2044.

Brunelli, M., V. F. Castellucci, and E. R. Kandel. 1976. Synaptic facilitation and behavioral sensitization in *Aplysia*: possible role for serotonin and cAMP. *Science* **194:** 1178–1181.

Byrne, J. H. 1983. Identification and initial characterization of a cluster of command and pattern-generating neurons underlying respiratory pumping in *Aplysia californica*. *J. Neurophysiol.* **49:** 491–508.

Carew, T. J., R. D. Hawkins, and E. R. Kandel. 1983. Differential classical conditioning of a defensive withdrawal reflex in *Aplysia californica*. *Science* **219:** 397–400.

Carew, T. J., and E. R. Kandel. 1977. Inking in *Aplysia californica*: neural circuit of an all-or-none behavioral response. *J. Neurophysiol.* **40:** 692–707.

Castellucci, V. F., H. Blumenfeld, P. Goelet, and E. R. Kandel. 1989. Inhibitor of protein synthesis blocks long-term behavioral sensitization in isolated gill-withdrawal reflex of *Aplysia*. *J. Neurobiol.* **20:** 1–9.

Castellucci, V. F., and E. R. Kandel. 1976. Presynaptic facilitation as a mechanism for behavioral sensitization in *Aplysia*. *Science* **194:** 1176–1178.

Castellucci, V. F., A. Nairn, P. Greengard, J. H. Schwartz, and E. R. Kandel. 1982. Inhibitor of adenosine 3′:5′-monophosphate-dependent protein kinase blocks presynaptic facilitation in *Aplysia*. *J. Neurosci.* **2:** 1673–1681.

Clark, G. A., and E. R. Kandel. 1984. Branch-specific heterosynaptic facilitation in *Aplysia* siphon sensory cells. *Proc. Nat. Acad. Sci. USA* **81:** 2577–2581.

Cleary, L. J., and J. H. Byrne. 1985. Interneurons contributing to the mediation and modulation of the tail withdrawal reflex in *Aplysia*. *Soc. Neurosci. Abstr.* **11:** 692.

Cleary, L. J., and J. H. Byrne. 1986. Associative learning of the gill and siphon withdrawal reflex in *Aplysia* interneurons mediating the unconditioned reflex. *Soc. Neurosci. Abs.* **12:** 397.

Dale, N., E. R. Kandel, and S. Schacher. 1987. Serotonin produces long-term changes in the excitability of *Aplysia* sensory neurons in culture that depend on new protein synthesis. *J. Neurosci.* **7:** 2232–2238.

Dash, P. K., B. Hoechner, and E. R. Kandel. 1990. Injection of the cyclic AMP responsive element into the nucleus of *Aplysia* sensory neurons blocks long-term facilitation. *Nature* **345:** 718–721.

Eskin, A., K. S. Garcia, and J. H. Byrne. 1989. Information storage in the nervous system of *Aplysia:* specific proteins affected by serotonin and cAMP. *Proc. Nat. Acad. Sci. USA* **86:** 2458–2462.

Frost, W. N., V. F. Castellucci, R. D. Hawkins, and E. R. Kandel. 1985. Monosynaptic connections made by the sensory neurons of the gill- and siphon-withdrawal reflex in *Aplysia* participate in the storage of long-term memory for sensitization. *Proc. Nat. Acad. Sci. USA* **82:** 8266–8269.

Frost, W. N., G. A. Clark, and E. R. Kandel. 1988. Parallel processing of short-term memory for sensitization in *Aplysia. J. Neurobiol.* **19:** 297–334.

Glanzman, D. L., S. L. Mackey, R. D. Hawkins, A. M. Dyke, P. E. Lloyd, and E. R. Kandel. 1989. Depletion of serotonin in the nervous system of *Aplysia* reduces the behavioral enhancement of gill withdrawal as well as the heterosynaptic facilitation produced by tail shock. *J. Neurosci.* **9:** 4200–4213.

Greenberg, S. M., V. F. Castellucci, H. Bayley, and J. H. Schwartz. 1987. A molecular mechanism for long-term sensitization in *Aplysia. Nature* **329:** 62–65.

Hammer, M., L. J. Cleary, and J. H. Byrne. 1989. Serotonin acts in the synaptic region of sensory neurons in *Aplysia* to enhance transmitter release. *Neurosci. Lett.* **104:** 235–240.

Hawkins, R. D., V. F. Castellucci, and E. R. Kandel. 1981. Interneurons involved in mediation and modulation of gill-withdrawal reflex in *Aplysia* II. Identified neurons produce heterosynaptic facilitation contributing to behavioral sensitization. *J. Neurophysiol.* **45:** 315–326.

Hawkins, R. D., and S. Schacher. 1989. Identified facilitator neurons L29 and L28 are excited by cutaneous stimuli used in dishabituation, sensitization, and classical conditioning of *Aplysia. J. Neurosci.* **9:** 4236–4245.

Hochner, B., M. Klein, S. Schacher, and E. R. Kandel. 1986. Action-potential duration and the modulation of transmitter release from the sensory neurons of *Aplysia* in presynaptic facilitation and behavioral sensitization. *Proc. Nat. Acad. Sci. USA* **83:** 8410–8414.

Kandel, E. R. 1979. *Behavioral biology of* Aplysia. W. H. Freeman, San Francisco.

Kandel, E. R., and J. H. Schwartz. 1982. Molecular biology of learning: modulation of transmitter release. *Science* **218:** 433–443.

Kistler, H. B., Jr., R. D. Hawkins, J. Koester, H. W. Steinbusch, E. R. Kandel and J. H. Schwartz. 1985. Distribution of serotonin-immunoreactive cell bodies and processes in the abdominal ganglion of mature *Aplysia. J. Neurosci.* **5:** 72–80.

Klein, M., J. S. Camardo, and E. R. Kandel. 1982. Serotonin modulates a new potassium current in the sensory neurons that show presynaptic facilitation in *Aplysia. Proc. Nat. Acad. Sci. USA* **79:** 5713–5717.

Koester, J. 1989. Chemically and electrically coupled interneurons mediate respiratory pumping in *Aplysia. J. Neurophysiol.* **62:** 1113–1126.

Kupfermann, I., T. J. Carew, and E. R. Kandel. 1974. Local, reflex and central commands controlling gill and siphon movements in *Aplysia. J. Neurophysiol.* **37:** 996–1019.

Lo, L. T., J. H. Byrne, and L. J. Cleary. 1987. Distribution of three modulatory transmitters within the pleural ganglion of *Aplysia. Soc. Neurosci. Abstr.* **13:** 1073.

Longley, R. D., and A. J. Longley. 1986. Serotonin immunoreactivity of neurons in the gastropod *Aplysia californica. J. Neurobiol.* **17:** 339–358.

Mackey, S. L., E. R. Kandel, and R. D. Hawkins. 1989. Identified serotonergic neurons LCB1 and RCB1 in the cerebral ganglia of *Aplysia* produce presynaptic facilitation of siphon sensory neurons. *J. Neurosci.* **9:** 4227–4235.

Montarolo, P. G., P. Goelet, V. F. Castellucci, J. Morgan, E. R. Kandel, and S. Schacher. 1986. A critical period for macromolecular synthesis in long-term heterosynaptic facilitation in *Aplysia. Science* **234:** 1249–1254.

Nazif, F. A., J. H. Byrne, and L. J. Cleary. 1991. cAMP induces long-term morphological changes in sensory neurons of *Aplysia. Brain Res.* **539:** 324–327.

Ocorr, K. A., and J. H. Byrne. 1985. Membrane responses and changes in cAMP levels in *Aplysia* sensory neurons produced by serotonin, tryptamine, FMRFamide and small cardioactive peptide B (SCP_B). *Neurosci. Lett.* **55:** 113–118.

Ocorr, K. A., and J. H. Byrne. 1986. Evidence for separate receptors that mediate parallel effects of serotonin and small cardioactive peptide B (SCP_B) on adenylate cyclase in *Aplysia californica. Neurosci. Lett.* **70:** 283–288.

Ocorr, K. A., M. Tabata, and J. H. Byrne. 1986. Stimuli that produce sensitization lead to elevation of cyclic AMP levels in tail sensory neurons of *Aplysia. Brain. Res.* **371:** 190–192.

Ono, J. K., and R. E. McCaman. 1984. Immunocytochemical localization and direct assays of serotonin-containing neurons in *Aplysia. Neuroscience* **11:** 549–560.

Perlman, A. J. 1979. Central and peripheral control of siphon-withdrawal reflex in *Aplysia californica. J. Neurophysiol.* **42:** 510–529.

Pinsker, H., I. Kupfermann, V. F. Castellucci, and E. R. Kandel. 1970. Habituation and dishabituation of the gill-withdrawal reflex in *Aplysia. Science* **167:** 1740–1742.

Pinsker, H. M., W. A. Hening, T. J. Carew, and E. R. Kandel. 1973. Long-term sensitization of a defensive withdrawal reflex in *Aplysia. Science* **182:** 1039–1042.

Pollock, J. D., L. Bernier, and J. S. Camardo. 1985. Serotonin and cyclic adenosine 3′:5′-monophosphate modulate the potassium current in tail sensory neurons in the pleural ganglion of *Aplysia. J. Neurosci.* **5:** 1862–1871.

Sacktor, T., and J. H. Schwartz. 1990. Sensitizing stimuli cause translocation of protein kinase C in *Aplysia* sensory neurons. *Proc. Nat. Acad. Sci. USA* **87:** 2036–2039.

Schacher, S., V. F. Castellucci, and E. R. Kandel. 1988. cAMP evokes long-term facilitation in *Aplysia* sensory neurons that requires new protein synthesis. *Science* **240:** 1667–1669.

Scholz, K. P., and J. H. Byrne. 1987. Long-term sensitization in *Aplysia:* biophysical correlates in tail sensory neurons. *Science* **235:** 685–687.

Scholz, K. P., and J. H. Byrne. 1988. Intracellular injection of cAMP induces a long-term reduction of neuronal K^+ currents. *Science* **240:** 1664–1666.

Schwartz, J. H., L. Bernier, V. F. Castellucci, M. Palazzolo, T. Saitoh, A. Stapleton, and E. R. Kandel. 1983. What molecular steps determine the time course of the memory for short-term sensitization in *Aplysia? Cold. Spring. Harbor. Symp. Quant. Biol.* **48:** 811–819.

Shuster, M. J., J. S. Camardo, S. A. Siegelbaum, and E. R. Kandel. 1985. Cyclic AMP-dependent protein kinase closes the serotonin-sensitive K^+ channels of *Aplysia* sensory neurons in cell-free membrane patches. *Nature* **313:** 392–395.

Shuster, M. J., and S. A. Siegelbaum. 1987. Pharmacological characterization of the serotonin-sensitive potassium channel of *Aplysia* sensory neurons. *J. Gen. Physiol.* **90:** 587–608.

Siegelbaum, S. A., J. S. Camardo, and E. R. Kandel. 1982. Serotonin and cAMP close single K^+ channels in *Aplysia* sensory neurons. *Nature* **299:** 413–417.

Sweatt, J. D., A. Volterra, B. Edmonds, K. A. Karl, S. A. Siegelbaum, and E. R. Kandel. 1989. FMRFamide reverses protein phosphorylation produced by 5-HT and cAMP in *Aplysia* sensory neurons. *Nature* **342:** 275–278.

Tritt, S. H., I. P. Lowe, and J. H. Byrne. 1983. A modification of the glyoxylic acid induced histofluorescence technique for demonstration of catecholamines and serotonin in tissues of *Aplysia californica*. *Brain Res.* **259:** 159–162.

Walsh, J. P. and J. H. Byrne. 1989. Modulation of a steady-state Ca^{2+}-activated, K^+ current in tail sensory neurons of *Aplysia*: role of serotonin and cAMP. *J. Neurophysiol.* **61:** 32–44.

Walters, E. T., and J. H. Byrne. 1983. Associative conditioning of single sensory neurons suggests a cellular mechanism for learning. *Science* **219:** 405–408.

Walters, E. T., J. H. Byrne, T. J. Carew, and E. R. Kandel. 1983a. Mechanoafferent neurons innervating tail of *Aplysia*. I. Response properties and synaptic connections. *J. Neurophysiol.* **50:** 1522–1542.

Walters, E. T., J. H. Byrne, T. J. Carew, and E. R. Kandel. 1983b. Mechanoafferent neurons innervating tail of *Aplysia*. II. Modulation by sensitizing stimulation. *J. Neurophysiol.* **50:** 1543–1559.

Walters, E. T., and M. T. Erickson. 1986. Directional control and the functional organization of defensive responses in *Aplysia*. *J. Comp. Physiol. A* **159:** 339–351.

Weiss, K. R., U. T. Koch, J. Koester, S. C. Rosen, and I. Kupfermann. 1982. The role of arousal in modulating feeding behavior of *Aplysia*: neural and behavioral studies. Pp. 25–57 in *The Neural Basis of Feeding and Reward*, B. G. Hoebel and D. Novin, ed. Haer Institute, New Brunswick, ME.

Zhang, Z. S., L. J. Cleary, D. M. Marshak, and J. H. Byrne. 1988. Serotonergic varicosities make apparent synaptic contacts with pleural sensory neurons of *Aplysia*. *Soc. Neurosci. Abstr.* **14:** 841.

Zwartjes, R. E., M. T. Crow, J. H. Byrne, and A. Eskin. 1990. Serotonin regulates the expression of mRNA in the pleural-pedal ganglia of *Aplysia*, as determined by *in vitro* translation. *Soc. Neurosci. Abstr.* **16:** 596.

Reference: *Biol. Bull.* **180:** 262–268. (April, 1991)

Studies of Behavioral State in *Aplysia*

IRVING KUPFERMANN, THOMAS TEYKE, STEVEN C. ROSEN, AND KLAUDIUSZ R. WEISS*

*Center for Neurobiology and Behavior, Columbia University College of Physicians and Surgeons; New York State Psychiatric Institute; and *Department of Physiology and Biophysics, Mt. Sinai School of Medicine, New York, New York*

Abstract. This paper reviews a series of studies on the neural organization and the cellular mechanisms underlying behavioral states; in these studies, feeding behavior in *Aplysia* was used as a model system. Feeding in *Aplysia* has similarities to motivated behaviors in other animals and is modulated by a number of interesting state variables, including arousal. Food-induced arousal manifests itself in two categories of feeding behavior: (1) appetitive responses (*e.g.*, head-up feeding posture and directed head turning), which orient the animal to potential goal objects such as food; and (2) consummatory responses (biting, swallowing), which obtain the goal object. The consummatory responses are rhythmic and relatively stereotyped, whereas the appetitive responses are highly variable. Our evidence suggests that one consummatory response, biting, appears to be controlled by command elements in the cerebral-ganglion, such as neuron CBI-2, which are capable of driving the behavior. One component of the appetitive behavior, head lifting, may be controlled (at least in part) by another cerebral neuron, C-PR. C-PR, however, affects numerous systems in the animal, but all the systems affected seem to be involved in the food-induced arousal state of the animal. We postulate that C-PR is, in some ways, analogous to command neurons that evoke behaviors. The C-PR, however, not only evokes a behavior, but also evokes a central motive state which aids in insuring that behavior is efficiently expressed.

Introduction

Mollusks have long been used for studies that are designed to investigate general neurobiological principles rather than the details of a single species. One important advantage of mollusks is the large size of their neurons. For many years, studies that were difficult or impossible in vertebrates could be approached by investigating the squid giant axon and the large somata of gastropod neurons. In recent years, the use of cell culture, brain slices, and other methodologies has made it possible to do many types of cellular studies on vertebrate neurons that could previously be done only in mollusks. However, it is still very difficult to study the integrative functions of the vertebrate nervous system and to relate cellular processes to behavior. For this reason, the presence of a relatively few neurons in gastropod mollusks has assumed increased importance.

We have been studying the marine mollusk *Aplysia* in order to understand the neural organization and the cellular mechanisms underlying behavioral states. We have concentrated on feeding behavior because our early studies indicated that the feeding responses of these animals are modulated by a number of interesting state variables, including arousal and satiation (Kupfermann *et al.*, 1982; Susswein *et al.*, 1978). This paper is a review of our work. It emphasizes studies of the appetitive aspects of feeding, and is not meant to be a general review of feeding in *Aplysia*.

Received 7 August 1990; accepted 6 November 1990.

Feeding Behavior in *Aplysia* has Similarities to Motivated Behaviors in Other Animals

To provide themselves with adequate nutrients, *Aplysia* has many of the same problems faced by most other animals. They must detect and locate appropriate food sources. They must approach the food and orient it to the buccal orifice. They must then bite and swallow the food. Finally, when a sufficient amount has been consumed, they need to stop feeding. These operations must all be carried out in a manner that is efficient in time and energy expenditure. One of the means by which the animals im-

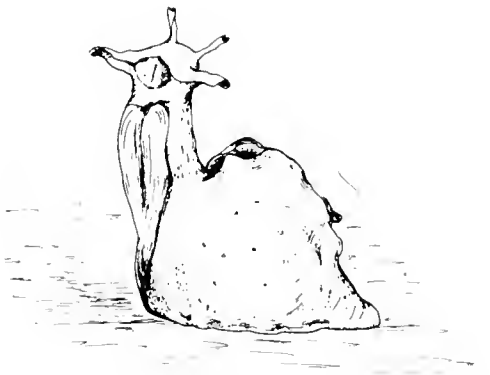

Figure 1. *Aplysia* in the feeding posture. In this position the animal shows directed turning responses to seaweed applied to the head.

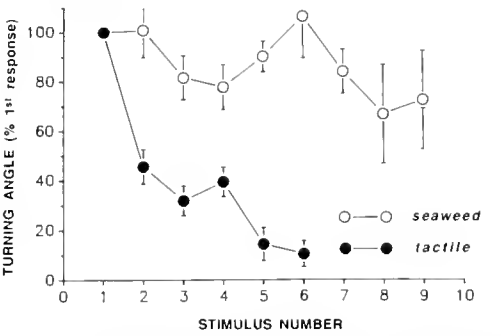

Figure 3. Turning angle evoked by repeated seaweed (open circles) or tactile (filled circles) stimuli. The animals (n = 5) were first induced into the feeding posture by means of seaweed. They were then stimulated at a locus 10° from the mouth, either with a purely tactile stimulus, or with seaweed. The stimulus was repeated every 10 s (10 successive stimuli; 3 series each). Final turning angles of the responses are shown as the percent of the final angle of the first response (means ± S.E.M.). Note the marked decline in the magnitude of the turning response evoked by repeated tactile stimulation and the relatively steady response magnitude upon repeated seaweed stimulation. Data from Teyke *et al.* (1990b).

prove the efficiency of their behavior is by regulating it according to particular internal states. These internal states are modulated by external and internal stimuli and by an internal endogenous process associated with a circadian activity rhythm. In higher animals, the constellation of state variables that regulate feeding are termed "hunger," and by analogy, a hunger-like state also appears to regulate feeding in *Aplysia*. As in higher animals, feeding in *Aplysia* is greatly potentiated by pre-exposing the animals to food; *i.e.*, the animal exhibits incentive motivation. When a quiescent *Aplysia* is first stimulated with seaweed, it becomes activated after a relatively long delay (up to a minute). We refer to this activated state as "food-induced arousal."

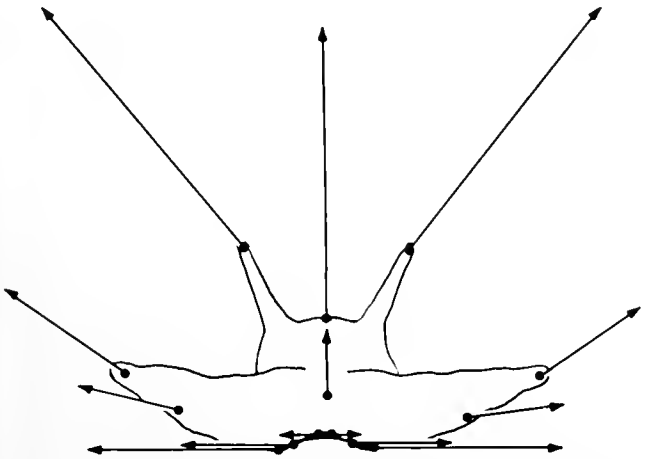

Figure 2. Vectors indicating the magnitude and direction that the head turns in response to tactile stimuli briefly presented (open loop) to different points on the rhinophores and tentacles. The movements turn the head in the direction of the stimulus. In the open loop condition the animal greatly overshoots the stimulus. If, however, the stimulus is maintained in place (closed loop), when the animal begins the response, the movement is represented by the indicated vectors, but as the animal turns, the response progressively decreases in magnitude so that the mouth comes to be accurately centered over the stimulus. Data from Teyke *et al.* (1990b)

Food-induced arousal in *Aplysia* manifests itself in at least two stages. First, appetitive behaviors (the orienting phase of motivated behaviors) are affected; second, consummatory responses are modified. Initial contact with food evokes a defensive withdrawal reflex of the head. The fast phase of this reflex appears to be controlled by the cerebral Bn neurons (Teyke *et al.*, 1989), which receive powerful tactile input, and which evoke withdrawal movements of the head and tentacles. After the initial defensive response, the animal ceases to withdraw. The response appears to be habituated, but unlike other forms of habituation in *Aplysia* (Castellucci *et al.*, 1970, see also Fig. 3), the response decrement occurs very rapidly, typically following just a single application of the stimulus. A subsequent brief food stimulus elicits an orienting response, instead of eliciting withdrawal. The animal gets into a characteristic feeding posture in which the posterior part of the foot is attached to the substrate, and the neck, head, and anterior part of the foot are lifted (Fig. 1). In addition, there are signs of "autonomic" arousal, such as an increase in blood pressure and heart rate (Koch *et al.*, 1984). The feeding posture is maintained even when the food is removed, indicating that the appetitive arousal has a "memory" component. From the feeding posture the animal can readily move its head toward a source of food. When the tentacles of the food-aroused animal make physical contact with food (seaweed), the animal moves its head so as to direct its mouth towards the stimulus (Fig. 2). For a brief (open loop) stimulus within the receptive field, the animal greatly overshoots the food, and the amount of overshoot is proportional to the angular

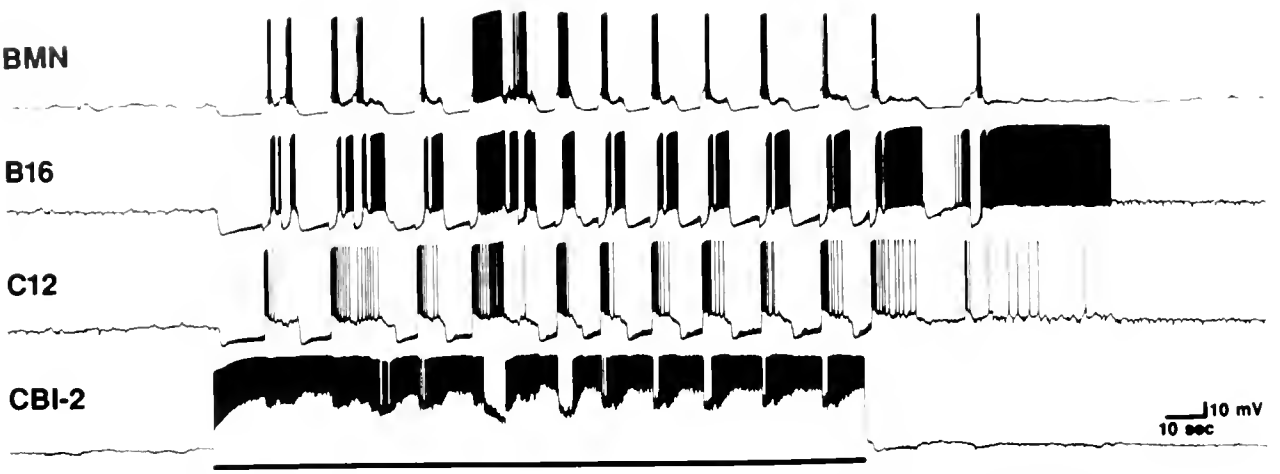

Figure 4. Example of the motor program driven by CBI-2. CBI-2 was fired by a constant depolarizing current (dark horizontal line). The rhythmic program incorporated neurons in the cerebral and buccal ganglia. The buccal program is reflected in the activity of an identified ARC muscle motor neuron, B16. Another buccal motor neuron, BMN, illustrates that the program is present in numerous other buccal neurons. C12 is a cerebral ganglion neuron that controls movements of the lips, and it is one of several cerebral neurons that is recruited by the buccal program that is driven by CBI-2. CBI-2 also shows periodic synaptic input driven by the buccal program. Note that when CBI-2 stops firing, the program briefly persists and then terminates. The data are from Rosen *et al.* (1987, 1988).

distance of the stimulus from the mouth. If, however, the stimulus is maintained in position so that it provides continuous feedback during the movement (closed loop), the food is accurately centered over the mouth (Teyke *et al.*, 1990b). Seaweed provides the animal with two distinct types of stimuli: tactile and chemical. Surprisingly, the stimulus that results in the animal turning toward the food is the tactile component. A purely chemical stimulus, provided by an aqueous extract of seaweed, is not very effective in eliciting turning. On the other hand, if the animal is first aroused with a chemical stimulus, a purely tactile stimulus (provided by a glass rod) very effectively evokes a turning response. If, however, the tactile stimulus is repeated without intermittent chemical stimulation, the turning response habituates until no response at all is evoked (Fig. 3). Thus, the chemical component of the seaweed maintains the arousal level of the animal, while the tactile component directs the response.

When the animal turns toward the stimulus, contact with food to the region immediately around the mouth (perioral zone) initiates consummatory behaviors and a new set of arousal responses. The consummatory arousal is characterized by a progressive build-up of the rate and magnitude of the rhythmic biting response that occurs when food touches the perioral zone (Kupfermann, 1974; Weiss *et al.*, 1982). Whereas the appetitive feeding responses are highly variable, the consummatory biting response is more stereotyped, although it consists of several components (Kupfermann, 1974; Weiss *et al.*, 1986): (1) There is a forward movement (cocking) of the whole buccal mass. The forward position is maintained during the whole meal. (2) The whole buccal mass undergoes forward and backward movements. These movements occur on a background of the maintained forward movement. (3) The radula rotates forward and backward. (4) The radula halves open and close. The latter two movements cause the food to be grasped and deposited into the buccal cavity. The relatively small backward movement, which deposits the food in the buccal cavity during biting behavior, can be distinguished from a larger backward movement (swallowing) that is triggered by the presence of food in the buccal cavity, and which results in the food being moved into the esophagus (Kupfermann, 1974). Biting movements, which are elicited by food contacting the perioral zone, thus consist of a large forward component of the radula, followed by a relatively small backward movement. Swallowing, which is elicited by food in the buccal cavity, consists of a relatively small forward movement and a large backward movement. The swallowing movements are associated with an inhibition of the biting movements; *i.e.*, as long as food is present in the buccal cavity, stimulation of the perioral zone never elicits a large forward movement of the radula.

Biting Responses are Elicited by the Activity of Individual Neurons Located in the Cerebral Ganglion

In a number of species, including gastropod mollusks, stereotyped responses are elicited by the activity of individual cells or small groups of cells (Kupfermann and

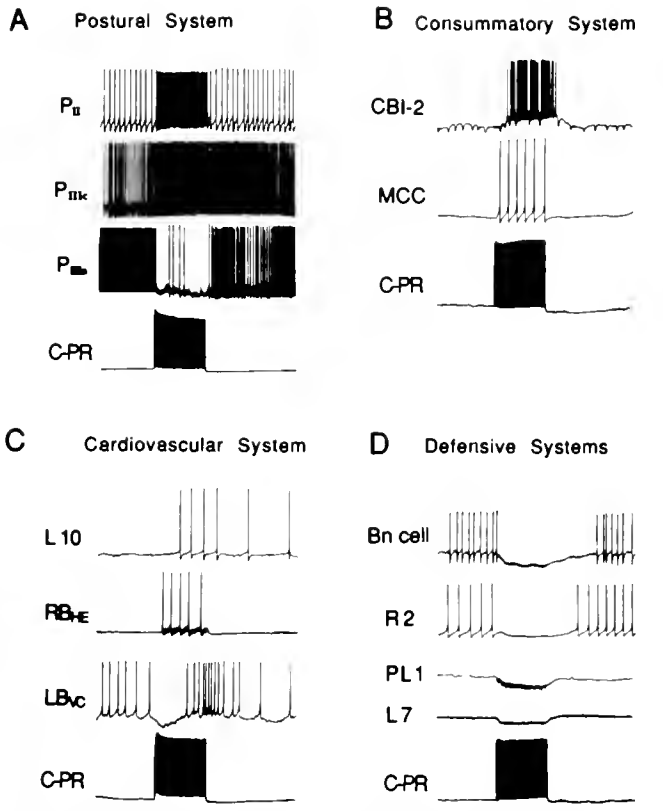

Figure 5. The various effects of firing C-PR on different systems associated with food-induced arousal. For each experiment, C-PR was intracellularly stimulated at 20 Hz for 5 s. For illustrative purposes, multiple follower cells of the C-PR are shown for each part of the figure, but the data for each trace were obtained in separate experiments. (A) Examples of the effects of firing C-PR on different pedal ganglion neurons, that may be part of the postural control system. (B) Effects of C-PR on cerebral ganglion neurons that control consummatory feeding responses (biting command element, CBI-2, and the modulatory neuron, metacerebral cell, MCC). (C) Effects of C-PR on abdominal ganglion neurons that control the cardiovascular system (command element L10, heart exciter RBHE, and vasoconstrictor LBVC. (D) Effects of C-PR on various neurons that participate in defensive responses [head withdrawal neuron, Bn cell (Teyke *et al.*, 1989); gill withdrawal motor neurons, L7; defensive secretion neurons, R2 and PL1]. Calibration: 2 s, 20 mV, except 5 mV for cells R2 and PL1 in part D. Data are from Teyke *et al.* (1990a).

Weiss, 1978; Gillette *et al.*, 1982; McClellan, 1986; Benjamin and Elliott, 1989; McCrohan and Kyriakides, 1989; Delaney and Gelperin, 1990). To determine the critical control elements for the consummatory phase of feeding in *Aplysia*, we back-filled the cerebral-buccal connectives and located a population of cerebral neurons that send their axons to the buccal ganglion. Several of these cells had been previously identified, including the serotonergic metacerebral cells (MCCs) and ICBM mechanosensory cells (Rosen *et al.*, 1989a,b). In addition, two small populations of cells were found in anterior and lateral positions. Firing of one of the cells (cerebral to buccal interneuron two, or CBI-2) within the anterior cluster, produced a robust and reliable rhythmic motor program of the buccal ganglion (Fig. 4) (Rosen *et al.*, 1987). CBI-2 receives chemosensory input from the perioral zone. In addition, when it elicits a buccal motor program it receives rhythmic synaptic input from the buccal ganglion, and thus it fires in phase with the buccal motor program. If, however, the synaptic feedback from the buccal ganglion is blocked by placing the cerebral ganglion in seawater containing cobalt ions, the firing of CBI-2 still evokes rhythmic activity in the buccal ganglion, in the absence of rhythmic activity in CBI-2 (Rosen *et al.*, 1988). For a discussion of recent work on the central pattern generating circuitry intrinsic to the buccal ganglion of *Aplysia*, see Kirk (1989), Nagahama and Takata (1989), and Susswein and Byrne (1988).

Using a semi-intact preparation, we found that the firing of CBI-2 can evoke rhythmic movements of the buccal mass and radula, and the movements are similar to the repetitive biting responses seen in the intact animal. The responses do not resemble swallowing or rejection. The firing of two other cerebral to buccal interneurons also evokes coordinated buccal ganglion activity, but the motor programs are different for each of the CBIs. Thus we hypothesize that the CBIs in *Aplysia*, as in other gastropods (Gillette *et al.*, 1982; Benjamin and Elliott, 1989; McCrohan and Kyriakides, 1989; Delaney and Gelperin, 1990), may constitute a command system, the conjoint activity of which drives consummatory feeding responses.

Activity of an Identified Cerebral Neuron Appears to Elicit Elements of Appetitive Arousal

Although stereotyped consummatory responses are driven by a relatively few command-like elements, it is difficult to imagine how the highly variable responses that constitute appetitive behavior could be similarly driven by a small number of neurons. Nevertheless, we set out to determine whether the nervous system contains neurons that can evoke appetitive feeding behavior. Backfills of the cerebral-pedal connectives revealed a small subset of cerebral ganglion neurons that send their axons to the pedal or pleural ganglia (Teyke *et al.*, 1990a). The firing of these neurons revealed a single (bilateral) cerebral neuron that can influence the activity of numerous neurons in the abdominal, pedal, and cerebral ganglia. We termed this neuron the cerebral to pedal regulator [to avoid confusion with the caudal photoreceptor (CPR) interneuron of crayfish, we abbreviate this neuron C-PR, although previously we did not use the hyphen].

The pedal ganglion in particular contains a large number of neurons that are excited by C-PR (Fig. 5). A smaller number of pedal ganglion neurons are inhibited by C-PR. Each neuron that is affected by C-PR activity receives input following the firing of either the left or right C-PR,

Figure 6. Example of a prolonged excitatory response in C-PR and the MCC to a brief seaweed stimulus. Calibration: 5 s, 20 mV. Data from Teyke *et al.* (1990a).

suggesting that C-PR is probably not directly involved in the directed head turning response, which is very strongly lateralized. Nevertheless, head turning does not occur unless the animal is first aroused, so that C-PR activity may enable head turning. Some of the effects of C-PR are monosynaptic, whereas others are mediated by interneurons. Firing of many of the pedal cells that are affected by the activity of C-PR causes the muscles of the anterior-dorsal region of the neck to contract (Teyke *et al.*, 1990a), which suggests that C-PR may evoke movements that cause the head to be lifted into the feeding posture. Consistent with a role of C-PR in eliciting head-lifting in response to food, we found that seaweed applied to the tentacles evokes strong activity in C-PR (Fig. 6). Furthermore, preliminary studies involving extracellular recordings from the cerebral-pedal connectives, support the idea that C-PR is active just before and during the time that the animal lifts its head into the feeding posture (Teyke *et al.*, 1990c). Thus, the total complex of appetitive feeding responses may consist of two components: a stereotyped postural head-lifting response and a more varied directed turning response.

We have formulated a simple neural model (Teyke *et al.*, 1990b) whose input-output functions are similar to the behavioral results concerning the directed head turning component of appetitive feeding behavior. The model is based on reflex circuits and does not contain command elements. By contrast, the head lifting response may be importantly controlled by a small number of neurons, such as C-PR, that have command-like properties. C-PR, however, affects responses other than head lifting. In fact,

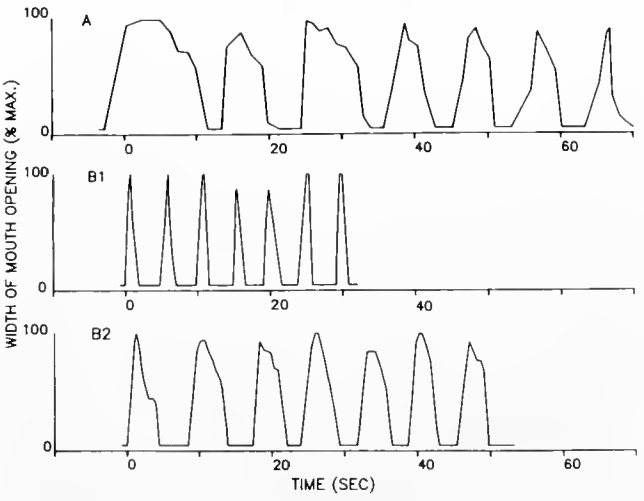

Figure 7. Sequence of mouth openings and closings during seven repetitive biting responses, in two animals that have had bilateral chronic lesions (protease injected) of the MCCs. The sequence is based on a videotaped analysis of biting. Width of the mouth opening is expressed as a percentage of the maximum. A, An example, illustrating "stuck" radula in a MCC lesioned animal, in which the radula stays protracted for an abnormally long duration. B, Responses of a normal animal (B1), and of the same animal (B2) following lesion of the MCCs. Data from Rosen *et al.* (1989a).

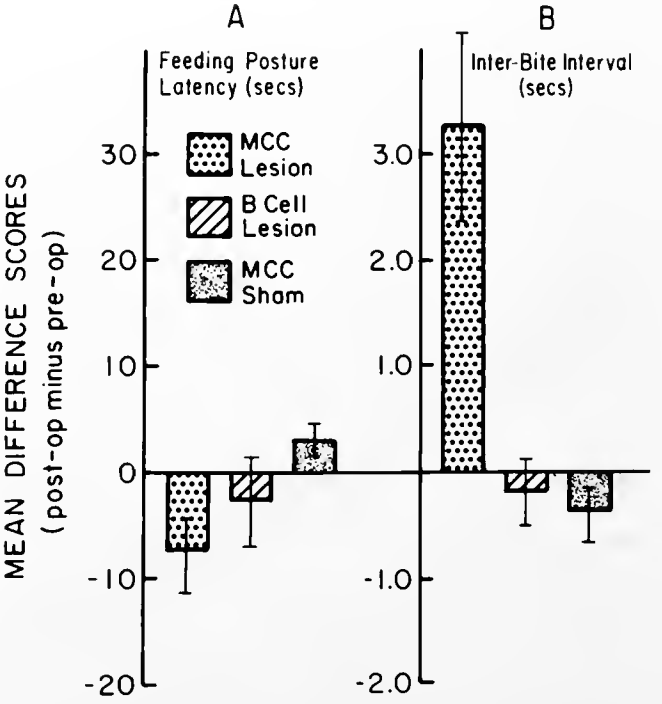

Figure 8. MCC lesion (n = 6), B cell control lesion (n = 7), and dye injection MCC control (n = 6) group mean difference scores (postoperative overall mean, minus preoperative scores, ± SEMs) for latency to assume feeding posture (A) and for interbite interval (B). Bites were elicited by continually stimulating the lips with seaweed, without allowing the animal to obtain the food. Data from Rosen *et al.* (1989a).

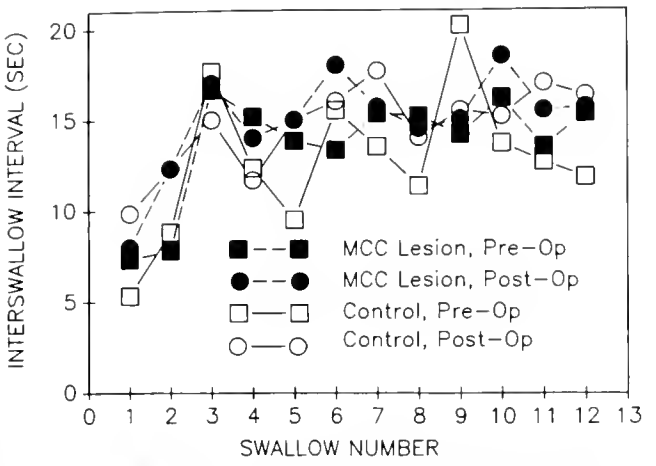

Figure 9. MCC lesion and control groups mean interswallow intervals, measured during ingestion of strips of seaweed. No significant group differences were found. Data from Rosen *et al.* (1989a).

we found that C-PR activity affects neurons involved in three other types of responses: defensive withdrawal reflexes (Fig. 5D), consummatory biting (Fig. 5B), and cardiovascular responses (Fig. 5C). The neurons involved in defensive responses were inhibited by the firing of C-PR, and in semi-intact preparations we showed that the firing of head withdrawal neurons in response to a strong tactile stimulus to the head was reduced when the C-PR neuron was permitted to fire. The rapid depression of withdrawal responses following contact with seaweed may therefore be due either in part, or wholly, to an active inhibition, rather than to low frequency depression, as appears to be the case for habituation of the gill and siphon reflex to tactile stimulation (Castellucci *et al.*, 1970).

Firing of C-PR evokes complex mixtures of excitatory and inhibitory synaptic responses in abdominal ganglion neurons controlling the heart and blood vessels (Fig. 5C). These effects could contribute to aspects of cardiovascular responses that occur during food-induced arousal.

The cerebral ganglion neurons involved in consummatory behaviors generally receive pure excitation when C-PR is fired. These neurons include command-like elements for biting (CBI-2) and the metacerebral cells (MCCs). The MCCs modulate the muscles and neurons that effectuate biting and account, in part, for the build-up of the speed and magnitude of successive bites, which occurs during consummatory arousal (Rosen *et al.*, 1989a). In contrast to the C-PR, the modulatory effects of the MCC are very restricted. It only modulates consummatory responses, and only the bite component. For example, if the MCCs are destroyed, there is no change in the capacity to elicit the feeding posture (Fig. 8) (Rosen *et al.*, 1989a), but there is an increase in the bite latency and inter-bite intervals (Fig. 7, 8B). Inter-swallow intervals are unchanged (Fig. 9).

When C-PR is fired at physiological rates, its excitatory effect on neurons involved in biting responses is never strong enough to drive the neurons at a rate sufficient to evoke biting. C-PR appears to function to increase the excitability of these neurons without directly driving consummatory responses.

By cutting various connectives we could localize the ganglia that contain the interneurons that produce the effects of C-PR on the various non-postural systems. We found that all of these effects are mediated by the activity of the pedal-pleural ganglia. It may be significant that these ganglia mediate the postural responses associated with food arousal. Thus appetitive arousal may involve a primary effect on a postural system, which, in turn, modulates the activity of the numerous other systems that will eventually come into play during feeding. In the vertebrate brain, indeed, neurons thought to be concerned with regulation of consciousness and arousal are concentrated in the brain stem in regions intimately involved with postural regulation (Hobson and Brazier, 1980). Because virtually all behaviors require a particular posture for their execution, the postural neural system may serve a primary role in arousal in highly diverse species.

Some of the effects of C-PR, such as those on the elements of consummatory responses, could enhance these responses. Other effects, such as those on Bn neurons, may suppress responses that are incompatible with feeding behavior. We postulate that C-PR is, in some ways, analogous to command neurons, which evoke behaviors. The C-PR, however, not only evokes a behavior (head lifting), but also evokes a central motive state that aids in insuring that behavior is efficiently expressed. A behavioral action such as feeding is made up of a number of different behavioral acts (*e.g.*, head lifting, biting, swallowing). Thus, a consideration of the ways in which behavioral efficiency is maximized raises two fundamental questions. First, how are multiple responses of the organism coordinated with one another, and second, how are the individual behavioral acts which make up a behavioral action modulated so as to optimize their speed and minimize energy expenditure? Our evidence suggests that one means of coordinating diverse responses directed toward a single goal is to affect diverse neuronal systems through the activity of a relatively few neuronal elements. Data presented elsewhere indicate that maximization of the efficiency of individual responses is accomplished, in part, by the activity of subordinate specialized neurons such as the MCC (Weiss *et al.*, 1978; Rosen *et al.*, 1989a). In addition, individual responses may be regulated by neuromodulators that occur as cotransmitters in motorneurons innervating the muscles that effectuate feeding responses (Lloyd *et al.*, 1985; Cropper *et al.*, 1987a,b, 1988, 1990). The motor neurons are subordinate to the modulatory effects of the MCC, which, in turn, is modulated by C-PR. Thus the

final motor activity appears to be regulated by modulatory neurons of progressively higher order. We are beginning to reduce the elusive concept of motivational state to explanations in terms of the actions of ordinary neural mechanisms, operating in networks of appropriately interconnected neurons.

Literature Cited

Benjamin, P. R., and C. J. H. Elliott. 1989. Snail feeding oscillator: the central pattern generator and its control by modulatory interneurons. Pp. 173–214 in *Neuronal and Cellular Oscillators*, J. W. Jacklet, ed. Marcel Dekker, Inc., New York and Basel.

Castellucci, V., H. Pinsker, I. Kupfermann, and E. R. Kandel. 1970. Neuronal mechanisms of habituation and dishabituation of the gill-withdrawal reflex in *Aplysia*. *Science* **167**: 1745–1748.

Cropper, E. C., R. Tenenbaum, M. A. Gawinowicz Kolks, I. Kupfermann, and K. R. Weiss. 1987a. Myomodulin: a bioactive neuropeptide present in an identified cholinergic buccal motor neuron of *Aplysia*. *Proc. Natl. Acad. Sci. USA* **84**: 5483–5486.

Cropper, E. C., P. E. Lloyd, W. Reed, R. Tenenbaum, I. Kupfermann, and K. R. Weiss. 1987b. Multiple neuropeptides in cholinergic motor neurons of *Aplysia*: evidence for modulation intrinsic to the motor circuit. *Proc. Natl. Acad. Sci. USA* **84**: 3486–3490.

Cropper, E. C., M. W. Miller, R. Tenenbaum, M. A. Gawinowicz Kolks, I. Kupfermann, and K. R. Weiss. 1988. Structure and action of buccalin: a modulatory neuropeptide localized to an identified small cardioactive peptide-containing cholinergic motor neuron of *Aplysia californica*. *Proc. Natl. Acad. Sci. USA* **85**: 6177–6181.

Cropper, E. C., M. W. Miller, F. S. Vilim, R. Tenenbaum, I. Kupfermann, and K. R. Weiss. 1990. Buccalin is present in the cholinergic motor neuron B16 of *Aplysia* and it depresses accessory radula closer muscle contractions evoked by stimulation of B16. *Brain Res.* **512**: 175–179.

Delaney, K., and A. Gelperin. 1990. Cerebral interneurons controlling fictive feeding in *Limax maximus*. I. Anatomy and criteria for re-identification. *J. Comp. Physiol. [A]* **166**: 297–310.

Gillette, R., M. P. Kovac, and W. J. Davis. 1982. Control of feeding motor output by paracerebral neurons in brain of *Pleurobranchaea californica*. *J. Neurophysiol.* **47**: 885–908.

Hobson, J. A., and M. A. B. Brazier, eds. 1980. *The Reticular Formation Revisited. Specifying Function for a Nonspecific System.* Raven Press, New York. 552 pp.

Kirk, M. D. 1989. Premotor neurons in the feeding system of *Aplysia californica*. *J. Neurobiol.* **20**: 497–512.

Koch, U. T., J. Koester, and K. R. Weiss. 1984. Neuronal mediation of cardiovascular effects of food arousal in *Aplysia*. *J. Neurophysiol.* **51**: 126–135.

Kupfermann, I. 1974. Feeding behavior in *Aplysia*: a simple system for the study of motivation. *Behav. Biol.* **10**: 1–26.

Kupfermann, I., L. Shkolnik, and K. R. Weiss. 1982. Modulatory synaptic actions of neurotransmitters in circuits controlling feeding in *Aplysia*. Pp. 517–531 in *Cytochemical Methods in Neuroanatomy*. Alan R. Liss, Inc., New York.

Kupfermann, I., and K. R. Weiss. 1978. The command neuron concept. *Behav. Brain Sci.* **1**: 3–10.

Lloyd, P. E., A. C. Mahon, I. Kupfermann, J. L. Cohen, R. H. Scheller, and K. R. Weiss. 1985. Biochemical and immunocytological localization of molluscan small cardioactive peptides in the nervous system of *Aplysia californica*. *J. Neurosci.* **5**: 1851–1861.

McClellan, A. D. 1986. Command systems for initiating locomotion in fish and amphibians: parallels to initiation systems in mammals. Pp. 3–20 in *Neurobiology of Vertebrate Locomotion*, S. Grillner, R. Herman, P. Stein, D. Stuart, eds. MacMillan Press, London.

McCrohan, C. R., and M. A. Kyriakides. 1989. Cerebral interneurones controlling feeding motor output in the snail *Lymnaea stagnalis*. *J. Exp. Biol.* **147**: 361–374.

Nagahama, T., and M. Takata. 1990. Neural mechanism generating firing patterns in jaw motoneurons during the food-induced response in *Aplysia kurodai*. II. Functional role of premotor neurons on generation of firing patterns in motoneurons. *J. Comp. Physiol. [A]* **166**: 277–286.

Rosen, S. C., M. W. Miller, K. R. Weiss, and I. Kupfermann. 1987. Control of buccal motor programs in *Aplysia* by identified neurons in the cerebral ganglion. *Soc. Neurosci. Abs.* **13**: 1060.

Rosen, S. C., M. W. Miller, K. R. Weiss, and I. Kupfermann. 1988. Activity of CBI-2 of *Aplysia* elicits biting-like responses. *Soc. Neurosci. Abs.* **14**: 608.

Rosen, S. C., K. R. Weiss, R. S. Goldstein, and I. Kupfermann. 1989a. The role of a modulatory neuron in feeding and satiation in *Aplysia*: effects of lesioning of the serotonergic metacerebral cells. *J. Neurosci.* **9**: 1562–1578.

Rosen, S. C., A. J. Susswein, E. C. Cropper, K. R. Weiss, and I. Kupfermann. 1989b. Selective modulation of spike duration by serotonin and the neuropeptides, FMRFamide, SCP_B, buccalin and myomodulin in different classes of mechanoafferent neurons in the cerebral ganglion of *Aplysia*. *J. Neurosci.* **9**: 390–402.

Susswein, A. J., K. R. Weiss, and I. Kupfermann. 1978. The effects of food arousal on the latency of biting in *Aplysia*. *J. Comp. Psychol.* **123**: 31–41.

Susswein, A. J., and J. H. Byrne. 1988. Identification and characterization of neurons initiating patterned neural activity in the buccal ganglion of *Aplysia*. *J. Neurosci.* **8**: 2049–2061.

Teyke, T., K. R. Weiss, and I. Kupfermann. 1989. A subpopulation of cerebral B cluster neurones of *Aplysia californica* is involved in defensive head withdrawal but not appetitive head movements. *J. Exp. Biol.* **147**: 1–20.

Teyke, T., K. R. Weiss, and I. Kupfermann. 1990a. *In vivo* firing pattern of the food arousal neuron CPR in *Aplysia*. *Soc. Neurosci. Abs.* **16**: 627.

Teyke, T., K. R. Weiss, and I. Kupfermann. 1990b. Appetitive feeding behavior of *Aplysia*: behavioral and neural analysis of directed head turning. *J. Neurosci.* **10**: 3922–3934.

Teyke, T., K. R. Weiss, and I. Kupfermann. 1990c. An identified neuron (CPR) evokes neuronal responses reflecting food arousal in *Aplysia*. *Science* **247**: 85–87.

Weiss, K. R., J. L. Cohen, and I. Kupfermann. 1978. Modulatory control of buccal musculature by a serotonergic neuron (metacerebral cell) in *Aplysia*. *J. Neurophysiol.* **41**: 181–203.

Weiss, K. R., U. T. Koch, J. Koester, S. C. Rosen, and I. Kupfermann. 1982. The role of arousal in modulating feeding behavior in *Aplysia*: neural and behavioral studies. Pp. 25–57 in *The Neural Basis of Feeding and Reward*, B. G. Hoebel, and D. Novin, eds. Haer Institute, Brunswick, ME.

Weiss, K. R., H. J. Chiel, U. Koch, and I. Kupfermann. 1986. Activity of an identified histaminergic neuron, and its possible role in arousal of feeding behavior in semi-intact *Aplysia*. *J. Neurosci.* **6**: 2403–2415.

Reference: *Biol. Bull.* **180**: 269–275. (April, 1991)

A Comparison of Bursting Neurons in *Aplysia*

A. ALEVIZOS[1,3], M. SKELTON[1], K. R. WEISS[1,2], AND J. KOESTER[1,2]

[1]*Center for Neurobiology and Behavior,* [2]*Department of Psychiatry, and* [3]*Department of Physiology and Cellular Biophysics, College of Physicians and Surgeons, Columbia University, 722 W. 168 St., New York, New York 10032*

Abstract. Five types of bursting neurons have been described in *Aplysia:* three types of individual bursters—the LUQ cells, L10, and R15, plus two types of population bursters—the bag cells and the R25/L25 cells. Individual bursters can burst without any synaptic input, while bursts generated by the population bursters are shaped largely by their synaptic interactions. In this paper we review what is known about the burst mechanisms of these five classes of neurons and attempt to relate them to the roles of the five cell types in the control of autonomic function.

Introduction

Molluscan neurons that have endogenous burst generating capabilities are useful experimental preparations for the study of burst generation and modulation. This is particularly true for *Aplysia.* Because the neural circuitry of *Aplysia* has been studied extensively, one can attempt to relate the functional properties of bursting neurons to their roles in the control of behavior, and to begin a comparative study of different types of bursters within the same organism. In this paper we will compare and contrast the burst mechanisms and functional roles of five different types of bursting neurons, all of which are found in the abdominal ganglion, and all of which have unique properties: the bag cells, the R25/L25 cells, cell L10, the LUQ cells, and cell R15. Particular attention is given to R15, which has been the focus of our recent studies. The interactions between these five classes of bursting cells, as well as some of their outputs, are shown schematically in Figure 1.

The Bag Cells

The neuroendocrine bag cells consist of two symmetrical clusters of about 400 neurosecretory cells each, which are strongly coupled to one another electrically. They have only one mode of firing—a synchronous population burst in all 800 cells that lasts approximately 15–30 min (Kupfermann and Kandel, 1970). This burst is necessary and sufficient to trigger normal egg laying behavior (Pinsker and Dudek, 1977; Dudek *et al.,* 1979). Oviposition is a complex, stereotyped behavior that lasts from one to a few hours and typically occurs at an interval of one or more days (Cobbs and Pinsker, 1982; Ferguson *et al.,* 1989). The physiological stimulus that triggers a population burst in the bag cells is unknown, but when the bag cells are excited experimentally, the intraburst firing frequency and the duration of the burst are independent of the intensity of the triggering stimulus (Kupfermann and Kandel, 1970). This all-or-none burst triggers the release of a dose of egg-laying hormone into the circulatory system. This hormone then initiates the release of mature oocytes from the ovotestis (Dudek *et al.,* 1980; Rothman *et al.,* 1983b). The population burst has an exceptionally long refractory period, lasting on the order of 18–24 h, which limits the rate of occurrence of egg laying (Kaczmarek and Kauer, 1983).

The all-or-none nature of the bag cell burst results from a positive feedback, reverberatory interaction within the population. In addition to releasing egg laying hormone, the bag cells also release three neuropeptides, α-, β-, and γ-bag cell peptides, which are autoexcitatory (Rothman *et al.,* 1983a; Brown and Mayeri, 1989). Even weak excitation of the bag cells can lead to an all-or-none burst, as the cells excite one-another by these slow, chemically mediated interactions. Not only do these peptides depolarize the bag cells, they also down-regulate voltage-sensitive K^+ channels and up-regulate Ca^{++} channels, rendering the cells more excitable and resulting in enhanced spike duration. These effects contribute to prolonging the burst, thus ensuring that a suprathreshold dose of egg-

Received 22 August 1990; accepted 6 November 1990.

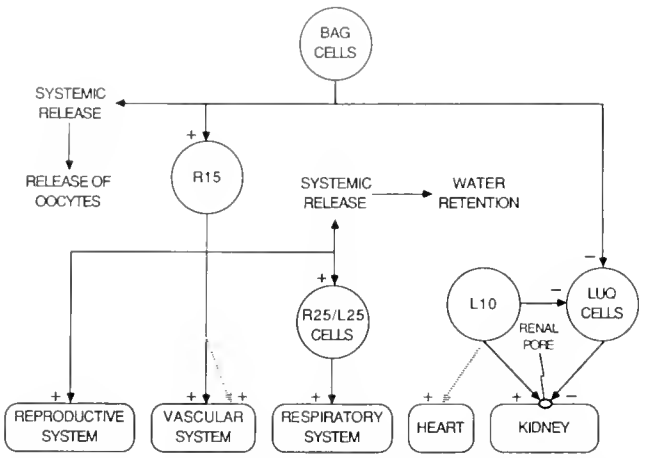

Figure 1. Summary of the interactions between bursting cells in the abdominal ganglion of *Aplysia*. The dashed lines represent indirect connections. The bag cells, L10, and the R25/L25 cells are known to make several other connections to neurons that are not shown here for simplicity (Koester and Kandel, 1977; Mayeri and Rothman, 1985; Segal and Koester, 1982).

laying hormone is released into the blood. These effects on ion channels are apparently mediated in part by activation of A-kinase and C-kinase (Strong and Kaczmarek, 1986; Strong *et al.*, 1987; De Riemer *et al.*, 1985; Conn *et al.*, 1988). An initial decrease in the levels of cyclic AMP, followed at a longer latency by a decrease in sensitivity to cyclic AMP, contribute to termination of the burst as well as to the refractory period that follows the burst (Kauer and Kaczmarek, 1985).

The R25/L25 Neurons

The R25 and L25 cells are two interconnected clusters of approximately 15 cells each, which act as trigger cells for respiratory pumping. They connect directly to the motoneurons that drive the behavior. A population burst in the R25/L25 network is necessary and probably sufficient for triggering the complete behavior (Byrne, 1983; Koester, 1989). Like egg laying, respiratory pumping often occurs episodically and in an all-or-none fashion (Pinsker *et al.*, 1970; Eberly and Pinsker, 1984). Unlike egg laying, each episode of respiratory pumping is brief, consisting of synchronous contractions of the mantle organs accompanied by heart inhibition (Pinsker *et al.*, 1970; Byrne and Koester, 1978). The motor effects typically last only 5–10 s. Individual episodes can occur spontaneously or in response to tactile or noxious stimuli (Pinsker *et al.*, 1970; Walters and Erickson, 1986). Respiratory pumping can also occur repetitively—either in a stationary rhythm with a period of a few minutes (unpub. obs.) or in a decelerating "seizure" pattern (Kanz and Quast, 1990). These repetitive episodes of respiratory pumping can occur spontaneously or in response to various environmental stimuli (Eberly *et al.*, 1981; Croll, 1985; Kanz and Quast, 1990). The functional significance of respiratory pumping appears to vary with the context in which it occurs. It has been hypothesized that respiratory pumping may function to enhance defensive withdrawal (Pinsker *et al.*, 1970), to expel defensive secretions or debris from the mantle cavity (Kupfermann and Kandel, 1969), to increase respiratory exchange (Byrne and Koester, 1978), or to contribute to the systemic circulation of hormones (Kanz and Quast, 1990).

The basic mechanism of burst generation in the R25/L25 network resembles that of the bag cells. Low frequency firing leads to a regenerative, all-or-none stereotyped burst that results from positive feedback interactions between cells in the R25/L25 network. Conventional facilitating chemical EPSPs, as well as electrical coupling, mediate these mutually excitatory connections. This positive feedback state can be accessed by two separate pathways—slow pacemaker potentials that are endogenous to the R25/L25 cells or excitatory chemical EPSPs that are generated by afferent input. Termination of the all-or-none population burst in these cells is mediated largely by synaptic interactions—slowly developing mutual synaptic inhibition and heterosynaptic depression of the mutually excitatory chemical connections (Byrne, 1983; Koester, 1989).

The LUQ Neurons

The left upper quadrant (LUQ) cells are a cluster of five similar neurons (Frazier *et al.*, 1967). A subset of the LUQ cells project to the kidney, where they ramify extensively. On the basis of their axonal projections they are thought to have extensive effects on kidney function. The only effects of these cells that have been examined in detail are on the renal pore, which they cause to close. The synaptic actions of the LUQ cells on this pore have very slow onsets and offsets, on the order of several seconds (Koester and Alevizos, 1989).

Unlike the bag cells and the R25/L25 cells, individual LUQ cells burst independently of one another. Their endogenous burst properties have been analyzed in detail (Kramer and Zucker, 1985a,b; Thompson *et al.*, 1986). The depolarizing pacemaker potential of each burst is initiated by the activation of voltage-dependent Ca^{++} channels. When the cell reaches action potential threshold, the Ca^{++} influx during each action potential causes a buildup of cytoplasmic free Ca^{++}, which has three effects. The initial effect is to activate Ca^{++}-dependent, non-specific cation-selective channels, which contribute to burst acceleration. Eventually the two slower effects of intracellular Ca^{++}-buildup predominate: (1) Ca^{++}-dependent inactivation of the Ca^{++} channels that initiated the depo-

larizing pacemaker potential leads to a phase of regenerative repolarization. (2) Activation of Ca^{++}-dependent K^+ channels also contributes to the repolarization, particularly at low temperatures.

Neuron L10

L10 also bursts endogenously (Kandel, 1976; Kleinfeld *et al.*, 1990). It is a multiaction interneuron and motoneuron that is thought to play a major role in integrating various aspects of renal function. It makes direct and indirect connections to the renal pore that oppose the synaptic actions of the LUQ cells—*i.e.*, it causes the pore to open. *In vitro* these openings occur at a rate of about one per minute. This peripheral antagonism is complemented by direct inhibitory projections from L10 to the LUQ cells. L10 also ramifies extensively in the kidney and is presumed to modulate other aspects of renal function (Koester and Alevizos, 1989). One way in which L10 may modulate renal excretion is by its excitatory connection to the heart excitatory motoneuron RB_{HE} (Koester *et al.*, 1974). The bulk filtration that gives rise to renal fluid is thought to occur within a specialized structure, the cristae aorta, which lies in series with the heart in the pericardial sac (Andrews, 1988). Therefore the increase in heart rate caused indirectly by L10 activity may increase renal filtration.

The mechanism that underlies spontaneous bursting in L10 has not been studied in detail. However, preliminary results suggest that many of the spikes that occur during a spontaneous burst are generated in peripheral axonal processes, far outside the ganglion (unpub. obs.).

Neuron R15

R15 is an endogenously bursting peptidergic neuron that is thought to play a role in integrating various aspects of egg laying. It was observed several years ago that spontaneous burst generation by R15 is enhanced by the bag cells when they fire in their population burst (Branton *et al.*, 1978). More recently, using an *in vitro* preparation, it has been found that R15 has several synaptic actions that may contribute to efficient egg laying behavior. (1) When R15 bursts spontaneously, it increases the frequency of respiratory pumping via its excitatory connections to the R25/L25 cells (Alevizos *et al.*, 1991a). (2) R15 causes contraction of the pleuroabdominal connectives by its excitatory connection to motoneuron L7 (Alevizos *et al.*, 1991b). (3) R15 increases the rate of anterograde peristalsis of the large hermaphroditic duct via its peripheral axonal processes (Alevizos *et al.*, 1991c). (4) R15 also sends processes to the left pedal-parapodial artery, by which it causes local vasoconstriction of this branch of the arterial tree (Skelton, in prep.).

It has been postulated that R15 integrates five different aspects of egg laying behavior: (1) The increase in respiratory pumping rate may enhance respiratory exchange (Alevizos *et al.*, 1991a). Alternatively, the vigorous pressure surges that occur in the arterial system as the result of gill contractions may assist in circulating egg laying hormone throughout the body (Kanz and Quast, 1990). (2) L7 is a multiaction excitatory neuron that connects to muscle in a variety of organs, as well as to neurons in the peripheral nervous system (reviewed by Umitsu *et al.*, 1987; Alevizos *et al.*, 1989). At the low rates of L7 firing elicited by R15 bursting *in vitro*, the only synaptic action that L7 expresses is excitation of the sheath muscle of the paired pleuroabdominal connectives. Each connective consists of a central axonal core surrounded by a connective tissue sheath that contains vascular channels into which the bag cells release their peptides and hormones. The accordion-like folding of the connectives in response to L7 activity may increase the fluid resistance of their vascular channels, thereby delaying the washout of the autoexcitatory peptides and ensuring that mutual excitation of the bag cells is maximally expressed (Alevizos *et al.*, 1991b). (3) The increase in peristalsis of the hermaphroditic duct presumably contributes to the mixing of the eggs with the secretory products of the duct, as well as assisting the cilia within the duct in moving the eggs to the caudal end of the genital groove (Alevizos *et al.*, 1991c). (4) The constriction of the left pedal/parapodial artery shunts arterial blood to the right pedal/parapodial artery, which perfuses the genital groove. Such an effect could help support the metabolic activity of the cilia lining the groove, which move the eggs several cm up the groove to its anterior orifice, from which they are deposited on the substrate. (5) In addition to its direct synaptic actions, R15 is also thought to have a neurosecretory action that influences water balance. R15 synthesizes R15α1 peptide, a 38 amino acid neuropeptide that causes an increase in net water retention when injected into the animal (Weiss *et al.*, 1989). R15 has numerous varicosities that appear to release into systemic vascular spaces (Rittenhouse and Price, 1985), leading to the suggestion that R15 may increase net water uptake when it is excited by the bag cells (Alevizos *et al.*, 1991c). Such an effect may be required to counter the water lost in egg formation, for the eggs are fertilized and packaged into gelatinous egg capsules on demand—*i.e.*, in response to the bag cell burst (Thompson, 1976). It will be necessary to record R15's firing pattern during spontaneous egg laying in the intact animal to determine the actual contributions of these different effects of R15 activity to egg laying behavior.

Each of the four direct synaptic actions of R15 can be mimicked by R15α1 peptide, and the peptide probably mediates them when R15 bursts. These synaptic actions are unusual in that they decay quite rapidly with repeated

activation of R15. An example of this synaptic decrement is shown in Figure 2, for the R15-R25/L25 connections. Prolonging the R15 burst period to greater than 10 min has no added effect on the excitation of the R25/L25 cells. The fact that the response of the R25/L25 cells to direct application of R15α1 peptide decreases in a similar fashion argues against depression of release being critical for the decrement in synaptic transmission. In addition, the R25/L25 cells respond normally to another excitatory transmitter when the response to R15 is depressed, ruling out non-specific refractoriness or postsynaptic inhibition as contributing to this synaptic decrement. Thus, postsynaptic desensitization appears to be the most likely explanation for the decay of R15's direct synaptic actions on the R25/L25 network. A similar conclusion is drawn from the actions of R15 on L7, on the hermaphroditic duct and on the arterial muscle. However, in the case of the two peripheral tissues, one cannot rule out muscular fatigue as a contributor to response decrement (Alevizos *et al.*, 1991c).

The direct synaptic actions of R15 are difficult to observe *in vitro* without taking special precautions. They are normally chronically depressed by the profound desensitization that results from the fact that R15 fires spontaneously at a high rate *in vitro*. Only if R15 is silenced by injecting hyperpolarizing current for 1–2 h does the desensitization decay, unmasking the four synaptic actions described above (Alevizos *et al.*, 1991a,b,c). This observation has two important implications. First, the synaptic actions of other spontaneously active neurons may be masked if they undergo profound depression. It may be necessary to silence such cells for a long time to restore their synaptic connections to a level where they can be detected. Second, the observation that R15's synaptic actions rapidly become completely depressed results in a paradox. How can these actions ever be expressed, given that R15 bursts continuously in *in vitro* experiments? Are its synaptic connections constantly desensitized? This question was addressed in chronic recording experiments, in which the axon of R15 was recorded from in intact, freely moving animals (Alevizos *et al.*, 1991a). It was found that R15 does not burst spontaneously in the intact animal (Fig. 3). Given that R15 is inactive in the intact animal and is excited by the bag cells *in vitro*, it has been suggested that R15 is a conditional burster that is switched to the bursting mode by the bag cell burst that triggers egg laying (Alevizos *et al.*, 1991a). Although preliminary results support this hypothesis, it has not yet been determined whether R15 fires during a spontaneous egg laying episode in the intact animal.

The mechanism that generates spontaneous bursts in R15 has been studied extensively (Adams, 1985; Adams and Levitan, 1985; Lewis, 1988; Thompson *et al.*, 1986). In its broad details it resembles the burst generating mechanism described above for the LUQ cells. Kramer and Levitan (1990) have demonstrated that modulation of R15 bursting by egg laying hormone is most effective when R15 is inactive, consistent with the observation that R15 is silent in the intact animal.

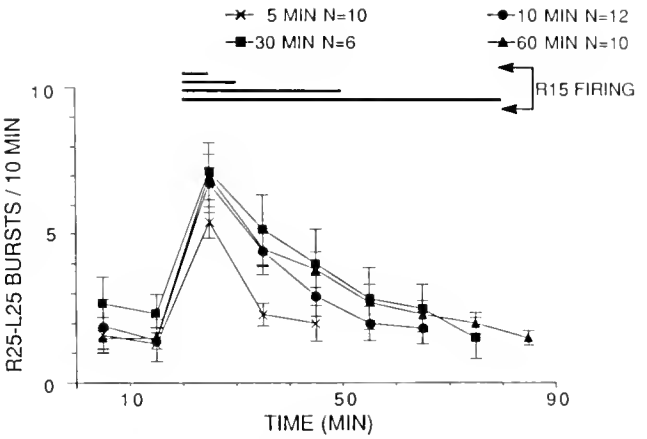

Figure 2. Modulation of the frequency of respiratory pumping by R15 decays during prolonged R15 activity. When R15 was allowed to burst spontaneously for various amounts of time after a 2-h period of hyperpolarization, it produced a long-lasting increase in the frequency of respiratory pumping. The amplitudes of the maximum effect and the time courses of decay of these increases were not significantly different for the 10-, 30-, and 60-min firing periods, while the effect produced by the 5-min firing was significantly smaller in both amplitude and duration. These data indicate that the maximum effect of R15 bursting is exerted within the first 5–10 min of R15 bursting, beyond which the response is independent of R15 activity. There was no trend for the firing rate of R15 to slow down over the course of the long burst periods (Alevizos *et al.*, 1991a).

Conclusions

It is interesting to see whether a comparison of these five types of bursting neurons leads to any conclusions about how the properties of each class relates to its functional role. Even with this relatively small sample of cell types, a few generalizations do emerge from such a comparison.

Is there a difference between individual bursters, which are not coupled to other bursting cells (L10, the LUQ cells, and R15) and population bursters, which fire as part of a population burst (the bag cells and the R25/L25 cells)? The two classes are alike in one respect—both individual bursters and population bursters can have endogenous pacemaker mechanisms (the LUQ cells, L10, R15 and the R25/L25 cells). They differ, however, in their ability to generate episodic bursts. In the *in vitro* preparations that have been examined so far, individual bursters do not seem to fire in isolated bursts. The population bursters (the bag cells and the R25/L25 cells), however, by virtue of the positive feedback chemical and electrical connec-

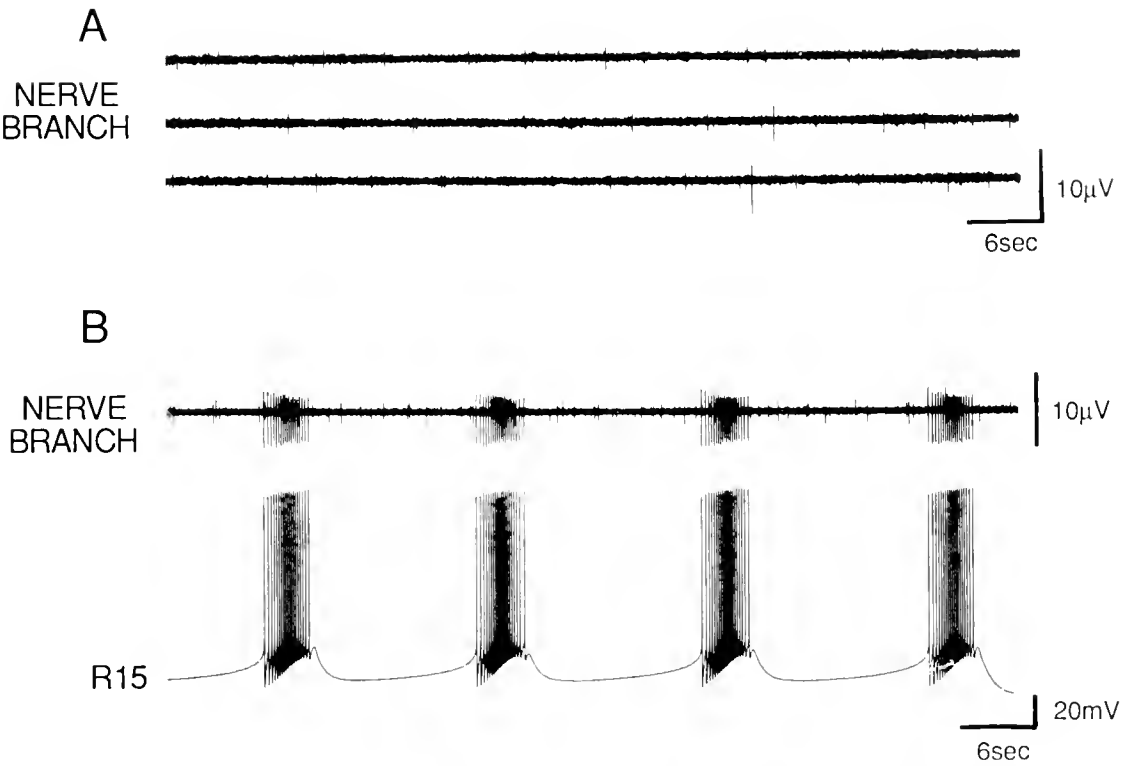

Figure 3. R15 does not burst spontaneously in the intact animal. An extracellular electrode chronically implanted in the subject was used to record activity from a small branch of the pericardial nerve that contains R15 processes. (A) In the intact animal there was no bursting activity of R15 recorded from the nerve branch. Three random 1.5-min samples are shown from a 2-h recording. (B) At the end of the experiment the animal was sacrificed, and the abdominal ganglion was dissected from the animal, along with the electrode still attached to the nerve branch. Bursting activity appeared in the nerve of the isolated ganglion. Intracellular recording from the R15 soma confirmed that the bursting activity in the nerve was due to R15 (n = 9) (Alevizos *et al.*, 1991a).

tions within each population, are well adapted to generate single bursts in response to brief volleys of excitatory synaptic input.

The excitatory and inhibitory chemical synaptic connections between members of a population of bursting cells also appear to extend the range of possible burst durations and intensities. While typical burst durations for the individual bursters are about 5–30 s (at 15°C), the bag cell bursts last 15–30 min. At the other extreme, although the burst duration of the R25/L25 network is quite variable, the high frequency terminal phase of the burst, which actually drives the motoneurons, lasts only 1–2 s. The excitatory synaptic connections between the R25/L25 cells also contribute significantly to the high firing frequencies that these cells attain during a burst—as high as 25–40 Hz. In contrast, individual bursters generally reach peak firing frequencies of only 1–3 Hz during a burst. The role of chemical connections in shaping the burst can also be extended to controlling the refractory period by the activation of second messenger systems that generate long-lasting effects. In the case of the bag cells, the refractory period can be made to last as long as 18–24 h in this way.

The shaping of the duration of the population bursts of the bag cells and the R25/L25 cells seems to have clear functional consequences. In the case of the bag cells, the long-lasting bursts with the gradual increase in spike width appear to provide a large safety margin for release of an effective dose of egg laying hormone into the circulation. For the R25/L25 cells, the very brief, high frequency burst is well suited for driving intense, synchronous contractions of the mantle organs, thereby optimizing the pumping action.

It is more problematic to understand the significance of the bursting patterns of the individual bursters. The bursts generated by one of them, L10, does have an obvious function. Each burst elicits a phasic opening of the renal pore. But whether the pore actually opens this way *in vivo* remains to be determined. In addition, it is not clear why the other two classes of individual bursters fire in a bursting mode. The synaptic actions generated by R15 and the LUQ cells are so slow that their follower

cells effectively integrate their firing patterns. That is, there is no reflection of the phasic bursting patterns of R15 and the LUQ cells on any of the nerve or muscle cells on which they synapse. This raises the question of why R15 and the LUQ cells burst, rather than firing in steady trains. Three possible explanations come to mind: (1) They may have other, more phasic synaptic actions. For example, R15 has transient synaptic actions on other neurons in the abdominal ganglion. These effects are not observed in all preparations, however, suggesting that they may be gated by some undetermined physiological variable (Alevizos and Koester, 1986; Brown and Mayeri; 1987). (2) The release properties of these cells may be such that brief bursts of activity are the most efficient for optimizing release. (3) Synaptic release in *Aplysia* is strongly influenced by the level of membrane potential immediately preceding initiation of an action potential. Hyperpolarization depresses release and depolarization enhances release (Shimahara and Peretz, 1978; Shapiro *et al.*, 1980). Perhaps the slow depolarizing waves of membrane potential that generate the bursts in these cells are conducted electrotonically to the terminals, where they may modulate spike-evoked release. However, it seems unlikely that such changes in resting potential would be conducted to terminals in the periphery. Therefore, a cell like R15, which makes both central and peripheral synapses, may have quite different release properties at its synapses within the ganglion compared to those in the periphery. If there does exist a difference between central and peripheral release sites, it may be amplified by modulatory inputs to R15 such as the one from the bag cells. When they fire in a population burst, the bag cells increase the depth of the depolarizing pacemaker waves recorded from the soma of R15 (Mayeri *et al.*, 1979). Thus, within the ganglion, the bag cells may influence release of peptides from R15 by two mechanisms: an increase in spike frequency and modulation of the slower membrane potential trajectory between bursts. The terminals in the periphery, however, are likely to experience only the increase in spike frequency.

Acknowledgments

This work was supported by NIH grant NS14385.

Literature Cited

Adams, W. B. 1985. Slow depolarizing and hyperpolarizing currents which mediate bursting in *Aplysia* neurone R15. *J. Physiol.* **360:** 51–68.

Adams, W. B., and I. B. Levitan. 1985. Voltage and ion dependence of the slow currents which mediate bursting in *Aplysia* neurone R15. *J. Physiol.* **360:** 69–93.

Alevizos, A., and J. Koester. 1986. Identified gill motoneuron L7 of *Aplysia* is a multimodal motoneuron that also innervates the cardiovascular system. *Soc. Neurosci. Abstr.* **12:** 499.

Alevizos, A., C. H. Bailey, M. Chen, and J. Koester. 1989. Innervation of vascular and cardiac muscle of *Aplysia* by multimodal motoneuron L7. *J. Neurophysiol.* **61:** 1053–1063.

Alevizos, A., K. R. Weiss, and J. Koester. 1991a. Synaptic actions of identified peptidergic neuron R15 in *Aplysia*: I. Activation of respiratory pumping. *J. Neurosci.* (in press).

Alevizos, A., K. R. Weiss, and J. Koester. 1991b. Synaptic actions of identified peptidergic neuron R15 in *Aplysia*. II. Contraction of pleuroabdominal connectives mediated by motoneuron L7. *J. Neurosci.* (in press).

Alevizos, A., K. R. Weiss, and J. Koester. 1991c. Synaptic actions of identified peptidergic neuron R15 in *Aplysia*: III. Activation of the large hermaphroditic duct. *J. Neurosci.* (in press).

Andrews, E. B. 1988. Excretory systems of molluscs. Pp. 381–448 in *The Mollusca*, Vol. 11, A. S. M. Saleuddin and K. M. Wilbur, eds. Academic Press, Inc., New York.

Branton, D. W., E. Mayeri, P. Brownell, and S. S. Simon. 1978. Evidence for local hormonal communication between neurones in *Aplysia*. *Nature* **274:** 70–72.

Brown, R. O., and E. Mayeri. 1987. Central actions of R15, a putative peptidergic neuron in *Aplysia*. *J. Neurobiol.* **18:** 3–13.

Brown, R. O., and E. Mayeri. 1989. Positive feedback by autoexcitatory neuroendocrine bag cells of *Aplysia*. *J. Neurosci.* **9:** 1443–1451.

Byrne, J. 1983. Identification and initial characterization of a cluster of command and pattern-generating neurons underlying respiratory pumping in *Aplysia californica*. *J. Neurophysiol.* **49:** 491–508.

Byrne, J., and J. Koester. 1978. Respiratory pumping: neuronal control of a centrally commanded behavior in *Aplysia*. *Brain Res.* **143:** 87–105.

Cobbs, J. S., and H. M. Pinsker. 1982. Role of bag cells in egg deposition of *Aplysia brasiliana*. I. Comparison of normal and elicited behaviors. *J. Comp. Physiol.* **147:** 523–535.

Conn, P. J., J. S. Strong, E. M. Azhderian, A. C. Nairn, P. Greengard, and L. K. Kaczmarek. 1988. Protein kinase inhibitors selectively block phorbol ester or forskolin-induced changes in excitability of *Aplysia* neurons. *J. Neurosci.* **9:** 480–487.

Croll, R. P. 1985. Sensory control of respiratory pumping in *Aplysia californica*. *J. Exp. Biol.* **117:** 15–27.

De Riemer, S. A., J. A. Strong, K. A. Albert, P. Greengard, and L. K. Kaczmarek. 1985. Enhancement of calcium current in *Aplysia* neurons by phorbol ester and protein kinase C. *Nature* **313:** 313–316.

Dudek, F. E., J. S. Cobbs, and H. M. Pinsker. 1979. Bag cell electrical activity underlying spontaneous egg laying in freely behaving *Aplysia brasiliana*. *J. Neurophysiol.* **42:** 804–817.

Dudek, F. E., G. Weir, J. Acosta-Urquidi, and S. S. Tobe. 1980. A secretion from neuroendocrine bag cells evokes release *in vitro* from ovotestis of *Aplysia californica*. *Gen. Comp. Endocrinol.* **40:** 241–244.

Eberly, L., J. Kanz, C. Taylor, and H. Pinsker. 1981. Environmental modulation of a central pattern generator in freely behaving *Aplysia*. *Behav. Neural Biol.* **32:** 21–34.

Eberly, L. B., and H. M. Pinsker. 1984. Neuroethological studies of reflex plasticity in intact *Aplysia*. *Behav. Neurosci.* **98:** 609–630.

Ferguson, G. P., A. Ter Maat, D. W. Parsons, and H. M. Pinsker. 1989. Egg laying in *Aplysia*: I. Behavioral patterns and muscle activity of freely behaving animals after selectively elicited bag cell discharges. *J. Comp. Physiol. A* **164:** 835–847.

Frazier, W. T., E. R. Kandel, I. Kupfermann, R. Waziri, and R. E. Coggeshall. 1967. Morphological and functional properties of identified neurons in the abdominal ganglion of *Aplysia californica*. *J. Neurophysiol.* **30:** 1288–1351.

Kaczmarek, L. K., and J. A. Kauer. 1983. Calcium entry causes a prolonged refractory period in peptidergic neurons of *Aplysia*. *J. Neurosci.* **3:** 2230–2239.

Kandel, E. R. 1976. *The Cellular Basis of Behavior* Freeman, San Francisco.

Kanz, J. E., and W. D. Quast. 1990. Respiratory pumping seizure: a newly discovered spontaneous stereotyped behavior pattern in the opisthobranch mollusc *Aplysia californica*. *J Comp. Physiol. A* **166:** 619–627.

Kauer, J. A., and L. K. Kaczmarek. 1985. Peptidergic neurons of *Aplysia* lose their response to cAMP during a prolonged refractory period. *J. Neurosci.* **5:** 1339–1345.

Kleinfeld, D., T. D. Parsons, F. Raccuia-Behling, B. M. Salzberg, and A. L. Obaid. 1990. Foreign connections are formed *in vitro* by *Aplysia californica* interneurone L10 and its *in vivo* followers and non-followers. *J. Exp. Biol.* **154:** 237–255.

Koester, J. 1989. Chemically and electrically coupled interneurons mediate respiratory pumping in *Aplysia*. *J. Neurophysiol.* **62:** 1113–1126.

Koester, J., and A. Alevizos. 1989. Innervation of the kidney of *Aplysia* by L10, the LUQ cells, and an identified peripheral motoneuron. *J. Neurosci.* **9:** 4078–4088.

Koester, J., and E. R. Kandel. 1977. Further identification of neurons in the abdominal ganglion of *Aplysia* using behavioral criteria. *Brain Res.* **121:** 1–20.

Koester, J., E. Mayeri, G. Liebeswar, and E. R. Kandel. 1974. Neural control of circulation in *Aplysia*. II. Interneurons. *J. Neurophysiol.* **37:** 476–496.

Kramer, R. H., and R. S. Zucker. 1985a. Calcium-dependent inward current in *Aplysia* bursting pacemaker neurones. *J. Physiol* **362:** 107–130.

Kramer, R. H., and R. S. Zucker. 1985b. Calcium-induced inactivation of calcium current causes the inter-burst hyperpolarization of *Aplysia* bursting neurones. *J Physiol.* **362:** 131–160.

Kramer, R. H., and I. B. Levitan. 1990. Activity-dependent neuromodulation in *Aplysia* neuron R15: intracellular calcium antagonizes neurotransmitter responses mediated by cAMP. *J. Neurophysiol.* **63:** 1075–1088.

Kupfermann, I., and E. R. Kandel. 1969. Neuronal controls of a behavioral response mediated by the abdominal ganglion of *Aplysia*. *Science* **164:** 847–850.

Kupfermann, I., and E. R. Kandel. 1970. Electrophysiological properties and functional interconnections of two symmetrical neurosecretory clusters (bag cells) in abdominal ganglion of *Aplysia*. *J. Neurophysiol* **33:** 865–876.

Lewis, D. V. 1988. Calcium-activated inward spike after-currents in bursting neurone R15 of *Aplysia*. *J Physiol* **396:** 285–302.

Mayeri, E., P. Brownell, W. D. Branton, and S. B. Simon. 1979. Multiple, prolonged actions of neuroendocrine bag cells on neurons in *Aplysia*. I. Effects on bursting pacemaker neurons. *J. Neurophysiol.* **42:** 1165–1184.

Mayeri, E., and B. S. Rothman. 1985. Neuropeptides and the control of egg-laying behavior in *Aplysia*. Pp. 285–301 in *Model Neural Networks and Behavior*, A. I. Selverston, ed. Plenum Press, New York.

Pinsker, M. H., and F. E. Dudek. 1977. Bag cell control of egg laying in freely behaving *Aplysia*. *Science* **197:** 490–493.

Pinsker, H., I. Kupfermann, V. Castellucci, and E. R. Kandel. 1970. Habituation and dishabituation of the gill-withdrawal reflex in *Aplysia*. *Science* **167:** 1740–1742.

Rittenhouse, A. R., and C. H. Price. 1985. Peripheral axons of the parabolic burster neuron R15. *Brain Res.* **333:** 330–335.

Rothman, B. S., E. Mayeri, R. O. Brown, P.-M. Yuan, and J. E. Shively. 1983a. Primary structure and neuronal effects of alpha-bag cell peptide, a second candidate neurotransmitter encoded by a single gene in bag cell neurons of *Aplysia*. *Proc. Nat. Acad. Sci. USA* **80:** 5753–5757.

Rothman, B. S., G. Weir, and F. E. Dudek. 1983b. Egg laying hormone: direct action on the ovotestis of *Aplysia*. *Gen. Comp. Endocrinol.* **52:** 131–141.

Segal, M. M., and J. Koester. 1982. Convergent cholinergic neurons produce similar postsynaptic actions in *Aplysia*: implications for neural organization. *J. Neurophysiol* **47:** 742–759.

Shapiro, E., V. F. Castellucci, and E. R. Kandel. 1980. Presynaptic membrane potential affects transmitter release in an identified neuron in *Aplysia* by modulating the Ca^{++} and K^{+} currents. *Proc. Nat. Acad. Sci. USA* **77:** 629–633.

Shimahara, T., and B. Peretz. 1978. Some potential of an interneurone controls transmitter release in a monosynoptic pathway in *Aplysia*. *Nature* **273:** 158–160.

Strong, J. A., and L. K. Kaczmarek. 1986. Multiple components of delayed potassium current in peptidergic neurons of *Aplysia*: modulation by an activator of adenylate cyclase. *J. Neurosci.* **6:** 814–822.

Strong, J. A., A. P. Fox, R. W. Tsien, and L. K. Kaczmarek. 1987. Stimulation of protein kinase C recruits covert calcium channels in *Aplysia* bag cell neurons. *Nature* **325:** 714–717.

Thompson, T. E. 1976. *Biology of Opisthobranch Molluscs*. Vol. I. The Ray Society, London.

Thompson, S., S. J. Smith, and J. W. Johnson. 1986. Slow outward currents in molluscan bursting pacemaker neurons: two components differing in temperature selectivity. *J. Neurosci.* **6:** 3169–3176.

Umitsu, Y., H. Matsumoto, and H. Koike. 1987. Active contraction of nerve bundle and identification of a nerve-contractor motoneuron in *Aplysia*. *J. Neurophysiol.* **58:** 1016–1034.

Walters, E. T., and M. T. Erickson. 1986. Directional control and the functional organization of defensive responses in *Aplysia*. *J. Comp. Physiol. A* **159:** 339–351.

Weiss, K. R., H. Bayley, P. E. Lloyd, R. Tenenbaum, M. A. Gawinowicz Kolks, L. Buck, E. C. Cropper, S. C. Rosen, and I. Kupfermann. 1989. Purification and sequencing of neuropeptides contained in neuron R15 of *Aplysia californica*. *Proc. Nat. Acad. Sci. USA* **86:** 2913–2917.

Reference: *Biol. Bull.* **180**: 276–283. (April, 1991)

Contraction, Serotonin-Elicited Modulation, and Membrane Currents of Dissociated Fibers of *Aplysia* Buccal Muscle

JEFFREY L. RAM, FENG ZHANG, AND LI-XIN LIU

Department of Physiology, Wayne State University, Detroit, Michigan 48201

Abstract. Feeding muscles of the buccal mass of *Aplysia* are innervated by cholinergic and serotonergic neurons. Buccal muscle I5 contracts in response to acetylcholine (ACh). During feeding arousal, ACh-elicited contraction of muscle I5 is potentiated by serotonin (5-HT). This paper demonstrates a dissociated cell preparation of muscle I5 in which cellular mechanisms regulating contraction can be investigated.

Dissociated muscle fibers contracted in response to both KCl and ACh. Serotonin (10^{-6} *M*) significantly potentiated the shortening caused by both KCl and ACh. Potentiation lasted at least 4 min, similar to potentiation in intact muscles.

Four types of currents recorded by patch clamp methods are illustrated. With 540 m*M* KCl in the patch electrode, stretch-activated channels having a chord conductance of 150 pS are observed in on-cell patches. In whole cell configuration, ACh elicits inward current at a holding potential of −60 mV. With high potassium in the electrode, depolarization elicits an outward current. The voltage-dependent outward current is blocked with cesium in the electrode and 4-aminopyridine and tetraethylammonium outside the cells. The remaining voltage-dependent inward current is calcium dependent. The voltage-dependent inward and outward currents are activated within the range of depolarization produced by ACh and may therefore play roles in regulating contractile responses elicited by ACh.

Introduction

Neurotransmitters can cause both direct and modulatory effects on target tissues. A "modulatory effect" of a neurotransmitter is one in which the transmitter has no immediate effect, but rather, it modifies the influence of other effectors. These modulatory influences appear to fine-tune the nervous system and the muscles it controls for switching between different behavioral tasks. The same circuits can subserve several different behaviors; the behavioral output depends on the relative weighting of different synapses and the excitability of circuit elements. Modulation of muscle is part of this integrated scheme. Although the relative strength of contractions appropriate for different behaviors could be manipulated by discrete relative changes in motoneuron activity, an additional, possibly more efficient method may be to give different "global commands" that change the relative strengths of contractile responses in ways appropriate for particular behaviors. An example of a modulatory effect of a neurotransmitter mediating a change in behavior is the potentiating effect of serotonin (5-HT) on buccal mass muscles of *Aplysia*, which is believed to mediate, in part, feeding arousal.

The buccal mass muscles of *Aplysia* are smooth muscles used in voluntary feeding movements. These muscles are innervated by cholinergic, peptidergic, and serotonergic neurons. Acetylcholine (ACh) is the direct effector of these muscles, as exemplified by the contractile response to ACh of buccal muscle I5. Muscle I5, also known as the accessory radular closer muscle (Cohen *et al.*, 1978), is the most intensively studied *Aplysia* muscle. I5 is innervated by buccal ganglion neurons B15 and B16 (Cohen *et al.*, 1978; Ram, 1983), both of which synthesize ACh (Cohen *et al.*, 1978) as well as several peptides (Cropper *et al.*, 1987, 1988). In addition, I5 is innervated by the serotonergic metacerebral giant cell (MCG). Activity of MCG causes no direct response of the muscle; however, it potentiates subsequent contractile responses to B15 and B16. This modulation is achieved largely through post-synaptic actions on the muscle (Weiss *et al.*, 1978). In isolated I5

Received 9 August 1990; accepted 6 November 1990.

Figure 1. Typical dissociated buccal muscle fiber. At the right is a patch electrode pointing to the fiber. Scale: calibration marks are 7.8 μm apart.

muscles 5-HT produces no contractile response itself but does potentiate ACh-elicited contractions (Ram *et al.*, 1981). MCGs are active during feeding (Weiss *et al.*, 1978). Lesion of serotonergic neurons changes (although does not completely block) feeding motor activity (Rosen *et al.*, 1983, 1989). Thus, the modulatory effect of the serotonergic MCG neurons on feeding muscles appears to have an important role in feeding arousal.

Although previous experiments on mechanisms mediating the modulatory effect of 5-HT on buccal muscles have suggested roles for cyclic AMP (Mandelbaum, 1980; Ram *et al.*, 1983, 1984a) and calcium (Ram *et al.*, 1984b; Ram and Parti, 1985), the cellular targets of these mediators have not been determined. For example, it is unknown whether cyclic AMP or calcium modify membrane mechanisms such as ion channels or change the sensitivity or activity of contractile proteins. For studying effects on contractile proteins, this laboratory developed a skinned muscle preparation, which is described elsewhere (Ram and Patel, 1989). To study membrane mechanisms, we developed a dissociated muscle fiber preparation. This paper describes the contractile properties of this dissociated muscle preparation, including its modulatory response to 5-HT, and demonstrates its suitability for patch clamp analysis of single channel and whole cell ionic currents. Preliminary descriptions of some of these data have appeared previously (Ram and Liu, 1990; Zhang and Ram, 1990).

Materials and Methods

Individuals of *Aplysia californica* (200–400 g) were obtained from Marinus (Long Beach, California) and maintained at 18°C in Instant Ocean with a 12:12 L:D light cycle. To obtain dissociated muscle fibers, a modification of the methods of Ishii *et al.* (1986), previously used to dissociate muscle fibers in *Mytilus*, was used. Both I5 buccal muscles were dissected from the animal, teased into thin strips, and incubated for 2–4 h at 28°C in Instant Ocean containing 10 m*M* HEPES (pH 7.0, adjusted with NaOH), 0.15% collagenase (Sigma Type I), 0.1% soybean trypsin inhibitor (Sigma Type I-S), and 1 μg/ml leupeptin

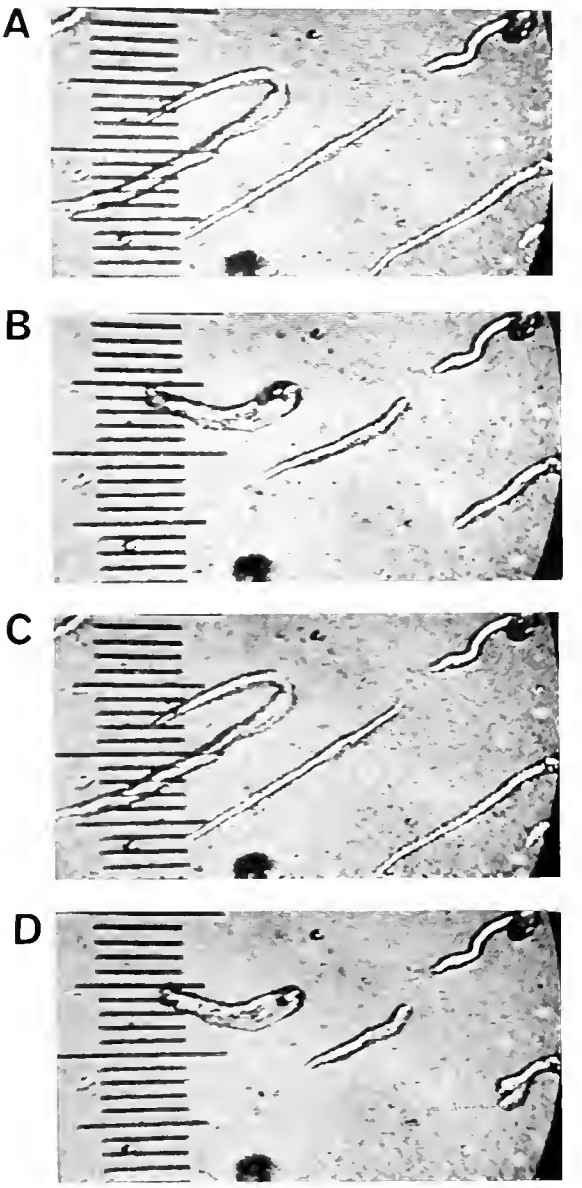

Figure 2. Serotonin (5-HT) potentiates high potassium-elicited contraction. Dissociated muscle fibers in a small chamber (0.4 ml volume) were constantly superfused with artificial seawater (ASW) at 5.5 ml/min. (A) Fibers at rest. (B) Contractile response to a 3-s pulse of ASW containing 100 m*M* KCl. All but the fiber in the upper right contracted. Fibers returned to rest length at the end of the pulse of KCl. (C) Fibers at the end of 1 min superfusion with ASW containing 10^{-6} *M* 5-HT. Fibers remained at rest length. (D) Contractile response to a 3-s pulse of 100 m*M* KCl ASW, identical to that given in (B), immediately after 1 min superfusion with 10^{-6} *M* 5-HT ASW. All contracting fibers shortened more after 5-HT treatment. Scale: calibration marks are 12 μm apart.

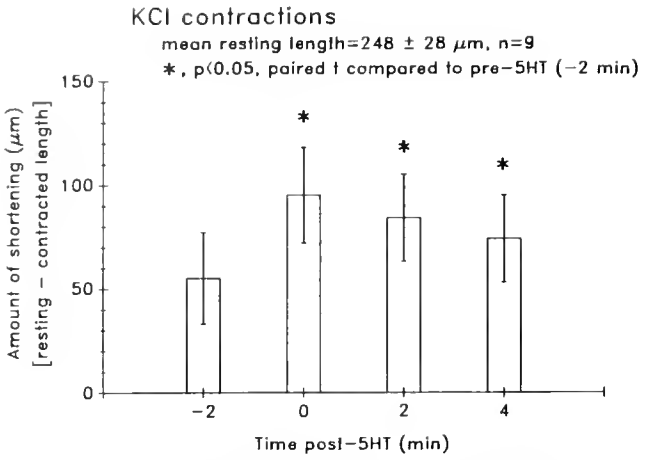

Figure 3. Magnitude and time course of 5-HT potentiation of KCl-elicited contractions. Fibers were measured in images similar to those illustrated in Figure 2. High potassium (100 m*M* KCl ASW) pulses were given every two min. Fibers were exposed to 5-HT (10^{-6} *M* in ASW) for 1 min immediately prior to the 0 time point.

(Sigma). When cells began appearing in the medium, fibers in remaining muscle pieces were dispersed by gentle trituration. The resultant dissociated cells were washed by centrifuging and resuspending them in wash medium containing all ingredients of the dissociating medium except collagenase. Washed cells were plated onto glass coverslips in 30-mm plastic petri dishes and stored at 4°C in a humidified chamber. Cells were usually used within 1–4 days, although viable, contractile cells have survived for as long as 10 days under these conditions. Experiments were done at room temperature (20–24°C) after allowing the cells to warm gradually for at least 30 min.

A plexiglass insert having a central hole approximately 1 cm in diameter was clamped into the 30-mm petri dish. The insert formed a small chamber, approximately 0.4 ml in volume. Medium was constantly pumped into the chamber (5.5 ml/min) and removed by suction from a surface wick opposite the inflow. The dish was mounted on a movable stage of an inverted microscope. The shape and movement of muscle fibers were recorded by a VHS camcorder (RCA CC310). A videotape demonstrating many of the contractile and electrophysiological responses reported in this paper ("Dissociated Muscle Fibers of *Aplysia*," by J. L. Ram) is available from the authors upon request. Morphometric analysis was done by measuring still-images on the tape playback. Photographs were made by oscilloscope camera directly off the TV monitor.

A Dagan 8900 Patch Clamp-Whole Cell Clamp was used for single channel and whole cell recording. Data were filtered by the 1 kHz low-pass filter in the Dagan amplifier. Electrodes were fabricated from Fisher non-heparinized hematocrit glass, polished to bubble number 3–4 (Corey and Stevens, 1985), and coated with Sylgard. Pipet solutions are described in relevant figure captions. Electrical stimuli and digital recording of currents were controlled by pCLAMP software (Axon Instruments, Burlingame, California).

Results

Morphology and contraction

The typical appearance of a dissociated fiber from buccal muscle I5 is illustrated in Figure 1. Dissociated muscle fibers were spindle-shaped and ranged from 5 to 25 μm in diameter and up to a mm in length. The widest diameter usually occurred near the middle of the fiber, adjacent to the nucleus, and averaged 13.6 ± 0.9 μm (mean ± S.E., n = 19). The average diameter of the fibers, measured every 20 μm along the length of the fiber, was 10.8 ± 0.7 μm. The average length of fibers at rest was 270 ± 10 μm (n = 37).

Dissociated muscle fibers contracted in response to KCl. In response to a 2- or 3-s pulse of ASW containing 100 m*M* KCl, 22 fibers that had average resting lengths of 262 ± 13 μm shortened to 218 ± 12 μm. An illustration of a subset of these fibers is shown in Figure 2, in which Figure 2A shows the fibers at rest and Figure 2B shows the max-

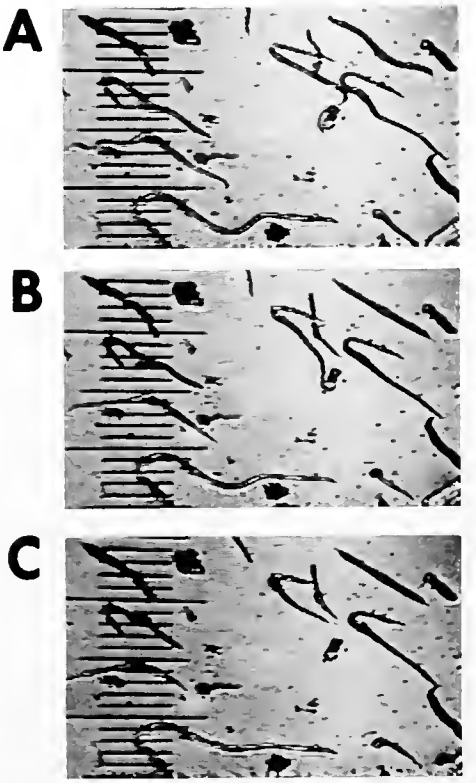

Figure 4. Serotonin (5-HT) potentiates ACh-elicited contractions. The procedure is identical to that of Figure 2 except that contraction was elicited by a 3-s pulse of 10^{-4} *M* ACh. (A) Fibers at rest. (B) Contractile response to ACh. (C) Contractile response to identical pulse of ACh as in (B) immediately after 1 min superfusion with 10^{-6} *M* 5-HT ASW. Scale: calibration marks are 20 μm apart.

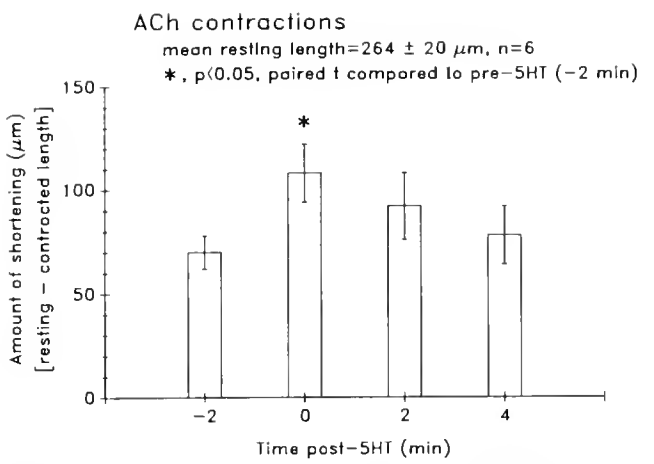

Figure 5. Magnitude and time course of 5-HT potentiation of ACh-elicited contractions. Fibers were measured on the field in Figure 4 and subsequent images. ACh pulses were given every 2 min. Fibers were exposed to 5-HT (10^{-6} *M* in ASW) for 1 min immediately prior to the 0 time point.

imal contraction produced by a 3-s pulse of KCl. Following the KCl pulse, fibers relaxed to their resting lengths within a few seconds.

Serotonin potentiated the contractile response to KCl (Fig. 2D). Figure 3 summarizes data from nine fibers that were exposed to 10^{-6} *M* 5-HT for 1 min. The amount of shortening produced by KCl pulses was almost doubled following 5-HT, and the effect lasted at least 4 min, similar to the long-lasting potentiation in intact muscles produced by 5-HT (Ram *et al.*, 1981). The fibers remained relaxed during the 5-HT application (Fig. 2C).

Similarly, ACh caused contraction of dissociated fibers, which could be potentiated by 5-HT. Figure 4 shows ACh-elicited contractions prior to 5-HT and immediately following one min 10^{-6} *M* 5-HT. Data from six fibers, summarized in Figure 5, show the significant increase in shortening caused by 5-HT and the similar time course of recovery from the effects of 5-HT to KCl-elicited contractions.

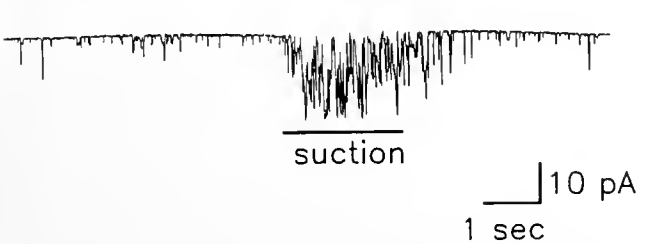

Figure 6. Channel activity in on-cell patches. The electrode contained (in m*M*) 406 KCl, 20 NaCl, 2 $MgCl_2$, 10 ATP, 0.1 GTP, 10 glutathione, and 100 HEPES, pH 7.0 with KOH. Electrode potential was identical to the bath potential, and the cell was at resting potential (not measured for this cell). Suction increased the opening of at least one population of large channels, conducting approximately 10 pA per unitary channel opening.

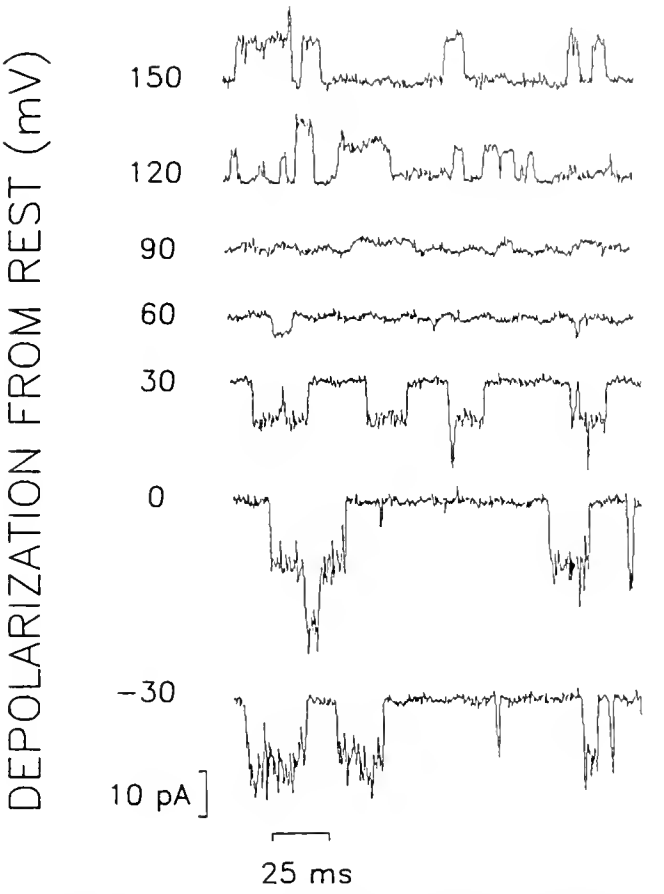

Figure 7. Current through stretch-activated channels in an on-cell patch, measured over a range of membrane potentials. The electrode contained 540 m*M* KCl. Stretch sensitivity of these channels was demonstrated during another part of the experiment (not illustrated here). Membrane potential was varied by changing the potential of the patch electrode, and the membrane potential is given as the change from resting potential. Pipet potential was held at each potential for at least 20 s. Channel current reversed at approximately 87 mV; chord conductance was approximately 150 pS; and channel opening probability was independent of membrane potential.

Single channel and whole cell patch clamp recording

Dissociated buccal muscle fibers were suitable for forming gigaseals for single channel and whole cell recording. With high potassium in the patch electrode, on-cell patches revealed the presence of a variety of channels conducting inward current at resting potential, including at least one prominent channel that could be activated by increased suction on the electrode (Fig. 6). The frequency of the opening of suction-activated channels increased with negative pressures of 50–100 cm H_2O (approximately 40–80 mm Hg), as measured by a water manometer (n = 3; see also Ram *et al.*, 1990). The current through unitary channel openings of the most prominent channel activated by suction, with the fiber at resting potential and the electrode at bath potential, averaged 12 ± 1 pA (n = 7 patches). The chord conductance of this

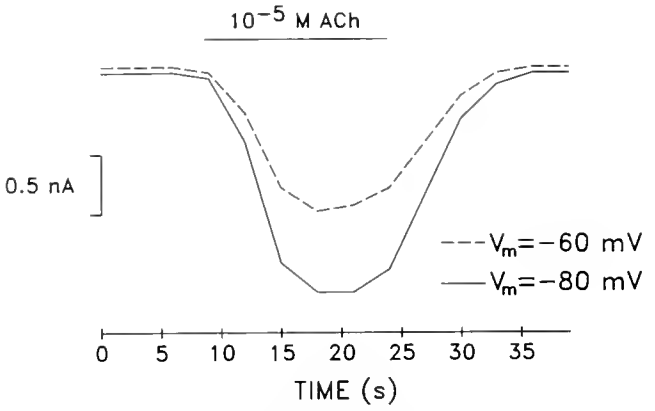

Figure 8. Response to ACh in whole-cell recording configuration. Pipet solution contained (in m*M*) 20 NaCl, 406 KCl, 2 $MgCl_2$, 100 HEPES, 5 EGTA, 5 MgATP, 0.1 NaGTP, 10 glutathione, pH 7.0 (adjusted with KOH). Fibers were constantly superfused with artificial seawater. Holding potential was −80 mV and was moved to −65 mV every 3 s. A 15-s pulse of 10^{-5} *M* ACh elicited inward current at both membrane potentials.

suction-activated channel, determined by eliciting channel activity at several different holding potentials, averaged 140 ± 20 pS (n = 3), as exemplified by the patch illustrated in Figure 7.

After gigaseal formation, whole cell configuration could be achieved by applying greater suction than is necessary to activate suction-activated channels. With a pipet solution containing high potassium and other ingredients meant to mimic the normal intracellular milieu of the fibers (complete composition is given in the caption to Fig. 8), ACh elicited an inward current (Fig. 8). The peak current elicited by 10^{-5} *M* ACh at a holding potential of −80 mV was −2.4 ± 0.5 nA (n = 20); at a holding potential of −60 mV, the peak current averaged −1.4 ± 0.4 nA (n = 20). Under the same ionic conditions, depolarization activated outward current (Fig. 9). In observations of more than 20 cells, a net voltage dependent inward current was never seen under conditions of having high potassium in the pipet and normal sea water outside. Occasionally, there was a slight delay in activation of outward current (not seen in Fig. 9), possibly indicating an initial counterbalancing inward current.

Voltage-dependent inward current can, however, be seen under conditions that block potassium channels. With cesium in the electrode and 4-aminopyridine and tetraethylammonium in the extracellular solution, depolarization elicited an inward current. The peak inward current averaged 2.4 ± .4 nA (n = 11 fibers). As illustrated in Figure 10, the voltage dependent inward current was dependent upon calcium in the extracellular medium.

Discussion

This paper demonstrates that smooth muscle fibers dissociated from buccal muscles of *Aplysia* are a suitable preparation for studying mechanisms regulating contraction and its modulation. First, isolated fibers have appropriate contractile responses: They contract in response to both high potassium and ACh, and the contractions to both are potentiated by 5-HT. Second, the dissociated fibers are suitable for patch clamp analysis of single channel and whole cell currents.

Previous studies have used indirect methods for investigating the roles of specific ion channels in regulating contraction of molluscan muscles. One set of questions that arise concerns the sources of activator calcium in the physiological responses to neurotransmitters. Is contraction dependent upon the influx of extracellular calcium? If so, are the channels receptor operated or voltage dependent, and are they specific for calcium? Many molluscan muscles are highly dependent upon extracellular calcium to trigger contraction. For example, ACh-elicited contractions of buccal muscle E1 (another muscle of the *Aplysia* buccal musculature whose contraction is potentiated by 5-HT) fail within two minutes of removal of extracellular calcium (Ram *et al.*, 1984b). Similarly, calcium-dependence of ACh-elicited contractions have also been demonstrated in a non-spiking muscle of *Aplysia* gill (Reilly and Peretz, 1987) and in four different pro-

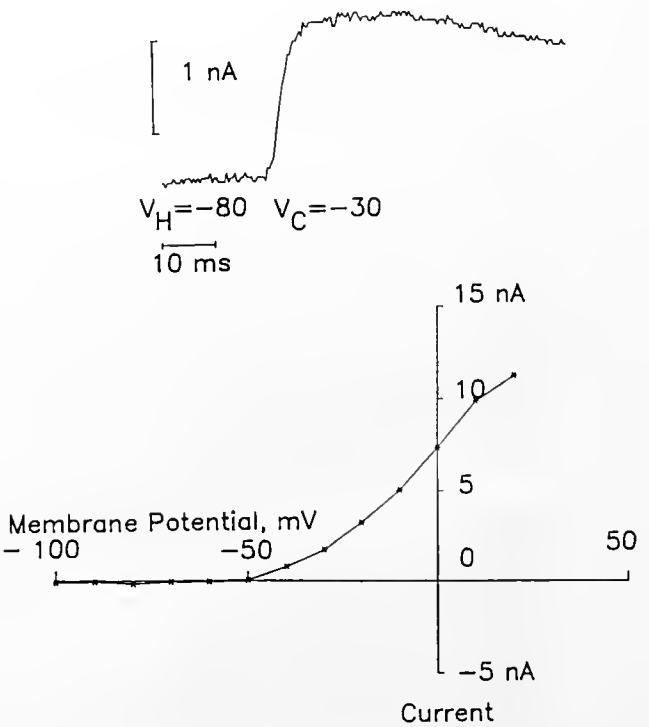

Figure 9. Voltage-dependent outward current in whole-cell configuration. Pipet solution and external medium were the same as in Figure 8. Holding potential was −80 mV. Currents were elicited by 60-ms pulses to various potentials, from −100 mV to +20 mV, given at intervals of 1.2 s. Linear leak and capacitative transients have been subtracted. (Upper) Typical response to −30 mV. (Lower) Current voltage relationship for peak current during the pulse.

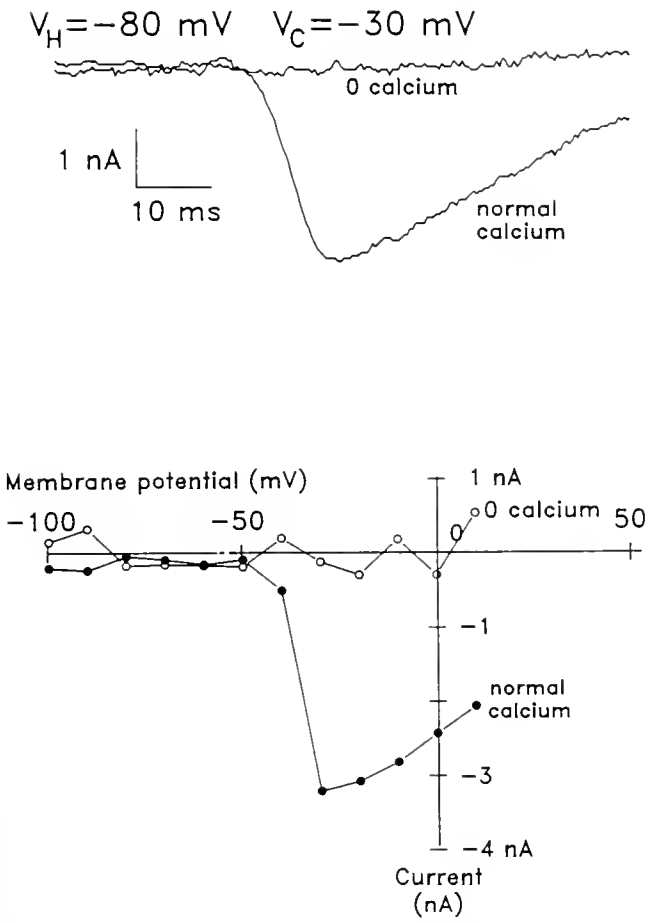

Figure 10. Voltage-dependent calcium current in whole-cell configuration. Pipet solution contained (in m*M*) 20 NaCl, 406 CsCl, 2 $MgCl_2$, 100 HEPES, 5 EGTA, 5 MgATP, 0.1 NaGTP, 10 glutathione, pH 7.0 (adjusted with CsOH). External medium was artificial seawater containing (in m*M*) 50 tetraethylammonium, 5 4-aminopyridine, 485 NaCl, 25 $MgSO_4$, 25 $MgCl_2$, 10 KCl, 10 $CaCl_2$, and 10 HEPES, pH 7.8 (adjusted with NaOH). For 0 calcium medium, the $CaCl_2$ was left out and all other ingredients increased in concentration by 1%. Holding potential was −80 mV. Currents were elicited by 60 ms pulses to various potentials, from −100 mV to +10 mV at intervals of 1.2 s. Linear leak and capacitative transients have been subtracted. (Upper) Typical responses to depolarization to −30 mV in the presence and absence of calcium. (Lower) Current-voltage relationships for peak current in the presence and absence of calcium.

boscis muscles of the marine snail *Busycon* (Huddart and Hill, 1988; Huddart *et al.*, 1990a, b; Hill and McDonald-Ordzie, 1979; Hill *et al.*, 1970). Another molluscan muscle, the anterior byssus retractor muscle (ABRM) seems less dependent upon extracellular calcium because ACh-elicited contractions of ABRM are not abolished by the removal of extracellular calcium for up to 10 min (Sugi and Yamaguchi, 1976). Recent investigations of intracellular calcium levels in ABRM using the calcium-sensitive fluorescent indicator FURA-2 have shown that although extracellular calcium may account for the majority of the rise in intracellular calcium in response to cholinergic activation, about 30% of the increase in intracellular free calcium may be attributed to the release of stored calcium (Ishii *et al.*, 1988).

Studies on the influx of calcium-45 in response to ACh have been used to determine whether calcium dependence of contraction involves physical movement of calcium into the cell. ACh stimulates influx of calcium-45 into *Aplysia* buccal muscles E1 and I5 (Ram and Parti, 1985; Gole *et al.*, 1987); however, ACh does not significantly increase calcium-45 influx into ABRM (Tameyasu and Sugi, 1976). The lack of significant ACh-stimulated calcium-45 influx in ABRM not only contrasts with the observations in *Aplysia* muscles but also stands in apparent contradiction with FURA-2 measurements showing a significant extracellular dependence of the ACh-stimulated rise in intracellular calcium in ABRM (see above). Calcium-45 influx measurements are inherently more variable than FURA-2 measurements. Therefore, the lack of significant effect of ACh on calcium-45 influx in ABRM probably reflects a relatively lower importance of calcium influx in ABRM compared to *Aplysia* buccal muscles rather than a complete absence of ACh-stimulated influx.

A possible route for calcium entry into muscle cells during the response to ACh is via voltage-dependent calcium channels. As discussed below, ACh causes depolarization of molluscan muscles. Previous evidence that depolarization could activate voltage dependent calcium channels included demonstrating that another depolarizing stimulus, a high potassium medium, causes contraction. High potassium induces contractions of *Busycon* proboscis retractor muscles (*e.g.*, Huddart *et al.*, 1990a, b), ABRM (*e.g.*, Twarog and Muneoka, 1972), and *Aplysia* buccal muscles (Ram, unpub. data). Furthermore, high potassium elicits contraction of isolated fibers, as described in *Aplysia* buccal muscle (Figs. 2 and 3, this paper) and in ABRM (Ishii *et al.*, 1986), unambiguously proving that contraction elicited by high potassium is a direct effect on single fibers and is not dependent upon either release of neurotransmitters from nerve endings in the muscle or mechanical or electrical coupling between fibers. Ishii *et al.* (1988) has also used FURA-2 to show that high potassium causes an increase in intracellular calcium that is completely dependent upon extracellular calcium.

Blockers of voltage-dependent calcium channels reduce the contractile responses produced by both ACh and high potassium. Thus, Huddart *et al.* (1990b) found that diltiazam, verapamil, and nifedipine all decrease ACh-elicited contractions of *Busycon* proboscis muscles. Similarly, nifedipine reduces ACh-elicited contraction of *Aplysia* buccal muscle (Ram and Liu, 1990).

The above indirect evidence for the existence of voltage-dependent calcium channels is now supported in the present paper by voltage clamp recordings of a voltage-dependent inward current that is dependent on extracellular calcium (Fig. 10). As described in a preliminary re-

port (Ram and Liu, 1990), we have also demonstrated that this current is partially inhibited by nifedipine and completely blocked by lanthanum.

For voltage-dependent calcium channels to play a role in mediating ACh responses, it must also be shown that the range of membrane potentials at which a voltage-dependent calcium current can be activated is within the range of membrane potentials caused by ACh. As illustrated in Figure 10, voltage-dependent calcium current begins to activate with depolarizations to −40 mV. In other cells (data not shown), voltage-dependent calcium current has been activated with depolarization to as little as −50 mV. As discussed below, ACh can depolarize cells to approximately −35 mV. Thus, the membrane potential required to activate voltage-dependent calcium channels is clearly within the range of depolarization produced by ACh in *Aplysia* buccal muscles. This paper provides the strongest evidence yet that activator calcium enters molluscan muscle fibers during cholinergic stimulation by voltage-dependent calcium channels.

This paper also initiates the analysis of receptor-operated channels activated by ACh. ACh causes depolarization of molluscan muscle fibers in clam heart (Wilkens and Greenberg, 1973), ABRM (Twarog, 1954), *Busycon* proboscis muscles (Huddart *et al.*, 1990b; Hill and Licis, 1985; Hill and McDonald-Ordzie, 1979), *Aplysia* gill muscle (Reilly and Peretz, 1987) and *Aplysia* buccal muscles (Ram *et al.*, 1990). Detailed quantitative studies of *Aplysia* buccal muscle revealed (a) an average resting potential of −65 mV (Gole *et al.*, 1987), (b) no contraction elicited with depolarizations less than approximately 10 mV above rest, (c) a non-linear relationship between contraction and depolarization in which increasing ACh beyond a certain concentration was accompanied by increasing contraction with little or no further increase in depolarization, and (d) maximal ACh-elicited depolarization of approximately 30 mV above rest (Ram *et al.*, 1990).

The limit on depolarization produced by ACh to only 30 mV above rest may result from several mechanisms. One possibility is that the reversal potential for ACh-activated channels is only 30 mV above rest. An alternative explanation is that depolarization activates voltage-dependent potassium channels that act as an effective brake on further depolarization even in the face of activation of more ACh-activated channels. Data in this paper show that analysis of this question is feasible. As expected for a depolarizing stimulus, ACh activates inward current (Fig. 8). The reversal potential of the ACh response is under investigation (Ram and Liu, 1990). Furthermore, Figure 9 demonstrates that the voltage-dependent outward current is activated within the voltage range elicited by ACh. The voltage-dependent outward current is undoubtedly potassium because it is blocked by TEA and 4-AP outside the cell and Cs in the electrode (Fig. 10).

This paper also demonstrates that buccal muscle fibers contain stretch-activated channels. Because these channels were observed with on-cell patch electrodes containing only KCl, the inward currents illustrated are almost certainly due to potassium current. Similarly, stretch-activated channels conducting primarily potassium ions have been reported previously in molluscan neurons (Morris and Sigurdson, 1989; Sigurdson and Morris, 1989) and cardiac muscle (Brezden and Gardner, 1986; Sigurdson *et al.*, 1987). Stretch-activated channels that are somewhat less selective for potassium have been reported in various mammalian tissues, including skeletal muscle (Guharay and Sachs, 1984) and smooth muscle (Kirber *et al.*, 1988).

In future experiments it should be possible to determine whether 5-HT potentiates contraction of dissociated muscle fibers by modifying the ionic currents illustrated here. One indication in a molluscan muscle that 5-HT may change membrane currents of molluscan muscles is that, in ABRM, 5-HT potentiates the rise in intracellular calcium caused by 100 m*M* KCl (Ishii *et al.*, 1989). The rise in intracellular calcium in response to KCl is completely dependent upon extracellular calcium (Ishii *et al.*, 1988) and is presumed to be due to voltage-dependent calcium current, similar to the current described in this paper in Figure 10. In addition, 5-HT might also be modifying potassium channels, receptor-operated channels, and stretch-activated channels.

Acknowledgments

This work was supported by the Muscular Dystrophy Association and NIH grant RR-08167. I am indebted to R. B. Hill for his critical comments on the manuscript.

Literature Cited

Brezden, B. L., and D. R. Gardner. 1986. A potassium selective channel in isolated *Lymnaea stagnalis* heart muscle cells. *J. Exp. Biol.* **123:** 175–189.

Cohen, J. L., K. R. Weiss, and I. Kupfermann. 1978. Motor control of buccal muscles in *Aplysia*. *J. Neurophys.* **41:** 157–180.

Corey, D., and C. S. Stevens. 1985. Science and technology of patch-recording electrodes. Pp. 53–68 in *Single Channel Recording*, B. Sakmann and E. Neher, eds. Plenum Press, New York.

Cropper, E. C., M. W. Miller, R. Tenenbaum, M. A. G. Kolks, I. Kupfermann, and K. R. Weiss. 1988. Structure and action of buccalin: a modulatory neuropeptide localized to an identified small cardioactive peptide-containing cholinergic motor neuron of *Aplysia californica*. *Proc. Nat. Acad. Sci.* **85:** 6177–6181.

Cropper, E. C., R. Tenenbaum, M. A. G. Kolks, I. Kupfermann, K. R. Weiss. 1987. Myomodulin: a bioactive neuropeptide present in an identified cholinergic buccal motor neuron of *Aplysia*. *Proc. Nat. Acad. Sci.* **84:** 5483–5486.

Gole, D., L. Munday, M. Kreiman, and J. L. Ram. 1987. Caffeine effects on buccal muscles of *Aplysia*. *Comp. Biochem. Physiol.* **88C:** 313–318.

Guharay, F., and F. Sachs. 1984. Stretch-activated single ion channel currents in tissue-cultured embryonic chick skeletal muscle. *J. Physiol.* **352:** 685–701.

Hill, R. B., M. J. Greenberg, H. Irisawa, and H. Nomura. 1970. Electromechanical coupling in a molluscan muscle, the radula protractor of *Busycon canaliculatum*. *J. Exp. Zool.* **174:** 331–348.

Hill, R. B., and P. Licis. 1985. Lanthanum and caffeine affect both membrane responses and force in a molluscan muscle, the radular protractor of *Busycon canaliculatum*. *Comp. Biochem. Physiol.* **82C:** 363–376.

Hill, R. B., and P. E. McDonald-Ordzie. 1979. Ionic dependence of the response to acetylcholine of a molluscan buccal muscle: the radula protractor of *Busycon canaliculatum*. *Comp. Biochem. Physiol.* **62C:** 19–30.

Huddart, H., D. D. Brooks, R. B. Hill, and R. Lennard. 1990a. Diversity of mechanical responses and their possible underlying mechanisms in the proboscis muscles of *Busycon canaliculatum*. *J. Comp. Physiol. B* **159:** 717–725.

Huddart, H., D. D. Brooks, R. Lennard, and R. B. Hill. 1990b. Unusual responses of proboscis muscles of *Busycon canaliculatum* to some calcium antagonist agents. *J. Comp. Physiol. B* **159:** 727–738.

Huddart, H., and R. B. Hill. 1988. Electrochemical uncoupling in a molluscan muscle examined by the sucrose gap technique. The effect of calcium antagonist and agonist agents. *J. Comp. Physiol. B* **158:** 501–512.

Ishii, N., T. Takakuwa, and K. Takahashi. 1986. Isolation of acetylcholine-sensitive smooth muscle cells from a molluscan catch muscle. *Comp. Biochem. Physiol.* **84C:** 1–6.

Ishii, N., A. W. M. Simpson, and C. C. Ashley. 1988. Carbachol and KCl-induced changes in intracellular free calcium concentration in isolated, fura-2 loaded smooth-muscle cells from the anterior byssus retractor muscle of *Mytilus edulis*. *Biochem. Biophys. Res. Comm.* **153:** 683–689.

Ishii, N., A. W. M. Simpson, and C. C. Ashley. 1989. Effects of 5-hydroxytryptamine (serotonin) and forskolin on intracellular free calcium in isolated and fura-2 loaded smooth-muscle cells from the anterior byssus retractor (catch) muscle of *Mytilus edulis*. *Pflugers Archiv* **414:** 162–170.

Kirber, M. T., J. V. Walsh, Jr., J. J. Singer. 1988. Stretch-activated ion channels in smooth muscle: a mechanism for the initiation of stretch-induced contraction. *Pflugers Archiv* **412:** 339–345.

Mandelbaum, D. E. 1980. Studies of the role of cyclic AMP and protein phosphorylation in the mediation of food arousal in *Aplysia*. Ph.D. thesis. Columbia University. 154 pp.

Morris, C. E., and W. J. Sigurdson. 1989. Stretch-inactivated ion channels coexist with stretch-activated ion channels. *Science* **243:** 807–809.

Ram, J. L. 1983. Neuropeptide activation of an identifiable buccal ganglion motoneuron in *Aplysia*. *Brain Res.* **288:** 177–186.

Ram, J. L., G. S. Ajimal, D. Gole, K. A. Haller, and A. Williams. 1984a. Serotonin and forskolin enhance both magnitude of contraction and relaxation rate of *Aplysia* dorsal extrinsic muscle independently of acetylcholine receptor. *Comp. Biochem. Physiol.* **79C:** 455–459.

Ram, J. L., S. Barmatoski, L.-X. Liu, and S. C. Mahaffey. 1990. Structure, contraction, and electrophysiological properties of intact and dissociated smooth muscle fibers of *Aplysia*. Pp. 651–658 in *Frontiers in Smooth Muscle Research Progress in Clinical and Biological Research, Vol. 327*, N. Sperelakis and J. D. Wood, eds. Wiley-Liss, New York.

Ram, J. L., D. Gole, U. Shukla, and L. Greenberg. 1983. Serotonin-activated adenylate cyclase and the possible role of cyclic AMP in modulation of buccal muscle contraction in *Aplysia*. *J. Neurobiol.* **14:** 113–121.

Ram, J. L., and L.-X. Liu. 1990. Ion channels in *Aplysia* smooth muscle: currents activated by voltage and acetylcholine (ACh). *Soc. Neurosci. Abstr.* **16:** 675.

Ram, J. L., and R. Parti. 1985. Regulation of calcium influx into buccal muscles of *Aplysia* by acetylcholine and serotonin. *J. Neurobiol.* **16:** 57–68.

Ram, J. L., and S. Patel. 1989. Skinned muscle fibers of *Aplysia*: potentiation of contraction by "background" calcium and lack of effect of cyclic AMP. *Comp. Biochem. Physiol.* **93A:** 745–749.

Ram, J. L., U. A. Shukla, and G. S. Ajimal. 1981. Serotonin has both excitatory and inhibitory modulatory effects on feeding muscles in *Aplysia*. *J. Neurobiol.* **12:** 613–621.

Ram, J. L., U. A. Shukla, R. Parti, and R. L. Goines. 1984b. Extracellular calcium dependence of contracture and modulation by serotonin in buccal muscle E1 of *Aplysia*. *J. Neurobiol.* **15:** 197–206.

Reilly, W. M., and B. Peretz. 1987. Excitation-contraction coupling in a non-spiking smooth muscle in the gill of *Aplysia*. *J. Comp. Physiol.* **157B:** 659–666.

Rosen, S. C., I. Kupfermann, R. S. Goldstein, and K. R. Weiss. 1983. Lesion of a serotonergic modulatory neuron in *Aplysia* produces a specific defect in feeding behavior. *Brain Res.* **260:** 150–155.

Rosen, S. C., K. R. Weiss, R. S. Goldstein, and I. Kupfermann. 1989. The role of a modulatory neuron in feeding and satiation in *Aplysia*: effects of lesioning of the serotonergic metacerebral cells. *J. Neurosci.* **9:** 1562–1578.

Sigurdson, W. J., and C. E. Morris. 1989. Stretch-activated ion channels in growth cones of snail neurons. *J. Neurosci.* **9:** 2801–2808.

Sigurdson, W. J., C. E. Morris, B. L. Brezden, and D. R. Gardner. 1987. Stretch activation of a K^+ channel in molluscan heart cells. *J. Exp. Biol.* **127:** 191–209.

Sugi, H., and T. Yamaguchi. 1976. Activation of the contractile mechanism in the anterior byssal retractor muscle of *Mytilus edulis*. *J. Physiol., Lond.* **257:** 531–547.

Tameyasu, T., and H. Sugi. 1976. Effect of acetylcholine and high external potassium ions on ^{45}Ca movements in molluscan smooth muscle. *Comp. Biochem. Physiol.* **53C:** 101–103.

Twarog, B. M., and Y. Muneoka. 1972. Calcium and the control of contraction and relaxation in a molluscan catch muscle. *Cold Spring Harbor Symp. Quant. Biol.* **37:** 489–503.

Twarog, B. M. 1954. Responses of a molluscan smooth muscle to acetylcholine and 5-hydroxytryptamine. *J. Cell. Comp. Physiol.* **44:** 141–164.

Weiss, K. R., J. L. Cohen, and I. Kupfermann. 1978. Modulatory control of buccal musculature by a serotonergic neuron (metacerebral cell) in *Aplysia*. *J. Neurophysiol.* **41:** 181–203.

Wilkens, L. A., and M. J. Greenberg. 1973. Effects of acetylcholine and 5-hydroxytryptamine and their ionic mechanisms of action on the electrical and mechanical activity of molluscan heart smooth muscle. *Comp. Biochem. Physiol.* **45A:** 637–651.

Zhang, F., and J. L. Ram. 1990. Serotonin (5-HT) potentiates contraction of dissociated fibers of *Aplysia* smooth muscle. *Soc. Neurosci. Abstr.* **16:** 1227.

Reference: *Biol. Bull.* **180**: 284–294. (April, 1991)

Photoresponsiveness of *Aplysia* Eye is Modulated by the Ocular Circadian Pacemaker and Serotonin

JON W. JACKLET

Department of Biological Sciences, Neurobiology Research Center, State University of New York at Albany, Albany, New York 12222

Abstract. The eye of the sea hare, *Aplysia*, contains a circadian pacemaker that controls rhythmic behaviors of the animal. This report shows that the pacemaker controls the photoresponsiveness of the eye as well. The electroretinogram (ERG) of the isolated eye-optic nerve preparation, evoked by brief green light pulses in otherwise dark conditions, was recorded regularly, while the circadian rhythm of compound action potential activity was continuously recorded from the optic nerve. The waveform of the ERG changed systematically and rhythmically during the circadian cycle. One wave component of the ERG was prominent during the subjective night phase of the rhythm when the compound action potential frequency was minimal; and it was inconspicuous during the subjective day phase of the rhythm when the compound action potential frequency was maximal. Because eyes attached to the central nervous system and isolated eyes both exhibited the same rhythmic ERG changes, the circadian pacemaker in the eye is responsible for modulation of the ERG. Addition of serotonin, a putative efferent transmitter, to the bathing saline induced the ERG wave component characteristic of the subjective night phase of the rhythm. The threshold serotonin concentration was 10^{-7} *M*, and serotonin had a long lasting effect.

Introduction

Each eye of *Aplysia* contains a circadian pacemaker (Jacklet, 1969a) that produces a circadian rhythm in the frequency of optic nerve (ON) autonomous compound action potentials (CAPs). The CAP activity is produced by the synchronous firing of a population of retinal pacemaker neurons (Jacklet *et al.*, 1982), the axons of which enter the optic nerve and project to the central ganglia (Olson and Jacklet, 1985). This rhythm of CAP activity is known to control rhythmic behaviors, such as locomotor activity-rest, because eyeless animals lack the well defined circadian rhythm of activity-rest that normal animals display (Strumwasser *et al.*, 1979; Lickey *et al.*, 1977). Feeding behavior also exhibits a circadian rhythm (Kupfermann, 1974), but the contribution of the ocular circadian pacemaker to that rhythm has not been tested. The ocular circadian pacemaker probably controls rhythmic behavior by neural connections to central motor control centers, or by affecting physiological processes in the eye itself, although the mechanisms are not yet known.

An eye contains the photoreceptors needed to entrain the ocular circadian rhythm to the solar day light-dark cycles, because the rhythm is entrained by light-dark cycles (Eskin, 1971), and the phase of the CAP frequency rhythm is shifted by light pulses given during the subjective night, yielding a phase response curve (Jacklet, 1974). The specific ocular photoreceptor responsible for the phase shifts have not been identified. The eyes and other cephalic photoreceptors also mediate simple phototactic behaviors (see Jacklet, 1980).

The electroretinogram (ERG) has been recorded from the eye by an extracellular pipette placed in the retina (Jacklet, 1969b) and by a suction electrode placed on the cornea (Eskin, 1977; Eskin and Maresh, 1982). The ERG amplitude is increased by serotonin treatment or by ON stimulation, which presumably releases serotonin from the terminal in the eye of the efferent neurons (Eskin and Maresh, 1982). Eyes contain several types of photoreceptors, in addition to the pacemaker neurons involved in the circadian rhythm. The largest and most numerous type is the R photoreceptor (Jacklet and Rolerson, 1982)

Received 9 August 1990; accepted 28 December 1990.

Non-standard abbreviations: CAP, compound action potential; ON, optic nerve; CT, circadian time; ERG, electroretinogram; CM, culture medium.

that responds to light with a graded prolonged depolarization. The light response of this receptor is largely responsible for the ERG (Jacklet, 1969b).

Rhythmic changes in the ERG of *Aplysia*, or any other gastropod, have not been reported, to my knowledge, even though ERG circadian rhythms of other animals are well known. For example, the ERG amplitude rhythm of the compound eye of *Limulus* has been intensively studied (Barlow, 1983). Photosensitivity increases by 20–100 fold during the night, and the rhythm, driven by a central nervous system circadian pacemaker, is mediated by efferent innervation. The efferent transmitter appears to be octopamine (Battelle *et al.*, 1989; Kass and Barlow, 1984).

I report here that the ERG waveform recorded from the isolated *Aplysia* eye changes rhythmically, and the rhythm maintains a stable phase relationship with the circadian rhythm in CAP frequency. Thus, the ocular circadian pacemaker affects physiological processes within the eye itself. The waveform of the ERG that is characteristic of subjective night is induced by the addition of serotonin to the bathing saline during subjective day, mimicking the influence of the circadian pacemaker during subjective night.

Materials and Methods

Individuals of *Aplysia californica* were obtained from Marinus, Inc., Long Beach, California, and kept in Instant Ocean tanks maintained at 16°C under light-dark cycles of 12:12. Two isolated preparations were used: the eye-ON, and the eye attached to the cerebral ganglion by the ON. They were placed in a recording dish (100 ml) equipped with tubing (polyethylene, PE) electrodes embedded in the RTV silicone rubber base. Preparations were maintained in a dark box at 18°C for several days of recording. The ON was drawn, by negative pressure applied by a syringe, into one electrode (PE 10) that was used to record CAPs, and the eye was drawn into another electrode (PE 50) for ERG recording. The negative pressure was released, and the eye and ON remained in place for recording. The eye was drawn completely into the electrode so that the activity of all retinal cells could be recorded.

The eye is spherical and about 0.7 mm in diameter. It has a central lens, a poorly developed cornea, and a complex retina containing photoreceptors and neurons (see Jacklet *et al.*, 1982; Herman and Strumwasser, 1984). ERG electrode recordings routinely picked up small CAPs. Activity was amplified with an A-M Systems model 1700 (gain, ×1000; bandpass 0.1–1000 Hz.) and displayed on a Tektronix 5300 oscilloscope. ERGs and CAPs were recorded and stored with Asystant+ software in an IBM AT computer, and the data were plotted with a Hewlett-Packard model 7470A plotter. The latencies of the ERGs and CAPs were measured from computer generated plots of the recordings.

Pairs of eyes from eight animals were used in the circadian rhythm study. Four eyes attached to the cerebral ganglion yielded 11 circadian cycles of data, and 7 isolated eyes yielded 12 circadian cycles of data. Eyes produced three to four cycles of CAP rhythm data routinely, but complete ERG data were not collected from all eyes. Pairs of eyes from seven animals were used in the serotonin experiments.

Light pulses were produced by driving an Archer green LED with 1–2 s (15, 30 or 70V) pulses from a Grass model S88 stimulator. Pulses were given at regular intervals of 10 min, 30 min, or 1 h in otherwise constant darkness. The LED was positioned 3 cm away and directly over the eye drawn into the PE tubing. The intensity incident on the eye was measured by placing the sensor of a radiometer/photometer (United Detector Corp., Model 40X) 3 cm from the LED. Light intensities for voltage pulses used to drive the LED were 0.6 $\mu W/cm^2$ at 15 V, 0.8 $\mu W/cm^2$ at 30 V, and 3 $\mu W/cm^2$ at 70 V. The *Aplysia* eye has high sensitivity to green light and the threshold intensity is about 0.06 $\mu W/cm^2$ at 500 nm (Jacklet, 1980).

Artificial seawater (ASW) was made up of the following salts in millimoles/liter: NaCl, 425; KCl, 10; $CaCl_2$, 10; $MgCl_2$, 22; $MgSO_4$, 26; $NaHCO_3$, 2.5; adjusted to pH 7.8. Culture medium (CM) was composed of ASW, 20% *Aplysia* blood, and 100 U/ml penicillin, 0.1 mg/ml streptomycin. Serotonin (Sigma, creatinine sulfate) was added to the CM to final concentrations of 10^{-7}, 10^{-6}, or 10^{-5} *M*. A 10-ml chamber fitted with polyethylene tubing for changing solutions inside the dark box was used for the serotonin experiments. The CM was removed entirely by applying suction to the polyethylene tubing and was replaced within a few seconds with the serotonin solution. The statistically significant differences between average latencies were determined using a two tailed *t* test. The level of significance used was $\alpha = .05$.

Results

Rhythmic changes in the ERG

The basic ERG waveform recorded in these experiments was triphasic, even though the entire eye was pulled into the tubing electrode. The waveform consisted of a sharply rising wave, followed by a slower wave of opposite polarity and a weak slow third phase. There was no obvious "off" response. This triphasic ERG waveform is very similar to the ERG recorded by Eskin (1977) on a Grass polygraph using a suction electrode applied on or near the cornea.

The latency of the ERG in the present study was about 0.9 s in response to a 1 $\mu W/cm^2$ green light pulse. This compares well with the latency of about 0.9 s obtained

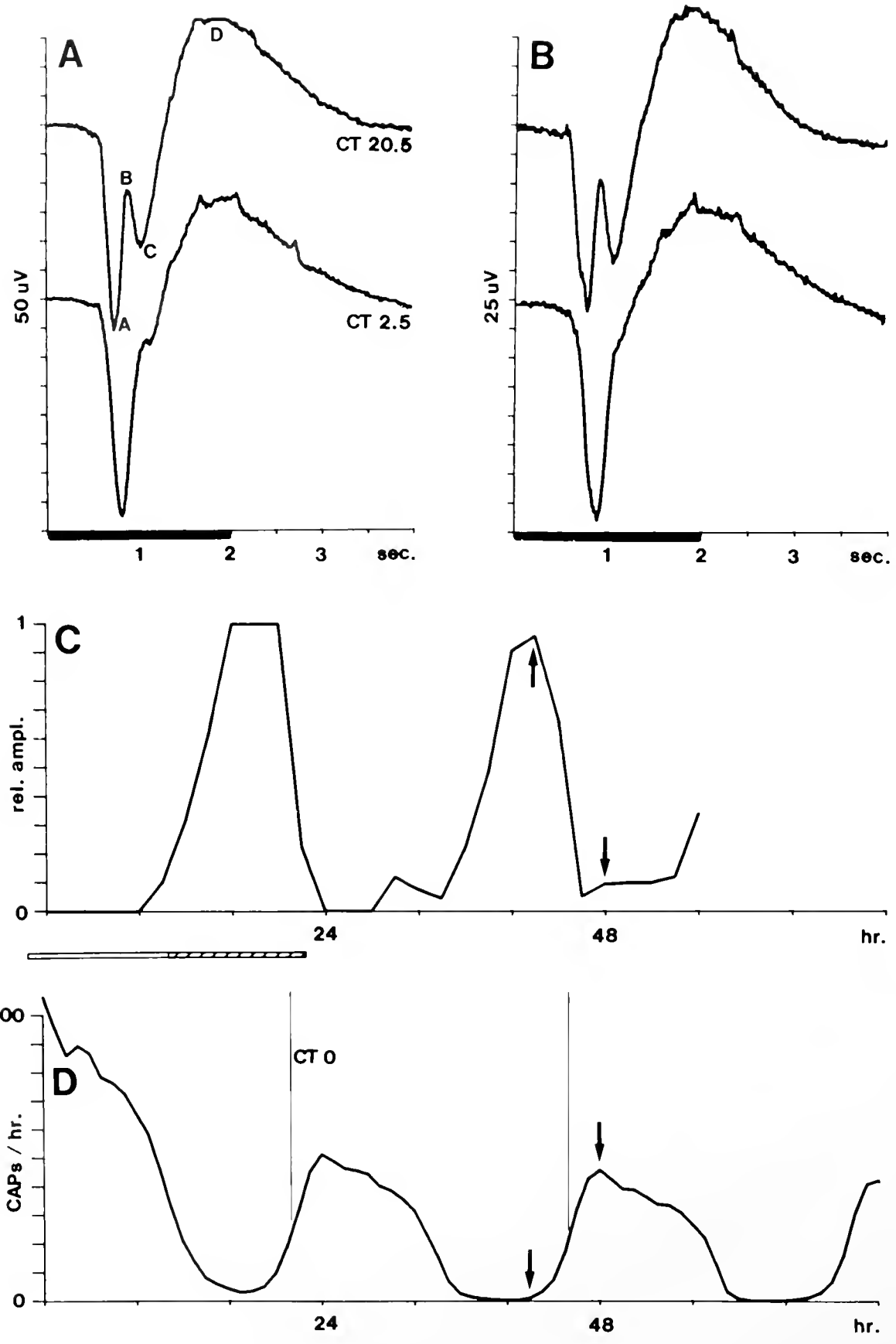
A
D
CT 20.5
B
C
A
CT 2.5
50 uV
1
2
3
sec.
B
25 uV
1
2
3
sec.
C
1
rel. ampl.
0
24
48
hr.
D
500
CT 0
CAPs / hr.
0
24
48
hr.

earlier in response to about 6 lux (<1 $\mu W/cm^2$) white light (Jacklet, 1969b). This is a rather long latency, but similar to those of other gastropod eyes under similar conditions. Latency is 1–3 s for *Otala*, a land snail (Gillary and Wolbarsht, 1967), and 0.2–0.5 s for the well-formed eye of *Strombus*, another marine gastropod (Gillary, 1974). The *Aplysia* eye latency is about 0.4 s in response to 600 lux white light (Jacklet, 1969b).

The ERG waveform was usually smooth during the subjective day, as shown in Figure 1A at CT 2.5. CT refers to circadian time, which is measured from the actual period of the free-running circadian rhythm of interest, in this case the CAP frequency rhythm shown in Figure 1D. The period is divided into 24 equal units. Circadian time 0–12 is subjective day, and CT 12–24 is subjective night. The phase point in the CAP rhythm corresponding to subjective dawn (CT 0) is the CAP frequency at ½ maximum marked in Figure 1D. During subjective night, the waveform developed a notch following the initial wave, as shown in Figure 1A at CT 20.5. For convenience, the waveform has been labeled in the figure. The initial wave is A, followed by the B-C wave or notch, followed by the slower D wave. The B-C wave has not previously been reported. This waveform is typical of the ERGs recorded during subjective night in these experiments.

The ERGs shown in Figure 1A were recorded from the same isolated eye at different phases (CT 20.5 and CT 2.5) in the circadian cycle. Similar ERGs were recorded from the other eye of the same animal at the same phases, even though the eye was attached to the cerebral ganglion by the ON (Fig. 1B). Being attached to the cerebral ganglion made no apparent difference in the waveform of the ERG or in the rhythmic changes in the waveform. In general, eye pairs exhibited very similar ERG waveforms, whether or not the eye was attached to the cerebral ganglion.

The ERG B-C wave changed rhythmically during the circadian cycle. It virtually disappeared during subjective day and reappeared during subjective night. The relative amplitude of the B-C wave, measured from the peak of the B to the peak of the C wave, cycled continuously, as shown in Figure 1C for the B-C wave of the isolated eye used in Figure 1A. When the cycling of the relative amplitude of the B-C wave is compared to the CAP frequency rhythm plotted in Figure 1D, the maximum B-C wave amplitude seems to occur at about CT 20 and to coincide with minimal CAP frequency during subjective night. The period of both rhythms is about 24 hours.

A few eyes exhibited weak rhythmic changes in the A wave of the ERG, but either they did not persist over two cycles, or they were not sufficiently robust to be considered true rhythms. The D wave was very stable and showed no rhythmicity.

The ERG waveform recorded from eyes of different animals varied somewhat, but the basic waveform could always be observed. One of the most extreme waveforms is shown in Figure 2A, B. This eye was attached to the cerebral ganglion, but the paired isolated eye exhibited the same ERG waveform and changed rhythmically. The A, B, C, and D waves are readily apparent. But the A wave is relatively small and the B-C wave is huge. The relative amplitude of the B-C wave changed rhythmically, but it never completely disappeared. It remained in the appropriate phase relationship with the CAP frequency rhythm for many cycles (Fig. 2C, D). The period of both rhythms is about 23 hours.

In most preparations, the latency (time from stimulus onset to ½ peak of A wave) of the ERG A wave was shorter during the subjective night, when the B-C wave was prominent, than during the subjective day. For example, in Figure 1A and B the latency is about 100 ms shorter during subjective night. The ERG latencies for light pulses given at CT 19–22, during subjective night, were compared to latencies obtained at CT 1–4, during subjective day, for 12 circadian cycles for both isolated eyes and eyes attached to the cerebral ganglion. Mean latency and the standard error of the mean (SEM) were calculated, and *t* tests were performed to determine whether mean differences were statistically significant. The average latency for isolated eyes was 1000 ms (SEM, 20; N, 34) during CT 19–22, and 1050 ms (SEM, 10; N, 39) during CT 1–4. The means were significantly different at the .05 level. The average latency for eyes attached to the cerebral ganglion was 920 ms (SEM, 20; N, 36) during CT 19–22, and

Figure 1. Rhythmic changes in the ERG. ERG waveforms recorded from the same isolated eye during subjective night (CT 20.5) and during subjective day (CT 2.5) are shown in A. The A, B, C, and D waves are labeled. The 2-s light pulse (3 $\mu W/cm^2$) is indicated by the black bar. The other eye from the same animal, but attached to the cerebral ganglion, exhibited the ERG waveform shown in B taken at CT 20.5 and CT 2.5 as in A. Vertical scales in A and B are 50 μV and 25 μV per division. The changes in relative amplitude of the B-C wave of the ERGs recorded from the isolated eye are plotted in C using the same time scale as the CAP frequency rhythm shown in D. Arrows identify the relative amplitude points of the B-C wave in C, and the CAP frequency in D corresponding to the ERGs in panel A taken at CT 20.5 and CT 2.5. Time reference for CT 0 is the thin labeled line in D that occurs at ½ the maximum CAP frequency. The projected light-dark cycle experienced by the animal before dissection is shown by the white/crosshatched bar.

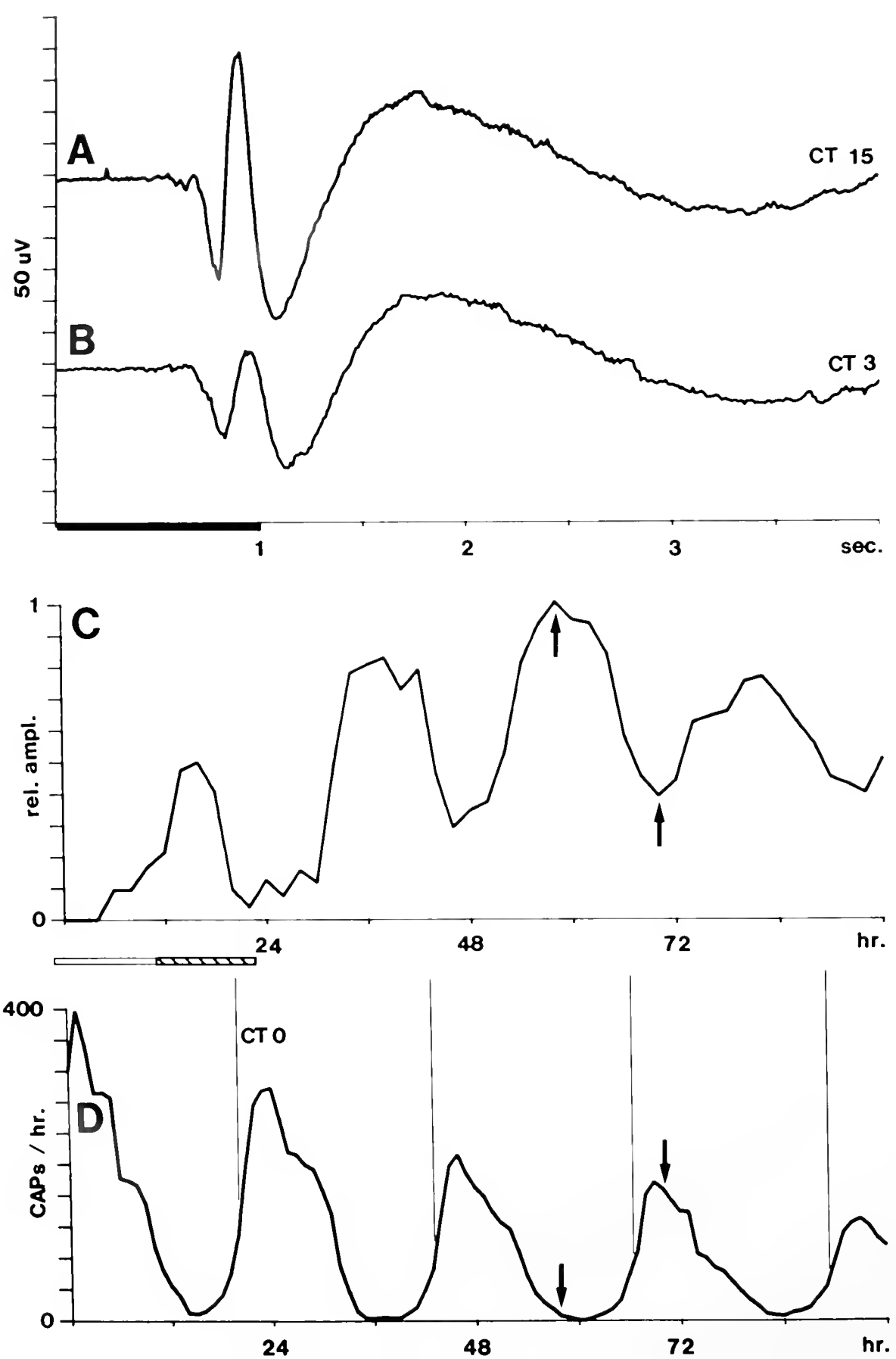
A
CT 15
50 uV
B
CT 3
1
2
3
sec.
C
1
rel. ampl.
0
24
48
72
hr.
400
CT 0
D
CAPs / hr.
0
24
48
72
hr.

970 ms (SEM, 20; N, 34) during CT 1–4. The means were significantly different at the .05 level. Although the mean A wave latencies are shorter for attached eyes than for isolated eyes, both show similar shifts in ERG latency during the circadian cycle.

To test for the involvement of chemical synapses in the circadian pacemaker modulation of the ERG waveform, two eyes were subjected to ASW containing 10^{-4} *M* Ca^{++} and 10^{-1} *M* Mg^{++}. This treatment drastically reduced the ERG as expected (Eskin, 1977). Thus, a reliable test for the involvement of chemical synapses was not possible.

Removal of the ON from the isolated eye did not interrupt cycling of the ERG waveform, but it did reduce the number of cycles that an eye exhibited. The ON was cut away from four eyes at the bases of their retinas, and ERGs were recorded as usual. Small CAPs recorded with the ERG electrode verified that the CAP circadian rhythm continued. Two of the eyes remained active for two cycles, and both exhibited cycling of the B-C wave, suggesting that the ON itself is not necessary for circadian cycling of the ERG.

Serotonin induces the ERG B-C wave

Serotonin induced the B-C wave in eyes at circadian times when it was not normally expressed. The induced B-C wave closely resembled the wave characteristic of subjective night. As shown in the example of Figure 3, the B-C wave was well developed at CT 20, as expected, and it became inconspicuous later, at CT 0.5, during subjective day. A short time later at CT 2.0, and just 13 min after the addition of 10^{-6} *M* serotonin to the bathing solution by perfusion, the induced B-C wave (Fig. 3C) was nearly identical to the B-C wave recorded at CT 20 (Fig. 3A). Continued exposure to serotonin enhanced the B-C wave (Fig. 3D) beyond the amplitude of the subjective night B-C wave. The effects of serotonin were long lasting and reached a maximum in about 1 h. Once induced, the B-C wave required several hours of washout before it returned to normal. Serotonin also enhanced the B-C wave of eyes tested during subjective night when the wave was already present.

During exposure to serotonin, the autogenous CAP frequency was reduced as expected from previous work (Corrent *et al.*, 1978; Eskin and Maresh, 1982). The number of CAPs evoked by the light pulse, especially those evoked several seconds after the pulse, were also reduced as shown in Figure 4B. However, compared to the response just before the addition of 10^{-6} *M* serotonin, there was no change in the latency of the initial CAP produced by a light pulse. The mean latency for the initial CAP in the light response was 1.40 s (SEM, 0.14; N, 7) before serotonin treatment, and 1.36 s (SEM, 0.05; N, 7) 15 min after serotonin treatment. A *t* test showed that these means were not significantly different. The initial CAP occurs at about the same time as the B-C wave, and small deflections on the ERG waveform caused by CAPs are clearly visible (Fig. 4A, B). During serotonin treatment, the CAP deflections on the ERG waveform, as well as the size and timing of the initial CAP during the light response, remained the same. Thus, changes in the light-evoked activity of the pacemaker neurons that produce the CAPs are not likely to account for the B-C wave induced by serotonin.

Serotonin shortened the latency of the ERG and occasionally increased the amplitude of the A wave. Both Figures 3 and 4 show a substantial decrease in the latency and increase in the A wave. The average ERG latency before serotonin was 960 ms (SEM, 20; N, 9); 15 min after the addition of 10^{-6} *M* serotonin it was 900 ms (SEM, 30; N, 9), and 45 min after an addition of serotonin it was 860 ms (SEM 40; N, 7). The difference in mean latency was not significant at 15 min, but at 45 min it was significantly different at the .05 level. The average amplitude of the A wave increased only 1.1 times at 45 min. At the threshold concentration (10^{-7} *M*) for ERG B-C wave induction, the average latency decreased by only 25 ms (N, 4), and the A wave amplitude did not change.

Discussion

ERG waveform changes

A major finding of our study is that the ERG changes systematically and rhythmically during the circadian cycle of CAP frequency. One component of the ERG, the B-C wave, is prominent during the subjective night phase of the rhythm when the CAP rate is minimal, and inconspicuous during the subjective day phase when the CAP

Figure 2. Rhythmic changes in the ERG of an eye attached to the cerebral ganglion. Waveforms characteristic of subjective night (CT 15) and subjective day (CT 3) for the same eye attached to the cerebral ganglion by the ON are shown respectively in A and B. The 1-s light pulse (3 $\mu W/cm^2$) is indicated by the black bar. Vertical scales in A and B are 50 μV per division. The B-C wave became very prominent in the eyes of this animal after several days of recording. C shows the changes in relative amplitude of the B-C wave plotted on the time scale of the CAP frequency rhythms in D. Arrows in C and D mark the times at which the ERGs shown in A and B were taken. Time reference for CT 0 is the thin labeled line in D at ½ the maximum CAP frequency. The projected light-dark cycle experienced by the animal before dissection is shown by the white/crosshatched bar. Light pulse is indicated by black bar in panels A, B.

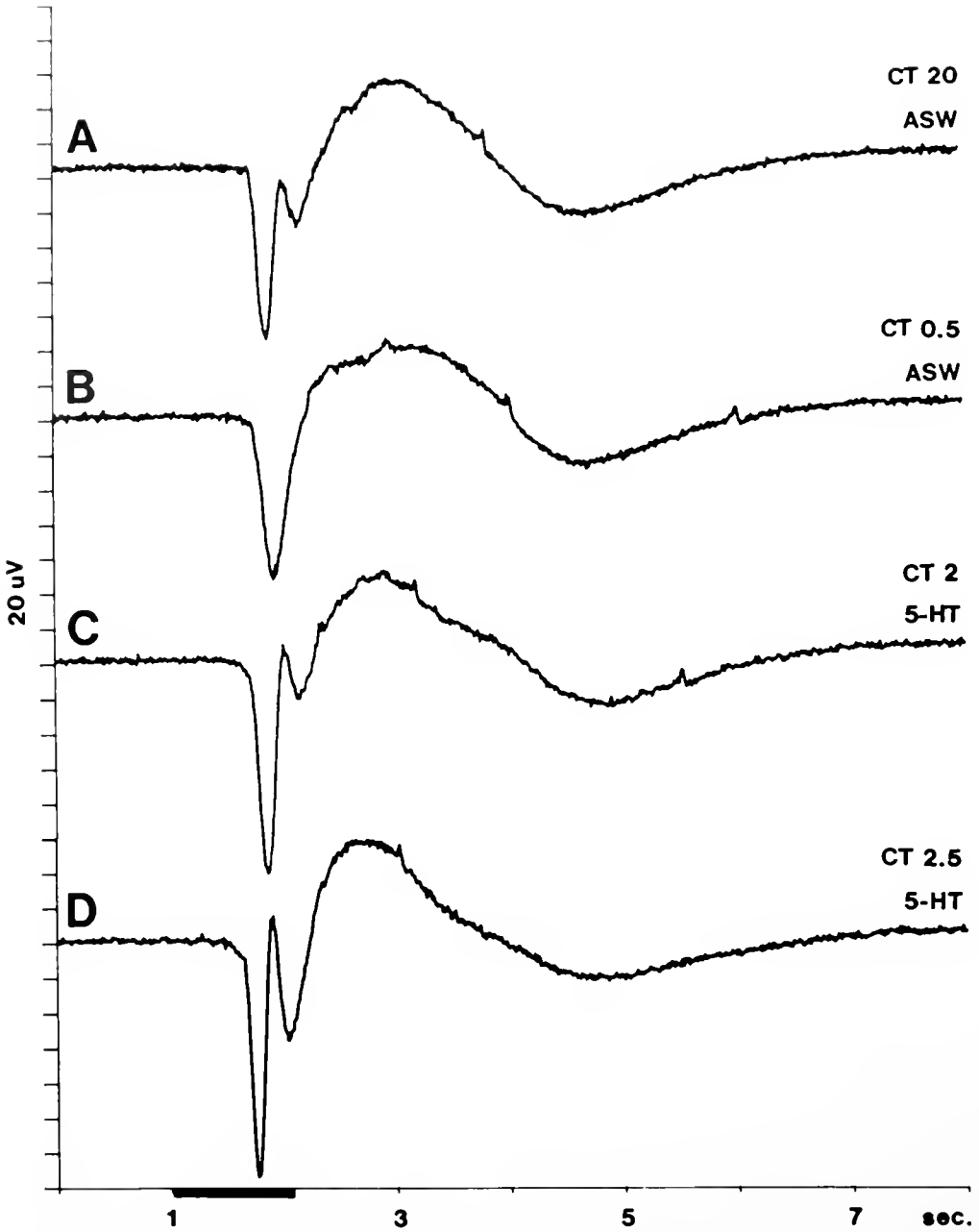

Figure 3. Changes in the ERG of an isolated eye induced by serotonin. The ERG waveform recorded at CT 20 with a characteristic B-C wave is shown in A. At CT 0.5 the ERG had changed to the subjective day waveform, lacking the B-C wave. Thirteen min after the addition of 10^{-6} *M* serotonin, the ERG shown in C with a prominent B-C wave was recorded. The B-C wave progressively increased until the maximum response in D was observed at 43 min after the addition of serotonin. At that time the latency of the A wave had decreased about 100 ms, and the A wave amplitude had increased 140%. Vertical scale is 20 μV per division. The black bar on the time scale marks the 1-s light (.8 μW/cm^2) pulse.

rate is maximal. Thus, the maximal B-C wave occurs during minimal CAP rate in an antiphase relationship. The B-C wave decreases in size sharply during the increase in CAP rate at subjective dawn, suggesting that a high CAP rate might suppress the B-C wave. However, the causal relationship between these events has not been determined. Isolated eyes, and eyes attached to the cerebral ganglion, exhibited similar ERG rhythms suggesting that the B-C wave pacemaker resides within the eye and that it is likely to be the CAP circadian pacemaker. The induction of the B-C wave by serotonin is an intriguing observation that will be addressed later in this discussion.

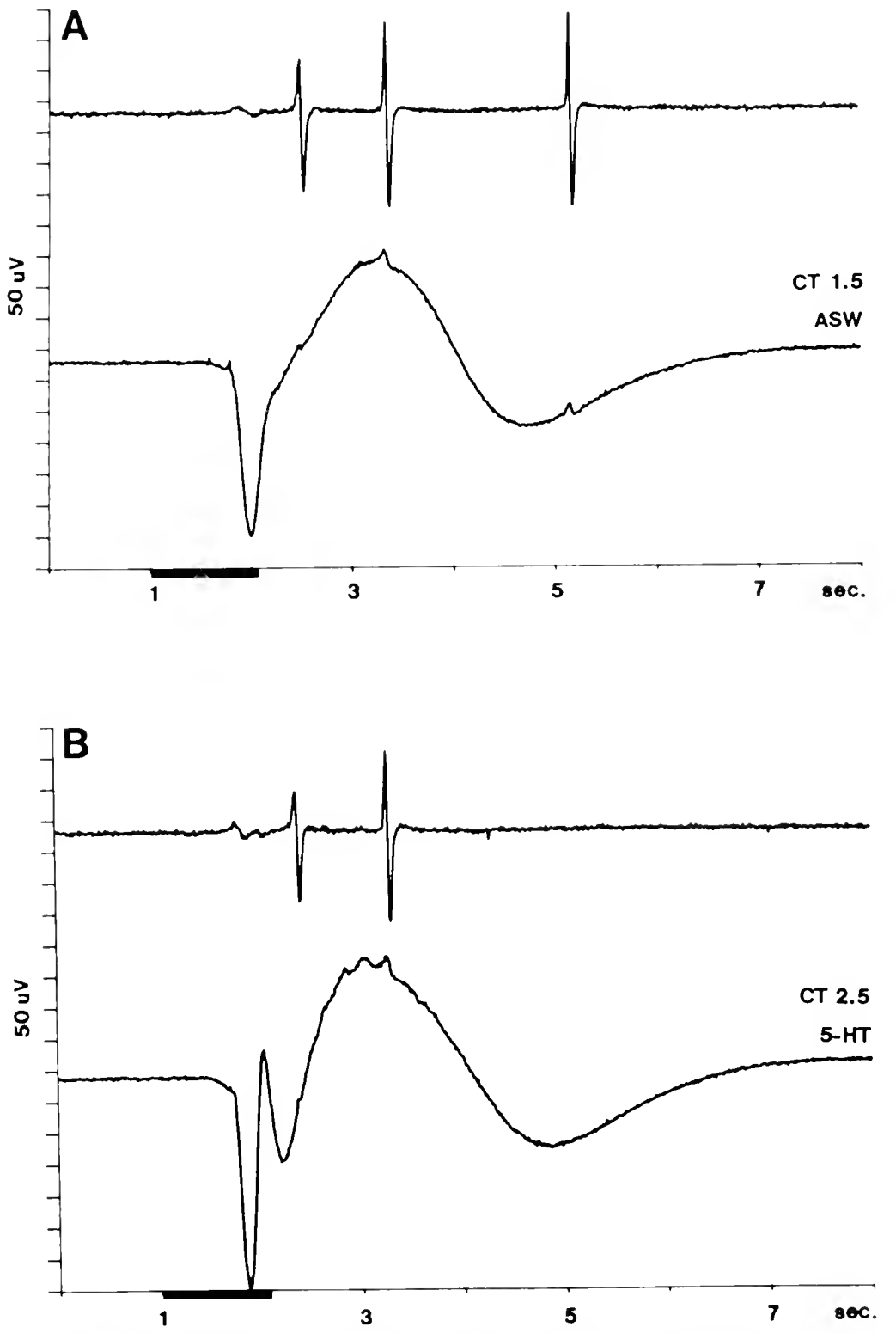

Figure 4. Changes in the ERG and CAP frequency induced by serotonin. Simultaneous recordings were made of CAPs (upper traces) and the ERG (lower trace) in response to 1-s light pulses (dark bar). Responses at CT 1.5 appear in A. CAPs appear on the ON trace and as small deflections on the ERG trace as well. At CT 2.5, 43 min after addition of 10^{-6} *M* serotonin, the B-C wave seen in B was prominent, the latency had decreased about 100 ms, and the number of CAPs evoked decreased. Black bars on time scale mark the 1-s light (.8 $\mu W/cm^2$) pulse. Vertical scales are 50 μV per division.

The ERG B-C wave characteristic of subjective night has not been previously reported. Several years ago, I looked for rhythmic changes in the ERG A wave amplitude because ERG amplitude changes are well known in other animals (see Barlow, 1983), but did not find consistent rhythms. In the present study, the use of computer assisted recording to compare ERG waveforms soon revealed that the B-C wave occurs and changes rhythmically. It also revealed that the A wave latency changes rhythmically, but that the A wave amplitude does not. Average latency differences of 50 ms during the cycle were found for both isolated and attached eyes.

The ERG recordings were made from eyes completely pulled into the tubing electrode, so signals could be recorded from any of the responding cell types in the eye, including cells in the basal retina. Previous work had shown that the largest photoresponses, recorded with a glass pipette in the retina, were corneal negative and were obtained near the distal segments of the large photoreceptors (Jacklet, 1969b). In the present study, light from the LED reached all surfaces of the isolated eye and was not restricted to the pathway through the cornea and lens.

The photoreceptor organization of the *Aplysia* retina was investigated with localized illumination by Block and McMahon (1983). They illuminated (100 lux, white light) the distal segments of the photoreceptors surrounding the lens and, as a result, unitary ON activity without CAPs was evoked in the ON. Illumination of the basal retina produced CAPs. Block and McMahon concluded that chemical synaptic inhibition, especially the inhibitory action of the receptor layer onto the CAP generating neurons, shapes in part the light responses of the isolated eye. Other evidence of synaptic inhibition in the retina is provided below.

Retinal cells that may contribute to the ERG B-C wave

The ERG consists of a sharply rising A wave, a rhythmically changing B-C wave, and a stable D wave. The A wave is likely to be caused by the R type photoreceptors with microvillous distal segments adjacent to the lens (Jacklet, 1969b; Jacklet and Rolerson, 1982). Intracellular recordings show that dark adapted R photoreceptors respond to white light pulses of 600 lux after a latency of 400 ms, comparable to the ERG latency of 400 ms at that intensity (Jacklet, 1969b); the response is a prolonged depolarization of 60–70 mV (Jacklet and Rolerson, 1982). Light adapted, but not dark adapted, R photoreceptors have a notch on the rising phase of the depolarization. The notch is probably not responsible for the B-C wave because it occurs early during the A wave, and because ERGs were recorded at interstimulus intervals of up to 1 h when the R photoreceptor are dark adapted and not expected to have a notch. Some R photoreceptors display prolonged hyperpolarization following the initial depolarization (see Fig. 3 in Jacklet and Rolerson, 1982). However this hyperpolarization is also unlikely to cause the B-C wave because it continues much longer than the B-C wave. Responses from R photoreceptors have not been studied throughout the circadian cycle, especially not during the subjective night when the B-C wave occurs, so changes that might account for the B-C wave have not been observed.

Light responses of R photoreceptors are not completely blocked by low Ca^{++} and high Mg^{++} ASW, but the resting potential is decreased, and the light-evoked depolarization is reduced and prolonged (Jacklet and Rolerson, 1982). This should account for the reduction of the ERG in low Ca^{++} and high Mg^{++} ASW previously observed (Eskin, 1977) and confirmed in this study.

The pacemaker neurons (or secondary neurones, Jacklet *et al.*, 1982) responsible for the CAPs also respond to light. They depolarize and fire synchronous action potentials that are correlated 1:1 with the ON CAPs. As shown in this study, CAPs produce small but observable deflections on the ERG waveform at all phases of the circadian cycle, but they are tiny compared to the B-C wave, and none are synchronized with the B-C wave. The light responses of the pacemaker neurons themselves seem unlikely to contribute to the B-C wave. However, the B-C wave is most conspicuous during the phase of the circadian cycle when the autogenous CAP frequency is low or absent. Perhaps low autogenous CAP activity creates the conditions necessary for the B-C wave to occur. The relationship between autogenous CAP activity and expression of the B-C wave has not yet been tested directly.

A retinal cell type that may contribute to the ERG B-C wave is the H photoreceptor (Jacklet and Rolerson, 1982). Its typical light response is a volley of action potentials followed by brisk hyperpolarization, and then depolarization accompanied by action potentials. The hyperpolarization occurs just after the initial photoresponse, at about the time that the B-C wave of the ERG is occurring. The H cell hyperpolarization appears to be synaptically evoked, because electrical stimulation of the ON evokes a similar sharp hyperpolarization (Jacklet and Rolerson, 1982). This cell type may be involved in shaping the light responses observed by Block and McMahon (1983) during selective illumination. The ERG B-C wave might be produced by enhanced inhibitory synaptic interactions within the retina controlled by the circadian pacemaker. Such enhanced interactions might improve the visual performance of the eye.

A determination of the retinal cell types in *Aplysia* that contribute to the rhythmic B-C wave must await a systematic intracellular study of cellular light responses throughout the circadian cycle, preferably with simultaneous ERG recordings.

The eye of a marine gastropod, *Strombus*, may share some of the features of the *Aplysia* eye photoresponses, including the B-C wave. The ERG exhibits two peaks of negativity that are separable under certain conditions of light and temperature (Gillary, 1974). The second peak resembles the B-C wave. This eye is 3 times the diameter, and contains about 100 times as many cells, as the *Aplysia* eye. It appears to lack circadian pacemaker neurons, and changes in the photoresponse during the circadian cycle have not been explored to my knowledge. This retina contains two types of depolarizing cells and one hyperpolarizing type (Quandt and Gillary, 1979), similar to the *Aplysia* retina. One depolarizing cell type (Type II) exhibits two peaks of depolarization that are similar, but of opposite polarity, to the ERG waveform (Quandt and Gillary, 1980).

Role of serotonin

Serotonin has been shown by Eskin and Maresh (1982) to increase the first wave (A wave in this study) of the *Aplysia* ERG when it is recorded with a suction electrode applied to the cornea. They did not see a B-C wave. That may be due to differences in recording methods, because they made polygraph recordings and did not report latencies. They found an average increase in the ERG amplitude of 63% after 20 min in 10^{-6} *M* serotonin, and a threshold concentration near 10^{-7} *M*. Dopamine, acetylcholine, and octopamine were tested but did not produce consistent ERG changes. They also reported a 20% increase in the ERG in response to ON stimulation and proposed that the stimulation might cause the release of serotonin from efferent terminals in the eye. Terminals have been identified by serotonin antisera (Goldstein *et al.*, 1984; Takahashi *et al.*, 1989).

The effect of serotonin on the ERG suggests that cyclic nucleotide second messengers may be involved. Cyclic AMP mediates many of the serotonin effects on short- and long-term central synapses in *Aplysia* (Kandel and Schwartz, 1982), and serotonin phase shifts the CAP rhythm (Corrent *et al.*, 1978) by a mechanism involving cAMP (Eskin *et al.*, 1982). In addition, cGMP mimics the effect of light on the circadian pacemaker by inducing phase shifts of the CAP rhythm (Eskin *et al.*, 1984). During the cGMP treatment, the membrane potentials of R photoreceptors were not altered, but changes in photoresponsiveness were not explored. A ten minute exposure to light increased the cGMP level by 50%. Cyclic GMP may be elevated, either as a consequence of photoresponses, or because it is involved in the phototransduction process (Eskin *et al.*, 1984). If any rhythmic changes in the levels of cyclic nucleotides occur, they might be involved in the B-C wave and the A wave latency changes.

Serotonin does not appear to induce the B-C wave by a direct effect on the initial light response of pacemaker neurons, because the initial CAP that most nearly coincides temporally with the B-C wave is unaffected by serotonin. Thus, serotonin does not allow expression of the B-C wave by suppressing the light-induced pacemaker neuron activity. However, the phase of the circadian cycle during low or zero CAP frequency is associated with expression of the B-C wave, and serotonin does suppress autogenous CAP activity. Serotonin may create the necessary conditions for expression of the B-C wave, in part, by suppressing autogenous CAP activity.

Because serotonin induces the ERG B-C wave and the reduction of the A wave latency, one may ask how it might be involved in circadian control of the ERG. Serotonin may just be mimicking a natural process, but because there are efferent synaptic terminals containing serotonin in the eye, they may well be involved. Because isolated eyes show circadian rhythms in the B-C wave, the control of serotonin release from the efferent terminals by central neurons is eliminated. But how then might serotonin be released by activity within the eye? Could processes controlled by the circadian pacemaker in the eye release serotonin? Because the appearance of the B-C wave is associated with minimal CAP frequency, release cannot be a direct effect of CAP activity. To produce the appropriate response, autogenous CAP activity would have to suppress serotonin release, and inactivity would have to promote release. Otherwise another process controlled by the circadian pacemaker must be involved.

Acknowledgments

I thank Mark Goldberg for excellent technical assistance. Research supported by NSF grant BNS 88-19773 to J.W.J.

Literature Cited

Barlow, R. B., Jr. 1983. Circadian rhythms in the *Limulus* visual system. *J. Neurosci.* **3:** 856–870.

Battelle, B-A., J. A. Evans, and S. C. Chamberlain. 1982. Efferent fibers to *Limulus* eyes synthesize and release octopamine. *Science* **216:** 1250–1252.

Block, G., and D. McMahon. 1983. Localized illumination of the *Aplysia* and *Bulla* eye reveals new relationships between retinal layers. *Brain Res.* **265:** 134–137.

Corrent, G., D. McAdoo, and A. Eskin. 1978. Serotonin shifts the phase of the circadian rhythm from the *Aplysia* eye. *Science* **202:** 977–979.

Eskin, A. 1971. Properties of the *Aplysia* visual system: *in vitro* entrainment of the circadian rhythm and centrifugal regulation of the eye. *Z. vergl. Physiologie* **74:** 353–371.

Eskin, A. 1977. Neurophysiological Mechanisms involved in photoentrainment of the circadian rhythm from the *Aplysia* eye. *J. Neurobiol.* **8:** 273–299.

Eskin, A., and R. Maresh. 1982. Serotonin or electrical optic nerve stimulation increases the photosensitivity of the *Aplysia* eye. *Comp. Biochem. Physiol.* **73C:** 27–31.

Eskin, A., J. S. Takahashi, M. Zatz, and G. D. Block. 1984. Cyclic guanosine 3′:5′-monophosphate mimics the effects of light on a circadian pacemaker in the eye of *Aplysia*. *J. Neurosci.* **4:** 2466–2471.

Eskin, A., G. Corrent, C. Y. Lin, and J. McAdoo. 1982. Mechanism for shifting the phase of a circadian rhythm by serotonin: involvement of cAMP. *Proc. Nat. Acad. Sci. USA* **79:** 660–664.

Gillary, H. L. 1974. Light-evoked electrical potentials from the eye and optic nerve of *Strombus*: response waveform and spectral sensitivity. *J. Exp. Biol.* **60:** 383–396.

Gillary, H. L., and M. L. Wolbarsht. 1967. Electrical responses from the eye of a land snail. *Rev. Can. Biol.* **26:** 125–134.

Goldstein, R., H. B. Kistler, H. W. M. Steinbusch, and J. H. Schwartz. 1984. Distribution of serotonin-immunoreactivity in juvenile *Aplysia*. *J. Neurosci.* **11:** 535–547.

Herman, K. G., and F. Strumwasser. 1984. Regional specializations in the eye of *Aplysia*, a neuronal circadian oscillator. *J. Comp. Neurol.* **230:** 593–613.

Jacklet, J. W. 1969a. Circadian rhythm of optic nerve impulses recorded in darkness from isolated eye of *Aplysia*. *Science* **164:** 562–563.

Jacklet, J. W. 1969b. Electrophysiological organization of the eye of *Aplysia*. *J. Gen. Physiol.* **53:** 21–42.

Jacklet, J. W. 1974. The effect of constant light and light pulses on the circadian rhythm in the eye of *Aplysia*. *J. Comp. Physiol.* **90:** 33–45.

Jacklet, J. W. 1980. Light sensitivity of the rhinophores and eyes of *Aplysia*. *J. Comp. Physiol.* **136:** 257–262.

Jacklet, J. W., and C. Rolerson. 1982. Electrical activity and structure of retinal cells of the *Aplysia* eye. II. Photoreceptors. *J. Exp. Biol.* **99:** 381–395.

Jacklet, J. W., L. Schuster, and C. Rolerson. 1982. Electrical activity and structure of retinal cells of the *Aplysia* eye. I. Secondary neurones. *J. Exp. Biol.* **99:** 369–380.

Kandel, E. R., and J. H. Schwartz. 1982. Molecular biology of learning: Modulation of transmitter release. *Science* **218:** 433–443.

Kass, L., and R. B. Barlow, Jr. 1984. Efferent neurotransmission of circadian rhythms in *Limulus* lateral eye. *J. Neurosci.* **4**(4): 908–917.

Kupfermann, I. 1974. Feeding behavior of *Aplysia*: A simple system for the study of motivation. *Behav. Biol.* **10:** 1026.

Lickey, M., J. Wozniak, G. Block, D. Hudson, and G. Augter. 1977. The consequences of eye removal for the circadian rhythm of behavioral activity in *Aplysia*. *J. Comp. Physiol.* **118:** 121–143.

Olson, L., and J. W. Jacklet. 1985. The circadian pacemaker in the eye of *Aplysia* sends axons throughout the central nervous system. *J. Neurosci.* **5**(12): 3214–3227.

Quandt, F. N., and H. L. Gillary. 1979. Classes of light-evoked response in the retina of *Strombus*. *J. Exp. Biol.* **80:** 287–297.

Quandt, F. N., and H. L. Gillary. 1980. Separable phases of light-evoked depolarizations in the retina of *Strombus*. *J. Exp. Biol.* **84:** 137–148.

Strumwasser, F., R. Alvarez, D. Viele, and J. Woolum. 1979. Structure and function of a circadian oscillator system. Pp. 51–56 in *Biological Rhythms and their Central Mechanisms*, M. Suda, O. Hayaishi, and H. Nakagawa, eds. Elsevier/North Holland Biomedical Press.

Takahashi, J. S., D. E. Nelson, and A. Eskin. 1989. Immunocytochemical localization of serotonergic fibers innervating the ocular circadian system of *Aplysia*. *Neuroscience* **28:** 139–147.

Reference: *Biol. Bull.* **180**: 295–300. (April, 1991)

Control of Central and Peripheral Targets by a Multifunctional Peptidergic Interneuron

DAVID J. PRIOR

Department of Biological Sciences, Northern Arizona University, Flagstaff, Arizona 86011

Abstract. In the terrestrial slug, *Limax maximus*, feeding activity and cardiovascular function have been shown to be correlated. For example, in intact animals, both feeding responsiveness and heart activity are suppressed during dehydration (Grega and Prior, 1986). The paired peptidergic buccal ganglion neurons RB1 and LB1 have dramatic modulatory effects on both the feeding motor program (FMP) and the force of heart contraction (Welsford and Prior, 1991). The B1 neurons appear to contain the small cardioactive peptides (SCPs). Observations have a frequency dependent excitation of both the FMP and the heart demonstrated by intracellular stimulation of B1. Thus, interneuron B1 may serve to mediate the coincident modulation of multiple responses to physiological stresses.

Introduction

Environmental stress or a change in the physiological state of an organism very often results in a concerted array of regulatory responses. Such responses usually include modification of behavioral patterns, or the level of behavioral responsiveness, as well as changes in physiological functions such as cardiac output and respiratory activity. With the use of certain invertebrate organisms, recent research has addressed the question of the control of such concerted response patterns (Prior, 1989; Teyke *et al.*, 1990; Frugal and Brownell, 1987).

Terrestrial gastropods, such as *Limax maximus*, are remarkably susceptible to environmental stresses such as dehydration. In a drying environment, they can lose 30–40% of their body weight within a few hours (see Prior *et al.*, 1983; Riddle, 1983; Prior, 1985, for reviews). Among the array of regulatory responses displayed by dehydrating slugs are contact-rehydration (Prior, 1984; Prior and Uglem, 1984), modifications in respiratory function (Dickinson *et al.*, 1988), alterations in feeding responsiveness (Prior, 1983; Phifer and Prior, 1985) and modifications in cardiovascular function (Grega and Prior, 1986; Welsford and Prior, 1991). As such, *Limax* represents a useful model for the analysis of the integration of multiple regulatory responses.

The concerted control of feeding behavior and cardiovascular function in *Limax* has been a focus of recent work (see Grega and Prior, 1985; Prior and Welsford, 1989). Rhythmic feeding behavior in this organism involves alternating protraction and retraction of the toothed radula against a food source. Feeding bouts often last many minutes and can involve hundreds of bite cycles (see Gelperin *et al.*, 1978). In semi-intact or isolated preparations of the central nervous system (CNS: Fig. 1), chemical stimuli applied to the lips or electrical stimulation of the lip nerves can elicit a prolonged pattern of efferent neural activity that underlies the feeding movements. This feeding motor program (FMP; Prior and Gelperin, 1977; Gelperin *et al.*, 1978) consists of alternating bursts of activity in protractor and retractor motoneurons (Fig. 1, 2). In addition to activation of the major buccal musculature, the FMP involves synchronized activation of the accessory salivary system. During feeding, the activity of the fast salivary burster neurons (FSBs), which are the motoneurons to the salivary ducts, becomes phase-locked with protraction (Fig. 2).

SCP_B Modulation of Feeding and Heart Function

In gastropods, the small cardioactive peptides (SCPs) have an excitatory effect upon both the musculature (see Lloyd and Willows, 1988; Lloyd, 1989) and the neural networks underlying patterned feeding activity (see Willows *et al.*, 1988). In several species, SCP_B can initiate patterned efferent activity in isolated CNS preparations (*e.g.*, *Helisoma*, Murphy *et al.*, 1985; *Tritonia*, Willows

Received 14 December 1990; accepted 30 January 1991.

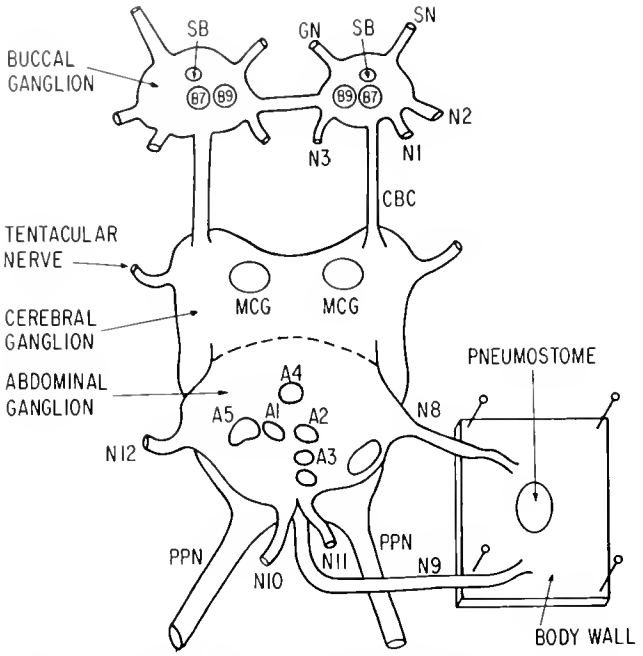

Figure 1. A diagram of the isolated central nervous system of *Limax* including: the paired buccal ganglia and the fused cerebral and abdominal ganglia; the pneumostome region; abdominal nerves N8–N12 and the posterior pedal nerves, PPN; buccal nerves N1–N3; gastric nerve, GN; salivary nerve, SN; buccal protractor motoneuron B7; fast salivary burster neuron, SB; cerebrobuccal connective, CBC; metacerebral giant cell, MCG.

et al., 1988). In *Limax*, however, SCP_B has a modulatory role, increasing the responsiveness of the central pattern generator to stimuli (Prior and Watson, 1987). In the presence of 10^{-7} to 10^{-6} *M* SCP_B, otherwise ineffective stimuli can initiate full expression of the feeding motor program.

Among the neurons in *Limax* that are responsive to SCP_B are the paired fast salivary bursters. The rate of endogenous burst activity in these motoneurons is enhanced by application of SCP_B in a concentration-dependent manner (Fig. 3, 4). Short-term application of SCP_B results in a slow increase in FSB burst frequency and an even slower decrement of the effect follows initiation of a saline wash. In addition, continuous perfusion of a preparation for 20–30 min reveals no indication of desensitization of the effect. In 10^{-6} *M* SCP_B, the burst frequency was sustained at 14 bursts/min compared with a control frequency of 1 burst/min (see Prior and Watson, 1987). It has been determined that this excitatory effect is mediated by an increase in the rate of the interburst depolarization rather than a general decrease in resting potential (Hess and Prior, 1989). Thus the effects of SCP_B on the *Limax* feeding system include modulation of the responsiveness of the FMP in addition to direct excitation of specific motoneurons.

To assess further the potential role of an SCP_B-like peptide in the regulation of feeding responsiveness, exogenous

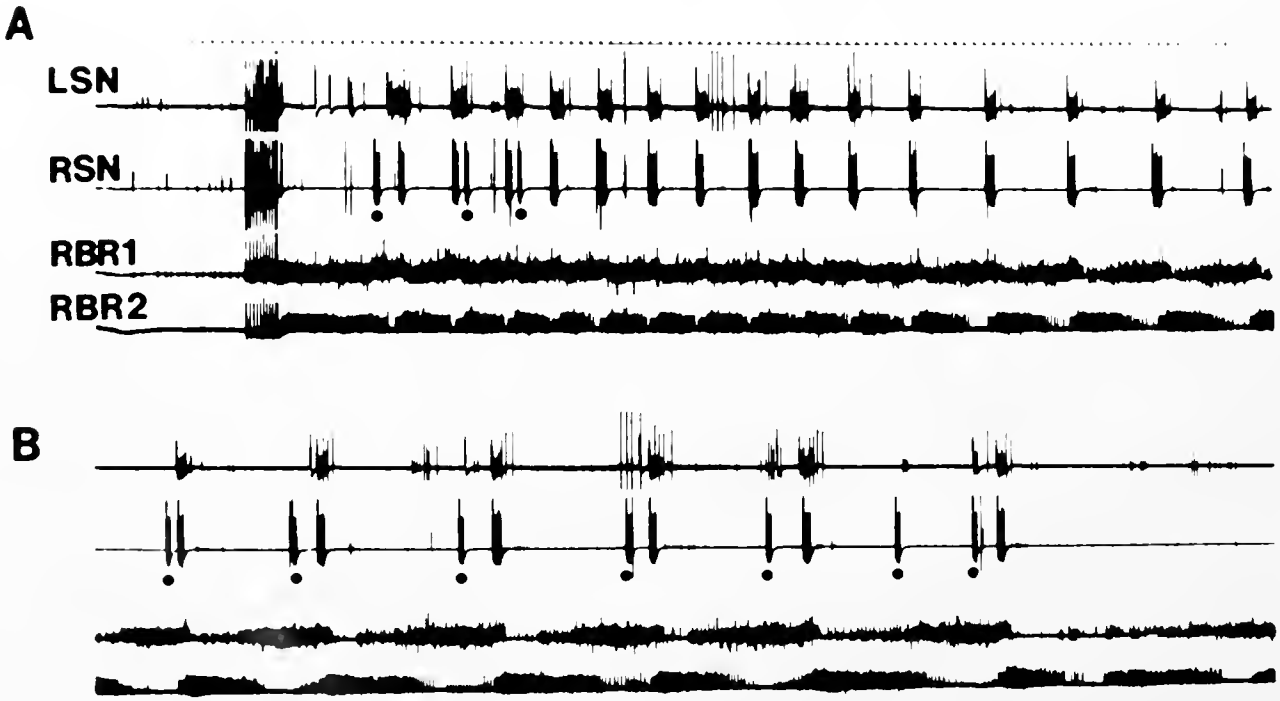

Figure 2. Activation of the feeding motor program (FMP) in an isolated buccal ganglia-brain preparation by electrical stimulation of an external lip nerve (artifacts at beginning at A). The FMP is characterized by alternation of efferent bursts correlated with protraction (buccal nerve 1; RBR1; and the right and left salivary nerves: RSN, LSN), and retraction (buccal nerve 2; RBR2). The nonfeeding endogenous bursts of the right FSB are noted with dots. The upper calibration trace indicates one mark/second. (From Prior and Watson, 1987)

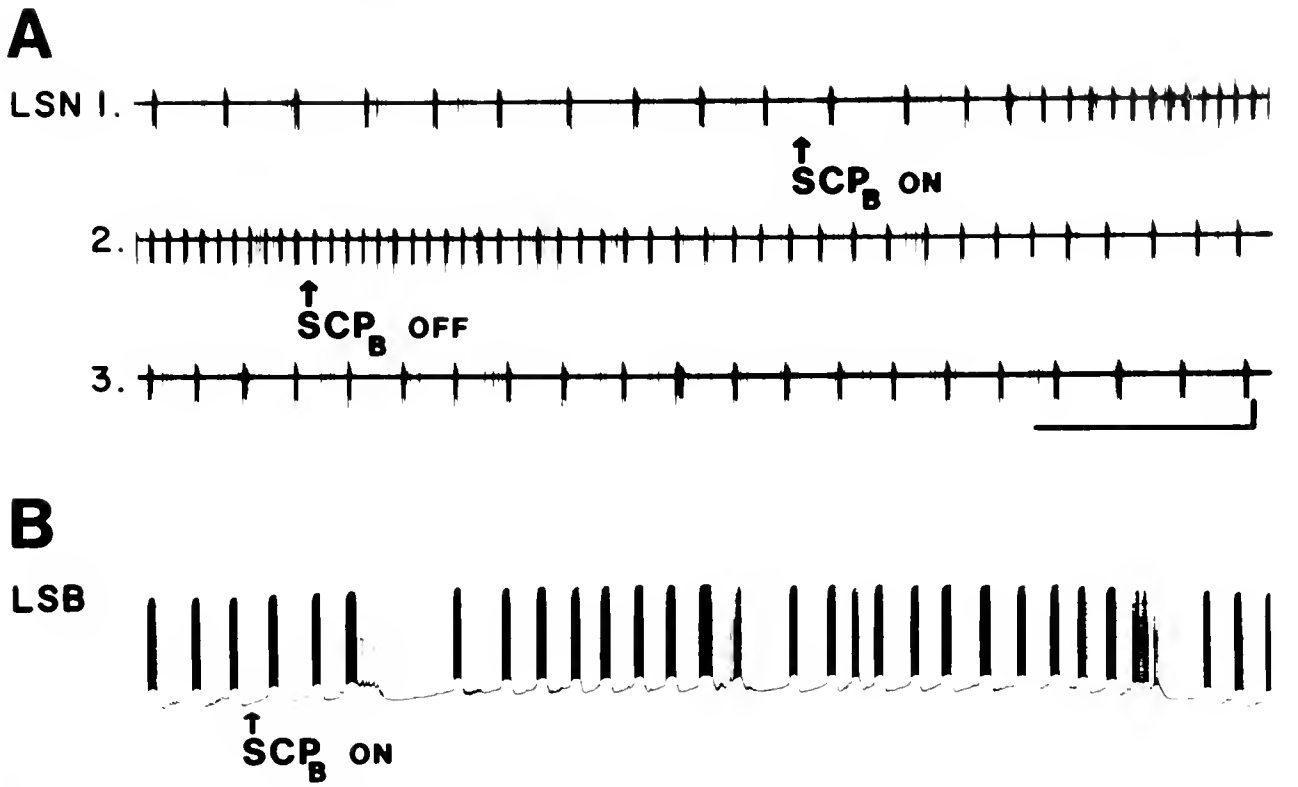

Figure 3. (A) A continuous extracellular recording from the left salivary nerve (LSN) of an isolated buccal ganglia-brain preparation is shown in 1–3. The prominent bursting unit in this record is the fast salivary burster (FSB; each burst consists of 12–15 spikes). Within 20 s of the application of 2×10^{-6} *M* SCP_B to the preparation (first arrow), the burst frequency of the FSB increases. Following removal of SCP_B from the superfusion medium (second arrow), burst frequency of the FSB returns to the pretreatment level. (B) an intracellular recording from the fast salivary burster neuron (FSB) showing the increase in burst frequency and, in this case, progressive depolarization, in response to 2×10^{-6} *M* SCP_B (the dashed line indicates the level of the interburst hyperpolarization before exposure to SCP_B). Bar = 30 s (A) and 20 mV (B). (From Prior and Watson, 1988)

SCP_B was injected into intact animals and their feeding responsiveness measured. As shown in Table 1., SCP_B can initiate the apetetive phases of feeding behavior including: (1) cessation of locomotion, (2) tentacular retraction, (3) lip eversion, and (4) lip movement. That the consumatory phase of feeding was not regularly initiated was not unexpected, in that in isolated CNS preparations SCP_B did not initiate feeding, but rather, increased responsiveness to stimuli. Nevertheless, this would appear to be the first demonstration of an orderly effect of injected SCP_B in an intact organism. This result certainly supports the notion that an SCP_B-like peptidergic system is involved in the control of the feeding system in *Limax*.

The small cardioactive peptides have been shown to have an excitatory effect on the musculature of numerous systems, including *Helix* heart (Lloyd 1978, 1982), *Aplysia* and *Tritonia* buccal mass and gut (Lloyd *et al.*, 1984; Lloyd and Willows, 1988), and *Limax* ventricle (Welsford and Prior, 1991; Lloyd, 1979; 1989). In *Limax*, both SCP_B and SCP_A cause a concentration-dependent increase in the force of ventricular contraction (Welsford and Prior, 1991). At a concentration of 10^{-6} *M*, SCP_B can cause a 150% increase in the force of ventricular contractions. Although lower concentrations of SCP_B (10^{-9} to 10^{-7} *M*) can cause a slight increase in heart rate, there does not appear to be a consistent effect (Prior and Welsford, 1989).

The excitatory effects of SCP_B on heart and the feeding system of *Limax*, together with the stress-induced coincident changes in feeding and cardiovascular function observed in intact animals (Grega and Prior, 1985), are indicative of the possibility of coincident control of these two systems.

Multifunctional Modulatory Interneuron B1

In that exogenous SCP_B can simultaneously modify feeding and cardiovascular function, immunohistochemical techniques were used in an effort to identify central

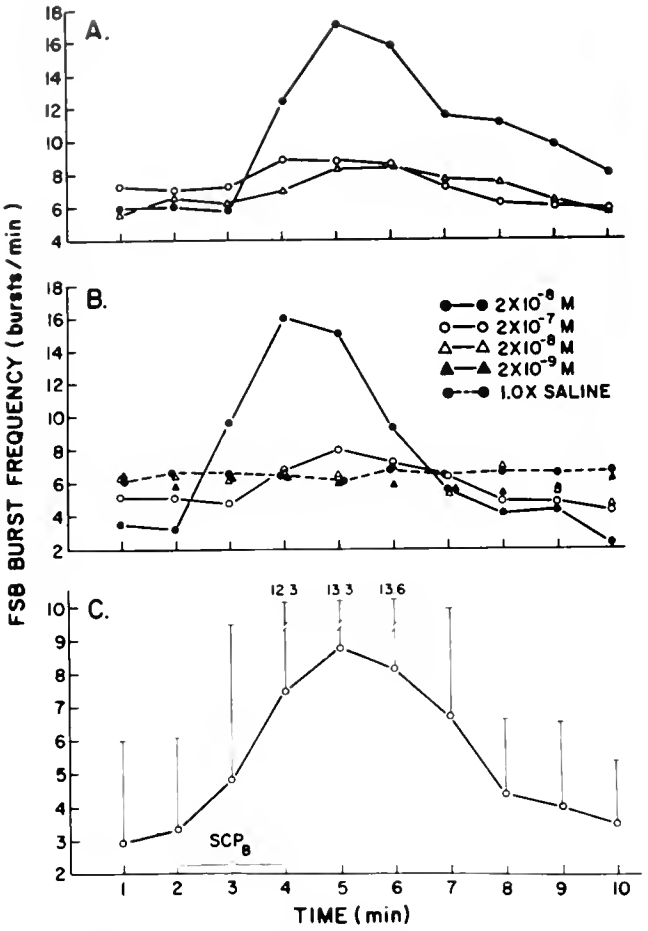

Figure 4. The responses of the fast salivary burster neuron (FSB) to varying concentrations of SCP_B are presented by plotting burst frequency as a function of time during the experiment. In each case, SCP_B was superfused over an isolated buccal ganglion-brain preparation between minutes 2 and 4. The preparation was superfused with saline for 20 min between each trial. (A) The responses obtained in three trials with the same preparation using various concentrations of SCP_B are shown. Each point represents the burst frequency of the FSB in the preceding 60 s. (B) The responses of a second preparation to SCP_B. In this case four different concentrations of SCP_B were used as well as a control saline trial. (C) The extent of the variability between preparations is illustrated by plotting the mean (±SD) burst frequency at each time point for 29 trials in 12 preparations during exposure to 2×10^{-6} *M* SCP_B. (From Prior and Watson, 1987)

neurons containing SCP_B-like-immunoreactive-material (SLIM) that might be involved. Among the most prominent SLIM-reactive neurons were the right and left B1 buccal neurons (Prior and Watson, 1987). In addition to those neurons that clearly contain SCP_B immunoreactive material, there are numerous cell bodies that are enmeshed by networks of immunoreactive fibers (*e.g.*, B7, FSB), which is suggestive of peptidergic endings near the target feeding neurons.

The morphology of B1 was examined by intracellular injection of horseradish peroxidase (Fig. 5a). There are

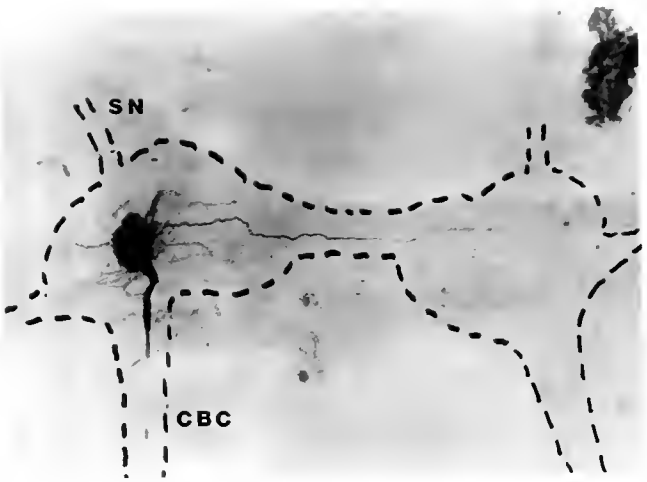

Figure 5a. A photomicrograph of a preparation of paired buccal ganglia (outlined) showing the morphology of the left B1 neuron injected with horseradish peroxidase. Cerebrobuccal connective, CBC; salivary nerve, SN; this preparation was made by K. Delaney)

two major axonal projections and an extensive dendritic arborization in the lateral lobe of the buccal ganglion. A small axon projects across the buccal-buccal commissure.

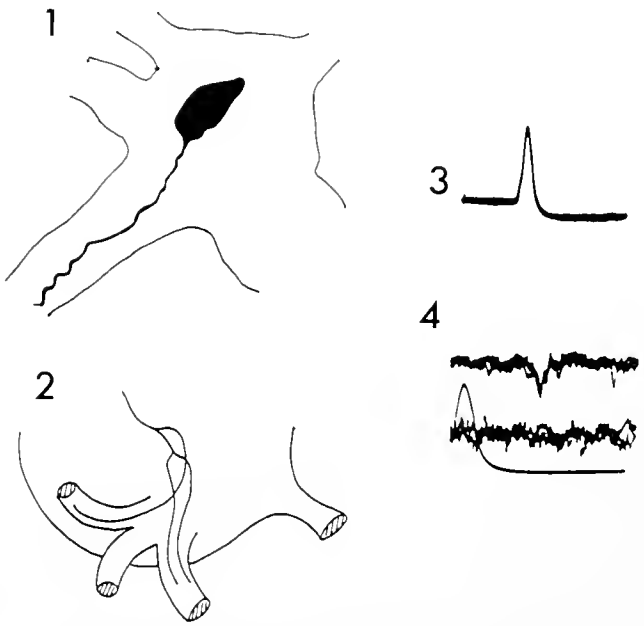

Figure 5b. Panel 1 is a camera lucida drawing of the soma of LB1 following injection of Co^{++} showing the major axon exiting the buccal ganglion in the ipsilateral cerebrobuccal connective. Panel 2 is a camera lucida drawing of the abdominal ganglion showing the continued axonal projection of the injected LB1, with one axonal branch in abdominal ganglion nerve 9 and two axonal branches in nerve 11. Panel 3 illustrates antidromic activation of B1 in response to repetitive stimulation of the cardiac branch of nerve 9. Panel 4 shows repetitive intracellular stimulation of B1 causing in a constant-latency axonal impulse recorded in nerve 9.

Table I

Behavioral effects of SCP_B injections in Limax maximus

Treatment	Behavioral observations			
	Tentacular locomotion	Lip retraction	Lip eversion	Lip movement
Saline	83.0%	8.0%	0.0%	0.0%
10^{-7} moll^{-1} SCP_B	83.0%	25.0%	17.0%	8.0%
10^{-6} moll^{-1} SCP_B*	92.0%	33.0%	42.0%	25.0%
10^{-5} moll^{-1} SCP_B**	17.0%	83.0%	100%	58.0%

The percentage of animals that displayed each behavior is presented in each case.
Each animal received injections of each concentration of SCP_B and the saline control.
The 0.05 probability level was accepted as significant (determined by a Friedman's test and a non-parametric multiple comparisons procedure).
All concentrations of SCP_B are the calculated final hemolymph concentrations.
The results with 1^{-5} and 10^{-6} moll^{-1} SCP_B injection were significantly different from those with injection of control saline and 10^{-7} moll^{-1} SCP_B. Furthermore, the results with 10^{-5} moll^{-1} SCP_B injection were significantly greater than those observed with injection of 10^{-6} moll^{-1} SCP_B.
* $P < 0.05$, ** $P < 0.01$, n = 12.
(From Schagene *et al.*, 1989)

Although the dendritic arborizations occur primarily in the lateral lobe, they do span into the medial lobe, including the region containing both retractor and protractor feeding motoneurons. The major axon projects out the ipsilateral cerebrocuccal connective, through the cerebral ganglion, into the abdominal ganglion and out abdominal nerves 9 and 11, which innervate the heart and kidney complex, respectively (Fig. 5b). Rapid stimulation (5Hz) of a cardiac branch of nerve 9 resulted in antidromic activation of the soma of B1. Correspondingly, repetitive activation of the soma of B1 by intracellular current injection was followed by a constant latency impulse in the cardiac branch of nerve 9 (Fig. 5a).

The immunohistochemical results together with the basic morphology of B1, including significant arborizations in the region of the feeding neurons, and, remarkably, a major axonal projection to the heart, were suggestive of a role for B1 in the concerted control of feeding and cardiovascular functions.

Intracellular stimulation of B1 at quite low frequencies results in a progressive increase in the activity of the fast

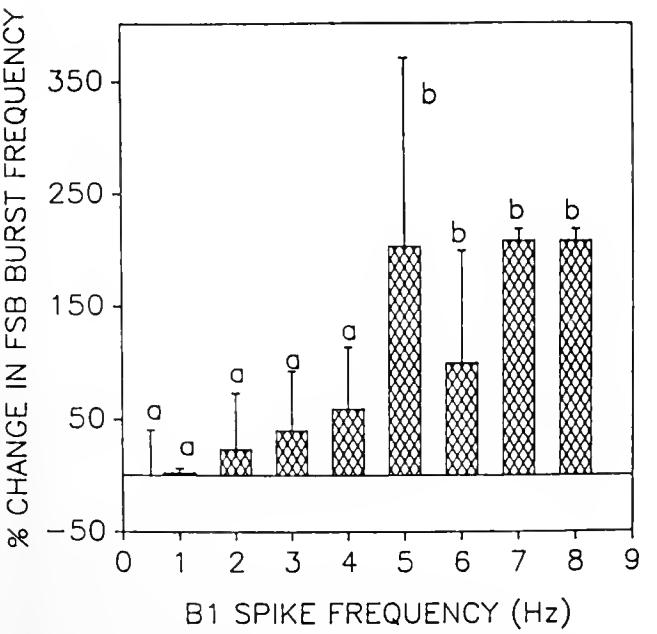

Figure 6. A summary of the change in the burst frequency of the fast salivary burster neuron initiated by intracellular stimulation of the ipsilateral B1 neuron at different impulse frequencies. The apparent threshold frequency for B1 is 2–4 Hz with the maximal effect occurring at about 7 Hz. Changes in the FSB burst frequency were normalized as a percentage of the pre-stimulation level of activity in each preparation. Each bar represents the mean (±SD) response of five buccal ganglion-brain preparations. (From Prior and Welsford, 1989)

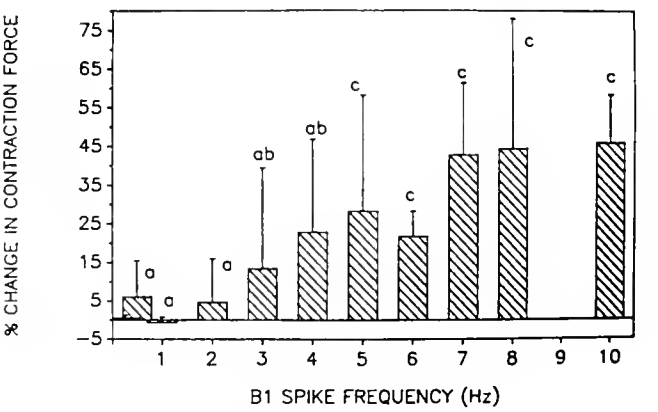

Figure 7. The effect of unilateral stimulation of B1 on the force of ventricular contraction. The bars represent the mean (±SD) response from 56 trials. Ten action potentials were elicited at each frequency. The a, b, c notation refers to significant differences (*e.g.*, C's are significantly, $P < 0.001$, different from a's and b's). (Redrawn from data of Welsford and Prior, 1991)

salivary bursters. As shown in Figure 6, driving B1 at 5 impulses/s can result in a 50% increase in FSB burst frequency. Even two to three impulses at low frequencies are sufficient to elicit a transient increase in FSB burst frequency. These effects are sustained in high Mg^{++}, high Ca^{++} saline indicating the possibility of monosynaptic connection.

To assess the potential role of B1 in the control of heart function, semi-intact preparations of the CNS and innervated heart were used, which allowed intracellular stimulation of B1 and measurement of ventricular activity. Stimulation of B1 at low frequencies resulted in an increase in the force of contraction of the heart (Fig. 7). It is of interest that B1 frequencies of 5 to 7 impulse/s were the most effective in the activation of both the FSB and the heart.

When this experiment was repeated with the CNS bathed in high Mg^{++}, high Ca^{++} saline, there was no change in the effectiveness of B1 to increase heart function. This suggests that B1 has a direct effect on peripheral targets rather than acting via additional CNS neuronal pathways.

Thus, it would appear that buccal neuron B1 may be a multifunction peptidergic interneuron capable of simultaneously modulating the central feeding motor program and cardiovascular function. As such, B1, along with other similar neurons, is positioned to control the synchrony of multiple behavioral responses normally observed in response to environmental stress and changes in the physiological state of an organism.

Acknowledgments

The work described in this paper was supported, in part, by grants from the Arizona Disease Control Research Commission (#82-0698) and The National Institutes of Health (M.B.R.S.# 2 SO3 RR03401-03).

Literature Cited

Dickinson, P. S., D. J. Prior, and C. Avery. 1988. The pneumostome closure rhythm in slugs: a response to dehydration controlled by hemolymph osmolality and peptide hormones. *Comp. Biochem. Physiol.* **89A**(4): 579–586.

Furgal, S. M., and P. H. Brownell. 1987. Ganglionic circulation and its effects on neurons controlling cardiovascular functions in the *Aplysia californica*. *J. Exp. Zool.* **244:** 347–364.

Gelperin, A., J. J. Chang, and S. Reingold. 1978. Feeding motor program in *Limax maximus:* neuromuscular correlates and control by chemosensory input. *J. Neurobiol.* **9:** 285–300.

Grega, D. S., and D. J. Prior. 1985. The effects of feeding on heart activity in the terrestrial slug, *Limax maximus:* central and peripheral control. *J. Comp. Physiol.* **156A:** 539–545.

Grega, D. S., and D. J. Prior. 1986. Modification of heart activity in response to dehydration in the terrestrial slug. *Limax maximus. J. Exp. Biol.* **237:** 185–190.

Hess, S. D., and D. J. Prior. 1989. Small cardioactive peptide B modulates feeding motoneurons in *Limax maximus. J Exp Biol.* **142:** 473–478.

Lloyd, P. E. 1978. Distribution and molecular characteristics of cardioactive peptides in the snail, *Helix aspersa. J Comp. Physiol.* **128:** 269–276.

Lloyd, P. E. 1979. Central peptide containing neurons modulate gut activity in *Tritona. Soc. Neurosci. Abstr.* **5:** 252.

Lloyd, P. E. 1982. Cardioactive neuropeptides in gastropods. *Fed. Proc.* **41:** 2948–2852.

Lloyd, P. E. 1989. Peripheral actions of the SCPs in *Aplysia* and other gastropod molluscs. *Am. Zool.* **29:** 1265–1274.

Lloyd, P. E., I. Kupfermann, and K. R. Weiss. 1984. Evidence for parallel actions of a molluscan neuropeptide (SCP_A) and serotonin in mediating arousal in *Aplysia. Proc. Nat. Acad. Sci. USA* **81:** 2934–2937.

Lloyd, P. E., and A. O. D. Willows. 1988. Multiple transmitter neurons in *Tritonia* II. Control of gut motility. *J. Neurobiol.* **19**(1): 55–67.

Murphy, A. D., K. Lukowiak, and W. K. Stell. 1985. Peptide modulation of patterned motor activity in identified neurons of *Helisoma. Proc. Nat. Acad. Sci. USA* **82:** 7140–7144.

Phifer, C. B., and D. J. Prior. 1985. Body hydration and haemolymph osmolality affect feeding and its neural correlate in the terrestrial gastropod, *Limax maximus. J Exp. Biol.* **118:** 405–426.

Prior, D. J. 1983. Hydration-induced modulation of feeding responsiveness in terrestrial slugs. *J. Exp. Zool.* **227:** 15–22.

Prior, D. J. 1984. Analysis of contact-rehydration in terrestrial gastropods: osmotic control of drinking behaviour. *J. Exp. Biol.* **111:** 63–73.

Prior, D. J. 1985. Water-regulatory behaviour in terrestrial gastropods. *Biol. Rev.* **60:** 403–424.

Prior, D. J., and G. L. Uglem. 1984. Analysis of contact-rehydration in terrestrial gastropods: absorption of ^{14}C-inulin through the epithelium of the foot. *J. Exp. Biol.* **111:** 73–80.

Prior, D. J. 1989. Neuronal control of osmoregulatory responses in gastropods. Pp. 1–24 in *Advances in Comparative Environmental Physiology,* R. Gilles, ed. 5. Springer-Verlag, New York.

Prior, D. J., and A. Gelperin. 1977. Autoactive molluscan neuron: reflex function and synaptic modulation during feeding in the terrestrial slug, *Limax maximus. J. Comp. Physiol.* **114:** 217–232.

Prior, D. J., and W. H. Watson. 1987. The molluscan neuropeptide, SCP_B, increases the responsiveness of the feeding motor program of *Limax maximus. J. Neurobiol.* **19**(1): 87–105.

Prior, D. J., and I. G. Welsford. 1989. The role of small cardioactive peptide, SCP_B, in the regulatory responses of terrestrial slugs. *Am. Zool.* **29:** 1255–1263.

Prior, D. J., M. Hume, D. Varga, and S. D. Hess. 1983. Physiological and behavioural aspects of water balance and respiratory function in the terrestrial slug, *Limax maximus. J. Exp. Biol.* **104:** 111–127.

Riddle, W. A. 1983. Physiological ecology of land snails and slugs. Pp. 431–461 in *The Mollusca,* W. D. Russell-Hunter, ed. *Ecology,* **6.** Academic Press, New York.

Schagene, K. A., I. G. Welsford, D. J. Prior, and P. A. Banta. 1989. Behavioral effects of injection of small cardioactive peptide, SCP_B, on the slug *Limax maximus. J. Exp. Biol.* **143:** 553–557.

Teyke, T., K. R. Weiss, and I. Kupfermann. 1990. An identified neuron (CPR) evokes neuronal responses reflecting food arousal in *Aplysia. Science* **247:** 85–87.

Welsford, I. G., and D. J. Prior. 1991. Modulation of heart activity in the terrestrial slug *Limax maximus* by the feeding motor program, small cardioactive peptides and stimulation of buccal neurone B1. *J. Exp. Biol.* **155:** 1–19.

Willows, A. O. D., P. E. Lloyd, and B. P. Masinovsky. 1988. Multiple transmitter neurons in *Tritonia* III. Modulation of central pattern generator controlling pattern. *J. Neurobiol.* **19**(1): 69–86.

Reference: *Biol. Bull.* **180**: 301–309. (April, 1991)

Opioid Systems and Magnetic Field Effects in the Land Snail, *Cepaea nemoralis*

MARTIN KAVALIERS AND KLAUS-PETER OSSENKOPP

Division of Oral Biology, Faculty of Dentistry, and Department of Psychology, University of Western Ontario, London, Ontario, Canada N6A 5C1

Abstract. Accumulating evidence shows that magnetic fields can affect a variety of opioid-mediated behavioral and physiological functions. The idea that endogenous opioids are involved in the mediation of fundamental behavioral responses in invertebrates is also gaining support. Evidence exists for opioid involvement in the mediation of nociceptive and antinociceptive ("analgesic") responses of the land snail, *Cepaea nemoralis*, and other mollusks, in a manner comparable to that in vertebrates. Exposure to various magnetic stimuli, including weak 60 Hz magnetic fields, has significant inhibitory effects on exogenous opiate-induced analgesia and endogenous opioid-mediated nociceptive responses of *Cepaea* in a manner analogous to that described for vertebrates. These effects of the magnetic stimuli are evident under both laboratory and natural conditions and include disruptions of the day-night rhythms of opioid-mediated nociception. These similar effects in *Cepaea* and rodents raise the possibility of a phylogenetic continuity in the effects of magnetic fields on basic opioid-mediated biological responses.

Introduction

Results of field and laboratory studies show that the behavioral, cellular, and physiological functions of animals can be affected by magnetic stimuli (see reviews in Adey, 1981; Gould, 1984; Ossenkopp and Kavaliers, 1988). These diverse actions have led to speculation on the possible modes of action of magnetic fields on biological systems (Leask, 1977; Semm *et al.*, 1980; Adey, 1981; Kirschvink and Gould, 1981; Liburdy *et al.*, 1987; Liboff and McLeod, 1988; Blackman *et al.*, 1989).

Evidence has accumulated that endogenous opioid systems and opioid peptides, which are involved in the modulation of a broad range of basic functions (Akil *et al.*, 1984), can be affected by magnetic stimuli. Substantial data now indicates that time-varying magnetic fields, especially those in the extremely low frequency (ELF) range (0.10–100 Hz), affect endogenous opioid systems and the actions of exogenous opiates such as morphine (Kavaliers and Ossenkopp, 1984, 1986, 1987; Miller *et al.*, 1985; Ossenkopp and Kavaliers, 1987; Prato *et al.*, 1987). Opioid systems may, thus, be an integral part of the mechanism(s) whereby magnetic fields exert their diverse behavioral and physiological effects (Ossenkopp and Kavaliers, 1988).

Although interest has primarily focused on vertebrates, there is evidence that magnetic fields affect a variety of behavioral physiological processes in invertebrates (Gould, 1984). Recently, opioid-mediated behaviors that are sensitive to magnetic stimuli have been demonstrated in a gastropod mollusk, the land snail *Cepaea nemoralis* (Kavaliers *et al.*, 1983; Kavaliers and Ossenkopp, 1989). This paper briefly describes (i) opioid modulation of behavioral responses in mollusks and (ii) the effects of magnetic fields on opioid mediated responses and their day-night rhythms in the snail, *Cepaea*.

Opioid Systems and Molluscs

General aspects

In vertebrates, endogenous opioid peptides co-exist with diverse hormones in endocrine glands and with classical or peptide transmitters in peripheral autonomic and sensory neurones. In addition, opioid peptides are widely distributed in the central nervous system where they function as transmitters or neuromodulators. Three families of endogenous opioid peptides derived from three precursor peptides are known to date: the pro-opiomelanocortin (POMC), the pro-enkephalin, and the pro-dynorphin system. These precursors undergo differential

Received 19 July 1990; accepted 6 November 1990.

processing in various regions of the central and peripheral nervous systems, and the major cleavage products have different affinities to the three major types of opioid receptors: μ, δ, and κ (Hollt, 1986).

These opioid peptides and receptors have now been identified in a variety of invertebrate taxa, strongly suggesting a phylogenetic conservation of opioid peptide structure and function (Kream *et al.*, 1980; Leung and Stefano, 1984, 1987; Scharrer *et al.*, 1988; Zisper *et al.*, 1988; Leung *et al.*, 1990; Santoro *et al.*, 1990). Results of behavioral, electrophysiological, immunological, and pharmacological studies have shown that endogenous opioid peptides and exogenous opiate agonists and antagonists have behavioral and physiological actions in invertebrates resembling those induced in mammals (Stefano, 1982, 1989; Leung and Stefano, 1987; Stefano *et al.*, 1989).

Behavioral aspects

Nociception. One of the primary roles of vertebrate opioid systems is the modulation of nociception and behavioral responses to aversive and stressful stimuli (Besson and Chaouch, 1987; Kavaliers, 1989a). In nature, animals commonly encounter aversive stimuli that can influence their survival. To effectively respond to these stimuli, organisms require: (i) a mechanism for recognizing aversive stimuli, (ii) a set of effectors that can react to the noxious stimulus, and (iii) a system for producing coordinated and directed movements and behavior in response to the stimuli. The ability of animals to recognize and physically react to aversive or noxious stimuli that can compromise their integrity is embodied in the term "nociception" (Sherrington, 1906). Nociceptors are preferentially sensitive to either a noxious stimulus or to an aversive stimulus that would become noxious if prolonged, and they code the intensity of the stimulus (Besson and Chaouch, 1987). In addition, the responses from the effectors are appropriate to the input from the receptors. Nociception can be used to provide an index of an animal's sensitivity to aversive environmental conditions and, thus, can allow for the determination of the capacity to execute adaptive behavior. Measurements of alterations in nociceptive-related responses (decreases in sensitivity-antinociception or analgesia when considered in terms of pain) are widely used to determine the behavioral and physiological status of animals following exposure to aversive, or potentially aversive, stimuli. In rodents, laboratory measures of nociception include recording of limb flexion or withdrawal (lifting a foot off an aversive, usually thermal surface); active avoidance (flinch jump, jumping, or moving from an aversive situation); and removal of the tail away from a thermal stimulus (tail-flick) (Kavaliers, 1989a).

Assays for invertebrate nociception have been developed, and nociceptive responses have been observed in invertebrates as well as vertebrates (Kavaliers, 1989a). For example, within a few seconds after *Cepaea* is placed on a surface warmed to 40°C, the snail lifts the anterior portion of its fully extended foot away from the aversive surface (Fig. 1). The behavioral end point used is the time at which the foot reaches its readily discernible maximum elevation. This "foot-lifting" behavior is not observed in snails that are exposed to temperatures normally present in their natural habitats, but becomes increasingly evident as the temperature is raised towards 40°C. This nociceptive response is comparable to the foot-lifting response exhibited by rodents when placed on a warmed surface. Similar, thermally induced nociceptive responses have also been reported for the snail, *Helix aspersa*, and the slug, *Arion alter* (Leung and Stefano, 1987; Dalton and Widdowson, 1989). A nociceptive function is also indicated for specific mechanoafferent neurons innervating the tail, parapodia, and much of the foot and body wall of the marine mollusk *Aplysia californica* (Walters and Erickson, 1986). These neurons display increasing discharge frequency in response to progressively increasing pressure, with maximal responses occurring to stimuli that could cause tissue damage (Walters, 1987). A similar graded pattern of response has been used to define the activity of classical mammalian nociceptors (Besson and Chaouch, 1987).

Opioid mediation of nociception and antinociception. Antinociception has been widely documented in experimental animals following exposure to diverse environmental stimuli, with both opioid and non-opioid mechanisms being implicated (Rodgers and Randall, 1988). Furthermore, it now seems clear that environmentally induced pain inhibition is an important component of an organism's defensive repertoire and hence has high adap-

Figure 1. Thermal 'nociceptive' response of a hydrated individual *Cepaea nemoralis* placed on a 40°C surface. The behavioral end point used is the maximum elevation of the anterior portion of the fully extended foot.

tive value (Amit and Galina, 1986). In vertebrates, the tonic activity of endogenous opioid systems can be increased by a range of environmental stimuli. In laboratory rodents, this "stress"—or environmentally induced analgesia (Amit and Galina, 1984)—can be recorded as an increased latency of a foot-lift or tail-flick response. Administration of either endogenous opioid peptides, such as enkephalin or exogenous opiate antagonists, such as the prototypic μ opiate agonist, morphine, produces similar analgesic effects. Prototypic exogenous opiate antagonists, such as naloxone or naltrexone, can reverse or attenuate these analgesic effects, and, in certain cases, can reduce nociceptive responses and induce hyperanalgesia (Martin, 1984).

Similar evidence for opioid involvement in the mediation of antinociception or analgesia and nociception is present for mollusks. Morphine, as well as the endogenous opioids β-endorphin and methionine-enkephalin, enhance, in a dose-dependent manner, the latency of the nociceptive responses of *Cepaea* and the slug, *Arion*, to a warmed surface (Dalton and Widdowson, 1989; Kavaliers *et al.*, 1983, 1985). As in mammals, maximum antinociceptive effects of morphine in *Cepaea* are seen 15–30 min after injection, with a decline to basal thermal response latencies by 60–120 min (Kavaliers *et al.*, 1983). These antinociceptive effects occur without any evident effects on the spontaneous locomotor activity or motor abilities of the animals. The antinociceptive effect of morphine is also produced by the benzomorphan levorphanol, but not by the stereoisomer dextrophan, suggesting that the receptor that interacts with these opiates has stereospecific requirements (Hirst and Kavaliers, 1987). Naloxone suppresses, and dose-dependently reverses, the analgesic effects of morphine in *Cepaea*, and reduces the response times (hyperalgesia) of particular morphological types of *Cepaea* that display elevated nociceptive responses (Kavaliers *et al.*, 1983; Kavaliers, 1989b). This further supports opioid involvement in the mediation of antinociception and nociception in *Cepaea*.

The specific μ and δ opioid agonists, (D-Ala^2-Me-Phe^5, Gly-ol)-enkephalin (DAMGO) and (D-Ala^2, D-Leu^4) enkephalin (DADLE), respectively, also have significant antinociceptive effects in *Cepaea* and *Arion*, suggesting the presence of μ and δ opioid receptors (Dalton and Widdowson, 1989; Kavaliers *et al.*, 1985). In addition, the specific κ opiate agonist U-50,488H, has significant antinociceptive effects in *Cepaea* (Kavaliers and Ossenkopp, 1989). As in mammals, the duration of effect of U-50,488H is longer than that of morphine, and there is a low sensitivity to reversal by naloxone. Taken together with the demonstrations of κ opioid binding sites and the immunocytochemical localization of the endogenous κ ligand dynorphin, in invertebrates (Ford *et al.*, 1986), these antinociceptive effects raise the possibility of a κ opioid-mediated antinociceptive system in *Cepaea*.

Day-night rhythms of nociception. Significant day-night rhythms are exhibited in the nociceptive responses and analgesic effects of morphine in *Cepaea*. These nocturnally and crepuscularly active snails display elevated night-time levels of nociception and morphine-induced analgesia under both field and laboratory conditions (Kavaliers *et al.*, 1990). The elevated nocturnal response latencies to a thermal stimulus are reduced by naloxone and the diel rhythm of nociception can be disrupted by pretreatment with the irreversible μ opioid receptor alkylating agent, β-funaltrexamine (β-FNA) (Kavaliers and Ossenkopp, 1991). This suggests that endogenous μ opioid systems may be involved in the generation or expression of the day-night rhythm of this measure of nociception in *Cepaea*.

Stress-induced analgesia. In rodents, diverse stimuli have been shown to increase endogenous opioid activity and induce integrated adaptive behavioral responses, including analgesia (Amit and Galina, 1986). Similar environmentally induced opioid activation and analgesia is also evident in mollusks and other invertebrates (Kavaliers, 1987; Maldonado and Miralto, 1987; Dalton and Widdowson, 1989; Valeggia *et al.*, 1989). Exposure to either heat, centrifugal rotation, or novel chemical stimuli has been shown to increase thermal nociceptive thresholds of *Cepaea* (Kavaliers, 1987, 1989a). The warm-stress-induced analgesia is blocked by naloxone and the δ opioid antagonist ICI 154,129, and is suppressed by a 24-h pretreatment with β-FNA (Kavaliers, 1987). Brief body (tail) pinch stress of the slugs *Arion* and *Limax* also resulted in significant increases in their response latencies (Kavaliers and Hirst, 1986; Dalton and Widdowson, 1988). The analgesic response of *Limax* was blocked by naloxone, while that of *Arion* was reduced in a dose-dependent manner by naltrexone and the δ opiate antagonist ICI 148,164. Moreover, the duration of the stress-induced analgesia in *Arion* could be prolonged by the injection of enkephalinase inhibitors (Dalton and Widdowson, 1988). This further supports the involvement of endogenous opioid peptides in the mediation of a number of forms of stress-induced analgesia in gastropod mollusks. It should be noted, however, that although these antinociceptive responses are opioid-mediated, it would be desirable to demonstrate cross-tolerance to exogenous opiate-induced analgesia, as well as to show changes in endogenous opioid peptide levels and receptor binding.

Mechanisms. At a biochemical and cellular level, there is evidence to suggest that the antinociceptive effects of opiates, in both *Cepaea* and rodents, are associated with alterations in calcium channel activity. Calcium channels are reported to be involved in the regulation of neuronal functions in mollusks in a manner similar, but not nec-

essarily identical, to that in vertebrates (Akaike *et al.*, 1981; Gerschenfeld *et al.*, 1986; Hammond *et al.*, 1987; Miller, 1987). In vertebrates, the activation of μ or δ opioid receptor types increases potassium channel conductance and indirectly reduces calcium channel conductance, while activation of κ receptors causes a direct reduction in voltage dependent calcium conductance (North, 1986). In both cases, the net result is a reduction in neuronal discharge frequency and the amount of transmitter released. In both rodents and *Cepaea*, the dihydropyridine (DHP) and non-DHP calcium channel antagonists diltiazem, verapamil, and nifedipine can reduce exogenous opiate and stress-induced opioid analgesia (Kavaliers and Ossenkopp, 1987, 1989). This suggests similar roles for calcium-channel-related mechanisms in the mediation of opiate-induced analgesia in mammals and mollusks. In addition, pharmacological reductions of G protein activity by pertussis toxin pretreatment have similar inhibitory effects on morphine-induced analgesia in *Cepaea* and rodents (Yu and Kavaliers, 1991). This suggests that similar intermediary messenger systems are involved in the mediation of opiate effects in *Cepaea* and rodents. Moreover, data also indicate that opiates have similar inhibitory effects on dopamine and possibly other monoamine systems in rodents and mollusks (Stefano, 1982). These observations suggest similar modes of action and sensitivities of opioid systems in vertebrates and mollusks.

Magnetic Fields and Opioid Systems

General aspects

Research on the roles of geomagnetic information in avian and invertebrate orientation and migration has provided some of the most convincing results on the biological effects of magnetic fields (Ossenkopp and Barbeito, 1978; Gould, 1984; Wiltschko and Wiltschko, 1990). A variety of other biological effects produced by exposure to magnetic fields have also been documented in both invertebrates and vertebrates (reviews in Adey, 1981; Gould, 1984; Ossenkopp and Kavaliers, 1988). In mollusks, these effects of magnetic fields include alterations in neuronal activity and orientation behaviors (Brown and Webb, 1960; Brown *et al.*, 1960 a,b; Brown, 1971; Lohmann and Willows, 1987; Azanza, 1989; Balaban *et al.*, 1990).

As previously indicated, among the more dramatic actions of magnetic stimuli in mammals are reversible modifications in the effects of exogenous opiates and endogenous opioids. Natural geomagnetic disturbances arising from intense solar activity, earth strength, 0.5–1.5 gauss 60 Hz magnetic fields, relatively weak rotating magnetic fields, and stronger magnetic fields associated with diagnostic magnetic resonance imaging have all been shown to reduce the analgesic effects of morphine in mice (Kavaliers and Ossenkopp, 1984, 1986; Miller *et al.*, 1985; Ossenkopp *et al.*, 1983; Prato *et al.*, 1987).

Results of recent investigations with the snail *Cepaea*, have extended these inhibitory effects of magnetic stimuli on opioid systems to mollusks (Kavaliers and Ossenkopp, 1989). These, and additional findings from *in vitro* preparations (Golding *et al.*, 1985), avian orientation (Papi and Luschi, 1991), and spatial learning in rodents (Kavaliers *et al.*, 1991a), which relate the effects of magnetic fields to alterations in opioid activity, suggest that a broad range of fundamental opioid-mediated functions may be sensitive to magnetic stimuli.

Magnetic fields and opioid-mediated nociception in Cepaea

Rotating magnetic fields. Results of investigations of the effects of exposure to a 0.5 Hz rotating magnetic field (RMF) on morphine-induced antinociception in *Cepaea* provided the first direct evidence that magnetic stimuli could affect opioid systems in an invertebrate (Kavaliers and Ossenkopp, 1989). As in rodents (Kavaliers and Ossenkopp, 1986, 1987), exposure for 15–30 min to a heterogenous time-varying magnetic field (0.15–9.0 mT or 1.5–90 gauss, produced by two rotating horseshoe magnets) of about 0.5 Hz significantly reduced day-time morphine-induced analgesia in *Cepaea* without any evident effects on the basal nociceptive responses of saline-treated control animals. The rotating magnetic fields also attenuated the analgesic effects of the κ opiate agonist U-50,488H. In addition, and as in rodents, exposure to the rotating magnetic fields reduced stress-induced opioid analgesia in *Cepaea*. These findings show that time-varying magnetic fields can significantly alter both exogenous opiate- (μ and κ) and endogenous opioid-induced analgesia in an invertebrate. These observations also raise the possibility that exposure to magnetic stimuli may compromise the expression of adaptive opioid-mediated behavioral and physiological responses to environmental stresses. It should be noted that in control sham exposure conditions, where dummy weights rather than horseshoe magnets were used, there were no effects on opioid-mediated antinociception. In these studies there was an equivalent electric field in the sham and magnetic field exposure conditions. This minimizes the potential involvement of electric fields in the inhibition of opioid analgesia.

60 Hz magnetic fields. Increasing concerns about the possible health effects due to exposure to high-voltage transmission lines and electrical appliances in the home have been expressed (Ahlboom, 1988). There have been numerous reports documenting biological effects in vertebrates following exposure to 50 or 60 Hz magnetic fields, although relatively little is known about the possible effects

in invertebrates. The effects in vertebrates have included retardation in embryological development, changes in behavioral activity levels and inhibition of chemically and electrically kindled seizures. These effects are compatible with alterations in the functioning of endogenous opioid systems (review in Ossenkopp and Kavaliers, 1988). This speculation of opioid involvement is encouraged by the observation that acute (30-min) exposure to low intensity 60 Hz magnetic fields markedly reduces morphine-induced analgesia levels in mice, with a functional relationship between magnetic field intensity and the degree of inhibition of analgesia (Ossenkopp and Kavaliers, 1987).

Recently, it was observed that exposure of *Cepaea* to low intensity (1.0 gauss, rms) 60 Hz magnetic fields in a Helmholtz coil apparatus, as shown in Figure 2, also resulted in an attenuation of morphine-induced analgesia (Kavaliers *et al.*, 1990). Various durations of exposure (0.50, 2, 12, 48, or 120 h) to the 60 Hz fields reduced the levels of morphine-induced analgesia in both the light and dark periods of a 12 h light:12 h dark cycle, with the magnetic stimuli having significantly greater inhibitory effects in the dark period. The inhibitory effects of the magnetic fields were reversible. Twenty-four hours after exposure, the levels of morphine-induced analgesia were not significantly different from pre-exposure levels (Kavaliers *et al.*, 1990). These effects in *Cepaea* are consistent with the day-night rhythms in the inhibitory effects of naloxone and 60 Hz and rotating magnetic fields on morphine-induced analgesia in nocturnal rodents (Kavaliers and Ossenkopp, 1984; Ossenkopp and Kavaliers, 1987). The weak 60 Hz magnetic fields also significantly reduced the levels of the elevated naloxone-sensitive dark period nociceptive response latencies in *Cepaea*, while not affecting the lower level light period responses. Moreover, the degree of attenuation of the analgesic and nociceptive response latencies was related to the duration of exposure to the 60 Hz magnetic fields.

Determinations were also made of the effects of 60 Hz magnetic fields on opioid-mediated responses outside the laboratory under natural conditions. Exposure to 1.0 gauss 60 Hz magnetic fields under field conditions significantly attenuated morphine-induced antinociception and nociceptive responses of *Cepaea*, with the degree of attenuation being related to the duration of exposure to the magnetic fields (Tysdale *et al.*, 1991). The 60 Hz fields also disrupted the day-night rhythm of nociception, with particularly marked alterations in responses occurring during the rapidly changing light levels of the twilight periods as shown in Figure 3. These field observations suggest a possible relation between light reception or changes and magnetic field reception in *Cepaea*. A connection between magnetic field and light reception has been previously theoretically postulated (Leask, 1977) and experimentally indicated in several species of arthropods and vertebrates (Leucht, 1984, 1990; Olcese *et al.*, 1985, 1988; Phillips, 1987). However, it has not been established whether light itself is a prerequisite for reception of the magnetic field.

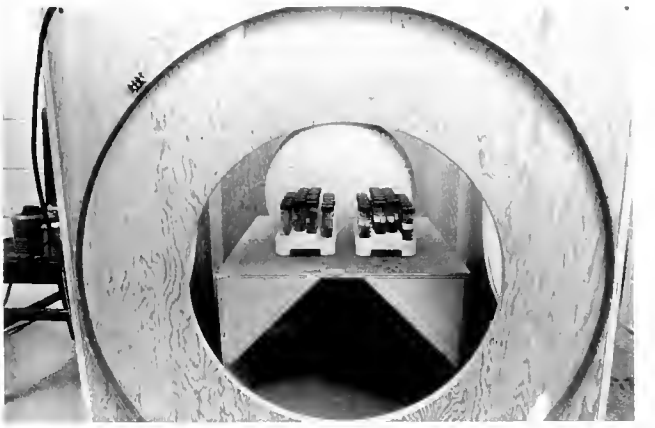

Figure 2. Helmholtz coil apparatus used for generation of 60 Hz magnetic fields to which the *Cepaea nemoralis* were exposed. Snails were held individually in translucent polypropylene 50 ml centrifuge tubes (10 · 2.5) containing a saturated atmosphere and natural vegetation. The tubes were placed upright on a platform (exposure volume) in the Helmholtz coil apparatus. The Helmholtz coils consisted of 100 turns of no. 24 motor enamel wire with a resistance of about 25 Ω per coil. The coils were 100 cm in diameter spaced 103 cm apart on the Z-axis and attached to the outside of a plywood frame. The coils were covered with a resin coating which immobilized the wires in the coils and prevented them from vibrating when they were carrying current. Line current (60 Hz) from standard outlets was applied to the coils and regulated with two variable autotransformers. The experimental exposure volume (30 × 30 × 330 cm) in which the snails in the tubes were placed was centered between the energized coils on the Z-axis. By altering the voltage input to the two coils, 60 Hz fields with linear polarity and field intensities up to 1.5 gauss (rms) could be generated [a field intensity of 1.0 gauss (rms) was used in the studies described in the text]. A sham field exposure condition was produced by turning off the current to the coils and placing test animals in the same exposure volume.

These observations with *Cepaea* show that exposure to weak 60 Hz magnetic fields significantly affects the diel rhythms of opioid-mediated responses in both the laboratory and under natural environmental conditions. They also show that the degree of inhibition of opioid-mediated responses is affected by both the duration and timing (day-night variations) of exposure to 60 Hz magnetic fields. These latter findings are particularly significant in view of the growing reports of associations between prolonged exposures to low intensity 50 and 60 Hz magnetic fields and the occurrence of various types of neoplasms (*e.g.*, Savitz *et al.*, 1988) and the evidence that opioid systems can modulate tumorigenesis (Zagon and McLaughlin, 1987). In this regard, it is of interest that the snails exposed to the 60 Hz magnetic fields showed, over a two-week period following exposures, increased levels of mortality relative to control sham-field exposed animals, and that night-time exposures resulted in greater mortality levels than day-time exposures (Ossenkopp *et al.*, 1990). This

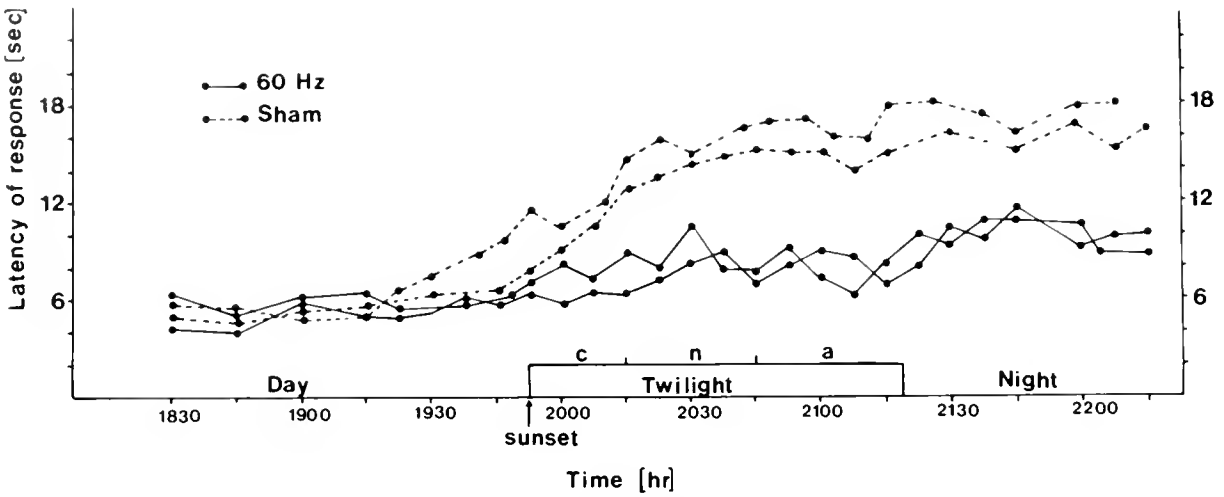

Figure 3. Examples of daytime, nighttime and twilight period thermal (40°C) response latencies (nociceptive responses) of *Cepaea nemoralis* held under natural summer (August) outdoor (Environmental Sciences Center, London, Ontario, 43° 4′ 30″ and 81° 18′ 30″ W) light conditions and exposed to either a 60 Hz magnetic field (1.0 gauss, rms, as described in Fig. 2) or a sham magnetic field (sham). Each point shown represents the mean nociceptive response of 18–24 snails. Different groups of snails were tested on each of the four days shown. For ease of presentation standard errors are excluded.

Exposure to the 60 Hz magnetic fields had no significant effects on the daytime (pre-sunset) nociceptive responses, but significantly ($P < 0.01$, repeated measures analysis of variance for 2200 h) reduced the nighttime response latencies as compared to the sham exposed snails and other control animals (not shown). Exposure to the magnetic fields also significantly ($P < 0.05$, for 2000 and 2100 h) attenuated the marked increases in thermal response latencies that occurred during the decreasing light levels of the twilight periods [civil (c), nautical (n) and astronomical (a) twilights; defined by the sun at −6°, −12° and −18°, respectively, from the horizon]. The greatest effects of the 60 Hz magnetic field on nociceptive responses occurred during the nautical and astronomical portions of the twilight period.

The temperatures and light intensities that the snails were exposed to ranged from 22 to 28°C and 100 to 200 $\mu w/cm^2$ (20–40 $\mu w/cm^2$ in the tubes) in the daytime, and from 14 to 22°C and 0.01 to 10 $\mu w/cm^2$ (0.001–1.0 $\mu w/cm^2$ in the tubes) in the twilight transitions and nighttime. These light (tubes) and temperature values were similar to the conditions present in the natural habitat of the snails (Kavaliers, 1989b). The background geomagnetic field had a daytime horizontal (H) intensity of 0.48 gauss, a vertical (Z) intensity of 0.24 gauss, and inclination (I) of 75. The Helmholtz coils were oriented with the x-axis oriented almost directly towards magnetic north.

is of relevance in view of the suggestions of synergistic effects between exposure to magnetic fields and environmental pollutants in the induction of neoplasms (Adey, 1987, 1990).

Mechanisms of action of magnetic stimuli on opioid systems

The inhibitory effects of the magnetic stimuli observed in both the day- and night-time may arise from the increased levels of the magnetic field as compared to earth strength fields or fluctuations in field strength. Although data has been presented to suggest that both of these components can influence biological systems (Adey, 1981; Cremer-Bartels *et al.*, 1984), evidence is accumulating that the biological effects of magnetic fields are primarily due to fluctuations in field strength (Blackman *et al.*, 1985, 1989; Prato *et al.*, 1987). Furthermore, data indicate that the extent of the biological effects of weak magnetic fields are dependent on the relative intensity and orientations of both the steady state [local geomagnetic field, which varies on a day-night basis (Cremer-Bartels *et al.*, 1984) and oscillating field (Blackman *et al.*, 1985; Prato *et al.*, 1987)]. However, it should be noted that many behavioral and physiological responses show no evidence of sensitivity to fluctuating magnetic fields (Ossenkopp and Kavaliers, 1988).

Magnetic fields have been proposed to alter the properties and stability of biological membranes, their transport characteristics, and the intra- and extra-cellular distributions and flux of calcium ions (Bawin and Adey, 1976; Adey, 1981, 1989; Liboff *et al.*, 1987; Carson *et al.*, 1990). Blackman *et al.* (1985, 1989) indicated that exposure to various combinations of time-varying and local geomagnetic fields caused significant changes in the efflux of calcium ions from *in vitro* preparations of chick brain

tissue. They speculated that this effect of magnetic fields on calcium ion efflux might involve a general property of biological tissue.

There is evidence that the inhibitory effects of the magnetic fields on opioid analgesia also involve changes in the levels, flux, and distribution of calcium ions, alterations in the functioning of calcium channels, along with modifications in the coupling between opioid receptors and calcium channels. This is supported by the findings that the DHP and non-DHP calcium channel antagonists diltiazem, nifedipine, and verapamil significantly reduce, while the DHP calcium channel agonist BAY K8644, significantly enhances the inhibitory effects of rotating magnetic fields on morphine-induced analgesia in *Cepaea* and mice (Kavaliers and Ossenkopp, 1987, 1989). In addition, the inhibitory effects of rotating magnetic fields on murine morphine-induced analgesia are reduced by the calcium chelator EGTA, and potentiated by the ionophore A21387 (Kavaliers and Ossenkopp, 1986).

Magnetic stimuli could affect calcium channel activation and conductance either directly or indirectly through alterations of intermediary effector or messenger systems. The second messenger system most commonly associated with opioid receptors and changes in ion transport involves inhibition of adenyl cyclase through G proteins (North, 1986; Stryer and Bourne, 1986). Administrations of pertussis toxin, which deactivates G proteins, reduce opiate-induced analgesia in both rodents and *Cepaea* (Parenti *et al.*, 1986; Przewlocki *et al.*, 1987; Yu and Kavaliers, 1990). Whether magnetic fields affect G protein activity is not known.

Calcium-activated, phospholipid-dependent protein kinase (protein kinase C; PKC) also plays an important role in relaying transmembrane signalling in diverse calcium-dependent cellular processes (Kaczmarek, 1987). Results of studies with PKC activators and inhibitors have shown that modulation of ion channel activity is an important function of PKC (DeRiemer *et al.*, 1985; Kaczmarek, 1987; Strong *et al.*, 1987; Conn *et al.*, 1989). Relatively little is known about the relations between PKC and opioid receptor activity, although results of a recent study indicate that stimulation of PKC with phorbol esters attenuates opioid activity through a decrease in G protein activity (Louie *et al.*, 1990).

There is, however, accumulating evidence linking magnetic fields and PKC activity. Magnetic stimuli have been reported to augment the effects of phorbol esters (PKC activators) and increase PKC activity in a number of cell culture preparations (Byus *et al.*, 1987; Adey, 1987, 1990). In *Cepaea*, the isoqinoline sulfonamides H-7 and H-9, which are specific inhibitors of PKC, reduce the inhibitory effects of 60 Hz magnetic fields on morphine-induced analgesia, whereas administration of the PKC activator SC-9 augments the effects of the magnetic fields (Kavaliers *et al.*, 1991b). This suggests that the inhibitory effects of magnetic fields on opiate-induced analgesia in *Cepaea* may include increases in PKC activity. Whether this involves effects on G proteins remains to be determined.

These mechanisms of action encompass a broader range of effects than just that of the opioid systems. However, in view of the broad range and phylogentic conservation of fundamental processes in which opioid systems are involved, these findings suggest that some of the biological effects of magnetic fields may arise through alterations of opioid activity.

Acknowledgments

We thank Susan Lipa and Donna Tysdale for their technical assistance and twilight determinations. The research described here was supported by Natural Science and Engineering and Research Council of Canada grants to M.K. and K.P.O.

Literature Cited

Adey, W. R. 1981. Tissue interactions with non-ionizing electromagnetic fields. *Physiol. Rev* **61:** 435–513.

Adey, W. R. 1987. Cell membranes: the electromagnetic environment and cancer promotion. *Neurochem. Res.* **13:** 671–677.

Adey, W. R. 1990. Joint actions of environmental nonionizing electromagnetic fields and chemical pollution in cancer promotion. *Environ. Health Perspec.* **86:** 297–305.

Ahlboom, A. 1988. A review of the epidemiologic literature on magnetic fields and cancer. *Scan. J. Work Enviro. Health* **14:** 337–343.

Akaike, N., A. M. Brown, K. Nishi, and Y. Tsuda. 1981. Actions of verapamil, diltiazem and other divalent cations on the calcium current of *Helix* neurons. *Br. J. Pharmacol.* **74:** 87–95.

Akil, H., S. J. Watson, M. E. Lewis, H. Khachaturian, and M. J. Walker. 1984. Endogenous opioids: biology and function. *Ann. Rev. Neurosci.* 7: 22–256.

Amit, Z., and G. H. Galina. 1986. Stress-induced analgesia: adaptive pain suppression. *Physiol Rev.* **66:** 1091–1120.

Azanza, M. J. 1989. Steady magnetic fields mimic the effect of caffeine on neurons. *Brain Res.* **489:** 195–198.

Balaban, P. M., N. I. Bravarenko, and A. N. Kuznetzov. 1990. Influence of a stationary magnetic field on bioelectric properties of snail neurons. *Bioelectromagnetics* **11:** 13–25.

Bawin, S. M., and W. R. Adey. 1976. Sensitivity of calcium binding in cerebral tissue to weak environmental electric fields oscillating at low frequency. *Proc. Nat. Acad. Sci. USA* **73:** 1999–2003.

Besson, J.-M., and A. Chaouch. 1987. Peripheral and spinal mechanisms of nociception. *Physiol. Rev.* **67:** 68–186.

Blackman, C. F., S. G. Beane, R. J. Rabinoowicz, D. R. House, and W. T. Joines. 1985. A role for the magnetic field in the radiation-induced efflux of calcium ions from brain tissue in vivo. *Bioelectromagnetics* **6:** 327–339.

Blackman, C. F., L. S. Kinney, D. E. House, and W. T. Joines. 1989. Multiple power-density windows and their possible origin. *Bioelectromagnetics* **10:** 115–128.

Brown, F. A., Jr. 1971. Some orientational influences of non-visual terrestrial electromagnetic fields. *Ann. N.Y. Acad. Sci.* **188:** 224–241.

Brown, F. A., Jr., and H. M. Webb. 1960. A "compass-direction" effect for snails in constant conditions and its lunar modulation. *Biol. Bull.* **119:** 65–74.

Brown, F. A., Jr., M. F. Bennett, and H. M. Webb. 1960a. A magnetic compass response of an organism. *Biol. Bull.* **119:** 65–74.

Brown, F. A., Jr., W. J. Brett, M. F. Bennett, and F. H. Barnwell. 1960b. Magnetic response of an organism and its solar relationships. *Biol. Bull.* **118:** 367–381.

Byus, C. V., S. E. Pieper, and W. R. Adey. 1987. The effects of low-energy 60 Hz environmental electromagnetic fields upon the growth-related enzyme ornithine decarboxylase. *Carcinogenesis* **8:** 1385–1389.

Carson, J. J. L., F. S. Prato, D. J. Prost, L. D. Diesbourg, and S. J. Dixon. 1990. Time-varying magnetic fields increase cytosolic free Ca^{2+} in HL60 cells. *Am. J. Physiol.* **28:** C687–C692.

Chiles, C., E. Hawrot, J. Gore, and R. Byck. 1989. Magnetic field modulation of receptor binding. *Magnetic Resonance in Medicine* **10:** 241–245.

Conn, J. P., J. A. Strong, and L. K. Kaczmarek. 1989. Inhibitors of protein kinase C prevent enhancement of calcium current and action potentials in peptidergic neuron of *Aplysia*. *J. Neurosci.* **9:** 480–487.

Cremer-Bartel, G., K. Krause, G. Mitoskas, and D. Brodersen. 1984. Magnetic fields of the earth as additional zeitgeber for endogenous rhythms. *Naturwissenschaften* **71:** 567–574.

Dalton, L. M., and P. S. Widdowson. 1989. The involvement of opioid peptides in stress-induced analgesia in the slug *Arion ater*. *Peptides* **10:** 9–13.

De Riemer, S. A., J. A. Strong, K. A. Albert, P. Greengard, and L. K. Kaczmarek. 1985. Enhancement of calcium current in *Aplysia* neurons by phorbol ester and kinase C. *Nature* **313:** 313–316.

Ford, R., D. M. Jackson, L. Tetrault, J. C. Torres, P. Assanh, J. Harper, M. K. Leung, and G. B. Stefano. 1986. A behavioral role for enkephalins in regulating locomotor activity in the insect *Leucophaea maderae*: evidence for high affinity kappa-like opioid binding sites. *Comp. Biochem. Physiol.* **85C:** 61–66.

Gerschenfeld, H. M., C. Hammond, and D. Paupardin-Tritsch. 1986. Modulation of the calcium current of molluscan neurones by neurotransmitters. *J. Exp. Biol.* **124:** 73–91.

Golding, G. P., L. Newboult, J. M. H. Rees, and B. R. Varlow. 1985. The effects of 50 Hz magnetic fields on opioid peptide mediated inhibition of guinea pig ileum. *Neuropeptides* **5:** 357–358.

Gould, J. 1984. Magnetic field sensitivity in animals. *Ann. Rev. Physiol.* **4:** 585–598.

Hammond, C., D. Paupardin-Tritsch, A. C. Narin, P. Greengard, and H. M. Gerschenfeld. 1987. Cholecystokinin induces a decrease in Ca^{++} current in snail neurons that appears to be mediated by protein kinase C. *Nature* **325:** 809–811.

Hirst, M., and M. Kavaliers. 1987. Levorphanol but not dextrophan suppresses the foot-lifting response to an aversive stimulus in the terrestrial snail (*Cepaea nemoralis*). *Neuropharmacology* **26:** 121–123.

Hollt, V. 1986. Opioid peptide processing and receptor selectivity. *Ann. Rev. Pharmacol. Toxicol.* **26:** 59–77.

Kaczmarek, L. K. 1987. The role of protein kinase C in the regulation of ion channels and neurotransmitter release. *Trends Neurosci.* **10:** 30–34.

Kavaliers, M. 1987. Evidence for opioid and non-opioid forms of stress-induced analgesia in the snail, *Cepaea nemoralis*. *Brain Res.* **410:** 111–115.

Kavaliers, M. 1989a. Evolutionary and comparative aspect of nociception. *Brain Res. Bull.* **6:** 923–931.

Kavaliers, M. 1989b. Polymorphism in opioid modulation of the thermal responses of the land snail *Cepaea nemoralis*. *Can. J. Zool.* **67:** 2721–2724.

Kavaliers, M., and M. Hirst. 1986. Naloxone-reversible stress-induced feeding and analgesia in the slug (*Limax maximus*). *Life Sci.* **38:** 203–209.

Kavaliers, M., M. Hirst, and G. C. Teskey. 1983. A functional role for an opiate system in snail thermal behavior. *Science* **220:** 99–101.

Kavaliers, M., M. Hirst, and G. C. Teskey. 1985. The effects of opioid and FMRF-amide peptides on thermal behavior in the snail. *Neuropharmacology* **24:** 621–626.

Kavaliers, M., and K.-P. Ossenkopp. 1984. Exposure to rotating magnetic fields alters morphine-induced behavioural responses in two strains of mice. *Neuropharmacology* **89:** 440–443.

Kavaliers, M., and K.-P. Ossenkopp. 1986. Magnetic field inhibition of morphine-induced analgesia and behavioral activity in mice: evidence for involvement of calcium ions. *Brain Res.* **379:** 830–838.

Kavaliers, M., and K.-P. Ossenkopp. 1987. Calcium channel involvement in magnetic field inhibition of morphine-induced analgesia. *Naunyn-Schmiedebergs Arch. Pharmakol.* **336:** 308–315.

Kavaliers, M., and K.-P. Ossenkopp. 1989. Magnetic fields inhibit opioid-mediated 'analgesic' behaviours of the terrestrial snail, *Cepaea nemoralis*. *J. Comp. Physiol. A.* **162:** 551–558.

Kavaliers, M., and K.-P. Ossenkopp. 1991. Magnetic fields, opioid systems and day-night rhythms of behavior. In *Electromagnetic Fields and Circadian Rhythms, Vol. I. Advances in Circadian Physiology*. M. Moore-Ede and S. Campbell, eds. Binkhauser, Boston, (in press).

Kavaliers, M., K.-P. Ossenkopp, and S. Lipa. 1990. Day-night rhythms in the inhibitory effects of 60 Hz magnetic fields on opiate-mediated 'analgesic' behaviors of the land snail, *Cepaea nemoralis*. *Brain Res.* **517:** 276–282.

Kavaliers, M., L. Eckel, K.-P. Ossenkopp, and N. Yu. 1991a. Enhanced learning of a sexually dimorphic spatial task in meadow voles following brief exposure to 60 Hz magnetic fields. *Soc. Neurosci. Abstr.* **21** (in press).

Kavaliers, M., K.-P. Ossenkopp, and D. M. Tysdale. 1991b. Evidence for the involvement of protein kinase C in the modulation of morphine-induced 'analgesia' and the inhibitory effects of exposure to 60Hz magnetic fields in the land snail, *Cepaea nemoralis*. *Brain Res.* (in press).

Kirschvink, J. L., and J. L. Gould. 1981. Biogenic magnetite as a basis for magnetic field detection in animals. *Biosystems* **13:** 181–201.

Kream, R. M., R. S. Zukin, and G. B. Stefano. 1980. Demonstration of two classes of opiate binding sites in the nervous tissue of the marine mollusc, *Mytilus edulis*. *J. Biol. Chem.* **225:** 9218–9224.

Leask, M. J. M. 1977. A physiochemical mechanism for magnetic field detection by migratory birds and homing pigeons. *Nature* **267:** 144–145.

Leucht, T. 1984. Responses to light under varying magnetic conditions in the honey bee, *Apis mellificia*. *J. Comp. Physiol. A.* **154:** 865–870.

Leucht, T. 1990. Ineractions of light and gravity reception with magnetic fields in *Xenopus laevis*. *J. Exp. Biol.* **148:** 325–334.

Leung, M. K., and G. B. Stefano. 1984. Isolation and identification of enkephalins in pedal ganglia of *Mytilus edulis* (Mollusc) *Proc. Nat. Acad. Sci. USA* **81:** 955–958.

Leung, M. K., and G. B. Stefano. 1987. Comparative neurobiology of opioids in invertebrates with special attention to senescent alterations. *Prog. Neurobiol.* **28:** 131–159.

Leung, M. K., H. H. Boer, J. van Minnen, J. Lundy, and G. B Stefano. 1990. Evidence for an enkephalinergic system in the nervous system of the pond snail, *Lymnaea stagnalis*. *Brain Res.* **531:** 66–71.

Liboff, A. R., R. J. Rozek, M. L. Sherman, B. R. McLeod, and S. D. Smith. 1987. ^{45}Ca cyclotron resonance in human lymphocytes. *J. Bioelect.* **6:** 13–22.

Liboff, A. R., and B. R. McLeod. 1988. Kinetics of channelised membrane ions in magnetic fields. *Bioelectromagnetics* **9:** 39–51.

Liburdy, R. P., R. Tenforde, and R. L. Magin. 1986. Magnetic-field induced drug permeability in liposome vesicles. *Radiat. Res.* **108:** 102–111.

Lohmann, K. J., and A. O. D. Willows. 1987. Lunar-modulated geomagnetic orientation by a marine mollusk. *Science* **235:** 231–235.

Louie, A. K., E. S. Bass, J. Zahn, P. E. Law, and H. H. Loh. 1990. Attenuation of opioid receptor activity by phorbol esters in neuroblastoma X Glioma NG 108-15 Hybrid cells. *J. Pharmacol. Exp. Therp.* **253:** 401–407.

Maldonado, H., and A. Miralto. 1987. Effects of morphine and naloxone on a defensive response of the mantis shrimp, *Squilla mantis*. *J. Comp. Physiol.* **A147:** 455–459.

Martin, W. R. 1984. Pharmacology of opioids. *Pharmacol. Rev.* **35:** 283–323.

Miller, R. J. 1987. Multiple calcium channels and neuronal function. *Science* **325:** 46–52.

Miller, D. B., C. F. Blackman, and J. S. Alie. 1985. Behavioral responses of morphine-treated mice to ELF magnetic fields. *Bioelectromagn. Soc. Meet. Abstr.* **1985:** 54.

North, R. A. 1986. Opioid receptor types and membrane ion channels. *TINS* **9:** 114–117.

Olcese, J., S. Reuss, and L. Vollrath. 1985. Evidence for the involvement of the visual system in mediating magnetic field effects on pineal melatonin synthesis in the rat. *Brain Res.* **333:** 382–384.

Olcese, J., S. Reuss, J. Stehle, S. Steinlecher, and L. Vollrath. 1988. Response of the mammalian retina to experimental alteration of the ambient magnetic field. *Brain Res.* **448:** 325–330.

Ossenkopp, K.-P., and R. Barbeito. 1978. Bird orientation and the geomagnetic field: a review. *Neurosci. Biobehav. Rev.* **2:** 255–270.

Ossenkopp, K.-P., and M. Kavaliers. 1987. Morphine-induced analgesia and exposure to 60 Hz magnetic fields: inhibition of nocturnal analgesia is a function of magnetic field intensity. *Brain Res.* **418:** 356–360.

Ossenkopp, K.-P., and M. Kavaliers. 1988. Clinical and applied aspects of magnetic field exposure: a possible role for the endogenous opioid systems. *J. Bioelect.* **7:** 189–208.

Ossenkopp, K.-P., M. Kavaliers, and M. Hirst. 1983. Reduced morphine analgesia in mice following a geomagnetic disturbance. *Neurosci. Lett.* **40:** 321–325.

Ossenkopp, K.-P., M. Kavaliers, and S. M. Lipa. 1990. Increased mortality in land snails (*Cepaea nemoralis*) exposed to powerline (60-Hz) magnetic fields and effects of the light-dark cycle. *Neurosci. Lett.* **114:** 89–94.

Papi, F., and P. Luschi. 1991. Pigeon navigation: naloxone injection and magnetic disturbance have a similar effect on initial orientation. *Rend. Acc. Naz. Lincei* (in press).

Parenti, M., F. Tirone, G. Giagnoni, N. Pecora, and D. Parolaro. 1986. Pertussis toxin inhibits the antinociceptive action of morphine in the rat. *Eur. J. Pharmacol.* **124:** 357–359.

Phillips, J. B. 1987. Specialized visual receptors respond to magnetic field alignment in the bowfly (*Calliphora vicina*). *Soc. Neurosci. Abstr.* **13:** 397.

Prato, F. S., K.-P. Ossenkopp, and M. Kavaliers. 1987. Nuclear magnetic resonance inhibition of morphine-induced analgesia in mice: differential effects of the static, radio-frequency and time-varying magnetic field components. *Mag. Reson. Imag.* **5:** 9–14.

Przewlocki, R., T. Costa, J. Lang, and A. Herz. 1987. Pertussis toxin abolishes the antinociception mediated by opioid receptors in rat spinal cord. *Eur. J. Pharmacol.* **144:** 91–93.

Rodgers, R. J., and J. I. Randall. 1988. Environmentally-induced analgesia: situational factors, mechanisms, and significance. Pp 107–147 in *Endorphins, Opiates and Behavioural Processes*, R. J. Rodgers and S. J. Cooper, eds. Wiley, Chichester.

Santoro, C., L. M. Hall, and R. S. Zukin. 1990. Characterization of two classes of opioid binding sites in *Drosophila melanogaster* head membranes. *J. Neurochem.* **54:** 154–170.

Savitz, D. A., H. Watchel, F. A. Barnes, E. M. John, and J. G. Tvrdik. 1988. Case-control study of childhood cancer and exposure to 60-Hz magnetic fields. *Am. J. Epidemiol.* **128:** 21–38.

Scharrer, B., G. B. Stefano, and M. K. Leung. 1988. Opioid mechanisms in insects, with special attention to *Leucophaea maderae*. *Cell. Mol. Neurobiol.* **8:** 269–284.

Semm, P., T. Schneider, and L. Vollrath. 1980. The effects of an earth-strength magnetic field on the electrical activity of pineal cells. *Nature* **288:** 607–608.

Sherrington, C. S. 1906. *The Integrative Action of the Nervous System.* Yale University Press, New Haven.

Stefano, G. B. 1982. Comparative aspects of opioid-dopamine interaction. *Cell. Mol. Neurobiol.* **2:** 167–182.

Stefano, G. B. 1989. Role of opioid neuropeptides in immunoregulation. *Prog. Neurobiol.* **33:** 149–153.

Stefano, G. B., M. K. Leung, X. Zhao, and B. Scharrer. 1989. Evidence for the involvement of opioid neuropeptides in the adherence and migration of immunocompetent invertebrate hemocytes. *Proc. Nat. Acad. Sci. USA* **86:** 626–630.

Strong, J. A., A. P. Fox, R. W. Tsien, and L. K. Kaczmarek. 1987. Stimulation of protein kinase C recruits covert calcium channels in *Aplysia* bag cell neurons. *Nature* **325:** 714–717.

Stryer, L., and H. R. Bourne. 1986. G proteins: a family of signal transducers. *Ann. Rev. Cell. Biol.* **2:** 391–419.

Tysdale, D., S. M. Lipa, K.-P. Ossenkopp, and M. Kavaliers. 1991. Inhibitory effects of 60Hz magnetic fields on opiate-induced 'analgesia' in the land snail, *Cepaea nemoralis*, under natural conditions. *Physiol. Behav.* **49:** 53–56.

Valeggia, C., E. Ferandez-Duque, and H. Maldonado. 1989. Danger stimulus-induced analgesia in the crab *Chasmagnethus granulatus*. *Brain Res.* **481:** 304–308.

Walters, E. T. 1987. Site-specific sensitization of defensive reflexes in *Aplysia:* a simple model of long-term hyperalgesia. *J. Neurosci.* **7:** 400–407.

Walters, E. T., and M. T. Erickson. 1986. Directional control and the functional organization of defensive responses in *Aplysia*. *J. Comp. Physiol. A.* **159:** 339–351.

Wiltschko, W., and R. Wiltschko. 1990. Magnetic orientation and celestial cues in migratory orientation. *Experentia* **46:** 342–352.

Yu, N., and M. Kavaliers. 1991. Pertussis toxin reduces the day-night rhythm of nociception and opioid mediated antinociception in the land snail *Cepaea nemoralis*. *Peptides* (in press).

Zagon, I. S., and P. J. McLaughlin. 1989. Opioid antagonist modulation of murine neuroblastoma: a profile of cell proliferation and opioid peptides and receptors. *Brain Res.* **480:** 16–28.

Zisper, B., M. R. Ruff, J. B. O'Neill, C. C. Smith, W. J. Higgins, and C. B. Pert. 1988. The opiate receptor: a single 110 kDa recognition molecule appears to be conserved in *Tetrahymena* leech and rat. *Brain Res.* **463:** 296–304.

Reference: *Biol. Bull.* **180**: 310–317. (April, 1991)

Oxidative Breakdown Products of Catecholamines and Hydrogen Peroxide Induce Partial Metamorphosis in the Nudibranch *Phestilla sibogae* Bergh (Gastropoda: Opisthobranchia)

ANTHONY PIRES AND MICHAEL G. HADFIELD

Kewalo Marine Laboratory, P.B.R.C., University of Hawaii, 41 Ahui St., Honolulu, Hawaii 96813

Abstract. Veliger larvae of the aeolid nudibranch *Phestilla sibogae* metamorphose in response to a soluble factor from their prey coral, *Porites compressa*. Metamorphosis begins with destruction of the velum, a ciliated structure used for swimming and feeding. Previous investigation had shown that *P. sibogae* larvae exposed to certain catecholamines lost the velum, but then failed to complete any subsequent steps characteristic of natural coral-induced metamorphosis. Because catecholamines oxidize rapidly in seawater, we have re-examined morphogenic effects of catecholamines using superfusion chambers that allow periodic replacement of test solutions. We report that fresh, unoxidized catecholamines do *not* induce velar loss, but that this morphogenic activity develops in aged, oxidized solutions of a variety of catecholamines and other catechol compounds. Evidence is presented that this activity is attributable to hydrogen peroxide, a byproduct of catechol autoxidation. Hydrogen peroxide induces velar loss at 10^{-4} *M*. The possible relationship of peroxide-induced velar loss to natural coral-induced metamorphosis is discussed.

Introduction

Chemical and neural mechanisms governing metamorphosis in marine invertebrates have long been of interest both to ecologists seeking to understand recruitment of larvae into adult populations, and to more reductionist biologists who view invertebrate larvae as excellent model systems for exploring the regulation of development (Hadfield, 1986). Larvae of the aeolid nudibranch *Phestilla sibogae* metamorphose upon exposure to a water-soluble factor derived from the stony coral *Porites compressa*, *P. sibogae*'s adult prey. Efforts to isolate and identify the coral-derived metamorphic inducer (CI, Hadfield and Pennington, 1990) have been accompanied by the screening of a wide range of chemical species for their capacity to induce metamorphosis (Hadfield, 1984; Hirata and Hadfield, 1986; Yool *et al.*, 1986; Pennington and Hadfield, 1989). Any such morphogens discovered by this second approach can be evaluated as possible structural analogues of CI, or as molecules involved in internal transduction of the CI signal, or as regulators of developmental mechanisms that normally unfold as a consequence of metamorphic induction by CI. Known neurotransmitters and neurohormones are among the plausible candidates for all three of these roles (D. E. Morse, this symposium; Bonar *et al.*, 1990). If a morphogenic response can be induced by application of a known neuroactive compound, certain plausible hypotheses may be made about what sorts of receptors and internal transduction systems might mediate natural metamorphosis, and appropriate experiments designed to test the implicated mechanisms.

Hadfield (1984) reported that larvae exposed to the catecholamines epinephrine (10^{-4} *M*) or norepinephrine (10^{-3} *M*) would often undergo a partial metamorphosis restricted to loss of the velum (a ciliated larval swimming and feeding organ), not followed by any of the subsequent steps in the morphogenic sequence characteristic of nat-

Received 14 August 1990; accepted 6 November 1990.

Abbreviations: CI: natural coral-derived metamorphic inducer; ASW: artificial seawater; FSW: filtered seawater; EP: (−)epinephrine; NE: (−)norepinephrine; IP: (−)isoproterenol; DA: dopamine; DOPA: L-B-3, 4-dihydroxyphenylalanine; DOPAC: 3,4-dihydroxyphenylacetic acid; DOMA: 3,4-dihydroxymandelic acid; DOB: 1,2-dihydroxybenzene; HVA: homovanillic acid; OCT: octopamine.

ural metamorphosis (described in Bonar and Hadfield, 1974; Hadfield, 1978). A difficulty in the interpretation of this result was that catechols autoxidize rapidly to quinones in alkaline aqueous solutions, in a multi-step reaction that generates hydrogen peroxide (H_2O_2). Figure 1 shows the net result of this reaction; its mechanism, the nature of intermediate products and regulation by pH and various catalysts have been explored for several catecholamines and are the subject of an extensive literature (Heacock, 1959; Hawley *et al.*, 1967; Misra and Fridovich, 1972; Graham, 1978; Cohen, 1983). At 25°C, a 10^{-4} *M* solution of epinephrine in MBL artificial seawater (ASW; Cavanaugh, 1956) Tris-buffered to pH 8.2 begins to turn visibly pink within 15 min due to the appearance of the quinone oxidation intermediate, adrenochrome. Maximum adrenochrome concentration, measured spectrophotometrically, is attained within 3 h (Pires and Hadfield, unpub. data). We therefore decided to re-examine morphogenic effects of catecholamines and related compounds using superfusion chambers that permit rapid periodic replacement of test solutions to control for catechol autoxidation. Our goal was to determine whether the previously reported partial metamorphosis was indeed due to catecholamines, or to some product of catecholamine oxidation.

We report that partial metamorphosis (velar loss) is induced in *P. sibogae* by solutions of any of several catechol compounds aged in ASW or by H_2O_2 but not by fresh catecholamines. We also provide evidence that the morphogenic potency of aged catechols is due to H_2O_2 or a derivative oxygen species generated as a consequence of catechol autoxidation. These results emphasize the need for caution in interpreting biological effects of bath-applied catecholamines and other unstable chemical species. Our results also suggest testable hypotheses concerning possible roles of H_2O_2 and oxygen radicals in natural coral-induced metamorphosis.

Materials and Methods

Larval culture

All larvae used in these experiments were taken from our laboratory culture system. Adult *P. sibogae* were kept together with field-collected heads of their prey coral *P. compressa* in outdoor sea tables supplied with running unfiltered seawater (~25°C). Egg masses deposited on the coral were collected daily and transferred to .22 μm filtered seawater (FSW). Eggs developed at 25°C in aerated glass beakers in an incubator and were mechanically hatched at day 6 post-fertilization. Subsequent culture procedures were as previously described (Miller and Hadfield, 1986) except that larval culture chambers continued to be maintained in an incubator at 25°C after hatching.

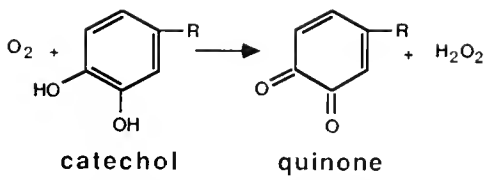

Figure 1. Generalized autoxidation of a catechol to a quinone, with the production of hydrogen peroxide (H_2O_2). For catecholamines, this reaction may also involve cyclization of the side chain R.

Experiments were conducted on 10-day-old (post-fertilization), unfed larvae. These larvae are facultative planktotrophs; under our culture conditions nearly all 10-day-old veligers are competent for metamorphosis without having to feed (Kempf and Hadfield, 1985; Miller and Hadfield, 1986).

Preparation of test solutions

(−)Epinephrine (EP), (−)norepinephrine (NE), (−)isoproterenol (IP), dopamine (DA), L-B-3, 4-dihydroxyphenylalanine (DOPA), 3,4-dihydroxyphenylacetic acid (DOPAC), 3,4-dihydroxymandelic acid (DOMA), catechol (1,2-dihydroxybenzene, DOB), homovanillic acid (HVA), octopamine (OCT), acetylsalicylic acid (aspirin), and thymol-free bovine catalase were purchased from Sigma Chemical Co. (St. Louis, Missouri). The first eight compounds above, all of which contain a catechol group, are sometimes referred to generically in the text as "catechol compounds" or "catechols." To avoid confusion, catechol itself is referred to as 1,2-dihydroxybenzene (DOB). All monoamines were obtained as hydrochloride salts except for EP (bitartrate) and DOPA (free acid). Pharmaceutical 3% H_2O_2 (Parke-Davis) was purchased locally. Stock solutions of test compounds were made fresh daily in deionized water at 10 times the desired final concentration and then diluted into 1.1× normal strength MBL ASW (Cavanaugh, 1956) buffered to pH 8.1–8.2 with 10 m*M* Trizma® (Sigma). This practice yielded ASW solutions of test compounds that were ionically equivalent to normal strength (1.0×) MBL ASW.

Many of the experiments presented in this paper were conducted to assay morphogenic potencies of fresh *versus* aged (oxidized) solutions of various catechol compounds. Aged solutions of test compounds in ASW were prepared as above and allowed to stand 10–14 h at 23–25°C. Fresh solutions were prepared in the same way from test compound stocks and 1.1× MBL ASW but were mixed immediately before use, as were ASW solutions of H_2O_2 for experiments on morphogenic effects of H_2O_2.

Experimental chambers

Experimental chambers (Fig. 2) were designed to permit rapid, frequent replacement of test solutions during ex-

periments. Each chamber is assembled from two symmetrical halves, constructed as follows. The body of each half-chamber is made from the base of a disposable plastic spectrophotometer cuvette cut to a volume of 1 cm^3. An 18-gauge hypodermic needle, cut to a length of 1–2 mm, is inserted through a small hole in the base of the half-chamber and cemented in place with silicone rubber aquarium sealant (Dow-Corning or equivalent). This feature allows replacement of test solutions with a syringe. Silicone rubber gaskets on the open rim of each half-chamber seal a mesh barrier (100 μm Nitex®) that separates the two halves. The halves are clamped together with rubber bands.

Our method for making the gaskets is generally useful for the construction of small watertight apparatuses. First, silicone rubber aquarium sealant is applied to the gasket-bearing surface to a slightly greater depth than the desired thickness of the finished gasket. Then a microscope slide (or other piece of smooth flat glass) smeared with a very thin film of silicone stopcock grease is laid down on the wet sealant and lightly pressed down until good contact is visible between sealant and glass along the entire surface of the gasket. After the sealant has cured, the glass can be "popped" off the finished gasket with a razor blade.

Comparisons of morphogenic potencies of fresh and aged test solutions (Figs. 4 and 6) were carried out in the superfusion chambers according to the following protocol. Each chamber was loaded with 17–112 larvae using a pipet. After the chamber halves were assembled, each chamber was flushed with 10 ml (=5× chamber volume) of test solution. Thereafter, test solutions were replaced in the same manner every 30 min until a total exposure time of 7 h had elapsed. Then the chambers were flushed with FSW and larvae washed out into Stender dishes. Larvae were scored for velar loss 16–24 h later (criteria below). In these experiments one set of 3 or 4 chambers was run with fresh test solutions (prepared as above for each solution change), while another set was run simultaneously with aged solutions (prepared as above the night before the experiment). The solution changing procedure, as well as other aspects of physical manipulation of the larvae, was identical in fresh solution and aged solution treatments.

Experiments on dose-dependent morphogenic effects of H_2O_2 and of aged DA (Figs. 5 and 7) were performed in 6 cm Stender dishes. Larvae (53–220 per dish) were exposed to several concentrations of H_2O_2 in ASW for 7 h without solution changes, and then washed into FSW for scoring as above.

Scoring of velar loss

Different degrees of velar loss are described and illustrated below. For scoring purposes, larvae able to swim freely and climb through the water column were considered to be intact. Such individuals never showed any evidence of velar reduction when examined at 50× magnification. Larvae lying on the bottom of the dish or swimming, but failing to clear the bottom, were scored as "velum lost" if any of the large ciliated cells at the velar margin were missing, or if the velar lobes were noticeably shortened. Instances of partial (Fig. 3B) and complete (Fig. 3C) velar loss were combined and divided by the total number of larvae to obtain a frequency of velar loss for each trial.

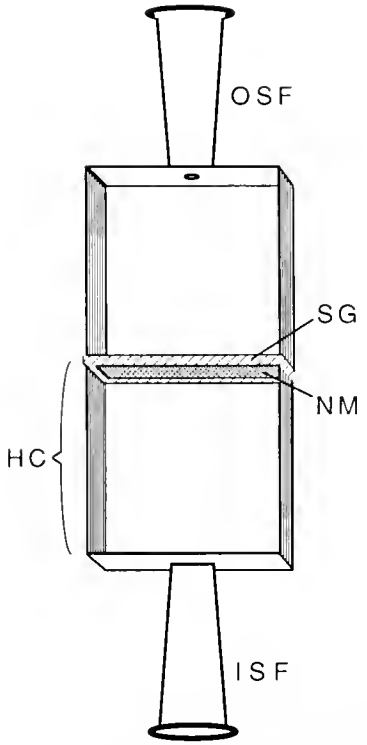

Figure 2. Superfusion chamber used in experiments comparing morphogenic potencies of fresh *versus* aged solutions of catechols. Larvae are retained in the lower half-chamber (HC) by a Nitex mesh barrier (NM), held in place by silicone rubber gaskets (SG). Inlet and outlet syringe fittings (ISF and OSF) allow periodic flushing with a syringe containing test solution. Total chamber volume is 2 cm^3. Half-chambers are held together during use by rubber bands (not shown).

Results

Induction of velar loss by aged catechols and H_2O_2

Loss of the velum, one of the major morphological transformations occurring during metamorphosis, can be considered a partial metamorphosis (Bonar and Hadfield, 1974; Hadfield, 1984). We consistently found that high proportions of larvae lost some or all of the velum (except for small remnant clumps of cephalic supportive cells) when exposed for 7 h to aged solutions of any of the cat-

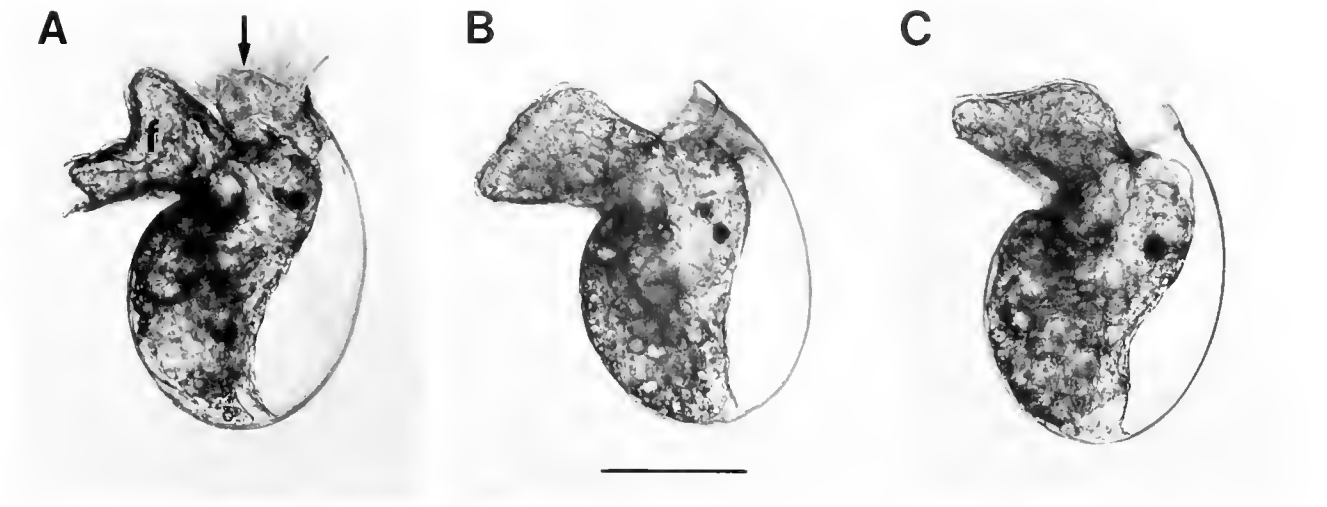

Figure 3. Velar loss in *Phestilla sibogae*. A. Lateral view of 11-day-old, untreated larva. Animal was photographed with intact velum (arrow) partly withdrawn into the larval shell to keep velum in same plane of focus as the rest of the animal; foot (f) is partly extended. Outlines of large ciliated cells are visible along the velar margin. B. Partial velar loss in an 11-day-old larva treated with 10^{-4} *M* H_2O_2 on day 10. C. Complete velar loss in an 11-day-old larva treated with 2×10^{-4} M H_2O_2 on day 10. Differences between larvae in shape of foot represent a range of movement independent of velar loss. Scale bar = 100 μm.

echol compounds tested, or to H_2O_2, but not when exposed to fresh catecholamines. Figure 3 illustrates velar loss in response to H_2O_2 but it could just as well indicate the results obtained with aged solutions of catechols. An 11 day-old untreated larva with intact velum is shown in Figure 3A. Velar loss induced by H_2O_2 or by aged catechols (or by Cl) begins with the detachment of the large ciliated cells at the velar margin. These cells are cast off intact, and their cilia continue to beat for some time after detachment. After separation of these cells begins, regression of non-ciliated supportive cells of the velar lobes becomes apparent. This state of partial velar loss is depicted in Figure 3B. This state is stable in that velar loss will proceed no further in larvae washed out of the H_2O_2 or aged catechol treatment into FSW. If the above treatments are applied in sufficiently high concentration (see below), 7-h treatment results in detachment of all the large ciliated velar cells and detachment or regression of remaining tissues, leaving small cephalic mounds of supportive cells where the velar lobes had been (Fig. 3C). Velar loss in response to these treatments, like that seen in natural coral-induced metamorphosis, is highly tissue-specific. Other ciliated epithelia (of the foot, for example) remain intact. When velar loss is induced with H_2O_2 or aged catechols, metamorphosis does not proceed beyond this point. However, if such larvae are then exposed to Cl, many will right themselves on the foot, take up the settled posture characteristic of natural metamorphosis (Hadfield, 1978), and complete metamorphosis in an apparently normal fashion.

Comparison of effects of fresh and aged catechols

Morphogenic effects of fresh and aged solutions of the catecholamines EP, NE, and IP (2×10^{-4} *M*) and DA (10^{-4} *M*) were quantitatively compared (Fig. 4). Dramatically different results were obtained in parallel trials using aged and fresh solutions of the same compounds, replaced every 30 min during the 7-h exposure period. Most larvae lost some or all of the velum after exposure to aged catecholamines. After exposure to fresh catecholamines, larvae rarely showed any indication of velar

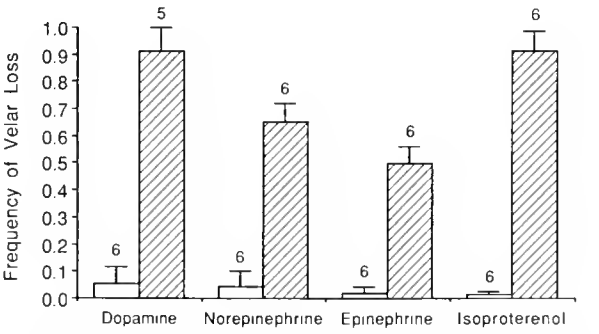

Figure 4. Frequencies of velar loss after 7-h exposure to fresh (open bars) or aged (hatched bars) solutions of catecholamines. Concentrations are 2×10^{-4} *M* except for dopamine (10^{-4} *M*). Ordinate values and error bars are means and standard deviations, respectively, calculated from arcsine transformed data. Numbers above error bars indicate the number of replicate trials, each involving a chamber containing 17–96 larvae. Trials for each compound were conducted on at least two different batches of larvae.

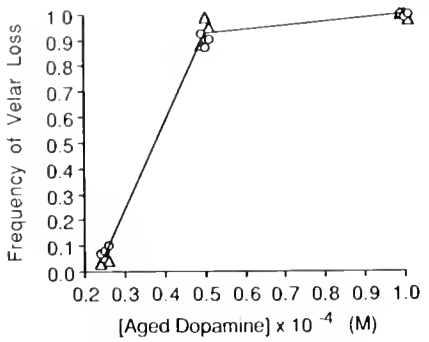

Figure 5. Frequencies of velar loss after 7-h exposure to varying concentrations of aged dopamine solutions. Triangles and circles represent two assays conducted in triplicate on two different batches of larvae. Each symbol represents a trial involving 53–220 larvae. Lines connect grand means of velar loss at each concentration, calculated from arcsine transformed data.

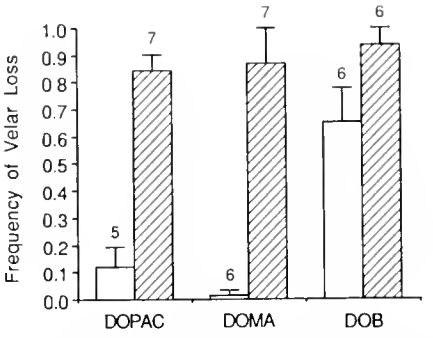

Figure 6. Frequencies of velar loss after 7-h exposure to fresh (open bars) or aged (hatched bars) solutions of the catechol compounds dihydroxyphenylacetic acid (DOPAC), dihydroxymandelic acid (DOMA), and dihydroxybenzene (DOB). Concentrations are 2×10^{-4} *M* except for DOB (10^{-4} *M*). Ordinate values and error bars are means and standard deviations, respectively, calculated from arcsine transformed data. Numbers above error bars indicate the number of replicate trials, each involving a chamber containing 18–112 larvae. Trials for each compound were conducted on at least two different batches of larvae.

loss and were generally indistinguishable in morphology and behavior from untreated animals. Larvae exposed to a higher concentration of fresh DA (2×10^{-4} *M*) according to this protocol did sometimes metamorphose completely by the time the experiment was scored, but at low frequency (0–.25, typically .10–.15), as suggested by earlier experiments conducted without solution replacement (Hadfield, 1984). However, in the current work, we used 10^{-4} *M* DA for the aged *versus* fresh comparison because aged solutions at higher concentrations proved somewhat toxic under these conditions. Complete metamorphosis was observed at very low frequency (≤.05) after exposure to fresh 10^{-4} *M* DA.

The frequency of velar loss in response to varying concentrations of aged DA is given in Figure 5. Concentration threshold for velar loss after 7-h exposure to fresh DA appears to lie between .25 and .5 $\times$ 10^{-4} *M*.

Experiments to test morphogenic effects of other catechol compounds yielded similar results (Fig. 6). Aged solutions of the deaminated catecholamine metabolites DOPAC or DOMA (both 2×10^{-4} *M*) as well as of DOB (10^{-4} *M*) consistently yielded high frequencies of velar loss. Fresh solutions of DOPAC and DOMA were relatively ineffective. Fresh DOB caused most larvae to show some evidence of velar loss, but this was invariably confined to the loss of a few large ciliated cells at the velar margin. Aged DOB, in contrast, nearly always resulted in detachment of all the ciliated velar cells and substantial regression of the velar lobes. DOPA, a catechol amino acid precursor of the catecholamine neurotransmitters, also caused a high mean frequency of velar loss (.67) in aged 10^{-4} *M* solutions, but a quantitative comparison could not be made with fresh solutions. Larvae treated with fresh DOPA tended to withdraw completely into the shell, and although vela appeared to be intact, accurate scoring of velar condition was not possible. OCT (NE minus one ring hydroxyl group) and HVA (DOPAC with one ring hydroxyl group methylated) do not oxidize as easily as their related catechol compounds, and had no morphogenic effects in aged or fresh 2×10^{-4} *M* solutions.

Quantification of H_2O_2-induced velar loss and abolition of effects of H_2O_2 and aged catechols by catalase

Because autoxidation of catechols in water yields H_2O_2 (Graham *et al.*, 1978), we tested the ability of H_2O_2 in ASW solutions to induce velar loss. Exposure to H_2O_2 for 7 h reliably induced velar loss at a concentration threshold in the range of .25–.5 $\times$ 10^{-4} *M* (Fig. 7). Solutions of .25 $\times$ 10^{-4} *M* H_2O_2 were never sufficient to cause observable velar loss; these animals were indistinguishable from untreated individuals (Fig. 3A). A large but variable fraction

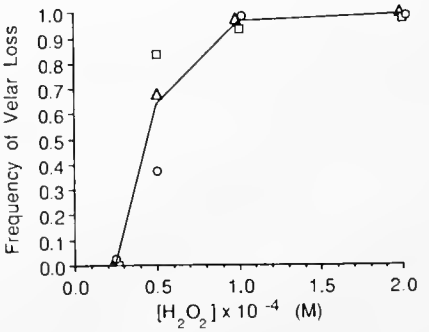

Figure 7. Frequencies of velar loss after 7-h exposure to varying concentrations of H_2O_2. Triangles, circles and squares represent three assays conducted on three different batches of larvae. Each symbol represents a trial involving 54–123 larvae. Lines connect grand means of velar loss at each concentration, calculated from arcsine transformed data.

of larvae tested at $.5 \times 10^{-4}$ *M* H_2O_2 showed clear indications of partial velar loss. In 10^{-4} *M* H_2O_2 nearly all larvae experienced at least partial velar loss; a typical instance is shown in Figure 3B. In 2×10^{-4} *M* H_2O_2, most larvae lost the entire velum except for small mounds of cephalic supportive cells (Fig. 3C).

Morphogenic potencies of H_2O_2 and aged solutions of all of the above catechol compounds were completely abolished by 10 min incubation with purified bovine catalase (5 μg/ml), prior to addition of larvae. The presence of H_2O_2 in aged solutions of catechols was confirmed by measuring an increase in dissolved oxygen concentration upon catalase treatment, with a Clark-type oxygen meter. (Catalase catalyzes the decomposition of H_2O_2 to water and molecular oxygen.) Hydrogen peroxide-induced velar loss was not inhibited by acetylsalicylic acid (aspirin) in any concentration between 10^{-6} and 10^{-3} *M*. [Aspirin, an inhibitor of prostaglandin endoperoxide synthetase, inhibits H_2O_2-induced spawning in the abalone *Haliotis rufescens* (Morse *et al.*, 1977).]

Discussion

Relationship of velar loss induced by H_2O_2 and by aged catechols to velar loss in natural metamorphosis

Velar loss in larvae of *P. sibogae* can be induced by application of H_2O_2 or aged solutions of catechols in the tenth-millimolar concentration range (Figs. 3–7). The stoichiometry of catechol autoxidation (Fig. 1), together with our observation that similar concentrations of H_2O_2 or aged catechols are required to induce velar loss, suggests the hypothesis that morphogenic activity of aged catechols is due to H_2O_2 produced upon autoxidation or to some other reactive species derived from H_2O_2 such as the hydroxyl radical $HO^{\cdot}$ (for discussions of H_2O_2 metabolism and oxygen radical biochemistry see Fridovich, 1978; Imlay and Linn, 1988; Cadenas, 1989; Kontos, 1989; Gutteridge *et al.*, 1990). Direct evidence for this hypothesis is the fact that morphogenic activity of aged catechol solutions is lost on incubation with catalase, an enzyme that selectively degrades H_2O_2 to molecular oxygen and water. However, we have not yet rigorously excluded cooperative effects of quinone oxidation products of catechols in velar destruction.

Natural coral-induced metamorphosis is preceded by settlement behavior in which the larva takes up a characteristic posture, attached by the foot to the substratum (Bonar and Hadfield, 1974; Hadfield, 1978). This behavior is not elicited by H_2O_2 or aged catechols. In natural metamorphosis, velar loss ensues in this settled position. Larvae treated with H_2O_2 or aged catechols begin to lose the velum while swimming; after enough large ciliated velar cells have been lost, larvae sink to the bottom of the experimental chamber and typically lie on a side of the shell in an extended posture.

Although the behavioral contexts for natural and artificially induced velar loss are different, the morphological phenomena share several common features. Both begin with the detachment of the large ciliated cells at the velar margin. Natural and artificially induced velar loss are both highly tissue-specific in that cell separation and tissue regression are confined to the velum and are not manifested in other ciliated epithelia. Following loss of the ciliated velar cells, clumps of nonciliated supportive cells remain as cephalic mounds (Fig. 3C). Partial metamorphosis induced by H_2O_2 or aged catechols does not proceed beyond this point. However, no loss of metamorphic competence has occurred, because such larvae can resume metamorphosis once exposed to Cl.

Further experiments are required to test the hypothesis that H_2O_2 or derivative oxygen radicals mediate velar loss in natural metamorphosis. Several techniques exist that are potentially applicable to detection of H_2O_2 or oxygen radical production in metamorphosing tissues (Freeman and Crapo, 1981; Radzik *et al.*, 1983; Ruch *et al.*, 1983; Kontos, 1989). Chemical scavengers of free radicals and of H_2O_2 can also be used to interfere with radical-dependent mechanisms (Cadenas, 1989; Kontos, 1989). We were unable to inhibit coral-induced metamorphosis with catalase, but that result is difficult to interpret because catalase is not expected to penetrate cells to reach potential sites of endogenous H_2O_2 generation or action. Future experiments will include other more penetrant scavengers. It is important to note that even if H_2O_2 or oxygen radicals are implicated in the mechanism of natural metamorphosis, there are many biological sources of these oxygen species other than oxidation of catechols (Cohen, 1983; Kontos, 1989).

Possible modes of action of H_2O_2

Hydrogen peroxide is well-known for its cytotoxic properties, which render it useful as a topical disinfectant. Mechanisms of cell damage by H_2O_2 and oxygen radicals have been subjects of several recent discussions (Imlay and Linn, 1988; Kontos, 1989; Gutteridge and Halliwell, 1990). Indeed, significant lysis of certain cultured vertebrate epithelial cells occurs upon exposure to H_2O_2 concentrations only slightly higher than those demonstrated to cause velar loss in the present study (Hayden *et al.*, 1990; Polansky *et al.*, 1990). However, the question of whether H_2O_2-induced velar disintegration in *Phestilla* larvae is a cytotoxic response remains. The facts that ciliated cells appear to be shed intact with cilia still beating and that other epithelial tissues show no evidence of injury at morphogenically active concentrations, might argue otherwise. Close structural examination of shed velar cells

in both H_2O_2-induced and coral-induced velar loss will be instructive in this regard. Non-toxic regulatory effects of H_2O_2 mimic the effects of insulin on glucose, carbohydrate, and lipid metabolism in vertebrate cells, possibly by stimulating phosphorylation of the insulin receptor (Heffetz *et al.*, 1990). This mechanism of action may warrant investigation in *Phestilla*, particularly in light of the recent discovery of a preproinsulin-related peptide in growth-regulating neuroendocrine cells of the gastropod *Lymnaea stagnalis* (Smit *et al.*, 1988) and the growing appreciation of insulin's role in cellular differentiation during embryogenesis (Alemany *et al.*, 1990). In another gastropod, the abalone *H. rufescens*, H_2O_2 induces spawning, probably by activating prostaglandin endoperoxide synthetase (Morse *et al.*, 1977). This particular pathway is unlikely to be involved in velar loss in *Phestilla* because H_2O_2 induction of velar loss is not blocked by aspirin, a potent inhibitor of that enzyme. One might speculate that H_2O_2 could also regulate the activity of a factor involved in epithelial cell adhesive interactions, perhaps akin to the "scatter factor" recently described as a promoter of cell-cell separation in cultured mammalian epithelia (Stoker and Gherardi, 1989).

Implications for other taxa

Our study points out the need for caution in the interpretation of behavioral and morphogenic effects of bath-applied catecholamines on marine animals. In the bivalve *Crassostrea gigas*, sufficient physical controls and corroborating pharmacological evidence have been marshalled in support of the hypothesis that dopaminergic and adrenergic neural pathways, mediate settlement and morphogenesis, respectively (Coon and Bonar, 1987; Bonar *et al.*, 1990). There are also brief reports of metamorphic induction by DOPA in the mussel *Mytilus edulis* (Cooper, 1982), and by DA in the mud snail *Ilyanassa obsoleta* (Levantine and Bonar, 1986), but details of the methods are not given. Certain catecholamines have been reported to induce metamorphosis in the scallops *Patinopecten yessoensis* (Kingzett *et al.*, 1990) and *Pecten maximus* (Cochard *et al.*, 1989), but in both of these studies the problem of catechol oxidation was not thoroughly resolved. DOPA induces a low frequency of metamorphosis in the polychaete *Phragmatopoma californica* (Jensen, 1987), but that work has implicated cross-linked quinoid derivatives of DOPA residues in proteins, rather than catecholamine neurotransmitters, in the inductive pathway (Jensen and Morse, 1990). To our knowledge the only other published example of catecholamine induction of larval metamorphosis is in the echinoid *Dendraster excentricus* (Burke, 1983). Whole larvae and excised larval arms metamorphosed in response to DA, but not to EP or NE. The response specificity suggests that DA did not act as a source of H_2O_2 in those experiments, but the protocols are not detailed enough to permit clear resolution of this issue.

Our results should not be interpreted to mean that catecholamines do not act as neurotransmitters mediating metamorphosis in *P. sibogae*. Bath-applied substances might not reach their target tissues in the proper concentration, or the co-activation of receptors on many cells throughout the nervous system may result in net inhibition of circuits that effect metamorphosis. We do hope that this study sounds a cautionary note to others investigating chemical control of metamorphosis, and prompts consideration of a possible morphogenic role for H_2O_2.

Acknowledgments

We thank Esther Leise for critically reading the manuscript, and Leonard Deal for competent and reliable technical assistance. Supported by NSF grant DCB89-03800 to M.G.H.

Literature Cited

Alemany, J., M. Girbau, and F. de Pablo. 1990. Insulin action and insulin receptors in embryogenesis of vertebrates and invertebrates. Pp. 198–204 in *Progress in Comparative Endocrinology: Proceedings of the Eleventh International Symposium on Comparative Endocrinology*, A. Epple, C. G. Scanes, and M. H. Stetson, eds. Wiley-Liss, New York.

Bonar, D. B., S. L. Coon, M. Walch, R. M. Weiner, and W. Fitt. 1990. Control of oyster settlement and metamorphosis by endogenous and exogenous chemical cues. *Bull. Mar. Sci.* **46:** 484–498.

Bonar, D. B., and M. G. Hadfield. 1974. Metamorphosis of the marine gastropod *Phestilla sibogae* Bergh (Nudibranchia: Aeolidacea). I. Light and electron microscopic analysis of larval and metamorphic stages. *J. Exp. Mar. Biol. Ecol.* **16:** 227–255.

Burke, R. D. 1983. Neural control of metamorphosis in *Dendraster excentricus*. *Biol. Bull.* **164:** 176–188.

Cadenas, E. 1989. Biochemistry of oxygen toxicity. *Ann. Rev. Biochem.* **58:** 79–110.

Cavanaugh, G. M. 1956. *Formulae and Methods VI of the Marine Biological Laboratory Chemical Room.* Marine Biological Laboratory, Woods Hole, Massachusetts.

Cochard, J. C., L. Chevolot, J. C. Yvin, and A. M. Chevolot-Mageur. 1989. Induction de la metamorphose de la coquille Saint Jacques *Pecten maximus* L. par des derives de la tyrosine extraits de l'algue *Delesseria sanguinea* Lamouroux ou syntheliques. *Halitotis* **19:** 259–274.

Cohen, G. 1983. The pathobiology of Parkinson's disease: biochemical aspects of dopamine neuron senescence. *J. Neural Transmission, Suppl.* **19:** 89–103.

Coon, S. L., and D. B. Bonar. 1987. Pharmacological evidence that alpha-1 adrenoceptors mediate metamorphosis of the Pacific oyster, *Crassostrea gigas*. *Neuroscience* **23:** 1169–1174.

Cooper, K. 1982. A model to explain the induction of settlement and metamorphosis of planktonic eyed-pediveligers of the blue mussel *Mytilus edulis* L. by chemical and tactile cues. *J. Shellfish Res.* **2:** 117.

Freeman, B. A., and J. D. Crapo. 1981. Hyperoxia increases oxygen radical production in rat lungs and lung mitochondria. *J. Biol. Chem.* **256:** 10986–10992.

Fridovich, I. 1978. The biology of oxygen radicals. *Science* **201:** 875–880.

Graham, D. G. 1978. Oxidative pathways for catecholamines in the genesis of neuromelanin and cytotoxic quinones. *Mol. Pharmacol.* **14:** 633–643.

Graham, D. G., S. M. Tiffany, W. R. J. Bell, and W. F. Gutknecht. 1978. Autoxidation versus covalent binding of quinones as the mechanism of toxicity of dopamine, 6-hydroxydopamine, and related compounds toward C1300 neuroblastoma cells *in vitro*. *Mol. Pharmacol.* **14:** 644–653.

Gutteridge, J. M. C., and B. Halliwell. 1990. The measurement and mechanism of lipid peroxidation in biological systems. *T I B S.* **15:** 129–135.

Gutteridge, J. M. C., I. Zs.-Nagy, L. Maidt, and R. A. Floyd. 1990. ADP-iron as a Fenton reactant: radical reactions detected by spin trapping, hydrogen abstraction, and aromatic hydroxylation. *Arch. Biochem. Biophys.* **277:** 422–428.

Hadfield, M. G. 1978. Metamorphosis in marine molluscan larvae: an analysis of stimulus and response. Pp. 165–175 in *Settlement and Metamorphosis of Marine Invertebrate Larvae*, F.-S. Chia and M. Rice, eds. Elsevier/North-Holland, New York.

Hadfield, M. G. 1984. Settlement requirements of molluscan larvae: new data on chemical and genetic roles. *Aquaculture* **39:** 283–298.

Hadfield, M. G. 1986. Settlement and recruitment of marine invertebrates: a perspective and some proposals. *Bull. Mar. Sci.* **39:** 418–425.

Hadfield, M. G., and J. T. Pennington. 1990. Nature of the metamorphic signal and its internal transduction in larvae of the nudibranch *Phestilla sibogae*. *Bull. Mar. Sci.* **46:** 455–464.

Hawley, M. D., S. V. Tatawawadi, S. Pickarski, and R. N. Adams. 1967. Electrochemical studies of the oxidation pathways of catecholamines. *J. Am. Chem. Soc.* **89:** 447–450.

Hayden, B. J., L. Zhu, D. Sens, M. J. Tapert, and R. K. Crouch. 1990. Cytolysis of corneal epithelial cells by hydrogen peroxide. *Exp. Eye Res.* **50:** 11–16.

Heacock, R. A. 1959. The chemistry of adrenochrome and related compounds. *Chem. Rev.* **59:** 181–237.

Heffetz, D., I. Bushkin, R. Dror, and Y. Zick. 1990. The insulinomimetic agents H_2O_2 and vanadate stimulate protein tyrosine phosphorylation in intact cells. *J. Biol. Chem.* **265:** 2896–2902.

Hirata, K. Y., and M. G. Hadfield. 1986. The role of choline in metamorphic induction of *Phestilla* (Gastropoda: Nudibranchia). *J. Comp. Biochem. Physiol.* **84C:** 15–21.

Imlay, J. A., and S. Linn. 1988. DNA damage and oxygen radical toxicity. *Science* **240:** 1302–1309.

Jensen, R. A. 1987. Factors affecting the settlement, metamorphosis and distribution of larvae of the marine polychaete *Phragmatopoma californica* (Fewkes). Ph.D. dissertation, University of California, Santa Barbara, California. 175 pp.

Jensen, R. A., and D. E. Morse. 1990. Chemically induced metamorphosis of polychaete larvae in both the laboratory and ocean environment. *J. Chem. Ecol.* **16:** 911–930.

Kempf, S. C., and M. G. Hadfield. 1985. Planktotrophy by the lecithotrophic larvae of a nudibranch, *Phestilla sibogae* (Gastropoda). *Biol. Bull.* **169:** 119–130.

Kingzett, B. C., N. Bourne, and K. Leask. 1990. Induction of metamorphosis of the Japanese scallop *Patinopecten yessoensis* Jay. *J. Shellfish Res.* **9:** 119–124.

Kontos, H. A. 1989. Oxygen radicals in CNS damage. *Chem.-Biol. Interactions* **72:** 229–255.

Levantine, P. L., and D. B. Bonar. 1986. Metamorphosis of *Ilyanassa obsoleta*: natural and artificial inducers. *Am. Zool.* **26:** 14A.

Miller, S. E., and M. G. Hadfield. 1986. Ontogeny of phototaxis and metamorphic competence in larvae of the nudibranch *Phestilla sibogae* Bergh (Gastropoda: Opisthobranchia). *J. Exp. Mar. Biol. Ecol.* **97:** 95–112.

Misra, H. P., and I. Fridovich. 1972. The role of superoxide anion in the autoxidation of epinephrine and a simple assay for superoxide dismutase. *J. Biol. Chem.* **247:** 3170–3175.

Morse, D. E., H. Duncan, N. Hooker, and A. Morse. 1977. Hydrogen peroxide induces spawning in mollusks, with activation of prostaglandin endoperoxide synthetase. *Science* **196:** 298–300.

Pennington, J. T., and M. G. Hadfield. 1989. Larvae of a nudibranch mollusc (*Phestilla sibogae*) metamorphose when exposed to common organic solvents. *Biol. Bull.* **177:** 350–355.

Polansky, J. R., D. J. Fauss, T. Hydorn, and E. Bloom. 1990. Cellular injury from sustained *vs.* acute hydrogen peroxide exposure in cultured human corneal endothelium and human lens epithelium. *C.L.A.O. J.* **16(1 Suppl.):** S23–S28.

Radzik, D. M., D. A. Roston, and P. T. Kissinger. 1983. Determination of hydroxylated aromatic compounds produced via superoxide-dependent formation of hydroxyl radicals by liquid chromatography/electrochemistry. *Anal. Biochem.* **131:** 458–464.

Ruch, W., P. H. Cooper, and M. Baggiolini. 1983. Assay of H_2O_2 production by macrophages and neutrophils with homovanillic acid and horse-radish peroxidase. *J. Immunol. Methods* **63:** 347–357.

Smit, A. B., E. Vrenghdenhil, R. H. M. Ebberink, W. P. M. Geraerts, J. Klootwijk, and J. Joose. 1988. Growth-controlling molluscan neurons produce the precursor of an insulin-related peptide. *Nature* **331:** 535–538.

Stoker, M., and E. Gherardi. 1989. Scatter factor and other regulators of cell mobility. *Br. Med. Bull.* **45:** 481–491.

Yool, A. J., S. M. Grau, M. G. Hadfield, R. A. Jensen, D. A. Markell, and D. E. Morse. 1986. Excess potassium induces larval metamorphosis in four marine invertebrate species. *Biol. Bull.* **170:** 255–266.

Reference: *Biol Bull* **180**: 318–327. (April, 1991)

cDNA Sequences Reveal mRNAs for Two Gα Signal Transducing Proteins from Larval Cilia

LISA M. WODICKA AND DANIEL E. MORSE

Department of Biological Sciences and the Marine Biotechnology Center, University of California, Santa Barbara, California 93106

Abstract. In planktonic larvae of the gastropod mollusk, *Haliotis rufescens* (red abalone), settlement behavior and subsequent metamorphosis are controlled by two convergent chemosensory pathways that report unique peptide and amino acid signals from the environment. The integration of signals from these two sensory pathways provides for variable amplification, or fine-tuning, of larval responsiveness to the inducers of settlement and metamorphosis. These pathways may be analogous to the neuronal and molecular mechanisms of facilitation and long-term potentiation characterized in other (adult) molluscan systems. Recently, the chemosensory receptors and signal transducers apparently belonging to the regulatory pathway (including a G protein and protein kinase C) have been identified in cilia purified from *H. rufescens* larvae. These elements retain their sequential receptor-dependent regulation in the isolated cilia *in vitro*. As a first step toward the molecular genetic dissection of the receptors, transducers, and the mechanisms of their control of settlement behavior and metamorphosis, we present evidence that the cilia purified from these larvae contain polyadenylated mRNA corresponding to unique signal transducers. Purification of this mRNA, enzymatic synthesis of the corresponding cDNAs, amplification by the polymerase chain reaction, cloning, and sequence analysis reveal that the ciliary mRNA includes sequences that apparently code for two Gα signal transducing proteins. One of these is highly homologous to members of the G_q family, recently shown in other systems to control the activity of phospholipase C; the other is more closely related to G_i and G_o. These results extend the tractability of the *Haliotis* system to analyses of cDNA and protein sequences of chemosensory elements from isolated cilia. This is the first time that mRNA has been purified from isolated cilia, and the corresponding cDNA synthesized and characterized.

Received 9 July 1990; accepted 28 January 1991.

[1] Abbreviations: GITC, guanidinium isothiocyanate; SDS, sodium dodecyl sulfate; IPTG, isopropyl-β-thiogalactoside; X-gal, bromo-, chloro-indolylgalactoside; AMV, avian myeloblastosis virus; Tris, tris-hydroxymethylaminomethane; EDTA, ethylenediamine-tetra-acetic acid; TE, Tris-EDTA; TBE, Tris-borate-EDTA; TAE, Tris-acetate-EDTA; bp, base-pair(s). The standard one-letter amino acid code is used.

Introduction

Larvae of the gastropod mollusk, *Haliotis rufescens* (red abalone), undergo a dramatic behavioral change when they encounter a specific chemical cue at the surfaces of crustose red algae: the planktonic larvae cease swimming, attach to the algal surface, and commence metamorphosis and plantigrade locomotion and feeding. This behavioral transition is controlled by the integration of two convergent chemosensory pathways that respond to chemical signals from the environment: a *morphogenetic pathway* activated by a GABA-mimetic morphogen encountered by the larvae on surfaces of recruiting algae, and a *regulatory* or *amplifier pathway* stimulated by lysine in seawater (Morse *et al.*, 1984; Trapido-Rosenthal and Morse, 1985, 1986a, b; Baxter and Morse, 1987; Morse 1990a). Activation of the morphogenetic pathway receptors is thought to trigger an efflux of chloride or other anions across the membrane of the primary chemosensory cell, apparently resulting in excitatory depolarization (Baloun and Morse, 1984). This transduction of the exogenous chemical signal to one that can be propagated by the larval nervous system is evidently sufficient to induce the change in larval behavior culminating in settlement, attachment, and the start of metamorphosis. Activation of the amplifier pathway receptors increases the sensitivity or output of the morphogenetic pathway by as much as 100-fold. The

receptors of the amplifier pathway are activated when they bind lysine, lysine polymers, or certain lysine analogs (Trapido-Rosenthal and Morse, 1985, 1986b). Experiments *in vivo* demonstrated that the amplifier pathway is controlled by chemosensory receptors and signal transducers distinct from those of the morphogenetic pathway, and that the lysine receptors of the amplifier pathway activate a sequential G protein-(phospholipase C) diacylglycerol-protein kinase C signal transduction cascade (Baxter and Morse, 1987). This system of dual control, in which the integration of two different kinds of chemosensory signals from the environment modulates the settlement behavior of the *Haliotis* larvae, fine-tunes larval responsiveness to exogenous settlement cues. The result of this integration may enhance the site-specificity of larval settlement and metamorphosis in potentially favorable habitats (Trapido-Rosenthal and Morse, 1985, 1986b; Morse, 1990a, b).

Because both the morphogenetic and amplifier pathways can be activated by macromolecular (protein-associated or polypeptide) ligands that are presumably impermeant (Morse *et al.*, 1984; Trapido-Rosenthal and Morse, 1985, 1986b), it was suspected that the chemosensory receptors controlling these two pathways might be located on externally accessible epithelia (Morse, 1985, 1990a, b). Epithelial cilia are known to carry chemosensory receptors in a wide variety of systems, including the well-characterized olfactory epithelia of frogs, fish, and mammals (*e.g.*, Rhein and Cagan, 1980; Chen and Lancet 1984; Pace *et al.*, 1985; Pace and Lancet, 1986; Lancet and Pace, 1987; Anholt, 1987; Anholt *et al.*, 1987). Epithelial cilia also have long been suspected to carry the chemosensory structures that mediate substratum recognition and thereby control settlement behavior and metamorphosis in various molluscan larvae (Raven, 1958; Fretter and Graham, 1962; Bonar, 1978a, b; Chia and Ross, 1984; Yool, 1985).

Recently, epithelial cilia isolated from *H. rufescens* larvae were shown to contain the lysine receptors and signal transducers that may control the amplifier pathway *in vivo* (Baxter and Morse, in prep.). These elements retain their functional coupling in the isolated cilia *in vitro*: *i.e.*, the specific and saturable binding of lysine to sodium-independent lysine receptors activates sequentially a G protein and diacylglycerol-stimulated protein kinase C (Baxter, 1991; Baxter and Morse, in prep.). The lysine-binding receptor was found to be reciprocally regulated by its tightly coupled G protein in the cilia *in vitro* (Baxter and Morse, in prep.); similar behavior is exhibited by other members of the rhodopsin and β-adrenergic G protein-coupled transmembrane receptor superfamily.

The tools of molecular genetics are required to further resolve the mechanisms by which the chemosensory and neuronal receptors, transducers, and pathways are integrated to control behavior in these small larvae (Morse, 1990a). As a first step toward that objective, we report here the amplification, cloning, and partial sequence analysis of cDNAs apparently corresponding to two Gα signal transducing proteins, from mRNA purified from the isolated cilia.

Materials and Methods

Cilia isolation

Larvae of *Haliotis rufescens* were produced in the laboratory by hydrogen peroxide-induced spawning of gravid adults (Morse *et al.*, 1977). Larvae were maintained at 15°C in 5 μm-filtered, UV-sterilized running seawater until 7 days post-fertilization; at this time they become developmentally competent to metamorphose in response to inducer (Morse *et al.*, 1979, 1980). Cilia were purified by differential centrifugation, after abscision induced by exposure of the larvae to a mild calcium-ethanol shock (Baxter and Morse, in prep.). This method is a modification of that used for the purification of functional receptor-bearing cilia from olfactory epithelia (Rhein and Cagan, 1980; Chen and Lancet, 1984) and other sources (Watson and Hopkins, 1962; Linck, 1973). Electron micrograph examination reveals the purified cilia to be intact and completely free of cell bodies and debris; the cilia are heterogeneous, and include short (*ca.* 0.5 μm) spatulate cilia similar to the sensory cilia found in other invertebrate systems, and long (≥10 μm) propulsive cilia from the larval velum (Baxter and Morse, in prep.).

RNA isolation

We isolated total RNA from cilia freshly purified from *Haliotis rufescens* larvae, using a single-step extraction with an acid guanidinium isothiocyanate (GITC[1])-phenol-chloroform mixture (Chomczynski and Sacchi, 1987). Poly A^+ mRNA was purified using oligo (dT) cellulose columns either centrifuged (Clontech, Palo Alto, California) or used with a syringe (Stratagene, La Jolla, California) in a modification of the technique described by Aviv and Leder (1972).

RNA was purified from bovine retina to provide a positive control enriched for G protein (transducin) mRNA. For this purpose, fresh bovine eyes were obtained from Federal Meat Market (Vernon, California). Retinas were immediately dissected on ice in Tris-buffered saline (Maniatis *et al.*, 1982) and placed on dry ice for transport to a nearby laboratory. There, half the samples were frozen in liquid nitrogen, and half were homogenized in GITC; these samples then were transported to Santa Barbara in GITC or on dry ice. RNA was isolated by the GITC-cesium chloride centrifugation method (Chirgwin *et al.*, 1979), and mRNA was then purified as described above.

Total RNA from both sources was analyzed by electrophoresis on formaldehyde gels (Maniatis *et al.*, 1982) with ethidium bromide added to the sample buffer, or was denatured at 65°C for 15 min, quickly chilled on ice, electrophoresed on 1% agarose/TBE gels (Han *et al.*, 1987) and visualized by UV-excited fluorescence after ethidium bromide staining (Maniatis *et al.*, 1982). Purity of total and poly A^+ RNA was confirmed by the ratio of absorbances at 260 and 280 nm and concentrations estimated from the A_{260}.

Synthesis of cDNA and oligonucleotide primers

Reverse transcriptase from avian myeloblastosis virus (AMV) (Invitrogen, San Diego, CA) was used to synthesize first strand cDNA. Cilia mRNA (100–500 ng) or bovine mRNA (1 μg) was used for each 50 μl reaction.

For polymerase chain reaction (PCR) amplifications, two kinds of oligonucleotide primers were made: degenerate primers (D) were used for the first amplifications of the cDNA, and (once the exact sequence of the Gα cDNA was determined) specific primers (S) were used to amplify the genomic sequences from sperm DNA. Oligonucleotides used as primers for PCR were synthesized (as the trityl-derivatives) by an automated oligonucleotide synthesizer (Applied Biosystems Inc., Foster City, California). To reduce the degeneracy of the primers, *Haliotis rufescens* condon usage frequencies (Groppe and Morse, 1989) were taken into consideration, and two separate pools of the downstream primer were synthesized (D_2 and D_3). Degenerate oligonucleotide primer sequences corresponding to the conserved *G* and *G′* domains (Lochrie and Simon, 1988) of G protein α subunits are: D_1: 5′ GAAGGATCCAAGTGGATCCA(GC)TG(CT)TTT 3′; D_2: 5′ CTCAAGCTTTCCT(TG)CTT(AG)TT(TG)AG-(AG)AA 3′; D_3: 5′ CTCAAGCTTTCTT(TG)CTT(AG)-TT(CA)AG(AG)AA 3′. D_1 corresponds to the conserved *G′* domain amino acid sequence, KWI(HQ)CF; D_2 and D_3 correspond to the conserved *G* domain sequence FLNK(KQ)D. Amino acid sequences chosen for these domains were based on the findings of Strathmann *et al.* (1989), with inclusion of a degeneracy representing additional sequences determined for yeast. In addition, these primers include oligonucleotide sequences (indicated by underlining) corresponding to the BamH I (D_1) and Hind III (D_2 and D_3) restriction enzyme targets; these sequences were added as linkers to facilitate cloning of the amplified products. A shorter variant of D_1 also was produced without the 9-nucleotide linker. Specific (non-degenerate) primer sequences based on the cDNA sequence subsequently determined for the *Haliotis* cilia Gα1 (see below) are: S_1: 5′ GCAGGATCCACGTCCATCATGTTCTTA 3′; and S_2: 5′ CTCAAGCTTCGGGTAGGTGA-TAATCGT 3′. These primers also have 9-nucleotide long 5′-linkers with a BamH I site (S_1) or a Hind III site (S_2).

After synthesis, oligonucleotides were deprotected at 55°C in ammonia overnight; they were then purified and detritylated by reverse-phase chromatography (Oligonucleotide Purification Cartridges from Applied Biosystems). The oligonucleotides were dried down, resuspended in sterile water, and concentration was estimated by absorbance at 260 nm.

PCR amplification

For amplification of cDNA, 50 pmol of each primer and 40% (20 μl) of the reverse transcription reaction were added directly to 100 μl PCR reactions. All other reaction components, including Taq DNA polymerase, were purchased from Perkin Elmer-Cetus Corp. (Norwalk, Connecticut) and used as suggested by that manufacturer. The number of amplification cycles was varied from 25 to 45 with the following parameters: denaturation at 94°C, 1 min; annealing at 37°C, 1 min; extension at 72°C, 3 min. For amplification of genomic DNA using specific primers, 0.3 μg *Haliotis rufescens* sperm DNA, 0.75 μg *Tetrahymena thermophila* DNA, 0.5 μg *Vibrio harveyi* DNA, or 1 μg salmon sperm DNA were added to otherwise identical amplification reactions. (The *Haliotis*, *Tetrahymena*, and *Vibrio* genomic DNA samples were generously provided by Jay Groppe, Jennifer Ortiz, and Richard Showalter, respectively.) All DNA samples were tested for amplification at amounts equal to or greater than the number of genome equivalents of the *Haliotis* DNA. Because DNA samples were in TE buffer, additions were adjusted such that the total amount of TE (and thus the concentration of EDTA) in all PCR reactions was equal. Optimum magnesium concentration, primer concentration, and cycling parameters were determined empirically. For amplification of genomic DNA, 25 pmol of each specific primer was used; the final concentration of magnesium was increased from the standard 1.5 m*M* to 2 m*M*; and a total of 30 amplification cycles was performed as before, except that the annealing temperature was raised to 45°C for the 2nd cycle and to 55°C for the 3rd–30th cycles. A 5 min extension step (72°C) was added after the last cycle.

Gel electrophoresis for analysis and purification of PCR reaction products

PCR reaction products were analyzed by electrophoresis on agarose gels (3% Nuseive agarose plus 1% Seaplaque agarose in TBE for cDNA-PCR reactions and 1.5% agarose/TAE buffer for genomic reactions), run at 2–6 v/cm, and stained with ethidium bromide. For analysis on the higher percentage gels, samples were loaded into wells cast from 0.7% agarose. One μg of restriction enzyme-digested plasmid (PBR322-BstN 1, from New England Biolabs Inc., Beverly, Massachusetts) was included for molecular weight markers.

For purification, amplified cDNA was electrophoresed on 3% low melting temperature agarose (Mermaid, from Bio 101 Corp., La Jolla), and DNA bands were excised while visualized on a 365 nm light box. DNA then was removed from the agarose by binding to glass beads (Glass Fog, from Bio 101 Corp.). Genomic products were run on 1.5% agarose gels as described above; bands were excised, and DNA was purified by binding to glass beads (Geneclean, from Bio 101 Corp.).

DNA cloning

Purified PCR products and a recombinant plasmid vector (*p*Bluescript KSII+, from Stratagene Corp.) were digested at 37°C for 1 h in 20 μl volumes with HindIII followed by BamHI (enzymes from New England Biolabs). Digested products were purified by gel electrophoresis as described above. The purified, linearized vector (100 ng) then was ligated to an approximately equimolar amount of PCR product insert; this reaction was catalyzed by T4 DNA ligase overnight at 4°C. Controls with no added insert were treated identically. Transformation of recipient bacteria (Epicurian Coli XL-1 Blue, from Stratagene Corp.) was performed by the method of Hanahan (1983), with modifications recommended by Stratagene Corp. After transformation, colonies with recombinant plasmids were identified on the antibiotic-containing agar medium with the chromogenetic substrate, X-gal. Each clone was then subcultured in 5 ml of LB containing ampicillin and tetracycline (37°C, overnight). Plasmid DNA was purified from these cultures after lysis with alkalai, using the miniprep procedure (Maniatis *et al.*, 1982).

Cloned plasmid DNA was digested as above with BamH I and Hind III simultaneously, and separately with BssH II (for which the plasmid has two sites, flanking the BamH I and Hind III sites). Restriction digests were analyzed by agarose gel electrophoresis. Plasmid DNA was purified by centrifugation chromatography (Sephacryl S-400 Miniprep Spun Columns, from Pharmacia, Piscataway, New Jersey).

DNA sequence analysis

Di-deoxy sequencing reactions were performed with modified T7 DNA polymerase (Sequenase II; United States Biochemical, Cleveland, Ohio) and 5′ [α-^{35}S]dATP, 1100 Ci/mmol (Amersham) by procedures modified from Sanger *et al.* (1977). Primers used for sequencing were plasmid primers T7, T3, KS, and SK (purchased from Stratagene) and the specific primers S_1 and S_2, described above. Reactions were analyzed by electrophoresis on 8% polyacrylamide-50% urea wedge sequencing gels. Gels were washed in 10% acetic acid-10% methanol, dried with vacuum at 80°C, and subjected to autoradiography. The autoradiograms were read with a sonic digitizer, and the resulting sequences analyzed with the aid of the Pustell Sequence Analysis software (IBI Macintosh).

Results

PCR amplification of cilia Gα cDNA

Poly A^+ mRNA was isolated from the purified cilia of 7–9-day-old, competent larvae of *Haliotis rufescens*, as described in the Methods. Starting with about 10^6 larvae, typical yields were 300–400 mg (wet weight) cilia, 50 μg total RNA, and 1 μg of poly A^+ mRNA (=2% of total RNA). AMV reverse transcriptase was used to catalyze random-hexamer primed synthesis of first strand cDNA from the purified mRNA, and the resulting mRNA-cDNA duplex was then used as template for PCR amplification with the degenerate primers corresponding to the conserved *G* and *G′* domains, as described in the Methods.

The primers used clearly directed the amplification of a 196 bp product from the cDNA templates prepared from the larval cilia (Fig. 1a). The size of this product is within the range predicted for a Gα cDNA domain lying between the highly conserved *G* and *G′* domains. This result suggests that the cilia purified from *Haliotis rufescens* larvae may contain mRNA coding for a Gα protein.

The positive result shown in Figure 1a allowed us to further optimize the primers used for PCR-amplification. The upstream primer used in the first PCR amplifications was relatively short, consisting of a degenerate pool of 17-mers. This primer only weakly amplified the positive control template, cDNA from bovine retina, a tissue highly enriched for the Gα known as transducin (results not shown). The addition of nine nucleotides containing the sequence of the BamHI restriction endonuclease site to the 5′-end of the 17-mers, to generate the D_1 primers (see Materials and Methods), makes efficient amplification of the control Gα sequence from bovine retina cDNA possible (Fig. 1b). [Similarly, we had found earlier that addition of the nine nucleotides containing the sequence of the Hind III restriction site to the 5′-end of short downstream primers, to generate the 26-mer D_2 and D_3 pools, also significantly enhanced the efficiency of these oligonucleotides as primers. These non-matching nucleotides do not reduce primer specificity. Similar observations have been reported by others (*e.g.*, Mack and Sninsky, 1988).] The results in Figure 1b show the downstream primers in the degenerate pool D_2 are more effective than those in D_3 for detecting and amplifying Gα cDNA sequences from both bovine retina and *Haliotis rufescens* larval cilia. Primer D_3 differs from D_2 by two nucleotides and apparently fails to hybridize efficiently to the target G protein cDNA sequence. Agarose gel electrophoresis of PCR products amplified with the optimized 26-mer primers (D_1 and D_2) reveals the expected 205 bp product from

cDNAs from both the larval cilia and bovine retina. The product is nine nucleotides longer than that seen in Figure 1a, as expected because the upstream primer (D_1) is nine nucleotides longer than that used in the first experiment. The cilia cDNA required more cycles of amplification (35) than did the bovine retina cDNA (25) before the product on an ethidium bromide stained gel could be visualized. Thus, there may be greater primer-template mismatch, or the target mRNA may be less abundant, in the larval cilia.

A control PCR reaction with no added DNA template, a test for DNA contamination of reagents, yielded no detectable PCR products amplified after 45 cycles (Fig. 1b). In addition, no amplified PCR products were observed in the following control reactions (not shown): (a) no primers in the PCR reaction; (b) no Taq polymerase in the PCR reaction; and (c) no reverse transcriptase in the cDNA reaction.

Cloning and sequence analysis of Gα cDNA

The 205 bp PCR product from the cilia cDNA was cloned in the plasmid vector as described in Materials and Methods. Twelve transformant colonies were picked and subcultured; gel electrophoresis of the restriction enzyme-digested plasmid DNA showed that 11 of these clones contained inserts of the correct size.

Sequence analysis of three of the cloned cilia PCR products revealed two unique cDNA sequences (Fig. 2). As shown, both of these share a number of the highly conserved residues of other Gα proteins in the *G–G′* region. Two out of the three clones proved to have identical nucleotide (and deduced protein) sequences over the 51 amino acid region between the primers. This *Haliotis* G protein α subunit (Gα1) differs in the region analyzed by only one amino acid from the sequence of mouse brain Gα11, a member of the newly discovered G_q class of α subunits (Strathmann *et al.*, 1989; Strathmann and Simon, 1990). This sequence differs significantly in the region analyzed from all other known classes of G protein α subunits (G_s, G_t, G_{olf}, G_o, G_i, G_x) from mammals, *Drosophila*, and yeast. The second G protein sequence from the larval cilia (*Haliotis* Gα2) is most homologous to G_o and G_i from *Drosophila*.

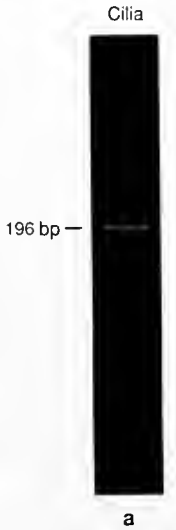

Figure 1(a). G protein α subunit cDNA from cilia, amplified by PCR. Product from 50 cycles of amplification; primers were a 17-mer variant of D_1 (without the BamHI site) and D_2. Number of base-pairs in product is indicated. Details in Materials and Methods.

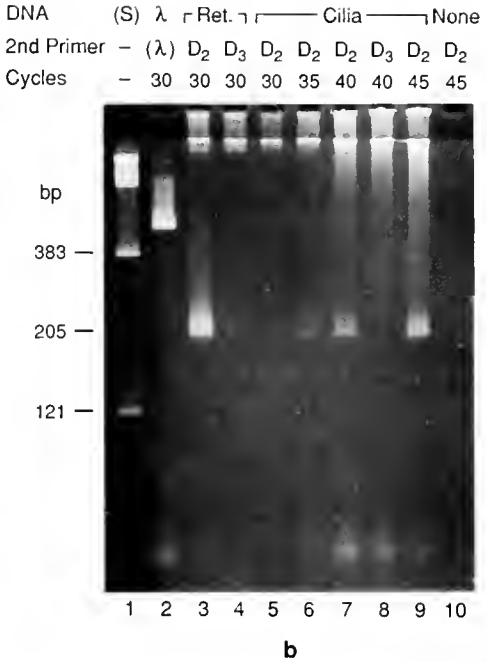

Figure 1(b). PCR amplification of larval cilia cDNA using degenerate primers D_1 and either D_2 or D_3. Lanes: (1) molecular weight standards; (2) λ DNA and primers as PCR control; (3) bovine retina cDNA, primers D_1 and D_2, 30 cycles; (4) bovine retina cDNA, primers D_1 and D_3, 30 cycles; (5) cilia cDNA, primers D_1 and D_2, 30 cycles; (6) cilia cDNA, primers D_1 and D_2, 35 cycles; (7) cilia cDNA, primers D_1 and D_2, 40 cycles; (8) cilia cDNA, primers D_1 and D_3, 40 cycles (9) cilia cDNA, primers D_1 and D_2, 45 cycles; (10) no DNA template, primers D_1 and D_2, 45 cycles.

Amplification, cloning, and sequence analysis of Gα from Haliotis *genomic DNA*

The nucleotide sequence from the *Haliotis rufescens* larval cilia Gα1 clone was used to design specific (*i.e.*, non-degenerate) primers to amplify the corresponding region of Gα from *H. rufescens* sperm genomic DNA. The specific primers (S_1 and S_2) were based on regions of the *Haliotis* sequence that differed significantly from other Gα protein sequences (Fig. 5; *cf.* Fig. 2).

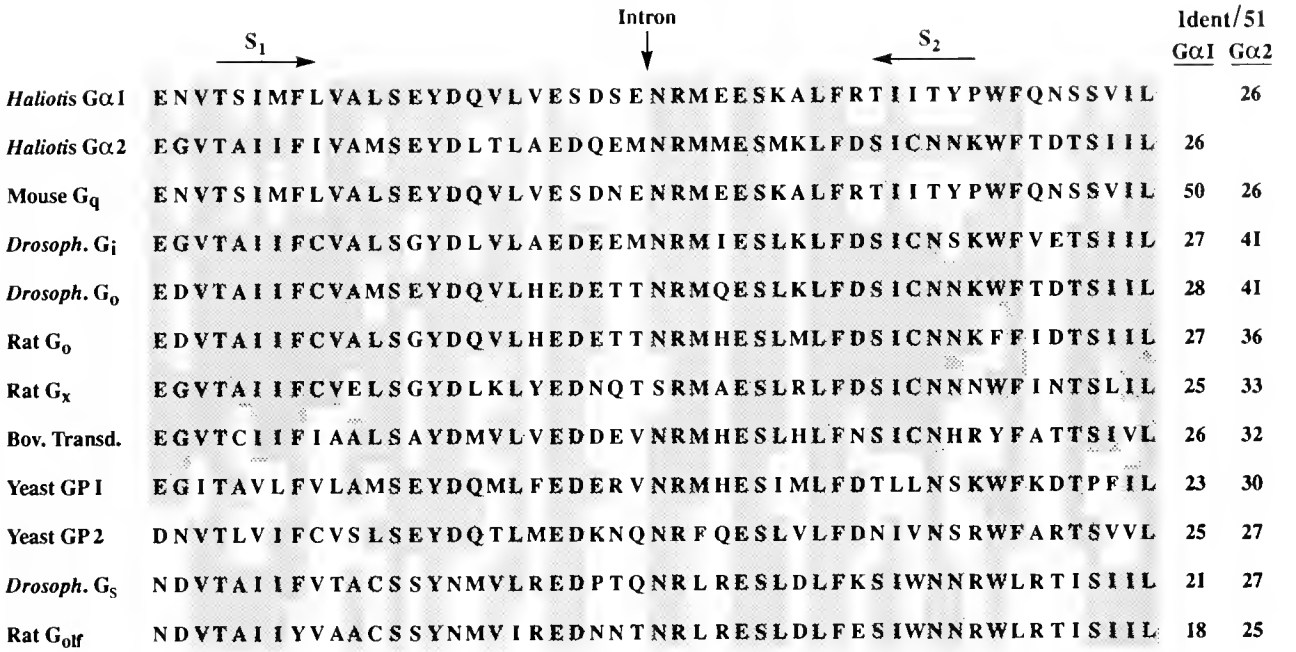

Figure 2. Gα sequences from cilia. Deduced amino acid sequences of the cloned PCR products (Gα1 and Gα2) from *Haliotis rufescens* cilia cDNA are compared with the corresponding regions of other Gα subunits. Residues highly homologous in several Gα proteins are indicated by shading. Region shown is between (not including) degenerate primers D_1 and D_2. The number of amino acids identical to *Haliotis* Gα1 and Gα2 (of 51 total) is shown for each Gα. Sequences used to design specific primers S_1 and S_2 are shown by arrows; position of the intron in genomic DNA is indicated. Standard (IUPAC) one-letter amino acid code is used.

Two distinct DNA products were seen when *Haliotis* genomic DNA was amplified by PCR reactions with the S_1 and S_2 primers, and the products were analyzed on an agarose gel (Fig. 3). The specificity of these primers for *Haliotis* DNA is evident by their failure to direct amplification of genomic DNA sequences from *Tetrahymena, Vibrio,* or salmon sperm in otherwise identical PCR reactions.

The 1.25 kb and 1.45 kb *Haliotis* genomic PCR products were electrophoretically purified, separately amplified again, and analyzed electrophoretically (Fig. 4). The successful purification of the two genomic PCR products is shown by the lack of visible contamination after this second round of amplification and gel electrophoresis. Each purified PCR product was cloned as described above, and the cloned inserts were then sequenced using primers matched to the vector.

During the cloning step we discovered that the larger of the two genomic PCR products had an internal Hind III site not found in the smaller product. This difference apparently resides in an intron, a non-coding sequence not present in the cDNA (see below). Although the resulting Hind III-Hind III fragment was not cloned, a partial sequence for this region was obtained from the direct sequencing of the uncloned PCR products using S_1 and S_2 as primers for the sequencing reaction. While this method of direct sequencing proved useful in this case, the quality of the sequencing reactions was highly variable (*cf.* McCabe, 1989).

The genomic PCR product sequences were identical to the Gα1 cDNA sequence from the cilia, and to one another, in the putative coding regions. But both of the cloned genomic sequences contain an intron that interrupts the coding sequence. The exact position of this intron between exons 6 and 7 is conserved in the genomic sequences corresponding to the *Haliotis* Gα1 and the G_o and G_i of mammals and *Drosophila* (Figs. 2, 5). The two *Haliotis* genomic sequences prove to be highly homologous to one another at both ends of the introns that are adjacent to the coding regions (corresponding to exons 6 and 7 in other species; *cf.* Fig. 5); however, the two introns differ in length by about 200 bp.

Discussion

The larvae of *Haliotis rufescens* provide a uniquely tractable model system for resolving and analyzing the chemosensory receptors and signal transducers, and the mechanisms of their functional integration, controlling behavior and development in response to chemical signals

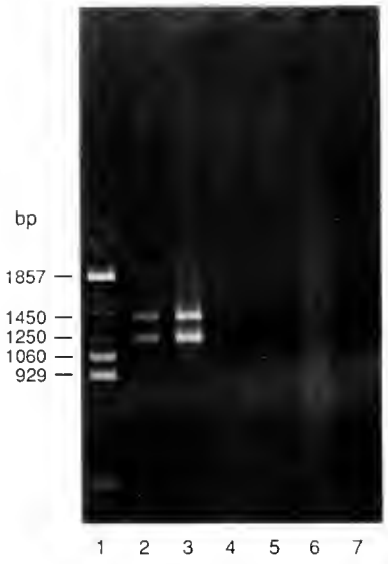

Figure 3. PCR amplification of genomic DNA using *Haliotis*-specific primers S_1 and S_2 (30 cycles). Lanes: (1) molecular weight standards; (2) and (3) 0.3 μg *Haliotis* sperm DNA; (4) 0.75 μg *Tetrahymena* DNA; (5) 0.5 μg *Vibrio* DNA; (6) 1 μg salmon sperm DNA; (7) no DNA. Other details in Materials and Methods.

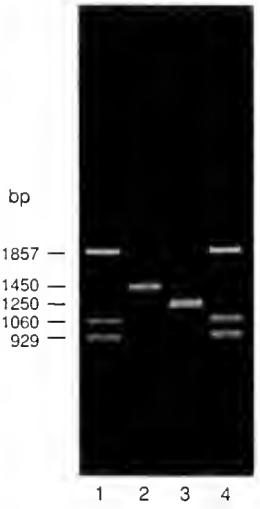

Figure 4. *Haliotis* genomic PCR products after gel purification and 30 additional cycles of amplification with specific primers S_1 and S_2. Lanes: (1) molecular weight standards; (2) *ca.* 1.45 kb genomic PCR product; (3) *ca.* 1.25 kb genomic PCR product; (4) molecular weight standards.

from the environment (Morse, 1990a, b). Purification of cilia in milligram quantities from the cultured larvae has allowed us to analyze the chemosensory receptors and signal transducers *in vitro* (Baxter, 1991; Baxter and Morse, in prep.), and (as shown here) to isolate mRNAs encoding some of these elements and conduct analyses at the cDNA sequence level. We have shown here that cilia purified from *H. rufescens* larvae contain polyadenylated mRNA, and that this mRNA includes sequences corresponding to two Gα signal transducing proteins.

The central role of the G proteins as chemosensory signal transducers was confirmed by *in vitro* studies of olfactory cilia isolated from frog (Pace *et al.*, 1985). Jones and Reed (1989) recently have identified a unique G_{olf} from the ciliated sensory epithelium of the rat olfactory mucosa; the sequence of this G protein α subunit was determined by analysis of its cDNA. G protein also acts as the primary chemosensory signal transducer in taste receptor cells in the frog; this G protein controls the activation of adenyl cylase, with the resulting sequential activation of a protein kinase and membrane depolarization (Avenet *et al.*, 1988). G protein transduction of chemosensory stimulation in catfish controls an inositol triphosphate (protein kinase) cascade (Huque *et al.*, 1987).

Although distal localization of mRNA has been observed in other systems (Merlie and Sanes, 1985; Garner *et al.*, 1988; Kosik *et al.*, 1989), the results reported here are the first of which we are aware in which mRNA has been purified, and the corresponding cDNA synthesized, amplified, cloned, and sequenced from purified cilia. Because the mRNA from which the G protein sequences were identified was extracted from cilia that had been purified and washed by four sequential cycles of differential centrifugation, it was probably not contaminated by free RNA released from the larvae. Electron microscopy shows no other cell fragments or cells contaminating the purified cilia (Baxter, 1991; Baxter and Morse, in prep.). *In situ* hybridization will be required, however, to verify the intraciliary localization of the Gα mRNA. Three independent lines of evidence confirm that the source of

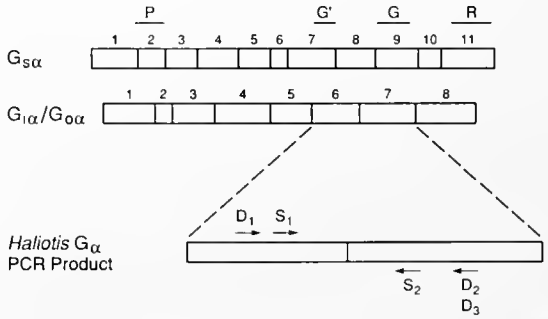

Figure 5. Genomic organization of mammalian G protein α subunits (after Kaziro *et al.*, 1990). Exons (coding regions) are numbered; vertical lines indicate introns. Conserved domains P (GTP hydrolysis), G′ and G (GTP binding) and R are shown above. [In the convention of Halliday (1984), domain G also is designated G, but the other domains are designated differently.]. The region of the *Haliotis* G protein corresponding to mammalian G_o and G_i exons 6 and 7 is expanded to show relative positions and orientations of PCR primers. D_1, D_2, and D_3 are degenerate primers used for cDNA amplification; S_1 and S_2 are the *Haliotis*-specific primers used for genomic amplification.

the G protein sequences characterized could not have come from bacterial contamination: (1) the mRNA selected was poly A^+; (2) the sequence of Gα1 determined corresponds exactly to a sequence in the genomic DNA (from sperm) of *Haliotis rufescens;* and (3) that genomic sequence contains an intron (at the expected position) that would be lacking from bacterial DNA. That these sequences were from *Haliotis* mRNA, and not from possible contaminants, was further confirmed by the failure of the unique ciliary sequences to direct amplification of any homologous sequences in control samples of bacterial, protozoan, or fish DNA, under conditions in which the perfectly homologous sequences were detected and amplified from *Haliotis* genomic (sperm) DNA.

The cDNA sequences that we obtained from mRNA purified from the cilia isolated from *Haliotis rufescens* larvae reveal two apparent G protein α subunit sequences. Although definitive characterization must await completion of the entire translated sequences, our identification of these sequences as members of the G protein family is strengthened by the finding that Gα1 is virtually identical (50/51 residues) to $G_q\alpha$ in the region sequenced, and the observation that the most highly conserved amino acids in this region of the other known Gα proteins also are conserved in the Gα1 and Gα2 sequences from the *Haliotis* larvae (Fig. 2). The genomic sequences that we thus far have characterized correspond exactly to their cDNAs, and contain the intron at the same position between the *G* and *G'* domains as those found in mammalian G protein genes.

The two Gα sequences obtained from the cilia of *Haliotis* larvae are clearly related to the Gα sequences from other species (Fig. 2) (and unrelated to tubulin, for example). Yet the two sequences differ significantly from one another. The larval cilia Gα1 sequence is highly homologous to that of the corresponding domain of the alpha subunit of the mammalian G_q. This is of particular interest, in light of the finding that G_q is a pertussis toxin-insensitive regulator of phospholipase C (Strathmann and Simon, 1990; Smrcka *et al.,* 1991), and our observation that the lysine-dependent regulatory pathway in *Haliotis* larvae is mediated by a pertussis toxin-insensitive G protein-phospholipase C-protein kinase cascade (Baxter and Morse, 1987; Baxter, 1991; Baxter and Morse, in prep.). Gα1 is markedly different from G_i, G_s, G_o, G_x, and G_{olf} characterized from other systems, whereas the larval cilia Gα2 sequence is significantly more closely related to G_i and G_o (from *Drosophila* and rat) than it is to the G_s and G_{olf} from these species. We are now in the process of identifying the Gα sequence corresponding to the transducing protein specifically activated by the lysine receptors in the isolated cilia. These experiments are facilitated by the observation that lysine binding to the ciliary receptors activates the associated Gα protein, increasing its radioactive labeling with ADP-ribose catalyzed by cholera toxin (Baxter and Morse, in prep.).

In molluscan larvae, the cilia of the cephalic apical tuft and of the propodium have been suggested to mediate chemosensory substratum-recognition and the resulting control of metamorphosis (Raven, 1958; Fretter and Graham, 1962; Bonar, 1978a, b; Chia and Koss, 1984; Yool, 1985). Ciliary receptors have been implicated in this process in other invertebrate larvae as well (*e.g.,* Laverack, 1968; Carthy and Newell, 1968; Chia and Spaulding, 1972; Siebert, 1974; Zimmer and Wollacott, 1977; Eckelbarger, 1978; Reed and Cloney, 1982; Reed, 1987). The ciliated cells of the apical tufts of *Haliotis* larvae are stellate neurons that appear anatomically to be primary chemosensory receptor cells (Yool, 1985). These neurons project axons to the cephalic ganglia; they also send lateral dendrites to a pair of adjacent mucus gland cells that are stimulated to secrete their contents in one of the first cellular changes observed in metamorphosis (Morse *et al.,* 1980a; Yool, 1985). These neurons and their cilia disappear from the organism after induction of metamorphosis; the time of this loss coincides with the time of loss of the labeled morphogenic receptors (Trapido-Rosenthal and Morse, 1986a), supporting the suggestion that some of the biochemically labeled chemosensory receptors controlling metamorphosis may be located on these cells or their cilia.

Our finding that sufficient mRNA can be obtained from the cilia of *Haliotis* larvae to establish a cDNA library opens this system to analyses, similar to that reported here, of the cDNAs for the receptors and other signal transducers of the morphogenetic and amplifier pathways that control metamorphosis. These analyses should provide insights into the mechanisms of action, functional integration, and evolution of the chemoreceptors and their associated signal-transducers in the molluscan larvae.

Acknowledgments

This research was supported by grants from the National Science Foundation (DCB-87-18224), the Office of Naval Research Molecular Biology Program (N00014-87-K-0762), and the University of California at Santa Barbara Training Grant in Marine Biotechnology. We especially appreciate the expert advice, and time and effort provided by Jay C. Groppe. We also gratefully acknowledge the helpful suggestions provided by Mel Simon, Thomas T. Amatruda, and John Sninsky; gifts of genomic DNA samples provided by Richard Showalter, Jennifer Ortiz, and Jay Groppe; and expert instruction and assistance in the dissection of retinas, provided by Page Erickson.

Literature Cited

Anholt, R. R. H. 1987. Primary events in olfaction. *Trends Biochem. Sci.* **12:** 58–62.

Anholt, R. R. H., S. M. Mumby, D. A. Stoffers, P. R. Girard, J. F. Kuo, and S. H. Snyder. 1987. Transduction proteins of olfactory receptor cells: identification of guanine nucleotide binding proteins and protein kinase C. *Biochemistry* **26:** 788–795.

Avenet, P., F. Hofmann, and B. Lindemann. 1988. Transduction in taste receptor cells requires cAMP-dependent protein kinase. *Nature* **331:** 351–354.

Aviv, H., and P. Leder. 1972. Purification of biologically active globin messenger RNA by chromatography on oligothymidylic acid-cellulose. *Proc. Nat. Acad. Sci. USA* **69:** 1408.

Baloun, A. J., and D. E. Morse. 1984. Ionic control of settlement and metamorphosis in larval *Haliotis rufescens* (gastropoda). *Biol. Bull.* **167:** 124–138.

Baxter, G. 1991. Chemosensory signal transduction in larvae of the mollusc, *Haliotis rufescens.* Doctoral Dissertation, University of California, Santa Barbara. 94 pp.

Baxter, G., and D. E. Morse. 1987. G protein and diacylglycerol regulate metamorphosis of planktonic molluscan larvae. *Proc. Nat. Acad. Sci. USA* **84:** 1867–1870.

Bonar, D. B. 1978a. Ultrastructure of a cephalic sensory organ in larvae of the gastropod *Phestilla sibogae* (Aeolidacea: Nudibranchia). *Tissue Cell* **10:** 153–165.

Bonar, D. B. 1978b. Morphogenesis at metamorphosis in opistobranch molluscs. Pp. 177–196 in *Settlement and Metamorphosis of Marine Invertebrate Larvae,* F.-S. Chia and M. E. Rice, eds. Elsevier/North Holland Biomedical Press, New York.

Carthy, J. D., and G. E. Newell, eds. 1968. *Invertebrate Receptors.* Academic Press, London.

Chen, Z., and D. Lancet. 1984. Membrane proteins unique to vertebrate olfactory cilia: candidates for sensory receptor molecules. *Proc. Nat. Acad. Sci. USA* **81:** 1859–1863.

Chia, F.-S., and R. Koss. 1984. Fine structure of the cephalic sensory organ in the larva of the nudibranch *Rostanga pulchra* (Mollusca: Opistobranchia, Nudibranchia). *Zoomorphology* **104:** 131–139.

Chia, F.-S., and J. G. Spaulding. 1972. Development and juvenile growth of the sea anemone, *Tealia crassicornis. Biol. Bull.* **142:** 206–218.

Chirgwin, J. M., A. E. Przybyla, R. J. MacDonald, and W. J. Rutter. 1979. Isolation of biologically active ribonucleic acid from sources enriched in ribonuclease. *Biochemistry* **18:** 5294.

Chomczynski, P., and N. Sacchi. 1987. Single-step method of RNA isolation by acid guanidinium thiocyanate-phenol-chloroform extraction. *Anal. Biochem.* **162:** 156–159.

Eckelbarger, K. J. 1978. Metamorphosis and settlement in the Sabellariidae. Pp. 145–164 in *Settlement and Metamorphosis of Marine Invertebrate Larvae,* F.-S. Chia and M. E. Rice, eds. Elsevier, New York.

Fretter, V., and A. Graham, eds. 1962. *British Prosobranch Molluscs.* Ray Society, London.

Garner, C. C., R. P. Tucker, and A. Matus. 1988. Selective localization of messenger RNA for cytoskeletal protein MAP2 in dendrites. *Nature* **336:** 674–677.

Groppe, J., and D. E. Morse. 1989. Molecular cloning of novel serine protease cDNAs from abalone. Pp. 285–288 in *Current Topics in Marine Biotechnology,* S. Miyachi, I. Karube, and Y. Ishida, eds. Japan Soc. Mar. Biotechnol., Tokyo.

Halliday, K. R. 1984. Regional homology in GTP-binding proto-oncogene products and elongation factors. *J. Cyclic Nucleotide Res.* **9:** 435–448.

Han, J. H., C. Stratowa, and W. J. Rutter. 1987. Isolation of full-length putative rat lysophospholipase cDNA using improved methods for mRNA isolation and cDNA cloning. *Biochemistry* **26:** 1617–1625.

Hanahan, D. 1983. Studies on transformation of *Escherichia coli* with plasmids. *J. Mol. Biol.* **166:** 557–580.

Huque, T., J. G. Brand, J. L. Rabinowitz, and D. L. Bailey. 1987. Phospholipid turnover in catfish barbel (taste) epithelium with special reference to phosphatidylinositol-4,5-bisphosphate. *Chem. Senses* **12:** 666–667.

Jones, D. T., and R. R. Reed. 1989. G_{olf}: an olfactory neuron-specific G protein involved in odorant signal transduction. *Science* **244:** 790–795.

Kaziro Y., H. Itoh, and M. Nakafuku. 1990. Organization of genes coding for G-protein α subunits in higher and lower eukaryotes. Pp. 63–76 in *G Proteins,* R. Iyengar and L. Birnbaumer, eds. Academic Press, San Diego.

Kosik, K. S., J. E. Crandall, E. J. Mufson, and R. L. Neve. 1989. Tau *in situ* hybridization in normal and Alzheimer brain: localization in the somatodenditic compartment. *Ann. Neurol.* **26:** 352–361.

Lancet, D., and U. Pace. 1987. The molecular basis of odor recognition. *Trends Biochem. Sci.* **12:** 63–66.

Laverack, M. S. 1968. On superficial receptors. *Symp. Zool. Soc. Lond.* **23:** 299–326.

Linck, R. W. 1973. Comparative isolation of cilia and flagella from the lamellibranch mollusc, *Aequipecten irradians. J. Cell Sci.* **12:** 345–367.

Lochrie, M. A., and M. J. Simon. 1988. G protein multiplicity in eukaryotic signal transduction systems. *Biochemistry* **27:** 4957–4965.

Mack, D. H., and J. J. Sninsky. 1988. A sensitive method for identification of uncharacterized viruses related to known virus groups: hepadnavirus model system. *Proc. Nat. Acad. Sci. USA* **85**(18): 6977–6981.

Maniatis, T., E. F. Fritsch, and J. Sambrook. 1982. *Molecular Cloning: A Laboratory Manual.* Cold Spring Harbor Laboratory, Cold Spring Harbor, New York.

McCabe, P. C. 1989. Asymmetric polymerase chain reaction. *Amplifications* **3:** 1–3.

Merlie, J. P., and J. R. Sanes. 1985. Concentrations of acetylcholine receptor mRNA in synaptic regions of adult muscle fibres. *Nature.* **317:** 66–68.

Morse, A. N. C., C. Froyd, and D. E. Morse. 1984. Molecules from cyanobacteria and red algae that induce larval settlement and metamorphosis in the mollusc *Haliotis rufescens. Mar. Biol.* **81:** 293–298.

Morse, D. E. 1985. Neurotransmitter-mimetic inducers of settlement and metamorphosis of marine planktonic larvae. *Bull. Mar. Sci.* **37:** 697–706.

Morse, D. E. 1990a. Recent progress in larval settlement and metamorphosis: closing the gaps between molecular biology and ecology. *Bull. Mar. Sci.* **46:** 465–483.

Morse, D. E. 1990b. Molecular mechanisms controlling metamorphosis in abalone larvae. In *Abalone,* M. Tegner and S. Shepherd, eds. Blackwell (in press).

Morse, D. E., H. Duncan, N. Hooker, and A. Morse. 1977. Hydrogen peroxide induces spawning in molluscs, with activation of prostaglandin endoperoxide synthetase. *Science* **196:** 298–300.

Morse, D. E., N. Hooker, H. Dunan, and L. Jensen. 1979. γ-aminobutyric acid, a neurotransmitter, induces planktonic abalone larvae to settle and begin metamorphosis. *Science* **204:** 407–410.

Morse, D. E., H. Duncan, N. Hooker, A. Baloun, and G. Young. 1980. GABA induces behavioral and developmental metamorphosis in planktonic molluscan larvae. *Fed. Proc.* **39:** 3237–3241.

Pace, U., and D. Lancet. 1986. Olfactory GTP-binding protein: signal-transducing polypeptide of vertebrate chemosensory neurons. *Proc. Nat. Acad. Sci. USA* **83:** 4947–4951.

Pace, U., E. Hanski, Y. Salomon, and D. Lancet. 1985. Odorant-sensitive adenylate cyclase may mediate olfactory reception. *Nature* **316:** 255–258.

Raven, C. P. 1958. *Morphogenesis, the Analysis of Molluscan Development.* Pergamon Press, New York.

Reed, C. G. 1987. The organization and isolation of the ciliary locomotory and sensory organs of marine bryozoan larvae. Pp. 397–408 in *Marine Biodeterioration,* R. Turner and R. Nagabhushanam, eds., Oxford Press, New Delhi.

Reed, C., and R. A. Cloney. 1982. The larval morphology of the marine bryozoan *Bowerbankia gracilis* (Ctenostomata: Vesicularioidea). *Zoomorphology* **100:** 23–54.

Rhein, L. D., and R. H. Cagan. 1980. Biochemical studies of olfaction: isolation, characterization, and odorant binding activity of isolated cilia from rainbow trout olfactory rosettes. *Proc. Nat. Acad. Sci. USA* **77:** 4412–4416.

Sanger, F., S. Nicklen, and A. R. Coulson. 1977. DNA sequencing with chain-terminating inhibitors. *Proc. Nat. Acad. Sci. USA* **74:** 5463–5467.

Siebert, A. E. 1974. A description of the embryology, larval development and feeding of the sea anemones *Anthopleura elegantissima* and *A. xanthogrammica. Can. J. Zool.* **52:** 1383–1388.

Smrcka, V., J. R. Hepler, K. O. Brown, and P. C. Sternweis. 1991. Regulation of polyphosphoinositide-specific phospholipase C activity by purified G_q. *Science* **251:** 804–807.

Strathmann, M., and M. I. Simon. 1990. G protein diversity: a distinct class of α subunits is present in vertebrates and invertebrates. *Proc. Nat. Acad. Sci. USA* **87:** 9113–9117.

Strathmann, M., T. M. Wilkie, and M. I. Simon. 1989. Diversity of the G-protein family: sequences from five additional α subunits in the mouse. *Proc. Nat. Acad. Sci. USA* **86:** 7407–7409.

Trapido-Rosenthal, H. G., and D. E. Morse. 1985. L-α, ω-Diamino acids facilitate induction of settlement and metamorphosis in larvae of a gastropod mollusc (*Haliotis rufescens*). *J. Comp. Physiol. B* **155:** 403–414.

Trapido-Rosenthal, H. G., and D. E. Morse. 1986a. Availability of chemosensory receptors is down-regulated by habituation of larvae to a morphogenetic signal. *Proc. Nat. Acad. Sci. USA* **83:** 7658–7662.

Trapido-Rosenthal, H. G., and D. E. Morse. 1986b. Regulation of receptor-mediated settlement and metamorphosis in larvae of a gastropod mollusc (*Haliotis rufescens*). *Bull. Mar. Sci.* **39:** 383–392.

Watson, M. R., and J. M. Hopkins. 1962. Isolated cilia from *Tetrahymena pyriformis. Exp. Cell. Res.* **28:** 280–295.

Yool, A. J. 1985. Physiological analysis of the induction of metamorphosis in larvae of *Haliotis rufescens* (Gastropoda: Mollusca). Ph.D. Thesis, University of California, Santa Barbara. 111 pp.

Zimmer, R. L., and R. M. Woolacott. 1977. Metamorphosis, ancestrulae, and coloniality in bryozoan life cycles. Pp. 91–142 in *Biology of Bryozoans,* R. M. Woolacott and R. L. Zimmer, eds., Academic Press, New York.

CONTENTS

Volume 180 Number 3

THE BIOLOGICAL BULLETIN

JUNE, 1991

Published by the Marine Biological Laboratory

THE
BIOLOGICAL BULLETIN

PUBLISHED BY
THE MARINE BIOLOGICAL LABORATORY

JUNE, 1991

Printed and Issued by
LANCASTER PRESS, Inc.
PRINCE & LEMON STS.
LANCASTER, PA

THE BIOLOGICAL BULLETIN

THE BIOLOGICAL BULLETIN is published six times a year by the Marine Biological Laboratory, MBL Street, Woods Hole, Massachusetts 02543.

Subscriptions and similar matter should be addressed to Subscription Manager, THE BIOLOGICAL BULLETIN, Marine Biological Laboratory, Woods Hole, Massachusetts 02543. Single numbers, $25.00. Subscription per volume (three issues), $72.50 ($145.00 per year for six issues).

Communications relative to manuscripts should be sent to Michael J. Greenberg, Editor-in-Chief, or Pamela L. Clapp, Managing Editor, at the Marine Biological Laboratory, Woods Hole, Massachusetts 02543. Telephone: (508) 548-3705, ext. 428. FAX: 508-540-6902.

POSTMASTER: Send address changes to THE BIOLOGICAL BULLETIN, Marine Biological Laboratory, Woods Hole, MA 02543.

Second-class postage paid at Woods Hole, MA, and additional mailing offices.
ISSN 0006-3185

INSTRUCTIONS TO AUTHORS

The Biological Bulletin accepts outstanding original research reports of general interest to biologists throughout the world. Papers are usually of intermediate length (10–40 manuscript pages). A limited number of solicited review papers may be accepted after formal review. A paper will usually appear within four months after its acceptance.

Very short, especially topical papers (less than 9 manuscript pages including tables, figures, and bibliography) will be published in a separate section entitled "Research Notes." A Research Note in *The Biological Bulletin* follows the format of similar notes in *Nature*. It should open with a summary paragraph of 150 to 200 words comprising the introduction and the conclusions. The rest of the text should continue on without subheadings, and there should be no more than 30 references. References should be referred to in the text by number, and listed in the Literature Cited section in the order that they appear in the text. Unlike references in *Nature*, references in the Research Notes section should conform in punctuation and arrangement to the style of recent issues of *The Biological Bulletin*. Materials and Methods should be incorporated into appropriate figure legends. See the article by Lohmann *et al.* (October 1990, Vol. **179**: 214–218) for sample style. A Research Note will usually appear within two months after its acceptance.

The Editorial Board requests that regular manuscripts conform to the requirements set below; those manuscripts that do not conform will be returned to authors for correction before review.

1. ***Manuscripts.*** Manuscripts, including figures, should be submitted in triplicate. (Xerox copies of photographs are not acceptable for review purposes.) The original manuscript must be typed in no smaller than 12 pitch, using double spacing (*including* figure legends, footnotes, bibliography, etc.) on one side of 16- or 20-lb. bond paper, 8½ by 11 inches. Please, no right justification. Manuscripts should be proofread carefully and errors corrected legibly in black ink. Pages should be numbered consecutively. Margins on all sides should be at least 1 inch (2.5 cm). Manuscripts should conform to the *Council of Biology Editors Style Manual*, 4th Edition (Council of Biology Editors, 1978) and to American spelling. Unusual abbreviations should be kept to a minimum and should be spelled out on first reference as well as defined in a footnote on the title page. Manuscripts should be divided into the following components: Title page, Abstract (of no more than 200 words), Introduction, Materials and Methods, Results, Discussion, Acknowledgments, Literature Cited, Tables, and Figure Legends. In addition, authors should supply a list of words and phrases under which the article should be indexed.

2. ***Title page.*** The title page consists of: a condensed title or running head of no more than 35 letters and spaces, the manuscript title, authors' names and appropriate addresses, and footnotes listing present addresses, acknowledgments or contribution numbers, and explanation of unusual abbreviations.

3. ***Figures.*** The dimensions of the printed page, 7 by 9 inches, should be kept in mind in preparing figures for publication. We recommend that figures be about 1½ times the linear dimensions of the final printing desired, and that the ratio of the largest to the smallest letter or number and of the thickest to the thinnest line not exceed 1:1.5. Explanatory matter generally should be included in legends, although axes should always be identified on the illustration itself. Figures should be prepared for reproduction as either line cuts or halftones. Figures to be reproduced as line cuts should be unmounted glossy photographic reproductions or drawn in black ink on white paper, good-quality tracing cloth or plastic, or blue-lined coordinate paper. Those to be reproduced as halftones should be mounted on board, with both designating numbers or letters and scale bars affixed directly to the figures. All figures should be numbered in consecutive order, with no distinction between text and plate figures. The author's name and an arrow indicating orientation should appear on the reverse side of all figures.

4. ***Tables, footnotes, figure legends, etc.*** Authors should follow the style in a recent issue of *The Biological Bulletin* in preparing table headings, figure legends, and the like. Because of the high cost of setting tabular material in type, authors are asked to limit such material as much as possible. Tables, with their headings and footnotes, should be typed on separate sheets, numbered with consecutive Roman numerals, and placed after

the Literature Cited. Figure legends should contain enough information to make the figure intelligible separate from the text. Legends should be typed double spaced, with consecutive Arabic numbers, on a separate sheet at the end of the paper. Footnotes should be limited to authors' current addresses, acknowledgments or contribution numbers, and explanation of unusual abbreviations. All such footnotes should appear on the title page. Footnotes are not normally permitted in the body of the text.

5. ***Literature cited.*** In the text, literature should be cited by the Harvard system, with papers by more than two authors cited as Jones *et al.*, 1980. Personal communications and material in preparation or in press should be cited in the text only, with author's initials and institutions, unless the material has been formally accepted and a volume number can be supplied. The list of references following the text should be headed Literature Cited, and must be typed double spaced on separate pages, conforming in punctuation and arrangement to the style of recent issues of *The Biological Bulletin*. Citations should include complete titles and inclusive pagination. Journal abbreviations should normally follow those of the U. S. A. Standards Institute (USASI), as adopted by BIOLOGICAL ABSTRACTS and CHEMICAL ABSTRACTS, with the minor differences set out below. The most generally useful list of biological journal titles is that published each year by BIOLOGICAL ABSTRACTS (BIOSIS List of Serials; the most recent issue). Foreign authors, and others who are accustomed to using THE WORLD LIST OF SCIENTIFIC PERIODICALS, may find a booklet published by the Biological Council of the U.K. (obtainable from the Institute of Biology, 41 Queen's Gate, London, S.W.7, England, U.K.) useful, since it sets out the WORLD LIST abbreviations for most biological journals with notes of the USASI abbreviations where these differ. CHEMICAL ABSTRACTS publishes quarterly supplements of additional abbreviations. The following points of reference style for THE BIOLOGICAL BULLETIN differ from USASI (or modified WORLD LIST) usage:

A. Journal abbreviations, and book titles, all underlined (for *italics*)

B. All components of abbreviations with initial capitals (not as European usage in WORLD LIST *e.g. J Cell. Comp. Physiol.* NOT *J. cell. comp. Physiol.*)

C. *All* abbreviated components must be followed by a period, whole word components *must not* (*i.e. J. Cancer Res.*)

D. Space between all components (*e.g. J Cell. Comp. Physiol.*, not *J Cell Comp.Physiol.*)

E. Unusual words in journal titles should be spelled out in full, rather than employing new abbreviations invented by the author. For example, use *Rit Vísindafjélags Islendinga* without abbreviation.

F. All single word journal titles in full (*e.g. Veliger, Ecology, Brain*).

G. The order of abbreviated components should be the same as the word order of the complete title (*i.e. Proc.* and *Trans.* placed where they appear, not transposed as in some BIOLOGICAL ABSTRACTS listings).

H. A few well-known international journals in their preferred forms rather than WORLD LIST or USASI usage (*e.g. Nature, Science, Evolution* NOT *Nature, Lond., Science, N.Y.; Evolution, Lancaster, Pa.*)

6. ***Reprints, page proofs, and charges.*** Authors receive their first 100 reprints (without covers) free of charge. Additional reprints may be ordered at time of publication and normally will be delivered about two to three months after the issue date. Authors (or delegates for foreign authors) will receive page proofs of articles shortly before publication. They will be charged the current cost of printers' time for corrections to these (other than corrections of printers' or editors' errors). Other than these charges for authors' alterations, *The Biological Bulletin* does not have page charges.

CONTENTS

No. 1, February 1991

BEHAVIOR

DEVELOPMENT AND REPRODUCTION

ECOLOGY AND EVOLUTION

PHYSIOLOGY

No. 2, April 1991

No. 3, June 1991

DEVELOPMENT AND REPRODUCTION

ECOLOGY AND EVOLUTION

ENVIRONMENTAL PHYSIOLOGY

PHYSIOLOGY

RESEARCH NOTE

Reference: *Biol Bull* **180:** 329–331. (June, 1991)

The Rime of the Ancient Scientist

EDWARD A. KRAVITZ*

(With apologies to Coleridge, Tennyson, Gray, Blake, and others too numerous to mention)

Part the First

In which the ancient Scientist detaineth and praiseth his beloved.

It was an ancient Scientist,
And he choseth one of three.
"By thy horned rim glass and balding pate,
Now wherefore choos't thou me?

Yon lobster pot is opened wide
And stuffèd full with kin;
Choose mollusk, moth or fruity fly,
Blood-sucking leech or fishy fin."

He holds him with his skinny hand,
"Biochemist trained was't I;
Thou art the best of all the rest,
I'll give thee reasons why.

Hail to thee most noble of crustaceans!
Worthy of Homaric ode,
Behemoth of a briny deep,
Traveler, of a wet, sandy road.

Photo by Robert Huber

* The author is the *George Packer Berry Professor of Neurobiology at Harvard Medical School, 220 Longwood Avenue, Boston, MA 02115.*

No predator dare match thy might;
Who choose with thee to fight?
No spindly jaws or furry paws
Dare tamper with thy mega-claws.

Along the way, limbs that are lost
Can be replaced, no extra cost.
How practical, how devine;
How cute thou art, how truly fine.

Inventor of contraception! Thou scoff? Thou doubt?
What other creature neatly packs all its sperm cells up in sacs?
Thou matest but once a year, tis true,
But that one time is quite a time!

If after all, one's going to breed,
Why one? Why two? Like lowly man.
Fifty thousand is the plan.
Cute little larval brood
(of course, to mom they're mostly food),
Which also makes good sense, thou see'st,
If mom didn't help by munching some,
The sea woulds't be a lobster slum
With millions and millions of the beasts;
No room for fish, crabs or other feasts.

Is't thy color really red?
Only when thou'rt really dead.

This poem was recited for the first time on November 2, 1989, at the annual meeting of the Society for Neurosciences, in Phoenix, Arizona. The occasion was an Invertebrate Neurobiology social which had as its theme: "Toasts to the Invertebrates." The organizer (M. J. Greenberg) had invited W. B. Kristan, I. Kupfermann, J. G. Hildebrand, and E. A. Kravitz to extol the advantages, utility, and other virtues of their favorite experimental animals, respectively, the leech, the sea slug, the moth, and the lobster. Stirring words were spoken that evening, and emotions ran high. Not one to take a challenge lightly, nor to miss an opportunity to discuss the virtues of other animals (and with a little help from Alice and a college textbook of literature) E. A. Kravitz produced "The Rime."

Greenish brown is more thy hue;
Not a bit like me or you.

Lobster, lobster, cooking red,
Boiling water, seaweed bed;
What happy hand or eye
Dare'st match drawn butter, lemon juice, and lobster pie?

Boiled *Aplysia,* tastes like rubber;
Sauteed leech, makes me shudder!
Marinated *Manduca,* scales for free,
Did he who cooked the lobster, cook thee?

Half a leg, half a leg,
Half a leg onward.
Back to the lobster tank each time
Till 8 or 10 appendages goneward

Thoughtful economical friend!

Nerve cells here, the muscles there,
The hormones all around;
Big cells thou art, and pluckable,
Over and over can'st be found.

Transmitters peptides and the like
For studies fundamental.
O joyous day! Callooh! Callay!
The data're transcendental."

"I fear thee, ancient Scientist!
I fear thy skinny hand."
"Fear not! Fear not! Thou noble beast!
List, while on others, I expand."

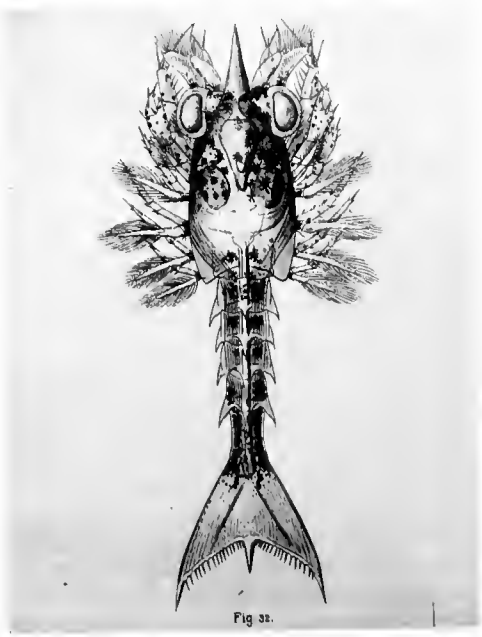

From: Herrick, F. H. 1911. Natural history of the American lobster. Bull. U. S. Eur. Fish. 1909, 29: 149–408.

Part the Second

In which the ancient Scientist compareth lowly beasties to precious lobster.

"First there's *Aplysia;* sea hare 'tis called.
Sea hare? Hare indeed! Some jokester must have been in need
Of immortality for selecting the beast least like the bunny,
Who's really cute and very funny (can'st imagine Bugs *Aplysia?*).

Molluscan mass of pulpy flesh!
Slimy inking shell-less blob!
Learner of Kandelian puzzles that aren't hard:
'Cause what's to train, in a slug without a brain?

But I digress and must continue.

Flies can fly, tis true. So what?
It really doesn't mean a lot:
So can frisbees, jets and kites:
Mostly what flies does is bites .

They're things to trap, and squash, and shoo
With sticky paper, swatters, and fancy kung-fu.
Their names are inelegant, crude and lewd,
Like houseflies, blowflies, horseflies and gnats;
I'd almost rather work with cats.

Their genes are cloned, they are well bred,
I'll grant thee that. But when that's said,
What good are they, these beasts so small?
Their whole brain can set
In one of thy glorious neurons, pet.

Guesseth whom I describeth next!

Eat n'eat n'eat n'eat n'eat n'eat n'eat n'eat,
n'eat n'eat n'eat n'eat n'eat n'eat n'eat n'eat n'molt.

Can'st yet tell? Nay? Then I go on!

Eat n'eat n'eat n'eat n'eat n'eat n'eat n'eat,
n'eat n'eat n'eat n'eat n'eat n'eat n'eat n'eat n'molt.

Art bored yet? Can'st bear more?
I'll spare thee that!

Now twice or thrice more say the same;
It doesn't matter which thee claim.
For now a change! O frabjous day!
Can't hardly wait! Can't barely stay!

Eat, etcetera and molt. And find a hole,
lie around, and turn to goo;
fly away and live a day,
Make 500 more like you.

Most interesting,
Ah, well.
They art a lovely shade of green;
Whilst dull, they're pretty to be seen.

Leeches, locusts, bees and ants

Have their precious sycophants,
Praising that ungainly lot
of vampires, swarms, and crop destroyers,
And fat queens of interest but to voyeurs.

Can'st not thou see thou art the best?
Ne'er another passeth test
Of beauty, wit, charm, intellect, and learning.
Accepteth me, for thee I'm yearning.

Part the Third

The noble beast agreeeth; the ancient Scientist getteth tenure.

"I see thy point old craggy beak;
I fear thee not, no more.
I am so good, its understood
All others but me foreswore.

Collect from my nerves;
Find all my cells;
Inject hormones by the score.
I'll behave for thee, and fight, not flee,
To please thee even more.

I warn thee, though, to leave me not,
Though funding turneth lean.
For if thou doth my chelipeds
Will teareth thee to tiny shreds.
My gastric mill will grind thy bones
Till nothing doth remain.
I'll chomp! I'll chew! I'll eat thee up!
Thou'll never be the same."

"Fear not, fear not, my precious pet,
I'll never leave thee cold.
I am so happy I could dance,
If I could be so bold."

In Xanadu did E A K
A stately lobster-palace plan,
Where Homar, with his next of kin,
In burrows with two entrances in,
Hides from his nemesis, man.

Twilight tolls the knell of parting day,
The blowing winds wind slowly o'er the sea,
The lobstermen homeward plod their weary way,
And leave the world to darkness, and to thee.

Reference: *Biol. Bull.* **180**: 332–345. (June, 1991)

Embryogenesis and Larval Development of the Asteroid *Patiriella regularis* Viewed by Light and Scanning Electron Microscopy

M. BYRNE[1] AND M. F. BARKER

School of Biological Sciences, Zoology A08, University of Sydney, N.S.W. 2006, Australia; and Department of Zoology, University of Otago, Dunedin, New Zealand

Abstract. The sea star *Patiriella regularis* (Verrill, 1867) has indirect development through bipinnaria and brachiolaria larvae. Development of this species is typical of asteroids with planktotrophic larvae and takes 9–10 weeks. The embryos develop through a wrinkled blastula and hatch as early gastrulae. In contrast to most asteroids, a third enterocoel forms on the left side of the stomach of the bipinnaria. This structure gives rise to the left posterior coelom; its significance is discussed. We suggest that this coelom is homologous to the trunk coelom in enteropneust embryology. The surface features of the larvae were examined by scanning electron microscopy. Newly hatched gastrulae are covered by cilia, and the bipinnaria have bands of cilia that follow the contours of the larval processes. A previously undescribed plug-like structure positioned on the post-oral surface appears to function as a seal for the mouth. Brachiolaria larvae have three brachiolar arms and a centrally located adhesive disc. Each arm is covered by adhesive papillae. Raised epithelial cells that dot the surface of the papillae and adhesive disc may be batteries of secretory cells. The brachiolar arms have an extracellular coat that may serve as a protective cover for the adhesive surfaces. Competent brachiolaria swim along the substratum and exhibit searching behavior with flexure of the median brachium. They settle on the undersides of natural shell substrata and do not respond to a primary algal film. Shade appears to be an important factor in settlement and metamorphosis in *P. regularis*. Metamorphosis takes 5–6 days, and the post-larvae take up a free existence at a diameter of 450–500 μm. The indirect development of *P. regularis* contrasts with the lecithotrophic and viviparous modes of development of other *Patiriella* species and provides the comparative basis to determine the ontogenic changes involved with evolution of direct development in the genus. The use of the divergent life histories of *Patiriella* as a model system for the study of evolutionary change in development is discussed.

Received 20 November 1990; accepted 8 March 1991.

[1] Present address: Department of Histology and Embryology, F-13, University of Sydney, N.S.W. 2006.

Introduction

The spinulosan sea star *Patiriella regularis* (Verrill, 1867) is common in New Zealand waters, ranging from the intertidal zone to 100 m depth (Mortensen, 1921; Crump, 1971). This species is a member of the *Patiriella* group of which there are eleven species in the Australia-New Zealand region (Dartnall, 1971; Keough and Dartnall, 1978). A remarkable feature of these asteroids is the diversity of life histories that they exhibit, ranging along a continuum from indirect to direct development (Dartnall, 1971; Lawson-Kerr and Anderson, 1978; Byrne, 1991; Table I). *P. regularis* spawns small eggs and develops indirectly through planktotrophic bipinnaria and brachiolaria larvae (Mortensen, 1921; Crump, 1971). These feeding larvae are typical of the Asteroidea and are considered to be of great antiquity (Strathmann, 1978a). In contrast, all the Australian species examined thus far are direct developers. *P. calcar, P. pseudoexigua,* and *P. gunnii* have large yolky eggs and develop directly through a non-feeding planktonic brachiolaria (Lawson-Kerr and Anderson, 1978; Grice and Lethbridge, 1989; Byrne, 1991; Chen and Chen, 1991). *P. exigua* oviposits large eggs that develop through a modified benthic brachiolaria (Lawson-Kerr and Anderson, 1978; Byrne, 1991). At the end of the indirect-direct continuum of development exhibited

Table I

Life history traits of Patiriella *species from Australia and New Zealand**

Species	Oocyte diameter (mm)	Developmental pattern	Larvae
P. regularis	150	Indirect/planktotrophic	Bipinnaria and brachiolaria
P. gunnii	360	Direct/lecithotrophic	Planktonic brachiolaria
P. calcar	400	Direct/lecithotrophic	Planktonic brachiolaria
P. pseudoexigua	—	Direct/lecithotrophic	Planktonic brachiolaria
P. exigua	400	Direct/lecithotrophic	Benthic brachiolaria
P. vivipara	120	Direct/viviparous	Intraovarian brooder No larva
P. parvivipara	100	Direct/viviparous	Intraovarian brooder No larva

* Data from: Dartnall (1969); Crump (1971); Keough and Dartnall (1978); Lawson-Kerr and Anderson (1978); Byrne (1991); Chen and Chen (1991).

by *Patiriella,* are the intraovarian brooders, *P. vivipara* and *P. parvivipara,* which give birth to crawl-away juveniles (Dartnall, 1969; Chia, 1976; Keough and Dartnall, 1978; Byrne, 1991).

Several nomenclatural systems have been suggested for the diverse developmental patterns in the Asteroidea (Chia, 1968, 1974; Oguro *et al.,* 1976, 1988). In one system, development through a bipinnaria and brachiolaria larvae is termed indirect, whereas development only through a brachiolaria is termed direct (for review, Oguro *et al.,* 1988). This system is most appropriate for *Patiriella.* Other systems make the distinction between indirect-planktotrophic larvae with a functional gut and direct-lecithotrophic larvae without a functional gut (Chia, 1968). The recent finding, however, of an intermediate pattern of asteroid development, through a larva that has both planktotrophic and lecithotrophic features, obscures this distinction (Bosch, 1989).

Comparative embryology of closely related species is a powerful tool for the investigation of developmental processes in evolution because homologous characters can be compared (Raff, 1987). This approach has attracted renewed interest, particularly with respect to echinoids, where recent studies have revealed that direct development arose through heterochronies in the appearance of adult features (Raff, 1987; Wray and Raff, 1989). Heterochronies, changes in the relative timing or rate of ontogenic events, are considered to be an important means of effecting evolutionary change (Anderson, 1987). The range of life histories in *Patiriella* listed in Table I presents an ideal system with which to investigate the modifications involved with the shift to direct development within a monogeneric group. In *P. vivipara,* direct development is achieved by heterochrony in suppression of larval characters and accelerated development of adult features (Byrne, 1991).

In the evolutionary sequence of developmental change in *Patiriella,* the planktotrophic development of *P. regularis* represents the ancestral mode of development in the genus, and, in this investigation, is described in detail. Particular attention is paid to the pattern of larval ciliation and the structure of the larval arms, features often modified in lecithotrophic larvae (Strathmann, 1978a). Settlement behavior and metamorphosis are also described. The ontogeny of *P. regularis* will provide the chronological

Table II

Chronology of development of Patiriella regularis *at 18–22°C*

Time	Stage
0	Fertilization
15–60 s	Elevation of fertilization membrane
40–60 min	First cleavage
1–1.5 h	Second cleavage
2–2.5 h	Third cleavage
3 h	Fourth cleavage
3.5–5 h	Early blastula
6–9 h	Wrinkled blastula
15–17.5 h	Late blastula/early gastrula
25 h	Hatching, gastrula with elongating archenteron
30–35 h	Advanced gastrula, budding of mesenchyme cells from terminal expansion of archenteron
45–55 h	Early bipinnaria, enterocoel and stomodeum formation, archenteron bent towards oral surface to complete gut, the posterior enterocoel starts as a thickening of the left side of the archenteron
55–60 h	Bipinnaria, ciliary bands distinct, gut regions differentiate
65–75 h	Bipinnarial arms well-developed, posterior enterocoel is vesicular, posterior elongation of right and left enterocoels, hydropore open, fusion of left enterocoel with posterior enterocoel
4–5 days	Anterior growth of enterocoels into oral hood and fusion to form the axohydrocoel
6 days	Extension of axohydrocoel into oral hood, right and left enterocoels continue to grow posteriorly, posterior enterocoel forms part of the left posterior coelom, formation of the ventral horn
10–14 days	Advanced bipinnaria, fusion of the ventral horn with the right enterocoel, the axohydrocoel with two lateral extensions for brachia
4–6 weeks	Early brachiolaria, growing brachiolar arms
8 weeks	Advanced brachiolaria, arms and adhesive disc well-developed, five lobes of the hydrocoel present, formation of adult primordium and skeleton
9–10 weeks	Larvae competent to metamorphose

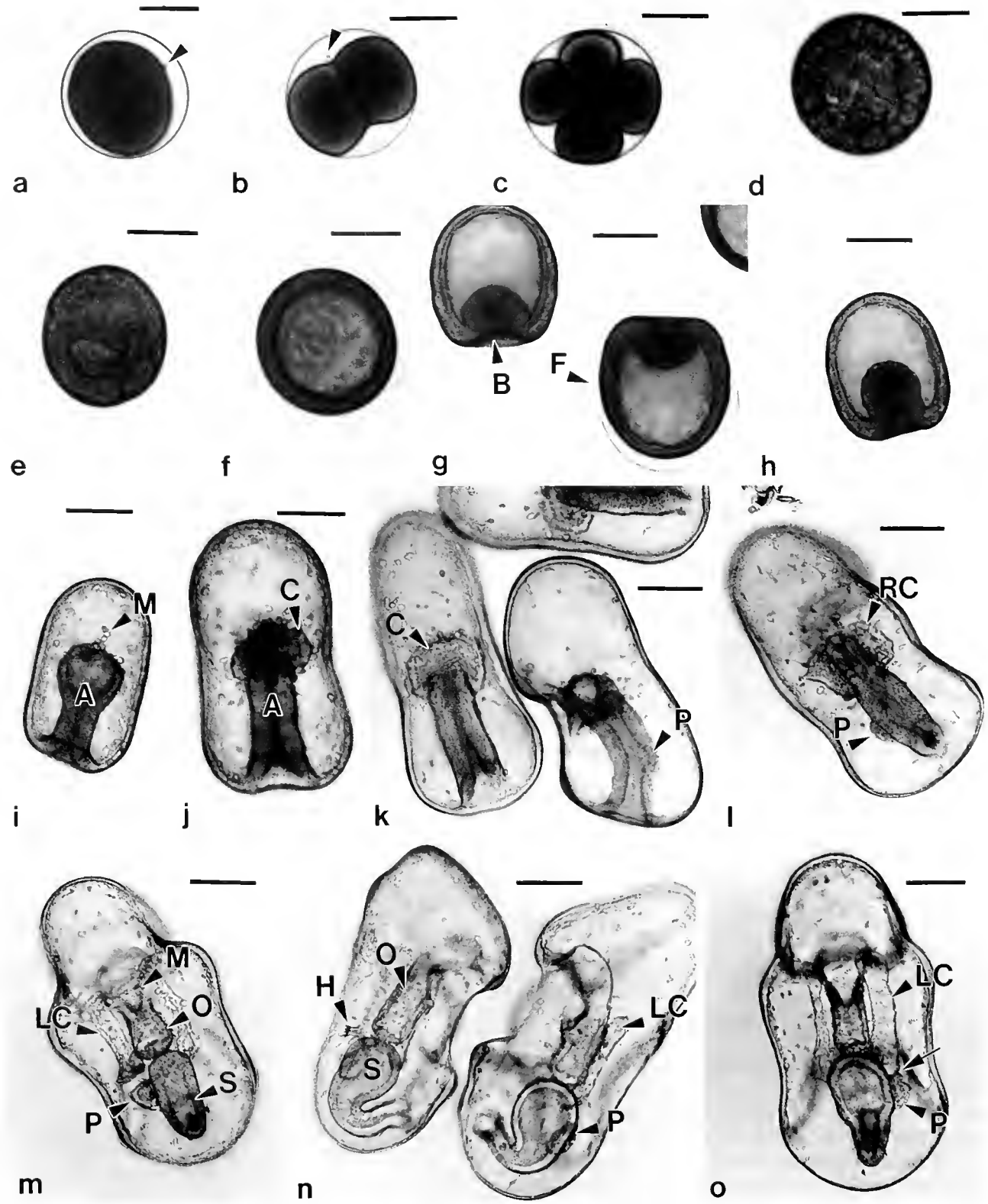

Figure 1. Development through the bipinnaria stage. a. Egg shortly after fertilization with an elevated fertilization membrane and one polar body (arrowhead). b. One hour, first cleavage, two polar bodies are evident (arrowhead). c. One and a half hours, second cleavage. d. Four hours, early blastula. e. Eight hours,wrinkled blastula. f. Sixteen hours, late coeloblastula rotating in membrane. g. Twenty-five hours,

basis required to determine the morphological and heterochronic changes underlying the evolution of direct development within the genus.

Materials and Methods

Specimens of *Patiriella regularis* were collected during slack water at 5–10 m depth from Otago Harbour, New Zealand (45°49.7′S; 170°38.4′E), near the Portobello Marine Laboratory, in January 1990. This species is gonochoric, and ovaries and testes were dissected from mature specimens. The testes were stored dry at 4°C, and the ovaries were placed in a 10^{-5} *M* solution of 1-methyladenine in filtered seawater (Kanatani, 1969). Following ovulation, the ova were transferred to beakers of 1.0 μm filtered seawater and washed gently through several changes of filtered seawater. For fertilization, the eggs were placed approximately one cell deep in 250-ml beakers, and a few drops of diluted sperm were added. After 5–10 min, the eggs were washed in fresh seawater to remove excess sperm, and the fertilized eggs were placed in 5-l beakers of filtered seawater. The cultures were stirred gently by motor-driven paddles. When the embryos attained the swimming gastrula stage, the cultures were filtered and placed in fresh seawater. Thereafter, the seawater in the cultures was changed once a week. Just prior to the early bipinnaria stage, feeding of the larvae commenced. The larvae were fed from unialgal cultures of the flagellate *Dunaliella primolecta* Butcher. The temperature of the culture room ranged from 18° to 22°C.

Embryogenesis and larval development of *Patiriella regularis* were documented by light and scanning electron microscopy (SEM). For SEM, the embryos and larvae were fixed in 2.5% glutaraldehyde in 0.45 μm filtered seawater for 1 h at room temperature. Once the bipinnaria stage was attained, larvae fixed by this method were first relaxed in 6.8% $MgCl_2$ in distilled water before being placed in the primary fixative. Following primary fixation, the specimens were washed in 2.5% sodium bicarbonate (pH 7.2) and post-fixed in 2% OsO_4 in 1.25% sodium bicarbonate for 1 h at room temperature. The specimens were then washed in distilled water and dehydrated in ethanol. After dehydration, the specimens were critical point dried, sputter coated, and viewed with a Joel JSM-35C scanning electron microscope. In addition, the fixation method of Barker (1978a) was also used. According to this method, larvae placed in a small drop of seawater were initially fixed by the addition of Bouin's fluid. The larvae were then transferred to 3% glutaraldehyde in 0.2 *M* cacodylate buffer for 1 h at room temperature. Following a rinse in the same buffer, the specimens were post-fixed in 2% OsO_4 in cacodylate buffer. Although the introduction of Bouin's caused the larvae to contract slightly, this method resulted in good preservation of the extracellular coat of the larvae. After fixation, the larvae were rinsed in distilled water and processed as described above.

Results

Spawning

Spawning of *Patiriella regularis* was observed *in situ* on 25 January 1990. Approximately 20 individuals, both males and females, were observed releasing gametes. The sperm exited from the gonopores as a narrow plume that dissipated 5–10 cm above the spawning individual. For the females, the eggs rolled on to the aboral surface after exiting from the gonopore. The shortest distance between spawning individuals ranged from 0.5 to 1.0 m, while the longest distance ranged from 4 to 5 m. These observations were recorded during the day under sunlit conditions and coincided with slack water.

In the laboratory, the ovaries of *Patiriella regularis* exhibited a long hormone-dependent period. It took 3–5 h before oocyte maturation; ovulation and spawning was induced by 1-methyladenine. The spawned ova were green and 150 μm in diameter (±9 μm; n = 20).

Embryogenesis

The chronology of the development of *Patiriella regularis* is outlined in Table II. A fertilization membrane forms 15–60 s after the introduction of sperm into the beakers containing ova, and the two polar bodies are given off within 20 min (Fig. 1a, b). Cleavage is radial and ho-

hatching gastrulae. B, blastopore; F, fertilization membrane. h. Twenty-five hours, swimming gastrula. i. Thirty-five hours, advanced gastrula, mesenchyme cells (M) are budding off into the blastocoel. A, archenteron. j. Fourty-five hours, early bipinnaria, right and left enterocoels are starting to form (C). A, archenteron. k. Fourty-seven hours, bipinnaria, enterocoels are forming (C), archenteron is complete. A small bulge on the archenteron is the beginning of the posterior enterocoel (P). l. Fifty-five hours, the right (RC) and left enterocoels grow posteriorly. On the left side of the achenteron, a small group of cells form the posterior enterocoel (P). m. Seventy hours, dorsal view. LC, left enterocoels; M, mouth; P, posterior enterocoel; O, oesophagus; S, stomach. n. Seventy hours, bipinnaria in side view, gut regions and hydropore (H) are evident. LC, left anterior enterocoel; O, oesophagus; P, posterior enterocoel; S, stomach. o. Seventy-five hours, ventral view. The arrow points to the fusing left anterior (LC) and posterior (P) enterocoels. The right and left anterior enterocoels have started to grow into the oral hood. Scale bars = 100 μm.

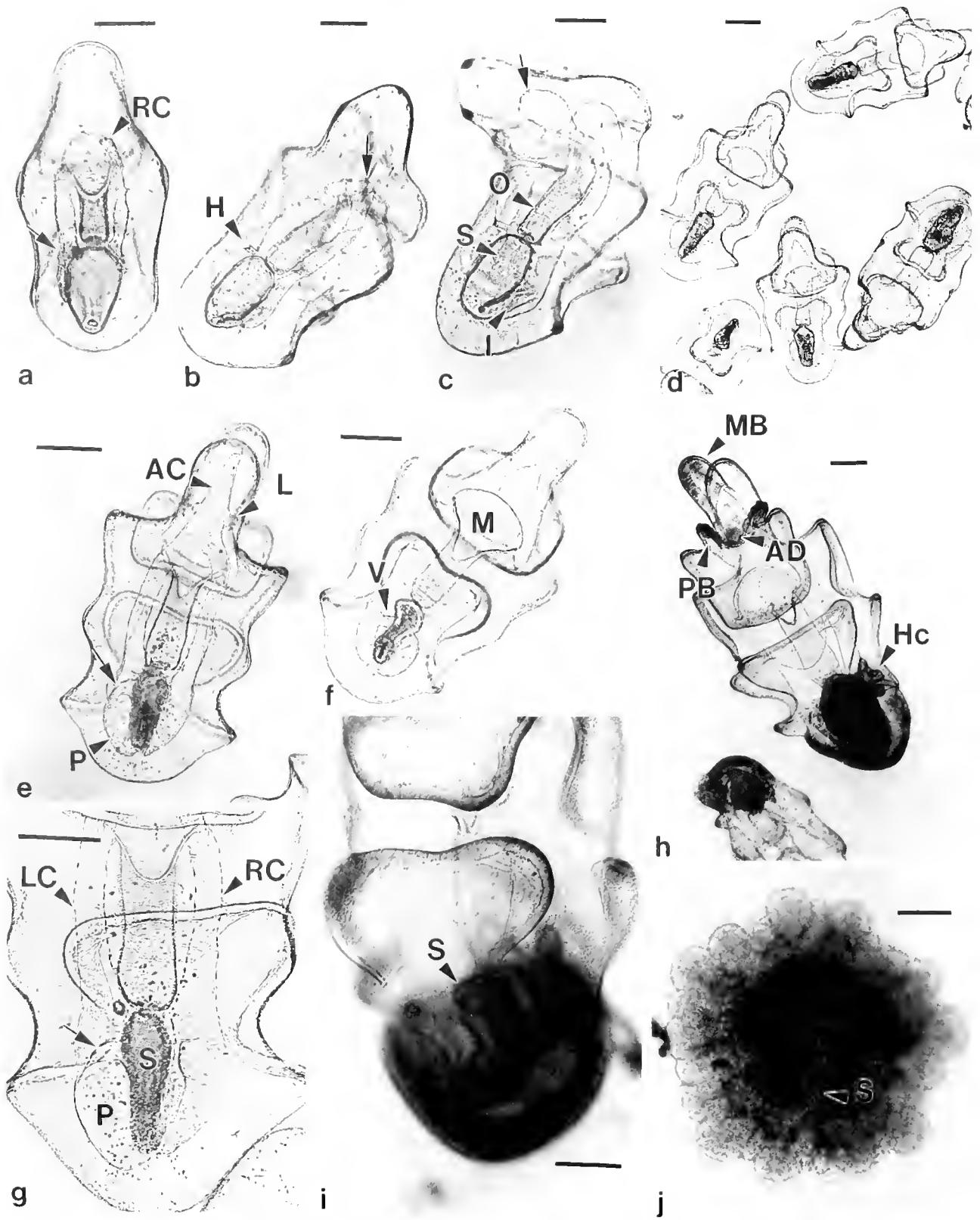

Figure 2. Development through metamorphosis. a. Eighty-eight hours, dorsal view. Growth of the right enterocoel (RC) into the oral hood. At the position where the two left enterocoels have met, tissue derived from fusion of their end walls is evident (arrow). b. Four and a half days, side view of a bipinnaria showing

loblastic (Fig. 1b–d). The first cell division occurs 40–60 min after fertilization, and the early blastula stage is reached witnin 4 h. By 4 h, asynchrony was evident in all cultures, with some embryos at a more advanced stage than others. Five hours post-fertilization, the embryos are well-developed blastulae 164 μm in diameter (±7 μm; n = 10) (Fig. 1d). The blastulae rotate within their close-fitting fertilization membranes, propelled by their ciliary covering. Blastular wrinkling starts 6 h after fertilization with folding of the blastoderm into the blastocoel. The furrows of the wrinkled blastulae are most apparent in 8-h larvae (Fig. 1e). Subsequently, the furrows smooth out and 18-h cultures contain late blastulae with a smooth surface and early gastrulae (Fig. 1f, g). Hatching ensues through rupture of the fertilization membrane, and the gastrulae become free-swimming larvae (Fig. 1g, h). At hatching, the larvae are round to elongate and have a shallow blastopore. They continue to elongate with growth of the archenteron into the blastocoel. The blind end of the archenteron expands and mesenchyme cells detach from its tip, moving into the blastocoel (Fig. 1i). At this stage, the larvae are 197 μm long (±1.2 μm, n = 10).

Early bipinnaria are present by the end of the second day. The right and left enterocoels form as pouches off the expanded tip of the archenteron (Fig. 1j). A shallow stomodeum is present, and the blind end of the archenteron bends towards the oral surface. During this stage, the posterior region bends ventrally, and from this time the blastopore can be regarded as the larval anus. By 55 h, the archenteron fuses with the stomodeal invagination, thereby completing the larval gut (Fig. 1k). With development of the ciliated bands, algal food was introduced into the cultures. The larvae now have a distinct peroral hood region. In addition, a shallow evagination, destined to form the posterior enterocoel, is evident on the left-hand wall of the archenteron; this soon grows to form a small thickening of cells (Fig. 1k, l).

By the end of the third day, the bipinnaria are feeding and have well-defined pre- and postoral ciliary bands. At this stage, the bipinnarial processes—lateral and anterior projections of the larval body wall—start to form. The regions of the gut differentiate with the expansion of the stomach and the separation of the stomach from the oesophagus by the cardiac sphincter (Fig. 1m). In three-day-old bipinnaria, the right and left enterocoels increase in length as they grow posteriorly, and the hydropore exits on the dorsal surface (Fig. 1n). During the fourth day of development, the small thickening on the archenteron wall grows to form a solid ball of cells attached to the stomach. A central cavity forms in this structure, thereby forming a posterior enterocoel on the left side of the larvae (Fig. 1n, o). This posterior enterocoel increases in size and is a conspicuous feature of all the larvae examined from five different cultures. When the advancing left anterior enterocoel reaches the posterior enterocoel, the two enterocoels fuse (Figs. 1o, 2a). In some larvae, fusion of the two left coelomic pouches was complete 75 h after fertilization. With subsequent development, it was evident that the posterior enterocoel forms part, if not all, of the left posterior coelom. Where the two enterocoels meet, a partition derived from fusion of their tissues forms (Fig. 2e, g). During the fourth day of development, the right and left enterocoels extend anteriorly into the oral hood (Figs. 1o, 2a). The larval length is now 630 μm (±5.8 μm; n = 10).

In 4.5 day larvae, the anterior extensions of the right and left enterocoels fuse to form the axohydrocoel in the oral hood (Fig. 2b). This anterior coelom grows to form an extension into the hood where the median-dorsal process develops (Fig. 2c–e). Five-day-old larvae are well-developed bipinnaria and the ciliary tracts increase in length following the edges of the bipinnarial processes. The bipinnaria exhibit muscular movements including contraction of the cardiac sphincter and dorsal and ventral flexure of the oral hood, which results in broadening and closure of the oral cavity (Fig. 2c). Internally, the fused left enterocoels extend below the gut, while growth of the right enterocoel is slower. The partition derived from fusion of the two left enterocoels divides the left enterocoel into anterior and posterior regions (Fig. 2e, g). Partition

---

the anterior coelom (arrow) in the oral hood formed through fusion of the right and left enterocoels. H, hydropore. c. Six days, bipinnaria from the side, exhibiting dorsal flexure, the anterior coelom has grown into the oral hood (arrow). I, intestine, O, oesophagus, S, stomach. d. Four-week-old culture containing late bipinnaria. e. Ten days, dorsal view, late bipinnaria/early brachiolaria. The anterior coelom (AC) has grown to form the lumen of the future median brachium, two small lateral branches at the base of this coelom (L) are destined to be the coelomic lumina of the posterior brachia. The left posterior enterocoel (P) has grown below the gut. A septum-like structure (arrow), partitions the left coelom into anterior and posterior sections. f. Four weeks, ventral view, early brachiolaria, the ventral horn (V) of the left posterior coelom has grown around the gut and fused with the right enterocoel. M, mouth. g. Four weeks, detail of the septum (arrow) dividing the left anterior (LC) and posterior coelom (P). RC, right enterocoel, S, stomach. h. Eight weeks, ventral view, late brachiolaria, the median (MB) and posterior (PB) brachia and the adhesive disc (AD) are well-developed. The lobes of the hydrocoel (Hc) are evident. i. Eight weeks, ventral view, adult primordium of a late brachiolaria, primary spicules (S) lie along the lobes of the hydrocoel. j. Nine weeks, metamorphosing larva from the aboral surface. S, skeleton. Scale bars: a,h,c,g,i,j = 100 μm. Scale bars: d,e,f,h; = 150 μm.

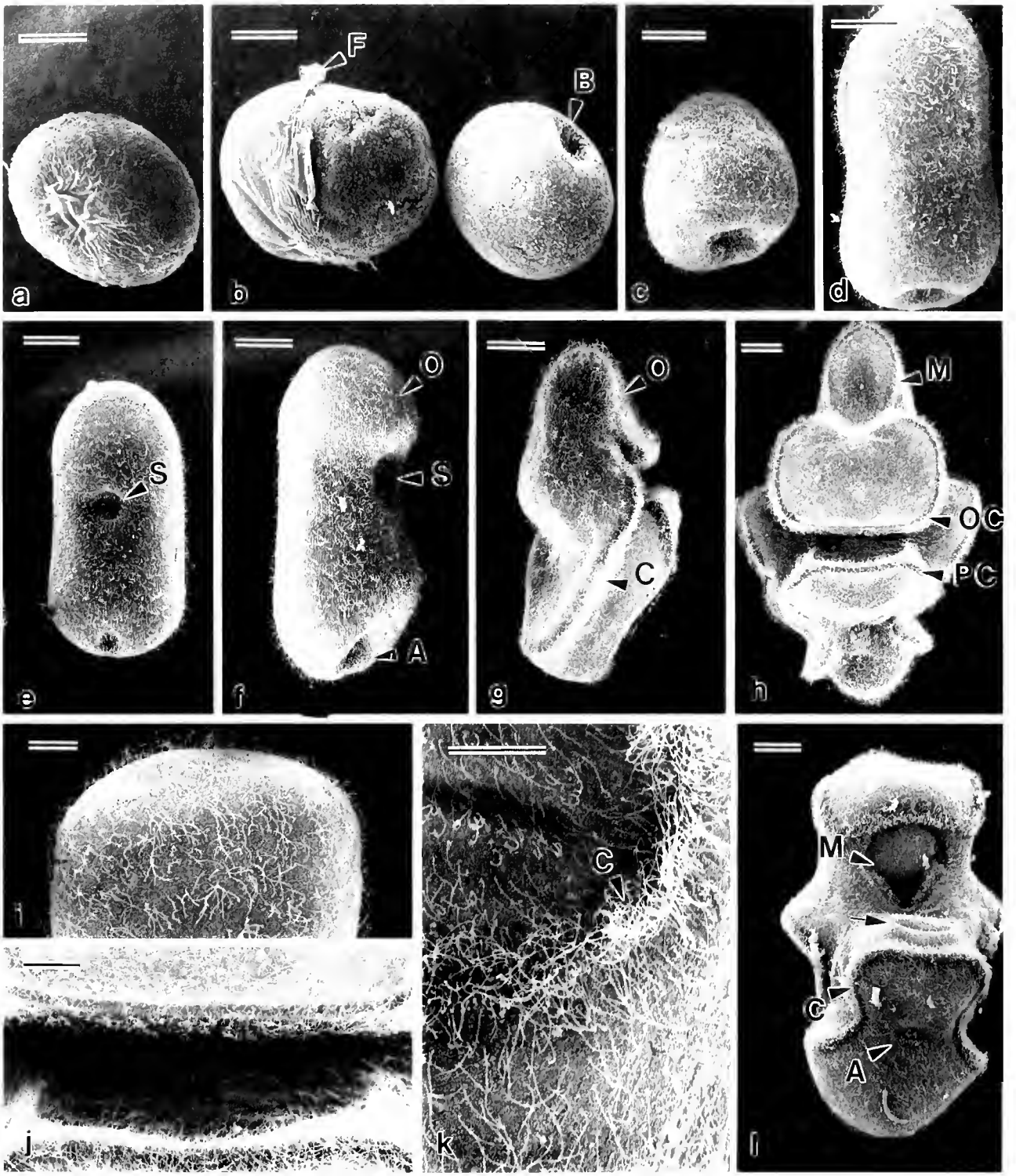

Figure 3. SEM of development through the bipinnaria stage. a. Late blastula within the fertilization membrane. b. Hatching and newly hatched gastrulae. B, blastopore; F, fertilization membrane. c. Gastrula starting to elongate. d. Elongate gastrula. e. Early bipinnaria forming the stomodeal invagination (S). f. Bipinnarial shape starting to develop, the stomodeum (S) has enlarged and the blastopore has moved to a ventral position to form the anus (A). O, forming oral hood. g. Bipinnaria side view with a distinct oral hood (O) and ciliary tracts (C). h. Late bipinnaria ventral view with oral- (OC) and postoral (PC) ciliary tracts. M, mouth. i. Ciliary field covering gastrula. j. Detail of bipinnaria in Figure 3h, showing the ciliary tracts around mouth and scattered cilia covering the larva. k. Ciliary tract (C) of a bipinnaria. l. Bipinnaria fixed in the dorsally-flexed position showing the plug-like structure on the post-oral surface (arrow). A, anus; M, mouth; C, ciliary tract. Scales: Fig. 3a–h, l = 50 μm; Fig. 3i–k = 20 μm.

of the right enterocoel was not observed. By day 6, the ventral horn of the left posterior coelom forms and extends between the stomach and the intestine. Eight-day-old larvae are 790 μm in length (±85 μm; n = 20).

Ten-day-old larvae are advanced bipinnaria (length, 990 ± 150 μm; n = 20). By day 14, the ventral horn completes its growth fusing with the right enterocoel (Fig. 2f). In the preoral hood, the coelom extends anteriorly beyond the median-dorsal process, forming the lumen of the future median brachiolar arm. At the base of the median-dorsal process, the anterior coelom gives rise to two lateral extensions destined to be the coelomic lumina of the posterior brachiolar arms (Fig. 2e).

The larvae grow as advanced bipinnaria through the first month of development. By week five, early brachiolaria are present with three brachiolar arms or brachia. The longest brachium extends from the median-dorsal process and contains the main branch of the anterior coelom. On either side are two small brachia into which the lateral coelomic extensions grow. Each of these brachiolar arms are contractile. Advanced brachiolaria were present in eight-week-old cultures (Fig. 2h). These larvae have a well-developed brachiolar complex comprised of the three brachia and a centrally located adhesive disc. The adult primordium develops the posterior region of the brachiolaria (Fig. 2h, i). On the left side of the larvae, the five lobes of the hydrocoel are evident (Fig. 2h). The first adult spicules form as small rods positioned along each lobe of the hydrocoel (Fig. 2i). By week nine, the larvae were competent to metamorphose at a length of 1430 μm (±194 μm; n = 20). This appears to be the upper growth limit of the larvae, as three-month-old brachiolaria were similar in length.

Metamorphosis

Advanced brachiolaria extend their arms and attach them to the bottom of the culture dishes in what appears to be searching behavior. The large median brachium bends at a 90° angle to the larval body, bringing the two posterior brachia and the adhesive disc into contact with the substratum. The larva then adhere temporarily to the bottom of the dish by means of the arm and then detach and continue swimming. To induce metamorphosis, glass slides with a primary algal film or natural shell substrata were placed in finger bowls, and competent larvae were introduced. The brachiolaria did not respond to the slides, but attached to the undersurfaces of the shells within a few hours of introduction. During temporary attachment, larvae moved over the surface of the substratum and exhibited searching behavior, with the brachiolar arms attaching and detaching as the larvae "walked" over the substratum. Following this exploratory phase, the larvae ceased to move, attached permanently with their brachia and adhesive disc, and started to metamorphose. During metamorphosis, the larval body is shortened and resorbed to a thin stalk. The adult primordium develops with formation of a pentamerous shape. The hydrocoel expands, and the first adult tube feet form on the oral surface. These tube feet are used for attachment and locomotion. Eventually, the post-larvae break free of their attachment stalks taking up an independent existence at a diameter of 450–500 μm five to six days after settlement (Fig. 2j). Development continues with completion of the adult digestive tract. Newly detached post-larvae do not have a mouth or an anus.

Scanning electron microscopy

Examination of the surface of hatching gastrulae of *Patiriella regularis* shows that they are covered by a uniform field of cilia (Fig. 3b). The wrinkled appearance of the fertilization membrane is probably due to the collapse of the membrane during fixation and drying (Fig. 3a, b). On hatching, the gastrulae start to elongate (Fig. 3b–d, i). With the development of the bipinnaria, pre- and postoral portions of the larvae are evident with a slight depression between them where the stomodeal invagination arises (Fig. 3e, f). As the larvae grow, the bipinnarial processes and the pre- and postoral ciliary tracts form (Fig. 3g, h). These tracts, a conspicuous feature of the larvae, are sinuous ridges of dense cilia that follow the contours of the bipinnarial processes (Fig. 3j, k). In addition to the ciliary tracts, the bipinnaria are also covered by a uniform field of cilia (Fig. 3j, k). Bipinnaria preserved in the dorsally flexed position reveal the presence of a plug-like structure on the postoral surface (Fig. 3l). On contraction of the larva, this structure would function as a seal over the mouth.

Formation of the brachiolar complex is evident with the appearance of the median brachiolar arm and two small lateral projections (Fig. 4a). Ridges on the median arm are developing papillae (Fig. 4a). In advanced brachiolaria, the arms take on their distinctive shape and are covered by adhesive papillae (Fig. 4b, c). An adhesive disc is positioned at the base of the arms (Fig. 5a). Like the bipinnaria, the brachiolaria has ciliary tracts and is covered by cilia (Fig. 4b, c). In addition to the preoral ciliary tract on the median-dorsal process, a lateral ciliary tract is present along the median brachium (Fig. 4b, i, j).

Preservation of the brachiolaria larvae differed with the two fixation methods used. An external coat covers the adhesive surface of the arms of brachiolaria fixed with the Bouin's method (Fig. 4a–j), whereas this coat is not present in larvae fixed with the glutaraldehyde-seawater method (Fig. 5a–h). The coat is a thin mesh-like material on the surface of the brachia that gives the arms a smooth appearance (Fig. 4b–j). Due to contraction of the larvae, it

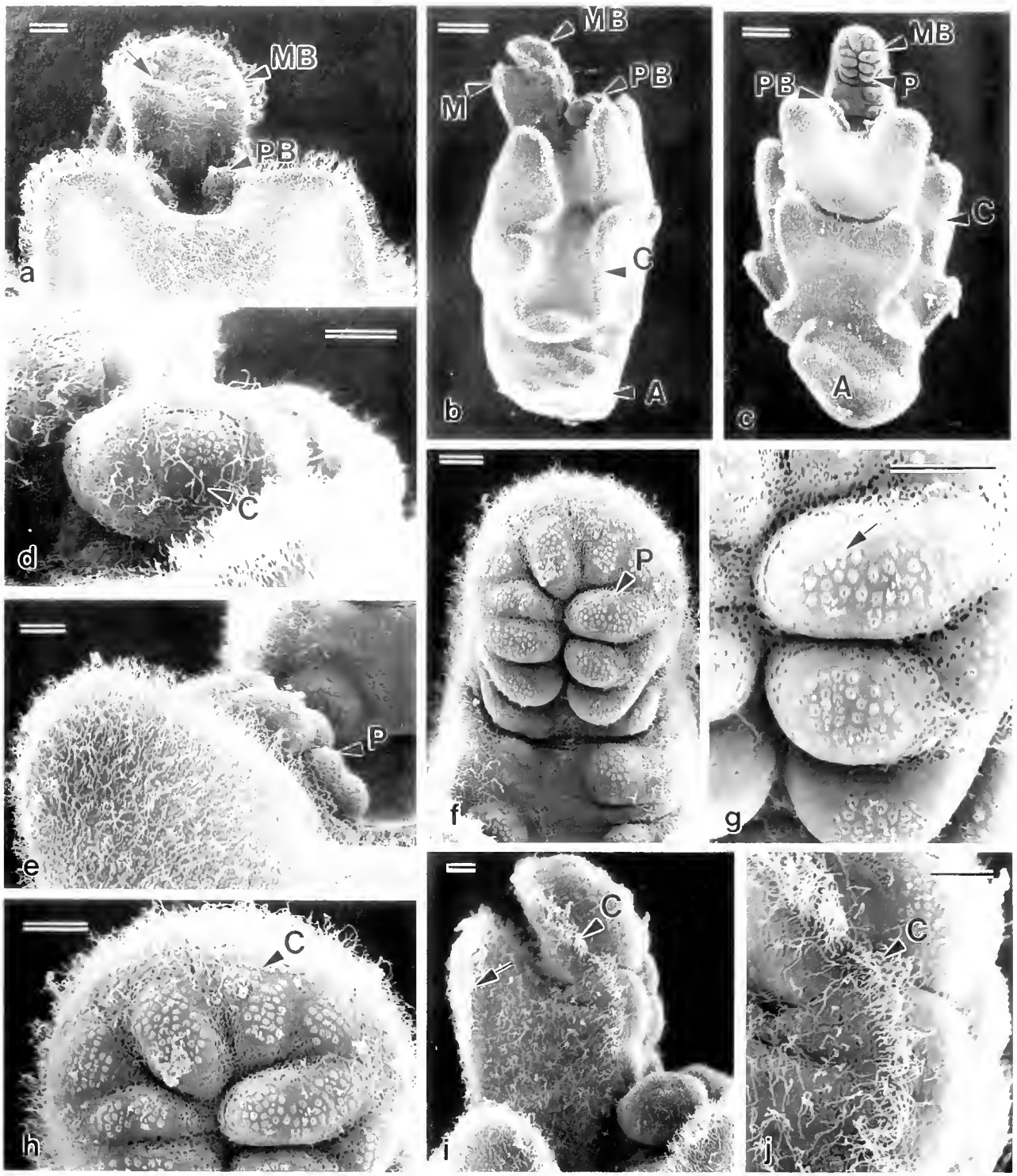

Figure 4. SEM of development through the brachiolaria stage of larvae fixed initially with Bouin's. a. Early brachiolaria. The two posterior arms (PB) are starting to form at the base of the median brachium (MB). Ridges (arrow) on the surface of the median brachium are developing papillae. b. Brachiolaria side view. The median brachium (MB) emerges from the median-dorsal process (M) and the posterior brachia (PB). A, developing adult primordium; C, ciliary tract. c. Late brachiolaria ventral view. Note the smooth surface of the median brachium (MB), which has two rows of papillae (P), and the cilia covering of the larva. The adult primordial (A) region is evident posteriorly. PB, posterior brachium. d. Detail of the brachiolaria shown in Figure 2b. The posterior brachium has a smooth extracellular coat through which cilia (C) emerge. e. Detail of the advanced brachiolaria shown in Figure 2c showing the posterior brachium and

is not possible to determine whether the adhesive disc has an extracellular covering. The rest of the brachiolar surface does not have this coat (Fig. 4b–j).

The removal of the extracellular coat by the glutaraldehyde-seawater method reveals the underlying structure of the brachiolar complex (Fig. 5a–g). Papillae cover the brachia down to their bases and surround the adhesive disc (Fig. 5a, b). The median brachium is considerably longer than the other two and has 9–16 papillae arranged in two rows. A cluster of papillae covers the surface of the posterior arms (Fig. 5c). Nodular arrays of raised epithelial cells dot the surface of the papillae (Fig. 5b,d–f). In side-view, these nodules are raised structures that have a fuzzy tip, probably comprised of microvilli (Fig. 5e). In brachiolaria with an intact extracellular coat, small elevations of the coat indicate the position of the underlying nodules (Fig. 4g, h). Cilia on and around the papillae occasionally protrude through the glycocalyx (Figs. 4d, h; 5d, e). The adhesive disc is a round, flat structure with raised epithelial cells similar to those seen on the papillae (Fig. 5b, g). In larvae fixed with the glutaraldehyde-seawater method, smooth patches of material apparently secreted by the papillae are evident on the surface of the brachia (Fig. 5c).

Competent brachiolaria have a distinct adult rudiment at the posterior end of the larvae and scattered cilia cover the future aboral surface (Fig. 5h). The reduction of the larval body to a thin attachment stalk is shown in the whispy tissue attached to the metamorphosing larva in Figure 5i. Post-larvae have two pairs of tube feet per arm, and cilia are present on the epidermis (Fig. 5j).

Discussion

Development of *Patiriella regularis* is similar to other asteroids that develop indirectly through planktotrophic bipinnaria and brachiolaria larvae (Dan, 1968; Strathmann, 1987). The bipinnarial processes of *P. regularis* larvae, characteristic of spinulosan asteroids, are relatively short in comparison with those of forcipulate larvae, which develop into long and slender extensions of the larval body (Gemmill, 1914; Strathmann, 1971; Barker, 1978b).

The wrinkled blastula has been widely reported in asteroid embryology for both indirect and direct developers (Mortensen, 1921; Chia, 1968; Komatsu, 1972, 1976; Oguro *et al.*, 1976; Byrne, 1991). A wrinkled blastula occurs in *Patiriella regularis*, which has small eggs, and it also occurs in the Australian species, *P. exigua*, *P. calcar*, and *P. gunnii*, which have large ova 350–400 μm in diameter (Lawson-Kerr and Anderson, 1978; Byrne, 1991). Blastular wrinkling in each of these *Patiriella* species results from the folding of the blastoderm into the blastocoel with subsequent smoothing out at the advanced blastula stage (Lawson-Kerr and Anderson, 1978; Byrne, 1991). In echinoids, wrinkled blastulae are only reported in species with large eggs (Williams and Anderson, 1975; Amemiya and Tsuchiya, 1979; Raff, 1987; Parks *et al.*, 1989), and the wrinkled blastula may be a consequence of the shift from indirect to direct development (Raff, 1987; Parks *et al.*, 1989). There is no evidence of a relationship between blastular wrinkling and egg size in asteroids, and infolding of the blastoderm may be associated with the mechanics of cleavage (Anderson, pers. comm.). Up to the early blastula stage, cleavage gives rise to large cuboidal blastomeres held within a close-fitting fertilization membrane. As development continues, the embryo may not be able to accommodate additional cuboidal cells in a spherical shape due to insufficient space within the fertilization membrane, resulting in the onset of wrinkling. In asteroids and echinoids that have a wrinkled blastula in their development, smoothing of advanced blastula corresponds with the transition from a cuboidal to a columnar blastomere organization (Parks *et al.*, 1989; Byrne, pers. obs.). Compared with cuboidal blastomeres, this columnar organization may be more readily accommodated in a spherical shape. But not all asteroids have a wrinkled blastula (Dan, 1968; Strathmann, 1987), and for these species, the spatial relationship between the blastular surface and the fertilization membrane during the cuboidal-columnar transition should be documented. Recent work suggests that wrinkling of lecithotrophic echinoid embryos may also be a mechanical phenomenon (Henry, pers. comm.).

The posterior enterocoel that forms on the left side of the archenteron in the early bipinnaria of *Patiriella regularis* is not a general feature of asteroid embryology (Dan, 1968; Strathmann, 1987). Homologous structures are reported in the bipinnaria of *Asterias rubens* and *Marthasterias glacialis*, where similar masses of cells may arise on the right or left side of the archenteron (Gemmill,

papillae (P).The arm has an extracellular coat that gives it a smooth appearance. f. Median brachium and papillae (P). The arm has an extracellular coat that gives it a smooth appearance. g. Detail of the papillae of the medium brachium and the smooth mesh-like extracellular coat. Raised bumps on the papillae (arrow) indicate the position of underlying raised epithelial cells (see Fig. 5b). h. Papillae at the tip of the median brachium with cilia (C) emerging through the surface coat. i. Anterior portion of brachiolaria shown in Figure 2b, showing the pre-oral ciliary tract on the median dorsal process (arrow) and the ciliary tract (C) on the median brachium. j. Detail of the ciliary tract (C) along the median brachium. Scales: Fig. 4a, d–j = 20 μm; Fig. 4b, c = 100 μm.

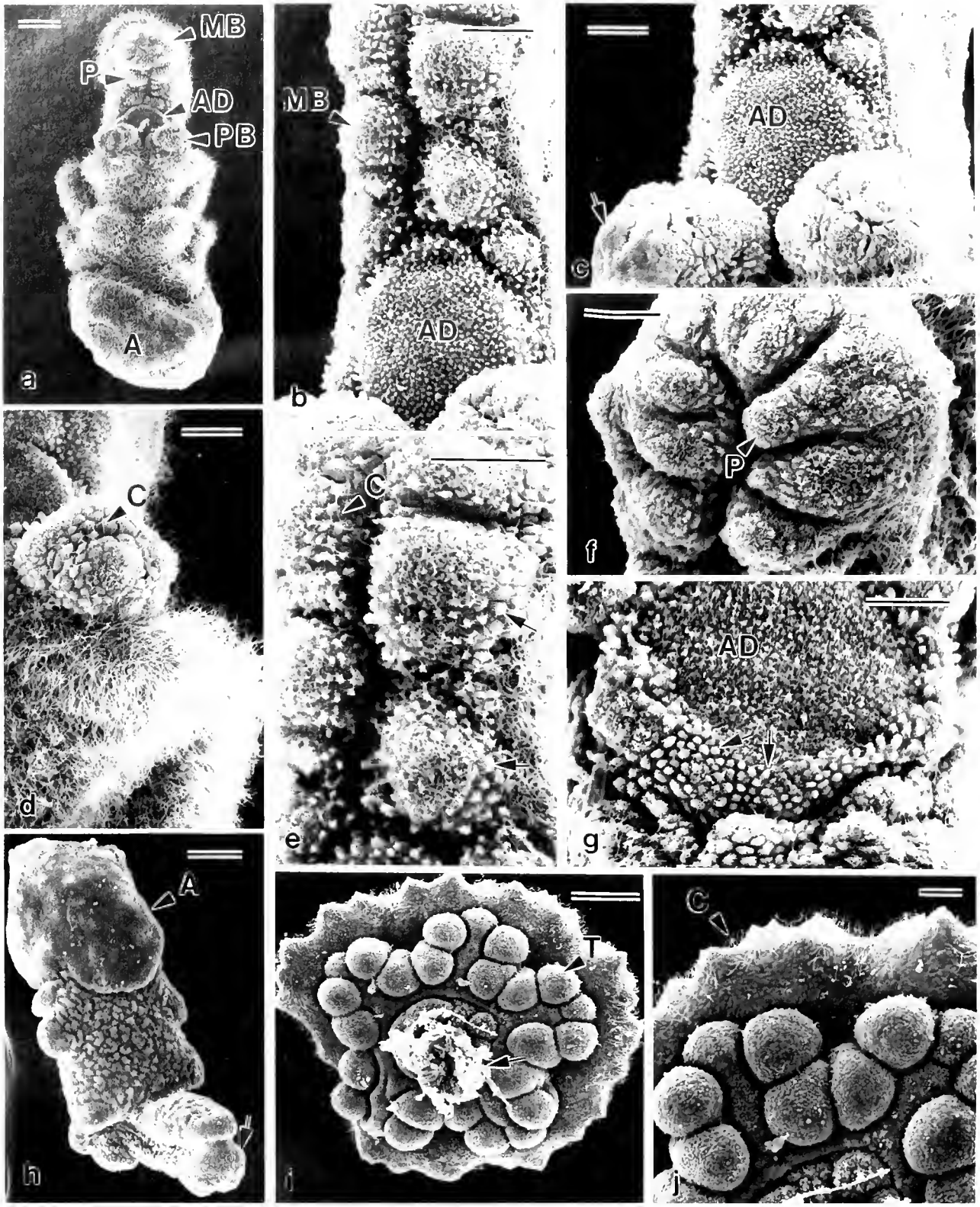

Figure 5. SEM of development through metamorphosis of larvae fixed by the glutaraldehyde-seawater method. a. Brachiolaria ventral view. Note the median (MB) and posterior brachia (PB) and the adhesive disc (AD). Cilia cover the larva, and the adult primordium is evident posteriorly (A). b. Median brachium (MB) with two rows of papillae. Note the absence of an extracellular coat. The papillae and adhesive disc (AD) are dotted by raised epithelial cells. c. Posterior brachium with a patch of secreted material on its surface (arrow). AD, Adhesive disc. d. Detail of the brachiolaria shown in Figure 5a. Cilia cover the larva and are also present on and around the papillae (C). Note the absence of an extracellular coat on the posterior

1914). In these species, this cell mass detaches from the gut and either breaks up into mesoderm or fuses with the advancing right or left enterocoel; in *M. glacialis* a central cavity occasionally forms (Gemmill, 1914). A similar situation to that seen in *P. regularis* occurs in the other asterinid species *Asterina miniata* and *A. pectinifera* (Heath, 1917; Newman, 1925; Komatsu, pers. comm.). As in *P. regularis*, a posterior enterocoelic growth arises on the left side of the archenteron of *A. miniata* and *A. pectinifera*, forming a third enterocoel that fuses with the anterior left enterocoel (Heath, 1917; Newman, 1925). In *P. regularis* and *A. miniata*, the posterior enterocoel is a functionally important structure that grows during development and gives rise to the posterior coelom (Newman, 1925). This contrasts with typical asteroid development, where the posterior coelom is derived from partition of the left anterior enterocoel (Gemmill, 1914; Dan, 1968; Strathmann, 1987). There is speculation as to the significance of the presence of a posterior enterocoelic growth and a third enterocoel (Gemmill, 1914; Heath, 1917; Newman, 1925). In the development of *A. miniata*, Newman (1925) considered the posterior enterocoel to be a vestigial feature. Gemmill (1914) and Heath (1917) considered the thickening of the archenteron wall in some asteroids, and the third enterocoel in others, to be rudiments of a posterior coelom present in the larvae of a common enteropneust-echinoderm ancestor. Thus, as suggested by Gemmill (1914), the posterior enterocoel of *P. regularis* may be homologous to the trunk coelom in enteropneust embryology.

The plug-like structure on the post-oral surface of the bipinnaria of *Patiriella regularis* has not been described before. This structure is evident only in bipinnaria fixed in the dorsally flexed posture and appears to serve as a seal for the mouth on ventral contraction of the larvae. In this manner it may function as a mechanism to prevent undesirable particles from entering the mouth. It was not seen in live specimens examined with the light microscope. Although this mouth seal has not been reported in the bipinnaria of other asteroids, its presence may be revealed by scanning electron microscopy.

The ultrastructure of the brachiolar complex has been described for the forcipulate asteroids *Stichaster australis* and *Coscinasterias calamaria* (Barker, 1978a). In comparison with these species, the median brachiolar arm of *Patiriella regularis* is well-supplied with adhesive papillae. In *S. australis* and *C. calamaria*, adhesive papillae are limited to the tip of the brachia, and the stem of the median brachium is smooth (Barker, 1978a). Like the brachiolaria of these species, cilia are also present on the papillae of *P. regularis* and may have a sensory role in the location of suitable substrata for settlement (Barker, 1978a). The raised epithelial nodules on the brachial papillae and adhesive disc of *P. regularis* appear to correspond to the batteries of secretory cells revealed by transmission electron microscopy of the brachiolar complex of *S. australis* and *C. calamaria* (Barker, 1978a).

Temporary attachment of *P. regularis* brachiolaria is achieved by the median brachium as it extends over substratum, assisted by adhesion of the posterior arms. The patches of smooth material on the brachia may be used for adhesion. For *P. regularis*, as reported for *S. australis* and *C. calamaria* (Barker, 1978a), it appears that permanent attachment is achieved by secretion of a cement-like material by the adhesive disc. Early descriptions of brachiolaria refer to the attachment disc as a 'sucker' because it was thought to effect attachment by means of suction with the edge of the disc forming a seal (Gemmill, 1914; Mortensen, 1921).

The difference in preservation of the brachiolaria by the two fixation methods is striking. Brachiolaria fixed initially with Bouin's fluid have a glycocalyx-like material covering their brachia, whereas larvae fixed with the glutaraldehyde-seawater method do not. Removal of surface coats by conventional fixation methods is reported for several echinoderms (Cameron and Holland, 1983; McKenzie, 1987). An extracellular coat similar to that on the brachiolar complex of *P. regularis* is present on the larvae of *Asterina miniata* (Cameron and Holland, 1983). In *A. miniata*, however, this coat covers the entire surface of the larva (Cameron and Holland, 1983). The preservation of a glycocalyx on the brachia, but not on the rest of the larval surface of *P. regularis*, suggests that it may function in association with the brachiolar complex as a protective covering for the attachment surface.

The searching behavior, settlement, and metamorphosis of *Patiriella regularis* is characteristic of asteroid brachiolaria (Gemmill, 1914; Barker, 1977). In contrast to that reported for *Coscinasterias calamaria*, the presence of a primary algal film is not sufficient to induce metamorphosis of *P. regularis* (Barker, 1977). The attachment and metamorphosis of the brachiolaria on the undersides of

brachium. e. Detail of the median brachium showing raised epithelial cells (arrows) on the papillar surface. Cilia are present on and around the papillae (C). f. Papillae (P) at the tip of the median brachium. g. Adhesive disc (AD), the arrows point to raised epithelial cells. h. Late brachiolaria ventral view. The larva is in the exploratory/attachment posture with the median brachium extended 90° to the larval body (arrow). A, adult primordium. i. Metamorphosing larva detached from its stalk, which appears as wispy material (arrow). Two pairs of tube feet (T) are present in each radius. j. Detail of the metamorphosing larva. The future adult surface is covered by cilia (C). Scales: Fig. 5a, h, i = 50 mm; Fig. 5b–g, j = 20 mm.

shells and not on the film-covered slides, suggests that shade and a rough-textured surface may be an important factor in selecting a site for metamorphosis in this species. Crump (1969) also reported attachment and metamorphosis of *P. regularis* brachiolaria on the undersides of introduced substrata.

The observation of simultaneous spawning of male and female *Patiriella regularis* in the field is similar to that reported for several asteroids (Minchin, 1987; Pearse *et al.*, 1988). The nearest distance between spawning *P. regularis*, however, is considerably longer than for *Marthasterias glacialis*, which gathers in spawning assemblages prior to gamete release (Minchin, 1987). Although some of the *P. regularis* releasing gametes were 0.5 m from an adjacent spawner, several individuals appeared to be spawning in isolation, as reported by Pearse *et al.* (1988). At this distance, and particularly for those individuals spawning in isolation, gamete dilution would reduce the chance of fertilization. Echinoid zygote production in the field decreases dramatically if females are more than 20 cm apart from spawning males (Pennington, 1985). There is evidence, however, that asteroid sperm and sperm of other echinoderms are attracted to conspecific ova, and this, to some extent, may ameliorate the problem of gamete dilution (Miller, 1989; Byrne, 1990). The collection site is subject to strong currents, and it seems that the chances of fertilization would be enhanced by the slack water conditions that coincided with spawning, as noted for breeding in holothuroids (McEuen, 1988).

From laboratory culture at 18–22°C, the pelagic period of *Patiriella regularis* has a duration of 9–10 weeks; it may be longer in the field, where ambient sea surface temperatures of 16–18°C in Otago Harbour coincide with the planktonic period of this species. This duration of larval life is similar to that of other temperature planktotrophic asteroids, although it is somewhat shorter than that of asteroids from the northern Pacific, where ambient temperatures range from 7 to 13°C (Strathmann, 1978b). Latitudinal differences in larval life undoubtedly reflect differences in ambient temperature, with the longest planktonic period of 22 weeks recorded for the antarctic asteroid *Odontaster validus* at sea temperatures of −2–−1°C (Pearse and Bosch, 1986).

Development of *Patiriella regularis* through feeding bipinnaria and brachiolaria larvae is typical of asteroid embryogenesis and contrasts with the development of the Australian *Patiriella. P. exigua, P. pseudoexigua, P. calcar,* and *P. gunnii* have completely lost the bipinnarial stage and develop directly through a non-feeding brachiolaria (Mortensen, 1921; Lawson-Kerr and Anderson, 1978; Byrne, 1991; Chen and Chen, 1991). Also in contrast to *P. regularis*, these species have large ova, the evolution of which is considered to be a pre-adaptive trait for the shift to direct development (Chia, 1968). Larvae derived from such eggs would no longer be obligate planktotrophs, resulting in the loss of structures required for feeding (Strathmann, 1978a). The development of *P. regularis* provides the basic reference for comparison with the direct developers. Features that are particularly important for comparison include the mode and timing of archenteron and coelom formation in *P. regularis*, and the morphology of larval feeding structures. As documented for echinoids (Raff, 1987), the evolution of direct development in *Patiriella* may involve heterochronic changes in these features. Together with the developmental chronologies of the other *Patiriella* species, the ontogeny of *P. regularis* presented here will be used to determine the changes underlying the shift to direct development within the genus and to assess the pathways by which feeding larvae were lost. The use of *Patiriella* as a tool with which to examine developmental processes in evolution is the subject of ongoing research.

Acknowledgments

We thank Professor John Jillett, Director of the Portobello Marine Laboratory (PML), for the use of facilities. The staff of the PML also provided technical assistance. In particular we thank Mr. Michael Stuart. Thanks also to Ms. Pia Laegdsgaard for technical assistance. Special thanks to Dr. V. B. Morris for reading the manuscript. This work was supported by a grant from the Australian Research Council.

Literature Cited

Anderson, D. T. 1987. Developmental pathways and evolutionary rates. Pp. 143–155 in *Rates of Evolution,* K. S. W. Campbell and M. F. Day, eds. Allen and Unwin, Sydney.

Amemiya, S., and T. Tsuchiya. 1979. Development of the echinothurid sea urchin *Athenosoma ijimai*. *Mar. Biol.* **52:** 93–96.

Barker, M. F. 1977. Observations on the settlement of the brachiolaria larvae of *Stichaster australis* (Verrill) and *Coscinasterias calamaria* (Gray) (Echinodermata: Asteroidea) in the laboratory and on the shore. *J. Exp. Mar. Biol. Ecol.* **30:** 95–108.

Barker, M. F. 1978a. Structure of the organs of attachment of the brachiolaria larvae of *Stichaster australis* (Verrill) and *Coscinasterias calamaria* (Gray) (Echinodermata: Asteroidea). *J. Exp. Mar. Biol. Ecol.* **33:** 1–36.

Barker, M. F. 1978b. Descriptions of the larvae of *Stichaster australis* (Verrill) and *Coscinasterias calamaria* (Gray) (Echinodermata: Asteroidea) from New Zealand, obtained from laboratory culture. *Biol. Bull.* **154:** 32–46.

Bosch, I. 1989. Contrasting modes of reproduction in two antarctic asteroids of the genus *Porania*, with a description of unusual feeding and non-feeding larval types. *Biol. Bull.* **177:** 77–82.

Byrne, M. 1990. Annual reproductive cycles of the commercial sea urchin *Paracentrotus lividus* from an exposed intertidal and a sheltered subtidal habitat on the west coast of Ireland. *Mar. Biol.* **104:** 275–289.

Byrne, M. 1991. Developmental diversity in the starfish genus *Patiriella*. In *Proceedings 7th International Echinoderm Conference,* N. Suzuki, ed. Balkema, Rotterdam.

Cameron, R. A., and N. D. Holland. 1983. Electron microscopy of extracellular materials during the development of a sea star, *Patiria miniata* (Echinodermata: Asteroidea). *Cell Tissue Res.* **234:** 193–200.

Chen, B., and C. Chen. 1991. Reproductive cycle, larval development, juvenile growth and size distribution of *Patiriella pseudoexigua* Dartnall (Echinodermata: Asteroidea). In *Proceedings 7th International Echinoderm Conference*, N. Suzuki, ed. Balkema, Rotterdam.

Chia, F. S. 1968. The embryology of a brooding starfish, *Leptasterias hexactis* (Stimpson). *Acta Zool.* **49:** 321–364.

Chia, F. S. 1974. Classification and adaptive significance of developmental patterns in marine invertebates. *Thalassia Jugoslav.* **10:** 121–130.

Chia, F. S. 1976. Reproductive biology of an intraovarian brooding starfish *Patiriella vivipera* Dartnall, 1969. *Am. Zool.* **16:** 181.

Crump, R. G. 1969. Aspects of the biology of some New Zealand echinoderms. Ph.D. thesis, University of Otago, Dunedin, New Zealand.

Crump, R. G. 1971. Annual reproductive cycles in three geographically separated populations of *Patiriella regularis* (Verrill), a common New Zealand asteroid. *J. Exp. Mar. Biol. Ecol.* **7:** 137–162.

Dan, K. 1968. Asteroidea. Pp. 303–308 in *Invertebrate Embryology*, H. H. Kume and K. Dan, eds. NOLIT Publishing House, Belgrade, Yugoslavia.

Dartnall, A. J. 1969. A viviparous species of *Patiriella* (Asteroidea, Asterinidae) from Tasmania. *Proc. Linn. Soc. NSW* **93:** 294–296.

Dartnall, A. J. 1971. Australian sea stars of the genus *Patiriella* (Asteroidea, Asterinidae). *Proc. Linn. Soc. NSW* **96:** 39–51.

Gemmill, J. F. 1914. The development and certain points in the adult structure of the starfish *Asterias rubens*, L. *Philos. Trans. R. Soc. Lond. Ser. B* **205:** 213–294.

Grice, A. J., and R. C. Lethbridge. 1989. Reproductive studies on *Patiriella gunnii* (Asteroidea: Asterinidae) in south-western Australia. *Aust. J. Mar. Freshwater Res.* **39:** 399–407.

Heath, H. 1917. The early development of a starfish *Pateria (Asterina) Minceata*. *J. Morphol.* **29:** 461–469.

Kanatani, H. 1969. Induction of spawning and oocyte maturation by 1-methyladenine in starfishes. *Exp. Cell Res.* **57:** 333–337.

Keough, M. J., and A. J. Dartnall. 1978. A new species of viviparous asterinid asteroid from Eyre Peninsula, South Australia. *Rec. S. Aust. Mus.* **17:** 407–416.

Komatsu, M. 1972. On the wrinkled blastula of the sea-star *Asterina pectinifera*. *Zool. Mag.* **81:** 227–231.

Komatsu, M. 1976. Wrinkled blastula of the sea-star *Asterina minor* Hayashi. *Dev. Growth Differ.* **18:** 435–438.

Lawson-Kerr, C., and D. T. Anderson. 1978. Reproduction, spawning and development of the starfish *Patiriella exigua* (Lamarck) (Asteroidea, Asterinidae) and some comparisons with *P. calcar* (Lamarck). *Aust. J. Mar. Freshwater Res.* **29:** 45–53.

McEuen, F. S. 1988. Spawning behaviors of northeast Pacific sea cucumbers (Holothuroidea: Echinodermata). *Mar. Biol.* **98:** 565–585.

McKenzie, J. D. 1987. The ultrastructure of the tentacles of eleven species of dendrochirote holothurians studied with special reference to the surface coats and papillae. *Cell Tissue Res.* **248:** 187–199.

Miller, R. L. 1989. Evidence for the presence of sexual pheromones in free-spawning starfish. *J. Exp. Mar. Biol. Ecol.* **130:** 205–221.

Minchin, D. 1987. Sea-water temperature and spawning behaviour in the seastar *Marthasterias glacialis*. *Mar. Biol.* **95:** 139–143.

Mortensen, T. 1921. *Studies on the Development and Larval Forms of Echinoderms*. G.E.C. Gad., Copenhagen. 216 pp.

Newman, H. H. 1925. An experimental analysis of asymmetry in the starfish, *Patiria miniata*. *Biol. Bull.* **49:** 111–138.

Oguro, C., M. Komatsu, and Y. T. Kano. 1976. Development and metamorphosis of the sea-star *Asteropecten scoparius* Valenciennes. *Biol. Bull.* **151:** 560–573.

Oguro, C., M. Komatsu, and Y. T. Kano. 1988. Significance of the nonbrachiolarian type of development in sea-stars. Pp. 241–246 in *Echinoderm Biology*, R. Burke, P. Lambert, and R. Parsley, eds. Balkema, Rotterdam.

Parks, A. L., B. W. Bisgrove, G. A. Wray, and R. R. Raff. 1989. Direct development in the sea urchin *Phyllacanthus parvispinus* (Cidaroidea): phylogenetic history and functional modification. *Biol. Bull.* **177:** 96–109.

Pearse, J. S., and I. Bosch. 1986. Are the feeding larvae of the commonest antarctic asteroid *Odontaster validus* really demersal? *Bull. Mar. Sci.* **39:** 477–484.

Pearse, J. S., D. J. McClary, M. A. Sewell, W. C. Austin, A. Perez-Ruzafa, and M. Byrne, 1988. Simultaneous spawning of six species of echinoderms in Barkley Sound, British Columbia. *Inv. Reprod. Dev.* **14:** 279–288.

Pennington, J. T. 1985. The ecology of fertilization of echinoid eggs: the consequences of sperm dilution, adult aggregation, and synchronous spawning. *Biol. Bull.* **169:** 417–430.

Raff, R. A. 1987. Constraint, flexibility, and phylogenetic history in the evolution of direct development in sea urchins. *Dev. Biol.* **119:** 6–19.

Strathmann, M. F. 1987. *Reproduction and Development of Marine Invertebrates of the Northern Pacific Coast*. University of Washington Press, Seattle. Pp. 535–555.

Strathmann, R. R. 1971. The feeding behaviour of planktotrophic echinoderm larvae: mechanisms, regulation, and rates of suspension-feeding. *J. Exp. Mar. Biol. Ecol.* **6:** 109–160.

Strathmann, R. R. 1978a. The evolution and loss of feeding larval stages of marine invertebrates. *Evolution* **32:** 894–906.

Strathmann, R. R. 1978b. Length of pelagic period of echinoderms with feeding larvae from the northeast Pacific. *J. Exp. Mar. Biol. Ecol.* **34:** 23–27.

Williams, D. H. C., and D. T. Anderson. 1975. The reproductive system, embryonic development, larval development and metamorphosis of the sea urchin *Heliocidaris erythrogramma* (Val.) (Echinodermata: Echinometridae). *Aust. J. Zool.* **23:** 371–403.

Wray, G. A., and R. A. Raff. 1989. Evolutionary modification of cell lineage in the direct-developing sea urchin *Heliocidaris erythrogramma*. *Dev. Biol.* **132:** 458–470.

Reference: *Biol. Bull.* 180: 346–354. (June, 1991)

Abnormal Sea Urchin Fertilization Envelope Assembly in Low Sodium Seawater

SOU-DE CHENG[1], PATRICIA S. GLAS[2], AND JEFFREY D. GREEN*

Department of Anatomy, Louisiana State University Medical Center, New Orleans, Louisiana 70112

Abstract. The structuralization of the sea urchin fertilization envelope (FE), a model for extracellular macromolecular assembly, was found to require sodium ions, the predominant cation of seawater. Eggs from *Strongylocentrotus purpuratus* activated in sea waters with sodium chloride substitutes (choline or Tris chloride) elevated incomplete FEs. In addition, the conversion of the microvillar casts of the FE from blunt (I-form) to angular (T-form) did not occur. The permeability of the abnormal FEs was also compromised, as approximately eight times more protein than normal was released into the ambient seawater. There were also significant increases in the escape of two cortical granule (CG) enzymes, β-1,3-glucanase and ovoperoxidase. Furthermore, FEs elevated in choline chloride (ChCl) seawater appeared to be deficient in the incorporation of ovoperoxidase, an enzyme that is normally bound to the FE and that cross-links structural proteins in the nascent FE. The morphology of FEs elevated in potassium chloride-substituted seawater was similar to those in normal sodium seawater. Thus, it appears that sodium, or at least a similar ion, is necessary for the proper functioning of ovoperoxidase and structural proteins in the elevation and normal assembly of the sea urchin FE.

Introduction

Sea urchin fertilization has been intensively studied for the dramatic intra- and extracellular events concomitant with the change from egg to embryo. The irreversible transformation of the relatively thin, soft vitelline layer (VL = glycocalyx), investing the unfertilized egg, into a hardened, insoluble fertilization envelope (FE), elevated from the egg surface, is a critical step for the protection of the developing embryo. Furthermore, this process has been the subject of numerous investigations as an example of regulated extracellular matrix assembly. Several recent reviews (Kay and Shapiro, 1985; Shapiro *et al.*, 1989; Somers and Shapiro, 1989) contain the details of such investigations; therefore, the process will be summarized only briefly here.

Transglutaminase has an important role in the earliest stages of VL modification (Battaglia and Shapiro, 1988). It is located on the egg surface and catalyzes the incorporation of primary amines into the nascent FE during the first 4 min of egg activation. This process is apparently related to the I-T transition of the microvillar projections of the VL (in *S. purpuratus*), because the transition does not occur in the presence of transglutaminase inhibitors. During the next few minutes, ovoperoxidase secreted from the cortical granules (CG) catalyzes the insertion of structural proteins from the CGs into the VL by cross-linking tyrosyl residues between polypeptides (Foerder and Shapiro, 1977; Hall, 1978). Besides this catalytic reaction, ovoperoxidase itself is incorporated into the nascent FE via a specific interaction with another CG protein, proteoliaisin (Weidman *et al.*, 1985). These enzyme activities result in a hardened, insoluble, fully formed FE within the first 10 min following egg activation.

Several recent reports have been concerned with ionic requirements for FE formation. Carroll and Endress (1982) demonstrated that formation of mature FEs requires the normal 9 m*M* [Ca^{2+}] and 48 m*M* [Mg^{2+}] in the seawater. By omitting these ions they could produce an "intermediate envelope" that was much thinner than the normal FE and did not incorporate structural proteins.

Received 29 August 1990; accepted 24 January 1991.

[1] Genetics Division, Children's Hospital, 300 Longwood Avenue, Boston, MA 02115.

[2] Department of Zoology and Physiology, Louisiana State University, Baton Rouge, LA 70803.

Abbreviations: SW (artificial seawater); CG (cortical granule); ChCl (choline chloride); FE (fertilization envelope); FP (fertilization product); VL (vitelline layer).

* To whom correspondence should be sent.

Deficiency of Cl^-, the most abundant anion in seawater, not only interferes with the normal I-T transformation, but also increases the permeability of the FE (Lynn *et al.*, 1988; Green *et al.*, 1990). Furthermore, the normal external Na^+ concentration (419 m*M*) is not only essential for preventing polyspermy and hardening the FE, but also for the normal embryonic development of the sea urchins *Arbacia punctulata* and *Strongylocentrotus purpuratus* (Schuel *et al.*, 1982).

To better understand the mechanism of FE elevation—an important early event of embryonic development—we concentrated on the effect of Na^+ deficiency on the formation of the FE. In the present study, the elevation and morphology of FEs from normal and low sodium (2 m*M*) seawaters were investigated. Envelopes were observed with phase, scanning, and transmission electron microscopy. Total soluble secreted protein and the enzymatic activities of ovoperoxidase (Foerder and Shapiro, 1977; Hall, 1978) and β-1,3-glucanase (Schuel *et al.*, 1972; Wessel *et al.*, 1987) in the fertilization products (FP) were compared. Portions of this investigation have been presented in a preliminary form (Cheng *et al.*, 1989).

Materials and Methods

Handling of gametes

Sea urchin (*S. purpuratus*) eggs were collected and acid dejellied as described previously (Green *et al.*, 1990). Eggs were divided into four equal portions, the three low Na^+ groups: KCl-, Tris-, and ChCl-substituted seawaters (SW) and the control: normal Na^+-SW group. They were washed and incubated in the appropriate SW for 15–40 min. All seawater formulations were based on Cavanaugh (1956). For the low Na^+-SWs, equimolar concentrations of KCl, Tris HCl, or ChCl (Sigma) replaced NaCl, yielding a calculated residual [Na^+] of approximately 2 m*M*. Normal and low Na^+ SWs were buffered with 10 m*M* TAPS (Sigma) and adjusted to pH 8.3 with NaOH or KOH, respectively. To avoid contamination from sperm proteins and secretions, eggs were activated by adding the Ca^{2+} ionophore A23187 (Chambers *et al.*, 1974; Steinhardt and Epel, 1974) to a final concentration of 38 μ*M* in 1% dimethyl sulfoxide (DMSO). Experiments were performed at 20°C.

Light microscopy

Eggs activated in normal and low Na^+-SWs were observed continuously on a 1 × 3 inch microscope slide under a coverslip supported by a ring of petroleum jelly. Photographs were taken with phase contrast optics on Kodak Technical Pan Film 2415.

Ovoperoxidase localization

Activated eggs of the control group (normal Na^+-SW) were rinsed at *15 min postactivation* with 0.45 *M* NaCl–0.1 *M* Tris HCl (Klebanoff *et al.*, 1979). Ten percent egg suspensions (v/v) were made and incubated in 5.6 m*M* 3,3-diaminobenzidine (DAB; Sigma) in 0.45 *M* NaCl–0.1 *M* Tris HCl in an ice bath for *10 min*. The experimental eggs (low Na^+) were handled identically except that NaCl was replaced with ChCl. Activated eggs were then fixed and prepared for TEM as described below.

Transmission electron microscopy

Eggs were fixed with 2% glutaraldehyde in the appropriate seawaters for 1 h at room temperature and washed with 0.1 *M* sodium cacodylate (pH 7.4). Postfixation with 1% osmium tetroxide (OsO_4) was performed for 30 min. Eggs were washed with double distilled water and dehydrated in ascending concentrations of ethanol. Ethanol was replaced with propylene oxide and eggs were infiltrated with EM bed-812 (Electron Microscopy Sciences). The blocks were cured at 58–60°C for 3 days. Sections were cut with glass knives on a Reichert-Jung Ultracut E; mounted on copper grids; stained with lead citrate (Reynolds, 1963) and uranyl acetate; and observed with a Philips 301 transmission electron microscope at 60 kV.

Scanning electron microscopy

Fixations were accomplished at 20°C by mixing equal volumes of eggs with 4% glutaraldehyde in seawater (with 10 m*M* TAPS pH 8.3) before activation and at 1, 3, 10, 30, and 60 min postactivation. Eggs were fixed for 1 h and washed in 0.1 *M* sodium cacodylate (pH 7.4). Postfixation took place in 1% OsO_4 in 0.1 *M* sodium cacodylate (pH 7.4) for 30 min. They were then washed with double distilled water and dehydrated in an ascending series of ethanol. Absolute ethanol was replaced gradually by acetone. Eggs were transferred to porous containers (Bio-Rad) and processed for CO_2 critical point drying (Samdri-790, Tousimis Research Corp.). The eggs were then attached to aluminum mounts coated with colloidal silver liquid (Ted Pella, Inc.) for sputter coating with gold: palladium (60:40; Electron Microscopy Sciences) for 3 min in a Hummer VI (Technics). Eggs were observed with a JEOL JSM-35CF scanning electron microscope at 25 kV and a condenser lens setting of 3. The photos were taken with Polaroid type 55 (4 × 5 in.) positive/negative instant sheet film.

Total protein assay

Ionophore-activated eggs were allowed to settle for approximately 10 min and the supernatant (secreted FP) was collected and centrifuged by hand to remove the few remaining eggs. Ionophore activation resulted in at least 95% elevated FEs. For protein determination the proteins in 1.0 ml of FP (5% egg suspension, v/v) were precipitated

by adding 110 μl ice-cold 50% trichloroacetic acid (TCA) and centrifuged for 20 min at 8800 × *g* (Eppendorf centrifuge 5413) at 10°C. Tubes were drained by inversion and the protein pellets air dried. Bovine serum albumin (BSA; Sigma) was the standard. All the precipitates were assayed according to Lowry *et al.* (1951). As a control, protein determinations were performed with BSA in each of the seawaters to ascertain their influences, if any, on the Lowry procedure.

β-1,3-glucanase assay

Glucanase activity was measured according to Green and Summers (1980). The FP was collected as described above. FP (0.2 ml; 5% egg suspension, v/v), normal Na^+- or ChCl-substituted SW (0.2 ml), and laminarin (0.2 ml of a 2.5 mg/ml SW solution) were incubated for 1 h at 37°C. Then 0.2 ml of this mixture, 0.4 ml enzyme solution (0.4 ml glucose oxidase and 3 mg horseradish peroxidase in 50 ml of 25 m*M* phosphate buffer, pH 6) and 0.4 ml o-dianisidine (40 mg in 50 ml double distilled water) were incubated for 10 min at 37°C. The reaction was stopped by the addition with rapid vortexing of 0.8 ml 4 *N* sulfuric acid. Spectrophotometric readings were taken at 530 nm. Controls lacking the substrate laminarin were used to check for the presence of glucose (the product of the glucanase-laminarin reaction) in the FP. Glucose was generated *only* in the presence of both the FP and laminarin. A glucose solution was the standard. Control glucose determinations were performed in normal Na^+-SW and ChCl-substituted-SW to ascertain the effects, if any, of ChCl substitution on the glucose oxidase-peroxidase reaction. All the chemicals for this assay were purchased from Sigma.

Ovoperoxidase assay

Ovoperoxidase assays were performed in 1 ml containing 18 m*M* guaiacol (Sigma), 0.3 m*M* H_2O_2 (Sigma), and 10 m*M* TAPS at pH 8.0 and 20°C (Deits *et al.*, 1984). The reaction was started by adding enzyme (in the FP), and the increase in absorbency at 436 nm was recorded spectrophotometrically with a strip chart recorder. All reported values are initial rates, because the reaction slows after 15–30 s. A unit of ovoperoxidase was defined as that which is required to oxidize 1 μmole of guaiacol per min in a 1-ml assay volume (Deits *et al.*, 1984).

FP including the ovoperoxidase was collected from a 5% (v/v) suspension of activated eggs. Ten minutes after activation, eggs were settled by low speed centrifugation and the supernatant (FP) was removed for the assay.

Statistics

Statistical analyses for total protein, β-1,3-glucanase and ovoperoxidase assays were performed using the Student's *t* test.

Results

Observations with light microscopy

The elevation of FEs in normal and low Na^+-SWs are compared in Figure 1. Figure 1A–D depicts eggs at 1 min postactivation. Although difficult to quantify from the photomicrographs in the normal Na^+-SW control group (Fig. 1A, E), the FE appeared relatively thin at the end of the first minute and thickened with increasing time. However, it appeared thicker (more refractive) than the low Na^+ groups, especially Tris and ChCl (Fig. 1C, D). At later time points, the FE of the control group remained more refractive than those of the low Na^+ groups. These differences were more striking at 3 min postactivation when the FE of ChCl eggs began to shrink and some collapsed, while those of the control remained spherical. By 30 min postactivation, the FEs remained robust in the normal and K^+-substituted SWs (Fig. 1E, F), while those of the Tris- and choline-substituted SWs had collapsed back nearer to the egg surface (Fig. 1G, H).

An interesting attribute of the activated eggs is that of their increased stickiness in the Tris and ChCl groups. In the first 3 min there was no apparent difference among the 4 groups. At approximately 4 min postactivation, however, the eggs of the Tris and ChCl groups formed extensive clumps.

Ultrastructural changes

Unactivated eggs incubated in normal Na^+- or ChCl-substituted-SWs and observed by SEM displayed similar surface morphology (Fig. 2A, E). At 1 min postactivation, the FEs in both SWs were elevated with rounded (I-form) microvillar projections (Fig. 2B, F). In contrast to FEs in ChCl-substituted SW (Fig. 2G), the typical I-T ("Igloo-Tent") transformation of *S. purpuratus* FEs in normal Na^+-SW was completed by 3 min (Fig. 2C) and resembled those of later time points (Fig. 2D). However, ChCl FEs did not undergo the transformation even by 30 min (Fig. 2H).

As judged with TEM (Fig. 3), FEs that elevated in normal Na^+-SW resulted in the well-defined, angular T-form projections (Fig. 3A) characteristic of this species. However, those in K^+-substituted-SW appeared to be intermediate in form (Fig. 3B), compared to those in Tris- and ChCl-substituted SWs, which were similar to each other in retaining rounded projections (Fig. 3C, D).

The above observations of the "soft" FEs (incomplete formation) suggested that their permeability, as well as their morphology, might be altered. Therefore, several measurements of permeability were undertaken.

Total protein secretion

Soluble secreted protein that leaked through the FEs of eggs activated in normal or low Na^+ SWs was measured

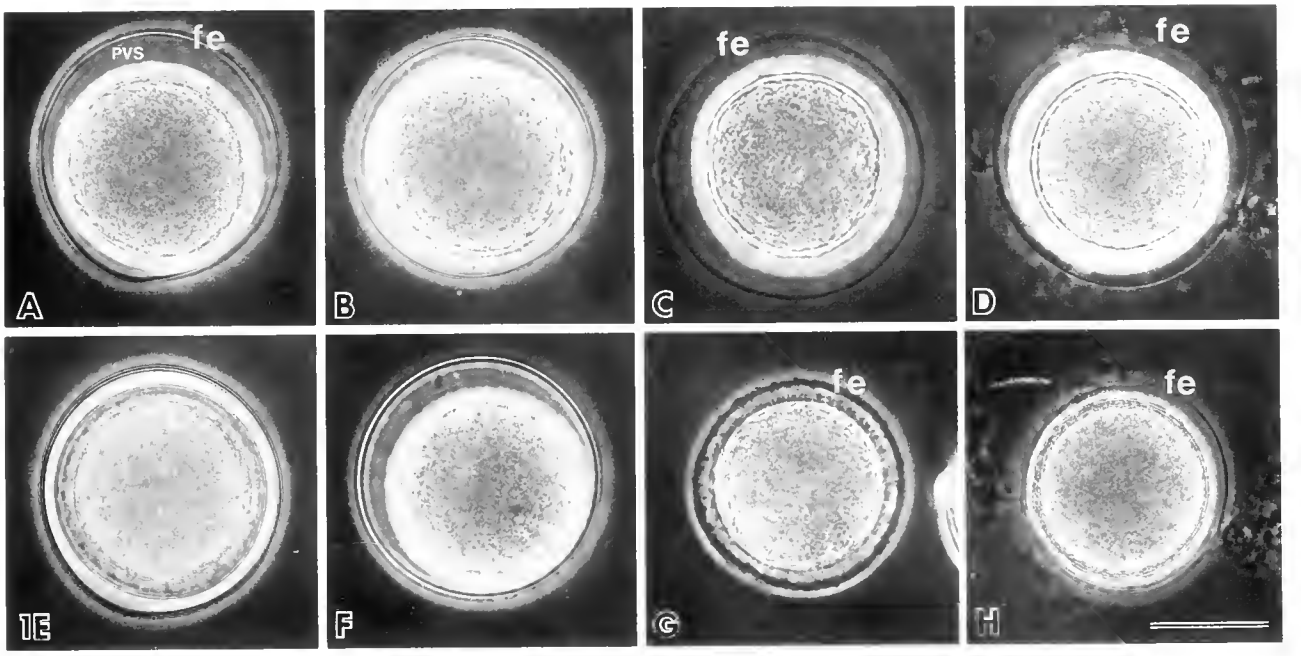

Figure 1. Phase microscopy of *Strongylocentrotus purpuratus* eggs activated in normal (A, E) and Na^+ depleted SWs (B–D and F–H). A, E: Normal Na^+-SW. B, F: KCl-substituted-SW. C, G: Tris-substituted-SW. D, H: ChCl-substituted-SW. A–D: 1 min postactivation. E–H: 30 min. These micrographs were taken focusing on the fertilization envelopes. fe = fertilization envelope; PVS = perivitelline space. Scale bar = 50 μm.

(Fig. 4). FPs were collected at 10 min postactivation from eggs pooled from several females. The FPs of the normal and K^+-substituted SW eggs had 22.7 ± 1.8 μg and 22.2 ± 5.7 μg (Mean ± S.E.M.) of protein/ml FP, respectively. They were not significantly different. However, the FPs of Tris- and ChCl-substituted SWs contained 162.1 ± 25.9 μg and 168.7 ± 3.4 μg, respectively. This 7- to 8-fold increase over normal and KCl was highly significant ($P < 0.0001$).

Control assays demonstrated no significant difference (95% confidence level) in TCA-precipitable BSA between normal and low Na^+ SWs. Therefore, the various SWs had no adverse effects on the Lowry assay. In addition, supernatant protein from *unactivated* eggs in DMSO was measured and found to contribute little to the total (~1.4 μg/ml; see also Green *et al.*, 1990).

β-1,3-glucanase secretion

Glucanase activity was measured (in normal and ChCl SWs) by the amount of glucose hydrolyzed from the β-1,3-glucan polysaccharide laminarin by egg-derived-glucanase in the FP (Fig. 5). Aliquots of FP of experimental and control groups were taken at 10 min postactivation. The glucose measurements from ChCl and normal SW were 1.62 ± 0.19 and 0.93 ± 0.19 μmoles glucose per ml of FP, respectively. Approximately 75% more glucanase activity was found in the FP from the ChCl eggs. This difference was significant ($P < 0.05$).

Control incubations of glucose were assayed in normal and ChCl-substituted SWs, and no significant differences (95% confidence level) were observed. Therefore, it is unlikely that the ChCl interfered with the glucose determination.

Ovoperoxidase secretion

Ovoperoxidase released from ChCl-SW eggs (3.72 ± 0.78 μmoles guaiacol oxidized/min/ml of FP) had significantly higher activity (see Fig. 6) than that released from normal SW eggs (0.82 ± 0.21 μmole/min/ml). Peroxidase activities in KCl-SW (1.09 ± 0.30 μmoles/min/ml) and Tris-SW (1.68 ± 0.30 μmoles/min/ml) FPs were intermediate between control and ChCl groups. There were significant differences between normal and ChCl ($P < 0.001$), and Tris ($P < 0.05$). However, ovoperoxidase release was not significantly different between normal and KCl ($P > 0.35$).

Ovoperoxidase localization

Because ovoperoxidase is incorporated into the FE (Somers *et al.*, 1989) and more enzyme activity was observed in the FP of the low Na^+ treatments (see above), it is possible that the higher activity was not only due to

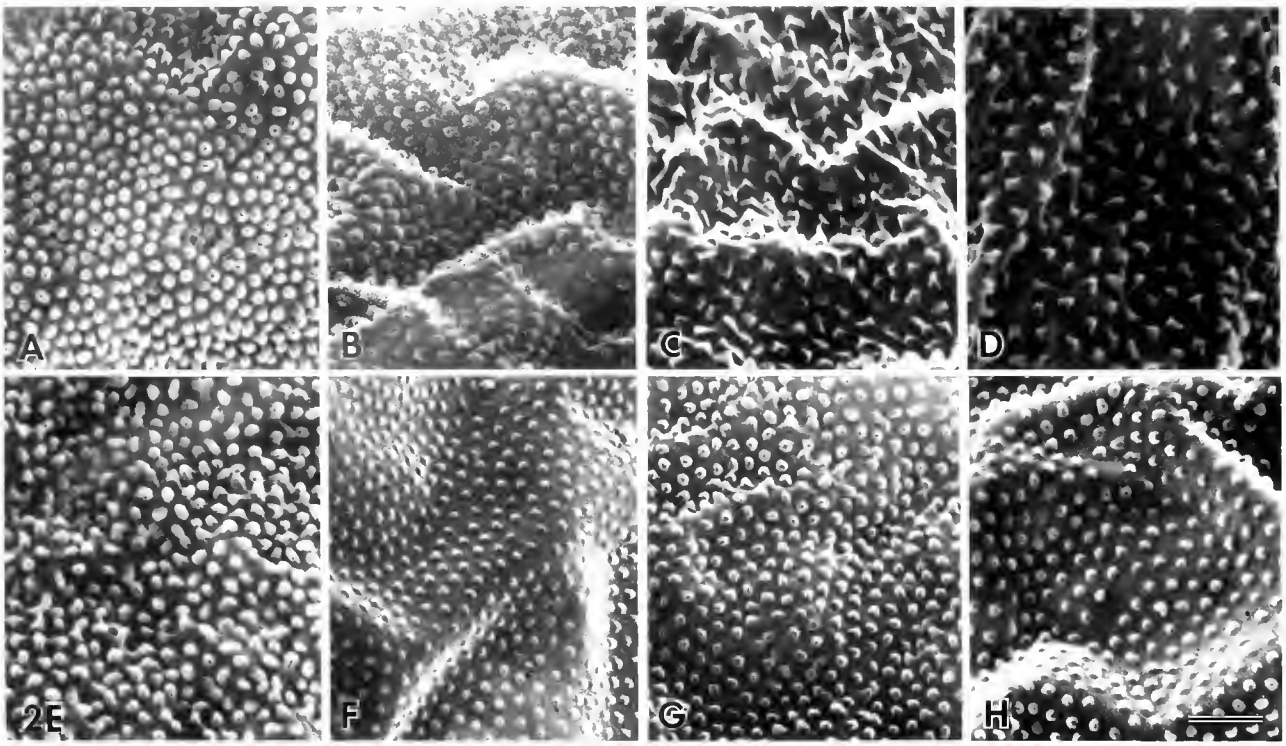

Figure 2. SEM of *Strongylocentrotus purpuratus* egg surfaces. A. VL of egg (unactivated) in normal Na^+-SW. B–D. FEs of normal Na^+-SW eggs at 1,3, and 60 min postactivation. E. VL of egg (unactivated) in ChCl-substituted-SW. F–H. FEs of ChCl-substituted-SW eggs at 1,3, and 30 min. The microvillar projections of the ChCl-substituted-SW eggs did not undergo the I–T transformation. Scale bar = 1 μm.

FE permeability, but that the ovoperoxidase was not incorporated efficiently into the structure of the FE. Therefore, DAB localization of ovoperoxidase was performed.

Comparing the TEM micrographs (Fig. 7) of FEs after DAB incubation, the normal SW FE (Fig. 7C) is conspicuously darker than that of the ChCl FE (Fig. 7D). Although both normal and ChCl FEs stained more intensively than the controls (Fig. 7A, B), the intensity of staining was higher in the normal FEs. Presumably, there was more ovoperoxidase incorporated into the FEs in normal Na^+-SW than in ChCl-substituted SW.

Discussion

Sea urchin eggs are excellent material for many biological studies because they can be harvested in large numbers, cultured in a well-defined medium (artificial seawater), and they develop synchronously. They are well suited for the study of extracellular self-assembly (Kay and Shapiro, 1985; Somers and Shapiro, 1989; Shapiro *et al.*, 1989). The complexity of the transition of the vitelline layer (VL) glycoprotein to the FE tempts one to try to dissect the myriad of sequential processes involved. The VL is not merely an inert cell coat, but it serves as a template or scaffolding upon which other proteins are assembled and intercalated under the influence of several enzymes. A requisite for proper structuralization is the presence of several ions in the seawater, *e.g.*, Ca^{2+}, Mg^{2+} (Carroll and Endress, 1982), Cl^- (Lynn *et al.*, 1988; Green *et al.*, 1990), and Na^+ (Schuel *et al.*, 1982). In the present study, we focused on the effects of Na^+-depletion on the elevation and structuralization of the FE.

There is some information on the sea urchin egg during fertilization in Na^+-depleted seawater. It was found that the fast block to polyspermy decayed concurrently with the retardation of the depolarization of the egg plasma membrane, a Na^+-dependent process (Jaffe, 1980; Schuel and Schuel, 1981). Additional investigations have shown that Na^+ accounts for the release of acid from the egg, resulting in an increased intracellular pH. This increase is necessary for increased protein synthesis, DNA synthesis, and cell division (Nishioka and Cross, 1978). In relation to the assembly of the FE, Schuel *et al.* (1982) demonstrated that low Na^+ (19 m*M*), ChCl-substituted seawater resulted in FEs that collapsed and failed to undergo normal structuralization, including the I to T transformation of the microvillar casts. The inhibition of the normal hardening process was attributed to the failure of CG structural proteins to impregnate or insert into the VL. However, this impairment of the hardening process is dis-

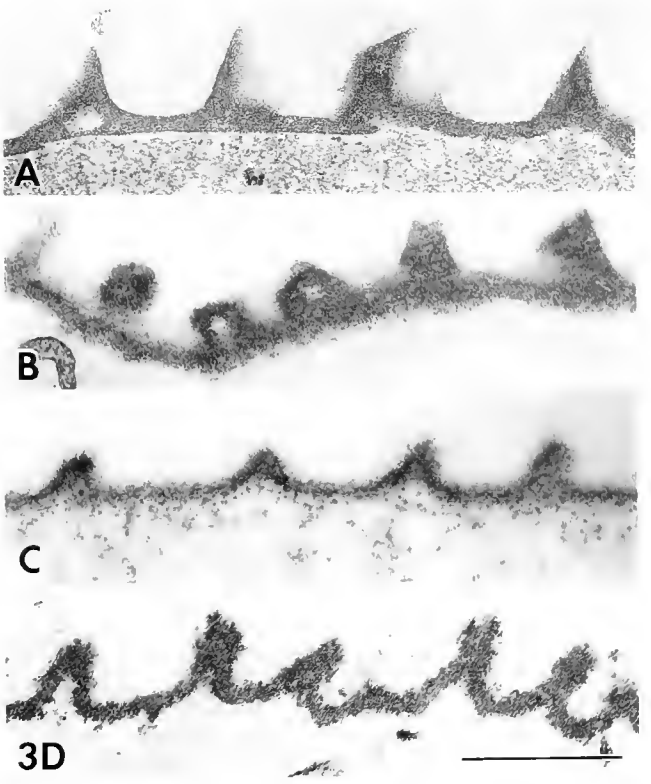

Figure 3. TEM of *Strongylocentrotus purpuratus* FEs. Eggs were fixed 15 min postactivation in the following SWs: A. normal Na^+. B. KCl. C. Tris. D. ChCl. Scale bar = 0.5 μm.

tinct from the phenomenon of "cross-linking," in that the latter is assayed by the disruption of FEs in urea. In their experiments, cross-linking was not affected. Furthermore, K^+ and Li^+ substituted for Na^+ in normal structuralization, while ChCl and Tris did not.

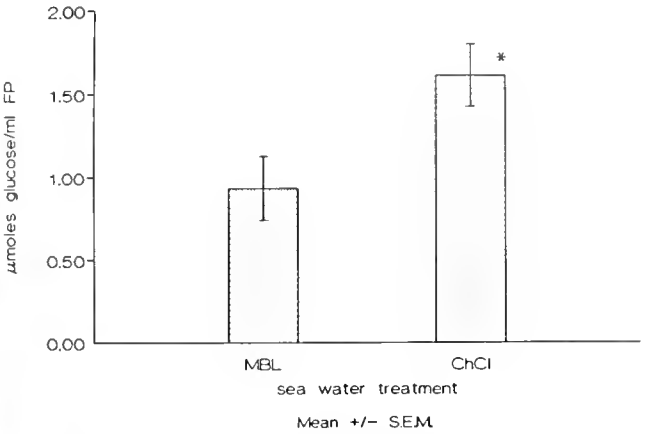

Figure 5. β-1,3-glucanase secretion. Glucanase activity released through FEs was assayed as described in Materials and Methods. The Mean ± S.E.M. are shown for four trials. The * denotes a statistically significant difference from the control, normal SW.

In the present study we lowered the Na^+ concentration to approximately 2 m*M* and observed an earlier collapse of the FE, 3 min as opposed to 30 min. It is not surprising that our FEs collapsed earlier than those of Schuel *et al.* (1982), because our Na^+ concentration was ten-fold less. Additional evidence of the failure of the sodium-deficient FEs to harden is that initially they expanded more than the normal FEs. This greater distension may also be related to the failure of proteins to insert into the FE, thereby raising the hydrostatic pressure in the perivitelline space (Schuel *et al.*, 1974; Green and Summers, 1980). However, within a few minutes, the FE began to shrink, suggesting that the FE was permeable to the secreted proteins, and this allowed for a decrease in the hydrostatic pressure

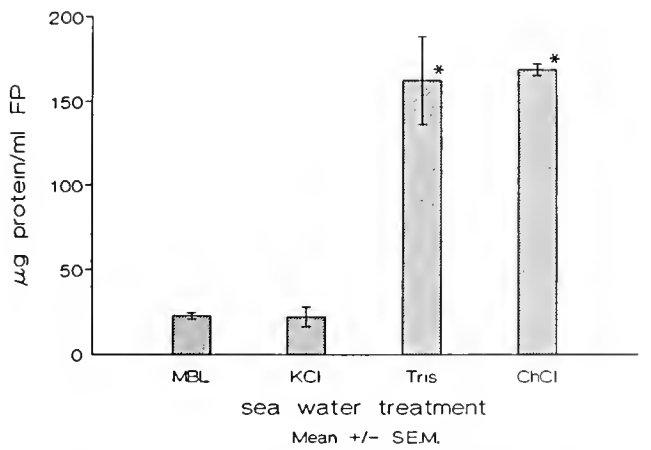

Figure 4. Protein release through FEs. Protein concentrations were determined by the Lowry assay. Each measurement represents the Mean ± S.E.M. of three trials. The * denotes a statistically significant difference from the control, normal SW.

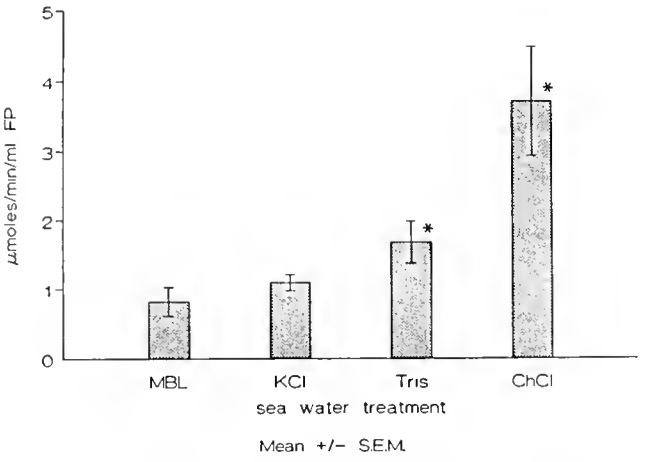

Figure 6. Ovoperoxidase secretion. Ovoperoxidase activity released through FEs was measured as described in Materials and Methods. Mean ± S.E.M. are shown (n = 3–7) and * denotes statistically significant differences from the control, normal SW.

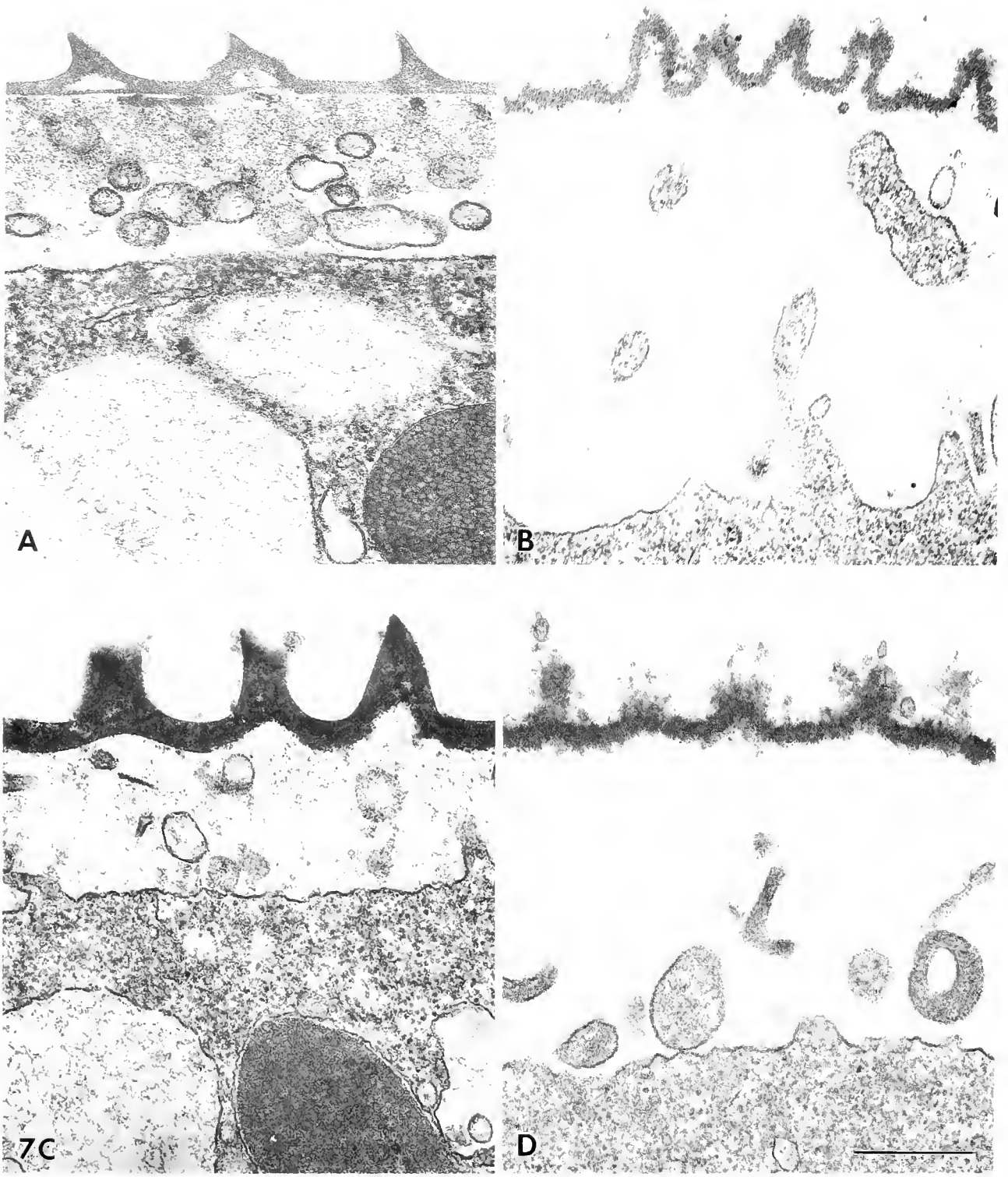

Figure 7. Ultrastructural localization of ovoperoxidase. The pointed T-form microvillar projections on normal Na^+-FE (15 min after activation) and the rounded I-form microvillar projections on ChCl-FE are demonstrated (A and B, respectively). After DAB localization of ovoperoxidase the FEs (C, normal Na^+; D, ChCl) stained more intensely than those of the controls (A and B) in both normal Na^+ and ChCl-substituted-SW. Furthermore, the staining of the normal Na^+ was darker than that of the ChCl. This suggests that less ovoperoxidase was incorporated into the FE of eggs activated in ChCl-substituted SW. D is a montage showing the FE and cortex of the same egg. Scale bar = 0.5 μm.

within the perivitelline space. This conclusion is strengthened by the fact that we observed a greater (approx. eightfold) increase in total proteins secreted into the ambient seawater in Tris and ChCl seawaters. Glucanase and ovoperoxidase secretions also increased significantly. Because ovoperoxidase is normally incorporated into the FE (Somers and Shapiro, 1989), the increase in soluble ovoperoxidase activity is probably related to both increased permeability and decreased incorporation of this enzyme into the nascent FE. The substitution of K^+ for Na^+ did not significantly interfere with hardening (structuralization), nor did it change protein or ovoperoxidase secretion significantly. This observation is consistent with the normal FE formation in K^+- or Li^+-substituted seawaters (Schuel *et al.*, 1982).

The results reported herein are similar to those obtained in Cl^--deficient seawaters (Lynn *et al.*, 1988; Green *et al.*, 1990). Moreover, our results are strikingly similar to those of Battaglia and Shapiro (1988), who reported similar findings when they inhibited egg surface transglutaminase activity with primary amines. This similarity suggests that both Cl^- and Na^+ may be important for the transglutaminase-catalyzed early cross-linking that occurs before the ovoperoxidase-catalyzed cross-linking. However, we can not ignore the possibility that the observed effects may be the result of ChCl or Tris **addition,** rather then exclusion of Na^+. This is a drawback to any substitution experiment. The size of the substituted ionic species may be important because K^+ and Li^+ are closer in size to Na^+ than are either Tris or ChCl. This question, too, remains to be resolved.

Another interesting observation of these experiments was the apparent paucity of hyalin in the perivitelline space of eggs activated in ChCl-substituted-SW (*e.g.*, Figs. 3A, D and 7A, B). This observation and the increased glucanase activity in the ambient sodium-deficient seawater may be related to the possibility that glucanase performs its major function on the hyaline layer of the egg (Wessel *et al.*, 1987) in a Na^+-dependent manner. This possibility awaits further experimentation.

Our results demonstrate that the ionic composition of the seawater significantly influences the formation of the FE in the sea urchin *S. purpuratus*. These results are consistent with other published reports. Moreover, the phenomenon of regulated extracellular assembly remains an intriguing field of study, to which the study of sea urchin FE formation can contribute.

Acknowledgments

The authors wish to thank Drs. Frank N. Low and Joseph B. Delcarpio for their SEM technical assistance, and Drs. William J. Swartz and John W. Lynn for their suggestions regarding this paper. This work was supported by an Edward G. Schlieder Educational Foundation Grant to J.D.G.

Literature Cited

Battaglia, D. E., and B. M. Shapiro. 1988. Hierarchies of protein cross-linking in the extracellular matrix: involvement of an egg surface transglutaminase in early stages of fertilization envelope assembly. *J. Cell Biol.* **107:** 2447–2454.

Carroll, E. J., and A. G. Endress. 1982. Sea urchin fertilization envelope: uncoupling of cortical granule exocytosis from envelope assembly and isolation of an envelope intermediate from *Strongylocentrotus purpuratus* embryos. *Dev. Biol.* **94:** 252–258.

Cavanaugh, G. M., ed. 1956. Pp. 67–69 in *Formulae and Methods of the Marine Biological Laboratory Chemical Room.* Marine Biological Laboratory, Woods Hole, MA.

Chambers, E. L., B. C. Pressman, and B. Rose. 1974. The activation of sea urchin eggs by the divalent ionophores A23187 and X-537A. *Biochem. Biophys. Res. Comm.* **60:** 126–132.

Cheng, S.-D., P. S. Glas, and J. D. Green. 1989. Enzymatic and morphological analysis of fertilization envelope (FE) assembly in low Na^+ sea water. *J. Cell Biol.* **109:** 128a.

Deits, T., M. Farrance, E. S. Kay, L. Medill, E. E. Turner, P. J. Weidman, and B. M. Shapiro. 1984. Purification and properties of ovoperoxidase, the enzyme responsible for hardening the fertilization membrane of the sea urchin egg. *J. Biol. Chem.* **21:** 13,525–13,533.

Foerder, C. A., and B. M. Shapiro. 1977. Release of ovoperoxidase from sea urchin eggs hardens the fertilization membrane with tyrosine crosslinks. *Proc. Natl. Acad. Sci. USA* **74:** 4214–4218.

Green, J. D., and R. G. Summers. 1980. Formation of the cortical concavity at fertilization in the sea urchin egg. *Dev. Growth Differ.* **22**(6): 821–829.

Green, J. D., P. S. Glas, S.-D. Cheng, and J. W. Lynn. 1990. Fertilization envelope assembly in sea urchin eggs inseminated in chloride-deficient sea water: II. Biochemical effects. *Mol. Reprod. Dev.* **25:** 177–185.

Hall, H. G. 1978. Hardening of the sea urchin fertilization envelope by peroxidase-catalyzed phenolic coupling of tyrosines. *Cell* **15:** 343–355.

Jaffe, L. A. 1980. Electrical polyspermy block in sea urchin eggs: nicotine and low sodium experiments. *Dev. Growth Differ.* **22:** 503–507.

Kay, E. S., and B. M. Shapiro. 1985. The formation of the fertilization membrane of the sea urchin egg. Pp. 45–80 in *Biology of Fertilization, Vol. 3, The Fertilization Response of the Egg.* C. B. Metz and A. Monroy, eds. Academic Press, Orlando.

Klebanoff, S. J., C. A. Foerder, M. Eddy, and B. M. Shapiro. 1979. Metabolic similarities between fertilization and phagocytosis. *J. Exp. Med.* **149:** 938–953.

Lowry, O. H., N. J. Rosebrough, A. L. Farr, and R. J. Randall. 1951. Protein measurement with the folin phenol reagent. *J. Biol. Chem.* **193:** 265–275.

Lynn, J. W., R. L. Goddard, P. Glas, and J. D. Green. 1988. Fertilization envelope assembly in sea urchin eggs inseminated in Cl^--deficient sea water: I. Morphological effects. *Gamete Res.* **21:** 135–149.

Nishioka, D., and N. Cross. 1978. The role of external sodium in sea urchin fertilization. Pp. 403–413 in *Cell Reproduction: In Honor of D. Mazia,* E. R. Dirksen, D. M. Prescott, and C. F. Fox, eds. Academic Press, New York.

Reynolds, E. S. 1963. The use of lead citrate at high pH as an electron opaque stain in electron microscopy. *J. Cell Biol.* **17:** 208–212.

Schuel, H., W. L. Wilson, R. S. Bressler, J. W. Kelly, and J. R. Wilson. 1972. Purification of cortical granules from unfertilized sea urchin egg homogenates by zonal centrifugation. *Dev. Biol.* **29:** 307–320.

Schuel, H., J. W. Kelly, E. R. Berger, and W. L. Wilson. 1974. Sulfated acid mucopolysaccharides in the cortical granules of eggs. Effects of quaternary ammonium salts on fertilization. *Exp. Cell Res.* **88:** 24–30.

Schuel, H., and R. Schuel. 1981. A rapid sodium-dependent block to polyspermy in sea urchin eggs. *Dev. Biol.* **87:** 249–258.

Schuel, H., R. Schuel, P. Dandekar, J. Boldt, and R. G. Summers. 1982. Sodium requirements in hardening of the fertilization envelope and embryonic development in sea urchins. *Biol. Bull.* **162:** 202–213.

Shapiro, B. M., C. E. Somers, and P. J. Weidman. 1989. Extracellular remodeling during fertilization. Pp. 251–276 in *The Cell Biology of Fertilization*, H. Schatten and G. Schatten, eds. Academic Press, San Diego.

Somers, C. E., D. E. Battaglia, and B. M. Shapiro. 1989. Localization and developmental fate of ovoperoxidase and proteoliaisin, two proteins involved in fertilization envelope assembly. *Dev. Biol.* **131:** 226–235.

Somers, C. E., and B. M. Shapiro. 1989. Insights into the molecular mechanisms involved in sea urchin fertilization envelope assembly. *Dev. Growth Diff.* **31**(1): 1–7.

Steinhardt, R. A., and D. Epel. 1974. Activation of sea urchin eggs by calcium ionophore. *Proc. Natl. Acad. Sci. USA* **71:** 1915–1919.

Weidman, P. J., E. S. Kay, and B. M. Shapiro. 1985. Assembly of the sea urchin fertilization membrane: isolation of proteoliaisin, a calcium-dependent ovoperoxidase binding protein. *J. Cell Biol.* **100:** 938–946.

Wessel, G. M., M. R. Truschel, S. A. Chambers, and D. R. McClay. 1987. A cortical granule-specific enzyme, β-1,3-glucanase, in sea urchin eggs. *Gamete Res.* **18:** 339–348.

Reference: *Biol. Bull.* **180**: 355–371. (June, 1991)

Embryonic Development of the American Lobster (*Homarus americanus*): Quantitative Staging and Characterization of an Embryonic Molt Cycle

S. M. HELLUY AND B. S. BELTZ

Department of Biological Sciences, Wellesley College, Wellesley, Massachusetts 02181

Abstract. The growth of a single brood of lobsters (*Homarus americanus* Milne-Edwards 1837) maintained at constant temperature is studied from the naupliar stage to hatching, and the sequence of appearance of morphological, anatomical, and behavioral characteristics observed. A percent-staging system based upon Perkins' eye index (1972) is presented, and ten equally spaced embryonic stages are illustrated and characterized at different levels of resolution: whole eggs, dissected embryos, antennulae and telsons. The tegumentary and setal changes in the telson show that a complete molt cycle takes place in the egg starting at about 12% embryonic development (E12%) with the molt of the nauplius into the metanauplius and ending just after hatching when the metanauplius molts into a first stage larva (L1, first zoea). At E30%, the cuticle begins to separate from the setae in the telson; this signals the start of Drach's (1939) stage D_0 of the metanaupliar embryonic molt cycle. At that time, the first sign of organogenesis of the L1, the formation of the endopod of the antennulae, becomes visible; presumed sensory neurons and their axons are observed at the tip of the exopod of the antennulae where a giant sensillum is differentiating. During D_0 the setae of the first larval stage are forming proximally and medially in the bilobed telson under the metanaupliar cuticle. At E90%, these setae are retracting, and the embryo has entered stage D_1. After hatching (E100%), the telson of the free metanauplius (prelarva) shows the characteristics of stage D_{2-3} and ecdysis soon follows. The arrested development observed at constant temperature in the experimental brood occurred at stage D_0 of the metanaupliar molt cycle, whereas development was resumed as the embryos entered stage D_1. These changes in developmental pace from D_0 to D_1 in the embryonic molt cycle are parallel to those occurring in older lobsters (Aiken, 1973). The quantitative staging of lobster development from extrusion to hatching, and the description of the embryonic molt cycle will facilitate future investigations on particular aspects of the embryogenesis of *Homarus* such as neural differentiation.

Received 3 December 1990; accepted 8 March 1991.

Introduction

Studies on lobsters and other crustaceans have made a significant contribution to our understanding of neural organization and the control of behavior (see Wiese *et al.*, 1990). There is increasing interest in examining the ontogenesis of particular behaviors and the cellular architecture that is the basis for those behaviors (Kravitz, 1988; Govind, 1989; Sandeman and Sandeman, 1990). Research on neural development at the embryonic level in *Homarus* is flourishing (Cole and Lang, 1980; Beltz and Kravitz, 1987; Beltz *et al.*, 1990; Helluy and Beltz, 1990; Meier and Reichert, 1990), but progress has been limited by the lack of adequate documentation on the general development of this organism in the egg, as well as by the absence of a staging system for the total embryonic period. These two problems are addressed in this paper.

Recent developmental studies in *Homarus* have dealt primarily with the perihatching period (Davis, 1964; Ennis, 1975; Charmantier and Aiken, 1987), and larval and postlarval life (Phillips and Sastry, 1980; Charmantier, 1987), whereas most of the literature concerned with the prehatching period dates back to the nineteenth century (Bumpus, 1891; Herrick, 1895). The latter studies are a remarkable achievement of patient and detailed observation and are illustrated by elegant drawings (Herrick, 1895), but the modern microscopic and photographic methods used in this study are necessary to provide added resolution. The nineteenth century studies also tend to focus on early embryogenesis while providing little or no information about middle and late development in the

egg, and the embryonic molt cycle. A deeper knowledge of lobster embryology could also provide more insight and understanding of studies that examine particular aspects of development, such as the influence of temperature on growth rate (Templeman, 1940; Perkins, 1972), population dynamics (Schuur *et al.* 1976; Hepper and Gough, 1978), the chemical composition and calorific content of the eggs (Pandian 1970a, b; Sasaki, 1984; Sasaki *et al.* 1986), or the differentiation of particular organs or systems, such as heart and gut (Burrage, 1978; Burrage and Sherman, 1979), and, again, nervous system.

The principal features involved in the reproduction and early development of the lobster *Homarus americanus* are well known. After copulation, spermatozoa are stored by the female for several months until oviposition and fertilization occur (Aiken and Waddy, 1980). In New England waters, egg development spans about 10 months, from egg extrusion in July or August to hatching the following May or June (Bumpus, 1891; Herrick, 1895). Following extrusion, the eggs are carried on the abdomen of the mother, attached to the pleopods. *Homarus* has relatively large, telolecithal eggs. Superficial cleavage leads to the formation of a blastoderm, and the central mass of yolk remains undivided (Bumpus, 1891). After only a few days, the naupliar organization is apparent. The nauplius, which is a developmental hallmark of crustaceans, is characterized by the presence of a median eye and three pairs of appendages: the antennulae, antennae, and mandibles (Shiino, 1988). The metanauplius arises from the differentiation and growth of the postmandibular appendages. *Homarus* hatches as a mature metanauplius (prelarva, prezoea) that molts rapidly into the first larval stage (Davis, 1964). There are three pelagic larval stages swimming with the feathery exopodites of six pairs of thoracic limbs. A metamorphosis leads to the formation of a postlarva (fourth stage) with most of the adult characteristics (Charmantier, 1987). The postlarva, which swims in a fully extended posture using its pleopods, later settles on the substrate. The duration of larval life, in the order of a few weeks, depends largely on temperature.

For the present study, behavioral, morphological, anatomical, and morphometric data were gathered from whole eggs and dissected embryos. A percent-staging scheme using the size of the pigmented area in the lateral eyes [the eye index (Perkins, 1972)] was adopted. Subsequently, ten equally spaced developmental stages were documented in detail with the eggs of different females. Particular attention was given to the growth and differentiation of the antennulae and telson. The antennulae, which are lined with aesthetascs (olfactory sensilla) in postembryonic animals from second larval stage on, were examined to gain insight into the ontogeny of the olfactory sensory apparatus. The telson was studied to elucidate how the round bilobed telson of the embryo is transformed into the triangular telson of the first larval stage.

Materials and Methods

Lobster and egg maintenance

Egg-bearing female lobsters *Homarus americanus* (Crustacea, Malacostraca, Decapoda, Reptantia, Astacidea, Nephropidae) were obtained from the Massachusetts State Lobster Hatchery on Martha's Vineyard, Massachusetts, and kept in recirculating artificial seawater. In addition, eggs detached from the mother's abdomen were provided by the New England Aquarium in Boston, Massachusetts, where lobsters were reared in filtered, temperature-controlled seawater. These detached eggs were maintained in our laboratory in free-floating net enclosures in artificial seawater. We found that hanging the clumps of eggs with surgical thread, and allowing them to float, led to good survival rates. Three tanks were maintained at temperatures of 10 ± 2°C, 18 ± 2°C, and 20 ± 2°C, to slow or accelerate the rate of development of the eggs, at a salinity between 27 and 32 ppt in a 12:12 light:dark cycle.

The experimental brood

We have not had any success promoting egg extrusion in females held in recirculating tanks, probably because of the variety of complex environmental factors necessary for this event (Waddy and Aiken, 1984). Therefore, in mid-October, the egg-bearing female containing the youngest eggs was chosen from a collection of approximately 200 gravid females collected by fishermen for the State Lobster Hatchery. The earliest stage observed in the experimental brood was a cleavage stage. The approximate date of extrusion was calculated as follows: in Templeman's (1940) experiments, the period from the late nauplius to the first appearance of pigment in the lateral eyes (26 days) lasted about 45% of the time required for the development from extrusion to appearance of eye pigment (58 days) at 12–13°C, and 41% (11/27) in Herrick's experiments (1895, p. 56) at 21°C. In the lobster (Templeman, 1940; Perkins, 1972) and in insects (Bentley *et al.*, 1979), developmental events are more condensed or expanded in time depending on temperature, but the proportion of the total duration of embryogenesis devoted to each developmental event does not change with temperature. In the present study at 18°C, the development from late nauplius to the first appearance of eye pigment took 9 days; therefore, by extrapolation from the data of Templeman (1940) and Herrick (1895), the period from extrusion to first appearance of eye pigment would be predicted to last 20–22 days. Thus, the estimated date of extrusion was calculated to be 21 days prior to the appearance of eye pigment. Note that extrusion did occur in the wild in water at seasonal temperatures.

Observations were made on the experimental brood kept at 18 ± 2°C for five months (mid-October to mid-

March, see Table I). The female died in mid-January, when the eggs were at 66% development; she was stripped of eggs and the spawn was suspended in nets in the tank. The eggs were agitated daily to try to replace the vigorous beating of the pleopods of the mother. In the experimental brood, the majority of the eggs attained the hatching stage but very few actually hatched into free metanaupliae; still fewer molted into first larval stages. Those larvae that did emerge were perfectly normal animals. The smoothness of growth curves of the experimental brood (see Results) and numerous observations on the progeny of other females confirmed that the free eggs of the experimental brood followed a normal course of development after the death of the mother.

Five live eggs from the experimental brood were examined every two or three days for the first two months, then once a week until hatching. As soon as the heart was formed, the heart beat was confirmed in each embryo to ensure that the observed eggs were alive. During each observation period, the width and length of the pigmented area in the lateral eyes (Fig. 1) and the greatest axis of the egg were measured in intact eggs; following dissection, the length of the cephalothorax was measured ventrally from the median eye to the anterior margin of the abdomen (Fig. 2). Behavioral observations, such as antennal twitching or tail flipping during dissection, were also noted. Photographs of whole eggs and dissected embryos were taken with a Zeiss stereomicroscope.

Developmental staging system

A developmental scale was designed that used the eye index (Perkins, 1972) as a marker of developmental progress. The eye index is defined as the average of the length and the width of the brown screening pigment spot (in micrometers) in the lateral eyes. The first measurable eye pigment spot had an eye index of 70 μm (Perkins, 1972; present study). Therefore, development prior to the appearance of eye pigment was characterized using time rather than the eye index. The estimated duration of development of the experimental brood was 159 days (Table I). Eye pigment first appears at 13.2% of the total time from extrusion to hatching, while the eye index at first appearance of pigment (70 μm) is 12.2% of the eye index of the experimental brood at hatching (578 μm) (Table I). These values indicate that there is little difference during early embryogenesis between staging based on time and that based on the eye index; time-staging was used prior to, and eye index-staging after 15% development (Table I). Later in embryogenesis, because of the period of developmental arrest (see Results), staging based upon time is no longer valid; the morphometric marker (eye index) must then be used.

Table I

Dates of observation of the experimental brood of Homarus americanus *maintained at 18°C, age, eye index, and percent-staging system. The dotted line signals the transition between percent of total time from extrusion to hatching and percent of eye index at hatching*

Date 88–89	Embryonic age (days)	Eye index (μm)	Stage (%)
10–08	0		0
10–16	8		5.3
10–18	10		6.3
10–20	12		7.6
10–23	15		9.4
10–25	17		10.7
10–27	19		12.0
10–29	21	70.6	13.2
10–31	23	72.5	14.5
11–02	25	98.0	17.0
11–04	27	139.2	24.1
11–06	29	145.0	25.1
11–08	31	156.8	27.1
11–11	34	160.7	27.8
11–18	41	213.6	37.0
11–24	47	248.9	43.1
12–01	54	282.2	48.8
12–08	61	307.7	53.2
12–15	68	329.3	57.0
12–23	76	352.8	61.0
12–29	82	366.5	63.4
01–05	89	386.1	66.8
01–12	96	382.2	66.1
01–19	103	425.3	73.6
01–26	110	447.0	77.3
02–02	117	441.0	76.3
02–09	124	458.6	79.3
02–16	131	466.5	80.7
02–23	138	474.3	82.1
03–02	145	474.3	82.1
03–09	152	542.9	93.9
03–16	159	578.2	100.0

Characterization of ten embryonic stages and of the embryonic molt cycle

Following the adoption of the percent-staging system, eggs from different broods were studied in more detail at every 10% increment in development. The eye index at hatching was estimated at 570 ± 20 μm (see Discussion), and therefore each 10% increment in developmental maturity was characterized by an increase of 57 μm in the eye index. The stage described as 10% was reached on day 16 in the experimental brood: the late egg-nauplius. Eggs were also examined when their eye indices measured 114 ± 6 μm (E20%), 171 ± 4 μm (E30%), 228 ± 7 μm (E40%), 285 μm ± 14 (E50%), 342 ± 11 μm (E60%), 399 ± 17 μm (E70%), 456 ± 5 μm (E80%), 513 ± 20 μm (E90%), 570 ± 20 μm (E100%). The varying range for each stage reflected embryo availability and limitations

imposed by the precision of the ocular micrometer. Twenty micrometers represents 3.5% of the total development scale. To characterize each of the ten stages and the early postembryonic stages, the same protocol described earlier for the experimental brood was used. Photographs of whole eggs (Figs. 3, 4) and dissected embryos (Fig. 5) were taken with a Zeiss stereomicroscope. In addition, antennulae (Fig. 6) and telsons (Fig. 7) were also severed, examined fresh, and photographed using a Zeiss IM35 photoinvertoscope equipped with modulation contrast optics (Hoffman, 1977).

Drach (1939) and Drach and Tchernigovtzeff (1967) designated the phases of ecdysis in crustaceans by letters from A to E: A and B are the postmolt periods, C the intermolt, D the premolt period, and E the ecdysis proper. In the present study, this system was used to characterize the molt cycle of *Homarus* that occurs within the egg envelopes. The period of the embryonic molt cycle was determined by matching setal changes in the telson of embryos (Figs. 7 and 8) with the setal changes in the telson previously documented in larvae of *Homarus americanus* (Rao *et al.*, 1973; Sasaki, 1984) and in the pleopods in juveniles (Aiken, 1973; 1980) during molt cycles. The subdivisions of stage D (D_0, D_1, D_{2-3}) and their distinguishing features are those described by Sasaki (1984).

Terminology

More than 70 terms have been used to refer to the various embryonic and larval stages of decapods (Gore, 1985). The form that arises from the differentiation and growth of the postmandibular appendages in the American lobster egg has been called a "post-nauplius" by Herrick (1895) or "postnauplius" by Helluy and Beltz (1990). In the present study "metanauplius" is used, a term commonly assigned to the form developing just past the naupliar stage (Wear, 1974; Williamson, 1982; Shiino, 1988). The form that is released from the egg envelopes and rapidly molts into the first larval stage is usually called a "prelarva" or "prezoea"; however, the term "mature metanauplius" seems more biologically relevant (see Discussion). The first larval stage of *Homarus* is sometimes referred to as a "mysis" (Shiino, 1988) based on the number of its appendages, or a first "zoea" because it locomotes with its thoracic appendages (Anderson, 1982; Williamson, 1982). Finally, "embryogenesis," "prehatch," and "egg development" are used interchangeably, although the latter part of egg development in *Homarus* is devoted to larval organogenesis rather than to embryogenesis strictly defined.

Results

I. Timing of development, sequence of events, and characterization of embryonic and early postembryonic stages

In the following account of the embryogenesis of *Homarus americanus*, the sequence of developmental events and morphometric data on eye index (EI) and cephalothoracic length (Figs. 1, 2) were obtained by studying the experimental brood, whereas the illustration and characterization of equally spaced embryonic and early postembryonic stages was achieved by studying many clutches

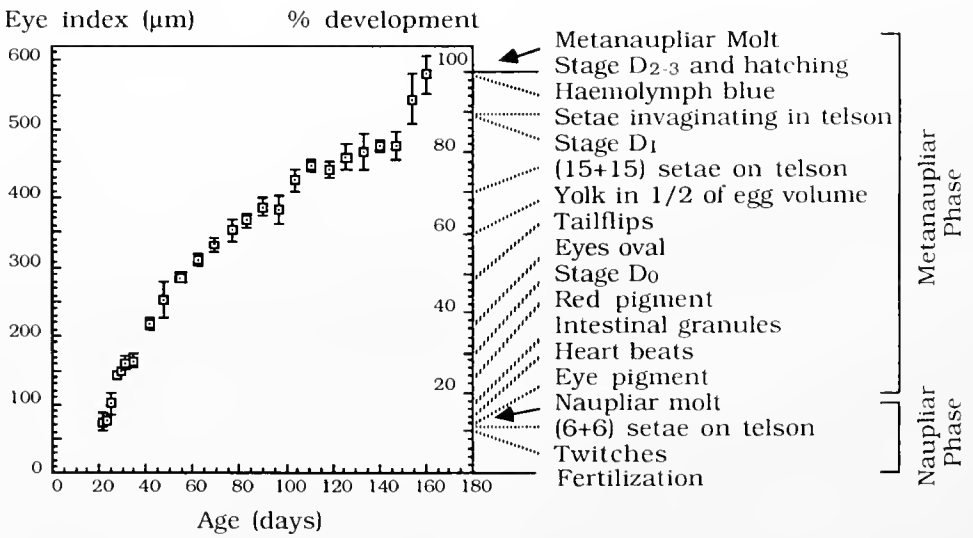

Figure 1. Eye index *versus* age of the experimental brood of *Homarus americanus*, maintained at 18°C. Developmental landmarks are indicated along a percent-scale based on the eye index. Perkins' eye index (1972) is the mean of the length and the width of the screening pigment spot in the lateral eyes. Each data point represents the mean of measurements on five individuals of the experimental brood ± one standard deviation.

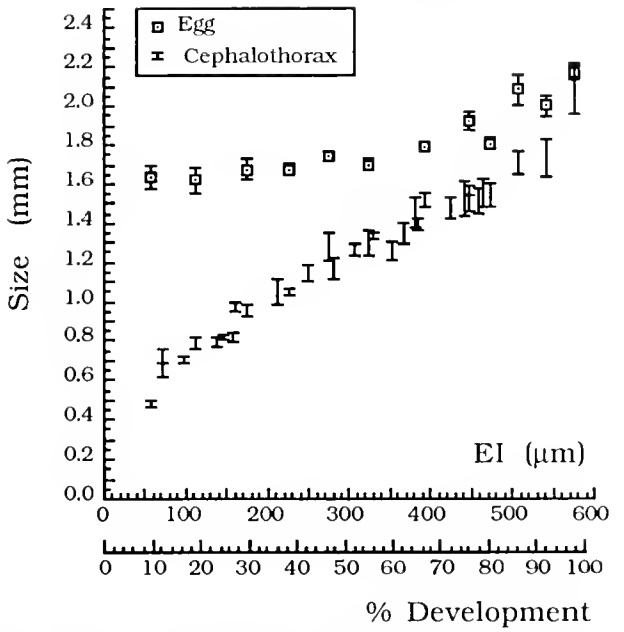

Figure 2. Greatest axis of egg and cephalothoracic length *versus* eye index and percent-development scale, in *Homarus americanus*. Greatest axis of egg: each data point represents the mean of five measurements ± one standard deviation (data points from different broods). Cephalothoracic length: the length of each bar represents one standard deviation on each side of the mean of five measurements (all individuals from experimental brood).

of eggs at different levels of resolution [whole eggs (Figs. 3, 4), dissected embryos (Fig. 5), antennulae (Fig. 6), and telsons (Figs. 7, 8)]. The stage of appearance of developmental events is expressed in percent-development of total embryogenesis. The percent-staging scheme is explained in "Materials and Methods." Dates of observation of the experimental brood, age, eye index, and percent-staging system are related in Table I and in Figure 1. The metanaupliar molt cycle is described in the second part of "Results."

Sequence of events prior to 10% development. The first organized structure to appear at the surface of the green yolk at 5% development (E5%, estimated day 8 of the experimental brood) is a typical crustacean nauplius with three pairs of appendages: the antennulae, the antennae, and the mandibles. The mandibles are first visible as two dots medial to the endopods of the antennae. This is equivalent to stage "M" of Bumpus with the eye lobes and the thoracoabdominal process still undefined. At E6% (day 10), the optic lobes appear as a white cloud of cells, and the thoracoabdominal process is clearly outlined. At E8% (day 12, stage "N" of Bumpus) the optic lobes are also delineated, and the embryo is easily separated from the yolk. The dorsal side of the embryo is apposed to the yolk, and the abdomen grows folded on the ventral side of the thorax. The tip of the abdomen reaches the level of the mandibles and is beginning to part medially at E9% (day 15, stage "O" of Bumpus); the buds of four pairs of post mandibular appendages line the trunk.

10% development (no eye pigment present: Figs. 3A, 5A, 6A, 7A). At E10%, the yolk occupies approximately 95% of the volume of the egg (Fig. 3A) whose greatest axis measures about 1.6 mm. The antennulae are uniramous and end with five setae whereas the antennae are biramous with five setae at the tip of the exopods and three setae at the tip of the endopods (Fig. 6A). The extremity of the abdomen nearly reaches the level of the labrum; the telson is beginning to part but setae are not yet present at its tip. This stage is equivalent to stage "O" of Bumpus (1891).

Sequence of events from 10% to 20% development. At E11% (day 17) at least 8 appendages are formed past the mandibles and at about this time, the first twitches in the two pairs of antennae occur upon dissection. Pigment is then visible in the median eye under the compound microscope. At about E12%, when pigment is already visible in the median eye but not yet in the lateral eyes, an embryonic molt occurs (see II, below). At least two envelopes surround the antennulae (Fig. 6B), and one envelope is stretched at the tip of the six setae (6 + 6) on each side of the telson indicating the occurrence of a molt (Figs. 7B, 8A). At about E13% (day 21), pigment is seen in the lateral eyes as a small dark crescent lining the posterior part of the lobes; the eye index at that stage is approximately 70 μm. At E14% (day 23), the first heartbeats are seen in approximately 10% of the embryos examined. By E17% (EI 98) heartbeats are seen in half of the eggs, and small refringent granules are present in the intestine.

20% development (EI = 114 μm; Figs. 3B, 5B, 6C, 7C). Muscular twitches are readily observed in the antennae, around the mouth, and in the abdomen, and the heart is beating. Between 10 and 20% of embryonic development, the nauplius has molted into a metanauplius (see II, below). This stage is equivalent to stage "P" of Bumpus (1891), defined as the stage when the tips of the third pair of maxillipeds reach the point of insertion of the antennulae and the telson reaches the level between the mouth and the median eye. The telson is provided with 6–7 setae on each of the two lobes (Fig. 7C).

Sequence of events from 20% to 30% development. At E24% (EI 139), red pigment spots (chromatophores) appear on each side of the brain. At E25% (EI 145) the telson reaches the anterior edge of the optic lobe (stage "Q" of Bumpus). The full complement of appendages present in the metanauplius is formed by E27% (EI 157), and by E28% (EI 161) the telson reaches beyond the optic lobes.

30% development (EI = 171 μm; Figs. 3C, 5C, 6D, 7D). The cephalothorax of the embryo is nearly 1 mm long. Red chromatophores are present on each side of the brain. A cluster of presumed sensory neurons has formed in the exopod of each antennula and their axons follow

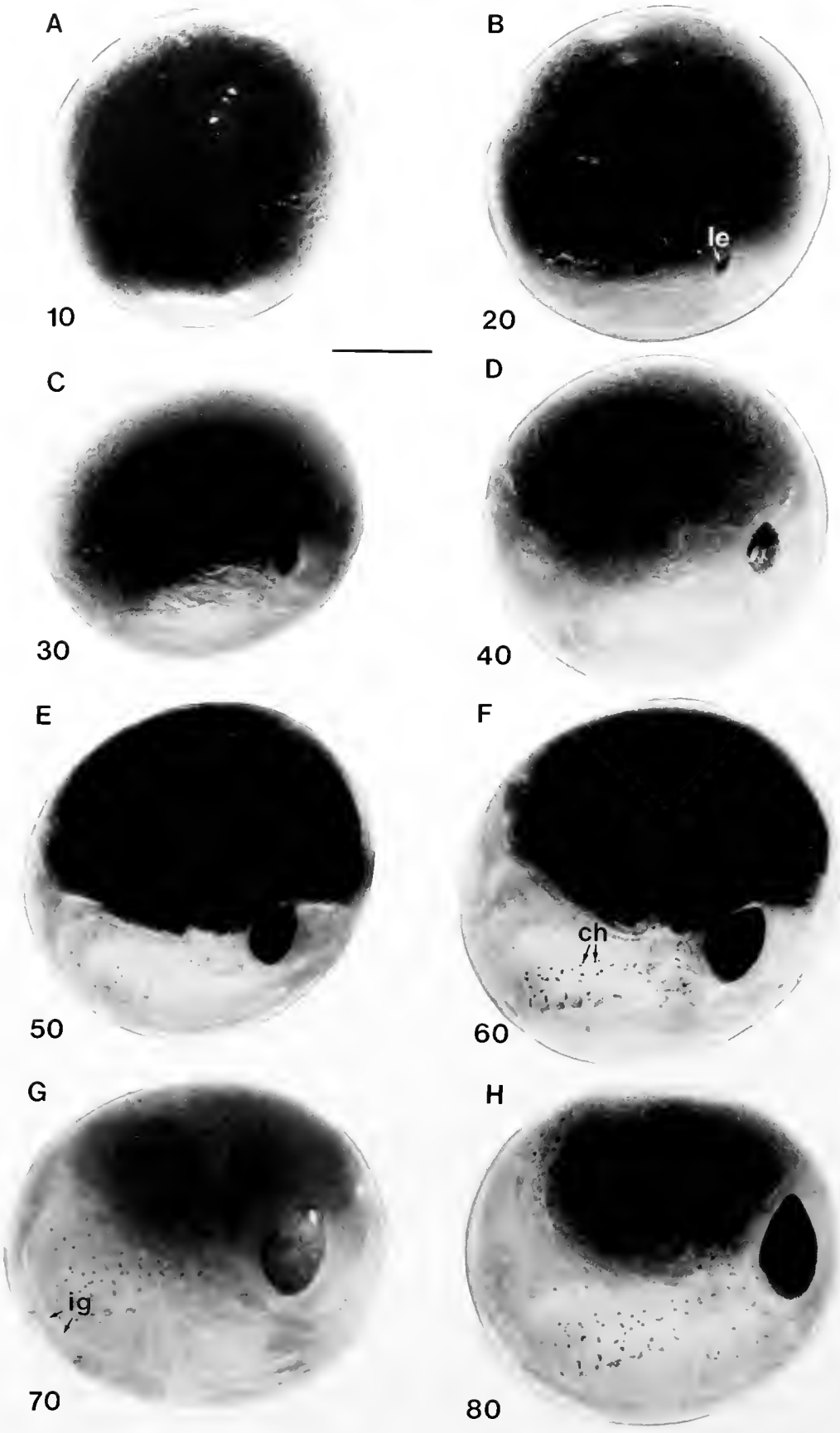
A
10
B
le
20
C
30
D
40
E
50
F
ch
60
G
ig
70
H
80

the anterior edge of these appendages in a bundle of a few micrometers (Fig. 6D). Serial plastic sections have shown that the bundle of axons projects to the olfactory lobes (in the deutocerebrum), which measure about 40 μm in diameter at that stage (unpub. results). The cluster of neurons is very similar to the cluster of bipolar sensory neurons that innervate each aesthetasc (olfactory sensillum) in the antennulae of spiny lobsters (Grünert and Ache, 1988). At E30% also, the endopod of each antennula tipped with a pointed seta, is visible under the cuticle (Fig. 6D). The endopods are freed after hatching when the metanauplius molts into a first larval stage (L1). The appearance of the endopod of the antennulae is the first visible sign of the formation of the L1 under the cuticle of the metanauplius. All postmandibular appendages are present and the trunk is lined with six pairs of prominent appendages: a pair of third maxillipeds and five pairs of walking legs. During the metanaupliar phase, the trunk appendages, which are uniramous, cannot be separated from each other. The tips of the third maxillipeds reach a level between the point of insertion of the antennulae and the anterior edge of the optic lobes whereas the telson is at the level of the anterior edge of the optic lobes [stage "Q" of Bumpus (1891)]. In the telson, the metanaupliar cuticle begins to separate from the side of the setae but the tip of these setae is still attached to the cuticle (Fig. 7D); this signals the start of the premolt stage D_0 of the metanaupliar molt cycle (see II, below).

Sequence of events from 30% to 40% development. Stage "R" of Bumpus is reached between E30% and E37% when the tip of the third maxillipeds is at the level of the antennae and the telson grows beyond the optic lobes. By E37%, the eye pigment spots have become oval rather than crescent-shaped, and red pigment granules line the sides of the nerve cord.

40% development (EI = 228 μm; Figs. 3D, 5D, 6E, 7E). A giant sensillum (260 μm) is visible as a long straight rod inverted at the tip of the exopod of each antennula. Setae are present at the extremities of trunk appendages. Red chromatophores are seen on the sides of the nerve cord, on the anterior edge of the optic lobes, and on the growing carapace. The third maxillipeds reach the anterior edge of the optic lobes, and the telson reaches anteriorly to the optic lobes. This stage is more advanced than stage "R," the most advanced stage described by Bumpus (1891).

Sequence of events from 40% to 50% development. The red chromatophores have invaded the appendages and the growing carapace by E43% and the abdomen by E49%.

50% development (EI = 285 μm; Figs. 3E, 5E, 7F). By E50%, some embryos perform very clear tailflips after removal of egg envelopes; also, the first caeca of the paired digestive glands (hepatopancreas) are seen, with the stereomicroscope, at the anterior end of the midgut where it comes in contact with the mass of yolk. The rostrum of the differentiating L1 is folded ventrally between the optic lobes and is visible upon dissection. The gap between the cuticle and the six or seven most distal and lateral setae on each side of the telson has widened, but the tips of these setae are still in contact with the cuticle (Fig. 7F). Other setae are growing more medially and more proximally beneath the cuticle of the telson. By now, the distal ends of the third maxillipeds, as well as the telson, reach anteriorly to the level of the optic lobes.

Sequence of events from 50% until hatching. There are no obvious changes in the general external morphology of the embryo from E50% until hatching (E100%). However, the embryo grows dramatically and the structures typical of the L1 are forming progressively beneath the cuticle of the metanauplius.

60% development (EI = 342 μm; Figs. 3F, 5F, 6F, 7G). At this stage the yolk occupies about half the volume of the egg. At least 10 setae are formed on each side of the telson (Fig. 7G).

70% development (EI = 399 μm; Figs. 3G, 5G, 7H, 8B). The full complement of setae (14 or 15 on each side) of the first larval stage is present on the telson under the metanaupliar cuticle; the median spine begins to differentiate (Figs. 7H, 8B).

80% development (EI = 456 μm; Figs. 3H, 5H, 6G, 7I). In the telson, only the most medial setae are in contact with the metanaupliar cuticle. These setae have not yet assumed the shape of spines, and the embryos are still in stage D_0 of the metanaupliar molt cycle (Fig. 7I).

90% development (EI = 513 μm; Figs. 4A, 5I, 6H, 7J, 8C). The egg is now enlarging rapidly, and its largest axis measures about 2.0 mm (Fig. 2). The yolk is turning yellow (Fig. 4A). The telson manifests a number of dramatic changes (Figs. 7J, 8C). The cuticle has lifted entirely from the setae and also from the epidermis on the lateral sides of the telson. The two most lateral setae are now pointed and sharp like spines, and they begin to retract. About a third of each seta is visible beneath the tegument. The

Figure 3. Unfixed, intact eggs of *Homarus americanus* at (A) 10, (B) 20, (C) 30, (D) 40, (E) 50, (F) 60, (G) 70, and (H) 80% embryonic development. The figures in the lower left corners refer to the percentage of development. In all photographs, the dorsal side is at the top, and the head and telson of the embryo are on the right. At 10% development (E10%), the embryo is seen as a small halo at the bottom part of the egg. The eye pigment is visible in the lateral eyes (le) by E20%. The red chromatophores (ch) already present by E40% are labeled at E60%. The intestinal granules (ig) are particularly clear at E70%. Scale bar: 500 μm.

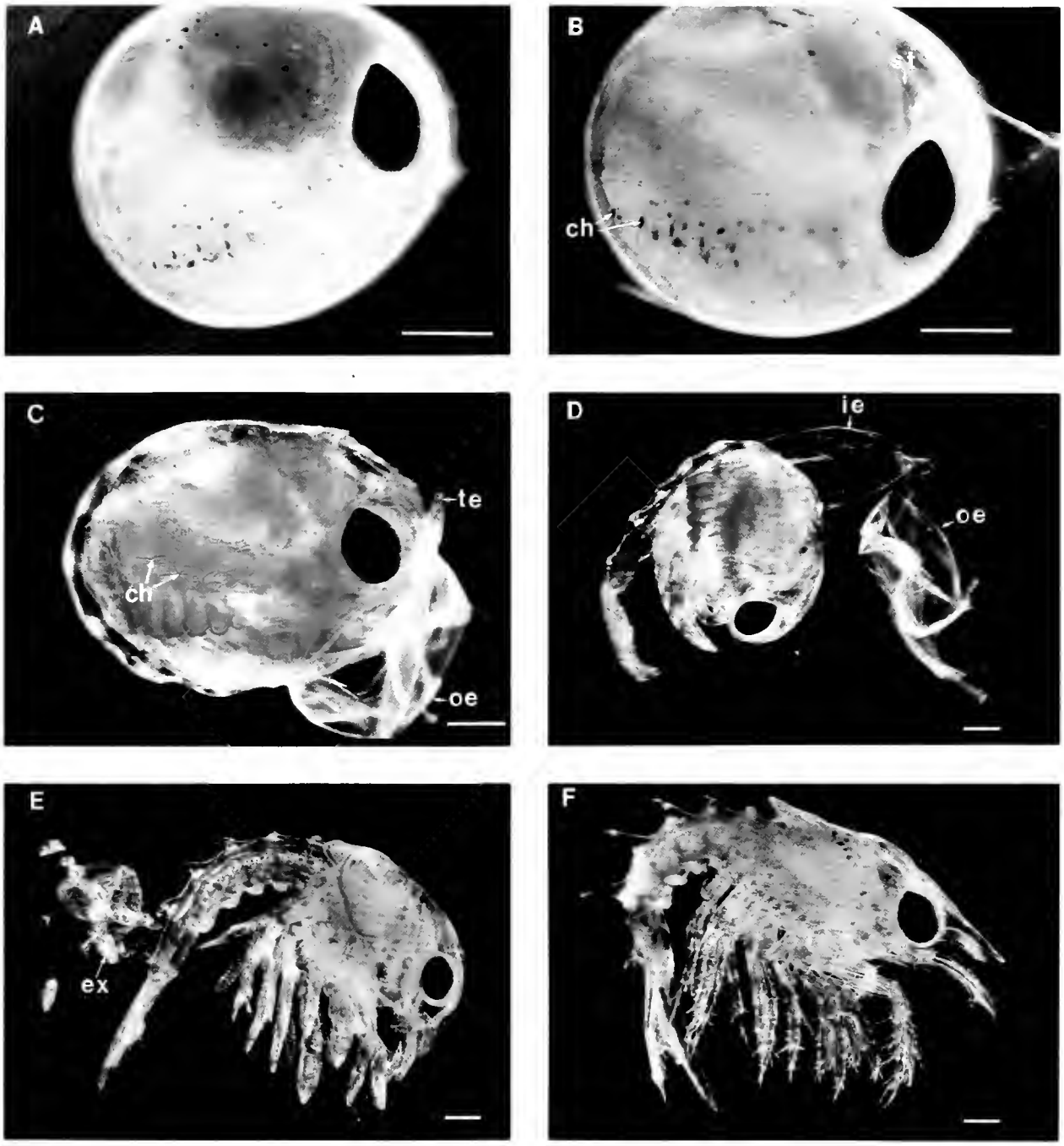

Figure 4. Perihatching development of *Homarus americanus*. In all these photographs of unfixed specimens, dorsal side is at the top, and anterior is right. (A) 90% embryonic development. (B) Embryo just prior to hatching (100%, blue embryo): note the blue tinge of the hemolymph, the blue stomach (st) and the red chromatophores (ch) in which the pigment is still concentrated. (C) Hatchling: the outer (oe) egg envelope has burst, and the telson (te) is piercing the inner egg envelope; the red pigment has spread in the star-shaped chromatophores (ch). (D) The metanauplius (prelarva, prezoea) is now free of both outer (oe) and inner (ie) egg envelopes. (E) Early first larval stage (first zoea): the exuvia (ex) of the metanauplius has been sloughed. (F) Mature first larval stage: rostrum, abdominal spines, and other acuminate structures are now erect. Scale bars: 500 μm.

epidermis forms papillae around each seta, and appears scalloped. Retraction of setae and scalloped epidermis are characteristic of stage D_1 (Sasaki, 1984).

100% development (EI = 570 μm; Figs. 4B, 7K). At this stage, just prior to hatching, the egg (2.2 mm) is brightly colored (Fig. 4B). The stomach is deep blue and the hemolymph pale blue. The yolk, which has been nearly entirely absorbed, is yellow or pale green. The two pairs of yolk caeca that were filling the egg earlier are attached to the digestive tube dorsally by this time, between the pyloric stomach and the numerous tubular digestive glands. The bilateral spines of the telson are entirely retracted, whereas the setae are only partially so.

Eclosion of the metanauplius (hatchling) (Figs. 4C, 6I, 7L, 8D). The outer egg envelope has burst. The red pigment disperses in star-shaped chromatophores (Fig. 4C). The giant sensillum is everted and projects from the exopods of the antennulae, but is still confined within the cuticle of the metanauplius (Fig. 6I). The spines and setae of the telson begin to expand (Figs. 7L and 8D). The epidermis becomes very distinct and forms a pronounced bulging around the invaginated setae; these are two characteristics of stage D_{2-3} of Sasaki (1984).

Free metanauplius (prelarva, prezoea; Fig. 4D). The metanauplius is freed of the two external egg envelopes; it is mostly still, but occasionally performs strong tail-flips. These movements presumably facilitate the molting process. Within hours after the egg membranes are shed, the metanauplius molts into a first larval stage.

Molt of the metanauplius and emergence of first larval stage (Figs. 4E and F, 6J, 7M). The exuvia peels away from the metanauplius. Slowly the rostrum, the abdominal spines, and all the other acuminate structures become erect. The telson opens like a fan into a triangular structure (Fig. 7M). The setae evaginate. The endopod of each antennula is released (Fig. 6J), as well as the feathery exopodites of the six pairs of thoracic appendages. Each antennula at hatching has one giant sensillum (550 μm) and three setae at the tip of the exopod, and one seta at the tip of the endopod (Fig. 6J) as reported by Herrick (1895). In brief, the curvaceous metanauplius molts into an angular larva ready to assume a pelagic life.

II. Metanaupliar embryonic molt cycle, growth curves and developmental plateau

Metanaupliar embryonic molt cycle. At about E12%, an envelope is seen enshrouding the telson (Figs. 7B and 8A), stretched at the tips of the 12 (6 + 6) bilaterally paired setae on the telson of the nauplius. This envelope is thought to be the exuvia of the naupliar stage; it is flat and was formed in the nauplius when the tip of the abdomen had not yet acquired any setae. The metanauplius that emerges at the naupliar molt has been forming during the naupliar stage. From this molt until the emergence of the first larval stage after hatching (metanaupliar molt), a complete molt cycle is observed in the setal changes of the telson. The cuticle begins to lift away from the telson at about E30% (Fig. 7D) when the metanauplius enters stage D_0. The shape of the 6 + 6 setae on the telson of the metanauplius is well defined on this cuticle. Setae form then medially and proximally, and by E70% (Fig. 7H, 8B), the full complement of setae of the first larval stage (15 + 15) is formed. Between E80% (Fig. 7I) and E90% (Fig. 7J), dramatic setal and tegumentary changes occur as the metanauplius enters stage D_1. Particularly striking is the transformation of the most lateral setae into straight and sharp spines (compare Figs. 7I and J, 8B and C). These spines are invaginating as well as all the setae. In addition, the epidermis becomes scalloped, and the cuticle lifts from the sides of the telson. Just prior to hatching (E100%), retraction of spines and setae is maximal. When the outer egg envelope ruptures, the bulging of the epidermis around the setae is pronounced, and the metanauplius has entered stage D_{2-3}. After hatching, the metanauplius molts into the first stage larva and the cuticle which is discarded still has the typical metanaupliar shape with the imprint of the (6 + 6) metanaupliar setae.

Growth curves and developmental plateau. The greatest axis of the egg increases gradually from 1.6 mm at E10% to about 1.8 mm at E80% and more rapidly to 2.2 mm at hatching (Fig. 2). In the experimental brood raised at 18°C, both the eye index (Fig. 1) and the cephalothoracic length showed a logarithmic growth from the first time these variables could be measured to approximately day 110. In Figure 2, cephalothoracic length appears linear because it is expressed as a function of the eye index. The eggs of the experimental brood reached a developmental plateau at an eye index of about 474 (E82%). Until this stage, development of the eggs was synchronous with little interindividual variability within the brood. This was shown by the low standard deviation of the eye index and of the cephalothoraxic length (Figs. 1, 2). Until 82%, all eggs were "green" and taken at random. However, after E82%, the population was no longer homogeneous, and the naked eye could distinguish by size and color three categories of eggs: "green," "yellowish" (Fig. 4A), and "blue" (Fig. 4B). In addition, the eggs hatched over a period of about a month, again indicating significant variability between eggs in a single brood. After E82% it was no longer possible to choose eggs randomly for observation; to assign an approximate age to each of these stages, "yellowish eggs" were examined on day 152 when the majority of eggs had reached this stage, and "blue eggs" (the hatching stage) were examined a week later. Individual eggs took about two weeks to change from "green" to "blue" eggs at 18°C.

Discussion

In the present paper, different aspects of the embryonic development of *Homarus americanus* are examined from

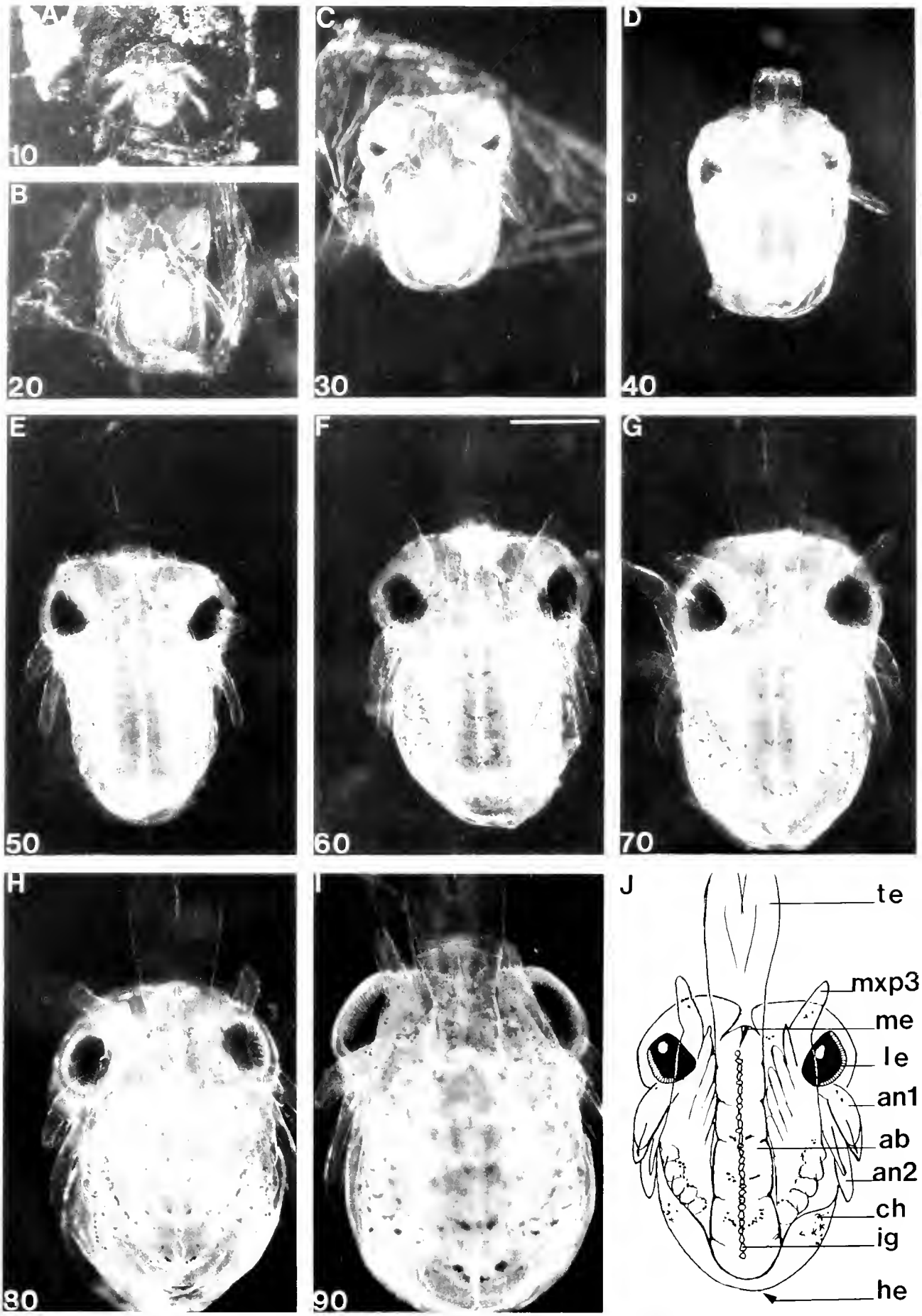
A
10
B
20
C
30
D
40
E
50
F
60
G
70
H
80
I
90
J
te
mxp3
me
le
an1
ab
an2
ch
ig
he

the formation of the naupliar stage until the emergence of the first larval stage. In the discussion that follows, the percent-staging scheme presented is compared to that used in other invertebrate systems, and anatomical and morphological observations of earlier authors are related to that staging system. The developmental plateau in the growth curve of the eggs is discussed in the context of the embryonic molt cycle. The occurrence of embryonic molt cycles in other crustaceans is reviewed and the significance of the prelarva debated.

Staging system

Embryonic studies on invertebrates have used staging systems based upon particular developmental events, and arbitrary notations such as letters or figures (Bumpus, 1891; Figueiredo and Barraca, 1963; Fernandez, 1980) to demarcate stages. Nevertheless, when intermediate stages are likely to be needed, a continuous rather than incremental staging system, and in particular a percent-staging system, is more flexible and communicable (Bentley *et al.*, 1979). In addition, a percent-staging method takes into account the entire embryonic life of the organism without ignoring periods when no particular biological events seem noticeable. For example, Bumpus (1891), Herrick (1895), and Templeman (1940) observed *Homarus* eggs only until the lateral eye pigment spots became oval, about 40% embryonic development in the present study.

Age in warm-blooded animals is generally a good indicator of the stage of development, but in invertebrates the rate of development is strongly dependent on temperature. To circumvent this problem, some methods have relied on a percent-staging scale of total embryonic time (*Schistocerca:* Bentley *et al.*, 1979; *Helisoma:* McKenney and Goldberg, 1989; *Cherax:* Sandeman and Sandeman, in press). In these studies, the staging scale is "calibrated" at a given constant temperature. The time from fertilization to hatching is then transformed into a percent-staging scale. This scale is applicable to animals raised at other temperatures because all developmental events are compressed or expanded proportionally, depending upon the temperature.

However, as pointed out by Bentley *et al.* (1979), a staging system based on percent of total time of embryogenesis cannot be applied in species with a period of developmental arrest. *Homarus* embryos manifest a period of arrested development in natural conditions (Perkins, 1972) and at constant temperature (present study) and these results indicate that factors other than temperature have a strong influence on the rate of embryonic development in lobsters. Therefore, we have used a morphometric index, the size of the screening pigment spot in the lateral eyes (the eye index of Perkins, 1972), as the basis for a percent-staging scheme. The eye index has been used as an indicator of developmental stage in a number of embryonic studies (Schuur *et al.*, 1976; Hepper and Gough, 1978; Cole and Lang, 1980; Sasaki, 1984; Sasaki *et al.*, 1986; Beltz and Kravitz, 1987; Beltz *et al.*, 1990; Helluy and Beltz, 1990; Meier and Reichert, 1990).

There are two obvious limitations of a staging system based upon the eye index. First, the eye pigment does not appear until approximately three weeks after egg extrusion, and at the first possible measurement is about 70 μm. To calibrate the relatively brief period from extrusion to appearance of eye pigment, a time-staging analysis has been used (see Materials and Methods). Thus, a percent-staging system has been established that covers the entire embryonic period, from extrusion until hatching. The second drawback of the proposed method is related to the variation of the eye index at hatching. Perkins (1972) reported that the eye index at hatching is 560 μm. Just prior to hatching in four broods that we have examined, it ranged from 570 μm to 586 μm and, taking into account Perkins' figure of 560 μm, 570 $\pm$ 20 μm was chosen as the eye index at hatching. This figure was used as the end point in establishing the percent-staging scale. The 20 μm variation represents a small proportion (3.5%) of the total percentage scale. The variation of the eye index at hatching could be due to a combination of factors such as genetic variability or perturbations due to environmental conditions. For instance, it has been reported that molting and development of morphological characteristics proceed somewhat independently in decapods (Gore, 1985), and it is conceivable that the physiological changes that regulate hatching and molting could be advanced or delayed with respect to morphogenesis and growth.

Growth curves and the developmental plateau

Lobster egg masses kept at seasonal water temperature show a developmental plateau when the temperature is low during the winter months (Perkins, 1972). More surprising is the fact that our experimental brood, which was

Figure 5. Ventral view of embryos of *Homarus americanus* dissected from the yolk and unfixed at (A) 10, (B) 20, (C) 30, (D) 40, (E) 50, (F) 60, (G) 70, (H) 80, and (I) 90% development. In all photographs, the head is at the top and the abdomen is folded ventrally onto the thorax. The figures in the lower left corners refer to the percentage of development. The line drawing (J) represents a schematic metanauplius. Abbreviations, ab: abdomen, anl: antennula, an2: antenna, ch: chromatophores, he: heart, ig: intestinal granules, le: lateral eye, me: median eye, mxp3: third maxilliped, te: telson. Scale bar in (F), valid from (A) to (I): 500 μm.

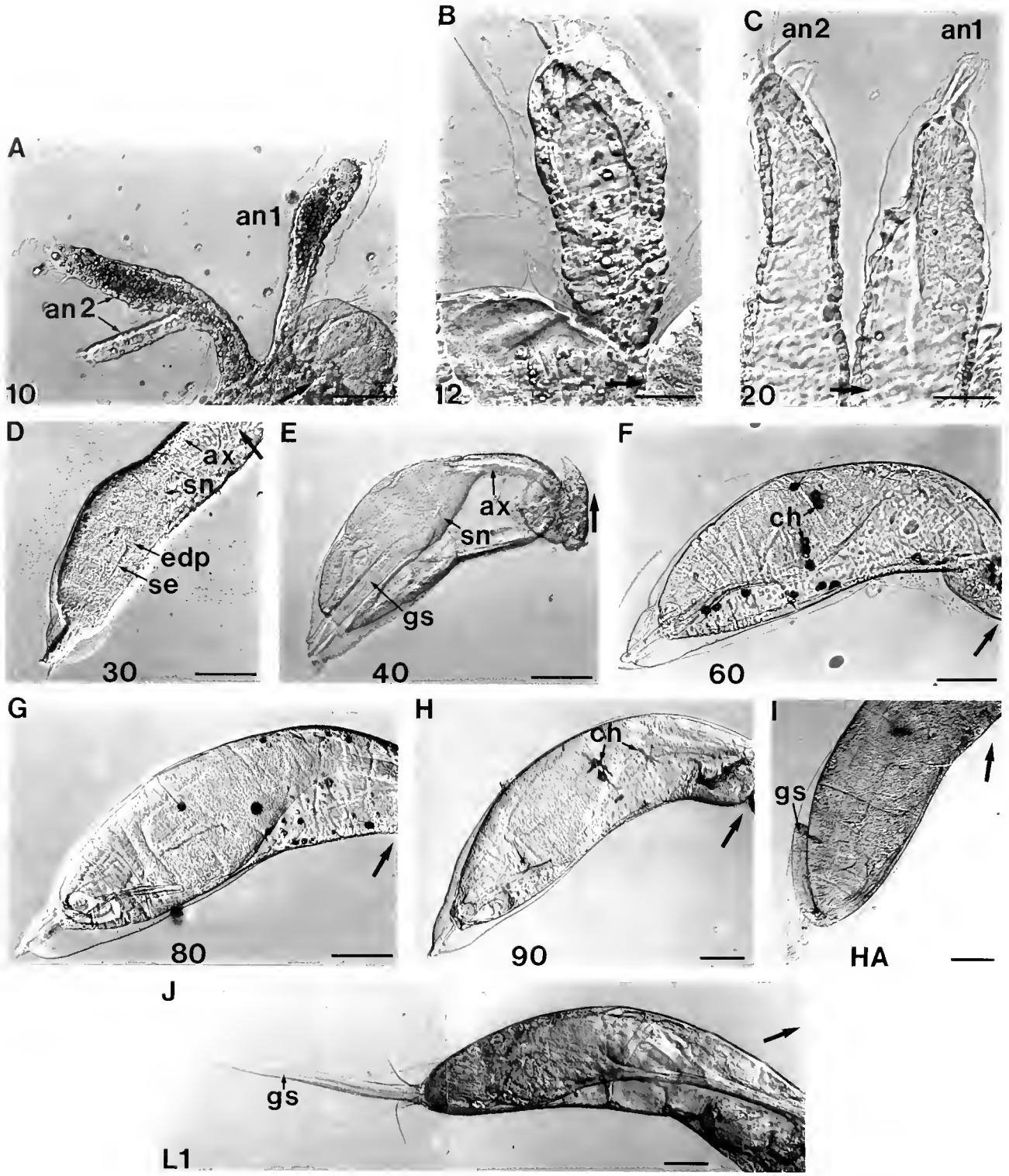

Figure 6. Unfixed antennulae of embryos of *Homarus americanus* at (A) 10, (B) 12, (C) 20, (D) 30, (E) 40, (F) 60, (G) 80, and (H) 90% development, in (I) a hatchling (HA) and in (J) a first larval stage (L1). In all photographs, the figures in the lower left corners refer to the percentage of development. Thick arrows point at the anterior end of the animals. The antenna (an2) is also shown in (A) and (C) in addition to the antennula (an1). By 30% development (E30%), a cluster of presumed sensory neurons (sn) and their axons (ax) are present in the antennula and are particularly visible at E40%. At E30%, the endopod (edp) of the antennula and the seta (se) at its tip are growing: the organogenesis of the first larval stage has already started. The endopod

raised at constant temperature, also showed a developmental plateau. The arrest in development characterized by a lack of growth in either the eye index or the cephalothoracic length, occurred at E82% development (EI 474). At E80%, the eggs are green and the metanauplii are still at stage D_0, whereas by E90% eggs are yellowish and have entered stage D_1. The heterogeneity of the egg population and the changes in pace of development observed in the experimental brood prior to hatching were therefore related to the transition from D_0 to D_1 of the metanaupliar molt cycle.

Developmental plateaus also occur during stage D_0 of the molt cycle in juvenile lobsters (Aiken, 1973). The arrest in development takes place at different times during stage D_0, from the first indication of epidermal retraction to maximal epidermal retraction. Lobsters pause in their development during the cold winter months, and the transition to the irreversible stage D_1 does not proceed until the water warms up in the spring. Aiken (1973) shows that when a lobster has passed beyond pleopod stage 2.5—and therefore entered stage D_1—development then proceeds at a rate regulated by temperature. It is possible that the embryonic metanauplius goes through the same cycle. Indeed, developmental plateaus have been observed at different eye indices during stage D_0 (from 350 μm to 450 μm) in different broods of eggs (Thomann, Beltz, and Helluy, unpub. results). Additionally, Perkins (1972) notes that during the winter months development is arrested in older eggs (extruded early in the summer) and still continues in younger eggs extruded later. It appears, therefore, that in the wild the eggs may spend a variable amount of time in stage D_0 (shorter in younger eggs); in the spring, internal and external cues could trigger the transition from D_0 to D_1. This could explain why extrusion of eggs is a prolonged event in a population of females in the wild, whereas hatching occurs during a more limited period (Herrick, 1895; Perkins, 1972).

Embryonic molt cycles

In the present study, evidence is presented for two molts occurring in *Homarus* prior to the first larval stage and associated with the beginning and the end of the embryonic metanaupliar stage. Other crustaceans are also known to pass through molt cycles within the egg envelopes (Wear, 1974; Goudeau, 1976; Goudeau and Lachaise, 1983). Graf (1972) characterizes the embryonic molt cycle of an amphipod on the basis of changes in the epidermis, setae, and calcium storage; these changes parallel those occurring during juvenile and adult molt cycles. In *Homarus* both Herrick (1895) and Bumpus (1891) mention the existence of embryonic molts. Based on the number of membranes enclosing the embryo, Herrick (1895, p. 183) presumes that at least three embryonic molts have occurred by the time the pigment appears in the lateral eyes and predicts that many more may take place during the long embryonic life. Bumpus (1891) notes that the cuticle lifts from the embryo in the region of the compound eye between stages N and O, and that a true ecdysis follows; this molt is probably the same as that observed in the present study around E12%, which is slightly after stage O of Bumpus. Goudeau *et al.* (1990), using electron microscopy, detect five envelopes originating from the embryo of *Homarus gammarus* secreted beneath the inner and outer egg envelopes and show that the secretion of the embryonic envelopes is associated with high titers of ecdysteroids; however, the embryos are not staged and the timing of secretion is not studied. The fact that the metanaupliar cuticle that begins to lift from the telson at 30% development possesses the imprint of the 6 + 6 setae that were present at the naupliar molt, and the fact that this same metanaupliar cuticle with the imprint of the 6 + 6 setae is discarded at the metanaupliar molt, demonstrate that there is only one instar during that period, not the many that were predicted by Herrick (1895). The progressive setal changes observed in the metanaupliar telson also support this conclusion. The several envelopes seen at the level of the antennulae (Fig. 6B) and antennae at stage E12% may indicate that additional molts occur prior to E12%, during the naupliar phase.

Whereas the setal changes occurring in the telson of the metanauplius seem very similar to those occurring during the molt cycle of larval and juvenile lobsters (Aiken, 1973; Rao *et al.*, 1973; Aiken, 1980; Sasaki, 1984), the cellular and biochemical changes in the epidermis and cuticle must be somewhat different. In the growing metanauplius there is no fixed postecdysial volume as there is in postembryonic animals. Indeed, the cephalothorax of the embryo grows by a factor of about 4 from the early 12% molt to the hatch molt (Fig. 2). Therefore, we presume that there is no mineralization of the metanaupliar cuticle. In that respect, it has also been noted before (see review in Gore, 1985) that the prezoeal cuticle is different from the exuvia of older lobsters.

---

of the antennula is also seen under the cuticle of the metanauplius at E80%, at E90%, and in the hatchling but is out of focus in the photographs of other stages. The giant sensillum (gs) at the tip of the exopod of the antennula is clearly seen forming inverted at E40% development, everted in the hatchling under the cuticle of the metanauplius, and free and erect with three other setae at the tip of the exopod in the antennula of the first larval stage. The red pigment in the chromatophores (ch) is seen concentrated at E60% and E80% and dispersed at E90%. Scale bars, A: 100 μm, B and C: 50 μm, D to J: 100 μm.

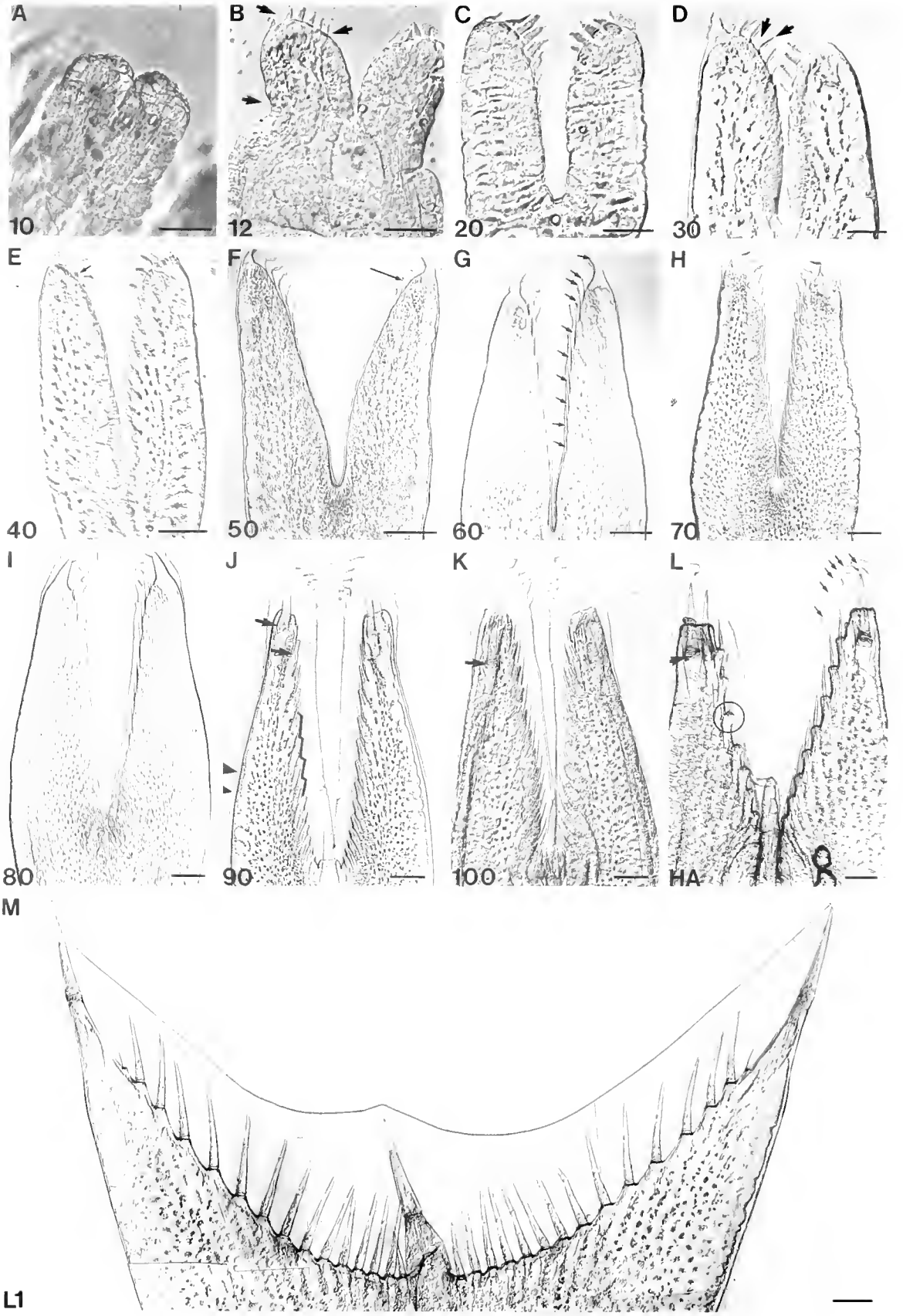
A
10
B
12
C
20
D
30
E
40
F
50
G
60
H
70
I
80
J
90
K
100
L
HA
M
L1

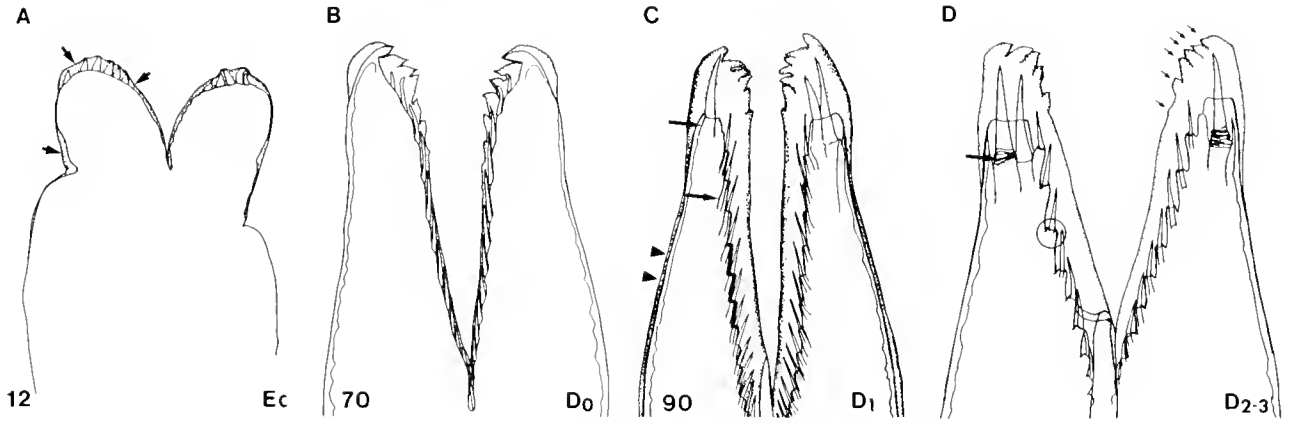

Figure 8. Line drawings of telsons of *Homarus americanus* at (A) 12, (B) 70, (C) 90% development, and (D) in a hatchling showing the naupliar ecdysis (Ec) and representative stages D_0, D_1, D_{2-3}. For photographs of those stages and legend, see Figure 7.

Lobster embryonic development in perspective

In the present study, the metanaupliar molt cycle and the organogenesis of the first larval stage of *Homarus* are examined. This aspect of development is generally ignored in the literature. For example, Bumpus (1891) studies the early embryology of *Homarus* only until stage R (between E30% and E40% development). Herrick (1895, p. 209) implies that the organogenesis of the L1 is extremely brief and takes place just prior to eclosion when he observes that the antennulae "remain single until just before the time of hatching when the inner branch of the flagellum begins to grow." In the present study the endopod (inner branch of the flagellum) of the antennulae is first seen at about 30% development. Therefore, our examination of both the antennulae and the telson indicate that the organogenesis of L1 begins early and continues throughout the embryonic molt cycle.

Overlooking the embryonic metanaupliar molt cycle has led to some confusion as to the status of the prezoea (prelarval form). The existence of a prezoea has been noted in many families of decapods, but its significance has been largely debated (see review in Gore, 1985). We agree with Wear (1974), who observes that "in decapods which hatch at a zoea stage, the prezoeal cuticle is associated with the metanauplius stage relegated to embryonic life, rather than to the preceding nauplius." This is clearly the case in *Homarus:* the ephemeral prelarva (prezoea) *is* the mature metanauplius between the moment it is freed of the two external egg envelopes and the time it molts (Fig. 4D).

Figure 7. Telsons of embryos of *Homarus americanus* (unfixed) at (A) 10, (B) 12, (C) 20, (D) 30, (E) 40, (F) 50, (G) 60, (H) 70, (I) 80, (J) 90, (K) 100% development, in (L) a hatchling (HA), and (M) a first larval stage (L1). Panel M is a montage. In all photographs, distal is at the top. The figures in the lower left corners refer to the percentage of development. The tegumentary and setal changes typical of different stages of the molt cycle as described by Aiken (1973 and 1980), Rao *et al.* (1973), and Sasaki (1984) in larval, juvenile, and adult lobsters are indicated with an asterisk in the following text. At about 12% development (E12%), an embryonic exuvia is lifting from the telson of the nauplius (arrows). The telson of the metanauplius forming under that exuvia is provided with 6 + 6 setae. At E30%, the metanaupliar cuticle begins to separate from the side of the setae* but the tips of these setae are still attached to the cuticle (arrows); this stage is equivalent to the premolt stage D_0 of the molting cycle of older lobsters. During the metanaupliar molt cycle, the setae present on the triangular telson of the first larval stage (first zoea) are forming gradually, proximally and medially in the telson of the metanauplius. By E60% at least 10 + 10 setae (arrows) are visible under the metanaupliar cuticle. At E70%, the full complement of setae of the first larval stage (15 + 15) is formed. Between E80% and E90%, dramatic setal and tegumentary changes occur. At E90% the epidermis is scalloped* (black line); setae and lateral spines are invaginating* (arrows) and the cuticle lifts from the sides of the telson (arrowheads); this stage is equivalent to D_1. Just prior to hatching (E100%) retraction of spines and setae is maximum. Note the crumpled tissue at the base of the lateral spines (arrow). In the hatchling (HA), this tissue forms a dark ring (arrow), the lateral spines are half extended, the epidermis is very distinct* and the bulging of the epidermis around the setae is pronounced* (circle) which is characteristic of stage D_{2-3}. Ecdysis takes place thereafter, and the metanaupliar cuticle bearing the shape of the 6 + 6 metanaupliar setae (arrows) is shed. After ecdysis the triangular telson of the first larval stage (L1) unfolds. Note that two individuals (J and L) had two lateral spines on one side. Scale bars, A to D: 50 μm, E to M: 100 μm.

One interpretation of the coupling of hatching and molting is that hatching is actually a by-product of the molting process. For instance, the extension of the lateral spines of the telson (Fig. 7L) could provoke the breaking of the inner and outer egg envelopes (Fig. 4C, D). Indeed, the lateral setae of the telson are smooth and extended until 80% development (Fig. 7I), begin to invaginate as soon as they become sharp (Figs. 7J, 8C), are entirely invaginated in the blue embryo (E100%) just prior to hatching (Fig. 7K), and are seen half evaginated in the hatchling (Figs. 7L, 8D) whose telson has just pierced the egg envelopes (Fig. 4C). No other part of the mature metanauplius is quite as hard and sharp as the lateral spines of the telson and it is therefore possible that the extension of these spines triggers the rupture of the egg envelopes. By this means, the metanauplius at the end of its molt cycle would precipitate hatching, and the beating of the pleopods of the mother would help the larva to slip out of its swaddling envelopes.

Molt cycles in postembryonic crustaceans are under hormonal control, and it is likely that embryonic molt cycles are regulated in a similar way. The circulating molting hormone is an ecdysteroid whose titers increase in D_0 and peak in D_2–D_3 in *Homarus* (Snyder and Chang, 1991) and in D_1 in *Penaeus* (Chan *et al.*, 1988). Because steroids influence neuronal development and survival in other systems (Weeks and Truman, 1986), the awareness of embryonic molts and the prediction of the timing of potential changes in steroid levels could be critical for future developmental neurobiological studies.

The nauplius is a form common to all crustaceans, and in some taxa (*e.g.*, Cirripedia, Anostraca) eggs hatch as naupliі. In other species, the naupliar stage is followed within the egg envelopes by the organogenesis of a more complex body form characterized by the morphogenesis and growth of the postmandibular region (Anderson, 1979, 1982; Weygoldt, 1979; Williamson, 1982; Gore, 1985; Schram, 1986; Shiino, 1988). It has been shown in several taxa [amphipods: Graf (1972); isopods: Goudeau (1976); decapods: Wear (1974), and the present study] that envelopes equated to embryonic exuvia are found during embryonic life as the postmandibular region differentiates. In amphipods (Graf, 1972) and decapods (present study), embryonic molt cycles are demonstrated with the progressive setal and tegumentary changes occurring in the telson. The existence of embryonic molt cycles in different taxa suggests that the relegation of larval stages to life in the egg, or, rather, the delay of hatching with regard to molting, is a widespread and distinctive evolutionary strategy in crustaceans. Besides leading to evolutionary considerations, the characterization of the metanaupliar molt cycle and the percent-staging scheme for lobster eggs should lend added insight in future investigations of neural, physiological, and ecological aspects of *Homarus* embryonic life.

Acknowledgments

We wish to thank Maureen Ruchhoeft for her kind and skillful help, Joe Gagliardi and Kay Leland for printing photographic plates, Michael Syslo and Kevin Johnson from the Massachusetts State Lobster Hatchery who provided the egg-bearing female lobsters, as well as Colleen Boggs and Tom Coffee who maintained them at the New England Aquarium. (Supported by NSF-BNS-8718938, NIH-NS 25915, and NSF- Presidential Young Investigator Award BNS- 8958169 to B.S.B.)

Literature Cited

Aiken, D. E. 1973. Proecdysis, setal development, and molt prediction in the American lobster (*Homarus americanus*). *J. Fish. Res. Board Can.* **30:** 1337–1344.

Aiken, D. E. 1980. Molting and growth. Pp. 91–163 in *The Biology and Management of Lobsters*, Vol. 1, J. S. Cobb and B. F. Phillips, eds., Academic Press, New York.

Aiken, D. E., and S. L. Waddy. 1980. Reproductive biology. Pp. 215–276 in *The Biology and Management of Lobsters*, Vol. 1, J. S. Cobb and B. F. Phillips, eds., Academic Press, New York.

Anderson, D. T. 1979. Embryos, fate maps, and the phylogeny of arthropods. Pp. 59–105 in *Arthropod Phylogeny*, A. P. Gupta, ed., Van Nostrand-Reinhold, Princeton, NJ.

Anderson, D. T. 1982. Embryology. Pp. 1–41 in *The Biology of Crustacea*, vol. 2, *Embryology, Morphology, and Genetics*, L. G. Abele, ed. Academic Press, New York.

Beltz, B. S., and E. A. Kravitz. 1987. Physiological identification, morphological analysis, and development of identified serotonin-proctolin containing neurons in the lobster ventral nerve cord. *J. Neurosci.* **7:** 533–546.

Beltz, B. S., M. S. Pontes, S. M. Helluy, and E. A. Kravitz. 1990. Patterns of appearance of serotonin and proctolin immunoreactivities in the developing nervous system of the American lobster. *J. Neurobiol.* **21:** 521–542.

Bentley, D., H. Keshishian, M. Shankland, and A. Toroian-Raymond. 1979. Quantitative staging of embryonic development of the grasshopper, *Schistocerca nitens*. *J. Embryol. Exp. Morphol.* **54:** 47–74.

Bumpus, H. C. 1891. The embryology of the American lobster. *J. Morphol.* **5:** 215–262.

Burrage, T. G. 1978. Fine structural development and activity in the heart and midgut of the embryonic lobster, *Homarus americanus* (Milne-Edwards). Ph. D. thesis, Clark University, Worcester, MA.

Burrage, T. G., and R. G. Sherman. 1979. Formation of sarcomeres in the embryonic heart of the lobster. *Cell Tissue Res.* **198:** 477–486.

Chan, S.-M., S. M. Rankin, and L. L. Keeley. 1988. Characterization of the molt stages in *Penaeus vannamei*: setogenesis and hemolymph levels of total protein, ecdysteroids, and glucose. *Biol. Bull.* **175:** 185–192.

Charmantier, G. 1987. Le développement larvaire et la métamorphose chez les Homards (Crustacea, Decapoda). *Oceanis* **13:** 137–165.

Charmantier, G., and D. E. Aiken. 1987. Osmotic regulation in late embryos and prelarvae of the American lobster *Homarus americanus* H. Milne-Edwards, 1837 (Crustacea, Decapoda). *J. Exp. Mar. Biol. Ecol.* **109:** 101–108.

Cole, J. J., and F. Lang. 1980. Spontaneous and evoked postsynaptic potentials in an embryonic neuromuscular system of the lobster, *Homarus americanus*. *J. Neurobiol.* **11:** 459–470.

Davis, C. C. 1964. A study of the hatching process in aquatic invertebrates. XIII. Events of eclosion in the American lobster, *Homarus americanus* Milne-Edwards (Astacura, Homaridae). *Am. Midl. Nat.* **72:** 203–210.

Drach, P. 1939. Mue et cycle d'intermue chez les Crustacés Décapodes. *Ann. Inst. Oceanogr.* **19:** 103–392.

Drach, P., and C. Tchernigovtzeff. 1967. Sur la méthode de détermination des stades d'intermue et son application générale aux crustacés. *Vie Milieu A* **18:** 595–610.

Ennis, G. P. 1975. Observations on hatching and larval release in the lobster *Homarus americanus*. *J. Fish. Res. Board Can.* **32:** 2210–2213.

Fernandez, J. 1980. Embryonic development of the glossiphoniid leech *Theromyzon rude*: characterization of developmental stages. *Dev. Biol.* **76:** 245–262.

Figueiredo, M. J., and I. F. Barraca. 1963. Contribuicao para o conpecimento da pesca e da biologia do Lagostim (*Nephrops norvegicus* L.) na Costa Portuguesa. *Notas Estud. Inst. Biol. Marit. (Lisb.)* **28:** 1–28.

Gore, R. H. 1985. Molting and growth in decapod larvae. *Crust. Issues* **2:** 1–65.

Goudeau, M. 1976. Secretion of embryonic envelopes and embryonic molting cycles in *Hemioniscus balani* Buchholtz, Isopoda, Epicaridea. *J. Morphol.* **148:** 427–451.

Goudeau, M., and F. Lachaise. 1983. Structure of the egg funiculus and deposition of embryonic envelopes in a crab. *Tissue and Cell* **15:** 47–62.

Goudeau, M., F. Lachaise, G. Carpentier, and B. Goxe. 1990. High titers of ecdysteroids are associated with the secretory process of embryonic envelopes in the European lobster. *Tissue and Cell* **22:** 269–281.

Govind, C. K. 1989. Asymmetry in lobster claws. *Am. Sci.* **77:** 468–474.

Graf, F. 1972. Stockage de calcium et formation des soies chez l'embryon d'*Orchestia* (Crustacé, Amphipode, Talitridé). Notion d'intermue embryonnaire. *C. R. Acad. Sc. Série D* **275:** 1669–1672.

Grünert, U., and B. W. Ache. 1988. Ultrastructure of the aesthetasc (olfactory) sensilla of the spiny lobster, *Panulirus argus*. *Cell Tissue Res.* **251:** 95–103.

Helluy, S., and B. S. Beltz. 1990. Stages in the embryonic development of the American lobster *Homarus americanus* with special emphasis on its nervous system. Pp. 530–536 in *Frontiers in Crustacean Neurobiology*, K. Wiese, W. D. Krenz, J. Tautz, H. Reichert and B. Mulloney, eds. Birkhaüser, Basel, Boston.

Hepper, B. T., and C. J. Gough. 1978. Fecundity and rate of embryonic development of the lobster, *Homarus gammarus* (L), off the coast of North Wales. *J. Cons. Int. Explor. Mer* **38:** 54–57.

Herrick, F. H. 1895. The American lobster: a study of its habits and development. *Bull. U.S. Fish. Commission* **15:** 1–252.

Hoffman, R. 1977. The modulation contrast microscope: principles and performance. *J. Microsc.* **110:** 205–222.

Kravitz, E. A. 1988. Hormonal control of behavior: amines and the biasing of behavioral output in lobsters. *Science* **241:** 1775–1781.

McKenney, K., and J. I. Goldberg. 1989. *Helisoma* embryogenesis: morphological, behavioral and neural development. *Soc. Neurosci. Abstr.* **15:** 1016.

Meier, T., and H. Reichert 1990. Neuronal development in the crustacean nervous system studied by neuron-specific antibody labelling. Pp. 523–529 in *Frontiers in Crustacean Neurobiology*, K. Wiese, W. D. Krenz, J. Tautz, H. Reichert, and B. Mulloney, eds. Birkhaüser, Basel, Boston.

Pandian, T. J. 1970a. Ecophysiological studies on the developing eggs and embryos of the European lobster *Homarus gammarus*. *Mar. Biol.* **5:** 154–167.

Pandian, T. J. 1970b. Yolk utilization and hatching in the Canadian lobster *Homarus americanus*. *Mar. Biol.* **7:** 249–254.

Perkins, H. C. 1972. Developmental rates at various temperatures of embryos of the northern lobster (*Homarus americanus* Milne-Edwards). *Fish. Bull.* **70:** 95–99.

Phillips, B. F., and A. N. Sastry. 1980. Larval Ecology. Pp. 11–57 in *The Biology and Management of Lobsters*, Vol. 2, J. S. Cobb and B. F. Phillips, eds. Academic Press, New York.

Rao, K. R., S. W. Fingerman, and M. Fingerman. 1973. Effects of exogenous ecdysones on the molt cycles of fourth and fifth stage American lobsters, *Homarus americanus*. *Comp. Biochem. Physiol. A* **44:** 1105–1120.

Sandeman, R., and D. C. Sandeman. 1990. Development and identified neural systems in the crayfish brain. Pp. 498–508 in *Frontiers in Crustacean Neurobiology*, K. Wiese, W. D. Krenz, J. Tautz, H. Reichert, and B. Mulloney, eds. Birkhaüser, Basel, Boston.

Sandeman, R., and D. C. Sandeman. 1991. Stages in the development of the embryo of the freshwater crayfish *Cherax destructor*. *Roux's Arch. Dev. Biol.* (in press).

Sasaki, G. C. 1984. Biochemical changes associated with embryonic and larval development in the american lobster *Homarus americanus* Milne-Edwards. Ph. D. thesis, Massachusetts Institute of Technology/Woods Hole Oceanographic Institution, WHOI-84-8.

Sasaki, G. C., J. M. Capuzzo, and P. Biesiot. 1986. Nutritional and bioenergetic considerations in the development of the American lobster *Homarus americanus*. *Can. J. Fish. Aquat. Sci.* **43:** 2311–2319.

Schram, F. R. 1986. *Crustacea*. Oxford University Press, New York.

Schuur, A., W. S. Fisher, J. C. Van Olst, J. Carlberg, J. T. Hughes, R. A. Shleser, and R. F. Ford. 1976. Hatchery methods for the production of juvenile lobsters (*Homarus americanus*). *Inst. Mar. Res. California* **48:** 1–20.

Shiino, S. M. 1988. Crustacea. Pp. 333–388 in *Invertebrate Embryology*, M. Kumé, and K. Dan, eds. Garland Publishing, New York.

Snyder, M. J., and E. S. Chang. 1991. Ecdysteroids in relation to the molt cycle of the American lobster, *Homarus americanus*. I. Hemolymph titers and metabolites. *Gen. Comp. Endocrinol.* **81:** 133–145.

Templeman, W. 1940. Embryonic developmental rates and egg laying of Canadian lobsters. *J. Fish. Res. Board Can.* **5:** 71–83.

Waddy, S. L., and D. E. Aiken. 1984. Broodstock management for year-round production of larvae for culture of the american lobster. *Can. Tech. Rep. Fish. and Aqua. Sc.* No 1272.

Wear, R. G. 1974. Incubation in British decapod crustacea, and the effects of temperature on the rate and success of embryonic development. *J. Mar. Biol. Assoc. U.K.* **54:** 745–762.

Weeks, J. C., and J. W. Truman. 1986. Steroid control of neuron and muscle development during the metamorphosis of an insect. *J. Neurobiol.* **17:** 249–267.

Weygoldt, P. 1979. Significance of later embryonic stages and head development in arthropod phylogeny. P. 107 in *Arthropod Phylogeny*, A. P. Gupta, ed. Van Nostrand-Reinhold, Princeton, NJ.

Wiese K., W. D. Krenz, J. Tautz, H. Reichert, and B. Mulloney. 1990. *Frontiers in Crustacean Neurobiology*. Birkhaüser, Basel, Boston.

Williamson, D. I. 1982. Larval morphology and diversity. Pp. 43–110 in *The Biology of Crustacea*, Vol. 2, *Embryology, Morphology, and Genetics*, L. G. Abele, ed. Academic Press, New York.

Reference: *Biol. Bull.* **180:** 372–386. (June, 1991)

How Do Temperature and Salinity Affect Relative Rates of Growth, Morphological Differentiation, and Time to Metamorphic Competence in Larvae of the Marine Gastropod *Crepidula plana*?

KERRY M. ZIMMERMAN AND JAN A. PECHENIK[1]

Biology Department, Tufts University, Medford, Massachusetts 02155

Abstract. The influence of environmental conditions on rates of larval growth has been documented many times for various marine mollusks. But the factors that influence rates of morphological and physiological differentiation, particularly the rate at which larvae within a population become competent to metamorphose, remain obscure. In four experiments, we reared larvae of the gastropod *Crepidula plana* at 29°C, 25°C, and 20°C at 30 ppt salinity, and in two other experiments, in salinities between 4–30 ppt at 25°C. Rates of shell growth and morphological differentiation, and rates of becoming competent within populations were recorded. Larvae were considered to be competent to metamorphose if they could be stimulated to metamorphose by exposure to a high concentration of KCl (20 m*M* above ambient). Larvae consistently became competent faster at higher temperatures, but in only one of four experiments did temperature also consistently increase the rates of growth and morphological differentiation. Larvae took longer to become competent when reared at lower salinities, but the effects were poorly predicted by the influence of salinity on rates of growth and morphological differentiation. Competent larvae could also not be recognized by shell length; many individuals were competent at shell lengths of 600–800 μm, while many other individuals were still not competent at sizes exceeding 1000 μm. At 29°C, many individuals became competent at smaller sizes than those reared at lower temperatures. Presence of gill filaments or shell brims also did not correlate with individual metamorphic competence. The data suggest that growth rate, rate of morphological differentiation, and time required for larvae of *C. plana* to become competent can be uncoupled markedly by shifts in rearing conditions.

Received 26 February 1990; accepted 9 January 1991.

[1] Please address reprint requests to J. A. Pechenik.

Introduction

Competence is a differentiated state in which larvae of benthic marine invertebrates first become capable of metamorphosing in response to environmental cues (Crisp, 1974; Scheltema, 1974; Chia, 1978; Hadfield, 1978; Miller and Hadfield, 1986; Coon *et al.*, 1990; Fitt *et al.*, 1990). Metamorphosis of gastropod larvae is most easily defined by the loss of the larval velum, an organ responsible for larval feeding, swimming, and gas exchange. This transformation marks the transition from a swimming planktonic stage to a largely sedentary benthic stage. The time required for a larva to become competent thus determines the obligate planktonic dispersal period (Scheltema, 1978; Jackson and Strathmann, 1981).

Larvae are often designated as competent based on their size, age, or the presence of particular morphological characteristics (Bayne, 1964; Bayne, 1965; Bayne, 1971; Hickman and Gruffydd, 1971; Switzer-Dunlap and Hadfield, 1977; Hadfield, 1978; Pechenik, 1984; Lima and Pechenik, 1985; Butman *et al.*, 1988). In at least some molluscan species, however, such criteria may be poor indicators of an individual's competence to metamorphose. In the bivalves *Mytilus edulis* and *Crassostrea gigas*, for example, neither shell size, age, nor the presence of eye spots guarantee that larvae will metamorphose in response to apparently appropriate cues (Eyster and Pechenik, 1987; Coon *et al.*, 1990). Similarly, size is an

inadequate indicator of metamorphic competence for the gastropod *Crepidula fornicata;* larvae from a single larval culture became competent to metamorphose at shell lengths ranging between 700 and 1000 μm (Pechenik and Heyman, 1987, in response to elevated KCl concentrations). Neither did behavioral changes successfully signal the time at which larvae of the opisthobranch *Phestilla sibogae* became metamorphically competent in the experiments of Miller and Hadfield (1986). There is growing reason to doubt, then, that the time required for a larva to become metamorphically competent is directly coupled to the rate at which the larva grows or develops most other conspicuous traits.

To date, few workers have rigorously documented the rate at which larvae in a population become competent to metamorphose, or have considered the influence of environmental factors on that rate. In addition, the correspondence between the rates of larval growth and of attaining metamorphic competence have been poorly explored. Under what conditions do larvae become competent more quickly, and to what extent can this accelerated attainment of competence be predicted from the influence of those conditions on rates of growth or morphological differentiation? Because larval metamorphosis can, for a number of species, be triggered by elevating KCl ambient concentration (Yool *et al.,* 1986; Pechenik and Heyman, 1987), the rate and sizes at which larvae of those species become competent can be determined experimentally. The larvae of *Crepidula fornicata* can be induced to metamorphose by elevated KCl concentrations at about the same age and size that larvae become responsive to adult-conditioned seawater and surfaces bearing microbial films (Pechenik, 1980; Pechenik and Heyman, 1987). The latter probably serve as metamorphic cues in the field (McGee and Target, 1989), but the active constituents have not been isolated.

In this paper, we report the effects of temperature and salinity on the rate of larval growth, the rate of morphological differentiation, and the time required for larvae of the prosobranch gastropod *Crepidula plana* to become metamorphically competent (as indicated by their response to elevated potassium concentration). In *Crepidula plana,* virtually all larvae eventually metamorphose "spontaneously"—no cue is deliberately provided—in glassware that is cleaned and acid-rinsed daily (Lima and Pechenik, 1985). Thus, the *maximum* dispersal potential for these larvae depends on how long metamorphosis can be delayed after they first become competent. We therefore also monitored the timing of "spontaneous" metamorphosis in relationship to the onset of metamorphic competence. We have thus been able to directly determine the influence of temperature on the length of time that metamorphosis can be delayed under laboratory conditions.

Materials and Methods

Maintenance of adults and larvae of Crepidula plana

Adult *Crepidula plana* were collected near Woods Hole, Massachusetts. We maintained adults at room temperature (21–25°C) in 1 μm filtered seawater (collected at Nahant, Massachusetts), changing the seawater daily. We fed adults the green unicellular alga *Dunaliella tertiolecta* (clone *DUN*) daily, until larval release. After their release, the larvae were isolated on a 150 μm sieve and transferred to 0.45 μm filtered seawater (29–30 ppt salinity). In each of the six experiments conducted, the larvae were all released on the same day, but not necessarily from one female.

Larvae were fed the naked flagellate *Isochrysis* sp. (Tahitian strain, clone *T-ISO*) daily; seawater was changed every other day. At the start of an experiment (2–9 days after hatching), known numbers of larvae were randomly assigned to either a 20°C, 25°C, or 29°C temperature incubator (Percival Manufacturing) stable to 0.1°C. Larvae of *C. plana* grow very slowly at temperatures below 20°C, and 29°C seems to be near the upper lethal temperature limit for this species (Lima and Pechenik, 1985). All larvae were cultured on a 11L:13D light cycle. Larval concentrations were maintained below one larva · ml^{-1} in all experiments (I–VI); the aim was to maximize growth rates and minimize competition for food. Larvae were fed 1.8×10^5 cells · ml^{-1} of *T-ISO* every other day in Experiments I and II, and daily in all subsequent experiments. A hemacytometer was used to determine algal cell concentrations. To monitor survival, we removed dead or moribund larvae from the cultures at each water change. Glassware was cleaned with Bon Ami and rinsed with deionized water at each water change.

Determining the influence of temperature on rates of growth and morphological differentiation

In four experiments, we examined how temperature affects the relationship between rates of larval growth, rates of morphological differentiation, and rates of becoming competent to metamorphose. In Experiments I and II, 1100–1600 larvae were reared at each tested temperature (20°C, 25°C, and 29°C) in batch culture. Thirty actively swimming larvae were collected daily (25°C and 29°C), or every other day (20°C) from the batch cultures. Seawater volumes were adjusted after larval collection to maintain larval densities. In Experiments III and IV, we determined the growth rates of larvae reared in individual glass bowls, at densities also below 1 larva · ml^{-1}.

Larval shell lengths were measured at 50× using a dissecting microscope equipped with an ocular micrometer;

Table I

Influence of temperature and salinity on rates of larval shell growth, morphological differentiation and becoming competent for larvae of Crepidula plana

Experiment number	Temperature (°C)	Salinity (ppt)	Growth rate ($\mu m \cdot day^{-1}$)	Days to 50% of the population competent	Days to 50% of the population gilled	Days to 50% of the population brimmed	% Mortality (n)
I	29	30	28.4 ($r^2 = 0.96$)	12.2	—	—	4.0 (1620)
I	25	30	40.0 ($r^2 = 0.96$)	19.0	—	—	7.0 (1120)
I	20	30	33.8 ($r^2 = 0.96$)	23.4	—	—	13.0 (1620)
II	29	30	27.9 ($r^2 = 0.88$)	12.3	—	—	2.5 (1300)
II	25	30	22.5 ($r^2 = 0.93$)	17.0	—	—	8.0 (1300)
II	20	30	19.2 ($r^2 = 0.91$)	19.0	—	—	15.0 (1300)
III	29	30	59.1 ($r^2 = 0.99$)	9.7	9.7	10.4	1.0 (1000)
III	25	30	52.0 ($r^2 = 0.89$)	13.4	10.3	13.7	2.0 (1000)
IV	29	30	40.5 ($r^2 = 0.79$)	11.0	9.6	11.3	1.0 (720)
IV	25	30	43.0 ($r^2 = 0.91$)	12.6	11.6	12.0	1.0 (720)
IV	20	30	29.4 ($r^2 = 0.89$)	18.6	15.4	18.2	4.0 (720)
V	25	29	39.1 ($r^2 = 0.96$)	—	—	—	18.0 (48)
V	25	25	27.1 ($r^2 = 0.97$)	—	—	—	16.0 (49)
V	25	19	15.4 ($r^2 = 0.91$)	—	—	—	17.5 (52)
VI	25	30	43.6 ($r^2 = 0.96$)	14.3	12.5	14.4	2.0 (620)
VI	25	25	35.1 ($r^2 = 0.94$)	17.6	13.3	14.6	2.0 (620)
VI	25	20	38.9 ($r^2 = 0.94$)	>22.0	14.0	15.2	1.0 (620)

In Experiments I and II, larvae were fed every other day, in all other experiments larvae were fed every day. Dashes indicate sampling from batch culture (Expts. I and II) or data not available (Expt. V).

the maximum shell length was measured with the larva lying on its left side. The presence of gill filaments and the lateral shell brims characterizing advanced larvae of this species (Pechenik and Lima, 1984) were also noted. Growth rates (μm shell growth $\cdot day^{-1}$) were determined by linear regression analysis of changes in shell length through time (SPSS Inc., 1988). The percentage of the larval population that was gilled or brimmed was plotted against time. From these plots we estimated the number of days necessary after larvae were released from their egg masses for 50% of the larvae in a population to become gilled or brimmed.

Table II

Influence of salinity on larval survival and rate of becoming competent in Experiment V

Salinity (PPT)	% Mortality	% population competent after 7 days in each salinity treatment $\bar{X} \pm$ SD (n)
29	18%	37% ± 4.0 (3)
25	16%	10.3% ± 9.3 (3)
19	17.5%	3.3% ± 2.9 (3)
14.5	31%	20% ± 7.2 (3)
8	85%	0% ± 0.0 (3)
4	100% in 3 days	—

At the time of KCl exposure, larvae were 16 days old. Larvae were introduced to the reduced salinities after 9 days of culture at full-strength salinity (29 ppt).

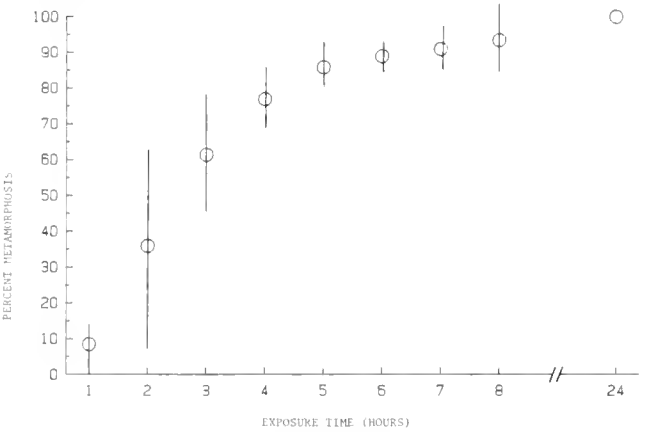

Figure 1. Influence of time exposed to elevated KCl concentration on metamorphosis of competent *Crepidula plana* larvae. KCl concentrations were elevated by 20 m*M* at 22–24°C. Larvae were examined for loss of velar lobes hourly for 8 h, then at 10 h and 24 h. Each point represents the mean of five replicates, with 20–21 larvae per replicate. Vertical bars represent one standard deviation. Average larval shell length (±SD) was 777 μm ± 97.8 (n = 100).

Larvae collected from batch culture were preserved in 10% formalin buffered with sodium borate (BORAX) (pH ~ 8.0), for later determination of larval organic weight; larvae reared at different temperatures were stored separately. Larval organic weights were determined as follows: one or more larvae of known shell lengths were placed into pre-weighed aluminum pans; the preserved animals were first rinsed three times with distilled water to remove preservatives and salts. The animals were dried overnight at 60°C in a drying oven, then weighed to determine initial total (inorganic and organic) dry weights. The animals were weighed to the nearest microgram (μg) with a Cahn microbalance with desiccant present in the weighing chamber to prevent rehydration. The pans were reweighed after sample combustion in a muffle furnace at 550°C for 6 h; combustion did not change the weight of the aluminum pans. The weight lost in combustion is equivalent to the larval organic weight. Individual body weights were

Table III

Results of ANACOVAs for shell size, % of the population competent to metamorphose, % fully gilled, or fully brimmed for each experiment by temperature and salinity with age as a covariate

Experiment I:	Influence of temperature (at 30 ppt) on growth rate	25°C > 20°C > 29°C
	Rate at which the population became competent	29°C > 25°C > 20°C
	Rate at which the population became gilled	29°C = 25°C = 20°C
	Rate at which the population became brimmed	29°C = 25°C = 20°C
Experiment II:	Influence of temperature (at 30 ppt) on growth rate	29°C > (25°C = 20°C)
	Rate at which the population became competent	29°C > 25°C > 20°C
	Rate at which the population became gilled	29°C = 25°C = 20°C
	Rate at which the population became brimmed	29°C = 25°C = 20°C
Experiment III:	Influence of temperature (at 30 ppt) on growth rate	29°C > 25°C
	Rate at which the population became competent	29°C > 25°C
	Rate at which the population became gilled	29°C > 25°C
	Rate at which the population became brimmed	29°C > 25°C
Experiment IV:	Influence of temperature (at 30 ppt) on growth rate	25°C > 29°C > 20°C
	Rate at which the population became competent	29°C > 25°C > 20°C
	Rate at which the population became gilled	29°C > 25°C > 20°C
	Rate at which the population became brimmed	29°C > 25°C > 20°C
Experiment VI:	Influence of salinity (at 25°C) on growth rate	30 ppt > 20 ppt > 25 ppt
	Rate at which the population became competent	30 ppt > 25 ppt > 20 ppt
	Rate at which the population became gilled	30 ppt > (25 ppt = 20 ppt)
	Rate at which the population became brimmed	30 ppt > 25 ppt > 20 ppt

All differences are significant at $P < 0.05$, and most were significant at $P < 0.001$.

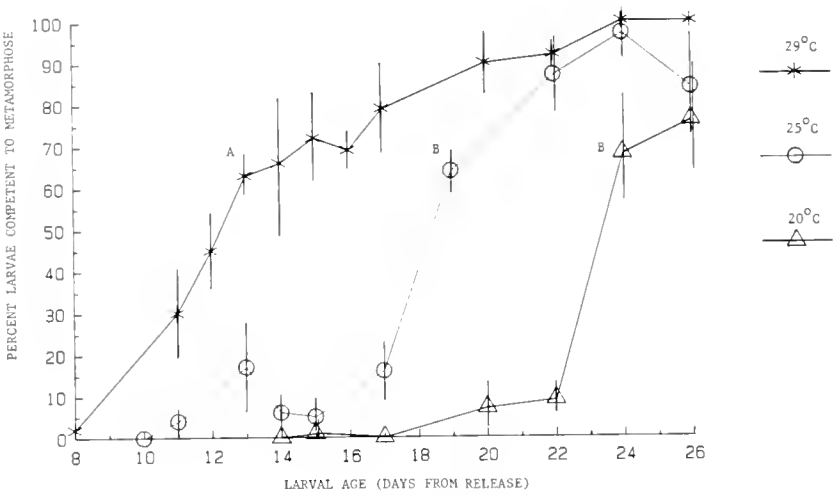

Figure 2. Influence of rearing temperature on the rate at which larvae became competent to metamorphose in Experiment 1. Each point represents the mean percentage metamorphosing in three bowls, with 34–40 larvae per bowl. Vertical bars represent one SD about the mean. Different letters represent larval populations with different mean growth rates (A < B).

determined for larvae longer than 700 μm; larvae less than 700 μm were pooled for weight determinations.

Determining the effect of temperature on the rate of becoming competent to metamorphose

Pechenik and Heyman (1987) found that elevating the KCl levels in natural seawater by 20 m*M* induced competent larvae of *C. fornicata* to metamorphose within 7 h. To determine whether the larvae of *C. plana* would respond similarly, we exposed advanced larvae of this species (22-day-old, 770 ± 98 μm shell length, n = 100) to a 20 m*M* increase in KCl concentration. We checked hourly for larval metamorphosis for the first 8 h, then at 10 h and 24 h; newly metamorphosed larvae were removed at each observation. The experiment was conducted at 22°C, with 5 replicates (21 larvae per replicate).

To determine the effect of temperature on the rate at which larvae in a given population became competent to metamorphose, we monitored larvae from a temperature treatment until some individuals reached shell lengths of about 600 μm. At 1–3 day intervals, we then transferred all larvae from three randomly chosen bowls into 3 bowls of seawater with elevated KCl concentrations; 30 to 45 glass bowls of larvae (20–40 larvae per bowl, depending on the experiment) were used for each temperature treatment during the course of an experiment. After exposing larvae to the elevated KCl for 6 h, we determined the number of individuals that had metamorphosed in each bowl, and measured the shell lengths of those that had metamorphosed and of those that had not. We also determined whether individuals had gills or shell brims. We conducted *t*-tests to determine whether there were differences in the mean shell lengths of competent and precompetent larvae in each temperature treatment. The rate at which larvae in each population became competent was determined by linear regression analysis. Significant regression coefficients (r) were obtained in all experiments. For regressions with correlation coefficients (r^2) greater than 0.80, the number of days for 50% of the larval population to become competent was determined from the regression. For data with r^2 values less than 0.80, the number of days for the populations to become 50% competent was estimated by eye.

Determining the influence of temperature on maximum length of larval life

Larvae of *C. plana* eventually undergo "spontaneous" metamorphosis in the laboratory, even when maintained in frequently cleaned glassware (Lima and Pechenik, 1985). Three bowls (20–40 larvae per bowl, depending on experiment) at each temperature were washed and acid-rinsed daily, at each change of algal suspension. Larvae were examined daily; we counted, removed, and measured newly metamorphosed snails. These data were compared with observations on the mean age and size, at metamorphosis, of individuals cultured in bowls cleaned only every 48 h ("filmed bowls"). The aim was to determine whether biological films building up over the 48-h period would induce a greater number of larvae to metamorphose. Such biological surface films have been implicated as metamorphic inducers in many marine invertebrates (Meadows and Campbell, 1972; Scheltema, 1974; Kirchman *et al.*, 1982; Lima, 1983; Coon *et al.*, 1985; Weiner *et al.*, 1989).

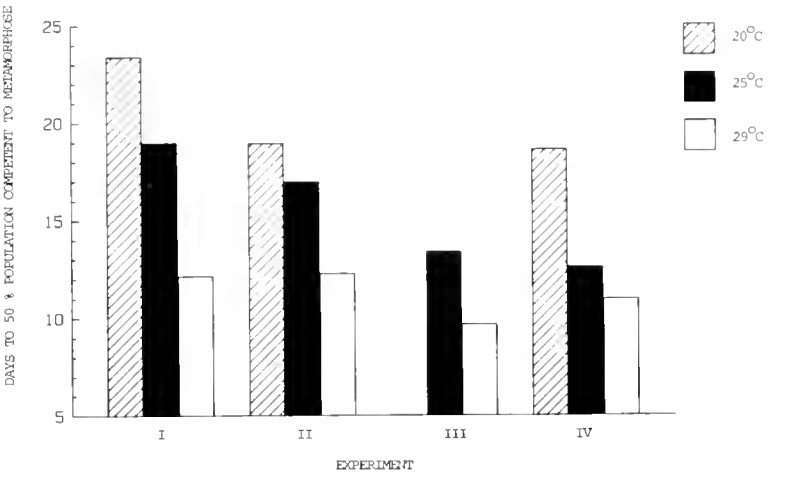

Figure 3. Influence of rearing temperature on the number of days for 50% of the larvae in each treatment population to become competent to metamorphose in Experiments I–IV.

The time required for 50% of the population to metamorphose in the bowls cleaned daily, minus the time required for 50% of the larvae to become competent in parallel experiments, was used as an index of capacity for delaying metamorphosis. This cannot be used to predict dispersal potential in the field, but should enable us to assess the influence of temperature and salinity on the physiological capacity for prolonging larval life, and will permit future interspecific comparisons of the physiological capacity for delaying metamorphosis.

Determining the effects of salinity on rates of growth, morphological differentiation, and rates of becoming competent

In two experiments, we examined how salinity affected the relationship between rates of growth, morphological differentiation, and becoming competent. In the first experiment, six salinities [29, 25, 19, 14.5, 8, and 4 parts per thousand (ppt)] were used to determine the salinity tolerance of larval *C. plana;* these salinities are equivalent to osmotic concentrations of 821, 708, 557, 403, 223, and 116 mOsm, respectively. The five lowest salinities were made by mixing 0.45 μm filtered seawater with deionized water; the 29 ppt seawater was composed solely of undiluted 0.45 μm filtered seawater. Osmotic concentrations were measured with a freezing point depression osmometer (Advanced Instruments, Inc.). This experiment was conducted at 25°C, with three replicate bowls of 20 larvae per bowl in each salinity treatment. Water and food were replaced daily. All larvae were reared in full-strength seawater for 9 days, and then acclimated to lower salinities in stages during 1 h. Shell-less, moribund, or dead larvae were counted and removed daily. Shell lengths were measured non-destructively (Pechenik, 1984) each day for growth rate determinations. All larvae were exposed to an increase of 20 m*M* KCl on the seventh day of the experiment (the 16th day of larval life) to determine the percentage of larvae competent to metamorphose in each salinity.

Based on the results of the first experiment, a second experiment (Experiment VI) was conducted at 30, 25, 20 ppt (again at 25°C) to examine more fully the effect of salinity on rates of growth and differentiation. We reared 25 larvae per bowl with 31 bowls per treatment. To minimize the effects of food supply on salinity—algae are cultured at about 30 ppt—the algae were concentrated by centrifugation at 3000 $\times$ *g* for 12 min and then resuspended in seawater of the appropriate test salinity (Pechenik and Fisher, 1979). Algal cells remained alive and motile in all salinities. Every day, larval shell lengths were measured non-destructively from randomly selected bowls at each salinity; presence or absence of gill filaments and shell brims were simultaneously noted.

Periodically, three bowls of larvae from each salinity treatment were randomly selected and all individuals (20–30 larvae per bowl) were exposed to elevated KCl concentrations in seawater to assess metamorphic competence. Larvae reared at 30 or 25 ppt were exposed to an increase of 20 m*M* KCl while those reared in 20 ppt seawater were exposed to either a 20 or a 23 m*M* KCl increase, to compensate for the lower baseline KCl concentration at the reduced salinity. All individuals exposed to KCl were measured, whether or not they metamorphosed, and were examined for the presence of gill filaments and shell brims.

Statistical analyses

Analyses of covariance (ANACOVA) were conducted for each experiment. Either temperature or salinity were

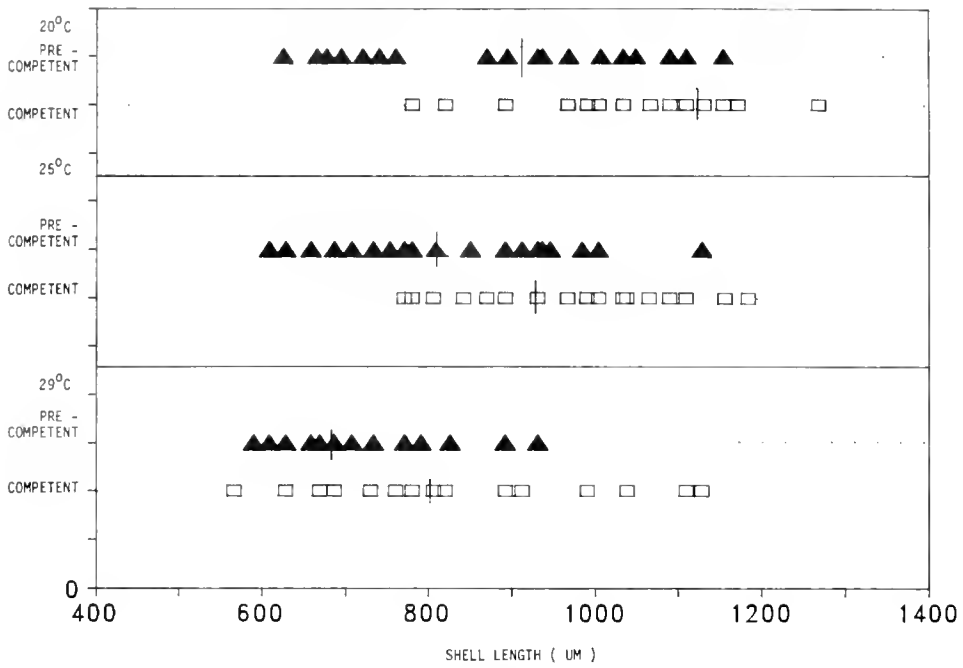

Figure 4. A comparison of the shell lengths of competent (□) and pre-competent (▲) larvae of *Crepidula plana* from Experiment IV. The points within each treatment represent the response of larvae from three bowls (~60 larvae per bowl). Data were taken when larvae at 29°C were 11 days old ($\bar{x}$ = 50.0% larvae competent; SD = 4.3); larvae at 25°C were 13 days old ($\bar{x}$ = 54.6% competent; SD = 6.4); larvae at 20°C were 19 days old ($\bar{x}$ = 51.3% competent; SD = 14.1).

used as independent variables; age (days from hatch) was the covariate; and one of the following was taken as the dependent variable: percent of the larval population competent to metamorphose, percent of the larval population gilled, percent of the larval population with a complete shell brim, or shell length (Table I) (Kleinbaum *et al.*, 1988; SPSS, Inc. 1988). In Experiments I and II, the gill, shell brim, and shell length data were obtained from larvae in batch culture, whereas the rate at which larvae became competent to metamorphose was determined with larvae reared in glass bowls. In Experiments III–VI, all data were obtained from the larvae reared in glass bowls. Percentage data were arcsine transformed prior to subsequent analysis, using the formula for proportions with unequal sample sizes (Draper and Smith, 1981).

Results

Effects of temperature and salinity on survival

Larval survivorship was high at all temperatures in Experiments I–IV, with the best survival, greater than 96%, occurring at the highest temperature tested (29°C) (Table I).

However, larvae were intolerant of very low salinities (Table II). Within the first two hours at 4 and 8 ppt, larvae were found clumped together with mucus, mainly on the bottoms of the rearing bowls, with their velar lobes extended and velar cilia moving; all treatment bowls at higher salinities (14.5, 19, 25, 29 ppt) contained swimming larvae. On the second day, at 4 and 8 ppt, velar lobes appeared smaller and velar cilia were less visible. By the third day, all larvae in the 4 ppt seawater had died and only two larvae out of the initial 65 survived at 8 ppt. Larval survivorship was good at salinities of 19 ppt and above, particularly in the second salinity experiment (Table I, Experiment VI).

Effects of temperature on rates of growth and morphological differentiation

Temperature had no significant effect on size-specific organic weight at 20 and 25°C and at 20 and 29°C (*t*-tests between slopes, $P > 0.10$, $t = 0.69$, d.f. = 30 and $t = 0.26$, d.f. = 42, respectively). Thus, a given change in shell length reflected comparable growth (in organic weight) for larvae at 20 and 25°C, and at 20 and 29°C. However, a given change in shell length reflected greater growth (in organic weight) for larvae at 25°C as compared to larvae reared at 29°C (*t*-tests, $P < 0.05$, $t = 2.05$, d.f. = 50).

The effect of temperature on larval growth rate varied markedly among experiments (Experiments I–IV, Tables I and III). There were differences both in the average

Table IV

Influence of temperature on age and size at spontaneous metamorphosis in glassware cleaned daily (clean bowls) and the delay period (number of days between when 50% of the population was competent and the mean age at metamorphosis in clean bowls)

Experiment number	Temperature (°C)	Mean age (days) at spontaneous metamorphosis (clean) $\bar{X} \pm SD$ (n)	Delay period (days)
I	29	19.32 ± 4.9 (75) A	7.16
I	25	24.66 ± 3.8 (98) B	5.67
I	20	28.66 ± 3.8 (100) C	5.26
II	29	18.09 ± 5.4 (99) A	5.79
II	25	26.86 ± 4.9 (44) B	9.86
II	20	30.96 ± 3.2 (73) C	12.00
III	29	14.49 ± 2.2 (306) A	4.79
III	25	16.81 ± 1.6 (214) B	3.40
IV	29	16.79 ± 1.7 (24) A	5.79
IV	25	18.54 ± 1.4 (24) B	5.90
IV	20	24.85 ± 2.6 (39) C	6.21

Within each column, letters following sample sizes signify significantly ($P < 0.05$) different means within experiments.

amount of daily growth at a temperature and in how temperature affected relative growth rates. For example, larvae grew the slowest (28 $\mu m \cdot day^{-1}$) at 29°C in Experiment I, but grew the fastest at 29°C (28 $\mu m \cdot day^{-1}$) in Experiment II (Table I). Over all experiments, average growth rates ranged between 19 $\mu m \cdot day^{-1}$ (Experiment II, 20°C) and 59 $\mu m \cdot day^{-1}$ (Experiment III, 29°C).

Larvae generally developed gill filaments and shell brims more rapidly at higher rearing temperatures, although rates of gill and brim formation were independent of temperature in the first two experiments (Table III). Note that in Experiment IV the effects of temperature on growth rates did not parallel those on morphological differentiation rates. These data indicate that gill formation, brim formation, and growth rate were affected similarly by rearing temperature in only one of the four experiments (Experiment III); only two temperature treatments were tested in that experiment.

Larvae typically became gilled between about 620–820 μm and brimmed between about 710–850 μm, with no consistent influence of rearing temperature or feeding frequency. Some larvae within the populations were fully gilled and brimmed before other larvae in the same population became gilled, indicating much individual variation in rates of morphological development within each temperature treatment.

All but seven metamorphosed individuals—out of thousands of metamorphosed snails examined in these experiments—had conspicuous gills, suggesting that most larvae developed gills before they became competent to metamorphose. The seven gill-less juveniles were all found at 29°C (Experiments I and II).

Elevated KCl concentration stimulates metamorphosis

Response to elevated KCl was rapid. Of those 22-day-old individuals (22°C) that eventually responded, increasing KCl concentrations by 20 m*M* induced at least 90% to metamorphose within 6 h (Fig. 1). Thus, in all subsequent experiments, larvae were exposed to elevated KCl concentrations for 6 h to assess metamorphic competence, defined here by the response to elevated potassium.

Effect of temperature on rates of becoming competent to metamorphose

Despite the unpredictable effects of rearing temperature on rates of growth and morphological differentiation, increasing larval rearing temperature significantly increased ($P < 0.001$) the rates at which larvae became competent to metamorphose in all experiments (Tables I, III; Figs. 2, 3).

Larval shell length was a poor indicator of whether a larva was competent to metamorphose. Although competent larvae were, on average, significantly larger ($P < 0.0001$) than pre-competent larvae of the same age and rearing history, shell lengths of competent and pre-competent larvae overlapped in all experiments, as exemplified by Experiment IV (Fig. 4).

Effect of temperature on the maximum length of larval life and period of delayed metamorphosis

At higher temperatures, larvae consistently exhibited "spontaneous" metamorphosis sooner than at lower temperatures (Table IV and Fig. 5). However, average growth rates failed to predict rates of spontaneous metamorphosis within a population. In Experiment I, for example, larvae reared at 20°C or 25°C grew at equivalent rates but metamorphosed faster at the higher temperature (Fig. 5). Even

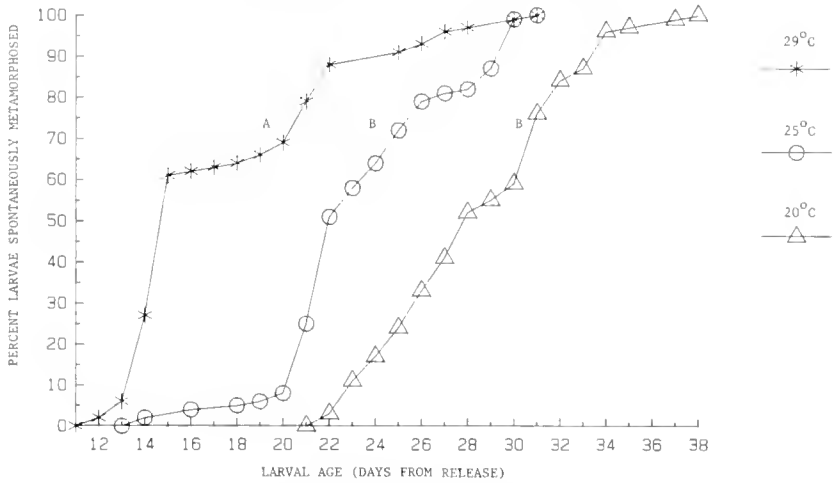

Figure 5. Maximum length of larval life for *Crepidula plana* maintained in glass bowls, acid-washed daily (Experiment I). Each point represents the mean of three replicates (110 larvae per treatment). Different letters signify larval populations differing significantly in mean growth rates (A < B < C).

so, individuals exhibiting faster growth within a temperature treatment tended to metamorphose sooner than slower growing larvae reared at the same temperature, confirming previous results (Lima and Pechenik, 1985) (Fig. 6; regression analysis of log growth rate). Within each temperature, faster growing individuals also tended to metamorphose at larger shell lengths, although the data do show considerable scatter (Fig. 7; $P < 0.05$ at each temperature). Individual growth rates were estimated using age and size at metamorphosis (Lima and Pechenik, 1985).

Generally, larvae maintained in bowls cleaned only every 48 h metamorphosed significantly sooner ($P < 0.05$; *t*-test), by about 5–10 days, than larvae maintained in bowls cleaned every 24 h, and at smaller shell lengths [smaller by about 100–300 μm (Zimmerman, 1989)]. This indicates that microbial films formed over 48 h could trigger larvae of *C. plana* to metamorphose, supporting previous reports (Lima, 1983).

The average delay period, defined here by the difference (in days) between (a) mean age at "spontaneous" metamorphosis in bowls cleaned daily and (b) when 50% of a larval population was competent to metamorphose, varied between experiments, and was markedly altered by temperature only in Experiment II (Table IV).

Effect of salinity on rates of growth and morphological differentiation

The effects of salinity on growth rate differed in the two experiments. In Experiment V (Table I), larvae grew more quickly at higher salinities (by about 12 $\mu m \cdot day^{-1}$ for each salinity increase above 19 ppt). In the three lowest salinities (4, 8, and 14.5 ppt), larvae suffered high mortality (85–100% at 4 and 8 ppt) and exhibited no detectable growth. In Experiment VI, salinity significantly affected mean growth rates, but not as dramatically as in Experiment V, and not in direct proportion to salinity. Larvae reared at 20 ppt grew significantly faster than larvae at 25 ppt in Experiment VI (Tables I, III). In both salinity experiments, larvae reared in full strength seawater (either 29 or 30 ppt) grew at rates comparable to those of larvae reared under comparable conditions (25°C, full strength seawater) in Experiments I–IV (Table I).

Salinity over the range of 20–30 ppt had negligible effects on rates of gill formation (Tables I, V) and on the shell sizes at which larvae became either gilled or brimmed. Larvae became gilled and brimmed at shell sizes between 628–728 μm and 699–790 μm, respectively, regardless of rearing salinity. However, every increase in rearing salinity increased rates of shell brim formation (Table III). The pattern of significant salinity effects on rates of growth and on rates of gill and brim formation (Table III) indicates that rates of growth and morphological differentiation were not affected similarly by changes in salinity.

The relative effect of salinity on rates of becoming competent to metamorphose and rates of growth

Despite the erratic influence of salinity on rates of growth, gill, and shell brim formation, larvae reared at higher salinities typically became competent to metamorphose sooner than those reared at lower salinities in both Experiments V and VI (Tables I–III). These results suggest that changes in salinity may uncouple rates of growth, rates of morphological differentiation, and rates of becoming competent to metamorphose. In Experiment

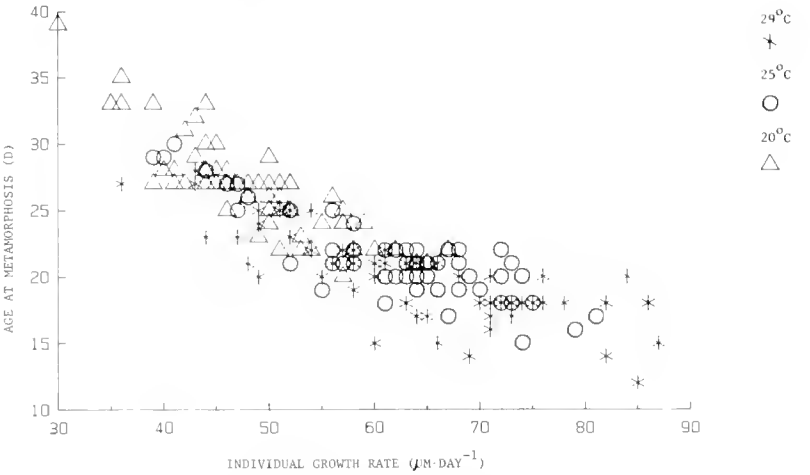

Figure 6. Maximum length of larval life as a function of estimated individual growth rate ($\mu m \cdot day^{-1}$) in Experiment IV ($r^2 = 0.74$, $y = -16.4(\ln x) + 88.7$). Individual growth rates were estimated from the size and age at which each individual underwent spontaneous metamorphosis in glass bowls that were cleaned daily. Larvae were cultured at three temperatures, as indicated (n = 64, 62, and 63 larvae per treatment at 29°C, 25°C and 20°C, respectively).

VI, for example, larvae grew more rapidly at 20 ppt than at 25 ppt, but took longer to become competent at the lower salinity (Table III and Fig. 8). Experiment VI was terminated before all larvae were allowed to metamorphose, so calculation of age and size at metamorphosis was not possible.

There was no significant difference ($P > 0.05$) in the percentage of larvae induced to metamorphose when KCl concentrations were elevated by 20 *versus* 23 m*M* at 20 ppt. Thus, the dilution of full strength seawater to make 20 ppt and 25 ppt seawater did not significantly affect the ability of KCl to induce larval metamorphosis.

Discussion

The primary goal of these experiments was to determine, for *Crepidula plana,* whether changes in temperature and salinity alter rates of growth, morphological differentiation, and the onset of competence equally. We must first consider the effects of temperature and salinity on each of these three components of development individually.

Larvae grew significantly faster at progressively higher temperatures (Table I) in only one experiment (Experiment III). Lima and Pechenik (1985) also found an in-

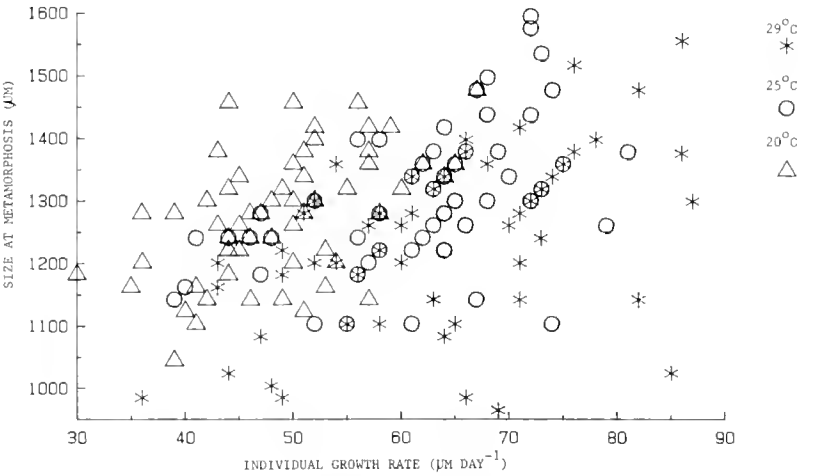

Figure 7. Size at metamorphosis as a function of individual larval growth rate ($\mu m \cdot day^{-1}$) (Experiment IV). Faster growing larvae tended to spontaneously metamorphose at larger shell sizes ($P < 0.05$; r = 0.549 at 29°C, n = 64; r = 0.512 at 25°C, n = 62; r = 0.511 at 20°C n = 63; combined r = 0.249, n = 189). Growth rates were estimated from size and age at spontaneous metamorphosis. Larvae were reared at three temperatures, as indicated.

Table V

Influence of temperature and salinity on percent changes in rates of shell growth, morphological differentiation, becoming competent to metamorphose, and spontaneous metamorphosis for all experiments

Experiment number	Temperature, salinity (°C) (ppt)	Growth rate ($\mu m \cdot day^{-1}$)	1·(Time to 50% competent)$^{-1}$	1·(Time to 50% gilled)$^{-1}$	1·(Time to 50% brimmed)$^{-1}$	1·(Time to 50% spontaneously metamorphosed)$^{-1}$
I	20°C, 30 ppt	—	—	—	—	—
	25°C, 30 ppt	+18%	+19%	—	—	+21%
	29°C, 30 ppt	−16%	+48%	—	—	+48%
II	20°C, 30 ppt	—	—	—	—	—
	25°C, 30 ppt	+17%	+10%	—	—	+11%
	29°C, 30 ppt	+45%	+35%	—	—	+48%
III	25°C, 30 ppt	—	—	—	—	—
	29°C, 30 ppt	+14%	+28%	+6%	+24%	+18%
IV	20°C, 30 ppt	—	—	—	—	—
	25°C, 30 ppt	+46%	+32%	+25%	+34%	+22%
	29°C, 30 ppt	+38%	+41%	+38%	+38%	+29%
V	25°C, 8 ppt	—	—	—	—	—
	25°C, 14.5 ppt	+12%	+20%	—	—	—
	25°C, 19 ppt	+233%	+3.3%	—	—	—
	25°C, 25 ppt	+334%	+10%	—	—	—
	25°C, 29 ppt	+438%	+37%	—	—	—
VI	25°C, 20 ppt	—	—	—	—	—
	25°C, 25 ppt	−9%	+20%	+5%	+4%	—
	25°C, 30 ppt	+12%	+35%	+11%	+6%	—

Each percent change was calculated relative to the lowest temperature, salinity treatment in a particular experiment.

consistent effect of temperature on larval growth rate for larvae of *C. plana* fed *T-ISO*, and the larval growth rates reported here for *C. plana* are generally comparable to those previously reported by Lima and Pechenik (1985) for larvae reared at identical food concentrations and temperatures. In our Experiment III, however, larvae reared at 29°C and 25°C grew 1.5–2.0 times faster than those reared by Lima and Pechenik (1985) under the same conditions. Lima and Pechenik (1985) reported comparably high larval growth rates (exceeding 50 $\mu m \cdot day^{-1}$) for *C. plana* reared at 25°C and 29°C on a different naked flagellate, *Isochrysis galbana* (clone ISO). Larvae of the congener *C. fornicata* also grow at rates exceeding 50 $\mu m \cdot day^{-1}$, at temperatures above 24°C (Lucas and Costlow, 1979; Pechenik, 1984; Pechenik and Lima, 1984).

Salinity also influenced larval growth rates, although the effects were often inconsistent between the two experiments (Tables I, III). Larvae grew faster at progressively higher salinities in Experiment V, but not in Experiment VI (Tables I, III). As with other molluscan larvae, including the congener *C. fornicata* (Davis, 1958; Davis and Ansell, 1962; Davis and Calabrese, 1964; Scheltema, 1965; Calabrese and Rhodes, 1974; Robert *et al.*, 1988; His *et al.*, 1989), those of *C. plana* grew poorly at salinities below about 20 ppt.

The influence of temperature on rates of morphological differentiation also varied from one experiment to the next (Table III). This contrasts with results reported for *C. fornicata* by Pechenik and Lima (1984) and Pechenik (1984), who found that larvae always tended to develop gills and shell brims more rapidly at higher temperatures. We have no way of knowing whether the inter-experiment variation we report for *C. plana* reflects genetic differences in the larval populations used, subtle differences in rearing conditions among experiments, or differences in the physiological history of the adults that released the larvae used in these experiments (Bayne *et al.*, 1975). Increases in salinity did not predictably alter rates of gill formation in Experiment VI (Table III), but shell brims formed more rapidly at higher salinities.

As reported previously for larvae of *C. plana* and *C. fornicata* (Pechenik and Lima, 1984; Lima and Pechenik, 1985), and for larvae of the blue mussel *M. edulis* (Pechenik *et al.*, 1990), temperature apparently altered rates of growth and morphological development to different degrees. In our studies, this is suggested by the fact that larvae tended to develop shell brims and visible gill filaments at different sizes when reared at different temperatures. For example, in Experiment I, larvae formed visible gill filaments on average between 681 and 721 μm,

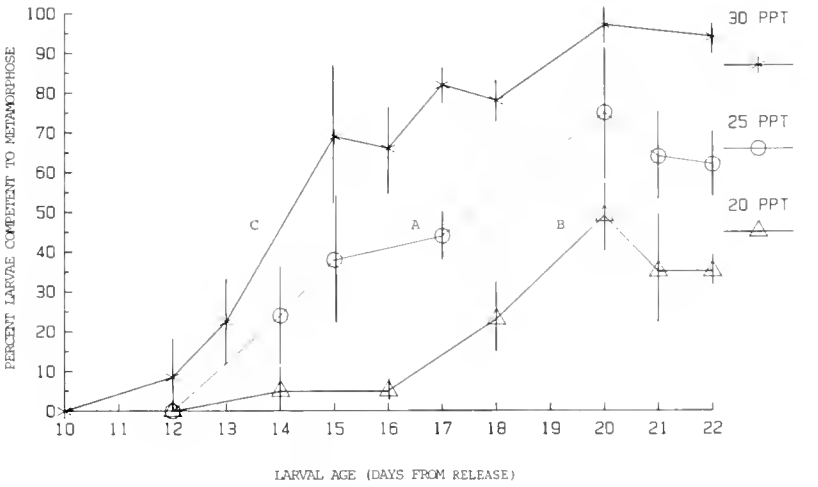

Figure 8. Influence of salinity on the rate at which larvae became competent to metamorphose in Experiment VI. Each point represents the mean percentage of larvae competent in three bowls, with 20–23 larvae tested per bowl. Vertical bars represent one SD about the mean. Different letters represent larval populations with different mean growth rates (A < B < C).

between 675 and 817 μm, and between 742 and 786 μm, at 29°C, 25°C, and 20°C, respectively. Rates of shell growth would have to be altered by temperature in exact proportion to any changes in rates of morphological development if larvae are to form gills and shell brims at comparable average sizes in all rearing conditions (Pechenik and Lima, 1984; Pechenik *et al.*, 1990).

Rates of shell growth and morphological differentiation were also affected to different degrees by salinity. For example, in Experiment VI, larvae grew significantly faster at 20 ppt than at 25 ppt, but the salinity decrease did not affect rate of gill formation. Indeed, rate of gill formation was not affected by salinity over the range tested. In contrast, shell brims formed faster at the higher salinity.

Despite the generally unpredictable effects of temperature on rates of larval growth and morphological differentiation both among and, often, within experiments, the influence of temperature on the rates at which larvae became competent to metamorphose was remarkably consistent among all four experiments; larvae always became competent to metamorphose faster when reared at higher temperatures (Table III and Fig. 3). Rates of becoming competent to metamorphose were clearly uncoupled from rates of morphological differentiation and shell growth. In Experiment I, for example, larvae reared at 29°C became competent significantly sooner (and often at smaller sizes) than larvae reared at 20°C or 25°C, despite significantly slower average growth for larvae reared at the higher temperature (Figs. 2, 4). In addition, larvae reared at 25°C became competent significantly sooner than larvae at 20°C, even though these larvae did not grow at significantly different rates at the two temperatures.

The same was true of the experiments (V and VI) examining the influence of salinity. Here again, larvae reared at higher salinities generally became competent faster, while rates of growth and morphological differentiation were not so predictably affected. For example, in Experiment VI, larvae reared at 20 ppt grew significantly faster than larvae at 25 ppt, but those larvae reared at 20 ppt became competent at slower rates (Table III and Fig. 8). The influence of temperature or salinity on the amount of time required for larvae in a population to become competent clearly cannot be predicted from the effects of environmental change on rates of growth (Table V). Individual competence also cannot be predicted on the basis of shell length (Fig. 4) or the presence of a shell brim or visible gill filaments; at least some gill-less larvae were induced to metamorphose by elevating KCl concentration (at 29°C, Experiments I and II). Also, in every experiment, at every temperature, some larvae without shell brims could be induced to metamorphose. Similarly, neither shell size nor morphological indicators were adequate predictors of whether individual blue mussel larvae would or would not attach to filamentous substrates in the laboratory (Eyster and Pechenik, 1987), or when oyster larvae (*Crassostrea gigas*) would exhibit settlement behavior in response to L-DOPA (Coon *et al.*, 1990).

Variation in the rates at which individuals became competent to metamorphose within treatments (as in Figs. 2 and 8) may be a natural phenomenon that encourages larvae released from an individual female to metamorphose at different times, likely increasing the spread of siblings among different populations (Strathmann, 1974; Hadfield, 1977) and minimizing their competition for food and space as juveniles.

In our experiments, larvae consistently underwent

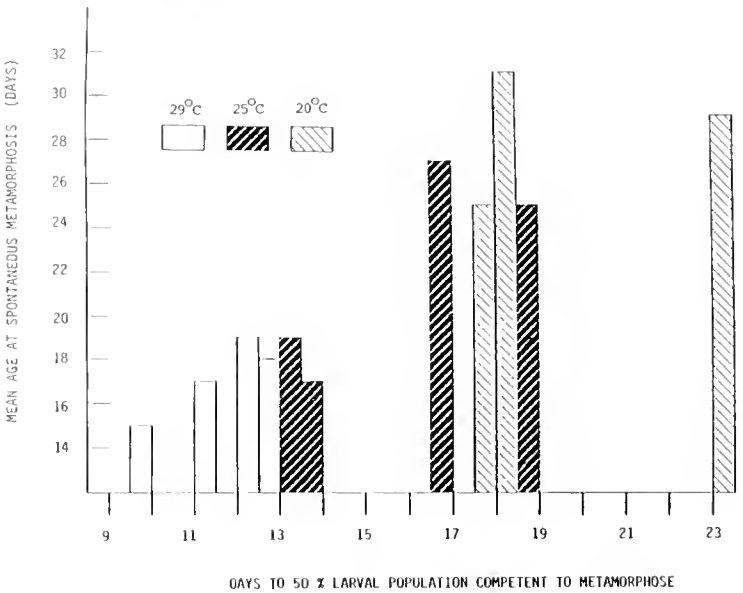

Figure 9. Influence of temperature on the relationship between the maximum length of larval life and the time required for 50% of a population to become competent. Larvae of *Crepidula plana* were reared at three temperatures, as indicated. For each temperature, different bars represent data from different experiments.

"spontaneous" metamorphosis sooner at higher temperatures (Fig. 5 and Table IV). This phenomenon of molluscan larvae metamorphosing sooner in warmer temperatures has been noted previously (Loosanoff, 1959; Davis and Ansell, 1962; Davis and Calabrese, 1964; Bayne, 1965; Pechenik, 1984; Pechenik and Lima, 1984; Lima and Pechenik, 1985). This relationship is consistent with the hypothesis that the timing of spontaneous metamorphosis is determined by the rate at which larvae progress through a developmental program with a fixed endpoint (Pechenik, 1980, 1984; Pechenik and Lima, 1984); the endpoint could be determined by some endogenous controlling factor or, as suggested recently by Coon *et al.* (1990), could reflect a gradually increasing sensitivity of receptors for an external chemical cue present naturally in extremely low concentrations. Although mean growth rates were not adequate indicators of the rates at which larvae within a population would undergo spontaneous metamorphosis (Fig. 5), faster growing individuals did tend to exhibit spontaneous metamorphosis sooner than slower growing individuals (Fig. 6). These results are similar to those reported previously for this species (Lima and Pechenik, 1985), for the congener *C. fornicata* (Pechenik, 1984; Pechenik and Lima, 1984), and for the bivalves *Mercenaria mercenaria* (Loosanoff, 1959) and *M. edulis* (Beaumont and Budd, 1982).

Despite the pronounced influence of temperature on rates of becoming competent and rates of spontaneous metamorphosis (Tables III, IV), temperature had a minor influence on the length of time that larvae of *C. plana* delayed metamorphosis in frequently cleaned glass bowls in all but one experiment (Table IV and Fig. 9). Only in Experiment II did temperature affect delay period by more than one or two days (Table IV). Thus, although larvae of *C. plana* will have a longer pre-competent period at lower temperatures, the capacity for delaying metamorphosis in the absence of suitable substrate may be affected to a much lesser degree.

In our experiments, larvae metamorphosed "spontaneously" about 3.5–12 days after becoming competent, with most delay periods lying between about 5 and 7 days (Table IV). These data are comparable to earlier laboratory estimates of delay potential for larvae of this species reared at comparable temperatures (Lima and Pechenik, 1985: their Table II), and seem to confirm the reduced capacity of *C. plana* for postponing metamorphosis relative to that exhibited by larvae of *C. fornicata;* the maximum delay period of about 20–30 days suggested for *C. fornicata* (Pechenik, 1984) is only an estimate, however, and has not yet been confirmed. The estimates of delay potential for *C. plana* reared at different temperatures given by Lima and Pechenik (1985) were based on the assumption that competence is attained at a particular shell length. The good agreement between their estimates and our more direct determinations suggest that although individual larvae clearly do not become competent to metamorphose at a particular size, the simplifying assumption of length-related competence may permit adequate predictions at the population level.

Clearly, the various aspects of morphological and

physiological development are affected to different degrees in *C. plana* by temperature and salinity changes. In only one experiment (Experiment III) did increased rearing temperature significantly increase all components of developmental rate that were monitored: shell and tissue growth, timing of gill differentiation and shell brim development, and onset of metamorphic competence. The likely impact of environmental factors on larval dispersal periods therefore cannot be estimated from data on rates of growth or morphological development, but clearly must be determined directly. Our data suggest that changes in temperature and salinity will have a more consistent influence on duration of pre-competent and competent periods of development than on either rates of shell growth or rates of morphological differentiation.

Acknowledgments

This research was completed in partial fulfillment of the requirements for the degree of Master of Science to K. M. Zimmerman. Summer support for K. M. Zimmerman was provided by NSF Grant OCE-8500857 to J. A. Pechenik. We thank Durwood Marshall for advising on analysis of covariance and Carol Valente and Valerie Ricciardone for typing the manuscript. The manuscript has benefited from the suggestions of two anonymous reviewers.

Literature Cited

Bayne, B. L. 1964. The responses of the larvae of *Mytilus edulis* L. to light and to gravity. *Oikos* **15:** 162–174.

Bayne, B. L. 1965. Growth and delay of metamorphosis of the larvae of *Mytilus edulis* L. *Ophelia* **2**(1): 1–47.

Bayne, B. L. 1971. Some morphological changes that occur at the metamorphosis of the larvae of *Mytilus edulis*. Pp. 259–280 in *Fourth European Marine Biology Symposium*, D. J. Crisp, ed. Cambridge University Press, Cambridge.

Bayne, B. L., P. A. Gabbott, and J. Widdows. 1975. Some effects of stress in the adult on the eggs and larvae of *Mytilus edulis* L. *J. Mar. Biol. Assoc. U.K.* **55:** 675–689.

Beaumont, A. R., and M. D. Budd. 1982. Delayed growth of mussel (*Mytilus edulis*) and scallop (*Pecten maximus*) veligers at low temperatures. *Mar. Biol.* **71:** 97–100.

Butman, C. A., J. P. Grassle, and C. M. Webb. 1988. Substrate choices made by marine larvae settling in still water and in a flume flow. *Nature* **333:** 771–773.

Calabrese, A., and E. W. Rhodes. 1974. Culture of *Mulinia lateralis* and *Crepidula fornicata* embryos and larvae for studies of pollution effects. *Thalassia Jugoslav.* **10**(1/2): 89–102.

Chia, F. S. 1978. Perspectives: settlement and metamorphosis of marine invertebrate larvae. Pp. 283–285 in *Settlement and Metamorphosis of Marine Invertebrate Larvae*, F. S. Chia and M. E. Rice, eds. Elsevier, New York.

Coon, S. L., D. B. Bonar, and R. M. Weiner. 1985. Induction of settlement and metamorphosis of the pacific oyster, *Crassostrea gigas* (Thunberg), by L-DOPA and catecholamines. *J. Exp. Mar. Biol. Ecol.* **94:** 211–221.

Coon, S. L., W. K. Fitt, and D. B. Bonar. 1990. Competency and delay of metamorphosis in the Pacific oyster *Crassostrea gigas*. *Mar. Biol.* **106:** 379–387.

Crisp, D. J. 1974. Factors influencing the settlement of marine invertebrate larvae. Pp. 177–265 in *Chemoreception in Marine Organisms*, P. T. Grant and A. M. Mackie, eds. Academic Press, New York.

Davis, H. C. 1958. Survival and growth of clam and oyster larvae at different salinities. *Biol. Bull.* **114**(3): 296–307.

Davis, H. C., and A. D. Ansell. 1962. Survival and growth of larvae of the european oyster, *O. edulis*, at lowered salinities. *Biol. Bull.* **122:** 33–39.

Davis, H. C., and A. Calabrese. 1964. Combined effects of temperature and salinity on development of eggs and growth of larvae of *M. mercenaria* and *C. virginica*. *U. S. Fish Wild. Fish. Bull.* **63**(3): 643–655.

Draper, N. R., and H. Smith. 1981. *Applied Regression Analysis*. John Wiley and Sons, Inc., New York. 567 pp.

Eyster, L. S., and J. A. Pechenik. 1987. Attachment of *Mytilus edulis* L. larvae on algal and byssal filaments is enhanced by water agitation. *J. Exp. Mar. Biol. Ecol.* **114:** 99–110.

Fitt, W. K., S. L. Coon, M. Walch, R. M. Weiner, R. R. Colwell, and D. B. Bonar. 1990. Settlement behavior and metamorphosis of oyster larvae (*Crassostrea gigas*) in response to bacterial supernatants. *Mar. Biol.* **106:** 389–394.

Hadfield, M. G. 1977. Chemical interactions in larval settling of a marine gastropod. Pp 403–413 in *Marine Natural Products Chemistry*, D. J. Faulkner & W. H. Fenical, eds. Plenum Publishing Corp., New York.

Hadfield, M. G. 1978. Metamorphosis in marine molluscan larvae; an analysis of stimulis and response. Pp. 165–175 in *Settlement and Metamorphosis of Marine Invertebrate Larvae*, F. S. Chia and M. E. Rice, eds. Elsevier, New York.

Hickman, R. W., and I.L. D. Gruffydd. 1971. The histology of the larva of *Ostrea edulis* during metamorphosis. Pp. 281–294 in *Fourth European Marine Biology Symposium*, D. J. Crisp, ed. Cambridge University Press, Cambridge.

His, E., R. Robert, and A. Dinet. 1989. Combined effects of temperature and salinity on fed and starved larvae of the Mediterranean mussel *Mytilus galloprovincialis* and the Japanese oyster *Crassostrea gigas*. *Mar. Biol.* **100:** 455–463.

Jackson, G. A., and R. R. Strathmann. 1981. Larval mortality from offshore mixing as a link between precompetent and competent periods of development. *Am. Nat.* **118**(1): 16–26.

Kirchman, D., S. Graham, D. Reish, and R. Mitchell. 1982. Bacteria induce settlement and metamorphosis of *Janua (Dexiospira) brasiliensis* Grube (Polychaeta:Spirorbidae). *J. Exp. Mar. Biol. Ecol.* **56:** 153–163.

Kleinbaum, D. G., L. L. Kupper, and K. E. Muller. 1988. *Applied Regression Analysis and Other Multivariate Methods*. PWS-Kent, Boston. 718 pp.

Lima, G. M. 1983. The relationship of temperature on growth rates and the length of larval life of the gastropod, *Crepidula plana* Say. Master's Thesis, Tufts University, Medford, MA. 115 pp.

Lima, G. M., and J. A. Pechenik. 1985. The influence of temperature on growth rate and length of larval life of the gastropod, *Crepidula plana* (Say). *J. Exp. Mar. Biol. Ecol.* **90:** 55–71.

Loosanoff, V. L. 1959. The size and shape of metamorphosing larvae of *Venus (Mercenaria) mercenaria* grown at different temperatures. *Biol. Bull.* **117:** 308–318.

Lucas, J. S., and J. D. Costlow, Jr. 1979. Effects of various temperature cycles on the larval development of the gastropod mollusc *Crepidula fornicata*. *Mar. Biol.* **51:** 111–117.

McGee, B. L., and N. M. Targett. 1989. Larval habitat selection of *Crepidula* (L.) and its effect on adult distribution patterns. *J. Exp. Mar. Biol. Ecol.* **131:** 195–214.

Meadows, P. S., and J. I. Campbell. 1972. Habitat selection by aquatic

invertebrates. Pp. 271–361 in *Advances in Marine Biology*, F. S. Russell and M. Yonge, eds. Academic Press, New York.

Miller, S. E. and Hadfield, M. G. 1986. Ontogeny of phototaxis and metamorphic competence in larvae of the nudibranch *Phestilla sibogae* Bergh (Gastropoda:Opisthobranchia). *J. Exp. Mar. Biol. Ecol.* **97:** 95–112.

Pechenik, J. A. 1980. Growth and energy balance during the larval lives of three prosobranch gastropods. *J. Exp. Mar. Biol. Ecol.* **44:** 1–28.

Pechenik, J. A. 1984. The relationship between temperature, growth rate, and duration of planktonic life for larvae of the gastropod *Crepidula fornicata* (L.). *J. Exp. Mar. Biol. Ecol.* **74:** 241–257.

Pechenik, J. A., and N. S. Fisher. 1979. Feeding, assimilation and growth of mud snail larvae, *Nassarius obsoletus* (Say), on three different algal diets. *J. Exp. Mar. Biol. Ecol.* **38:** 57–80.

Pechenik, J. A., and G. M. Lima. 1984. Relationship between growth, differentiation, and length of larval life for individually reared larvae of the marine gastropod, *Crepidula fornicata*. *Biol. Bull.* **166:** 537–549.

Pechenik, J. A., and W. D. Heyman. 1987. Using KCl to determine size at competence for larvae of the marine gastropod *Crepidula fornicata* (L.). *J. Exp. Mar. Biol. Ecol.* **112:** 27–38.

Pechenik, J. A., L. S. Eyster, J. Widdows, and B. L. Bayne. 1990. The influence of food concentration and temperature on growth and morphological differentiation of blue mussel *Mytilus edulis* L. larvae. *J. Exp. Mar. Biol. Ecol.* **136:** 47–63.

Rohert, R., E. His, and A. Dinet. 1988. Combined effects of temperature and salinity on fed and starved larvae of the European flat oyster *Ostrea edulis*. *Mar. Biol.* **97:** 95–100.

Scheltema, R. S. 1965. The relationship of salinity to larval survival and development in *Nassarius obsoletus* (Gastropoda). *Biol. Bull.* **65:** 340–354.

Scheltema, R. S. 1974. Biological interactions determining larval settlement of marine invertebrates. *Thalassia Jugslav.* **10**(1/2): 263–296.

Scheltema, R. S. 1978. On the relationship between dispersal of pelagic veliger larvae and the evolution of marine prosobranch gastropods. Pp. 303–322 in *Marine Organisms*, B. Battaglia and J. A. Beardmore, eds. Plenum Publishing, New York.

SPSS, Inc. 1988. *SPSS-X User's Guide, Third Edition.* SPSS, Inc., Chicago. 1072 pp.

Strathmann, R. 1974. The spread of sibling larvae of sedentary marine invertebrates. *Am. Nat.* **108**(959): 117–123.

Switzer-Dunlap, M., and M. G. Hadfield. 1977. Observations on development, larval growth and metamorphosis of four species of Aplysiidae (Gastropoda: Opisthobranchia) in laboratory culture. *J. Exp. Mar. Biol. Ecol.* **29:** 245–261.

Weiner, R. M., M. Walch, M. P. Labare, D. B. Bonar, and R. R. Colwell. 1989. Effect of biofilms of the marine bacterium *Alteromonas colwelliana* (LST) on set of the oysters *Crassostrea gigas* (Thunberg, 1793) and *C. virginica* (Gmelin, 1791). *J. Shellfish Res.* **8**(1): 117–123.

Yool, A. J., S. M. Grau, M. G. Hadfield, R. A. Jensen, D. A. Markell, and D. E. Morse. 1986. Excess potassium induces larval metamorphosis in four marine invertebrate species. *Biol. Bull.* **170:** 255–266.

Zimmerman, K. M. 1989. Differential effects of temperature and salinity on the growth and differentiation of larvae of the marine gastropod *Crepidula plana*. Master's Thesis, Tufts University, Medford, MA. 89 pp.

Reference: *Biol. Bull.* **180**: 387–393. (June, 1991)

Predation Risk and Avoidance Behavior in Two Freshwater Snails

JAMES E. ALEXANDER, JR.[1] AND ALAN P. COVICH

Department of Zoology, University of Oklahoma, Norman, Oklahoma 73019

Abstract. We examined the predator avoidance behaviors of two common freshwater snails, *Physella virgata* and *Planorbella trivolvis*, to the crayfish *Procambarus simulans*. In response to crayfish predation, the snails crawled above the waterline for several hours, then returned to the water. A significant size-dependent relationship existed between crawlout (vertical migration above the waterline) and vulnerability to predation. All observed size classes of *P. virgata*, and small *P. trivolvis*, were vulnerable and crawled out in response to crayfish predation. Large, invulnerable *P. trivolvis* did not display any overt avoidance behavior, but relied instead on strong shell architecture for defense. We suggest that, in these species, crawling above the waterline reduces the probability of an encounter between vulnerable thin-shelled snails and crayfish. This behavior is an adaptive response to predation.

Introduction

Predation is an important cause of evolutionary change in many prey taxa (Vermeij and Covich, 1978; Vermeij, 1982a, b). Predators influence their prey populations in various ways; one aspect of predation in freshwater systems that is receiving increasing attention is the behavioral interactions that occur between predator and prey (Peckarsky, 1984; Sih, 1984). The relative impact of invertebrate predators on freshwater snails, and the responses of the snails to their predators have frequently been studied (Townsend and McCarthy, 1980; Covich, 1981; Brown and DeVries, 1985; Lodge *et al.*, 1987; Brown and Strouse, 1988; Crowl and Covich, 1990; Crowl, 1990; Hanson *et al.*, 1990; Kesler and Munns, 1990; Alexander and Covich, 1991). Freshwater snails exhibit predator avoidance mechanisms, such as burying into substrata, and crawling into vegetation or above the waterline (Snyder, 1967; Townsend and McCarthy, 1980; Alexander and Covich, 1991).

Comparative studies on a variety of animals have shown that closely related or co-occurring species may respond differently to a predator. In other situations, juveniles or smaller individuals that are vulnerable to predators show stronger antipredator responses than larger, older, or other, relatively less vulnerable prey (Stein, 1977; Schmitt, 1982; Sih, 1982, 1986; Werner and Hall, 1988). In these studies, prey appear to assess the tradeoffs between predation risk and foraging for food; *i.e.*, the vulnerable species or size classes forage in different habitats, or at different times, than the invulnerable prey. Comparative studies, by revealing the variety and relative effectiveness of antipredator responses, help to elucidate the adaptive nature of a response. In this paper, we describe the predator avoidance response of two common, co-occurring freshwater snail species, *Physella virgata* (Pulmonata, Physidae, Fig. 1A) and *Planorbella trivolvis* (Pulmonata, Planorbidae, Fig. 1B, C), to their predator, the crayfish *Procambarus simulans* (Decapoda, Astacidae). In another paper (Alexander and Covich, 1991), we demonstrated that *Physella virgata* performs a chemically mediated predator avoidance behavior (crawling above the waterline for a minimum of 2 h) in response to an actively foraging crayfish predator. *Physella virgata* appears to react to chemicals emanating from crayfish and from injured conspecifics. In this study, we demonstrate a size-dependent avoidance response that corresponds to the relative vulnerability of a snail to crayfish predation.

Received 2 November 1990; accepted 19 March 1991.

[1] To whom communications should be sent. Present address: Department of Biology, Box 19498, The University of Texas at Arlington, Arlington, TX 76019.

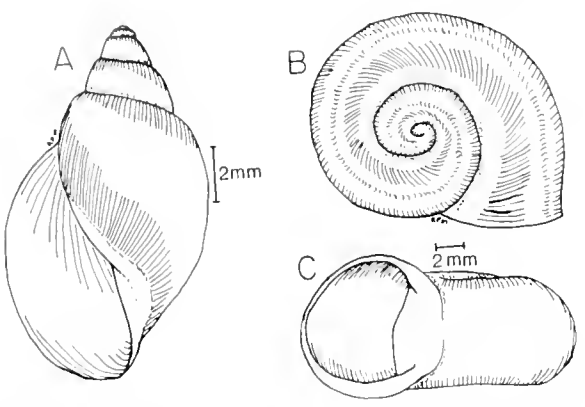

Figure 1. The shell morphology of *Physella virgata* (A) and *Planorbella trivolvis* (B and C). The size bar is 2 mm.

Materials and Methods

Study site and general methods

The snails and crayfish used in this study were collected from Oliver Wildlife Preserve (Norman, Oklahoma). Oliver Wildlife Preserve is a forested area on the South Canadian River floodplain that is inundated periodically by runoff and heavy spring rains. The middle third of the preserve typically remains under water throughout the late winter to early summer months (December to June) and supports large populations of *P. virgata*, *P. trivolvis*, and *P. simulans* (Alexander, 1987). Woody debris in Oliver Wildlife Preserve provide abundant substrata onto which the snails migrate to avoid predators; snails were observed above the waterline throughout the year at Oliver Wildlife Preserve and at other sites (pers. obs.).

Laboratory experiments were conducted at night, in darkness, simulating the natural conditions under which crayfish are most active. No substratum was included in these experiments. For the handling time and ingestion probability experiments (Experiment 1), where crayfish and snails were under continuous observation, low intensity red light was used to facilitate observations. In the second experiment, low intensity white light was used briefly to record observations. When not used in experiments, snails were maintained in 40–80-l aquaria and fed commercial fish food (TetraMin) and lettuce *ad libitum*. Crayfish were housed individually in 4-l plastic containers and fed fish food pellets and lettuce *ad libitum*. Crayfish were starved for at least 24 h prior to the start of the experiments.

Experiment 1: differential vulnerability of Physella *and* Planorbella

This experiment was aimed at examining the ability of *P. simulans* to handle and ingest different size classes of *P. virgata* and *P. trivolvis*. A 10-l aquarium was placed so that the actions of the crayfish and snails could be observed under low intensity red light illumination, regardless of their position in the aquarium. The snails were sorted according to shell length (SL), in 1-mm increments (±0.5 mm), ranging from 5 to 12 mm. For each observation, 50 snails of one size class and species were placed in the aquarium in 2 l of previously aerated tap water. One adult *P. simulans* [carapace length (CL) = 28–36 mm] was then added to the aquarium. Two variables were recorded during the observation period: (a) handling times (time spent consuming a prey), and (b) ingestion probabilities (if a snail was eaten, rejected, or had escaped from the predator once captured). The crayfish (n = 6) were tested with all size classes of both species, randomly, during 15-min observation times, over a 2-week period. Crayfish were observed feeding on one size class of one snail species in all observation periods. Handling time was defined as the period including the capture of the snail, the consumption of the snail, the crayfish cleaning its mouthparts, and the movement forward by the crayfish to continue foraging. Each snail capture was noted, as well as the number of snails that were either consumed or rejected. The ratio of number of snails eaten to the number of snails captured was defined as the ingestion probability.

Experiment 2: size-mediated predator avoidance

To examine the relationship between snail size, predation vulnerability, and avoidance behavior in both snail species, *P. virgata* and *P. trivolvis* were sorted into five size categories (4.1–6.0, 6.1–8.0, 8.1–10.0, 10.1–12.0, and 12.1–16.0 mm SL). A total of 100 snails of one species was added to each 40-l aquarium (25 × 50 × 30 cm) with 5 l of previously aerated tap water. Due to unequal numbers available from the field in each size class, the size class categories contained unequal numbers of snails. With *P. virgata*, the numbers of snails per size class added were: 10, 30, 30, 25, and 5 snails in each of the increasing size classes, respectively. With *P. trivolvis*, the numbers of snails per size class were: 30, 30, 20, 10, and 10 snails in each of the increasing size classes, respectively.

To half of the eight replicates per snail species, one adult (CL = 30–40 mm) *P. simulans* was added at 2200 h. The other four replicates served as predator-free controls. The crayfish were allowed to feed without interruption for 2 h in total darkness, then the number of snails out above the waterline, as well as the number of snails eaten, were determined for each size class and species. Because all five snail class sizes were included in each aquarium, a split-plot ANOVA examined the effects of the two independent variables (presence or absence of crayfish and snail size) on the number of snails killed in

each size class (dependent variable). A second ANOVA separately analyzed differences in the number of surviving snails in each size class found above the waterline as the dependent variable. Each snail species was analyzed separately. Because the data were expressed as proportions (proportion of the snails killed and the proportion of the surviving snails above waterline), the data were arc-sine transformed prior to analysis (Sokal and Rohlf, 1981).

Results

Experiment 1: differential vulnerability of Physella *and* Planorbella

Handling times increased exponentially with increasing snail size for both species (Fig. 2A). For *P. trivolvis*, handling times increased more rapidly with increasing shell size than did the handling times for *P. virgata*. For each snail prey, an exponential equation was fitted by least squares non-linear regression to the handling time data of each snail species. The resultant best-fit non-linear regression between shell length (SL) and handling times (HT) for *P. virgata* was $HT = 0.095\ e^{0.28(SL)}$ ($n = 279$, $r^2 = 0.75$), and for *P. trivolvis:* $HT = 0.118\ e^{0.42(SL)}$ ($n = 113$, $r^2 = 0.74$). For both species, the best-fit exponential equations fit the data well, explaining 74–75% of the observed variance in the samples.

The ingestion probabilities decreased more rapidly with increasing shell size for *P. trivolvis* than for *P. virgata* (Fig. 2). Approximately 60% of the smallest *P. trivolvis* (5–7 mm SL) were not eaten once captured, and few of the larger *P. trivolvis* (>8 mm SL) were picked up by the crayfish. In contrast, all small *P. virgata* (<8 mm SL) were eaten, once captured. The difference in vulnerability between the two snail species was significant; *P. virgata* were more likely to be eaten, once captured, at all size classes (Wilcoxin signed-ranks test, $T = 0$, $n = 5$, $P < 0.05$, Siegel, 1956). The snail size at which 50% of prey captured were rejected (called R^{50}) was calculated from linear regression analyses run for each individual crayfish, using the rejection data (log 10 transformed). The mean R^{50} for *P. trivolvis* was 6.5 mm, and the mean R^{50} for *P. virgata* was 10.7 mm. The R^{50} for *P. trivolvis* was larger than the R^{50} for *P. virgata* for each crayfish used in the experiment (Wilcoxin signed-ranks test, $T = 0$, $n = 6$, $P < 0.05$).

For both prey species, handling times decreased at the largest size class tested. The apparent decrease occurred because the three smaller crayfish used in the study could not consume snails greater than 8 mm SL (in *P. trivolvis*) and 12 mm SL (in *P. virgata*).

Experiment 2: size-mediated predator avoidance

Two-way analysis of variance results demonstrated that in *P. virgata*, only the presence of a predator had a significant effect on both dependent variables (the numbers of surviving snails above the waterline and the number of snails killed) (Fig. 3A, B, Table I). No significant effect of snail size was observed in *P. virgata;* all sizes of *P. virgata* were equally vulnerable and were equally likely to crawl above the waterline. In contrast, for *P. trivolvis*, both independent variables (predator presence, snail size) and the interaction between predator presence and snail size all were very significant (Fig. 4A, B, Table I). The significant size effect was due to the inverse relationship between size and both snail mortality and the number of surviving snails above the waterline. Smaller *P. trivolvis* were more likely than larger individuals to be eaten. In addition to being more vulnerable to *P. simulans* predation, small (4–6 mm SL) *P. trivolvis* displayed the most prominent crawlout response, with most of the surviving snails above the waterline. Medium-sized specimens (6–12 mm SL) of *P. trivolvis* were intermediate in vulnerability and were less likely than smaller animals to display the crawlout response. Larger (12–16 mm SL) specimens of *P. trivolvis* were least vulnerable and did not display an increase in crawlout response over that seen in predator-free control aquaria. No significant level of mortality

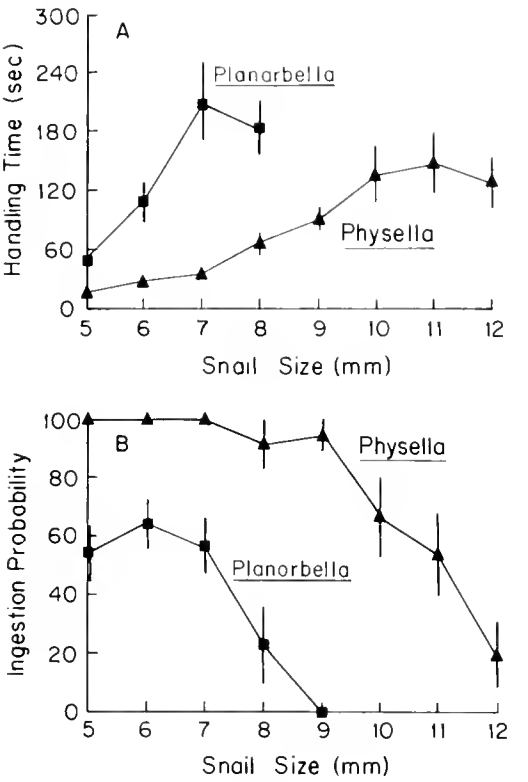

Figure 2. The influence of snail size (shell length) on handling times (A) and ingestion probabilities (B) in *Physella virgata* and *Planorbella trivolvis*, fed upon by *Procambarus simulans*. The error bars are standard errors of the mean.

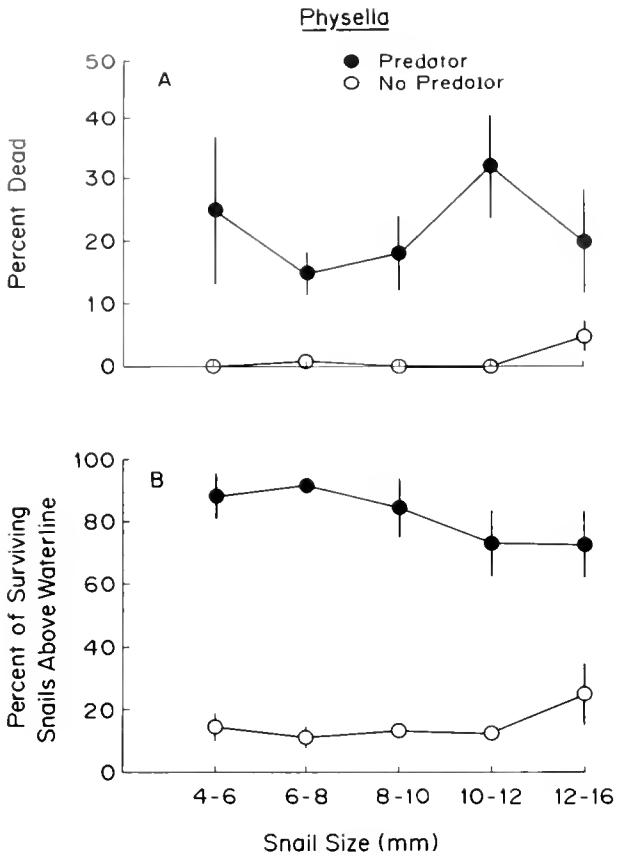

Figure 3. Size-mediated predator avoidance and death in *Physella virgata*. The upper figure (A) is the percentage of dead snails in each size class (shell length), the lower figure (B) represents the percentage of surviving snails in each size class above the waterline, in both predator (darkened circles) and predator-free control (open circles) treatments (n = 4 in both treatments). The error bars are standard errors of the mean.

or crawlout was observed in the predator-free control aquaria in either species.

Of the 315 surviving *P. trivolvis*, 23 (7.3%) had some shell damage due to crayfish. The damaged shells were not randomly distributed among the size classes. In the two largest size classes, 8.3% and 5.1% of the surviving 10–12 mm and 12–16 mm SL size classes were damaged, respectively. The two smallest (4–6 mm and 6–8 mm SL) size classes had fewer damaged shells than expected (1.3% and 6.3%, respectively), based on the number of snails originally available in each size class, while the intermediate (8–10 mm SL) sized class had more damaged shells than expected, 15.7% (χ^2 goodness-of-fit test, $\chi^2 = 10.9$, d.f. = 4, $P < 0.05$). In marked contrast, only one out of the 314 surviving *P. virgata* (in the 8–10 mm SL size class) showed shell damage due to crayfish manipulation.

There was no difference in the predation intensity in aquaria housing *P. trivolvis* or *P. virgata;* the crayfish consumed equal numbers of *P. virgata* (86) and *P. trivolvis* (85) among the four replicates in each treatment, suggesting that there was no difference in hunger motivation in the predators used. On average, each crayfish consumed

Table I

The influence of snail size on crawlout behavior in Physella virgata *and* Planorbella trivolvis

	Variable: % dead		Variable: % crawlout	
Factor (d.f.)	*P. trivolvis* F	*P. virgata* F	*P. trivolvis* F	*P. virgata* F
Predator presence (1, 6)	119.3***	18.8**	160.5***	146.5***
Snail size (4, 24)	3.0*	0.4	15.5***	0.3
Predator × Size (4, 24)	3.8*	1.0	12.7***	0.7

The table describes the summary of the ANOVA analyses. Each of the dependent variables (percent dead, percent surviving snails above the waterline) were analyzed separately, for each species. (Significance levels are as follows: $*P < 0.05$; $**P < 0.01$; and $***P < 0.001$.)

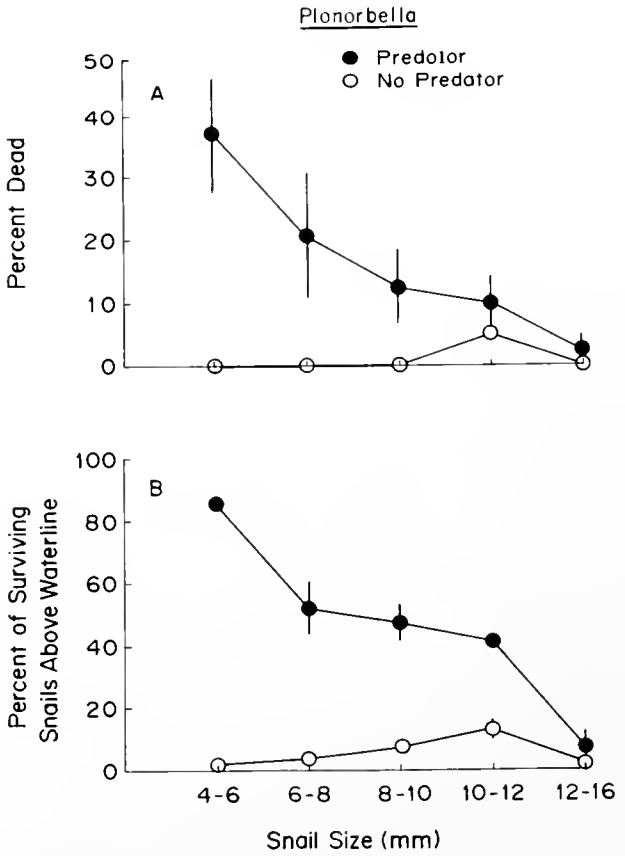

Figure 4. Size-mediated predator avoidance and death in *Planorbella trivolvis*. The treatments and symbols are the same as in Figure 3.

slightly more than 21 snails of either prey species during the 2-h observation period.

Discussion

In marine systems, gastropod anti-predator structures and behaviors are common. Marine snails rely either on strong shell architecture (Palmer, 1979; Bertness *et al.*, 1981; Schmitt, 1982; Blundon and Vermeij, 1983; Lowell, 1986) or on escape and avoidance behavior. Many marine snails crawl towards or above the waterline to temporarily escape from or avoid their predators, such as crabs, sea stars, and predatory gastropods (Feder, 1963; Ansell, 1969; Phillips, 1976; Vaughn and Fisher, 1988). Like many marine gastropod species, the crawlout responses in *P. virgata* and *P. trivolvis* represent the active use of a potential refuge (the terrestrial environment) that temporarily protects these freshwater snails from crayfish predation.

In this study, handling times (time spent consuming prey) and the ingestion probabilities (probability of consuming a prey) were expected to differ between the two prey, because differences in vulnerability existed due to differences in relative shell thickness and shell shape between the two snail species. From these results, it was clear that *P. virgata* were much more vulnerable to crayfish than similar-sized *P. trivolvis*. Crayfish could not consume large *P. trivolvis*, because they could not either crush the thicker planispiral shell or manipulate the shell to a position where the mouthparts could crush it or chip the thickened aperture lip (pers. obs.). Crayfish often dropped large *P. trivolvis* (SL > 6 mm) after lengthy handling periods, and subsequently ignored large *P. trivolvis* after several unsuccessful predation attempts. In contrast, in all size classes, the thinner, elongated spiral shell of *P. virgata* could be manipulated and crushed by the same crayfish, strongly suggesting that specimens of *P. virgata* were more vulnerable to crayfish predation than *P. trivolvis*. Crayfish either crushed the shell at the body whorl, chipped away at the aperture lip, or had broken off the shell spire (pers. obs.). Because their shells provided little structural defense, specimens of all size classes of *P. virgata* were equally vulnerable to crayfish predation and thus were equally likely to crawl above the waterline (Fig. 3).

In examining the surviving snails from the second experiment, only one living specimen of *P. virgata* with a damaged shell was observed in the experiment, strong indirect evidence that, once a specimen of *P. virgata* was captured, the snail was usually eaten. In addition, when foraging on *P. virgata*, crayfish almost always were able to effectively handle and consume *P. virgata* encountered, as shown by the high ingestion probabilities (Fig. 2). For *P. trivolvis*, 23 (7.3%) of the surviving animals recovered in the second experiment were observed with some damage, suggesting that they survived a predatory encounter with the crayfish.

At any given size, specimens of *P. trivolvis* required 2–4 times the handling time by crayfish for successful predation than did similar-sized *P. virgata* (Fig. 2A), indicating the much greater difficulty in crushing the *P. trivolvis* shells. Stein *et al.* (1984), comparing the prey value of a physid (*Physa* sp.) and a planorbid (*Helisoma* sp.) to redear sunfish (*Lepomis microlophus*), noted that redear sunfish weakly selected the physid over the planorbid, but that size selection did not occur within either genus. The force required to crush the physid (3 Newtons for 10 mm SL *Physa* lying aperture down) was less than that required to crush the planorbid (4 Newtons for 10 mm SL *Helisoma* lying on its side), but the difference in force was not dramatically different. The shells were crushed in this way because sunfish were observed orienting snails between their pharyngeal gill plates (their crushing surfaces) so as to crush the minimal dimension of the shell. Crayfish in our study crushed snail shells primarily by chipping with their mandibles at the shell aperture, holding the snail with their maxillipeds. Sometimes, crayfish appeared to use their chelae to balance and press the shell against their mandibles. Although we did not measure the force required for crayfish to crush *P. virgata* and *P. trivolvis* shells, nor did we measure the shell thicknesses, the data suggest that crayfish could more easily crush *P. virgata* shells than *P. trivolvis* shells, because crayfish primarily attempt to break the aperture lip, particularly in *P. trivolvis*, and not the entire shell.

Antipredator mechanisms may be quite dissimilar in closely related gastropod species. Two congeneric species of marine snails, *Tegula eiseni* and *T. aureotincta*, differ in their predator defenses; *T. aureotincta* performed avoidance behaviors to gastropod and asteroid predators, while *T. eiseni* depended more on shell morphology for defense (Schmitt, 1982). *Physella virgata* relies on behavioral avoidance much more exclusively than does *P. trivolvis*, which appears to rely more on predator avoidance when young, and on shell strength as larger adults.

The correspondence between the reactivity of snails of a given size class and their vulnerability was expected, if predator avoidance behavior (crawlout) has some costs associated with reacting inappropriately to the potential threat of predation. Crawling to or above the waterline could expose the snail to other predators, including birds, and certain insects, such as belostomatids (Crowl and Alexander, 1989; Kesler and Munns, 1990). Further costs to crawlout behavior include decreased foraging time (if the animals cannot forage on food above the waterline), decreased opportunities for reproduction, and desiccation (Alexander and Covich, 1991).

The differences in the antipredator responses between the two species may be influenced by differences in selective pressures caused by the distinct physiological adaptations used by the two snails in their respective microhabitats (McMahon, 1983). *Planorbella trivolvis,* with its well-developed neomorphic gill, and its more efficient respiratory pigment (hemoglobin), is much more aquatic than *P. virgata,* which retains an air-filled mantle cavity (lung) as the major organ of gas exchange. *Physella virgata* makes periodic excursions to the surface to renew its oxygen store, and subsequently is limited to shallow water near-shore habitats or those habitats with structure (*i.e.,* aquatic macrophytes or woody debris) extending above the waterline. *Planorbella trivolvis,* with a much greater capacity for aquatic gas exchange, makes excursions into much deeper water, where crawlout sites are likely to be unavailable. In *P. virgata,* physiologically restricted to shallow, near-shore waters, selective pressures may have caused a retention of a strong crawlout response to avoid predators and reduced pressure for the development of a structurally predator-resistant shell. In contrast, *P. trivolvis,* whose range (particularly in adults) extends into deeper water and consequently has little access to terrestrial refugia, selection pressures may have been towards development of a structurally predator-resistant shell and a reduced dependence on a crawlout response.

Because they can be the dominant primary consumers in some habitats, mollusks and decapod crustaceans play important roles in many aquatic communities. Many are herbivorous, detritivorous, or omnivorous, and are important for cycling nutrients and providing energy in the form of variously sized food items for higher trophic level consumers (Ansell, 1969; Momot *et al.,* 1978; Grimm, 1988). The study of the behavioral interplay between freshwater snails and crayfish is essential in understanding how these behavioral processes influence predator-prey dynamics and community composition. Rapid snail escape and avoidance behavior, and the subsequent decrease in encounter probabilities, suggest that in some structurally complex habitats, such as macrophyte-dominated littoral zones or forested wetland areas, vertical migration above the waterline is an adaptive response to crayfish predation.

Acknowledgments

The first author thanks his Ph.D. advisory committee: R. Mellgren, D. Mock, F. Sonleitner, and T. Yoshino, for their suggestions. Various versions of the manuscript and statistical analyses were improved by the efforts of T. Crowl, K. Brown, and P. Rutledge. We thank R. McMahon for his help with snail identification, figure drawings, for providing insight into the different physiological constraints on the two snails, and for critically evaluating the final manuscript. Two anonymous reviewers helped to evaluate the final manuscript. The research was supported by research and teaching assistantships from the Department of Zoology, University of Oklahoma, and by NSF grant BSR 8500773.

Literature Cited

Alexander, J. E., Jr. 1987. Predator-prey interactions between freshwater snails and crayfish. Ph.D. dissertation, University of Oklahoma.

Alexander, J. E., Jr., and A. P. Covich. 1991. Predator avoidance in the freshwater snail *Physella virgata* to the crayfish *Procambarus simulans. Oecologia* (in press).

Ansell, A. D. 1969. Defensive adaptations to predation in the mollusca. *Proc. Mar. Biol. Assoc. India Symp. Ser.* **3:** 487–512.

Bertness, M. D., S. D. Garrity, and S. C. Levings. 1981. Predation pressure and gastropod foraging: a tropical-temperate comparison. *Evolution* **35:** 995–1007.

Blundon, J. A., and G. J. Vermeij. 1983. Effect of shell repair on shell strength in the gastropod *Littorina irrorata. Mar. Biol.* **76:** 41–45.

Brown, K. M., and D. R. DeVries. 1985. Predation and the distribution and abundance of a pulmonate pond snail. *Oecologia* **66:** 93–99.

Brown, K. M., and B. H. Strouse. 1988. Relative vulnerability of six freshwater gastropods to the leech *Nephelopsis obscura* (Verrill). *Freshwater Biol.* **19:** 157–165.

Covich, A. P. 1981. Chemical refugia from predation for thin-shelled gastropods in a sulfide-enriched stream. *Verh. Int. Vereinigung Theoret. Angewandte Limnol.* **21:** 1632–1636.

Crowl, T. A. 1990. Life-history strategies of a freshwater snail in response to stream permanence and predation: balancing conflicting demands. *Oecologia* **84:** 238–243.

Crowl, T. A., and J. E. Alexander, Jr. 1989. Parental care and foraging ability in male waterbugs (*Belostoma flumineum*). *Can. J. Zool.* **67:** 513–515.

Crowl, T. A., and A. P. Covich. 1990. Predator-induced life-history shifts in a freshwater snail. *Science* **247:** 949–951.

Feder, H. M. 1963. Gastropod defensive responses and their effectiveness in reducing predation by starfishes. *Ecology* **44:** 505–512.

Grimm, N. B. 1988. Role of macroinvertebrates in nitrogen dynamics of a desert stream. *Ecology* **69:** 1884–1893.

Hanson, J. M., P. A. Chambers, and E. E. Prepas. 1990. Selective foraging by the crayfish *Orconectes virilis* and its impact on macroinvertebrates. *Freshwater Biol.* **24:** 69–80.

Kesler, D. K., and W. R. Munns, Jr. 1990. Predation by *Belostoma flumineum* (Hemiptera): an important cause of mortality in freshwater snails. *J. N. Am. Benthol. Soc.* **8:** 342–350.

Lodge, D. M., K. M. Brown, S. P. Klosiewski, R. A. Stein, A. P. Covich, B. K. Leathers, and C. Bronmark. 1987. Distribution of freshwater snails: spatial scale and the relative importance of physicochemical and biotic factors. *Am. Malacol. Union* **5:** 73–84.

Lowell, R. B. 1986. Crab predation on limpets: predator behavior and defensive features of the shell morphology of the prey. *Biol. Bull.* **171:** 577–596.

McMahon, R. F. 1983. Physiological ecology of freshwater pulmonates. Pp. 359–430 in *The Mollusca, Vol. 6, Ecology,* W. D. Russell-Hunter, ed. Academic Press, Inc., Orlando, FL.

Momot, W. T., H. Gowing, and P. D. Jones. 1978. The dynamics of crayfish and their role in ecosystems. *Am. Midl. Nat.* **99:** 10–35.

Palmer, A. R. 1979. Fish predation and the evolution of gastropod shell sculpture: experimental and geographic evidence. *Evolution* **33:** 697–713.

Peckarsky, B. L. 1984. Predator-prey interactions among aquatic insects. Pp. 196–254 in *The Ecology of Aquatic Insects*, V. H. Resh and D. M. Rosenberg, eds. Praeger Scientific, New York.

Phillips, D. W. 1976. The effect of a species-specific avoidance response to predatory starfish on the intertidal distribution of two gastropods. *Oecologia* **23:** 83–94.

Schmitt, R. J. 1982. Consequences of dissimilar defenses against predation in a subtidal marine community. *Ecology* **63:** 1588–1601.

Siegel, S. 1956. *Nonparametric Statistics For The Behavioral Sciences* McGraw-Hill, Inc., New York.

Sih, A. 1982. Foraging strategies and the avoidance of predation by an aquatic insect, *Notonecta hoffmanni*. *Ecology* **63:** 786–796.

Sih, A. 1984. The behavioral response race between predator and prey. *Am. Nat.* **123:** 143–150.

Sih, A. 1986. Antipredator responses and the perception of danger by mosquito larvae. *Ecology* **67:** 434–441.

Snyder, N. F. R. 1967. An alarm reaction of aquatic gastropods to intraspecific extract. *Cornell University Agricultural Experimental Station Memoir* 403.

Sokal, R. R., and F. J. Rohlf. 1981. *Biometry*, 2nd ed. W. W. Freeman and Co., San Francisco.

Stein, R. A. 1977. Selective predation, optimal foraging, and the predator-prey interaction between fish and crayfish. *Ecology* **58:** 1237–1253.

Stein, R. A., C. G. Goodman, and E. A. Marschall. 1984. Using time and energetic measures of cost in estimating prey value for fish predators. *Ecology* **65:** 702–715.

Townsend, C. R., and T. K. McCarthy. 1980. On the defence strategy of *Physa fontinalis* (L.), a freshwater pulmonate snail. *Oecologia* **46:** 75–79.

Vaughn, C. C., and F. M. Fisher. 1988. Vertical migration as a refuge from predation in intertidal marsh snails: a field test. *J. Exp. Mar. Biol. Ecol.* **123:** 163–176.

Vermeij, G. J. 1982a. Phenotypic evolution in a poorly dispersing snail after arrival of a predator. *Nature* **299:** 349–350.

Vermeij, G. J. 1982b. Unsuccessful predation and evolution. *Am. Nat.* **120:** 701–720.

Vermeij, G. J., and A. P. Covich. 1978. Coevolution of freshwater gastropods and their predators. *Am. Nat.* **112:** 833–843.

Werner, E. E., and D. J. Hall. 1988. Ontogenetic habitat shifts in bluegill: the foraging rate-predation risk trade-off. *Ecology* **69:** 1352–1366.

Reference: *Biol. Bull.* 180: 394–405. (June, 1991)

Shape Variation in Hydractiniid Hydroids

NEIL W. BLACKSTONE[1] AND LEO W. BUSS[1,2]

[1]*Department of Biology, and* [2]*Department of Geology and Geophysics, Yale University, New Haven, Connecticut 06511*

Abstract. Colonies of hydractiniid hydroids consist of feeding polyps connected by a common gastrovascular system. The gastrovascular system consists of stolons, which enclose gastrovascular canals. Stolons may be fused into a stolonal mat or extend from the periphery of the colony. *Hydractinia* forms a stolonal mat early in colony development; *Podocoryne*, on the other hand, does not. To facilitate comparisons of these taxa, we propose a simple shape metric, $perimeter/\sqrt{area}$, and show that this measure: (1) correlates closely with relative amounts of peripheral stolon and stolonal mat structures in *Hydractinia*, (2) permits analyses of within- and between-species variation of growth morphology in *Podocoryne* and *Hydractinia*, and (3) allows quantitative analysis of breeding studies of *Hydractinia*, both before and after stolonal mat formation in the progeny.

Introduction

Hydractiniid hydroids encrust hard substrata in the sea. *Hydractinia echinata* and related species are commonly found on the shells of hermit crabs and often exhibit a species-specific correlation with host hermit crabs (Buss and Yund, 1989; Cunningham *et al.*, in press). *Podocoryne carnea* also encrust hermit crab shells, but commonly inhabit other substrata as well (Edwards, 1972; Mills, 1976). Colony development in both taxa begins with the metamorphosis of the planula larvae into a primary polyp. Runner-like stolons extend from the primary polyp. Stolons encase fluid-filled, gastrovascular canals that are continuous with the gastrovascular cavity of the polyp. *Podocoryne* continues to develop in this way, *i.e.*, by lineal extension of the stolons, initiation of new stolon tips, and iteration of feeding polyps on the stolons (Braverman, 1963; McFadden, 1986). Stolons in *Hydractinia*, however, quickly fuse to form a continuous stolonal mat, which shows sheet-like growth, and from which extend varying amounts of peripheral stolons (McFadden *et al.*, 1984; Blackstone and Yund, 1989; Buss and Grosberg, 1990). Figure 1 provides rough schemata of the differences in form between these taxa.

While morphological variation within each taxon has been compared and related to ecological characteristics (*e.g.*, competitive ability; see McFadden *et al.*, 1984; McFadden, 1986; Yund, 1987; Buss and Grosberg, 1990), quantitative comparisons of between-taxa variation have been hampered by the differences in growth form, *i.e.*, the presence of a stolonal mat in *Hydractinia* and its absence in *Podocoryne*. For instance, competitive ability among strains of *Hydractinia* has been shown to correlate with relative amounts of peripheral stolon and stolonal mat structures (measured using several methods, see McFadden *et al.*, 1984; Yund, 1987; Buss and Grosberg, 1990), but such measures cannot be applied to *Podocoryne*.

To facilitate comparisons of biological traits between *Podocoryne* and *Hydractinia*, we propose a simple measure of morphology that can be used in both taxa. We show that this measure correlates with ratios of peripheral stolon and stolonal mat structures in *Hydractinia*, and we use this measure to examine morphological variation and its genetic basis both between and within *Podocoryne* and *Hydractinia*. Finally, we relate this variation to ecological, evolutionary, and developmental aspects of these species and discuss the relevance to other clonal taxa as well.

Materials and Methods

Growth morphology and shape

We suggest treating hydractiniid hydroids as geometric shapes for purposes of comparison. We prefer Bookstein's

Received 7 August 1990; accepted 19 February 1991.

(1978: p. 8) definition: ". . . a shape is an outline-with-landmarks from which all information about position, scale, and orientation has been drained," with the qualification that hydroid colonies have no reliable morphological landmarks. Further, the aspects of hydractiniid growth morphology of particular interest are essentially two-dimensional, comprising those portions of the colony that adhere to the substratum. Although there are sophisticated techniques available for the analysis of two-dimensional shapes-without-landmarks (*e.g.*, Lohman, 1983; Ferson *et al.*, 1985), we will take a simpler approach. The terms previously used to categorize hydractiniid growth morphology (many peripheral stolons = "net type," few peripheral stolons = "mat type," see Hauenschild, 1954) point out an intuitively obvious correlation between two-dimensional growth morphology and shape. Colonies with few peripheral stolons often show approximately circular growth forms, while colonies with many peripheral stolons exhibit more irregular shapes (Fig. 1).

An appropriate "size-free" metric to quantify these differences in shape is $perimeter/\sqrt{area}$ (*cf.*, Gould, 1973; Patton, 1975). We point out several properties of this measure, by way of introducing it to morphological studies of encrusting clonal organisms. First, regardless of scale, this measure is constant for a given geometric shape. For instance, this measure will equal $2\sqrt{\pi}$ for a circle, 4 for a square, ≈ 4.5 for an equilateral triangle, ≈ 5.4 for a "first-aid" sign, ≈ 5.7 for a cross (length of the long arm is twice that of the three short arms), and so on. In each case, these values are constant regardless of the actual size of the object as long as the same units are used to measure both perimeter and area. Second, while the same geometric shapes will have similar $perimeter/\sqrt{area}$ values, shapes with the same $perimeter/\sqrt{area}$ need not be the same. In fact, for encrusting clonal organisms, no two shapes are likely to be the same, yet many may have similar $perimeter/\sqrt{area}$ values. This shape metric thus only assesses the degree of circularity of a shape. Shapes with values close to $2\sqrt{\pi}$ approach perfect circularity, while highly non-circular shapes have much larger values. Third, $perimeter/\sqrt{area}$ has a minimum at $2\sqrt{\pi}$; possible values thus have a lower bound, and their distributions may be skewed. Note that this is not unusual; most morphometric measurements have a lower bound at zero and thus may form skewed distributions. Regardless of the lower bound (0 or $2\sqrt{\pi}$), a log-transformation usually provides distributions suitable for parametric analysis (see Sokal and Rohlf, 1981).

The utility of this measure may be visualized by comparing a plot of perimeter and area for two sibling *Hydractinia* colonies (Fig. 2) grown from primary polyps under standard conditions (see McFadden *et al.*, 1984). While the perimeter *versus* area trajectories fluctuate as stolons branch and fuse, it is clear that the colony with a greater amount of stolons projecting from the center has a larger perimeter for a given area and larger $perimeter/\sqrt{area}$ values. To assess quantitatively the capacity of this shape metric to assay the amount of peripheral stolons, we measured the correlation between $perimeter/\sqrt{area}$ and peripheral stolon development for the 242 *Hydractinia* colonies used in a breeding study (see protocol below). At age 50 days, each colony was measured using a digital image analysis system. Briefly, an Eyecom II camera attached to a Wild Makroskop was used to project each colony onto a black-and-white monitor (640×480 pixels; note that the pixels are orthogonal and that the length of a pixel is the same in either direction). Points on the video image of each colony were recorded with a digitizing tablet interfaced with a DEC PDP-11 minicomputer. The outline of each colony was traced with points at 5 pixel intervals, and the perimeter and area were computed. The outline of the stolonal mat, *i.e.*, the fused stolons (see Fig. 1), was also traced, and the perimeter and area were measured. Scales ranged from 150 pixels/mm for the smallest colonies to 25 pixels/mm for the largest colonies. Over this range of observation, these colonies are not fractal, *i.e.*, they do possess a characteristic scale and do not show self-similarity over the different scales of observation employed here (although self-similarity may be apparent using other scales of observation). Thus, while smaller colonies were measured with slightly greater resolution, this did not bias the results in a systematic fashion. Data were transferred to an IBM-PC and uploaded to an IBM 3083 mainframe where analysis was done using SAS software.

Comparing peripheral stolon development to colony shape entails methodologic problems. Logical measures of peripheral stolon development involve a measure of the total size of the colony divided by the size of the stolonal mat (*e.g.*, total colony perimeter/stolonal mat perimeter and total colony area/stolonal mat area). Given the nature of colony growth (*i.e.*, peripheral stolons projecting from a central area of stolonal mat, Fig. 1), the extent to which these ratios are greater than 1 will measure the amount of peripheral stolons. A straightforward procedure would be to correlate these ratios to the total perimeter divided by the square root of the total area (*i.e.*, the shape metric). However, this could result in autocorrelation, because both ratios necessarily contain measures of the overall size of the colony (either total perimeter or total area). We measured these correlations and then assessed the effects of autocorrelation by adjusting the correlated ratios to remove similar variables from each. For instance, the correlation of the ratio, colony perimeter/stolonal mat perimeter, to the ratio, $perimeter/\sqrt{area}$, can

be considered equivalent to the correlation of stolonal mat perimeter to $\sqrt{area}$ if there are no effects of autocorrelation. Further, we considered the biological meaning of correlations between stolonal mat size and total colony size and whether these correlations support our interpretation of the shape metric. Spearman's coefficient of rank correlation (r_s) was used; this coefficient is less sensitive to the statistical pecularities of ratios than parametric correlation coefficients (see Sokal and Rohlf, 1981), although here both coefficients were similar for all correlations.

Shape variation in Podocoryne *and* Hydractinia

The *perimeter*/$\sqrt{area}$ measure was used to compare morphological variation within and between field-collected colonies of *Podocoryne* and *Hydractinia* using the technique of clonal repeatibility, *i.e.*, comparing clonal replicates of the same colony to gauge broad-sense heritability (Falconer, 1981). Colonies were collected from an intertidal site near Guilford, Connecticut, where *Podocoryne carnea* and *Hydractinia symbiolongicarpus*, a sibling species of *H. echinata*, commonly co-occur (Buss and Yund, 1989), although *Podocoryne* is much less abundant than *Hydractinia*. When reproductive polyps are present, these species can be easily distinguished: *Podocoryne* produces free-swimming medusae, while *Hydractinia* lacks a medusoid stage and produces fixed gonophores (Mills, 1976). Using a dissecting microscope, *Podocoryne* colonies were identified from large collections of all hydroid-bearing hermit crab shells. Relatively few colonies contained reproductive polyps; hence, tentative identifications were made on the basis of general patterns of colony appearance (in this area, *Podocoryne* has few spines and usually co-occurs with algal epibionts) and feeding polyp morphology (in this area, *Podocoryne* tends to have smaller polyps, a more pronounced hypostome, and shorter, more tapered tentacles). In this way, 60 colonies were tentatively identified as *Podocoryne* and were labelled with numbered bee tags attached with cyanoacrylate adhesive. Colonies were maintained in 40-liter aquaria with undergravel filters (20 colonies per tank) at 16°C. Colonies were fed 3-day-old brine shrimp nauplii (also grown at 16°C) every other day, and 25% of the water was changed twice a week. In 1–2 weeks all colonies were reproductive (tentative identifications were correct in all cases). Medusae from each colony were isolated and raised in finger bowls at 16°C. Each day, medusae were examined under a dissecting microscope, fed brine shrimp, and transferred to fresh seawater. Medusae were raised to sexual maturity (7–14 days), and the sex of the parent colony was determined by the morphology of the gonads (Rees, 1941; Edwards, 1972; identity as *P. carnea* was also verified by examining the medusae, see Edwards, 1972; Mills, 1976). From the original 60 colonies, 10 male and 5 female colonies were selected using a pseudo-random number generator. Sixty *Hydractinia* colonies were haphazardly collected from the same site and maintained in the same fashion. Compared to *Podocoryne*, *Hydractinia* requires more time to mature (*cf.* Hauenschild, 1956; Braverman, 1963), but within two months all colonies were fully reproductive, whereupon they were sexed, labelled, and 10 male and 5 female colonies were selected with a pseudo-random number generator. Previous investigations (McFadden *et al.*, 1984; Buss and Grosberg, 1990) have shown that colony morphology does not differ on the basis of sex; nevertheless, equal numbers of each sex from each species were included in this study.

For morphological comparisons, colonies were surgically explanted onto 22 mm^2 glass cover slips and held in place with loops of thread until attachment whereupon the threads were removed (see McFadden *et al.*, 1984; explants of 3–5 feeding polyps were used). Because of the work involved, comparisons were made using five field-collected colonies of each species at a time. Five explants (hereafter "replicates") for each of the five field-collected colonies (hereafter "strains") for both *Podocoryne* and *Hydractinia* (hereafter "species") were grown in a floating rack at 16°C. Three "racks" were used over a two-month period; rack is thus a proxy for time effects. Each rack consisted of two side-by-side rows of slots; cover slips were arranged so that the five replicates for each strain occupied consecutive slots; strains of each species were randomly paired, alternating right and left sides. The formal analysis thus consists of a four-level nested analysis of variance (see Sokal and Rohlf, 1981). Replicates are nested within strains, which are nested within species, which are nested within racks. Such an analysis accounts for all sources of variation except position within racks. Position effects can be assessed by designating five positions within each rack; each position then contains the replicates from a pair of *Podocoryne* and *Hydractinia* strains. The analysis then becomes replicates within species within positions within racks. Outcome variables were analyzed in both ways.

Using the above protocols, *perimeter*/$\sqrt{area}$ measures were taken, and counts of polyps and total area measures were also recorded. Variables were measured at 7 and 14 days after explanting; specific growth rates (see Blackstone, 1987; Blackstone and Yund, 1989) for polyp (*polyp/polyp-day*) and area (mm^2/mm^2*-day*) were also calculated for this interval. Each rate was calculated by increment in number or area (for polyp number and total area respectively) per time increment per initial number or area. While technically "specific" refers to "divided by mass," any measure of size can be used, provided the same units are used in the numerator and denominator, since a specific growth rate has units of 1/time.

Breeding studies

While studies of clonal repeatibility can establish broad-sense heritabilities for a trait, breeding studies can provide further insight into the nature of the genetic variation underlying a trait (Falconer, 1981). With the same 5 female and 10 male *Hydractinia* colonies used above, 10 crosses (2 males per female) were designated using a pseudo-random number generator, and additional mating experiments were done to insure that all individuals belonged to the same species (see Buss and Yund, 1989). Matings were carried out every several days for a month. Pairs of male and female colonies were isolated in the dark overnight; morning light triggered gamete release (see Yund *et al.*, 1987, and references therein). Embryos were transferred to fresh seawater and kept for 3–4 days with a daily water change. By this time, embryos had developed into planulae competent to metamorphose (Plickert *et al.*, 1988). Metamorphosis was induced by ionic imbalance (Spindler and Muller, 1972; Weis and Buss, 1987). Competent planulae were transferred to a 53 m*M* CsCl solution in seawater. After approximately 4 h, planulae were placed on glass cover slips in seawater-filled six-well plates (1 planula per well). Attachment and metamorphosis occurred within 2 days. Six plates per cross (36 planulae total) were metamorphosed. Colonies were fed 3-day-old brine shrimp nauplii, followed by a complete water change each day.

Colonies were maintained in an incubator at 12.5°C for 50 days (to a mean size of 11 feeding polyps). The temperature conditions were chosen to reflect the ambient temperatures in Long Island Sound during the spring and early summer (Yund *et al.*, 1987). At this point in the seasonal cycle, sexual reproduction, recruitment, and intraspecific competition occur at high frequencies in this area (Buss and Yund, 1988). The duration of the experimental period was chosen for the purpose of assessing colony shape at small colony sizes. *Hydractinia* planulae display site-specific settlement on shells, hence the vast majority of intraspecific competitive encounters occur at small colony sizes (Yund *et al.*, 1987; Buss and Yund, 1988; Yund and Parker, 1989; see discussion below).

Using the protocols described above, colonies were measured for area and perimeter as soon as primary polyps and stolons developed after metamorphosis (<5 days). Each colony was measured at weekly intervals up to an age of 50 days (25–50% of the colonies of each cross failed to survive to this age). We analyzed the data using quantitative genetic techniques (Falconer, 1981). Because of the small size of the laboratory population, we suggest only very limited interpretation of our results with regard to the natural population of *Hydractinia*. Rather, we intended to gain further insight into the results suggested by the clonal repeatibility experiments; is shape largely genetically determined, *i.e.*, does shape variation have a large broad-sense heritability, and further, is there any evidence that the broad-sense heritability of shape variation in this laboratory population is due to narrow-sense heritability? Analyses were done on initial $perimeter/\sqrt{area}$ (age <5 days), on mean $perimeter/\sqrt{area}$ (for each colony, all shape measures up to age 50 days were averaged, and this mean value was used as the outcome), and on final $perimeter/\sqrt{area}$ (age = 50 days). These three comparisons correspond to before, during, and after stolonal mat formation.

Although our goals were somewhat different from typical quantitative genetic studies (*cf.*, Falconer, 1981), we used standard methods to examine the covariance of full sibs and the covariance of half sibs. Specifically, the between-female parent component of variance (i.e., $\sigma_{females}^2$, the variance between the means of the half-sib families) estimates COV_{HS} and measures additive genetic variance (*i.e.*, narrow-sense heritability, provided maternal effects are slight). The between-male parent component of variance, σ_{males}^2, estimates $COV_{FS} - COV_{HS}$ and measures a combination of additive and non-additive genetic variance (*i.e.*, broad-sense heritability, provided environmental effects are slight). Insight into additive and non-additive genetic variance can thus be obtained from a nested analysis of variance. The F-ratio of the male-parent mean square to the within-brood mean square will measure additive and non-additive genetic variance, while the F-ratio of the female-parent mean square to the male-parent mean square will measure additive genetic variance (see results below). We focus on qualitative interpretations of the analysis of variance rather than exact calculations of heritabilities because of the small size of the laboratory population and the limited goals of our breeding study (see Mitchell-Olds, 1986; Via, 1988).

To properly gauge the inheritance of shape, we attempted to reduce environmental effects in several ways. First, because we expected *a priori* that non-additive genetic variance would be large relative to additive genetic variance (*i.e.*, $COV_{FS} \gg COV_{HS}$, see discussion below), each female parent was mated to two male parents. Thus, any maternal or cytoplasmic effects (see discussion in Mazer, 1987) will inflate the covariance of the half sibs and inflate our estimate of additive genetic variance. Second, because matings were initiated at slightly different times and because between-mating environmental variation could inflate the covariance of the full sibs, environmental conditions were closely controlled. In addition to incubation at a constant temperature, seawater chemistry was monitored weekly, and nitrates and nitrites were maintained at low levels ($\leq$9.0 ppm and $\leq$0.01 ppm, respectively). Salinity was maintained at $\approx$26 ppt. Any

variation in environmental conditions was slight and showed no systematic trend over the time course of the experiment. Finally, colony position effects were assessed. Stacks of culture plates (6 per mating) were kept on a single shelf in an incubator and positions were varied daily in a random manner. Individual plates, however, were kept in descending order (1–6), and culture wells were also in fixed positions. Because there was only one colony per well, wells were pooled into left wells, center wells, and right wells based on their positions in the six-well plate. The complete analysis was thus well position nested within plate, plate nested within male parent, and male parent nested within female parent. This analysis was carried out for intial and average shape measures. By the age of 50 days, the 25–50% mortality for each cross rendered the analysis of well position effects and plate effects unreliable because of missing values, and the pooled within-broods mean square was used as the error variance.

Further insight into environmental effects was gained by two additional experiments. First, for one of the maternal half-sib families, three 50-day-old offspring from each paternal cross were explanted onto snail shells occupied by hermit crabs and cultured in the 40-liter aquaria until each colony covered its shell and was fully mature. The 6 colonies were then compared using the method of clonal repeatibility described above, *i.e.*, 5 explants from each colony were grown on cover slips in a floating rack at 16°C and *perimeter/√area* was measured at 10 days after explanting. These shape measures were then compared to the measures made on the colonies in their first 50 days of growth. Second, two colonies from each of three crosses were grown in the six-well plates as described above until they grew to the edge of the coverslip (60–120 days). Measures of *perimeter/√area* were made at roughly weekly intervals.

Results

Growth morphology and shape

For the 242 50-day-old *Hydractinia* colonies measured, indices of peripheral stolon development (total colony perimeter/stolonal mat perimeter and total colony area/stolonal mat area) correlate highly with total colony perimeter divided by the square root of total colony area (r_s = 0.95 and 0.91, respectively). Because the correlated variables contain similar measures of total colony size (total perimeter, total area, or the square root of total area), the possibility of autocorrelation exists. For two reasons, however, the underlying structure of the data suggests that autocorrelation has negligible effects.

First, adjusting the correlated ratios to remove similar variables from each does not alter the correlations. Stolonal mat perimeter is highly correlated with the square root of total colony area (r_s = 0.94; note that r_s is insensitive to transformations of the correlated variables so that the correlation of stolonal mat perimeter and total colony area is also 0.94). Additionally, total colony perimeter is highly correlated with the ratio (total colony area)$^{3/2}$/stolonal mat area (r_s = 0.92).

Second, either measure of stolonal mat size (perimeter or area) shows a high correlation with total colony area (r_s = 0.94 and 0.92, respectively) but much weaker correlations with total colony perimeter (r_s = 0.63 and 0.53, respectively). Stolonal mat size is thus indicative of total colony area, but less so of total colony perimeter. These results are consistent with the stolonal mat showing circular growth in these small colonies, and deviations from circular growth being caused by peripheral stolons.

Shape variation in Podocoryne *and* Hydractinia

Measures of *perimeter/√area* for both 7 and 14 days after explanting show that *Hydractinia* has more circular shapes than *Podocoryne* (Table I). To analyze these data, a natural logarithmic transformation was done to better meet the assumptions of the analysis of variance. The log-transformed data were first analyzed to assess the effects of the positions of the colonies within the racks, *i.e.*, replicates nested within species nested within positions nested within racks. Because of the different numbers of replicates

Table I

Shape variation in 15 strains of Podocoryne *and* Hydractinia[a]

	Podocoryne			*Hydractinia*		
Strain[b]	n	Age 7	Age 14	n	Age 7	Age 14
1	3	17.87 1.03	21.44 0.99	5	9.03 0.58	17.46 0.70
2	5	13.67 3.96	17.06 3.62	5	4.17 0.10	5.40 0.43
3	3	7.20 2.08	15.70 3.52	3	3.83 0.08	3.94 0.08
4	5	18.54 1.87	25.38 1.94	5	5.12 0.68	5.44 1.06
5	2	15.24 1.67	26.26 0.86	5	4.33 0.10	4.05 0.13
6	4	23.78 1.92	23.97 1.89	5	7.23 0.89	15.46 2.70
7	3	20.35 1.40	33.43 2.09	4	4.44 0.33	5.18 0.67
8	5	19.06 3.46	30.62 1.10	5	9.92 2.48	15.12 2.33
9	5	20.72 1.79	20.16 0.96	4	4.52 0.23	6.55 0.87
10	4	22.04 2.49	26.50 1.85	4	6.56 0.52	11.72 0.47
11	5	22.59 1.25	23.22 2.55	2	8.14 3.47	10.53 5.24
12	4	13.23 2.08	21.39 2.81	5	5.63 0.52	10.46 1.48
13	5	21.54 0.83	22.63 1.33	5	7.45 0.74	10.72 1.22
14	5	17.87 1.69	21.72 3.30	4	10.92 1.71	15.75 1.03
15	4	10.63 2.43	19.15 0.73	5	11.07 1.31	19.81 1.06

[a] Shape measures are *perimeter/√area*; means and standard errors are shown for n replicates of each strain, 7 and 14 days after explanting.

[b] For *Podocoryne*, strains 3, 7, 9, 13, and 15 are females, and for strain 3 at age 14 n = 2. For *Hydractinia*, strains 3, 5, 12, 14, and 15 are females, and for strain 14 at age 14 n = 3.

(some replicates were lost due to mortality, see Table I), the nested ANOVAs were unbalanced, although examination of the coefficients of the variance components indicated a high reliability of the F-tests carried out (see discussion in Sokal and Rohlf, 1981). At day 7, there is a strong effect of species ($F = 26.95$, d.f. = 15, 98, $P \ll 0.001$), but no effect of position ($F = 0.06$, d.f. = 12, 15, $P > 0.99$) or rack ($F = 1.05$, d.f. = 2, 12, $P > 0.35$). Similarly, at day 14, species shows a strong effect ($F = 26.96$, d.f. = 15, 96, $P \ll 0.001$), while position ($F = 0.19$, d.f. = 12, 15, $P > 0.99$) and rack ($F = 0.70$, d.f. = 2, 12, $P > 0.50$) do not. Based on this analysis, position effects were dropped from the model; this allowed including the strain effects (*i.e.*, replicates within strains within species within racks, see Table II). Again, because of the different numbers of replicates, this ANOVA is also unbalanced. Examination of the coefficients of the variance components (Table II) suggests that F-ratios should be reliable; in particular, the F-ratio assessing the effects of racks (i.e., $MS_{racks}/MS_{species}$) is highly reliable, while the F-ratio assessing the effects of species (*i.e.*, $MS_{species}/MS_{strains}$) is slightly conservative. The results are similar to the first analysis: there is no effect of racks ($F = 0.02$, d.f. = 2, 3, $P > 0.95$) and a strong effect of species ($F = 20.45$, d.f. = 3, 24, $P \ll 0.001$). Further, strains within species show significant variation ($F = 4.99$, d.f. = 24, 98, $P \ll 0.001$). Results at 14 days are similar; racks show no effect ($F = 0.03$, d.f. = 2, 3, $P > 0.95$), while species ($F = 12.94$, d.f. = 3, 24, $P \ll 0.001$) and strains ($F = 8.11$, d.f. = 24, 96, $P \ll 0.001$) show strong effects.

In addition to shape differences, *Podocoryne* exhibits faster growth rates than *Hydractinia* (Table III). Specific growth rates of polyps show no effect of racks ($F = 0.21$, d.f. = 2, 3, $P > 0.80$), but significant effects of species ($F = 11.75$, d.f. = 3, 24, $P \ll 0.001$) and of strains ($F = 3.79$, d.f. = 24, 96, $P \ll 0.001$). Similarly, specific growth rates of colony areas show no effect of racks ($F = 0.35$, d.f. = 2, 3, $P > 0.70$), a moderate effect of species ($F = 6.70$, d.f. = 3, 24, $P < 0.01$) and a strong effect of strains ($F = 2.90$, d.f. = 24, 96, $P \ll 0.001$).

Table II

Analysis of variance table for log-transformed shape measures at day 7 of the clonal repeatibility experiment

Source	d.f.	Mean square	Composition of mean square
Between racks	2	0.104	$\sigma_{error}^2 + 4.00\sigma_{strain}^2 + 20.00\sigma_{species}^2 + 40.00\sigma_{rack}^2$
Between species within racks	3	10.897	$\sigma_{error}^2 + 4.02\sigma_{strain}^2 + 20.08\sigma_{species}^2$
Between strains within species	24	0.497	$\sigma_{error}^2 + 4.22\sigma_{strain}^2$
Between replicates	98	0.099	σ_{error}^2

Table III

Specific growth rates for 15 strains of Podocoryne *and* Hydractinia[a]

	Podocoryne			*Hydractinia*		
Strain	n	Area	Polyp	n	Area	Polyp
1	3	0.211 0.01	0.197 0.01	5	0.181 0.01	0.184 0.01
2	5	0.181 0.05	0.169 0.02	5	0.034 0.01	0.00 0.00
3	2	0.110 0.09	0.071 0.07	3	0.059 0.06	0.013 0.04
4	5	0.226 0.01	0.166 0.02	5	0.038 0.01	0.035 0.02
5	2	0.130 0.06	0.069 0.04	5	0.102 0.01	0.113 0.02
6	4	0.195 0.01	0.138 0.02	5	0.092 0.03	0.074 0.03
7	3	0.203 0.01	0.170 0.03	4	0.124 0.01	0.123 0.01
8	5	0.220 0.01	0.197 0.01	5	0.176 0.02	0.101 0.02
9	5	0.184 0.03	0.171 0.02	4	0.063 0.01	0.071 0.03
10	4	0.174 0.02	0.166 0.03	4	0.113 0.03	0.100 0.02
11	5	0.191 0.01	0.215 0.01	2	0.050 0.03	0.019 0.08
12	4	0.101 0.06	0.220 0.03	5	0.100 0.01	0.079 0.01
13	5	0.192 0.02	0.207 0.01	5	0.102 0.01	0.148 0.02
14	5	0.112 0.03	0.181 0.02	3	0.144 0.01	0.042 0.03
15	4	0.158 0.03	0.137 0.02	5	0.192 0.01	0.079 0.02

[a] Specific growth rates (1/day) for total colony area and polyp number for 7 to 14 days after explanting; strains are designated by the same numbers as in Table I, and means and standard errors are shown for n replicates of each strain.

Breeding studies

For the breeding experiments conducted with *Hydractinia*, the shapes of the colonies initially and at 50 days (Table IV) show little correlation ($r_s = -0.06$, $P > 0.30$, for all 242 50-day-old colonies). This likely results from growth changes associated with stolonal mat formation (Fig. 1). Despite such variation, analyses of initial, average, and final colony shape all suggest a highly significant effect of the male parent and a non-significant effect of the female parent. For initial colony shape, there is no effect of the female parent ($F = 0.98$, d.f. = 4, 5, $P > 0.45$), a strong effect of the male parent ($F = 7.39$, d.f. = 5, 50, $P \ll 0.001$), and no effect of either plate ($F = 0.85$, d.f. = 50, 119, $P > 0.70$), or well position ($F = 0.95$, d.f. = 119, 173, $P > 0.60$). Similarly, for average colony shape there is no effect of the female parent ($F = 0.44$, d.f. = 4, 5, $P > 0.75$) and a strong effect of the male parent ($F = 15.21$, d.f. = 5, 50, $P \ll 0.001$). Again, there was no effect of either plate ($F = 0.88$, d.f. = 50, 119, $P > 0.65$) or well position ($F = 1.04$, d.f. = 119, 173, $P > 0.40$). For both initial and average shape analyses, the coefficients of the variance components (Table V) indicate a high reliability of the F-ratios. For final shape measures, missing values (because of mortality) rendered the analysis of position

Table IV

Descriptive statistics for the 10 crosses used in the breeding studies[a]

	Initial		Average		Final		
Parents[b]	n	Shape	n	Shape	n	Shape	Polyp
15 × 11	36	5.86 0.25	36	8.36 0.47	23	11.44 0.91	19.6 3.1
15 × 13	36	6.61 0.39	36	6.71 0.40	28	6.75 0.54	8.3 1.2
12 × 7	36	7.26 0.30	36	6.17 0.20	28	4.99 0.38	11.1 0.9
12 × 2	36	7.08 0.36	36	7.85 0.28	23	8.98 0.70	5.4 1.0
5 × 8	36	7.77 0.42	36	7.98 0.29	21	6.78 0.73	12.2 1.4
5 × 9	36	7.90 0.35	36	6.87 0.30	19	6.76 0.68	11.9 1.4
14 × 1	36	8.56 0.46	36	8.74 0.34	31	6.59 0.61	19.7 1.1
14 × 10	28	5.55 0.23	28	5.63 0.22	17	6.74 0.76	19.5 2.4
3 × 4	36	7.11 0.37	36	6.28 0.27	27	4.13 0.14	8.4 0.9
3 × 6	36	6.09 0.34	36	6.18 0.34	25	5.64 0.56	8.0 1.2

[a] Sample sizes (n), means and standard errors for shape measures ($perimeter/\sqrt{area}$) from initial colonies (primary polyps < 5 days old), average colonies (for each colony, all shape measures up to 50 days were averaged; this mean value was used for the descriptive statistics), and final colonies (50 days old). Data on polyp number (mean and standard error) is also presented for the final colonies.

[b] Numbers designating female parent and male parent respectively; the numbers correspond to the strains of *Hydractinia* from Tables I and III.

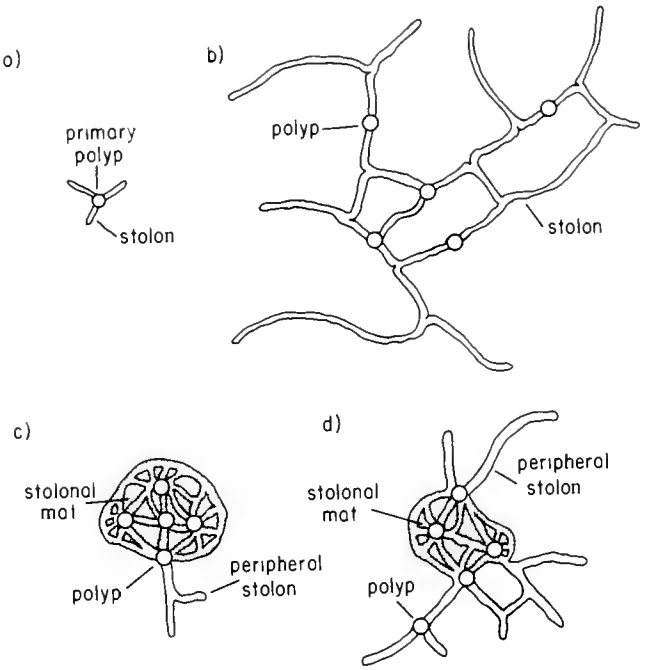

Figure 1. Rough schemata of (a) a primary polyp of a hydractiniid hydroid, (b) a small *Podocoryne* colony, and small *Hydractinia* colonies of the (c) "mat type," with few peripheral stolons, and the (d) "net type," with more peripheral stolons. Colonies are drawn as if encrusting the surface of the page; polyps would project up out of the plane of the paper. In the stolonal mat (the central portion of the *Hydractinia* colonies represented by the stipled pattern), the spaces between the stolons are filled with tissue; thus these stolons are fused together, while the peripheral stolons outside the stipled area (and those in *Podocoryne*) are unfused. Colonies are drawn to roughly the same scale; stolon width is approximately 70 microns.

effects unreliable; nevertheless, using the pooled within-broods mean square as the error variance, the data suggest a non-significant effect of the female parent ($F = 1.23$, d.f. = 4, 5, $P > 0.40$) and a large effect of the male parent ($F = 11.3$, d.f. = 5, 232, $P \ll 0.001$). Overall, the slight effect of the female parent (*i.e.*, a non-significant covariance of the half sibs) indicates that $\sigma_{females}^2$ is relatively small and that both maternal effects and additive genetic variance are correspondingly small. On the other hand, the large effect of the male parent suggests a large covariance of the full sibs, a relatively large σ_{males}^2, and likely a large non-additive genetic variance, given the closely controlled environmental conditions. The interpretation of these results should be limited to the small laboratory population on which the breeding studies were based (see Discussion).

While environmental effects could not be tested directly with this experimental design, the six offspring raised on hermit crab shells and then compared using clonal repeatibility allow an assessment of the sensitivity of *Hydractinia* colony morphology to environmental circumstances. These colonies were from crosses 15 × 11 and 15 × 13 (see Table IV); Figure 3 shows the shape measures for the 50-day ontogenies of the young colonies. After these young colonies were grown to maturity on hermit crab shells, explants were made; Figure 3 also shows the mean shape measures for five 10-day-old replicates from each of the mature colonies (means and standard errors for the 5 replicates of each colony are adjacent to the symbol for the 50-day shape measure for that colony). Comparing these shape data generated by different methods suggests that, despite different culture conditions, both methods generate roughly similar data for the same col-

Table V

Analysis of variance table for the analysis of the natural logarithms of average shape measures for each colony

Source	d.f.	Mean square	Composition of mean square
Between female parent	4	0.395	$\sigma_{error}^2 + 1.93\sigma_{well}^2 + 5.77\sigma_{plate}^2 + 34.60\sigma_{males}^2 + 69.21\sigma_{females}^2$
Between male parent	5	0.890	$\sigma_{error}^2 + 1.94\sigma_{well}^2 + 5.78\sigma_{plate}^2 + 34.65\sigma_{males}^2$
Between plate	50	0.059	$\sigma_{error}^2 + 1.95\sigma_{well}^2 + 5.82\sigma_{plate}^2$
Between well position	119	0.066	$\sigma_{error}^2 + 1.96\sigma_{well}^2$
Within well position	173	0.064	σ_{error}^2

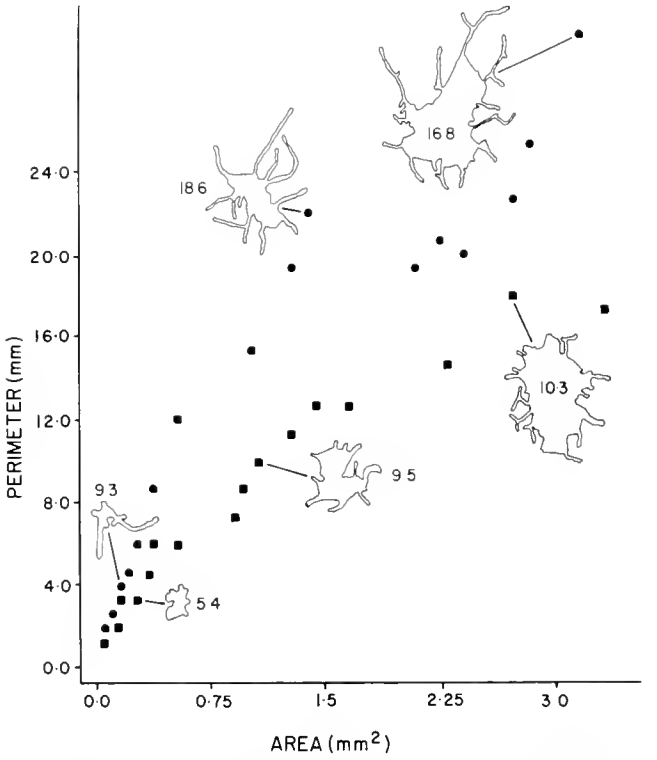

Figure 2. Perimeter versus area plots for two sibling *Hydractinia* colonies measured every other day for the first 5 weeks of ontogeny. Camera lucida tracings (not to scale) and shape measures ($perimeter/\sqrt{area}$) are shown for some of the data points. While shapes fluctuate as stolons branch and fuse, the two colonies exhibit distinct trajectories in perimeter versus area space.

ony, and, in particular, either method shows the differences between the crosses. At 50 days, cross 15 × 11 produced significantly more irregular shapes than cross 15 × 13 (Table IV); analysis of the clonal repeatibility data shows the same pattern. If the log-transformed shape data are analyzed as replicates nested within crosses nested within positions, there is an effect of cross ($F = 7.9$, d.f. = 3, 24, $P < 0.001$), but no effect of position ($F = 0.05$, d.f. = 2, 3, $P > 0.90$). Analyzing the data as replicates nested within strains nested within crosses provides a similar result (no significant effect of strains $F = 0.92$, d.f. = 4, 24, $P > 0.45$, but a significant effect of crosses $F = 22.7$, d.f. = 1, 4, $P < 0.01$). In either case, cross 15 × 11 exhibits significantly more irregular shapes than cross 15 × 13. This supports the findings of the breeding experiment and suggests that the differences between crosses are not the result of some undetected environmental factor varying over time.

The 6 colonies from 3 different crosses (12 × 7, 5 × 8, and 3 × 4 in Table IV) which were grown beyond 50 days (Fig. 4) show some variation in colony shape, but also suggest that differences among crosses are maintained at larger sizes. For instance, at 110 days, the 4 colonies which had not yet reached the edges of the cover slips suggest the same differences in shape, which were apparent for the complete crosses at 50 days (Table IV; for $perimeter/\sqrt{area}$, 5 × 8 > 12 × 7 > 3 × 4).

Discussion

These results have implications with regard to morphological variation in hydractiniid hydroids and in other clonal taxa as well. We discuss (1) the biological basis of shape in hydractiniid hydroids, (2) the implications of the *Hydractinia* breeding studies, (3) the general phenomenon of heterochrony in hydractiniid hydroids, and (4) the relevance of these results to other clonal taxa.

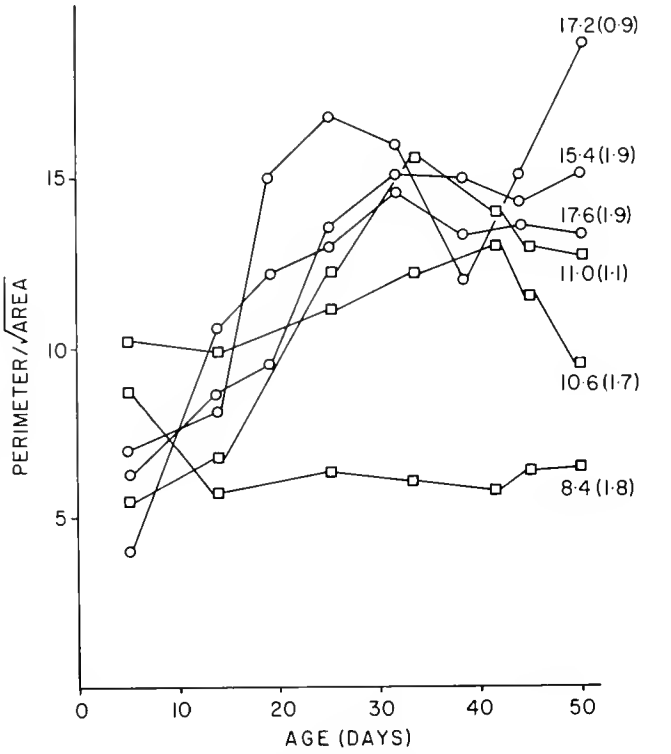

Figure 3. Shapes ($perimeter/\sqrt{area}$) of 6 colonies from one of the maternal half-sib families (3 from 15 × 11, shown by circles, 3 from 15 × 13, shown by squares; the crosses are designated as in Table IV) for the first 50 days of growth (lines connect points for each individual). These colonies were grown to maturity on hermit crab shells and then explanted and measured for shape again. Numbers adjacent to the symbol for the 50-day shape value show the means, with standard errors in parentheses, for 5 replicates of each colony 10 days after explanting. Despite differences in culture conditions, the clonal repeatibility shape measures and the shape measures for the first 50 days both suggest that colonies from 15 × 11 have more irregular shapes than those from 15 × 13.

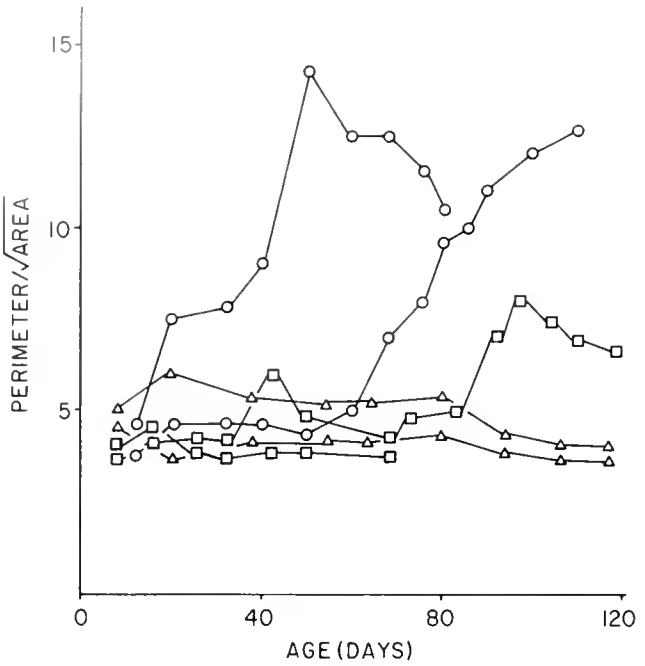

Figure 4. Two colonies from each of 3 crosses (5 × 8, circles; 12 × 7, squares; and 3 × 4, triangles; the crosses are designated as in Table IV) were grown beyond 50 days on glass cover slips and measured for shape (*perimeter/√area*). Lines connect values for each colony; 2 colonies reached the edges of the cover slips in <80 days; the remaining 4 were grown for over 100 days. While shapes fluctuate, at 110 days these 4 colonies suggest shape differences which were apparent for all colonies of each cross at 50 days (Table IV; 5 × 8 > 12 × 7 > 3 × 4).

The biological basis of shape

The results presented show a strong correlation between measures of peripheral stolon development and *perimeter/√area* in *Hydractinia*. Previous work (McFadden *et al.*, 1984; Yund, 1987; Buss and Grosberg, 1990) suggests that peripheral stolon development is correlated with competitive ability in *Hydractinia*. Thus, shape as measured by *perimeter/√area* will show a similar correlation. Further, *Podocoryne* shows more irregular shapes than *Hydractinia* and thus greater peripheral stolon development; this result agrees with its competitive dominance over *Hydractinia* in laboratory studies (McFadden, 1986). The correlations of shape with competitive ability can make measures of shape useful to biologists, but clearly shape differences are not causally related to competitive ability (see discussion below). Rather, shape, competitive ability, and peripheral stolon development are likely correlated consequences of the underlying dynamics of growth in these hydroids.

Shape measures bear a clearly interpretable relationship to these growth dynamics. Examining Figure 1 suggests that *perimeter/√area* will measure the degree to which stolons extend from a central ring stolon or network of ring stolons. Stolons encase the gastrovascular canals; the combined actions of stolons and, in particular, muscular polyps drive the gastrovascular fluid through the canals and nourish the colony (see Schierwater *et al.*, in press). Since the gastrovascular system is closed, peripheral stolons are essentially dead-end channels, and a considerable pressure is likely necessary to supply these stolons with fluid. Contrast this to the situation in a ring stolon or network of ring stolons well-supplied by polyps; here, flow can proceed from polyp to polyp with relatively little exertion of pressure. Hence, the amount of peripheral stolons and the degree of non-circularity of colony shape are likely to be measures of the ability of the colony to maintain the energetic and physiological costs of supplying these peripheral elements with gastrovascular flow.

Hydractinia *breeding studies*

Generally, the clonal repeatibility experiments and the breeding experiments produced compatible results for the 15 strains of *Hydractinia*, despite differences in culture conditions. For instance, the fastest and slowest growing strains (1 and 2, measured by polyp specific growth rates) produce the fastest and slowest growing offspring (14 × 1 and 12 × 2, measured by polyp number at 50 days), the strain with the most irregular shape (15) in one cross produced offspring with the most irregular shapes (15 × 11), and strains with nearly circular shapes (3 and 4) produced nearly circular offspring (3 × 4). The somewhat circular shape of colony 2 seems at variance with the irregular shapes of 12 × 2; however, this likely indicates the limitations of comparing developing colonies to clonal explants. Colony 2 shows extremely slow growth as do its offspring (12 × 2). It is likely that this slow growth reflects equally slow development of adult colony form and organization. The irregular shapes of young 12 × 2 colonies may indicate a slow transition from early colony development to adult morphology.

Despite the agreement of the results of the clonal repeatibility experiments and the breeding experiments, the latter can provide classes of information which are not available from the former. While only a small breeding study was carried out here, it is, to our knowledge, the first example of carefully controlled crosses for a clonal organism. To stimulate further such work, we will discuss the general value of such data. Clonal repeatibility studies demonstrate a significant broad-sense heritability of the shape variation (the strain-within-species effect in the ANOVAs). The breeding studies not only demonstrate a significant broad-sense heritability (the effect of the male parent in the ANOVAs), but also provide information on the sorts of genetic variation that constitute this broad-

sense heritability. For the three analyses (initial, average, and final shape measures), $MS_{females}/MS_{males}$ is roughly 1 (0.98, 0.44, and 1.23 respectively, see Results) and in each case is non-significant. This suggests that the covariance of the half-sibs is small, that is, progeny from the same maternal half-sib family are not appreciably more similar to each other than to unrelated progeny. On the other hand, the covariance of the full-sibs is high (hence the large effect of the male parent). If environmental effects are slight, these results suggest that non-additive genetic variance constitutes the bulk of the broad-sense heritability of shape in this small laboratory population. This result is bolstered by the additional study of one of the maternal half-sib families (progeny of female 15, *i.e.*, crosses 15 × 11 and 15 × 13). Using clonal repeatibility, this study shows that the difference between the full-sib families does not depend on some undetected environmental factor.

Thus, it is possible that within this small laboratory population of *Hydractinia*, the genes controlling shape variation show high levels of dominance and epistasis. This result is supported by examining the data qualitatively. In Table IV, paternal full-sib families are very similar (*e.g.*, note the low standard errors). Nevertheless, within a particular maternal half-sib family, full-sib families are often very different (*e.g.*, progeny of females 3, 12, and 15). Thus, the expression of the shape phenotype seems to depend on the interactions between the maternal and paternal genes (*i.e.*, dominance and epistasis). This result is intriguing in view of what is known about the ecology of this species. An increasing body of evidence suggests that competition for space has resulted in selection on growth morphology in *Hydractinia* species. Briefly, when two or more colonies of the same size encrust the same substratum, the colony with the greater peripheral stolon development will predominate (Buss *et al.*, 1984; Yund *et al.*, 1987; Buss and Grosberg, 1990), because peripheral stolons are capable of differentiating into a specialized aggressive organ, the hyperplastic stolon (Buss *et al.*, 1984; Lange *et al.*, 1989). Further, such competition is common in nature (Buss and Yund, 1988; Yund and Parker, 1989), and geographic variation in growth morphology correlates with the frequency of competition (Yund, 1987). Nevertheless, while this evidence suggests that natural selection favors colonies with extensive peripheral stolon development, colonies with little peripheral stolon development are present in the population of *Hydractinia symbiolongicarpus* sampled (see shape measures in Table I, and see McFadden *et al.*, 1984) and in other *Hydractinia* populations (Yund, 1987).

The results of the breeding experiment indicate a possible explanation for the maintenance of morphological variation in *Hydractinia* populations. While limits to the effects of natural selection are usually caused by countervailing selection, rather than exhaustion of additive genetic variance (see Lande, 1988), the latter has been implicated in a number of studies (*e.g.*, see Falconer, 1981; Lynch and Sulzbach, 1984; Hilbish and Koehn, 1985; Berven, 1987; Travis *et al.*, 1987; Emerson *et al.*, 1988; Gibbs, 1988). Possibly, this has occurred in *Hydractinia* populations, *i.e.*, natural selection has removed much of the additive genetic variation controlling peripheral stolon development, and what remains may be largely non-additive (*i.e.*, subject to epistatic and dominance effects) and thus masked from selection. We suggest this only as a possibility for directing future work; the small size of the laboratory population of *Hydractinia* precludes any firm generalization to natural populations.

Heterochrony in hydractiniid hydroids

Using morphological criteria, *Podocoryne* and *Hydractinia* have been grouped in the same family (*e.g.*, Mills, 1976), and mtDNA sequence data strongly support this interpretation (C. Cunningham, pers. comm.). In this phylogenetic context, variation between *Podocoryne* and *Hydractinia* can be described in terms of general patterns of heterochrony (Gould, 1977). As Gould points out, certain morphological traits often correlate with suites of life history characteristics. This seems to be the case with *Podocoryne* and *Hydractinia*. Relative to the latter, *Podocoryne* grow and mature rapidly (see Hauenschild, 1956; Braverman, 1963), produce energetically inexpensive medusae (*cf.*, Schierwater, 1989; Schierwater and Hauenschild, 1990), and disperse widely to new and varied substrata (*Podocoryne* have swimming medusae and larvae, while *Hydractinia* lack medusae and have crawling larvae). Further, the morphology of *Podocoryne* can be regarded as juvenilized relative to *Hydractinia*. When either hydroid fully covers the substratum, stolons form densely packed structures (a fused stolonal mat in *Hydractinia*, and a structure resembling a stolonal mat in *Podocoryne*). Such a structure is thus the final developmental stage in both taxa. *Hydractinia*, however, always forms some stolonal mat early in its colony development, and in many cases much of the young colony consists of stolonal mat (hence the nearly circular shapes of some *Hydractinia* strains). Very young (and sexually immature) *Hydractinia* thus attain a developmental stage (*i.e.*, fused stolonal mat and nearly circular shape) that is only approached by fully mature *Podocoryne*. The latter can thus be regarded as paedomorphic or the former peramorphic (see Alberch *et al.*, 1979).

Shape variation in clonal organisms

Many clonal plants, fungi, and invertebrate animals are composed of clonally iterated food-gathering units (*i.e.*,

ramets) connected by vascular canals (*e.g.*, stolons or rhizomes) that adhere to the substratum (Boardman *et al.*, 1973; Larwood and Rosen, 1979; Jackson *et al.*, 1985; Harper *et al.*, 1986). Clonal morphologies of this sort vary markedly in the development of peripheral stolons or rhizomes (Buss, 1979; Jackson, 1979; Lovett-Doust, 1981; Harper, 1985). The approach used here to measure variation in peripheral stolon development in hydractiniid hydroids may prove useful in other analyses of clonal form. Simple shape measures such as $perimeter/\sqrt{area}$ can easily be acquired from properly lighted specimens with a simple pixel gradient detector (provided by most commercially available image analysis software). Use of such characters may have considerable technical advantages for the analysis of ontogenetic and phylogenetic changes in colony form.

Acknowledgments

The Peabody Museum Morphometrics Laboratory, the Social Sciences Statistics Laboratory, and the Yale Computer Center were used for image analysis and data analysis. Comments were provided by M. Dick, R. Lange, B. Schierwater, and two reviewers. The National Science Foundation (BSR-88-05961) provided support.

Literature Cited

Alberch P., S. J. Gould, G. F. Oster, and D. B. Wake. 1979. Size and shape in ontogeny and phylogeny. *Paleobiology* **5:** 296–317.

Berven, K. A. 1987. The heritable basis of variation in larval developmental patterns within populations of the wood frog (*Rana sylvatica*). *Evolution* **41:** 1088–1097.

Blackstone, N. W. 1987. Specific growth rates of parts in a hermit crab: a reductionist approach to the study of allometry. *J. Zool. Lond.* **211:** 531–545.

Blackstone, N. W., and P. O. Yund. 1989. Morphological variation in a colonial marine hydroid: a comparison of size-based and age-based heterochrony. *Paleobiology* **15:** 1–10.

Boardman, R. S., A. H. Cheetam, and W. A. Oliver. 1973. *Animal Colonies. Development, and Function through Time.* Dowden, Hutchinson, and Ross, Stroundberg, PA.

Bookstein, F. L. 1978. *The Measurement of Biological Shape and Shape Change.* Lecture Notes in Biomathematics. No. 24. Springer-Verlag, New York.

Braverman, M. 1963. Studies of hydroid differentiation II. Colony growth and the initiation of sexuality. *J. Embryol. Exp. Morphol.* **11:** 239–253.

Buss, L. W. 1979. Habitat selection, directional growth, and spatial refuges: why colonial animals have more hiding places. Pp. 459–497 in *Biology and Systematics of Colonial Organisms*, G. Larwood and B. Rosen, eds. Academic Press, London.

Buss, L. W., and P. O. Yund. 1988. A comparison of recent and historical populations of the colonial hydroid *Hydractinia*. *Ecology* **69:** 646–654.

Buss, L. W., and P. O. Yund. 1989. A sibling species group of *Hydractinia* in the northeastern United States. *J. Mar. Biol. Assoc. U. K.* **69:** 857–874.

Buss, L. W., and R. K. Grosberg. 1990. Morphogenetic basis for phenotypic differences in hydroid competitive behavior. *Nature* **343:** 63–66.

Buss, L. W., C. S. McFadden, and D. R. Keene. 1984. Biology of hydractiniid hydroids. 2. Histocompatibility effector system/competitive mechanism mediated by nematocyst discharge. *Biol. Bull.* **167:** 139–158.

Cunningham, C. W., L. W. Buss, and C. Anderson. (in press). Molecular and geologic evidence of shared history between hermit crabs and the symbiotic genus *Hydractinia*. *Evolution.*

Edwards, C. 1972. The hydroids and the medusae *Podocoryne areolata*, *P. borealis*, and *P. carnea*. *J. Mar. Biol. Assoc. U. K.* **52:** 97–144.

Emerson, S. B., J. Travis, and M. Blouin. 1988. Evaluating a hypothesis about heterochrony: larval life-history traits and juvenile hind-limb morphology in *Hyla crucifer*. *Evolution* **42:** 68–78.

Falconer, D. S. 1981. *Introduction to Quantitative Genetics*, 2nd ed. Longman, London.

Ferson, S., F. J. Rohlf, and R. K. Koehn. 1985. Measuring shape variation of two-dimensional outlines. *Syst. Zool.* **34:** 59–68.

Gibbs, H. L. 1988. Heritability and selection on clutch size in Darwin's medium ground finches (*Geospiza fortis*). *Evolution* **42:** 750–762.

Gould, S. J. 1973. The shape of things to come. *Syst. Zool.* **22:** 401–404.

Gould, S. J. 1977. *Ontogeny and Phylogeny.* Harvard University Press, Cambridge, MA.

Harper, J. L. 1985. Modules, branches, and capture of resources. Pp. 1–33 in *Biology and Systematics of Colonial Organisms*, G. Larwood and B. Rosen, eds. Academic Press, London.

Harper, J. L., B. R. Rosen, and J. White (eds.). 1986. *The Growth and Form of Modular Organisms.* Royal Society Press, London.

Hauenschild, C. 1954. Genetische entwicklungphysiologische Untersuchungen uber Intersexualitat und Gewebevertraglichkeit bei *Hydractinia echinata*. *Roux's Archiv. fur Entwicklungsmech.* **147:** 1–41.

Hauenschild, C. 1956. Uber die Vererbung einer Gewebevertraglichkeit-Eigenschaft bei den Hydroidpolypen *Hydractinia echinata*. *Z. Naturforsch.* **11b:** 132–138.

Hilbish, T. J., and R. K. Koehn. 1985. Dominance in physiological phenotypes and fitness at an enzyme locus. *Science* **229:** 52–54.

Jackson, J. B. C. 1979. Morphological strategies of sessile animals. Pp. 499–555 in *Biology and Systematics of Colonial Organisms*, G. Larwood and B. Rosen, eds. Academic Press, London.

Jackson, J. B. C., L. W. Buss, and R. E. Cook (eds.). 1985. *Population Biology and Evolution of Clonal Organisms.* Yale University Press, New Haven, CT.

Lande, R. 1988. Quantitative genetics and evolutionary theory. Pp. 71–84 in *Quantitative Genetics*, B. S. Weir, E. J. Eisen, M. M. Goodman, and G. Namkoong, eds. Sinauer, Sunderland, MA.

Lange, R., G. Plickert, and W. A. Muller. 1989. Histoincompatibility in a low invertebrate, *Hydractinia echinata*: analysis of a mechanism of rejection. *J. Exp. Zool.* **249:** 284–292.

Larwood, G., and B. Rosen (eds.). 1979. *Biology and Systematics of Colonial Organisms.* Academic Press, London.

Lohman, G. P. 1983. Eigenshape analysis of microfossils: a general morphometric procedure for describing changes in shape. *Math. Geol.* **15:** 659–672.

Lovett-Doust, L. 1981. Population dynamics and local specialization in a clonal perennial (*Ranunculus repens*). I. The dynamics of ramets in contrasting habitats. *J. Ecol.* **69:** 743–755.

Lynch, C. B., and D. S. Sulzbach. 1984. Quantitative genetic analysis of temperature regulation in *Mus musculus*. II. Diallel analysis of individual traits. *Evolution* **38:** 527–540.

Mazer, S. J. 1987. Parental effects on seed development and seed yield

in *Raphanus raphanistrum*: implications for natural and sexual selection. *Evolution* **41:** 355–371.

McFadden, C. S. 1986. Laboratory evidence for a size refuge in competitive interactions between the hydroids *Hydractinia echinata* (Flemming) and *Podocoryne carnea* (Sars). *Biol. Bull.* **171:** 161–174.

McFadden, C. S., M. J. McFarland, and L. W. Buss. 1984. Biology of hydractiniid hydroids. 1. Colony ontogeny in *Hydractinia echinata* (Flemming). *Biol. Bull.* **166:** 54–67.

Mills, C. E. 1976. *Podocoryne selena*, a new species of hydroid from the Gulf of Mexico, and a comparison with *Hydractinia echinata*. *Biol. Bull.* **151:** 214–224.

Mitchell-Olds, T. 1986. Quantitative genetics of survival and growth in *Impatiens capensis*. *Evolution* **40:** 107–116.

Patton, D. R. 1975. A diversity index for quantifying habitat "edge." *Wildl. Soc. Bull.* **3:** 171–173.

Plickert, G., M. Kroiher, and H. Munk. 1988. Cell proliferation and early differentiation during embryonic development and metamorphosis of *Hydractinia echinata*. *Development* **103:** 795–803.

Rees, W. J. 1941. On life history and developmental stages of the medusa *Podocoryne borealis*. *J. Mar. Biol. Assoc. Plymouth* **25:** 309–316.

Schierwater, B. 1989. Experimentelle Studien zu den energetischen Kosten der Fortpflanzung bei sexuellem versus vegetativem Modus an *Eleutheria dichotoma* (Athecata, Hydrozoa) und *Stylaria lacustris* (Naididae, Oligochaeta). Ph.D. Thesis. University of Braunschweig, Braunschweig, FRG.

Schierwater, B., and C. Hauenschild. 1990. The position and consequences of a vegetative mode of reproduction in the life cycle of a hydromedusa and an oligochaete worm. Pp. 37–42 in *Advances in Invertebrate Reproduction 5*, M. Hoshi and O. Yamashita, eds. Elsevier, Amsterdam.

Schierwater, B., B. Piekos, and L. W. Buss. (in press). Hydroid stolon contractions mediated by contractile vacuoles. *J. Exp. Biol.*

Sokal, R. R., and F. J. Rohlf. 1981. *Biometry*, 2nd ed. W. H. Freeman, San Francisco.

Spindler, A. N., and W. A. Muller. 1972. Induction of metamorphosis by bacteria and by lithium pulse in the larvae of *Hydractinia echinata* (Hydrozoa). *Wilhelm Roux' Arch. Entwicklungsmech. Org.* **169:** 271–280.

Travis, J., S. B. Emerson, and M. Blouin. 1987. A quantitative genetic analysis of larval life history traits in *Hyla cruciter*. *Evolution* **41:** 145–156.

Via, S. 1988. Estimating variance components: reply to Groeters. *Evolution* **42:** 633–634.

Weis, V. M., and L. W. Buss. 1987. Ultrastructure of metamorphosis in *Hydractinia echinata*. *Postilla* **199.**

Yund, P. O. 1987. Intraspecific competition and the maintenance of morphological variation in the colonial marine hydroid *Hydractinia symbiocadianus*. Ph.D. Thesis. Yale University, New Haven, CT.

Yund, P. O., C. W. Cunningham, and L. W. Buss. 1987. Recruitment and postrecruitment interactions in a colonial hydroid. *Ecology* **68:** 971–982.

Yund, P. O., and H. M. Parker. 1989. Population structure of the colonial hydroid *Hydractinia* sp. nov. C in the Gulf of Maine. *J. Exp. Mar. Biol. Ecol.* **125:** 63–82.

Reference: *Biol. Bull.* 180: 406–415. (June, 1991)

Inducible Agonistic Structures in the Tropical Corallimorpharian, *Discosoma sanctithomae*

J. S. MILES

Marine Science Center, Northeastern University, Nahant, Massachusetts 01908

Abstract. The Corallimorpharia are a group of soft-bodied anthozoans closely related to the scleractinian corals. Although numerous reports have documented the agonistic behaviors of actiniarians and hard corals, only Chadwick (1987) has shown such behaviors in a corallimorph (*Corynactis california*). The following investigation confirms the use of inducible aggressive structures in space competition in the laboratory and in the field by *Discosoma sanctithomae*. This tropical corallimorph used both modified marginal tentacles and mesenterial filaments to damage adjacent scleractinians. All colonies of *Agaricia agaricites* transplanted near *D. sanctithomae* were damaged. Initially, *D. sanctithomae* adjacent to *Meandrina meandrites* were severely wounded. However, 67% recovered and retaliated within a one to six month period, causing damage to *M. meandrina* that persisted for at least twelve months.

Introduction

Many benthic cnidarians that reproduce asexually expand their colonies proximally and radially. New individuals require space on the substrate to become established and to grow. In a coral reef environment, however, space is limiting, and as an individual, or clone, expands, competitive interactions are common. These competitive encounters may have provided important selective pressures for the evolution of agonistic behaviors and structures to deal with these competition events. Abel (1954) first described acrorhagi, the inflatable sacks around the collar of certain Actiniaria. Francis (1973a) noticed a particular spatial pattern among conspecific anemone clones of *Anthopleura elegantissima;* individuals of a clone were closely aggregated, but groups of different clones were always separated by an "anemone-free zone." This led Francis to describe a series of behaviors in which *A. elegantissima* used acrorhagi during agonistic interactions with non-clonemates. Other researchers have investigated various aspects of aggressive behavior in members of the class Anthozoa (Bonnin, 1964; Williams, 1975; den Hartog, 1977; Purcell, 1977; Bigger, 1980; Kaplan, 1983; Sammarco *et al.*, 1983; Bak and Borsboom, 1984; Hidaka and Yamazato, 1984; Sebens, 1984; Chadwick, 1987). Knowledge has evolved from initial descriptions of straightforward, predictable results of spatial competition events (Lang, 1971, 1973; Francis, 1973b; Chornesky, 1983; Chornesky and Williams, 1983) to descriptions of more complex, dynamic interactions. The importance of temporal scale was recognized, and many competitive outcomes were discovered to be reversible (Bak *et al.*, 1982; Logan, 1984; Chornesky, 1985). The initial victor was not always the ultimate winner. Other factors such as size, attack angle, and previous aggressive history affected the outcome of competitions (Brace and Pavey, 1978; Brace, 1981; Bak *et al.*, 1982). Also, significant work has been done elucidating the systems of recognition required for these agonistic behaviors (Theodor, 1970; Hildemann, 1974; Bigger, 1980; Sauer *et al.*, 1986). The number of species known to exhibit specialized structures used in aggressive behaviors has also increased, including members from four different orders within the class Anthozoa (reviewed by Lang and Chornesky, 1988).

In addition to acrorhagi, certain species in the order Actiniaria employ a modified feeding tentacle as a fighting tentacle (= catch tentacles, Purcell, 1977). Functionally similar to the acrorhagi, this elongated tentacle can adhere to neighboring non-clonemate conspecifics, causing tissue necrosis and ultimately, if successful, retreat of the opposition. As with *A. elegantissimma*, these behaviors have been reported to produce single-clone aggregates separated by anemone-free zones (Purcell, 1977; Purcell and Kitting, 1982). One report indicated the mechanism also worked

Received 17 September 1990; accepted 24 January 1991.

on an intrasexual level, yielding anemone-free zones between clones of the same sex (Kaplan, 1983). Some scleractinians possess a structure similar to the actiniarians' fighting tentacle. Sweeper tentacles, so termed because they sweep the adjacent area, develop on polyps of certain reef corals (Richardson *et al.*, 1979; Chornesky, 1983; Chornesky and Williams, 1983; Hidaka and Yamazato, 1984). The development of sweeper tentacles is induced by the presence of, or aggression by, another coral (Chornesky, 1983). These interactions are primarily interspecific and are often used in conjunction with a second mechanism. Lang (1971, 1973) and Logan (1984) described the process of extracoelenteric digestion used by reef corals to avoid being overgrown and to acquire new space. The extrusion of mesenterial filaments through the mouth and body wall onto another coral results in partial mortality of the opposing colony.

Although the Octocorallia use allelochemicals in competitive interactions (Sammarco *et al.*, 1983, 1985; LaBarre, 1986; Pawlik *et al.*, 1987), until recently no member of this subclass was reported to have specialized structures used for aggression. Several reports described sweeper-like tentacles on species of Alcyonacea and Gorgonacea, but these tentacles are probably feeding apparati (Abel, 1970; Muzik, 1983). However, *Erythropodium caribaeorum* (Gorgonacea), develops sweeper tentacles and uses them for aggression (Sebens and Miles, 1988). These structures function in the same way as the sweeper tentacles of the scleractinians, but instead of only one or two tentacles per polyp becoming sweepers, all eight of the tentacles on many polyps elongate and are able to damage neighboring corals. It is of interest to note that *E. caribaeorum* is the only obligate encrusting gorgonian in the Caribbean. This growth form inevitably leads to interactions with a variety of other species requiring space on the primary substratum.

The Corallimorpharia are another order with members exhibiting agonistic behaviors. These soft-bodied members of the Hexacorallia resemble anemones, but are related more closely, morphologically and phylogenetically, to the scleractinians. Chadwick (1987) reported that the corallimorph *Corynactis californica* used mesenterial filaments against species of anemones and corals in agonistic interactions in the laboratory. Earlier, den Hartog (1977) described two types of tentacles along the rim of the oral disk of the corallimorph *Discosoma sanctithomae* (Duchassaing and Michelotti). Some of these marginal tentacles are thin and hair-like, whereas others are finger-like and bulbous. He found these bulbous tentacles to have larger and more dense holotrichous nematocysts than the thin counterparts and suggested that these might represent a morphological variant used in agonistic encounters, although no experimental work was done. Sebens (1976) examined this species in field and laboratory studies in Panama but found no evidence of agonistic behavior in short-term experiments. Here, I report the first field results demonstrating agonistic behavior in competitions between a corallimorph and several species of scleractinian corals. *D. sanctithomae* used both mesenterial filaments and enlarged marginal tentacles to damage the scleractinian corals *Agaricia agaricites* and *Meandrina meandrites*.

Materials and Methods

Site location and description

Field and laboratory experiments were completed at the Discovery Bay Marine Laboratory in Discovery Bay, Jamaica (18°30′N; 77°20′W). The reef crest along the north coast of Jamaica runs predominantly east to west, with spur and groove formations jutting out to the north. At Discovery Bay, the fore reef is separated from a well-developed lagoon by a conspicuous reef crest that has mounds of exposed coral rubble accumulated from Hurricane Allen in 1980. Spur and groove formations begin at 10 m on the fore reef and continue to the fore reef slope, which occurs at 21 m at some locations. The east back reef is predominantly a sandy bottom with *Thalassia* beds interspersed with patch reefs. Columbus Park is an area of the back reef with high concentrations of silt and of particulate matter that reduces visibility. Shallow areas are dominated by benthic soft-bodied zoantharians within a dead *Acropora cervicornis* framework. The deeper regions possess a rich sponge and mollusk community. For a more detailed description, see Goreau (1959), Goreau and Goreau (1973), and Liddell *et al.* (1984). Survey data were collected from the west back reef and Columbus Park, and from Long Term Study (LTS), Kinzie's Reef, and Lynton's Mine on the fore reef. Transplant experiments were located at all the fore reef survey sites between depths of 10 m and 20 m (Fig. 1).

Animal descriptions and collection

Discosoma sanctithomae is a corallimorpharian common throughout the Caribbean and Bermuda between depths of 1–20 m (den Hartog, 1980). Both solitary individuals and asexually produced clonal aggregates can be found living within the coral reef framework. The animal is orally-aborally flattened, with the oral disk averaging approximately 4 cm in diameter (Fig. 2A). A margin at the edge of the oral disk lacks tentacles and is often tucked up under the disk, but at other times is expanded well beyond the basal attachment area. The oral disk tentacles of *D. sanctithomae* are very short, stubby, and are often ramous. A second group of tentacles extends radially from the margin of the disk and are thus termed marginal tentacles.

Figure 1. Map of the fore reef at Discovery Bay, Jamaica. Areas marked with stars indicate sites of transplant experiments and fore reef survey sites.

Specimens of *Discosoma sanctithomae* used in the field experiments were never removed from the reef or disturbed in any way. Individuals were identified by tags placed on nearby coral rubble. *D. sanctithomae* used in laboratory experiments were collected along with pieces of the substrate, usually dead *Acropora cervicornis*, because attempts to scrape off individuals were always unsuccessful. The collected animals were placed in a running seawater table and allowed to acclimate for three to seven days before being used in experiments.

The scleractinian corals *Agaricia agaricites* (Pallas) and *Meandrina meandrites* (L) were used in the field transplants. Pieces of coral (approximately 6 × 8 cm) were collected using a rock hammer and chisel to release them at their base or at an area of dead coral skeleton. The corals were collected from the same reefs onto which they were to be transplanted. They were not brought to the surface, but were left for two to seven days before being transplanted. Corals were not used if they showed signs of tissue damage from the collection methods within this period. *A. agaricites* and *M. meandrites* used in the laboratory experiments were collected in a similar manner. However, these corals were transferred to running seawater tables and allowed to acclimate for three to seven days.

Field surveys

Field surveys of *Discosoma sanctithomae* were conducted to determine which organisms lived adjacent to the corallimorph and what interactions were occurring. The surveys were done by swimming parallel transects across depth contours throughout a designated area and recording every *D. sanctithomae* observed. Each of the *D. sanctithomae*'s neighbors were noted, and any damage on either *D. sanctithomae* or any neighbor was recorded. Percent-cover data were gathered from the same area as the *D. sanctithomae* survey. Survey procedures involved assigning random numbers to a chain-link transect that was haphazardly dropped within the study area. Species or substrate type that fell under each of the marked chain links was recorded (Rogers *et al.*, 1983). Information from

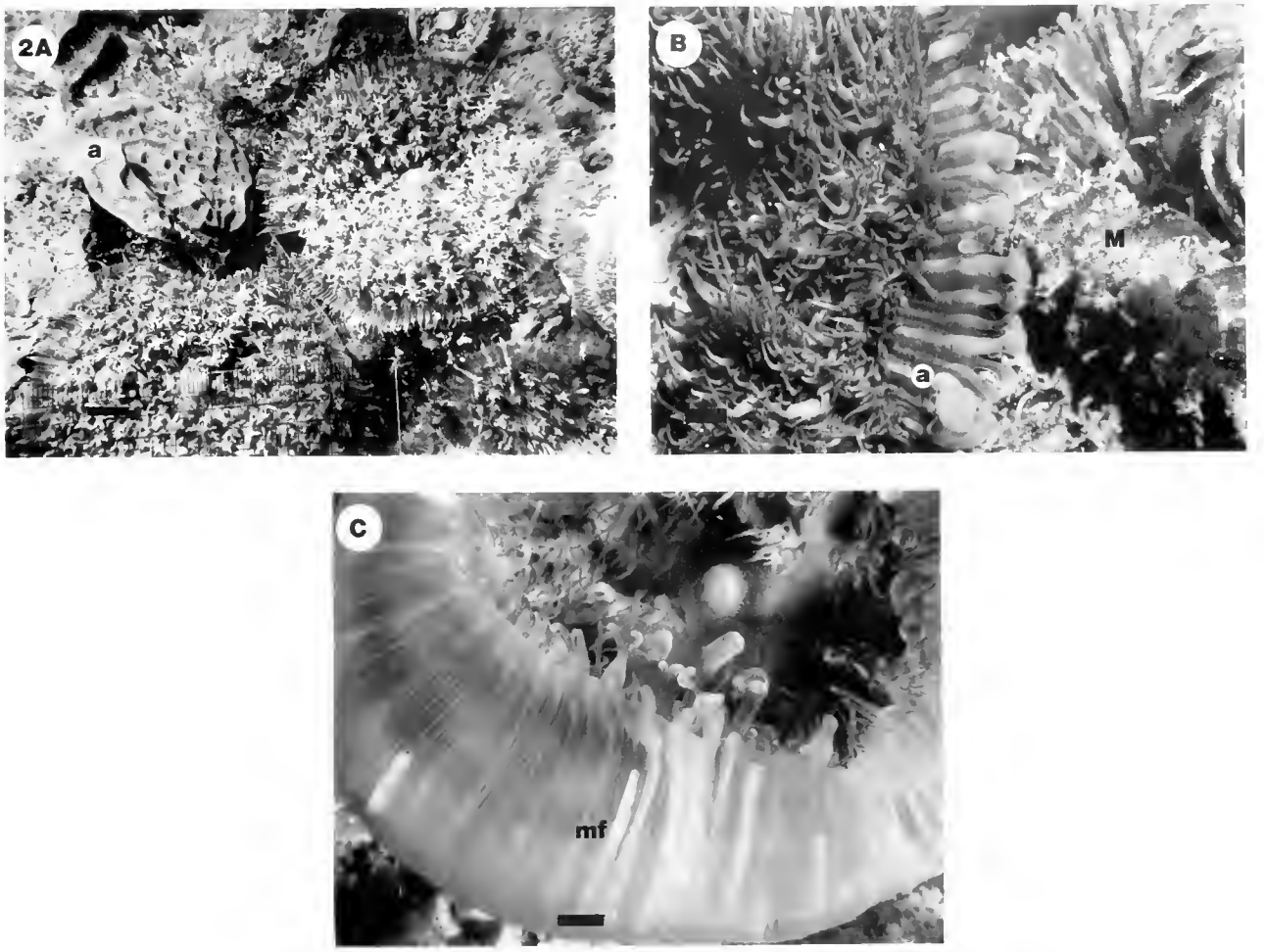

Figure 2. (A) *Agaricia agaricites* (a) transplanted next to a *Discosoma sanctithomae* with thin marginal tentacles (arrows). Scale = 1 cm. (B) *D. sanctithomae* adjacent to *Meandrina meandrites* (M) developed large swollen acrospheres (a) at the tips of the marginal tentacles. Areas of the rim have become enlarged also. Scale ≈ 2 mm. (C) *D. sanctithomae* with acrospheres. Mesenterial filaments (mf) can be seen in the area of the coelenteron leading to the marginal tentacles. Scale ≈ 2 mm.

the *D. sanctithomae* survey and the percent cover transects was compared to determine whether *D. sanctithomae*'s contact with neighbors was random or reflected some sort of selection for, or by, neighboring species.

Transplant experiments

Field. Manipulative experiments were done in the field to study the interactions of *Discosoma sanctithomae* and scleractinian corals. Pieces of coral were epoxied adjacent to, but not touching, individual *D. sanctithomae,* which were partially retracted. However, transplants were located so that fully expanded *D. sanctithomae* would touch the coral's tissue. The Pettit Underwater Patching Compound used to fix the corals in place was not toxic when applied only to the dead base of the coral. Corals showing a general tissue necrosis (possibly from handling) soon after the transplant (1–2 days) were removed from the study; this accounts for most of the discrepencies between initial and final sample sizes. Specific sets of transplants were designed to address the following questions: (1) Can *D. sanctithomae* damage scleractinian corals adjacent to them? (2) Are bulbous marginal tentacles with acrospheres associated with the damage to corals? (3) Do *D. sanctithomae* react differently depending on the species of coral that is next to them?

Three sets of transplants (Series I) were begun in January 1987. In the first set of transplants (T1) pieces of *Agaricia agaricites* (n = 19) were placed next to *D. sanctithomae* with filiform marginal tentacles (Fig. 2A). A second group of transplants (T2) paired *A. agaricites* (n = 16) with *D. sanctithomae* that had bulbous marginal tentacles. *A. agaricites* was chosen because it was found frequently next to *D. sanctithomae* in the field surveys. Both sets of

transplants were designed to examine *D. sanctithomae*'s tendency to damage corals. Also, if the bulbous tentacles were responsible for damage to the scleractinians, the corals in T2 would be expected to incur damage more quickly than the corals in T1. *Meandrina meandrites* (n = 18) was used in a third transplant experiment (T3) to test for any variation in response by *D. sanctithomae*. Unlike *A. agaricites*, this coral is known to use mesenterial filaments readily in aggressive encounters (Lang, 1973; Logan, 1984). All experimental pairs were monitored for damage to *D. sanctithomae* or to *A. agaricites*, and for any changes in the morphology of the marginal tentacles on *D. sanctithomae* once a week for five weeks, again after five months, then after one year. Several night dives were done to confirm damage to coral polyps and to check for development of sweeper tentacles (Chornesky, 1983). Photographs of experimental pairs were taken weekly with a Nikonos camera with a 2:1 extension tube, and a Minolta XL401 Super-8 movie camera was left on the reef for four days at a time, taking photographs at 1.5-min intervals. A second series of transplants (Series II) was started in February 1988. These experiments were identical to the 1987 T1 and T2 transplants except that they were monitored once a day for two and a half weeks to examine the interactions over a shorter time period.

Two types of controls were used to test for the effects of the transplantation process. Pieces of coral transplanted near *Discosoma sanctithomae* were always large enough so that at least half of their tissue area was out of reach of the *D. sanctithomae*, even when fully expanded (opposite-side controls). Additional pieces of coral were transplanted among the experimental pairs, but not within reach of any *D. sanctithomae*. These corals were regularly examined for any signs of damage. A control for *D. sanctithomae* acrosphere formation was done by observing the marginal tentacles of two sets of *D. sanctithomae* that were surrounded only by algae. One group of *D. sanctithomae* was monitored once every ten days for two months. The second group was monitored every day for up to twenty days. These individuals were studied to determine whether sporadic changes in the marginal tentacles occurred without contact with cnidarian neighbors.

Laboratory experiments. Transplant experiments similar to those in the field were done in the laboratory in running seawater tables. *Discosoma sanctithomae* individuals were paired with pieces of *Agaricia agaricites* (n = 5) and *Meandrina meandrites* (n = 5). None of the *D. sanctithomae* had enlarged marginal tentacles, nor did the corals have sweeper tentacles at the beginning of the experiment. When both members of an experimental pair were contracted, neither touched the other. Three pieces of *A. agaricites* and two of *M. meandrites*, as well as three individuals of *D. sanctithomae*, were out of reach of any other anthozoan and acted as the controls. These pairs were inspected for damage every hour for the first seven hours. Throughout the experiment a Super-8 movie camera with an intervalometer photographed individual pairs every 1.5 min. The experiment continued for eight days.

Results

Survey data

The neighboring species of more than 155 *Discosoma sanctithomae* were recorded (Fig. 3A, B). Approximately 37% (n = 238) of them were foliose or turf complex algae, the largest group total. The second most common group found adjacent to *D. sanctithomae* were crustose coralline

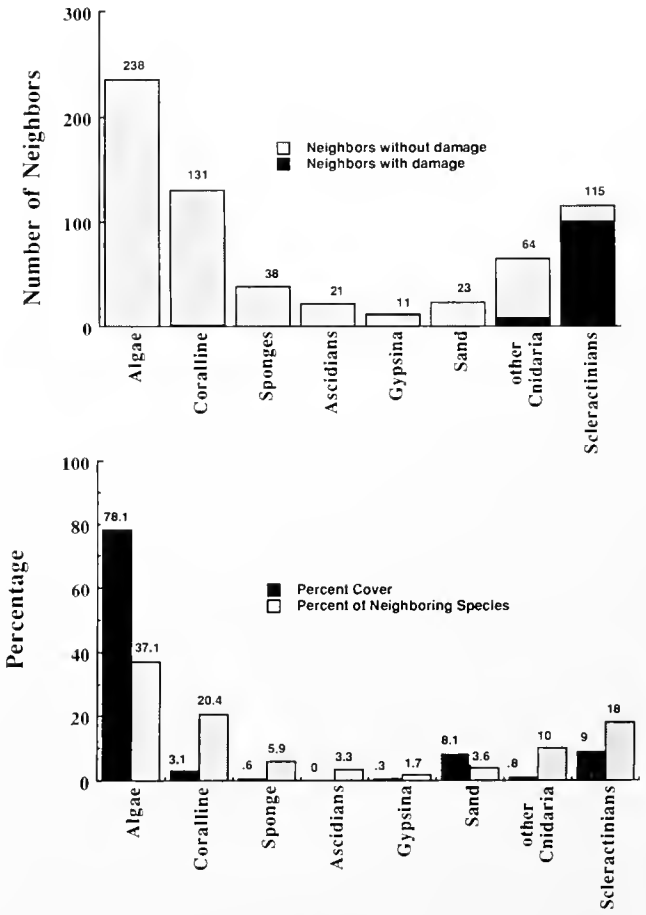

Figure 3. (Top) The area adjacent to individual *Discosoma sanctithomae* were surveyed at all transplant sites on the fore reef and in Columbus Park. Neighboring species and substrate type were counted and classified as damaged or not damaged; exact counts are reported above bars. Each organism and substrate type counted as "1" interaction regardless of size; this may underestimate the impact of larger organisms and overestimate those of smaller ones. (Bottom) Surveys of species percent-cover were done at all the neighbor survey sites. Sixteen transects were completed; 713 chain-link transect points were classified into the same eight catagories used for the neighbor survey. Numbers above each bar represent percentages for each group. Percent-cover results (black) are compared to percentage data of neighboring species (white; n = 641).

algae (20.4%), followed by the scleractinian corals (18%). The corals found most frequently adjacent to the corallimorphs were *Montastrea annularis, Siderastrea siderea,* and *Agaricia agaricites.* In more than 75% of the cases when *D. sanctithomae* was adjacent to a scleractinian, there were areas of dead coral associated with the area of contact. Damage was not readily apparent in any other group (Fig. 3A).

Although algae were also the most abundant organisms in the surveys of percent cover (n = 557, 78%), scleractinian corals (9%) and sand (8%) were the second and third most commonly occurring items, respectively (Fig. 3B). The complement of species and groups neighboring *D. sanctithomae* proved to be significantly different than the proportion of species expected from the percent cover survey using a G-test for independence ($G = 21.03$, $P < 0.05$). Algae have been dominant space occupiers in the fore reef community since the die-off of *Diadema antillarum* in 1983 (Liddell and Ohlhorst, 1983).

Field transplants

Series I. Sixteen of seventeen *Discosoma sanctithomae* originally with filiform tentacles had developed bulbous tentacles with acrospheres in the presence of *Agaricia agaricites* within six weeks. The mean time for acrosphere development was 17.3 ± 2.0 days (mean ± S.E.). During this time, all 17 of the *A. agaricites* colonies had been damaged; the mean time to damage from each colony was 17.9 ± 1.8 days (mean ± S.E.) (Fig. 4A). In comparison, only one opposite-side control was damaged. Formation of acrospheres and the occurrence of damage was significantly greater than that which might occur by chance (G-test with William's correction factor: G = 15.5; G = 23.0 resp.; $P < 0.05$). The time to acrosphere development was not significantly different from the average time for damage to occur to the corals (Mann-Whitney: $U' = 170.5$, $P < 0.05$).

All 12 *Agaricia agaricites* colonies placed next to the *Discosoma sanctithomae* that had acrospheres at the start of the experiment (T2) were damaged. The average time to damage (10.0 ± 1.7 days, mean ± S.E.) was significantly faster than the time to damage for the transplants that later formed acrospheres (T1) (Mann-Whitney: U = 204, $P < 0.05$) (Fig. 4A). Again, only one opposite-side coral control was damaged. Sweeper tentacles on *A. agaricites* occurred on only one colony. They formed after the interactions had progressed for about one month and after the coral had been initially damaged by the corallimorph. The corresponding *D. sanctithomae* did not reveal any damage.

The results of the *Discosoma sanctithomae* transplants with *Meandrina meandrites* were strikingly different. Within one week, 38% of the *D. sanctithomae* (n = 16) had suffered severe body lesions from the mesenterial filaments of *M. meandrites* (Fig. 4B). This increased to 63% within two weeks, culminating in the death of two *D. sanctithomae* individuals within the first month. The first incidence of damage to *M. meandrites* did not occur until almost one month had passed. However, of those *D. sanctithomae* that survived the first two months (n = 12), 67% went on to damage the *M. meandrites* over the next four months. Damage inflicted by these *D. sanctithomae* was still visible twelve months later (Fig. 5). None of the opposite-side coral controls were damaged.

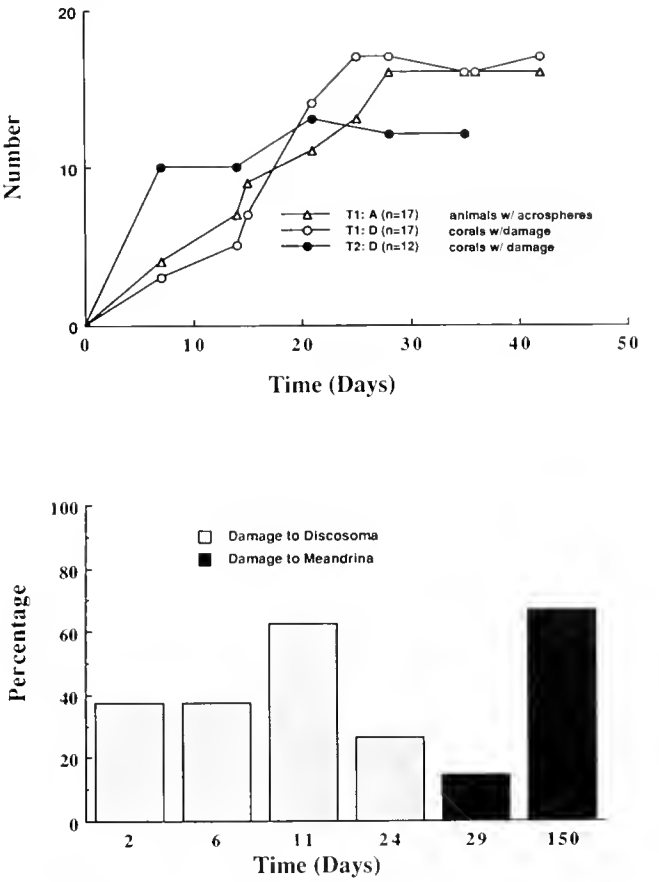

Figure 4. (Top) Results of two field transplant experiments (T1 & T2) are shown. In the first transplant (T1) 17 corals were placed next to *Discosoma sanctithomae* with thin marginal tentacles. T1:A (△) charts the progression of acrosphere development in *D. sanctithomae.* T1:D (○) tracks the development of damage to the corals. In T2, 12 corals were next to *D. sanctithomae* that possessed acrospheres. T2:D (●) records the damage incurred to the adjacent corals. (Bottom) Results of field transplant 3 (T3). Eighteen *Meandrina meandrites* were placed near *D. sanctithomae* with acrospheres. Initially 38% of the *D. sanctithomae* were severely injured; two died within the first month. Although none of the corals suffered damage before the end of the first month, 67% of the remaining transplants were damaged over the subsequent six-month period and remained damaged for at least twelve months.

Series II. Results of the Series II transplants were similar to Series I results. Ten of eleven *A. agaricites* corals placed

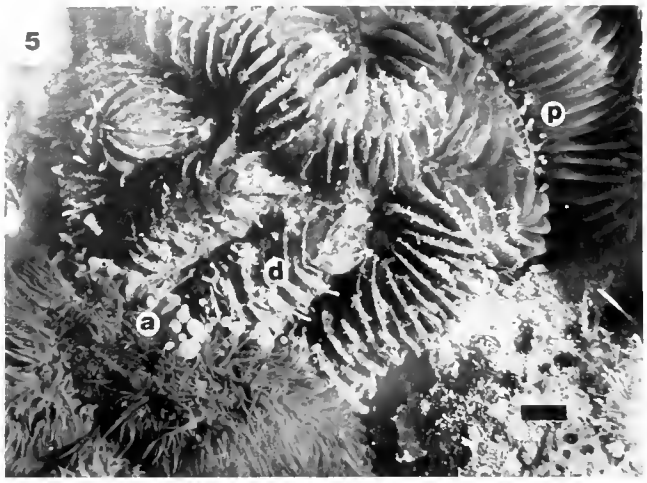

Figure 5. *Discosoma sanctithomae* vs. *Meandrina meandrites:* interaction after twelve months. Note the large acrospheres (a) and the algae-covered dead coral skeleton (d). Live coral polyps (p) can be seen out of reach of the *D. sanctithomae*'s tentacles. Scale ≈ 2.7 mm.

next to *Discosoma sanctithomae* with acrospheres were damaged in 12.0 ± 1.5 days (mean ± S.E.). Only two of the eleven corals adjacent to *D. sanctithomae* without acrospheres were clearly damaged (6.0 ± 5.0 days, mean ± S.E.). Only three of eleven had developed acrospheres within the trial period of 10 to 20 days. This short period before damage occurred reflects one coral that was extensively damaged after the second day by mesenterial filaments that were released through the marginal tentacles of the corallimorph. Mesenterial filaments were observed being extruded by *D. sanctithomae* through the tentacles on numerous other occasions, and were extruded frequently from the mouth and through the body wall as well.

Controls

None of the isolated coral controls experienced any tissue damage. The lack of incidences of damage to opposite-side coral controls were reported with the results for the particular transplant. The *D. sanctithomae* individuals acting as controls for random acrosphere development showed little change; no acrospheres were formed. There were, however, frequent influxes and effluxes of mesenterial filaments to and from the marginal tentacles. At times the filaments remained between the mesenteries in the coelenteron, and at other times they traveled into the tips of the marginal tentacles.

Laboratory experiments

The results of the laboratory experiments were a brief accelerated version of the field experiments. All the corals, and the *Discosoma sanctithomae* individuals, retracted their polyps when the experimental pairs were initially established. Although eight of ten corals partially expanded their polyps within 20 min, and all the *D. sanctithomae* adjacent to *A. agaricites* had relaxed within the first hour, there was no direct contact. The *D. sanctithomae* next to the *M. meandrites* remained contracted, with four of them extruding mesenterial filaments within the first seven hours.

Meandrina meandrites transplants were equally active. All five corals released mesenterial filaments onto the *Discosoma sanctithomae* within the first 7 h. *D. sanctithomae* near *A. agaricites* also extruded filaments but, in general, the severity of such attacks was greatly reduced compared to those with *M. meandrites*. Within 24 h, 4 *D. sanctithomae* had mucus layers covering body wounds inflicted by *M. meandrites'* mesenterial filaments. Body postures were strongly evasive, especially when compared to *D. sanctithomae* near *A. agaricites;* the latter often laid their marginal disks over the coral surfaces. By the end of the third day, four of the five corallimorphs near *M. meandrites* were dead. The fifth had severe body lesions and had partially released its hold on the substrate. None of the *M. meandrites* individuals were damaged.

None of the *Agaricia agaricites* individuals were observed releasing mesenterial filaments, nor using sweeper tentacles. A general pattern evolved for the *D. sanctithomae-A. agaricites* interactions of gradual expansion of the *D. sanctithomae* onto the coral's surface followed by retraction, and intermittent extrusion of mesenterial filaments by *D. sanctithomae. Discosoma sanctithomae* was able to damage *A. agaricites* in two separate cases, although the coral recovered its damaged area in one of these events. Three *D. sanctithomae* adjacent to *A. agaricites* died within eight days, but two of these deaths must be qualified. Two of the fatalities resulted from the *D. sanctithomae* releasing its hold near the *A. agaricites* and wandering into a colony of *M. meandrites*. None of the *D. sanctithomae* individuals formed marginal tentacles. All the control corals survived without damage, and one of the three control *D. sanctithomae* individuals died.

Discussion

Although lacking a hard skeleton, the soft-bodied relatives of the scleractinians, such as the Actiniaria, have proven to be able competitors for space (Francis, 1973a; Purcell, 1977; Purcell and Kitting, 1982; Chadwick, 1987). More recently, investigators have discovered that the Corallimorpharia possess aggressive abilities as well. During prolonged interspecific exposure, *Corynactis californica* killed polyps of the actiniarians *Anthopleura elegantissima* and *Metridium senile*, as well as the scleractinians *Astrangia lajollaensis* and *Balanophyllia elegans* by extruding mesenterial filaments (Chadwick, 1987). The

present study supplies evidence that another corallimorph, *Discosoma sanctithomae*, can compete successfully with scleractinian corals for primary space. Every colony of *Agaricia agaricites* transplanted next to *Discosoma sanctithomae* was damaged, whereas none of the associated *D. sanctithomae* were damaged. Most of the damage occurred within the first month of a 14-month experimental period. *D. sanctithomae* was able to cause severe necrosis of tissue on the coral *Meandrina meandrites*, which is considered to be near the top of the Caribbean coral competitive hierarchy due to its effective use of mesenterial filaments in damaging other scleractinians (Lang, 1973). Although many of the *D. sanctithomae* were initially inflicted with extensive body lesions by *M. meandrites*, many recovered and retaliated successfully, causing damage that persisted at least twelve months. This represents a clear and dramatic example of a competitive reversal and places *D. sanctithomae* near the top of a zoantharian competitive hierarchy.

Most of the agonistic behaviors of soft-bodied anthozoans (and some scleractinians) involve morphological modifications that provide the capability to inflict damage. Anemones in the family Actiniidae inflate acrorhagi (Abel, 1954; Francis, 1973a; Sebens, 1984); acontiate anemones in several families develop "fighting tentacles" from feeding tentacles (Purcell, 1977; Purcell and Kitting, 1982; Kaplan, 1983). *D. sanctithomae* uses marginal tentacles frequently filled with mesenterial filaments and ectoderm engorged with specialized nematocysts (den Hartog, 1977, 1980). The marginal tentacles changed from thin, filiform appendages to bulbous acrospheres in the presence of *A. agaricites* and *M. meandrites*. The initial increase in volume seems to be due to the influx of mesenterial filaments, which is later compounded by the ectoderm thickening with nematocysts (as seen by den Hartog, 1977). Unlike the acrorhagi (Bonnin, 1964; Bigger, 1980), which become inflated with each aggressive interaction, the marginal tentacles of *D. sanctithomae* remain bulbous once enlarged. In this study, the most extensive acrospheres were found closest to the site of interaction with the scleractinians. Acrospheres never developed in *D. sanctithomae* surrounded only by algae, nor were they found in *D. sanctithomae* adjacent to sponges, tunicates, or other noncnidarian neighbors in the field surveys.

Every incidence of damage to the experimental corals was associated with the presence of acrospheres except in one case. The association between acrospheres and damage is further supported by a decrease in the amount of time before damage appeared on the corals next to *D. sanctithomae* with acrospheres compared to those that developed acrospheres during the experiment. As the interactions progressed, algae may have acted as a buffer to contact with the acrospheres. After algae began to settle on the bare coral skeleton, the acrospheres did not intensify further.

Discosoma sanctithomae responded to the corals adjacent to them by developing acrospheres and by inflicting damage. However, the response was extremely graded. *D. sanctithomae* reacted to *Agaricia agaricites* much differently than it did to *Meandrina meandrites*. In general, the interactions with *A. agaricites* appeared to be much more gradual, progressing slowly, but ultimately resulting in the development of acrospheres on *D. sanctithomae* and damage to the coral. Conversely, the behavior of *D. sanctithomae* next to *M. meandrites* was much more dramatic, responding to the aggressive actions of *M. meandrites*. Within less than twenty-four hours, *D. sanctithomae* individuals had been damaged extensively and were withdrawn, some for several days. Those that later recovered and attacked *M. meandrites* did so with well-developed acrospheres. Often the marginal tentacles and even the rim of the oral disk were thickened and swollen (pers. obs.), presumably filled with potent nematocysts (den Hartog, 1977) (Fig. 2B).

The laboratory experiments and the Series II transplants served to elucidate the differences in *Discosoma sanctithomae*'s behaviors. *D. sanctithomae*'s response to adjacent *Meandrina meandrites* was immediate and severe. *M. meandrites'* quickness in extruding mesenterial filaments and inflicting damage deterred *D. sanctithomae* from approaching *M. meandrites*. In contrast, *D. sanctithomae* placed next to *Agaricia agaricites* repeatedly relaxed and expanded its disk directly on top of *A. agaricites'* living tissue. *D. sanctithomae* did not appear to be adversely affected by *A. agaricites*, although it did periodically retract away from contact with the coral. *D. sanctithomae* could cause small amounts of necrosis to *A. agaricites'* tissue which, at least in the early stages, was often recovered by the coral. However, sometime after prolonged exposure and repeated attacks, the *A. agaricites* was no longer able to regain lost tissue. Not long after this stage, algae (usually a green alga) began to settle on the bare coral skeleton. These dead areas persisted for the remainder of the study period.

The use of mesenterial filaments in competitive interactions is well documented for scleractinians. Some of the most aggressive corals use exclusively mesenterial filaments for defense (Lang, 1971, 1973; Logan, 1984). The corallimorph *Corynactis californica* extruded mesenterial filaments primarily out the mouth but also through the body wall and once through the tentacles during agonistic encounters (Chadwick, 1987). *Discosoma sanctithomae* invoked two mechanisms for inflicting damage that reflect its phylogenetic relationship with the scleractinians and its particular tentacle morphology. Like many hard corals, the corallimorph readily emitted mesenterial filaments out of the mouth and through the body wall when disturbed.

In addition, *D. sanctithomae* continually transferred mesenterial filaments into the discal and marginal tentacles, sometimes passing them out through the tips. It is not yet known whether there are permanent holes at the tips of these tentacles through which the mesenteries can pass. A similar movement of mesenterial filaments occurs in the discal tentacles of *Rhodactis howesii* (Corallimorpharia) during feeding behaviors (Hamner and Dunn, 1980).

This regular fluctuation of mesenterial filaments dispose *Discosoma sanctithomae* to be capable of quickly sending mesenterial filaments into and out of the tips of the marginal tentacles when it is involved in agonistic encounters with neighboring species. *D. sanctithomae* was observed to damage adjacent corals with mesenterial filaments from its marginal tentacles. Although most incidences of damage occurred after acrospheres had formed, some corals showed damage before this time that could have been caused by mesenterial filaments. By extruding the filaments out the tips of the marginal tentacles, *D. sanctithomae* increases the probability of the filaments landing on the tissue of the opposing organism. It is a behavior that the corallimorph can invoke quickly at the time of interaction because mesenterial filaments regularly fluctuate in and out of the marginal tentacles. Hence, there is less time between the recognition of a competitor and the commencement of an aggressive response than would be required to form sweeper or fighting tentacles.

Den Hartog (1977) determined that the size and density of holotrich nematocysts was greater in bulbous marginal tentacles than in the filiform type. This study confirms that interactions with scleractinians can induce the formation of bulbous tentacles. After a period of less than a week, thin transparent marginal tentacles of *Discosoma sanctithomae* became thickened and more opaque in the presence of the coral colonies. Some tentacles doubled in thickness and became opaque, while others more than tripled their girth and were associated with a greatly thickened oral rim. A few tentacles elongated, forming distinct tips with acrospheres (Fig. 2). All forms of these thickened marginal tentacles were able to cause necrosis of the coral tissue.

The combination of mesenterial filaments and acrospheres enabled *D. sanctithomae* to respond immediately, warding off imminent damage, and to develop an alternate form of defense that required more time to initiate. *D. sanctithomae* may use mesenterial filaments in response to adverse interactions of short temporal scale, and reserves acrosphere formation, involving the costly construction of new tissue and many nematocysts, for prolonged interactions. Its soft body allows it to avoid some acts of aggression from opponents by bending away and perhaps even by moving the base laterally. All such characteristics make *D. sanctithomae* an effective competitor, holding its own on the substratum of the reef against some of the most aggressive corals.

Acknowledgments

This work was supported partially by the Lerner-Gray Fund for Marine Research and by Sigma Xi Grants-in-Aid of Research. My research was aided by the field assistance of Lars Kula, Pete Edmunds, Ruth Gates, and many members of Northeastern University's East/West Program. P. Schultze provided insightful discussion on the statistical analysis. K. P. Sebens, J. Witman, M. P. Morse, and D. O'Brien, along with two anonymous reviewers critically reviewed the manuscript. Thank you all. This is contribution number 182, Marine Science Center, Northeastern University, Nahant, MA, and number 495, Discovery Bay Marine Laboratory, Discovery Bay, Jamaica.

Literature Cited

Abel, E. F. 1954. Ein Beitrag zur Giftwirkung der Aktinien und Funktion der Randsäckchen. *Zool. Anz.* **153:** 19–268.

Abel, E. F. 1970. Über den Tentakelapparat der Edelkoralle (*Corallium rubrum* L.) und seine Funktion beim Beutefangverhalten. *Oecologia* **4:** 133–142.

Bak, R. P. M., and J. L. A. Borsboom. 1984. Allelopathic interaction between a reef coelenterate and benthic algae. *Oecologia* **63:** 194–198.

Bak, R. P. M., R. M. Termaat, and R. Dekker. 1982. Complexity of coral interactions: influence of time, location of interaction and epifauna. *Mar. Biol.* **69:** 215–222.

Bigger, C. H. 1980. Interspecific and intraspecific acrorhagial aggressive behavior among sea anemones: a recognition of self and not-self. *Biol. Bull.* **159:** 117–134.

Bonnin, J. P. 1964. Recherches sur la "reaction d'aggression" et sur le fonctionnement des acrorrhages d'*Actinia equina* L. *Bull. Biol. Fr. Belg.* **98:** 225–250.

Brace, R. C. 1981. Intraspecific aggression in the color morphs of the anemone *Phymactis clematis* from Chile. *Mar. Biol.* **64:** 85–93.

Brace, R. C., and J. Pavey. 1978. Size dependent dominance hierarchy in the anemone *Actinia equina*. *Nature* **273:** 752–753.

Chadwick, N. 1987. Interspecific aggressive behavior of the corallimorpharian *Corynactis californica* (Cnidaria: Anthozoa): Effects on sympatric corals and sea anemones. *Biol. Bull.* **173:** 110–125.

Chornesky, E. A. 1985. Repeated reversals of competitive dominance during spatial competition between reef corals. *Ecology* **70(4):** 843–855.

Chornesky, E. A. 1983. Induced development of sweeper tentacles on the reef coral *Agaricia agaricites:* a response to direct competition. *Biol. Bull.* **165:** 569–581.

Chornesky, E. A., and S. L. Williams. 1983. Distribution of sweeper tentacles on *Montastrea cavernosa*. Pp. 61–67 in *The Ecology of Deep and Shallow Reefs*, M. L. Reaka, ed. Symp. Ser. Undersea Res., N.O.A.A. Nat. Undersea Res. Prog., 1.

den Hartog, J. C. 1980. Caribbean shallow water Corallimorpharia. *Zool. Verh.* **176:** 1–83.

den Hartog, J. C. 1977. The marginal tentacles of *Rhodactis sanctithomae* (Corallimorpharia) sweeper tentacles of *Montastrea cavernosa* (Scleractinia), their cnidom and possible function. *The Second Int. Coral Reef Symposium.* Univ. Miami Press, Miami, FL. **1:** 463–470.

Francis, L. 1973a. Clone specific segregation in the sea anemone *Anthopleura elegantissima*. *Biol. Bull.* **144:** 64–72.

Francis, L. 1973b. Intraspecific aggression and its effects on the distribution of *Anthopleura elegantissima* and some related sea anemones. *Biol. Bull.* **144:** 73–92.

Goreau, T. F. 1959. The ecology of Jamaican coral reefs I. Species composition and zonation. *Ecology* **40:** 67–90.

Goreau, T. F., and N. I. Goreau. 1973. The ecology of Jamaican coral reefs II. Geomorphology, zonation, and sedimentary phases. *Bull. Mar. Sci.* **23:** 399–464.

Hamner, W. M., and D. F. Dunn. 1980. Tropical Corallimorpharia (Coelenterata: Anthozoa): feeding by envelopment. *Micronesica*, vol **16**, June.

Hidaka, M., and K. Yamazato. 1984. Intraspecific interactions in a scleractinian coral, *Galaxea fascicularis* induced formation of sweeper tentacles. *Coral Reefs* **3:** 77–85.

Hildemann, W. H. 1974. Some new concepts in immunological phylogeny. *Nature* **250:** 116–120.

Kaplan, S. A. 1983. Intrasexual aggression in *Metridium senile*. *Biol. Bull.* **165:** 416–418.

LaBarre, S. 1986. Competitive strategies of soft corals (Coelenterata: Octocorallia): III. Spacing and aggressive interactions between alcyonaceans. *Mar. Ecol. Prog. Ser.* **28:** 147–156.

Lang, J. C. 1971. Interspecific aggression by scleractinian corals I. The rediscovery of *Scolymia cubensis* (Milne Edwards & Haime). *Bull. Mar. Sci.* **21:** 952–959.

Lang, J. C. 1973. Interspecific aggression by scleractinian reef corals II. Why the race is not only to the swift. *Bull. Mar. Sci.* **23:** 260–279.

Lang, J. C., and E. A. Chornesky. 1988. Competition between scleractinian reef corals: a review of mechanisms and effects. In *Ecosystems of the World: Coral Reefs*, Z. Dubinsky, ed. Elsevier Press, Amsterdam.

Liddell, W. D., and S. L. Ohlhorst. 1986. Changes in the benthic community composition following the mass mortality of *Diadema* at Jamaica. *J. Exp. Mar. Biol. Ecol.* **95:** 271–278.

Liddell, W. D., S. L. Ohlhorst, and A. G. Choates. 1984. *Modern and Ancient Carbonate Environments of Jamaica* Sedementa X. Miami Beach, Univ. of Florida Press. 99 pp.

Logan, A. 1984. Interspecific aggression in hermatypic corals from Bermuda. *Coral Reefs* **3:** 131–138.

Muzik, K. 1983. Zoom and focus: octocorals. *Newton Graphic Science Magazine (Japan)* **3:** 30–35.

Pawlik, S. R., M. T. Burch, and W. Fenical. 1987. Patterns of chemical defense among Caribbean gorgonian corals: a preliminary survey. *J. Exp. Mar. Biol. Ecol.* **108:** 55–66.

Purcell, J. E. 1977. Aggressive function and induced development of catch tentacles in the sea anemone *Metridium senile* Coelenterata: Actiniaria. *Biol. Bull.* **153:** 355–368.

Purcell, J. E., and C. L. Kitting. 1982. Intraspecific aggression and population distributions of the sea anemone *Metridium senile*. *Biol. Bull.* **162:** 345–359.

Richardson, C. A., P. Dustan, and J. C. Lang. 1979. Maintenance of living space by sweeper tentacles of *Montastrea cavernosa*, a Caribbean reef coral. *Mar. Biol.* **55:** 181–186.

Rogers, C. S., M. Gilnack, and H. C. Fitz III. 1983. Monitoring of coral reefs with linear transects: a study of storm damage. *J. Exp. Mar. Biol. Ecol.* **66:** 285–300.

Sammarco, P. W., J. C. Coll, and S. LaBarre. 1985. Competitive strategies of soft corals (Coelenterata: Octocorallia). *Coral Reefs* **1:** 173–178.

Sammarco, P. W., J. C. Coll, S. LaBarre, and B. Willis. 1983. Competitive strategies of soft corals (Coelenterata: Octocorallia): allelopathic effects on selected scleractinian corals. *J. Exp. Mar. Biol. Ecol.* **91:** 199–215.

Sauer, K. P., M. Muller, and M. Weber. 1986. Alloimmune memory for glycoproteid recognition molecules in sea anemones competing for space. *Mar. Biol.* **92:** 73–79.

Sebens, K. P. 1976. The ecology of Caribbean sea anemones in Panama: utilization of space on a coral reef. Pp. 67–77 in *Coelenterate Ecology and Behavior*, G. O. Mackie, ed. Plenum Publ., NY.

Sebens, K. P. 1984. Agonistic behavior in the intertidal sea anemone *Anthopleura xanthogrammica*. *Biol. Bull.* **166:** 457–472.

Sebens, K. P., and J. S. Miles. 1988. Sweeper tentacles in a gorgonian octocoral: morphological modifications for interference competition. *Biol. Bull.* **175:** 378–387.

Theodor, J. L. 1970. Distinction between "self" and "not self" in lower invertebrates. *Nature* **227:** 690–692.

Williams, R. B. 1975. Catch tentacles in sea anemones: occurrence in *Haliplanella luciae* (Verrill) and a review of current knowledge. *J. Nat. Hist.* **9:** 241–248.

Reference: *Biol. Bull.* 180: 416–431. (June, 1991)

Autotomy in Blue Crab (*Callinectes sapidus* Rathbun) Populations: Geographic, Temporal, and Ontogenetic Variation

L. DAVID SMITH[1,2] AND ANSON H. HINES[1]

[1]*Smithsonian Environmental Research Center, P.O. Box 28, Edgewater, Maryland 21037 and*
[2]*Department of Zoology, University of Maryland, College Park, Maryland, 20742*

Abstract. Blue crab (*Callinectes sapidus* Rathbun) populations were examined at four sites in Chesapeake Bay and three additional sites along the southeastern Atlantic coast and Gulf of Mexico; the aims were to assess the incidence of limb autotomy and to determine whether injury patterns varied temporally, geographically, and ontogenetically. These data, which include four years of information from one site (Rhode River, Maryland, a subestuary of central Chesapeake Bay), make this study the most extensive and intensive survey of limb autotomy yet conducted in arthropods. A substantial percentage (17–39%) of the blue crab populations were either missing or regenerating one or more limbs, suggesting that autotomy is an important mechanism for their survival. The frequency of limb autotomy varied, both within and between years, and over broad geographical scales. Injury levels were generally correlated positively with crab size. Limb autotomy was independent of sex and molt stage, and frequencies varied little among sites in the Rhode River. Patterns of limb injury in *C. sapidus* were remarkably consistent among all sites. The most frequent injury involved loss of a single cheliped. Swimming legs suffered the least damage. Severe multiple limb loss was rare. Right and left limbs were lost with equal frequency in most populations. This consistency of autotomy pattern suggests differential vulnerability of limbs and standard behavioral response by blue crabs to various injury-causing agents. The frequency of autotomy was density-dependent in the Rhode River, indicating that intraspecific interactions (*e.g.*, cannibalism) may be a major cause of limb loss in populations in the Rhode River subestuary and elsewhere.

Received 2 October 1990; accepted 27 December 1990.

Introduction

Many invertebrate and vertebrate species respond to injury or its threat by autotomizing (*i.e.*, severing) a body part along a breakage plane (Wood and Wood, 1932; Needham, 1953; Robinson *et al.*, 1970; Vitt *et al.*, 1977; McVean, 1982; McCallum *et al.*, 1989). While such behavior has immediate survival benefits (Dial and Fitzpatrick, 1983; Medel *et al.*, 1988; Smith, 1990a), autotomy may handicap individuals when foraging (Slater and Lawrence, 1980; Smith, 1990a), overwintering (Willis *et al.*, 1982); escaping predators (Vitt *et al.*, 1977; Dial and Fitzpatrick, 1984; Smith, 1990a), or competing for mates (Sekkelsten, 1988; Smith, 1990a) or shelter (Conover and Miller, 1978; Berzins and Caldwell, 1983). Energetic costs of regenerating body parts can reduce reproductive output (Maiorana, 1977) and growth (Kuris and Mager, 1975; Smith, 1990b). Theoretical models (Harris, 1989) have suggested that nonlethal injury could regulate population abundance, if injury rates were density-dependent and significantly reduced long-term survival or reproduction. Detailed knowledge of autotomy patterns and frequencies, for a single species, over both narrow and broad temporal and geographic scales, are needed to make more reliable inferences concerning the fitness benefits and consequences of autotomy.

Quantitative surveys of limb loss in decapod crustaceans exist for only a few species (*Cancer magister*, Durkin *et al.*, 1984; Shirley and Shirley, 1988; *Cancer pagurus*, Bennett, 1973; *Carcinus maenas*, Needham, 1953; McVean, 1976; McVean and Findlay, 1979; Sekkelsten,

1988, *Menippe mercenaria,* Sullivan, 1979; Simonson and Steele, 1981; Simonson, 1985; *Paralithodes camtschatica* and *Chionoecetes bairdi,* Edwards, 1972). The percentage of injury in these species ranged from 13–66%. Inferences from these data regarding the fitness consequences of autotomy have been limited, however, because field data have not been collected for more than one complete growing season; smaller individuals in commercial species frequently have not been sampled; chelipeds have often been the only limbs assessed; and collections have been geographically restricted. To understand how the incidence of autotomy varies within and among populations, multiple-year and -site data on injury are needed for a range of body sizes for both sexes.

Nonlethal injury often results from unsuccessful attacks by predators (Vermeij, 1982). Variation in injury levels among populations and species has been thought to reflect differences in predation intensity and efficiency over altitudinal gradients (Ballinger, 1979; Shaffer, 1978), ecological habitats (Schoener and Schoener, 1980); biogeographic regions (Vermeij, 1976); geologic time (Vermeij, 1977, 1983), life histories (Vitt *et al.,* 1977), and behaviors (Jaksic and Fuentes, 1980; Schall and Pianka, 1980). Although specific agents responsible for autotomy in nature are rarely identified (*cf.,* Robinson *et al.,* 1970; Jaeger, 1981; Smith, 1990a), such information is needed to understand the patterns and impact of injury in populations. Intraspecific predation is common in the animal kingdom (Fox, 1975; Polis, 1981; Stevens *et al.,* 1982; Reaka, 1987; Kurihara and Okamoto, 1987), and may be an important cause of autotomy in some taxa (*e.g.,* salamanders; Jaeger, 1981). Large *Callinectes sapidus* are known to prey on smaller conspecifics (Laughlin, 1982; Hines *et al.,* 1990; Peery, 1989; Smith, 1990a). If intraspecific interactions are chiefly responsible for autotomy in blue crabs, then injury levels should correlate positively with population densities over temporal and spatial scales.

Costs of nonlethal injury to individuals will depend on the type and number of missing limbs. The relative importance of different limbs to survival, in turn, may be indicated by the frequency of their repair in the population. Limb regeneration in arthropods occurs upon molting, and crabs may require a number of molts (*e.g.,* 1–3 in *Callinectes sapidus,* Smith, 1990b; >4 in *Paralithodes camtschatica,* Edwards, 1972) before full limb length is restored. For most limbs, evidence of past injury disappears once symmetry has been restored. Following the loss of a major (crusher) claw, however, normal cheliped dimorphism is often not reestablished (Smith, 1990b); thus, the absence of such dimorphism can serve as a measure of survival of past injury.

To assess the impact of autotomy in a population, it is necessary to: (1) document spatial, temporal, and ontogenetic variation in patterns and levels of injury; (2) identify causal agents; and (3) determine the various costs of injury to individuals. The present study examines incidences of autotomy in blue crabs (*Callinectes sapidus* Rathbun) at four sites in Chesapeake Bay and three additional sites along the southeastern United States Atlantic coast and the Gulf of Mexico. These data, which include four years of information from one site in central Chesapeake Bay, make this the most detailed survey yet conducted on autotomy in arthropods.

Materials and Methods

Sampling procedures

Callinectes sapidus individuals were collected from 1986 to 1989 in the Rhode River, Maryland; at three additional sites in the Chesapeake Bay in fall 1989; and at three sites along the southeastern Atlantic coast and the Gulf of Mexico of the United States (Figs. 1, 2) in spring 1989. At all locations, crabs were measured or examined for: (1) carapace width between tips of lateral spines, (2) sex, (3) sexual maturity in females (1986–89) and males (1988–89, only), (4) molt stage, (5) type and side of any missing or regenerating limbs, (6) lengths of limb buds, regenerating limbs, and contralateral intact limbs, and (7) side of the crusher claw.

Sexual maturity in female blue crabs was determined by examining differences in abdominal allometry (Van Engel, 1958). For males, sexual maturity was indicated by the ease with which the abdomen could be pulled away from the ventral surface of the cephalothorax (Van Engel, 1958; 1990). Molt stages were determined by assessing carapace hardness and by examining the propodus of the fifth pereopod for evidence of epidermal retraction (Van Engel, 1958; Johnson, 1980). A limb stump that was either scarred, or possessed a papilla or limb bud, was classified as a missing limb. A regenerating limb was considered to be a functional appendage that had undergone at least one molt since autotomy, but was shorter than the intact, contralateral limb. Crabs that possessed an unscarred stump wound, indicating possible injury caused during collection, were not measured. Limb length was measured as the distance from the autotomy plane in the basi-ischial segment to the dactyl tip of a fully extended limb.

Site descriptions and collection methods

Rhode River, Maryland. Callinectes sapidus individuals were collected from the Rhode River near Edgewater, Maryland (38°51′N, 76°32′W), between July and November in 1986, and from May to November each year from 1987 to 1989 (Figs. 1, 2). The Rhode River is a

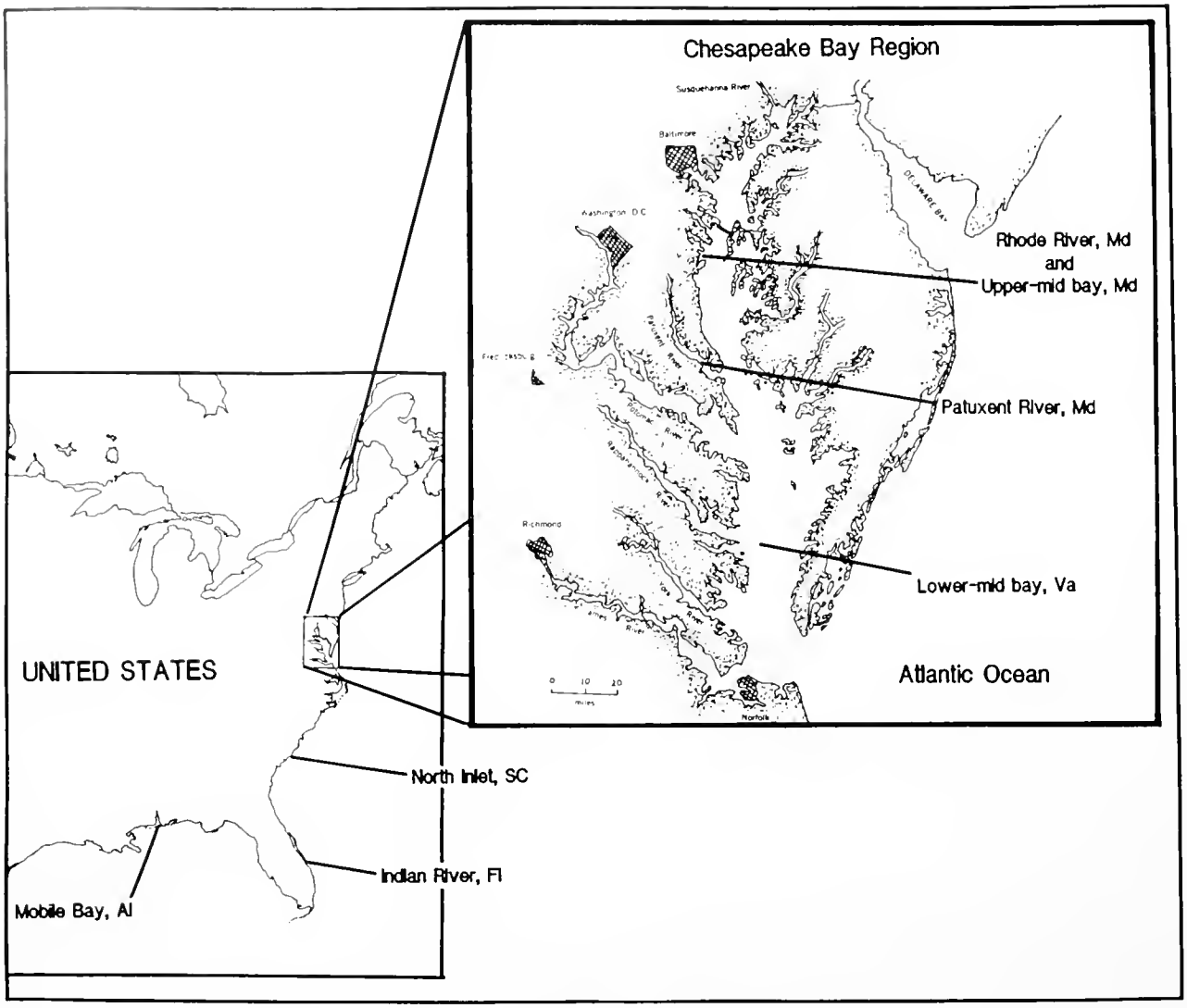

Figure 1. Map of the United States Atlantic coast and the Gulf of Mexico showing locations of blue crab sampling sites from 1986 to 1989.

shallow (maximum depth = 4 m), 485 ha mesohaline subestuary that empties into the western side of the upper-central Chesapeake Bay (Hines *et al.*, 1987a,b). Water temperatures ranged from 8°C to 34°C during the sampling period, with July temperatures averaging 28°C (±2.4). Salinities typically ranged from 4 to 14‰; but unusually low salinities (0–10‰) were recorded in 1989.

Several methods were used to sample blue crabs in the Rhode River as well as at other sites. Potential biases related to these different collection techniques were examined and are discussed below. In all four years, blue crabs were sampled monthly by otter trawl (3 m wide mouth; 5 mm mesh net body; 7 mm mesh cod end; with tickler chain; Hines *et al.*, 1987a) pulled for 900 m on two consecutive days at each of three stations in the Rhode River. Two stations were located at the river mouth, one over sandy substrate, and the other over muddy sediment; a third station was located at the river head over muddy sediment (Fig. 2).

From 1986 to 1988, blue crabs were also collected biweekly at a fish weir spanning the principal freshwater tributary (Muddy Creek) of the Rhode River. Crabs moving up- and downstream were captured separately in single hoop nets (7 mm mesh). No crabs were sampled at the weir in 1989 because of storm-related damage. Consequently, in 1989, crabs were collected biweekly at the river head (0.5–2 m depth); larger individuals were caught in baited commercial crab pots (57 mm mesh), and smaller crabs in specially designed crab pots (7 mm mesh). Blue

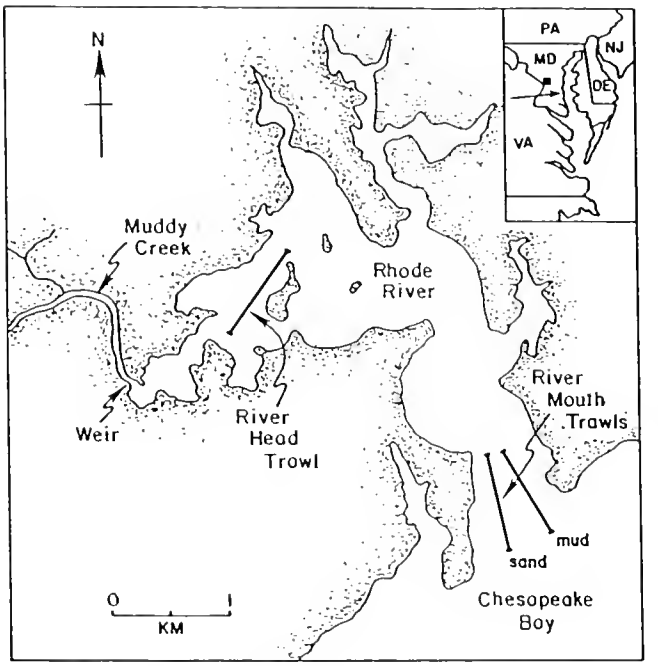

Figure 2. Map of the Rhode River subestuary, Maryland, showing sampling sites from 1986 to 1989. These include mouth sand and mouth mud trawl stations (1986–89) = River Mouth; river head trawl station (1986–89) and crab pot/seine sites (1989, only) = River Head; and Muddy Creek up- and downstream weir nets (1986–88) = Creek.

crabs were also sampled periodically in nearshore waters (depth 0.3–1.2 m) with a 10 m beach seine (7 mm mesh).

Non-Rhode River sites. Locations, dates, physical conditions (*e.g.*, depth, salinity), and sampling techniques for additional sites in Chesapeake Bay and for sites in South Carolina, Florida, and Alabama are summarized in Table I. Note that the upper-mid Chesapeake Bay site was only 1 km east of the mouth of the Rhode River, Maryland. Using a dipnet, blue crabs were collected from the sides of a commercial pound net at this site.

Statistical analyses

Data were treated as categorical, and frequencies were analyzed by logistic regressions (Cox, 1970; PROC CATMOD with maximum likelihood estimation, 0.5 added to all cells; SAS Institute, 1985) or two-way contingency tables. In the Rhode River, data were analyzed for only those months when 25 or more crabs were obtained. Locations in the Rhode River were combined into river mouth, river head, or creek sites, because differences in autotomy frequency were not detected between sample stations within each subregion (G-tests, $P > 0.05$). Crabs were divided into small (<61 mm carapace width), medium ($61 \leq CW \leq 110$ mm), and large (>110 mm CW) size classes. The division between medium and large size classes corresponded approximately with the onset of sexual maturity. Molt stages were classified as postmolt (stages A and B), intermolt (stage C), and premolt (stage D) (Johnson, 1980). Crabs in the act of molting (stage E) were very rare and were included as premolt animals.

The primary null hypothesis tested whether the frequency of injured crabs (*i.e.*, those animals missing or regenerating at least one limb) in a population was independent of one or more of the following independent variables: (1) year (Rhode River, only), (2) month (Rhode

Table I

Sampling sites, dates, physical conditions, and sampling methods used to collect blue crabs in 1989

Site	Location (Lat., Long.)	Sampling dates 1989	Depth (m)	Salinity (‰)	Temp. (°C)	Sampling method
Upper-Mid Chesapeake Bay, Maryland	38°50′N, 76°31′W	Aug.–Sept.	5	6–11	24–28	dip net
Patuxent River, Maryland	38°23′N, 76°36′W	Oct.	9–21	12–14	14	otter trawl
Lower-Mid Chesapeake Bay, Virginia	37°25′N-37°39′N 75°56′W-76°17′W	Oct.	4–18	19	19	otter trawl
North Inlet, South Carolina	33°21′N, 79°11′W	May	.2–3	21	31	crab pots, dip net
Indian River, Florida	27°50′N, 80°29′W	May	.5–5	23–26	29–32	crab pots, dip net
Mobile Bay, Alabama	30°15′N, 88°00′W	May	.5–5	24	27	crab pots, seine

Latitudinal and longitudinal range of sampling transects are given for the lower-mid Chesapeake Bay site. See text for description of 1986–1989 Rhode River surveys.

Table II

Frequencies and percentages of crabs missing, regenerating, and both missing and regenerating limbs in the Rhode River from 1986 to 1989

	Rhode River, Maryland							
	1986[a]		1987[b]		1988[b]		1989[b]	
Category	n	%	n	%	n	%	n	%
Total intact	1050	75.0	505	81.2	536	82.5	569	82.2
Total injured:	350	25.0	117	18.8	113	17.5	123	17.8
Missing[1]	211	15.1	56	9.0	53	8.2	68	9.8
Regenerating[2]	123	8.8	55	8.8	57	8.8	46	6.7
Miss. + Regen.[3]	16	1.1	6	1.0	3	0.5	9	1.3
Total caught	1400	100.0	622	100.0	649	100.0	692	100.0
Sex ratio M:F	67:33		81:19		83:17		76:24	
Size ratio S:M:L[4]	12:48:40		20:26:54		21:38:41		32:18:50	

[1] Missing = crabs with one or more scarred stumps, papillae, or limb buds.
[2] Regenerating = crabs possessing one or more functional but shortened appendages.
[3] Miss. + Regen. = crabs possessing both missing and regenerating limbs.
[4] Size ratio: (S < 61 mm carapace width, M = 61–110 mm CW, L > 110 mm CW) for all crabs (injured and intact).
Years with the same superscripted letter did not differ significantly in total autotomy frequency.

River, only), (3) subestuarine location (Rhode River, only), (4) body size, (5) sex, (6) sexual maturity, (7) molt stage, and (8) geographic location. All relevant two factor combinations of these independent variables were tested by logistic regression for their relationship to the binary response variable (*i.e.*, frequency of injured *versus* uninjured crabs). Expected cell frequencies of injured animals were often low (<1) and prevented more than two independent variables from being tested reliably in a single model. Significant two-way interactions were not recorded between independent variables in most instances; hence, these results, except when specified, are not discussed. If a test revealed nonindependence, unplanned multiple comparisons controlling for experimentwise type I error were used to distinguish differences among frequencies (simultaneous test procedures, STP tests; Sokal and Rohlf, 1981, pp. 728). Two-way contingency tables were used to examine frequencies of injury as a function of limb type and number, right *versus* left side, and missing *versus* regenerating limbs.

Median carapace widths of injured and uninjured animals were compared within sites by nonparametric procedures (Mann-Whitney U-test; Sokal and Rohlf, 1981), because variances for carapace widths were heteroscedastic (F-max test; Sokal and Rohlf, 1981) even after attempts at data transformation.

Results

Population structure

In the Rhode River, sex ratios were consistently male-dominated, but relative frequencies of males and females differed among all years except between 1987 and 1988 (STP test, 3 df; Table II). Annual size-frequency distributions differed among all years in the Rhode River and among all other sites in 1989 (Komolgorov-Smirnov two-sample tests, $P < 0.05$; Tables II, III). Outside the Rhode River, sex ratios were skewed towards females at all sites except South Carolina and the Patuxent River, Maryland (G-test, 5 df, $P < 0.05$; Table III). Collections from the upper-mid Chesapeake Bay were designed to capture females and larger individuals; therefore, these sex and size ratios should not be compared to those from other sites, which were sampled randomly.

Sampling methods

The frequency of autotomy in crabs collected from baited crab pots and seines at the Rhode River head (19%) did not differ from injury levels in otter trawls (22%) at that site in 1989 (G-test, 1 df, $P > 0.05$). No significant differences in injury were observed between otter trawl and fish weir collections from 1986 to 1988 (G-tests, 1 df, $P > 0.05$). At non-Rhode River sites, autotomy frequencies did not differ among crabs collected by otter trawl (Patuxent River, lower-mid Chesapeake Bay) and crab pots and seines (South Carolina, Florida, Alabama) (G-tests, $P > 0.05$).

Autotomy frequencies

Yearly and geographic variation. Frequencies of blue crabs missing or regenerating one or more limbs differed significantly among sites and years sampled (G-tests, P

Table III

Frequencies and percentages of crabs missing, regenerating, and both missing and regenerating limbs at sites in the Chesapeake Bay and along the southeastern United States in 1989

	Chesapeake Bay											
	Upper-Mid[a]		Patuxent R.[b]		Lower-Mid[b]		N. Inlet SC[b]		Indian R. FL[b]		Mobile B. AL[ab]	
Category	n	%	n	%	n	%	n	%	n	%	n	%
Total intact	549	80.9	63	61.2	150	67.0	139	68.1	132	65.7	191	73.5
Total injured:	130	19.1	40	38.8	74	33.0	65	31.9	69	34.3	69	26.5
Missing[1]	85	12.5	24	23.3	53	23.7	33	16.2	37	18.4	25	9.6
Regenerating[2]	39	5.7	11	10.6	17	7.6	27	13.2	32	15.9	40	15.4
Miss. + Regen.[3]	6	0.9	5	4.9	4	1.7	5	2.5	0	0.0	4	1.5
Total caught	679	100.0	103	100.0	224	100.0	204	100.0	201	100.0	260	100.0
Sex ratio M:F	40:60		51:50		26:74		61:39		32:68		37:63	
Size ratio S:M:L[4]	1:25:74		0:12:88		16:9:75		17:17:66		25:5:70		15:28:57	

[1] Missing = crabs with one or more scarred stumps, papillae, or limb buds.
[2] Regenerating = crabs possessing one or more functional but shortened appendages.
[3] Miss. + Regen. = crabs possessing both missing and regenerating limbs.
[4] Size ratio: (S < 61 mm carapace width, M = 61–110 mm CW, L > 110 mm CW) for all crabs (injured and intact).
Sites with the same superscripted letter did not differ significantly in total autotomy frequency.

< 0.01; Tables II, III). In the Rhode River subestuary, limb loss frequency was significantly higher in 1986 (25.0%) than in 1987–89 (STP test, 3 df, $P < 0.01$; Table II). Levels of injury in the latter three years did not differ significantly. The frequency of limb loss from 1986 to 1989 was positively correlated with estimated annual mean densities of crabs based on trawl net collections (Hines *et al.*, 1990) (Pearson's correlation coefficient, $r = 0.99$, $P < 0.05$).

Frequencies of limb loss in the Rhode River in spring (20.9%) and fall (19.1%) 1989 did not differ significantly from the overall frequency (17.8%) for the entire sampling season (May to October). This yearly value is used for comparison with injury levels at non-Rhode River sites in spring and fall 1989. The frequency of limb loss in the Rhode River subestuary in 1989 was identical to that recorded at the nearby upper-mid Chesapeake Bay site, but much lower than autotomy frequencies at two other sites in Chesapeake Bay (STP test, 2 df, $P < 0.01$; Tables II, III). Similarly, the frequency of limb loss in the Rhode River in 1989 was significantly lower than springtime injury levels recorded at sites in South Carolina (31.9%) and Florida (34.3%), but not in Alabama (26.5%) (STP test; 3 df; $P < 0.01$; Tables II, III). The incidence of limb autotomy did not differ significantly among Patuxent River, lower-mid Chesapeake Bay, South Carolina, Florida, or Alabama sites (STP test, 4 df, $P > 0.05$), despite temporal and geographic differences among these samples.

Missing versus *regenerating limbs.* At all sites in the Chesapeake Bay and in two of four years in the Rhode River (1986, 1989), blue crabs were missing limbs more often than they were regenerating them (G-tests, 1 df, $P < 0.05$; Tables II, III). Blue crabs collected from Mobile Bay, Alabama, showed the opposite trend, missing limbs less often than they were regenerating them (G-test, 1 df, $P < 0.05$; Table III). No significant differences in frequencies of individuals missing or regenerating appendages were observed in Indian River, Florida; North Inlet, South Carolina; or the Rhode River, Maryland, in 1987 and 1988. Animals simultaneously missing and regenerating limbs were rare in all years and sites (Tables II, III).

Size and sex. Of all variables measured, body size correlated most often with autotomy frequencies (Figs. 3, 4). In the Rhode River, large animals were missing or regenerating limbs significantly more often than small or medium size individuals for all years except 1988 (Fig. 3). Limb loss frequencies did not differ significantly between small and medium size classes in any year (STP tests, 2 df, Fig. 3). Injury frequencies did not vary significantly among years in the smallest size class, but between-year variation in injury levels was observed in both medium and large size classes (G-tests, 3 df, $P < 0.05$; Fig. 5). Median carapace widths of all injured crabs were significantly larger than those of all intact individuals in each year (Mann-Whitney U-tests, $P < 0.001$). The frequency of autotomy was independent of sex for all years in the

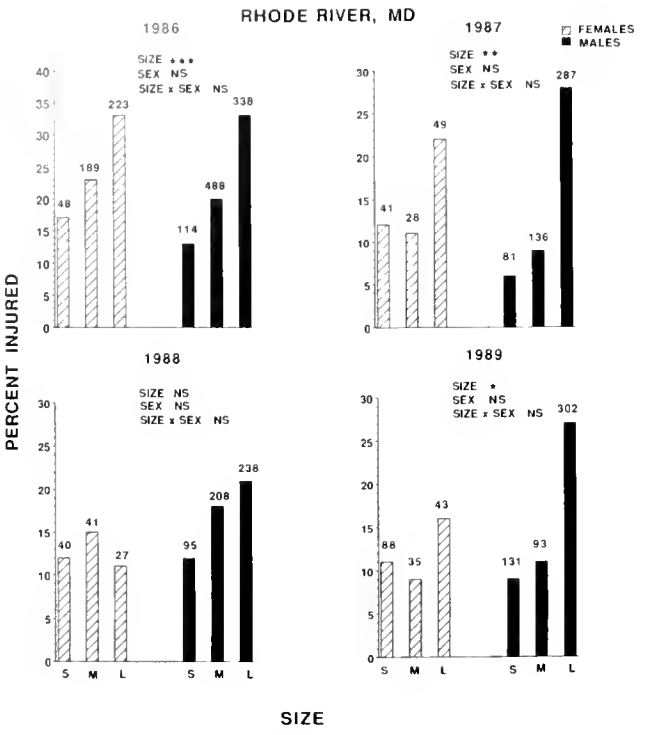

Figure 3. Histograms of the percentage of crabs injured in Rhode River, Maryland, as a function of size and sex for each year (1986–1989). S, M, and L represent small (carapace width < 61 mm), medium (61–110 mm), and large (>110 mm) size classes of crabs, respectively. Sample sizes of total crabs (*i.e.*, injured + uninjured animals) in each category are presented above each bar. Results of logistic model testing for association of size, sex, and the interaction of size and sex with injury frequency are presented for each year. NS, not significant; *, $P < 0.05$; **, $P < 0.01$; ***, $P < 0.001$.

Rhode River and size differences were the same for both sexes (Fig. 3).

Outside the Rhode River, opposite size-related trends in autotomy frequencies were observed at upper-mid Chesapeake Bay and South Carolina sites (Fig. 4). Patterns at the upper-mid Chesapeake Bay site resembled those of the Rhode River, with large animals showing highest incidences of limb loss. In contrast, large crabs showed the least amount of limb loss in North Inlet, South Carolina and males were injured significantly more often than females (STP test, $P < 0.05$). The frequency of injury was independent of size and sex at Patuxent River, lower-mid Chesapeake Bay, Indian River, and Mobile Bay sites (Fig. 4). At non-Rhode River sites, with one exception, median carapace widths of injured and intact crabs did not differ (Mann-Whitney U-tests, $P > 0.05$). At the upper-mid Chesapeake Bay site, patterns again were similar to ones observed in the Rhode River; injured crabs were larger than uninjured animals (Mann-Whitney U-test, $P < 0.002$).

Reproductive maturity. In the Rhode River, limb loss and reproductive maturity were significantly correlated for females in 1986 (male reproductive maturity was not measured) and for both sexes in 1989. In 1986, mature female crabs showed greater frequency of limb loss (34%; n = 132) than juvenile females (25%; n = 312) (G-test, 1 df, $P = 0.05$). In 1989, adults of both sexes (26%; n = 324) suffered higher levels of limb loss than did juveniles (10%; n = 359) (logistic regression, 4 df, $P < 0.001$). No significant differences in injury were observed between juveniles and adults in the Rhode River in 1987 and 1988, or at Chesapeake Bay and southeastern sites with the exception of South Carolina (logistic regression, 4 df, P

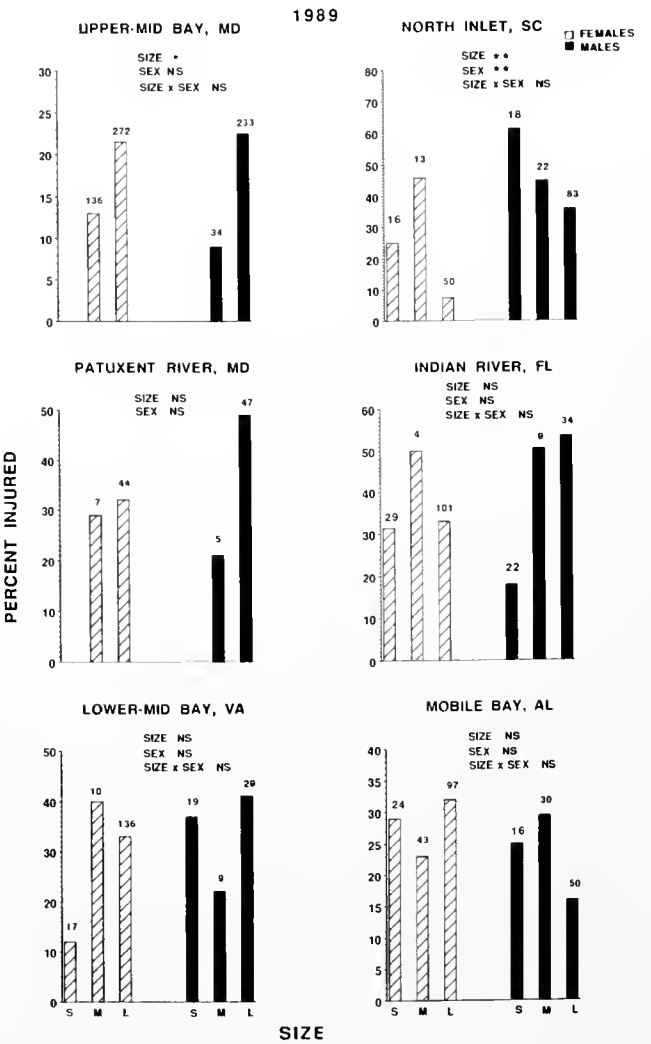

Figure 4. Histograms of the percentage of crabs injured at sites in the Chesapeake Bay, South Carolina, Florida, and Alabama as a function of size and sex in 1989. Size categories and statistical tests are as described in Figure 3. In the Patuxent River site, separate tests were used to compare effects of (1) sex, and (2) size among females. Sample sizes were too low to test for the interaction of size and sex.

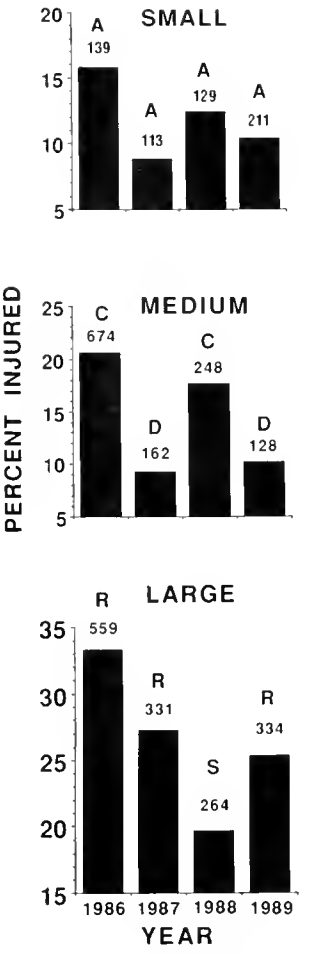

Figure 5. Between-year comparisons of percentages of crabs missing, regenerating, and both missing and regenerating limbs in the Rhode River by size from 1986 to 1989. Years with the same superscripted letter did not differ significantly in total autotomy frequency (STP tests, $P > 0.05$).

< 0.006). At North Inlet, juvenile crabs showed anomalously high levels of limb loss (44%) compared to adults (25%).

Season. The percentage of injury for large crabs and for combined size classes in the Rhode River varied significantly over the season in 1987 and 1989 only (G-tests, $P < 0.05$, Fig. 6). In these years, overall levels of autotomy were high early in the season, declined in mid-summer (July–August), increased in September, and dropped again in October. These late season declines in injury level were due primarily to an influx of smaller, undamaged crabs into the subestuary (Hines *et al.*, 1987a, 1990). Large crabs continued to have high levels of damage in late fall (Fig. 6). No significant seasonal trends in autotomy frequency were observed for small or medium size crabs in any year.

Subestuarine location. No significant differences in limb loss were found among sites within the Rhode River subestuary from 1986 to 1988. In contrast, crabs caught at the river head in 1989 were missing or regenerating limbs more than twice as often (20%) as those caught at the river mouth (9%) (G-test, 1 df, $P < 0.002$).

Molt stage. The frequency of limb loss was independent of molt stage for all years in the Rhode River and at all other sites, except South Carolina, where premolt animals were damaged almost twice as often as intermolt animals (G-test, 2 df, $P < 0.05$).

Patterns of autotomy

Limb number. Single limb loss was the most common form of autotomy for all sites and years (Figs. 7, 8). In

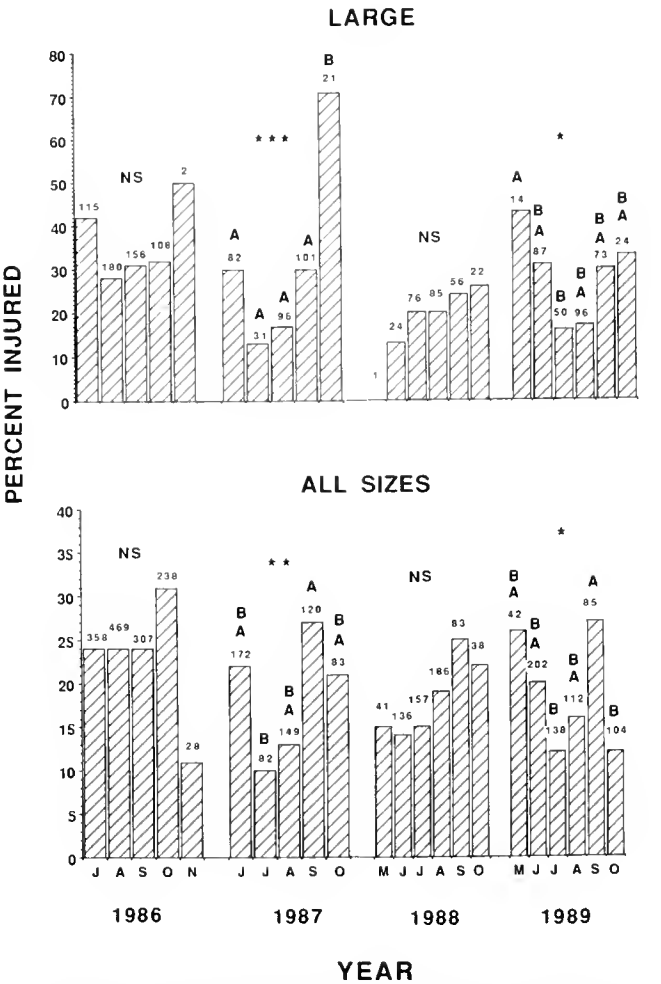

Figure 6. Percentage of crabs injured (*i.e.*, missing or regenerating at least one limb) by month in the Rhode River, Maryland from 1986 to 1989. Large crabs (>110 mm CW) and combined size classes are presented. Sample sizes and results of 2-way contingency tests are presented above each bar. NS = Not significant; *, $P < 0.05$; **, $P < 0.01$, ***, $P < 0.001$. For each year, months with the same letter were not significantly different (STP tests, $P > 0.05$).

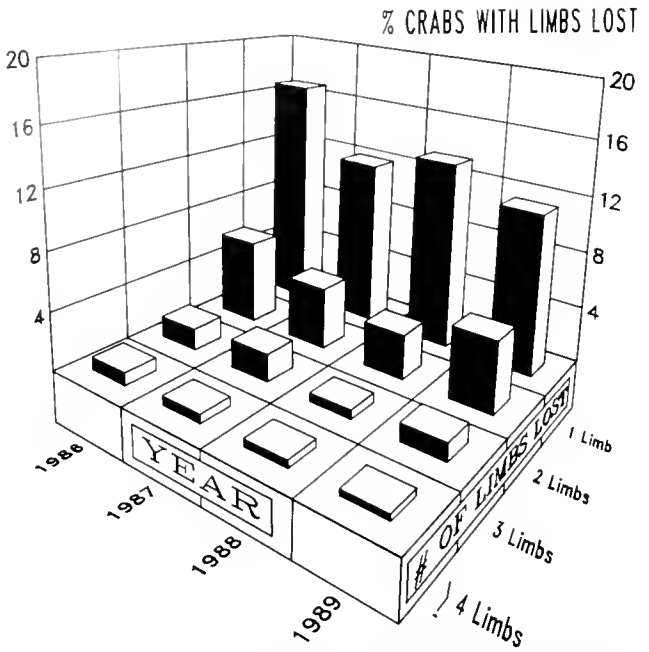

Figure 7. Histogram of the percentage of crabs missing or regenerating 1, 2, 3, or 4 or more limbs in the Rhode River, Maryland, from 1986 to 1989.

the Rhode River, 11–17% of the population were missing or regenerating a single limb, while injury to two appendages occurred less frequently (3–6%). Loss of three or more limbs was observed in less than 2.5% of the population in the Rhode River for any given year (Fig. 7). The maximum number of limbs missing or regenerating on a single crab was six. The mean number of limbs lost ranged from 1.3 to 1.6. The proportion of numbers of limbs (*i.e.*, 1, 2, 3, ≥4) lost among crabs in the Rhode River did not differ among years ($G^2 = 9.0$, 9 df, $P > 0.1$).

The relative numbers of limbs lost also did not differ among blue crabs in Alabama, Florida, upper- or lower-mid Chesapeake Bay (Fig. 8). In North Inlet, South Carolina, single limb loss was proportionately higher than double limb loss when compared to other sites (STP test, $P < 0.05$). In Patuxent River, injury to two limbs (15.5%) occurred nearly as often as single autotomy (19.4%). The proportion of crabs experiencing single *versus* multiple limb loss did not differ significantly with body size at any site (G-tests, 2 df, $P > 0.05$) with the possible exception of the Rhode River in 1986. In that year, only 13% of the injured small crabs were missing or regenerating two or more limbs; medium (33%) and large (36%) crabs showed considerably higher levels of multiple autotomy (G-test, 2 df, $P = 0.06$).

Although comparatively rare, in all years in the Rhode River and at upper- and lower-mid Chesapeake Bay sites, multiple autotomy occurred more often than would be expected based on a binomial distribution in which: (1) the probability of losing any one limb was assumed equal, and (2) limbs were independent with respect to damage (Table IV). In contrast, observed and expected frequencies of single and multiple limb loss did not differ significantly at South Carolina, Florida, and Alabama sites. Observed and expected frequencies of limb loss were marginally non-significant (G-test, 2 df, $P = 0.07$) in the Patuxent River.

Limb type. Chelipeds were the most common limbs lost in all populations (8–33%) (Figs. 9, 10). Few crabs were missing or regenerating the paddle-shaped fifth pereopod (1–5%). Different limb types were not lost with equal frequency at any site or in any year (G-tests, 4 df, $P < 0.02$). The proportions of injured limb types did not differ in the Rhode River among years ($G^2 = 18.3$, 12 df, $P > 0.1$). Damage to chelipeds was disproportionately high at Florida, lower-mid Chesapeake Bay, and Patuxent River sites when compared to other sites (STP tests, 20 df, $P < 0.05$, Fig. 10). With the exception of the South Carolina site and the Rhode River in 1988, there were no differences between the frequencies of right and left limbs lost. At both North Inlet in 1989 and Rhode River in 1988, right limbs were lost more often than left limbs (G-tests, 4 df, $P < 0.05$).

Cheliped morphology. The majority (63–87%) of crabs at all sites and in all years possessed a right crusher cheliped

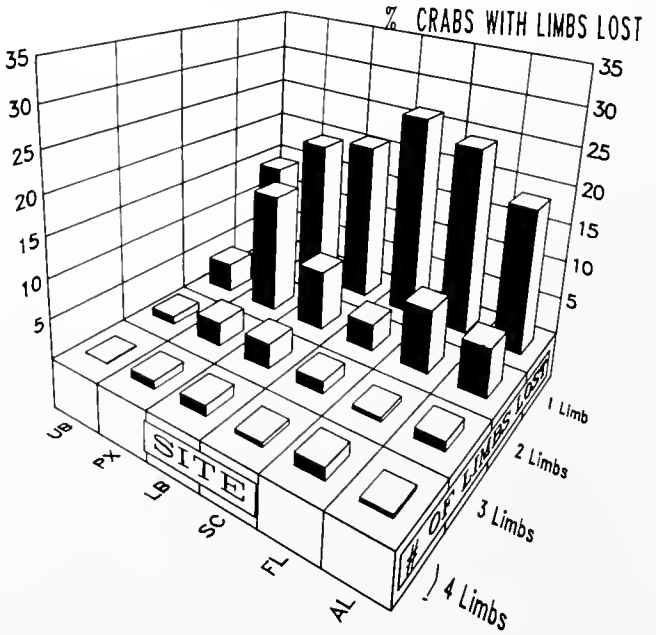

Figure 8. Histogram of the percentage of crabs missing or regenerating 1, 2, 3, or 4 or more limbs in the upper-mid Chesapeake Bay (UB); Patuxent River, Maryland (PX); lower-mid Chesapeake Bay (LB); North Inlet, South Carolina (SC); Indian River, Florida (FL); and Mobile Bay, Alabama (AL) in 1989.

Table IV

Comparisons of expected versus observed frequencies of intact crabs and those missing or regenerating 1, 2, 3, or 4 or more limbs in the Rhode River, Maryland from 1986 to 1989

	Rhode River, Maryland							
	1986		1987		1988		1989	
Injury status	Obs.	Exp.	Obs.	Exp.	Obs.	Exp.	Obs.	Exp.
Intact	1050	960	505	463	536	514	569	528
−1 Limb	234	369	75	138	86	122	78	145
−2 Limbs	83	64	26	18	20	13	34	18
−3 Limbs	21	6	12	2	4	1	8	1
− ≥4 Limbs	12	0.5	4	0.7	3	0.4	3	0.1
G-test	$P < 0.001$		$P < 0.001$		$P < 0.005$		$P < 0.001$	

Expected frequencies were generated from a binomial distribution in which the probability of loss of each of 10 limbs was the same. Limbs were assumed to be lost independently. The probability of losing any one limb = # limbs lost in the population/(10 × # crabs in the population). The final two categories (−3 and −4 or more limbs) were pooled for analysis. (G-tests, 2 df).

and a left cutter cheliped (Table V). The frequency of crabs with a right crusher/left cutter did not differ among years in the Rhode River. Frequencies of crabs with right crusher/left cutter morphology in the upper-mid Chesapeake Bay and Rhode River in 1989, however, were significantly higher than those from other sites in that year. Crabs with two cutters were relatively common (7–21%); whereas, left crusher/right cutter morphological patterns were observed less frequently (0.6–10%). Crabs possessing double crushers were extremely rare (≤1%).

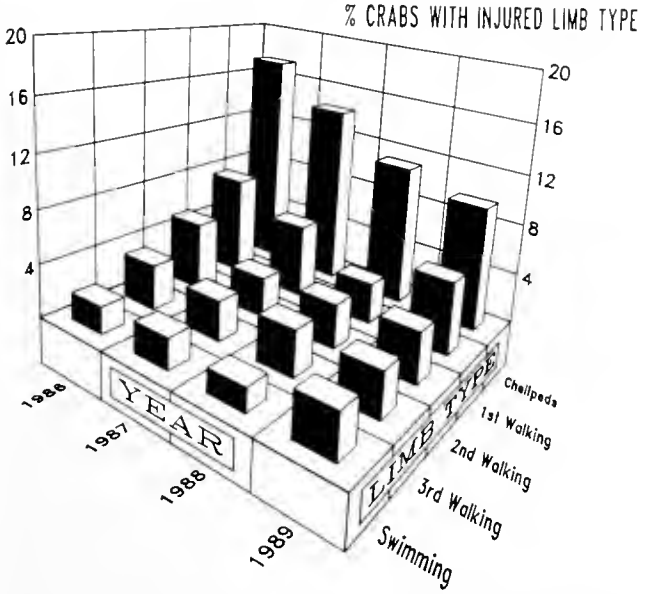

Figure 9. Histogram of the percentage of crabs missing or regenerating one or both chelipeds, 1st, 2nd, and 3rd walking legs and swimming legs in the Rhode River, Maryland, from 1986 to 1989.

Frequencies of crabs bearing right crusher/left cutter morphologies decreased as size increased in the Rhode River in all years (Fig. 11). The frequency of female crabs bearing a right crusher/left cutter was greater than males in three of four years ($P = 0.06$). Sex differences in the frequency of crusher/cutter patterns were generally consistent across size classes (but see 1986, size × sex interaction).

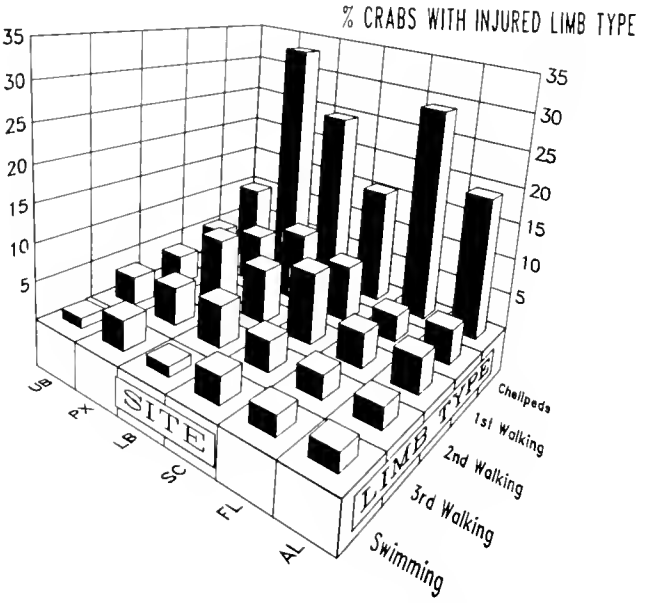

Figure 10. Histogram of the percentage of crabs missing or regenerating one or both chelipeds, 1st, 2nd, and 3rd walking legs and swimming legs in the upper-mid Chesapeake Bay (UB); Patuxent River, Maryland (PX); lower-mid Chesapeake Bay (LB); North Inlet, South Carolina (SC); Indian River, Florida (FL); and Mobile Bay, Alabama (AL) in 1989.

Table V

Frequencies and percentages of crusher and cutter cheliped morphologies from blue crabs collected in the Rhode River (1986-1989), and in the upper-mid Chesapeake Bay; Patuxent River; lower-mid Chesapeake Bay; North Inlet, SC; Indian River, FL, and Mobile Bay, AL in 1989

	Morphological Patterns of Crab Chelipeds				
Site & Year	Right crusher left cutter	Left crusher right cutter	Double cutters	Double crushers	Other
Rhode R. 86	1109 (79%)*	61 (4%)	148 (11%)	1 (.1%)	81 (6%)
Rhode R. 87	509 (82%)*	18 (3%)	68 (11%)	0 (0%)	27 (4%)
Rhode R. 88	537 (83%)*	4 (.6%)	88 (14%)	0 (0%)	20 (3%)
Rhode R. 89	576 (83%)* a	4 (.6%)	93 (13%)	0 (0%)	19 (3%)
Upper-Mid CB 89	593 (87%) a	20 (3%)	44 (7%)	2 (.3%)	20 (3%)
Patuxent R. 89	71 (69%) b	3 (3%)	12 (12%)	1 (1%)	16 (16%)
Lower-Mid CB 89	163 (73%) b	11 (5%)	21 (9%)	2 (1%)	27 (12%)
N. Inlet, SC 89	129 (63%) b	20 (10%)	42 (21%)	1 (.5%)	12 (6%)
Indian R., FL 89	146 (73%) b	11 (6%)	20 (10%)	1 (.5%)	23 (11%)
Mobile B., AL 89	192 (74%) b	20 (8%)	37 (14%)	2 (.8%)	9 (4%)

The category "other" included crabs missing one cheliped and possessing one cutter or crabs missing both chelipeds. Comparisons of frequency of crabs with a right crusher/left cutter for 4 years in the Rhode River (STP test, 3 df) and among all 1989 sites (STP test, 6 df) are presented. Sites with the same symbol or letter (to denote separate tests) are not significantly different ($P > 0.05$).

The relationship of size and sex to cheliped morphology was less consistent at sites outside the Rhode River. The frequency of crabs possessing a right crusher/left cutter did not vary significantly with size or sex at any Chesapeake Bay site or in Mobile Bay. Low sample sizes in the Patuxent River prevented testing the interaction between size and sex. Size differences were recorded in North Inlet and Indian River (G-tests; $P < 0.05$). At North Inlet, large males (47%; n = 84) possessed fewest right crushers. Regardless of size, *ca.* 69% of female blue crabs (n = 82) possessed a right crusher and left cutter. In Indian River, Florida, the incidence of right crusher/left cutters was lower in large individuals of both sexes when compared to small size classes.

Discussion

Causal agents

High frequencies of limb loss recorded over broad temporal and geographic scales indicate that autotomy is an important mechanism for survival in *Callinectes sapidus*. Eighteen to 25% of blue crabs surveyed over a four year period in the Rhode River, Maryland, and 19–39% of blue crabs at six other sites along the eastern coast of the United States in 1989 were missing or regenerating one or more limbs. Autotomy is an effective escape response to predators (Robinson *et al.*, 1970; Congdon *et al.*, 1974; Medel *et al.*, 1988; Smith, 1990a). Variation in injury levels in populations may indicate differential predation pressure (*e.g.*, Shaffer, 1978; Ballinger, 1979; Schall and Pianka, 1980; McCallum *et al.*, 1989) or predator efficiency (Schoener, 1979; Schoener and Schoener, 1980; Jaksic and Fuentes, 1980). In the Rhode River, significantly higher levels of limb loss were recorded in blue crabs in 1986 (25%) than in three subsequent years (18–19%). If partial predation is responsible for autotomy (Smith, 1990a), then these differences indicate either increased predation pressure, decreased predator efficiency, or both during 1986.

Several lines of evidence indicate that unsuccessful predation by conspecifics may be the principal source of nonlethal injury in blue crabs in the Rhode River. Based on trawl catches (Hines *et al.*, 1987a, 1990), the Rhode River subestuary lacks abundant fish predators or decapod species capable of capturing and killing medium-to-large, hard-shelled blue crabs. American eel (*Anguilla rostrata*) and oyster toadfish (*Opsanus tau*), both known predators of small blue crabs (Wenner and Musick, 1975; Wilson *et al.*, 1987), occur in very low densities in the subestuary (Hines *et al.*, 1990). Gut analysis (Laughlin, 1982; Hines *et al.*, 1990) and experimental work (Peery, 1989; Smith, 1990a) have shown that cannibalism is an important cause of mortality in blue crabs. A long-term study in Chesapeake Bay (Lipcius and Van Engel, 1990) suggested density-dependent regulation of blue crab populations by conspecifics. Increased encounter rates between conspecifics during years of high abundance should lead to increased levels of both lethal and nonlethal injury. In the present survey, the frequency of limb loss was positively correlated with annual blue crab abundances (correlation coefficient, r = 0.99) in the Rhode River. Mean abundances of crabs in the Rhode River between 1987 and

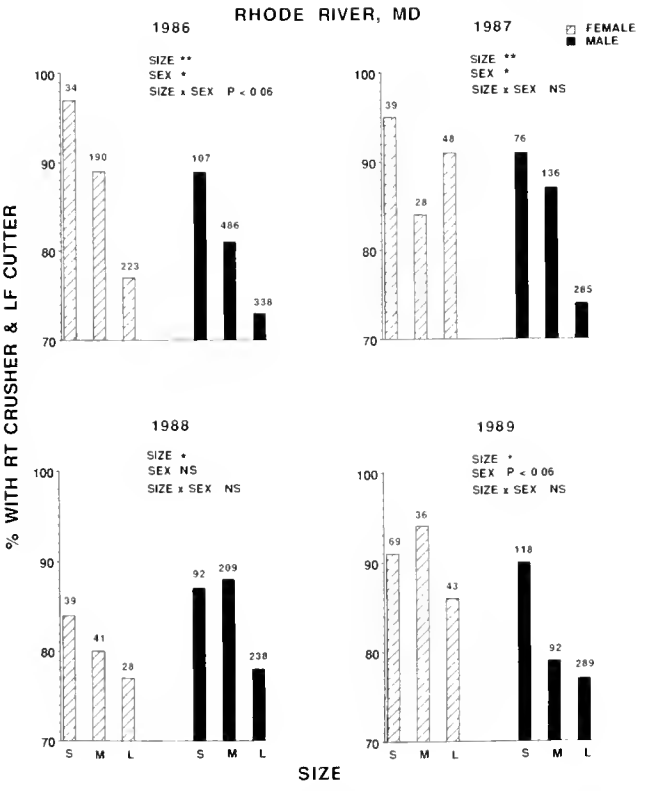

Figure 11. Histograms of the percentage of crabs possessing a right crusher and left cutter in the Rhode River, Maryland, as a function of size and sex for each year (1986–89). S, M, and L represent small (carapace width < 61 mm), medium (61–110 mm), and large (>110 mm) size classes of crabs, respectively. Sample sizes of total crabs (*i.e.*, animals with and without right crusher-left cutter combinations) in each category are presented above each bar. Results of logistic model testing for the association of size, sex, and their interaction with the frequency of crabs bearing a right crusher-left cutter combination are presented for each year. NS, not significant; *, $P < 0.05$; **, $P < 0.01$; ***, $P < 0.001$.

1989 (4–6 crabs/m^2) were significantly lower than in any of the five previous years surveyed (Hines *et al.*, 1990). Injury levels in the Rhode River between 1987 and 1989 remained remarkably constant, which suggests temporal coupling between injury-causing agents and victims.

Factors besides partial predation (*e.g.*, intraspecific competition, fisheries) could contribute to observed autotomy frequencies, but these sources are probably minor. In most brachyuran crabs, intraspecific competitive interactions are highly ritualized and do not usually result in limb autotomy (Hazlett, 1972; Jachowski, 1974; Hyatt and Salmon, 1978). In *Callinectes sapidus*, instances of limb loss were rare when size-matched males competed for a sexually receptive female in small arenas (<1%; Smith, 1990a). Limb autotomy can occur during ecdysis in blue crabs, but such instances were observed infrequently (Smith, pers. obs.). Handling by fisheries also could contribute to injury in certain size classes (*e.g.*, Kennelly *et al.*, 1990). Larger sublegal-size blue crabs (CW < 127 mm) may experience limb loss before being culled. Smaller crabs generally escape uninjured through the mesh of crab pots (Smith, pers. obs.), while larger, legal-sized crabs are harvested.

Autotomy frequencies were not biased by the various gear used to sample blue crabs. Severely injured (and potentially less mobile) animals should not have been underrepresented in collections, because active (otter trawls, seines) as well as passive (fish weir, crab pots) methods of capture were used. By using a variety of collection methods, a range of depths and habitats in the subestuary were sampled.

Size effects

Positive correlations between autotomy frequency and blue crab body size indicate ontogenetic differences in both repair rates and susceptibility to predation. The average percentage of injury in medium- and small-size crabs for four years in the Rhode River was 37% and 58% that of large crabs, respectively. Similar size-related trends have been observed in a shore crab, *Carcinus maenas* (McVean, 1976; McVean and Findlay, 1979; Sekkelsten, 1988). Predator inefficiency often increases with increased prey size (Murtaugh, 1981; Vermeij, 1982; Reaka, 1987; Peery, 1989), and tethering experiments (Smith, 1990a) have demonstrated that larger blue crabs suffered appendage loss proportionately more often than mortality compared to smaller crabs. In the present survey, median carapace widths of injured crabs in the Rhode River were greater than those of uninjured individuals. Evidence of limb loss will also remain for longer periods in large than small animals. Limb regeneration requires molting, and blue crab molting frequency declines as size increases (Leffler, 1972; Smith, 1990b). In St. Johns River, Florida, the average length of the molt interval (*ca.* 40 days) for large (>110 mm CW) crabs was 2.5 times that of small crabs (16 days; 20–59 mm CW) and 1.5 times that of medium crabs (27 days; 60–110 mm CW) (Tagatz, 1968; see also Smith, 1990b). Based on these molt intervals, estimated daily injury rates for crabs in a given size class (*i.e.*, % injury/molt interval) over four years in the Rhode River were similar (*ca.* 0.74%/day for small crabs, 0.64%/day for medium crabs, and 0.69%/day for large crabs). Although small crabs are more vulnerable to fatal attack from predators than medium or large crabs (Smith, 1990a), they will regenerate missing limbs more quickly after nonlethal injury. In female blue crabs, molting ceases when sexual maturity is reached (Millikin and Williams, 1984), so subsequent injuries accumulate.

Temporal variation

The lack of significant monthly variation in injury for small- and medium-size blue crabs within years in Rhode

River indicates that predator efficiency remained seasonally consistent for both size classes. Significant between-year differences among medium-size crabs, however, suggests that as annual predation levels change, medium-size animals may experience greater variability in survival than smaller animals. Injury levels in large crabs exhibited both significant within- and between-year variability. Higher frequencies of limb loss in the large size class late in the season (September-October) could have resulted from a combination of factors: (1) slower repair rates as average sizes increased over the summer; (2) decreasing molting frequency as water temperature declined (Leffler, 1972); and (3) increased levels of cannibalism as bivalve prey (*e.g., Mya arenaria, Macoma balthica*) became scarce (Hines *et al.,* 1990). High frequencies of limb loss seen at the beginning of each season may be a carryover from the previous fall. Because molt frequency declines over winter, regeneration is delayed.

Sex

Male and female blue crabs, regardless of stage of sexual maturity, appeared equally vulnerable to injury in the Rhode River. This is consistent with observations in *Carcinus maenas* (McVean and Findlay, 1979) and *Cancer magister* (Shirley and Shirley, 1988). Given that adult male blue crabs continue to molt, it is surprising that injury frequencies in mature females were not proportionately higher. It is possible that: (1) large adult males are molting so infrequently that they rarely restore limb symmetry; (2) behavioral differences are making mature females less prone to injury (but see Smith, 1990a); or (3) females are migrating to spawning areas in southern Chesapeake Bay, so their injuries are not observed in the Rhode River.

Spatial variation

Injury frequencies did not vary spatially within the Rhode River subestuary in three of four years. Hines *et al.* (1987a) have shown that blue crabs enter the Rhode River each spring and fall where they grow to maturity. Male crabs forage throughout the subestuary and use Muddy Creek as a molting habitat. These movement patterns may explain why observed injury levels are homogeneous across sites.

Significant differences among autotomy frequencies in the Rhode River region, other sites in the Chesapeake Bay, and southeastern United States indicate that these regions differ in the type, degree, or efficiency of injury-causing agents. Injury levels recorded in the Rhode River and upper-mid Chesapeake Bay in 1989 were markedly lower than at any other site (except Alabama) for that year. Higher frequencies of limb loss and regeneration outside the Rhode River cannot be attributed to differences in sex ratio or size distributions among sites, because the elevated injury levels were maintained for most categories of size and sex. The relatively low salinities and shallow depths found in the Rhode River may limit the abundances and diversity of predators so that the subestuary serves as a refuge. Qualitative observations of trawl catches at the Patuxent River, lower-mid Chesapeake Bay, and Alabama sites showed higher diversity and abundances of large, known crab predators (*e.g.,* striped bass, *Morone saxatilis;* oyster toadfish, *Opsanus tau;* white catfish, *Ictalurus catus,* Millikin and Williams, 1984) than were found in the Rhode River (Hines *et al.,* 1990).

Surprisingly, no significant differences in injury frequency existed among populations from the Patuxent River, Maryland south to Mobile Bay, Alabama, even though these populations spanned two biogeographic provinces (cold-temperate North Atlantic and warm-temperate Northwest Atlantic; Vermeij, 1978), were sampled in different seasons, and were subjected to different suites of predators. These data contrast with studies showing increased predation pressure at lower latitudes (Bertness *et al.,* 1981; Vermeij *et al.,* 1980; Heck and Wilson, 1987).

Patterns of autotomy

The consistency of limb loss pattern observed in this study is probably due to limb function and the behavioral response to the injury-causing agent. Chelipeds were lost most often, followed by first walking legs. Similar patterns have been observed in other brachyuran crabs (*e.g., Carcinus maenas,* McVean, 1976; McVean and Findlay, 1979; *Cancer magister,* Durkin *et al.,* 1984; Shirley and Shirley, 1988). Crabs respond to threats from predators or competitors with outstretched claws (Schone, 1968; Robinson *et al.,* 1970; Jachowski, 1974; Vannini, 1980) making anterior limbs particularly vulnerable to injury. Strikes from behind may often prove fatal, so fewer crabs will be found missing swimming legs. Additionally, the autotomy response in swimming legs is greatly reduced in larger crabs; even severe damage to these limbs often would not result in autotomy (Smith, pers. obs.). Small and medium-sized crabs, however, autotomize all limb types readily. Escape responses by blue crabs showed no consistent directionality (Smith, 1990a), and the symmetry of limb loss suggests that the injury-causing agent is striking randomly. Similarity in injury frequency between right and left sides has also been observed in Dungeness crabs, *Cancer magister* (Durkin *et al.,* 1984).

Multiple autotomies could be caused either by single events damaging more than one leg or by cumulative damage from independent events. While single limb loss

was most common at all sites and in all years in *Callinectes sapidus* (also in *Carcinus maenas*, McVean and Findlay, 1979; *Cancer magister*, Shirley and Shirley, 1988), multiple limb loss was more frequent than chance predicts. McVean (1976) interpreted a similar pattern in *C. maenas* to indicate that injured animals are more susceptible to attack than intact individuals. Tethering studies in *C. sapidus* suggest that multiple limb loss occurs in a single attack event (Smith, 1990a). The percentage of animals simultaneously missing and regenerating limbs was rare (*ca.* 1%) in all years in the Rhode River, indicating that previous limb loss, in most instances, does not make an animal more vulnerable to future attacks.

Cheliped regeneration

Substantial percentages of regenerating chelipeds were observed in all populations, which suggests that, despite their importance (*e.g.*, defense, foraging), crabs could compensate temporarily for their loss. In many crustacean taxa, loss of the major claw results in the transformation of the opposing minor claw into a major claw over several molts (Hamilton *et al.*, 1976). The autotomized limb is simultaneously replaced by a minor claw. In blue crabs, transformation can be incomplete even after three molts (Smith, 1990b); consequently, those crabs losing a right crusher claw bear symmetrical, double cutters following regeneration. Presence of a left crusher/right cutter, double cutters, or double crushers is evidence of previous limb loss. In the Rhode River, frequencies of animals bearing a right crusher/left cutter generally declined as size increased. Up to 25% of large crabs (*e.g.*, 1986; Fig. 11) showed evidence of having lost a right crusher during their lifetime, which suggests that survival following loss of a right crusher was high. Frequencies of these atypical claw morphologies were even higher in South Carolina (32%) and Florida (35%). Interestingly, the percentage of male crabs bearing a right crusher and left cutter was lower than in females in three out of four years in the Rhode River, which suggests that males were suffering greater incidence of cheliped injury during their lifetime.

Conclusions

By examining the frequency of injury over both temporal and geographic scales, our study provides the most complete analysis to date on autotomy in any species. The magnitude of this data set allows inferences about causal agents of autotomy and about the impact of autotomy on blue crab survival following attack. Four years of autotomy data in the Rhode River, Maryland, provide evidence that: (1) the frequency of nonlethal injury in the population is positively correlated with density and is probably due to unsuccessful conspecific predation; (2) the rate of autotomy is similar over the lifespan of the individual, but differences in molting rate and predator efficiency result in higher injury levels in larger animals; (3) chances of survival subsequent to single or double limb loss are good; and (4) lower frequencies of autotomy in the Rhode River compared to other sites indicate geographic differences in the intensity or efficiency of injury-causing agents. The high incidence of limb loss in all age groups, and in both sexes over broad temporal and geographic scales, indicates that autotomy is an important adaptation for avoiding predation.

Acknowledgments

We wish to thank the many individuals who have assisted us in this study. We extend our sincere appreciation to Dr. D. Allen, J. Dimitry, J. Dindo, A. Fanning, P. Geer, M. Haddon, J. Harding, L. Johnson, W. Lee, D. Lello, Dr. S. Morgan, D. Palmer, H. Reichardt, Dr. M. Rice, R. Speers, G. Tritaik, and L. Wiechert, for their assistance in collecting and measuring animals; and Dr. E. Russek-Cohen for her statistical advice. This manuscript has benefited from critical comments by Dr. J. Dineen, D. Lello, Dr. M. Raupp, Dr. M. Reaka, Dr. G. Vermeij, and two anonymous reviewers. We are grateful to them all. The project has been supported by the Lerner-Gray Fund; Sigma Xi Grants-in-Aid of Research, the Department of Zoology's Chesapeake Bay Fund at the University of Maryland, and a Smithsonian Predoctoral Fellowship, all to L. D. Smith, and grants to A. H. Hines from the Smithsonian Environmental Sciences Program, Smithsonian Scholarly Studies Program, and the National Science Foundation OCE-8700414. This paper was submitted in partial fulfillment of a Doctor of Philosophy at the University of Maryland.

Literature Cited

Ballinger, R. E. 1979. Intraspecific variation in demography and life history of the lizard, *Sceloporus jarrovi*, along an altitudinal gradient in southeastern Arizona. *Ecology* **60:** 901–909.

Bennett, D. B. 1973. The effect of limb loss and regeneration on the growth of the edible crab, *Cancer pagurus* L. *J. Exp. Mar. Biol. Ecol.* **13:** 45–53.

Bertness, M. D., S. D. Garrity, and S. C. Levings. 1981. Predation pressure and gastropod foraging: a tropical-temperate comparison. *Evolution* **35:** 995–1007.

Berzins, I. K., and R. L. Caldwell. 1983. The effect of injury on the agonistic behavior of the stomatopod, *Gonodactylus bredini* (Manning). *Mar. Behav. Physiol.* **10:** 83–96.

Congdon, J. D., L. J. Vitt, and W. W. King. 1974. Geckos: adaptive significance and energetics of tail autotomy. *Science* **184:** 1379–1380.

Conover, M. R., and D. E. Miller. 1978. The importance of the large chela in the territorial and pairing behaviour of the snapping shrimp, *Alpheus heterochaelis*. *Mar. Behav. Physiol.* **5:** 185–192.

Cox, D. R. 1970. *Analysis of Binary Data.* Metheun, London. 142 pp.

Dial, B. E., and L. C. Fitzpatrick. 1983. Lizard tail autotomy: function and energetics of postautotomy tail movement in *Scincella lateralis*. *Science* **219**: 391–393.

Dial, B. E., and L. C. Fitzpatrick. 1984. Predator escape success in tailed *versus* tailless *Scincella lateralis* (Sauria:Scincidae). *Anim. Behav.* **32**: 301–302.

Durkin, J. T., K. D. Buchanan, and T. H. Blahm. 1984. Dungeness crab leg loss in the Columbia River estuary. *Mar. Fish. Rev.* **46**: 22–24.

Edwards, J. S. 1972. Limb loss and regeneration in two crabs: the king crab *Paralithodes camtschatica* and the tanner crab *Chionoecetes bairdi*. *Acta Zool.* **53**: 105–112.

Fox, L. R. 1975. Cannibalism in natural populations. *Ann. Rev. Ecol. Syst.* **6**: 87–106.

Hamilton, P. V. 1976. Cheliped laterality in *Callinectes sapidus* (Crustacea: Portunidae). *Biol. Bull.* **150**: 393–401.

Harris, R. N. 1989. Nonlethal injury to organisms as a mechanism of population regulation. *Am. Nat.* **134**: 835–847.

Hazlett, B. A. 1972. Responses to agonistic postures by the spider crab *Microphrys bicornutus*. *Mar. Behav. Physiol.* **1**: 85–92.

Heck, K. L., Jr., and K. A. Wilson. 1987. Predation rates on decapod crustaceans in latitudinally separated seagrass communities: a study of spatial and temporal variation using tethering techniques. *J. Exp. Mar. Biol. Ecol.* **107**: 87–100.

Hines, A. H., R. N. Lipcius, and A. M. Haddon. 1987a. Population dynamics and habitat partitioning by size, sex, and molt stage of blue crabs *Callinectes sapidus* in a subestuary of central Chesapeake Bay. *Mar. Ecol. Prog. Ser.* **36**: 55–64.

Hines, A. H., P. J. Haddon, J. J. Miklas, L. A. Wiechert, and A. M. Haddon. 1987b. Estuarine invertebrates and fish: sampling design and constraints for long-term measurements of population dynamics. Pp. 140–164 in *New Approaches to Monitoring Aquatic Ecosystems, ASTM STP 940*, T. P. Boyle, ed. American Society for Testing and Materials, Philadelphia.

Hines, A. H., A. M. Haddon, and L. A. Wiechert. 1990. Guild structure and foraging impact of blue crabs and epibenthic fish in a subestuary of Chesapeake Bay. *Mar. Ecol. Prog. Ser.* **67**: 105–126.

Hyatt, G. W., and M. Salmon. 1978. Combat in the fiddler crabs *Uca pugilator* and *U. pugnax*: a quantitative analysis. *Behaviour* **65**: 182–211.

Jachowski, R. L. 1974. Agonistic behaviour of the blue crab, *Callinectes sapidus* Rathbun. *Behaviour* **50**: 232–253.

Jaeger, R. G. 1981. Dear enemy recognition and the costs of aggression between salamanders. *Am. Nat.* **117**: 962–974.

Jaksic, F. M., and E. R. Fuentes. 1980. Correlates of tail losses in twelve species of *Liolaemus* lizards. *J. Herpetol.* **14**: 137–141.

Johnson, P. T. 1980. *Histology of the Blue Crab,* Callinectes sapidus. *A Model for the Decapoda.* Praeger Sci. Publ. Co., New York. 440 pp.

Kennelly, S. J., D. Watkins, and J. R. Craig. 1990. Mortality of discarded spanner crabs *Ranina ranina* (Linnaeus) in a tangle-net fishery—laboratory and field experiments. *J. Exp. Mar. Biol. Ecol.* **140**: 39–48.

Kuris, A. M., and M. Mager. 1975. Effect of limb regeneration on size increase at molt of the shore crabs *Hemigrapsus oregonensis* and *Pachygrapsus crassipes*. *J. Exp. Zool.* **193**: 353–360.

Kurihara, Y., and K. Okamoto. 1987. Cannibalism in a grapsid crab, *Hemigrapsus penicillatus*. *Mar. Ecol. Prog. Ser.* **41**: 123–127.

Laughlin, R. A. 1982. Feeding habits of the blue crab, *Callinectes sapidus* Rathbun, in the Apalachicola estuary, Florida. *Bull. Mar. Sci.* **32**: 807–822.

Leffler, C. W. 1972. Some effects of temperature on the growth and metabolic rate of juvenile blue crabs, *Callinectes sapidus*, in the laboratory. *Mar. Ecol. Prog. Ser.* **41**: 123–127.

Lipcius, R. N., and W. A. Van Engel. 1990. Blue crab population dynamics in Chesapeake Bay: variation in abundance (York River, 1972–1989) and stock-recruit functions. *Bull. Mar. Sci.* **46**: 180–194.

Maiorana, V. C. 1977. Tail autotomy, functional conflicts and their resolution by a salamander. *Nature* **265**: 533–535.

McCallum, H. I., R. Endean, and A. M. Cameron. 1989. Sublethal damage to *Acanthaster planci* as an index of predation pressure. *Mar. Ecol. Prog. Ser.* **56**: 29–36.

McVean, A. 1976. The incidence of autotomy in *Carcinus maenus* (L.). *J. Exp. Mar. Biol. Ecol.* **24**: 177–187.

McVean, A. 1982. Autotomy. Pp. 107–132 in *The Biology of Crustacea*, Vol. 4, D. E. Bliss, ed. Academic Press, Inc., New York.

McVean, A., and I. Findlay. 1979. The incidence of autotomy in an estuarine population of the crab *Carcinus maenas*. *J. Mar. Biol. Assoc. U.K.* **59**: 341–354.

Medel, R. G., J. E. Jimenez, S. F. Fox, and F. M. Jaksic. 1988. Experimental evidence that high population frequencies of lizard tail autotomy indicate inefficient predation. *Oikos* **53**: 321–324.

Millikin, M. R., and A. B. Williams. 1984. Synopsis of biological data on the blue crab, *Callinectes sapidus* Rathbun. *NOAA Technical Report NMFS 1. FAO Fisheries Synopsis* No. 138.

Murtaugh, P. A. 1981. Inferring properties of mysid predation from injuries to *Daphnia*. *Limnol. Oceanogr.* **26**: 811–821.

Needham, A. E. 1953. The incidence and adaptive value of autotomy and of regeneration in Crustacea. *Proc. Zool. Soc. London* **123**: 111–122.

Peery, C. A. 1989. Cannibalism experiments with the blue crab (*Callinectes sapidus* Rathbun): potential effects of size and abundance. Master's thesis. College of William and Mary, Williamsburg, Virginia.

Polis, G. A. 1981. The evolution and dynamics of intraspecific predation. *Ann. Rev. Ecol. Syst.* **12**: 225–251.

Reaka, M. L. 1987. Adult-juvenile interactions in benthic reef crustaceans. *Bull. Mar. Sci.* **41**: 108–134.

Robinson, M. H., L. G. Abele, and B. Robinson. 1970. Attack autotomy: a defense against predators. *Science* **169**: 300–301.

SAS Institute. 1985. *SAS User's Guide: Statistics.* Version 5 Edition. SAS Institute Inc., Cary, North Carolina. 956 pp.

Schall, J. J., and E. R. Pianka. 1980. Evolution of escape behavior diversity. *Am. Nat.* **155**: 551–566.

Schoener, T. W. 1979. Inferring the properties of predation and other injury-producing agents from injury frequencies. *Ecology* **60**: 1110–1115.

Schoener, T. W., and A. Schoener. 1980. Ecological and demographic correlates of injury rates in some Bahamian *Anolis* lizards. *Copeia* **1980**: 839–850.

Schone, H. 1968. Agonistic and sexual display in aquatic and semiterrestrial brachyuran crabs. *Am. Zool.* **8**: 641–654.

Sekkelsten, G. I. 1988. Effect of handicap on mating success in male shore crabs *Carcinus maenas*. *Oikos* **51**: 131–134.

Shaffer, H. B. 1978. Relative predation pressure on salamanders (Caudata:Plethodontidae) along an altitudinal transect in Guatemala. *Copeia* **1978**: 268–272.

Shirley, S. M., and T. C. Shirley. 1988. Appendage injury in dungeness crabs, *Cancer magister* in southeastern Alaska. *Fish. Bull.* **86**: 156–160.

Simonson, J. L. 1985. Reversal of handedness, growth, and claw stridulatory patterns in the stone crab *Menippe mercenaria* (Say) (Crustacea:Xanthidae). *J. Crust. Biol.* **5**: 281–293.

Simonson, J. L., and P. Steele. 1981. Cheliped asymmetry in the stone crab, *Menippe mercenaria*, with notes on claw reversal and regeneration. *Northeast Gulf Sci.* **5**: 21–30.

Slater, A., and J. M. Lawrence. 1980. The effect of arm loss on feeding and growth rates in *Lytechinus variegatus*. *Fla. Sci.* **43**: 16.

Smith, L. D. 1990a. The frequency and ecological consequences of limb autotomy in the blue crab, *Callinectes sapidus* Rathbun. Ph.D. Dissertation. University of Maryland, College Park. 259 pp.

Smith, L. D. 1990b. Patterns of limb loss in the blue crab, *Callinectes sapidus* Rathbun, and the effects of autotomy on growth. *Bull. Mar. Sci.* **46**: 23–36.

Sokal, R. R., and F. J. Rohlf. 1981. *Biometry*. W. H. Freeman, New York. 859 pp.

Stevens, B. G., D. A. Armstrong, and R. Cusimano. 1982. Feeding habits of the Dungeness crab *Cancer magister* as determined by the index of relative importance. *Mar. Biol.* **72**: 135–145.

Sullivan, J. R. 1979. The stone crab, *Menippe mercenaria*, in the southwest Florida fishery. *Fl. Mar. Res. Publ. No. 36*

Tagatz, M. E. 1968. Growth of juvenile blue crabs, *Callinectes sapidus* Rathbun, in the St. Johns River, Florida. *Fish. Bull.* **67**: 281–288.

Van Engel, W. A. 1958. The blue crab and its fishery in the Chesapeake Bay. Part 1—Reproduction, early development, growth and migration. *Commer. Fish. Rev.* **20**: 6–17.

Van Engel, W. A. 1990. Development of the reproductively functional form in the male blue crab, *Callinectes sapidus*. *Bull. Mar. Sci.* **46**: 13–22.

Vannini, M. 1980. Notes on the behaviour of *Ocypode ryderi* Kingsley (Crustacea, Brachyura). *Mar. Behav. Physiol.* **7**: 171–183.

Vermeij, G. J. 1976. Interoceanic differences in vulnerability of shelled prey to crab predation. *Nature* **260**: 135–136.

Vermeij, G. J. 1977. The Mesozoic marine revolution: evidence from snails, predators and grazers. *Paleobiology* **3**: 243–258.

Vermeij, G. J. 1978. *Biogeography and Adaptation: Patterns of Marine Life*. Harvard University Press, Cambridge, MA. 332 pp.

Vermeij, G. J. 1982. Unsuccessful predation and evolution. *Am. Nat.* **120**: 701–720.

Vermeij, G. J. 1983. Shell-breaking predation through time. Pp. 649–669 in *Biotic Interactions in Recent and Fossil Benthic Communities*, M. J. S. Tevesz and P. L. McCall, eds. Plenum, New York.

Vermeij, G. J., E. Zipser, and E. C. Dudley. 1980. Predation in time and space: peeling and drilling in terebrid gastropods. *Paleobiology* **6**: 352–364.

Vitt, L. J., J. D. Congdon, and N. A. Dickson. 1977. Adaptive strategies and energetics of tail autotomy in lizards. *Ecology* **58**: 326–337.

Wenner, C. A., and J. A. Musick. 1975. Food habits and seasonal abundance of the American eel, *Anguilla rostrata*, from the lower Chesapeake Bay. *Chesapeake Sci.* **16**: 62–66.

Willis, L., S. T. Threlkeld, and C. C. Carpenter. 1982. Tail loss patterns in *Thamnophis* (Reptilia:Colubridae) and the probable fate of injured individuals. *Copeia* **1982**: 98–101.

Wilson, K. A., K. L. Heck, Jr., and K. W. Able. 1987. Juvenile blue crab, *Callinectes sapidus*, survival: an evaluation of eelgrass, *Zostera marina*, as refuge. *Fish. Bull.* **85**: 53–58.

Wood, F. D., and H. E. Wood, II. 1932. Autotomy in decapod crustacea. *J. Exp. Zool.* **62**: 1–55.

Reference: *Biol. Bull.* 180: 432–439. (June, 1991)

Hydration State, Metabolism, and Hatching of Mono Lake *Artemia* Cysts

LAURIE E. DRINKWATER* AND JOHN H. CROWE

Department of Zoology, University of California, Davis, California

Abstract. *Artemia monica*, the only macrozooplankton in Mono Lake, California, is unique among brine shrimp in that it produces encysted diapause embryos that sink to the lake bottom where they overwinter. Currently, the lake's salinity is about twice as high as it was 40 years ago and, at equilibrium, it is projected to fluctuate between 169–248 g/l. Here we describe the effects of salinity on the termination of diapause, hatching, carbohydrate metabolism, and hydration of the cysts. As expected, hatching is much more sensitive to salinity than is termination of diapause. Carbohydrate metabolism, which involves the conversion of trehalose to glycerol and is required for hatching, responds to increasing salinity as reported in other *Artemia* species: increasing amounts of glycerol must be synthesized as salinity is raised. The unfreezable water in these embryos is 0.29 g H_2O/gram dry weight (gdw) cysts, similar to values reported for other biological systems. This result and previous studies suggest that water probably becomes limiting at hydration levels of about 0.60 g H_2O/gdw cysts. In Mono Lake water, the cysts reach this critical hydration at a salinity between 140–160 g/l, equivalent to approximately 3780–4330 mOsm/kg. We conclude that *Artemia monica* will cease to exist within this salinity range and doubt that it can hatch beyond this limit, which is imposed by the requirement of metabolic processes for minimal amounts of cellular water.

Introduction

The relationships between external salinity, metabolic activity, and the physical state of cellular water have been studied extensively in the encysted diapause embryo of *A. franciscana* (Clegg, 1964, 1978, 1986; Glasheen and Hand, 1989). In their natural environment, the cysts are frequently subjected to extreme fluctuations in salinity and complete desiccation. Rupture of the cyst wall during hatching is thought to be an osmotic process, brought about by the synthesis of glycerol and the resulting increase in turgor pressure (Clegg, 1964, 1976a). Although the cysts can hatch in a wide range of salinities by increasing the amount of glycerol produced as salinity increases, they reach a point where hatching is completely inhibited due to inadequate cellular water (Clegg, 1964).

The critical hydration levels that limit metabolism in *A. franciscana* have been investigated by Clegg and colleagues (1974, 1976a, b, c; 1977; Clegg and Cavagnaro, 1976; Clegg and Lovallo, 1977). In an elegant series of studies, they report that the shutdown of metabolism due to water loss occurs in a step-wise fashion, with distinct metabolic transitions corresponding to changes in the physical state of water remaining in the cysts. The metabolic characteristics and hydration levels of these three metabolic domains are shown in Table I. Cysts with water contents lower than about 0.60 H_2O g/gdw (gram dry weight) exhibit a dramatic decrease in their metabolic capabilities. Further studies suggest that a significant bulk aqueous phase is not present until the cysts contain more than 0.6 g H_2O/gdw. Clegg has hypothesized that, as hydration levels fall below 0.60 g H_2O/gdw, metabolic pathways are disconnected, resulting in a restricted metabolism that does not permit hatching of the cyst (for reviews of the model see Clegg, 1978, 1986). Another metabolic transition occurs at hydration levels of 0.3 g H_2O/gdw and lower. This water is considered to be the "bound water," and at water contents of 0.3 g/gdw and lower, the only metabolic activity evident is a slow decline in ATP.

An atypical species of brine shrimp, *A. monica*, inhabits Mono Lake, California—a large, deep, termial lake on the eastern side of the Sierra Nevada. Unlike *A. francis-*

Received 26 March 1990; accepted 27 December 1990.

* Current address: Department of Vegetable Crops, University of California, Davis, CA 95616.

Table 1

Hydration-dependence of cellular metabolism in Artemia *cysts*

Cyst hydration (g H_2O/gdw cysts)	Metabolic events initiated
0 to 0.1	None observed
0.1	Decrease in ATP concentration
0.1 to 0.3 ± 0.05	No additional events observed
0.3 ± 0.05	Metabolism involving several amino acids, Krebs-cycle and related intermediated, short chain aliphatic acids, pyrimidine nucleotides, slight decrease in glycogen concentration
0.3 to 0.6 ± 0.07	No additional events observed
0.6 ± 0.07	Cellular respiration, carbohydrate synthesis, mobilization of trehalose, net increase in ATP, major changes in the free amino acid pool, hydrolysis of yolk protein, RNA and protein synthesis, resumption of embryonic development
0.6 to 1.4	No additional events observed

The two critical levels of hydration where large changes in metabolic capacity occur are shown in bold typeface. After Clegg (1978).

cana cysts, Mono Lake cysts are not subjected to desiccation, and rarely experience drastic changes in salinity. The thin cyst shell permits the cysts to sink to the lake bottom where they are activated (diapause is terminated) by the cold temperatures. They remain on the lake bottom for 6–7 months, until late February to early March, when they begin hatching (Lenz, 1980, 1983).

The future viability of this species is of concern, because water exports from the Mono Lake basin have caused a decline in the lake level. The lake's salinity has more than doubled over the past 40 years and, at equilibrium, it is predicted to fluctuate between 169 and 248 g/l (Vorster, 1985). The shrimp are the only macrozooplankton in the lake, and serve as a food source for the large population of California gulls that have a major rookery on the lake. Thus, *A. monica* occupies a key position in the Mono Lake ecosystem (Mason 1967; Winkler, 1977; Lenz, 1980).

This study examines the effects of salinity of the metabolism and hydration of the cysts in *Artemia monica*. The results indicate that in terms of their response to elevated salinity, *A. monica* is very similar to the well-studied brine shrimp, *A. franciscana*, despite pronounced differences in the habitats of these two species.

Materials and Methods

Collection of cysts

Gravid females collected from Mono Lake were held in the laboratory for 1–2 weeks while they released their cysts. Conditions approximated those of Mono Lake in the summer: temperature was 18°C, and Mono Lake water (MLW) containing 50 g solids/l (1300 mOsm/kg) was used; no food was provided. Before being used, the cysts were stored anaerobically in this medium at 14°C. The newly released diapause cysts will not hatch, even when placed in conditions normally favorable for hatching; they require a cold treatment (≤5°C) of about 90 days (Dana, 1981; Drinkwater and Crowe, 1987). Storage at 14°C, as described above, had previously maintained the diapause state and yielded viable cysts (Drinkwater and Crowe, 1987).

Osmolality of Mono Lake water

The physiologically relevant measurement of the dissolved solids in this water is osmolality, as we will show in the Results section. However, previous workers have represented their results in terms of grams of dissolved solids per liter of water (g/l). To facilitate a comparison of the present results with those of previous studies, we will report data here in both forms. Furthermore, previous workers have referred to the measurement g/l as "salinity" even though this is not the precise oceanographic meaning of this word. We will continue this usage.

It is not possible to reconstitute Mono Lake water from the salts collected by complete evaporation because some insoluble salts are formed during precipitation. Consequently, we produced the desired salinities by partially evaporating water collected from the lake and determining the salt content of subsamples gravimetrically. Adjustments were made to the non-desiccated stock by dilution with distilled water to yield MLWs of varying salinity. The osmolality of these solutions was determined by measurements of freezing point depression. Samples of the solutions were frozen in an ethylene glycol bath chilled to about −20°C. The temperature was monitored, and the equilibrium freezing point was recorded during the release of the latent heat of fusion as the samples froze. These measurements were repeated four times on each sample.

Metabolic studies

Preliminary analyses indicated that the carbohydrate profile of *A. monica* cysts was essentially identical to those of other *Artemia* cysts: prior to development the embryos contained high levels of trehalose and glycogen, and low levels of glycerol. Therefore, we expected that trehalose would be mobilized for glycerol production during pre-emergence development (PED).

In the first experiment, we determined when trehalose degradation is initiated. Diapause cysts were incubated aerobically and anaerobically at two temperatures, 14°C and 4°C. We knew from our previous work that the cysts

in the 14°C incubations would not break diapause and, consequently, would not hatch. However, the 4°C treatment would permit the cysts to break diapause, and they would begin hatching if adequate oxygen were present (Drinkwater and Crowe, 1987). The inclusion of the anaerobic treatments allowed us to break diapause but inhibit hatching, as aerobic metabolism is obligatory for hatching to occur (Clegg and Conte, 1980). Because the cysts could break diapause and hatch in the aerobic 4°C incubation, we set up parallel groups such that the percent hatch under these conditions could be monitored (Drinkwater and Crowe, 1987). This first experiment enabled us to compare the carbohydrate metabolism of cysts remaining in diapause (14°C) to that of cysts which had terminated diapause (4°C) and resumed development.

The effects of salinity on carbohydrate metabolism were studied as follows. Diapause cysts were incubated aerobically at 4°C in MLW of four salinities: 50, 80, 100, and 125 g/l (1300, 2100, 2690, and 3370 mOsm/kg). Two petri dishes of cysts were set up at each salinity and maintained in hygrostats over water of the same salinity. The media were monitored with a refractometer to assure constant salinity. Under these conditions, cysts can break diapause and begin hatching, thus percent hatch was monitored as described above. In addition, to separate the effects of salinity on termination of diapause from those on hatching, subsamples were periodically taken and placed under favorable hatching conditions: 14°C, in MLW of 50 g/l (1300 mOsm/kg).

Carbohydrate assays

Samples of cysts were removed and decapsulated by exposure to 2% hypochlorite (diluted household bleach), at 4°C, until examination under a dissecting microscope showed that the cyst shell had been removed (Sorgeloos *et al.*, 1977). This usually required 5 to 10 min. Each sample was divided into three subsamples and weighed after desiccation over $CaSO_4$. Trehalose, glycerol, and glucose were extracted by grinding cysts in a tissue homogenizer in 60% ethanol. Soluble sugars were separated by high pressure liquid chromatography (HPLC) on a HPX-87H anion exchange column (Bio-Rad; Schwarzenbach, 1982) and were quantified with a Knauer differential refractometer. The pellet was analyzed for glycogen according to the anthrone method (Umbreit *et al.*, 1972).

Calorimetry: determination of unfreezable water

A Perkin-Elmer DSC2-C Differential Scanning Calorimeter, supplemented with a Perkin-Elmer 3600 data station and TADS thermal analysis software, was used to determine the amount of unfreezable water in hydrated cysts of *A. monica* and *A. franciscana*. Decapsulated cysts were hydrated to varying degrees, either by submersion in distilled water, or by exposure to water vapor in individual hygrostats (Clegg, 1974). Cysts hydrated in the liquid phase required thorough blotting to remove all water on their surfaces. We sometimes observed two endothermic spikes due to water on the surface of the cysts; these samples were discarded.

The majority of the data presented in this paper are from cysts hydrated from the vapor phase. Samples (8 mg) were placed in pre-weighed aluminum calorimetry pans and sealed. The pans were weighed and the amount of freezable water was then measured by freezing the cysts, allowing them to reach thermal equilibrium at −63°C, and running calorimetry scans from −63°C to 27°C.

Frozen water in the cysts was quantified by comparing the enthalpy of the melting endotherm for water in the frozen cysts (calculated by the Perkin-Elmer TADS software), with enthalpy of known standards treated in the same way. After calorimetry, the pans were punctured to permit desiccation of the cysts by lyophilization. The samples were reweighed after equilibrating over $CaSO_4$. The water content of the samples was determined as the difference between the wet and dry weights.

Hydration of cysts in Mono Lake water

The water content of cysts as a function of the salinities of MLW was determined according to the method of Clegg (1974). Cysts were placed in individual chambers constructed of 35 ml covered vials and hydrated from the vapor phase over MLW of 50, 80, 100, 125, 140, 160, and 200 g/l. Six days were needed for cysts in the vapor phase to reach equilibrium at 2°C (Clegg, 1974). After being weighed, the cysts were lyophilized and then brought to equilibrium over $CaSO_4$ for 10 h in individual desiccators; the dry weight was then determined.

Results and Discussion

Salinity of Mono Lake water: a clarification

The salinities of MLW and its dilutions have, in the past, been compared with those of solutions of entirely different ionic compositions such as seawater or NaCl solutions (Dana, 1981; Dana and Lenz, 1986). Mono Lake water has an unusual salt composition, with high levels of carbonates and sulfates (Cole and Brown, 1967). Because the cysts respond to the chemical potential of water, we clearly cannot make direct comparisons of solutions containing different ionic species on a g/l basis. Such comparisons have led to considerable confusion in the literature. Our careful measurements of the osmolality of diluted Mono Lake water and NaCl solutions illustrate this point (Fig. 1). The osmolality of MLW is lower than a solution of NaCl containing the same amount of salts by weight. Thus, the water content of cysts in Mono Lake

water is higher than those in the NaCl solution containing the same amount of salts on a g/l basis. This seemingly simple point is exceedingly important, in that interpretation of data based on dissolved solutes can lead to incorrect conclusions, as illustrated by the following discussion.

Previous workers have shown that *A. monica* can hatch in MLW of 133 g/l (Dana and Lenz, 1986). Limits for many *Artemia* populations are between 70–99 g NaCl/l, and because the highest salinity for hatching (*A. franciscana*, Utah population) is reported as >99 g NaCl/l (d'Agostino, 1965, as cited by Collins, 1977), Dana and Lenz concluded that *A. monica* is unusual in its ability to hatch at increased salinities. However, Figure 1 shows that 133 g/l MLW is equivalent to a NaCl solution of about 105 g/l (3500 mOsm)—very similar to the highest reported salinity permitting hatching in *A. franciscana*. We conclude that *A. monica* is not unusual with regard to its hatchability as a function of osmolality of the bathing solution.

Salinity effects on the hatching mechanism in A. monica

As shown in Figure 2, breakdown of trehalose into glycerol only occurs under aerobic conditions in cysts that are able to break diapause and hatch. Therefore, the same osmotic mechanism proposed for hatching in *A. franciscana* is likely present in *A. monica*.

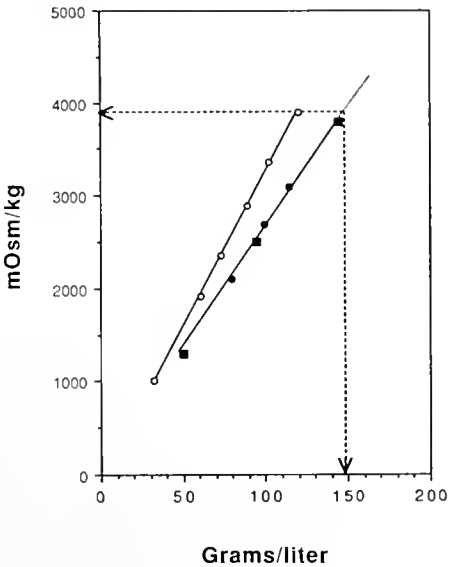

Figure 1. Osmolality of NaCl solutions and Mono Lake water of equal salt content on a g/l basis. Dotted arrows indicate that a 2.0 *M* (117 g/l) NaCl solution is the osmotic equivalent of about 150 g/l Mono Lake water. NaCl data are from Weast (1983). Data for Mono Lake water are from two sources using different methods: (squares) our data, obtained by freezing point depression; (circles) Herbst and Dana (1980), determined by vapor pressure osmometry.

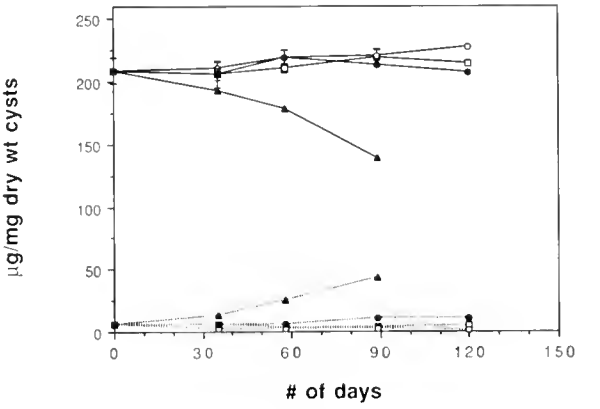

Figure 2. Trehalose (solid lines) and glycerol (broken lines) contents of cysts incubated under the following conditions: 4°C, aerobic (triangles); 4°C, anaerobic (closed circles); 14°C, aerobic (open circles); 14°C, anaerobic (squares). The 4°C, aerobic incubation is the only treatment which permitted both activation and hatching; the cysts were not sampled after 90 days because the majority of them had hatched. Note the significant decline in trehalose as glycerol increases. The other three incubations exhibited no hatching; cysts in the 4°C, anaerobic incubation could break diapause, but could not hatch in the absence of oxygen. Points are $\bar{x} \pm SD$, $n = 3$.

Having shown that the synthesis of glycerol proceeds with hatching, we incubated cysts in several salinities of MLW to determine the effect of salinity on carbohydrate metabolism. Simultaneously, we monitored termination of diapause and hatching. Increasing salinities resulted in faster synthesis of glycerol (Fig. 3a), while trehalose breakdown is slower at higher salinities (Fig. 3b). Figure 3c shows that, at the lowest salinity (50 g/l), glycogen is synthesized in addition to glycerol, suggesting that at this salinity some of the trehalose is being converted to glycogen. However, glycogen shows net degradation in the higher salinities, indicating that an osmotic regulatory mechanism may control the amount of glycerol and glycogen synthesized by the embryo in response to changes in salinity. The decline of glycogen may, in part, also explain the lower hatch seen in Figure 4 at higher salinities. If the embryo must synthesize more glycerol to hatch as salinity increases, fewer carbohydrate reserves will be available for other necessary developmental processes.

Salinity effects on termination of diapause

Figure 5 indicates that there is only a slight inhibition of diapause termination in the highest salinity used in these experiments. The percent hatch is essentially the same in three of the salinities, with only a 20% lower hatch in the cysts from the 125 g/l (3370 mOsm/kg) treatment. When data from the metabolic studies are combined with the hatching data from this study and others (Dana and Lenz, 1986), we can conclude that the decrease

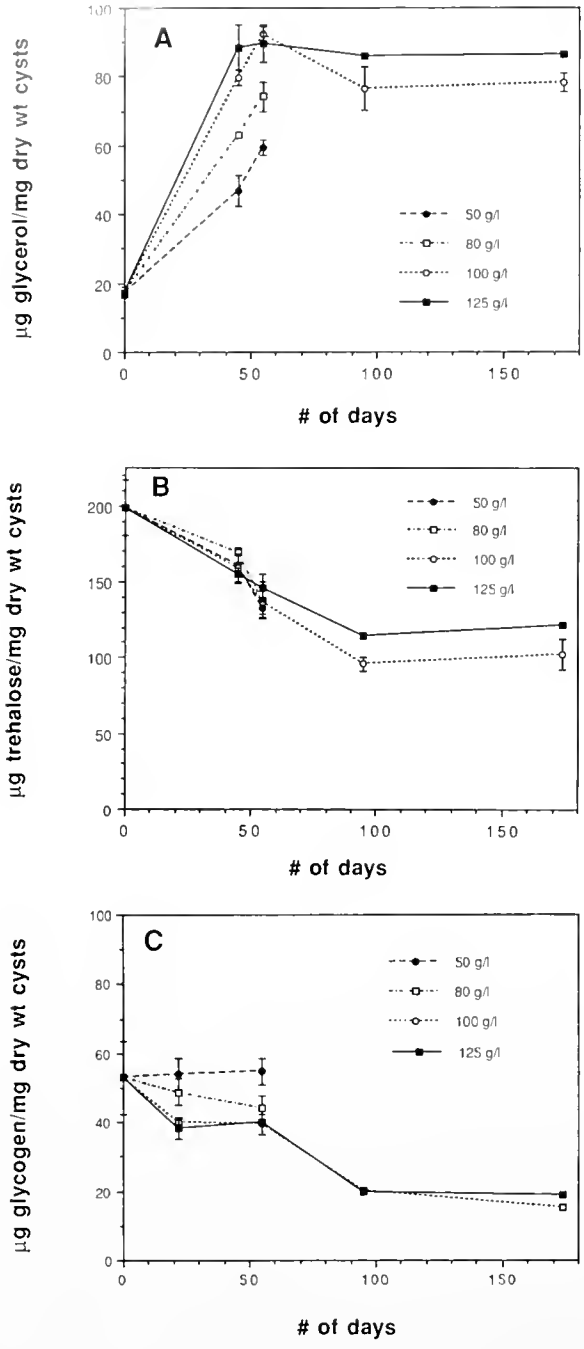

Figure 3. Changes in carbohydrate levels of cysts incubated aerobically in four salinities of Mono Lake water at 4°C. (A) Glycerol synthesis is faster at higher salinities. (B) Trehalose breakdown is faster in the lower salinities. (C) Glycogen levels; only the lowest salinity, 50 g/l (1300 mOsm/kg), shows a net increase in glycogen. Points are x ± SD, n = 3. Refer to Figure 4 to determine percent hatch during the experiment.

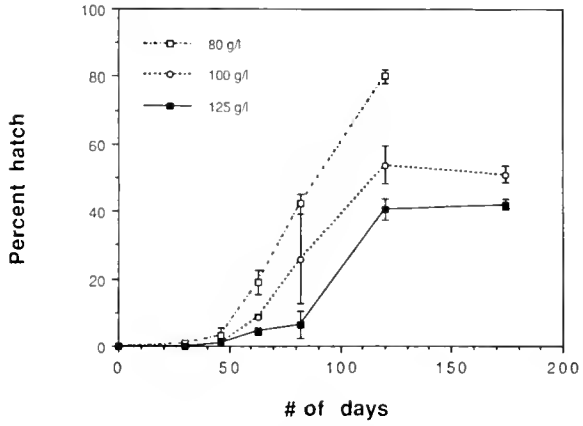

Figure 4. Percent hatch of *Artemia monica* during the experiment described in Figure 3. Hatching in the 50 g/l (1300 mOsm/kg) treatment was essentially the same as the 80 g/l (2100 mOsm/kg) treatment and is not shown. Each point represents x ± SD, n = 3.

in hatching observed at the higher salinities used in these experiments primarily results from interference with hatching rather than release from diapause. Thus, termination of diapause is less susceptible to increasing salinities, because salinities that only impair cyst activation completely inhibit hatching (Dana and Lenz, 1986; Drinkwater and Crowe, 1987).

Unfreezable water and hydration of Mono Lake cysts

Previous experiments indicate that the hatching limit of *A. monica* is somewhere between 133–159 g/l MLW (Dana and Lenz, 1986). Based on our metabolic data and studies of the hydration dependence of metabolism, we assume that, at this limiting salinity, conventional metabolism can no longer occur, and degradation of trehalose therefore stops. However, the potential for adaptations permitting the cysts to hatch at higher salinities is a possibility to which several researchers working at Mono Lake have alluded (Dana, pers. comm.). We have attempted to

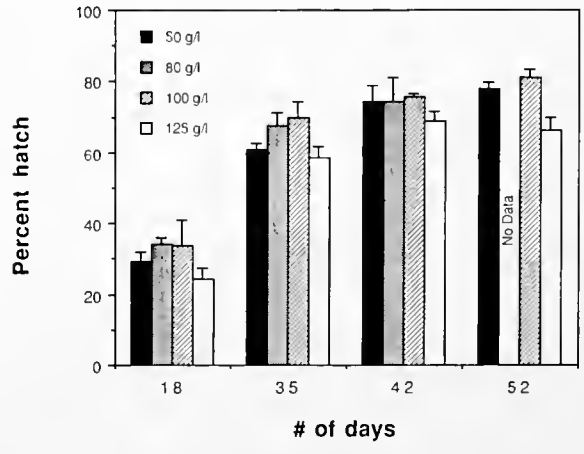

Figure 5. Percent hatch of cysts removed from the treatment salinity and hatched in 50 g/l (1300 mOsm/kg) at 14°C to determine the number of activated cysts. x ± SD of three determinations are graphed.

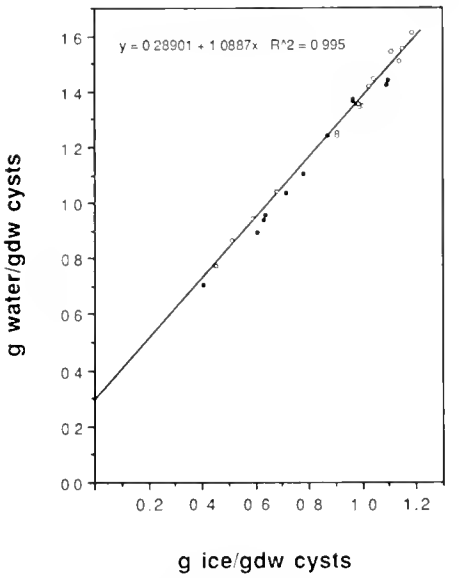

Figure 6. Unfreezable water in *Artemia monica* (open circles) and *A. franciscana* (closed circles). The line represents a linear regression on the *A. monica* data; the *A. franciscana* data are included for comparison. The y-intercept (unfreezable water) is 0.29 g H_2O/gdw cysts.

determine the physical limitation of conventional metabolism in these organisms by studying their hydration properties and unfreezable water content.

The amount of unfreezable water in *A. monica* cysts corresponds closely with our data for *A. franciscana* (Fig. 6). The y-intercept gives the estimated amount of unfreezable water, in this case, 0.29 g H_2O/gdw for *A. monica* cysts. A few *A. franciscana* samples were run for comparison. Linear regression of these points estimates unfreezable water to be 0.28 g/gdw cysts, very close to our value for *A. monica*. These values for unfreezable water coincide closely with the critical hydration at which the transition to the ametabolic state occurs, about 0.3 g/gdw (Table I; Clegg, 1978, review). Below this water content, the cysts are considered to be ametabolic. Thus, the unfreezable water content represents a physiologically significant hydration feature of the cells.

Comparing the quantity of bound water contained in these two species (0.28–0.29 g/gdw) with figures reported for a wide range of biological systems, we find close agreement; amounts range from 0.3 to 0.5 g/gdw (Williams, 1970; Cooke and Kuntz, 1974, Garlid, 1978; O'Dell and Crowe, 1979; Crowe *et al.*, 1983). Our results do not agree with previous findings for a now extinct population of *A. franciscana* previously located in Brazil; freezable water in that study was about 0.6 g/gdw (Crowe *et al.*, 1981). However, because the phase transition curve for the *A. franciscana* cysts was reported to be curvilinear rather than linear, the cysts probably had water in their outer porous shells, causing the internal water content to appear higher

Table II

Water content (g H_2O/grams dry weight) of decapsulated Artemia monica *cysts in Mono Lake water of salinities ranging from 50 to 200 g/l*

Salinity (g/l)	Cyst hydration g H_2O/gdw cysts
50	1.16 ± 0.06
80	1.04 ± 0.08
100	0.97 ± 0.15
125	0.76 ± 0.01
140	0.66 ± 0.02
160	0.55 ± 0.04
200	0.39 ± 0.02

Data reported as $\bar{x}$ ± S.D., n = 3.

than it actually was. In the previous experiments with *Artemia* (Crowe *et al.*, 1981), the cysts were hydrated by immersion in water, whereas in our present experiments, hydration was achieved by exposure to the vapor phase, eliminating this potential source of error.

Salinity and water content of Mono Lake cysts

Finally, the water contents of *A. monica* cysts in varying concentrations of Mono Lake water were determined to assess the point at which hatching would be limited by insufficient intracellular water. In Table II, the hydration levels of *A. monica* cysts equilibrated in MLW of 50–200 g/l are reported. To permit comparison with *A. franciscana*, previously published data have been corrected for the presence of the shell and have been graphed with *A. monica* in Figure 7; a close correspondence in water contents is demonstrated. *A. monica* cysts reach a critical hydration of 0.6–0.67 g/gdw in salinities between 140–

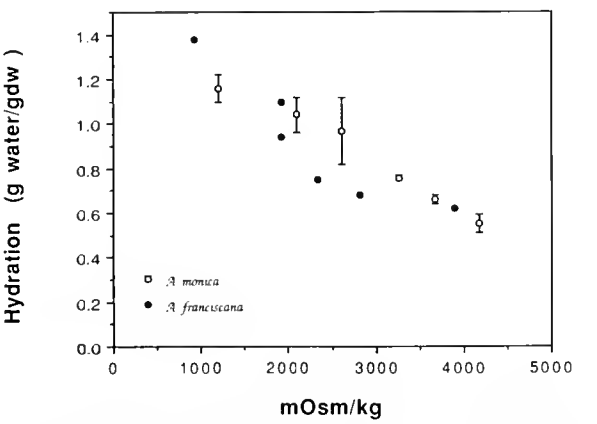

Figure 7. Hydration of *Artemia monica* cysts compared to *A. franciscana* cysts as a function of osmolality. Data from *A. franciscana* have been corrected for shell weight (from Clegg, 1974, 1976a).

160 g/l MLW, equivalent to NaCl solutions of approximately 1.9–2.1 *M* (3600–4050 mOsm/kg).

Clegg (1978) has not detected conventional metabolism in *A. franciscana* cysts hydrated in 2.0 molal NaCl. More recently, Glasheen and Hand (1989) have used microcalorimetry to demonstrate that heat dissipation, and thus metabolism, in *A. franciscana* from the Great Salt Lake is severely depressed by 2.0 *M* NaCl. We suggest that *A. monica* also experiences a critical hydration at this salinity, and submit that conventional metabolism will not occur in these cysts at a limiting salinity between 140–160 g/l MLW. We must stress, however, that at salinities somewhat lower that these, which actually impose a physical limit to conventional metabolism, hatching will be impaired; *i.e.*, a smaller proportion of cysts will hatch, and hatching will take longer (Jennings and Whitaker, 1941; Clegg, 1964; Dana and Lenz, 1986).

Conclusions

Several lines of evidence presented here suggest that cysts of *A. monica* possess limits to development that are similar to those found in *A. franciscana*. (1) Hatching is correlated with the synthesis of glycerol and, as in *A. franciscana*, synthesis of this compound is probably required for hatching. Glycerol synthesis increases when the cysts are incubated at higher salinities. (2) The amounts of unfreezable water in *A. monica* and *A. franciscana* are similar, suggesting that the hydration levels at which metabolic transitions occur are the same. (3) At salinities of about 150 g/l MLW (equivalent to 4060 mOsm/kg), the water content of *A. monica* cysts is less than 0.6 g/gdw, thus conventional metabolism and development will not be possible.

We conclude that, while *A. monica* can hatch in salinities in the upper range of those reported for *Artemia* cysts, they are not unique in this ability, and they have no unusual adaptive potential with respect to salinity thresholds. All available evidence suggests that these limits on metabolism are imposed by the biophysical interactions inherent in the hydration of cellular components and the effects of this water of hydration on the functioning of macromolecular assemblages (Clegg, 1986; Glasheen and Hand, 1989).

Thus, these organisms probably cannot adapt to Mono Lake salinities above about 150 g/l (4060 mOsm/kg) by extending their hatching limit beyond that level. Biological adaptation, powerful as it is, cannot overcome the basic principles of eukaryotic metabolism which require the presence of minimal amounts of cellular water. It follows then, that *A. monica* will become extinct when salinity rises to between 140–160 g/l—even before the lake reaches equilibrium. Certainly, *A. monica* will not exist in Mono Lake when it reaches its projected equilibrium, since salinity will then be 169–248 g/l, well above 4000 mOsm/kg (Fig. 1).

Finally, should the salinities in Mono Lake be allowed to reach these levels, we doubt that another brine shrimp species could be successfully introduced due to the characteristics of this lake that make it unique among *Artemia* habitats (Lenz, 1980; Dana, 1981; Bowen *et al.*, 1985; Drinkwater and Crowe, 1987). First, because of its ionic composition, Mono Lake water is toxic to many *Artemia* populations, including the most well-known North American species, *A. franciscana* (Bowen *et al.*, 1985). Second, in order for a species to persist in the lake, its life-cycle would need to be synchronized with the conditions in Mono Lake; *i.e.*, diapause induction and termination must occur at the appropriate times. In addition, the Mono Lake ecosystem probably cannot mimic other hypersaline lakes, such as the Great Salt Lake, in which floating cysts are deposited on the shore as the lake recedes and are then swept back into the lake by spring rains. The average annual precipitation in the Mono basin is 33 cm, compared to 52 cm for the Great Salt Lake. And in the spring, average precipitation for Mono Lake is only 4 cm (April, May, and June), while the Great Salt Lake receives 16 cm during these same months (NOAA, 1985, 1986). These observations illustrate some of the specific difficulties involved in attempting to introduce a replacement brine shrimp species into Mono Lake.

Acknowledgments

Appreciation is extended to Gail Dana for her essential assistance early in the project. We are sincerely grateful to Dr. James Clegg for his contribution of many enlightening discussions and for reviewing the manuscript prior to submission. This research was supported in part by Los Angeles Department of Water and Power.

Literature Cited

Bowen, S. T., E. A. Fogarino, K. N. Hitchner, G. L. Dana, V. H. S. Chow, M. R. Buoncristiani, and J. R. Carl. 1985. Ecological isolation in *Artemia*: population differences in tolerance of anion concentrations. *J. Crust. Biol.* **5**: 126–129.

Clegg, J. S. 1964. The control of emergence and metabolism by external osmotic pressure and the role of free glycerol in developing cysts of *Artemia salina*. *J. Exp. Biol.* **41**: 879–892.

Clegg, J. S. 1974. Interrelationships between water and cellular metabolism in cysts. I. Hydration-dehydration from liquid and vapor phases. *J. Exp. Biol.* **61**: 291–308.

Clegg, J. S. 1976a. Interrelationships between water and metabolism in *Artemia* cysts. II. Carbohydrates. *Comp. Biochem. Physiol.* **53a**: 83–87.

Clegg, J. S. 1976b. Interrelationships between water and cellular metabolism in *Artemia* cysts. III. Respiration. *Comp. Biochem. Physiol.* **53a**: 89–92.

Clegg, J. S. 1976c. Interrelationships between water and cellular metabolism in *Artemia* cysts. V. $^{14}CO_2$-incorporation. *J. Cell. Physiol.* **89**: 369–380.

Clegg, J. S. 1977. Interrelationships between water and cellular metabolism in *Artemia* cysts. VI. RNA and protein synthesis. *J. Cell. Physiol* **91:** 143–154.

Clegg, J. S. 1978. Hydration-dependent metabolism transitions and the state of cellular water in *Artemia* Pp. 117–154 in *Dry Biological Systems*, J. H. Crowe and J. S. Clegg, eds. Academic Press, New York.

Clegg, J. S. 1986. The physical properties and metabolic status of *Artemia* cysts at low water contents: the "water replacement" hypothesis. Pp. 169–185 in *Membranes, Metabolism and Dry Organisms*, A. C. Leopold, ed. Cornell University Press, Ithaca, NY.

Clegg, J. S., and F. P. Conte. 1980. A review of the cellular and developmental biology of *Artemia*. Pp. 11–54 in *The Brine Shrimp Artemia, Vol. 2. Physiology, Biochemistry, Molecular Biology*. G. Persoone, P. Sorgeloos, O. Roels, and E. Jaspers, eds. Universa Press, Wetteren, Belgium.

Clegg, J. S., and J. Cavagnaro. 1976. Interrelationships between water and cellular metabolism in *Artemia* cysts. IV. Adenosine 5'-triphosphate and cysts hydration. *J. Cell. Physiol.* **88:** 159–166.

Clegg, J. S., and J. Lovallo. 1977. Interrelationships between water and cellular metabolism in *Artemia* cysts. VII. Free amino acids. *J Cell. Physiol.* **93:** 161–168.

Cole, G. A., and R. J. Brown. 1967. The chemistry of *Artemia* habitats. *Ecology* **48:** 858–861.

Collins, N. C. 1977. Ecological studies of terminal lakes: their relevance to problems in limnology and population biology. Pp. 411–420 in *Desertic Terminal Lakes, Proceedings*. D. C. Greer, ed. Utah Water Research Laboratory, Utah.

Cooke, R., and I. D. Kuntz. 1974. The properties of water in biological systems. *Annu. Rev. Biophys. Bioeng.* **3:** 95–126.

Crowe, J. H., L. M. Crowe, and S. J. O'Dell. 1981. Ice formation during freezing of *Artemia* cysts of variable water contents. *Mol Physiol.* **1:** 145–152.

Crowe, J. H., S. J. Jackson, and L. M. Crowe. 1983. Nonfreezable water in anhydrobiotic nematodes. *Mol. Physiol.* **3:** 99–105.

D'Agostino, A. 1965. Comparative studies of *Artemia salina* (development and physiology). Ph.D. Diss. New York University. Cited by Collins, 1977.

Dana, G. 1981. Comparative population ecology of the brine shrimp, *Artemia*. M. A. Thesis, San Francisco State University.

Dana, G. L., and P. H. Lenz. 1986. Effects of increasing salinity on an *Artemia* population from Mono Lake, California. *Oecolgia* **68:** 428–436.

Drinkwater, L. E., and J. H. Crowe. 1987. Regulation of embryonic diapause in *Artemia:* environmental and physiological signals. *J. Exp. Zool.* **241:** 297–307.

Garlid, K. D. 1978. Overview of our understanding of intracellular water in hydrated cells. Pp. 3–19 in *Dry Biological Systems*, J. H. Crowe and J. S. Clegg, eds. Academic Press, New York.

Glasheen, J. S., and Hand, S. C. 1989. Metabolic heat dissipation and internal solute levels of *Artemia* embryos during changes in cell-associated water. *J. Exp. Biol.* **145:** 263–282.

Herbst, D. B., and G. L. Dana. 1980. Environmental physiology of salt tolerance in an alkaline salt lake population of *Artemia* from Mono Lake, California, U.S.A. Pp. 157–167 in *The Brine Shrimp Artemia Vol. 2. Physiology, Biochemistry, Molecular Biology*, G. Persoone, P. Sorgeloos, O. Roels, and E. Jaspers, eds. Universa Press, Wetteren, Belgium.

Jennings, R. H., and D. M. Whitaker. 1941. The effect of salinity upon the rate of excystment of *Artemia*. *Biol. Bull* **80:** 194–201.

Lenz, P. H. 1980. Ecology of an alkali-adapted variety of *Artemia* from Mono Lake, California, USA. Pp. 79–96 in *The Brine Shrimp Artemia. Vol. 3. Ecology, Culturing, Use in Aquaculture*, G. Persoone, P. Sorgeloos, O. Roels, and E. Jaspers, eds. Universa Press, Wetteren, Belgium.

Mason, D. T. 1967. Limnology of Mono Lake, California. *University of California Publications in Zoology Vol. 83.* University of California Press, Berkeley.

NOAA, National Climatic Data Center. 1985. Climatology of the US. No. 20; Climatic Summaries of Selected Sites 1951–80; Utah.

NOAA, National Climatic Data Center. 1986. Climatological Data: California Section; Annual Summary. 90:13.

O'Dell, S. J., and J. H. Crowe. 1979. Freezing in nematodes: the effects of variable water contents. *Cryobiology* **16:** 534–541.

Schwarzenbach, R. 1982. High-performance liquid chromatography of carboxylic acids. *J. Chromatogr.* **251:** 339–358.

Sorgeloos, P., E. Bossuyt, E. Lavina, M. Baeza-Mesa, and G. Peronne. 1977. Decapsulation of *Artemia* cysts: a simple technique for the improvement of the use of brine shrimp in aquaculture. *Aquaculture* **12:** 311–315.

Umbriet, W. M., R. H. Burris, and J. F. Stauffer, eds. 1972. *Manometric and Biochemical Techniques.* 5th ed. Burgess Publishing Co., Minneapolis, MN.

Vorster, P. T. 1985. A water balance forecast model for Mono Lake, California. Masters thesis, California State University, Hayward, CA.

Weast, R. C., ed. 1983. *CRC Handbook of Chemistry & Physics.* CRC Press, Boca Raton, FL.

Williams, R. J. 1970. Freezing tolerance in *Mytilus edulis*. *Comp. Biochem. Physiol.* **35:** 145–161.

Winkler, D. W., ed. 1977. An ecological study of Mono Lake, California. Institute of Ecology, University of California, Davis, Publ. No. 12.

Reference: *Biol. Bull.* 180: 440–446. (June, 1991)

Ultrastructure and Neuronal Control of Luminous Cells in the Copepod *Gaussia princeps*

MARK R. BOWLBY[1] AND JAMES F. CASE

Marine Science Institute and Department of Biological Sciences, University of California, Santa Barbara, California 93106

Abstract. The physiology of light production in copepods is largely unknown. The mesopelagic copepod *Gaussia princeps* possesses luminous glands, each consisting of a single large cell discharging through a cuticular pore. Slow flashes external to the cuticle are triggered from excised abdomens by electrical stimulation of the ventral nerve cord. Each luminous cell contains UV fluorescent secretory vesicles distally, which are secreted through a valved cuticular pore. Each luminous cell, except for the most proximal portion, is surrounded by a cellular sheath, which appears to form the distal valve. Luminous cells have a stem containing small, electron-lucent precursors to secretory vesicles proximal to the fluorescent vesicles. Nerve terminals, filled with large synaptic vesicles, are associated with the unsheathed proximal cell membrane. Gap junctions interconnect the nerve terminals, and possibly serve to accelerate conduction to the luminous cell to achieve a synchronous effector output.

Introduction

Many marine copepods produce brilliant luminous secretions. Despite many investigations (Barnes and Case, 1972; Herring, 1988; Bannister and Herring, 1989; Latz *et al.*, 1990), much remains to be understood about the physiology of light production.

Copepod luminescence was first thought to involve the expulsion of luciferin and luciferase from separate glands through a common pore, with mixing and light emission occurring externally to the cuticle (Clarke *et al.*, 1962). Recent studies, however, refute this theory (Herring, 1988; Bannister and Herring, 1989; Bowlby and Case, 1989), as does this investigation. Individual light glands in some Metridinidae consist of a single cell type occurring in a unitary relationship with cuticular pores (Herring, 1988; Bannister and Herring, 1989). There is little evidence, other than in some ostracods, for the separate cellular packaging of luciferin and luciferase in any luminous organism (Harvey, 1952).

Control of luminous glands in copepods has not previously been investigated, although the short latency between stimulus and light emission indicates a probable nervous involvement (Barnes and Case, 1972; Latz *et al.*, 1987, 1990). Many other organisms, such as crustaceans (Dennell, 1940), teleost fish (Nicol, 1967; Baguet and Case, 1971; Anctil and Case, 1977), fireflies (Buck and Case, 1961; Case and Buck, 1963; Smith, 1963; Linberg and Case, 1982), coelenterates (Anderson and Case, 1975; Bassot *et al.*, 1978), and annelids (Herrera, 1977), possess demonstrated or suspected neuronal control pathways of luminous glands (reviewed by Case and Strause, 1978). Experiments on euphausiids suggest that serotonin may be involved in neurotransmission to the photophores (Kay, 1965, 1966). The ophiuroids have undergone an extreme specialization of generating and propagating luminescence within modified nerve cells of the radial nerve cord (Brehm, 1977).

Luminous cells in copepods fluoresce when excited with ultraviolet (UV) light (Barnes and Case, 1972; Herring, 1988; Bannister and Herring, 1989), due to absorption by luciferin and subsequent re-emission in the visible region of the spectrum. This technique, in conjunction with image intensification of luminous sites, has allowed identification of at least 14 luminous sites on the antennae, cephalothorax, thorax, mandibular palps, and urosome of *G. princeps* (Clarke *et al.*, 1962; Barnes and Case, 1972; Bannister and Herring, 1989; Bowlby and Case, in press), along with a similar distribution of sites in *Pleuromamma*

Received 21 December 1990; accepted 8 March 1991.

[1] Present address: Department of Neurobiology, Harvard Medical School, 220 Longwood Ave., Boston, MA 02115.

xiphias and *Metridia princeps* (Bannister and Herring, 1989).

The mesopelagic calanoid copepod *G. princeps* (T. Scott) occurs below 400 m during the day, and vertically migrates to an upper limit of 200 m at night. They occur in numbers up to approximately 25 individuals · 1000 m^{-3} (Childress, 1977).

In this investigation, the physiology of light production was studied in the mesopelagic copepod *Gaussia princeps*. Light, scanning, and transmission electron microscopy were used to elucidate luminous cell ultrastructure and associated neuroeffector junctions. This may ultimately lead to a more complete understanding of the adaptive significance bioluminescence serves in the midwater environment.

Materials and Methods

Specimen collection

Adult male and female specimens of *Gaussia princeps* (T. Scott) (mean total body length 1 cm) were collected from 1986 through 1989 from the San Clemente Basin, off the coast of California, at approximately 32°N, 117°W. Collections were made from the R. V. *New Horizon* and R. V. *Point Sur*, with an opening-closing Tucker trawl (length, 30 m; mouth, 10 m^2). The trawl was equipped with an insulated cod end (Childress *et al.*, 1978), and towed between 400 and 800 m depth. Specimens were sorted and maintained in filtered seawater at 6°C until testing. Animals were fed *Artemia* nauplii or an unsorted zooplankton/phytoplankton mixture, collected locally at 10 m depth, twice per week. Individuals survived for up to 6 months in this regime.

Physiological experiments

Adult *Gaussia princeps* were anesthetized with 2-phenoxyethanol and held non-invasively, using fine U-shaped pins, in a Sylgard-lined petri dish filled with chilled seawater. Specimens remained dark and undisturbed for 4 h, to allow recovery from the anesthetic and partial restoration of bioluminescent reserves. The abdomen was subsequently isolated by bisection at abdominal segment 1 (A1), and used for all subsequent trials. Secondary longitudinal incisions were often performed, to permit localized stimulation of different tissues. Bioluminescence was elicited with single 10–70 V square wave pulses of 1–100 ms duration, using a 5 to 10 Mohm resistance tungsten microelectrode and an indifferent bath electrode. Luminescence was recorded with a photomultiplier tube (PMT) with a 5 mm diameter input fiber optic attached to a micromanipulator. The PMT signal was recorded and stored on a Nicolet digital oscilloscope. Radiometric calibration was not performed, owing to the variable input geometry of the manipulated fiber optic.

Microscopy

Epifluorescence microscopy was conducted on intact specimens and excised abdominal tissue from 20 anesthetized specimens using ultraviolet light from a mercury lamp filtered with 365 nm excitation, 395 nm dichroic, and 420 nm barrier filters. Ultraviolet and broadband visible light were separately or simultaneously used.

Primary fixation for light microscopy, transmission electron microscopy (TEM), and scanning electron microscopy (SEM) was done in 1% paraformaldehyde and 3% glutaraldehyde in 0.2 *M* sodium phosphate buffer with 5% glucose. Secondary fixation was carried out in 2% OsO_4

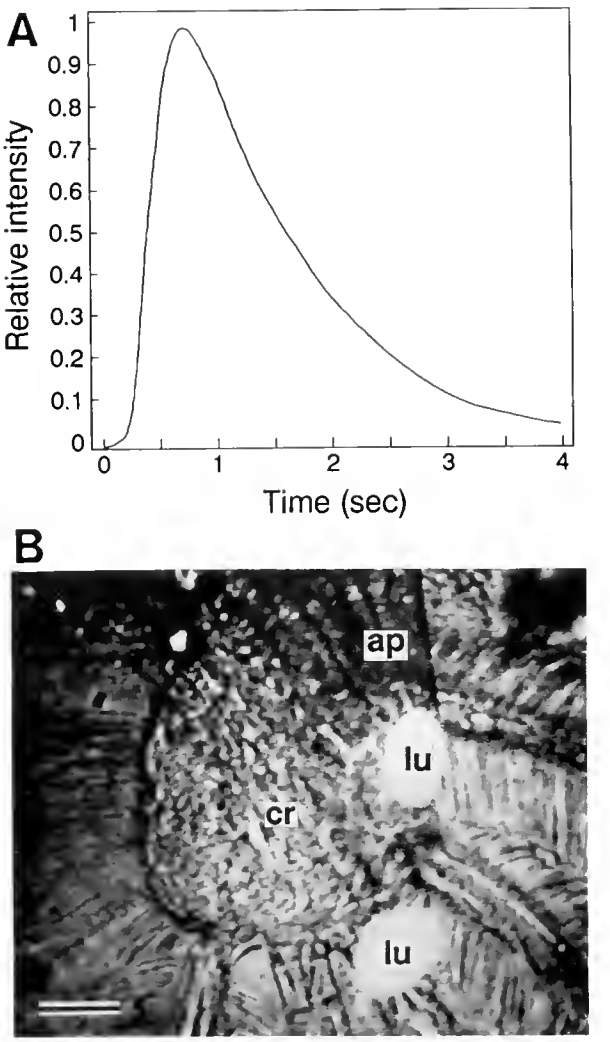

Figure 1. Bioluminescence produced by excised *Gaussia princeps* abdominal preparations. The ventral nerve cord at abdominal segment 1 was electrically stimulated with single 10–70 V square wave pulses. (A) Photomultiplier record of a slow flash. Mean flash latency is 109 ms. (B) Image intensified video frame of the abdominal anal segment papilla and caudal rami luminous cells. Luminescence is produced exclusively external to the cuticle. Scale = 100 μm. ap, anal papilla; cr, caudal rami; lu, luminous secretion.

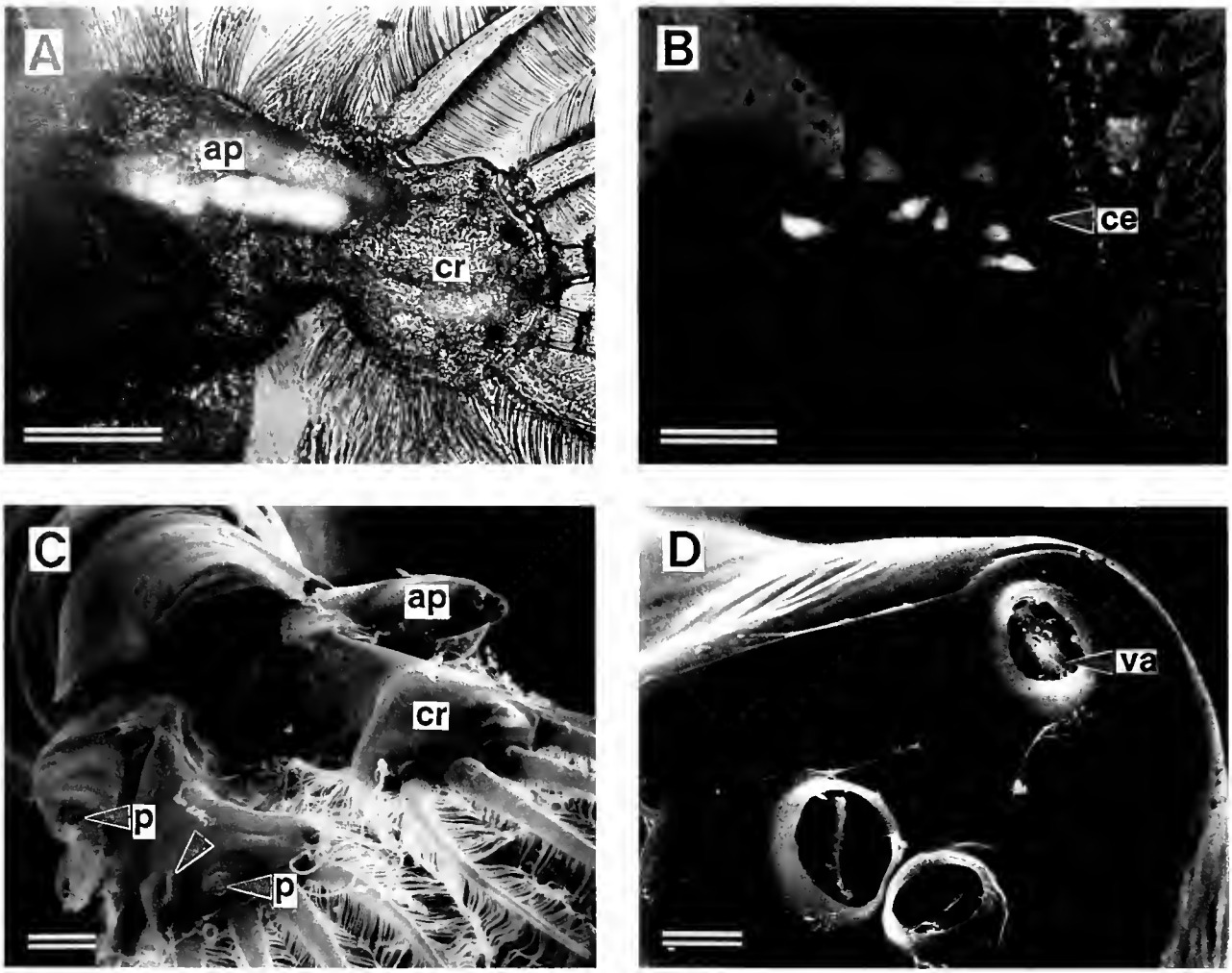

Figure 2. Structure of *Gaussia princeps* luminous glands. (A) Epifluorescence microscopy of luminous cells. The anal papilla and caudal rami each contain three luminous cells filled with fluorescent secretory vesicles. The third luminous cell is positioned below the visible cells. Scale = 300 μm. (B) Solitary fluorescent luminous cells located on the cephalothorax. Cells are much smaller than those of (A), with fewer secretory vesicles. Scale = 300 μm. (C) SEM of the abdominal anal papilla and caudal rami luminous cell cuticular pores (dorsal view). Each structure contains three cuticular pores. Pores not associated with fluorescent/luminescent sites occur on the caudal rami (unlabeled arrowhead). Scale = 100 μm. (D) Luminous cell pores (10 μm) of one anal papilla. Each pore contains a closed valve in the aperture. Valve shrinkage occurred in two of the three pores. Scale = 10 μm. ap, anal papilla; ce, cephalothorax; cr, caudal rami; p, pore; va, valve.

in 0.2 *M* sodium phosphate buffer. Fixed material was rinsed and dehydrated through an increasing ethanol series. Specimens prepared for light microscopy and TEM were transferred into propylene oxide and infiltrated with increasing concentrations of Araldite or Spurr's resin over 3 days. Serial thick (0.5–1 μm) and thin (0.1 μm) transverse and longitudinal sections were cut on a Sorvall Porter-Blum ultramicrotome with glass knives for light microscopy and TEM. Light microscopy was performed using a Zeiss IM35 inverted microscope, while TEM was done on a Philips 300. Following dehydration, specimens prepared for SEM were critical point dried, sputter coated with gold-palladium, and viewed with an Hitachi S-415A.

Whole-mount preparations of excised abdominal tissue were made by primary fixation in the presence of 0.1% methylene blue for 2 h. Tissues were rinsed, dehydrated, and mounted on glass slides in Permount and examined with a Zeiss IM35 inverted microscope.

Image intensification

Low light level video images of luminescent activity in excised abdominal preparations were made with an ISIT

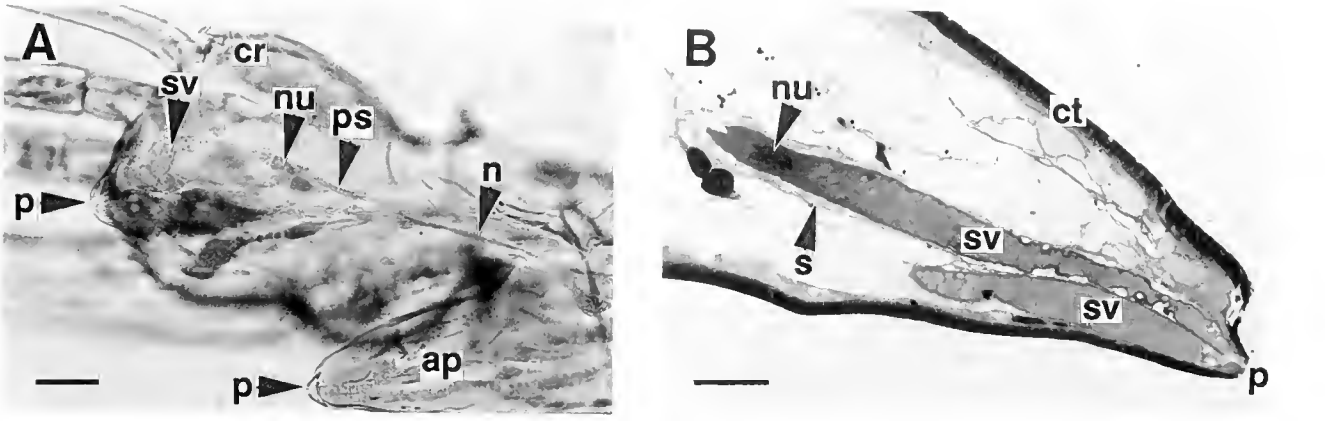

Figure 3. Light microscopy of abdominal luminous cell structure. Total luminous cell length is approximately 500 μm. (A) Abdominal whole mount stained with 0.1% methylene blue. Note the neural process terminating on the luminous cell proximal stem. Scale = 100 μm. (B) Longitudinal section through the anal papilla. Two luminous cells, filled with secretory vesicles and leading to separate cuticular pores, are shown. Luminous cell nucleus is located at the proximal border of the secretory vesicles. A sheath encloses the luminous cell. Scale = 50 μm. ap, anal papilla; ct, cuticle; cr, caudal rami; p, pore; ps, proximal stem; n, nerve; nu, nucleus; s, sheath; sv, secretory vesicles.

video camera, an F/0.95 lens, and a Zeiss IM35 inverted microscope. Video images were viewed at slow speed to analyze the luminescent patterns, and enhanced with a Megavision 1024XM image analysis system for final presentation. Bioluminescence was elicited using 50 V, 100 ms square pulses delivered through tungsten glass insulated microelectrodes.

Results

Physiology

Focal electrical stimulation for 100 ms at 10 V near the ventral nerve cord of the bisected abdomen induced luminescence from the caudal rami and anal segment papillae. (Fig. 1A). Luminescence appeared predominantly as a slow flash with a mean duration of 3 s and a mean latency of 109 ms. Nerve cord involvement was confirmed by stimulation at 70 V of adjacent longitudinal muscle groups without eliciting luminescence. Muscle tissues were also separated from the ventral nerve cord by longitudinal incisions from segments A1 to A3. Stimulation near the ventral nerve cord in such preparations continued to elicit luminescence, while muscle stimulation remained ineffective.

The excised abdomen produced luminescence only external to the cuticle (Fig. 1B). Light was never emitted intracellularly within luminous cells. Light appeared as a localized glow near the cuticular pores of the luminous cells. Details of excitation behavior in intact specimens are presented elsewhere (Bowlby and Case, in press).

Luminous cell structure

Epifluorescence microscopy revealed spherical, green fluorescent, secretory vesicles within each luminous cell (Fig. 2A, B). Three cells occur in each anal segment papilla and caudal ramus (Fig. 2A), while solitary luminous cells occur in the cephalothorax (Fig. 2B), thorax, basal 8 antennule segments, and mandibular palps. Secretory vesicles were visually confirmed to be discharged through associated cuticular pores in several specimens. It was unclear if secretory vesicles were discharged intact or if secretion involved vesicle membrane lysis.

Three pores (10 μm) are located on each anal papilla and caudal ramus (Fig. 2C) corresponding to discharge sites of the fluorescent secretory vesicles. Single pores are located near the fluorescent/luminescent sites on the thorax, cephalothorax, mandibular palps, and antennule segments. A closed valve-like structure is located in the aperture of each cuticular pore (Fig. 2D). Pore size and valve morphology were similar for luminous cells on the cephalothorax and thorax. Some valves appear as a partition dividing the pore aperture rather than as a valve, although it is suspected this is due to asymmetrical shrinkage of the valve away from the cuticle.

Abdominal luminous glands consist of a single long cell (approximately 500 μm), containing secretory vesicles distally, a nucleus at the proximal margin of the secretory vesicles, and a long stem proximal to the nucleus (Fig. 3A, B). Long nerve processes projecting from the midline of the specimen are associated with luminous cells (Fig. 3A).

Distal to the nucleus, large (4 μm) secretory vesicles have amorphous contents (Fig. 4A, B). Endoplasmic reticulum and mitochondria closely surround the secretory vesicles. A cellular sheath surrounds all except the proximal end of the luminous cell (Figs. 3B; 4A, B). This sheath consists of layers of cells with clear cytoplasm, whose

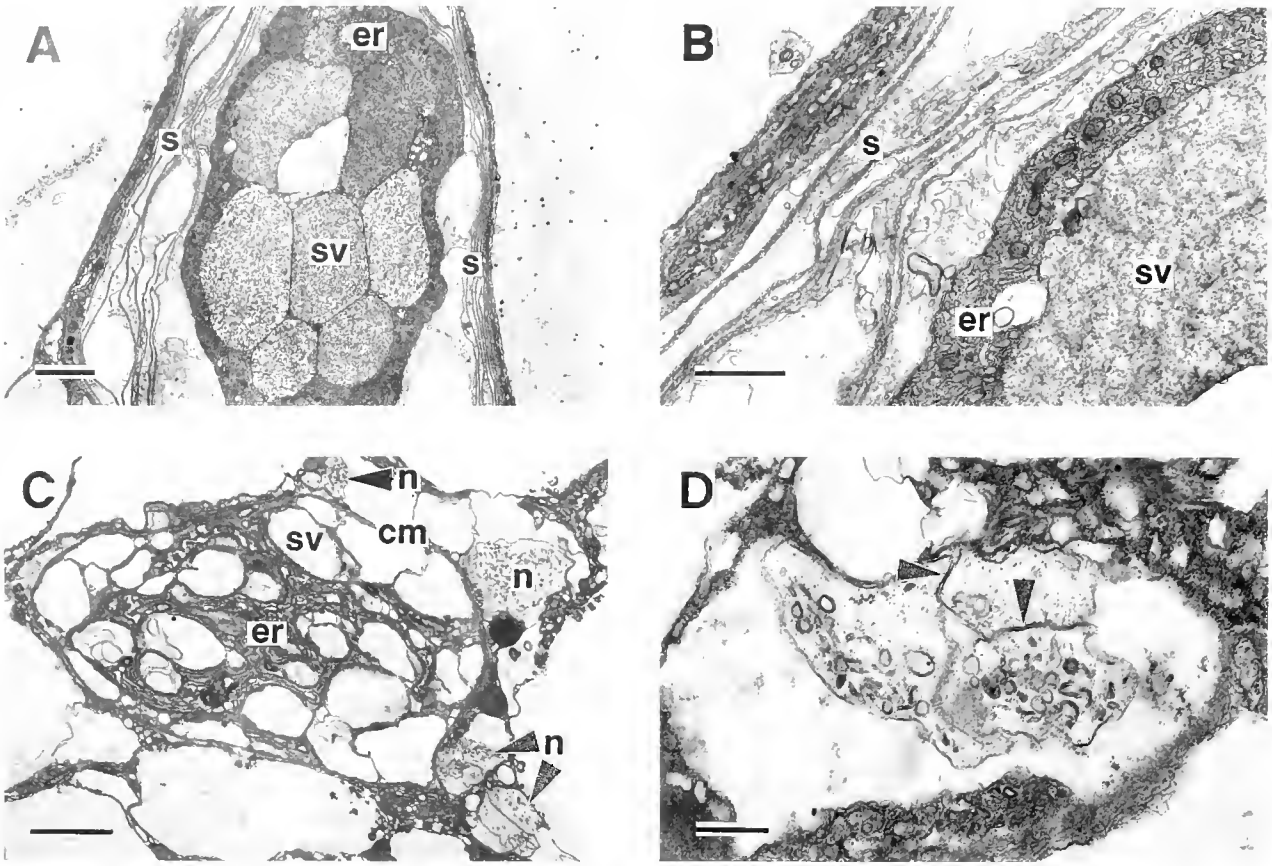

Figure 4. TEM of luminous cells. (A) Transverse section of an abdominal luminous cell distal to the nucleus. Secretory vesicles (4 μm), containing an amorphous material, are surrounded by endoplasmic reticulum. Scale = 2 μm. (B) Transverse section of the peripheral components of the luminous cell. The luminous cell is surrounded by a sheath consisting of layers of thin cells. Note mitochondria within the endoplasmic reticulum. Scale = 1 μm. (C) Proximal stem near the proximal limit of the luminous cell, containing endoplasmic reticulum and 2 μm electron-lucent precursors to secretory vesicles, but no cellular sheath. Nerve terminals filled with synaptic vesicles are associated with the luminous cell membrane. Scale = 3 μm. (D) Nerve terminals containing 110 nm synaptic vesicles and interconnected by 5 nm gap junctions (arrowheads). Scale = 0.5 μm. cm, cell membrane; er, endoplasmic reticulum; n, nerve; s, sheath; sv, secretory vesicles.

membranes are separated by a thin extracellular space containing fibrous material (Fig. 4B).

The proximal limit of the luminous cell consists of endoplasmic reticulum and smaller (2 μm) electron-lucent precursors to secretory vesicles, but no cellular sheath (Fig. 4C). Nerves are associated only with this region of the luminous cell. Nerves often contain large light and dense staining synaptic vesicles, and appear in close association with the cell membrane (Fig. 4C, D). Synaptic vesicles are either ovoid (mean largest diameter = 97 nm) or spherical (mean diameter = 116 nm). Nerve cells are interconnected in several locations by 5 nm gap junctions (Fig. 4D).

A composite drawing of a hypothetical *Gaussia princeps* luminous cell indicates the predominance of secretory vesicles in the distal region (Fig. 5). Secretory vesicles are expelled through a valve in the pore, which have been observed open or closed in other genera (Herring, 1988; Bannister and Herring, 1989). The valve appears to be formed from the sheath, which surrounds all except the proximal region of the luminous cell. Nerve terminals, filled with synaptic vesicles, are associated with the proximal, unsheathed portion of the cell.

Discussion

Luminescence in *Gaussia princeps* occurs by expulsion of secretory vesicles through a cuticular pore. The luminescent process presumably involves at least three steps: (1) neural activation of the luminous cell, (2) expulsion of secretory vesicles through cuticular pores, culminating in (3) initiation of swimming movements and displace-

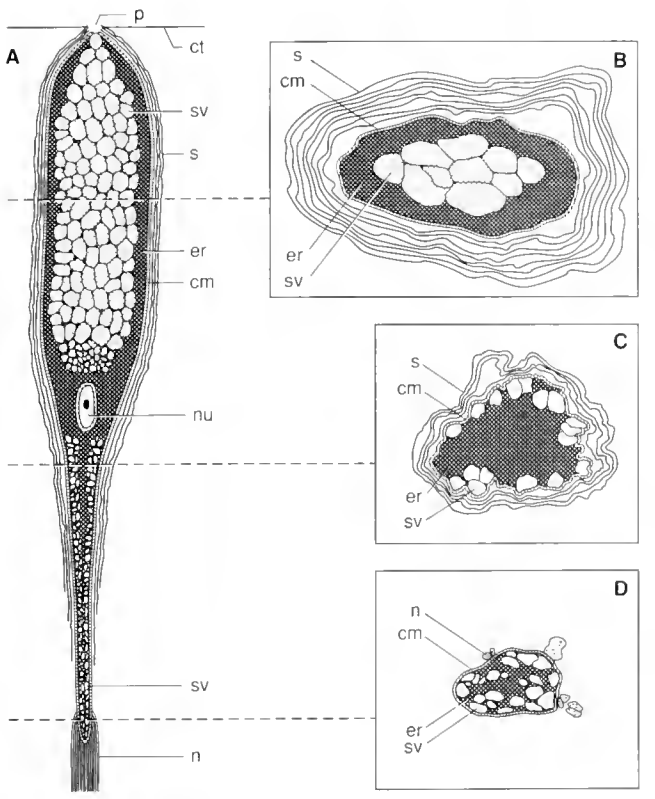

Figure 5. *Gaussia princeps.* Diagrammatic illustration of a luminous cell. (A) Longitudinal view of all portions of the cell. (B) Transverse view of the secretory vesicle containing portion of the cell. (C) and (D) Transverse views of the proximal stem. cm, cell membrane; ct, cuticle; er, endoplasmic reticulum; n, nerves; nu, nucleus; p, pore; s, sheath; sv, secretory vesicles.

ment of the animal away from the persistently luminous bolus.

Luminous cells consist largely of secretory vesicles contained within an endoplasmic reticulum matrix. Precursors to secretory vesicles may be produced in the proximal stem of the luminous cell and transported to the distal region of the cell, where they fuse and acquire amorphous material, forming large secretory vesicles. The single luminous cell type of *G. princeps* appears similar to those in other members of the Metridinidae (Herring, 1988; Bannister and Herring, 1989). *Pleuromamma xiphias* and *Metridia princeps* have luminous cells filled distally with secretory vesicles and enclosed within a sheath. In the Augaptilidae, in contrast, a pair of luminous cells discharge through a common pore (Bannister and Herring, 1989). Secretory vesicles are morphologically very different from the Metridinidae, containing paracrystalline contents.

Fluorescence from the secretory vesicles indicates the probable presence of luciferin or its precursors. In the absence of a second type of differentially staining intracellular organelles, the secretory vesicles also presumably contain, or have associated with them, luciferase. The absence of necessary cofactor(s) such as oxygen, ATP, Ca^{+2}, Mg^{+2}, or Cu^{+2} (Campbell, 1988, 1989), may prevent luminescence from being expressed within the luminous cell. Many of these cofactor(s) are likely to be present in the seawater, and thus could initiate light generation once expulsion occurs. The slow decay of light when secretory vesicles are not dispersed by appendage movement may result from the slow diffusion of cofactor(s) into the bolus of secreted material. Similarly, luminescence induced by mechanical pressure on a light gland may be due to ruptures of the luminous cell and cuticle, allowing entry of seawater and cofactor(s) into the gland (Barnes and Case, 1972; Bannister and Herring, 1989). Alternatively, changes in permeability or breakdown of vesicular bounding membrane upon excretion may permit the luminescence reaction to proceed.

Neuroeffector junctions occur only on the proximal region of the luminous cell. While classical membrane active zones were not found, large synaptic vesicles fill the terminals. Gap junctions among peripheral nerves may serve to ephaptically accelerate conduction to the luminous cell and achieve simultaneous effector output. The mechanism of material expulsion from the luminous cells cannot be related to the action of muscle fibers or microfilaments, due to their absence near the cells (Herring, 1988; Bannister and Herring, 1989; present study). Because luminous expulsion occurs from excised abdomens, changes in coelomic hydrostatic pressure are also not responsible for the expulsion process. Release of neurotransmitter from the neuroeffector junction synaptic vesicles in response to neural stimulation is assumed to cause changes in luminous cell membrane conductance, leading to ionic changes within the cell and luminescent vesicle release to the exterior.

Electrically induced flashes from excised abdominal preparations were predominantly of the slow flash type described in Bowlby and Case (in press). The latent period, however, is 10 times shorter in excised tissue than in intact specimens. This difference may be due to the absence of receptor delay, central nervous system processing, and to a shorter final motor pathway. The absence of the other flash types in excised preparations is not due to incapacity on the part of the abdominal photocytes, as they produce fast, long, and compound responses in intact specimens. Rather, we suspect that central nervous system temporal patterning of command motor impulses may regulate flash patterns.

Copepods generally live under conditions of high kinematic viscosity and low Reynolds numbers (Vogel, 1981). The ejection of luminous material beyond the boundary layer of the integument presents a problem under these conditions. Experiments with scale copepod

models in flow tanks indicate that an artificial secretion of a short pressure pulse produces a torus of secretory product that escapes from the boundary layer (Herring, 1988). Luminous cells in excised *G. princeps* abdomens were able to eject luminescent material beyond the cuticular boundary layer. Thus luminescent material is apparently secreted from the abdominal luminous cells as a short pressure pulse. Intact specimens also commonly flex the abdomen and burst/escape swim to further eject luminous material and displace themselves from the luminous secretion (Bowlby and Case, in press).

Acknowledgments

The authors wish to thank the captains and crews of the R. V. *New Horizon* and R. V. *Point Sur*. J. Childress generously provided ship time, and M. Latz, A. Grutter, and K. Linberg provided technical assistance. Supported by the Office of Naval Research (Contracts N00014-84-K-0314 and N00014-87-K-0044).

Literature Cited

Anctil, M., and J. F. Case. 1977. The caudal luminous organs of lantern fishes: general innervation and ultrastructure. *Am J Anat.* **149:** 1–22.

Anderson, P. A. V., and J. F. Case. 1975. Electrical activity associated with luminescence and other colonial behavior in the pennatulid *Renilla kollikeria*. *Biol. Bull.* **149:** 80–95.

Baguet, F., and J. Case. 1971. Luminescent control in *Porichthys* (Teleostei): excitation of isolated photophores. *Biol. Bull.* **140:** 15–27.

Bannister, N. J., and P. J. Herring. 1989. Distribution and structure of luminous cells in four marine copepods. *J. Mar. Biol. Assoc. UK* **69:** 523–533.

Barnes, A. T., and J. F. Case. 1972. Bioluminescence in the mesopelagic copepod, *Gaussia princeps* (T. Scott). *J. Exp. Mar. Biol. Ecol.* **8:** 53–71.

Bassot, J. M., A. Bilbaut, G. O. Mackie, L. M. Passano, and M. Pavans De Ceccatty. 1978. Bioluminescence and other responses spread by epithelial conduction in the siphonophore *Hippopodius*. *Biol. Bull.* **155:** 473–479.

Bowlby, M. R., and J. F. Case. 1989. Endogenous bioluminescent characteristics of a mesopelagic copepod. *Am. Zool.* **29:** 37A. (Abstract)

Bowlby, M. R., and J. F. Case. in press. Flash kinetics and spatial patterns of bioluminescence in the copepod *Gaussia princeps*. *Mar. Biol.*

Brehm, P. 1977. Electrophysiology and luminescence of an ophiuroid radial nerve. *J. Exp. Biol.* **71:** 213–227.

Buck, J., and J. F. Case. 1961. Control of flashing in fireflies. I. The lantern as a neuroeffector organ. *Biol. Bull.* **121:** 234–256.

Campbell, A. K. 1988. *Chemiluminescence: Principles and Application in Biology and Medicine.* VCH/Horwood, Chichester.

Campbell, A. K. 1989. Living light: biochemistry, function and biomedical applications. *Essays Biochem.* (Biochemical Soc., Lond.) **24:** 41–81.

Case, J. F., and J. Buck. 1963. Control of flashing in fireflies. II. Role of central nervous system. *Biol. Bull.* **125:** 234–250.

Case, J. F., and L. G. Strause. 1978. Neurally controlled luminescent systems. Pp. 331–366 in *Bioluminescence in Action*, P. J. Herring, ed. Academic Press, New York.

Childress, J. J. 1977. Effects of pressure, temperature and oxygen on the oxygen-consumption rate of the midwater copepod *Gaussia princeps*. *Mar. Biol.* **39:** 19–24.

Childress, J. J., A. T. Barnes, L. B. Quetin, and B. H. Robison. 1978. Thermally protecting cod ends for the recovery of living deep-sea animals. *Deep-Sea Res.* **25:** 419–422.

Clarke, G. L., R. Conover, C. David, and J. Nicol. 1962. Comparative studies of luminescence in copepods and other pelagic marine animals. *J. Mar. Biol. Assoc. UK* **42:** 541–564.

Dennell, R. 1940. On the structure of the photophores of some decapod Crustacea. *Discovery Rep.* **20:** 307–382.

Harvey, E. N. 1952. *Bioluminescence.* Academic Press, New York.

Herrera, A. A. 1977. The physiology of bioluminescence in polynoid worms. Ph.D. Dissertation, University of California, Los Angeles.

Herring, P. J. 1988. Copepod luminescence. *Hydrobiologia* **167/168:** 183–195.

Kay, R. H. 1965. Light-stimulated and light-inhibited bioluminescence of the euphausid *Meganyctiphanes norvegica* (G. O. Sars). *Proc. R. Soc. Lond. (B)* **162:** 365–386.

Kay, R. H. 1966. The inhibition of optically stimulated bioluminescence in *Meganyctiphanes norvegica*. George Allen and Unwin Ltd., London.

Latz, M. I., M. R. Bowlby, and J. F. Case. 1990. Recovery and stimulation of copepod bioluminescence. *J. Exp. Mar. Biol. Ecol.* **136:** 1–22.

Latz, M. I., T. M. Frank, M. R. Bowlby, E. A. Widder, and J. F. Case. 1987. Variability in flash characteristics of a bioluminescent copepod. *Biol. Bull.* **173:** 489–503.

Linberg, K., and J. F. Case. 1982. Comparative ultrastructure of adult light organs in synchronously and asynchronously flashing fireflies. MA. Thesis, University of California, Santa Barbara.

Nicol, J. A. C. 1967. The luminescence of fish. *Symp. Zool. Soc. Lond.* **19:** 27–55.

Smith, D. S. 1963. The organization and innervation of the luminescent organ in a firefly, *Photuris pennsylvanica* (Coleoptera). *J. Cell Biol.* **16:** 323–359.

Vogel, S. 1981. *Life in Moving Fluids.* The University Press, Princeton, NJ.

Reference: *Biol. Bull.* **180**: 447–452. (June, 1991)

Short-Term Metallothionein and Copper Changes in Blue Crabs at Ecdysis

DAVID W. ENGEL[1] AND MARIUS BROUWER[2]

[1]*National Marine Fisheries Service, NOAA, Southeast Fisheries Center, Beaufort Laboratory, Beaufort, North Carolina 28516, and Duke University Marine Laboratory, Marine Biomedical Center, Beaufort, North Carolina 28516*

Abstract. We have previously demonstrated that the small metal-binding protein, metallothionein (MT), plays an important role in the metabolism of Cu and Zn during the molt cycle of the blue crab, *Callinectes sapidus*. To further delineate the role of MT in the regulation of both metals, the distribution of copper and zinc was examined immediately after ecdysis in the blue crab. Hemolymph, digestive gland, and stomach were analyzed, by atomic absorption spectrophotometry (AAS), for total metal concentration in crabs at different molt stages, from premolt (D_3) through paper shell (B_2), and including intermolt (C_4). Cytosolic extracts were prepared from digestive glands of individual crabs and analyzed, by gel filtration chromatography and AAS, for MT, copper, and zinc. The short-term changes in metal concentrations in the tissues, and those in MT and metals in the cytosol were dramatic. Transient changes in the metals bound to MT correlated well with the loss of copper from the hemolymph and the digestive gland. The observed changes occurred over a period of 90 min after ecdysis. The data suggest that copper is stripped from hemocyanin in the digestive gland after ecdysis, displacing zinc from MT in the cytosolic pool. We hypothesize that the copper/zinc-MT complex may then be sequestered in lysosomes and eliminated into the gut and out in the feces. A discriptive flow model showing the involvement of MT in copper and zinc partitioning after ecdysis in the blue crab has been constructed.

Introduction

Recent investigations have demonstrated that molting in the blue crab, *Callinectes sapidus*, profoundly affects the tissue and cytosolic concentrations and partitioning of copper and zinc (Engel, 1987; Engel and Brouwer, 1987). At molt the concentration of circulating hemocyanin, the copper-containing respiratory protein of crustaceans, decreases dramatically. In the blue crab this decrease is about 60% (Mangum *et al.*, 1985; Engel, 1987). Because hemocyanin is a large copper-containing protein that occurs in high concentrations (~50 mg/ml corresponding to 0.67 m*M* protein and 1.33 m*M* of copper), its degradation releases significant amounts of copper into the cytosolic metal pools. The rapidity of the events, and the reactivity of the copper, dictate that some mechanism must be present to detoxify the copper and to assist in the excretion or storage of the metal. In our earlier investigations, we have attempted to account for the fate of the released copper, but have been unable to find any pool of the metal stored in the tissues of animals in the papershell or early hard crab stages. These results suggested that the excess copper may be excreted.

The low molecular weight metal-binding protein, metallothionein (MT), also changes in concentration and in metal composition in relation to the molt cycle (Engel, 1987; Engel and Brouwer, 1987). The changes that have been observed in MT correlate with the metabolic requirements for copper and the synthesis and turnover of hemocyanin (Engel and Brouwer, 1987; Brouwer *et al.*, 1989). Cu-MT from marine crustaceans can be separated into three different forms (Brouwer *et al.*, 1986). The Cu-MT(1) and Cu-MT(2) isoforms cannot reactivate apohemocyanin *in vitro* (Brouwer *et al.*, 1989). However, Cu-MT(3), which differs in amino acid composition from MT(1) and MT(2), can serve as a copper donor for apohemocyanin, and can reconstitute its oxygen-binding function (Brouwer *et al.*, 1989).

Received 22 August 1990; accepted 27 December 1990.

We suspected that, during the breakdown of hemocyanin, the liberated copper is bound to MT and excreted from the crab. To test this hypothesis, we examined blue crabs just prior to, during, and immediately after ecdysis to determine how the copper is excreted, and to elucidate the mechanism and time course of the process.

Materials and Methods

All of the premolt and postmolt crabs used in these experiments were obtained from commercial blue crab shedding operations at Beaufort, North Carolina. The premolt crabs were selected at the site and transported to the laboratory for sampling of tissues. Tissue samples from postmolt animals were collected on site at different times after ecdysis. Hemolymph samples were placed on ice, and the digestive gland samples were frozen on dry ice. The molt stages that were sampled in this investigation were: premolt, D_3 and D_4; soft crab, A_1 and A_2; and papershell B_1 and B_2. The timed tissue samples were taken from A_1 stage crabs at 0, 15, 45, 60, and 90 min after ecdysis.

The concentrations of copper and zinc were determined in samples of digestive gland, stomach, and hemolymph from individual blue crabs. The hemolymph samples were collected by severing an appendage between two joints and collecting the hemolymph in polyethylene vials. Hemolymph was analyzed for hemocyanin, copper, and zinc concentrations (Engel and Brouwer, 1987). Digestive glands and stomachs were collected for total metal analysis. Portions of the digestive glands were stored at −70°C for the determination of the cytosolic distribution of metals and metallothioneins.

Tissue samples used for metal analysis were dried at 100°C for 24 to 48 h and wet ashed with concentrated HNO_3 at 90°C. The residue was dissolved in 0.25 *N* HCl, and the concentrations of copper and zinc were measured by flame atomic absorption spectrophotometry. Preparative and measurement techniques were calibrated against the National Bureau of Standards, Oyster Reference Material #1566.

The cytosolic distribution of copper, zinc, and MT was determined by gel filtration chromatography with Sephadex G-75 (Engel, 1987). In these investigations, a computer program was developed that allows for the averaging of elution profiles so that there is less subjectivity in the evaluation of results. The program requires the use of uniform methodologies, and provides metal concentrations in each fraction in terms of micromoles of metal per kilogram wet weight of tissue.

Data on molt-induced changes in tissue metal concentrations were tested for significance ($P < 0.05$) by analysis of variance and Tukey's studentized range test. The cytosolic distributions of copper and zinc were analyzed with the assistance of a computer program developed in our Laboratory that gave average elution profiles.

Results

The concentrations of hemocyanin, copper, and zinc in the hemolymph, and of copper and zinc in the digestive gland, varied with molt stage (Figs. 1, 2). Significant changes occurred throughout the molt cycle, in the level of hemocyanin, and in the concentrations of copper and zinc in the hemolymph and digestive gland (ANOVA, $P < 0.05$). In the hemolymph, concentrations of hemocyanin, copper, and zinc decreased significantly ($P < 0.05$) at ecdysis, between D_4 and A_1, and remained at reduced levels throughout the papershell stage. There was some indication that the hemocyanin concentration was increasing at the end of the papershell stage (Fig. 1). In the digestive gland, a transient, significant ($P < 0.05$) increase in copper concentration occurred in stage A_1 relative to stages D_4 and A_2 (Fig. 2). This increase in copper concentration in the digestive gland coincides with the decreases in the concentrations of both hemocyanin and copper in the hemolymph. The subsequent decrease in copper concentration in A_2 suggests that the copper is being lost from the tissue.

The transient increase in copper during A_1 is not seen with zinc (Figs. 1, 2). When the changes in copper and zinc in the digestive gland are compared on a molar basis, an increase of about 0.3 m*M*/kg in copper is revealed between D_4 and A_1, and a concomitant 0.3 m*M*/kg decrease occurs in zinc (Fig. 2). However, this copper/zinc relation does not hold as the crabs go from A_1 to A_2. The data suggest that, during those stages of the molt cycle, both copper and zinc are lost from the digestive gland.

To determine the possible route of metal loss by the crabs during the period following ecdysis, stomachs of hard (C_4), soft (A_1–A_2), and papershell (B_1–B_2) crabs were examined for concentrations of copper and zinc (Fig. 3). The data from these measurements show that the stomachs of soft crabs have significantly higher concentrations of copper and zinc ($P < 0.05$) than those of either hard crabs or papershell crabs, which were not significantly different. Such information supports the idea that the pathway for the loss of copper and zinc following ecdysis leads from the digestive gland to the gut, and that the metals are excreted in the feces (*e.g.*, digestive gland → stomach → gut → feces).

Because the changes in copper and zinc concentrations in the digestive gland apparently occur quite rapidly, short-term measurements were made of the cytosolic partitioning of copper and zinc (*i.e.*, the portion of metals bound to MT). Although the total amount of copper changed, the partitioning of copper was similar at each sampling time. The maximum amount of copper was bound to MT

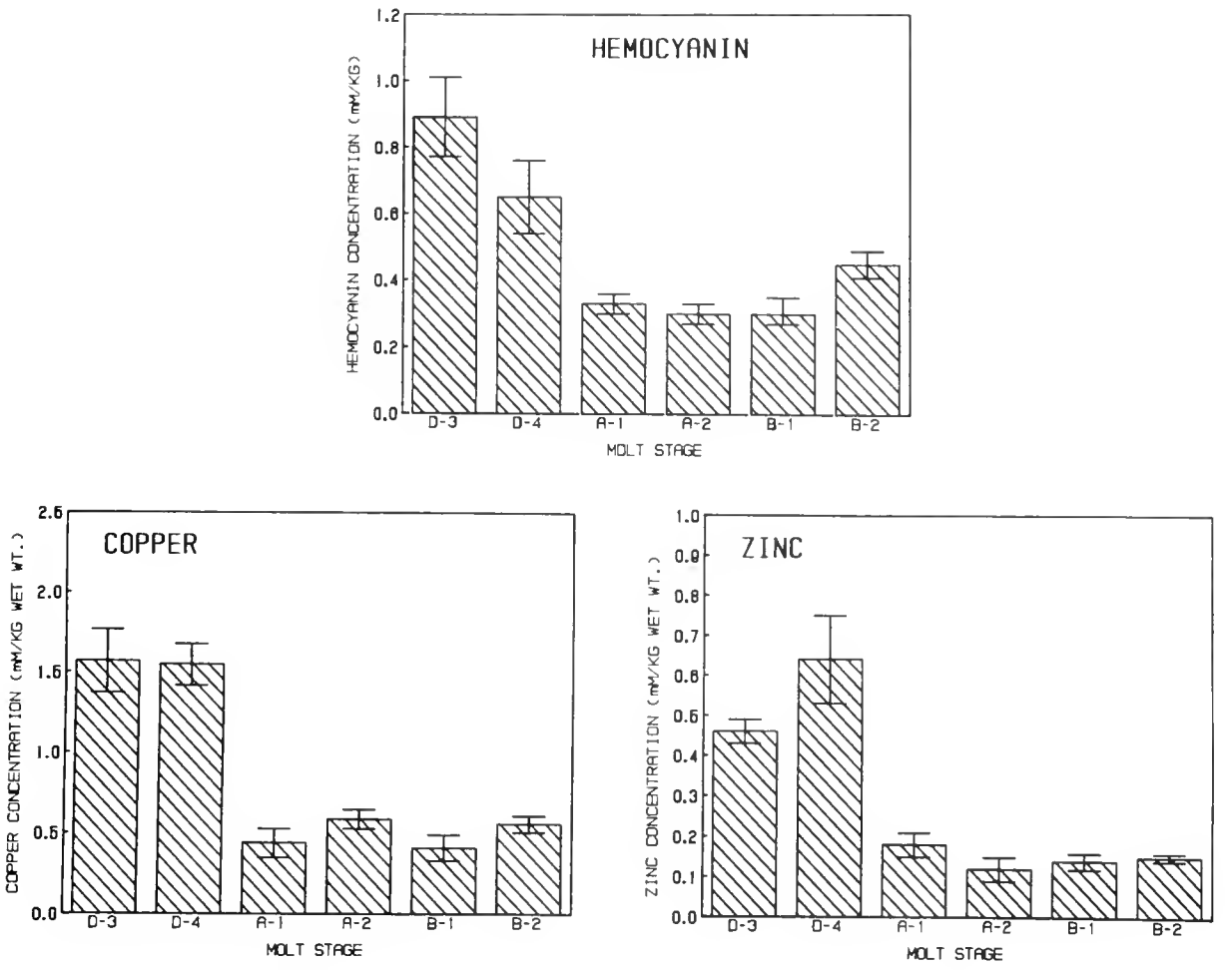

Figure 1. Histograms showing the average concentrations of hemocyanin, copper and zinc in the hemolymph at selected stages of the molt cycle. All concentrations of hemocyanin, copper and zinc are reported in millimoles/kilogram wet weight of sample. Each bar represents the mean of six crabs and the vertical lines above and below the mean describe one standard error.

60 min after ecdysis (Fig. 4). While the amount of Cu-MT increased in the cytosol from 15 through 60 min after ecdysis, the amounts of Zn-MT decreased over the same period. In the period between 45 and 60 min after ecdysis, there was about a 10 micromolar increase in copper bound to MT and a similar decrease in the amount of bound zinc. This observation suggests that zinc was displaced from the MT by copper released during the rapid degradation of hemocyanin following ecdysis. Cytosolic copper concentrations were initially low, but had increased five fold by 60 min after ecdysis (Fig. 5), which correlates well with the observed increase in copper bound to MT (Fig. 4). There was very little change in cytosolic zinc concentration for the first 60 min after ecdysis, but it did decrease between 60 and 90 min. These decreases in both Cu and Zn-MT and in total cytosolic copper between 60 and 90 min suggests again that metal was lost from the digestive gland at this time.

Discussion

From the data collected in our current and earlier experiments (Engel, 1987; Engel and Brouwer, 1987) on the mechanisms of copper and zinc metabolism during the molt cycle of the blue crab, we have constructed a diagram showing the relationships between the breakdown of hemocyanin and the changes in the concentrations of Cu-MT and Zn-MT (Fig. 6). Three significant changes occur in the metals bound to MT during the molt cycle. The first is at the beginning of premolt when the metals bound to MT change from predominantly copper to zinc. The second occurs within 90 min after ecdysis when there is a transient pulse of copper bound to the predominantly zinc-MT. The third change occurs during stages B_1 and B_2 when the MT once again becomes primarily a copper protein, and this change is correlated with synthesis of hemocyanin (Engel and Brouwer, 1987).

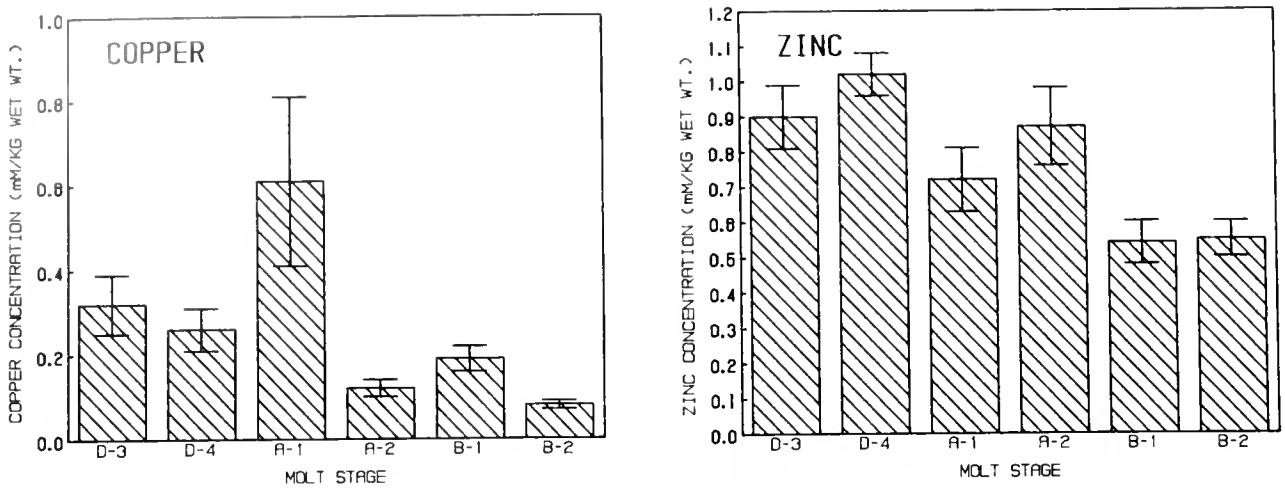

Figure 2. Histograms showing the copper and zinc concentrations in digestive glands of blue crabs at selected stages of the molt cycle. All concentrations and error designations are the same as described in Figure 1.

At the end of the intermolt stage, C_4, and the beginning of premolt, D_1, the metal bound to MT changes from predominantly copper to zinc. The trigger for this change has yet to be demonstrated. We hypothesize, however, that the reduction in the concentrations of Cu-MT is correlated with reduced hemocyanin synthesis and an increased rate of Zn-carbonic anhydrase synthesis in preparation for molting. These types of changes, which preceed molting, could be initiated by increases in the concentration of the molting hormone, ecdysteroid (Soumoff and Skinner, 1983). While the magnitude of the changes in the metals bound to MT are large, from 90% copper to 90% zinc (Engel, 1987), no information is available on either the timing or rate of the change.

The transient pulse of copper bound to MT in the digestive gland cytosol immediately after ecdysis (*i.e.*, within 90 min) is undoubtedly correlated with the catabolism of hemocyanin. Because there is roughly a 60% decrease in hemocyanin concentration in the hemolymph shortly after molt (Fig. 1) (Mangum *et al.*, 1985; Engel, 1987), a large quantity of copper should be released into the cytosol of the digestive gland in a relatively short time. The observed pulse of Cu-MT, therefore, represents the detoxification of the liberated copper by an *in situ* processes in the digestive gland cytosol. To more fully describe our hypothesis, a flow diagram has been developed that shows the interaction between the released copper and the cytosolic pool of Zn-MT present at ecdysis (Fig. 7). The mechanism of copper detoxification may be a straightforward substitution process involving the pool of Zn-MT already present in the digestive gland. This large concentration of Zn-MT in the cytosol acts as a sink for the copper that is released during the degradation of hemocyanin. Because copper has a higher binding affinity for MT than does zinc, it simply displaces the zinc already bound to MT. This process would account for the rapid kinetics, because *de novo* synthesis of MT is unlikely to occur rapidly (Hildebrand and Enger, 1980). This substitution process will not result in an all-copper protein. After the substitution, a significant portion of the Cu/Zn-MT complex is excreted via lysosomes into the digestive tract and out in the feces, and the remainder may serve as the initial copper donor for renewed hemocyanin synthesis. The excess zinc not bound to MT can either be excreted

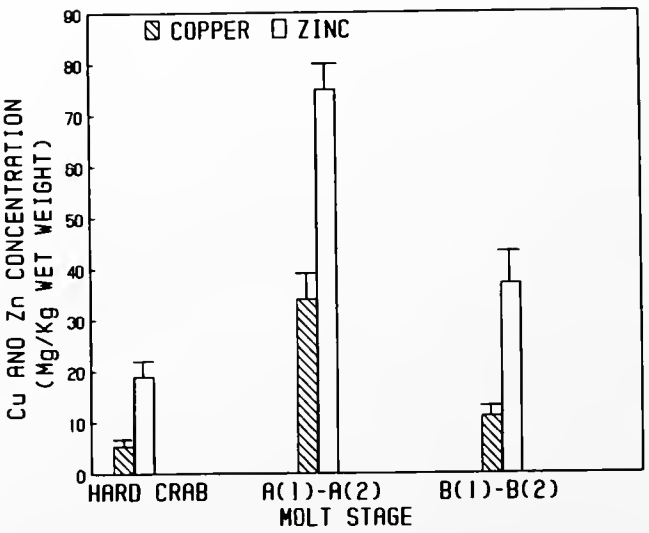

Figure 3. Histograms showing the copper and zinc concentrations in the stomachs of hard crabs [n = 8], soft crabs (A_1 and A_2) [n = 5], and papershell crabs (B_1 and B_2) [n = 6]. Concentrations are given as milligrams of metal per kilogram of tissue plus and minus one standard error of the mean.

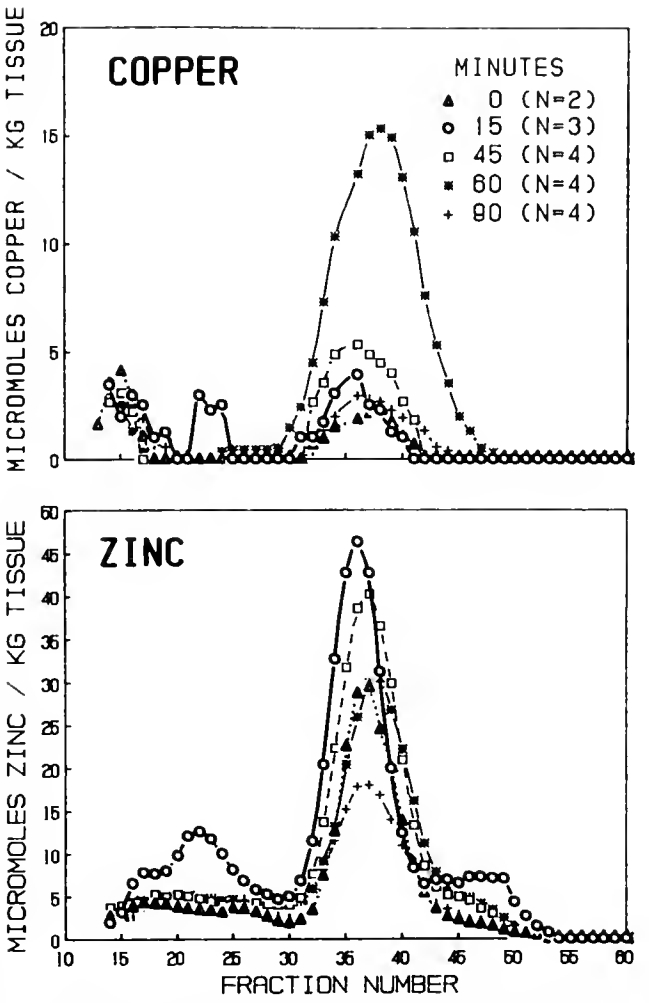

Figure 4. Average elution profiles of protein bound copper and zinc in digestive gland cytosols at five specific times after ecdysis (0, 15, 45, 60, and 90 min). Each elution profile is a computer generated average of from 2 to 4 individual crabs. The concentrations of copper and zinc are normalized to the wet weight of the tissue used and to the amount of cytosol applied to the column.

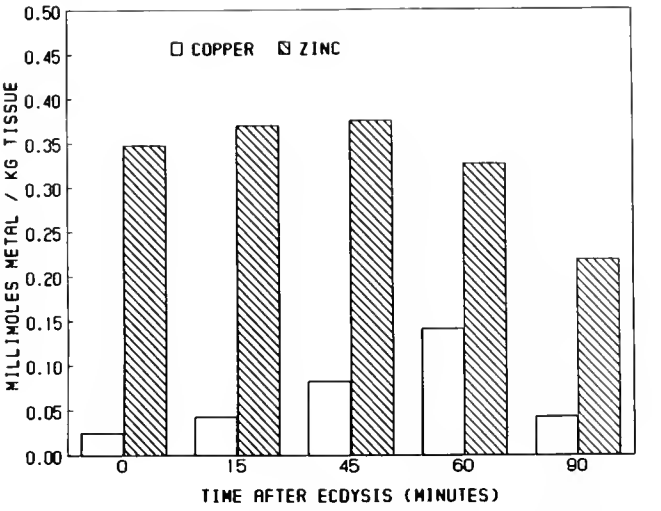

Figure 5. Histograms showing the average cytosolic concentrations of copper and zinc (*i.e.*, millimoles/kg) in digestive glands at five times after ecdysis (0, 15, 45, 60, and 90 min). These metal concentrations are calculated from the cytosolic samples applied to the Sephadex G-75 column.

in lysosomes via the gut, or via the green gland in the urine.

Our functional model of copper detoxification agrees with the observations made by Al-Mohanna and Nott (1989) on the shrimp *Penaeus semisulcatus*. In their electron microscopic examination of the shrimp hepatopancreas during the molt cycle, they demonstrated the presence of copper and sulfur containing granules in the R cells of the hepatopancreas using EDAX energy dispersive microanalysis. These granules are released to the lumen of the hepatopancreas through cellular degeneration and sloughing. The occurrence of these copper containing granules may be associated with the synthesis and turnover of hemocyanin.

The conversion of the MT back to a copper protein occurs later in the postmolt period, B_1 and B_2, and precedes the resynthesis of hemocyanin (Engel, 1987; Engel and Brouwer, 1987), strongly suggesting that Cu-MT may act, directly or indirectly, as the source of copper for hemocyanin synthesis (Fig. 7). Brouwer and coworkers (1986, 1989) have demonstrated that Class-I Cu-MTs [*i.e.*, related in primary structure to equine renal MT (Fowler *et al.*, 1987)] isolated from the hepatopancreas of the American lobster cannot transfer their copper to hemocyanin. However, a third copper-protein, which has a lower molecular weight than the Class-I MTs, contains less cysteine, and is much more acidic, has been isolated from the lobster hepatopancreas. This copper-protein,

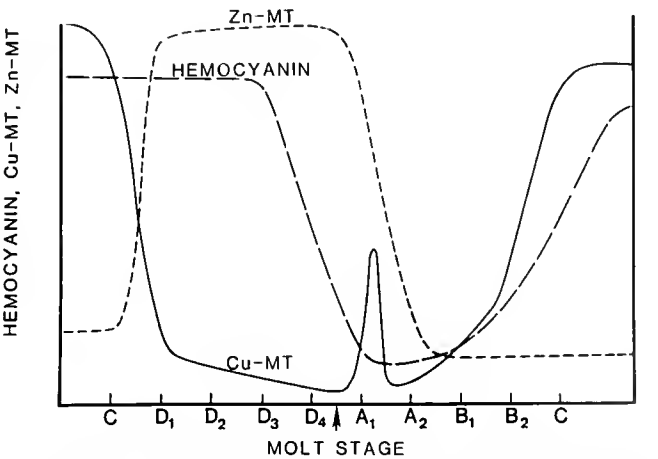

Figure 6. A descriptive diagram showing the relationships between hemocyanin in the hemolymph and copper and zinc MT during the molt cycle of the blue crab. The arrow denotes the time of ecdysis.

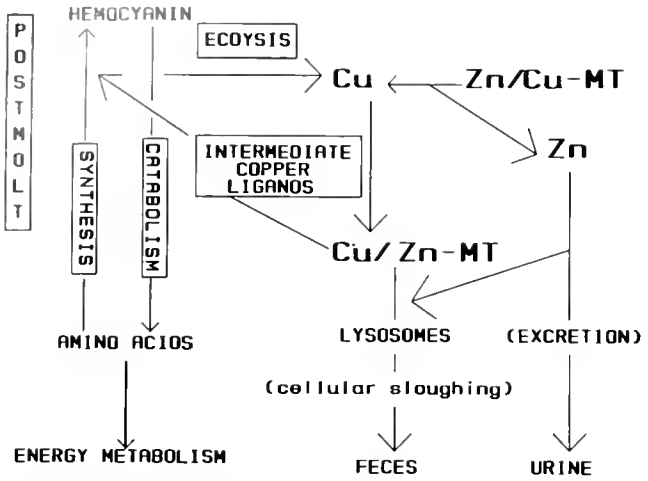

Figure 7. A flow diagram of the synthetic and catabolic pathways for hemocyanin and the interactions between copper, zinc, and copper/zinc-MT in the digestive gland of the blue crab immediately after ecdysis and during the later postmolt recovery period. The diagram includes the pathways for detoxification of copper released from hemocyanin, excretion of copper and zinc (Engel, 1987; Engel and Brouwer, 1987; and Al-Mohanna and Nott, 1989), and the presence of a lower molecular weight compound that is active in the transfer of copper to the apoprotein during hemocyanin synthesis (Brouwer, unpub. data).

tentatively classified as a Class II-MT, has been found effective in restoring the oxygen binding capacity of apohemocyanin (Brouwer *et al.*, 1989). Whether copper exchange occurs between the Class I and II-MTs remains to be demonstrated.

This investigation gives further support to the hypothesis that the function of metallothionein in normal organisms is in the regulation of nutritional metals. Through the use of the normal crustacean growth process of molting, we have been able to identify some of the functional mechanisms of cytosolic metal regulation involving MT. These data also serve to point out that if a protein such as MT is to be used as an indicator of animal health, the processes that control its abundance and turnover must be demonstrated.

Acknowledgments

The authors thank Mr. William J. Bowen, III for his efforts to collect the tissue samples from molting blue crabs at the desired times, and the local crab shedders for their cooperation (*i.e.*, Mr. Garry Culpepper, Hooper Family Seafood, and Pitmann Seafood). The authors also acknowledge the assistance of the ADP/Biometrics Unit in the statistical analysis of the data and in the development of the computer program for averaging elution profiles. This research was supported by the National Marine Fisheries Service and by the National Institutes of Health Grant ESO 4074 (M.B.).

Literature Cited

Al-Mohanna, S. Y., and J. A. Nott. 1989. The accumulation of metals in the hepatopancreas of the shrimp *Penaeus semisulcatus* de Hann (Crustacea: Decapoda) during the molt cycle. Pp. 195–207 in *Proceedings of the First Arabian Conference on Environment and Pollution.* Allen Press, Oxford.

Brouwer, M., D. R. Winge, and W. R. Gray. 1989. Structural and functional diversity of copper-metallothionein from the American lobster, *Homarus americanus. J. Inorg. Biochem.* **35:** 289–303.

Brouwer, M., P. Whaling, and D. W. Engel. 1986. Copper-metallothioneins in the American lobster, *Homarus americanus:* potential role as Cu(I) donors to apohemocyanin. *Environ. Health Perspect.* **65:** 93–100.

Engel, D. W. 1987. Metal regulation and molting in the blue crab, *Callinectes sapidus:* copper, zinc, and metallothionein. *Biol. Bull.* **172:** 69–82.

Engel, D. W., and M. Brouwer. 1987. Metal regulation and molting in the blue crab, *Callinectes sapidus:* metallothionein function in metal metabolism. *Biol. Bull.* **173:** 237–249.

Fowler, B. A., C. E. Hildebrand, Y. Kojima, and M. Webb. 1987. Nomenclature of metallothionein. *Experientia Suppl.* **52:** 19–22.

Hildebrand, C. E., and M. D. Enger. 1980. Regulation of Cd^{2+}/Zn^{2+}-stimulated metallothionein synthesis during induction, deinduction, and superinduction. *Biochemistry* **19:** 5850–5857.

Mangum, C. P., B. R. McMahon, P. L. DeFur, and M. G. Wheatly. 1985. Gas exchange, acid-base balance, and the oxygen supply to the tissues during a molt of the blue crab, *Callinectes sapidus. J. Crust. Biol.* **5:** 188–206.

Soumoff, C., and D. M. Skinner. 1983. Ecdysteroid titers during the molt cycle of the blue crab resembled those of other crustacea. *Biol. Bull.* **165:** 321–329.

Reference: *Biol. Bull.* **180**: 453–465. (June, 1991)

Musculature Associated with the Water Canals in Freshwater Mussels and Response to Monoamines *In Vitro*

DAVID B. GARDINER, HAROLD SILVERMAN, AND THOMAS H. DIETZ

Department of Zoology and Physiology, Louisiana State University, Baton Rouge, Louisiana, 70803

Abstract. The gills of freshwater mussels perform many functions that depend on water flow through the water canals and channels. Regulation of water flow depends in part on ciliary activity and in part on the contraction of musculature underlying the gill filament and water channel epithelium. Obliquely striated muscles control water canal openings (ostia) at the base of the filaments and also at the entry into the water channel (internal ostia, IO). The muscles adjacent to the ostia are oriented in an anterior-posterior direction (perpendicular to gill filaments), and those controlling the internal ostia are oriented in a dorso-ventral direction (parallel to gill filaments). Small bundles of fibers radiate from the major dorso-ventral IO muscle bands and appear to insert at the base of the water canal epithelial cells at the canal-channel junction. Both muscular bands are closely associated with the branchial nerves in the gill. When gills are exposed to 10^{-5} *M* serotonin *in vitro*, both ostial openings dilate and gill ciliary activity increases. The net result of serotonin treatment is an increase in ciliary activity, a maximal opening of the water canal ostia, and, presumably, an increase in water flow through the gill.

Introduction

The gill in freshwater mussels is responsible for many of the functions associated with water flow through the animal. For example, ion transport, feeding, reproduction, and respiration are all dependent on the pattern of water flow through the gill. The gill ciliary activity generates the force for water flow (Riisgard and Mohlenberg, 1979; Jorgensen, 1982, 1989; Paparo, 1988; Silvester, 1988; Sleigh, 1989), and water flow has been calculated from data characterizing ciliary activity (Jorgensen 1989; Sleigh, 1989). The pattern of flow through the gill begins with water moving across the gill filaments and through the ostial (O) openings that lead into the water canals. From the canals, water flow is directed through the internal ostia (IO), into the central water channels that conduct water into the suprabranchial chamber, and then out through the excurrent siphon (see Fig. 1).

The specializations found in the various gill epithelia indicate that ion transport and perhaps respiration take place across the internal epithelial lining the water canals and channels (Kays *et al.*, 1990). The epithelial cells of the gill showing the most enzymatic activity for carbonic anhydrase are located on the internal epithelial surfaces (Kays *et al.*, 1990). In addition, the cells showing the most oxidative activity form the epithelia lining the canals. The ciliated epithelia lining the filaments do not appear to contain any of the specializations associated with ion transporting cells and are larger (apical to basal surface) than one would expect for gas exchange. They appear to be providing protection, as well as the driving force for water flow.

While ciliary activity may be the principal driving force for water flow, the pattern of flow may be regulated by the muscles present in the gill tissue. In oysters, the gill musculature and vascular changes control the diameter of the ostia (Galtsoff, 1964; Nelson, 1941; Nelson and Allison, 1940) and influence the rate of water flow through the gill (Nelson, 1941; Nelson and Allison, 1940). Similar regulation of ostial diameter by muscles in unionid gills

Received 12 December 1990; accepted 8 March 1991.

Abbreviations: Acetylcholine (ACh); Epinephrine (Epi); Gamma Aminobutyric Acid (GABA); Internal Ostia (IO); Norepinephrine (Norepi); Ostia (O); Scanning Electron Microscopy (SEM); Transmission Electron Microscopy (TEM)

would control water flow in response to the osmoregulatory (Dietz and Graves, 1981), respiratory, and even the reproductive needs of the animal (Silverman, 1989; Richard *et al.*, 1991). Muscular control also offers the possibility of blocking flow into the water channels. Previously we showed that the water channels of the Lampsilinae are functionally occluded during reproduction (Silverman *et al.*, 1987).

In the research reported here, we have used morphological techniques to describe the musculature associated with the water canals of the freshwater unionid gills. We have also demonstrated that serotonin, a well-known inhibitor of muscle contraction in a number of molluscan systems (Twarog 1954; Cambridge, 1959; Twarog and Cole, 1972; Jorgensen, 1976; Satchell and Twarog, 1978; Kobayashi and Hasimoto, 1982), causes the canal musculature to relax, allowing the water canals to expand. Serotonin increases ciliary activity in a variety of marine mussels (Gosselin *et al.*, 1962; Aiello and Guideri, 1966; Aiello, 1970; Paparo and Murphy, 1975; Jorgenson, 1976; Capatane *et al.*, 1978; Paparo, 1980; Sanderson and Satir, 1982; Sanderson *et al.*, 1985), and dopamine depresses ciliary activity in marine bivalves (Catapane *et al.*, 1978; Paparo, 1980). However, we report here that both serotonin and dopamine increase gill ciliary activity in the freshwater unionids.

Materials and Methods

Animal maintenance

The unionid mussels *Anodonta grandis* and *Ligumia subrostrata* were collected from ponds near Baton Rouge, Louisiana. The animals were maintained in aerated artificial pondwater (0.5 m*M* NaCl, 0.4 m*M* $CaCl_2$, 0.2 m*M* $NaHCO_3$, and 0.05 m*M* KCl) at 25°C and were allowed to acclimate to laboratory conditions for a week before being used. The mussels were only studied during the nonreproductive season so the gills were not being employed to brood larvae.

Preparation of gills for light and transmission electron microscopy

We opened the clams by cutting the adductor muscles, thereby exposing the lateral and medial demibranch (gill) pairs. The gills were excised and placed in a Ringer's solution designed for freshwater mussels (5.0 m*M* $CaCl_2$, 0.5 m*M* KCl, 5.0 m*M* NaCl, 5.0 m*M* $NaHCO_3$ and 5.0 m*M* Na_2SO_4) or a 30 m*M* tris(hydroxymethyl)aminomethane (tris-HCl) buffer solution, pH 7.8. After several minutes, the gills were removed and flattened on a polystyrene petri dish or pinned to a wax base.

Gills were fixed in 2% glutaraldehyde (EM grade) in 30 m*M* tris-HCl containing 1 m*M* ethylenediaminetetraacetic acid (EDTA), pH 7.8 (Silverman *et al.*, 1983, 1987). Alternatively, glutaraldehyde was added directly to the gills in freshwater mussel Ringer's solution with or without EDTA. Gills were exposed to the fixative for 2 h. During fixation, the gills were cut dorso-ventrally (parallel to gill filaments) into strips of 5–8 mm. Following fixation, gill strips were washed three times for 5 min each in either 30 m*M* tris-HCl or phosphate buffer, pH 7.8, and post-fixed in 1% aqueous osmium tetroxide for 1 h. After osmication, the gill strips were washed three times for 10 min each in deionized water and then dehydrated in a graded ethanol series (10 min in 50%, 70%, 80%, 90%, 95%, and 3 × 10 min in 100%). Two resins, Spurr's low viscosity (Polysciences, Inc.) and LR White hard grade (EMS, Inc.), were used. Gill strips to be embedded in LR White were placed in a 1:1 resin/ethanol mixture for 20 min and then into 100% LR White resin for 24 h. Fol-

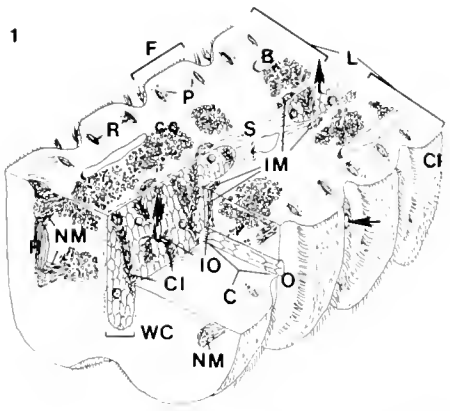

Figure 1. A schematic representation of the gill of *Ligumia subrostrata* modified from Kays *et al.* (1990). The gill consists of an ascending and descending lamella (L) organized as filaments (F) surrounding central water channels (WC). The lamellae are joined by connective tissue septa (S). The filaments are supported by discontinuous calcified chitinous rods (R) and an associated mucopolysaccharide matrix (P). Extensive extracellular calcium concretions (cc) are located in the connective tissue underlying the filaments. Blood sinuses (B) also occur in this region. Water enters the gill through ostia (O) located at the base of the filaments. The ostia open into water canals (C) which lead into the WC. The opening of the water canal into the WC is designated as the internal ostia (IO). Water moves into the WC, and is directed dorsally to the suprabranchial chamber. The general direction of water flow through the gill is indicated by the arrows. Associated with the rods are anterior-posterior oriented bands of muscle (NM); these bands are associated with nerve fibers which are oriented in the same direction. This musculature flares and inserts onto adjacent chitinous rods at discontinuities in the rods. The muscle bands alternate with ostial openings at the base of the filaments. Associated with the internal ostia are bands of muscle (IM) oriented in the dorsal-ventral direction; these bundles of muscle also are associated with nerve fibers. Water canal epithelial cells are non-ciliated microvillar cells. Ciliated cells (Cl) are oriented in rows in the water channel; the epithelial cells forming the border of the IO are also ciliated (not to scale; the top and bottom of the figure are dorsal and ventral, respectively; anterior is to the left and posterior to the right).

lowing the overnight incubation, fresh LR White resin was added, and the gill strips were embedded flat in aluminum pans at 60°C for 48 h. Gill strips embedded in Spurr's resin were initially placed in 100% propylene oxide, 3 × 20 min, followed by graded propylene oxide/resin series (20 min at 1:1, 1:2, 1:3, 1:4, 3 × 1 h at 100% resin, and 100% for 24 h) and final embedding in fresh resin at 60°C for 48 h.

Gills were sectioned for light microscopy with a Reichert-Jung Ultracut E ultramicrotome at 0.5–2.0 μm thickness with glass knives and for transmission electron microscopy (TEM) at 60–90 nm thickness with a diamond knife. Sections for light microscopy were stained according to a tribasic staining procedure developed by Grimley (1964). The gill was sectioned in two planes: (1) anterior-posterior cross-sections, and (2) frontal sections (*en face*) across the surface of the filaments. Sections for light microscopy were examined and photographed with a Nikon Microphot-FXA microscope. Sections for TEM were stained with 3% uranyl acetate for 2 min followed by Reynolds' (1963) lead citrate for 2–5 min. The sections were examined with a JOEL 100 CX transmission electron microscope operating at 80 kV.

The light micrographs of isolated chitinous rods were prepared by cutting gills into 5–6 mm longitudinal strips along the filaments and incubating the strips in calcium-free Ringer's solution containing 1000 U/ml collagenase IV (Sigma, St. Louis). After 12 h, the rods were collected by repeated centrifugations of the collagenase treated gill at 50 × *g* for 5 min and viewed with an Nikon Diaphot inverted microscope.

Neurotransmitter application

Gills were excised and placed in individual polystyrene petri dishes containing freshwater mussel Ringer's, pH 7.8. Gills were cut in half dorso-ventrally, and incubated in the Ringer's solution for 30 min with changes every 10 min. The diameter of the ostia and the internal ostia, and gill movement, were monitored with an inverted Nikon Diaphot microscope for 5 min before fixing. One of the gill halves was fixed without being exposed to putative transmitter substances by the addition of an equal volume of fixative (4% formalin and 4% glutaraldehyde in mussel Ringer's, pH 7.8) directly onto the tissue. Before fixing the control, we placed the other half of the bisected gill in a mussel Ringer's solution containing 10^{-5} *M* neurotransmitter [acetylcholine, dopamine, gamma aminobutyric acid (GABA), epinephrine, norepinephrine, or serotonin], pH 7.8.

Preparation of gills for scanning electron microscopy

After fixation, the gills were washed in a 30 m*M* tris-HCl or phosphate buffer, pH 7.8, for 15 min with changes every 5 min, and then osmicated in 1% aqueous osmium tetroxide for 1 h. After osmication, gills were washed in deionized water for 15 min with changes every 5 min. Fine micro-dissection tools were used to separate the opposing gill lamellae by severing the interlamellar septa and exposing the central water channel epithelium (see Fig. 1). Gills were cut dorsal-ventrally (parallel to filaments) every 6–10 mm and dehydrated in the graded ethanol series. The tissues were then stacked perpendicular to one another and wrapped in lens paper to ensure that they would remain flat during critical point drying. Gills were critical point dried (Denton Vacuum, Inc.) and mounted on stubs. The water channel epithelium was oriented as the facing surface. Specimens were sputter coated with gold/palladium (20 nm) and viewed with a Hitachi S-500 scanning electron microscope (SEM) with a working distance of 30 mm, operated at 25 kV.

Neurotransmitter effect on the canal ostial diameter

The dimensions of the internal ostia of gills exposed to transmitter substance were obtained from scanning electron micrographs and assessed quantitatively. Samples for scanning electron microscopy were selected at random from control and treated tissues that had remained flat after critical point drying. Three or more tissues were selected from each treatment group, and three low magnification micrographs of each sample were taken from the first three separate fields of the water channel region brought into view. Image-analysis was performed on the resulting SEM negatives. Ostial surface area and other average ostial dimensions (*i.e.,* perimeter and diameter) were calculated from digitized images using densitometry and stereology software (Image-1/AT IM5000). Statistics are based on paired Student's t-tests with significance set at $P < 0.05$.

Assay of gill ciliary activity

While the gross muscular responses in the gill to various neurotransmitters was being monitored, ciliary activity was observed to increase when the gills were exposed to serotonin or dopamine. The changes in lateral ciliary activity in *Ligumia* gills were assayed by the procedures of Paparo (1980). Ciliary beats per second was determined by synchronizing the activity with the rate of flashing of a calibrated strobe light. Gills were placed in dishes designed to allow pondwater to flow through at a rate of 0.5 ml/min. Initial measurements of the rate of ciliary beating in pondwater over 60 min were used as control values. The effect of serotonin or dopamine on the ciliary activity was analyzed after the petri dish contents were replaced with fresh pondwater containing either serotonin or dopamine and then continuing the flow at 0.5 ml/min with

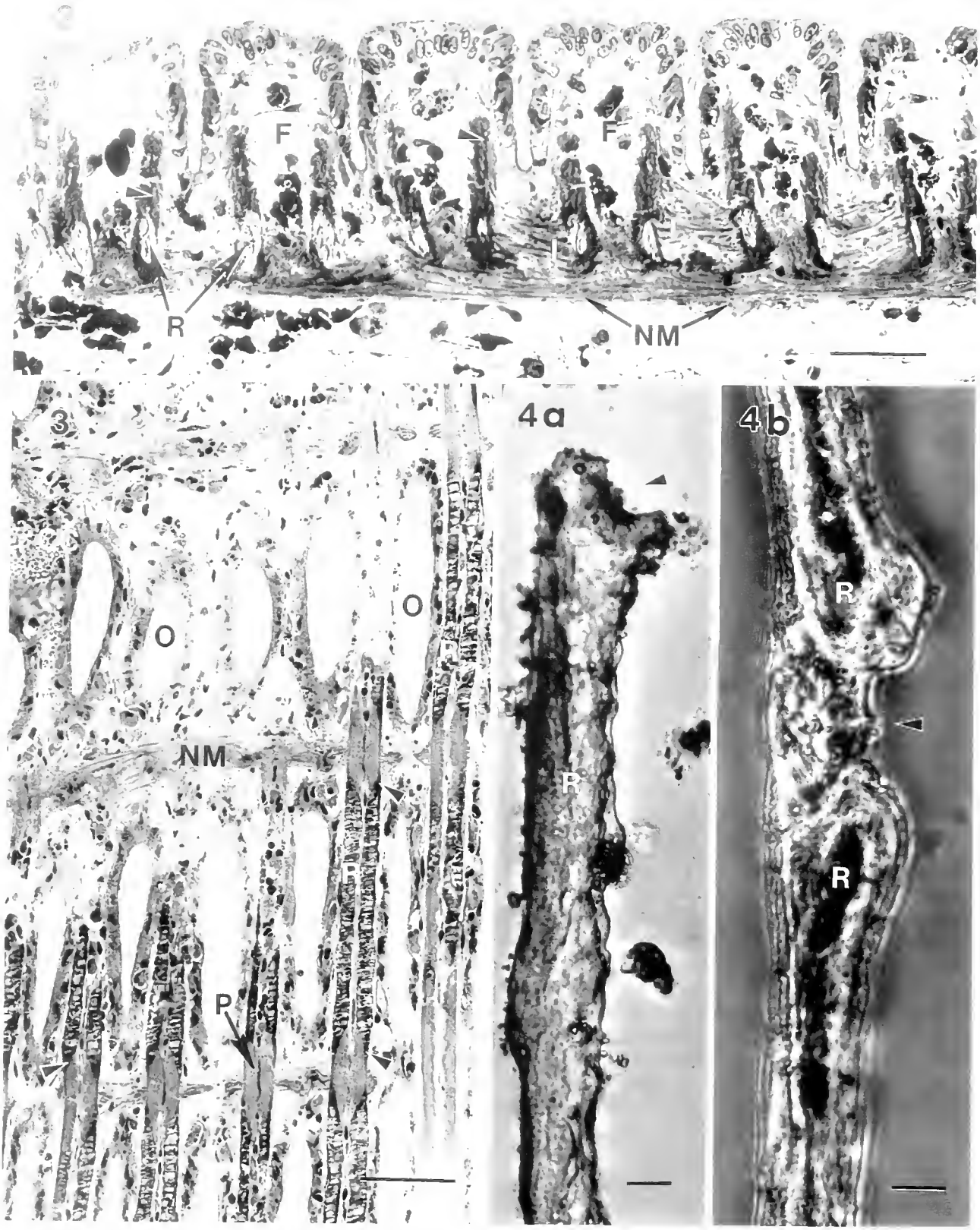

Figure 2. Light micrograph of a cross-section of the gill of *Anodonta* (anterior/posterior to the left/right). Underlying the filaments (F) is the muscular band (NM) that traverses in an anterior-posterior direction. The muscles insert (I) onto the calcified chitinous rods (R) that support the filaments. The insertion occurs as fibers of muscle extend from the main band and contacts each rod. The rods are surrounded by a mu-

fresh pondwater containing the appropriate neurotransmitter. This application of the neurotransmitter solution was maintained for 1 h; then the pondwater was removed and replaced by fresh pondwater lacking neurotransmitter, and the gill was monitored for another hour. The concentrations of serotonin and dopamine tested ranged from 10^{-6} to 10^{-4} *M*.

Rhodamine-123 treatment of gill explants

Mitochondrial activity in epithelial cells of the water canal was demonstrated with a mitochondrial fluorescence stain, rhodamine-123 (Johnson *et al.*, 1980), a positively charged lipophilic molecule that interacts specifically with mitochondrial membranes. Isolated gills were examined with a confocal imaging system supplied by Bio-Rad Laboratories (Richmond, California). Gills were excised from animals, and the interlamellar septa were cut to expose the central water channel. The gills were incubated for 20 min in pondwater containing 10 μg/ml rhodamine-123. Following incubation, the gills were placed on glass slides and covered with coverslips with petroleum jelly at the corners. The samples were viewed under a Nikon Microphot-FXA microscope equipped for confocal imaging. Serial images along the length of the water canals were captured by digitizing on the image enhancement computer.

Results

Canal-associated musculature

Two bands of musculature are directly associated with the water canals of the gill. Located at the base of the filaments are relatively thick bands of musculature, 70–72 μm and 20–23 μm in diameter for *Anodonta* and *Ligumia*, respectively. These muscle bands underlie the filaments and are oriented in the anterior-posterior direction along the entire length of the gill (Fig. 2). The muscle bands occur periodically, alternating with rows of ostia located at the base of the filaments (Fig. 3). Muscle bands occur approximately every 335 μm and every 180 μm in *Anodonta* and *Ligumia*, respectively. The rows of ostial openings connect the mantle cavity to the water canal at the base of the filaments (Figs. 1–3). The muscle bands lie perpendicular to, and run between, septations in the parallel calcified chitinous rods that support the filaments (Figs. 3, 4). The muscle appears to be attached to the end of the rods (Fig. 4). Indentations are observed at the separation points along the individual discontinuous chitinous rods. Contraction of the muscle bands pulls the rods of adjacent filaments together, reducing the water canal opening to a slit oriented in the dorsal-ventral direction. There is little musculature located in the underlying connective tissue in the vicinity of the water canal (Fig. 2) except where the water canal approaches the basal surface of the central water channel epithelium.

Another distinct band of musculature is located at the base of the canal near the opening of the water canal into the water channel (Fig. 5). These muscular bands are approximately 21 μm in thickness in *Ligumia* and are oriented dorso-ventrally (Fig. 6). The muscle bands are on either side of rows of canals and send muscle fibers into the base of the canal epithelium, that forms the IO (Figs. 6–9). This musculature appears to have the ability to control the diameter of the IO (Fig. 9).

Neurotransmitter effects on canal-associated musculature

The two muscular systems described above responded similarly to the exogenous putative neurotransmitters to which the gills were exposed. The addition of serotonin to the gills *in vitro* resulted in an immediate relaxation of

copolysaccharide substance that appears darkly stained in this micrograph (arrowheads). Ostia are not visible in this micrograph as they alternate with muscular bands along the base of the filaments (see Fig. 3). Bar = 50 μm.

Figure 3. Light micrograph of a gill from *Anodonta* cut across the face of the filaments in the dorso-ventral plane. This section is below the base of the filaments and demonstrates the alternation of water canal ostia (O) with nerve-muscle bands (NM). The periodicity of this alternation of structures is readily apparent. Note that the section is cut through the calcified rods (R). The rods taper (arrowheads) and become discontinuous every 335 μm, and it is at this tapered site that the muscle bands interact with the rods. Mucopolysaccharide (Silverman *et al.*, 1983) material (P) associated with the rods is evident at the tapered sites. A few calcium concretions (CC) are seen in the connective tissue of this micrograph. Bar = 100 μm.

Figure 4. Whole mounts of calcified chitinous rods from gills digested with collagenase. (a) Is a portion of a rod in which soft tissue has been completely digested away. Rods are discontinuous allowing the nerve muscle tract to pass in the anterior-posterior direction between adjacent filaments. The ends of the rods where muscles attach are flared and indented (arrowhead). (b) Is partially digested with collagenase and the remains of soft tissue/mucopolysaccharide (arrowhead) can be seen inserting on two rods (R) oriented end to end. The internal darker portion of the rod is calcified. The less dense perimeter contains layers of less calcified mucopolysaccharide. Bars in a and b = 2 μm.

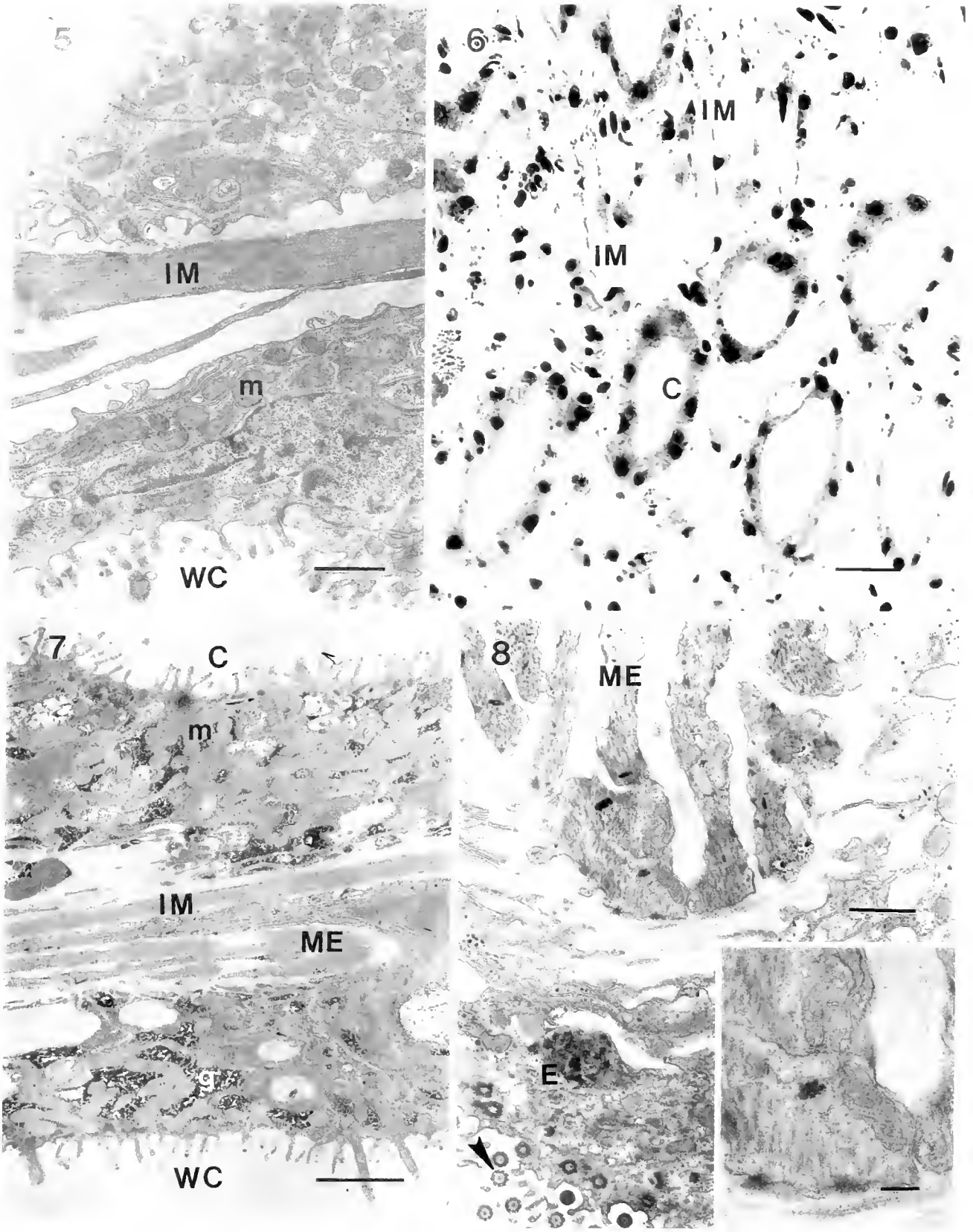

Figure 5. A TEM of the base of the water channel of a *Liguania* gill. The water channel (WC) is located at the bottom of the micrograph. The epithelium of a water canal near its junction with the water channel is located at the top of the micrograph. Note the major obliquely striated muscle band (IM) located in the connective tissue at the base of the water channel epithelium. Mitochondria (m) are indicated in the mi-

the external and internal musculature, thereby increasing the diameter of the ostia (Fig. 10) and the internal ostia (Fig. 11). These results were visible by gross observation of the preparations with an inverted light microscope (Fig. 10). The relaxation was maintained throughout the 5-min observation period. In contrast, none of the other transmitters tested appeared to have any visible effect.

The internal ostia were examined by SEM and the average dimensions of the internal ostia were measured in control and experimental treatment groups (Table I). The average dimensions of the internal ostia in a serotonin-treated gill are 2–3 fold larger than controls (Table I, Fig. 11). The internal ostia of the controls have a distinct long axis (height) showing indented edges (Figs. 11, 12). The fully relaxed serotonin-treated ostia have a smooth, uniform oval to circular shape (Figs. 11, 13). The addition of acetylcholine, dopamine, GABA, epinephrine, or norepinephrine caused no observable changes in the size of the internal ostia, implying that the contractile state of the gill musculature was not affected by these agents (Table I).

Rhodamine-123 treatment

The muscular control of canal ostia, and the regulation of water flow through the canal, are consistent with our hypothesis that the water canal epithelial cells are a major site of ion transport in the gill. When gills were incubated in rhodamine-123, fluorescence was specifically localized with the mitochondria-rich cells of the canal epithelium. When the intact living gill was visualized with confocal optics, the cells lining the water canals displayed the greatest fluorescence because of their high mitochondrial content (Fig. 14). Optical sectioning shows that this high activity is in every water canal epithelial cell and extends along the entire length of the water canal.

Gill ciliary activity

In vitro, gills incubated in pondwater showed a consistent rate of ciliary activity (15 beats/s) during the 1-h control observation (Fig. 15). Addition of 10^{-4} *M* serotonin caused an immediate increase in ciliary activity that peaked within 20 min at 24 beats/s. The high ciliary rate was maintained until serotonin was removed 40 min later, and the ciliary beat returned to base line about 40 min thereafter.

Dopamine had an effect on ciliary activity, but it differed from that of serotonin (Fig. 15). The increased ciliary activity peaked at 20 beats/s upon the addition of 10^{-4} *M* dopamine, but 40 min were needed to reach the peak ciliary rate. After dopamine was removed, the ciliary activity immediately dropped to baseline. The response to both dopamine and serotonin was dose-dependent as shown in Figure 16.

Discussion

Most studies of water flow through eulamellibranch gills stress the role of ciliary activity as the driving force for water flow (Jorgenson, 1982; Silvester 1988; Sleigh, 1989). Indeed, many flow measurements and coupled mathematical analyses indicate that ciliary activity is sufficient to account for the water flow (Jorgenson, 1989; Sleigh, 1989). These models treat water canals as hollow tubes of fixed dimensions for the calculations. While such models are useful for studying water flow through gill systems, they are constrained by the underlying assumptions. The measured 2–3 fold difference in the internal ostia dimensions between control and serotonin-treated gills indicates that effective water canal size and its regulation are potentially important factors to be considered for water flow through the gill of unionids. The substantial increase in ostial size coupled to the increase in ciliary activity known

tochondria-rich water canal epithelial cells. Bar = 1 μm.

Figure 6. A light micrograph of a face section through the gill of *Ligumia*. The section is cut through the gill just above the base of the water channel epithelium. Located between and associated with the canals (C) are bands of muscle (IM) traversing in a dorsal/ventral direction. These muscle bands alternate with rows of canals and send fibers to the base of the canal epithelial cells. Muscle bands are not seen in every location between water canals as the section is at a slightly oblique plane. Bar = 60 μm.

Figure 7. Low magnification TEM of *Ligumia* gill indicating that the major internal muscle band (IM) lying at the base of the water channel (WC) epithelium branches and has numerous muscular extensions (ME). These extensions eventually end in the region of the internal ostia with several muscle fibers inserting at the base of the water canal (C) epithelium (see Fig. 8). Most of the cytoplasm of the two epithelia observed is occupied by glycogen (g) and mitochondria (m). Bar = 2 μm.

Figure 8. Higher magnification TEM of *Anodonta* gill showing that the muscle extensions end in thin, finger-like processes consisting of only a few muscle fibers. These fibers are obliquely striated fibers, and the inset indicates the presence of thick and thin filaments. The muscle is inserting in the basal region of the water canal near the water channel epithelium (E) and has hemidesmosome-like electron-dense material at the muscle-connective tissue interface (inset). Note that in this region of the water channel epithelial cells are ciliated (arrowhead). Bar = 1 μm; inset bar = 0.25 μm.

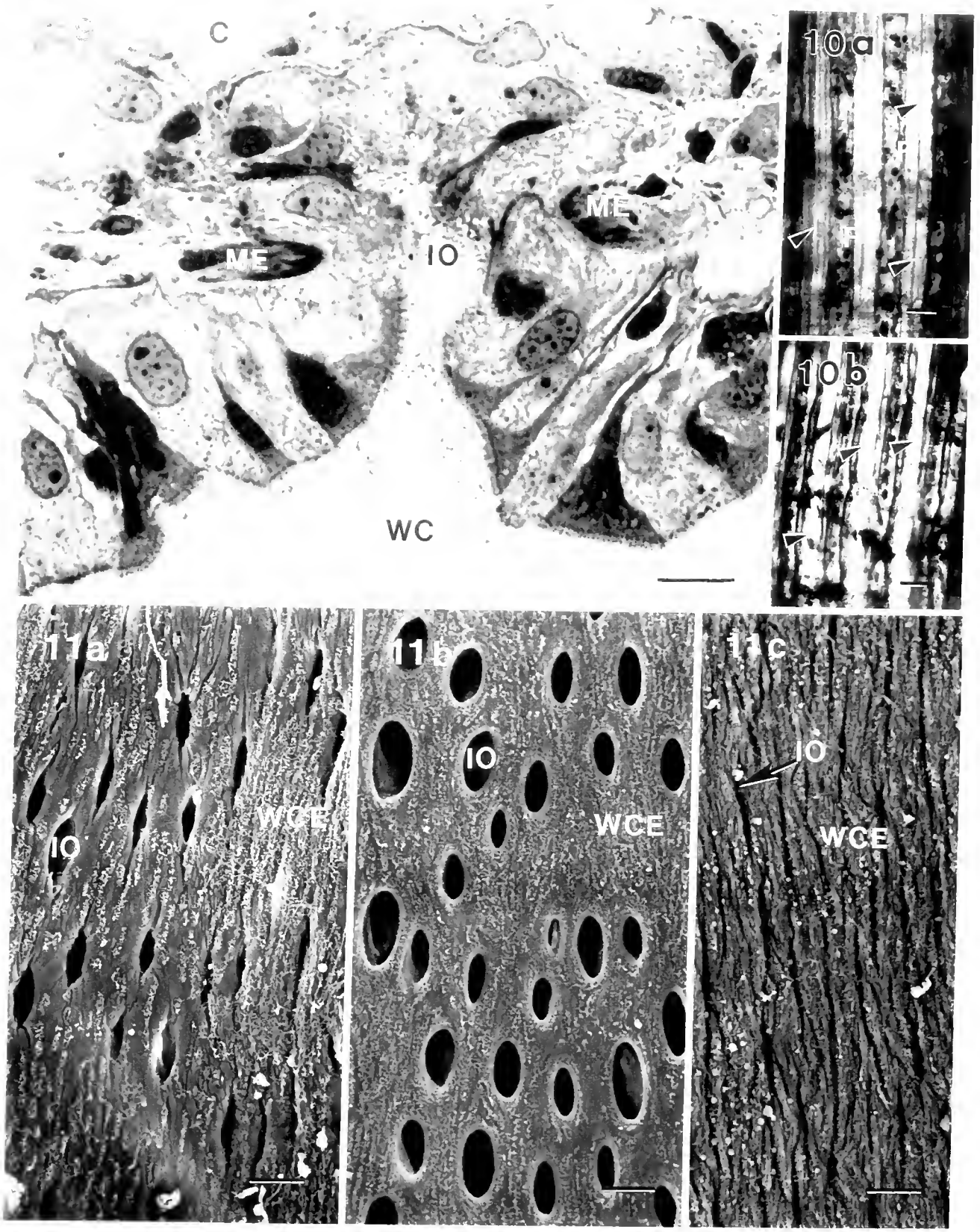

Figure 9. A light micrograph from *Anodonta* gill showing the finger-like muscle extensions (ME) on either side of a water canal (C) at the base of the epithelial cells where the canal enters the water channel (WC) at the internal ostia (IO). Bar = 60 μm.

to occur with serotonin in some bivalves (Gosselin *et al.*, 1962; Aiello and Guideri, 1966; Aiello, 1970; Paparo and Murphy, 1975; Jorgenson, 1976; Capatane *et al.*, 1978; Sanderson and Satir, 1982; Sanderson *et al.*, 1985; this study) makes canal size regulation an important, underestimated contributor to water flow regulation. The threefold difference in ostia dimensions with serotonin treatment may be an over-estimate of the normal conditions based on the potential for some partial contraction of the muscle. We developed our methods to minimize fixation artifact, but the microscopic preparations would likely lead to reduced ostial dimensions (shrinkage) rather than enlargement. Our data demonstrate the potential range within which the mussels can regulate canal openings and water flow with the ostial musculature.

The general orientation of the musculature associated with the ostia and internal ostia was the same in the two unionid genera we examined and is thus likely to be the generalized pattern for the unionids. These muscles are obliquely striated and have not been well-characterized (Ridewood, 1903; Ortmann, 1911; Kays *et al.*, 1990; Richard *et al.*, 1991). Their organization and their association with the ostia suggest that the axes for movement and for regulation of the two openings are different. The ostia are regulated by the muscles. When they contract, adjacent chitinous rods of adjacent filaments are pulled toward one another closing the ostia. During relaxation, the tension on the rods is released, allowing the filaments to separate and the ostia located at the base of the filaments to open. Such a mechanism suggests that the gill as a whole would have a "postural tone" under normal conditions. This can be confirmed by watching the accordion-like movements of the gill due to spontaneous contractions, and the expansion of the gill when relaxed following the addition of serotonin. The muscle bands at the IO are perpendicular to the muscle bands at the ostia. They are oriented dorso-ventrally along the gill axis and in close proximity to the IO; they exert control by sending a few muscle fibers to the base of the epithelial cells surrounding the IO. When these muscle bands contract, the inserting fibers pull on the IO, creating an elongated shape, and causing an indented appearance on the edges of the IO. Increased muscular contraction elongates and closes the opening. The SEM, TEM, and bright field images, comparing control to serotonin-treated gills, are all consistent with this proposed mechanism of action.

The results reported here indirectly suggest that serotonin is a relaxing agent for the muscle bands we have described. While the results have not been confirmed electrically, they are consistent with such experiments in other molluscan systems (Cambridge, 1959; Twarog and Cole, 1972; Satchell and Twarog, 1978; Kobayashi and

Table I

Average internal ostia size in Ligumia subrostrata *gills following exogenous treatment with biogenic amines*

	Height	Width	Perimeter
ACh	39.7 ± 8.0	12.1 ± 3.2	93.9 ± 21.2
ACh-control	33.1 ± 9.1	12.3 ± 2.9	82.2 ± 22.1
Dopamine	24.3 ± 0.9	12.3 ± 1.5	65.9 ± 3.3
Dopamine-control	30.6 ± 0.9	10.3 ± 0.5	75.6 ± 1.9
Epi	34.5 ± 5.3	11.3 ± 1.4	81.9 ± 11.9
Epi-control	27.4 ± 5.3	10.2 ± 1.4	67.2 ± 11.5
Norepi	29.9 ± 4.6	9.4 ± 1.3	71.4 ± 11.2
Norepi-control	31.9 ± 1.9	11.3 ± 2.9	74.9 ± 7.5
GABA	22.5 ± 1.8	15.9 ± 1.9	64.6 ± 6.3
GABA-control	23.8 ± 4.5	13.2 ± 1.2	60.4 ± 9.0
Serotonin	57.9 ± 2.7*	24.4 ± 1.1*	147.3 ± 6.9*
Serotonin-control	33.1 ± 3.8	10.0 ± 0.9	78.3 ± 8.2

All measurements are in microns. Height and width refer to the longest and shortest axes of the oval shaped ostia, respectively. Data are means ± standard error ($n \geq 3$). ACh = Acetylcholine, Epi = Epinephrine, GABA = Gamma Aminobutyric Acid, Norepi = Norepinephrine.

* Significantly different from controls, $P < 0.01$.

Figure 10. Comparison of whole mount light micrographs of control (a) and serotonin-treated (b) *Anodonta* gills. The micrographs show the surface of the filaments, allowing observation of the ostia (arrowheads). In (a), the control gill ostia are barely discernable as the lighter areas because the adjacent filaments (F) are pulled toward one another closing the space between filaments. Gills in this condition have few ostial openings. In contrast, a gill treated with 10^{-5} *M* serotonin (b) shows filaments that are farther from one another allowing ostial openings to enlarge. Bars in a and b = 50 μm.

Figure 11. Scanning electron micrographs of the water channel epithelium (WCE) of *Ligumia* showing the internal ostia (IO) as they enter the water channel. (a) Is an untreated control gill. Note both the size and shape of the IO openings. The long axis (height) has a dorsal/ventral orientation. Their edges, particularly those on the dorsal and ventral ends, tend to have an indented appearance. (b) Is a gill that has been treated with 10^{-5} *M* serotonin. Relaxation of musculature allows the IO to fully expand. The ostia still have a dorsal-ventral orientation although not nearly as pronounced. The ostia have an oval to round shape and the indentations seen in (a) are absent. The oval orientation is likely due to the orientation of the underlying musculature. (c) Is a gill that has been treated with pH 5 buffer to stimulate full contraction. Note the exaggerated dorsal-ventral orientation and deep indentations of the ostial edges oriented in the same direction. The "pull" by the underlying musculature has occluded the IO opening. Bars in a, b and c = 10 μm.

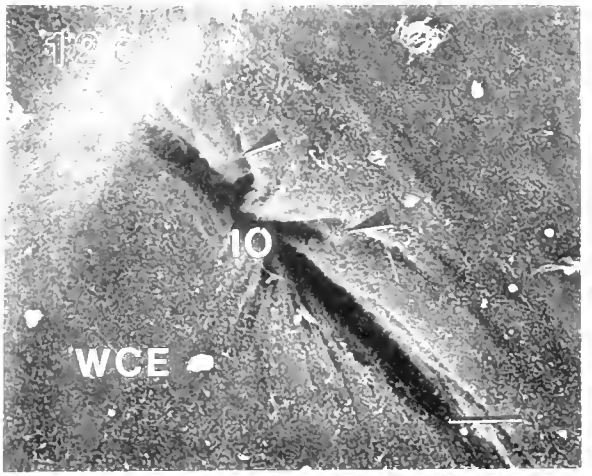

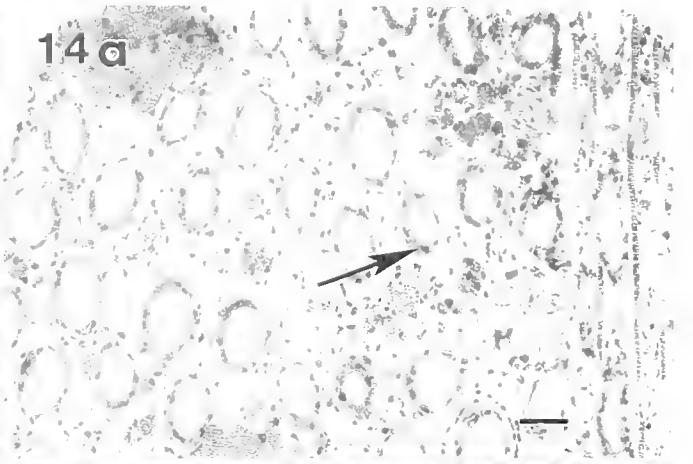

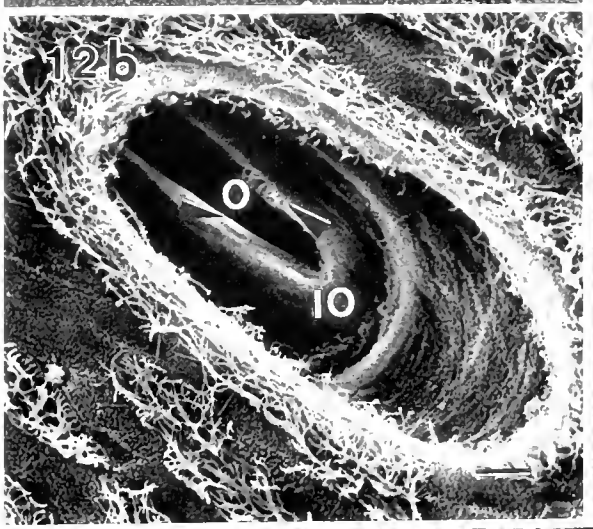

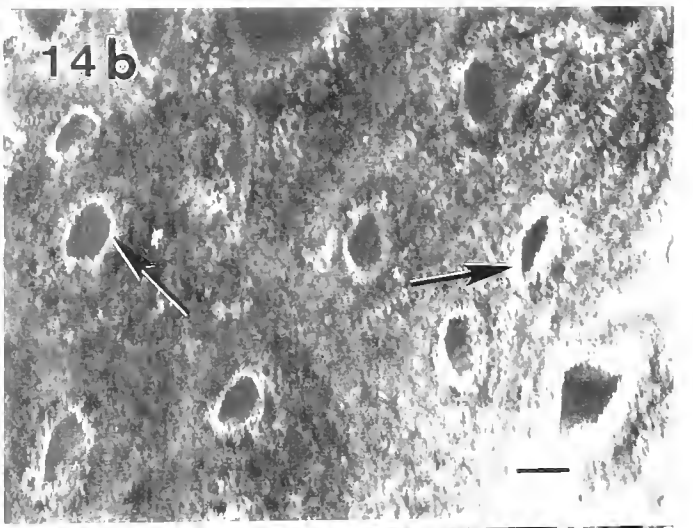

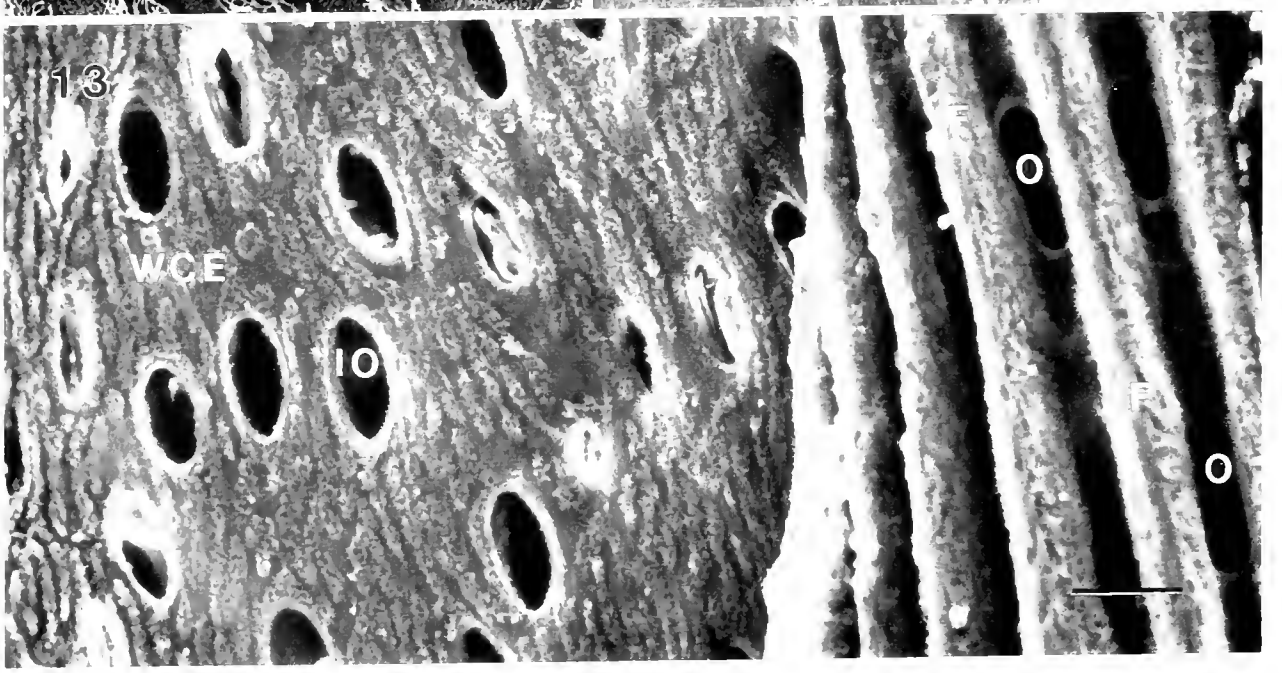

Figure 12. High magnification SEM micrographs of *Ligumia* gills viewing the water channel epithelium (WCE). (a) Is from a control gill showing the elongation in the dorsal-ventral direction. This internal ostium is almost completely occluded. The indentations of the IO border are evident (arrows) as well. (b) Is an internal ostium from a serotonin-treated (10^{-5} M) gill. The dorsal-ventral longitudinal orientation is evident.

Hasimoto, 1982). Acetylcholine, dopamine, norepinephrine, epinephrine, and GABA were neither excitatory nor inhibitory in our bioassay. These results clearly do not exclude any of these substances as putative excitatory transmitters because bath application may not allow these agents to reach their targets. We were able to demonstrate a dose-response relationship of ciliary beat for both serotonin and dopamine, but our bioassay was not sufficiently sensitive, and so no dose-response relationship for serotonin-induced muscular relaxation was demonstrated only an all-or-none relaxation response occurred.

Although these muscles have previously been ignored, their importance to the functions of the unionid gill should not be overlooked. Evidence demonstrating that the gill is the predominant site of ion regulation in unionid mussels is convincing (Dietz and Findley, 1980; Dietz and Graves, 1981; Dietz and Hagar, 1990). Further, more evidence is accumulating (Kays *et al.*, 1990; this study) that the epithelial cells of the water canals are important osmoregulatory cells. The high mitochondrial content and activity (as demonstrated here by rhodamine-123 experiments), surface area calculations, considerable basal and lateral membrane infolding, and the high levels of cytochrome oxidase activity (Kays *et al.*, 1990) shown by these cells all suggest osmoregulatory function. Coordinated muscle and ciliary activity may allow finer control and a wider range of regulation, including a shut-down of water flow. The coordinated control of ciliary and muscular activity is apparent, at least in response to serotonin.

No-flow conditions do occur in some unionid species during reproduction. In the Lampsilinae, the central water chambers housing embryos are physiologically isolated from the water flow through the mantle cavity (Silverman

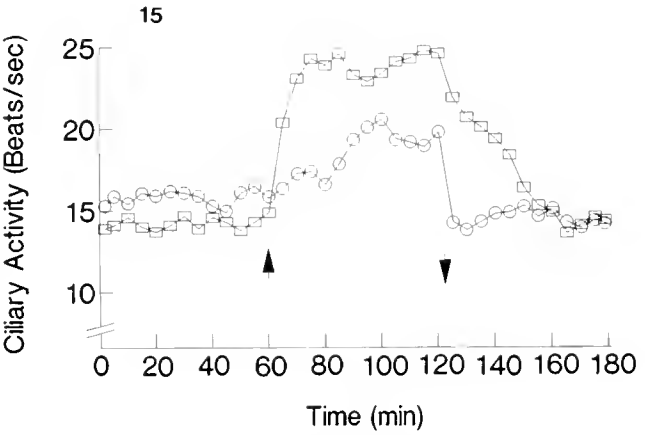

Figure 15. Lateral ciliary activity of a representative (of 5) *Ligumia* gill in response to application of exogenous serotonin and dopamine. Gills were exposed either to 10^{-4} *M* serotonin (open squares) or 10^{-4} *M* dopamine (open circles) for 1 h. Initiation of the treatment is indicated by the upward pointing arrow and termination by the downward pointing arrow.

et al., 1987; Richard *et al.*, 1991). We speculate that the mechanism for reduced water flow into the brood chamber is, in part, regulation by canal ostial musculature.

Mathematical treatments of the hydrodynamics of water flow through mussel gills do not completely fit the available data. Silvester (1988) has recently concluded, after an elegant treatment of *Mytilus* gill ciliary mechanics, that faster flow than can be accounted for by known ciliary activity actually occurs. Indeed, his final statement, "one should perhaps be alert to the possibility that other systems in the mussel may be contributing to the pumping performance" (Silvester, 1988), could allude to the possibility

The IO opening is not indented as seen in (a). This field allows a clear view through the IO and into the water canal. At the filament side of the water canal is an ostium that is delimited by the filaments on either side of the ostium. This is evident by the dorsal-ventral, straight edges (arrowheads) of the ostium. The muscle bands underlying the two ostial openings lie perpendicular to one another (not shown), but both bands work to close their respective opening in the dorsal-ventral direction. Bars in a and b = 10 μm.

Figure 13. An SEM micrograph of *Ligumia* gill exposed to 10^{-5} *M* serotonin. The gill has been prepared so that the left hand side of the micrograph has one lamella removed to expose the water channel epithelium (WC) while the right side of the micrograph contains an intact lamella and filaments (F). Between the filaments, the ostia (O) are visible and fully open, displaying the dorsal-ventral long-axis orientation. They clearly demonstrate the limitations on their size being set by the inter-filament distance. The space between filaments is controlled by muscle inserting on the chitinous rods supporting the filaments. The internal ostia (IO) show the same orientation. Bar = 50 μm.

Figure 14. Face view of *Ligumia* gills showing the mid-region of the water canals (C) passing from the gill filaments into the water channel. (a) Is a control light micrograph of fixed tissue similar to that seen in Figure 6. Note the size of the water canal epithelial cells (arrow). These cells have previously been shown to be high in cytochrome oxidase activity (Kays *et al.*, 1990). (b) Is an optical section through a living gill accomplished using confocal imaging techniques. The gill has been treated with rhodamine-123 to highlight mitochondrial location. The major fluorescence corresponds to the cytoplasm of the water canal epithelial cells (arrows). The canal cells are the major site of active mitochondria. There is some auto-fluorescence associated with other epithelia of the gill, but it is minor compared with that seen in the water canal epithelia cells. Bars in a and b = 50 μm.

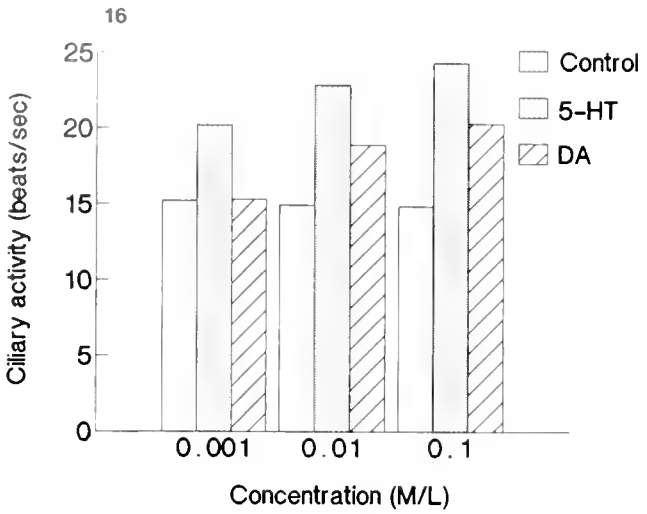

Figure 16. Dose-response relationship of lateral ciliary beat in *Ligumia* gills following the application of serotonin or dopamine. The last three ciliary rate measurements of the initial control and treatment periods were averaged for each gill, and the average of five gills are presented (standard error < 0.5 beats/s).

of muscular activity aiding ciliary function. Indeed, the anterior-posterior and dorsal-ventral contractions of the muscle bands in the gill may provide additional driving force through an accordion-like motion. The current study indicates that these muscles are likely to be important contributors to water flow dynamics across the molluscan gill, at least for the unionids.

Acknowledgments

We thank Dr. A. Paparo for determination of ciliary activity, Ms. Beckey Demler of the LSU Basic Sciences Microscopy Center for technical help, and Ron Bouchard for photographic assistance. All image analysis was done in the Microscopy Facility. This work comprises a portion of an MS thesis (Louisiana State University) by DBG. This work was supported by a NSF grant DCB88-02320.

Literature Cited

Aiello, E. 1970. Nervous and chemical stimulation of gill cilia in bivalve molluscs. *Physiol. Zool.* **43:** 60–70.

Aiello, E., and G. Guideri. 1966. Relationship between 5 hydroxytryptamine and nerve stimulation of ciliary activity. *J. Pharmacol. Exp. Ther.* **154:** 517–523.

Cambridge, G. W., J. A. Holgate, and J. A. Sharp. 1959. A pharmacological analysis of the contractile mechanism of *Mytilus* muscle. *J. Physiol.* **148:** 451–464.

Catapane, E. J., G. B. Stefano, and E. Aiello. 1978. Pharmacological study of the reciprocal dual innervation of the lateral ciliated gill epithelium by the CNS of *Mytilus edulis* (Bivalvia). *J. Exp. Biol.* **74:** 101–113.

Dietz, T. H., and A. M. Findley. 1980. Ion-stimulated ATPase activity and NaCl uptake in the gills of freshwater mussels. *Can. J. Zool.* **58:** 917–923.

Dietz, T. H., and S. Y. Graves. 1981. Sodium influx in isolated gills of the freshwater mussel *Ligumia subrostrata*. *J. Comp. Physiol.* **143:** 185–190.

Dietz, T. H., and A. F. Hagar. 1990. Chloride uptake in isolated gills of the freshwater mussel *Ligumia subrostrata*. *Can. J. Zool.* **68:** 6–9.

Galtsoff, P. S. 1964. The American oyster *Crassostrea virginia* Gmelin. *U. S. Fish Wildlife Serv. Fish. Bull.* **64:** 1–480.

Gosselin, R. E., K. E. Moore, and A. S. Milton. 1962. Physiological control of molluscan gill cilia by 5-hydroxytryptamine. *J. Gen. Physiol* **46:** 277–296.

Grimley, P. 1964. A tribasic stain for thin sections of plastic-embedded, OsO_4-fixed tissue. *Stain Tech.* **39:** 229–233.

Johnson, L. V., M. L. Walsh, and L. B. Chen. 1980. Localization of mitochondria in living cells with rhodamine-123. *Proc. Natl. Acad. Sci. USA* **77:** 990–994.

Jorgensen, C. B. 1976. Comparative studies on the function of gills in suspension feeding bivalves, with special reference to effects of serotonin. *Biol. Bull.* **151:** 331–343.

Jorgensen, C. B. 1982. Fluid mechanics of the mussel gill: the lateral cilia. *Mar. Biol.* **70:** 275–281.

Jorgensen, C. B. 1989. Water processing in ciliary feeders, with special reference to the bivalve filter pump. *Comp. Biochem. Physiol.* **94A:** 383–394.

Kays, W. T., H. Silverman, and T. H. Dietz. 1990. Water channels and water canals in the gill of the freshwater mussel, *Ligumia subrostrata:* ultrastructure and histochemistry. *J. Exp. Zool.* **254:** 256–269.

Kobayashi, M., and T. Hasimoto. 1982. Antagonistic responses of the radular protractor and retractor to the same putative neurotransmitters. *Comp. Biochem. Physiol.* **72C:** 343–348.

Nelson, T. C. 1941. On the locus of action of diantlin upon the oyster's gills as revealed by the effects of acetylcholine, eserine, and adrenalin. *Anat. Rec.* **81:** 88.

Nelson, T. C. and J. B. Allison. 1940. On the nature and action of diantlin; a new hormone-like substance carried by the spermatozoa of the oyster. *J. Exp. Zool.* **85:** 299–338.

Ortmann, A. E. 1911. A monograph of the Najades of Pennsylvania. *Mem. Carnegie Mus.* **4:** 279–347.

Paparo, A. 1980. The regulation of intracellular calcium and the release of neurotransmitters in the mussel, *Mytilus edulis*. *Comp. Biochem. Physiol.* **66A:** 517–520.

Paparo, A. 1988. Ciliary activity on the ctenidium of bivalve molluscs. *Comp. Biochem. Physiol.* **91C:** 99–110.

Paparo, A., and J. A. Murphy. 1975. The effect of Ca on the rate of beating of lateral cilia in *Mytilus edulis* I. A response to perfusion with 5-HT, DA, BOL, and PBZ. *Comp. Biochem. Physiol.* **50C:** 9–14.

Reynolds, E. S. 1963. The use of lead citrate at high pH as an electron-opaque stain in electron microscopy. *J. Cell. Biol.* **17:** 208–213.

Richard, P. E., T. H. Dietz, and H. Silverman. 1991. Structure of the gill during reproduction, *Anodonta grandis, Ligumia subrostrata* and *Carunculina parva texasensis*. *Can. J. Zool.* (in press).

Ridewood, W. G. 1903. On the structure of the gills of the Lamellibranchia. *Phil. Trans. Roy. Soc. London* **195:** 147–284.

Riisgard, H. U., and F. Mohlenberg. 1979. An improved automatic recording apparatus for determining the filtration rate of *Mytilus edulis* as a function of size and algal concentration. *Mar. Biol.* **52:** 61–67.

Sanderson, M. J., E. R. Dirksen, and P. Satir. 1985. The antagonistic effects of 5-hydroxytryptamine and methylxanthine on the gill cilia of *Mytilus edulis*. *Cell Motil.* **5:** 293–309.

Sanderson, M. J., and P. Satir. 1982. Multiple effects of ethanol and 5-hydroxytryptamine on the gill cilia of *Mytilus edulis*. *Cell Motil.* **2:** 215–224.

Satchell, D. G. and B. M. Twarog. 1978. Identification of 5-hydroxytryptamine (serotonin) released from the anterior byssus retractor muscle of *Mytilus californianus* in response to nerve stimulation. *Comp. Biochem. Physiol.* **59C:** 81–85.

Silverman, H. 1989. Form and function of calcium concretions in unionids. Pp. 367–384 in *Origin, Evolution, and Modern Aspects of Biomineralization in Plants and Animals. Proceedings of the Fifth International Symposium on Biomineralization*, R. Crick, ed. Plenum Press, New York.

Silverman, H., W. T. Kays, and T. H. Dietz. 1987. Maternal calcium contribution to glochidial shells in freshwater mussels (Eulamellibranchia: Unionidae). *J. Exp. Zool.* **242:** 137–146.

Silverman, H., W. L. Steffens, and T. H. Dietz. 1983. Calcium concretions in the gills of a freshwater mussel serve as a calcium reservoir during periods of hypoxia. *J. Exp. Zool.* **227:** 177–189.

Silvester, N. 1988. Hydrodynamics of flow in *Mytilus* gill. *J. Exp. Mar. Biol. Ecol.* **120:** 171–182.

Sleigh, M. 1989. Adaptations of ciliary systems for the propulsion of water and mucus. *Comp. Biochem. Physiol.* **94A:** 359–364.

Twarog, B. M. 1954. Responses of a molluscan smooth muscle to acetylcholine and 5-hydroxytryptamine. *J. Cell. Comp. Physiol.* **44:** 141–163.

Twarog, B. M., and R. A. Cole. 1972. Relaxation of catch in a molluscan smooth muscle II. Effects of serotonin, dopamine and related compounds. *Comp. Biochem. Physiol.* **43A:** 331–335.

Reference: *Biol. Bull.* 180: 466–474. (June, 1991)

On the Nature of Paddle Cilia and Discocilia

GRAHAM SHORT* AND SIDNEY L. TAMM**

Boston University Marine Program, Marine Biological Laboratory, Woods Hole, Massachusetts 02543

Abstract. Cilia with paddle-shaped or disc-shaped tips enclosing a curved end of the axoneme (paddle cilia or discocilia) have been described in a variety of marine invertebrates. Although numerous studies, in which fixed specimens were used, claimed that paddle cilia and discocilia are genuine structures of unknown function, several studies, in which fresh living material was used, reported that modified cilia are artifacts. We have re-investigated a recent SEM report that paddle cilia are genuine organelles in veliger larvae of marine bivalves (Campos and Mann, 1988). Using high-speed video and electronic flash DIC microscopy, we find no paddle cilia in living larvae of *Spisula solidissima* and *Lyrodus pedicellatus*. Hypotonic seawater, however, induces formation of paddle cilia and vesiculations of the ciliary membrane in these veligers, as does the hypotonic SEM fixative used by Campos and Mann (1988). Fixatives that are isosmotic with seawater, on the other hand, do not induce paddle cilia. We conclude that paddle cilia are artifacts, and we propose a unifying mechanism to explain their production in various animals under different conditions.

Introduction

Cilia with a distal expansion of the ciliary membrane enclosing a looped end of the axoneme (paddle cilia or discocilia) have been described in a variety of marine invertebrates (Tamarin *et al.*, 1974; Oldfield, 1975; Bergquist *et al.*, 1977; Dilly, 1977a, b; Ehlers and Ehlers, 1978; Heimler, 1978; Storch and Alberti, 1978; Arnold and Williams-Arnold, 1980; Bone *et al.*, 1982; Matera and Davis, 1982; Pfannenstiel, 1982; Nielsen, 1987; Campos and Mann, 1988; Durfot *et al.*, 1990). In spite of older cytological evidence to the contrary (Hartmann, 1953; Lewin and Meinhart, 1953; Preer and Preer, 1959; Child, 1961; Pitelka and Child, 1964), many investigators believe that paddle cilia are genuine organelles. Various functions have been proposed for paddle cilia, including serving as micro-spatulae for application of adhesive material or secretions to the substrate (Tamarin *et al.*, 1974; Dilly, 1977b), increasing the efficiency of the power stroke and the effectiveness of water and feeding currents (Bergquist *et al.*, 1977; Dilly, 1977a; Arnold and Williams-Arnold, 1980), increasing membrane surface area for trapping food particles (Dilly, 1977a), acting as chemoreceptors (Matera and Davis, 1982; Campos and Mann, 1988), and transporting unknown materials along the cilium from base to tip (Dilly, 1977a, b).

However, the few studies that have carefully compared fresh living material to chemically fixed or quick-frozen material have concluded that paddle cilia and discocilia are artifacts caused by osmotic stress, non-physiological conditions, or fixatives and fixation additives (Ehlers and Ehlers, 1978; Bone *et al.*, 1982; Pfannenstiel, 1982; Nielsen, 1987).

To examine the status of paddle cilia anew, we have re-investigated a recent SEM report that paddle cilia are genuine structures in veliger larvae of marine bivalves (Campos and Mann, 1988). We used high-speed video and electronic flash DIC microscopy of living larvae of *Spisula solidissima* and *Lyrodus pedicellatus* in normal seawater and in hypotonic seawater, together with light microscopy and SEM of larvae fixed in solutions of different osmolarities and composition.

We find that paddle cilia are indeed artifacts, and propose a new mechanism to account for their formation in various animals. A preliminary account of this work has appeared (Short and Tamm, 1989).

Materials and Methods

Organisms

Spisula solidissima adults were obtained from Marine Resources at the Marine Biological Laboratory (MBL)

Received 7 February 1991; accepted 22 March 1991.

* Present address: Cell, Molecular, Neuroscience Program, University of Hawaii, Honolulu, Hawaii 96822.

** To whom reprint requests should be sent.

and maintained in cold running seawater (15°C) at the Environmental Studies Laboratory (ESL) of the Woods Hole Oceanographic Institution (WHOI); *Lyrodus pedicellatus* larvae were obtained from adults maintained at ESL. *Spisula* adults were spawned by dissection of gonads or by thermal stimulation at 22°C, and the larvae reared following methods of Gallager and Mann (1986). Larvae were fed monocultures of *Isochrysis galbana* at a concentration of 10,000 cells per ml.

Light microscopy and video recording

Living veliger larvae of *Spisula solidissima* and *Lyrodus pedicellatus* were observed in slide wells of normal seawater under Zeiss DIC and phase contrast optics with a Dage 67 video camera modified for high field rates (120, 180, 240 Hz) and synchronized with a strobex flash (Chadwick-Helmuth). Images were recorded with a GYYR model 2051 video recorder allowing still-field playback and analysis. Films (35 mm; Kodak Tech Pan 2415) of larvae were taken with Zeiss DIC and phase contrast optics using an Olympus OM-2N camera and an Olympus T-32 electronic flash tube positioned in the illumination path.

Fixation and scanning electron microscopy

Umbo stage larvae of *Spisula* and *Lyrodus* were rinsed in 0.45 μm filtered seawater and fixed in three ways. *Method 1* (Campos and Mann, 1988): larvae were siphoned from the culture container and retained on a 50 μm nylon mesh screen, then transferred to filtered seawater and relaxed in 8% (w/v) $MgCl_2$. Larvae were concentrated by centrifugation and fixed in 2.5% glutaraldehyde, 0.1 *M* Na cacodylate, pH 7.2 (total osmolarity of 409 mOsmols as determined by Wescor 5100C vapor pressure osmometer) at 4°C for 2 h. Larvae were rinsed 3 times in 0.1 *M* Na cacodylate, 0.25 *M* NaCl, pH 7.2, for 30 min each, and post-fixed in 1% OsO_4, 0.19 *M* NaCl, 0.1 *M* Na cacodylate for 1 h. Larvae were rinsed in 0.1 *M* Na cacodylate, 0.15 *M* NaCl and stored overnight at 4°C. *Method 2:* the same glutaraldehyde solution as above was used, but with 0.29 *M* NaCl added to make it isosmotic with MBL seawater (920 mOsmols). *Method 3:* concentrated larvae were relaxed in 6.82% $MgCl_2$ and fixed in unbuffered 2.5% glutaraldehyde, 0.13 *M* NaCl, 50% seawater (isosmotic; 920 mOsmols) at 4°C for 30 min.

For light microscopy, larvae were observed on slides after glutaraldehyde fixation. For SEM, fixed larvae were dehydrated through a graded ethanol series, critical point dried (Samdri-78A), sputtered with gold palladium (Samsputter-2a), and examined with a JSM-840 SEM. Photographs were taken on Polaroid positive-negative film.

Results

Light microscopy of living and fixed larvae

The velum of *Spisula solidissima* and *Lyrodus pedicellatus* consists of four ciliary bands: inner and outer pretrochal bands, an adoral band, and a metatrochal band. The pretrochal bands are responsible for obtaining food and for locomotion, and the adoral and metatrochal bands convey food particles to the mouth. The pretrochal bands consist of compound cilia; the adoral and metatrochal bands contain simple cilia. Figures 1A and 1B are flash photographs of living umbo stage larvae of *Spisula* (two weeks old) and *Lyrodus* (two days old), respectively, in normal seawater. No paddle cilia or vesiculated ciliary membranes are evident in any of the ciliary bands of either larva. High-speed flash-synchronized video microscopy of swimming *Spisula* and *Lyrodus* larvae also failed to show modifications of ciliary structure.

The hypotonic glutaraldehyde fixative of Campos and Mann (1988) (Method 1), with or without OsO_4 postfixation, induced swelling of the tips of pretrochal cilia of *Spisula* larvae (Fig. 1C) and vesiculation along pretrochal ciliary membranes of *Lyrodus* larvae (Fig. 1D). The terminal swellings of *Spisula* cilia and vesiculations along the shafts of *Lyrodus* cilia were about 2 μm in diameter. Because these modifications of ciliary structure were observed directly in fixed larvae by light microscopy, they are not induced by subsequent procedures used for SEM and TEM.

Addition of NaCl to make this fixative isosmotic with MBL seawater (Method 2) resulted in no paddle cilia in *Spisula* larvae, nor vesiculation of ciliary membranes in *Lyrodus* larvae. Instead, the cilia appeared uniformly smooth and cylindrical. Similarly, an unbuffered isosmotic glutaraldehyde fixative containing 50% seawater (Method 3) did not induce paddle cilia or vesiculations in either species (Fig. 1E, F).

Treatment of living, 2-week-old larvae of *Spisula* with 45% seawater (420 mOsmols) caused swelling of the distal tips of the pretrochal cilia within 2 min. These paddle cilia resembled those induced by hypotonic fixatives (Fig. 1C). Treatment of *Lyrodus* veligers with 45% seawater resulted in vesiculation of the membrane along the entire shaft of the pretrochal cilia within 10 min. Again, these vesiculated cilia resembled those induced by hypotonic fixatives (Fig. 1D). The majority of the modified cilia in both species remained attached to the velum. However, treatment with 45% seawater for longer times caused detachment and loss of cilia. Upon transfer of larvae to 100% seawater, many cilia of both species regained their normal appearance within 5–10 min, indicating that tip swelling or vesiculation is a reversible osmotic phenomenon.

In a subsequent experiment using 2-day-old *Spisula* veligers, we found that 45% seawater was ineffective in producing paddle cilia, but that 15–20% seawater was re-

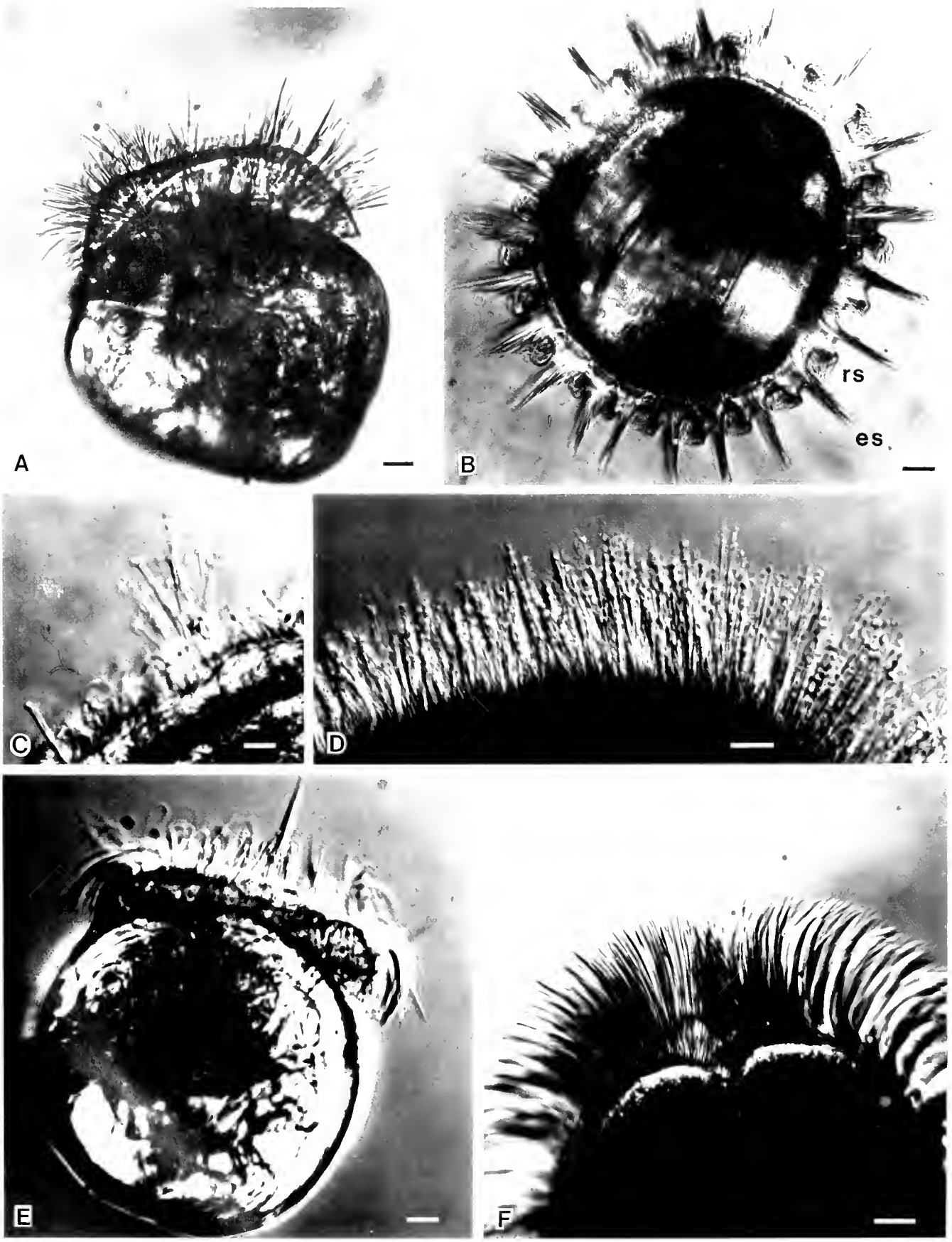
A
B
rs
es
C
D
E
F

quired to induce swelling of the ciliary tips in these younger larvae. The paddle cilia were immotile or only weakly beating and were easily detached, resulting in poor swimming ability of the larvae. Upon transfer to 100% seawater, many of the larvae resumed swimming. DIC microscopy of these larva showed that some velar cilia regained a normal appearance, but that others had detached and were missing.

Scanning electron microscopy of larvae

Larvae of *Spisula* and *Lyrodus* treated with the isosmotic fixative containing 50% seawater (Method 3) and processed for SEM, showed uniformly cylindrical velar cilia without terminal swellings or vesiculations (Figs. 2A, C, 3A, C). However, swollen cilia were present in both species when fixed by the hypotonic fixative of Campos and Mann (1988) (Method 1) (Figs. 2B, D, 3B, D). In contrast to light microscopic images of Method 1-fixed *Lyrodus* larvae (Fig. 1D), those processed for SEM showed terminal paddles on pretrochal cilia rather than vesiculation along the ciliary length (Fig. 3B, D). The modified cilia induced in *Spisula* and *Lyrodus* are similar to those observed by Campos and Mann (1988). The distal swellings measure 1–1.15 μm in diameter in both species, and often result in fraying of the compound organelles into individual cilia. The paddle cilia observed in *Spisula* are not restricted to the pretrochal ciliary bands; metatrochal cilia also exhibit terminal swellings in response to the hypotonic fixative of Campos and Mann (1988) (Fig. 2B). However, the metatrochal ciliary blebs measure about 1.0 μm in diameter and are located about 1 μm proximal to the ciliary tips. The adoral cilia, in contrast, do not exhibit dilations at the tips (Fig. 2B).

Discussion

We have reinvestigated the report by Campos and Mann (1988) that paddle cilia and discocilia are genuine structures in the velum of molluscan bivalve larvae. Campos and Mann (1988) did not examine living larvae, but used a hypotonic fixative (409 mOsmols; Method 1) to prepare larvae of *Spisula solidissima* and *Mullina lateralis* for SEM.

We imaged beating velar cilia in larvae of *Spisula solidissima* and *Lyrodus pedicellatus* by electronic flash and high-speed video light microscopy. No paddle cilia or discocilia were observed in normal seawater. Other high-speed video microscopic studies also have not found modified cilia in living larvae of *Spisula*, *Lyrodus*, and *Mercenaria* (Gallager, 1988; pers. comm.).

We could reversibly induce swelling of the ciliary membrane by treatment of living larvae with hypotonic (15–45%) seawaters. In addition, paddle cilia were observed using the hypotonic glutaraldehyde fixative of Campos and Mann (1988) (Method 1), but not in fixatives made isosmotic with seawater (Methods 2 and 3). We therefore conclude that paddle cilia and discocilia in *Spisula* and *Lyrodus* are not genuine structures, but are artifacts.

Of the numerous reports of paddle cilia and discocilia in various animals (Mecklenburg *et al.*, 1974; Tamarin *et al.*, 1974; Oldfield, 1975; Bergquist *et al.*, 1977; Dilly, 1977a, b; Ehlers and Ehlers, 1978; Heimler, 1978; Storch and Alberti, 1978; Arnold and Williams-Arnold, 1980; Bone *et al.*, 1982; Matera and Davis, 1982; Pfannenstiel, 1982; Nielsen, 1987; Campos and Mann, 1988; Durfot *et al.*, 1990), only a handful of investigators concluded that modified cilia are artifacts (Mecklenburg *et al.*, 1974; Ehlers and Ehlers, 1978; Pfannenstiel, 1982; Bone *et al.*, 1982; Nielsen, 1987). These investigators, in contrast to the others, did not rely mainly on fixed material, but used fresh living specimens and compared the effects of stress and various TEM and SEM preparative procedures on ciliary structure.

For example, Ehlers and Ehlers (1978) found that living, untreated marine Turbellaria do not possess paddle cilia or discocilia, but that these structures could be induced by the addition of certain fixative buffers and chemicals to the seawater. Osmolality also influenced the extent of paddle cilia formation (Ehlers and Ehlers, 1978).

Similarly, Pfannenstiel (1982) did not observe modified cilia in living polychaetes, but could produce paddle cilia or discocilia by glutaraldehyde and osmium fixatives, or by $MgCl_2$ solutions of different osmolarities. When $MgCl_2$-treated specimens were returned to seawater, the modified cilia regained their normal cylindrical appearance, "revealing that they are transient structures" (Pfannenstiel, 1982).

In addition, Bone *et al.* (1982) found that the median endostylar cilia of *Ciona* usually have straight tips in fresh

Figure 1. DIC flash photographs. A. Living *Spisula* veliger in normal seawater. No paddle cilia are present. Scale bar, 20 μm. B. Living *Lyrodus* veliger in normal seawater. Metachronal waves of pretrochal cilia circle the velum (es, cilia in effective stroke; rs, cilia in recovery stroke). No paddle cilia are evident. Scale bar, 30 μm. C. *Spisula* pretrochal cilia fixed in the hypotonic solution of Campos and Mann (1988) (our Method 1). Cilia have paddle tips. Scale bar, 10 μm. D. *Lyrodus* pretrochal cilia in the hypotonic fixative of Campos and Mann (1988) (Method 1). Vesiculation occurs along the length of the ciliary membranes. Scale bar, 20 μm. E. *Spisula* pretrochal cilia in isosmotic fixative containing 50% seawater (Method 3). No paddle cilia are present. Scale bar, 20 μm. F. *Lyrodus* pretrochal cilia in isosmotic fixative containing 50% seawater (Method 3). No vesiculation of ciliary membranes is evident. Scale bar, 20 μm.

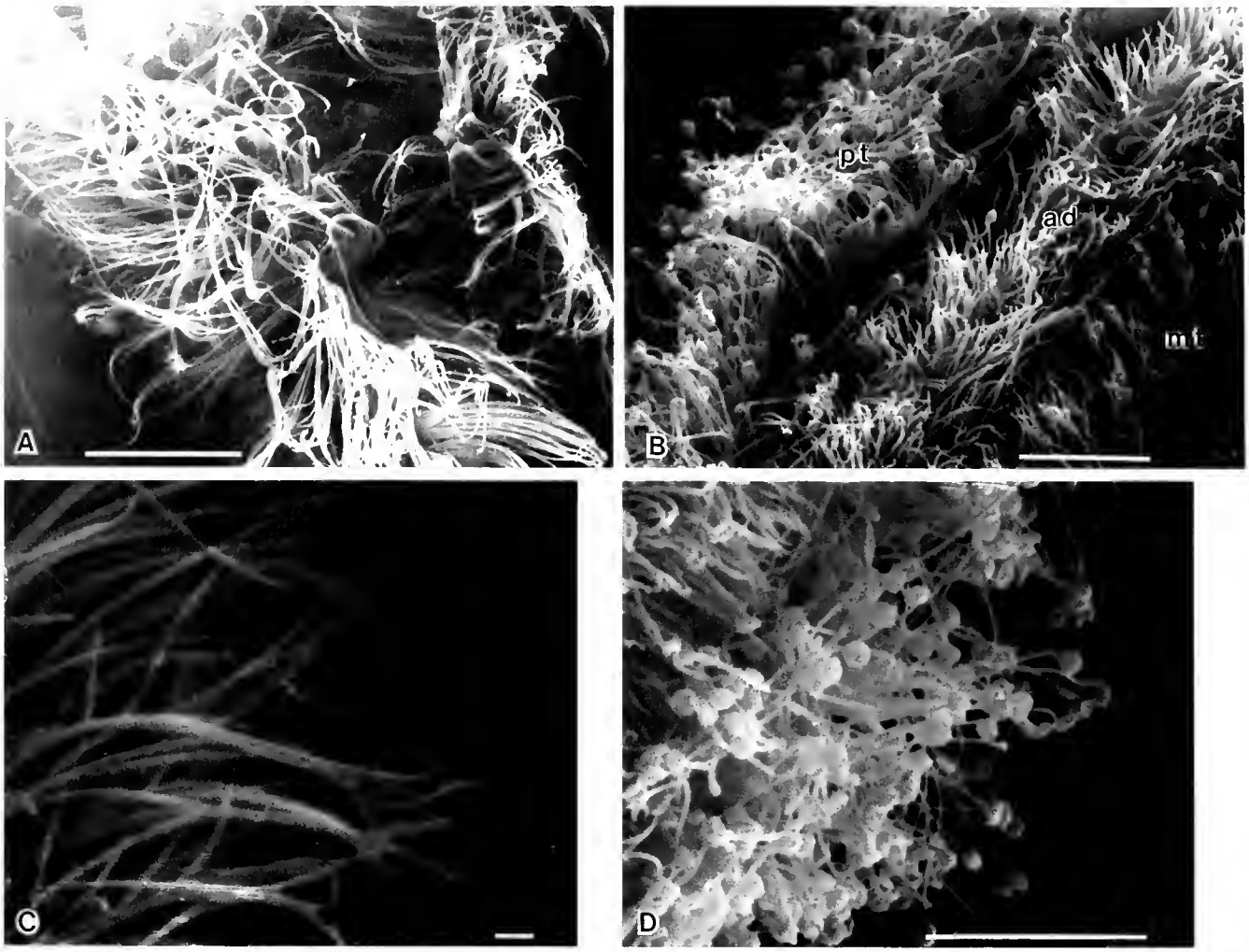

Figure 2. Scanning electron micrographs of velar cilia in *Spisula solidissima* larvae. A, C. Isosmotic fixative containing 50% seawater (Method 3). No paddle cilia are present. B, D. Hypotonic fixative of Campos and Mann (1988) (Method 1). Paddle cilia occur in pretrochal (pt) and metatrochal (mt) bands, but not in the adoral cilia (ad). Scale bars: A, 10 μm; B, 10 μm; C, 1 μm; D, 10 μm.

living preparations. However, the addition of buffered or unbuffered glutaraldehyde fixatives induced rapid coiling of the ciliary tips, resulting in many concentric axonemal coils piled around each other within the ciliary membrane. Coiled ciliary tips were not observed in SEM material that had been quenched in liquid nitrogen and freeze-dried.

The few reports of paddle cilia or discocilia in living preparations in seawater (Heimler, 1978; Arnold and Williams-Arnold, 1980; Matera and Davis, 1982) have been attributed to osmotic stress, anoxia, or other non-physiological conditions in the microscopic slide chambers used for observation (Bone *et al.*, 1982; Pfannenstiel, 1982). In fact, Matera and Davis (1982) induced reversible transitions between paddle cilia and cylindrical cilia by perfusions of hypotonic and hypertonic solutions. In a comprehensive review of the structure of ciliary bands in more than 15 phyla of invertebrates, Nielsen (1987) reported that paddle cilia and discocilia only occur "in specimens which have not been treated with sufficient care." Nielsen (1987) concluded that "until further evidence in favor of paddle cilia in unstressed animals has been presented, I prefer to regard these structures as artifacts."

In this regard, cell physiologists have long recognized that the ciliary membrane is the weakest part of the cilium, and that osmotic stress or non-physiological conditions readily cause coiling or curving of the axoneme within a distal expansion of the ciliary membrane (Hartmann, 1953; Lewin and Meinhart, 1953; Preer and Preer, 1959; Child, 1961; Pitelka and Child, 1964; Mecklenburg *et al.*, 1974). For example, Mecklenburg *et al.* (1974) found that moderate heat exposure caused club-shaped vesicular protrusions of the distal ends of rabbit tracheal cilia. Child

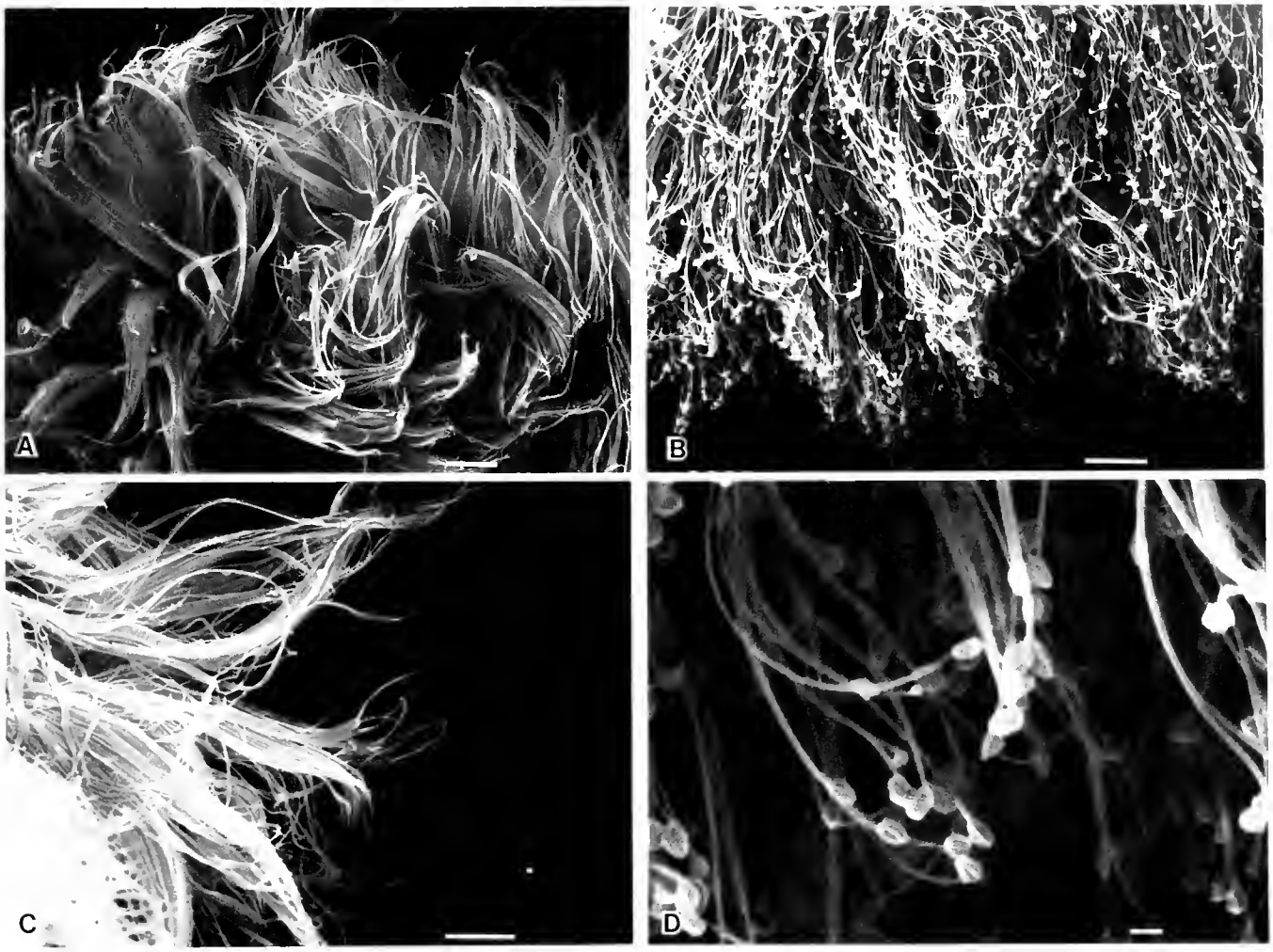

Figure 3. Scanning electron micrographs of velar cilia in *Lyrodus pedicellatus* larvae. A, C. Isosmotic fixative containing 50% seawater (Method 3). No paddle cilia are present. B, D. Hypotonic fixative of Campos and Mann (1988) (Method 1). Paddle cilia are present. Scale bars: A–C, 10 μm; D, 1 μm.

reported that swelling of isolated sucrose-treated cilia of *Tetrahymena* begins first at the tip, and progressively spreads to the base, indicating a "proximal-distal reduction in the strength of connections between the axoneme and the membrane" (Pitelka and Child, 1964, p. 149). Various types of bridges linking the ciliary or flagellar membrane to the outer doublet microtubules have recently been studied biochemically and by electron microscopy (Dentler, 1981). A new mutant of *Chlamydomonas reinhardtii* with disc-shaped flagellar tips (loop-1) similar in appearance to paddle cilia has recently been isolated, indicating a possible genetic defect in the binding between the axoneme and flagellar membrane (Nakamura *et al.*, 1990).

It is commonly observed that paddle cilia and discocilia are limited in distribution within a given specimen; *i.e.*, certain ciliary bands or body regions exhibit modified cilia, whereas other types of cilia in the same animal appear normal (Dilly, 1977a, b; Ehlers and Ehlers, 1978; Heimler, 1978; Arnold and Williams-Arnold, 1980; Bone *et al.*, 1982; Matera and Davis, 1982; Pfannenstiel, 1982; Campos and Mann, 1988; our results). This restricted distribution of paddle cilia and discocilia has been used to argue against their artifactual nature, on the grounds that artifactual production should effect all cilia uniformly (Bergquist *et al.*, 1977; Matera and Davis, 1982; Campos and Mann, 1988). However, Matera and Davis (1982) admitted that, "at the very least, these findings imply some unique properties of the tips of paddle cilia, although they do not alone disprove that the dilations are artifacts."

In fact, workers in the field have long recognized that "different cilia—even on the same organism—are not equally sensitive to stress and some cilia are indeed difficult to fix in a normal shape" (Nielsen, 1987). Our results on differences between ciliary types of veligers in response to hypotonic fixatives supports this finding. It is well-docu-

mented that various types of locomotory and sensory cilia differ in their lipid and protein composition, as well as in the kinds of structures linking the axonemal microtubules to the membrane (Dentler, 1981; Bloodgood, 1990). Therefore, absence of paddle cilia or discocilia in certain types of cilia or body regions of an animal does not mean that modified cilia observed elsewhere on the organism are genuine structures.

The mechanism(s) responsible for the formation of paddle cilia and discocilia is not understood. Our results on living and fixed veligers of *Spisula* and *Lyrodus* suggest that osmotic stress, not the buffers or fixatives used for electron microscopy, is the cause of modified cilia. However, Ehlers and Ehlers (1978) claimed that certain buffers and fixation additives play an important role in generating modified cilia in marine turbellarians. Surprisingly, they found that increasing the osmolality of the fixatives *increased* the numbers of paddle cilia formed.

Convincing evidence that osmotic changes themselves are not required for formation of paddle cilia is Pfannenstiel's (1982) finding that isotonic $MgCl_2$ solution induced paddle cilia in polychaetes. Nevertheless, he also found that the number and time of appearance of modified cilia were inversely related to the concentration of $MgCl_2$.

Bone *et al.* (1982) also discounted osmotic effects as the cause of coiling of ciliary tips in *Ciona*, because the total osmolarity of their glutaraldehyde fixatives was greater than that of seawater, and therefore should have induced a transient shrinkage preceding fixation.

We propose a unifying mechanism for the production of paddle cilia that accounts for many of these seemingly contradictory findings (Fig. 4). We suggest that the primary cause of paddle cilia and discocilia is a conformational change of ciliary doublet microtubules that results in the coiling of the axonemal tip within the distal membrane. Indeed, previous studies indicated that doublet microtubules have an intrinsic tendency to coil when not constrained within the axoneme (Summers and Gibbons, 1971; Zobel, 1973), and that physiological changes in Ca concentration or pH can induce reversible changes in the coiling parameters of isolated doublet microtubules in solution (Miki-Noumura and Kamiya, 1976, 1979; Takasaki and Miki-Noumura, 1982). We recently showed that increased concentrations of Ca, Ba, or Sr induce sharp curvatures of the distal end of axonemes in detergent-extracted macrocilia of *Beroë* (Tamm and Tamm, 1990). This tip curling response is independent of ATP-powered microtubule sliding, and is believed to be caused by Ca/Ba/Sr-induced helical changes in doublet microtubules, some of which are prevented from sliding (Tamm and Tamm, 1990).

In this regard, many of the conditions that induce paddle cilia and discocilia may initially increase Ca or proton flux across the distal ciliary membrane. For example, hypotonic swelling of the tip of the ciliary membrane, where membrane-microtubule bridges are the weakest (Child, 1961; Pitelka and Child, 1964), should increase membrane tension and open stretch-activated ion channels, if present (Guharay and Sachs, 1984; Sachs, 1988). Because stretch-activated channels are cation-selective, and some are Ca-permeable (Christensen, 1987; Lansman *et al.*, 1987), a resulting influx of Ca or change in pH at the ciliary tip might induce a conformational alteration of doublet microtubules that results in coiling of the axonemes (Fig. 4A). Secondly, certain fixatives or chemicals may cause an initial breakdown or permeabilization of the ciliary membrane, leading to similar Ca influx or pH changes which also might trigger conformational changes of the axonemal tip (Fig. 4B). This pathway, it should be noted, would not require distal swelling of the ciliary membrane, and would account for cases of paddle cilia formation under isosmotic or hyperosmotic conditions. Alternatively, disruption of the intact axonemal structure by proteolysis during fixation or handling may remove cross-linking constraints (nexin links, radial spokes) and allow spontaneous conformational alterations of the doublet microtubules, resulting in the coiling of the axoneme (Zobel, 1973) (Fig. 4C). These three possible pathways need not be mutually exclusive; for example, destruction of restraining elements within the axoneme may facilitate Ca or proton-induced alterations in microtubule conformation.

Indeed, Bone *et al.* (1982) found that Ca-blocking agents, such as Co and Mn, reversibly *uncoiled* discocilia in *Ciona*. These authors concluded that discocilia are caused by coiling of axonemes within the ciliary membrane, but believed that such conformational changes were brought about primarily by asymmetrical contraction of the axoneme after cross-linking by glutaraldehyde.

Regardless of the precise pathway(s) involved, the novel feature of the proposed mechanism is an induced or intrinsic conformational change of the doublet microtubules that leads to coiling of the tip of the axoneme (Fig. 4). Dilation or expansion of the ciliary membrane around the looped end of the axoneme would then be merely a passive secondary effect, and not the cause of coiling. Osmotic swelling of the ciliary membrane is thus one method for triggering an ion flux that would induce a conformational change of the doublet microtubules, but membrane tension itself would not be responsible for the coiling of the axoneme.

Our theory for the production of paddle cilia is readily testable. For example, the swollen membrane at the ciliary tip could be disrupted or removed. If the end of the axoneme still remained coiled, then membrane tension is not responsible for maintenance of the paddle. If, on the other hand, the distal end of the axoneme uncoiled and straightened upon disruption of the enclosing membrane, then membrane tension, not intrinsic shape changes of axonemal microtubules, is likely

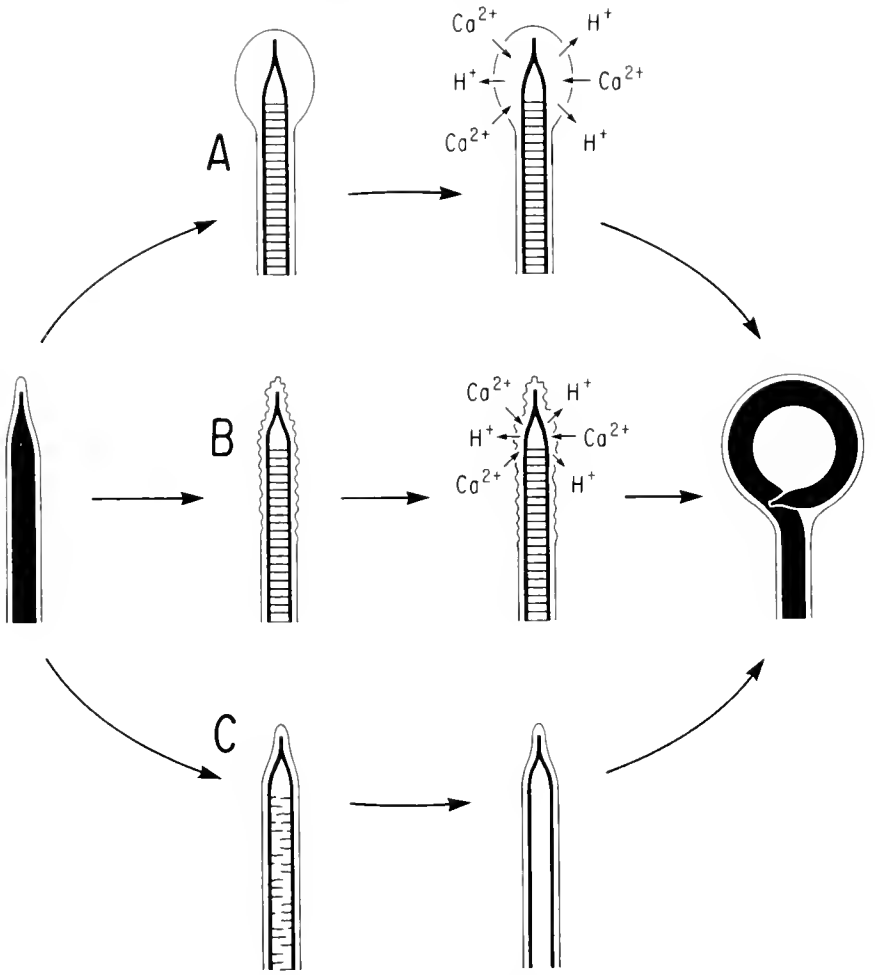

Figure 4. Proposed mechanism of formation of paddle cilia and discocilia. Three possible pathways lead from normal cylindrical ciliary structure (left, straight black axoneme within ciliary membrane) to an induced (A, B) or spontaneous (C) coiling of the axoneme within a distal expansion of the ciliary membrane (right). A. Osmotic swelling by hypotonic solutions or fixatives stretches the distal membrane and opens stretch-activated cation channels; Ca influx or proton efflux trigger conformational changes of the axoneme. B. Fixation or stress initially weakens the ciliary membrane and allows Ca influx or proton efflux, resulting in coiling of the axoneme as in A. No osmotic swelling is necessary. C. Abnormal conditions or fixation lead to weakening or destruction of internal cross-linking restraints (nexin links, radial spokes?), allowing spontaneous conformational alterations of doublet microtubules and coiling of the axoneme. These three pathways need not be mutually exclusive (see text).

to be the cause. Further experiments along these lines are planned.

In conclusion, we believe that our work, together with previous studies, convincingly shows that discocilia and paddle cilia are not genuine structures, but are artifacts. The unifying mechanism we propose to account for their formation suggests that these modifications may be useful for investigating the structural and mechanical properties of axonemal microtubules, as well as the nature of microtubule-membrane interactions in cilia.

Acknowledgments

We thank Scott Gallager, WHOI, for use of facilities, technical assistance, and helpful discussion and advice. We are also grateful to Louie Kerr, MBL EM facility, for SEM assistance, and to Ms. Dorothy Hahn for patiently and skillfully processing these words. This work was supported by a Woods Hole Marine Science Consortium fellowship to G.S. and NIH Grant GM27903 to S.L.T.

Literature Cited

Arnold, J. M., and L. D. Williams-Arnold. 1980. Development of the ciliature pattern on the embryo of the squid *Loligo pealei*: a scanning electron microscope study. *Biol. Bull.* **159:** 102–116.

Bergquist, P. R., C. R. Green, M. E. Sinclair, and H. S. Roberts. 1977. The morphology of cilia in sponge larvae. *Tissue Cell* **9:** 179–184.

Bloodgood, R. A. 1990. *Ciliary and Flagellar Membranes.* Plenum Press, New York. 431 pp.

Bone, Q., K. P. Ryan, and A. Pulsford. 1982. The nature of complex discocilia in the endostyle of *Ciona* (Tunicata: Ascidiacea). *Mikroskopie (Wien.* 39: 149–153.

Campos, B., and R. Mann. 1988. Discocilia and paddle cilia in the larvae of *Mulinia lateralis* and *Spisula solidissima* (Mollusca: Bivalvia). *Biol. Bull.* **175:** 343–348.

Child, F. M. 1961. Some aspects of the chemistry of cilia and flagella. *Exp. Cell Res. Suppl.* **8:** 47–53.

Christensen, O. 1987. Mediation of cell volume regulation by Ca^{2+} influx through stretch-activated channels. *Nature* **330:** 66–68.

Dentler, W. L. 1981. Microtubule-membrane interactions in cilia and flagella. *Int. Rev. Cytol.* **72:** 1–47.

Dilly, P. N. 1977a. Material transport within specialized ciliary shafts on *Rhabdopleura* zooids. *Cell Tissue Res.* **180:** 367–381.

Dilly, P. N. 1977b. Further observations of transport within paddle cilia. *Cell Tissue Res.* **185:** 105–113.

Durfot, M., E. Sagrista, M. G. Bozzo, M. Poquet, J. Garcia Valero, M. J. Amor, J. Ferrer, and E. Ribes. 1990. Modified cilia in vibratil epithelia of mussels infected by *Mytilicola intestinalis* and *Modiolicola gracilis* (Crustacea, Copepoda). *4th Internat. Colloq. Pathol. Marine Aquacul.*, Vigo, Spain. Pp. 108–109.

Ehlers, U., and B. Ehlers. 1978. Paddle cilia and discocilia—genuine structures? *Cell Tissue Res.* **192:** 489–501.

Gallager, S. M. 1988. Visual observations of particle manipulation during feeding in larvae of a bivalve mollusc. *Bull. Mar. Sci.* **43:** 344–365.

Gallager, S. M., and R. Mann. 1986. Growth and survival of *Mercenaria mercenaria* (L.) and *Crassostrea virginia* (Gmelin) relative to broodstock conditioning and lipid content of eggs. *Aquaculture* **56:** 105–121.

Guharay, F., and F. Sachs. 1984. Stretch-activated single ion channel currents in tissue-cultured embryonic chick skeletal muscle. *J. Physiol., Lond.* **352:** 685–701.

Hartmann, M. 1953. *Allgemeine Biologie.* Gustav Fischer Verlag, Stuttgart. P. 143.

Heimler, W. 1978. Discocilia—a new type of kinocilia in the larvae of *Lanice conchilega* (Polychaeta, Terebellomorpha). *Cell Tissue Res.* **187:** 271–280.

Koltzoff, N. 1953. Abschnitt. Dynamik. Pp. 140–143 in *Allgemeine Biologie*, M. Hartmann, ed. Gustav Fischer Verlag, Stuttgart.

Lansman, J. B., Hallam, T. J., and T. J. Rink. 1987. Single stretch-activated ion channels in vascular endothelial cells as mechanotransducers? *Nature* **325:** 811–813.

Lewin, R. A., and J. O. Meinhart. 1953. Studies on the flagella of algae. III. Electron micrographs of *Chlamydomonas moewusii*. *Can. J. Bot.* **31:** 711–717.

Matera, E. M., and W. J. Davis. 1982. Paddle cilia (discocilia) in chemosensitive structures of the gastropod mollusk *Pleurobranchaea californica*. *Cell Tissue Res.* **222:** 25–40.

Mecklenburg, C. V., U. Mercke, C. H. Hakansson, and N. G. Toremalm. 1974. Morphological changes in ciliary cells due to heat exposure. *Cell Tissue Res.* **148:** 45–56.

Miki-Noumura, T., and R. Kamiya. 1976. Shape of microtubules in solutions. *Exp. Cell Res.* **97:** 451–453.

Miki-Noumura, T., and R. Kamiya. 1979. Conformational change in the outer doublet microtubules from sea urchin sperm flagella. *J. Cell Biol.* **81:** 355–360.

Nakamura, S., M. Watanabe, K. Hatase, and M. K. Kojima. 1990. Light inhibits flagellation in a *Chlamydomonas* mutant. *Plant Cell Physiol.* **31:** 399–401.

Nielsen, C. 1987. Structure and function of metazoan ciliary bands and their phylogenetic significance. *Acta Zool. (Stockh.)* **68:** 205–262.

Oldfield, S. C. 1975. Surface fine structure of the globiferous pedicellariae of the regular echinoid, *Psammechinus miliaris* (Gmelin). *Cell Tissue Res.* **162:** 377–385.

Pfannenstiel, H. D. 1982. Modified axonemes and ciliary membranes in three polychaete species. *Cell Tissue Res.* **224:** 181–188.

Pitelka, D. R., and F. M. Child. 1964. The locomotor apparatus of ciliates and flagellates: relations between structure and function. Pp. 131–198 in *Biochemistry and Physiology of Protozoa*, vol. III, S. H. Hutner, ed. Academic Press, New York.

Preer, J. R., and L. B. Preer. 1959. Gel diffusion studies on the antigens of isolated cellular components of *Paramecium*. *J. Protozool.* **6:** 88–100.

Sachs, F. 1988. Mechanical transduction in biological systems. *CRC Crit. Rev. Biomed. Eng.* **16:** 141–169.

Short, G., and S. L. Tamm. 1989. Paddle cilia occur as artifacts in veliger larvae of *Spisula solidissima* and *Lyrodes pedicellatus*. *Biol. Bull.* **177:** 314.

Storch, V., and G. Alberti. 1978. Ultrastructural observations on the gills of polychaetes. *Helgol. Wiss. Meeresunters.* **31:** 169–179.

Summers, K. E., and I. R. Gibbons. 1971. Adenosine triphosphate-induced sliding of tubules in trypsin-treated flagella of sea-urchin sperm. *Proc. Natl. Acad. Sci. USA* **68:** 3092–3096.

Takasaki, Y., and T. Miki-Noumura. 1982. Shape of the ciliary doublet microtubule in solution. *J. Mol. Biol.* **158:** 317–324.

Tamarin, A., P. Lewis, and J. Askey. 1974. Specialized cilia of the byssus attachment plaque forming region in *Mytilus californianus*. *J. Morphol.* **142:** 321–327.

Tamm, S. L., and S. Tamm. 1990. Ca/Ba/Sr-induced conformational changes of ciliary axonemes. *Cell Motil. Cytoskel.* **17:** 187–196.

Zobel, C. R. 1973. Effect of solution composition and proteolysis on the conformation of axonemal components. *J. Cell Biol.* **59:** 573–594.

Reference: *Biol. Bull* **180**: 475–484. (June, 1991)

Metabolism and Excretion of Injected [^{3}H]-Ecdysone by Female Lobsters, *Homarus americanus*

MARK J. SNYDER[1] AND ERNEST S. CHANG[2]

Bodega Marine Laboratory, University of California, P.O. Box 247, Bodega Bay, California 94923

Abstract. The dynamics of ecdysteroid metabolism and excretion were followed in adult lobsters, *Homarus americanus*. Females at five different molt stages were injected with [^{3}H]-ecdysone. Levels of [^{3}H]-20-hydroxyecdysone (20E), converted from [^{3}H]-ecdysone, rose rapidly and remained significantly higher in premolt stages D_0 and D_1. In contrast, significant increases in the levels of highly polar ecdysteroid metabolites (HP) occurred primarily in stages A and C. Changes in the hemolymph levels of 20E and HP in hemolymph over the molt cycle suggest additional metabolic mechanisms by which the titers of active molting hormones can be regulated.

Excretion of [^{3}H]-ecdysteroids was slower during early premolt stages D_0 and D_1, suggesting that this reduced rate may be an additional mechanism for regulating ecdysteroid titers. Study of [^{3}H]-ecdysteroids indicated that metabolism proceeds primarily to HP that are excreted in the urine with unaltered ecdysteroids. An additional ecdysteroid metabolic route was found in the midgut gland; this route removes ecdysteroids from the hemolymph and transforms them into apolar metabolites prior to their excretion in the feces. This route is similar to that previously found for ingested [^{3}H]-ecdysone, which was converted to apolar conjugates without further absorption.

Introduction

The first ecdysteroid isolated from a decapod crustacean was 20-hydroxyecdysone (20E) by Hampshire and Horn (1966). Since that report, nearly 20 different ecdysteroids have been identified from over 25 crustacean species (see Chang, 1989, for review). 20E has been reported to be the putative active molting hormone, because it specifically alters premolt changes in kinase activities and protein synthesis in epidermal tissues (Christ and Sedlmeier, 1987; Traub *et al.*, 1987).

The primary ecdysteroid product of the molting gland, or Y-organ, is thought to be ecdysone (Chang and O'Connor, 1977). Additional evidence suggests that the Y-organ secretes other ecdysteroids, namely 25-deoxyecdysone (Lachaise *et al.*, 1989) and 3-dehydroecdysone (Spaziani *et al.*, 1989). A single hydroxylation step converts ecdysone and 25-deoxyecdysone to the more active products 20E and ponasterone A (P), respectively. Further metabolism proceeds by additional hydroxylation steps, formation of acids, and conjugation to form polar and apolar products (McCarthy, 1980, 1982; Lachaise and Lafont, 1984; Connat and Diehl, 1986; Snyder and Chang, 1991a, b).

Many decapod tissues absorb [^{3}H]-ecdysone or [^{3}H]-20E from the hemolymph (Kuppert *et al.*, 1978; McCarthy, 1980, 1982) and metabolize these injected ecdysteroids *in vitro* (Lachaise and Lafont, 1984). The metabolism of ecdysteroids has been studied in greater detail in insects, and the structural identities of many metabolites have been confirmed by mass spectrometry, nuclear magnetic resonance, and other chemical techniques (reviewed by Koolman and Karlson, 1985).

A characteristic pattern of hemolymph ecdysteroid titers defines the crustacean molt cycle; *i.e.*, titers are low until the final large premolt peak, and this peak is followed by a rapid decline just prior to ecdysis (Chang, 1989). Recently, the decapods *Uca pugilator* and *Homarus americanus* were reported as having other significant titer variations during their molt cycles (Hopkins, 1986; Snyder and Chang, 1991a). Hemolymph 20E levels in the lobster

Received 2 October 1990; accepted 5 February 1991.

[1] Current address: Department of Entomology, University of Arizona, Tucson, AZ 85721.

[2] To whom all correspondence should be addressed.

Abbreviations: 20,26E, 20,26-dihydroxyecdysone; 20E, 20-hydroxyecdysone; 20EA, 20-hydroxyecdysonoic acid; HP, highly polar ecdysteroid metabolites; HPLC, high-performance liquid chromatography; P, ponasterone A; RP, reverse phase; T, triol (22,25-dideoxyecdysone).

H. americanus drop precipitously in late premolt, and the drop is associated with an increase in the titer of highly polar metabolites (Snyder and Chang, 1991a). The titers of hemolymph ecdysteroids decrease both in late premolt and when regenerating limb buds autotomize. These changes are explicable by increases in both the metabolism of ecdysteroids to polar conjugates and the excretion of ecdysteroids (McCarthy, 1980, 1982). Other than control of the Y-organ by molt-inhibiting hormone, additional controlling mechanisms for the regulation of ecdysteroid titers are little known in crustaceans (Chang, 1989).

Excretion pathways for ecdysteroids in crustaceans have received little attention. When decapods were injected with [^{3}H]-ecdysone, [^{3}H]-20E, or [^{3}H]-P, much of the radiolabel appeared in the surrounding water within 1 to 48 h (Lachaise *et al.*, 1976; Kuppert *et al.*, 1978; Buchholz, 1982; Lachaise and Lafont, 1984). We recently cannulated both the antennal gland and anus and found that ecdysteroids are excreted both in urine and feces, although urine is the major route (Snyder and Chang, 1991b). The gut also excretes ecdysteroids from the hemolymph, in addition to playing an important role in detoxifying (by apolar conjugation) and excreting ingested ecdysteroids (Snyder and Chang, 1991b). That the gut metabolizes ecdysteroids, whether ingested, endogenous, or injected, has been found in several arthropods (Isaac and Slinger, 1989).

We have injected ecdysteroids into lobsters at five stages in the molt cycle, and have determined the levels of metabolites produced. These studies have revealed the changes in ecdysteroid metabolism that occur during the molt cycle. In addition, we have cannulated the anus and urinary pores, collected the radiolabeled metabolites, and thus elucidated the excretory routes for injected ecdysteroids.

Materials and Methods

Animals

Adult female *Homarus americanus* (420–570 g wet wt.) were either obtained from a seafood supplier (Net Result, Martha's Vineyard, Massachusetts) or were reared at the Bodega Marine Laboratory (Chang and Conklin, 1983; Conklin and Chang, 1983). No differences were observed between the lobsters obtained from these two sources. Only non-reproductive lobsters were used in this study to avoid ovarian influences on ecdysteroid dynamics (Lachaise *et al.*, 1981). They were maintained in a flow-through system at 12 ± 3.5°C on a 16L:8D photoperiod and fed a mixed diet of frozen fish, shrimp, and live mussels thrice weekly. The lobster premolt stages $D_0^{1.0}$, D_1', D_1'', D_1''', D_2', and D_2'' of Aiken (1973) are reported here as stages D_0^1, D_1^1, D_1^2, D_1^3, D_2^1, and D_2^2, respectively. Staging of postmolt and early intermolt was made according to the degree of softness of the carapace and chelae as reported by Stevenson (1968).

Cannulation was accomplished as follows. A lobster was restrained on its dorsum on a bed of ice. Both antennal gland pores were then externally cannulated by the methods of Holliday (1977). In addition, a cannula was inserted into the anus and held in place with cyanomethacrylate glue. The cannula (3.18 × 4.76 × 80 mm, i.d. × o.d. × l) was open-ended and initially filled with air. When properly attached, water did not enter the cannula. When the lobster defecated, the feces expelled air distally from the cannula. The remaining air in the cannula protected the feces from being contaminated by seawater. Feces were collected from the cannula after it was removed from the animal.

Injections

[23,24-^{3}H]-ecdysone (89 Ci/mmol, New England Nuclear) was purified by high-performance liquid chromatography (HPLC), dissolved in lobster saline (Mykles, 1980), and 3–4 μCi injected into the hemocoel at the base of the fourth pereiopod. The injected ecdysone did not raise the levels of circulating ecdysteroids above those previously observed (Snyder and Chang, 1991a). Injected animals were in stages A–B, C_4, D_0^1, D_1^1, and D_2^2–D_3^1. The hemolymph was sampled at 1, 4, 12, 24, 48, 72, and 96 h after injection, and all excreta were collected daily. Each of the collected samples was extracted in methanol and prepared for HPLC and liquid scintillation spectrometry, as described previously (Snyder and Chang, 1991a,b).

In one experiment, juvenile female lobsters (stage C_4, 29–46 g wet wt.) were injected with 1 μCi of [^{3}H]-ecdysone. At 1 h and 10 days, four lobsters were sacrificed, and the midgut glands, ovaries, abdominal muscles, hindguts, antennal glands, epidermal tissues of the cephalothorax, and the remaining carcasses were extracted in 100% methanol. Following two re-extractions and centrifugations (10 min, 4100 × *g*), portions of the resultant supernatants were subjected to liquid scintillation spectrometry for the determination of total radioactivity per tissue. Because the sample extracts were highly diluted, no variations in counting efficiency were observed. As a positive control, we added [^{3}H]-ecdysone to non-radiolabeled tissues prior to the extraction steps and thus determined that our tissue extraction efficiencies were 80–90%.

HPLC

Samples of individual hemolymph, urine, and fecal extracts were dissolved in the appropriate solvent, centrifuged, and the supernatant injected directly onto a Waters C_{18} μBondapak column (3.9 mm I.D. × 30 cm). One of the following reverse phase elution conditions was used:

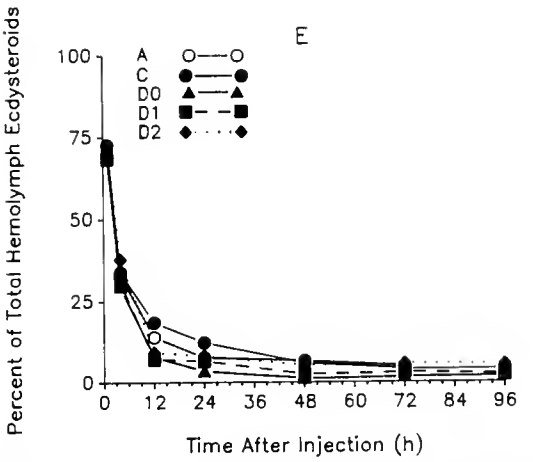

Figure 1. Changes in the hemolymph level of injected [^{3}H]-ecdysone (E) as a function of time and molt stage. [^{3}H]-ecdysone was injected at time zero. Concentration of labeled ecdysone in the hemolymph of lobsters is expressed as a percentage of the total [^{3}H]-ecdysteroids, and determined by methanolic extraction of hemolymph samples followed by scintillation counting of reverse phase-HPLC fractions. Samples were separated with gradient systems #1 or #2 (see text) with either (or both, for some samples) methanol or acetonitrile as the solvent. Molt stages A, C, D_0, D_1, and D_2 refer to the morphological designations of Aiken (1973). Sample sizes were as given for Table I with the addition of n = 3 for stage A. Standard deviation bars are omitted for clarity.

(1) a 35 min linear gradient of 20–100% methanol in water at 1.0 ml/min (1.0 min fractions); (2) a linear gradient of 20–100% acetonitrile in 20 m*M* Tris, pH 7.5, at 1.0 ml/min (1.0 min fractions collected); or (3) a linear gradient of 20–100% methanol in 20 m*M* Tris, pH 7.5, at 1.0 ml/min (1.0 min fractions collected). In all cases, we employed a Waters HPLC system. Duplicate samples from each fraction were analyzed by scintillation spectrometry. The sum of the radioactive ecdysteroids recovered in the HPLC-fractions was equal to 70–85% of the total, unfractionated radioactivity. The amount of each [^{3}H]-ecdysteroid metabolite was expressed as the percentage of the total radioactivity, and the values at each time point were compared statistically by ANOVA and Scheffé tests of arcsine transformed values (Sokal and Rohlf, 1969).

Enzymatic hydrolysis

The fractions resulting from HPLC that contained ecdysteroids of greater polarity than 20E are designated "polar fractions." The polar fractions from individual samples of urine and feces were pooled and then incubated, at 37°C for 24 h, in 1.0 ml sodium acetate buffer (50 m*M*, pH 5.5) containing 3.0 mg/ml type H-2 *Helix pomatia* sulfatase (Sigma). Apolar fractions from fecal samples were dissolved in ethanol (5% v/v in final hydrolysis mixture) with or without addition of enzymes, and incubated for 72 h (Whiting and Dinan, 1988). These modifications increased the hydrolysis of apolar material (Whiting and Dinan, 1988; Snyder and Chang, 1991b). After the addition of three volumes of methanol to terminate the reactions, the samples were centrifuged at 4100 × *g*, re-extracted twice, and the pooled supernatants evaporated under reduced pressure and analyzed by HPLC-scintillation spectrometry.

Results

Hemolymph ecdysteroids

Changes in hemolymph ecdysteroid metabolites were followed for 96 h after the injection of [^{3}H]-ecdysone. Figure 1 shows the rate of disappearance of ecdysone from the hemolymph. The loss of ecdysone, as a percentage of the total hemolymph [^{3}H]-ecdysteroids, was not significantly different from one molt stage to another. Within 1 h, ecdysone levels had fallen to about 70% of the total. Levels dropped dramatically to 6.5–12.2% by 24 h. Levels of [^{3}H]-ecdysone did not fall to zero and were still 2.5–5.5% of the total at 96 h.

Hemolymph [^{3}H]-20E levels were also followed after the injection of [^{3}H]-ecdysone (Fig. 2). By 1 h, [^{3}H]-20E percentages were 17–27% of the total [^{3}H]-ecdysteroids and not significantly different among the different molt stages. At 4 and 12 h, lobsters in stages D_0 and D_1 had higher percentages of labeled 20E (relative to other ecdysteroids) than at other molt stages. Levels of 20E for both stages (≥75% of the total) were consistently higher

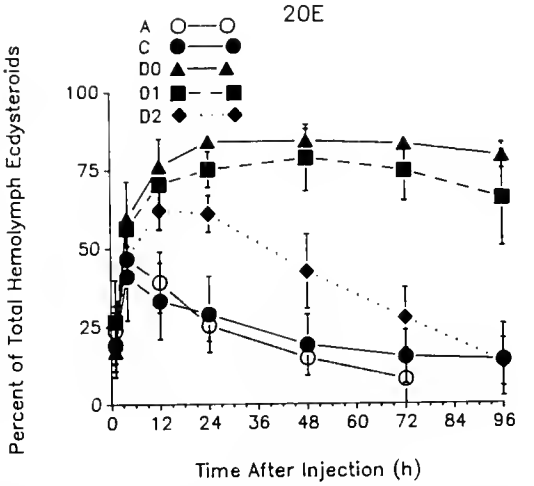

Figure 2. Change in the hemolymph level of radiolabeled 20-hydroxyecdysone (20E) as a function of time and molt stage. [^{3}H]-ecdysone was injected at time zero. Concentration of labeled 20E in the hemolymph of lobsters is expressed as a percentage of the total [^{3}H]-ecdysteroids. Separation and quantification conditions are as listed in Figure 1 and Materials and Methods. Sample sizes are as given for Table I with the addition of n = 3 for stage A. Bars indicate one standard deviation from the mean.

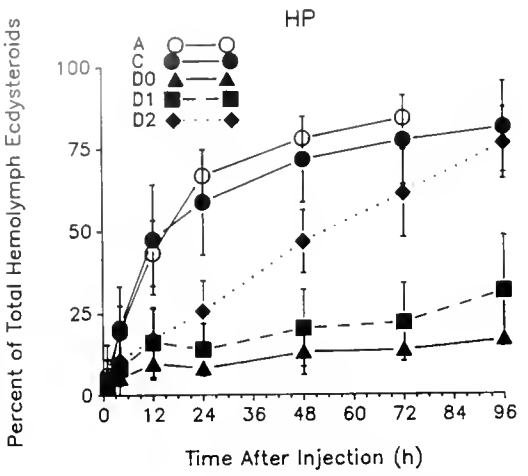

Figure 3. Change in the hemolymph level of radiolabeled highly polar ecdysteroid metabolites (HP) as a function of time and molt stage. [^{3}H]-ecdysone was injected into lobsters at time zero. Concentration of labeled HP in the hemolymph is expressed as a percentage of the total [^{3}H]-ecdysteroids. Separation and quantification conditions are as listed in Figure 1 and Materials and Methods. Sample sizes are as given for Table I with the addition of n = 3 for stage A. Bars indicate one standard deviation from the mean.

than those of other stages through 96 h. Premolt lobsters in stages D_1 and D_2 had similar 20E percentages at least until 12 h post-injection of [^{3}H]-ecdysone. By 24 h, the [^{3}H]-20E in the D_2 lobsters started to drop dramatically, reaching, by 72–96 h, levels equivalent to those in stages A and C. Levels of [^{3}H]-20E were significantly lower in D_2 than either D_0 or D_1 lobsters by 24 h. The concentrations of [^{3}H]-20E in stages A and C changed together throughout the 96 h experiment. Levels for those two stages peaked (41–47%) at 4 h, and then dropped to 7.9–11.1% of the total [^{3}H]-ecdysteroids by 72 h. Stage A and C [^{3}H]-20E levels were significantly lower than those of all other stages until 96 h post-injection, when stage D_2 lobsters had similar values. These data indicate that the rate of 20E loss becomes significantly faster as lobsters approach stage D_3.

Changes with time in the percentages of highly polar ecdysteroid metabolites (HP) were the converse of those in 20E (Fig. 3). All molt stages were similar from 1–4 h post-injection of [^{3}H]-ecdysone. The hemolymph percentages of [^{3}H]-HP in stages D_0 and D_1 lobsters barely increased. This is because [^{3}H]-20E percentages remain high in these two stages through 96 h (Fig. 2). The percentage of [^{3}H]-HP in late premolt stage D_2 lobsters was equivalent to those in D_0 and D_1 animals through 12 h (8–17% of the total), then rose to a significantly higher level by 48 h. At 72 h, stages D_2, A, and C had similar [^{3}H]-HP percentages. Stage A and C lobsters both showed rapid increases in [^{3}H]-HP percentages that were significantly higher (increasing to >75% of the total) than those in other molt stages.

Ecdysteroid excretion

Table I gives the data for total excretion of [^{3}H]-ecdysteroids, as a percentage of the injected dose, during the first 6 or the first 15 days after injection of [^{3}H]-ecdysone. Lobsters in stages D_0 and D_1 excreted significantly less ecdysteroids (12%) in the first 6 days after injection than those in stages C or D_2 (30%). By 15 days, D_0 lobsters had excreted significantly less [^{3}H]-ecdysteroids (28%) than those in stage D_1 (39%) and C (45%). Urine was always the major route for ecdysteroid excretion (Table I). In stages C and D_2, 90–96% of the radiolabel was excreted in the urine. Significantly more [^{3}H]-ecdysteroids were excreted in the feces of stage D_0 and D_1 lobsters than at stages C or D_2.

Ecdysteroid metabolites

Lobsters in stages C through D_1 were injected with [^{3}H]-ecdysone. Ninety-six hours later, the profiles of ecdysteroid metabolites in hemolymph, urine, and feces were examined. The data for injections into stages C (Fig. 4) and D_1 (Fig. 5) were similar to those for injections into stages D_2 and D_0, respectively. Therefore, profiles for the latter injections are not shown. At least four HP were resolved by RP-HPLC. Besides 20E, ecdysone, and P, two of these HP were tentatively identified as epimers of 20-hydroxyecdysonoic acid (20EA) and 20,26-dihydroxyecdysone (20,26E). The characterizations were based on co-elution with authentic standards in at least two different solvent systems; normal phase separations were also performed on some samples (data not shown). In addition, two other ecdysteroid metabolites were designated as "highly polar

Table I

Percentage of radioactivity recovered from excreta of adult lobsters following injection of [^{3}H]-ecdysone

		Urine plus feces[2]		Days 1–15[3]	
Molt stage[1]	n	Days 1–6	Days 1–15	Urine	Feces
C	5	30.0 ± 4.1[a]	45.2 ± 3.7[a]	90.2 ± 2.9[a]	9.8 ± 2.9[a]
D_0	3	11.5 ± 2.8[b]	28.2 ± 4.7[b]	80.6 ± 0.8[b]	19.4 ± 0.8[b]
D_1	4	12.0 ± 2.1[b]	38.7 ± 5.0[a]	73.3 ± 3.5[c]	26.7 ± 3.5[c]
D_2	4	30.6 ± 3.9[a]	—	95.5 ± 2.1[d]	4.5 ± 2.1[d]

[1] Molt stage designations are those of Aiken (1973). Postmolt stages A and B were not monitored for [^{3}H] excretion. Values with different superscript letters (within a column) indicate significant differences ($P < 0.05$).

[2] Sum of the radioactivity excreted in both the urine and feces in either the first 6 or the first 15 days following [^{3}H]-ecdysone injection. Late premolt stage D_2 lobsters were followed only for the first 6 days (after which they molted).

[3] Percentages of total radioactivity recovered in either the urine or feces over the entire experiment (days 1–15).

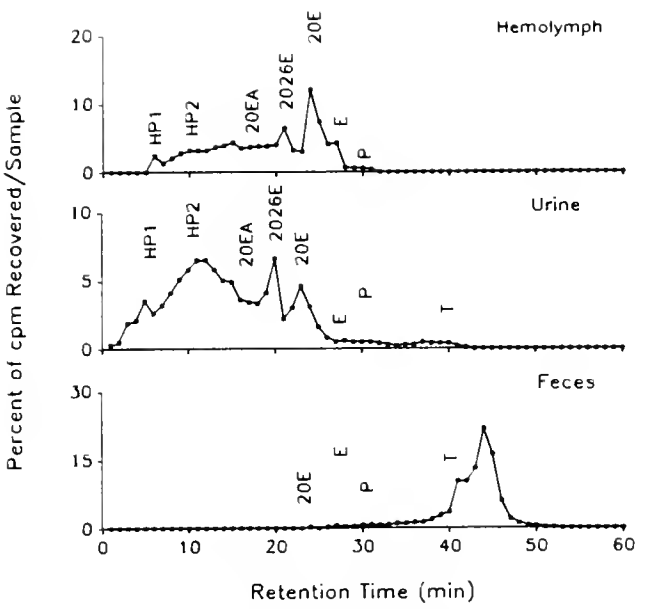

Figure 4. Reverse phase-HPLC-scintillation spectrometric analyses of hemolymph, urine, and fecal [^{3}H]-ecdysteroids. Samples were obtained from a stage C_4 lobster 96 h after injection of [^{3}H]-ecdysone. Separation conditions are described in Figure 1. The retention times of authentic 20-hydroxyecdysonoic acid epimers (20EA), 20,26-dihydroxyecdysone (20,26E), 20-hydroxyecdysone (20E), ecdysone (E), ponasterone A (P), and 22,25-dideoxyecdysone (triol, T) are shown. Two highly polar ecdysteroid products, which include conjugates and non-enzyme-hydrolyzable metabolites, are labeled as HP1 and HP2.

1" (HP1) and "highly polar 2" (HP2). The most polar metabolite, HP1, was a mixture of conjugates of 20EA, 20,26E, and 20E and also contained *Helix pomatia* enzyme-resistant compounds. The urine of stage D_2 lobsters contained significantly more HP1 material as enzyme-hydrolyzable conjugates than any other molt stage. This result indicates that ecdysteroid conjugation may increase in the late premolt stage. Hydrolysis of HP2 also yielded 20EA, 20,26E, 20E, and non-hydrolyzable material. Raising both the concentration of enzymes and incubation times failed to increase the hydrolysis of HP1 and HP2, supporting the idea that they may also contain other types of ecdysteroid metabolites. There were no significant differences between any of the molt stages in 20E and ecdysone excretion as percentage of the total ecdysteroids excreted per day in urine. But, since the excretion rates in stages C and D_2 were significantly higher in days 1–6 (Table II) than those in D_0 and D_1, more free 20E and ecdysone were excreted in the urine of the former stages.

The hemolymph of stage C lobsters, 96 h after injection, contained mainly HP2, 20EA, 20,26E, and 20E. Smaller quantities of HP1, ecdysone, and P were also present. The urine of stage C animals contained almost 90% HP with HP2, 20,26E, and 20E in similar proportions. The feces contained >95% apolar material; one component eluted with a retention time similar to that of 22,25-dideoxyecdysone (triol, T). Only small percentages of [^{3}H]-20E, ecdysone, and P were ever found in the feces of any molt stage.

Metabolite profiles for stage D_2–D_3 are shown in Figure 5. The major hemolymph ecdysteroid at this stage was 20E, with smaller amounts of HP1, HP2, 20,26E, and ecdysone. The urinary profile is also shown. Fecal [^{3}H]-ecdysteroids were >99% apolar products. Hydrolysis of the fecal apolar material yielded a number of products (Fig. 6). The profiles of fecal ecdysteroid conjugates varied according to molt stage. Figure 6 shows the profile of a premolt stage D_1 lobster fecal sample 10 days post-injection; at this time, 20E was the major hemolymph metabolite. Hydrolysis yielded a large percentage of 20E, and smaller amounts of HP1, ecdysone, P, T, and unhydrolyzed apolar components. During intermolt stage C, hydrolysis of fecal apolar ecdysteroids resulted in a higher percentage of free HP (data not shown).

The uptake and metabolism of [^{3}H]-ecdysone injected into hemolymph was studied in juvenile lobsters in intermolt stage C (Table II). By 1 h after injection, only 33% of the radiolabel remained in the hemolymph. Tissues such as hindgut, antennal glands, immature ovaries, and epidermis all contained <1% of the injected dose at 1 h. Only abdominal muscle (3.7%), midgut gland (4.5%), and

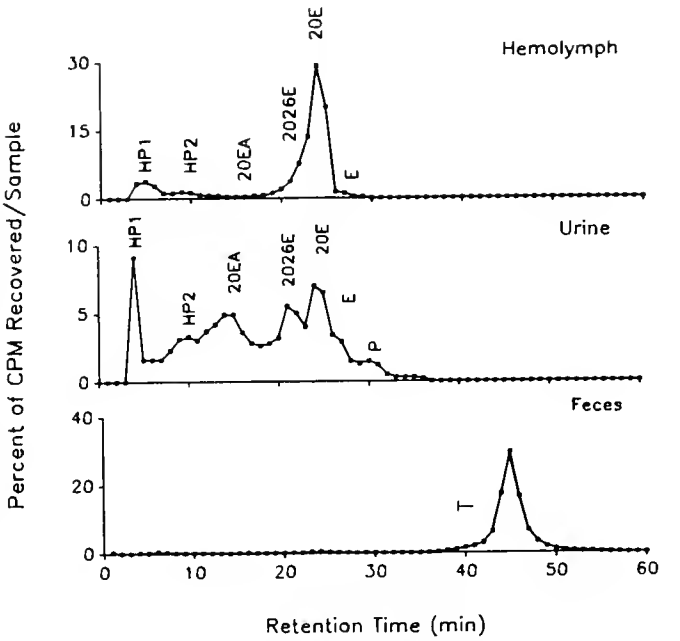

Figure 5. Reverse phase-HPLC-scintillation spectrometric analyses of hemolymph, urine, and feces from a lobster at stage D_2–D_3 (when the hemolymph ecdysteroids reach a maximum). The animal was injected with [^{3}H]-ecdysone in stage D_1 and sampled 96 h later. Separation conditions are described in Figure 1. Abbreviations for the various ecdysteroids are as in Figure 4.

carcass (45%) contained appreciable radioactivity at 1 h. When calculated as percentage of dose per gram wet weight of tissue, the largest amounts were found (after 1 h) in the antennal glands (16%) and ovaries (11%). The smallest quantities on a per weight basis were found (after 1 h) in muscle (1.5%) and carcass (1.8%).

By 10 days post-injection, about 41% of the injected dose had been lost due to excretion. Concomitantly, most tissues had very low levels of radioactivity; hindgut, antennal glands, epidermis, ovaries, and muscle all contained 0.1–0.2% of the initial label. Higher levels were found in hemolymph (1.0%), midgut gland (5.2%), and carcass (14%). On a wet weight basis, significantly higher levels were associated with hindgut, antennal glands, and midgut gland (30–32%). Clearly, by 10 days, the midgut gland had concentrated much more [^{3}H]-ecdysteroids than any other single tissue examined.

At 1 h and 10 days, 11% and 38% of the injected dose, respectively, could not be accounted for by either losses in methanol extraction (81% efficiency), leakage from the injection site (about 2.5%, as judged from counts of absorbent paper held on the wound for 30 s after injection, and from counts of the seawater bath 1 h later), or from adherence to the injection needle (about 5%). Possible explanations for these unexplained losses are [^{3}H] exchange or the activity of side-chain cleaving enzymes; the latter has been suggested to occur in decapod crustaceans (Lachaise and Lafont, 1984) and in other arthropods (Koolman and Karlson, 1985).

Some tissue extracts from 1 h and 10 days after injection of juvenile lobsters were also studied by RP-HPLC (Fig. 7). In 1 h, the largest amount of [^{3}H]-ecdysteroids in hemolymph remained as ecdysone, followed by smaller quantities of 20E and P. Only about 2% of the dose was found as HP in hemolymph 1 h after injection. Abdominal muscle contained higher levels of 20E than hemolymph, but ecdysone was still the major ecdysteroid at 1 h. At 1 h, muscle contained slightly higher (about 5%) levels of HP than did hemolymph. Large amounts of 20,26E, and

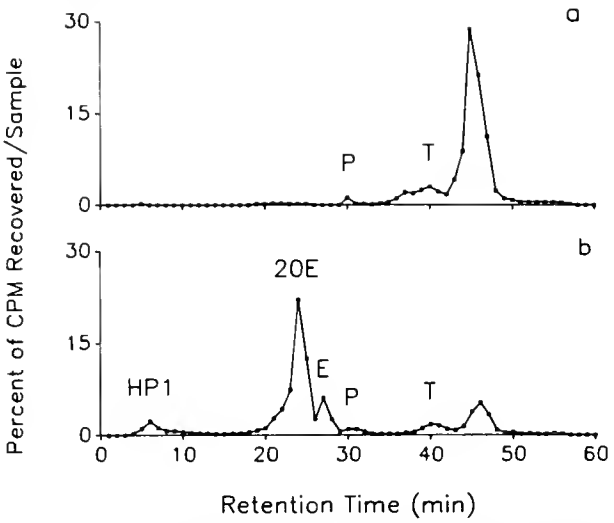

Figure 6. Enzyme treatment of fecal [^{3}H]-ecdysteroids from a stage D_1 lobster. Ecdysteroids were isolated from feces and incubated without (a) or with (b) *Helix pomatia* sulfatase. The samples were then analyzed by reverse phase-HPLC. Separation conditions are described in Figure 1. Abbreviations for the various ecdysteroids are as in Figure 4.

Table II

Recovery of radioactivity in tissues of juvenile lobsters injected with [^{3}H]-ecdysone[1]

Sample	n	H	HG	AG	EP	OV	M	MG	C
1 h[2]	4								
% of injected dose		33.1 ± 3.0^e	0.2 ± 0^a	0.4 ± 0.1^b	0.9 ± 0.1^c	0.9 ± 0.2^c	3.7 ± 0.8^d	4.5 ± 0.6^d	45.4 ± 6.1^f
%/g wet wt.		3.3 ± 1.0^{a,c}	3.5 ± 0.8^{a,c}	15.6 ± 6.1^b	3.8 ± 1.0^a	10.8 ± 2.1^b	1.5 ± 0.8^{c,d}	2.8 ± 0.9^{a,c,d}	1.8 ± 0.2^d
10 days[2]	4								
% of injected dose		1.0 ± 0.2^c	0.2 ± 0.1^a	0.1 ± 0^a	0.1 ± 0^a	0.1 ± 0^a	0.4 ± 0^b	5.2 ± 1.1^d	13.7 ± 2.4^e
%/10 g wet wt.		1.1 ± 0.2^a	30.3 ± 25.4^d	32.4 ± 1.7^d	4.0 ± 1.3^b	11.7 ± 7.8^b	5.2 ± 9.1^{a,b,c}	32.3 ± 5.1^d	6.0 ± 0.4^c

[1] Lobsters were injected with [^{3}H]-ecdysone, sacrificed at either 1 h or 10 days; methanolic extracts were then made of the various tissues: (H = hemolymph, HG = hindgut, AG = antennal glands, EP = epidermis of cephalothorax, OV = ovaries, M = abdominal muscle, MG = midgut gland, and C = remaining carcass). The radioactivity recovered from extracts was computed from determinations on aliquots and expressed as a percentage of the total injected dose.

[2] The data are presented, either as a percentage of the injected dose, or as a percentage of the dose per gram (for 1 h), or per 10 g (for 10 days) of wet tissue. Values are means (±1 standard deviation). Different superscript letters denote values that are significantly different ($P < 0.05$) from each other (within a row); analysis by ANOVA followed by Scheffé tests of the aresine transformations of the percentage values (Sokal and Rohlf, 1969).

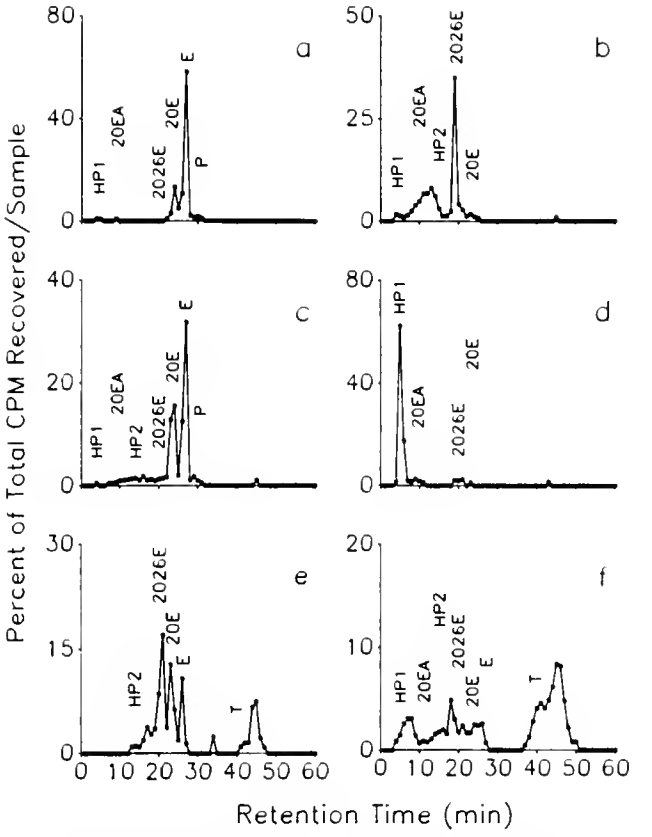

Figure 7. Reverse phase-HPLC chromatograms of extracts of tissues from juvenile stage C_4 lobsters. Hemolymph (a,b), abdominal muscle (c,d), and midgut gland (e,f) were taken at either 1 h (a,c,e) or 10 days (b,d,f) after injection with [^{3}H]-ecdysone. Samples were separated using gradient #3. Abbreviations for the various ecdysteroids are as in Figure 4.

approximately equivalent amounts of 20E, ecdysone, and apolar products were present in midgut gland at 1 h after injection. Smaller amounts of HP2, and a peak eluting between P and T, were also found in the midgut gland at 1 h.

By 10 days, hemolymph contained mostly HP with a large peak of 20,26E and smaller quantities of HP1, 20EA, HP2, and 20E. In contrast, a large peak of HP1 and very small amounts of 20EA, 20,26E, and 20E were present in the muscle at 10 days. A large amount of apolar material and smaller quantities of HP1, 20EA, 20,26E, 20E, and ecdysone were found in the midgut gland at 10 days.

Discussion

At all molt stages, ecdysone was very rapidly eliminated from lobster hemolymph. The rapid loss of [^{3}H]-ecdysone was not unexpected, because ecdysone titers in *H. americanus* (as determined by RIA) were never more than 19% of the total ecdysteroids in hemolymph (Snyder and Chang, 1991a). Ecdysone also has a short half-life in the crab *Gecarcinus lateralis* (McCarthy, 1980, 1982) and in several insect species (reviewed by Koolman and Karlson, 1985; Koolman and Walter, 1985). The activity of ecdysone 20-monooxygenase, which converts ecdysone to 20-hydroxyecdysone (20E), probably has a role in changing the levels of ecdysone in lobsters, as it does in several insects (Smith *et al.*, 1983; Mitchell and Smith, 1988). Young (1976) treated blowflies with supraphysiological doses of ecdysone, and demonstrated that alterations in the conversion rates of ecdysone to 20E could not be explained by saturation of metabolizing sites. Lachaise *et al.* (1976) reported that the rate of conversion of ecdysone to 20E was slower in postmolt and intermolt than in premolt stage crabs. Soumoff and Skinner (1988) demonstrated that enzyme activity varied with molt cycle in *G. lateralis* and that the variations were lowest in late premolt and postmolt. Additionally, Chang and O'Connor (1978) showed that 20-hydroxylation activity increased by four times in the testes of crabs (*Pachygrapsus crassipes*) that had undergone eyestalk ablation. The variation in ecdysone 20-monooxygenase during the crustacean molt cycle is still not understood.

Coincident with the drop in [^{3}H]-ecdysone were increases in [^{3}H]-20E. The primary metabolite of ecdysone in other crustaceans has been shown to be 20E (Lachaise *et al.*, 1976; Chang and O'Connor, 1978; Kuppert *et al.*, 1978; McCarthy, 1980, 1982; Buchholz, 1982). The relative amounts of [^{3}H]-20E, following the peak of conversion from [^{3}H]-ecdysone at 4–12 h, were significantly higher in the premolt stages of lobsters. In the late premolt stage D_2, there was a rapid loss of [^{3}H]-20E after 24 h similar to that exhibited in stages A and C after 4 h. These results are suggestive of a mechanism that regulates ecdysteroid metabolism around the time of the late premolt peak in the hemolymph (Snyder and Chang, 1991a). McCarthy (1982) reported long hemolymph 20E half-lives for *G. lateralis* in early-mid premolt. Long half-lives for 20E in early premolt crabs were significantly reduced by the autotomy of partially regenerated limbs, suggesting that other controls of ecdysteroid metabolism exist (McCarthy, 1980). Others have reported that 20E catabolism in insects can vary over larval-pupal stages (reviewed by Lehmann and Koolman, 1989). As in the lobster molt cycle, 20E was lost at a faster rate when molting hormone titers were increasing in the blowfly *Calliphora vicina* (Young, 1976; Young and Young, 1976; Koolman and Walter, 1985) and in the tobacco hornworm *Manduca sexta* (reviewed by Gilbert, 1989). The potential roles of 20E catabolic activity in the regulation of crustacean ecdysteroid titers require further study.

Levels of highly polar [^{3}H]-ecdysteroid metabolites (HP), such as 20-hydroxyecdysonoic acid (20EA), 20,26-dihydroxyecdysone (20,26E), and conjugates, increased

in hemolymph after increases in 20E. In *H. americanus*, hemolymph metabolites appeared in the following order: ecdysone → 20E → HP. The metabolism of a single injected dose of [^{3}H]-ecdysone appeared to mimic normal ecdysteroid metabolism in lobsters. Highly polar metabolites were the major circulating ecdysteroids in all lobster molt stages, except during mid-late premolt, the period when the major peak of ecdysteroids occurs in the hemolymph (Snyder and Chang, 1991a). However, of the metabolites detected by RIA in lobster hemolymph, urine, and feces (Snyder and Chang, 1991a,b), not all were found after the injection of [^{3}H]-ecdysone. A few unidentified metabolites eluting from the RP column between ecdysone and P were absent in the present study. Gilbert (1989) advised caution in the interpretation of [^{3}H]-ecdysone injection experiments, as similar incomplete ecdysteroid profiles were found in *Manduca sexta*.

Injections of [^{3}H]-ecdysone into cannulated lobsters confirmed that the likely route for excretion of ecdysteroid metabolites (HP, and unconjugated 20E, ecdysone, and P) from hemolymph is via the urine in all molt stages. Equivalent results were found when excreta were assayed by RIA throughout the molt cycle (Snyder and Chang, 1991b). Others have shown that HP were formed by decapod crustaceans following the injection of [^{3}H]-ecdysone or [^{3}H]-P (Lachaise *et al.*, 1976; Kuppert *et al.*, 1978; McCarthy, 1980, 1982; Buchholz, 1982; Lachaise and Lafont, 1984). Some of these metabolites, including conjugates, have also been found in the seawater surrounding the animals (Buchholz, 1982; Lachaise and Lafont, 1984). The only differences related to the molt cycle that were discovered in lobster urine were in the amounts of HP conjugates, which were much higher in late premolt (stage D_2) lobsters. It may be that highly polar conjugates are destined for excretion only in non-reproductive lobsters, and that excretion is more significant during the rapid decline in ecdysteroid titer just prior to ecdysis. Lachaise and Lafont (1984) found similar increases in highly polar ecdysteroid conjugates in late premolt crabs (*Carcinus maenas*) after injection of ponasterone A. Polar conjugates are loaded into vitellogenic ovaries, and thus may be potential sources of ecdysteroids for developing crustacean embryos (Lachaise *et al.*, 1981; Spindler *et al.*, 1987).

The data on excretion rates (Table I), suggest that lobsters have an additional mechanism for regulating ecdysteroid levels. Initial excretion rates were higher for intermolt (stage C) and late premolt (stage D_2) lobsters after the final hemolymph peak. Additionally, the excretion rate increased in mid-premolt (stage D_1), in the latter part of the 15-day observation period, at a time after injection equivalent to stage D_2 lobsters. The data indicate that excretion rates vary with the stage of the molt cycle; regulation of these excretion rates may therefore be an additional means of altering ecdysteroid titers. These results agree with earlier studies on insects. Hoffmann *et al.* (1974) and Koolman and Walter (1985) provided evidence that excretion rates varied and were lowest at times of peak hormone titer in locusts and blowflies. The role of excretion in regulating ecdysteroid titers in crustaceans remains obscure.

Excretion of [^{3}H]-ecdysteroids in lobster feces was detected following injection of [^{3}H]-ecdysone into hemolymph. These data confirm those from earlier RIA data (Snyder and Chang, 1991b), indicating that the lobster gut can absorb ecdysteroids from hemolymph and transform them into apolar conjugates prior to their excretion in feces. Apolar ecdysteroid conjugates were also found in larval crabs after the injection of [^{3}H]-ecdysone (Connat and Diehl, 1986). The apolar material in lobster feces consisted of conjugates of HP metabolites and 20,26E, 20E, ecdysone, and P. Apolar ecdysteroid-conjugating enzymes in the gut are, therefore, not specific for particular metabolites. Conjugating enzymes are similarly non-specific in spiders (Connat *et al.*, 1988c), ticks (Connat *et al.*, 1988b), mealworms (Delbecque *et al.*, 1988), and crickets (Whiting and Dinan, 1988). The apolar metabolites have been identified as long-chain fatty acid esters in a variety of arthropods, but their definitive identification in crustaceans awaits further study (Hoffman *et al.*, 1985; Kubo *et al.*, 1987; Whiting and Dinan, 1989). The failure of others to find apolar conjugates as major ecdysteroid metabolites of arthropods has been attributed to losses in purification or in the choice of HPLC conditions (Connat and Diehl, 1986).

When ingested by lobsters, [^{3}H]-ecdysone is converted to apolar conjugates without further metabolism to other ecdysteroids or absorption from the gut (Snyder and Chang, 1991b). Similarly, ingested ecdysteroids are efficiently "detoxified" to apolar metabolites in a variety of arthropods including spiders (Connat *et al.*, 1988c), ticks (Connat *et al.*, 1988a), and tobacco budworms (Kubo *et al.*, 1987). The role of the lobster midgut gland in apolar ecdysteroid conjugation was confirmed by injection of [^{3}H]-ecdysone (Table II; Fig. 7). Appreciable amounts of apolar conjugates were only found in the midgut gland. This finding parallels results derived from *in vitro* studies of the lobster (Snyder and Chang, 1992) and crayfish midgut glands (Gorell *et al.*, 1972). Appreciable amounts of apolar conjugates were also found in the crayfish midgut gland after injection of [^{3}H]-ecdysone into the hemolymph (Kuppert *et al.*, 1978). The function of the midgut gland is still unclear in relation to its role in ecdysteroid metabolism; it might be the slow release of apolar conjugates into the feces, or the provision, after hydrolysis, of an additional source of active hormone. Both Sehnal *et al.* (1981) and Williams (1987) have shown that the insect pupal midgut contains a mobilizable source of ecdysteroids that is sufficient to drive the pupal-adult transition

in the absence of prothoracic glands. The lack of appreciable absorption of [^{3}H]-ecdysone after ingestion by *H. americanus* argues that the sole function of this ecdysteroid metabolic route in crustaceans may be for excretion.

Apolar ecdysteroid conjugates have been found in ovaries and embryos in other arthropods, such as ticks (Connat *et al.*, 1988b), cockroaches (Slinger and Isaac, 1988), and crickets (Whiting and Dinan, 1988, 1989). Similar studies should be conducted on crustaceans to determine the presence of these apolar conjugates in ovaries and embryos.

In conclusion, the metabolism of [^{3}H]-ecdysteroids in *H. americanus* involves both polar and apolar pathways. The overall metabolic routes of lobster ecdysteroids are therefore similar to those found in a variety of other arthropods.

Acknowledgments

We gratefully acknowledge the gifts of ponasterone A from Dr. J. D. O'Connor (University of North Carolina, Chapel Hill), and 20,26-dihydroxyecdysone and 20-hydroxyecdysonoic acid from Dr. M. J. Thompson (U. S. Department of Agriculture, Beltsville, Maryland). We also thank Drs. B. L. Lasley and J.-H. Cheng for helpful discussions and the Editors and anonymous reviewers whose suggestions improved this paper. This work was supported by the NOAA, National Sea Grant College Program, Department of Commerce, under Grant NA85AA-D-SG140, Project R/A-80, through the California Sea Grant College Program (to E.S.C.). The U. S. Government is authorized to reproduce and distribute copies for governmental purposes.

Literature Cited

Aiken, D. E. 1973. Proecdysis, setal development, and molt prediction in the American lobster (*Homarus americanus*). *J. Fish. Res. Board Can.* **30:** 1337–1344.

Buchholz, F. 1982. The metabolism of ecdysone and its putative role as the female sex-pheromone in the green shore crab *Carcinus maenas* L. *Publ. Cent. Natl. Exploit. Oceans Actes Colloq.* **14:** 35–46.

Chang, E. S. 1989. Endocrine regulation of molting in Crustacea. *Rev. Aquatic Sci.* **1:** 131–157.

Chang, E. S., and D. E. Conklin. 1983. Lobster (*Homarus*) hatchery techniques. Pp. 271–275 in *CRC Handbook of Mariculture*, Vol. 1, J. P. McVey, ed. CRC Press, Boca Raton.

Chang, E. S., and J. D. O'Connor. 1977. Secretion of α-ecdysone by crab Y-organs *in vitro*. *Proc. Natl. Acad. Sci. USA* **74:** 615–618.

Chang, E. S., and J. D. O'Connor. 1978. *In vitro* secretion and hydroxylation of α-ecdysone as a function of the crustacean molt cycle. *Gen. Comp. Endocrinol.* **36:** 151–160.

Christ, B., and D. Sedlmeier. 1987. Variations in epidermal cyclic nucleotide-dependent protein kinase activity during moult cycle of the crayfish *Orconectes limosus* and hormonal control of kinase activity by 20-hydroxyecdysone. *Int. J. Biochem.* **19:** 79–84.

Conklin, D. E., and E. S. Chang. 1983. Grow-out techniques for the American lobster, *Homarus americanus*. Pp. 277–286 in *CRC Handbook of Mariculture*, Vol. 1, J. P. McVey, ed. CRC Press, Boca Raton.

Connat, J. L., and P. A. Diehl. 1986. Probable occurrence of ecdysteroid fatty acid esters in different classes of arthropods. *Insect Biochem.* **16:** 91–97.

Connat, J. L., E. M. Dotson, and P. A. Diehl. 1988a. Apolar conjugates of ecdysteroids are not used as a storage form of molting hormone in the argasid tick *Ornithodoros moubata*. *Arch. Insect Biochem. Physiol.* **9:** 221–235.

Connat, J. L., E. M. Dotson, and P. A. Diehl. 1988b. Metabolism of ecdysteroids in the female tick *Amblyomma hebraeum* (Ixodoidea, Ixodidae): accumulation of free ecdysone and 20-hydroxyecdysone in the eggs. *J. Comp. Physiol. B* **157:** 689–699.

Connat, J. L., P. A. Fürst, and M. Zweilin. 1988c. Detoxification of injected and ingested ecdysteroids in spiders. *Comp. Biochem. Physiol.* **91B:** 257–265.

Delbecque, J. P., J. L. Connat, and R. Lafont. 1988. Polar and apolar metabolites of ecdysteroids during the metamorphosis of *Tenebrio molitor*. *J. Insect Physiol.* **34:** 619–624.

Gilbert, L. I. 1989. The endocrine control of molting: the tobacco hornworm, *Manduca sexta*, as a model system. Pp. 448–471 in *Ecdysone: From Chemistry to Mode of Action*, J. Koolman, ed. Georg Thieme Verlag, Stuttgart.

Gorell, T. A., L. I. Gilbert, and J. B. Siddall. 1972. Binding proteins for an ecdysone metabolite in the crustacean hepatopancreas. *Proc. Natl. Acad. Sci. USA* **69:** 812–815.

Hampshire, F., and D. H. S. Horn. 1966. Structure of crustecdysone, a crustacean molting hormone. *Chem. Commun.* **2:** 37–38.

Hoffmann, J. A., J. Koolman, P. Karlson, and P. Joly. 1974. Molting hormone titer and metabolic fate of injected ecdysone during the fifth larval instar and in adults of *Locusta migratoria* (Orthoptera). *Gen. Comp. Endocrinol.* **22:** 90–97.

Hoffmann, K. H., D. Bulenda, E. Thiry, and E. Schmid. 1985. Apolar ecdysteroid esters in adult female crickets, *Gryllus bimaculatus*. *Life Sci.* **37:** 185–192.

Holliday, C. W. 1977. A new method for measuring the urinary rate of a brachyuran crab. *Comp. Biochem. Physiol.* **58A:** 119–120.

Hopkins, P. M. 1986. Ecdysteroid titers and Y-organ activity during late anecdysis and proecdysis in the fiddler crab, *Uca pugilator*. *Gen. Comp. Endocrinol.* **63:** 362–373.

Isaac, R. E., and A. J. Slinger. 1989. Storage and excretion of ecdysteroids. Pp. 250–253 in *Ecdysone: From Chemistry to Mode of Action*, J. Koolman, ed. Georg Thieme Verlag, Stuttgart.

Koolman, J., and P. Karlson. 1985. Regulation of ecdysteroid titer: degradation. Pp. 343–361 in *Comprehensive Insect Physiology Biochemistry and Pharmacology*, Vol. 7, G. A. Kerkut and L. I. Gilbert, eds. Pergamon Press, Oxford.

Koolman, J., and J. Walter. 1985. Ecdysteroids in insects: how are their concentrations regulated? Pp. 198–220 in *Metamorphosis: British Society for Developmental Biology Symposium*, Vol. 8, M. Balls and M. Bownes, eds. Clarendon Press, Oxford.

Kubo, I., S. Komatsu, Y. Asaka, and G. De Boer. 1987. Isolation and identification of apolar metabolites of ingested 20-hydroxyecdysone in frass of *Heliothis virescens* larvae. *J. Chem. Ecol.* **13:** 785–794.

Kuppert, P., M. Buchler, and K.-D. Spindler. 1978. Distribution and transport of molting hormones in the crayfish, *Orconectes limosus*. *Z. Naturforsch.* **33C:** 437–441.

Lachaise, F., and R. Lafont. 1984. Ecdysteroid metabolism in a crab: *Carcinus maenas* L. *Steroids* **43:** 243–259.

Lachaise, F., M. Lagueux, R. Feyereisen, and J. A. Hoffmann. 1976. Métabolisme de l'ecdysone au cours du développement de *Carcinus maenas* (Brachyura, Decapoda). *C. R. Acad. Sci. Paris* **283:** 943–946.

Lachaise, F., M. Goudeau, C. Hetru, C. Kappler, and J. A. Hoffmann. 1981. Ecdysteroids and ovarian development in the shore crab, *Carcinus maenas*. *Hoppe-Seyler's Z. Physiol. Chem.* **363:** 1059–1067.

Lachaise, F., G. Carpenter, G. Sommé, J. Colandeau, and P. Beydon. 1989. Ecdysteroid synthesis by crab Y-organs. *J. Exp. Zool.* **252:** 283–292.

Lehmann, M., and J. Koolman. 1989. Regulation of ecdysone metabolism. Pp. 217–220 in *Ecdysone: From Chemistry to Mode of Action*, J. Koolman, ed. Georg Thieme Verlag, Stuttgart.

McCarthy, J. F. 1980. Ecdysone metabolism and the interruption of proecdysis in the land crab, *Gecarcinus lateralis*. *Biol. Bull.* **158:** 91–102.

McCarthy, J. F. 1982. Ecdysone metabolism in premolt land crabs (*Gecarcinus lateralis*). *Gen. Comp. Endocrinol.* **47:** 323–332.

Mitchell, M. J., and S. L. Smith. 1988. Ecdysone 20-monooxygenase activity throughout the life cycle of *Drosophila melanogaster*. *Gen. Comp. Endocrinol.* **72:** 467–470.

Mykles, D. L. 1980. The mechanism of fluid absorption at ecdysis in the American lobster, *Homarus americanus*. *J. Exp. Biol.* **84:** 89–101.

Sehnal, F., P. Maroy, and J. Mala. 1981. Regulation and significance of ecdysteroid titre fluctuations in lepidopterous larvae and pupae. *J. Insect Physiol.* **27:** 535–544.

Slinger, A. J., and R. E. Isaac. 1988. Synthesis of apolar ecdysone esters by ovaries of the cockroach *Periplaneta americana*. *Gen. Comp. Endocrinol.* **70:** 74–82.

Smith, S. L., W. E. Bollenbacher, and L. I. Gilbert. 1983. Ecdysone 20-monooxygenase activity during larval-pupal development of *Manduca sexta*. *Mol. Cell. Endocr.* **31:** 227–251.

Snyder, M. J., and E. S. Chang. 1991a. Ecdysteroids in relation to the molt cycle of the American lobster, *Homarus americanus*. I. Hemolymph titers and metabolites. *Gen. Comp. Endocrinol.* **81:** 133–145.

Snyder, M. J., and E. S. Chang. 1991b. Ecdysteroids in relation to the molt cycle of the American lobster, *Homarus americanus*. II. Excretion of metabolites. *Gen. Comp. Endocrinol.* (in press).

Snyder, M. J., and E. S. Chang. 1992. Role of the midgut gland in the metabolism and excretion of ecdysteroids by lobsters. *Homarus americanus*. *Gen. Comp. Endocrinol.* (in press).

Sokal, R. R., and F. J. Rohlf. 1969. *Biometry*. W. H. Freeman, San Francisco. 776 pp.

Soumoff, C., and D. M. Skinner. 1988. Ecdysone 20-monooxygenase activity in land crabs. *Comp. Biochem. Physiol.* **91C:** 139–144.

Spaziani, E., H. H. Rees, W. L. Wang, and R. D. Watson. 1989. Evidence that Y-organs of the crab *Cancer antennarius* secrete 3-dehydroecdysone. *Mol. Cell. Endocr.* **66:** 17–25.

Spindler, K.-D., A. Van Wormhoudt, D. Sellos, and M. Spindler-Barth. 1987. Ecdysteroid levels during embryogenesis in the shrimp, *Palaemon serratus* (Crustacea Decapoda): quantitative and qualitative changes. *Gen. Comp. Endocrinol.* **66:** 116–122.

Stevenson, J. R. 1968. Metecdysial molt staging and changes in the cuticle in the crayfish *Orconectes sanborni* (Faxon). *Crustaceana* **14:** 169–177.

Traub, M., G. Gellissen, and K.-D. Spindler. 1987. 20(OH)ecdysone-induced transition from intermolt to premolt protein biosynthesis patterns in the hypodermis of the crayfish, *Astacus leptodactylus*, *in vitro*. *Gen. Comp. Endocrinol.* **65:** 465–477.

Whiting, P., and L. Dinan. 1988. The occurrence of apolar ecdysteroid conjugates in newly-laid eggs of the house cricket, *Acheta domesticus*. *J. Insect Physiol.* **34:** 625–631.

Whiting, P., and L. Dinan. 1989. Identification of the endogenous apolar ecdysteroid conjugates present in newly-laid eggs of the house cricket (*Acheta domesticus*) as 22-long-chain fatty acyl esters of ecdysone. *Insect Biochem.* **19:** 759–765.

Williams, C. M. 1987. Midgut of lepidopteran pupae is a major depot of sequestered, mobilizable, ecdysteroids. *Memor. Instit. Oswaldo Cruz* **82:** 47–49.

Young, N. L. 1976. The metabolism of ^{3}H-molting hormone in *Calliphora erythrocephala* at the mature larval and white puparial stages. *Insect Biochem.* **6:** 1–12.

Young, N. L., and P. R. Young. 1976. Biochemical control of moulting hormone titer in *Calliphora erythrocephala* during puparium formation. *Insect Biochem.* **6:** 169–177.

Reference: *Biol. Bull.* **180**: 485–488. (June, 1991)

New Calcitonin Isolated from the Ray, *Dasyatis akajei*

Y. TAKEI[1]*, A. TAKAHASHI[2], T. X. WATANABE[3], K. NAKAJIMA[3], S. SAKAKIBARA[3], Y. SASAYAMA[4], N. SUZUKI[4], AND C. OGURO[4]

Departments of [1]Physiology and [2]Molecular Biology, Kitasato University School of Medicine, Sagamihara, Kanagawa 228, [3]Peptide Institute Inc., Protein Research Foundation, Minoh, Osaka 562, and [4]Department of Biology, Faculty of Science, Toyama University, Toyama 930, Japan

Abstract. Calcitonin causes hypocalcemia by inhibiting the resorption of calcium from the bone in mammals. Calcitonin has now been isolated from the ultimobranchial gland of a cartilaginous fish, the ray (*Dasyatis akajei*), and its amino acid has been determined to be H-Cys-Thr-Ser-Leu-Ser-Thr-Cys-Val-Val-Gly-Lys-Ser-Gln-Gln-Leu-His-Lys-Leu-Gln-Asn-Ile-Gln-Arg-Thr-Asp-Val-Gly-Ala-Ala-Thr-Pro-NH_2. Although its basic structure is well conserved, the amino acid sequence of ray calcitonin is considerably different from that of other calcitonins sequenced to date. Because the ray lacks calcified bones, an examination of the effect of calcitonin in this fish may elucidate a new role for calcitonin in vertebrates.

Introduction

Calcitonins were first isolated from the thyroid glands of mammals, and amino acid sequences have now been determined in five species (Neher *et al.*, 1968; Potts *et al.*, 1968, 1971; Brewer and Ronan, 1969; Raulais *et al.*, 1976). Although calcitonin-like immunoreactivity was also identified in the ultimobranchial glands of all classes of non-mammalian vertebrates (Van Noorden and Pearse, 1971; Tisserand-Jochem *et al.*, 1977; Sasayama *et al.*, 1984; Treilhou-Lahille *et al.*, 1984), structures have been determined for only one species of bird and two teleost fishes (Niall *et al.*, 1969; Noda and Narita, 1976; Homma *et al.*, 1986). The mammalian calcitonins fall into two groups according to the homology of their amino acid sequences, and the difference between the amino acid sequences of these two mammalian groups is greater than that between the bird and the teleosts (Fig. 1). As for function, non-mammalian calcitonins have a much greater hypocalcemic effect in the rat than do the mammalian calcitonins (Homma *et al.*, 1986).

Recently, immunoreactive calcitonin was demonstrated in the ray, *Dasyatis akajei* (Sasayama *et al.*, 1984). Because the osteocytes are the principal site of action of calcitonin in mammals (Friedman and Raisz, 1965), a new action of calcitonin should be expected in this cartilaginous fish. Indeed, mammalian calcitonin has been shown to lack a hypocalcemic effect in some non-mammalian species (Pang *et al.*, 1980). Thus, the roles of calcitonin in the cartilaginous fish may provide a new insight into the fundamental actions of calcitonin common to all vertebrates. As the essential step toward discovering such roles, an attempt was made to isolate calcitonin from the ray and to determine its amino acid sequence. The molecular structure of calcitonin in this phylogenetically primitive fish may provide new evidence for the evolution of the calcitonin molecule in vertebrate phylogeny.

Materials and Methods

The rays (*Dasyatis akajei*) were caught in Toyama Bay and anesthetized with 1/3,000 (v/v) of tricaine methanesulfonate (Sigma) in seawater. The ultimobranchial glands were resected under a dissecting microscope, immediately frozen, and kept at −50°C until used.

Calcitonin was extracted from ray ultimobranchial glands and purified as follows. Two hundred deep-frozen glands (2.2 g) were pulverized in a stainless-steel crusher with a hammer, immediately boiled for 5 min with 7 volumes of water, acidified with acetic acid to make a final concentration of 1 *M*, and homogenized in a Polytron homogenizer for 90 s at 4°C at maximum speed (Takei *et al.*, 1989). The homogenate was centrifuged at 25,000 × *g* for 30 min at 4°C, and the high molecular weight proteins and lipids were removed from the supernatant

Received 22 February 1991; accepted 27 March 1991.

* To whom correspondence should be sent.

```
Fowl CT      CASLSTCVLGKLSQELHKLQTYPRTDVGAGTP-NH2
Eel CT       CSNLSTCVLGKLSQELHKLQTYPRTDVGAGTP-NH2
Salmon CT    CSNLSTCVLGKLSQELHKLQTYPRTNTGSGTP-NH2

Rat CT       CGNLSTCMLGTYTQDLNKFHTFPQTSIGVGAP-NH2
Human CT     CGNLSTCMLGTYTQDFNKFHTFPQTAIGVGAP-NH2

Porcine CT   CSNLSTCVLSAYWRNLNNFHRFSGMGFGPETP-NH2
Bovine CT    CSNLSTCVLSAYWKDLNNYHRFSGMGFGPETP-NH2
Ovine CT     CSNLSTCVLSAYWKDLNNYHRYSGMGFGPETP-NH2
```

Figure 1. Amino acid sequences of the mammalian and non-mammalian calcitonins (CTs) that have been sequenced to date. The identical amino acids within the same group are boxed.

with 67% and 98.5% acetone, respectively, at 4°C. The extract was then subjected to reverse-phase high performance liquid chromatography (HPLC) on an ODS-120T column (4.6 × 250 mm; Tosoh, Tokyo) with a linear gradient elution from 20% to 80% CH_3CN in 0.1% trifluoroacetic acid (pH 2.0), and each fraction was examined for the presence of immunoreactive calcitonin by immunoblotting. Each immunoreactive fraction was finally purified on the same column with a solvent of a different pH (ammonium acetate buffer, pH 4.6).

The fractions were lyophilized and a small portion of each, or synthetic salmon calcitonin (1 ng–1 μg), was dissolved in 10 μl of a mixture of 0.1 *M* Na_2CO_3 (pH 9.5) and methanol (4:1, v/v), and blotted onto an Immobilin PVDF transfer membrane (Millipore Co. Ltd., Tokyo). The membrane was soaked in 100% methanol for 3 s, and washed 3 times in 10 m*M* phosphate-buffered saline (pH 7.2) containing 0.05% Tween 20 (PBST) for 5 min. The membrane was washed twice more in PBST containing 1% normal goat serum, and then three times again in PBST. The membrane was then incubated with an antiserum raised against salmon calcitonin (Sasayama *et al.*, 1989) (1/40,000 dilution) for 2 h at room temperature. The unbound antiserum was removed by three washes in PBST, and the membrane was immunostained with a Vectastain ABC kit (Vector Laboratories, California) according to the protocol included with the kit.

A portion of purified ray calcitonin was subjected to reduction and S-carboxymethylation, as reported previously (Takei *et al.*, 1989), and further purified by reverse phase HPLC. The amino acid sequence of the purified peptide was determined with a protein sequencer (Applied Biosystems, Model 470A/120A). The sequence thus determined was verified by the amino acid analysis (15), and by coelution of the purified and synthetic peptides in reverse-phase HPLC with two different solvent systems (Takei *et al.*, 1990). The ray calcitonin was synthesized by a peptide synthesizer (Applied Biosystems, Model 430A) as reported previously (Takei *et al.*, 1989). The correct sequence of the synthetic peptide was confirmed by amino acid analysis, and by the sequencer.

Results

At first, 1/10 of the crude acid extract of ray ultimobranchial glands was subjected to reverse phase HPLC, and several fractions showed immunoreactivity to the antibody raised against salmon calcitonin (Fig. 2). Each positive fraction was further chromatographed with a solvent of different pH, and only one immunoreactive peak was detected from one of the positive fractions (Fig. 3). No immunoreactive material was recovered from the other fractions. The height of the peak was equivalent to 12.2 nmoles of salmon calcitonin. Thus, the ultimobranchial gland of the ray contains at least 60 nmoles/g tissue of calcitonin. The amino acid sequence of the purified material was determined by sequencer (Fig. 4).

The ray calcitonin was also purified from the remaining 9/10 of the crude extract. This material was then reduced and S-carboxymethylated, and 1/10 of the carboxymethylated peptide was subjected to amino acid analysis to verify the sequence. The ray calcitonin was composed of

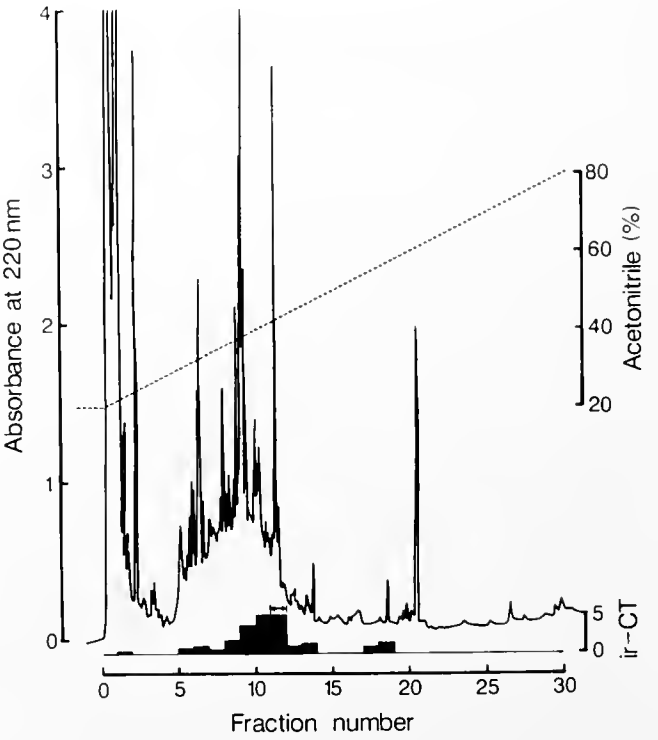

Figure 2. Reverse phase HPLC on an ODS-120T column. Sample, crude acid extract of ultimobranchial glands of the ray; flow rate, 1 ml/min; fraction size, 2 ml/tube. Solvent system: linear-gradient elution from 20 to 80% CH_3CN in 0.1% trifluoroacetic acid for 60 min. The immunoreactive calcitonin (ir-CT) was quantified by scores from 0 to 5. Arrows indicate the fraction within which ray calcitonin was eluted.

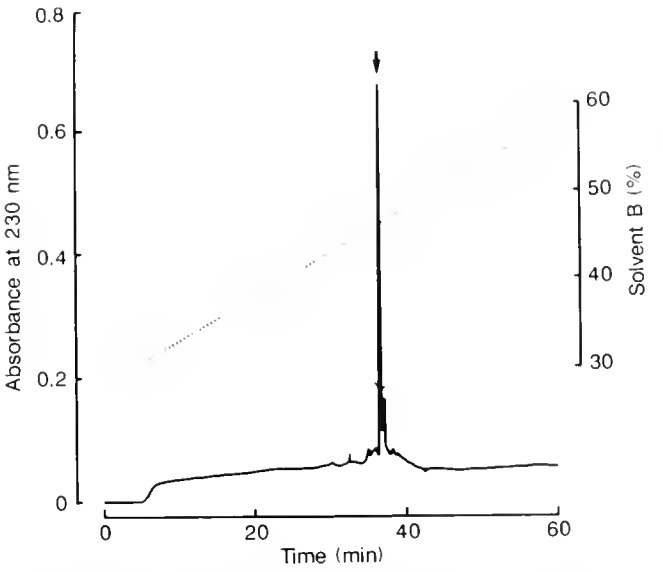

Figure 3. Reverse phase HPLC on an ODS-120T column. Sample, fraction 12 in Figure 2; flow rate, 1 ml/min. Solvent system: linear-gradient elution from solvent A (H_2O : CH_3CN : 1 M NH_4OAc, pH 4.6 = 72 : 8 : 1, v/v) to B (H_2O : CH_3CN : 1 M NH_4OAc, pH 4.6 = 25 : 100 : 1, v/v) for 40 min. Fraction was collected at each peak. Immunoreactivity appeared only in the peak marked by the arrow.

32 amino acid residues: Asp, 2.0 (2); Glu, 4.6 (4); CM-Cys, 1.3 (2); Ser, 3.0 (3); Gly, 2.2 (2); His, 1.0 (1); Arg, 1.1 (1); Thr, 4.2 (4); Ala, 2.2 (2); Pro, 1.1 (1), Val, 2.4 (3), Ile, 1.0 (1), Leu, 4.2 (4), Lys, 2.0 (2); the numbers in parentheses were deduced from the sequencing. Since the cysteine residue was undetectable without carboxymethylation in a sequencer, the carboxymethylated material was also subjected to the sequencer and the presence of cysteine residues at the first and the seventh position was confirmed. The amidation of the proline residue at the C-terminus was determined by co-chromatography with a synthetic peptide in reverse-phase HPLC.

Discussion

In this study, a large amount of calcitonin (more than 60 nmoles/g tissue) has been detected in the ultimobranchial glands of the ray (*Dasyatis akajei*), and sequenced. This is the first elasmobranch calcitonin to have been characterized.

In mammals, calcitonin is a hypocalcemic hormone that inhibits the reabsorption of calcium from the bone (Friedman and Raisz, 1965). Among non-mammals, calcitonin-like immunoreactivity has been detected in selected species from all classes, and calcitonin has been isolated in a bird and teleosts (Niall *et al.*, 1969; Van Noorden and Pearse, 1971; Noda and Narita, 1976; Tisserand-Jochem *et al.*, 1977; Sasayama *et al.*, 1984; Treilhou-Lahille *et al.*, 1984; Homma *et al.*, 1986), but the physiological roles of the hormone in these species are not fully understood. Because a hypocalcemic effect is not common in non-mammalian species (Pang *et al.*, 1980), cartilaginous fishes, which appear to have large amounts of calcitonin, may be good material with which to investigate those roles of the hormone that have been retained throughout the vertebrates. The use, in such studies, of the native hormone, now available, is important because mammalian hormones often have little biological effect in fishes (Takei *et al.*, 1989, 1990).

The calcitonins sequenced to date can be classified into three groups according to their structural similarity (Fig. 1). The sequence homology among the calcitonins within each group is 88–94% (Table 1). Ray calcitonin is apparently more homologous to non-mammalian calcitonins, but the homology is less than that within any of the groups. In particular, the calcitonins from fowl and ray are more similar than the two types of mammalian calcitonins. Non-mammalian calcitonins generally have greater hypocalcemic effects in the rat than do mammalian calcitonins (Homma *et al.*, 1986). Indeed, our preliminary

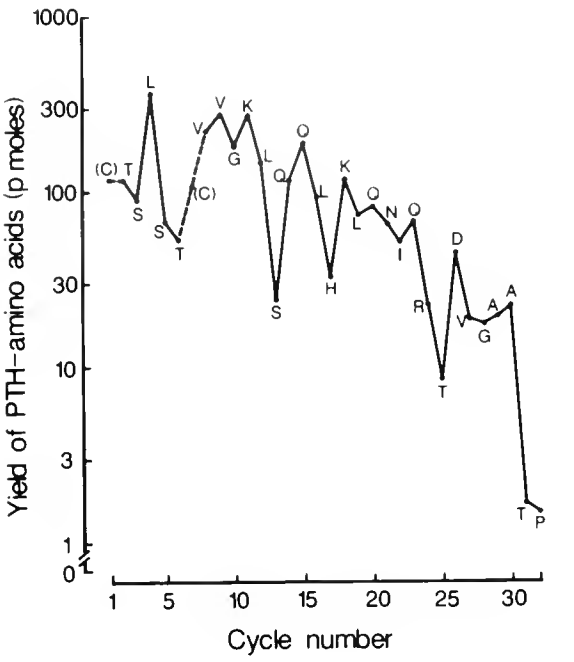

Ray CT CTSLSTCVVGKLSQQLHKLQNIQRTDVGAATP–NH_2

Figure 4. Automatic sequencer analysis of the purified peak of ray calcitonin immunoreactivity shown in Figure 3. The yield of phenylthiohydantoin-derivitized (PTH) amino acid is plotted for each cycle of Edman degradation. The cystine residues (C) at cycles 1 and 7 were not determined in this analysis, which was carried out without prior carboxymethylation (see Results). The complete amino acid sequence, finally verified by amino acid analysis and by co-chromatography with synthetic peptide, is set out below the plot.

Table 1

*The sequence homology of amino acids (above *) and of nucleotides (below *) between two calcitonins from different species*

	Ray	Fowl	Eel	Salmon	Rat	Human	Pig	Ox	Sheep
Ray	*	78	75	66	38	34	31	31	31
Fowl	–	*	94	88	50	47	44	44	41
Eel	–	–	*	94	53	50	41	41	44
Salmon	–	74	–	*	59	56	41	44	41
Rat	–	66	–	60	*	94	47	47	44
Human	–	68	–	60	91	*	44	44	41
Pig	–	–	–	–	–	–	*	91	88
Ox	–	–	–	–	–	–	–	*	94
Sheep	–	–	–	–	–	–	–	–	*

Numbers are homologies expressed in terms of percentage. –; not examined. For nucleotide sequences, see Craig *et al.*, 1982; Rosenfeld *et al.*, 1984; Lasmoles *et al.*, 1985; Poeschl *et al.*, 1987.

results show that when rats are injected with 1 pmol of ray calcitonin, the plasma calcium concentration decreases by 15.3 ± 1.5% after 30 min, whereas injection with the same dose of human and porcine calcitonin causes a decrease of 9.8 ± 1.2% and 3.5 ± 0.7%, respectively (n = 10 in each case). Thus, ray calcitonin is apparently more hypocalcemic in the rat than mammalian calcitonins. Ray calcitonin may have a clinical application, as is the case for eel calcitonin (Orimo, 1979).

Acknowledgments

The authors are grateful to Dr. David A. Price of The Whitney Laboratory, University of Florida, for the critical reading of this manuscript. We also thank Miss S. Nishida for artwork. This investigation is supported in part by the Terumo Foundation.

Literature Cited

Brewer, H. B., Jr., and R. Ronan. 1969. Amino acid sequence of bovine calcitonin. *Biochemistry* **63:** 940–947.

Craig, R. K., L. Hall, M. R. Edbrooke, J. Allison, and I. MacIntyre. 1982. Partial nucleotide sequence of human calcitonin precursor mRNA identifies flanking cryptic peptides. *Nature* **295:** 345–347.

Friedman, J., and L. G. Raisz. 1965. Thyrocalcitonin: inhibition of bone resorption in tissue culture. *Science* **150:** 1465–1467.

Homma, T., M. Watanabe, S. Hirose, A. Kanai, K. Kangawa, and H. Matsuo. 1986. Isolation and determination of amino acid sequence of chicken calcitonin I from chicken ultimobranchial glands. *J. Biochem.* **100:** 459–467.

Lasmoles, F., A. Jullienne, F. Day, S. Minvielle, G. Milhaud, and M. S. Moukhtar. 1985. Elucidation of the nucleotide sequence of chicken calcitonin mRNA: direct evidence for the expression of a lower vertebrate calcitonin-like gene. *EMBO J.* **4:** 2603–2607.

Neher, R., B. Riniker, W. Rittel, and H. Zuber. 1968. Menschliches calcitonin. III. Struktur von calcitonin M und D. *Helv. Chim. Acta* **51:** 1900–1905.

Niall, H. D., H. T. Keutmann, D. H. Copp, and J. T. Potts, Jr. 1969. Amino acid sequence of salmon ultimobranchial calcitonin. *Proc. Natl. Acad. Sci. USA* **64:** 771–778.

Noda, T., and K. Narita. 1976. Amino acid sequence of eel calcitonin. *J. Biochem.* **79:** 353–359.

Orimo, H. 1979. Clinical application of calcium-regulating hormone. *Clin. Endocrinol.* **28:** 269–274.

Pang, P. K. T., A. D. Kenny, and C. Oguro. 1980. Evolution of endocrine control of calcium regulation. Pp. 323–356 in *Evolution of Vertebrate Endocrine Systems*, P. K. T. Pang, and A. Epple, eds. Texas Tech. Press, Lubbock.

Poeschl, E., I. Lindley, E. Hofer, J. M. Seifert, W. Brunowsky, and J. Besemer. 1987. The structure of procalcitonin of the salmon as deduced from its cDNA sequence. *FEBS Lett.* **226:** 96–100.

Potts, J. T., Jr., H. D. Niall, H. T. Keutmann, H. B. Brewer, Jr., and L. J. Deftos. 1968. The amino acid sequence of porcine thyrocalcitonin. *Proc. Natl. Acad. Sci. USA* **59:** 1321–1328.

Potts, J. T., Jr., H. D. Niall, H. T. Keutmann, and R. M. Lequin. 1971. Chemistry of calcitonin; species variation plus, structure-activity relations and pharmacologic implications. Pp. 121–127 in *Calcium, Parathyroid Hormone and the Calcitonin*, R. V. Talmage and P. L. Munson, eds. Excerpta Medica, Amsterdam.

Raulais, D., J. Hagaman, D. A. Ontjes, R. L. Lundblad, and H. S. Kingdon. 1976. The complete amino-acid sequence of rat thyrocalcitonin. *Eur. J. Biochem.* **64:** 607–611.

Rosenfeld, M. G., S. G. Amara, and R. M. Evans. 1984. Alternative RNA processing events as a critical developmental regulatory strategy in nonendocrine gene expression. *Biochem. Soc. Symp.* **49:** 27–44.

Sasayama, Y., C. Oguro, R. Yui, and A. Kanbegawa. 1984. Immunohistochemical demonstration of calcitonin in ultimobranchial glands of some lower vertebrates. *Zool. Sci.* **1:** 755–758.

Sasayama, Y., K. Matsuda, C. Oguro, and A. Kambegawa. 1989. Immunohistochemical study of the ultimobranchial gland of chum salmon fry. *Zool. Sci.* **6:** 607–610.

Takei, Y., A. Takahashi, T. X. Watanabe, K. Nakajima, and S. Sakakibara. 1989. Amino acid sequence and relative biological activity of eel atrial natriuretic peptide. *Biochem. Biophys. Res. Commun.* **164:** 537–543.

Takei, Y., A. Takahashi, T. X. Watanabe, K. Nakajima, S. Sakakibara, T. Takao, and Y. Shimonishi. 1990. Amino acid sequence and relative biological activity of a natriuretic peptide isolated from eel brain. *Biochem. Biophys. Res. Commun.* **170:** 883–891.

Tisserand-Jochem, E. M., A. Eyquem, J. Peignoux-Deville, and C. Calmettes. 1977. Calcitonine du corps ultimobranchial de' Anguilles (*Anguilla anguilla* L.): localisation cytologique par immunofluorescence indirecte a l'aide d'un anticorps humain anti-calcitonine de Saumon. *C. R. Acad. Sci. Ser. D* **258:** 81–84.

Treilhou-Lahille, F., A. Jullienne, M. Aziz, A. Beaumont, and M. S. Moukhtar. 1984. Ultrastructural localization of immunoreactive calcitonin in the two cell types of the ultimobranchial gland of the common toad (*Bufo bufo* L.). *Gen. Comp. Endocrinol.* **53:** 241–251.

Van Noorden, S., and A. G. E. Pearse. 1971. Immunofluorescent localization of calcitonin in the ultimobranchial gland of *Rana temporaria* and *Rana pipiens*. *Histochemie* **26:** 95–97.

Reference: *Biol. Bull* **180**: 489–495. (June, 1991)

Carbon Budgets for Two Species of Benthonic Symbiont-Bearing Foraminifera

B. H. TER KUILE[1,*] AND J. EREZ[2]

[1]*The Interuniversity Institute of Eilat, The Hebrew University of Jerusalem, P. O. Box 469, Eilat 88103, Israel, and* [2]*Department of Geology, The Hebrew University of Jerusalem, Jerusalem 91904, Israel*

Abstract. Carbon budgets are presented for two symbiont-bearing foraminifera: *Amphistegina lobifera*, a perforate species, and the imperforate species *Amphisorus hemprichii*. Both species have a potential for autotrophy with respect to carbon, because the translocation from symbionts to host is sufficient to account for the increase in measured biomass. Experimentally determined feeding rates exceed the supposed amount of food retained as calculated by balancing the budget by a factor of up to ten. When feeding does not occur, the carbon budget of *A. lobifera* is almost exactly balanced, whereas the budget of *A. hemprichii* can be balanced within the precision of the measurements. Carbon for calcification by *A. lobifera* is initially concentrated in an internal pool that derives approximately 10% of its content from organic matter respired by the host. Carbon of organic origin was not incorporated into the skeleton of *A. hemprichii*.

Introduction

Carbon budgets have been constructed for various invertebrates bearing algal symbionts, such as corals (Muscatine *et al.*, 1981, 1984; Falkowski *et al.*, 1984) and zoanthids (Steen and Muscatine, 1984), but not for foraminifera. One of the reasons for this is that carbon budgets can only be formulated once the flows of carbon and the mechanisms involved in directing these flows are known qualitatively. Then a scheme integrating all fluxes can be drawn up, so that research aimed at quantifying these fluxes can be properly interpreted. Earlier research within this framework showed that the perforate and imperforate groups of foraminifera have widely different mechanisms for uptake of inorganic carbon and for calcification (ter Kuile and Erez, 1987, 1988; ter Kuile *et al.*, 1989). Therefore, two conceptually different budgets must be constructed for foraminifera: one for a representative of the perforate, and one for an imperforate species. The species we have chosen for this study are: *Amphistegina lobifera* (perforate) and *Amphisorus hemprichii* (imperforate).

In earlier studies on carbon budgets of symbiont-bearing calcifying systems, the contribution of the symbionts to the carbon requirements of the host was considered a key feature of the host-symbiont relationship and was, therefore, often emphasized. Determination of the carbon translocation from symbionts to host is difficult because it involves measurements within an organism. Another disputed parameter is the relative contribution of feeding to the carbon requirements of the host. Lee and coworkers (Lee and Bock, 1976; Lee *et al.*, 1980) estimated that, in foraminifera, carbon from feeding exceeds carbon from photosynthesis by a factor of 10, but ter Kuile *et al.* (1987) found a ratio of 0.5–2. Feeding rates are difficult to measure because feeding is episodic, and because egested algae do not resuspend well. At least in foraminifera, feeding seems to provide nutrients rather than carbon (ter Kuile *et al.*, 1987). Hence, minimum feeding rates can be estimated by calculating the nutrient requirements of the host symbiont-system by assuming a constant ratio of carbon to nutrients. One purpose of this study is to estimate the two uncertain parameters: translocation of carbon from symbionts to host, and the contribution of feeding to the carbon budget. The calculated values, estimated by balancing the budget so that no carbon is unaccounted for,

Received 19 April 1989; accepted 8 January 1991.

* Present address: ICP-TROP 74.39, Avenue Hippocrate 74, B-1200 Brussels, Belgium.

are used as a control on the experimentally obtained values.

Based on stable isotope experiments with corals and foraminifera, Goreau (1977) and Erez (1977, 1978) suggested that inorganic carbon is initially taken up in an internal inorganic carbon pool. According to this view, some respired carbon of organic origin may be taken up by the inorganic pool and afterwards incorporated into the skeleton. Later, experimental evidence was found for the existence of the inorganic carbon pool in perforate, but not in imperforate foraminifera (ter Kuile and Erez, 1987, 1988). Such pools have not been included in the earlier proposed budgets for corals (Falkowski *et al.*, 1984). We believe, however, that the internal inorganic carbon pool is important for overall carbon cycling, at least in perforate foraminifera. Therefore, the second purpose of this study is to understand the role of the pool in the carbon cycling of the perforate species.

The following observations have to be taken into account while formulating carbon budgets for foraminifera. First, the important taxonomical differences between the perforate and imperforate groups of foraminiferal species are reflected in widely different calcification mechanisms (ter Kuile *et al.*, 1989). Therefore two different models are proposed, one for each group.

Perforate species

Inorganic carbon (Ci) is initially taken up from seawater in one flow in the form of bicarbonate. In the cytoplasm, CO_2 is photoassimilated by the symbionts, and $CO_3^=$ is concentrated in the internal inorganic carbon pool (hereafter called "pool"), which serves for calcification only and not for photosynthesis. About 10% of the carbon incorporated into the skeleton consists of carbon originally photoassimilated by the symbionts and respired by the host. Feeding seems to provide nutrients, phosphate and nitrogen compounds, rather than carbon, to the host-symbiont system. (Leutenegger, 1977; Leutenegger and Hansen, 1979; ter Kuile and Erez, 1987, 1988; ter Kuile *et al.*, 1987, 1988, 1989).

Imperforate species

Inorganic carbon is taken up from seawater in two separate flows that do not interfere with each other. Carbonate is taken up by a diffusion-limited process into vacuoles where calcification occurs. The symbionts use either CO_2 or HCO_3^-. Some carbon derived from feeding may be assimilated in the host organic matter, but not in the skeleton. Internal recycling of respired carbon from organic origin into the skeleton does not occur (Hemleben *et al.*, 1986; ter Kuile and Erez, 1987, 1988; ter Kuile *et al.*, 1987, 1989).

We present carbon budgets for two species of foraminifera, based on rates determined in a large number of experiments; some of the data were obtained from other studies (ter Kuile and Erez, 1987, 1988; ter Kuile *et al.*, 1987).

Materials and Methods

Amphistegina lobifera (perforate) and *Amphisorus hemprichii* (imperforate) were collected from *Halophila* sp. plants, 24 h before each experiment. We checked the foraminifera for viability by observing their overnight upward mobility in glass jars (ter Kuile and Erez, 1984, 1987). The budget presented for *A. lobifera* comprises measurements of specimens with average weights of 66 to 72 μg (Table I); specimens of *A. hemprichii* weighed 385 μg on average, ranging from 242 to 523 μg. Long-term kinetic and pulse-chase experiments involving ^{14}C tracer techniques (ter Kuile and Erez, 1987, 1988) were used throughout the study. Incubations were carried out in 100 ml erlenmeyer flasks near a north-oriented window in natural light/dark cycles. The maximum light intensity was 750 $\mu E\ m^{-2}s^{-1}$, which corresponds to a depth of 15 m, similar to the depth of the sample location. Twenty to 40 mg of organisms were used for each incubation.

Determination of compartment biomass

The biomass of the following compartments was measured: total dry weight, biomass of the organic matter, dry weight of the skeleton, and the carbon content of internal inorganic carbon pool. Determinations of protein and chlorophyll content were used to estimate symbiont biomass.

Total dry weight of foraminifera was determined with a Cahn 25 electrobalance. Biomass of organic matter was measured as the additional weight of a Nuclepore (0.4 μ) filter on which the particulate organic matter of a sample whose shell was dissolved in 8.5% H_3PO_4 had been collected. The organic matter of *Amphistegina lobifera* was, on the average, 8.0% ($\pm$0.6, n = 48) of the total dry weight, and *Amphisorus hemprichii* contained 5.2% ($\pm$0.6) organic matter. The dry weight of the skeleton was determined by substracting the dry weight of the organic matter from the total dry weight. The internal inorganic carbon pool size of *A. lobifera* was measured by ^{14}C radiotracer methods, in combination with pulse-chase experiments (ter Kuile and Erez, 1988).

The protein content of finely crushed, dried specimens was determined by the Lowry method, as modified by Peterson (1977). The contribution of the symbionts to the organic matter could be estimated from the chlorophyll content measured after extraction in methanol (Strickland

and Parsons, 1972); this was possible because we found no change in the chlorophyll to protein ratio in samples obtained at depths less than 35 m. Sizes of compartments are given in μg C/mg foram (total dry weight of skeleton and organic matter).

Fluxes between the compartments

The following five fluxes were measured; the methods used were exactly those of the papers cited in each case. (1) The uptake of inorganic carbon from the medium—consisting of photoassimilation, uptake into the skeleton, uptake into the pool and, by addition, total uptake—was measured as $H^{14}CO_3^-$ uptake (ter Kuile and Erez, 1987, 1988). (2) Translocation of photosynthates from symbionts to host was calculated from pulse-chase experiments (ter Kuile and Erez, 1987). (3) Incorporation of metabolic carbon (initially taken up photosynthetically) into the skeleton was also derived from pulse-chase experiments, (ter Kuile and Erez, 1987, 1988). (4) Respiration was again derived from pulse-chase experiments. (5) Uptake and rejection of carbon derived from feeding on algae in the environment (not their own symbionts) was determined in time-course and pulse-chase experiments as previously reported (ter Kuile *et al.*, 1987). All rates are given in μg C/mg foram/24 h in a natural light/dark cycle.

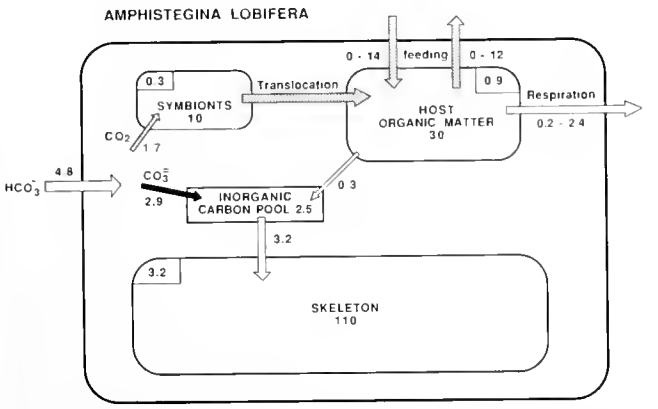

Figure 1. Carbon budget for *Amphistegina lobifera*. The compartments and the fluxes between them were qualitatively described in earlier studies (see Introduction). The names and sizes of different compartments are given in large letters and numbers; the names of processes and the amounts of carbon transferred are in small lettering. Open arrows indicate transfer of inorganic carbon, striped arrows indicate transfer of organic carbon, and closed arrows indicate the active transport of carbonate. Numbers framed in compartment corners indicate daily increase in size of that compartment. Units: sizes of compartments in μg C/mg foram. Rates of fixation and transfer, and daily increase, in μg C/mg foram/24 h in a natural light/dark cycle.

Table I

Rates of carbon fixation and pool size in Amphistegina lobifera *in a natural light/dark cycle*

Org. wt. (μg)	Total	Photo	Skeleton	Pool size (μg C/mg foram)
	(μg C/mg foram/24 h)			
66	4.9	2.0	2.9	
68	4.8	1.6	3.2	2.5[a]
68	5.1	1.7	3.4	
70	5.5	1.9	3.6	
72	3.9	1.2	2.7	
	—	—	—	
Average:	4.8	1.7	3.2	

[a] In experiments not reported here, a pool size of 2.2 to 2.9 μg C/mg foram was measured in foraminifera with an organism weight of about 70 μg.

Abbreviations: Org. wt = organism weight; Total = total carbon uptake; Photo = carbon uptake for photosynthesis by the symbionts; Skeleton = carbon uptake for calcification; Pool size = carbon content of the internal inorganic carbon pool for calcification. The standard deviation of a large number of measurements on identical samples, which were made using our methodology, was around 5% of the reported value (ter Kuile and Erez, 1987).

Results

Budget descriptions

The carbon budget for *Amphistegina lobifera* is presented in Figure 1. The compartments are defined and their size determined as described above in Materials and Methods. The existence of the fluxes between them was demonstrated in earlier studies (ter Kuile and Erez, 1987, 1988; ter Kuile *et al.*, 1989, see Introduction). The uptake rates used to construct the budget are given in Table I. The organic compartment makes up 8.0% of the total dry weight. About half of organic dry weight is carbon (Sverdrup *et al.*, 1942; Parsons and Takahashi, 1973), which amounts to 40 μg C/mg foram. The ratio of chlorophyll to protein is roughly 1:39 (Table II); a usual ratio for algae is 1:10 (Parsons and Takahashi, 1973). Thus, the symbionts comprise about one quarter of the total organic matter. The organic matter compartments of symbionts and host contain about 10 and 30 μg C/mg foram, respectively. The skeleton comprises 92% of the total dry weight, which amounts to 110 μg C/mg foram. The inorganic carbon pool size (ter Kuile and Erez, 1988) depends on the calcification rate, which in turn depends on the size of the specimens. For specimens of roughly 70 μg, a pool size of approximately 2.5 μg C/mg foram (Table I) was found in the experiments performed for this study. In other studies we found similar values (2.2–2.9 μg C/mg foram) (ter Kuile and Erez, 1988).

Total uptake of inorganic carbon (Ci) by *Amphistegina lobifera* was, on average, 4.8 μg C/mg foram/24 h (Table

Table II

Protein and chlorophyll measurements of Amphistegina lobifera *and* Amphisorus hemprichii *(duplicate measurements on different size groups)*

	Protein (μg/mg foram)	Organism weight (μg)
A. lobifera	33.92	340
	32.10	340
	40.05	60
	39.40	60
A. hemprichii	20.88	1107
	17.10	1107
	26.30	283
	23.49	283
	Ratio protein/ chlorophyll (μg/μg)	**Organism weight (μg)**
A. lobifera	39.7	>250
	37.4	75–250
	40.1	<75
A. hemprichii	45.2	>2000
	34.7	>2000
	40.8	<500
	41.4	<500

1). Under the experimental conditions, specimens of the size range used in this study (around 70 μg) grew at a daily rate of about 3%/day. This rate was determined optically, by converting size increase to weight increase (ter Kuile and Erez, 1984), and by the incorporation of $^{14}CO_3^{2-}$ into the skeleton. Approximately 1.7 (1.2–2.0) μg C/mg foram/24 h net is fixed photosynthetically by the symbionts. The chlorophyll:protein ratio does not change with size (Table II), indicating that the symbionts grow in proportion to the organic matter. When growing at a rate of 3% a day, the symbionts need 0.3 μg C/mg foram/24 h for growth. Hence, a net amount of 1.4 μg C/mg foram/24 h will be available for translocation to the host. Calculations based on the results of pulse-chase experiments indicate a transfer of 1.3 μg C/mg foram/24 h. At the measured growth rate, the host needs 0.9 μg C/mg foram/24 h for growth. Transfer of respired Ci to the skeleton amounts to 0.3 μg C/mg foram/24 h. Loss of respired Ci to the environment is roughly 0.2 μg C/mg foram/24 h. Incorporation into the skeleton is 3.2 μg C/mg foram/24 h (Table I). This carbon is initially concentrated in the pool which, in turn, derives 0.3 μg C/mg foram/24 h from respired carbon (see above) and, by balance, 2.9 μg C/mg foram/24 h is taken up directly from seawater. When no feeding occurs, the budget is balanced with respect to uptake, growth, and respiration. During feeding experiments, large amounts of labeled algae (up to 14 μg C/mg foram/24 h) were rapidly ingested, but most of this food was egested in organic form within 24 h (ter Kuile *et al.*, 1987). Approximately 8% of the carbon in the food was respired. Less than 2% of the label taken up through feeding was incorporated into the skeleton (ter Kuile *et al.*, 1987). Feeding rates depend on the conditions during preincubation and the availability of suitable food. Therefore, the values given in Figure 1 must be considered minimum and maximum rates, rather than long-term averages. Consequently, the value for respiration is at a minimum when no feeding occurs and organisms grow slowly, and at a maximum when feeding rates, and thus growth rates, are high.

Amphisorus hemprichii *budget*

A similar budget for the carbon cycling of *Amphisorus hemprichii* is presented in Figure 2. This budget differs strongly, not only quantitatively, but qualitatively as well, from the budget of *A. lobifera*, reflecting the widely different calcification mechanisms found in perforate and imperforate foraminifera, respectively (see Introduction). Because of the large size range, the variation in the data was also large (Table III). The organic matter was 5.2% of the total weight (dry weight/dry weight). Symbiont biomass is about one quarter of the total organic matter, estimated from the chlorophyll:protein ratio (1:40.5 ± 4.3; ter Kuile and Erez, 1984; this study, Table II). When converted to carbon weight, the sizes of the organic compartments are 7.5 μg C/mg foram for symbionts, and 22.5 μg C/mg foram for the host. Skeleton contains 113 μg C/mg foram. *A. hemprichii* does not contain an internal inorganic carbon pool for calcification (ter Kuile and Erez, 1987, 1988).

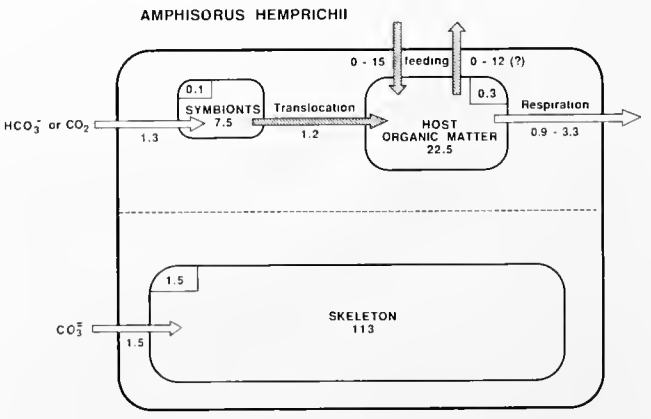

Figure 2. Carbon budget for *Amphisorus hemprichii*. This budget differs from that of *Amphistegina lobifera* due to differences in the calcification mechanisms (see Introduction). Units as in Figure 1.

Table III

Rates of carbon fixation in Amphisorus hemprichii *in a natural light/dark cycle. No internal inorganic carbon pool is observed in* A. hemprichii

Org. wt. (μg)	Total	Photo (μg C/mg foram/24 h)	Skeleton
243	2.5	1.5	1.0
362	2.9	1.1	1.8
409	2.5	1.0	1.5
523	3.7	1.7	2.0
	—	—	—
Average *	2.9	1.3	1.6
116	3.3	1.2	2.1
149	3.0	1.2	1.8
3000	2.2	1.3	0.9
3500	2.8	1.6	1.2

* Light and heavy specimens, not used in Figure 2.
Abbreviations and units as in Table I.

In the experiments for this budget, a net average of 1.3 μg C/mg foram/24 h (Table III) was fixed photosynthetically. Because *Amphisorus hemprichii* grew roughly 1.5%/day in the laboratory (ter Kuile and Erez, 1984, 1987), the symbionts and the host organic matter compartments increase 0.1 and 0.3 μg C/mg foram/24 h, respectively. By balance, 0.9 μg C/mg foram/24 h should be respired. The respiration rate calculated from pulse-chase experiments (ter Kuile and Erez, 1987) was 1.1 μg C/mg foram/24 h. Translocation, estimated from pulse-chase experiments, was 1.5 μg C/mg foram/24 h. The calculated rate is 1.2 μg C/mg foram/24 h, which is within the precision of the measurement. Up to 15 μg C/mg foram/24 h is taken up through feeding (ter Kuile *et al.*, 1987). In one pulse-chase experiment, 25% of the amount initially ingested was still present after one week. Thus, feeding may contribute considerable amounts of reduced carbon for the growth of *A. hemprichii*. About half of the food that was not retained was respired, and the rest was egested, both in roughly equal rates of about 1.5 μg C/mg foram/24 h. Egestion is difficult to measure in *A. hemprichii*, because the fecal pellets do not resuspend. At present, the budget is not balanced with respect to carbon derived from feeding, because the estimated egestion is too low (ter Kuile *et al.*, 1987). To balance the budget, the egestion rate should be 12 μg C/mg C/24 h. Uptake into the skeleton was, on the average, 1.5 (1.0–2.0) μg C/mg foram/24 h (Table III). Even though uptake for photosynthesis and calcification occurs in roughly equal rates, about four times more carbon is accumulated in the skeleton than in the organic matter, because most of the photosynthates are respired. Specimens weighing less than 150 μg have higher rates of calcification than of photosynthesis, whereas specimens heavier than 3000 μg have lower rates of calcification than of photosynthesis. In the medium range, the calcification:photosynthesis ratio was constant, roughly 1:1 (comparison in Table III).

Discussion

Carbon budgets for benthonic symbiont-bearing foraminifera can best be compared to a similar budget for corals developed by Falkowski and coworkers (1984). The relative sizes of the compartments in corals and foraminifera differ: in *Amphistegina lobifera*, the symbionts, host organic matter, and skeleton contain approximately 7, 20, and 73% of the total carbon, respectively. For *Amphisorus hemprichii* these numbers are: 5, 16, and 79%. Corals contain about 1–2% organic matter (dry weight/dry weight) (Erez, 1978), which amounts to 5% of the carbon in organic form and 95% in the skeleton. The symbionts constitute only 3.7–4.5% of the total organic matter (Falkowski *et al.*, 1984), giving a final distribution of 0.2%, 4.8%, and 95% for carbon in the symbionts, host organic matter, and the skeleton.

In calcareous algae, 70–90% of the total dry weight is $CaCO_3$ (Pentecost, 1980); therefore, the ratio of carbon in the organic matter to carbon in the skeleton is about 1:1. Coccolithophores form coccoliths depending on the environmental conditions, and may shed them after formation. The relative amount of carbon in the skeleton is therefore difficult to estimate, but it is probably 1:1 as well (Sikes *et al.*, 1980; Van der Wal, 1984).

Therefore, corals contain the least amount of organic carbon per unit of inorganic (calcareous) carbon, foraminifera are intermediate, and calcareous algae contain the most. This suggests that corals need to take up fewer nutrients in the form of nitrogen or phosphorous compounds from their surroundings per unit total carbon (both organic and calcareous), foraminifera need more, and calcareous algae require still more than the symbiotic systems. This has consequences for the carbon cycling of foraminifera, because feeding may be the primary source of nutrients, at least in *A. lobifera* (ter Kuile *et al.*, 1987). Determination of feeding rates was the least reliable measurement of our budget, because feeding is a discontinuous process, and because egestion cannot be measured well. Assuming that foraminifera obtain all their nutrients from food and have the same C:N:P ratio as the food, the amount of nutrients retained can be estimated. The total daily increase of organic matter of *A. lobifera*, host and symbionts, is 1.2 μg C/mg foram/24 h, which can be provided by photoassimilation by the symbionts. The maximum feeding rate is about ten times higher. Thus, about 10% of the nutrients present in the food are retained, while almost all of the carbon derived from feeding is respired or egested (ter Kuile *et al.*, 1987). The general

"black box" observation that the efficiency of retention between trophic layers is usually around 10% further supports the validity of the high experimental rates. Based on the carbon budget, we expect that long-term feeding rates are much lower, unless feeding is very inefficient, or the feeding efficiency varies with the food concentration.

The photosynthetic rates of *Amphistegina lobifera* and *Amphisorus hemprichii* measured in this study are similar to those found by Erez (1978), but are an order of magnitude lower than those of planktonic foraminifera (Erez, 1983; Jorgensen *et al.*, 1985). Photosynthetic rates of corals, when normalized to the total weight of the organism, are similar (Erez, 1978), or much lower (Falkowski *et al.*, 1984). Total weight may not be a useful normalization factor for corals. The symbionts of foraminifera and light-adapted corals translocate sufficient reduced carbon to the host to sustain respiration and growth (Jacques and Pilson, 1980; Muscatine *et al.*, 1981, 1984; Falkowski *et al.*, 1984; Davies, 1984; Edmonds and Spencer Davies, 1986). Therefore, these systems have a potential for autotrophy with respect to carbon, but not to nutrients that must be provided by feeding (Falkowski *et al.*, 1984; ter Kuile *et al.*, 1987). Besides nutrients, planktonic foraminifera and shade-adapted corals require additional reduced carbon from feeding (Falkowski *et al.*, 1984; Jorgensen *et al.*, 1985). Excretion of mucus by corals has been well documented (Crossland *et al.*, 1980a, b; Muscatine *et al.*, 1984; Crossland, 1987), but we found no evidence that foraminifera lose photosynthetically fixed carbon in the form of mucus. Cycling of respired carbon into the skeleton has been demonstrated for both corals (Crossland *et al.*, 1980a) and foraminifera (ter Kuile and Erez, 1987).

Corals and perforate foraminifera may have another common feature, the internal inorganic carbon pool. First predicted in corals to explain the stable isotope composition of the calcium carbonate skeleton by Goreau (1977), this pool was demonstrated experimentally in perforate foraminifera, but not in imperforate species (ter Kuile and Erez, 1988). This pool functions solely as a carbon reservoir for calcification in which carbonate is concentrated in an energy-dependent process (ter Kuile *et al.*, 1989). More uptake in the pool occurs when metabolic rates supported by symbiont activity are high, but no carbon from the pool is photoassimilated (Fig 1). This correlation between uptake by the pool and photosynthetic activity may explain the lighter than expected isotopic composition of rapidly photosynthesizing corals and foraminifera (Erez, 1978). The occurrence of the same phenomenon in both classes of organisms suggests that the pool of corals may operate similarly to that of perforate foraminifera.

Acknowledgments

This study was supported by the United States-Israel Binational Science Foundation, Project 3418/83. The authors wish to thank Drs. Z. Reiss and B. Luz for fruitful discussions.

Literature Cited

Crossland, C. J. 1987. *In situ* release of mucus and DOC-lipid from the corals *Acropora variabilis* and *Stylophora pistillata* in different light regimes. *Coral Reefs* **6:** 35–42.

Crossland, C. J., D. J. Barnes, T. Cox, and M. Devereux. 1980a. Compartmentation and turnover of organic carbon in the staghorn coral *Acropora formosa*. *Mar. Biol.* **59:** 181–187.

Crossland, C. J., D. J. Barnes, and M. A. Borowitzka. 1980b. Diurnal lipid and mucus production in the staghorn coral *Acropora acuminata*. *Mar. Biol.* **60:** 81–90.

Davies, P. S. 1984. The role of zooxanthellae in the nutritional energy requirements of *Pocillopera eydouxi*. *Coral Reefs* **2:** 181–186.

Edmunds, P. J., and P. Spencer Davies. 1986. An energy budget for *Porites porites* (Scleractinia) *Mar. Biol.* **92:** 339–347.

Erez, J. 1977. Influence of symbiotic algae on the stable isotope composition of hermatypic corals: a radioactive tracer approach. *Proc. 3rd. Int. Coral Reef Symp.* **2:** 563–569.

Erez, J. 1978. Vital effect on stable-isotope composition seen in foraminifera and coral skeletons. *Nature* **273:** 199–202.

Erez, J. 1983. Calcification rates, photosynthesis and light in planktonic foraminifera. Pp. 307–313 in *Biomineralization and Biological Metal Accumulation*, P. Westbroek and E. J. de Jong, eds. Reidel, Dordrecht.

Falkowski, P. G., Z. Dubinsky, L. Muscatine, and J. W. Porter. 1984. Light and the bioenergetics of a symbiotic coral. *Bioscience* **34:** 705–709.

Goreau, T. J. 1977. Coral skeletal chemistry: physiological and environmental regulation of stable isotopes and trace metals in *Montastrea annularis*. *Proc. R. Soc. Lond. B* **196:** 291–315.

Hemleben, Ch., O. R. Anderson, W. Berthold, and M. Spindler. 1986. Calcification and chamber formation in Foraminifera—a brief overview. Pp. 237–249 in Special Volume 30: *Biomineralization in Lower Plants and Animals*. B. S. C. Leadbeater and R. Riding, eds. The Systematics Association, London.

Jacques, T. G., and M. E. Q. Pilson. 1980. Experimental ecology of the temperate scleractinian coral *Astrangia danae*. 1. Partition of respiration, photosynthesis and calcification between host and symbionts. *Mar. Biol.* **60:** 167–178.

Jorgensen, B. B., J. Erez, N. P. Revsbech, and Y. Cohen. 1985. Symbiotic photosynthesis in a planktonic foraminiferan, *Globigerinoides sacculifer* (Brady), studied with microelectrodes. *Limnol. Oceanogr.* **30:** 1253–1267.

Kuile, B. ter, and J. Erez. 1984. *In situ* growth rate experiments on the symbiont-bearing foraminifera *Amphistegina lobifera* and *Amphisorus hemprichii*. *J. Foram. Res.* **14:** 262–276.

Kuile, B. ter, and J. Erez. 1987. Uptake of inorganic carbon and internal carbon cycling in benthonic symbiont-bearing foraminifera. *Mar. Biol.* **94:** 499–510.

Kuile, B. ter, J. Erez, and J. J. Lee. 1987. The role of feeding in the metabolism of larger symbiont-bearing foraminifera. *Symbiosis* **4:** 335–350.

Kuile, B. ter, and J. Erez. 1988. The size and function of the internal inorganic carbon pool of the foraminifer *Amphistegina lobifera*. *Mar. Biol.* **99:** 481–487.

Kuile, B. ter, A. Kaplan, and J. J. Lee, 1988. Uptake of inorganic carbon by *Fragilaria shiloi*, symbiont of the foraminifer *Amphistegina lobifera*. *Symbiosis* **6:** 225–236.

Kuile, B. ter, J. Erez, and E. Padan. 1989. Mechanisms for the uptake

of inorganic carbon by two species of symbiont-bearing foraminifera. *Mar. Biol* **103:** 241–251.

Lee, J. J., and W. D. Bock. 1976. The importance of feeding in two species of soritid foraminifera with algal symbionts. *Bull Mar Sci* **26:** 530–537.

Lee, J. J., M. E. McEnery, and J. R. Garrison. 1980. Experimental studies of larger foraminifera and their symbionts from the Gulf of Elat on the Red Sea. *J Foram Res* **10:** 31–47.

Leutenegger, S. 1977. Ultrastructure de Foraminiferes perfores et imperfores ainsi que leurs symbiotes. *Cah. Micropaleontol (CNRS, Paris)* **3:** 1–52.

Leutenegger, S., and H. J. Hansen. 1979. Ultrastructure and radiotracer studies of pore function in foraminifera. *Mar. Biol.* **54:** 11–16.

Muscatine, L., L. R. McCloskey, and R. E. Marian. 1981. Estimating the daily contribution of carbon from zooxanthellae to coral animal respiration. *Limnol Oceanogr* **26:** 601–611.

Muscatine, L., P. G. Falkowski, J. W. Porter, and Z. Dubinsky, 1984. Fate of photosynthetic fixed carbon in light- and shade-adapted colonies of the symbiotic coral *Stylophora pistillata*. *Proc. R. Soc. Lond. B* **222:** 181–202.

Parsons, T. R., and M. Takahashi. 1973. *Biological Oceanographical Processes* Pergamon Press, New York. 186 pp.

Pentecost, A. 1980. Calcification in plants. *Int. Rev. Cyt.* **62:** 1–25.

Peterson, G. L. 1977. A simplification of the protein assay method of Lowry *et al.* which is more generally applicable. *Anal. Biochem* **83:** 346–356.

Sikes, S., R. D. Roer, and K. M. Wilbur. 1980. Photosynthesis and coccolith formation: Inorganic carbon sources and net inorganic reaction of deposition. *Limnol. Oceangr* **25:** 248–261.

Steen, R. G., and L. Muscatine. 1984. Daily budgets of photosynthetically fixed carbon in symbiotic zoanthids. *Biol Bull* **167:** 477–487.

Strickland, J. D., and R. Parsons. 1972. *A Practical Handbook of Seawater Analysis* 2nd ed. Fisheries Research Board of Canada. 310 pp.

Sverdrup, H. U., M. W. Johnson, and R. H. Fleming. 1942. *The Oceans, Their Physics, Chemistry and General Biology* Prentence-Hall, Englewood Cliffs, NJ. 1087 pp.

Wat, P. van der 1984. Calcification in two species of coccolithophorid algae. *Gua Papers Geol* **20:** 113 pp.

Reference: *Biol. Bull.* 180: 496–504. (June, 1991)

The Induction of Carbonic Anhydrase in the Symbiotic Sea Anemone *Aiptasia pulchella*

VIRGINIA M. WEIS*

Department of Biology, University of California, Los Angeles, California 90024

Abstract. The activity and nature of carbonic anhydrase (CA, EC 4.2.1.1.) was measured and described in the tropical sea anemone *Aiptasia pulchella*. The hypothesis that high CA activity in animal tissue is induced by the presence of symbiotic algae was tested. CA activity was positively correlated with the number of symbiotic dinoflagellates (zooxanthellae) present. CA activity in aposymbiotic anemone tissue was 2.5 times lower than that in control symbiotic animals or in aposymbiotic animals repopulated with algae. Polyclonal antisera against human CA were used to probe for the presence of CA in both symbiotic and aposymbiotic anemone tissue, and in freshly isolated and cultured zooxanthellae. The resulting immunoblots showed one band with a molecular weight of 30 kDa in symbiotic animal tissue and control mammalian CA lanes, no bands in the aposymbiotic animal lanes, and one band at a molecular weight of 22.5 kDa in freshly isolated and cultured zooxanthellae lanes. Because no 22.5 kDa band was detected in the symbiotic animal tissue lanes, the high CA activity found in symbiotic animal tissue is considered to be due to the induction of animal enzyme by the presence of algae. The lack of any band in the aposymbiotic lanes further supports the hypothesis that CA activity in *A. pulchella* is induced by the presence of algae.

Introduction

Symbiotic dinoflagellates ("zooxanthellae") residing in vacuoles within cells of marine cnidarians exhibit a high rate of photosynthesis (Falkowski *et al.*, 1984). When this rate exceeds the respiration rate of the association, the algae must draw on inorganic carbon (C_i) from the seawater pool to satisfy the high carbon demand. CO_2 is the C_i species preferred as a substrate for carbon assimilation by ribulose bisphosphate carboxylase/oxygenase (RUBISCO) in the zooxanthellae. Yet at an ambient pH of 8.2–8.3, C_i in seawater is present mostly as HCO_3^-. Additionally, the movement of HCO_3^- across unstirred boundary layers and the several animal and algal membranes to the site of photosynthesis could be relatively slow (Kerby and Raven, 1985).

Weis *et al.* (1989) hypothesize that the supply of CO_2 for photosynthesis in algal/cnidarian symbioses is augmented by the presence in the cnidarian tissue of carbonic anhydrase (CA, EC 4.2.1.1.), an enzyme that catalyzes the inter-conversion of HCO_3^- and CO_2. In the 22 species of cnidarians examined, CA activity in the animal tissue of symbiotic species was, on average, 29 times higher than in non-symbiotic species. In the symbiotic species, CA activity in the animal fraction was 2–3 times higher than that in the algae. These results suggest that CA activity in animal tissue is related to the presence of zooxanthellae.

Two other findings indicate that CA activity in symbiotic animal tissue is related to the presence of algae. First, CA activity is correlated with habitat irradiance in colonies of the coral *Stylophora pistillata* (Weis *et al.*, 1989). *S. pistillata* from high light habitats exhibited significantly higher rates of CA activity than did those living at lower light levels. Second, there are spatial differences in CA activity within the same individual (Weis *et al.*, 1989). Column tissue of the anemone *Condylactis gigantea*, which lacks symbionts, had very low activity compared to the tentacle tissue which contains symbionts.

In this study I present further evidence, from work on symbiotic and aposymbiotic *Aiptasia pulchella*, of a positive correlation between the CA activity in animal tissue and the number of zooxanthellae present. Additionally, I use the immunoblot technique to show that high CA

Received 2 October 1990; accepted 25 February 1991.

* Present address: Department of Biological Sciences, University of Southern California, Los Angeles, CA 90089.

activity in symbiotic animal tissue is the result of induction in the animal tissue by the presence of the algae.

Materials and Methods

Maintenance of experimental organisms

A clone of the anemone *Aiptasia pulchella* (Java clone) was maintained in laboratory in aquaria or large finger bowls containing Millipore-filtered seawater (MFSW) obtained from Santa Monica Bay. For at least 14 days prior to experimentation, anemones were kept in a Precision incubator at 25°C at an irradiance of 40 $\mu E \cdot m^{-2} \cdot s^{-1}$ on a 12 h light/dark cycle unless otherwise specified. Throughout the experiments the anemones were fed *Artemia* nauplii once weekly, and the finger bowls were cleaned and the water was changed daily.

Zooxanthellae isolated from the Java clone were grown in ASP-8A medium (Guillard and Keller, 1984) in 25 l clear plastic carboys. The carboys were incubated at room temperature at an irradiance of approximately 60 $\mu E \cdot m^{-2} \cdot s^{-1}$ (16 h light/8 h dark cycle). The cultures were aerated with air passed through a bacterial air filter (Gelman Bacteria air vent). One carboy would yield approximately 10 ml of wet packed cells after approximately 75 days. The cells were collected by centrifugation and stored at −70°C.

Aposymbiotic and repopulated animals

A three part study was designed to measure CA activity in symbiotic, aposymbiotic, and newly repopulated symbiotic animals. Fifteen animals were incubated under controlled maintenance conditions for 14 days. Five animals were then assayed for CA activity, as described below, which provided values for control symbiotic animal tissue.

Ten anemones were subjected to a low temperature shock, a treatment that rendered them aposymbiotic (Steen and Muscatine, 1987). The anemones were placed in the dark at 4°C, in pre-cooled MFSW, for 4 h and subsequently incubated at 25°C in the dark. As a result of this treatment, *A. pulchella* expelled 99% of its algae within a week. To insure that virtually all of the algae were expelled, these ten anemones were then maintained in the dark at 25°C for ten weeks.

After ten weeks in the dark, five aposymbiotic anemones were placed in the light (12 h light/dark at 40 $\mu E \cdot m^{-2} \cdot s^{-1}$) for repopulation by zooxanthellae. For the first two weeks of the repopulation period, one symbiotic anemone was placed in the bowl with the aposymbiotic anemones as a potential algae donor. After seven weeks, the repopulated anemones had regained their former brown color, indicating the presence of algae and were subsequently assayed for CA activity.

Change in CA activity with a change in numbers of algae

The kinetics of loss of algae and concomitant change in CA activity in the anemone fraction of the association was also quantified. Forty-two anemones were placed, for two weeks, under the control conditions described above. Three anemones were assayed for CA activity and sampled for algal numbers on day one, and another three were kept in control conditions for the duration of the experiment (32 days) and then sampled at the end. These sets were the controls. The remaining anemones were divided into two groups. Half of the anemones were subjected to a cold shock in the same fashion as described above and subsequently maintained in the dark at 25°C. The other half was simply placed in the dark at 25°C (dark treated). Three anemones in each group, cold shock and dark treated, were sampled for algal number and assayed for CA activity after 3, 6, 10, 17, 24, and 32 days in the dark.

Separation of algae and anemone tissue for the CA assay

Anemones were homogenized in a hand-held Teflon-glass tissue homogenizer in 3.5 ml of MFSW chilled to 2°C. The homogenate was transferred to a 10 ml conical centrifuge tube and centrifuged at 900 × *g* for 1 min to separate animal tissue (supernatant) from algae (pellet). There was no evidence that the supernatant was contaminated with algae. The animal tissue supernatant was decanted and diluted 1:1 (v/v) with cold 25 m*M* veronal buffer (2°C), containing 5 m*M* EDTA, 5 m*M* dithiothreitol (DTT) and 10 m*M* $MgSO_4$, adjusted to pH 8.2 (modified from Graham and Smillie, 1976). At this point, the animal tissue supernatant was ready for the CA assay.

Algal pellets were resuspended in MFSW and centrifuged several times, which removed most of the residual anemone debris. The algae were then resuspended in 1 ml of 10% formalin in MFSW, refrigerated and saved. Cell numbers were determined with a haemacytometer and indexed to the weight of soluble anemone protein (determined as described below).

In vitro *assay for CA activity*

The *in vitro* CA assay is described in detail by Weis *et al.* (1989). The CA activity in animal homogenates was measured by the decrease in pH, resulting from the hydration of CO_2 to HCO_3^- and H^+, after the addition of substrate. CO_2-saturated distilled H_2O served as substrate and was prepared prior to an experiment by passing gaseous CO_2 through an air-stone in 200 ml of distilled H_2O at 2°C for 10 min. The water was considered to have been saturated when the pH was below 3.5, and it was then stored in a tightly stoppered glass flask at 2°C.

The assay was run as follows. One milliliter of the buffered animal homogenate was further diluted with 1 ml of 50 m*M* veronal buffer, (adjusted to pH 8.2 with 1 *N* NaOH) and transferred to a small glass test tube. The mixture was stirred with a magnetically driven stir bar. One ml of substrate was then added rapidly, and the decrease in pH of the constantly stirred mixture was recorded with a Beckman combination Ag/AgCl pH probe immersed in the mixture and connected to a Beckman Model 45 pH meter. The meter was fitted to an Acorn BBC computer with an analog to digital (A/D) converter that converted the meter output to a digital record. The data were collected and analyzed by a customized software program (John Lighton, copyright 1985).

As a control for non-specific change in pH, the same procedure was carried out with animal homogenate which had been heated to boiling for 5 min, and then cooled to 2°C. This treatment eliminated most or all CA activity. There was no evidence of renaturation upon cooling. CA activity of native animal homogenate and heat-denatured control was measured in triplicate. Units of enzyme activity were normalized to the weight of soluble protein (Hartree, 1972) with bovine serum albumin (Sigma) as a standard. CA activity was expressed as ΔpH units · min^{-1} · mg soluble $protein^{-1}$ as determined from:

$$\frac{(\Delta\text{pH of native animal homogenate} - \Delta\text{pH of denatured control}) \cdot \text{min}^{-1}}{\text{mg soluble animal protein}}$$

Sample preparation for electrophoresis

Symbiotic and aposymbiotic anemones were homogenized in a 2.5 ml Teflon-glass tissue homogenizer, in an extraction buffer consisting of 10 m*M* phosphate buffer at pH 6.8 with 1 m*M* ethylenediaminetetraacetate (EDTA), 5 m*M* $MgSO_4$, 5 m*M* dithiothreitol (DTT), and 2 m*M* phenylmethyl-sulfonyl fluoride (PMSF), a protease inhibitor. The homogenate was centrifuged at 12,000 rpm in an Eppendorf microfuge for 7 min to pellet the zooxanthellae and animal debris. No evidence was found of contamination of the supernatant by algae. The algal pellet was cleaned three times; in each instance, the cells were suspended and centrifuged in MFSW. The pellet was then stored at −70°C until needed. The slightly milky supernatant, containing the animal tissue, was decanted and stored in a test tube on ice. Usually 8 animals, each with an oral disc diameter of 0.6–0.9 mm, were homogenized in 0.75 ml of buffer to yield a concentration of approximately 4000 μg protein/ml. Soluble protein was quantified using the method of Hartree (1972).

At least 0.2 ml of packed algae, cultured or freshly isolated, were required to yield enough protein for gel electrophoresis and immunoblotting. For the freshly isolated algae, many frozen pellets from different isolations had to be combined to yield 0.2 ml. The 0.2 ml of thawed algae were suspended in 5 ml of 2% Triton X-100 in MFSW for 10 min to permeabilize and weaken the cell wall and cell membrane. The algae were alternately centrifuged at 2000 rpm in a table top centrifuge, and washed with MFSW, until foam from the Triton was gone from the supernatant. The cells were then resuspended in 0.5 ml of the extraction buffer with approximately 0.3 ml of 425–600 μm diameter glass beads (Sigma). The mixture was "vortexed" vigorously in a test tube for 1 min and centrifuged, first at 2000 rpm for 1 min in a table top centrifuge, and then at 12,000 rpm for 7 min in a microfuge, to remove the beads, unbroken cells, and cell wall debris. The resulting clear, very deep orange supernatant was decanted and stored in a test tube on ice. This technique disrupted approximately 70% of the cells, as measured by haemacytometer cell counts of samples before and after the treatment, and produced 3500–4000 μg protein/ml.

Mammalian CA (Worthington Biochemical), used as a control, was dissolved in extraction buffer to a concentration of 500 μg/ml. Prestained rainbow molecular weight markers (Amersham) were used as standards.

Electrophoresis and immunoblotting

Immunoblots, with anti-CA as a probe, were performed on animal tissue and zooxanthellae to determine the nature of CA in the different fractions. SDS-polyacrylamide gel electrophoresis (PAGE) was carried out using techniques modified from Laemmli (1970). A 12.5% resolving gel and a 4.5% stacking gel were most commonly used. Gels, 6.5 cm long and 0.75 mm thick, were run on a Hoefer SE 250 slab gel apparatus with continuous cooling. Before being loaded, the samples were diluted 1:1 with a treatment buffer (Laemmli, 1970) and boiled for 90 s. Twenty μl of sample were loaded, equalling approximately 40–50 μg of protein/sample. The gels were run at a constant voltage (200 V) and were stained with either Coomassie blue (Hames and Rickwood, 1987) or silver nitrate (Johnstone and Thorpe, 1987).

Electrophoretic transfer of proteins from unstained gels onto nitrocellulose paper was carried out in a Hoefer TE 22 transfer apparatus for 2 h at 4°C at a constant current (200 mA) in a 25 m*M* Tris, 192 m*M* glycine, and 20% methanol buffer, pH 8.3. (Towbin *et al.,* 1979). Subsequently, the nitrocellulose was incubated for 1–2 h in a blocking buffer of 3% Carnation instant dry milk in Tris buffered saline (50 m*M* Tris, 150 m*M* NaCl) pH 7.4, and then, overnight, in the appropriate primary antiserum in blocking buffer at room temperature. For each blot, one of two polyclonal antisera was used: a sheep anti-human CA [from Bioproducts for Science (BPS)] at a dilution of 1:200, or a sheep anti-human CA (from ICN) at 1:1000.

The blots were washed in blocking buffer and incubated for 2 h in a 1:1000 dilution of the secondary antibody, an alkaline phosphatase-conjugated, donkey anti-sheep IgG (Sigma). In the development, nitro blue tetrazolium (NBT) and 5-bromo-4-chloro-3-indolyl phosphate (BCIP) were used as the substrates (Engvall, 1980; Johnstone and Thorpe, 1987).

Results

CA activity in symbiotic, aposymbiotic, and repopulated anemones

To determine whether CA activity in animal homogenate is correlated with the presence of algae in animal tissue, CA activity was measured in animal tissue from (1) control symbiotic anemones, (2) aposymbiotic anemones, and (3) repopulated anemones. Both control symbiotic and repopulated symbiotic anemones were light brown and had similar average CA activities of 1.82 ± 0.27 and 1.83 ± 0.40 ΔpH units · min^{-1} · mg $protein^{-1}$, respectively. In contrast, the aposymbiotic animals were white, almost transparent, and had a significantly lower average value of 0.75 ± 0.12 ΔpH units · min^{-1} · mg $protein^{-1}$ (Fig. 1).

Change in CA activity with a change in numbers of algae

To determine whether CA activity would change with a change in numbers of algae, anemones were sampled kinetically, as described above. The number of algae lost with increasing time in the dark was quantified in both cold shock and dark treated anemones (Fig. 2). After just

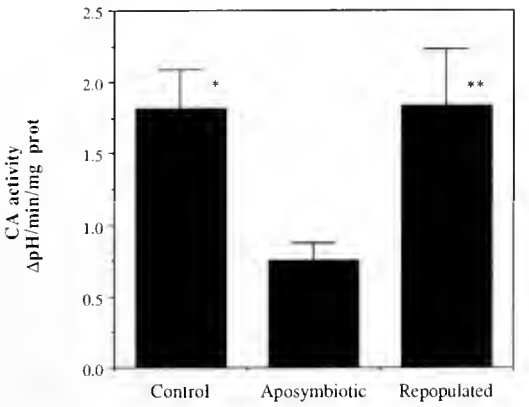

Figure 1. CA activity in control anemones, anemones rendered aposymbiotic by cold shock treatment and kept in the dark for 10 weeks, and anemones rendered aposymbiotic, kept in the dark, and subsequently reinfected with zooxanthellae. Each value is a mean ± SD of the mean (n = 5). * = different from aposymbiotic by $P \leq .0001$. ** = different from aposymbiotic by $.0001 < P \leq .005$ as calculated from a one way ANOVA.

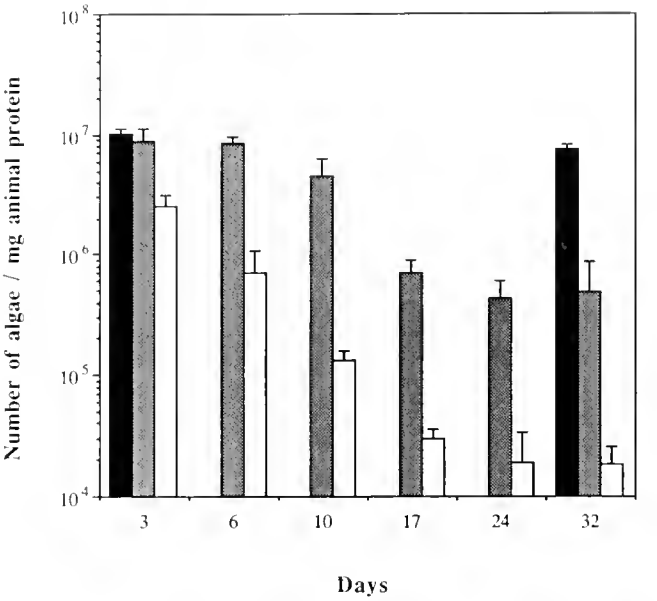

Figure 2. Number of zooxanthellae * mg animal $protein^{-1}$ *versus* days in the dark for control ■, dark-treated ▨ and cold shocked □ *Aiptasia pulchella*. Each value is a mean ± SD (n = 3).

3 days of darkness, the cold shocked anemones contained less than one third as many algae as the dark treated anemones (Table I). From days 3 to 10, cold shock treated anemones lost over 90% of their algae, compared to only 50% in dark treated anemones. By the end of the 32 day experiment, cold shocked animals had only about 4% of the number of cells/mg animal protein contained in dark treated animals (Table I). The numbers of algae in control anemones, at the beginning and at the end of the experiment, remained high (Table I). Initially, only cold shocked anemones had significantly fewer algae than the controls, but by the end of the experiment both dark treated and cold shocked anemones had lost significant numbers of cells compared to the light controls (Table I).

CA activity in the animal fraction of both dark and cold shock treated anemones was measured with increasing time in the dark (Fig. 3). CA activity in control animals at the beginning and end of the experiment were similar. CA activity in dark-treated anemones decreased modestly, while CA activity in cold shocked anemones decreased more dramatically (Table II). From days 3 to 10, CA activity decreased by 46% in cold shocked anemones, but by only 28% in dark-treated anemones. CA activity in cold shocked *versus* dark-treated animals was significantly different only at day 10 (ANOVA: $.005 < P \leq .01$). Yet at day 32, only CA activity in cold shocked anemones was significantly different (ANOVA) from the control (Table II).

The CA activity in the animal tissue was directly correlated with the number of algae present for both dark

Table I

Tests for differences in algae numbers between control and treated animals

Treatment	# of algae ($\times 10^6$) animal protein	Control, 3 days 10.20 ± 1.16	Control, 32 days 7.50 ± 0.72
Dark, 3 days	8.72 ± 2.40	$P > .25$	—
Cold shocked, dark, 3 days	2.53 ± 0.60	$.0001 < P \leq .005$	—
Dark, 32 days	.50 ± 0.36	—	$.0001 < P \leq .005$
Cold shocked, dark, 32 days	.02 ± 0.01	—	$.0001 < P \leq .005$

Significance values from one way ANOVA tests between the listed groups, each with n = 3, are given below along with a mean ± standard deviation for each treatment. The treatment type is listed with the number of days in the dark after the beginning of the experiment.

and cold shock treated anemones (Fig. 4). Most of the lower values were from the cold shock treated anemones.

Electrophoresis and immunoblotting

To determine the nature of CA in the association, symbiotic and aposymbiotic anemone tissue, as well as freshly isolated and cultured zooxanthellae, were probed for the presence of CA with polyclonal antisera against human CA. In the immunoblots, both the mammalian CA and symbiotic animal tissue lanes contained one band with an apparent molecular weight of 30 kiloDaltons (kDa) (Fig. 5). One band with an apparent molecular weight of 22.5 kDa appeared in the cultured zooxanthellae lane, and no reaction occurred in the aposymbiotic animal tissue lane (Fig. 5). Freshly isolated algae lanes also contained a single band at 22.5 kDa (data not shown), suggesting that their CA was similar to that in the cultured algae.

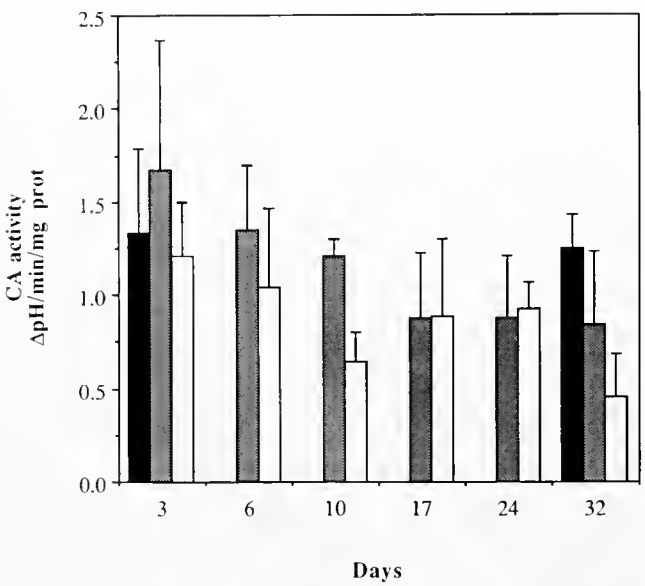

Figure 3. CA activity in animal tissue *versus* number of days in the dark for control ■, dark-treated ▨ and cold shocked □ *Aiptasia pulchella*. Each value is a mean ± SD of the mean (n = 3).

The symbiotic animal and cultured zooxanthellae had different relative signal strengths with the two antibodies used (Table III). The symbiotic animal lane gave roughly equal signals at 30 kDa with both the BPS anti-CA and the ICN anti-CA, whereas the algae at 22.5 kDa reacted only with the ICN anti-CA. Both anti-CA probes labeled mammalian CA well.

Discussion

Evidence for the correlation of CA activity with the presence of zooxanthellae

The significant decrease in CA activity in aposymbiotic *versus* control anemones and the subsequent increase in repopulated anemones to control levels (Fig. 1) show that CA activity in anemone tissue is correlated with the presence of algae. These findings are consistent with discovery of a spatial relationship between zooxanthellae and CA activity in the anemone *Condylactis gigantea* (Weis *et al.*, 1989). Additionally, the hypothesis that CA is functioning in the delivery of carbon to the zooxanthellae (Weis *et al.*, 1989) is further supported by these data. Thus, if algae are not present, the supply of CO_2 to the anemones requires no augmentation. Although CA activity is low in the aposymbiotic animals, it is not absent. CA is present in virtually all organisms and functions in intracellular pH maintenance (Wyeth and Prince, 1977).

The study of kinetics also reveals a correlation between CA activity and algal numbers. CA activity starts to decrease almost as soon as the cold shocked anemones begin to expel their algae, and it stops decreasing when algal numbers begin to stabilize. The similarity of the CA activity in cold shocked anemones after 32 days (Fig. 3) and ten weeks (Fig. 1) suggests that the decrease in CA activity is discontinued after 32 days. The relatively modest decrease in CA activity over time in dark treated anemones is consistent with the relative paucity of algae expelled from these anemones compared with the cold shocked animal (Fig. 2).

Table II

Tests for differences in CA activity between control and treated animals

Treatment	$\Delta pH \cdot min^{-1} \cdot mg\ protein^{-1}$	Control, 3 days 1.332 ± 0.457	Control, 32 days 1.248 ± 0.186
Dark, 3 days	1.672 ± 0.694	$P > .25$	—
Cold shock, dark, 3 days	1.208 ± 0.288	$P > .25$	—
Dark, 32 days	.842 ± 0.394	—	$.10 < P \leq .25$
Cold shock, dark, 32 days	.452 ± 0.237	—	$.01 < P \leq .025$

Significance values from one way ANOVA tests between the listed groups, each with n = 3, are given below along with a mean ± standard deviation for each treatment. The treatment type is listed with the number of days in the dark after the beginning of the experiment.

The nature of CA in A. pulchella

Animal CA, a zinc metalloenzyme, has a molecular weight of approximately 30 kDa, and has as many as six isozymes (Coleman, 1980; Lindskog *et al.*, 1971; Tashian, 1989). Plant CA has been less extensively studied, but occurs in a wide variety of terrestrial and aquatic plants and algae (Lamb, 1977; Poincelot, 1979; Reed and Graham, 1981; Graham *et al.*, 1984). Plant CA varies in molecular weight from about 40 to 250 kDa; it consists of up to 6 subunits ranging in size from approximately 25–34 kDa. Different numbers of subunits and molecular weights have been reported even for a single species (Graham *et al.*, 1984). This study indicates that anemone CA is a 30 kDa protein, whereas CA from freshly isolated or cultured algae is either a 22.5 kDa protein or a protein with several 22.5 kDa subunits (Fig. 5), a weight slightly below the 25–34 kDa range reported for other algae and higher plants (Graham *et al.*, 1984). The successful labeling of both cnidarian and zooxanthellae CA with anti-human CA indicates that at least some portions of the enzyme are highly conserved.

Because protein from freshly isolated algae was difficult to obtain (large quantities of anemones and extensive cleaning were needed to yield enough uncontaminated algal protein), most experiments were performed on cultured algae. The similar labeling of cultured and freshly isolated algae at 22.5 kDa suggests that they have CAs of identical molecular weight.

Induction of animal CA by the presence of algae

Induction or deinduction of an enzyme occurs when the factors controlling its synthetic pathway are removed or changed. Additionally, changes in rates of enzyme degradation can affect the relative activity of an enzyme. These processes can take from minutes to days to be manifested as a change in enzyme activity. Induction of CA activity in the animal tissue in the presence of zooxanthellae could account for the vastly different rates of CA activity in different regions of an individual of *Condylactis gigantea* or in symbiotic *A. pulchella* relative to aposymbiotic ones. In this study, CA activity decreased at a faster rate in the first ten days than in the last 22 in both cold shock and dark treated anemones (Fig. 3). This stabilization of CA activity by the end of the experiment suggests that the putative deinduction or increased degradation of the enzyme took place in the first ten days. A similar plateau in algal population size, although not as well pronounced (Fig. 2), remains consistent with the correlation of CA activity and the presence of zooxanthellae.

The immunoblots of the symbiotic animal tissue, aposymbiotic animal tissue and cultured algae (Fig. 5) suggest that high CA activity in symbiotic animal tissue exhibited in Figure 1 is due to induction of CA in the animal by the presence of the algae, rather than to the presence of algal CA. In Figure 5, anti-CA labeled a single band at 30 kDa in symbiotic animal tissue, whereas no such band appeared in aposymbiotic animals. This result is consistent

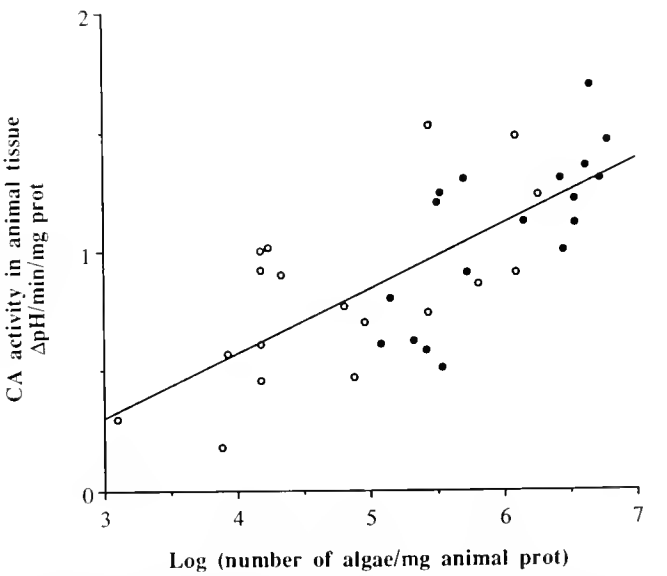

Figure 4. CA activity in animal tissue of dark-treated ● and cold shocked ○ anemones *versus* log (number of algae * mg animal protein^{-1}). Each point is a datum from a single animal. The $r^2 = 0.518$.

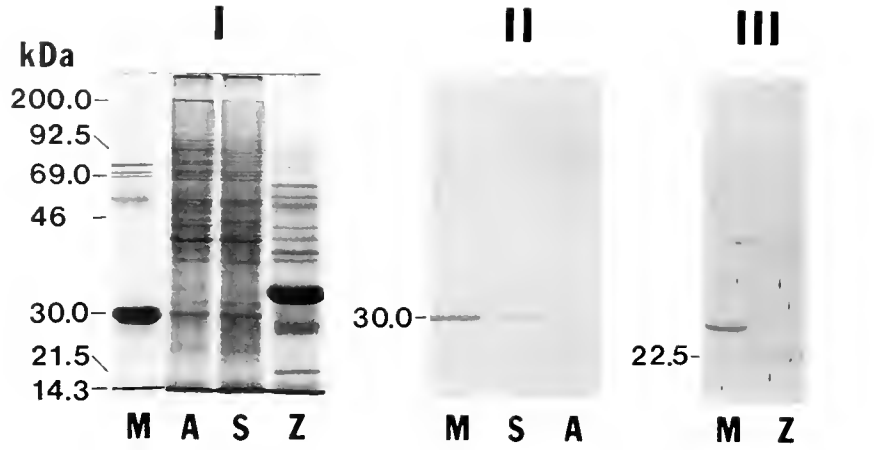

Figure 5. An SDS-polyacrylamide gel stained with Coomassie blue (I) and corresponding immunoblots (II and III). Blot II was probed with BPS anti-human CA and blot III with ICN anti-human CA. M = control purified mammalian CA, S = symbiotic animal extract, A = aposymbiotic animal extract, and Z = cultured zooxanthellae extract.

with the loss of enzyme activity in aposymbiotic anemones as compared to symbiotic and repopulated *A. pulchella* (Fig. 1; although there is low CA activity in aposymbiotic anemones, there is not enough protein in the gel to react with the anti-CA probe). The molecular weight of CA from freshly isolated and cultured algae was 22.5 kDa. No band at 22.5 kDa was detected in any symbiotic animal lanes. If algal CA were responsible for CA activity in symbiotic animal tissue, either by export of its CA to the perialgal space or further into the animal tissue, then it should appear on the gel in the symbiotic animal tissue lane.

Induction of CA activity has been studied in detail in mammalian tissues (see Deutsch, 1987, for review), but much less in invertebrates, plants, and algae. Such studies include the induction of CA activity during osmotic stress, to aid in osmoregulation, in various crustaceans (Henry and Cameron, 1983; Wheatly and Henry, 1987; Henry, 1988). CA activity can be induced in some microalgae. The chlorophytes *Chlamydomonas reinhardtii* (*e.g.*, Badger *et al.*, 1978; Coleman *et al.*, 1984, 1985) and *Chlorella vulgaris* (Hogetsu and Miyachi, 1979; Tsuzuki *et al.*, 1980), and the rhodophyte *Porphyridium* spp. (Dixon *et al.*, 1987; Yagawa *et al.*, 1987) show an increase in CA activity when switched from a high to a low CO_2 environment.

The mechanism of induction of CA activity is largely undescribed. In humans, the mechanism varies greatly depending on both the function of CA and the tissue or organ type (see Deutsch, 1987, for some examples). As mentioned above, CA is induced in *C. reinhardtii* by low [CO_2] but also by light (Dionisio *et al.*, 1989a, b). In algal/cnidarian symbioses, any number of factors related to presence of algae might induce CA activity in animal tissue, such as increased [O_2] or decreased [CO_2] due to photosynthesis, changes in intracellular pH resulting from different [CO_2], or products, such as glycerol or amino acids, translocated from alga to host (see Cook, 1983, for review).

The kinetics of CA induction or deinduction in animal systems has been studied infrequently. In microalgae, however, the kinetics of CA induction are well described and, in all cases, are shorter in duration than deinduction in *A. pulchella*. Within 24 h after placing *C. reinhardtii* in a low CO_2 environment, CA activity increased up to 2000% (Coleman *et al.*, 1984; Badour and Tan, 1987). CA has even been reported to be induced and deinduced at the transcriptional level on a diel cycle in *C. reinhardtii* when the chlorophyte is grown in 12 h light/dark cycle (Toguri *et al.*, 1989).

Other examples of induction in symbioses

There are several algal/cnidarian symbioses in which algae apparently induce enzyme activity or developmental phenomena in the animal. For example, the animal tissue

Table III

Relative signal strengths of the two polyclonal antisera used to probe the experimental samples

	ICN anti-human CA 1:1000 dilution	BPS anti-human CA 1:200 dilution
Purified mammalian CA	+++	+++
Symbiotic animal tissue	+	+
Cultured zooxanthellae	++	−

ICN sheep antiserum was purchased from ICN and BPS sheep antiserum from Bioproducts for Science.

of the symbiotic anemone *Anthopleura elegantissima* contains high levels of superoxide dismutase (SOD) activity compared with SOD in nonsymbiotic anemones. High SOD activity is interpreted as a mechanism for removal of damaging superoxide radicals produced during photosynthesis by the symbiotic algae (Dykens and Shick, 1982, 1984). Also, low molecular weight fractions from homogenates of symbiotic cnidarians suppress uptake of exogenous alanine by isolated zooxanthellae. Similar fractions from aposymbiotic animals fail to suppress uptake (Blanquet *et al.*, 1988). Metamorphosis (which involves complex changes in enzyme expression and activity) of scyphistomae of *Cassiopeia xamachana* and *Mastigias papua,* is induced by the presence of zooxanthellae (Sugiura, 1964; Trench, 1979; Hofmann and Kremer, 1981).

Enzyme induction has also been demonstrated in other symbioses. In the *Rhizobium*/legume symbiosis, the bacteroid nitrogenase activity and host glutamate synthetase activity are positively correlated. Further, the presence of the bacterial symbionts induces the synthesis of the leghemoglobin apoprotein (Smith and Douglas, 1987). In the bacteria/*Amoeba proteus* symbiosis, peribacterial vacuolar membranes contain a protein not found in food vacuolar membranes (Jeon, 1983). Jeon suggests that the synthesis of this protein is induced by the presence of the bacteria, and that the protein somehow prevents lysosomal fusion with the peribacterial vacuolar membrane and subsequent digestion of the bacteria.

This study describes another example of genome interaction between two partners in a symbiosis. Future studies on the molecular mechanisms of induction and regulation of CA should prove fruitful.

Acknowledgments

I thank S. Anandan and M. Harmon for valuable technical assistance, R. Gates, M. Harmon, G. Somero, and L. Muscatine for comments of the manuscript, and L. Muscatine for valuable suggestions and input. This study was supported by a research grant from the National Science Foundation (OCE-8510518 to L. Muscatine).

Literature Cited

Badger, M. R., A. Kaplan, and J. A. Berry. 1978. A mechanism for concentrating CO_2 in *Chlamydomonas reinhardtii* and *Anabaena variabilis* and its role in photosynthetic CO_2 fixation. *Carnegie Inst. Wash. Year Book* **77:** 251–261.

Badour, S. S., and C. K. Tan. 1987. Activities of carbonic anhydrase and carboxylating enzymes in *Chlamydomonas segnis* adapted and adapting to air levels of carbon dioxide. *Plant Cell Physiol.* **28**(8): 1485–1492.

Blanquet, R. S., D. Emmanuel, and T. A. Murphy. 1988. Suppression of exogenous alanine uptake in isolated zooxanthellae by cnidarian host homogenate fractions: species and symbiosis specificity. *J. Exp. Mar. Biol. Ecol.* **117:** 1–8.

Coleman, J. E. 1980. Current concepts of the mechanism of action of carbonic anhydrase. Pp. 133–150 in *Biophysics and Physiology of Carbon Dioxide* C. Bauer, G. Gros, and H. Bartels, eds. Springer Verlag, Berlin.

Coleman, J. R., J. A. Berry, R. K. Togasaki, and A. R. Grossman. 1984. Identification of extracellular carbonic anhydrase of *Chlamydomonas reinhardtii. Plant Physiol.* **76:** 472–477.

Coleman, J. R., L. S. Green, J. A. Berry, R. K. Togasaki, and A. R. Grossman. 1985. Adaptation of *Chlamydomonas reinhardtii* to air levels of CO_2 and the induction of carbonic anhydrase activity. Pp. 339–359 in *Inorganic Carbon Uptake by Aquatic Photosynthetic Organisms,* W. Lucas and J. Berry, eds. *Am. Soc. Plant Physiol.,* Rockville, MD.

Cook, C. B. 1983. Metabolic interchange in algae-invertebrate symbioses. *Int. Rev. Cytol.* **14:** 177–210.

Deutsch, H. F. 1987. Carbonic anhydrases. *Int. J. Biochem.* **19**(2): 101–113.

Dionisio, M. L., M. Tsuzuki, and S. Miyachi. 1989a. Light requirement for carbonic anhydrase induction in *Chlamydomonas reinhardtii. Plant Cell Physiol.* **30**(2): 207–213.

Dionisio, M. L., M. Tsuzuki, and S. Miyachi. 1989b. Blue light induction of carbonic anhydrase activity in *Chlamydomonas reinhardtii. Plant Cell Physiol.* **30**(2): 215–219.

Dixon, G. K., B. N. Patel, and M. J. Merrett. 1987. Role of intracellular carbonic anhydrase in inorganic-carbon assimilation by *Porphyridium purpureum. Planta* **172:** 508–513.

Dykens, J. A., and J. M. Shick. 1982. Oxygen production by endosymbiotic algae controls superoxide dismutase activity in their animal host. *Nature* **297:** 579–580.

Dykens, J. A., and J. M. Shick. 1984. Photobiology of the symbiotic sea anemone, *Anthopleura elegantissima.* defenses against photodynamic effects, and seasonal photoacclimatization. *Biol. Bull.* **167:** 683–697.

Engvall, E. 1980. Enzyme immunoassay ELISA and EMIT. *Meth. Enzymol.* **70:** 419–439.

Falkowski, P. G., Dubinsky, Z., and L. Muscatine. 1984. Light and the bioenergetics of a symbiotic coral. *BioScience* **34:** 705–709.

Graham, D., and R. M. Smillie. 1976. Carbonate dehydratase in marine organisms of the Great Barrier Reef. *Aust. J. Plant Physiol.* **3:** 113–119.

Graham, D., M. L. Reed, B. D. Patterson, D. G. Hockley, and M. R. Dwyer. 1984. Chemical properties, distribution, and physiology of plant and algal carbonic anhydrases. *Ann. N. Y. Acad. Sci.* **429:** 222–237.

Guillard, R. R. L., and M. D. Keller. 1984. Culturing dinoflagellates. Pp. 391–442 in *Dinoflagellates,* D. L. Spector, ed. Academic Press, New York.

Hames, B. D., and D. Rickwood. 1987. *Gel Electrophoresis of Proteins: A Practical Approach.* IRL Press, Oxford. 290 pp.

Hartree, E. F. 1972. Determination of protein: a modification of the Lowry method that gives a linear photometric response. *Anal. Biochem.* **48:** 422–427.

Henry, R. P. 1988. Multiple functions of carbonic anhydrase in the crustacean gill. *J. Exp. Zool.* **248:** 19–24.

Henry, R. P., and J. N. Cameron. 1983. The role of carbonic anhydrase in respiration, ion regulation and acid-base balance in the aquatic crab *Callinectes sapidus* and the terrestrial crab *Gecarcinus lateralis. J. Exp. Biol.* **103:** 205–223.

Hofmann, D. K., and B. P. Kremer. 1981. Carbon metabolism and strobilation in *Cassiopea andromedea* (Cnidaria: Scyphozoa): Significance of endosymbiotic dinoflagellates. *Mar. Biol.* **65:** 25–33.

Hogetsu, D., and S. Miyachi. 1979. Role of carbonic anhydrase in photosynthetic CO_2 fixation in *Chlorella. Plant Cell Physiol.* **20**(4): 747–756.

Jeon, K. 1983. Integration of bacterial endosymbionts in amoebae. *Int. Rev. Cytol. Suppl.* **14:** 29–47.

Johnstone, A., and R. Thorpe. 1987. *Immunocytochemistry in Practice.* Blackwell Scientific, Oxford. 306 pp.

Kerby, N. W., and J. A. Raven. 1985. Transport and fixation of inorganic carbon by marine algae. *Adv. Bot. Res.* **2:** 71–123.

Laemmli, U. K. 1970. Cleavage of structural proteins during the assembly of the head of bacteriophage T4. *Nature* **227:** 680–685.

Lamb, J. E. 1977. Minireview: plant carbonic anhydrase. *Life Sci.* **20:** 393–406.

Lindskog, S., L. E. Henderson, K. K. Kannan, A. Liljas, P. O. Nyman, and B. Strandberg. 1971. Carbonic anhydrase. Pp. 587–665 in *The Enzymes, Volume 5,* P. Boyer, ed. Academic Press, New York.

Poincelot, R. P. 1979. Carbonic anhydrase. Pp. 230–238 in *Encyclopedia of Plant Physiology. Photosynthesis II. Photosynthetic Carbon Metabolism and Related Processes,* M. Gibbs and E. Latzko, eds. Springer Verlag, Berlin.

Reed, M. L., and D. Graham. 1981. Carbonic anhydrase in plants: distribution, properties and possible physiological roles. *Prog. Phytochem.* **7:** 47–94.

Smith, D. C., and A. E. Douglas. 1987. Symbiosis between nitrogen-fixing prokaryotes and plant roots. Pp 64–92 in *The Biology of Symbiosis.* Edward Arnold Publishers, London.

Steen, R. G., and L. Muscatine. 1987. Low temperature evokes rapid exocytosis of symbiotic algae by a sea anemone. *Biol. Bull.* **172:** 246–263.

Sugiura, Y. 1964. On the life history of rhizostome medusae II. Indispensability of zooxanthellae for strobilation in *Mastigias papua. Embriologia* **8:** 223–233.

Tashian, R. E. 1989. The carbonic anhydrases: widening perspectives on their evolution, expression and function. *Bioessays* **10**(6): 186–192.

Toguri, T., S. Muto, S. Mihara, and S. Miyachi. 1989. Synthesis and degradation of carbonic anhydrase in a synchronized culture of *Chlamydomonas reinhardtii. Plant Cell Physiol.* **30**(4): 533–539.

Towbin, H., T. Staehelin, and J. Gordon. 1979. Electrophoretic transfer of proteins from polyacrylamide gels to nitrocellulose sheets: procedure and some applications. *Proc. Nat. Acad. Sci. USA* **76**(9): 4350–4354.

Trench, R. K. 1979. The cell biology of plant-animal symbiosis. *Ann. Rev. Plant Physiol.* **30:** 485–531.

Tsuzuki, M., Y. Shiraiwa, and S. Miyachi. 1980. Role of carbonic anhydrase in photosynthesis in *Chlorella* derived from kinetic analysis of $^{14}CO_2$ fixation. *Plant Cell Physiol.* **21**(4): 677–688.

Weis, V. M., G. J. Smith, and L. Muscatine. 1989. A "CO_2-supply" mechanism in zooxanthellate cnidarians: role of carbonic anhydrase. *Mar. Biol.* **100:** 195–202.

Wheatly, M. G., and R. P. Henry. 1987. Branchial and antennal gland Na^+/K^+-dependent ATPase and carbonic anhydrase activity during salinity acclimation of the euryhaline crayfish *Pacifastacus leniusculus. J. Exp. Biol.* **133:** 73–86.

Wyeth, P., and R. H. Prince. 1977. Carbonic anhydrase. *Inorg. Perspect. Biol. Med.* **1:** 37–71.

Yagawa, Y., S. Muto, and S. Miyachi. 1987. Carbonic anhydrase of a unicellular red alga *Porphyridium cruentum* R-1. I Purification and properties of the enzyme. *Plant Cell Physiol.* **28**(7): 1253–1262.

Reference: *Biol. Bull.* **180:** 505–507. (June, 1991)

Mitochondrial Activities of Phosphagen Kinases are Not Widely Distributed in the Invertebrates

W. ROSS ELLINGTON[1] AND AMY C. HINES

Department of Biological Science, B-157, Florida State University, Tallahassee, Florida 32306

A diverse array of phosphagen kinases [arginine kinase (AK), lombricine kinase (LK)], glycocyamine kinase (GK), taurocyamine kinase (TK), and creatine kinase (CK) is found in the animal kingdom (see ref. 1 for a review). These reactions appear to function in the temporal buffering of ATP in muscles during energy deficits such as might occur during burst contraction or anoxia (2, 3). In many vertebrate tissues, a distinct mitochondrial isoenzyme of CK is present, and it may play a special role in the intracellular transport of high energy phosphate (4). In this study, we investigated whether mitochondrial activities of phosphagen kinases are present in invertebrate muscles. Our results show that AK is present in mitochondria from a crustacean. However, phosphagen kinases are lacking in mitochondria from insect flight muscles, molluscan cardiac and smooth muscle, and polychaete and oligochaete body wall musculature. It appears that mitochondrial activities of phosphagen kinases are not widely distributed in the invertebrates. These data, in conjunction with previous studies on the physico-chemical nature of the interaction of phosphagen kinases with mitochondria (5, 6), suggest that mitochondrial compartmentation of phosphagen kinases may have evolved independently in two major animal groups.

Mitochondrial CK in vertebrate muscle constitutes the proximal end of the so-called phosphocreatine shuttle (4). According to the shuttle model, CK catalyzes the phosphorylation of creatine to phosphocreatine using newly synthesized ATP. The resulting phosphocreatine is then thought to diffuse from the mitochondrion to sites of ATP use (myofibrils, ion transport ATPases), where it is used to phosphorylate ADP to ATP. In effect, high energy phosphate is thought to be transported by phosphocreatine rather than ATP, which overcomes the diffusion limitations of the adenine nucleotides (4). The presence of mitochondrial CK is advantageous because it maximizes enzymatic potential in the compartment where it is needed (2). In contrast to the situation in vertebrate muscles, we show in the following results that mitochondrial activities of other phosphagen kinases are rather uncommon in the animal kingdom.

Tightly coupled mitochondria were isolated from the muscles of seven representative species of invertebrates, and the presence of phosphagen kinase activity was assessed by respirometric methods (Table I). Phosphagen kinase activities were not present in mitochondria from the body wall musculature of the earthworm *Lumbricus terrestris* and the polychaete *Nereis virens*. Mitochondria from the radula retractor muscle of the whelk *Busycon canaliculatum* and the systemic ventricle of the octopus *Octopus vulgaris* lacked AK activity, which is consistent with results from studies on other mollusks (8, 9, 10). AK was also not present in mitochondria from the flight muscles of the blowfly *Sarcophaga bullata* and moth *Manduca sexta*. AK also appears to be absent from the flight muscle mitochondria of the locust *Locusta migratoria* (11). Spectrophotometric assays (3) of phosphagen kinase activities in detergent extracts of *L. terrestris*, *N. virens*, and *M. sexta* mitochondria revealed only trace (<0.1 μmole/min · g wet wgt at 25°C), or no activity.

Only mitochondria isolated from the hearts of the crayfish *Procambarus clarkii* contained phosphagen kinase activity (Table I). Mitochondrial AK activity in *P. clarkii* was sufficiently high, as to facilitate stimulation of approximately 50% of state-3 respiration when 5 m*M* L-arginine was added to the respiration system (Fig. 1). Mitochondrial AK represented around 1.5% of the total AK

Received 9 October 1990; accepted 3 March 1991.

[1] To whom editorial correspondence and reprint requests should be sent.

Table I

Mitochondrial activities of phosphagen kinases in the muscles of a variety of invertebrates. A "+" or "−" indicates the presence or absence, respectively, of mitochondrial kinase activity. Quality of mitochondrial preparations is indicated by showing the range of values of the respiratory control ratios (RCR = State 3 respiration ÷ State 4 respiration). An RCR value greater than one indicates that mitochondria are coupled and show respiratory control behavior in response to the addition of ADP (see discussion below)

Organism and tissue	RCR	Phosphagen kinase	Mitochondrial activity
Lumbricus terrestris body wall (earthworm)	3–4	LK	−
Nereis virens body wall (polychaete)	4–5	GK	−
Busycon canaliculatum radula muscle (whelk)	3–5	AK	−
Octopus vulgaris systemic ventricle (octopus)	8–17	AK	−
Sarcophaga bullata flight muscle (blowfly)	4–7	AK	−
Manduca sexta flight muscle (moth)	5–10	AK	−
Procambarus clarkii heart (crayfish)	4–6	AK	+

N. virens and *B. canaliculatum* were obtained from the Marine Biological Laboratory (Woods Hole, Massachusetts). *L. terrestris*, *S. bullata*, and *M. sexta* were purchased from Carolina Biological Supply (Burlington, North Carolina). *O. vulgaris* and *P. clarkii* were collected locally. Mitochondria were isolated by gentle homogenization and differential centrifugation procedures (details available upon request). Mitochondrial respiration was monitored polarigraphically as previously described (6, 7). The addition of ADP to tightly coupled mitochondria respiring in the presence of substrate (state-4) leads to a dramatic increase in respiration (state-3) which will continue until all of the ADP has been phosphorylated to ATP. If a phosphagen kinase is present in the mitochondria, subsequent addition of the appropriate phosphagen acceptor (arginine, lombricine, glycocyamine, etc.) will lead to the formation of phosphagen and ADP by the following reaction:

Phosphagen kinase: $\text{Acceptor} + \text{ATP} \rightarrow \text{ADP} + \text{Phosphagen}$

Oxidative phosphorylation: $\beta O_2 + \text{ADP} + P_i \rightarrow \text{ATP} + \beta H_2O$

Net reaction: $\beta O_2 + \text{Acceptor} + P_i \rightarrow \text{Phosphagen} + \beta H_2O$

(Note: β is dependent on the P:O ratio)

The resulting ADP will stimulate respiration and ATP formation via oxidative phosphorylation (see above). The ATP will phosphorylate additional acceptor, producing more ADP which will stimulate state-3 respiration as long as acceptor is present (net reaction above). Thus, stimulation of state-3 respiration by phosphagen acceptor indicates the presence of mitochondrial phosphagen kinase activity (see Fig. 1, for example), providing that the mitochondria have been extensively washed, as was the case in this study. Most experiments were conducted on at least three independent preparations from each species. Because *O. vulgaris* was not readily available, only a single mitochondrion preparation was used for the experiments with this species.

activity in *P. clarkii* heart muscle (Fig. 1). AK has also been observed in the mitochondria of several other crustaceans (12, 13, 14). Furthermore, we have recently shown that heart mitochondria from the horseshoe crab *Limulus polyphemus* (a chelicerate arthropod) contain AK activity that is clearly intrinsic to the mitochondrion (6, 7).

Our rather limited survey, coupled with the results of others, suggests that mitochondrial phosphagen kinase activities are consistently present in the muscles of only three groups: AK in crustaceans, and also in the relic chelicerate *L. polyphemus*, and CK in vertebrates. The interaction between AK and these mitochondria is hydrophobic, in that detergents are required to solubilize enzyme activity (6, 14). In contrast, the interaction between CK and vertebrate mitochondria is clearly electrostatic and is easily disrupted by changes in ionic strength

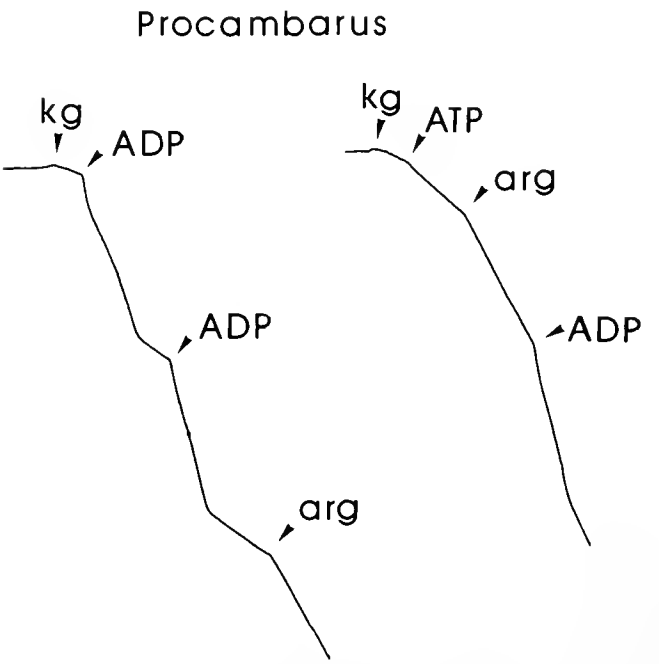

Figure 1. *Patterns of oxygen consumption (vertical-oxygen concentration; horizontal-time) of mitochondria from the heart of the crayfish* Procambarus clarkii. *Mitochondria were added to an isotonic respiration medium supplemented with 1.5 mM $MgCl_2$ and 5 mM potassium phosphate, and respiration was monitored at 25°C.* Left panel—*5 mM α-ketoglutarate (Kg) was initially added followed by two cycles of addition of 200 μM ADP. After return to state-4 respiration, 5 mM L-arginine (arg) was added to ascertain whether AK was present.* Right panel—*Respiration was initiated by the addition of 5 mM α-ketoglutarate followed by 200 μM ATP. Addition of 5 mM L-arginine resulted in stimulation of State-3 respiration via ADP production by the AK reaction. Respiration was further enhanced by addition of 200 μM ADP. In both sets of experiments, L-arginine was capable of stimulating respiratory activity equivalent to approximately 50% of the ADP-initiated state-3 rate. To verify the presence of AK activity,* P. clarkii *mitochondria were extracted in detergent (1% Triton X-100). AK activity was assayed in the mitochondrial extract using previously described spectrophotometric procedures (7). AK activity in crayfish mitochondria was 16 μmoles/min · g wet wgt at 25°C which represents approximately 1.5% of the total AK activity in this tissue. Since these mitochondria were washed four times, it is clear that AK activity is intrinsic to* P. clarkii *mitochondria and is not a cytoplasmic contaminant.*

(5). Given the broad phylogenetic distance between the crustacean and chelicerate arthropods and the vertebrates, the apparent lack of phosphagen kinase activities in the muscle mitochondria of the other major groups, and the dramatic differences in the physico-chemical interaction between these kinases and the mitochondria, we speculate that mitochondrial phosphagen kinase activities arose independently in the two groups where they are found.

Finally, we point out that, although insect flight muscles and cephalopod hearts develop the highest aerobic power outputs of any invertebrate muscles (15, 16), the functional capabilities of these muscles do not appear to be intrinsically limited or compromised by the absence of phosphagen kinase activities in their mitochondria.

Acknowledgments

We thank J. Otto for performing some of the initial mitochondrial isolation experiments using *N. virens* tissue. Supported by NSF Grant DCB-8710108 to WRE.

Literature Cited

1. **Watts, D. C. 1971.** Evolution of phosphagen kinases. Pp. 150–173 in *Biochemical Evolution and the Origin of Life*, E. Schoffeniels, ed. North Holland Publishing, New York.
2. **Meyer, R. A., H. L. Sweeney, and M. J. Kushmerick. 1984.** A simple analysis of the phosphocreatine shuttle. *Am. J. Physiol.* **246:** C365–C377.
3. **Ellington, W. R. 1989.** Phosphocreatine represents a thermodynamic and functional improvement over other muscle phosphagens. *J. Exp. Biol.* **143:** 177–194.
4. **Bessman, S. P., and P. J. Geiger. 1981.** Transport of energy in muscle. *Science* **211:** 448–452.
5. **Vial, C., B. Font, D. Goldschmidt, and D. C. Gauteron. 1979.** Dissociation and reassociation of creatine kinase with heart mitochondria: pH and phosphate dependence. *Biochim. Biophys. Acta* **88:** 1352–1359.
6. **Doumen, C., and W. R. Ellington. 1990.** Mitochondrial arginine kinase from the heart of the horseshoe crab, *Limulus polyphemus* I. Physicochemical properties and nature of interaction with the mitochondrion. *J. Comp. Physiol. B* **160:** 449–457.
7. **Doumen, C. and W. R. Ellington. 1990.** Mitochondrial arginine kinase from the heart of the horseshoe crab, *Limulus polyphemus*. II. Catalytic properties and studies of potential coupling with oxidative phosphorylation. *J. Comp. Physiol. B* **160:** 459–468.
8. **Storey, K. B. 1977.** Purification and characterization of arginine kinase from the mantle muscle of the squid, *Symplectoteuthis oualaniensis*. *Arch. Biochem. Biophys.* **179:** 518–526.
9. **Ballantyne, J. S., P. W. Hochachka, and T. P. Mommsen. 1981.** Studies on metabolism of the migrating squid *Loligo opalescens*. Enzymes of tissue and heart mitochondria. *Mar. Biol. Lett.* **2:** 75–85.
10. **Mommsen, T. P., and P. W. Hochachka. 1981.** Respiratory and enzymatic properties of squid heart mitochondria. *Eur. J. Biochem.* **120:** 345–350.
11. **Schneider, A., R. J. Niener, and M. K. Grieshaber. 1989.** On the role of arginine kinase in insect flight muscle. *Insect Biochem.* **19:** 471–480.
12. **Chen, C. H., and A. L. Lehninger. 1973.** Respiration and phosphorylation by mitochondria from the hepatopancreas of the blue crab. *Arch. Biochem. Biophys.* **154:** 449–459.
13. **Skorkowski, E. F., Z. Aleksandrowicz, T. Wrzolkowa, and J. Swierczyski. 1976.** Isolation and some properties of mitochondria from the abdomen muscle of the crayfish *Orconectes limosus*. *Comp. Biochem. Physiol.* **56B:** 493–500.
14. **Hird, F. J. R., and Y. Robin. 1985.** Studies on phosphagen synthesis by mitochondrial preparations. *Comp. Biochem. Physiol.* **80B:** 517–520.
15. **Ellington, C. P. 1985.** Power and efficiency of insect flight muscle. *J. Exp. Biol.* **115:** 293–304.
16. **Houlihan, D. F., C. Agnisda, N. M. Hamilton, and I. Trara-Genoino. 1985.** Oxygen consumption of the isolated heart of *Octopus*: effects of power output and hypoxia. *J. Exp. Biol.* **131:** 137–157.

INDEX

D

E

F

G

H

I

J

K

L

M

N

O

P

R

S

T

U

V

W

Y

Z

CONTENTS